Groundwater Hydrology

About the Author

Bhagu R Chahar earned his PhD degree in Civil Engineering from Indian Institute of Technology Roorkee. He completed his MTech (Civil Engineering) with specialization in Water Resources Engineering from the Indian Institute of Technology Kharagpur and received his bachelor's degree in Civil Engineering from MBM Engineering College, Jodhpur University, Jodhpur. He started his academic career in February 1992 as Assistant Professor in Civil Engineering, MBM Engineering College, Jodhpur. He then joined the Indian Institute of Technology Delhi (IIT-D) as Assistant Professor in Civil Engineering in 2003. Later in 2008, he became Associate Professor and was then elevated to Professor of Civil Engineering in 2012. He has teaching experience of over 22 years and has guided many masters and doctoral theses. His current areas of research include groundwater modeling, seepage, subsurface drainage, urban drainage, channel design, numerical methods, and so forth. He is recipient of several scholarships and awards including Visiting International Fellowship of EWRI of ASCE, Young Scientist of DST, and AICTE Career Award for Young Teachers. He is also author of more than 110 articles in reputed journals and proceedings and has presented many papers in national and international conferences. He is Fellow of ISH, IWWA and IWRS, and Life Member of ASCE, ISTE, IAH, and IE(I).

Groundwater Hydrology

Bhagu R Chahar
Professor
Department of Civil Engineering
Indian Institute of Technology Delhi
New Delhi

McGraw Hill Education (India) Private Limited
NEW DELHI

McGraw Hill Education Offices

New Delhi New York St Louis San Francisco Auckland Bogotá Caracas
Kuala Lumpur Lisbon London Madrid Mexico City Milan Montreal
San Juan Santiago Singapore Sydney Tokyo Toronto

McGraw Hill Education (India) Private Limited

Published by McGraw Hill Education (India) Private Limited
P-24, Green Park Extension, New Delhi 110 016

Groundwater Hydrology

Print Edition:
ISBN-13: 978-93-3920-463-1
ISBN-10: 93-3920-463-8

eBook Edition:
ISBN-13: 978-93-3920-464-8
ISBN-10: 93-3920-464-6

Managing Director: *Kaushik Bellani*

Head—Higher Education (Publishing and Marketing): *Vibha Mahajan*
Senior Publishing Manager (SEM & Tech. Ed.): *Shalini Jha*
Editorial Executive: *Harsha Singh*
Manager—Production Systems: *Satinder S Baveja*
Assistant Manager—Editorial Services: *Sohini Mukherjee*
Production Exécutive: *Anuj K Shriwastava*

Assistant General Manager—Higher Education (Marketing): *Vijay Sarathi*
Senior Graphic Designer—Cover: *Meenu Raghav*

General Manager—Production: *Rajender P Ghansela*
Manager—Production: *Reji Kumar*

Typeset at Mukesh Technologies Pvt. Ltd., Puducherry, India 605 008 and
printed at Rashtriya Printers, M-135, Panchsheel Garden, Naveen Shahdara, Delhi 110 032

Cover Printer:

To
My Teachers and Students

Contents

Preface

Groundwater is an important resource, and its exploration, planning, and management play a significant role in the effective utilization of it for domestic, irrigation, industrial, and other purposes. Groundwater hydrology deals with quality and quantity aspects of groundwater, and it is a broad field with many ramifications. There is an ever-increasing demand for information on groundwater hydrology by students and professionals in several fields. In this book, an attempt has been made to present the basic principles of groundwater movement in aquifers and management of groundwater. The principles of groundwater flow are presented through elaborate derivation of governing differential equations and their analytical solutions for simple boundary conditions. At the same time, the book incorporates sufficient theoretical material to grasp the concepts even by bypassing the clutter of mathematical equations. It has an appropriate focus on both aspects of groundwater: resource development as well as contamination transport and quality management. There is a separate chapter on groundwater flow solution by complex analysis, and the book contains substantial original material on solutions by the author to seepage from canals using conformal mapping, stream-depletion problem, flowing-well problem, and some case studies. The book has a broader scope due to comprehensive coverage on most aspects of groundwater, and it enables the readers to acquire a basic understanding of the groundwater hydrology for addressing groundwater issues. The book has been written to serve the needs of undergraduate and graduate students and professionals in hydrogeology, groundwater engineering, water resources engineering, agricultural engineering, earth sciences, water resources management, geotechnical engineering, and environmental sciences.

Salient Features of the Book

- Comprehensive coverage on most of the aspects of groundwater to suit undergraduate and postgraduate syllabi of different programs of various universities
- Principles of groundwater flow presented through elaborate derivation of governing differential equations and their analytical solutions for simple boundary conditions
- Incorporates sufficient theoretical material to grasp the concepts even by bypassing the clutter of mathematical equations
- Appropriate focus on both aspects of groundwater: resource development and contamination transport and quality management
- Contains substantial original material on solutions by author to seepage from canals using conformal mapping, stream-depletion problem, flowing-well problem, and some case studies

- Separate chapters on groundwater flow solution by complex analysis, and flow through unsaturated media
- Large number of solved examples and variety of numerical problems designed on semester and competitive examination patterns
- Rich pedagogy including illustrations, solved examples, numerical problems, and theory questions

Chapter Organization

The book contains 19 chapters, which are clubbed into four parts. Part I includes Chapters 1–4, which are related to groundwater occurrence, distribution, and exploration along with well construction and logging. Part II deals with theoretical aspects of groundwater flow comprising Chapters 5–9; whereas Part III is devoted to well hydraulics consisting Chapters 10–14. The groundwater management issues are incorporated in Part IV through Chapters 15–19. The following are the highlights of the individual chapters. Chapter 1 defines groundwater and its occurrence and distribution in porous media as well as properties of the porous media. Chapter 2 deals with aquifers in detail and groundwater scenario in India. Chapter 3 describes various techniques elaborately to investigate, target, and map the distribution and availability of groundwater in adequate quantity of good quality. Site selection for wells, different methods of well logging, well-construction techniques, and well-completion steps are discussed elaborately in Chapter 4, whereas Chapter 5 introduces principles of groundwater movement in porous media in a generalized way including Darcy's law and transformation of medium. Chapter 6 covers theory of groundwater flow which incorporates derivation of governing equations and analytical solutions for simple groundwater-flow problems. Chapter 7 presents contaminant transport in groundwater with emphasis on the origin and sources of contaminants in groundwater, classification of groundwater contamination, transport mechanism, and governing equations for contaminant transport in saturated porous media. Chapter 8 deals with functions of complex variables, different types of mappings and their application in solving groundwater-flow problems. Properties of unsaturated medium, water-retention characteristics, hydraulic conductivity relations, derivation of flow equations in unsaturated porous medium, and infiltration of surface water are incorporated in Chapter 9. Chapter 10 describes governing equations in radial coordinates and steady-state solutions to flow problems for cases of single wells, multiple wells and wells in uniform flow field; whereas Chapter 11 addresses solutions to problems for unsteady-state flow in confined aquifers toward fully penetrating wells such as single wells, multiple wells, and wells near different boundaries. Chapter 12 incorporates in detail the unsteady-state solutions to flow problems for special cases, namely wells in unconfined aquifers, wells in leaky aquifer, partially penetrating wells in confined aquifers, large diameter wells, flowing wells, wells in multiple-layer aquifers, and well losses. Estimation of aquifer parameters is one of the most important aspects of well hydraulics, and Chapter 13 explains pumping test and slug test techniques for estimating aquifer parameters for confined, unconfined, and leaky aquifers. Detailed description of aspects related to design, development, and maintenance of water wells is included in Chapter 14. The key issues and various methods of artificial recharge of groundwater are presented in Chapter 15; whereas Chapter 16 deals with the different concerns of saline-water intrusion in aquifers. Introduction and importance of groundwater modeling, classification and description of groundwater models, and finite difference method for groundwater modeling are covered in Chapter 17. Finally, the salient features of management of groundwater quantity and quality are incorporated in Chapters 18 and 19, respectively.

Online Learning Center

The text is accompanied by an exhaustive website accessible at *http://www.mhhe.com/chahar/gh1* which contains the following material.

For Instructors

- Solutions Manual
- Lecture PPTs

For Students

- Chapter-wise MCQs
- Exhaustive Bibliography

Acknowledgments

The approach in this textbook reflects the influence of my mentors combined with my own experiences in teaching and practicing groundwater hydrology. I am particularly grateful to Professor G C Mishra, who was the first to stimulate my interest in the area of seepage and groundwater during my PhD work; Professor P K Swamee, who instilled in me the gist for quality research and publication; and Professor Shashi Mathur, who mentored me in teaching groundwater hydrology after joining IIT Delhi. The current book evolved from my lecture notes built up over 20 years' experience in teaching groundwater hydrology mainly at the master's level. My students kept on requesting me to convert the lecture notes into a textbook. A good part of my lecture notes came from Todd and Mays (2005), Harr (1962), DeWiest (1965), Misstear et al. (2006), Bouwer (1978), Bear (1979), Swartz and Zang (2004), and Karamouz et al. (2011). I am indebted to these authors and their publishers and the relevant excerpts used have been duly acknowledged. Several problems and solutions have resulted from assignments and term papers submitted by students. I appreciate the students who provided feedback on my lecture notes and with whom I discussed much of the material and its presentation in this text for improving its clarity and focus. I am indebted to Devender, who prepared the solutions to several problems and assisted in preparing the manuscript. My hearty gratitude is due to Dr S K Sharma who provided material on case studies. I also acknowledge my advisees: Mahender, Ghanshyam, Shishir, Sridebi, Anand, and Boini, as their contributions find place in different forms in the book. I am thankful to my career in academia at IIT Delhi, which offered me the opportunity to write this book. Special thanks go to my school and college teachers, particularly Professor C R S Pillai, Professor Alam Singh, Sanwar Sharma, and Shivaji Singh, who nurtured me in choosing the academic career. The preparation of this manuscript diverted my attention from many other important activities, including spending time with my family. Special thanks are due to Dr Dhanya as she was always ready to share responsibilities in the department that made it possible to complete the book without taking sabbatical. Gratitude is also due to Professors V P Singh, R S Nirjar, O P Sharma, Santosh Satya, A K Gosain, etc., who inspired me in writing this book.

I also acknowledge the reviewers who took out time to go through the script and gave valuable suggestions. Their names are given below.

Mujib Ahmad Ansari	*ZHCET, Aligarh Muslim University, Uttar Pradesh*
Ramalinga Reddy	*Reva Institute of Technology and Management, Bangalore, Karnataka*
Amit Vishwakarma	*University Institute of Technology, Bhopal, Madhya Pradesh*
Javed Alam	*ZHCET, Aligarh Muslim University, Uttar Pradesh*
Dr.K.Krishne Gowda	*University BDT College of Engineering, Davangere, Karnataka*
Alok Sinha	*Indian School of Mines, Dhanbad, Jharkhand*
Dr. Deba Prakash Satapathy	*College of Engineering and Technology, Bhubaneswar, Odisha*
Sindhu Gomathy	*College of Engineering, Trivandrum, Thiruvananthapuram*

Many people contributed directly or indirectly to the completion of this book, which is thankfully acknowledged. I could not have completed this book without the blessings of my teachers and the unwavering support of my students; therefore, I dedicate this work to my teachers and students.

Feedback

I realize that the first edition is bound to have defects. I will appreciate suggestions directed toward the improvement of this book.

July 2014, New Delhi

Bhagu R Chahar

Publisher's Note

McGraw-Hill Education (India) invites suggestions and comments from you, all of which can be sent to *info.india@mheducation.com* (Kindly mention the title and author name in the subject line.)

Piracy-related issues may also be reported.

Chapter 1 Groundwater: Introduction, Occurrence, and Assessment

1.1 General

Groundwater hydrology may be defined as the science of the occurrence, distribution, and movement of water below the surface of the earth. *Geohydrology* has the same meaning, but *hydrogeology* differs by its greater emphasis on geology. Groundwater is an important source of water supply throughout the world. It serves as an important source in all climatic zones in general and in arid regions in particular. Its use for domestic, irrigation, and industrial purposes continue to increase due to its convenient availability near the point of use, excellent quality, and relatively low cost of development. Groundwater development in forms such as springs, wells, *qanats*, etc., dates from ancient times. *Qanats/kanats* are being used for the past 3,000 years. *Qanat* is a gently sloping tunnel (infiltration gallery) dug through alluvial material or soft sedimentary rock to collect water beneath the water table at its upper end and then allow water by gravity flow to a ground surface outlet at the other end. *Qanats* are still in use in Iran and Afghanistan, and they supply about 75 percent of all water used in Iran. Thus, the utilization of groundwater dates from ancient times, although an understanding of the occurrence and movement of subsurface water as part of hydrologic cycle is recent.

Most of the Earth's liquid freshwater is stored as groundwater. Groundwater would produce a layer 60 m deep if spread evenly over the land surface of the earth. Groundwater flows through permeable material that contains interconnected cracks or spaces that are both numerous and large enough to allow water to move freely. The large volume of groundwater and its slow movement make it a great buffer in the hydrological cycle. Some groundwater is very old and may have accumulated over geological time periods. In fact, groundwater may be as old as the rock containing it, having been trapped during the formation of water-bearing rock. Most of the groundwater is derived from precipitation. Other sources of groundwater include water from deep in the earth, which is carried upward in intrusive rocks and water that is trapped in sedimentary rocks during their formation. The quantities of such water are small and are often so highly mineralized that this groundwater is not suitable for irrigation and other purposes.

Groundwater is commonly understood to mean water occupying all the voids within a geologic stratum. It exists almost everywhere underground. It is found underground in the spaces between the rock and soil particles, or in crevices and cracks in rock. Water-bearing formations of the earth's crust act as conduits for transmission and as reservoirs for storing groundwater. Water-bearing formations that store water and act as natural pipelines for transmission are known as *aquifers*. Much of the freshwater is found in aquifers within 100–300 m below the earth's surface. At greater depths, because of the weight of overlying rock, these opening are much smaller, and thereby hold considerably smaller quantities of water.

Groundwater flows slowly through aquifers at different rates. In some places where groundwater has dissolved limestone to form caverns and large openings, its rate of flow can be relatively fast. In some permeable materials, groundwater may move several meters in a day; in other places, it moves only a few centimeters in a very slow manner through relatively impermeable materials such as clay and shale. Therefore, the residence time of groundwater is quite long; the overall average residence time is about 300 years. Groundwater may contain many constituents, including microorganism, gases, and inorganic and organic materials. Soils contain high concentration of carbon dioxide that dissolves in the groundwater, creating a weak acid capable of dissolving many silicate minerals. The eventual quality of the groundwater depends on temperature and pressure conditions, and on the kinds of rock and soil formations through which the groundwater flows. Because groundwater flows through an aquifer, it is naturally filtered. This filtering, combined with the long residence time underground, means that the groundwater is usually free from disease-causing microorganisms. Natural filtering also means that groundwater usually contains less suspended material and nondissolved solids than surface water.

Groundwater is an important source for public water supply, which plays a vital role in maintaining supplies during dry summers and prolonged droughts. Groundwater provides about 24 percent of global water supply. In many locations, groundwater is the only source of freshwater. Generally, it is the cheapest source of water and is preferred because of good quality and low cost of development. The total capital cost involved in developing a groundwater supply is low when compared to the cost involved in developing a new surface water resource. Operational costs are also favorable, because groundwater needs little treatment, and boreholes can be developed close to where they are needed; therefore, long pipelines and expensive transport systems are not required. Groundwater supports economic activity through its use in agriculture and industry, where there is a need for high quality and reliable source of water, for which groundwater is ideal.

Groundwater is also important apart from its value as a resource. Groundwater must also be taken into account when devising measures to control flooding. The environmental role of groundwater also has an economic value, for example, groundwater-maintained river flows are vital for the proper dilution of discharged wastewater. The study of groundwater is essential for engineers who construct dams, tunnels, water conveyance channel, mines, and other structures; in fact, it is a must when planning almost any kind of structure, be it above or below the ground. Groundwater must be considered whenever the stability of slopes is important, whether the slope is natured or constructed. The fluid pressure exerted by groundwater, for example, plays an important role in the occurrence of earthquake. The movement of water through underground geologic formations controls the migration and the accumulation of petroleum and the formation of some ore deposits. Groundwater may be used as a source of heat for energy-efficient commercial and residential heating/cooling systems.

1.2 Groundwater Vis-À-Vis Surface Water

Groundwater is distinctive from surface water in the following respects:

- Groundwater exists in voids in the subsurface and its movement is very slow.
- Pore geometry, soil or rock fracture, surface tension, and flow resistance fundamentally affect groundwater movement, both in saturated and unsaturated conditions.
- Topographic and geologic structures strictly govern groundwater flows.
- Soil, stratum, rock mineral, and geothermal conditions exert a great influence on the chemical properties of groundwater.

Table 1.1 lists the relative advantages and disadvantages of groundwater over surface water:

Table 1.1 *Advantages and disadvantages of groundwater and surface water*

Groundwater	*Surface water*
Advantages	*Disadvantages*
1. Many large-capacity sites are available	1. Few new sites available
2. Slight to no evaporation loss	2. High evaporation loss even in humid climate
3. Requires little land area	3. Requires large land area
4. Slight to no danger of catastrophic structural failure	4. Ever-present danger of catastrophic failure
5. Uniform water temperature	5. Fluctuating water temperature
6. High biological purity	6. Easily gets contaminated
7. Safe from immediate radioactive fallout	7. Easily gets contaminated by radioactive material
8. Serves as conveyance systems—canals or pipelines across lands of others unnecessary	8. Water must be conveyed
9. May be used as a source of heat	9. Cannot be used for such purpose
Disadvantages	*Advantages*
1. Water must be pumped	1. Water may be available by gravity flow
2. Suitable for storage and conveyance use only	2. Suitable for multiple uses
3. Water may be mineralized	3. Water is generally of relatively low mineral content
4. Minor flood control value	4. Maximum flood control value
5. Limited flow at any point	5. Large flows
6. Power head is usually not available	6. Power head is available
7. Difficult and costly to investigate, evaluate, and manage	7. Relatively easy to evaluate, investigate, and manage
8. Recharge opportunity usually dependent on surplus surface flows	8. Recharge dependent on annual precipitation
9. Recharge water may require expensive treatment	9. No treatment required of recharge water
10. Involves continuous expensive maintenance of recharge areas or wells	10. Little maintenance required of facilities

1.3 Groundwater: A Component of Hydrologic Cycle

The earth, an aquatic planet, has fresh and salt water in the hydrosphere (see Table 1.2). The hydrosphere includes land (a part of the earth crust), ocean, and a part of atmosphere. Land water is distributed in soil, rivers, lakes, and polar ice. Groundwater is a part of land water, and it consists of water held in voids in the earth crust. Table 1.2 shows that more than 99 percent of available source of liquid freshwater lies underground.

Table 1.2 *Distribution of water in hydrosphere*

S. No.	*Item*	*Volume (Mkm^3)*	*Total (%)*	*Freshwater (%)*
A	Oceans	1338.0	96.5	
B	Saline lakes	12.955	1.0	
C	Freshwater	35	2.5	100
1	Ice	24.363	1.725	69.6
2	Groundwater	10.53	0.76	30.1
3	Rivers	0.00212	0.0002	0.006
4	Lakes	0.091	0.007	0.26
5	Soil water	0.02	0.002	0.05
6	Atmosphere	0.0129	0.001	0.025

Source: Chow et al. (1988).

Groundwater does not stay underground forever, but it circulates as part of the *hydrologic cycle* (Figure 1.1). The hydrologic cycle is the series of trans-

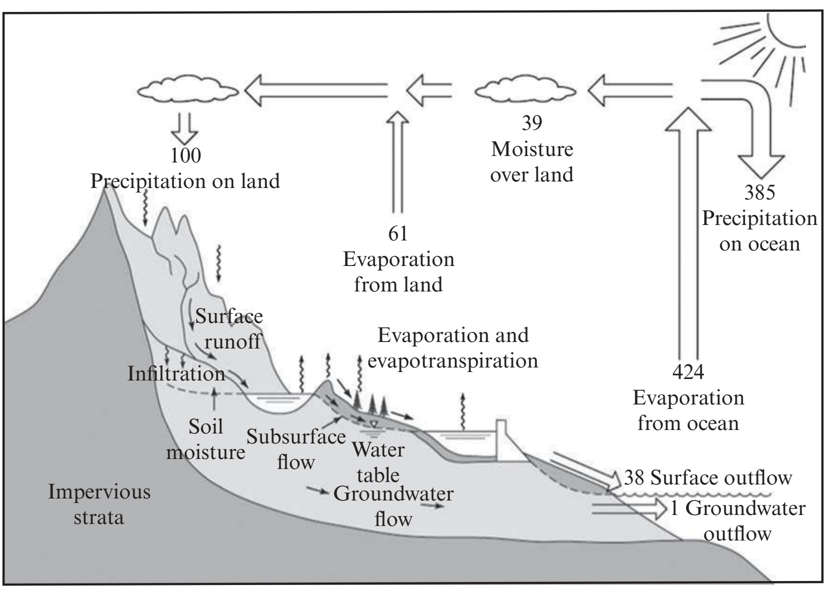

Figure 1.1 *Groundwater as a part of hydrologic cycle (Chow et al. 1988)*

formations that occur in the circulation of the surface and into the subsurface regions of the earth, and then back from the surface to the atmosphere, through evaporation and transpiration. When precipitation falls on the land surface, part of the water runs off into the lakes and rivers. Some part of the precipitation reaches groundwater aquifer as recharge. Due to very slow movement of the groundwater, the *residence time* of the groundwater—that is the length of time water spends in the groundwater portion of the hydrologic cycle—varies enormously. The discharge of groundwater occurs in two ways: (i) natural and (ii) artificial. The *natural discharge* occurs as flow in streams, rivers, marshes, lakes, and oceans; or, it may discharge in the form of springs and flowing wells. Pumping through wells constitutes the major *artificial discharge* of ground water. Figure 1.1 shows that participation of groundwater in the hydrologic cycle is less active (1 percent of total precipitation on the land surface).

1.4 Origin and Age of Groundwater

Precipitation is the main source of groundwater. The precipitated water may infiltrate directly into the ground, or it, as a runoff, may reach to streams or lakes and then seep into ground. A portion of rain falling on the earth's surface infiltrates into ground and travels down; and when checked by impervious layer to travel further down, forms groundwater. Such recharge of groundwater is typically about 30–50 percent of precipitation in temperate humid climates, 10–20 percent of precipitation in Mediterranean-type climates, and about 0–2 percent of precipitation in dry climates. Other sources of groundwater include water from deep inside the earth, which is carried upward in intrusive rocks and water that is trapped in sedimentary rocks during their formation. The quantities of such water are small and they are highly mineralized.

Age of groundwater refers to whether the groundwater is recharged over recent years or else contained in aquifers over a very long time. Most potable groundwater is recharged seasonally and annually as newer groundwater, which may be 1–10 years in age. Groundwater recharged from atmospheric precipitation is called *meteoric water*, which has been a recent (thousands of years) part of the hydrologic cycle. Old meteoric water often found in arid areas where most of the groundwater was formed during previous climatic periods with higher rainfall. The deeper confined groundwater recharged once in the history of hydrological cycle are old and fossil water. Much older groundwater that is of atmospheric precipitation origin but that may have been isolated from the hydrologic cycle for millions of years is called *connate water*. This type of groundwater was already present in the geologic formation when it was formed (such as the water in which alluvial material was deposited). Connate water is often found in the lower parts of deep aquifers and is normally of poor quality. *Juvenile* or *primary water* is groundwater that has never been part of the hydrologic cycle. It was formed within the earth itself and is of volcanic or magmatic origin. It has high mineral content and insignificant in quantity. *Magmatic waters* include volcanic (shallow magma) water and plutonic (deep magma) water. *Metamorphic water* is water that was in rocks during the period of metamorphism. *Marine water* is water that has moved into aquifers from oceans. Thus, the age of groundwater may range from a few years to millions of years or more. It can be estimated with the use of radioisotope tracers. The ion chromatography using isotope and geochemical methods is used in evaluating age of newer and old groundwaters. These methods also help in rediscovering palaeohydrological environment in the evaluation of present and ancient groundwaters and their sustainability.

1.5 Definition of Groundwater

Groundwater is that part of the water below the natural earth surface, which flows naturally out of the earth's surface or can be collected in wells. All *underground water* is not groundwater. If a well is dug, the soil may be dry in the initial portion, then moist soil is encountered, and finally the *water table* occurs. The water table divides the soil into saturated or unsaturated, and the pressure on it is equal to the atmospheric pressure as shown in Figure 1.2. In general, the soil above the water table is unsaturated, and it is saturated below the water table. If a well is dug in unsaturated zone, water does not flow to the well even though the soil may be wet. The water present in this part is not groundwater. If the well is extended below the water table, water will flow freely into the well and this water is groundwater. A well is connected to the atmosphere; hence, the pressure in the well is equal to the atmospheric pressure. Therefore, the pressure in the groundwater must be above atmospheric pressure if it is to flow freely into the well. On the contrary, the underground water that cannot flow into the well should have pressure less than atmospheric pressure. This part of underground water is known as *vadose* or *shallow water*. Thus, the groundwater is different from the rest of the underground water in terms of its pressure greater than atmospheric pressure. Figure 1.2 shows this contrast between groundwater and vadose water. Due to positive (above atmospheric) pressure, the groundwater moves freely under gravity into wells or springs; it is also called *free water* or *gravitational water*. The vadose water is under negative (below atmospheric) pressure and is held to the soil particles by capillary forces. This water can move within the unsaturated or vadose zone or can be extracted by the roots of plants, but it cannot move out

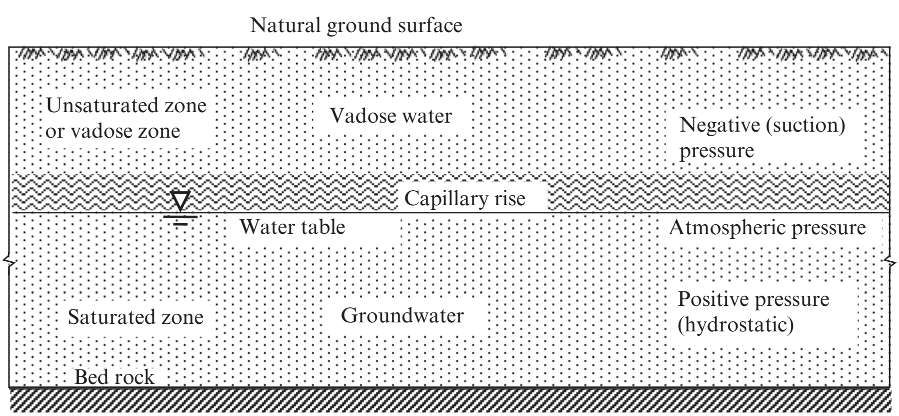

Figure 1.2 *Groundwater and vadose water*

of the zone into wells that are exposed to atmospheric pressure. The vadose zone may be saturated by capillary rise near the water table or by rainfall or irrigation near the ground surface, but the pressure of the water is below atmospheric pressure. In addition, the groundwater zone may be unsaturated due to the presence of air bubbles. Thus, the water table or atmospheric pressure is the dividing line between the two: vadose water below atmospheric pressure and groundwater above atmospheric pressure.

1.6 Porous Media Properties

Groundwater and/or vadose water exist everywhere under the ground, but the quantity of water present depends on the properties of the medium/geological formation. The medium (rock/soil) beneath the earth surface may be permeable or impermeable, but most soils are permeable although their degree of permeability varies. Soil and rock strata that permit water flow are called *porous media*. A porous medium is an interconnected structure of tiny conduits of various shapes and sizes. It is made up of a matrix of particles and embedded voids; thus, a portion of the soil cross-section is occupied by solid particles and the remainder by voids. Infiltration, groundwater movement, and storage occur in these void spaces. Those portions of a rock or soil not occupied by solid mineral matter can be occupied by groundwater. Because interstices serve as water conduits, they are of fundamental importance to the study of groundwater.

1.6.1 Porosity

The amount of groundwater stored in a porous media depends on porosity. The *porosity* of a rock or soil is a measure of the contained interstices or voids, or it is the amount of air space or void space between soil particles. It is expressed as the ratio of the volume of interstices/voids/pore space in a porous medium to the total volume of the given porous medium, thus

$$\eta = \frac{\text{Volume of voids}}{\text{Total volume}} = \frac{V_\mathrm{v}}{V} = \frac{V - V_\mathrm{s}}{V} = \frac{\rho_\mathrm{m} - \rho_\mathrm{d}}{\rho_\mathrm{m}} = 1 - \frac{\rho_\mathrm{d}}{\rho_\mathrm{m}} \tag{1.1}$$

where η is the porosity, V_v is the volume of voids (pore space/interstices), V_s is the volume of solids, V is the total volume (bulk volume), ρ_m is the density of mineral (solid) particles, and ρ_d is the bulk dry density. Porosity may also be expressed as a percentage by multiplying the resultant value by 100.

1.6.2 Void Ratio

Void ratio e is defined as the ratio of the volume of voids to the volume of solids, therefore

$$e = \frac{\text{Volume of voids}}{\text{Volume of solids}} = \frac{V_\mathrm{v}}{V_\mathrm{s}} = \frac{\eta}{1-\eta} \tag{1.2}$$

Void ratio is commonly used in soil mechanics; it is not used in groundwater flow. Porosity is always used in groundwater flow as it is more appropriate parameter, having measure of the water-bearing capacity of a formation and capability of a formation to transmit water.

Porosity of consolidated materials depends on the degree of cementation, the state of solution, and fracturing of rocks. On the contrary, porosity of unconsolidated materials depends on the packing of the grains, their shape, arrangement, and size distribution. The spherical particles that are stacked directly on top of each other (cubic packing) have higher porosity ($\eta = 0.476$) than the particles in a pyramid shape ($\eta = 0.26$), sitting on top of two other particles (rhombohedral packing). One important point is that the diameter size of the grain does not affect porosity. As the porosity is a ratio of void space to total volume, a room full of ping pong balls would have the same porosity as a room full of footballs, as long as the packing or arrangement are similar. In a porous medium of smaller particles mixed with larger particles (nonuniform size distribution or well graded), the smaller particles could fill in the void spaces between the larger particles, which would result in a lower porosity than the medium with well-sorted grains (uniform size distribution). Not all particles are spheres or round. Particles exist in many shapes, and these shapes pack in a variety of ways that may increase or decrease porosity. Generally, a mixture of grain sizes and shapes results in lower porosity.

Typically, pores/interstices are characterized by their size, shape, irregularity, and distribution. *Original interstices* are created by geologic processes governing the origin of the geologic formation and are found in sedimentary and igneous rocks (Figure 1.3). *Secondary interstices* develop after the rock is formed; examples include joints, fractures, solution openings, and openings formed by plants and animals (Figure 1.3). With respect to size, interstices may be classified as capillary, supercapillary, and subcapillary. *Capillary interstices* are sufficiently small that surface tension forces will hold water within them; *supercapillary interstices* are those that are larger than capillary ones; and *subcapillary interstices* are so small that water is held primarily by adhesive forces. Depending on the connection of interstices with others, they may be classified as communicating or isolated.

The term *effective porosity* refers to the amount of interconnected pore space available for fluid flow and is expressed as a ratio of interconnected interstices to total volume. For unconsolidated porous media and for many consolidated rocks, the two porosities are identical. The terms *primary* and *secondary porosity* are associated with original and secondary interstices, respectively. Porosities

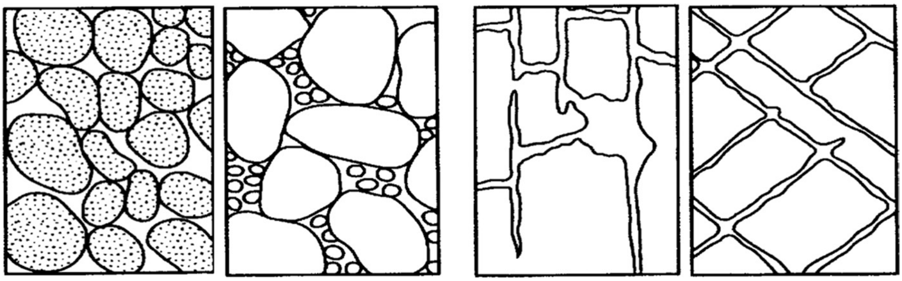

Figure 1.3 *Primary and secondary porosity*

in granular sedimentary deposits depend on the shape and arrangement of individual particles, distribution by size, and degree of cementation and compaction. In consolidated formations, the removal of mineral matter by solution and degree of fracture are also important. Porosities range from near zero to more than 50 percent, depending on the above factors and the type of material. Representative porosity values for various geologic materials are listed in Table 1.3. It should be recognized that porosities for a particular soil or rock can vary considerably from these values.

Table 1.3 *Representative values of porosity for various materials*

Material	*η (%)*	*Material*	*η (%)*
Gravel, coarse	28	Peat	92
Gravel, medium	32	Schist	38
Gravel, fine	34	Shale	6
Sand–gravel mix	20	Basalt	17
Sand, coarse/medium	39	Limestone	30
Sand, fine	43	Dolomite	26
Silt	46	Sandstone	35
Clay	42	Granite, weathered	45
Dune sand	45	Fractured rock	5
Till	32	Slate	<5
Loam	35	Granite	<1
Loess	49		

Aquifers are used as stores for water and natural pipelines for transmission. It would be expected that the value of a rock/formation as an aquifer would depend on the porosity only. Porosity is a geometric property and gives a measure about how much water a soil or rock stratum can store, but it may not be directly related to the hydraulic properties of the material. Two soils of uniform grain size, one larger than the other, but evenly packed, have the same pore volume. But the pore size is different, and hence the hydraulic properties differ. Not all the water stored in pore spaces becomes part of flowing or moving groundwater. Just as water clings to a glass, it also clings to soil particles due to surface tension, cohesion, or adhesion. It forms a thin film around a particle. Therefore, texture and structure also control the hydraulic properties concerned with water movement. Although clays have a high porosity, they hold water by electrochemical bonding and have small, poorly connected interstices; hence, much of the water held is unavailable and the rate at which available water can be abstracted is low.

1.6.3 Permeability

Permeability is a hydraulic property of a porous medium. Unlike porosity, permeability does depend on grain size and texture, and structure is also important. It is directly related to the size of pore space and interconnectivity of the pore spaces. Water can permeate/move between granular void or pore spaces, and fractures between rocks. Permeability is a measure of the ability of a porous medium to transmit a fluid. Low porosity always mean low permeability, but higher porosity may not always result in higher permeability. For example, clays have high porosity but less permeability due to their structure and ion exchange characteristics. In addition, the pore spaces are not well connected. For unconsolidated materials (sand and gravel), the permeability is directly proportional to the square of the grain size. The crystalline rock has low porosity because it contains very few openings, therefore water cannot pass through. However, volcanic rock may have high permeability if the openings are large and are well connected.

1.6.4 Moisture Content

A part of voids is occupied by water and the remainder by air. The volume occupied by water to the total volume of the given porous medium is defined by the *soil moisture content* θ as follows:

$$\theta = \frac{\text{Volume of water in voids}}{\text{Total volume}} = \frac{V_w}{V} \tag{1.3}$$

In soil mechanics, gravitational moisture content is used, which is defined as the ratio of weight of water to the weight of the solid particles of a given volume of porous medium. In groundwater hydrology, volumetric moisture content θ is used. The range of θ is $0 < \theta < \eta$, that is, when the soil is saturated, the soil moisture content is equal to the porosity. The porous medium is *unsaturated* when the medium still has some of its voids occupied by air ($\theta < \eta$) and *saturated* when voids are filled with water ($\theta = \eta$). Therefore, the *degree of saturation* = θ/η.

1.6.5 Specific Retention

The water-retentive property of a soil or rock is markedly influenced by its surface area. This area depends on particle size and shape and on the type of clay minerals present. Specific surface area refers to the area per unit weight of the material. Clay particles contribute the greatest amount of surface area in unconsolidated formations. The *specific retention* S_r of a soil or rock is the ratio of the volume of water it will retain after saturation against the force of gravity to its own volume, therefore

$$S_r = V_r/V \tag{1.4}$$

where V_r is the volume occupied by retained water and V is the bulk volume of the soil or rock. The value of V_r is same as field capacity in unsaturated zone.

1.6.6 Specific Yield

The specific yield S_y of a soil or rock is the ratio of the volume of water that, after saturation, can be drained by gravity to its own volume, thus

$$S_y = V_y/V \tag{1.5}$$

where V_y is the volume of water drained. Values of S_r and S_y can also be expressed as percentages. Because V_r and V_y constitute the total water volume in a saturated material, it is apparent for all interconnected pores that

$$\eta = V_v / V = \left(V_r + V_y\right) / V = S_r + S_y \tag{1.6}$$

Therefore, the specific yield is always less than porosity. Unlike porosity, specific yield is influenced by grain size. For example, if two soil samples have the same porosity, but different grain sizes (e.g. clay and sand), the sample with smaller grain sizes will have a lower specific yield. Clay has a greater surface area than sand; therefore, more water will remain behind, clinging to the clay particle surfaces. Values of specific yield also depend on shape and distribution of pores, compaction of stratum, and time of drainage. It should be noted that fine-grained materials yield little water, whereas coarse-grained materials permit a substantial release of water. Representative values of specific yield for various materials are listed in Table 1.4.

Table 1.4 *Representative values of specific yield for various materials*

Material	*S_y (%)*	*Material*	*S_y (%)*
Gravel, coarse	23	Loess	18
Gravel, medium	24	Peat	44
Gravel, fine	25	Schist	26
Sand, coarse/medium	27	Limestone	14
Sand, fine	23	Sandstone	24
Dune sand	38	Silt	8
Till	16	Clay	3

1.6.7 Storage Coefficient

Water recharged to or discharged from an aquifer represents a change in the storage volume within the aquifer. A *storage coefficient* or *storativity* is defined as the volume of water that an aquifer releases from or takes into storage per unit surface area per unit change in the component of head normal to that surface. The coefficient is a dimensionless quantity involving a volume of water per volume of aquifer. It may range from .01 to 0.3.

1.7 Vertical Distribution of Subsurface Water

Subsurface water flows below the ground surface. Natural topographic and geologic systems control the occurrence of groundwater. Unconsolidated deposits of sand and gravel are favorable for groundwater occurrence due to their high permeability. The water content in the geologic formations varies with depth below ground surface. The occurrence of subsurface water may be divided into zones of aeration and saturation. The zone of aeration consists of interstices occupied partially by water and partially by air. In the zone of saturation, all interstices are filled with water under hydrostatic pressure. On most of land masses of the earth, a single zone of aeration overlies a single zone of saturation and extends upward to the ground surface as shown in Figure 1.4.

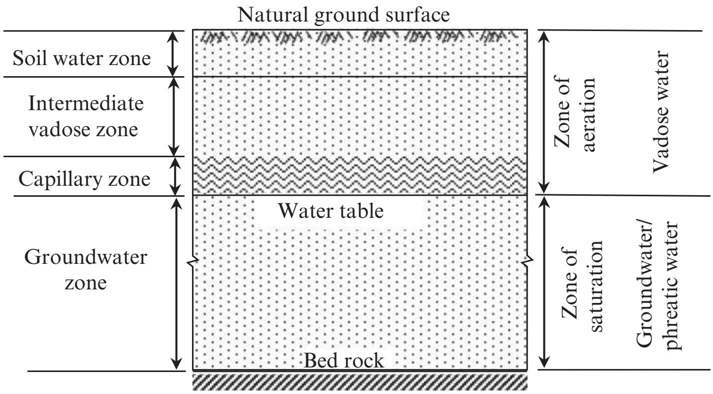

Figure 1.4 *Vertical distribution of underground water*

1.7.1 Zone of Aeration

In the zone of aeration, vadose water occurs. This general zone may be further subdivided into soil water zone, the intermediate vadose zone, and the capillary zone.

Soil Water Zone

The main characteristics of this zone are as follows:

- It is usually unsaturated, except temporarily when excessive water reaches the ground surface from rainfall or irrigation.
- The amount of water present in the soil water zone depends primarily on the recent exposure of the soil to moisture. The existing soil moisture is extracted by the plant roots due to evapotranspiration and soil dries out.
- It contains hydroscopic water, which sticks to soil and is unavailable to plants.
- It contains capillary water, which is held by surface tension and is available to plants.
- It contains gravitational water, which is excessive water and drains through the soil under the influence of gravity.
- Its thickness varies with soil type and vegetation. Soils absorb and retain water, which may be withdrawn by plants during periods between rainfalls and irrigations.

Because of the agricultural importance of soil water in supplying moisture to roots, agriculturist and soil scientists have studied soil moisture distribution and movement extensively. The *water-holding capacity* is defined by the available water, which is the range of plant available water, the moist end being the field capacity and the dry end the being the wilting point. *Field capacity* can be defined as the amount of water held in the soil after wetting and after subsequent drainage has become negligibly small. The negligible drainage rate is often assumed after two days; however, different soils possess varying drainage rates so that quantitative values may not be comparable. The *wilting point* defines the water content of soils when plants growing in that soil are reduced to a permanent wilted condition. Because factors such as soil type and volume and plant type and age influence wilting point, this moisture content can also be variable.

Intermediate Vadose Zone

An intermediate zone exists between the soil water zone and the capillary fringe. The thickness may vary from zero (water logged land) to more than 100 m under deep water table conditions in arid regions. This is a cushion zone through which temporary excess water from rainfall or irrigation in the soil water zone flows down to unconfined groundwater as gravitational water. Nonmoving vadose water (known as *pellicular water*) is held in place by hygroscopic and capillary forces.

Capillary Zone

The capillary zone (capillary fringe) extends from the water table up to the limit of capillary rise of water. If a pore space could be idealized to represent a capillary tube, the capillary rise h_c can be derived from equilibrium between surface tension of water and the weight of water raised. Thus,

$$h_c = \frac{2\sigma}{r\gamma}\cos\phi \tag{1.7}$$

where σ is the surface tension, γ is the specific weight of water, r is the tube radius, and ϕ is the contact angle between the meniscus and the wall of the tube. The thickness of the capillary zone will vary inversely with the pore size of a soil or rock. It can be approximated by

$$h_c = \frac{0.15}{r}\ \text{cm} \tag{1.8}$$

where effective size r is in centimeter.

Table 1.5 *Capillary rise in unconsolidated materials*

Material	*Grain size (mm)*	*Capillary rise (cm)*
Gravel, fine	2–5	2.5
Sand, very coarse	1–2	6.5
Sand, coarse	0.5–1	13.5
Sand, medium	0.2–0.5	24.6
Sand, fine	0.1–0.2	42.8
Silt	0.05–0.1	105.5
Silt, fine	0.02–0.05	200
Clay	<0.002	>200

The capillary rise is less than 2.5 cm for gravel, about 2 m for silt, and several meters for clay. Table 1.5 lists some representative values of capillary rise in unconsolidated materials. Soil material contains innumerable pores of a wide range in size; the upper boundary of the capillary zone will form a jagged limit, and there will be gradual decrease in water content with height. That is, just above the water table almost all the pores contain capillary water; higher, only a smaller connected pores contain water; and still higher, only the few smallest connected pores contain water lifted above the water table.

1.7.2 Zone of Saturation

The saturated zone extends from the water table down to underlying impermeable rock. Water table is the surface of atmospheric pressure and appears as the level at which water stands in a well penetrating the aquifer. In reality, saturation extends slightly above the water table due to capillary attraction; however, water is held there less than atmospheric pressure. Water occurring in the zone of saturation is commonly referred to as groundwater. In the zone of saturation, groundwater fills all of the interstices; hence, the (effective) porosity provides a direct measure of the water contained per unit volume. A portion of the water can be removed from subsurface strata by drainage or by pumping of a well; however, molecular and surface tension forces hold the remainder of the water in place.

1.8 Surface Water and Groundwater Interaction

Surface and subsurface water systems are in continuous dynamic interaction. They are the two components of hydrologic cycle. The water that flows directly on the top of the ground is called surface water such as streams, lakes, springs, and reservoirs. The shape of the water table follows that of the ground surface; therefore; it is a moderated version of the land surface. The overland flow is generated when the rate of rainfall exceeds the infiltration capacity of the soil. The main source of groundwater is infiltration of precipitation. Groundwater flows from areas where the water table is high, to areas where it is low. When the water table meets the ground surface, water leaves the aquifer, either as a spring or by seeping directly into rivers. The time the groundwater takes to travel to the river will depend on how permeable the rock is and on whether it follows a shallow or a deep path. Either way, it can be in the ground for a long time, from months, up to centuries in some cases.

Streams may either contribute water to aquifer or receive water from groundwater (Figure 1.5). Groundwater discharges to a stream when the water table is higher than the water level in the stream and the stream is a *gaining or effluent* stream (Figure 1.5(a)). The discharge received is called base flow. Stream loses water to groundwater through seepage from streambed when the water table is below the water level in the stream and the stream is a *losing or influent* stream (Figure 1.5(b) and (c)). Some streams may be gaining stream for a period and losing for the rest of period in a year, or may be gaining stream for some reaches and losing for the rest of the length. Losing streams may be

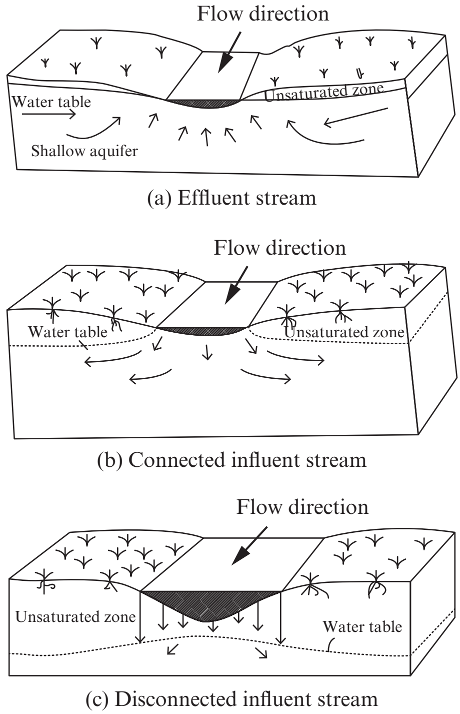

Figure 1.5 *Surface–subsurface water interaction: Gaining and losing streams*

connected (Figure 1.5(b)) to groundwater by a continuous saturated zone or may be disconnected (Figure 1.5(c)) from the groundwater by an unsaturated zone. A *spring* is a point/area through which groundwater emerges from an aquifer to the ground surface, and it may be the origin of a stream. Lakes also interact with groundwater and may be discharging lakes or recharging lakes. A discharge lake receives groundwater similar to base flow, and a recharge lake loses water as seepage to a groundwater flow system. Wetlands and waterlogged areas form when groundwater discharges to land surface or when conditions are such that the surface water is slow to drain away.

1.9 Groundwater Assessment

Groundwater is an annually replenishable resource, but its availability is nonuniform in space and time. The groundwater gets replenished every year due to high rainfall and good recharge conditions. Hence, the sustainable development of groundwater resources warrants precise quantitative assessment based on reasonably valid scientific principles. In the year 1982, the Government of India (CGWB 2009a, b) constituted "Ground Water Estimation Committee" (GEC) which recommended two approaches for groundwater resource assessment, namely (i) groundwater-level fluctuation and specific yield method and (ii) rainfall infiltration method.

1.9.1 Water-Level Fluctuation Method

The replenisable recharge is estimated based on premonsoon to postmonsoon water-level fluctuation (WLF). The monitoring of water-level network stations should be adequate in space and time, and analysis of data should be carried out keeping in view the hydrogeological situation. In this method, the change in storage is computed by multiplying WLF between premonsoon and postmonsoon seasons with the area of assessment and specific yield.

$$\textit{Change in storage} = h \times S_y \times A$$

where, h is the rise in water level due to monsoon (fluctuation between premonsoon and postmonsoon water level), A is the area for the computation of recharge, S_y is the specific yield that can be assumed to be 0.04–0.22 for unconsolidated formations (alluvium), 0.01–0.15 for semiconsolidated formations (sedimentary rocks), and 0.002–0.04 for consolidated formations (crystalline and other hard rocks).

1.9.2 Rainfall Infiltration Factor Method

In areas where ground-water level monitoring is not adequate in space and time, rainfall infiltration factor (RIF) may be adopted. The recharge from rainfall is estimated as given below:

$$\textit{Recharge from rainfall} = f \times A \times \textit{Normal monsoon rainfall}$$

where, f is the RIF. The same RIF should be used for computation of recharge due to rainfall during monsoon and nonmonsoon seasons. RIF can be assumed 0.08–0.25 for unconsolidated formations (alluvium), 0.03–0.14 for semiconsolidated formations (sedimentary rocks), and 0.01–0.12 for consolidated formations (crystalline and other hard rocks). These ranges of RIF are a guideline and should be adopted based on their applicability to prevalent hydrogeological situation.

The rainfall recharge should be computed by WLF and RIF methods. WLF value is used if the difference between the two methods is less than 20 percent; otherwise, rationalized RIF value is considered. Besides natural groundwater recharge estimation, recharge due to seepage from canals, return seepage from irrigated fields, seepage from tanks and lakes, potential recharge in water logged and flood prone areas are computed as follows:

- Seepage from unlined canals in normal type of soil with some clay content along with sand: 15–20 ha.m/d/10^6 m^2 of wetted area of canal.
- Seepage from unlined canals in sandy soils: 25–30 ha.m/d/10^6 m^2 of wetted area.
- Seepage from lined canals may be taken as 20 percent of the unlined canal values.
- Return flow from irrigation by surface water sources: 35 percent of water delivered at the outlet for application in the field and 40 percent of water delivered at outlets for paddy irrigation only.

- Return flow from irrigation by ground water sources: 30 percent of the water delivered at the outlet, and for paddy irrigation 35 percent as return seepage of the water delivered may be taken.
- The seepage from the tanks, ponds, lakes, and flood plains may be taken as 44–60 cm per year over the total water spread. The seepage from percolation tanks is higher and may be taken as 50 percent of its gross storage.
- Managed/artificial groundwater recharge can be estimated depending on the recharge method used.

The annual replenishable groundwater recharge includes all the components. Groundwater levels fluctuate based on the groundwater recharge and discharge (withdrawal/draft) from the aquifer. Groundwater levels are measured by specific agencies at regular interval. The database thus generated forms the basis for assessment and planning of groundwater resources and changes in the regime consequent to various development and management activities.

1.10 Climate Change and Groundwater

Climate is the accumulation of daily and seasonal weather conditions over a long period of time at a location or in a region. The climate and groundwater in a region are intimately related to each other. The climate change results in the variability in precipitation, temperature, evaporation, and soil moisture that affect groundwater recharge, demand, and other factors related to groundwater. It has been predicted that the regions closer to equator will become drier, whereas northern and southern hemispheres will receive more of precipitation and also experience extreme weather conditions. Huge quantity of groundwater extraction for agriculture and other purposes using electric and diesel pumps add to significant amount of carbon emission, which contributes to climate change. The greater the water head lift, the greater the energy consumption. The mining of static groundwater aquifers that are not recharged and lifted from greater depth, particularly in arid and semiarid regions, also multiply the carbon footprint of groundwater extraction. Extreme events such as floods, drought and diminishing snow cover, ice-melt water, and rising sea levels are some of the likely results of climate change. According to Intergovernmental Panel on Climate Change or IPCC (2001), Indo-Gangetic plain will have initially increased water availability due to meeting of snow, but it would face groundwater reductions later on. Erratic behavior of hydrologic cycle due to climate change will increase the groundwater critically in agriculture drought proofing as well as increase the threat to total availability of water resources. Many Indian states such as Delhi, Punjab, Haryana, Rajasthan, Gujarat, Andhra Pradesh, etc., are prone to this threat as the groundwater is already overexploited in these states. The change in temperature and precipitation affect natural groundwater recharge. The base flow contribution to streams and rivers is also diminishing due to consequent pumping of unconfined aquifers connected with streams. Due to climate change, the sea level may rise, which will result in saline water ingress into freshwater costal aquifers. In these events, the managements of groundwater resources would face greater significance. Various safeguard measures are required and must be adopted toward minimizing the impact of climate change on groundwater. Such measures include enhancing soil infiltration, preventing groundwater degradation and increasing agriculture water-use efficiencies. The managed groundwater recharging is one of the most important ways to adaptation and mitigation of impact of climate change on groundwater availability.

PROBLEMS

1.1. Define groundwater hydrology. Why do we study groundwater hydrology?

1.2. Describe porous media and the relevant properties.

1.3. Describe different types of water based on the origin.

1.4. What are the important properties of porous media affecting groundwater?

1.5. Why is groundwater preferred over surface water?

1.6. What is the difference between groundwater and vadose water?

1.7. What is the difference between field capacity and specific retention?

1.8. How is groundwater assessed?

1.9. What do you understand by surface and subsurface water interactions?

Chapter

2

Groundwater: Aquifers and Indian Scenario

2.1 General

Natural topographic and geologic systems control the occurrence of groundwater. Thus, groundwater has various types in flow systems based on the topographic and geologic conditions. The groundwater flow field mainly consists of rock masses or sediment formations. Most of the sediment formations are heterogeneous. This system consists of alternatively overlying permeable layers and less permeable layers and the bottom layer is close to the bedrock. Thus, groundwater may occur in many types of geologic formations. Water-bearing formations of the Earth's crust act as conduits for transmission and as reservoirs of storage of groundwater. Groundwater flows slowly through water-bearing formations at different rates. Soils may contain high concentration of carbon dioxide that dissolves in the groundwater, creating a weak acid capable of dissolving limestone to form caverns and large opening, wherein the rate of flow can be relatively fast.

Aquifer: Groundwater is stored in subsurface void spaces below the water table. Aquifers are used as stores for water and natural pipelines for transmission. Thus, the value of a geological formation as an aquifer should depend on the porosity only; however, although the porosity is an important variable, other factors also play a role in aquifer characterization. An *aquifer* is a saturated formation of permeable material that stores, transmits, and yields significant quantities of water to wells and springs. The key word is yield and also the ability to store and transmit water. Therefore, not all groundwater is stored in an aquifer. An aquifer transmits water relatively easily due to its high permeability. Good aquifers can comprise unconsolidated deposits of sand and gravel, sandstone, basalt, limestone, and dolomite, whereas fractured igneous or metamorphic rocks are only marginal aquifers. The aquifer is the primary unit in groundwater investigation. Aquifers are generally areally extensive with geologic formations, a group of formations, or part of formation and may be overlain or underlain by a confining bed, which may be defined as a relatively impermeable material stratigraphically adjacent to one or more aquifers. The following are the important types of confining beds:

Aquiclude: A saturated but relatively impermeable material that does not yield appreciable quantities of water to wells, although it may contain a large amount of water due to its high porosity, for example, clay.

Aquifuge: A relatively impermeable formation neither containing nor transmitting water (neither porous nor permeable), for example, solid granite.

Aquitard: A saturated but poorly permeable stratum that impedes groundwater movement and does not yield water freely to wells, but that may transmit appreciable water to or from adjacent aquifers and when sufficiently thick, may constitute an important groundwater storage zone, for example, sandy clay.

Figure 2.1 shows a typical groundwater system with aquifers and aquicludes maintained by natural recharge.

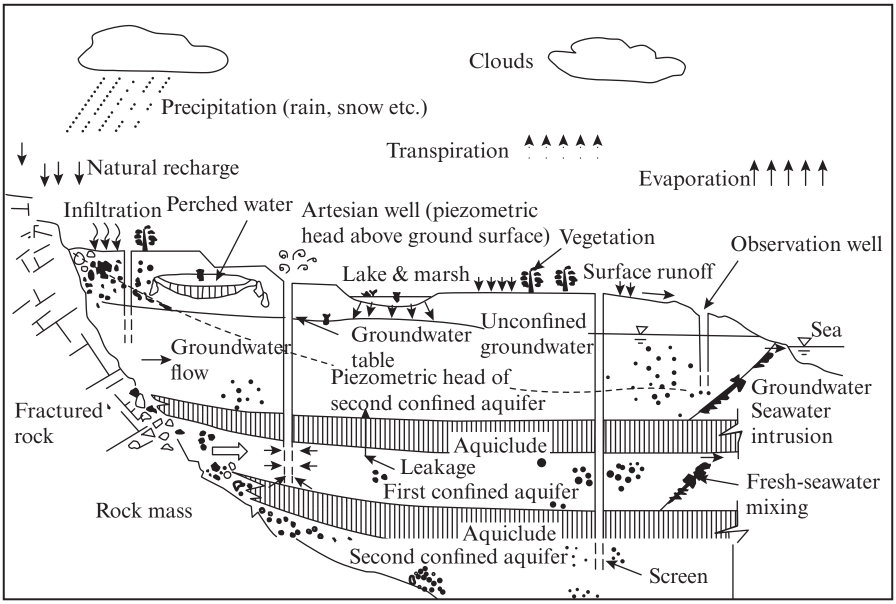

Figure 2.1 *Groundwater system*

2.2 Types of Aquifers

Aquifer is a saturated geologic formation that yields significant quantity of groundwater under gravity. The term significant quantity is relative, which means that a formation qualifying for an aquifer in one hydrogeological environment may or may not qualify for an aquifer in other hydrogeological environments. Most aquifers are of large areal extent and may be visualized as underground storage reservoirs. Water enters a reservoir from natural or artificial recharge; it flows out under action of gravity or is extracted by wells. Ordinarily, the annual volume of water removed or replaced represents only a small fraction of the total storage capacity. Aquifers may be classified as unconfined or confined, depending on the presence or absence of a water table, while a leaky aquifer represents a combination of the two types (Figure 2.2).

Unconfined Aquifer

An unconfined aquifer is one in which a water table varies in undulating form and in slope, depending on areas of recharge and discharge, pumpage from wells, and permeability. A well driven into an unconfined aquifer will indicate a water level corresponding to the water table level at that location. The rise and fall of water level in the water table correspond to change in the volume of

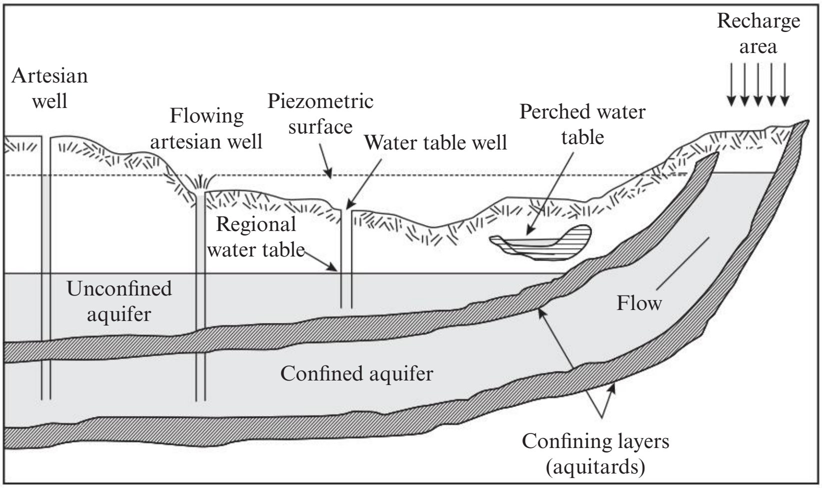

Figure 2.2 *Types of aquifers (Chow et al. 1988)*

water in storage within an aquifer. Only the saturated zone of this aquifer is of importance in groundwater studies. Recharge of this type of aquifer takes place through infiltration of precipitation from the ground surface.

Perched Aquifer

A special case of an unconfined aquifer involves perched water bodies. This occurs wherever a groundwater body is separated from the main groundwater by a relatively impermeable stratum of small areal extent and by the zone of aeration above the main body of groundwater. Clay lenses in sedimentary deposits often have shallow perched water bodies overlying them. A perched aquifer sits above the main water table. Wells tapping these sources yield only temporarily or small quantities of water.

Confined Aquifer

Confined aquifers (artesian or pressure aquifers) occur where groundwater is confined under pressure greater than atmospheric pressure by overlying relatively impermeable strata (aquiclude or aquitard). Often clays and silts, or rocks such as shale, comprise confining layers. Confining layers do not allow water to pass through or the rate of movement is extremely slow. In a well penetrating such an aquifer, the water level will rise above the bottom of the confining bed. Water enters a confined aquifer in an area where the confining bed rises to the surface; where the confining bed ends underground, the aquifer becomes unconfined. A region supplying water to a confined aquifer is known as a recharge area;

water may also enter by leakage through a confining bed. Rise and fall of water in wells penetrating confined aquifers result primarily from changes in pressure rather than changes in storage volumes. The piezometric/potentiometric surface of a confined aquifer is an imaginary surface coinciding with the hydrostatic pressure level of the water in the aquifer. If the potentiometric surface is above the land surface, then a flowing artesian well or spring may occur where water flows without the use of a pump. It should be noted that a confined aquifer becomes an unconfined aquifer when the piezometric surface falls below the bottom of the upper confining bed. Also, quite commonly an unconfined aquifer exists above a confined aquifer.

Leaky aquifer

Aquifers that are completely confined or unconfined occur less frequently than do leaky, or semi-confined, aquifers. These are a common feature in alluvial valleys, plains, or former lake basins where a permeable stratum is overlain or underlain by a semi-pervious aquitard, or semi-confining layer. Pumping from a well in a leaky aquifer removes water in two ways: (i) horizontal flow within the aquifer and (ii) vertical flow through the aquitard into the aquifer.

2.3 Geologic Formations as Aquifers

Although groundwater exists everywhere under the ground, some parts of the saturated zone contain more water than others. An aquifer is an underground formation of permeable rock or loose material that can produce useful quantities of water when tapped by a well. Groundwater scientists generally distinguish between two types of aquifers in terms of the physical attributes of the aquifer: *porous formations* and *fractured formations*. Porous formations have primary porosity from the time of deposition, whereas fractured formations have secondary porosity developed due to various geological and tectonic processes. Porous formations consist of aggregates of individual particles such as sand or gravel. The groundwater occurs in and moves through the openings between the individual grains. Porous media where the grains are not connected to each other are considered *unconsolidated*. Unconsolidated formations consist of alluvial sediments of river basins, and coastal and deltaic tracts. If the grains are cemented together, such aquifers are called *consolidated*, for example, sandstones. In consolidated rocks, the grains are held firmly together by cementation, compaction, and recrystallization. The porosity and permeability of consolidated rocks are due to fracturing and weathering. *Fractured aquifers* are rocks in which the groundwater moves through cracks, joints, or fractures in otherwise solid rock. Examples of fractured aquifers include granite and basalt. Chalk, made up of the remains of countless tiny shells, is also permeable mainly because there are cracks in the rock.

The nature and lateral and vertical extent of aquifers are controlled by the lithology, stratigraphy, and structure of the rock formations. *Aquifer mapping* may be adopted for delineation of primary and principal aquifers that are extensive, limited in extent, and/or local aquifers of reasonable extent. The primary and principal aquifers can be grouped under the following categories:

- porous (intergranular) rock aquifers including alluvial/sand dune aquifers
- fissured and fractured (hard rock) aquifers
- carbonate rock aquifers
- volcanic rock aquifers
- semi-consolidated rock aquifers

The aquifers can be characterized based on the well yield, thickness of aquifer, and other relevant parameters. The *well yield index* is the most used parameter. It is based on the following five categories:

- Category I : 0–5 gpm (gallon per minute)
- Category II : 5–25 gpm
- Category III : 25–100 gpm
- Category IV : 100–500 gpm
- Category V : >500 gpm

The aquifer may further be grouped under the following three broad categories based on the thickness:

- Category I : aquifer with thickness <30 m
- Category II : aquifer with thickness between 30 and 100 m
- Category III : aquifer with thickness >100 m

2.4 Fence Diagrams

A *Fence* (or *Panel*) diagram is a geologic cross section that allows easy visualization of the stratigraphic changes in subsurface conditions. The litholog or soil samples or rock cores obtained from borings data are used to create the fence diagrams. They are similar to cross sections, but rather than interpolating subsurface geology from a map, the geology between stratigraphic sections or cores drilled into the subsurface is interpolated. Fence diagrams are effective at demonstrating changes in unconformities, and other stratigraphic relationships occurring in a region. Their construction involves marking of the locations of each section on paper/map and choosing a vertical scale. Then draw a vertical line representing the length of the section, and mark off the stratigraphic boundaries along the line. The next step is to choose pairs of sections between which to draw the "fence" or panels. The selection of panels should be based on the relative locations of sections and the lithologic and stratigraphic variations. Once all of the useful panels are joined, the fence diagram shows the 3-D geometry of the various stratigraphic units. Figure 2.3 shows a simple representative fence diagram, while Figure 2.4 (see Plate 1) shows the fence diagram of upper Yamuna basin aquifers.

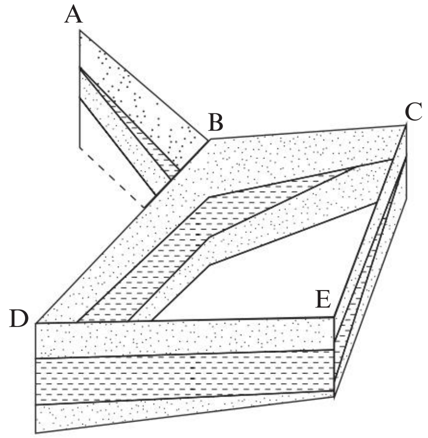

Figure 2.3 *Fence diagram*

Isopach (same thickness) map is a map of the thickness of a unit of interest for visualization tool for 3-D stratigraphic reconstructions. These maps consist of contours like a topographic map, but they represent the thickness of a unit rather than the elevation of the surface. They are all constructed by plotting the desired data on a base map and contouring it to identify systematic variations. The subsurface isopach map is based primarily on formation thicknesses determined from well cuttings, cores, or geophysical logs.

2.5 Aquifer Mapping

The national project on aquifer management (NAQUIM) is an initiative of the Ministry of Water Resources, Government of India, for mapping and managing the entire aquifer systems in the country. Its vision is to identify and map aquifers at the micro level, to quantify the available groundwater resources, and to propose plans appropriate to the scale of demand and aquifer characteristics, and institutional arrangements for participatory management (CGWB 2014). A major output is 1:50,000 scale (in selected areas 1:10,000 scale) multiple-layer digital maps of the areas. Aquifer mapping is needed to develop an understanding of the groundwater flow systems and to support better management of groundwater resources. The *aquifer mapping* can be defined as an interdisciplinary scientific process, wherein a combination of geologic, geophysical, hydrologic, and chemical field and laboratory analyses are applied to characterize the quantity, quality, and distribution of groundwater in aquifers (CGWB 2013b). It involves collection and compilation of groundwater-related data and analysis using various advanced tools of GIS and Spatial Analysis so as to produce the maps in two and three dimensions depicting the disposition of aquifers at suitable scale linked with their hydraulic properties. The resultant GIS database is useful for assessment of groundwater potential, and digital aquifer disposition maps facilitate a base for developing suitable numerical and management models. Aquifer mapping enhances the knowledge about groundwater occurrence and distribution in space and time and helps in resource assessment, planning, and management of groundwater at local as well as regional level.

Systematic aquifer mapping helps in improving understanding of the geologic framework of aquifers, their hydrologic characteristics, water levels in the aquifers and how they change over time, and the occurrence of natural and anthropogenic contaminants that affect the potability of groundwater. Aquifer mapping involves detailed analysis of the underlying geological formations and delineating the areas from which groundwater flows into the wells. The location and yield of aquifers are dependent on the following six factors: (i) geologic conditions such as rock type, (ii) thickness of formation, (iii) sorting of grains in unconsolidated formation, (iv) grain size of sediments, (iv) faulting, and (vi) degree of fractures present. The thickness of an aquifer may be few meters or hundreds of meters. An aquifer may be just below the land surface or hundreds of meters below. Aquifer mapping depicts all these information. A typical aquifer map includes the following:

- aquifer geometry maps
- contour maps for water table and hydrostatic heads of different aquifers
- groundwater flow maps
- maps on aquifer depths, saturated/total thickness, and estimated yield
- maps on spatial variation of hydraulic parameters
- maps on quality of groundwater in different aquifers
- hydrogeological cross sections and 3-D aquifer disposition diagrams
- depth of drilling, discharge, well spacing, and the limits
- level of exploitation of aquifers and annual recharge, vulnerable aquifers, their protection, and sites for their monitoring
- dynamic and static resource and aquifer-wise water budget, and
- areas for artificial recharge.

A multidisciplinary team consisting of experts on various aspects of groundwater and hydrology are required to map aquifer units and synthesize existing datasets with a view to integrate into map coverages. These maps can be grouped into three categories: aquifer maps, aquifer properties and vulnerability maps, and aquifer management option maps. Aquifer map preparation essentially involves the following activities:

- digitization of aquifer map and preparation of GIS datasets of aquifer thickness, depth of occurrences of water bearing zones, their water bearing and transmission properties, etc.
- digitization of the maps and preparation of GIS datasets depicting geophysical parameters, water quality parameters, status of groundwater resources, etc.
- preparation of conceptual model of the area and visualization of the aquifer units in three dimension including fence and cross-section preparation.

The output of these models is in the form of two-dimensional strip-logs, cross sections, and three-dimensional modeled fence diagrams. Technical maps are produced to support modeling and aquifer-based groundwater management. Besides these, descriptive maps are also produced at the block level or watershed level. These maps integrate the different thematic layers, that is, lineaments, soil types, surficial geology, hydrogeology, fence diagrams/cross sections, etc.

Once the aquifer mapping becomes available for whole of the country, it will provide detailed information on groundwater potential, groundwater flow systems, groundwater quality and quantity aspects, aquifer detailing, recharge status and vulnerability of aquifers, and many more things. Such information will help in resource assessment, planning, and management of groundwater at local as well as regional level.

2.6 Indian Aquifers

India has 14 principal aquifer systems and 42 major aquifers (CGWB 2012). Figure 2.5 (see Plate 2) shows the principal aquifer systems. The most productive aquifers are composed of (i) unconsolidated sand and gravel or (ii) fractured limestone and sandstone. Alluvium is the major aquifer system that covers around 31 percent of the entire country and available in Uttar Pradesh, Bihar, West Bengal, Assam, Odisha, and Rajasthan. In India, around 8 percent of the area in Chhattisgarh, Andhra Pradesh, Madhya Pradesh, Gujarat, Karnataka, and Rajasthan contain sandstone aquifer, while limestone aquifer cover around 2 percent mainly in Chhattisgarh, Andhra Pradesh, Karnataka, Gujarat, and the Himalayan states. The rest (around 60 percent area) of the country is covered with the other formations, that is, Basalt aquifer—17 percent, Shale aquifer—7 percent, Gneiss aquifers—20 percent, and Schist, Granite, Quartzite, Charnockite, Khondalite, Laterites, Intrusive, and so on aquifers—15 percent of the area of the country.

2.6.1 Alluvial Deposits

Probably 90 percent of all developed aquifers consist of unconsolidated rocks, chiefly gravel and sand. These are the most significant groundwater reservoirs for large-scale development in the high rainfall and recharge areas. They are not prolific in desert conditions with less rainfall recharge. These aquifers may be divided into four categories based on manner of occurrence: water courses, abandoned or buried valleys, plains, and intermontane valleys. *Water course* consists of the alluvium that forms and underlies stream channels, as well as forming the adjacent floodplains. *Abandoned* or *buried valleys* are valleys no longer occupied by the stream that formed them. Although such valleys may resemble water courses in permeability and quantity of groundwater storage, their recharge and perennial yield are usually less. Extensive *alluvial plains* underlain by unconsolidated sediments may exist at many places. In some places, gravel and sand beds form important aquifers under these plains; in other places, they are relatively thin and have limited productivity. The Indo-Gangetic Plains have alluvial deposits over 1000 m. Groundwater occurs under unconfined to confined conditions due to great variation in the nature and thickness of aquifers, clay, and kankar layers. *Intermontane* valleys or *valley fills* may be underlain by tremendous volumes of unconsolidated rock materials derived by erosion of bordering mountains. The sand and gravel beds of these aquifers produce large quantities of water most of which are replenished by seepage from streams into alluvial fans at the mouths of mountain canyons. Streams emerging from mountainous terrain carry loads of unsorted materials ranging from boulders to clay, which in the foothill region are deposited in the form of *alluvial cones* or *fans*. Most fan deposits are coarse grained and have a high specific yield and permeability. A combination of bed slope, topographic slope, and high recharge rate resulted in high-pressure artesian conditions known as *Tarai basin* along the Himalayan foothills. The *bhabar* is a steeply sloping belt of alluvial fan deposits and it merges with *tarai* forming a springline, which separates the flowing well area and recharge area. The mode of development of groundwater is primarily through dug wells, dug cum bore wells, tube wells, and cavity wells. With regard to groundwater potential, there are aquifers having enormous fresh groundwater reserve down to 600 m depth in the Indo-Ganga-Brahmaputra basin. This groundwater reservoir gets replenished every year and is being used heavily. In coastal areas, there are reasonably extensive aquifers but these are at a high risk of saline water intrusion. The alluvial aquifers have transmissivity values from 250 to 4000 m^2/d and hydraulic conductivity from 10 to 800 m/d. The well yields range upto 100 l/second (lps) and more, but yields of 40–100 lps are common. Many high-capacity (100 m^3/h) tube wells were installed in the Banas valley fill to supply water to big cities in semi-arid region of Rajasthan.

2.6.2 Limestone

Limestone varies widely in density, porosity, and permeability depending on degree of consolidation and development of permeable zones after deposition. Opening in limestone may range from microscopic original pores to large solution caverns forming subterranean channels sufficiently large to carry the entire flow of a stream. Large springs are frequently found in limestone areas. The dissolution of calcium carbonate by water causes prevailingly hard groundwater to be found in limestone aquifers; also, by dissolving the rock, water tends to increase the pore space and permeability with time. Solution development of lime stone forms a karst terrain characterized by solution channels, closed depressions, subterranean drainage through sinkholes, and caves. Such regions normally contain large quantities of groundwater.

Karst aquifers are composed of soluble rocks, for example, carbonate (limestone and dolomite) rocks and all their varieties and conglomerates with carbonate matrix. Karstification occurs by the chemical and mechanical action of water in a region of carbonate rocks. Thus, a nonhomogeneous underground water reservoir containing networks of interconnected cracks, caverns, and channels (formed by solution processes of water) is known as *karst aquifer*. Aquifers developed by erosive/weathering action instead of solution processes cannot be considered as karst. *Holokarst* (complete karst) develops in soluble carbonate rocks characterized by the vast, bare, and rocky land without arable land. *Merokarst* (incomplete karst) occurs in lower depths wherein carbonate sediments are covered with arable soil and with vegetation. A transitional type is formed in limestone isolated by impermeable and less soluble sediments. Due to fast movement of water and absence of filtering by soil layers, these aquifers are more prone to contamination. In addition, the calcium, magnesium, and bicarbonate ions existing in karst aquifers increase the hardness and alkalinity of water in these aquifers. Also, fecal material from septic tanks, leachate from landfills, agricultural chemicals, pesticides, etc., may reach groundwater in karst aquifer without any significant dilution by filtering through porous media. Karst aquifers are filled and emptied by water very fast due to large size and interconnectivity of cracks, caverns, and channels. The difference between maximum water level after rainy season and minimum water level after dry season can be very high. Water wells in karst aquifers should be carefully located and drilled on fracture intersections.

In the carbonate rocks, solution cavities lead to widely contrasting permeability within short distances, so no rock differs as widely in its water transmitting property as carbonate rocks. The permeability of large masses of rock may be negligible, but in caverns it may be very high. Groundwater flow in caverns and openings in limestone aquifers is not laminar but turbulent. Potential limestone aquifers are found to occur in Rajasthan and Peninsular India in which the yields range from 5 to 25 lps. Large springs exist in the Himalayan region in the limestone formations.

2.6.3 Aeolian Sediments

The deposition of Aeolian sediments follows a definite pattern that is largely dependent on the direction and velocity of wind, geology of source rock, topography of the host rocks, drainage, and climate (Karanth 1987). Aeolian sediments such as dune sand and loess are uniform in grain size distribution, mineral composition, and textural characteristics. These deposits have high infiltration rate. Many times well-cemented calcareous (known as kankar) pans are found in Aeolian deposits, which may result in confining bed or perched water table conditions. Loose aeolian deposits pose problems in well construction and drilling, but the presence of calcareous materials make possible digging of even open wells. The transmissivity, hydraulic conductivity, and yields of tube wells may range from 50 to 800 m^2/d, 3–20 m/d, and 25–100 m^3/h, respectively, in aeolian aquifers in Rajasthan.

2.6.4 Sandstone

Sandstone is the most productive among the semiconsolidated sedimentary rocks. Sandstone and conglomerate are cemented forms of sand and gravel. As such, their porosity and yield have been reduced by the cement. The best sandstone aquifers yield water through their joints. Conglomerates have limited distribution and are unimportant as aquifers. Potential semiconsolidated (sandstone) aquifers particularly those belonging to Gondwanas and Tertiaries have transmissivity values from 100 to 2300 m^2/d and the hydraulic conductivity from 0.5 to 70 m/d. Generally, the well yields in productive areas range from 10 to 50 lps. Lathi sandstone and Nagaur sandstone in Rajasthan and Tipam sandstone in Tripura State also form productive aquifers.

2.6.5 Volcanic Rock

Volcanic rock (such as basalt) can form highly permeable aquifer. The types of openings contributing to the permeability of basalt aquifers include interstitial spaces in clinkery lava at the tops of flows, cavities between adjacent lava beds, shrinkage cracks, lava tubes, gas vesicles, fissures resulting from faulting and cracking after rocks have cooled, and holes left by the burning of trees overwhelmed by lava. In India, the predominant types of volcanic rocks are the basaltic lava flows of Deccan Trap Plateau. The Deccan Traps have usually poor to moderate permeability depending on the presence of primary and secondary fractures.

2.6.6 Igneous and Metamorphic Rocks

In solids forms, igneous and metamorphic rocks are relatively impermeable and hence serve as poor aquifers. Where such rocks occur near the surface under weathered conditions, however, they have been developed into small wells for domestic water supply. The yield potential of the crystalline and metasedimentary rocks shows wide variations. Bore wells tapping the fracture systems generally yield less than 1–10 lps. The transmissivity value of the fractured rock aquifers vary from 10 to 500 m^2/d and the hydraulic conductivity varies from 0.1 to 10 m/d.

2.6.7 Clay and Shale

Clay and coarser materials mixed with clay are generally porous, but their pores are so small that they may be regarded as relatively impermeable. Clayey soils can provide small domestic water supplies from shallow, large-diameter wells. Shale is formed by consolidation and induration of clayey sediments. Fractured shale furnishes small water supplies. Dense shales devoid of fractures are practically impervious and form confining layers.

2.7 Groundwater Resources Status of India

India is the largest user of groundwater and irrigates about 39 million hectare land through groundwater. About 85 percent of India's rural domestic water requirements, 50 percent of its urban water requirements, and more than 50 percent of its irrigation requirements are being met from groundwater resources. The annual groundwater withdrawal is about 243 billion cubic meter (bcm) through 21 million groundwater extraction structures (wells, etc.), of which

91 percent is utilized for irrigation and the remaining 9 percent for domestic and industrial uses. Groundwater is annually replenishable resource, but its availability is non-uniform in space and time. As per assessment by CGWB (2011) in March 2009, the annual replenishable groundwater resource in India is about 431 bcm, out of which 396 bcm is considered to be available for extraction for various uses after keeping 35 bcm for natural discharge during the nonmonsoon period for maintaining environmental flows in springs, rivers, and streams. The following are the salient features:

- annual replenishable groundwater resources—431 bcm
- net annual groundwater availability—396 bcm
- annual groundwater draft for irrigation, domestic, and industrial uses—243 bcm
- stage of groundwater development—61 percent
- assessment units—blocks/*mandals*/*talukas*

The stage of groundwater development, computed as the ratio of groundwater draft to total replenishable resource, works out as about 61 percent for the country as a whole. However, the development of groundwater in the country is highly uneven and shows considerable variations from place to place as shown in the *Appendix A*. The status of groundwater development is very high (more than 100 percent) in the states of Delhi, Haryana, Punjab, and Rajasthan, where the annual groundwater consumption is more than the annual groundwater recharge. In the states of Gujarat, Tamil Nadu, Uttar Pradesh, UTs of Daman and Diu, Lakshadweep, and Puducherry, the stage of groundwater development is 70 percent and above. In rest of the country, the stage of groundwater development is below 70 percent. There has been an increase in the stage of groundwater development from 58 percent in 2004 to 61 percent in 2009.

There were 5842 groundwater assessment units (blocks/*talukas*/*mandals*) in India in 2009. As a part of the resource estimation following the groundwater estimation committee norms, the assessment units are categorized for groundwater development based on two criteria—(i) stage of groundwater development defined as (Gross Draft For All Uses/Net Annual Availability) × 100 and (ii) long-term trend of pre- and post-monsoon water levels. The long-term groundwater level trend is computed for a period of 10 years. The significant rate of water level decline is taken between 10 and 20 cm per year depending on the local hydrogeological conditions. Assessment units with stage of groundwater development below 70 percent are safe. In over-exploited blocks, the annual groundwater extraction exceeds the net annual groundwater availability and significant decline in long-term groundwater level trend happens either in pre or post-monsoon or both. In critical blocks, the stage of groundwater development is between 90 percent and 100 percent and significant decline is observed in the long-term water level trend in both pre- and post-monsoon periods. In semi-critical units, the stage of groundwater development is between 70 percent and 100 percent and significant decline in long-term water level trend is recorded in either pre- or post-monsoon periods. These four categories along with the number of assessment units and their percentage are listed in Table 2.1. Apart from these four categories, the remaining 71 (less than 1 percent) units having poor-quality groundwater are categorized as Saline blocks. The *Appendix B* tabulates state-wise details of these categories and Figure 2.6 (see plate 3) shows this categorization status of groundwater development of 5842 assessment units in India.

Table 2.1 *Categorization of blocks*

S. No.	*Category*	*No of blocks (out of 5842)*	*Stage of groundwater development*	*Significant long-term water-level decline trend*	
				Pre-monsoon	*Post-monsoon*
1	Safe	4277 (73%)	≤70%	No	No
2	Semicritical	523 (9%)	>70% and ≤100%	Yes	No
				No	Yes
3	Critical	169 (3%)	>90% and ≤100%	Yes	Yes
4	Overexploited	802 (14%)	>100%	Yes	No
				No	Yes
				Yes	Yes

The development of groundwater in different areas of the country has not been uniform as shown in Figure 2.6 (Plate 3). Numbers of over-exploited and critical units are significantly higher in Delhi, Gujarat, Haryana, Himachal Pradesh, Karnataka, Punjab, Rajasthan, Tamil Nadu, Puducherry, and Daman and Diu (see *Appendix B*). The overexploited areas are mostly concentrated in the North Western, Western, and Southern Peninsular parts of the country; for example, in the North Western part, namely, Punjab, Haryana, Delhi, and Western Uttar Pradesh, where although replenishable resources are abundant, there have indiscriminate withdrawals of groundwater mainly for irrigation purpose leading to over exploitation. In the Western part, namely, Rajasthan and Gujarat, over exploitation is caused by arid climate resulting in scanty and irregular rainfall and consequent less recharge. In the Southern Peninsular part, namely, Karnataka and Tamil Nadu, a large number of over-exploited blocks are caused because of hard rock terrain, which permits less recharge and thus results in water-stressed conditions.

In semi-critical areas, caution may be exercised in planning future development, with regard to quantum of additional groundwater withdrawal. In over-exploited areas, there should be intensive monitoring and evaluation and future groundwater development should be linked with water conservation measures. In fact, more widespread adoption of water conservation measures based on watershed management techniques is beneficial even in semi-critical and critical areas. In some areas of the country, good continuous rainfall and management practices such as groundwater augmentation and conservation measures through government and private initiatives have resulted in improvement in groundwater situation.

2.8 Groundwater Level

Groundwater levels fluctuate depending on the groundwater recharge and discharge (withdrawal/draft) from the aquifer. Groundwater levels are being measured by CGWB since 1969 four times a year during pre-monsoon, March/April/May, August, November, and January. At present, a network of 19,427 observation wells located all over the country are being monitored. Groundwater samples are being collected from these observation wells once a year during the months of March/April/May to obtain background information of groundwater quality changes on regional scale. The database thus generated forms the basis for assessment and planning of groundwater resources and changes in the regime consequent to various development and management activities. The groundwater level and quality monitoring is of particular importance in coastal aquifers. The groundwater level data for 2011 indicate that 4 percent wells had water level less than 2 m bgl, 25 percent wells had water level in the depth range 2–5 m bgl, 41 percent wells in the depth range 5–10 m bgl, 23 percent wells in the depth range 10–20 m bgl, 5 percent wells in the depth range 20–40 m, and remaining 2 percent wells had water level more than 40 m bgl (Figure 2.7, see Plate 4). The maximum depth to water level of 123.55 mbgl was observed in Rajasthan while the minimum was less than 1 mbgl (it was even zero in water-logged areas). The groundwater level falls if the annual draft is more than the recharge, but it will rise for decreased draft and increased recharge.

2.9 Trans-Boundary Aquifer Systems

The underground aquifers are major source of irrigation and drinking water supply worldwide and are exclusive source of supply in arid areas. Aquifers are of large areal extent. Many aquifers in various countries are sensitive because of over exploitation and/or pollution. Aquifers do not follow the geographical boundary between two countries. Due to its geological formation, an aquifer may span over more than one country, which is known as trans-boundary aquifer system. Such aquifers that transcend national boundaries deserve to be managed jointly on sustainable basis. Key features in trans-boundary aquifer system include precise identification and quantification of groundwater movement and its flow across boundaries, water transfer from one side of the boundary to the other, occurrence of majority of recharge and discharge on either side of boundary, and accurate estimate of aquifer resources and river boundaries vis-à-vis underlying aquifers and their interrelationship. UNESCO has brought out a hydrogeological map of shared aquifers, which delineates aquifer shared at least between two countries. It also depicts information about the rate of groundwater replenishment and water quality. There are 273 shared aquifers that include 68 in Americas, 38 in Africa, 155 in Europe, and 12 in Asia. The Guarani aquifer is by far the largest aquifer in the world shared between Brazil, Argentina, Paraguay, and Uruguay that extends over 1.2 million sq km. The UN General Assembly resolution on the law of trans-boundary aquifers encourages the member nations to make appropriate bilateral and regional arrangements for proper management of trans-boundary aquifers. The laws relate to general obligations of cooperation, equitable and reasonable utilization of shared groundwater resources, protection, preservation, and management of such aquifer systems, exchange of data and information on regular basis, bilateral and regional agreements and adoption of harmonized standards for aquifers by member nations, notification to each other of their planned activities that might impact shared aquifer systems, and fostering technical cooperation. It is obligatory for shared aquifer nations to prevent aquifers from any harm, prevent and control pollution being caused to them, if any, share groundwater data on a regular basis, and conduct harmonious development and management of shared aquifers. The digital satellite imagery, telemetry, and sensor network technologies can play absolute role in the monitoring of aquifer water levels and water quality from remote key monitoring wells that can be jointly established by nations sharing aquifer systems.

The sequence of steps in the process of making assessments of shared aquifers are delineation of aquifers along transnational boundaries, aquifer characterization, thickness, limit, and extent, the position of recharge/discharge zones, data credibility, and levels of data details and their scope of sharing. The aquifer name, type, extent, and countries sharing aquifers that transcend boundaries of nations in the subcontinent of India are shown in Figure 2.8.

The aquifer system in the northern corridor between bordering nations are of fissured and fractured type. These are local and discontinuous. Most are hilly and even nonaquiferous with very insignificant or low yield and are sources of local water supplies. Similar is the situation in the extreme eastern corridor where aquifers are discontinuous, and have relatively low permeability and yield potential along Indo-Myanmar boundary. Productive aquifers of significance and importance however exist along Indo-Bangladesh, Indo-Bhutan, and Indo-Nepal boundary areas. The aquifers along Indo-Pakistan boundary areas are highly productive, except in the northern belt where Tertiary rock aquifers locally have very low yield potential. Along lower western corridor in Thar Desert, the replenishable aquifers are discontinuous and variably brackish and saline with deeper groundwater being “fossil” water. In eastern corridor in the Indian state of West Bengal and bordering Bangladesh, the alluvial aquifers on either side contain arsenic in groundwater. Rest of the groundwater of trans-boundary aquifers is of high quality.

The water administration of trans-boundary aquifers is a relatively very new field. Locating and managing of the trans-boundary aquifer systems is becoming important due to competing stake holders. Many institutions responsible for the management of aquifers are also not well versed with the administration and governance of such shared aquifer systems. The competing uses of water resources and need for future have identified the urgency for harmonious and cooperative management of shared aquifers. The key issues include spatial distribution of aquifer parameters, hydraulics of groundwater flow, natural recharge and discharge areas, and vulnerability of aquifer to pollution. Such parameters assume varied significance over different parcels of land on either sides of the boundary. The focus areas that need attention for scientific development and management of shared aquifer resources are hydrogeological knowledge of

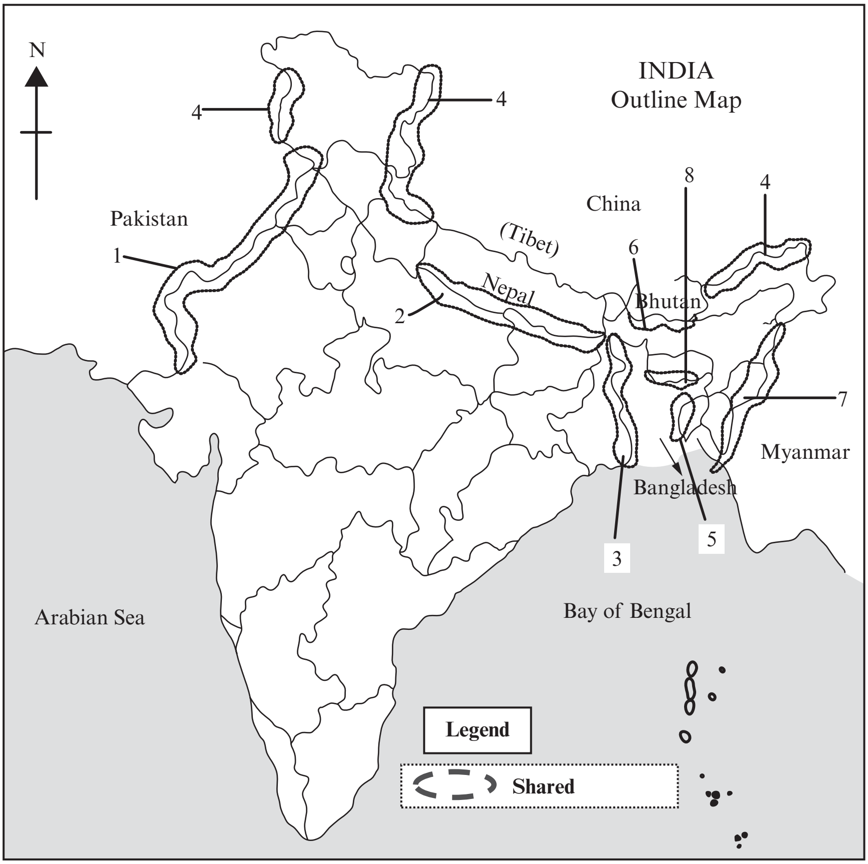

<u>AQUIFERS:</u>

1. Aeolian, Alluvial, & Tertiary Sandstone aquifers (India, Pakistan)—25–50 m^3/h
2. Upper Tertiary & Quaternary Alluvial (Bhabar–Tarai) aquifers (India, Nepal)— 120–250 m^3/h
3. Alluvial/deltaic aquifers (India, Bangladesh)—50–300 m^3/h
4. Tertiary sandstone/siltstone & Proterozoic (granite, phyllite, quartzite) aquifers (India, China, Pakistan)—5–25 m^3/h
5. Tertiary (Tipam Sandstone) aquifers (India, Bangladesh)—50–150 m^3/h
6. Older Alluvium aquifer (India, Bhutan)—50–100 m^3/h
7. Sandstone & siltstone aquifers (India, Myanmar)—10–25 m^3/h
8. Proterozoic (granite–gneiss) aquifers (India, Bangladesh)—5–25 m^3/h

Figure 2.8 *Trans-boundary aquifers of Indian subcontinent* shared aquifers that cut across boundaries, legal knowledge, and management for equitable share of such aquifers and socio-economic, institutional, and environmental aspects that under-pin the management of such aquifers.

PROBLEMS

2.1. What are the different types of geological formations?

2.2. What are the differences between confined and unconfined aquifers?

2.3. Why is aquifer mapping important?

2.4. How are trans-boundary aquifers important?

2.5. Describe the karst aquifer.

2.6. How does a groundwater block convert from safe to semi-critical to critical and then finally to overexploited?

2.7. What is a fence diagram? How is it different from isopach map?

PLATE 1

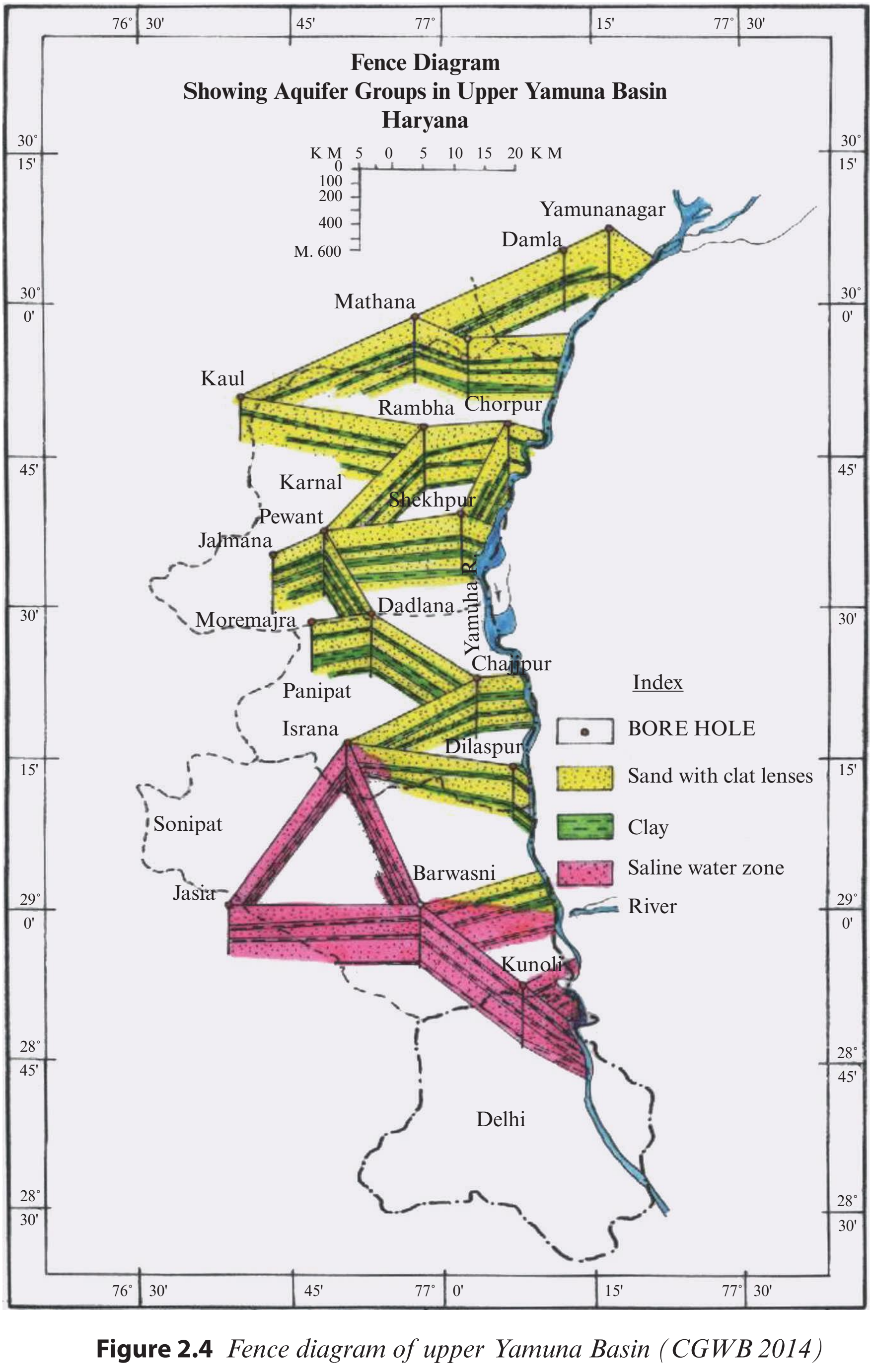

Figure 2.4 *Fence diagram of upper Yamuna Basin (CGWB 2014)*

PLATE 2

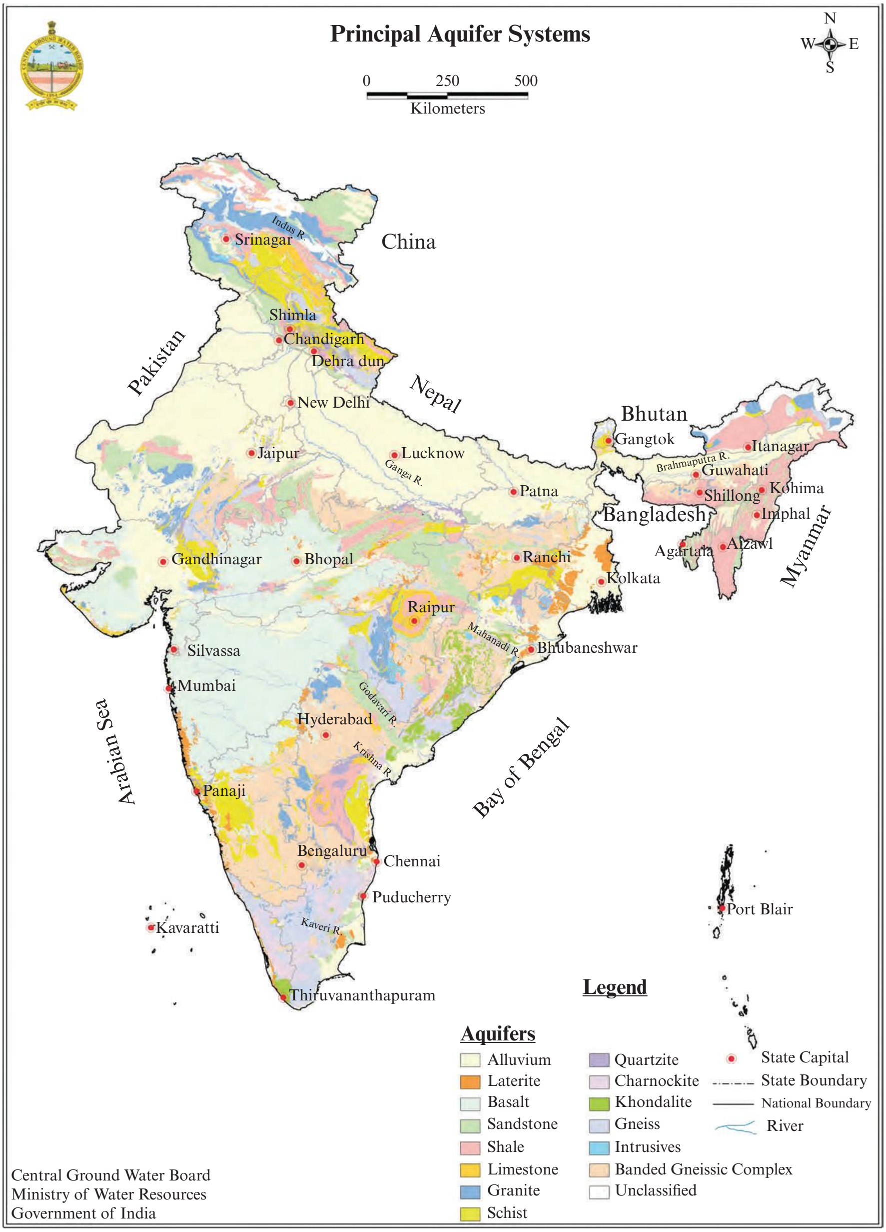

Figure 2.5 *Principal aquifers of India (CGWB 2012)*

PLATE 3

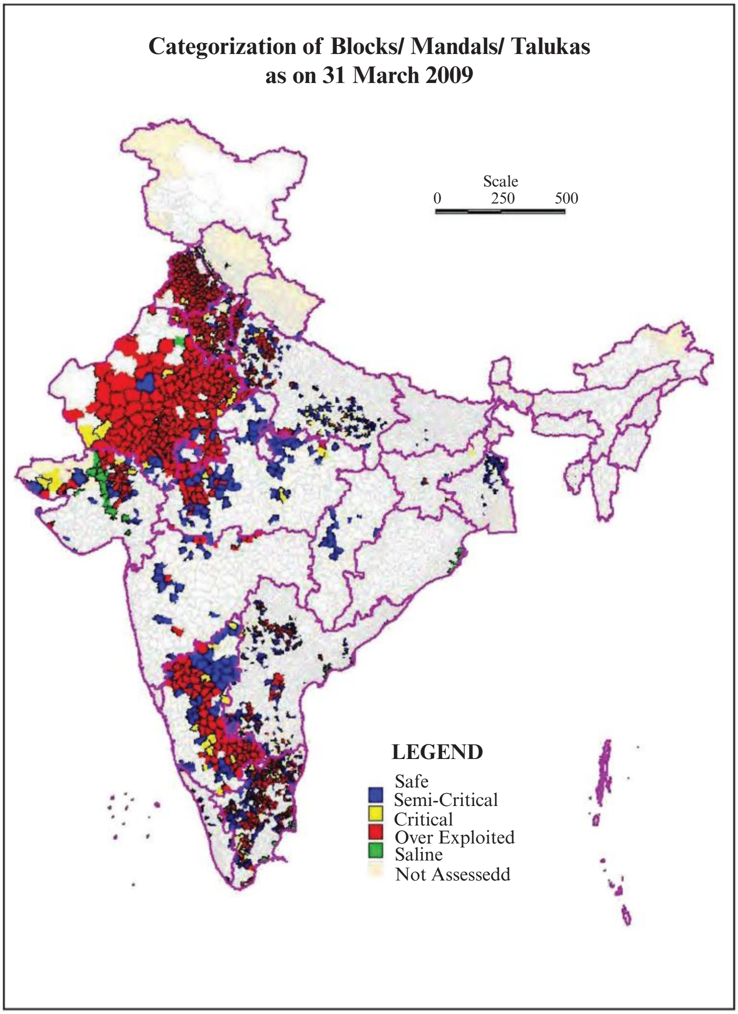

Figure 2.6 *Categorization of groundwater assessment units (CGWB 2011)*

PLATE 4

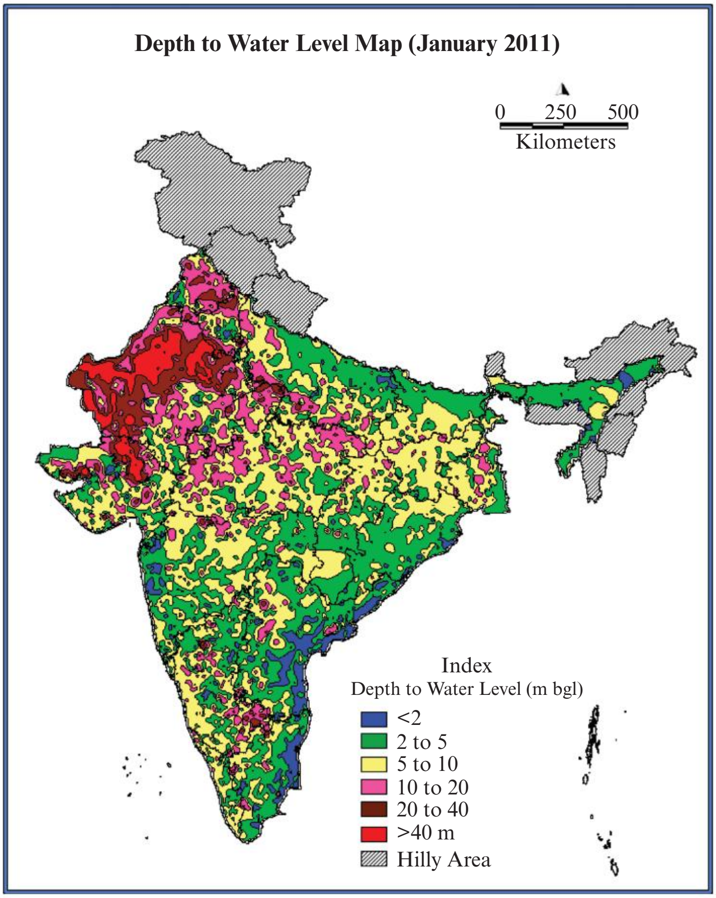

Figure 2.7 *Groundwater (below ground) levels in India (CGWB 2013a)*

Chapter 3

Groundwater Prospecting

3.1 General

Groundwater is a hidden source. We do not know where lays a good quantity along with good quality of groundwater. Making an intelligent assessment about groundwater requires the best possible knowledge of the distribution of water and geologic materials. The knowledge of the depositional and erosional events in an area may indicate the extent and regularity of water-bearing formations. The type of rock formation will suggest the magnitude of water yield to be expected. Stratigraphy and geologic history of an area may reveal aquifers unsuitability, interconnection of aquifer and continuity of aquifer, or important aquifer boundaries. The nature and thickness of overlying beds as well as the dip of water-bearing formation will enable estimates of drilling depths to be made. Investigating groundwater conditions is difficult and expensive because subsurface conditions pertaining to groundwater is buried deep out of sight. It is impossible to have a complete picture of the actual distribution of geologic materials, hydraulic properties, hydraulic heads, and chemical composition. In practice, explorations are done at isolated locations and interpolated/extrapolated for the entire area under consideration. Many techniques are available to investigate and map the distribution of groundwater and groundwater-bearing materials. Geophysical methods are based on the physical properties of material below the earth's surface. A variety of geophysical techniques are available to predict the availability of groundwater in adequate quantity of good quality. The procedure for predicting the availability of groundwater is known as *groundwater prospecting* or *groundwater investigation* or *groundwater exploration* or *groundwater targeting*. The objective of groundwater exploration is to locate aquifers capable of yielding water of suitable quality, in economic quantities for various purposes by using different techniques. The techniques used to access occurrence and quality of groundwater can be classified as (i) *surface investigation* and (ii) *subsurface investigation*. The type of investigation technique to be adopted is governed by several factors. Surface investigation methods include geologic, remote-sensing, and geophysical methods (such as electrical resistivity, seismic, magnetic, etc.), whereas subsurface investigation consist of well drilling and logging methods. Surface investigation methods are less costly than subsurface investigation methods. These methods involve collection of existing meteorological, hydrological, and geological data, such as topographical, geological, hydrogeological maps, maps on evapotranspiration and surface runoff, aerial and/or satellite photographs, and hydrometeorological maps. They also involve measurement of electric resistivity and seismic refraction. These methods might be partially successful in prospecting groundwater due to incomplete hydrogeologic picture of the potential aquifer. In India, majority of wells are constructed without exploration study because of unavailability of groundwater exploration services economically and at required time. Rather, the siting of wells is based on the historical success rate of wells in the neighborhood; therefore, small capacity wells generally do not pose big problems. However, for groundwater development at new locations, proper exploration studies are necessary.

3.2 Geologic Method

Preliminary conclusions related to many aspects of groundwater occurrence and yield can be drawn from the knowledge of the geology of the area. The geologic method enables large areas to be rapidly and economically investigated on preliminary basis for accessing potential for groundwater development. A geologic investigation begins with collection, analysis, and hydrogeologic interpretation of existing topographic maps, aerial photographs, geologic maps, logs, and the other records. If geologic and hydrogeologic maps are available, then a potential site of a well can easily be identified. This method is a first step for any investigation of subsurface water, and it involves a very less investment as no costly equipments are needed. Further, the data obtained from this method serve as preliminary data for detailed investigation. Mapping geology and geological structure have a great bearing on the shape and distribution of aquifers. Detection keys for alluvial areas include mapping of river bed forms, alluvial terraces, alluvial fans, meandering and braided belts, loosing and gaining reaches in streams, badland regions, previous river courses, channel fills, and back swamp areas. Indices of geomorphology for detection of aquifers and water-bearing prospecting horizons over hard rock include mapping of vertical geological barriers, weathering processes and zones of shallow and deep weathered landscapes, mapping of pediments, pediment slopes, and buried pediments. Identification of intratrappean beds, drainage anomaly, and vegetation alignment along certain zones are good indicators of groundwater aquifers.

3.3 Remote Sensing

Photograph of earth taken from an aircraft or satellite at various electromagnetic wavelength ranges can provide useful information regarding groundwater condition. Remote sensing enables hydrogeologist to view large areas instantly and achieve a prospective view, which is not possible through ground surveys and even with low-level aerial photographic techniques. Application of remote-sensing techniques with conventional hydrogeological surveys helps to narrow down the target areas and improves the rate of success in locating sites for production wells. The remote sensing depends on the wavelength of either emitted or reflected electromagnetic radiation from the surface or from a relatively shallow layer of the earth. Because of their underground dispositions, the groundwater aquifers cannot be detected directly through aerial photos or satellite imageries.

Satellite imageries and digital data are generally applied to decipher groundwater potential zones, using procedure of feature identification. Vegetation types and their affinity with lithology of rocks have great bearing on the occurrence/absence of groundwater. Vegetation clusters have affinity with shallow groundwater occurring as springs and seepages in the inland areas as well as with saline groundwater in coastal regions.

Stereoscopic examination of aerial photograph reveals observable patterns; colors and relief make it possible to distinguish differences in geology, soils, soil measure, vegetation, and use. Thus, photogeology can differentiate between soil and rock type and indicate their permeability and aerial distribution, and therefore areas of groundwater recharges and discharges. Ariel photographs also reveal fracture patterns in rocks, which can be related to porosity, permeability and high yield. Hydrobotanical studies of vegetation in photographs also gives an insight into groundwater potential beneath. Phreatophytes that transpire water from shallow water tables define depths to groundwater. Halophytes plant with a high tolerance for soluble salts and white efflorescence of salt at ground surface indicate the presence of shallow brackish or saline groundwater. Xerophytes desert plants subsisting on minimal water suggest a considerable depth of the water table. The nonvisible portion of electromagnetic spectrum also contributes to groundwater investigation, infrared imaginary that gives difference in apparent surface temperatures, enables information on soil moisture, groundwater circulation, and faults functioning as aquicludes to be obtained.

Remote-sensing data can be used to develop GIS layers for lithology of rock; structural geology (fracture, lineament and joints); topographic and drainage density; land use, land cover layer (vegetation layer), soil layer, etc. Application of high-resolution satellite data combined with information collected through geophysical and ground surveys thus helps in making different GIS layers. Subsequently, expert choice and relational methods are used in GIS environment to conjunctively analyze all layers to converge evidences and delineate promising and preferable regions of potential aquifer.

3.4 Geophysical Exploration

Geophysical exploration is the scientific measurement of physical properties of the earth's crust (subsurface formations and contained fluids) by instruments located on the surface for investigation of groundwater. Nowadays, the application of geophysical exploration to groundwater is becoming common. The success of these methods depends on how best the physical parameters deduced are interpreted in terms of aquifer parameters. As the geophysical characteristic or its range is not unique, the choice from more alternatives is based on experience on hydrogeology of the area. Thus, these methods are frequently inexact and are most useful when supplemented by other methods. Geophysical methods detect differences or anomalies of physical properties such as density, magnetism, elasticity, and electrical resistivity within the earth crust. The anomaly is interpreted in terms of subsurface inhomogeneity that may include variation in lithology or quantity and quality of water. Surface geophysical methods are commonly used to map features of the geological setting and the location of abandoned hazardous waste disposal sites.

3.5 Electric Resistivity Method

Surface electrical resistivity surveying is based on the principle that the distribution of electrical potential in the ground around a current-carrying electrode depends on the electrical resistivities and distribution of the surrounding soils and rocks. Electrical methods can be applied to describe the geologic setting and patterns of groundwater existence and its quality. In these methods, generally *electrical conductivity* (the ability of a material to conduct electricity) or *electrical resistivity* (the reciprocal of electrical conductivity) is measured. The common rock-forming minerals have very high resistivity. Rocks and sediments conduct electricity as a consequence of ions in solution in the pore fluid and the charged layer present on clay minerals. Electric resistivity of rock-formation limits the amount of current passing through the formation when an electric potential is applied. The conductance of electricity is controlled by the content of total dissolved solids (TDS) in groundwater and the relative abundance of clay minerals. The higher the TDS in the pore fluid in a formation, the lesser the electric resistivity. Similarly, the higher the clay content in the formation with the same pore water chemistry, the lesser the electric resistivity as the clay offers very low resistivity. Resistivity is higher in igneous rocks than in metamorphic rocks, and it is less in sedimentary rocks. The metamorphic rocks contain hydrous minerals and fabric, whereas the sedimentary rocks contain abundant pore space and fluids. In general, the resistivity of rock formations depends on material, density, porosity (pore size and shape), water content and quality, and temperature. Joints and fractures present in hard rocks, when saturated, results in low resistivity than the adjoining massive rock. There are no fixed limits for resistivity of various rocks; it varies over a wide range, and there is considerable overlapping of resistivity ranges of several rock types as shown in Table 3.1. In relative porous formation, the resistivity is controlled more by water content and quality of water within formation than by the rock resistivity. For aquifer containing unconsolidated materials, the resistivity decreases with the saturation and salinity of the groundwater.

Table 3.1: *Representative resistivity values of soil and rocks (adapted from different sources)*

Formation material	*Resistivity (Ω-m)*
Clay, soft shale	1–10
Wet to moist clayey soil and wet clay	1–80
Wet to moist silty soil and silty clay	Low 10s
Sand, wet to moist silty and sandy soils	50–400
Well-fractured to slightly fractured rock with moist-soil-filled cracks	100–900
Alluvium	10–800
Sandstone	100–1,000
Sand and gravel with layers of silt	Low 1,000s

(*Continued*)

Table 3.1: Continued

Formation material	*Resistivity (Ω-m)*
Coarse dry sand and gravel deposits	High 1,000s
Slightly fractured rock with dry, soil-filled cracks	Low 1,000s
Glacial moraine	10–5,000
Porous limestone	100–3,000
Dense limestone	$>10^4$
Igneous rocks	$500–10^6$
Metamorphic rocks	$500–10^7$
Magnetite ore	1–5,000
Massively bedded rock	High 1,000s

Mineral grains comprising soils and rocks are essentially nonconductive, except in some exotic materials such as metallic ores; therefore, the resistivity of soils and rocks is governed primarily by the amount of pore water, its resistivity, and the arrangement of the pores. To the extent that differences of lithology are accompanied by differences of resistivity, resistivity surveys can be useful in detecting bodies of anomalous materials or in estimating the depths of bedrock surfaces. In coarse, granular soils, the groundwater surface is generally marked by an abrupt change in water saturation, and thus by a change of resistivity. In fine-grained soils, however, there may be no such resistivity change coinciding with a piezometric surface. Generally, since the resistivity of a soil or rock is controlled primarily by the pore water conditions, there are wide ranges in resistivity for any particular soil or rock type, and resistivity values cannot be directly interpreted in terms of soil type or lithology. However, zones of distinctive resistivity can be associated with specific soil or rock units on the basis of local field or drill-hole information. The resistivity surveys can be used to extend field investigations into areas with very limited or nonexistent data. In addition, resistivity surveys may be used as a reconnaissance method to detect anomalies that can be further investigated by complementary geophysical methods and/or drill holes.

Geophysical resistivity techniques are based on the response of the earth to the flow of electrical current. In the field, the electric resistivity method consists of measuring the electric potential difference between two electrodes in an electric field as induced by two current electrodes. The electric resistivity may be defined as resistance in ohms between opposite faces of a unit cube of the material. If a material of resistance R has an area A and length L, then the resistivity σ (Ω-m) is

$$\sigma = R\frac{A}{L} \tag{3.1}$$

Actual resistivity is determined by *apparent resistivity*, which is computed from measurement of current and potential differences between pairs of electrodes placed in the ground surface. The apparent resistivity ρ_a can be calculated as follows:

$$\rho_a = C\frac{V}{I} \tag{3.2}$$

where V is the voltage difference, I is the electric current induced, and C is a geometric factor that depends on the spacing and pattern of electrodes, and it may be given by (Zohdy et al., 1974) the following equation:

$$C = 2\pi / \left(\left\{ \frac{1}{AM} - \frac{1}{BM} \right\} - \left\{ \frac{1}{AN} - \frac{1}{BN} \right\} \right) \tag{3.3}$$

In which AM, BM, AN, and BN are spacing between electrodes as shown in Figure 3.1. To avoid polarization, low-frequency alternating current (< 1 Hz) or reversing direct current is applied at potentials of up to about 200 V. Dry soil around current electrodes is wetted to obtain good electrical contact. The effective depth of current penetration increases with the increase in electrode spacing. If the material of formation is homogeneous and isotropic in nature, ρ_a may represent true resistivity. The *apparent resistivity* of anisotropic or layered formation depends on spacing and pattern of electrodes, as well as material properties, layer thickness, dip, and anisotropic properties of underlying formations. Although it is assumed that a given electrode spacing represents the depth of resistivity measurement, this rule of thumb may not be correct in majority of cases.

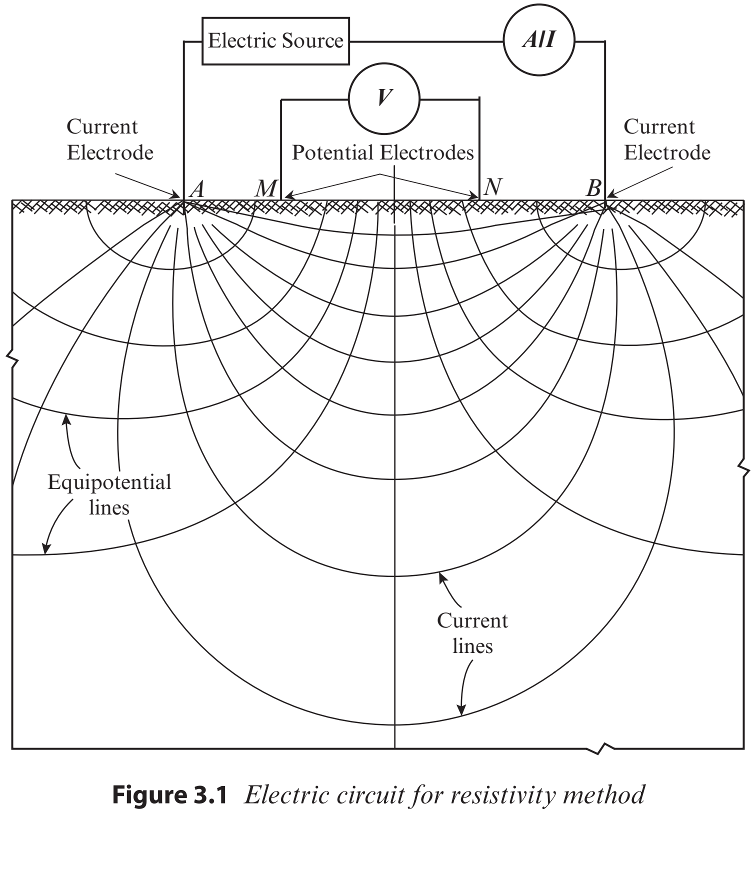

Figure 3.1 *Electric circuit for resistivity method*

Figure 3.1 shows the electrical field for a homogenous subsurface stratum. If the resistivity is uniform everywhere in subsurface zone beneath the electrodes, an orthogonal network of circular arcs will be formed by the current and equipotential lines as shown in Figure 3.1. Various standard electrode spacing arrangements can be adopted, but the most common arrangements are (Zohdy et al., 1974) as follows:

- Wenner arrangement
- Schlumberger arrangement
- Dipole–dipole array.

Wenner arrangement

The Wenner arrangement is shown in Figure 3.2 in which the potential electrodes (*M* and *N*) are placed in a line with the current electrodes (*A* and *B*). All four electrodes are located equidistant from each other. If *L* is the distance between the current electrodes, then $AM = MN = NB = L/3$ (i.e., spacing between two adjacent electrodes is equal to one-third of spacing between the current electrodes). Using $AM = MN = NB = L/3$ in Eqn. (3.3), the apparent resistivity for Wenner arrangement becomes

$$\rho_a = \pi \frac{2L}{3} \frac{V}{I} \tag{3.4}$$

The depth of investigation in an isotropic and homogeneous formation may be approximated to the spacing between two adjacent electrodes, that is, $L/3$.

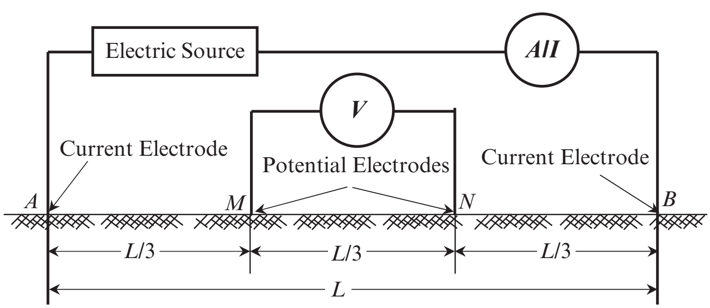

Figure 3.2 *Arrangement of electrodes in Warner method of resistivity determination*

Schlumberger arrangement

In Schlumberger arrangement shown in Figure 3.3, all four electrodes are placed in a line, but the spacing between the current electrodes *A* and *B* (= *L*) is several times than the spacing between the potential electrodes *M* and *N* (= *b*). Using $AB = L$ and $MN = b$ in Eqn. (3.3), the apparent resistivity for Schlumberger arrangement becomes

$$\rho_a = \pi \frac{L^2 - b^2}{4b} \frac{V}{I} \tag{3.5}$$

where *L* and *b* are the spacings between the current and potential electrodes, respectively. Theoretically, $L >> b$; but for practical applications, good result can be obtained if $L \geq 5\, b$. The main advantage of the Schlumberger arrangement over the Wenner arrangement is that the potential electrodes do not have to be moved each time corresponding to the spacing between the current electrodes is changed. The depth of investigation in an isotropic and homogeneous formation is approximately equal to half the spacing between the current electrodes.

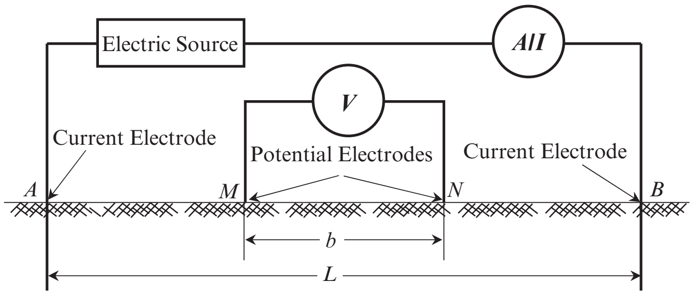

Figure 3.3 *Arrangement of electrodes in Schlumberger method of resistivity determination*

Dipole–dipole array

In dipole–dipole array, the current electrodes and potential electrodes are arranged in separate pairs or dipoles as shown in Figure 3.4. The electrode pairs can be arranged in several ways. The distance between the current electrodes and the potential electrodes is much less than the distance between the centers of the dipoles. The dipole–dipole array is more suitable for deep exploration.

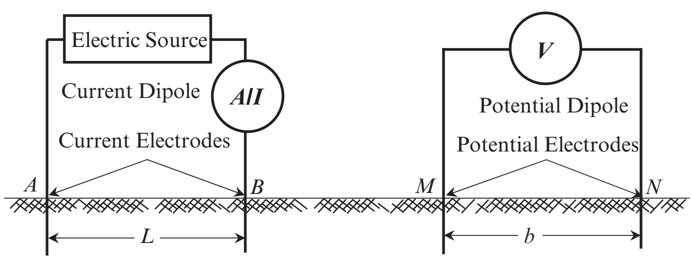

Figure 3.4 *Arrangement of electrodes in dipole–dipole method of resistivity determination*

Electric resistivity investigations cover vertical variations at selected locations by varying electrode spacing. More generally, they are conducted to obtain horizontal profiles of apparent resistivity of an area by adopting constant electrode spacing. There are two modes of field operations:

1. Profiling
2. Sounding

The electrode spacing is kept constant in the *profiling*, *lateral traversing* or *constant separation traversing* (CST) method. The Wenner arrangement is most convenient for profiling or CST. The apparent resistivity changes with electrode spacing, but the spacing is fixed in the profiling method, hence there is one resistivity value within a fixed volume of earth material; thus, only one measurement is made at each station. The investigation is conducted by moving from station to station along a cross section or a two-dimensional surface grid. By measuring the apparent resistivity along the same profile with different electrode spacings, lateral as well as vertical changes in the apparent resistivity can be determined. Once all the data are plotted, it is possible to interpret differences in the apparent resistivity as a function of geology of formation. The other two most common array types used for CST are the dipole–dipole and pole–dipole arrays. The *sounding* or *vertical electrical sounding* (VES) method involves making a series of measurements at a single station with increasing electrode spacing. The Schlumberger arrangement is most convenient and commonly used method for VES. Layers, dips and faults in formation, dykes, buried stream channels and fresh water–saline water zones are easily distinguished in resistivity profiles. It is also possible to differentiate low resistivity water-bearing formations from high-resistivity dry zones and impervious rocks. Fence and isopach diagrams can also be prepared from the profiling data collected by varying spacing between the electrodes along several sections.

The electric resistivity procedure involves measuring potential difference between two electrodes by supplying current by other two electrodes. As the spacing between the electrodes increases, the electrical field extends deeper into the earth to provide resistivity as a function of depth. The measurement of current and potential differences yields apparent resistivity over an unspecified depth. When apparent resistivity is plotted against electrode spacing for various spacing at one location, a smooth curve can be drawn through the points. The interpretation of this curve is difficult and complex. Generally, the actual subsurface resistivity vary with depth, hence apparent resistivity will change as

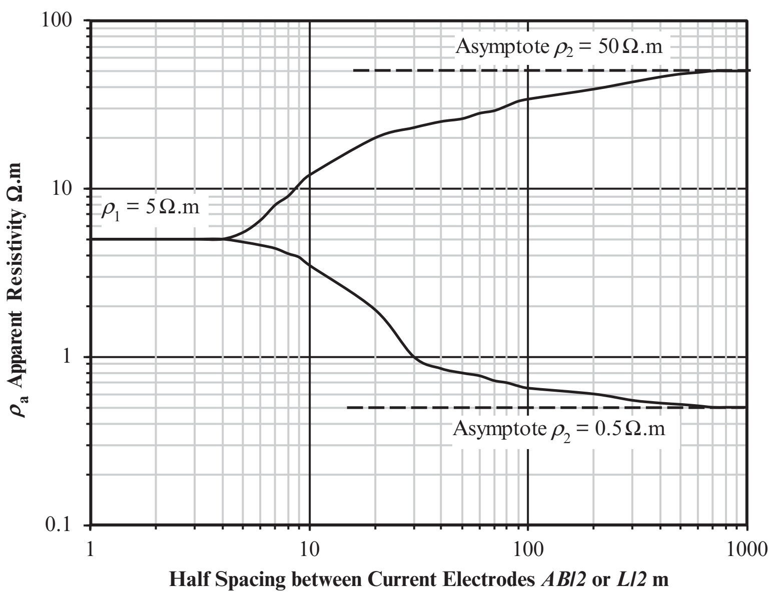

Figure 3.5 *Electric sounding curves for two layered system*

we increase the electrode spacing, but not in like manner as changes in depth at great depth have only slight change in resistivity as compared to change in shallow depths. Therefore, electric resistivity method is limited for a few 100 m or so. The information on layering and presence of water in the formation can be interpreted by plotting apparent resistivity versus electrode spacing curve on log–log graph known as electrical sounding curve. In horizontally stratified formations, the shape of the sounding curve depends on the electrode configuration, resistivity and thickness of formations beneath the sounding point. In a homogeneous and isotropic formation of infinite depth, the sounding curve is a straight line for all electrode spacings. For two-layered formation ($h_2 >> h_1$), the sounding curves are shown in Figure 3.5 for ρ_2/ρ_1 = 10 and 0.1.

Figure 3.6 presents Wenner array master curves for two-layer case ($h_2 >> h_1$). These master-type curves (theoretical curves of apparent resistivity for horizontal, isotropic, and homogeneous layers for various combinations of thicknesses and resistivities) are plotted on log–log scale. To reduce the number of graphs needed, master curves are normalized on both axes. To find the thickness of layer in a two-layer system, follow the steps listed below:

1. Plot the observed apparent resistivity values with spacing on log–log paper having same scale as the master curve.
2. Keep axes parallel and overlay the data plot on a master curve and then slide the data plot around until a curve on the master curve best matches majority of plotted data points.
3. Find the a/h_1 line on the master curve. Where this crosses, the data plot's x-axis is the layer thickness.

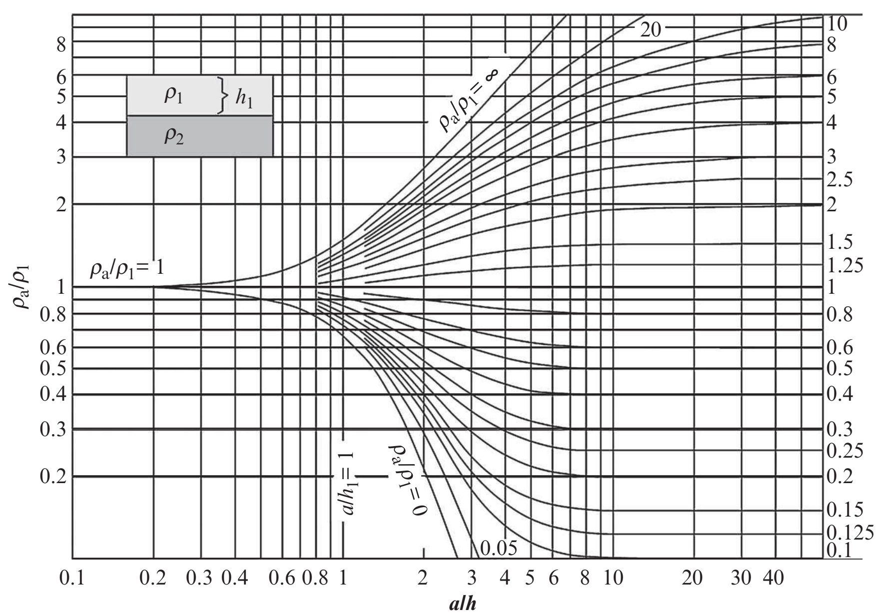

Figure 3.6 *Master curves for Wenner's method in two-layered system (Zohdy et al., 1974)*

4. Find the ρ_a/ρ_1 line on the master curve. Where this crosses, the data point's y-axis is the resistivity of the first layer.
5. Find the resistivity of the second layer by multiplying the first layer's resistivity by the best-fitting curve's ρ_a/ρ_1 ratio.

If the formation consists of three layers, there are four possible sounding curves (Zohdy et al., 1974) as follows:

(i) A-type section – $\rho_1 < \rho_2 < \rho_3$
(ii) H-type section – $\rho_1 > \rho_2 < \rho_3$
(iii) K-type section – $\rho_1 < \rho_2 > \rho_3$
(iv) Q-type section – $\rho_1 > \rho_2 > \rho_3$

These curves are shown in Figure 3.7.

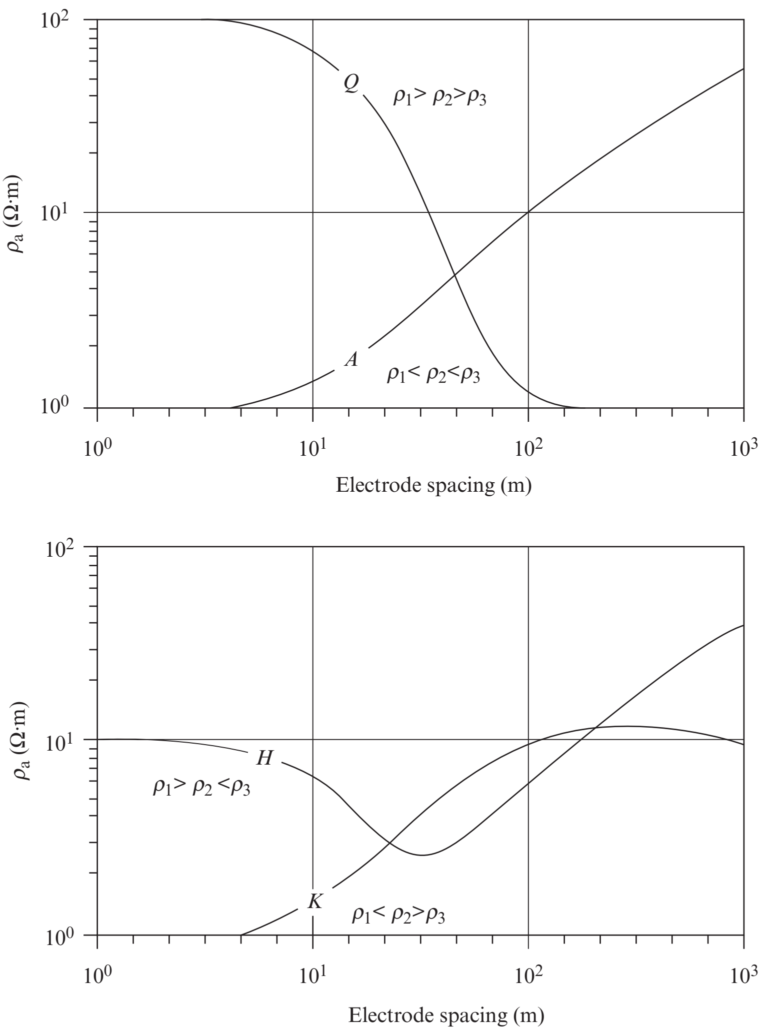

Figure 3.7 *Electric sounding curves for three-layered system*

Likewise, there will be eight possible relations in a four-layered medium and 16 possible relations in a five-layered medium. In general, the number of possible sounding curves = 2 no. of layers – 1. From the shape of the sounding curve, it is possible to decipher the number of layers and their resistivity relationships. The depth-wise variation in apparent resistivity can be related to parameters such as the depth to water table, thickness of unsaturated zone, thickness of water-bearing formation, stratification boundaries, bedrock, boundaries of geothermal zones, and fresh water–saline water interfaces. Curve matching of observed sounding curve with master-type curves may be adopted to estimate the thickness of different layers. When the data of several sections are available, they can be interpreted by depicting in maps the areal distribution of layers (fence and isopach diagrams). In a multilayered medium, the interpretation becomes more difficult. The availability of drilling data is useful to make test soundings near the well to calibrate/validate the resistivity parameters. Using these known resistivity parameters, the layer thickness can be determined for the area where there is lack of drilling information.

Of all other methods, electric resistivity method is applied extensively to groundwater studies. Its portable equipment and ease of operation enables a rapid measurement. The method is used for planning and in efficient and economic test drilling programs. When subsurface conditions are relatively homogenous, the technique can be used to detect the water table as the top of a relatively conductive layer. The anisotropism in the horizontal or lateral direction is distinguished by profiling, whereas the anisotropism in the vertical direction is distinguished by VES. Lateral resistivity changes can be interpreted in terms of aquifer limits and changes in groundwater quality, whereas VES may indicate aquifers, water tables, salinities, impermeable formations, and bedrock depths. It is very well adapted for locating subsurface saltwater boundaries because the decrease in resistance when salt water is encountered becomes apparent on the resistivity spacing curve. This method is unique in detecting fresh water–salt water interface, which other (gravity, magnetic, or seismic) methods cannot do. Clay layers can easily be detected in electric resistivity method. The method is also useful in prospecting for groundwater in hard rocks in which the distribution of aquifer is irregular. The resistivity of groundwater varies from 10 to 100 Ω-m, depending on the concentration of dissolved salts. The low resistivity (about 0.2 Ω-m) of sea water is because of the relatively high salt content. This makes the resistivity method an ideal technique for mapping the saline and fresh water interface in coastal areas.

Like all geophysical techniques of resistivity, electrical resistivity methods produce nonunique results as (i) data are compared to known geological data (e.g., boreholes), (ii) similar rocks have a wide range in resistivities based on the water content, (iii) lithology changes do not necessarily correspond to a resistivity change, and (iv) resistivity changes do not necessarily correspond to a lithology change. Resistivity values have a much larger range when compared with other physical quantities mapped by other geophysical methods. The resistivity of rocks and soils in a survey area can vary by several orders of magnitude. In comparison, density values used by gravity surveys usually change by less than a factor of 2, and seismic velocities usually do not change by more than a factor of 10. Hence, without sound geological knowledge, resistivity data may be misleading. Further, the electrical resistivity method has some inherent limitations that affect the resolution and accuracy that may be expected from it. Like all methods using measurements of a potential field, the value of a measurement obtained at any location represents a weighted average of the effects produced over a large volume of material, with the nearby portions contributing most heavily. This tends to produce smooth curves that do not lend themselves to high resolution for interpretations. Another feature common to all potential field geophysical methods is that a particular distribution of potential at the ground surface does not generally have a unique interpretation. Although these limitations should be recognized, the nonuniqueness or ambiguity of the resistivity method is scarcely less than that with the other geophysical methods. For these reasons, it is always advisable to use several complementary geophysical methods in an integrated exploration program rather than relying on a single exploration method. Moreover, the presence of highly conductive layer (saline water) or highly resistant layer at shallow depth makes this method ineffective. Any factor that disturbs the electric field in the vicinity of electrodes may invalidate the resistivity measurements. The maximum depth range of electric resistivity investigation is limited to 500 m.

3.6 Seismic Method

Seismic methods utilize both reflected and refracted energy waves to measure how fast and what paths these waves travel through different types of lithologic units. The seismic refraction method involves the creation of a small shock at a depth of about 1 m or so (known as shot/shock point) either by the impact of a heavy instrument or by a small explosive charge. The arrival of the shock waves at various distances is measured with sound detectors called geophones placed on the ground surface. The change in the velocity of seismic waves is governed by changes in the elastic properties of the formation. The travel time of seismic wave depends on the media through which it passes. The velocity seismic/sound wave in subsurface material increases with bulk density and water content. Porosity tends to decrease wave velocity, but water content increases it. In coarse alluvial materials, seismic velocity increases markedly from unsaturated to saturated zones. The velocities are greatest in solid igneous rocks (about 5,000 m/s) and least in loose unconsolidated unsaturated materials (about 250 m/s). Table 3.2 lists few representative values of seismic wave velocity. For deep unconsolidated saturated materials, the velocity may range from about 1,500 m/s to about 2,500 m/s. The greater the contrast of travel time or velocities of sound waves, the more clearly the formations and their boundaries can be identified. Thus, the measurements on travel time or velocities of sound waves can be interpreted in terms of type, porosity, and water content of the formation and depth of the various strata.

Table 3.2: *Representative values of wave velocity (adapted from different sources)*

Formation material	*Wave velocity (mls)*
Loose surface/top dry soil	100–300
Dry sand	300–500
Dry gravel	500–1,300
Saturated sand, gravel, silt, or clay	1,500–1,800
Granite weathered and fractured	1,000–2,000
Granite	4,000–6,000

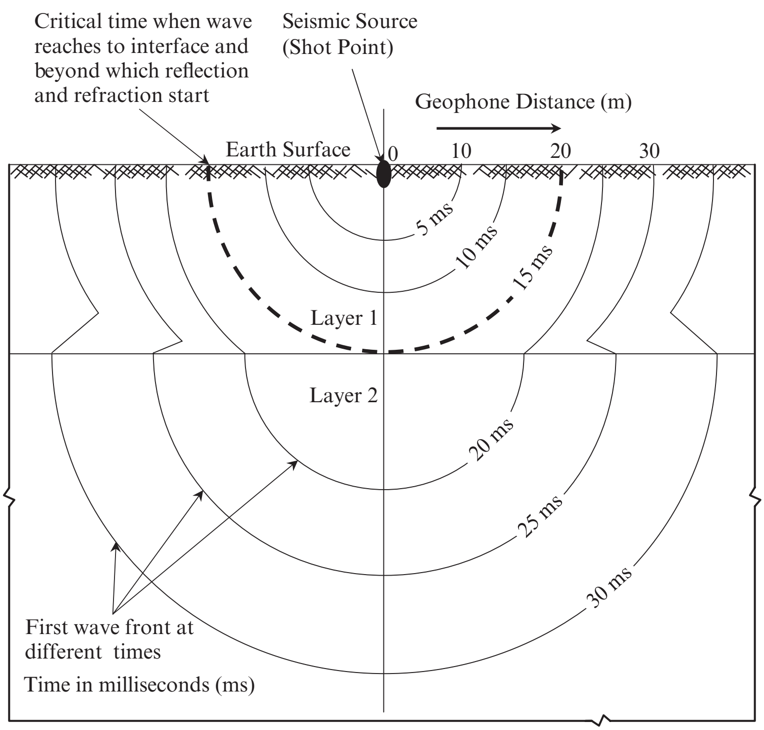

Figure 3.8 *Advance of wave front in seismic refraction method*

In a homogeneous and isotropic medium, the velocity of wave propagation is constant in all directions. The wave front in any given time is spherical, and the spherical wave expands outward from a shock point, as shown in Figure 3.8. It travels at a speed governed by the material through which it passes. Seismic waves follow the same laws of propagation as light rays; and if the medium is layered, the seismic waves are reflected or refracted based on the angle of incidence of the ray at any interface where velocity change occurs. Refraction of waves follow Snell's law ($\sin i/\sin r = V_1/V_2$) and at critical angle of incidence i_c: $\sin i_c = V_1/V_2$. When a wave strikes the interface/boundary more than the critical angle of incidence, it is totally reflected back (e.g., ray R_2 at point B in Figure 3.9). On the one hand, if a wave strikes the interface/boundary less than the critical angle of incidence, it is reflected back in the first medium with velocity V_1 and partly refracted into the second medium with velocity V_2. On the other hand, if a wave strikes the interface/boundary at the critical angle of incidence, a part (along AR) of the energy is reflected back in the first medium with velocity V_1 and a part is refracted and transmitted parallel to the interface of two mediums (along AC) with velocity in the second medium V_2 (see Figure 3.9). Travel times of various waves to reach from the shot point, S to the geophone, R are as follows:

1. For direct/surface waves along SR path:

$$t_d = \frac{SR}{V_1} = \frac{x}{V_1} \tag{3.6}$$

2. For reflected waves along SBR path:

$$t_i = \frac{SB + BR}{V_1} = \frac{x}{V_1 \sin i} = \frac{2D_1}{V_1 \cos i} = \frac{2}{V_1}\sqrt{(x/2)^2 + D_1^2} \tag{3.7}$$

3. For refracted waves at critical angle of incidence along SACR path:

$$t_r = \frac{SA+CR}{V_1} + \frac{AC}{V_2} = \frac{2D_1}{V_1 \cos i_c} + \frac{x - 2D_1 \tan i_c}{V_2} = \frac{x}{V_2} + \frac{2D_1}{V_1 V_2}\sqrt{V_2^2 - V_1^2} \tag{3.8}$$

where D_1 is the depth of the top layer and x is the distance from shot point to geophone.

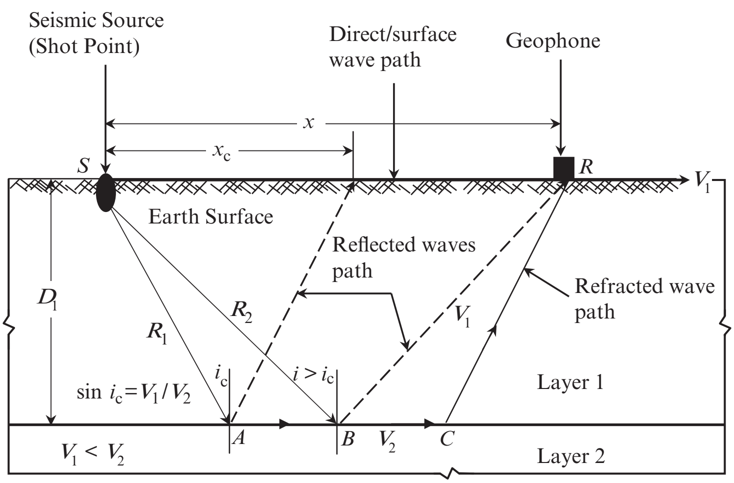

Figure 3.9 *Propagation of direct, reflected, and refracted seismic waves*

Thus, at the geophones closer to the shot point, the direct/surface waves arrive first. The reflected waves reach only after the direct waves, and their travel time curves are hyperbolic in nature. The refracted waves can appear only in geophones beyond some critical distance x_c from the shot point given by the following equation:

$$x_c = 2D_1 \tan i_c = \frac{2D_1 V_1}{\sqrt{V_2^2 - V_1^2}} \tag{3.9}$$

At remote locations on the surface, the first wave will arrive either directly from the shot point or from a refracted path depending on the velocities of sound waves in the layers. Refracted waves will reach the more remote geophones sooner than the straight travelling waves if the velocity of sound in the deeper layers is much greater than that in the surface materials. This happens when the geophones are located at a distance greater than x computed by equating Eqs (3.6) and (3.8) and solving as given by the following equation:

$$x = 2D_1\sqrt{\frac{V_2 + V_1}{V_2 - V_1}} \tag{3.10}$$

Figure 3.10 shows paths of seismic waves in a three-layered medium. These waves originated at source S reach to the receiver geophones as direct wave, reflected wave, or refracted wave at different times based on the geometric and material properties of the medium. For example, geophone at R_1 will receive direct wave and reflected wave; the refracted wave will not arrive at R_1. At R_2 direct wave and reflected and refracted (SBCR$_2$) waves from interface of layer 1 and layer 2 will arrive at different times, but it will not receive refracted wave from interface of layer 2 and layer 3. The receiver R_3 receives the direct wave along path **SR$_3$** at velocity V_1; the reflected wave from interface at point D along path SDR$_3$ at velocity V_1; the refracted wave from interface at points B and E along path SBER$_3$ with velocity V_1 for SB part, velocity V_2 for BE along interface and again velocity V_1 for ER$_3$ part; and the reflected wave from interface between layer 2 and layer 3 at point J along path SAJGR$_3$ at velocity V_1 for SA part, velocity V_2 for AJ and JG parts and again velocity V_1 for GR$_3$ part. Similarly, geophones subsequent to R_4 will receive direct wave, reflected and refracted waves from the interface between layer 1 and layer 2, and reflected and refracted waves from the interface between layer 2 and layer 3.

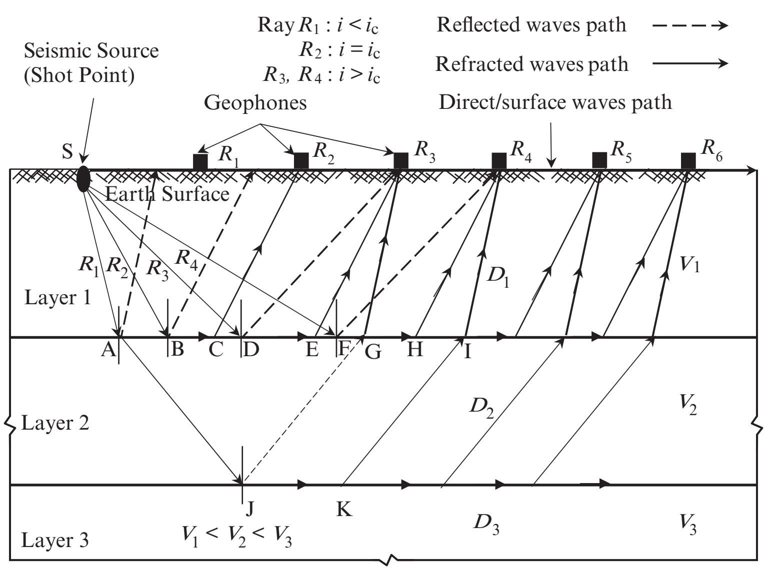

Figure 3.10 *Schematic of travel of sound waves in a layered medium*

There are two types of seismic investigations: lateral surveys called fan shooting and vertical surveys called refraction surveys. In fan shooting, the geophones are arranged on a circle around the shot point. It is suitable for locating buried valleys, salt domes, etc. In refraction seismic survey, the geophones are uniformly placed on a straight line from the shot point to record the arrival time of first shock waves. These waves may have travelled straight from the shot point to the geophone, or they may have been refracted and reflected in the deeper layers. For example, in a homogeneous unconsolidated material with water table when the wave reaches the water table, it will travel along the interface. As it travels, a series of waves is propagated back into the unsaturated layer. At any location on the surface, the first wave will arrive either directly from the shot point or from a refracted path.

By measuring the time interval of the first arrival at varying distances from the shot point, a time–distance graph can be plotted. The graph between the arrival time of the first shock wave at each geophone and the distance of geophone from shock point will be a succession of straight lines for a layered medium (see Figure 3.11). The first section represents the first or top layer, the second section the second layer, and so on. The velocity of wave in each layer is the reciprocal of the slope of the corresponding straight line section. Several equations are available to calculate the depth of various discontinuities or the thickness of the different layers. The thickness of a particular layer in a multilayered formation is given by (Bower, 1978) the following equation:

$$D_{\mathrm{i}} = \frac{V_i V_{i+1}}{2\sqrt{V_{i+1}^2 - V_i^2}} \left(t_{i+1} - 2D_1 \frac{\sqrt{V_{i+1}^2 - V_1^2}}{V_1 V_{i+1}} - 2D_2 \frac{\sqrt{V_{i+1}^2 - V_2^2}}{V_2 V_{i+1}} - \ldots - 2D_{i-1} \frac{\sqrt{V_{i+1}^2 - V_{i-1}^2}}{V_{i-1} V_{i+1}} \right) \tag{3.11}$$

where, D_{i} is the thickness of *i*th layer (for the top layer, $i = 1$), V_{i} is the wave velocity in *i*th layer (reciprocal of slope for *i*th straight line section of data curve), and t_{i} is the intercept of extended straight line for *i*th layer with time axis.

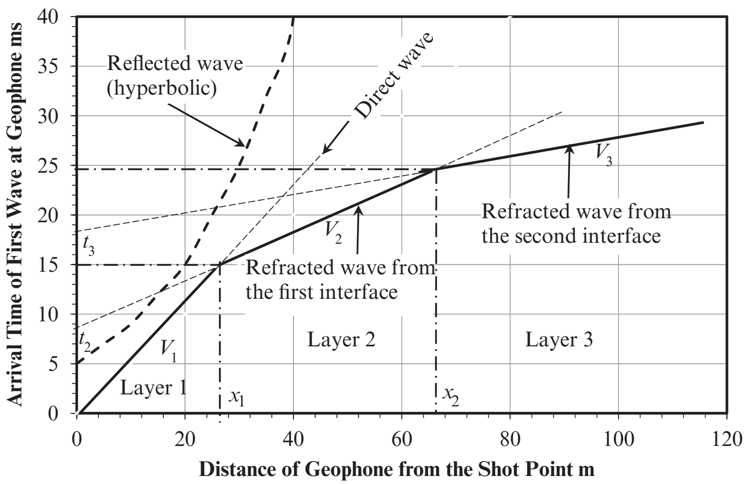

Figure 3.11 *Plot of arrival time of first wave at different geophones*

For the top layer $i = 1$, Eqn. (3.11) reduces to

$$D_1 = \frac{V_1 V_2}{2\sqrt{V_2^2 - V_1^2}} t_2 \tag{3.12}$$

Similarly, for the second layer $i = 2$, therefore Eqn. (3.11) reduces to

$$D_2 = \frac{V_2 V_3}{2\sqrt{V_3^2 - V_2^2}} \left(t_3 - 2D_1 \frac{\sqrt{V_3^2 - V_1^2}}{V_1 V_3} \right) \tag{3.13}$$

Alternatively rewriting Eqn. (3.10) gives the depth of the top layer as follows:

$$D_1 = \frac{x_1}{2} \sqrt{\frac{V_2 - V_1}{V_2 + V_1}} \tag{3.14}$$

and the depth of the second layer can be determined by (Bower, 1978) the following equation:

$$D_2 = \frac{x_2}{2} \sqrt{\frac{V_3 - V_2}{V_3 + V_2}} - \frac{D_1}{6} \tag{3.15}$$

where, x_1 is the horizontal distance of the first break point in the curve that is the distance from the shock point to the point at which the direct wave and the refracted wave arrive simultaneously, and x_2 is the horizontal distance of the second break point in the curve as shown in Figure 3.11.

The field procedure of seismic refraction investigations has been simplified with the help of compact efficient instruments. It is commonly used to map crosssections of alluvial valleys so that variations in thickness of unconfined aquifers can be determined. The seismic refraction method can eliminate rapidly and economically areas that are unfavorable for test drilling. The actual presence of groundwater is difficult to determine without supplementary information because velocities overlap in saturated and unsaturated zones. The depth range of refraction seismic surveys is usually on the order of 100 m. The depth range is restricted to the layer with the highest sound velocity (bedrock). Seismic velocities must increase with depth in order to obtain satisfactory results; thereby, a dense layer overlying an unconsolidated aquifer can mask the presence of the aquifer. It is not readily adapted to small areas. The local noise or vibrations from sources such as highways, airports, and construction sites interfere with seismic work. Lack of velocity contrast, small thickness of layers, undulating subsurface layers, variable compaction, etc., also limit the use of seismic methods. The seismic method is not commonly used as it requires sophisticated instruments and trained personnel for operation of instrument and interpretation.

3.7 Ground Penetrating Radar and Other Methods

Ground penetrating radar (GPR) is used to delineate features of the geologic setting, map the distribution of buried objects, define the configuration of the water table and stratigraphic boundaries, etc. GPR is based on the reflection of radio waves from discontinuities under the earth's surface. A transmitting antenna at the surface radiates short pulses of radio waves into the ground. A movable antenna at the surface detects the reflected waves from the subsurface.

The source of radar wave pulses and the receiver antenna are generally built into a single unit that tow across the ground surface. The intensity of the reflected waves returning to the surface is recorded as a function of time. As the radar unit is moved along the ground surface, a succession of intensity of the reflected waves versus time is plotted with distance known as wiggle trace plot. The wiggle trace provides a 2-D picture of subsurface features. It is even possible to visualize 3-D subsurface scenarios in GPR techniques. The resolution of GPR images is a function of the frequency bandwidth of the system; higher systems get higher resolution, but less penetration depth. In principle, GPR works like a reflection seismic method except that electromagnetic reflections rather than sound waves are recorded at the surface. Radio waves are reflected due to changes in dielectric constants and electrical conductivity as a result of variation in properties of the minerals present, degree of saturation, and material density. It is possible to obtain a continuous profile (in form of a wiggle trace plot) of the subsurface by moving the GPR system at a slow speed. The interpretation methods used for GPR data are similar to the method for seismic data. The investigative depth of the GPR method ranges from a few meters to about 100 m (generally less than 30 m). Because clayey sediments are highly conductive, GPR does not work well at sites underlain by moist lake clay or glacial till.

The *gravity method* measures differences in density on the earth's surface that may indicate geologic structure. This method is seldom used to explore groundwater as it is expensive. In addition, the difference in water content in subsurface strata seldom involves measurable difference in specific gravity. *Electromagnetic methods* induce a current in the ground with an alternating current-transmitting coil. The magnetic field around the coil induces an electrical field based on the properties of the medium, the moisture content, etc.; the resulting electrical conductivity can easily be measured. Terrain conductivity is a form of electromagnetic methods where the transmitting coil and receiver coil are mounted a fixed distance apart. The most important application of electromagnetic method is to detect buried features such as waste disposal sites and lost underground storage tanks and pipelines. This method is quicker than electric resistivity method. In *magnetic methods*, variations in the magnetic field of the earth in relation to subsurface geology is detected and measured. Magnetic anomalies are associated with magnetite, ilmenite-type rocks, whereas sedimentary rocks are either nonmagnetic or feebly magnetic. This method is fast and less expensive, but magnetic contrasts are seldom associated with groundwater occurrence.

3.8 Subsurface Investigation

A detailed and comprehensive study of groundwater and conditions under which it occurs can only be made by subsurface investigations. The aquifer data such as its permeability, location, thickness, and groundwater quality and quantity can be obtained from subsurface examination. These are comparatively expensive, but these are essential if data on quality and quantity of the groundwater are desired. After using the general sources and suitable surface investigation methods, it is possible to choose the best location for subsurface investigations. Manual excavation can be adopted to explore shallow unconsolidated materials. A variety of direct push methods are available. Small diameter probes and sensors are pushed directly down into unconsolidated materials without drilling out a borehole. Probes generally consist of a small drilling pipe with a cone-shaped tip on it. When compared with drilling, probes are a relatively quick and inexpensive way of exploring moderate depths, even below the water table. Probes work well in many sands, silts, and clays, but they have difficulty penetrating dense or cobble-bearing materials. Probes can explore as deep as 30 m or more in ideal settings with soft, fine-grained sediments. Some probes are equipped to collect small diameter soil core samples and some are equipped to collect pore gas and water through porous screens. Some probes contain sensors that measure the concentration of specific contaminants. On the contrary, some probes are equipped to make geophysical measurements such as electrical conductivity, which can be used to identify the water table and stratification. Probes can be used to measure hydraulic heads and hydraulic conductivities. In test drilling, one or more small diameter holes are drilled to supply information on the groundwater level and the geological substrata. The results of the drilling and sampling of material make it possible to establish a geological log with information from the different strata that is useful in verifying other means of investigation and to obtain assurance of underground condition prior to well drilling. The log can contain grain size. It is also possible to take groundwater samples for chemical analysis. If test hole gives good result, it is reamed to larger diameter to form a pumping well; otherwise, it is used as observation well. Geophysical logging techniques provide information on physical properties of geologic formations, water quality, and well construction. The last most informative step in an investigation for a groundwater well is a pumping test. The setting involves a pumping well and several observation wells. Test holes that may have been drilled earlier can be useful as observation wells. Pumping tests can be either short- (investigation of the vicinity of the hole) or long-time pumping (information from larger scale). Water sampling at suitable intervals for chemical analysis are done during the duration of the pumping time. Analysis of the data received from the pumping test provides information on permeability, transmissivity, yield of the well, and water quality. These will be dealt in the subsequent chapters.

Case Study

Sharma (2013) conducted Schlumberger VES survey at Jhiwana and Patan Kalan in Alwar district of Rajasthan. In sounding with Schlumberger configuration, the current electrodes are moved outward along a straight line, keeping the closely spaced potential electrodes fixed at the center till a measureable—determined by the sensitivity of instrument—potential difference is obtained. The resultant apparent resistivity values are listed in Table 3.3. The Schlumberger VES could have the maximum current electrode separation (AB) in the range of 200–400 m.

Table 3.3 *Schlumberger vertical electrical resistivity survey data*

Half spacing between current electrodes	*Apparent resistivity (Ωm)*	
AB/2 or L/2 (m)	**Jhiwana**	**Patan Kalan**
3	72.02	48.65
4	71.75	50.42
5	70.52	53.41
6	66.49	55.93
8	61.89	60.48
10	58.29	63.61
10	56.62	57.15
12	53.22	54.87
15	50.16	55.02
20	44.16	52.87
25	39.51	49.26
25	35.25	45.05
30	31.61	43.15
40	30.18	41.02
50	27.68	40.35
50	28.87	36.86
60	26.61	34.42
80	22.76	30.28
100	19.28	30.63
100	19.75	29.78
150	19.25	34.54
200	19.65	37.94

Based on available lithologs and electric logs of the existing exploratory wells, located in and around the area, constructed by State and Central Ground Water Departments and private owners, the gradation of electrical resistivity values have been made as listed in Table 3.4.

Table 3.4 *Standardization of electrical resistivity value in terms of subsurface lithology and groundwater quality*

Electrical resistivity range in Ω m	*Groundwater quality*	*Inferred lithology*
9–30	Dry zone	Top soil dry/moist. Sediments, consisting of coarse sands, clay/silt, and kankar (rocks fragments) in varying proportion.
15–35	Fresh	Sand and clay mixed sediments, carrying fresh water, suitable for drinking

(*Continued*)

Table 3.3 Continued

Electrical resistivity range in Ω m	*Groundwater quality*	*Inferred lithology*
10–15	Marginally fresh	Sand and clay-mixed sediments, carrying marginally fresh quality of water suitable for domestic, horticulture, and even for drinking water use with caution
5–10	Marginally brackish	Sand and clay-mixed sediments, carrying marginal brackish quality of water suitable for domestic and horticulture use. The water can also be used for drinking purpose after initial treatment.
< 5	Brackish/saline	Sediments consisting mixture of sand and clay, and carrying brackish quality of water suitable only for domestic use
100–400	Fresh water	Fractured/jointed quartzite
400–1,000	Fresh water	Partially fractured quartzite
> 1,000	Dry	Compact quartzite

The change in resistivity value in a particular VES and the trend of the curve play a significant role in determining the type of formation. The values of apparent resistivity ρ_a in Ω-m are plotted against the related half-current electrode separation AB/2 on double-log paper as shown in Figures 3.12 and 3.13 for Jhiwana and Patan Kalan, respectively. VES maps give 2-D image of subsurface variation of resistivity both vertically and laterally, and hence the variation of subsurface hydrogeological conditions of study area.

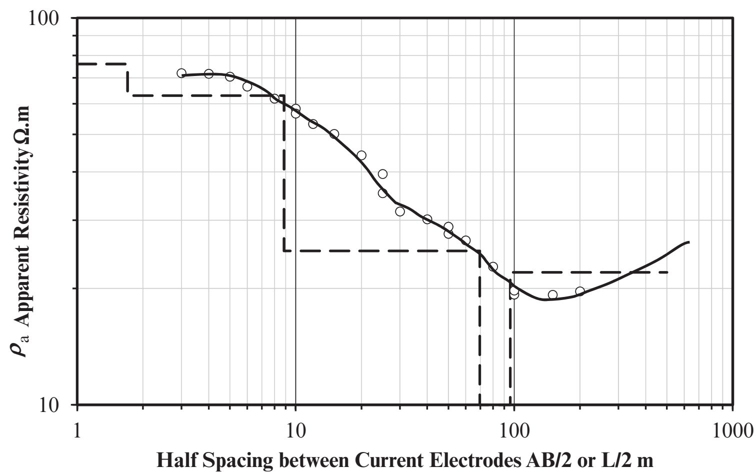

Figure 3.12 *Plot of Schlumberger apparent resistivity at Jhiwana*

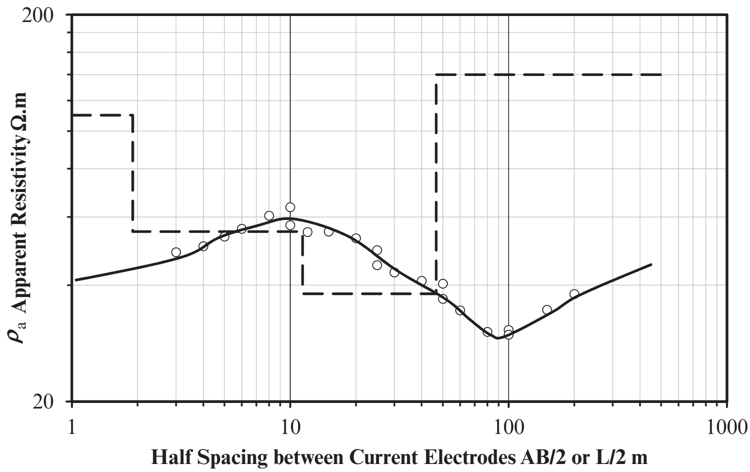

Figure 3.13 *Plot of Schlumberger apparent resistivity at Patan Kalan*

Analysis of Figure 3.12, Figure 3.13, and Table 3.4 resulted in Tables 3.5 and 3.6 for Jhiwana and Patan Kalan, respectively.

Table 3.5: *VES results at Jhiwana with AB/2 = 200 m*

True resistivity (Ω-m)	*Thick ness (m)*	*Depth range (m)*	*Inferences*	*Projected litholog*
76	1.7	0.00–1.70	Surface soil with sandy clay	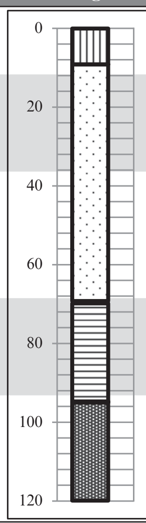
63	7.14	1.70–8.84	Dry, fine-grained sand with clay	
25	60.72	8.84–69.56	Fresh water saturated fine-grained sand predominant	
10	26	69.56–95.56	Marginal fresh water saturated sandy clay	
22	Continue	95.56–continued	Fresh water saturated fine-grained sand predominant	

The area is underlain by alluvium formation comprising silt/clay, sand medium to fine grained with pebbles of quartzite, occasionally overlying the basement of quartzite depth which could not be estimated being more than 95.56 m bgl. However, the depth to the basement of quartzite could be estimated to be

46.60 m bgl. Depending on the length spread available and nature of subsurface formation in the study area, the depth of investigation varies from 78.34 to 95.56 m bgl. Due to the presence of thick saturated silty/clayey layers, after certain depth at places, the resistivity values sink down to very low and restrict the depth of penetration of current. This results in limited depth of penetration, even though the current electrode separation is kept at its maximum. Therefore, at many places, detailed information of deeper depths where groundwater is occurring could not be picked up. The thickness of the alluvium is expected to be more than 95.56 m in the area. Formation comprising fine sand or clayey sand below the depth of 20 m bgl is likely to form good aquifers. In Jhiwana area, the depth to groundwater level is estimated to occur in the range of 20–25 m bgl. The unsaturated sand layer occurs in depth zone of 8.84–10.26 m. Groundwater quality is expected fresh (with EC = 400 and TDS =256) from 8.84 m to depth of 69.56 m bgl, marginally fresh (with EC = 1,000 and TDS = 640) from 69.56 to 95.56 m bgl and fresh (with EC = 455 and TDS =291) further below.

Table 3.6 *VES results at Patan Kalan (for AB/2 = 150 m)*

True resistivity	*Thickness*	*Depth range*	*Inferences*	*Litholog*
110	1.9	0.00–1.90	Surface soil with sandy clay	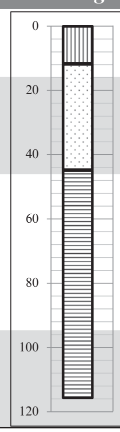
55	9.5	1.90–11.40	Dry fine grained sand with clay	
38	35.2	11.40–46.60	Fresh water saturated medium-grained sand predominant	
140	continue*	46.60–continued	Weathered/fractured quartzite	

The depth to basement (Quartzite bed rock) in Patan Kalan village area has been estimated to be 46.60 m bgl. The thickness of the alluvium is expected to be 46.60 m in the area. Formation comprising fine sand or clayey sand below the depth of 20 m bgl is likely to form good aquifers. The water level in the area under investigation is expected to vary in the range of 20–25 m bgl. The unsaturated zone exists up to 11.40 m bgl depth. The saturated fresh water medium sand aquifer exists between 11.40 and 46.60 m bgl. Groundwater quality is fresh (having EC = 263 and TDS = 168).

SOLVED EXAMPLES

Example 3.1: The following Table 3.7 lists representative seismic survey data

Table 3.7 *Seismic survey data*

Distance of geophone (m)	*Arrival time of first wave (ms)*	*Distance of geophone (m)*	*Arrival time of first wave (ms)*	*Distance of geophone (m)*	*Arrival time of first wave (ms)*
0	0	35	28	70	42
5	4	40	30	75	43
10	9	45	31	80	43
15	12	50	34	85	45
20	15	55	37	90	47
25	20	60	38	95	47
30	24	65	40	100	48

Estimate aquifer layering pattern.

Solution: Figure 3.14 shows a plot between the distance of geophones and the arrival of the first sound wave at different geophones.

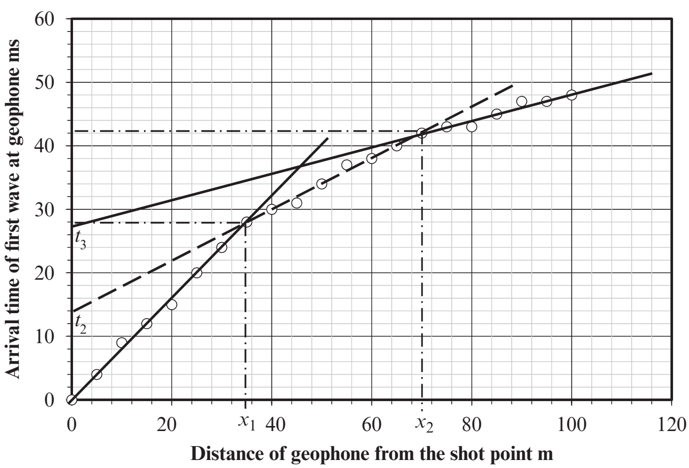

Figure 3.14 *Time v/s distance plot for example 3.1*

The first straight line section is response due to the top layer. The inverse of its slope is the velocity in the layer. As $x = 25$ m; $t = 20$ ms $= 0.02$ s, therefore $V_1 = 25/0.02 = 1{,}250$ m/s. The second straight line section is response of the second layer and the inverse of its slope is the velocity in the layer, therefore $V_2 = (60 - 40)/(0.038 - 0.03) = 2{,}500$ m/s. Similarly, the velocity in the third layer is $V_3 = (100 - 75)/(0.048 - 0.043) = 5{,}000$ m/s.

The location of the first breakpoint is $x_1 = 35$ m at time $= 28$ ms. The intercept of extended straight line for second layer with time axis is $t_2 = 14$ ms.

Therefore, the thickness of the top layer using Eqn. (3.12) is

$$D_1 = \frac{V_1 V_2}{2\sqrt{V_2^2 - V_1^2}} t_2 = \frac{1{,}250 \times 2{,}500}{2\sqrt{2{,}500^2 - 1{,}250^2}} \times 0.014 = 10.10 \text{ m}$$

and also using Eqn. (3.14),

$$D_1 = \frac{x_1}{2}\sqrt{\frac{V_2 - V_1}{V_2 + V_1}} = \frac{35}{2}\sqrt{\frac{2,500 - 1,250}{2,500 + 1,250}} = 10.10 \text{ m}$$

The location of the second breakpoint is x_2 = 70 m at time = 42 ms. The intercept of extended straight line for third layer with time axis is t_3 = 27.5 ms, therefore the thickness of the third layer by Eqn. (3.13) comes out:

$$D_2 = \frac{V_2 V_3}{2\sqrt{V_3^2 - V_2^2}}\left(t_3 - 2D_1\frac{\sqrt{V_3^2 - V_1^2}}{V_1 V_3}\right) = \frac{2,500 \times 5,000}{2\sqrt{5,000^2 - 2,500^2}}$$

$$\left(0.0275 - 2 \times 10.10\frac{\sqrt{5,000^2 - 1,250^2}}{1,250 \times 5,000}\right) = 17.10 \text{ m}$$

Alternatively, using Eqn. (3.15),

$$D_2 = \frac{x_2}{2}\sqrt{\frac{V_3 - V_2}{V_3 + V_2}} - \frac{D_1}{6} = \frac{70}{2}\sqrt{\frac{5,000 - 2,500}{5,000 + 2,500}} - \frac{10.10}{6} = 18.52 \text{ m}$$

In this example, the refracted waves can appear only in geophones beyond critical distance x_c from the shot point given by Eqn. (3.9):

$$x_c = \frac{2D_1V_1}{\sqrt{V_2^2 - V_1^2}} = \frac{2 \times 10.10 \times 1,250}{\sqrt{2,500^2 - 1,250^2}} = 11.67 \text{ m}$$

The reflected waves will reach at any geophone

$$t_i = \frac{2}{V_1}\sqrt{(x/2)^2 + D_1^2} = 0.0016\sqrt{(x/2)^2 + 102} \text{ s.}$$

and the refracted waves will reach at time

$$t_r = \frac{x}{V_2} + \frac{2D_1}{V_1V_2}\sqrt{V_2^2 - V_1^2} = \frac{x}{V_2} + t_2 = 0.014 + 0.0004x$$

PROBLEMS

3.1. Why do we need groundwater investigation?

3.2. How is remote sensing useful in groundwater targeting?

3.3. Explain the electric resistivity method of groundwater exploration.

3.4. After deriving expressions for the time taken by direct, reflected, and refracted waves from the source to reach a geophone station, describe the seismic method of locating water-bearing aquifers.

3.5. Explain the electric resistivity method of groundwater exploration along with Wenner and Schlumberger configurations.

3.6. What are differences in sounding and profiling methods in the electric resistivity technique of groundwater exploration? Where and how are these methods used?

3.7. Describe the merits and demerits of electric resistivity and seismic methods of groundwater exploration.

3.8. How is ground penetrating radar used in groundwater prospecting?

3.9. What are the advantages and disadvantages of surface and subsurface methods of groundwater investigation?

Chapter 4

Well Logging and Construction

4.1 General

A well is a hole or shaft that is usually vertical, excavated in the earth to extract water, oil or gas. Wells are also constructed for subsurface exploration, water-level observation, artificial recharge and waste disposal purposes. Groundwater is extracted through water wells for domestic, agricultural, industrial, and allied uses. Horizontal wells or *qanats* have been widely used for water supply and irrigation in the Middle East and western Asia since the first millennium BC and continue to be used today. The growth of many urban settlements in Europe in the industrial period was aided by use of groundwater. Wells continue to play a significant role as their use have increased in India and developing countries during the past 20–30 years due to increased water demand for industrial, agricultural, and domestic needs. Even developed countries are constructing new wells each year for domestic and other water supplies. In the past couple of decades, more wells are being constructed for artificial recharge of aquifers, aquifer cleanup, reuse, and recycle of treated waste water, geothermal source energy, construction dewatering, brine-mining, water injection to oil reservoirs, river support, etc. Wells and boreholes are also used extensively for monitoring water levels and groundwater quality and for different logging purposes.

There is some water under the earth's surface almost everywhere. The practical way for locating sites where the water occurs under favourable conditions is *groundwater exploration* that includes the application of scientific knowledge, drilling experience, and plain common sense. Certain clues are helpful in locating groundwater sites; for example valleys, gravel, sand, sandstone, and limestone are favourable signs, whereas clay, shale, and crystalline rocks are negative signs. The character of the formations beneath the earth's surface is obtained by test drilling and recording a log of the borehole. *Well-logging* consists of recording characteristic properties of the various strata in terms of depth. Thus, in production wells (for drinking water, irrigation, or other supply purposes), the first step is groundwater exploration to find locations where wells can be designed and constructed to supply the required demand of water, of a quality suitable for the intended use, at reasonable cost and with least impact to either fellow groundwater users or to the environment. Groundwater exploration is also an important step in locating other types of wells (aquifer cleanup, artificial recharge, groundwater monitoring, etc.).

Many methods exist for construction of wells; selection of a particular method depends on the purpose of the well, the yield of the well, depth to groundwater, geologic conditions, availability of drilling machinery, and economic factors. Open wells are dug manually. Shallow wells are dug, bored, driven, or jetted. Deep tube wells are drilled by cable tool or rotary methods. Site selection, logging, and construction techniques of wells are described in this chapter, whereas Chapter 14 deals with the design, development, and maintenance of water wells.

4.2 Type of Wells

Water wells may have different forms, orientations, and sizes. Traditionally, most water wells were excavated by hand as shallow large diameter shafts; nowadays, the majority is constructed as small diameter boreholes drilled by machines. They are typically vertical but can be horizontal (infiltration gallery), a combination of vertical and horizontal well (radial collector well), or sometimes inclined (Figure 4.1).

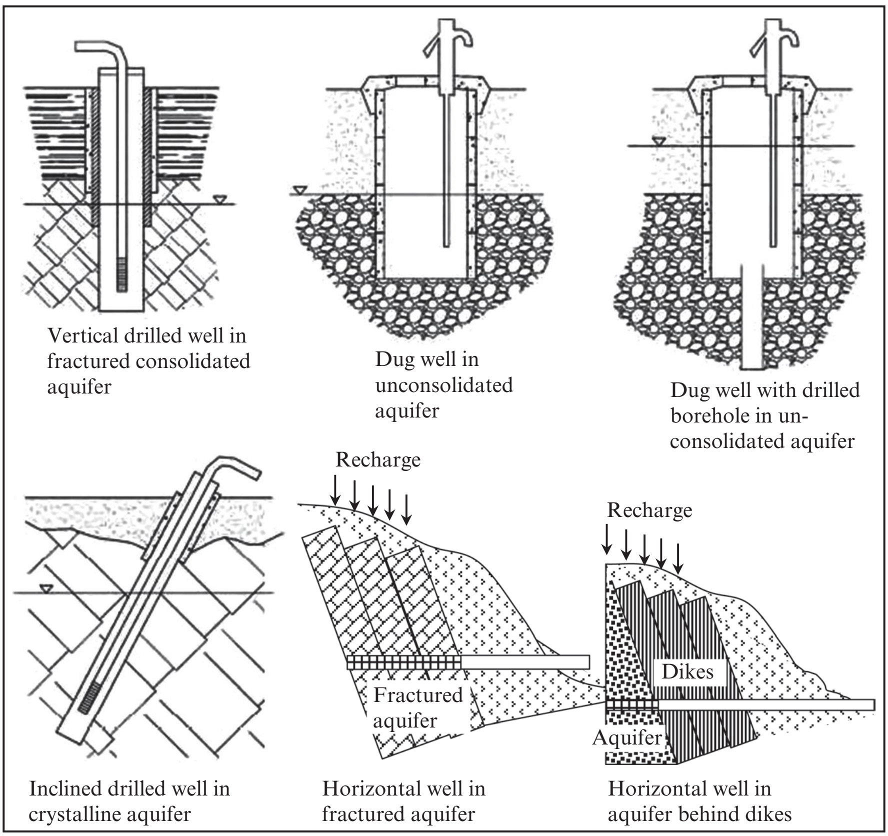

Figure 4.1 *Examples of different types of water wells*

There are various types of wells. The following is the list of selected type of wells:

(i) *Deep well* or *tube well* is constructed by drilling. They are also known as production well or production borehole.

(ii) *Dug* or *open well* is a large diameter, usually shallow water well constructed by manual labor.

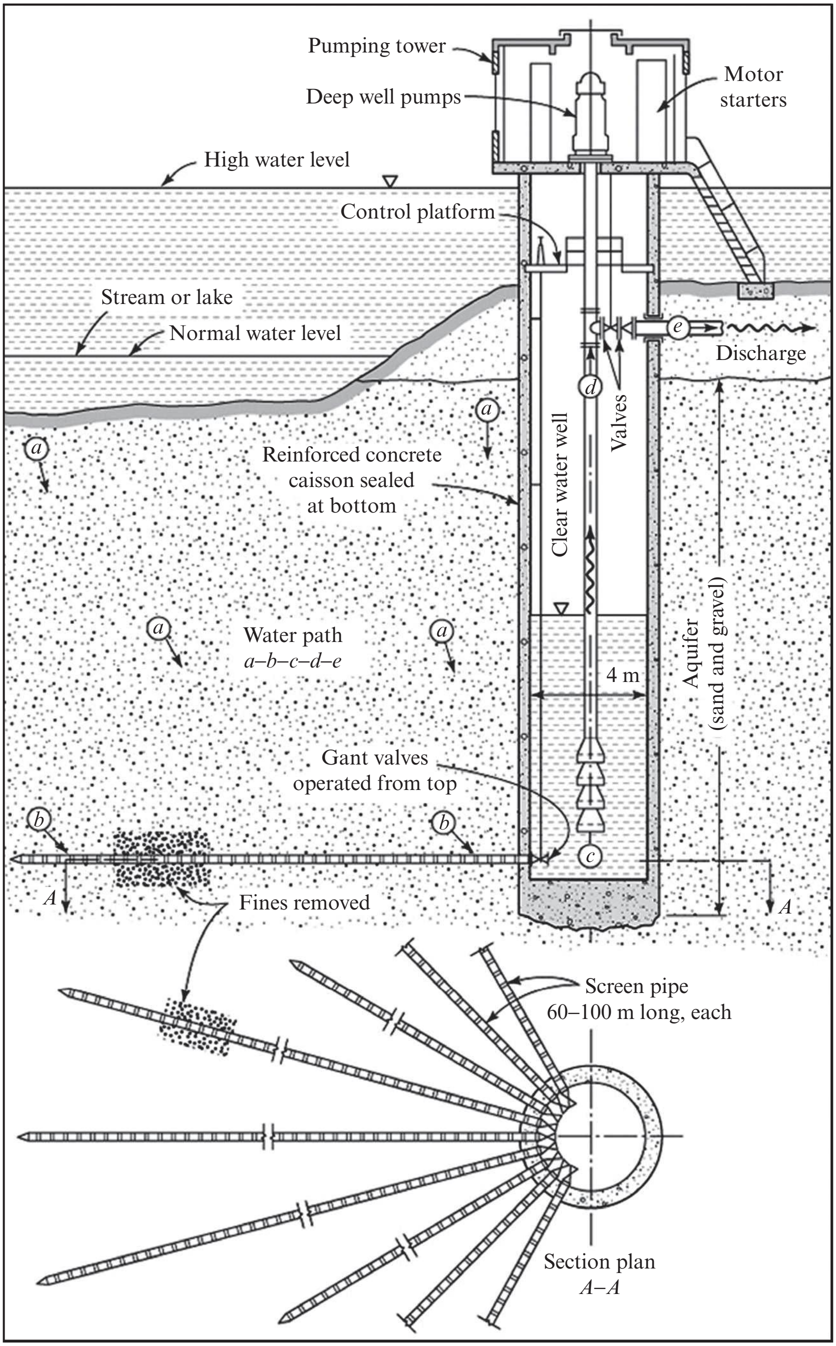

Figure 4.2 *Ranney (radial collector) well (Todd and Mays, 2005)*

(iii) *Exploratory borehole* is drilled for the specific purpose of obtaining information about the subsurface geology or groundwater.
(iv) *Observation well* or borehole is constructed to obtain information on variations in groundwater level or water quality.
(v) *Piezometer* is a small diameter borehole or tube constructed for the measurement of hydraulic head at a specific depth in an aquifer. In a piezometer, the section of the borehole (the screened section) in contact with the aquifer is usually very short.
(vi) *Test well* is a borehole drilled to test an aquifer by means of pumping tests.
(vii) *Infiltration gallery* is a shallow horizontal well usually constructed in the bed of a river or along a river bank in an alluvial aquifer.
(viii) *Horizontal well* is occasionally drilled in mountain sides to tap vertical bedding planes or fracture zones, groundwater behind dikes, etc. Such type of wells is free-flowing.
(ix) *Radial collector well* is a large diameter well with horizontal boreholes extending radially outward into the aquifer. Radial collector well is also known as *Ranney* well (Figure 4.2).
(x) *Qanat, ghanat, falaj, foggara, karez, or kariz* consists of one or more head wells (mother wells) located in saturated medium at higher elevation and gently sloping tunnel in which the water flows to the point of abstraction under gravity (Figure 4.3). Where the tunnel is below water table, it also functions as an infiltration gallery.

According to a method of drilling, wells are called dug wells, driven wells, and drilled wells. *Dug wells* and *driven wells* are constructed to extract shallow ground water. The *driven wells* are constructed by driving pipes in shallow porous sand and gravel aquifers, whereas deeper wells are machine drilled. Shallow wells often go dry, but deep wells constructed and designed scientifically seldom go dry. Figure 4.4 shows the components of a drilled well. The pump-chamber casing provides stability to the well and protects the pump against debris falling into the well from the sides of the borehole. The bottom/bail plug (or tailpipe) is a short length of casing, capped at the bottom, installed at the base of the well

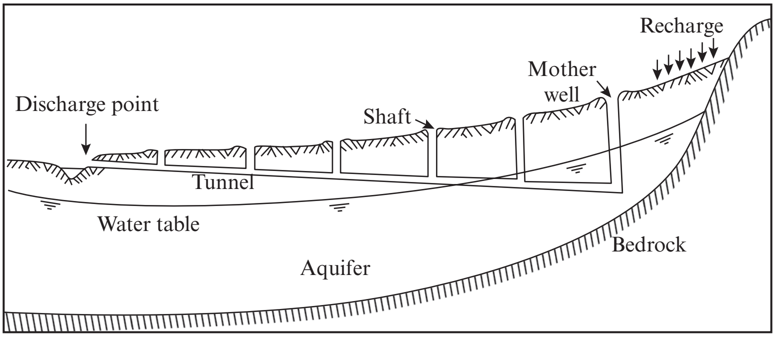

Figure 4.3 *Qanat, ghanat, falaj, foggara, or karez (gravity well)*

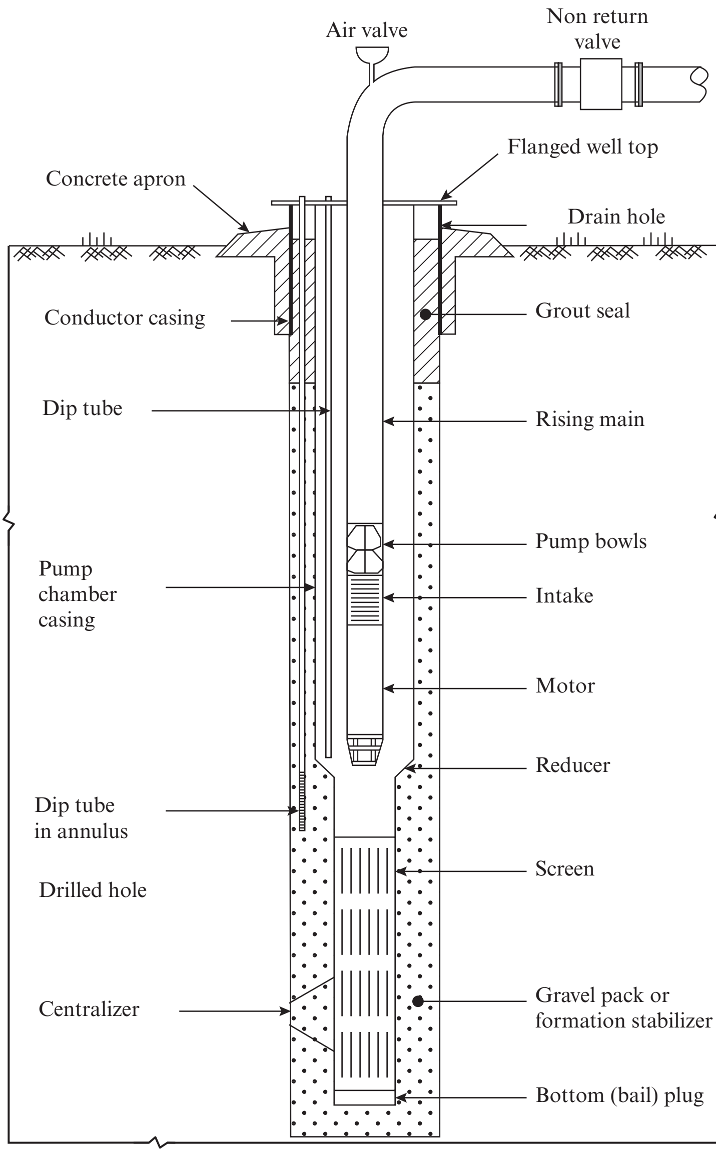

Figure 4.4 *Components of a drilled well (Misstear et al., 2006)*

screen to act as a sediment trap. The conductor casing in the upper few meters of the well provides stability during drilling; and if permanent, it may also support the weight of the pump. The grout seal around the conductor casing prevents movement of contaminants downwards from the surface through the annular space to the well and aquifer. Dip tubes are handy for monitoring water levels inside the well and in the gravel pack between the screen and borehole wall.

4.3 Selection of Well Site

The initial step in successful groundwater development is the selection of proper well sites, first ascertaining the presence of suitable aquifers and then finding the best place for the well from a standpoint of quantity, quality, depth of groundwater, and absence of potential contamination by polluted or other low-quality water. The sites are decided on the basis of topographic, soil, and geological conditions in relation to areas of recharge and discharge. The location for siting a well is decided by hydrogeologists and engineers, bearing the following points in mind (Misstear et al., 2006):

- The well should have sufficient yield to meet the demand.
- The water quality should be fit for the particular purpose.
- The well should be reliable, requiring little maintenance.
- The well should be durable, with a design life suited to its purpose.
- The construction and operating costs should not be excessive.
- The community should be involved if the local people are the potential beneficiaries of the new well.
- The well should not impact unacceptably on neighboring wells or on the environment, and therefore it should not violate local water resources, planning, or environmental legislation.

Environmental impacts to be avoided include (i) significant reductions in groundwater flow to ecologically important wetlands, spring areas, or baseflow supported rivers; (ii) saline intrusion in coastal aquifers; and (iii) ground subsidence caused by large drawdowns in unconsolidated, compressible aquifers or by dewatering organic rich subsoils or sediments.

The optimum location can often be determined without detailed studies, if wells already exist in the particular area, and the groundwater hydrology is fairly well known. In new areas, investigations and intensive studies are required to delineate the more promising groundwater areas and to determine optimum well sites. The sequence of groundwater investigations for locating well sites and planning a well scheme includes the following:

(1) Desk study
(2) Field reconnaissance
(3) Well survey
(4) Geophysical survey
(5) Test drilling and logging
(6) Pump testing

4.3.1 Desk Study

A desk study followed by a field reconnaissance may be sufficient for a small groundwater development in an extensive, homogeneous aquifer, where the groundwater resources and groundwater quality are clearly understood. The desk study includes answers to the following questions (Misstear et al., 2006):

- How much water is required?
- What water quality criteria apply—potable, livestock, irrigation, other?

- How many wells are likely needed?
- How much hydrogeological information is already available?
- What are the data gaps to be filled by additional investigations?
- What are the social, environmental, community, and land ownership criteria that will influence the siting and operation of the well scheme?

Potential data requirements involves topographic maps; bedrock geology maps; soils, subsoils and land use maps; hydrogeology and groundwater vulnerability maps; geology, hydrogeology, site investigation, and other relevant reports; aerial photographs, satellite imagery; well and borehole records; etc. Based on such information, it may be possible to detect sufficiently permeable strata that, by virtue of their relative elevation or depression, geologic history and hydrology could be water-bearing. Examples of possible well locations for a variety of aquifer situations are shown in Figure 4.5. In developed countries such geological and hydrogeological information is readily available, and therefore the collection and analysis of existing data may eliminate the need for a detailed field exploration survey. Hydrogeological data in many developing countries are sparse and more difficult to obtain.

It may be advantageous to use a geographical information system for storing and retrieving the data, including the preparation of maps and sections. Remote-sensing data (i.e. aerial photographs and satellite imagery) are useful for drawing inferences on groundwater conditions. The use of remote sensing is relevant when choosing well sites in crystalline aquifers and in some consolidated aquifers. In these situations, the best potential well sites may relate to "lineaments" that can be observed on the remote-sensing imagery. These lineaments may correspond to fracture zones, faults, or other hydrogeological features of significance, including lithological or hydraulic boundaries. However, the fractures may be infilled with low-permeability clays derived from hydrothermal alteration or weathering material, therefore the detection of a lineament on an aerial photograph or satellite image should preferably be followed up by ground investigations, such as geophysical surveys or exploratory drilling, but even these may not adequately distinguish between clay-filled and transmissive fracture zones.

4.3.2 Field Reconnaissance

The desk studies are followed by a reconnaissance of the project area before planning the detailed exploration survey. The field reconnaissance helps to (i) develop a better understanding of the hydrogeology of an area through existing wells and boreholes; (ii) find out whether there are any problems relating to well yields, water quality, or reliability; (iii) assess the practicalities involved in carrying out geophysical surveys; (iv) look for potential sources of pollution and estimate the groundwater vulnerability; and (v) identify and examine potential sites for exploratory boreholes. Although borehole sites are selected primarily on hydrogeological criteria, the field reconnaissance should consider issues such as land availability and community acceptance, access for a drilling rig, potential flooding problems, and borehole security with respect to vandalism.

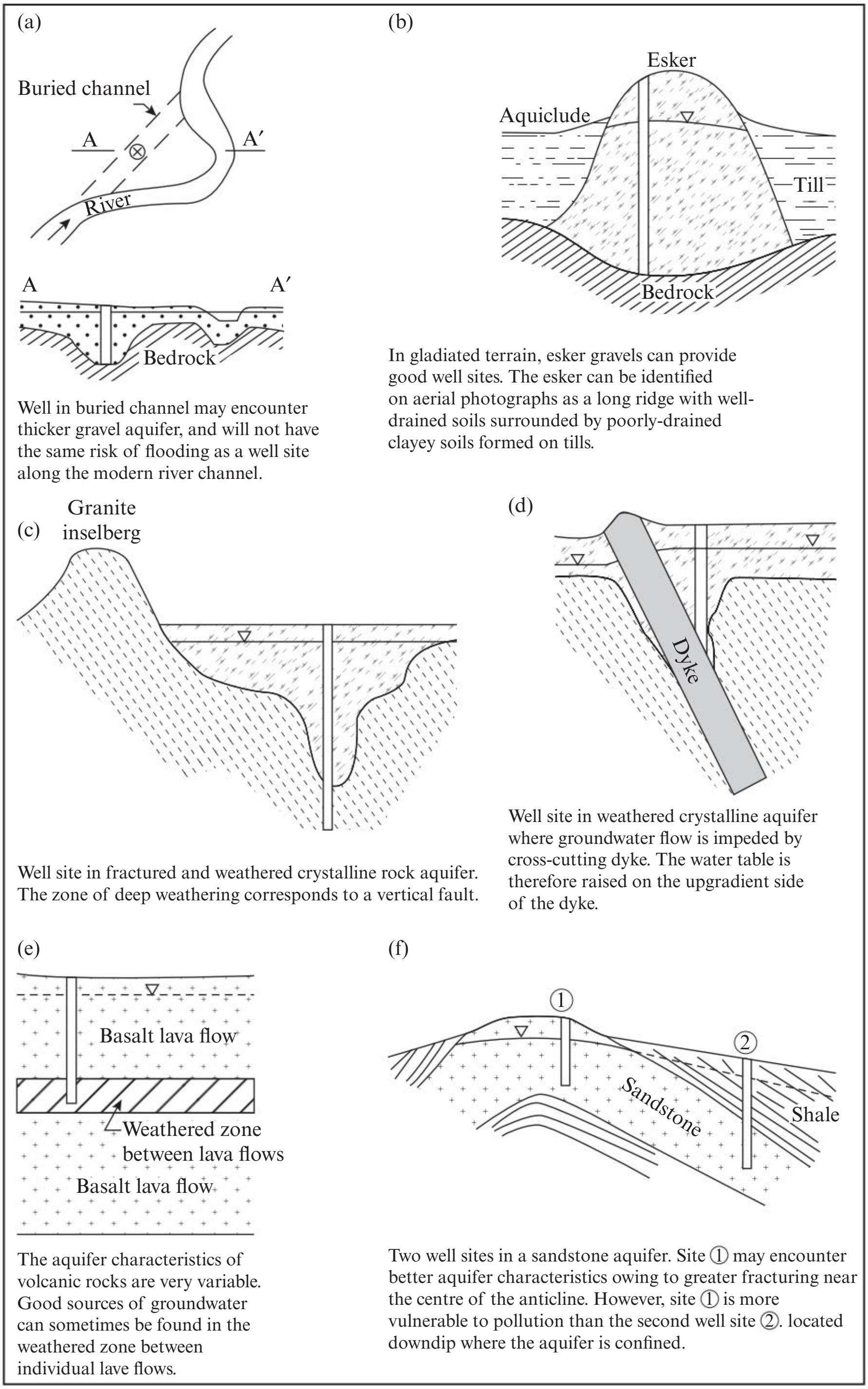

Figure 4.5 *Examples of well sites in a variety of hydrogeological situations (Misstear et al., 2006)*

4.3.3 Well Survey

The field reconnaissance is followed by a systematic survey of existing wells in the study area. The information collected is added to the project database or GIS. An essential requirement is to be able to record the locations of the wells accurately on the project maps. Global positioning systems (GPS) are very useful for mapping the coordinates of a well and the elevation of a suitable datum. The type of information that should be gathered during a well survey may include (i) number of wells and their coordinates; (ii) well details such as well owner, well type (drilled, hand-dug, radial collector), production well, or monitoring well, borehole log, depth and diameter of well, date and type of construction; (iii) aquifer type, depth to water level (static, pumping); (iv) pumping details—type and make of pump, pumping rate, pump setting depth, normal pumping periods, pumping test results; and (v) well water quality. Thus, the well survey provides the hydrogeologist information on groundwater levels (at rest and during pumping); well construction; present status and use of the well; pumping rates, hours pumped, groundwater use; and groundwater quality.

4.3.4 Geophysical Investigation

The next step is the geophysical investigation that can provide useful data on geology, aquifer geometry and water quality. Different methods provide data on different geophysical properties of the ground; therefore, the best survey results are usually achieved by using more than one method. The main geophysical methods used in groundwater exploration are described in Chapter 3. Geophysical surveys do not lead to a unique geological model; more than one interpretation of the data is possible. Borehole control is essential to reduce this ambiguity. Therefore, geophysical surveys should be carried out in conjunction with exploratory boreholes rather than as a replacement for a drilling program. The combined use of geophysics and drilling can produce results more cheaply than relying on drilling alone, since the number of exploratory boreholes can be reduced.

4.3.5 Test Drilling

The most accurate information about the geologic profile and the depth and quality of groundwater at the selected site is obtained by test well/hole drilling. The purpose of test drilling is to determine depths to groundwater, quality of water, and physical character and thickness of aquifers without the expense of a regular well, which might prove to be unsuccessful. Test wells are of relatively small diameter and can be drilled using cable tool, rotary, and jetting methods at a fraction of the cost of full-sized actual wells. The test drilling investigations often follow a phased approach, with initial exploration drilling followed by more detailed investigations. Exploration drilling is used to confirm the provisional interpretation of the hydrogeology derived from the desk studies, field reconnaissance, well survey, and geophysical surveys. The siting of the exploration boreholes in a situation where there are few data is difficult, but it should be governed by the principle that every borehole should be drilled to provide an answer to questions such as the following: Is there an aquifer? How thick is it? How thick are the cover materials? The amount of time, money, and effort that should be spent on a groundwater investigation (including test drilling, well logging, and pumping test) will depend on the size and nature of the proposed groundwater abstraction scheme, the complexity of the hydrogeology, the existing information, and the success rate of the exploration techniques that may be used. Where deep groundwater and/or consolidated materials make test drilling relatively expensive, or where the site is difficult to access for drilling rigs, it is better to get maximum possible information from geophysical investigations with the aim of minimizing test drilling sites. On the contrary, where groundwater is shallow in unconsolidated materials, test drilling is relatively inexpensive and it may be better to minimize geophysical investigations and rely more on test drilling to determine optimum well sites. Well loggings as described in the following section are also performed on test wells. Since the cost of test well drilling is a small fraction of actual production well, test drilling is usually economically justified in identifying well fields. When a test well appears suitable as a site for a finished well, it can easily be converted into a larger diameter, permanent production well by reaming/redrilling. Test wells also serve as observation wells for measuring water levels or for conducting pumping tests.

4.3.6 Pumping Tests

Values of the aquifer characteristics, transmissivity and storativity, are obtained by means of pumping tests on test wells. Test wells, with their satellite observation boreholes, are expensive installations, and their number in any particular investigation is likely to be limited by budgetary constraints. In a uniform aquifer, test wells can be widely spaced; but in an aquifer that is variable, test wells may have to be close together to predict aquifer behavior with confidence. The aquifer characteristics obtained from a pumping test is not perfect, and also aquifer behavior over several years may have to be predicted from observations taken over a period of only a few weeks. The exploration/observation boreholes can also be used to obtain water samples for analysis to measure the variation in regional groundwater quality. The quality of water from the test wells should be monitored on site during the tests, to detect any changes with time. At least one sample should be taken for full laboratory analysis to ascertain its suitability for the intended use. Seasonal trends, longer term natural trends, or likely trends in water quality induced by pumping may also need to be investigated. Although the design of a well field intended for a town water supply will inevitably require a comprehensive assessment of groundwater quality as part of the detailed investigation phase, a well scheme for construction dewatering, for example, may involve only a limited chemical sampling scheme to check on the likely corrosiveness of the water on the pumps and pipe work, and to satisfy the needs of the discharge consent. Having investigated the existing groundwater quality, we also need to assess the future risk of pollution at the proposed well site. Potential sources of pollutants are many and varied and include point sources such as waste disposal sites, industries, fuel storage tanks, latrines, septic tank systems and farmyards, and diffuse pollution sources such as intensive agricultural practices (inappropriate use of fertilizers, manures, and deep ploughing), road salting, and urbanized areas. When locating wells for drinking water, the risks from both chemical and microbial pollutants should be considered.

The pumping tests of the drilling investigation phase provide data on the aquifer characteristics and well performance. These tests generally only indicate the potential well yields in the short term. In designing a well or well field, the long-term sustainability of the supply must be considered. This requires an estimate of recharge and of the overall water balance of the aquifer system. In situations where the resource is under pressure, where adverse environmental impacts are possible or where there is insufficient information available to determine the extent of the resource and the possible impacts of the proposed well scheme, then an evaluation of the recharge and resource availability must be carried out.

Once a site is found appropriate for the location of a well, groundwater investigations may be carried out to ascertain for availability of desired quality and quantity of groundwater before the actual production well is constructed.

4.4 Well Logging

Before drilling an actual well in a new area, it is a pre-requisite to have groundwater prospecting through surface investigation methods as explained in Chapter 3. The next step is to select a proper site as described earlier in the previous section. Then, it is a common practice to drill a test well or hole. During drilling of a test well, a careful record, or log, is kept of the various geologic formations and the depths at which they are encountered known as *well logging*. Well loggings are also taken for production wells. During drilling samples corresponding to different depth and time of drilling are collected. These samples are analyzed to prepare logs pertaining to depth, color, character, size of material, and structure of the strata penetrated. Thus, information about the geology and groundwater conditions of the selected site is collected through well-logging techniques. The possible use of well logs in well design and aquifer parameters determination are as follows:

- Classifying lithology of rock layers drilled through a borehole
- Permeable and nonpermeable rock layers correlation with adjoining boreholes
- Obtaining information on electrical conductivity and seismic velocity data for modeling purposes
- Determining clay zone, porosity, and degree of water saturation
- Determining vertical flow in and around wells
- Determining water-quality parameters
- Determining presence of saline water in aquifer formation around a borehole

There exist different well-logging techniques, and different methods require specialized personnel and equipment. When well loggings are carried for a number of wells in a groundwater basin, the results can be correlated to yield a complete picture of the groundwater geology of the basin. Therefore, well-logging techniques are subsurface investigation methods for supplementing surface investigation methods for detailed and comprehensive study of groundwater and conditions under which it occurs. Whether the information needed concerns an aquifer (its location, thickness, composition, permeability, and yield) or groundwater (its location, movement, and quality), quantitative data can be obtained from well loggings or subsurface explorations. However, these subsurface explorations are conducted entirely by personnel on the surface who operate equipment extending underground. Proper identification of strata in the hydraulic rotary method requires careful analysis because drilling mud is mixed with each sample. A drilling-time log can be prepared relatively simpler and inexpensive way. Nowadays geophysical well-logging techniques are being widely used in water wells. As logging techniques become more sophisticated, the data they produce become more complex. The interpretation of many logs is more of an art than a science; log responses are governed by numerous environmental factors, making quantitative analysis difficult. In general, best results are obtained with experience and with supplemental hydrogeologic information.

4.4.1 Well-Logging Techniques

Well logging is the process by which physical, chemical and structural properties of aquifer formation are measured by borehole logging devices that are lowered in a borehole. The important purposes of a well log are to (Misstear et al., 2006)

- Assist in quality control and supervision of the drilling process, and to ensure the specifications of the materials being used during drilling. Is the well vertical? Is it being drilled at the specified diameter? Is grouting being carried out to an approved standard?
- Identify where water strikes are made during drilling, and how the well's water level changes during drilling. These observations may determine where a well screen or casing length should be installed, where a pump should be installed, or what the pumping regime of the well should be.
- Make a first assessment of water quality during drilling. Strong discoloration, odor or taste might indicate intervals of a well that should be cased out so that water of inferior quality does not enter the well. The progressive increase in salinity of groundwater during drilling may be an indication that drilling should not progress any deeper.
- Assess the geological succession being penetrated by the well or borehole. Where does the aquifer commence? Where does it finish? Where are the main water bearing horizons or fracture zones?
- Help decide where samples of formation or water should be taken for more detailed analysis and quality controlling the collection of such samples.
- Characterize the aquifer horizons being penetrated. The degree of cementation of the aquifer may determine whether a well screen is necessary or not. The grain size and its distribution will determine the need for a gravel pack, and will control the design and sizing of a well screen. It may be that rapid confirmation of the aquifer grain size is required for a specially designed well screen to be produced and delivered to the well site in a timely manner for installation.
- Provide information to regional or national environmental, hydrometric, or geological authorities for creating a valuable database resource for hydrogeologists and planners.

The most commonly used well-logging techniques include driller's log, geophysical logging, radiation logging, caliper logging, CCTV logging, etc. Different well-logging techniques are described in the subsequent sections.

4.4.2 Driller's Log

The most common well log is the driller's description of the geologic character and thickness of each stratum, the depth at which character changed and the depth to water table. A driller usually produces two types of logs based on his observations on hydrogeology as drilling progresses: geologic logs and drilling time logs. The driller can relate the well's geology and groundwater potential by observing the following drilling process:

- The drilling penetration rate
- The drill action and
- The behavior of the drilling fluid.

Geologic Log

A *geologic log* is constructed from sampling and examination of well cuttings collected at frequent intervals during the drilling of a well or test hole. Drill cuttings are often a mixture of material from the bottom of the hole, drilling mud, and material from higher layers that were still in the hole or that caved in from the wall. This type of log is the most important one, as it furnishes a description of the geologic character and thickness of each stratum encountered as a function of depth, thereby enabling aquifers to be delineated. Figure 4.6 shows a geologic log. The utility of geologic log depends on the experience and competence of the driller. The preparation of a good geologic log can be difficult because well cuttings are small and mixed with mud and material from higher layers, and also most geologic logs are prepared by well drillers, who may be untrained or busy with other activities during drilling operations. But a geologic log prepared carefully and completely by an experienced driller consultation with a hydrogeologist present during drilling is of very high quality.

Drilling Time Log

A *drilling-time log* consists of an accurate record of the time, in minutes and seconds, required to drill each unit depth of the hole. The drilling penetration rate provides a simple indication of the well's geology. Because, the texture of a stratum being penetrated largely governs the drilling rate, a drilling-time log may be readily interpreted in terms of formation types and depths. The technique is most practical with hydraulic rotary drilling although it is applicable to other methods as well. In general, the harder the rock, the slower the penetration using rotary, percussion, or auger drilling. There are no absolute penetration rates for individual drilling techniques in particular rock types. The penetration rate is influenced by many factors such as the type of equipment, the well depth, the drill diameter, the bit type, the weight on the bit, and the skill of the driller. Nonetheless, the penetration time log relates the type of lithology as well as to its hardness and is very useful and invariably used well-logging technique.

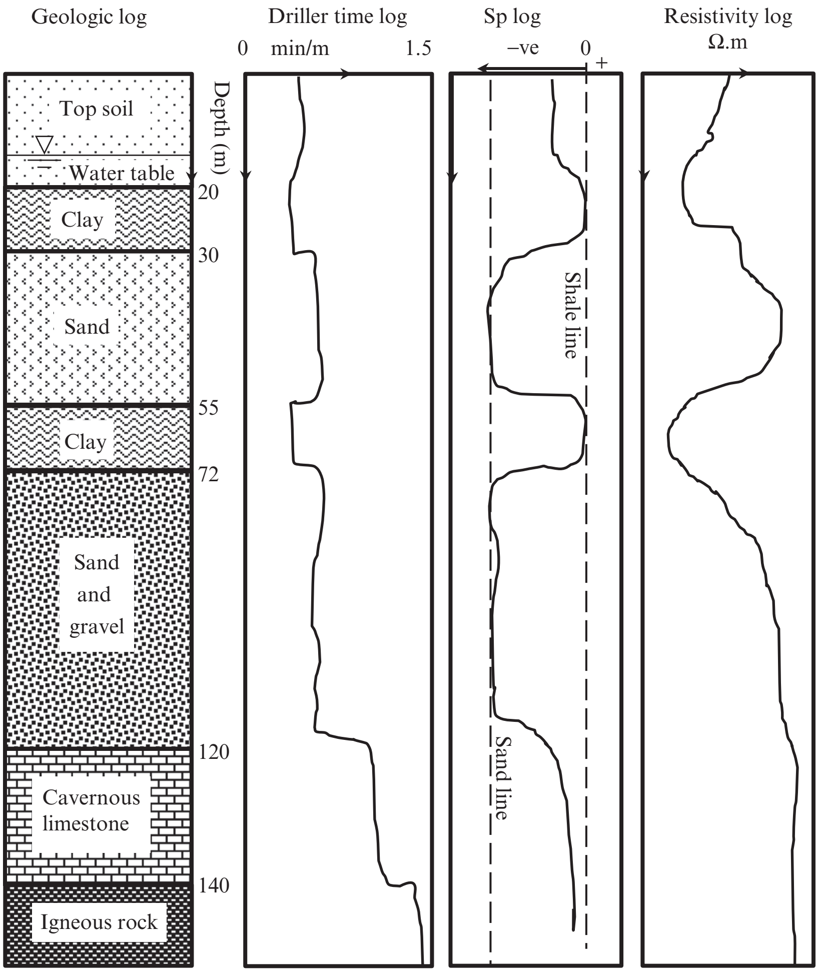

Figure 4.6 *Driller's log and resistivity logs (hypothetical)*

4.4.3 Sampling

The most precise and detailed information about subsurface materials is obtained from actual samples taken at the bottom of the bore hole at selected intervals during drilling. Formation samples are needed to establish the lithological succession at a site and to assess the hydrogeological characteristics of the aquifers. The establishment of a lithological section is a particularly important part of exploratory drilling, but it is also important in the construction of water wells and observation boreholes. The most common methods produce disturbed samples, which can be categorized as either bulk samples or representative samples. These are used to identify the formation and also the grain-size distribution in aquifer material. They are not suitable for measuring aquifer properties, and when samples are needed for laboratory tests of porosity and hydraulic conductivity, or even for better formation identification, then undisturbed samples must be obtained. Numerous techniques are available to obtain bore hole samples with minimum disturbances. Although it may be possible to obtain undisturbed samples from consolidated rock and gravel-free clays or fine sands, undisturbed samples of coarse sand and gravel are very difficult to obtain.

4.4.4 Geophysical Logging

Undisturbed sampling is an expensive procedure and will never be totally representative of in situ conditions. The best alternative way of measuring in situ conditions in an aquifer or well is to place the measuring instruments in the aquifer. *Geophysical logging* involves lowering sensing devices in a borehole and recording a physical parameter that may be interpreted in terms of formation characteristics; groundwater quantity, quality, and movement; or physical structure of the borehole. When it is performed by lowering a device in the bore hole, it is called downhole geophysical logging. Large quantity of data can be acquired by geophysical logging at relatively low cost. Geophysical logs furnish continuous records of subsurface conditions that can be correlated from one well to another. They serve as valuable supplements to geologic logs. Data from geophysical logs can be digitized, stored on magnetic tape, or transmitted by radio or telephone for interpretation. Graphic displays of log data permit rapid visual interpretations and comparisons in the field, hence decisions regarding completion and testing of wells can be made immediately. There are many reasons for carrying out geophysical logging (Misstear et al., 2006):

- To collect information on the well or borehole geology. If this is carried out in a mud-filled hole before installing casing and well-screen, it can be invaluable in assisting with screen design and placement.
- To determine physical properties (porosity, bulk density, formation resistivity, fluid resistivity) of aquifer units
- To identify inflow horizons and fractures, and to quantify water inflows
- To assess and check on the integrity and construction of completed or existing wells
- To assess the changes in the well's fluid properties with depth
- To determine geothermal gradient
- To correlate lithological and hydrogeological features between wells and boreholes
- To assist in diagnosing biofouling and other operational problems, thus aiding the maintenance of the well

Geophysical logging techniques provide information on physical properties of geologic formations, water quality, and well construction. The geophysical logging techniques were common in oil industry. These techniques are relatively expensive and hence are not routinely used for low-capacity wells. Most water wells are shallow, small-diameter holes for domestic water supply; logging costs would be relatively large and usually unnecessary. But for deeper and more expensive wells, such as for municipal, irrigation, or injection purposes, logging can be economically justified in terms of improved well construction and performance. Another deterrent to geophysical logging is the lack of experience among drillers, engineers, and geologists in the interpretation of logs.

The order in which the geophysical logs will be run depends on whether the well is newly drilled and full of drilling mud, or completed and full of representative groundwater. In the former case, the main purpose of geophysical logging will be to locate aquifer and aquitard horizons, assess their properties, and confirm the final well design, including the screen setting depths. Formation logs will typically be run at this stage, namely electrical resistivity logs and radiation logs.

Electrical Resistivity Logs

Electrical resistivity logs are run in fluid-filled boreholes in existing, completed wells, filled with natural formation water, but their use is restricted to unlined portions of the well. These types of logs measure the electrical resistivity of the formations and are used to distinguish aquifer and aquitard horizons and to assess their properties. The standard electrical resistivity logs do not function in dry, cased, or screened sections; however, they identify the base of casing below water level. Electrical resistivity is affected by a number of factors including clay content, porosity, fluid column conductivity, and pore water fluid conductivity, all of which are of interest in assessing aquifer properties. If appropriate geometric factors are taken into consideration, these intrinsic properties can often be deduced from the apparent resistivity measurements generated by electrical logs. Often, in hydrogeological studies, electrical tools are simply used to distinguish high-resistivity formations from low-resistivity formations. In crystalline rock settings, low resistivity may indicate a porous, fractured, weathered zone, whereas high resistivity may indicate intact rock (Figure 4.6). Electrical resistivity logs are of several basic types, but all of them comprise an array of potential (voltage) and current electrodes. Most of the electrodes are downhole, but some configurations often include electrodes at the surface. Current is passed between two electrodes (AB), and potential (voltage) difference is measured between two electrodes (MN). An apparent resistivity (ρ_a) is then calculated; the apparent resistivity may be affected by the resistivity of the borehole fluid (the wider the well diameter, the greater the effect), the geometry of the well relative to the log, and any resistance associated with the electrode/soil interface at the surface. The main resistivity log types are (Misstear et al., 2006) as follows:

Single-point resistance log Here, resistance is measured between a single current/potential electrode on the log, and another current/potential electrode at the well top. The single-point resistance (SPR) log is difficult to use quantitatively, but it has very good vertical resolution in narrow boreholes. In wider wells, its utility is more limited.

Short normal log In short normal electrode configuration, the current passes between a current electrode A at the base of the log and a second electrode B, at the top of the log (or, sometimes, at the surface). Potential difference is measured between an electrode M on the log (at a distance of 406 mm above current electrode A) and a second potential electrode N at the surface or sometimes higher on the log (Figure 4.7). This tool has relatively shallow penetration of the formation, but relatively good depth resolution. It is best used in moderately narrow wells.

Long normal log In long normal electrode configuration, the AM electrode spacing is 1626 mm (Figure 4.7). This has good penetration (due to wide electrode spacing) but poor depth resolution. It performs well in wide-diameter wells.

Lateral log In lateral or guard or focused electrical resistivity two guard electrodes straddle the log's current electrode (Figure 4.7). Their electric field focuses the main electric field out into the formation in a narrow beam, thus achieving good penetration and good depth resolution.

Microlog Here, the electrode array is very closely spaced (only a few centimeters apart) and mounted on a pad that is pressed by means of a sprung arm against the borehole wall. This achieves very high vertical resolution. Penetration is, however, very shallow, and the log is affected by any filter cake on the borehole wall, or by the penetration of any drilling fluid (mud filtrate) into the formation.

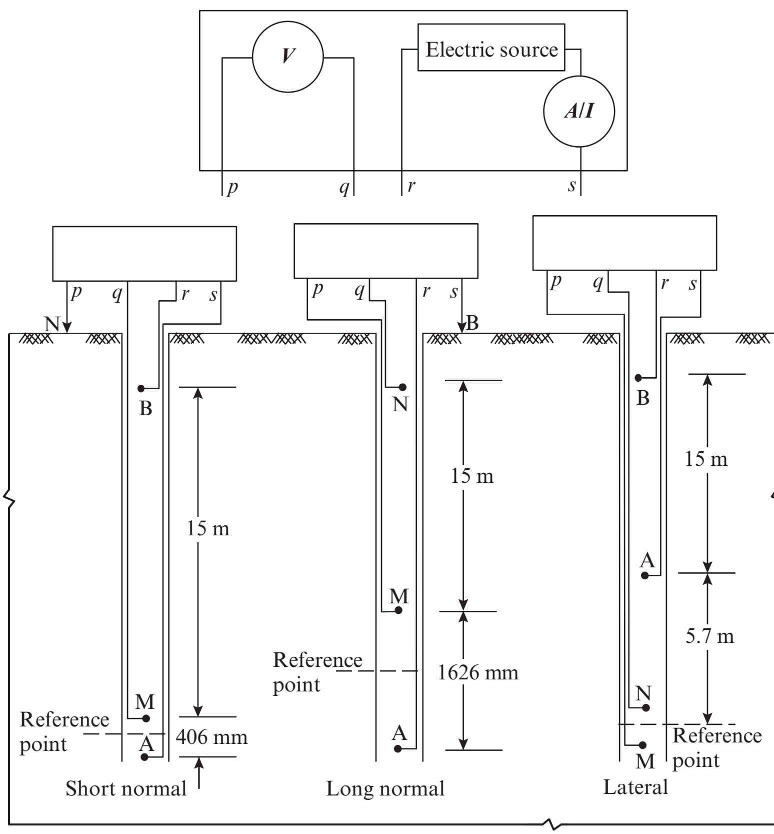

Figure 4.7 *Placing of electrodes in resistivity logging*

There are other electrical/magnetic logs that do not, strictly speaking, measure resistivity. The induction resistivity log, using induced electromagnetic fields, can be used in uncased dry sections and in plastic cased sections, whereas the casing collar locator is specifically designed for steel-cased wells.

Induction logs

These are essentially analogous to the application of electromagnetic induction in surface geophysics. The main advantage of this log is that it can be run in dry sections of a well or in sections lined by plastic casing.

Spontaneous/(self-potential) log

The spontaneous/self-potential (SP) log passively measures natural potential differences set up in the earth's stratigraphy at junctions, for example, between mudstone horizons and sandstone horizons. These can be very difficult to interpret unambiguously, especially in freshwater situations. The SP log is best run in mud-filled uncased holes, immediately following drilling. A log of the self- or spontaneous potential is obtained by recording the naturally occurring voltage difference between an electrode that is placed in the surface soil near the bore hole and another electrode that is lowered into the hole. Variations in the recorded voltage difference will occur as the hole electrode passes different formations. These variations are due to electrochemical effects between dissimilar layers, different streaming potentials, and other electrokinetic effects associated with movement of water through the various layers. The resulting recorder trace thus serves as a fairly accurate indicator of the depth of discontinuities and types of materials. In a formation, the clay or shale beds have approximately same potential, which is a vertical straight line in SP logs known as shale or clay line and treated as zero base line (Figure 4.6). Potential values range from zero to several hundred millivolts. By convention, potential logs are read in terms of positive and negative deflections from the baseline. The sign of the potential depends on the ratio of the salinity (or resistivity) of the drilling mud to the formation water. Extreme negative deflections joined by a straight vertical line parallel to shale line result to sand line (Figure 4.6). Potential logs indicate permeable zones but not in absolute terms; they can also aid in determining casing lengths and in estimating total dissolved solids in groundwater. The SP log is meaningless when no clay formations are encountered in the drilled depth. It is better to use SP log simultaneously with other logging results.

Casing-collar locator

A casing-collar locator (CCL) is a useful device for recording locations of casing collars, perforations, and screens. The CCL is a form of passive electromagnetic device. The instrument consists of a magnet wrapped with a coil of wire. Here, currents are induced in coils set within magnetic fields when the log passes any massive conducting object, such as the chunk of metal that is the collar or joint between strings of casing. The voltage fluctuations caused by changes in the mass of metal cutting the lines of flux from the magnet are recorded to form the log.

4.4.5 Radiation Logging

The nuclei of certain elements are unstable and tend to transform spontaneously, through various decay reactions, into nuclei of other elements, giving rise to isotopes. The process of decay of unstable isotopes to more stable elements is accompanied by emission of radiations consisting of alpha particles, beta particles, and gamma rays. Penetration ranges of alpha- and beta particles are few microns and millimeters, respectively, while gamma rays have penetration up to about a meter in solids. Because of their high penetrating power, gamma rays are used in radiation logging. *Radiation logging*, also known as *nuclear* or *radioactive logging*, involves the measurement of fundamental particles emitted from unstable radioactive isotopes. Different rocks contain characteristic amounts of radioactive minerals. Radiation logging can be (i) those that measure the difference in intensity of natural radioactivity and (ii) those that measure radiation reflected from or induced in the formation from an artificial source. Logs having application to groundwater are natural gamma, gamma–gamma, and neutron. The emissions can be detected by Geiger–Mueller counter, scintillation counter, ionization chamber, or neutron detector. Figure 4.8 shows a schematic arrangement of component parts of a radiation logging equipment. Radiation logs can be interpreted in terms of lithology, tops, and bottoms of beds and thickness, porosity, permeability, moisture content, and specific yield of formations. For interpretation in terms of lithology, a general idea of the geology of the area is required. An important advantage of these logs over most others is that they may be recorded in either cased or open holes that are filled with any fluid.

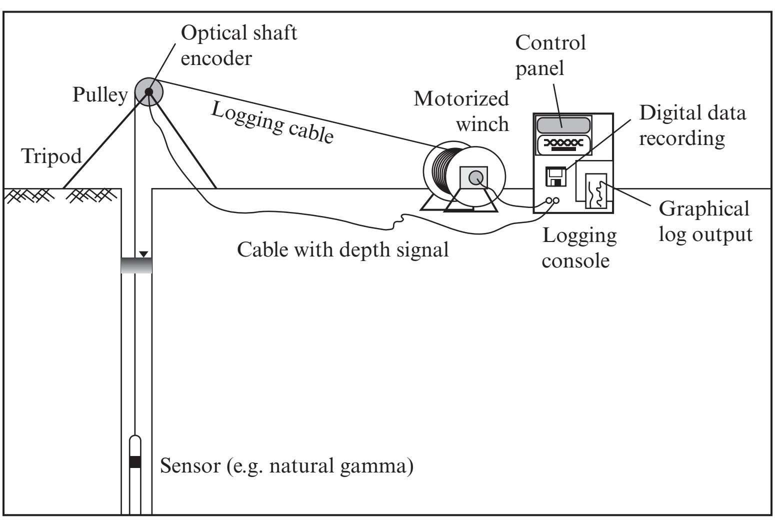

Figure 4.8 *Radiation logging equipment*

Natural Gamma Ray Logging

Because all rocks emit natural gamma radiation, a record of this constitutes a natural gamma log. The radiation originates from unstable isotopes of potassium, uranium, and thorium. Logs of the natural gamma ray emission of the various strata are obtained by lowering a gamma ray detector into the well and recording its output. Since gamma rays pass through metal, the technique can also be used in cased holes. The most important application to groundwater hydrology is the identification of lithology, particularly clayey or shale-bearing sediments that possess the highest gamma intensity. In general, clays and shales contain much more of the gamma-emitting elements than that of quartz sands and carbonate rocks (Figure 4.9). Thus, gamma rays can be used to distinguish between clay and nonclay materials, and hence to enhance the interpretation of electrical logs. Some drilling muds and mud additives contain radioactive elements, which can interfere with gamma logging. The gamma ray log should always be correlated with a driller's log and other logging results available.

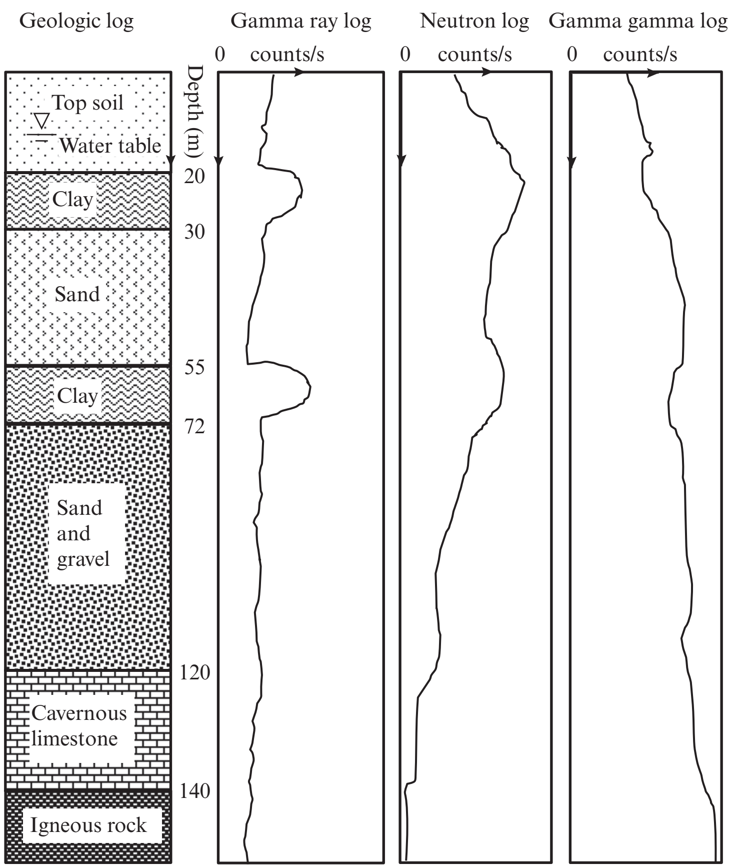

Figure 4.9 *Hypothetical radiation logs*

Neutron Logging

Neutron logs are obtained by lowering a single probe with a fast neutron source and detector into the bore hole and recording the intensity of the slow neutrons caused by backscatter and attenuation of the fast neutrons by hydrogen in the surrounding formation. The intensity of the slow neutrons, which is measured with a detector in the same probe, can then be related to the water content of the formation material around the probe. In formations, the hydrogen content is directly proportional to the interstitial water; therefore, neutron logs can measure moisture content above the water table and porosity below the water table. Neutrons have a relative mass of 1 and no electric charge; therefore, the loss of energy when passing through matter is by elastic collisions. Neutrons are slowed most effectively by collisions with hydrogen because the nucleus of a hydrogen atom has approximately the same mass as a neutron. Measured changes in water content may be helpful in locating water tables (Figure 4.9). By measuring moisture contents above and below the water table, the specific yield of unconfined aquifers can be determined. The lateral penetration of neutron logs is in the range 0.2–0.6 m. The method can be used on cased or uncased holes. Neutron log results are influenced by hole size; therefore, in large unease holes, information on hole diameter is required for proper interpretation.

Gamma–Gamma Logging

Gamma–gamma logs are obtained by lowering a probe with a gamma radiation source into the bore hole and recording the intensity of the backscattered and attenuated gamma rays with a detector in the same probe. This intensity is related to the density of the surrounding material, therefore that bulk density and porosity of formation material around the probe can be estimated. In addition, within the same geologic formation it is possible to estimate specific yield from the difference in bulk density measured above and below a water table. Finally, gamma–gamma logs can assist in locating casing, collars, grout, and zones of hole enlargement.

Neutron and gamma–gamma logs may be used to evaluate the removal of drilling mud from the aquifer around the well, which is necessary during well development. Because most of the gamma rays detected originate within 15–30 cm of the borehole wall, logs run before and after well development can reveal zones where clay and fine-grained material were removed. Borehole dimensions and fluid, casing, and gravel pack all exert minor influences on gamma probe measurements.

4.4.6 Other Subsurface Logging Methods

Besides the array of logging techniques, other subsurface methods can yield important information about hydrogeologic conditions of the formation and health of the well itself. In an existing groundwater-filled well, geophysical logs will typically be run in the following order:

- CCTV log to ensure well is safe and unobstructed.
- Caliper logging to check well construction and diameter. This is run in an uphole direction to ensure constant tension in the cable and better depth control.

- Fluid logs (temperature, conductivity, acoustic, etc.) require an undisturbed column of water and thus are typically run in a downhole direction before any other log.
- Other logs, for example, a log may contain both natural gamma and caliper tools.

CCTV Log

A convenient tool with increasing use for well construction log is a television camera lowered in a well. Specially designed wide-angle cameras are equipped with lights and provide continuous visual inspection of a borehole; with videotape, a record of the interior can be preserved. The CCTV log is typically used to inspect the well construction as well as for locating changes in geologic strata, pinpointing large pore spaces, inspecting the condition of the well casing, filter and screen, checking for debris in wells, locating zones of sand entrance, and searching for lost drilling tools. Most modern CCTV units allow color inspection and use light-sensitive chips to return a digital image. This feature in the CCTV may allow the identification of biofouling of well screens, geological features, fractures, or fissure horizons in limestones or crystalline rocks and the presence of macrofauna, such as leeches and cave-dwelling shrimps in water wells. Some modern cameras have a single, remotely controlled, three-axis, omnidirectional lens. Older models may have a choice of two lenses: (i) forward view that provides a view down the axis of the well and (ii) side view that uses a rotatable mirror at 45° to give a view of the borehole wall. Photographs taken within a well at close intervals, termed a photolog can be used for the same purposes.

Caliper Logging

A caliper log is a well construction log that provides a record of the average diameter of a borehole. The caliper log typically has three sprung arms that push outward against the borehole wall and track its contours. The caliper log can be run in a wet or dry well, but it must be empty of pump, rising main, and any other downhole equipment. It allows the user to identify the length and diameter of the casing, which will typically appear as a straight line of fixed diameter, possibly with small blips representing casing joints or welds. Well screen may be distinguished from plain casing by small outward deviations at regular intervals representing slots. Open-hole sections will typically be represented by more irregular lines. Weaker horizons (e.g. shales) may be washed out during drilling and therefore be represented by zones of larger diameter. Fissures or fractures in limestones or crystalline rock may be visible as sharp outward deviations in the caliper trace. These logs aid in the identification of lithology and stratigraphic correlation, in the location of fractures and other rock openings and in correcting other logs for hole diameter effects (Figure 4.10). During well construction, caliper logs indicate the size of casing that can be fitted into the hole and enable the annular volume for gravel packing to be calculated. Other applications include measuring casing diameters in old wells and locating swelling and caving zones.

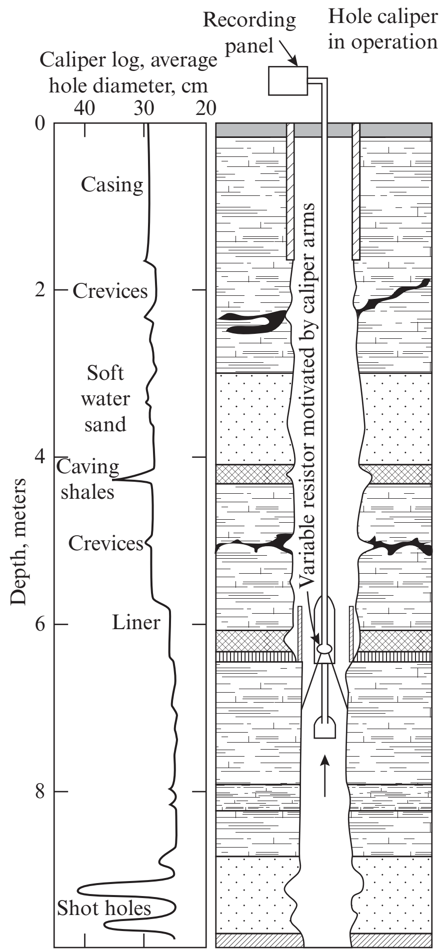

Figure 4.10 *Caliper logging (Todd and Mays, 2005)*

Temperature Logging

Normally, temperature increases with depth (at the rate roughly 3°C for each 100 m) in accordance with the geothermal gradient. Departures from this normal gradient may provide information on circulation or geologic conditions in the well. A recording resistance thermometer can be used to measure vertical traverse of groundwater temperature in a well. Abnormally cold temperatures may indicate the presence of gas or, in deep wells, may suggest recharge from ground surface. Likewise, abnormally warm water may occur from water of deep-seated origin. Temperatures may indicate waters from different aquifers intersected by a well. Temperature logs may detect the location of the new concrete plugging behind a casing, because the heat generated during setting produces a marked temperature increase of the water within the casing.

Fluid Conductivity Logging
A continuous record of the conductivity of fluid in a borehole is *a fluid conductivity log*. The probe measures the AC voltage drop across two closely spaced electrodes, which is governed by the resistivity of the fluid between the electrodes. The fluid conductivity log represents the resistivity of the fluid in a borehole while a resistivity log measures rock and fluid conditions outside a borehole. Temperature logs should be made in conjunction with fluid conductivity logs so that values can be corrected to a standard temperature. Fluid conductivity logs enable saline water zones to be located, furnish information on fluid flow within a well, and provide a means to extrapolate water sample data from a well.

Fluid Velocity Logging
Measurement of fluid movement within a borehole constitutes a *fluid velocity log*. Such data reveal strata contributing water to a well, flow from one stratum to another within a well, hydraulic differences between aquifers intersected by a well, and casing leaks. Several flowmeter designs have been developed for boreholes. The flowmeter should be compact and sensitive to small water movements and directions.

Acoustic Logging
Acoustic or *sonic logging* measures the velocity of sound through the rock surrounding an uncased, fluid-filled hole. Sound velocity in rock is governed by the velocity of the rock matrix and the fluid filling the pore space. The greater the porosity, the closer the measured sound velocity approaches that of the fluid. Main applications of the acoustic log include determining the depth and thickness of porous zones, estimating porosity, identifying fracture zones, and determining the bonding of cement between the casing and the formation.

Table 4.1 lists selected well-logging methods along with their applicability.

Table 4.1 *Well-Logging methods*

Type of log	*Specific well-logging device*	*Condition of bore hole under logging*	*Information obtained*
Nuclear log	Gamma ray Neutron–neutron	Open/cased holes with or without fluid	Rock lithology, porosity
Electromagnetic log (EM log)	Induction logging	Open and PVC-cased holes with or without fluid	Lithology and salinity of water
Electrical log	Self-potential/ resistivity	Open/screened hole with fluid	Lithology; location of screen
Acoustic amplitude (AA) log	Sonic log	Open holes with fluid	Lithology and porosity
Physical log	Caliper log	Open and cased holes with or without fluid	Diameter of borehole
Optical (television) logging	Bore hole TV Camera device	Open and cased hole with clear water	Caving, incrustation in pipes/screens, rock fractures

(*Continued*)

Table 4.1 (Continued)

Type of log	*Specific well-logging device*	*Condition of bore hole under logging*	*Information obtained*
Flow meter logging	Flow meter	Open and cased boreholes with fluid	Vertical flow in bore hole
Fluid logging	Water quality	Open and cased holes with fluid	EC, pH, Chloride, TDS, etc.

Tracer Techniques

The technique involves the introduction of a tracer to monitor the movement of water in the subsurface (direction and velocity). A tracer should be selected considering its behavior in the system to which it is to be introduced and its detection. A good tracer (Karanth, 1987):

- Should not be present in large concentration in the formation and water.
- Should be easily detectable.
- Should not be adsorbed by the media or react with water.
- Should not change the hydraulic characteristics of the aquifer.
- Should have low toxicity and be harmless.
- Should have a useful life long enough for the duration of observations otherwise minimum.

Dyes can be detected in extremely low concentration, but they are subject to considerable adsorption. Common salts are readily available and excellent tracers but high dosages are required. Radioisotope tracers have the advantage of being detectable in extremely low concentration, but their use requires safety regulations.

One or more boreholes may be used to determine the direction and velocity of groundwater flow in aquifers. In point dilution method, a tracer is injected in an isolated screened section of a well and its dissipation is observed to find the direction and velocity of groundwater movement. In two-well pulse technique, a tracer is injected into a nonpumping well, and it is monitored for arrival time in a pumping well to estimate porosity.

Water-Level Measurement

The determination of the depth to groundwater is one of the most common measurements in groundwater investigations in both existing and new wells. Groundwater-level data are needed to define groundwater flow directions, changes in water levels over time, and effects of pumping tests. Several techniques are available to measure water levels in pumping wells, observation wells, and piezometers. A simple, direct, and accurate method for obtaining water depth is lowering a steel tape into a well. For repeated measurements and for depths exceeding 50 m, an *electric water-level sounder* is preferred. A water-level sounder consists of a battery, a voltmeter, a calibrated two-wire cable on a reel, and an electrode. When the electrode contacts water, the circuit is completed and the voltmeter shows a deflection or light/buzzer turns on. The depth is read directly from graduations along the cable. See Figure 4.11. One disadvantage of this technique is the time required to lower the tape and to make an actual measurement. During the initial stages of an aquifer testing with several wells, it may be difficult for a single observer to measure all the wells frequently.

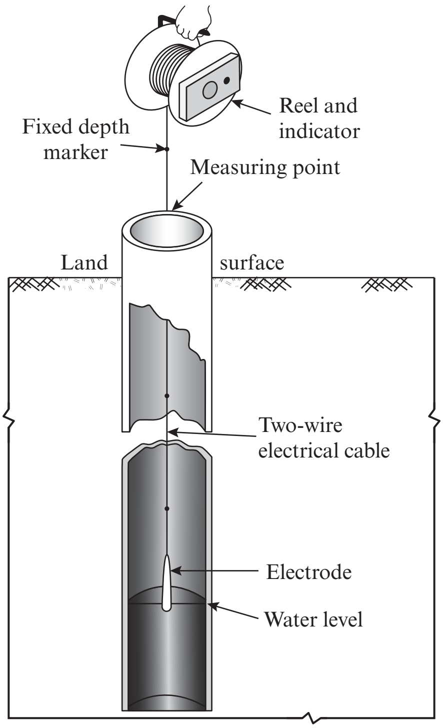

Figure 4.11 *Water-level recording*

Another convenient method for measuring water levels in deep wells is the *rock technique* based on time required for a ball to fall to the water surface plus the time for the sound of the splash to return to ground surface. *Automatic water-level recorders* or *pressure transducers* are other methods where short-term fluctuations in water levels are of interest, such as near intermittently operating wells or for pumping tests. Where multiple aquifers exist with differing water levels, individual observation wells screened in only one aquifer are often drilled.

4.5 Well Construction Techniques

Shallow wells, generally less than 15 m depth, are constructed by digging, boring, driving, or jetting. While some boreholes can be drilled by hand, using rotary, auger, or jetting techniques, manual methods are used mainly in the construction of open wells and shafts.

4.5.1 Manual Construction

Dug wells are the oldest way of water extraction dating back to early civilizations. Depths range up to 20 m or more, depending on the position of the water table, whereas diameters may range from 1 to 10 m. Dug wells should be extended a few meters below the water table. Dug wells can yield relatively large quantities of water from shallow sources and are most extensively used for individual water supplies in areas containing unconsolidated glacial and alluvial deposits. Their large diameters permit storage of considerable quantities of water if the wells extend some distance below the water table. In the past, all dug wells were excavated by hand, and even today the same method is widely used particularly in developing and underdeveloped countries. The major factors to be considered in hand-digging wells are methods to maximize the penetration rate and to minimize the danger to the excavators. The excavation in soft formations is usually by shovel, pick, and hoe. Loose material is hauled to the surface in a container by means of suitable pulleys and lines (bucket and hoist system). In hard rock, the rock has to be broken up before it can be extracted and this may require a chisel, jack-hammer, or even explosives. The diameter of the hole must be large enough for one, or possibly two, people to work down the hole (DTH), but it should be as small as possible to minimize the amount of debris to be excavated and corresponding volume of spoil to be removed. However, an open well of several meters in diameter may be drilled manually for increased yield and substantial water storage in the well. To complete the well below the water table, the excavation must be dewatered. This is normally achieved using a surface-mounted centrifugal pump or using pulley and bucket system through manual power or manual and animal power.

In unconsolidated sediments, for safety and to prevent caving, lining (or cribbing) of wood or sheet piling should be placed in the hole to brace the walls. A modem dug well is permanently lined to control sand entry and possible caving but with suitable openings for entry of water. Often, a casing string comprising reinforced concrete rings is used to support the well. Excavation takes place from underneath the lowermost ring (which may be equipped with a special shoe), such that the string of rings sinks as excavation progresses and new rings (or masonry layers) are added at the surface. Sometimes, a masonry lining is adopted wherein the lining is added in parts at the bottom as excavation progresses.

Large dug wells can be constructed rapidly with portable excavating equipment such as clamshell and orange-peel buckets. A properly constructed dug well can yield 2,500–7,500 m^3/d, although most domestic dug wells yield less than 500 m^3/d. A major limitation of large, open dug wells involves the ease of their pollution by surface water, airborne material, and objects falling or finding entrance into the wells. Accident may happen if the safety aspects of well digging are overlooked.

In the developing countries, where access for motorized drilling rigs is poor or where drilling is expensive, manual drilling is adopted. It is essentially a hand-powered auger and is best suited to relatively cohesive but unconsolidated sedimentary rocks, or to weathered crystalline rocks where large unweathered rock fragments are absent. Below the water table, if the sediment starts running into the base of the borehole, progress can be very slow. The method sounds crude; but under the right ground conditions, it can be surprisingly effective. Another method of manual drilling, much used in unconsolidated silty and sandy waterlogged sediments is sludging that involves sinking a simple string of narrow diameter galvanized steel or bamboo pipe by repeatedly jerking it up and down into the sediment.

4.5.2 Auger Drilling

Bored wells are constructed with hand-operated or power-driven earth augers where a groundwater exists at a shallow depth in an unconsolidated aquifer. Augers vary from small-diameter manual augers for soil sampling to large truck or crane-mounted augers used for drilling shafts for piles or piers that are more than a meter in diameter. Hand augers are available in several shapes and sizes, all operating with cutting blades at the bottom that bore into the ground with a rotary motion. The commonest auger design is the screw auger, with a blade welded in a spiral to a central solid drill stem. In small soil augers, the spiral may extend for the first few centimeters of the tip; but with continuous flight augers, the auger is supplied in sections, usually 1 m long, with the spiral blade extending the full length of each section. An alternative design of auger is the bucket auger, which cuts the soil with two blades on the base and then passes the soil up into the bucket. When the bucket is full, it has to be withdrawn for emptying and, as drilling proceeds, sections have to be added to the auger stem. Reamers can be attached to enlarge holes to diameters exceeding the auger size. A continuous flight auger is a common auger method for drilling exploration boreholes. When the blades are full of loose earth, the auger is removed from the hole and emptied; the operation is repeated until the desired hole depth is reached. Hand-bored wells seldom exceed 20 cm in diameter and 15 m in depth. A continuous-flight power auger has a spiral extending from the bottom of the hole to the surface (Figure 4.12). Cuttings are carried to the surface as on a screw conveyor, whereas sections of the auger may be added as depth increases. Power-driven augers will bore holes up to 1 m in diameter and, under favorable conditions, to depths

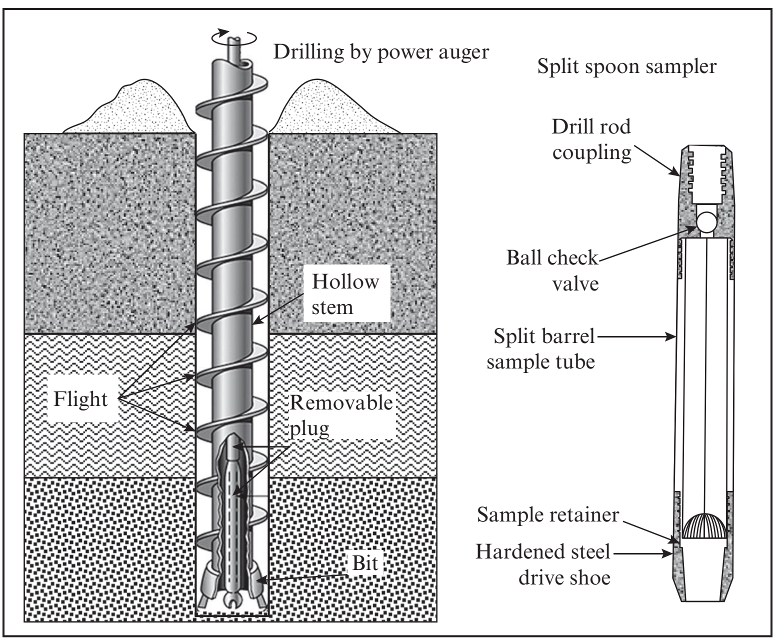

Figure 4.12 *Auger drilling and split sampler*

exceeding 30 m. The simple equipment, usually truck mounted, can be operated rapidly by one person and functions to depths exceeding 50 m in unconsolidated formations that do not contain large boulders.

In auger drilling, disturbed samples of the formation can be picked from the blades of the auger. Undisturbed core samples can be taken by hollow-stem augering. As augering progresses, a core of sediment is forced into the tube or hollow stem, to be recovered when the augers are withdrawn, or by wire-line if a wire-line core barrel is incorporated in the design. A split-spoon sampler can also be used. Thus, an auger drilling is a valuable method for rapid formation sampling at shallow depths.

Auger drilling is an inexpensive method for constructing small observation boreholes provided that the formation is soft and cohesive. Augers work best in formations that do not cave. Where loose sand and gravel are encountered in a large-diameter hole, or the boring reaches the water table, it may be necessary to lower a concrete or metal casing to the bottom of the hole and continue boring inside. After the desired depth is reached, the permanent well casing and screen are centered in the hole, the outer casing is removed, and the peripheral space is backfilled with gravel. Augers sometimes supplement other well-drilling methods where sticky clay formations are encountered; here augers are more effective than any other penetrating device. Augering is impractical in hard rocks, dry sand, coarse gravel, or in stiff boulder clay; below the water table, penetration can be difficult because of formation collapse.

4.5.3 Driven Wells

A *driven well* or *well-point* is a small diameter string of steel tubing driven by repeated impacts into the ground to below the water table. Diameters of driven wells are small, in the range of 3–10 cm. The depth of wellpoints is less than 15 m (sometimes more than 20 m). The bottom end is a pointed spike that can be driven into loose unconsolidated sediments. The lowermost section consists of slotted pipe (or screen) to allow the abstraction of water (Figure 4.13). Screens are available in a variety of opening sizes, the choice depending on the size of particles in the water-bearing stratum. To drive a well, the pipe casing and threads should be protected at the top with a drive cap. Driving can be done with a maul, sledge, drop hammer, or air hammer. Wellpoints can be readily installed by appropriately modified top hammer rigs if a pilot hole has been drilled by rotation jetting. Where the aquifer properties are suitable, well-points may also be installed permanently for groundwater abstraction. Yields from driven wells are small, with discharges of about 100–250 m^3/d. Driven wells are best suited for domestic supplies, for temporary water supplies, and for exploration and observation. Driven wells are limited to unconsolidated formations containing no large gravel or rocks that might damage the drive point.

Important advantages of driven wells are that they can be constructed in a short time, at minimum cost, and even by one person. Wellpoints can be very rapid means of exploring the hydraulic behavior of loose sedimentary (sand dunes or alluvial sands) aquifers with a shallow water table, as the wellpoints can be test pumped for short periods using surface-mounted suction pumps, and samples can be taken. Wellpoints may also be used as observation wells

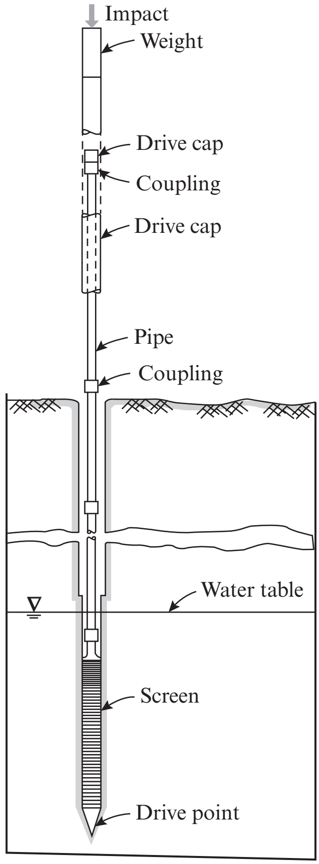

Figure 4.13 *Well driving (Todd and Mays, 2005)*

for monitoring of hydraulic responses during a large-scale pumping test. Once the testing, sampling, or period of observation is complete, the well point can be jacked out of the ground and reused elsewhere. Batteries of driven wells connected by a suction header to a single pump (known as *wellpoint systems*) are effective for localized lowering of the water table. Wellpoint systems are particularly advantageous for dewatering excavations for foundations and other subsurface construction operations.

4.5.4 Jetting

Jetted wells are constructed by the cutting action of a downward directed stream of water. The high-velocity stream washes the earth away, whereas the casing, which is lowered into the deepening hole, conducts the water and cuttings up and out of the well. Jetting is an effective means of constructing wells in shallow, unconsolidated aquifers. The method is rapid, can be carried out with relatively simple equipment, and is inexpensive. Well-jetting relies on a combination of percussion and fluid circulation. The drill pipe, which may be open ended or have a drill bit at its base, is driven into the shallow soil. Water is then pumped down the drill pipe, which fluidizes the unconsolidated formation, and helps the drill pipe to sink further. The water carries the cuttings up the annulus between the drill pipe and the borehole wall to a settlement pit on the surface, where the cuttings settle out and the water is recirculated through the pump. See Figure 4.14. Various types of jetting drill bits are used depending on the type of formation to be drilled. In penetrating clays and hardpans, the drill pipe is raised and lowered sharply, causing the bit to shatter the formation. During the jetting operation, the drill pipe is turned slowly to ensure a straight hole. If the formation being drilled is very unstable, temporary casing can be installed or some drilling mud can be added to the circulating water. To complete a shallow jetted well after the casing extends to below the water table, the well pipe with screen attached is lowered to the bottom of the hole inside the casing. The outer casing is then pulled, gravel is inserted in the outer space, and the well is ready for pumping. A simplification of the above procedure can be obtained by using a self-jetting well point. In jetted wells, the diameter ranges from 3 to 10 cm (sometimes up to 30 cm) and depth may be greater than 15 m. Jetted wells have only small yields and are best adapted to unconsolidated formations such as sand, clay, and silt. Because of the speed of jetting a well and the portability of the equipment, jetted wells are useful for exploratory test holes, observation wells, and well point systems. The method becomes impractical if large boulders are present, and it is not suitable for drilling in hard consolidated or crystalline aquifers. Jetting also does not allow collection of samples.

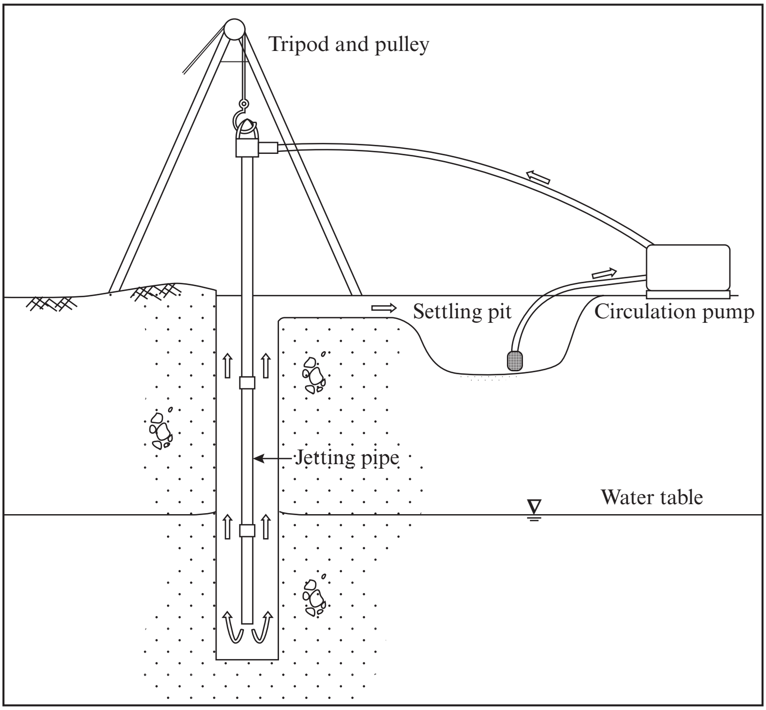

Figure 4.14 *Well construction by jetting (Misstear et al., 2006)*

Many top hammer or DTH rigs are able to operate without (or with minimal) hammer operation, and to sink boreholes in loose unconsolidated sediments by a combination of air or water jetting and a low rate of rotation. The use of eccentric bits allows for rapid construction of shallow wells in sandy or gravelly fluvial sediments.

4.5.5 Drilling

Most large, deep, high-capacity wells are constructed by drilling. There are many different drilling techniques, but most of them are classified as either percussion or rotary techniques depending on the predominant drill action. Each method has particular advantages. Jetting involves both a percussive and hydraulic drill action. The construction procedure of a successful well is dependent on local conditions encountered in drilling; hence, each well should be treated as an individual project. Construction methods differ from place to place and also from one driller to another. There are a number of considerations that influence the choice of drilling method, including (Misstear et al., 2006) the following:

- What is the purpose of the well, that is, for exploration, monitoring, or abstraction?
- In what kind of geology is it to be constructed, for example, unconsolidated, consolidated, or crystalline?
- What are the intended depth and diameter of the well?
- How should the well to be lined?
- What drilling equipment and expertise are available?
- What technique(s) have been successful in this area before?

For a drilling method to be suitable, it must be able to fulfil certain basic requirements for the given geological conditions, including the following:

- It must permit the efficient breaking up and removal of the soil or rock from the borehole.
- The hole must remain stable and vertical to the full depth.
- The drilling fluid should not cause excessive damage to the aquifer formation.
- The method should not have an adverse impact on groundwater quality (and special care needs to be taken when selecting a drilling method for constructing boreholes for investigating certain groundwater contaminants such as trace organics).
- The hole must be large enough to permit the installation of the casing and screen, including sufficient annular clearance for the grout seal and artificial gravel pack (if a pack is required).
- The method should allow the well to be completed in the required timeframe and at reasonable cost.

Types of Drilling

Each type may offer various methods of drilling and clearing borehole. The actual procedure or action, which breaks consolidated or unconsolidated materials, is called *hole-drilling method*. The procedure or action, which removes cuttings from the hole, is called *hole-clearing method*. The procedure or action, which keeps the hole open, preventing caving or collapse of the walls is known as *hole-stabilizing method*. Broadly, the types of drilling techniques are grouped into three categories as follows:

(1) Rotary drilling (rotary cutting action)
(2) Cable tool drilling (cable percussion action)
(3) DTH drilling (air percussion DTH hammer action)

Drilling can be classified according to

- the bore hole drilling action (whether the drilling action is a hammering or a rotatory)
- the bore hole clearing method (whether the hole is cleared by mechanical or fluid flushing methods)
- the bore hole stabilization method (whether it is stabilized using casing pipes, hydrostatic pressure of drilling fluid)

Percussion Drilling or Cable Tool Method

Percussion or cable tool drilling is a very old drilling method, having been used to construct wells in China as long ago as the first millennium BC. Wells drilled by the cable tool method are constructed with a standard well drilling rig, percussion tools, and a bailer. Drilling rig consists of a string of heavy cutting tools (a *swivel socket, a set of jars, a drill stem*, and *a drilling bit* as shown in Figure 4.15),

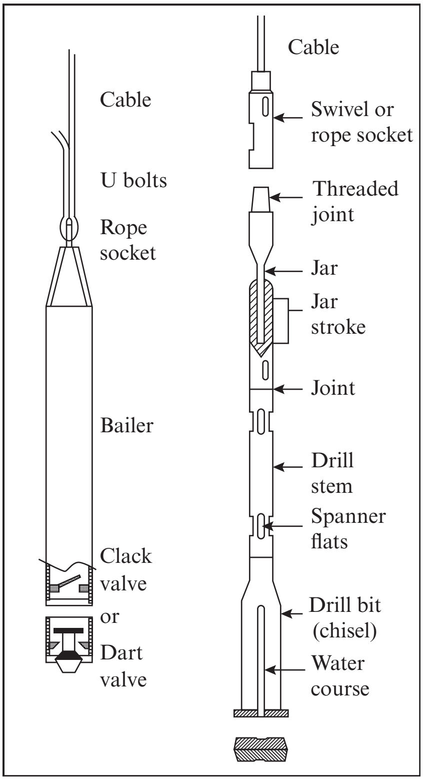

Figure 4.15 *Tool string for percussion drilling in hard rock (Misstear et al., 2006)*

which is suspended on a cable that passes over a pulley mounted on a mast. Tools are made of steel and are joined with tapered box-and-pin screw joints, and the total weight may be several thousand kilograms. The most important part of the string of tools is the bit, which does the actual drilling. Bits are manufactured in lengths of 1–3 m and weigh up to 1,500 kg. Variously shaped bits are made for drilling in different rock formations. The drill stem is a long steel bar that adds weight and length to the drill so that it will cut rapidly and vertically. A set of jars consists of a pair of narrow connecting links to assist in loosening the tools if they stick in the hole. The swivel socket attaches the drilling cable to the string of tools. Drill cuttings are removed from the well by a *bailer* or *sand bucket*. Although several models are manufactured, a bailer consists essentially of a section of pipe with a valve at the bottom and a ring at the top for attachment to the bailer line. When lowered into the well, the valve permits cuttings to enter the bailer but prevents them from escaping. After filling, the bailer is hoisted to the surface and emptied. Bailers are available in a range of diameters, lengths of 3–8 m, and capacities up to 0.25 m^3.

The drilling of a borehole is started by installing a short, large diameter conductor or starter pipe into the ground, either by drilling or by digging a pit 1–2 m deep. The function of the conductor pipe is to prevent the surface material beneath the rig from collapsing into the hole and to guide the tool in the initial drilling. The tool string is assembled and lowered into the conductor pipe, and then drilling begins. Drilling is accomplished by regular lifting and dropping of a string of tools. Power is normally supplied by a diesel engine. On the lower end, a bit with a relatively sharp chisel edge breaks the rock by impact. The driller can vary the number of strokes (20–40 strokes) per minute and the length of each stroke (40–100 cm) by adjusting the engine speed and the crank connection on the spudding arm. The tool string is held in such a position that the drill bit will strike the bottom of the hole sharply, and the cable is fed out at such a rate that this position is maintained. The drilling line is rotated so that the bit forms a round hole. Water should be added to the hole if none is encountered to form a paste with the cuttings, thereby reducing friction on the falling bit. After the bit has cut 1 or 2 m through a formation, the string of tools is lifted to the surface, and the hole is bailed. The actual procedure of drilling depends on the formation to be drilled. In unconsolidated formations, casing should be maintained to near the bottom of the hole to avoid caving. In drilling any deep well, it is important that proper alignment be maintained so as not to interfere with pump installation and operation. The greatest problem occurs in drilling through rock formations. The method is capable of drilling holes of 8–60 cm in diameter through consolidated rock materials to depths of 600 m.

The whole rig can be mounted on the back of a truck or trailer, and is quite mobile as shown in Figure 4.16. The simplicity of design, ruggedness, and ease of maintenance and repair of the rigs and tools are important advantages in isolated areas. In addition, less water is required for drilling than with other methods, a matter of concern in arid and semiarid regions. Furthermore, sampling and formation logging are simpler and more accurate with a cable tool rig. The cable tool rig is highly versatile in its ability to drill satisfactorily over a wide range of geologic conditions. In particular, cable tool rigs can drill through boulders and fractured, fissured, broken, or cavernous rocks, which often are beyond the capabilities of other types of equipment. However, in unconsolidated sand and gravel, especially quicksand, it is least effective because the loose material slumps and caves around the bit. Its major drawbacks are its slower drilling rate, its depth limitation, the necessity of driving casing coincidentally with drilling in unconsolidated materials, and the difficulty of pulling casing from deep holes.

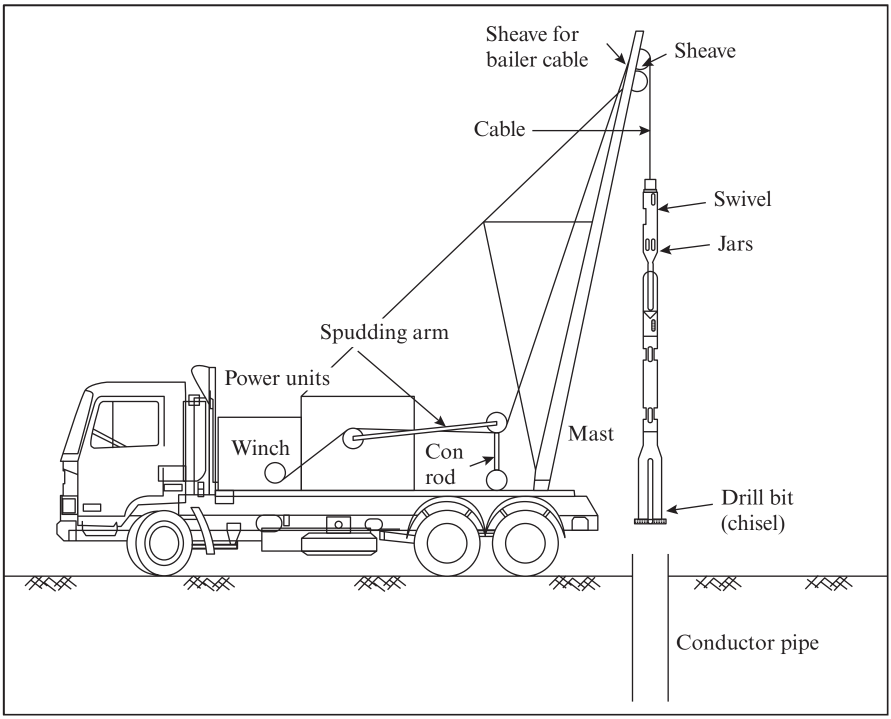

Figure 4.16 *Truck-mounted percussion drilling rig (Misstear et al., 2006)*

Rotary Drilling Method

Rotary drilling techniques were developed in the nineteenth and early twentieth centuries, partly to overcome the problem with percussion drilling of having to employ temporary casing in unstable formations. Instead, rotary methods use the hydrostatic pressure of circulating drilling fluids to support the borehole walls. This use of drilling fluids enables the boreholes to be drilled to much greater depths than can be achieved by percussion rigs. The drilling fluid may be a bentonite mud, clean water, air, a foam-based fluid, or a synthetic polymer (or some combination of these), depending on the properties required to stabilize the hole and bring the cuttings to the surface. Circulation of drilling fluid is occasionally lost when it goes into a permeable zone rather than back up the hole. It is necessary to plug off this permeable zone using drilling fluid thickened by additives. The plugged zone must be restored if it is subsequently tapped for groundwater. A rotary drilling technique can be direct circulation type or reverse circulation type. In direct circulation, the drilling fluid is pumped down the drill pipe and up through the annulus around the drill string to the surface; whereas in reverse circulation, the circulation medium flows DTH between the wall of the hole and the drill rods through the bit and up the inside of the drill rods.

Direct Circulation Rotary Drilling

Normal or *direct circulation* rotary is used when the circulation medium (air, water or drilling mud) is pumped under pressure down the drill rods, through drilling bit and carries drill cuttings to the surface between the wall of the hole and the drill rods. The drilling rig for a rotary outfit consists of a derrick, or mast from which the drill string is suspended, a rotating table, a pump for the drilling mud, a hoist, and a winch for raising or lowering the drill string. All these are mounted on a diesel-engined power unit (some smaller rigs have a power transfer from the vehicle engine). The drilling mud leaves the drill pipe through the bit, where it cools and lubricates the cutting surface, entrains drill cuttings, and carries the drill cuttings upward within the annular space between drill pipe and hole wall as the fluid returns to ground surface. The drilling mud then overflows into a ditch and passes into a settling pit. Here, the cuttings settle out; thereafter, the mud is picked up by the pump for recirculation in the hole.

The drilling mud is mixed in a mud pit or mud tank and is pumped by the mud pump through the Kelly hose to a water swivel at the top of the kelly. This swivel is the unit from which the entire drill string is suspended, and allows the mud to pass while the drill string rotates. The mud passes down the drill string to the bit which it leaves by ports in the bit faces, and then returns up the annulus between the borehole wall and drill pipe to the mud pits. A mud pit often has at least two chambers, the first and largest allows cuttings to settle from the mud, before it passes to a second chamber that acts as a sump for the mud pump. The mud pit should normally have a volume of about three times the volume of the hole to be drilled.

The drill bit assembly commonly consists of a bit, a drill collar (a length of large-diameter very heavy drill pipe), and a drill pipe that extends to the ground surface. The upper end of the drill pipe is attached to the kelly (a square section of drill rod). The drill is turned by a rotating table that fits closely around the kelly and allows the drill rod to slide downward as the hole deepens. Figure 4.17 shows the arrangement of parts of a direct circulation rotary drilling. The collar is designed to give weight to the drill string, improve its stability, and hence the hole verticality, as well as decreasing the annulus around the drill string, and so increasing the velocity of mud flow away from the bit. Drill bits are available in various forms. The commonest rotary bit is the tricone or rock-roller bit, which has three conical cutters which rotate on bearings. It is a group of conical roller gears with teeth that scrape, grind, and fracture the rock. The choice of drill bit depends on the formation to be drilled. In soft formations, a simple drag bit equipped with hardened blades can be used. The drilling fluid passes through ports that are placed to clean and cool the teeth as well as carry away the cuttings. The teeth on the cutters vary in size, shape, and number to suit the formation being drilled—small, numerous teeth for hard formations and larger teeth for soft formations. The bit operates by crushing the rock: by

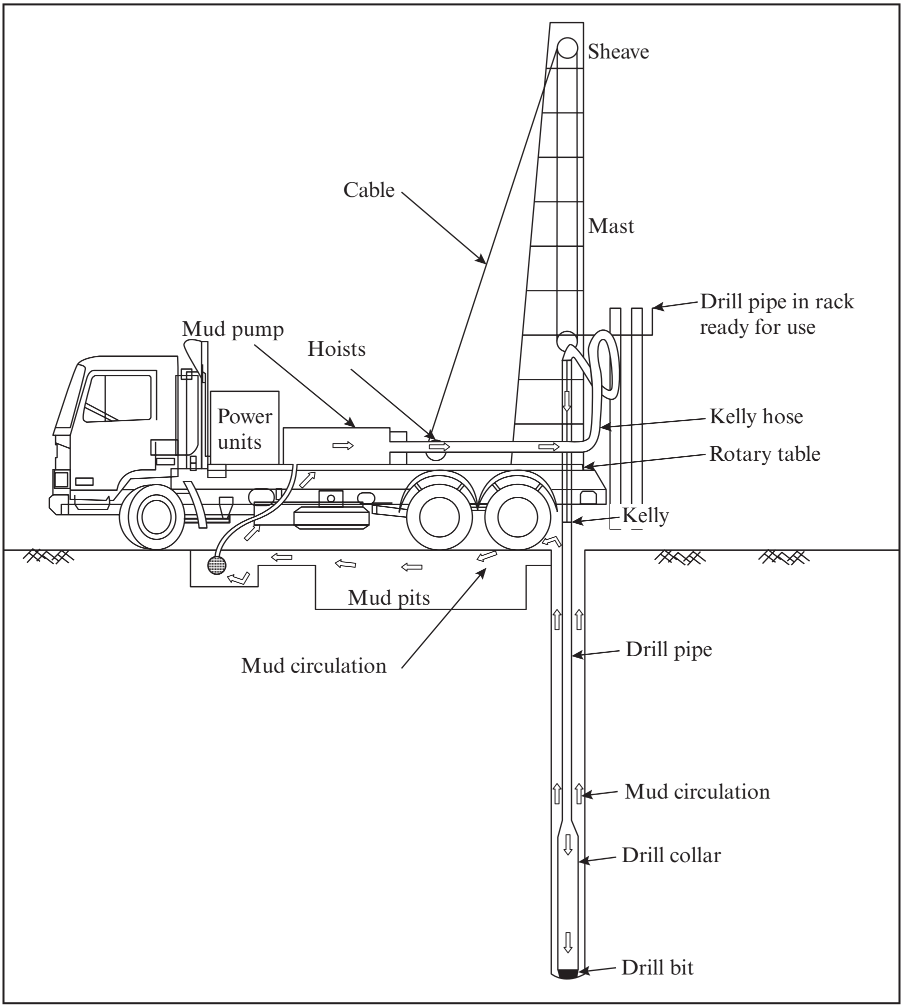

Figure 4.17 *Rotary (direct circulation) drilling rig (Misstear et al., 2006)*

overloading it at the points of the teeth and by tearing or gouging as the cones rotate. Sometimes, a pilot hole is drilled with a small-diameter bit, and then if water is successfully encountered, the hole is enlarged using a larger diameter reaming bit. Drag and tricone bits break the rock into fragments or cuttings, which are returned to the surface as "disturbed formation samples." Samples of undisturbed are not possible.

An important factor in direct circulation drilling is the choice of drilling fluid. The fluid can be air or clean water if the formations are hard and stable (crystalline and consolidated aquifers), or a mud or foam-based fluid where the borehole wall needs to be supported. Drilling fluid should not introduce pollutants into the aquifer and damage the aquifer formation. For instance, water used for mixing fluids should not contain harmful bacteria, and therefore untreated surface water is not suitable. The most common general-purpose drilling fluid for unconsolidated aquifers has traditionally been a mud based on natural bentonite clay. The mud fulfills several purposes such as the following:

- It keeps the hole clean by removing cuttings from the bit, carries them to the surface, and allows them to settle out in mud pits.
- It cleans, cools, and lubricates the drill bit and drill string.
- It forms a supportive mud cake (filter cake) on the borehole wall.
- It exerts a hydrostatic pressure through the filter cake to prevent caving of the formation.
- It retains cuttings in suspension while the drilling stops to add extra lengths of drill pipe.
- It supports the weight of the casing string in deep boreholes.

The properties of the mud which allow it to fulfill these functions are its velocity, viscosity, density, and gel strength (thixotropy). The mud is a suspension of clay in water. Under the hydrostatic pressure of the mud in the borehole, water is forced from the suspension into the adjacent formations. The water leaves the clay behind as a layer or cake of clay platelets attached to the borehole wall known as a *filter cake* or *mud cake*. No casing is ordinarily required during drilling because the mud cake forms a clay lining on the wall of the well. This seals the walls, thereby preventing caving, entry of groundwater, and loss of drilling mud. The hydraulic pressure exerted by the mud column depends on the mud density; and in severely caving formations, the mud density can be increased by the addition of heavy minerals such as barytes ($BaSO_4$). A heavy drilling mud may be used to counteract strong pore pressures in artesian aquifers. Great care must be taken, however, to avoid excessive filter cake build-up, because if it becomes too thick it can reduce the diameter of the borehole sufficiently to prevent withdrawal of the drill string. Organic additives that degrade with time and thereby cause the mud cake to break down within a few days may be advantageous.

Rotary drilling is invariably used for oil wells and its application to water-well drilling is steadily increasing. It is a rapid method for drilling in unconsolidated strata. Deep wells up to 45 cm in diameter, and even larger with a reamer, can be constructed. Advantages are the rapid drilling rate, the avoidance of placement of a casing during drilling, and the convenience for electric logging. Disadvantages include high equipment cost, more complex operation, the need to remove the mud cake during well development, and the problem of lost circulation in highly permeable or cavernous geologic formations.

Air Rotary Method

Drilling mud is replaced by compressed air in air rotary drilling method. The technique is rapid and convenient for small diameter holes in consolidated formations where a clay lining is unnecessary to support the walls against caving. Larger diameter holes can be drilled by employing foams and other air additives. Drilling depths can exceed 150 m under favorable circumstances. An important advantage of the air rotary method is its ability to drill through fissured rock formations with little or no water required.

Rotary-Percussion Method

A rotary-percussion procedure using air as the drilling fluid provides the fastest method for drilling in hard-rock formations. A rotating bit, with the action of a pneumatic hammer, delivers 10–15 impacts per second to the bottom of the hole. Penetration rates of as much as 0.3 m/min have been achieved.

Reverse-Circulation Rotary Method

Reverse circulation has the circulation medium flow DTH between the wall of the hole and the drill rods through the bit and up the inside of the drill rods as shown in Figure 4.18. The reverse circulation technique utilizes the hydrostatic pressure of the column of fluid in the hole or an outer tube to stabilize the wall primarily, although drilling mud may be introduced to provide wall-building characteristics. Of particular benefit are the low fluid velocities against the

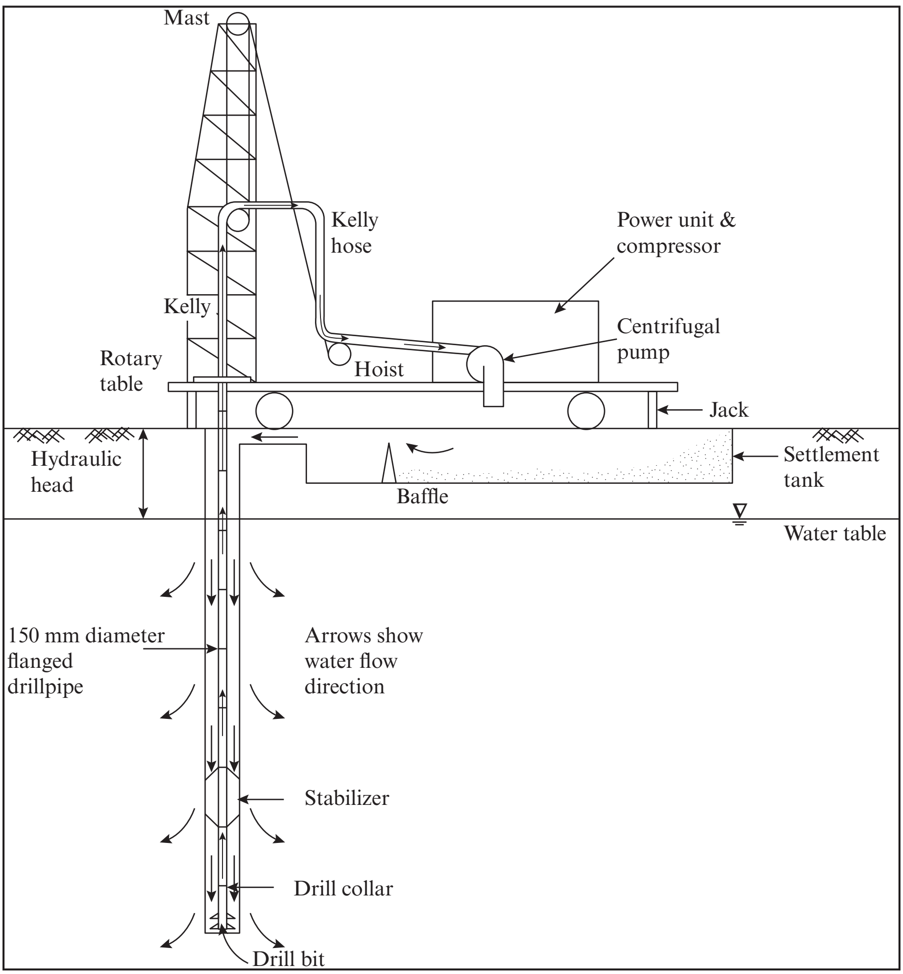

Figure 4.18 *Reverse circulation rotary drilling (Misstear et al., 2006)*

wall of the hole with high velocities carrying the cuttings inside the drill rods. Large-diameter boreholes can be drilled quickly with conventional reverse circulation for water supply or dewatering wells, requiring minimal development. Dual-tube reverse circulation in its numerous forms has many sampling and exploration uses.

The reverse-circulation rotary method is suitable for drilling large-diameter holes in unconsolidated formations. Water is pumped up through the drill pipe using a large-capacity centrifugal or jet pump. Discharge from the hole flows into a large pit where cuttings settle out. Thereafter, the water runs through a ditch and back into the hole so that the water level in the hole is maintained at ground surface. To avoid erosion of the sides of the hole, downward velocities must be restricted; therefore, the minimum hole diameter is about 40 cm. The velocity of water up the drill pipe usually exceeds 2 m/s. It requires a large volume of readily available water. Such rigs can drill to depths of 125 m or more. Rapid drilling rates are possible with diameters up to 40 cm and depths to 400 m. Because reverse-circulation holes have large diameters, completed wells are usually gravel packed. A particular advantage of the method is that continuous and accurate geologic and groundwater quality samples can be obtained as a function of depth.

Top-hole and DTH hammer drilling are essentially a combination of direct circulation rotary drilling and percussion, whereas auger drilling is a rotary method that does not use a circulating fluid. A particular drilling rig machine often permits the use of several types of drilling. A multipurpose rotary machine for example may be used for rotary air or mud, DTH hammer, diamond, or auger drilling. Percussion drilling is used most often at shallow depths and in unconsolidated sediments, or relatively soft rocks, whereas rotary methods (especially direct circulation rotary) predominate in the construction of deep boreholes or wells, and top-hole or DTH hammer drilling is the method of choice in hard crystalline rocks. Table 4.2 summarizes the advantages and disadvantages of various well construction methods.

Table 4.2 *Comparison of well construction methods*

Construction method	*Diameter and depth ranges and material best suited*	*Advantages*	*Disadvantages*
Manual	Diameter >1,000 mm Depth < 30 m Alluvium, clay, silt, sand and small gravel	• Uses low technology, and therefore is cheap where labor is cheap	• Hand-digging wells are slow. • It is restricted to shallow depths.
Augering	Diameter < 50–900 mm Depth < 10–50 m	• Inexpensive method for drilling exploration boreholes in unconsolidated aquifers	• Not suitable for very coarse formations or hard rock

(*Continued*)

Table 4.2 (Continued)

Construction method	*Diameter and depth ranges and material best suited*	*Advantages*	*Disadvantages*
	Alluvium, clay, silt, sand and small gravel.	• Good samples using a hollow-stem auger and core barrel	• Drilling difficult below the water table
Driving of wellpoints	Diameter 50–100 mm Depth < 15 m Alluvium, silt, sand and small gravel	• Rapid method of installing shallow wells in unconsolidated aquifers	• Not suitable for hard-rock formations • Limited to shallow water table
Jetting	Diameter 50–100 mm but can be up to 200 mm Depth < 30 m Alluvium, silt, sand, and small gravel	• Rapid, inexpensive method for constructing small-diameter wells in shallow unconsolidated aquifers	• May use large volumes of water in permeable formations • Poor samples
Percussion drilling or cable tool method	Diameter 100–600 mm Depth > 1,000 m (consolidated formations) but mostly < 100 m Alluvium and sedimentary rock (sandstone, shale quartzite, limestone, etc.)	• Low-technology rigs, and therefore relatively cheap mobilization, operation and maintenance • Suitable for a wide variety of lithologies • Needs small work area • Uses little water • Good samples • Water strikes easy to identify	• Drilling depth is limited in unconsolidated formations because of need for temporary casing • Slow method, especially in hard formations • Slow in alluvium and sandstone, fast in limestone
Rotary drilling	Diameter 100–750 mm Depth > 1,000 m possible Alluvium, silt, sand and small gravel, sedimentary rocks, soft to hard consolidated rock	• Very great drilling depths are possible • Suitable for a wide variety of lithologies • Fast drilling • Does not need temporary casing	• High-technology rig, so relatively expensive to mobilize and operate • May need a large working area for rig and mud pits • Can use a lot of water • Filter-cake build-up can make development difficult • Samples from conventional DC rotary can be poor (but good samples from coring)

(*Continued*)

Table 4.2 (Continued)

Construction method	*Diameter and depth ranges and material best suited*	*Advantages*	*Disadvantages*
			• Loss of circulation of drilling fluid in fissures • Sometimes difficult to identify aquifer
Reverse rotary	Diameter 400–1, 200 mm Depth up to 300 m Alluvium, silt, sand, gravel, and cobble	• Rapid drilling in coarse unconsolidated aquifers at large diameters • Leaves no filter cake • Quite good samples, especially with dual-tube reverse rotary	• Fast in alluvial sediments • May use great volumes of water • Not suitable for hard formations (unless used with a dual tube system and DTH hammer) • Large boulders can be problem
Rotary cum percussion	Diameter 300–500 mm Depth up to 600 m Alluvium, silt, sand, small size gravel, and soft to hard consolidated rock	• Very fast drilling • Fast in bouldary formations	
DTH	Diameter 100–450 mm Depth > 500 m possible in dry formations	• Crystalline hard rocks and carbonate rocks (granite, basalt, limestone, dolomite, gneiss, schist) • Hammer methods are very fast in hard formations • They do not need water • There is no invasion of aquifer by drilling mud • Water strikes easy to identify	• Hammer methods are not normally suitable for soft, clayey formations • Drilling depth below the water table is limited by hydraulic pressure • The use of lubricating oil for the DTH hammer could be a problem in a contamination investigation • Samples can be poor from standard hammer methods (but better samples can be obtained from reverse circulation, dual-tube, DTH hammer)

4.6 Well Completion

After a well has been drilled, it must be completed. This can involve placement of casing, cementing of casing, placement of well screens, and gravel packing; however, wells in hardrock formations can be left as open holes so that these components may not be required. Once the casing is installed, the well should be checked for its verticality and alignment, as these factors can have a significant influence on the successful operation of the well, especially for a deep well to be equipped with a line shaft turbine pump. Verticality and straightness are also important for submersible pumps: the pump should be located centrally in the well to maintain a cooling flow of water around the motor. Verticality can be measured with a plumb-bob. The methods of casing and screen installation in rotary drilled boreholes vary with the depth of the borehole and the ability to install the casing and screen in one operation. A borehole to be completed with a single string of casing and screen is drilled to the design depth and then is geophysically logged. The aquifer boundaries, upper and lower, are identified and the casing and screen string is assembled on the surface into lengths suitable for handling by the available rig. As the string is lowered DTH, each length is joined to the top of the previous one. The casing and screen string is lowered until the screen is opposite the target aquifer. The annulus is then filled either with an artificial gravel pack or formation stabilizer, or the formation is allowed to collapse against the screen during development. This method of installation can be used for single or multiple aquifers; in both cases, close control of the depth of the screen must be kept to avoid misplacing them. Wells are cemented by grouting in the annular space surrounding the casing to prevent entrance of water of unsatisfactory quality, to protect the casing against exterior corrosion, and/or to stabilize caving rock formations. Details of well casing and screen and gravel packing are given below.

4.6.1 Well Casings

Well casing serves as a lining to maintain an open hole from ground surface to the aquifer. It seals out surface water and any undesirable groundwater and also provides structural support against caving materials outside the well. Materials commonly used for well casings are wrought iron, alloyed or unalloyed steel, and ingot iron. Joints normally consist of threaded couplings or are welded, the object being to secure water tightness. Polyvinyl chloride pipe may be employed as casing for shallow, small-diameter observation wells. In cable-tool drilling, the casing is driven into place; in rotary methods, the casing is smaller than the drilled hole and hence can be lowered into place. *Surface casing* is installed from ground surface through upper strata of unstable or fractured materials into a stable and, if possible, relatively impermeable material. Such surface casing serves several purposes, including (i) supporting unstable materials during drilling, (ii) reducing loss of drilling fluids, (iii) facilitating installation or removal of other casing, (iv) aiding in placing a sanitary seal, and (v) serving as a reservoir for a gravel pack. This casing may be temporary during drilling or it may be permanent.

Pump chamber casing comprises all casing above the screen in wells of uniform diameter. The pump chamber casing should have a nominal diameter at least 5 cm larger than the nominal diameter of the pump bowls. Nonmetallic pipes (e.g. concrete, asbestos-cement, plastic, and fiberglass-reinforced plastic pipe) are sometimes used where corrosion or incrustation is a problem.

4.6.2 Well Screens

A *well screen* serves as the intake section of a well that obtains water from an aquifer and sometimes is called as the business end of the well to emphasize its importance in the efficient performance of the well as a hydraulic structure. In consolidated formations, where the material surrounding the well is stable, groundwater can enter directly into an uncased well without need of a well screen. However, well screens are required in unconsolidated formations. The well screen stabilizes the sides of the hole, prevents sand movement into the well, and allows a maximum amount of water to enter the well with a minimum of hydraulic resistance. A well screen is adequate only when it is capable of letting sand-free water flow into the well in ample quantity and with minimum loss of head. The desirable features of a properly designed well screen are as follows (Johnson, 1975):

(i) Openings in the form of slots that are continuous and uninterrupted around the circumference of the screen
(ii) Close spacing of slot openings to provide maximum per cent of open area without compromising with strength
(iii) V-shape slot openings that widen inwardly
(iv) Single metal construction to avoid galvanic corrosion
(v) Adaptability to different conditions
(vi) Ample strength to resist the forces to which the screen may be subjected during and after installation
(vii) Ready availability of accessories and end fittings

In the past, well casings were often perforated in place by a special cutting knife, but this practice is now discontinued because of the large irregular openings created, the small percentage of open area obtained, and the difficulty of controlling entry of sand with water during pumping. More common is the use of preperforated casing, constructed by sawing, machining, or torch-cutting slots in the casing. Openings by sawing or machining can be properly sized, whereas torch-cut slots tend to be large, irregular, and conducive to sand entry. A major factor in controlling head loss through a perforated well section is the percentage of open area. For practical purposes, a minimum open area of 15 percent is desirable; this value is readily obtained with many commercial screens but not with preperforated casing. Manufactured screens are preferred to preperforated casing because of the ability to tailor opening sizes to aquifer conditions and because of larger percentages of open area that can be achieved. Several types of well screens are available; few of them are described in the following paragraphs.

Continuous Slot Wire Wound Screens

The continuous slot type of well screen is made by winding of round or specially shaped (triangular) wire spirally around a cage of vertical rods. See Figure 4.19. At each point where the wire crosses the rods, the two members are securely joined by welding or so. A change in the size of openings can be made at will during fabrication. A single section of well screen may be made with one, two, or more different sizes of slot opening, if geologic conditions require these variations. The use of triangular wire results into V-shaped slot openings with narrowest at the outer face and widen inwardly, which make them nonclogging. This is because the opening allows only two-point contact by any grain of sand so that single particles retained by the screen cannot close off the openings, and the area of openings goes on increasing inward so that any grain of sand entering through the outer surface easily pass through the remaining screen slot without wedging in the opening. Such nonclogging shape is highly desirable in well developing stage. The continuous slot well screen provides maximum percentage of open area, least clogging from sand grains and incrustation, and least head loss and consequently more useful life of well. Although such screens are more expensive, they may prove to be more economical, especially for thin but highly productive aquifers as they are the most efficient, possess the largest open area, and can be closely matched to aquifer gradations.

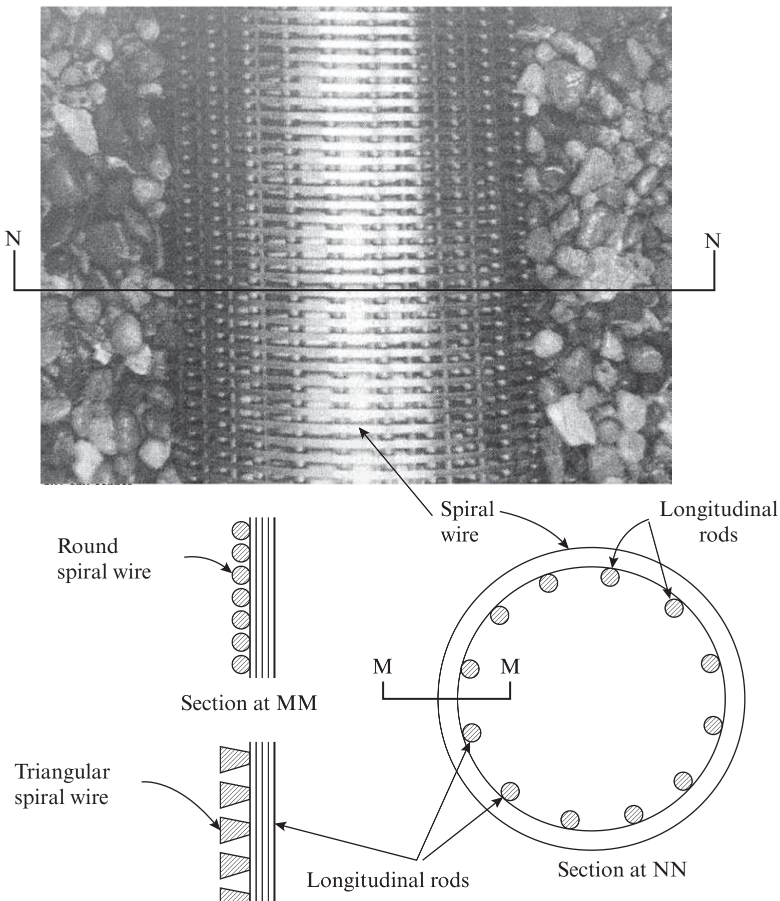

Figure 4.19 *Continuous slot well screen*

Louver or Shutter Screens
The shutter-type well screens have rows of louver sort of openings as shown in Figure 4.20. The openings may be oriented either at right angles or parallel to the axis of the screen. The openings are produced in the wall of a solid tube by a stamping operation through a power punch working against a die. The slot size (length and width of opening) and their number depend upon the series of die sets. A complete range of openings is not possible, and the percentage area of openings is limited. The shape of the louver openings is not suitable naturally developed well as they become blocked by sand grains during the development procedure. Therefore, the use of the shutter screens is confined to artificially gravel-packed wells. Louver screens are made in various materials including mild steel, stainless steel, and bronze.

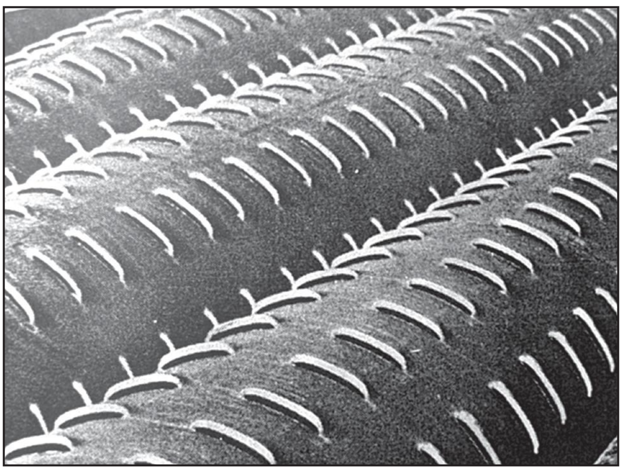

Figure 4.20 *Louver-type well screen*

Pipe Base Well Screen
The pipe base well screen is made by using a perforated steel pipe as a structural core with a continuous slot screen jacket mounted on the pipe base. The jacket can be made by winding a trapezoidal-shaped wire directly on the perforated pipe or by winding the wire over a series of longitudinal rods spaced as desired around the circumference of the pipe. These rods hold the wire away from the perforated pipe surface so that fewer of the openings are blocked. This type of well screen has two sets of openings. The total area of perforations in the pipe is usually less than the total area of slot opening on the jacket formed by wire winding, therefore the hydraulic performance of the screen depends on the percentage open area in the pipe, but which is low. To prevent galvanic corrosion (due to two metals construction), the same material for pipe and jacket should be used.

Slotted Well Screen
Pipe with slots can be used as a makeshift substitute for well screens. Slots may be cut with a saw or oxyacetylene torch, or they may be punched using chisel and die or casing perforator. The limitations of such screens are that the openings

cannot be closely spaced, percentage area of opening is low, openings are nonuniform in size and spacing, and small-size openings to control fine sand are impossible to produce. Slotting also speeds up the corrosion. Figure 4.21 shows a slotted PVC pipe and slots in bridge-type screen.

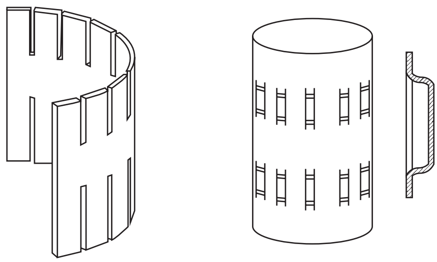

Slotted pipe   Bridge-slot screen

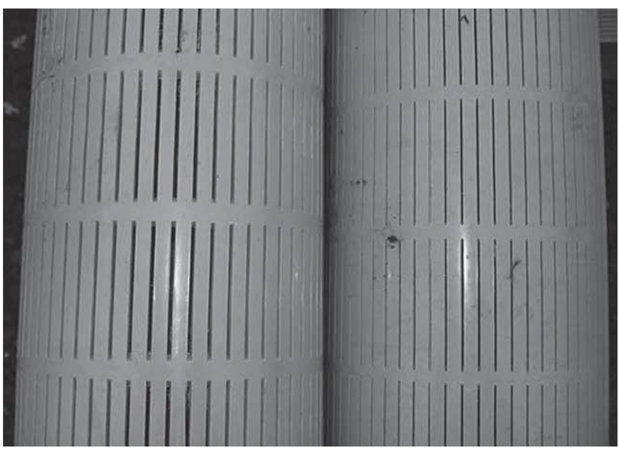

Slotted PVC pipe

Figure 4.21 *Other type of well screens*

Screen Material

Three things govern the choice of metal of which the screen should be made: mineral content of water and formation, the presence of bacterial slimes, and strength requirement of the screen. If the water has low pH (< 7), high dissolved oxygen (> 2 ppm), presence of hydrogen sulfide, high total dissolved solids (> 1,000 ppm), high carbon dioxide (> 50 ppm), or high chlorides (> 500 ppm), it is corrosive and the well screen should be made of corrosion resistant metals. Incrusting water tends to deposit minerals on the screen surface resulting into clogging of the screen. If the water has high pH (> 7.5), high carbonate hardness (> 300 ppm), high iron content (> 2 ppm), or high manganese (> 1 ppm), it has incrusting tendencies and the well screen should be made of corrosion-resistant metals to withstand the corrosive effect of the acid treatment for removing incrustation. Iron bacteria produce accumulations of slimy material of jelly-like consistency, and they oxidize and precipitate dissolved iron and manganese, leading to complete plugging of the well screen in a short time. The treatment includes the use of strong solution of chlorine and hydrochloric acid. The corrosiveness of these treatments should be kept in selecting material of the well screen. The screen should have adequate strength to resist the forces to which it will be subjected and maximum open area consistent with the strength requirements. Screens are made of a variety of metals and metal alloys, plastics, concrete, asbestos cement, fiberglass-reinforced epoxy, coated base metals, and wood. Because a well screen is particularly susceptible to corrosion and incrustation, nonferrous metals, alloys, and plastic are often selected to prolong well life and efficient operation. From strength requirement point of view, stainless steel is better than nonferrous metals, alloys, and plastic.

Screen Installation

Procedures for installing well screens vary with the method of well drilling. In the cable-tool method of drilling, screens are normally placed by the *pull-back method*. After casing is in place, the screen is lowered inside, and the casing is pulled up to near the top of the screen. The main requirement is to use casing of such kind, condition, and strength that it can be sunk to the full depth of the well and then pulled back to the length of the screen. A lead packer ring on the top of the screen is flared outward to form a seal between the inside of the casing and the screen. Alternatively, a self-sealing packer of flexible material may be used for this purpose. The main function of the seal is to keep sand out of well. If there is too much friction between the casing and the hole wall (as in deep wells in unconsolidated formations), it may be very difficult to pull the casing. The pull-back method of screen installation is also the most practical method to use in rotary drilled wells. For the rotary method of drilling without casing, screens are lowered into place as drilling mud is diluted and again are sealed by a lead packer to an upper permanent casing. When pull-out method does work or as an alternate method, screens are placed by the *bail-down method*, involving bailing out material below the screen until the screen section is lowered to the desired aquifer depth. Another method is the *wash-down method* wherein the jetting action loosens the sand and allows the screen to sink.

4.6.3 Gravel Packs

A *gravel-packed* well is the one that contains an artificially placed gravel screen or envelope surrounding the well screen. A gravel pack (i) stabilizes the aquifer, (ii) minimizes sand pumping, (iii) permits the use of a large screen slot with a maximum open area, and (iv) provides an annular zone of high permeability, which increases the effective radius and yield of the well. Gravel packs consist of uniform or graded material with maximum grain size of a pack near 1 cm, while the thickness in the range of 8–15 cm. The selected gravel should be washed and screened siliceous material that is rounded, abrasive resistant, and dense. Gravel should be placed in such a manner as to ensure complete filling of the annular space and to minimize segregation. Uniform gravel can be poured into bore hole from ground surface as long as bridging between screen and bore hole wall is avoided. Graded gravel cannot be dropped into the hole because the differently sized particles will segregate and form bands of predominantly fine and coarse materials in the envelope. This reduces the effectiveness of the gravel pack. Particle separation can be minimized by extending two tremie pipes to the bottom of the well on opposite sides of the screen. Gravel is poured, washed, or pumped into the tremie pipes; these are then withdrawn in stages as the pack is placed. In cable-tool holes, the inner casing and screen are set inside the blank outer casing, the annular space is filled with gravel, and thereafter the outer casing is pulled out of the well. In sandy aquifers, where a gravel pack is most essential, deep wells should be constructed by the rotary or reverse-circulation rotary method. The drilling fluid should be circulated and diluted with water before the gravel is introduced.

4.7 Piezometers and Water Table Observation Wells

Piezometer is a borehole or standpipe with a screen at the end of the casing that is installed in an aquifer to measure piezometric pressure/level. Water enters through the screen in the piezometer and rises up to stable water elevation, which is the hydraulic head at the point of measurement. Piezometer, as shown in Figure 4.22, has the following:

(i) A screen to create a relatively large surface for water to enter the standpipe
(ii) A sand pack around the screen to increase effective diameter
(iii) A seal above the screen to prevent water from leaking along the casing
(iv) A casing protector to finish the top of the piezometer and to prevent unauthorized access

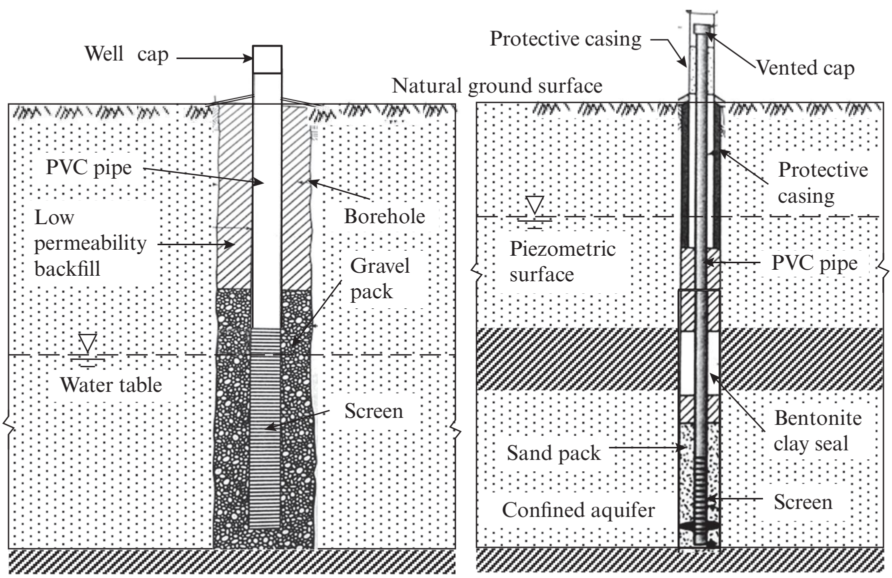

Figure 4.22 *Piezometer and water table observation wells*

A piezometer can work properly only if the water moving into or out of standpipe comes from the aquifer zone adjacent to the screen. If water leaks up or down, then hydraulic head and water-quality measurement can be erroneous. The seal prevents this leakage and is constructed from bentonite clay. Generally, the casing is made of 5.1 cm diameter PVC. After auger drilling in noncaving formations, the screen and casing can be lowered down the hole and proper sand packing and sealing are provided. In caving formation, auger drilling possesses problems, but hollow stem auger allows the casing down the hole center of the auger and back out of the auger results into collapsing of the hole around the casing providing natural sealing. Jetting, cable tool with temporary casing and rotary drilling with mud are alternate ways of caving formations. Piezometers greater than 30 m depth may have problems in placing sand pack and grout seal.

A water table monitoring well is similar to a piezometer well except for the length of screen and its placing as shown in Figure 4.22. A water table observation well has a long screen that extends above and below the water table; therefore, it provides the elevation of the water table and hydraulic head at the top of the groundwater system. If the water table level rises or falls, it will remain within the screened section. Providing a seal is less critical because the zone above the screen is unsaturated; however, a low-permeability backfill around the casing above the screen prevents surface drainage from moving down along the borehole.

Chapter 14 deals with the design, development, and maintenance of water wells.

PROBLEMS

4.1. What is a well? What are the types of wells?

4.2. What are the differences among test, exploratory, and observation wells?

4.3. Write a note on Ranney well.

4.4. What is meant by *qanat*? Explain.

4.5. What is the sequence of steps in planning a well scheme?

4.6. How are desk study, reconnaissance, and well survey different?

4.7. What are the reasons for carrying out geophysical logging?

4.8. Describe the conditions where jetting and driving can and cannot be used.

4.9. How is a good site for a well selected?

4.10. Why is test drilling important?

4.11. What do you understand by well logging?

4.12. What are the different types of well-logging techniques?

4.13. What are the different types of resistivity logs? Where is a particular log suitable?

4.14. What are the different types of radiation loggings? Where is a particular log suitable?

4.15. How are tracer techniques helpful in groundwater exploration?

4.16. What is the role of a drilling fluid, and how is it selected? Describe the advantages of mud over water as a drilling fluid.

4.17. How is drilling fluid lost? How is it overcome?

4.18. Explain the situations where Ranney wells may be a better choice than conventional vertical wells.

4.19. What are the benefits of gravel packing?

4.20. What is the purpose of cementing/grouting?

4.21. Explain the well construction steps in jetting, driving, and drilling?

4.22. Why is well casing required? How is it selected?

4.23. What are the functions of a well screen? Describe the different types of screen with their salient features.

Chapter 5

Principles of Groundwater Movement in Porous Media

5.1 Darcy's Experimental Law

Groundwater in its natural state is invariably moving. This movement is governed by established hydraulic principles. Darcy's law is a phenomenologically derived constitutive equation that describes the flow of a fluid through a porous medium. It states that the flow rate through porous media is proportional to the head loss and inversely proportional to the length of the flow path. Darcy's law along with the equation of conservation of mass is equivalent to the groundwater flow equation, one of the basic relationships of hydrogeology. It is also used to describe oil, water, and gas flows through petroleum reservoirs. The law was formulated by Henry Darcy based on the results of experiments on the flow of water through beds of sand. It also forms the scientific basis of permeability used in the earth sciences. It is analogous to Fourier's law in the field of heat conduction, Ohm's law in the field of electrical networks, or Fick's law in diffusion theory.

Darcy's law is analogous to pipe flow in which energy is dissipated over the distance to overcome frictional loss resulting from fluid viscosity. Darcy observed by conducting experiments that the volume per unit time passing through a porous medium is directly proportional to the area of cross section A (m^2) and the head difference between inlet and outlet (h_1–h_2) and inversely proportional to the length of the medium l (m) therefore,

$$\frac{Vol}{t} = Q \propto A(h_1 - h_2)\frac{1}{l} \tag{5.1}$$

which in terms of specific discharge q or discharge velocity or Darcy velocity v (m/s) is

$$q = v = \frac{Q}{A} = -K\frac{\partial h}{\partial l} = -K\,i \tag{5.2}$$

where constant of proportionality K = hydraulic conductivity (m/s) and $i = \partial h/\partial l$ = hydraulic gradient = rate of head loss per unit length of medium. The negative sign indicates that the total head is decreasing in the direction of flow because of friction or resistance.

Darcy's law is a simple mathematical statement which neatly summarizes several familiar properties that groundwater flowing in aquifers exhibits, including (i) if there is no hydraulic gradient (difference in hydraulic head over a distance), no flow occurs (this is hydrostatic conditions), (ii) if there is a hydraulic gradient, flow will occur from high head toward low head (opposite the direction of increasing gradient, hence the negative sign in Darcy's law), (iii) the greater the hydraulic gradient (through the same aquifer material), the greater the discharge, and (iv) the discharge may be different through different aquifer materials (or even through the same material, in a different direction) even if the same hydraulic gradient exists.

5.2 Hydraulic Head

The energy available for groundwater flow is given the name *hydraulic head*. It consists of three components, related to elevation, pressure, and velocity. The total energy head is expressed by the equation

$$h = z + \frac{p}{\rho g} + \frac{v^2}{2g} \tag{5.3}$$

where h is the hydraulic head (m), z is the elevation or datum head (m), p is the pressure exerted by water column (Pa), ρ is the density of fluid (kg/m^3), g is the acceleration due to gravity (m/sec^2), and v is velocity of flow (m/s). In groundwater flow, the velocity is so low that the energy contained in velocity can be neglected when computing the total energy. Thus, the hydraulic head is written as

$$h = z + \frac{p}{\rho g} \tag{5.4}$$

5.3 Velocity Potential

Velocity potential is analogous to a force potential whose directional derivative is the force in that direction. Hence, the *velocity potential* is a scalar function of space and time $\phi = f(x, y, z, t)$ such that partial derivative with respect to any direction gives the flow velocity in that direction, that is,

$$v_x = \frac{\partial \phi}{\partial x};\ v_y = \frac{\partial \phi}{\partial y};\ v_z = \frac{\partial \phi}{\partial z} \tag{5.5}$$

In groundwater the velocity potential may be defined as

$$\phi = -K\left(\frac{p}{\rho g} + z\right) + Const = -Kh + Const \tag{5.6}$$

For the points of equal hydraulic head the velocity potential function $\phi = f(x, y, z, t)$ = constant and the curve joining such points is known as *equipotential lines*. Equipotentials are defined as curves of constant potential. A plot of equipotentials, which are sometimes called potentiometric contours, shows the variation of the potential throughout a flow domain in much the same way as the contour lines on a topographic map show the ground elevations. In addition, both the direction and the magnitude of the discharge vector can be derived from a plot of equipotentials. The discharge vector is directed normal to the equipotentials.

5.4 Direction of Groundwater Flow

In an aquifer, it is likely that the head will decrease in some direction and increase in others. The direction of groundwater movement is from higher head to a lower head; however, with the above definition of velocity potential the groundwater flow is in the direction of increasing velocity potential. This is due to placement of datum, wherein the head is measured above the datum while the velocity potential is being measured below the datum. The *hydraulic gradient* is oriented in the direction of maximum head decrease; thus, the maximum gradient is perpendicular to the lines of equal hydraulic head (equipotential lines). At a minimum, it takes three hydraulic head measurements (say at *A*, *B*, and *C*) to determine the hydraulic gradient and the direction of groundwater flow. The procedure consists of (Figure 5.1)

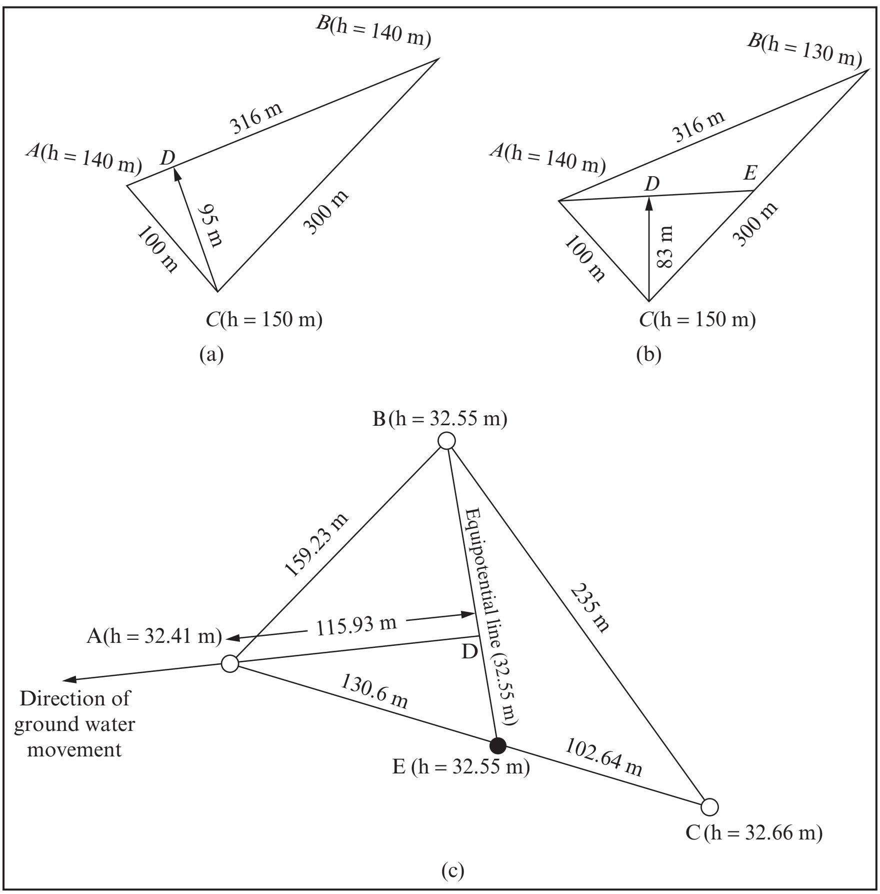

Figure 5.1 *Direction of groundwater movement*

(i) Make sure that the three hydraulic heads in three wells (A, B, and C) are not equal.

(ii) If the hydraulic heads at two of the wells (A and B) are equal as shown in Figure 5.1(a), draw a line through C and perpendicular to AB (with the intercept point D). If the hydraulic head at well C is greater than the hydraulic head at wells A and B, ground water will flow from C to D. The hydraulic gradient from C to D is

$$i_{CD} = \frac{h_C - h_D}{l_{CD}} \tag{5.7}$$

where, h_C and h_D are the hydraulic heads at wells C and D, and l_{CD} is the distance between C and D.

(iii) If the hydraulic heads are different at the three wells as shown in Figure 5.1(b), find a location (E) on the line connecting the well with the highest head (C) to the well with the lowest head (B), at which the head is the same as that in the intermediate well (A). Draw a line between A and E and another line through C, perpendicular to the line AE. The flow direction is from C to D as the arrow shows and again, the hydraulic gradient from C to D is as given by the previous equation. Figure 5.1(c) illustrates another example of determination of groundwater flow direction.

5.5 Hydraulic Conductivity and Intrinsic Permeability

A medium has a unit *hydraulic conductivity* if it will transmit in unit time a unit volume of groundwater at the prevailing kinematic viscosity through a cross section of unit area measured at right angles to the direction of flow, under a unit hydraulic gradient. It has units of velocity. The hydraulic conductivity of a soil or rock depends on a variety of physical factors, including porosity, particle size and distribution, shape of particles, arrangement of particles, and other factors. In general, for unconsolidated porous media, K varies with square of particle size; clayey materials exhibit low values of K, whereas sands and gravels display high values. The hydraulic conductivity in saturated zones can be determined by a variety of techniques, including calculation from formulas, laboratory methods, tracer tests, auger hole tests, and pumping tests of wells.

The hydraulic conductivity depends on both properties of the porous medium and the fluid (e.g., density and viscosity). For many groundwater studies, water is the fluid of interest, providing more or less constant values of density and viscosity (neglecting temperature dependencies). Thus, measurements of hydraulic conductivity are useful in comparing differences in hydraulic behavior of the actual materials. In looking more generally at systems where the fluids other than water are present (such as, air, oil, and gasoline), hydraulic conductivity becomes an awkward parameter because the density and viscosity of the fluid vary together with the medium properties.

A convenient alternative is to write Darcy's equation in a form of *intrinsic permeability* where the properties of the medium and the fluid are represented explicitly

$$v = -\frac{k\rho g}{\mu}\frac{\partial h}{\partial l} \tag{5.8}$$

where, k is the intrinsic permeability, and μ is the dynamic viscosity of fluid (Pa.s or kg/m/sec). The *intrinsic permeability* of a rock or soil is a measure of its ability to transmit fluid as the fluid moves through it. The intrinsic permeability is independent of the fluid moving through the medium and depends only upon the medium properties. The relation between hydraulic conductivity and intrinsic permeability, therefore, is

$$K = \frac{k\rho g}{\mu} \quad or \quad k = \frac{\mu}{\gamma} K \tag{5.9}$$

where, $\gamma = \rho g$ is the specific weight or weight density (N/m^3) of fluid. The intrinsic permeability is used primarily when the density or the viscosity of the fluid varies with position. The dimension of k is m^2, but it is so small that square micrometers $(\mu\ \mathrm{m})^2 = 10^{-12}\ \mathrm{m}^2$ is used. In the petroleum industry it is expressed in Darcy ($= 0.987\times10^{-12}\ \mathrm{m}^2$). Table 5.1 lists typical values of hydraulic conductivity and intrinsic permeability for different geological formations. For water, viscosity and density are functions of pressure and temperature. At 20° C and 1 atm pressure $\rho = 998.2$ kg/m^3 and $\mu = 1.002\times10^{-3}$ Pa.s or kg/m/sec. under these conditions

$$K = 9.77\times10^{6}\, k \qquad \text{or} \qquad k = 1.023\times10^{-7}\, K \tag{5.10}$$

Table 5.1 *Hydraulic conductivity for different geological formations (Todd and Mays 2005)*

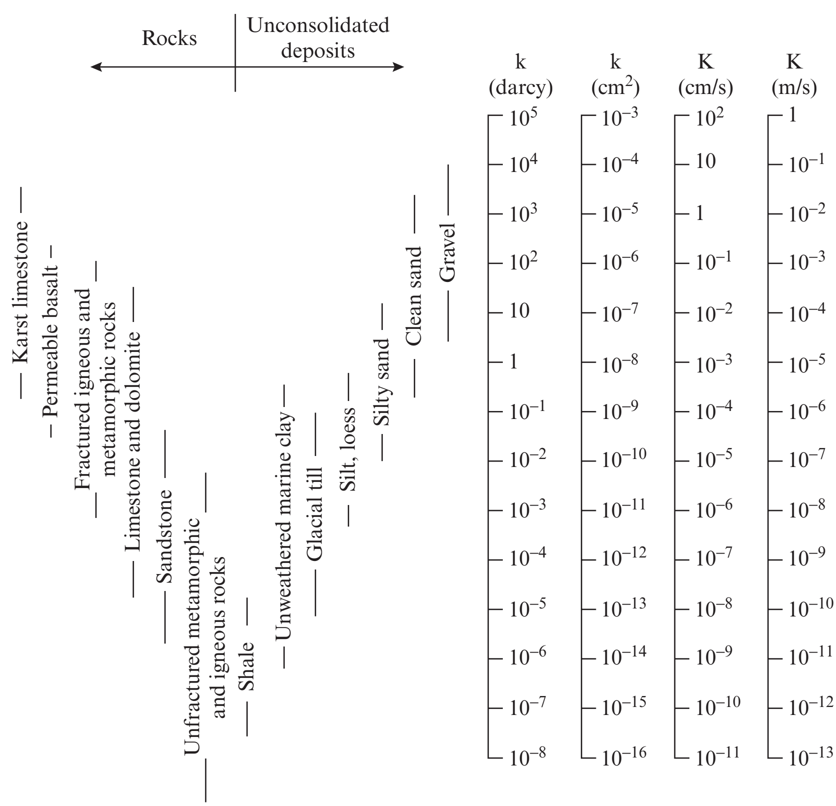

5.6 Relation Between Darcy Velocity and Interstitial Velocity

Darcy velocity v is the *apparent velocity* or *fictitious velocity* or *Darcy flux* (discharge per unit area). This value of velocity, often referred to as the apparent velocity, is not the velocity which the water traveling through the pores is experiencing. The velocity v is referred to as the Darcy velocity because it assumes that flow occurs through the entire cross section of the material without regard to solids and pores. Actually water can flow though pores only and the pore spaces vary continuously with location within the medium. Therefore, the actual velocity is nonuniform, involving endless accelerations, deceleration, and changes in direction. To define the *actual flow velocity* or *interstitial velocity*, one must consider the microstructure of the rock material. For naturally occurring geologic materials, the microstructure cannot be specified three-dimensionally; hence, actual velocities can only be quantified statistically.

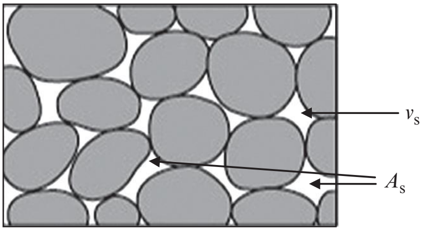

Figure 5.2 *Seepage velocity*

In reality, the flow is limited to the pores (white spaces in Figure 5.2) only so that the average interstitial velocity or actual velocity or *seepage velocity* (v_s) through pore space can be determined by applying continuity equation

$$Q = A_s v_s = Av \tag{5.11}$$

hence

$$v_s = v\frac{A}{A_s} = \frac{v}{\eta} \tag{5.12}$$

where, A = total area of soil specimen and A_s = area of pores only (Figure 5.2). The velocity is divided by porosity to account for the fact that only a fraction of the total aquifer volume is available for flow. The pore velocity is the velocity a conservative tracer/dye experiences if carried by water through the aquifer. This indicates that for a sand with a porosity of 33 percent the $v_s = 3v$.

5.7 Validity of Darcy's Law

Darcy's law is a generalized relationship for flow in porous media, which may be stated in several different forms depending on the flow conditions. It is valid for any Newtonian fluid. Although it was established under saturated flow conditions, it may be adjusted to account for unsaturated and multiphase flow. In applying Darcy's law, it is important to know the range of validity within which it is applicable. Darcy's velocity is proportional to the hydraulic gradient similar to the velocity in laminar flow is proportional to the first power of the hydraulic gradient (Poiseuille's law). This analogy indicates that Darcy's law applies to laminar flow in porous media. As inertial forces increase, turbulence occurs gradually. The turbulence occurs first in the larger pore spaces; with increasing velocity it spreads to the smaller pores. For fully developed turbulence, the head loss varies approximately with the second power of the velocity rather then linearly. The *Reynold's number* (a dimensionless parameter) serves as a criterion to distinguish between laminar and turbulent flow. Reynold's number for porous media flow may be expressed as

$$N_{\mathrm{R}} = \frac{\rho v d_{10}}{\mu} \tag{5.13}$$

where, d_{10} is the effective grain size. Darcy's law is valid for $N_{\mathrm{R}} < 1$ and does not depart seriously up to $N_{\mathrm{R}} = 10$. Fortunately, most natural underground flow occurs with $N_{\mathrm{R}} < 1$ so Darcy's law is applicable. Deviations from Darcy's law can occur where steep hydraulic gradients exist, such as near pumped wells; also, turbulent flow can be found in rocks such as basalt and limestone that contain large underground openings. Darcy's law has been found to be invalid for very slow water flow through dense clay; there the effects of electrically charged clay particles on water in the minute pores produce nonlinearity between flow rate and hydraulic gradient.

5.8 Derivation of Darcy's Law from N – S Equations

Although Darcy's law (an expression of conservation of momentum) was determined experimentally by Darcy, it has since been derived from the Navier – Stokes equations. The various forces that may influence the motion of a fluid are due to gravity, pressure, viscosity, turbulence, surface tension and compressibility. For the motion of fluid if we consider only gravity, pressure and viscous force, the equation of Newton's second law for motion of a fluid by considering these forces becomes

$$Ma = F_a + F_p + F_v \tag{5.14}$$

where, F_{g} = body force, F_{p} = pressure force, and F_{v} = viscous force. This equation is known as Navier – Stokes' equation which is useful in the analysis of viscous flow. In x-direction, Eqn. (5.14) can be written as

$$\frac{\partial v_x}{\partial t} + v_x \frac{\partial v_x}{\partial x} + v_y \frac{\partial v_x}{\partial y} + v_z \frac{\partial v_x}{\partial z} = -\frac{1}{\rho}\frac{\partial p}{\partial x} + \frac{\mu}{\rho}\nabla^2 v_x \tag{5.15}$$

For porous media $v = v_{\mathrm{x}}/\eta$ and so on, this equation for 2-D (x–y plane) case becomes

$$\frac{1}{\eta}\frac{\partial v_x}{\partial t} + \frac{v_x}{\eta^2}\frac{\partial v_x}{\partial x} + \frac{v_y}{\eta^2}\frac{\partial v_x}{\partial y} = -\frac{1}{\rho}\frac{\partial p}{\partial x} + \frac{\mu}{\eta\rho}\nabla^2 v_x \tag{5.16}$$

Similarly, in y-direction

$$\frac{1}{\eta}\frac{\partial v_y}{\partial t}+\frac{v_x}{\eta^2}\frac{\partial v_y}{\partial x}+\frac{v_y}{\eta^2}\frac{\partial v_y}{\partial y}=-\frac{1}{\rho}\frac{\partial p}{\partial y}+\frac{\mu}{\eta\rho}\nabla^2 v_y-g \tag{5.17}$$

From dimensional consideration

$$\nabla^2 v_x=\frac{-1}{C}\frac{v_x}{L^2}=\frac{-v_x}{Cd^2};\qquad \nabla^2 v_y=\frac{-v_y}{Cd^2} \tag{5.18}$$

where L = characteristic length = d (diameter of solid minerals particles). From the definition of velocity potential

$$v_x=\frac{\partial\phi}{\partial x};\ v_y=\frac{\partial\phi}{\partial y} \tag{5.19}$$

Therefore,

$$\frac{1}{\eta}\frac{\partial}{\partial t}\left(\frac{\partial\phi}{\partial x}\right)+\frac{1}{\eta^2}\frac{\partial\phi}{\partial x}\frac{\partial}{\partial x}\left(\frac{\partial\phi}{\partial x}\right)+\frac{1}{\eta^2}\frac{\partial\phi}{\partial y}\frac{\partial}{\partial y}\left(\frac{\partial\phi}{\partial x}\right)=-\frac{1}{\rho}\frac{\partial p}{\partial x}-\frac{\mu}{\eta\rho}\frac{1}{Cd^2}\frac{\partial\phi}{\partial x} \tag{5.20}$$

As ϕ is a continuos function of x, y, and t; the order of its partial derivatives may be changed, thus

$$\frac{1}{\eta}\frac{\partial}{\partial x}\left(\frac{\partial\phi}{\partial t}\right)+\frac{1}{2\eta^2}\frac{\partial}{\partial x}\left(\frac{\partial\phi}{\partial x}\right)^2+\frac{1}{2\eta^2}\frac{\partial}{\partial x}\left(\frac{\partial\phi}{\partial y}\right)^2=-\frac{1}{\rho}\frac{\partial p}{\partial x}-\frac{\mu}{\eta\rho}\frac{1}{Cd^2}\frac{\partial\phi}{\partial x} \tag{5.21}$$

Likewise

$$\frac{1}{\eta}\frac{\partial}{\partial y}\left(\frac{\partial\phi}{\partial t}\right)+\frac{1}{2\eta^2}\frac{\partial}{\partial y}\left(\frac{\partial\phi}{\partial x}\right)^2+\frac{1}{2\eta^2}\frac{\partial}{\partial y}\left(\frac{\partial\phi}{\partial y}\right)^2=-\frac{1}{\rho}\frac{\partial p}{\partial y}-\frac{\mu}{\eta\rho}\frac{1}{Cd^2}\frac{\partial\phi}{\partial y}-g \tag{5.22}$$

Integrating wrt to y

$$\frac{1}{\eta}\left(\frac{\partial\phi}{\partial t}\right)+\frac{1}{2\eta^2}\left(\frac{\partial\phi}{\partial x}\right)^2+\frac{1}{2\eta^2}\left(\frac{\partial\phi}{\partial y}\right)^2=-\frac{p}{\rho}-\frac{\mu}{\eta\rho}\frac{\phi}{Cd^2}-gy+F(x,t) \tag{5.23}$$

Considering steady state and neglecting inertial terms, that is,

$$\frac{\partial\phi}{\partial t}=0;\left(\frac{\partial\phi}{\partial x}\right)^2+\left(\frac{\partial\phi}{\partial y}\right)^2=0 \tag{5.24}$$

The equation becomes

$$\frac{p}{\rho}+\frac{\mu}{\eta\rho}\frac{\theta}{Cd^2}+gy=Const \tag{5.25}$$

Defining $\eta\ Cd^2 = k$ = Intrinsic permeability and $\frac{\gamma}{\mu}k = K$ = Hydraulic conductivity gives

$$\phi=-\frac{k\gamma}{\mu}\left(\frac{p}{\gamma}+y\right)+Const \tag{5.26}$$

$$\phi = -K\left(\frac{p}{\gamma} + y\right) + Const \tag{5.27}$$

Taking derivative and defining $\frac{p}{\gamma} + y = h$ = Total Head

$$\frac{\partial \phi}{\partial y} = -K\frac{\partial}{\partial y}\left(\frac{p}{\gamma} + y\right) = -K\frac{\partial h}{\partial y} \tag{5.28}$$

Therefore,

$$v_y = -K\frac{\partial h}{\partial y}; \qquad v_y = -Ki_y \tag{5.29}$$

which is Darcy's equation. Similarly, we can get for x-axis (where constant is different and $h = p/\gamma$ as the g term is zero)

$$\frac{\partial \phi}{\partial x} = -K\frac{\partial h}{\partial x}; \qquad v_x = -Ki_x \tag{5.30}$$

5.9 Homogeneity and Isotropy

If hydraulic conductivity is independent of position within a geologic formation then the formation is termed *homogeneous*. This means that the hydraulic conductivity does not vary spatially within the area. If hydraulic conductivity is dependent of the position within a geologic formation then the formation is termed *heterogeneous*. This means that the hydraulic conductivity varies spatially. If a formation has a hydraulic conductivity that is independent of the direction of measurement it is called *isotropic*. This means that the hydraulic conductivity would be the same if measured in the x, y, or z direction. If a formation has a hydraulic conductivity that is dependent on the direction of measurement it is called *anisotropic*. This means that the hydraulic conductivity varies depending on if it was measured in the x, y, or z direction. Moreover, if the soil has the same hydraulic conductivity at all points within the region of flow, the soil is said to be homogeneous and isotropic. If the hydraulic conductivity is dependent on the direction of the measurement and if this directional dependence is the same at all points of the flow region, the soil is said to be homogeneous and anisotropic. In homogeneous and anisotropic soils, the hydraulic conductivity is dependent on the direction of the measurement but independent of the space coordinates.

5.10 Generalized Darcy's Equations

In isotropic medium, one of the coordinate axis can be aligned along the direction of hydraulic gradient and the flow becomes 1-D in that direction and the Darcy's law can be applied. But the hydraulic conductivity of material at a point in an anisotropic medium exhibits directional dependency. To have a broader application (in anisotropic medium or 3-D flow), the 1-D Darcy's law must be generalized.

Darcy's law in anisotropic materials is expressed as

$$v = -K\Delta h \tag{5.31}$$

where v is the Darcy velocity vector, ∇h is the gradient of hydraulic head, K is hydraulic conductivity tensor.

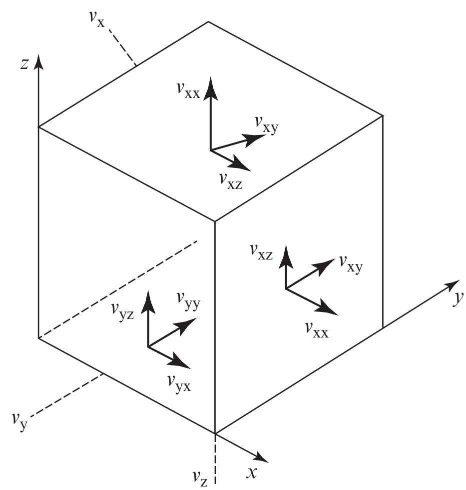

Figure 5.3 *Velocity components*

In Cartesian coordinates

$$v = v_x i + v_y j + v_z k \tag{5.32}$$

$$\nabla h = \left(i\frac{\partial}{\partial x} + j\frac{\partial}{\partial y} + k\frac{\partial}{\partial z} \right) h \tag{5.33}$$

$$K = \begin{bmatrix} K_{xx} & K_{xy} & K_{xz} \\ K_{yx} & K_{yy} & K_{yz} \\ K_{zx} & K_{zy} & K_{zz} \end{bmatrix} \tag{5.34}$$

where i, j, and k are unit vectors along x, y, and z directions, respectively. Hence, Darcy velocity components in x, y, and z directions (see Figure 5.3) are given by

$$v_x = -K_{xx}\frac{\partial h}{\partial x} - K_{xy}\frac{\partial h}{\partial y} - K_{xz}\frac{\partial h}{\partial z} \tag{5.35}$$

$$v_y = -K_{yx}\frac{\partial h}{\partial x} - K_{yy}\frac{\partial h}{\partial y} - K_{yz}\frac{\partial h}{\partial z} \tag{5.36}$$

$$v_z = -K_{zx}\frac{\partial h}{\partial x} - K_{zy}\frac{\partial h}{\partial y} - K_{zz}\frac{\partial h}{\partial z} \tag{5.37}$$

where

$$K_{xy} = K_{yx}; \qquad K_{xz} = K_{zx}; \qquad K_{yz} = K_{zy} \tag{5.38}$$

If the principal directions of anisotropy coincide with the x, y, and z directions, the nondiagonal components of hydraulic conductivity tensor are zero, that is,

$$K_{xy} = K_{yx} = K_{xz} = K_{zx} = K_{yz} = K_{zy} = 0 \tag{5.39}$$

and the Darcy velocities in the x, y, and z directions are simplified as

$$v_x = -K_{xx}\frac{\partial h}{\partial x} \tag{5.40}$$

$$v_y = -K_{yy}\frac{\partial h}{\partial y} \tag{5.41}$$

$$v_z = -K_{zz}\frac{\partial h}{\partial z} \tag{5.42}$$

5.11 Laplace Equation

Physically all flow systems extend in three dimensions. However, in many problems, the features of the groundwater motion are essentially planar, with the motion being substantially the same in parallel planes. Such problems can be considered 2-D and thereby reducing the complexity of the analysis. Fortunately, in civil engineering the vast majority of problems falls into this category. For an incompressible fluid if the flow is 2-D and steady then equation of continuity is

$$\frac{\partial v_x}{\partial x} + \frac{\partial v_y}{\partial y} = 0 \tag{5.43}$$

By using velocity potential function

$$\frac{\partial^2 \phi}{\partial x^2} + \frac{\partial^2 \phi}{\partial y^2} = 0 \Rightarrow \nabla^2 \phi = 0 \tag{5.44}$$

This is Laplace equation. Also this can be written in terms of h as

$$\frac{\partial}{\partial x}\left(-K\frac{\partial h}{\partial x}\right) + \frac{\partial}{\partial y}\left(-K\frac{\partial h}{\partial y}\right) = 0 \tag{5.45}$$

$$\frac{\partial^2 h}{\partial x^2} + \frac{\partial^2 h}{\partial y^2} = 0 \Rightarrow \nabla^2 h = 0 \tag{5.46}$$

5.12 Stream Function

Stream function is a scalar function of space and time $\psi = f(x, y, t)$ such that its partial derivative with respect to any direction gives the velocity component at right angles (in the clockwise direction) to this direction, thus,

$$v_x = \frac{\partial \psi}{\partial y}; \qquad v_y = -\frac{\partial \psi}{\partial x} \tag{5.47}$$

Equating the respective potential and stream functions of v_x and v_y,

$$\frac{\partial \phi}{\partial x} = \frac{\partial \psi}{\partial y}; \qquad \frac{\partial \phi}{\partial y} = -\frac{\partial \psi}{\partial x} \tag{5.48}$$

These are Cauchy – Riemann equations. Substituting stream functions of v_x and v_y, in continuity equation for 2-D study flow

$$\frac{\partial^2 \psi}{\partial x \partial y} - \frac{\partial^2 \psi}{\partial y \partial x} = 0 \tag{5.49}$$

This means that the $\psi = f(x, y)$ satisfies identically the equation of continuity.

Taking derivative of the first equation of Cauchy – Riemann equations wrt y and the second equation of Cauchy – Riemann equations wrt x

$$\frac{\partial^2 \phi}{\partial y \partial x} = \frac{\partial^2 \psi}{\partial y^2}; \qquad \frac{\partial^2 \phi}{\partial x \partial y} = -\frac{\partial^2 \psi}{\partial x^2} \tag{5.50 a, b}$$

Subtracting Eqn. (5.50 b) from Eqn. (5.50 a) results to

$$\frac{\partial^2 \psi}{\partial x^2} + \frac{\partial^2 \psi}{\partial y^2} = 0 \Rightarrow \nabla^2 \psi = 0 \tag{5.51}$$

This is also Laplace equation. Thus both ϕ and ψ satisfy Laplace's equation and hence they are the *conjugate harmonic functions* and that means the curves $\phi = f(x, y)$ = constant are the orthogonal trajectories of the curves $\psi = f(x, y)$ = constant. The Laplace equation for the stream function or velocity potential or head is linear, so that these functions may be superposed.

It should be noted that within a given region of flow the streamlines and equipotential lines are unique. That is, considering the total differential

$$d\psi = \frac{\partial \psi}{\partial x} dx + \frac{\partial \psi}{\partial y} dy \tag{5.52}$$

From Cauchy–Riemann equations

$$\psi = \int \left(\frac{\partial \phi}{\partial x} dy - \frac{\partial \phi}{\partial y} dx \right) \tag{5.53}$$

and

$$\phi = \int \left(\frac{\partial \psi}{\partial y} dx - \frac{\partial \psi}{\partial x} dy \right) \tag{5.54}$$

Hence, in solving groundwater problems we need to concern ourselves only with the determination of one of the functions, subject to the imposed boundary conditions. The other function will follow directly from the relationship between them. Laplace equation indicates that for conditions of steady-state, laminar flow, the form of the groundwater motion can be completely determined by solving one equation, subject to the boundary conditions of the flow domain. The solution to this equation for certain boundary conditions is unique.

5.13 Flownet

Solving groundwater flow problems amounts to solving the differential equation of Laplace with the appropriate boundary conditions. Only a few solutions to Laplace's equation in three dimensions exist. Fortunately, many practical flow problems either are 2-D or can be approximated by a 2-D analysis. If analytical solution is difficult to obtain then several problems can be solved graphically. The graphical solution of Laplace equation gives all data for plotting a flow net consisting of a set of flow lines orthogonal to a set of equipotential lines.

If the path of an individual particle in flow field is tracked then the tangent at any point gives the direction of velocity at that point and the locus of all points defines the path of flow of an individual particle known as *flow line* or *streamline*. The physical significance of streamlines can be established as follows. Consider a streamline *AB* in the flow field as shown in Figure 5.4, which gives:

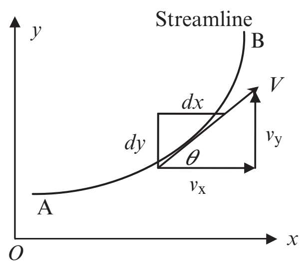

Figure 5.4 *Streamline*

$$\frac{v_y}{v_x} = \tan\theta = \frac{dy}{dx} \tag{5.55}$$

and hence,

$$v_y dx - v_x dy = 0 \tag{5.56}$$

Substituting v_x and v_y, in terms of stream functions

$$\frac{\partial\psi}{\partial x}dx + \frac{\partial\psi}{\partial y}dy = 0 \qquad \Rightarrow \qquad d\psi = 0 \tag{5.57}$$

Hence

$$\int d\psi = \psi = Const \tag{5.58}$$

Thus along a streamline the stream function is constant. Therefore we see that the curves $\psi = f(x, y)$ equal to a sequence of constants, are at all points tangent to the velocity vectors and hence a set of streamlines.

Discharge between two stream lines (another important physical property of the stream function) can be obtained by considering the flow between the two streamlines as shown in Figure 5.5. Elementary discharge between two stream lines through *dy*-section

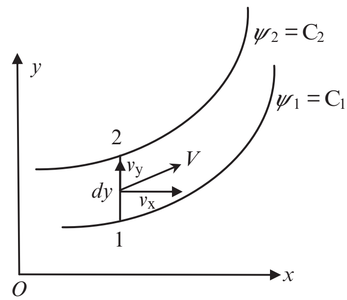

Figure 5.5 *Discharge between two streamlines*

$$dq = Vds = -v_y dx + v_x dy = \frac{\partial \psi}{\partial x} dx + \frac{\partial \psi}{\partial y} dy = d\psi \tag{5.59}$$

Total discharge between 1–2 section

$$q = \int dq = \int_{\psi_1}^{\psi_2} d\psi = \psi_2 - \psi_1 \tag{5.60}$$

Thus total discharge = $q = \psi_2 - \psi_1$ that the quantity of flow between two streamlines, called a *flow channel* is a constant, hence it behaves like a solid tube. Thus, once the streamlines of flow have been obtained, their plot not only shows the direction of flow but the relative magnitudes of the velocity along the flow channels, that is, the velocity at any point in the flow channel varies inversely with the streamline spacing in the vicinity of that point.

The discharge vector is normal to the equipotentials, the flow occurs in the direction of the steepest slope of the plot of potentiometric contours. Discharge streamlines are curves whose tangent at any point coincides with the discharge vector. For 2-D steady flow, the equipotential lines is $\phi = f(x, y) =$ constant. By total derivative

$$d\phi = \frac{\partial \phi}{\partial x} dx + \frac{\partial \phi}{\partial y} dy = 0 \tag{5.61}$$

Hence,

$$v_x dx + v_y dy = 0 \quad \Rightarrow \quad \frac{dy}{dx} = -\frac{v_x}{v_y} \tag{5.62}$$

For 2-D steady flow, along the stream line

$$v_y dx - v_x dy = 0 \quad \Rightarrow \quad \frac{dy}{dx} = \frac{v_y}{v_x} \tag{5.63}$$

Product of these two is −1 so they intersect each other orthogonally. The streamlines (ψ = constant) and equipotential lines (ϕ = constant) form a grid of curves called a *flow net* wherein all intersections are at right angles as shown in Figure 5.6.

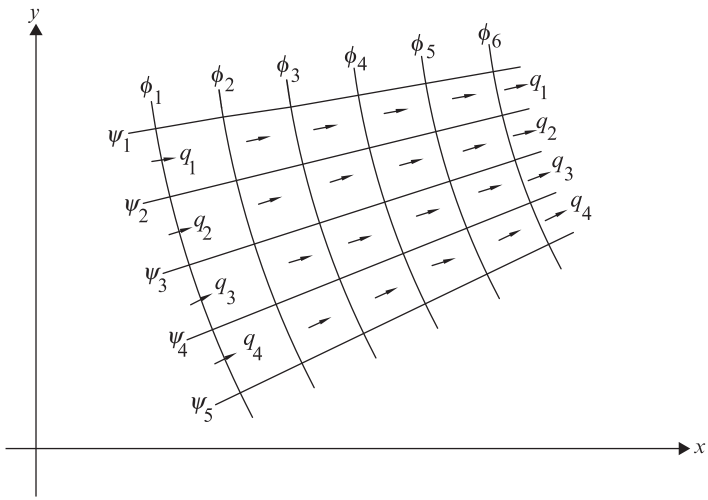

Figure 5.6 *Flownet*

An important distinction between ϕ and ψ functions lies in the fact that the ϕ functions exist only for *irrotational flow*. A particle of fluid is said to have zero net rotation or to be irrotational if the circulation, the line integral of the tangential velocity taken around the particle is zero. Assume the particles as a free body of fluid in the shape of a sphere. As fluid may be considered frictionless all surface forces act normal to the surface and hence through its mass center. Likewise gravity acts through the mass center, which for an incompressible fluid is coincidental with its geometric center. Thus, no torque can exist on the sphere and it remains without rotation. The circulation in rectangular element in 2-D flow is

$$v_x dx + \left(v_y + \frac{\partial v_y}{\partial x} dx \right) dy - \left(v_x + \frac{\partial v_x}{\partial y} dy \right) dx - v_y dy \tag{5.64}$$

Now if the circulation is zero, we have for irrotational flow,

$$\frac{\partial v_y}{\partial x} - \frac{\partial v_x}{\partial y} = 0 \tag{5.65}$$

Substituting for v_x and v_y,

$$\frac{\partial^2 \phi}{\partial x \partial y} - \frac{\partial^2 \phi}{\partial y \partial x} = 0 \tag{5.66}$$

which shows that the existence of the velocity potential implies that flow is irrotational.

A *flownet* for an isotropic and homogeneous system provides a graphical solution to the Laplace equation. Flownets are usually drawn only for a 2-D flow field. In heterogeneous media the flownet is not perfect squares. In anisotropic media, streamlines do not intersect equipotential lines at right angles except when flow is aligned with one of the principal directions of hydraulic conductivity. Several guidelines and procedures are available in the literature for drawing flownets for variety of problems.

5.14 Different Boundaries in a Porous Medium

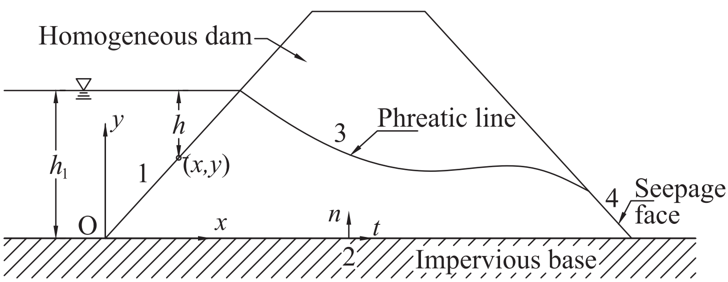

Figure 5.7 *Different type of boundaries*

5.14.1 Boundary 1: Interface Between Soil and Water or Boundaries of the Reservoirs

Along the boundaries of the reservoir the pressure distribution may be taken as hydrostatic. Therefore, the pressure at any point (x, y) on this boundary as shown in Figure 5.7 is

$$p_{(x,y)} = p_{atm} + \gamma_w h \tag{5.67}$$

But $h = h_1 - y$ so

$$\frac{p_{(x,y)}}{\gamma_w} = \frac{p_{atm}}{\gamma_w} + (h_1 - y) \tag{5.68}$$

$$\Rightarrow \frac{p_{(x,y)}}{\gamma_w} + y = \frac{p_{atm}}{\gamma_w} + h_1 \tag{5.69}$$

Therefore,

$$\phi = -K(\frac{p_{(x,y)}}{\gamma_w} + y) + C = -K(\frac{p_{atm}}{\gamma_w} + h_1) + C_1 = \text{Const.} \tag{5.70}$$

Hence, ϕ is constant at Boundary 1, which means Boundary 1 is an equipotential line.

5.14.2 Boundary 2: Impervious Boundary

At impervious boundaries the fluid can neither penetrate the boundary nor leave gaps; thus, the velocity component normal to the boundary at any point must vanish thus,

$$V_n = 0 \Rightarrow \frac{\partial \phi}{\partial n} = 0 \Rightarrow \phi = \text{Const} \tag{5.71}$$

Thus, ϕ is constant along n direction i.e. normal to the impervious boundary.

$$V_n = 0 \Rightarrow \frac{\partial \psi}{\partial t} = 0 \Rightarrow \psi = \text{Const} \tag{5.72}$$

Hence, ψ is constant along t direction (along the impervious boundary) that means Boundary 2 is a flow/stream line. Likewise, any streamline satisfies the condition for an impervious boundary and may be taken as such.

5.14.3 Boundary 3: Phreatic Line or Line of Seepage

The *line of seepage* or *phreatic line* is the upper most streamline in the flow domain. It separates the saturated region of flow from that part of the porous medium through which no flow occurs as shown in Figure 5.7. The determination of its locus is one of the major objectives of groundwater investigations. In addition to the requirement that this boundary is a streamline ψ = constant, it is evident that the pressure at every point along its surface is constant and equal to atmospheric pressure, thus along this line pressure is atmospheric, that is, $p = p_{\text{atm}}$. At any point on the streamline

$$\phi = -K(\frac{p_{(x,y)}}{\gamma_w} + y) + C \Rightarrow \phi = -K(\frac{p_{\text{atm}}}{\gamma_w} + y) + C \tag{5.73}$$

Therefore,

$$\Rightarrow \phi + Ky = -\frac{K_{\text{atm}}}{\gamma_w} + C \ = \text{Const} \Rightarrow \phi + Ky \ = \text{Const} \tag{5.74}$$

which demonstrates that the velocity potential (and the total head) along the line of seepage varies linearly with elevation head. Hence,

$$\phi_1 + Ky_1 = \phi_2 + Ky_2 \tag{5.75}$$

$$\frac{(\phi_2 - \phi_1)}{K} = y_1 - y_2 \tag{5.76}$$

Similarly,

$$\frac{(\phi_3 - \phi_2)}{K} = y_2 - y_3 \tag{5.77}$$

But

$$(\phi_2 - \phi_1) = (\phi_3 - \phi_2) \tag{5.78}$$

$$\Rightarrow y_1 - y_2 = y_2 - y_3 \tag{5.79}$$

$$\Rightarrow \Delta y_1 = \Delta y_2 = \text{Const} \tag{5.80}$$

This requires constant vertical intercepts at the points of intersection of the line of seepage with successive equipotential lines of equal drops ($\Delta\phi$ = constant). Hence, Boundary 3 is the top flow line (ψ is constant) and ϕ varies linearly.

5.14.4 Boundary 4: Interface Between Soil and Air (Seepage Face)

Seepage face is a boundary where the seepage leaving the flow region enters a zone free of both liquid and soil. As the pressure on this surface is constant and atmospheric similar to line of seepage thus,

$$\phi + Ky = \text{constant} \tag{5.81}$$

Therefore, the velocity potential varies linearly but $\psi \neq$ constant, So Boundary 4 is not a flow line.

5.15 Transformation of Inhomogeneous into Homogeneous Medium

An *equivalent transformed section* is a fictitious section such that the seepage discharge is the same as that for an actual anisotropic and/or inhomogeneous section of same dimensions (thickness and cross-sectional area) under same head loss. Let there are n homogeneous and isotropic layers of thicknesses d_1, d_2, d_3, …, d_n and hydraulic conductivities K_1, K_2, K_3,…, K_n respectively in a stratified (*inhomogeneous*) medium as shown in Figure 5.8. The equivalent transformed section has the hydraulic conductivities K_x along the stratification and K_y normal to the stratification and dimensions $L_e = L$ and $d_e = d_1 + d_2 + d_3 + \ldots + d_n$

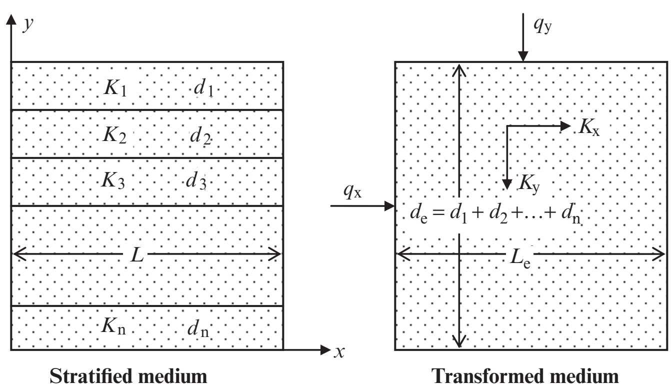

Figure 5.8 *Transformation of medium*

5.15.1 Flow Parallel to Stratification

First consider flow parallel to the stratification (x-direction). Seepage discharges per unit width of the medium in each layer are

$$q_1 = d_1K_1i_1\,; \quad q_2 = d_2K_2i_2\,; \quad q_3 = d_3K_3i_3\,; \;\ldots\; q_n = d_nK_ni_n \tag{5.82}$$

For the equivalent transformed section, let discharge, hydraulic conductivity, and hydraulic gradient in the x-direction are q_x, K_x, and i_x, respectively, so that

$$q_x = d_e K_x i_x = (d_1 + d_2 + d_3 + \ldots + d_n) K_x i_x \tag{5.83}$$

The conditions for this case are

$$i_1 = \frac{\partial h}{\partial l} = \frac{h_2 - h_1}{L} = i_2 = i_3 = \ldots = i_n = i_x \tag{5.84}$$

and

$$q_x = q_1 + q_2 + q_3 + \ldots + q_n \tag{5.85}$$

Therefore,

$$q_x = (d_1 + d_2 + d_3 + \ldots + d_n) K_x i_x = d_1 K_1 i_1 + d_2 K_2 i_2 + d_3 K_3 i_3 + \ldots + d_n K_n i_n \tag{5.86}$$

and, hence,

$$K_x = \frac{d_1 K_1 + d_2 K_2 + d_3 K_3 + \ldots + d_n K_n}{d_1 + d_2 + d_3 + \ldots + d_n} = \sum_{j=1}^{n} K_j d_j \bigg/ \sum_{j=1}^{n} d_j \tag{5.87}$$

5.15.2 Flow Normal to Stratification

Now consider flow normal to the stratification (y-direction). Seepage discharges per unit width of the medium in each layer are

$$q_1 = LK_1 i_1; \quad q_2 = LK_2 i_2; \quad q_3 = LK_3 i_3; \quad q_n = LK_n i_n \tag{5.88}$$

where hydraulic gradient in each layer is given by

$$i_1 = \frac{\partial h}{\partial l} = \frac{h_{L1}}{d_1}; \quad i_2 = \frac{h_{L2}}{d_2}; \quad i_3 = \frac{h_{L3}}{d_3}; \quad i_n = \frac{h_{Ln}}{d_n} \tag{5.89}$$

hence

$$h_{L1} = d_1 i_1; \quad h_{L2} = d_2 i_2; \quad h_{L3} = d_3 i_3; \quad h_{Ln} = d_n i_n \tag{5.90}$$

For the equivalent transformed section, let discharge, hydraulic conductivity, and hydraulic gradient in the y-direction are q_y, K_y, and i_y, respectively, so that

$$q_y = L_e K_y i_y = LK_y i_y \tag{5.91}$$

and

$$i_y = \frac{\partial h}{\partial l} = \frac{h_L}{d_e} = \frac{h_L}{d_1 + d_2 + d_3 + \ldots + d_n} \tag{5.92}$$

here the total head loss h_L is the sum of head losses in each layer, that is,

$$h_L = h_{L1} + h_{L2} + h_{L3} + \ldots + h_{Ln} \tag{5.93}$$

Therefore

$$(d_1 + d_2 + d_3 + \ldots + d_n)i_y = d_1 i_1 + d_2 i_2 + d_3 i_3 + \ldots + d_n i_n \tag{5.94}$$

but

$$i_y = \frac{q_y}{LK_y};\ i_1 = \frac{q_1}{LK_1};\ i_2 = \frac{q_2}{LK_2};\ i_3 = \frac{q_3}{LK_3};\ i_n = \frac{q_n}{LK_n} \tag{5.95}$$

and from the condition of continuity of flow in the y-direction

$$q_y = q_1 = q_2 = q_3 = \ldots = q_n \tag{5.96}$$

and hence

$$\frac{d_1 + d_2 + d_3 + \ldots + d_n}{K_y} = \frac{d_1}{K_1} + \frac{d_2}{K_2} + \frac{d_3}{K_3} + \ldots + \frac{d_n}{K_n} \tag{5.97}$$

or

$$K_y = \sum_{j=1}^{n} d_j \Big/ \sum_{j=1}^{n} (d_j / K_j) \tag{5.98}$$

5.15.3 Comparison of Hydraulic Conductivities Along and Normal the Stratification

The hydraulic conductivity along the stratification is always greater than the hydraulic conductivity normal to the stratification, that is, $K_x > K_y$ or

$$\sum_{j=1}^{n} K_j d_j \Big/ \sum_{j=1}^{n} d_j > \sum_{j=1}^{n} d_j \Big/ \sum_{j=1}^{n} (d_j / K_j) \tag{5.99}$$

To prove it consider a two-layer porous medium

$$\frac{K_1 d_1 + K_2 d_2}{d_1 + d_2} > \frac{d_1 + d_2}{\dfrac{d_1}{K_1} + \dfrac{d_2}{K_2}} \tag{5.100}$$

or

$$\left(K_1 d_1 + K_2 d_2\right)\left(\frac{d_1}{K_1} + \frac{d_2}{K_2}\right) > \left(d_1 + d_2\right)^2 \tag{5.101}$$

or

$$\frac{K_2}{K_1} + \frac{K_1}{K_2} > 2 \qquad \Rightarrow \qquad K_1^2 + K_2^2 > 2K_1 K_2 \tag{5.102}$$

and hence

$$\left(K_1 - K_2\right)^2 > 0 \tag{5.103}$$

which is always true so $K_x > K_y$. This can also be proved for three-layered or more layered soil medium.

5.16 Transformation of Anisotropic into Isotropic Medium

The transformation from anisotropic medium to isotropic medium takes the following steps. Consider Figure 5.9 as shown below, let s and n represent the directions of the tangent to the flow line and the normal to the equipotential line, respectively. In an isotropic flow medium, the flow lines and equipotential lines form an orthogonal system, hence the s and n directions are identical ($\beta = 0$). In anisotropic flow, the direction of the stream lines in general, will not coincide with the direction of the normal to the equipotential lines and hence $\beta \neq 0$.

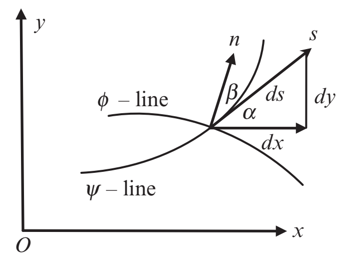

Figure 5.9 *Anisotropic medium*

From Darcy's law, the flow velocity along the steam line (s-direction) is given by

$$v_s = -K_\alpha \frac{dh}{ds} \tag{5.104}$$

where, K_α = hydraulic conductivity in the s-direction; v_s = velocity in s-direction. $\frac{dh}{ds}$ = hydraulic gradient in s-direction. Hence, the velocity components in the x and y-directions are

$$v_x = -K_x \frac{\partial h}{\partial x} \qquad v_y = -K_y \frac{\partial h}{\partial y} \tag{5.105}$$

The velocity components along x and y-directions are

$$v_x = v_s \cos\alpha \qquad v_y = v_s \sin\alpha \tag{5.106}$$

therefore,

$$v_x = -K_x \frac{\partial h}{\partial x} = v_s \cos\alpha \quad \Rightarrow \quad \frac{\partial h}{\partial x} = \frac{-v_s}{K_x}\cos\alpha \tag{5.107}$$

$$v_y = -K_y \frac{\partial h}{\partial y} = v_s \sin\alpha \quad \Rightarrow \quad \frac{\partial h}{\partial y} = \frac{-v_s}{K_y}\sin\alpha \tag{5.108}$$

Also, from Figure 5.9,

$$\frac{dx}{ds} = \cos\alpha \qquad \frac{dy}{ds} = \sin\alpha \tag{5.109}$$

As

$$\frac{dh}{ds} = \frac{\partial h}{\partial x}\frac{dx}{ds} + \frac{\partial h}{\partial y}\frac{dy}{ds} \tag{5.110}$$

By substituting the corresponding values from Eqs (5.107) to (5.109) in Eqn. (5.110),

$$\frac{dh}{ds} = \frac{-v_s}{K_\alpha} = \frac{-v_s}{K_x}\cos^2\alpha + \frac{-v_s}{K_y}\sin^2\alpha \tag{5.111}$$

Therefore,

$$\frac{1}{K_\alpha} = \frac{\cos^2\alpha}{K_x} + \frac{\sin^2\alpha}{K_y} \tag{5.112}$$

From rectangular coordinates, we have,

$$x = r\cos\alpha \qquad\qquad y = r\sin\alpha \tag{5.113}$$

Using Eqs (5.112)–(5.113)

$$\frac{r^2}{K_\alpha} = \frac{x^2}{K_x} + \frac{y^2}{K_y} \tag{5.114}$$

Eqn. (5.114) is the equation of an ellipse, which has major semi-axis = $\sqrt{K_x}$ and minor semi-axis = $\sqrt{K_y}$. If $\sqrt{K_x} = \sqrt{K_{max}}$ and $\sqrt{K_y} = \sqrt{K_{min}}$ as in case of a stratified medium with the x-direction parallel to the bedding plane, the hydraulic conductivity in any direction, making an angle α with the x-axis, can be obtained from the graphical construction, as shown in Figure 5.10, is called the *ellipse of direction*.

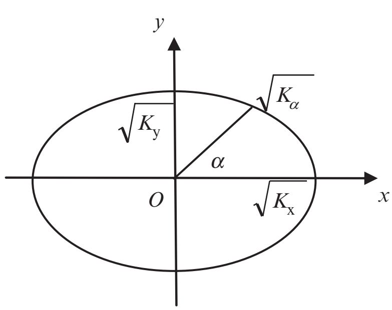

Figure 5.10 *Ellipse of direction*

Therefore, the square root of the directional hydraulic conductivity for a homogeneous and anisotropic layer when plotted from a point will generate an ellipse.

5.16.1 X-Transformation

The validity of the transformation of coordinates can be demonstrated in a more rigorous manner directly from the equation of continuity. Using velocity components from the velocity potential functions in the continuity equation,

$$\frac{\partial}{\partial x}\left(-K_{\mathrm{x}}\frac{\partial h}{\partial x}\right)+\frac{\partial}{\partial y}\left(-K_{\mathrm{y}}\frac{\partial h}{\partial y}\right)=0 \tag{5.115}$$

If the medium were homogeneous then

$$K_{\mathrm{x}}\frac{\partial^2 h}{\partial x^2}+K_{\mathrm{y}}\frac{\partial^2 h}{\partial y^2}=0 \quad\Rightarrow\quad \frac{K_{\mathrm{x}}}{K_{\mathrm{y}}}\frac{\partial^2 h}{\partial x^2}+\frac{\partial^2 h}{\partial y^2}=0 \tag{5.116}$$

$$\frac{\partial^2 h}{\partial\left(x\sqrt{K_{\mathrm{y}}/K_{\mathrm{x}}}\right)^2}+\frac{\partial^2 h}{\partial y^2}=0 \Rightarrow \quad \frac{\partial^2 h}{\partial X^2}+\frac{\partial^2 h}{\partial y^2}=0 \tag{5.117}$$

where,

$$X = x\sqrt{K_{\mathrm{y}}/K_{\mathrm{x}}} \tag{5.118}$$

Substituting this in direction of ellipse equation, we get,

$$\frac{r^2}{K_\alpha}=\frac{X^2}{K_{\mathrm{y}}}+\frac{y^2}{K_{\mathrm{y}}} \quad\Rightarrow\quad X^2+y^2=\frac{K_{\mathrm{y}}}{K_\alpha}r^2=R^2 \tag{5.119}$$

Therein,

$$R = r\sqrt{K_{\mathrm{y}}/K_\alpha} \tag{5.120}$$

If $r=\sqrt{K_\alpha}$ then $R=\sqrt{K_{\mathrm{y}}}$. Eqn. (5.119) is an equation of circle. This equation and Figure 5.11 demonstrate that, by the transformation of scale $X = x\sqrt{K_{\mathrm{y}}/K_{\mathrm{x}}}$ in the x-direction, the ellipse of direction will be transformed into a circle where the hydraulic conductivity will be an invariant with the direction.

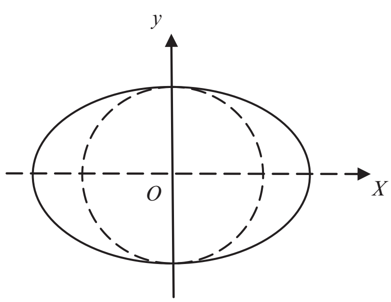

Figure 5.11 *X-Transformation*

5.16.2 Y-Transformation

Similarly as above transformation can be achieved in the y-direction as

$$\frac{\partial^2 h}{\partial x^2}+\frac{\partial^2 h}{\partial\left(y\sqrt{K_{\mathrm{x}}/K_{\mathrm{y}}}\right)^2}=0 \Rightarrow \quad \frac{\partial^2 h}{\partial x^2}+\frac{\partial^2 h}{\partial Y^2}=0 \tag{5.121}$$

where,

$$Y = y\sqrt{K_x/K_y} \tag{5.122}$$

Substituting this in direction of ellipse equation,

$$\frac{r^2}{K_\alpha} = \frac{x^2}{K_x} + \frac{Y^2}{K_x} \quad \Rightarrow \quad x^2 + Y^2 = \frac{K_x}{K_\alpha} r^2 = R^2 \tag{5.123}$$

Therein,

$$R = r\sqrt{K_x/K_s} \tag{5.124}$$

If $r = \sqrt{K_\alpha}$ then $R = \sqrt{K_x}$. Eqn. (5.123) represents a circle. Figure 5.12 demonstrates that, by the transformation of scale $Y = y\sqrt{K_x/K_y}$ in the y-direction, the ellipse of direction can be transformed in to a circle wherein the hydraulic conductivity is direction independent.

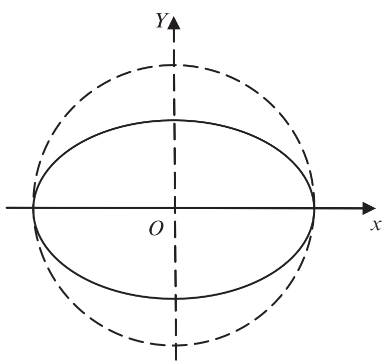

Figure 5.12 *Y-Transformation*

5.16.3 Equivalent Hydraulic Conductivity

If the medium is layered parallel to x-axis, then $K_x > K_y$ so $X = x\sqrt{K_y/K_x}$ transformation results into a contraction along X-axis to have the circle while $Y = y\sqrt{K_x/K_y}$ transformation results into an expansion along Y-axis to have the circle. Thus, by simple expansion or contraction of spatial coordinates, a given homogeneous and anisotropic flow region can be transformed into a fictitious isotropic region (see Figure 5.13) where in Laplace's equation is valid and consequently the potential theory is applicable. This fictitious flow region is called the transformed section. The equivalent hydraulic conductivity for the transformed section can be computed by equating seepage discharges in anisotropic (original) and isotropic (transformed/equivalent) mediums in x-direction as

$$q = AB\,K_x\,\frac{dh}{dx} = A'B'\,K_e\,\frac{dh}{dX} \tag{5.125}$$

in X-transformed case (Figure 5.14) where $X = x\sqrt{K_y/K_x}$ but $AB = A'B'$ as there is no change in y-dimensions thus,

$$K_x \frac{dh}{dx} = K_e \frac{dh}{dx}\sqrt{\frac{K_x}{K_y}} \qquad \Rightarrow \qquad K_e = \sqrt{K_x K_y} \tag{5.126}$$

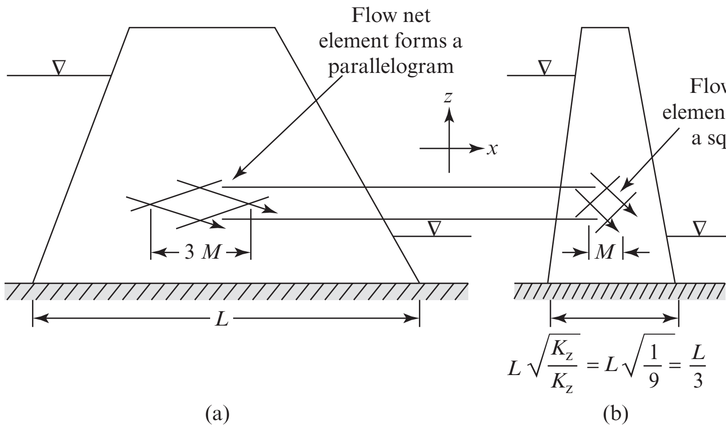

Figure 5.13 *Equivalent transformation (Todd and Mays 2005)*

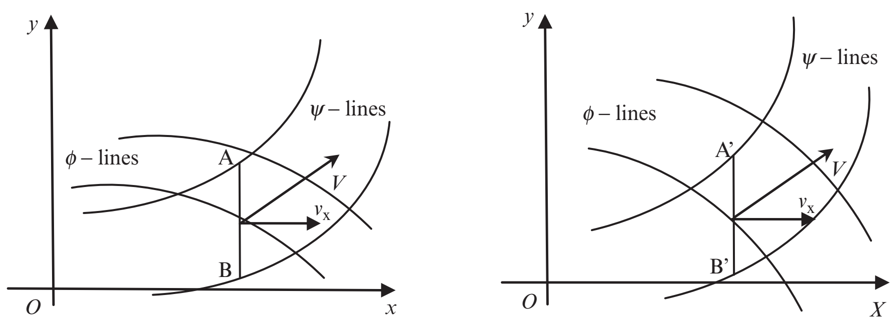

Figure 5.14 *X-Transformation*

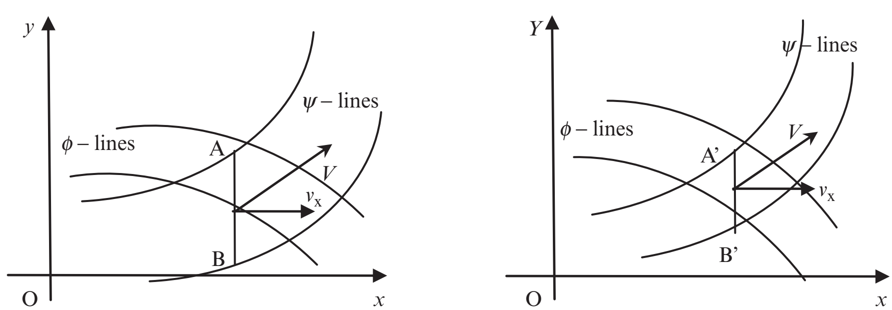

Figure 5.15 *Y-Transformation*

Similarly, for Y-transformed case (Figure 5.15), the seepage discharges in x-direction

$$q = AB\,K_x \frac{dh}{dx} = A'B'\,K_e \frac{dh}{dx} \tag{5.127}$$

where, $A'B' = AB\sqrt{K_x/K_y}$ but dh/dx is the same as there is no change in x-dimensions thus

$$AB\,K_x = K_e AB\sqrt{\frac{K_x}{K_y}} \qquad \Rightarrow \qquad K_e = \sqrt{K_x K_y} \tag{5.128}$$

Therefore, from both transformations, the equivalent hydraulic conductivity is same $K_e = \sqrt{K_x K_y}$. Once the problem has been solved for the transformed section, the solution for the natural medium can be obtained by applying the inverse of the scaling ratio. Thus, it will be shown that the effects of anisotropy can be taken into account by a simple transformation of spatial coordinates.

5.17 Flow Through Two Media (Flow Crossing Anisotropy)

Consider a case where flow passes from a region of hydraulic conductivity K_1 to other region of K_2 as shown in Figure 5.16. Due to difference in conductivities the direction of flow changes from α_1 in region K_1 to α_2 in region K_2, where α_1 and α_2 are angles of flow lines with normal in regions K_1 and K_2, respectively.

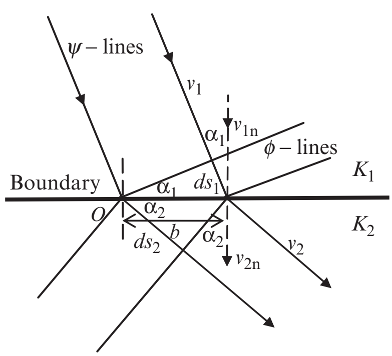

Figure 5.16 *Flow crossing boundary of two isotropic mediums*

The velocity potentials in regions K_1 and K_2 are given by

$$\phi_1 = -K_1 h_1 + C_1 = -K_1\left(\frac{p_1}{\gamma_w} + y_1\right) + C_1 \tag{5.129}$$

$$\phi_2 = -K_2 h_2 + C_2 = -K_2\left(\frac{p_2}{\gamma_w} + y_2\right) + C_2 \tag{5.130}$$

At the common point O at the interface, $p_1 = p_2$; $y_1 = y_2$ and $C_1 = C_2$, which may be assumed zero. With these conditions, dividing Eqn. (5.129) by Eqn. (5.130)

$$\frac{\phi_1}{\phi_2} = \frac{K_1}{K_2} \tag{5.131}$$

From continuity condition, the normal components of flow approaching and leaving the boundary/interface must be equal; hence the normal velocity components must be such that

$$v_{1\text{n}} = v_{2\text{n}} \tag{5.132}$$

or

$$v_1 \cos\alpha_1 = v_2 \cos\alpha_2 \tag{5.133}$$

Hence,

$$K_1 \frac{dh_1}{ds_1}\cos\alpha_1 = K_2 \frac{dh_2}{ds_2}\cos\alpha_2 \tag{5.134}$$

But between the same two equipotential lines $dh_1 = dh_2$ and also $ds_1 = b\sin\alpha_1$ and $ds_2 = b\sin\alpha_2$; thus,

$$K_1 \frac{\cos\alpha_1}{\sin\alpha_1} = K_2 \frac{\cos\alpha_2}{\sin\alpha_2} \quad \Rightarrow \quad \frac{K_1}{K_2} = \frac{\tan\alpha_1}{\tan\alpha_2} \tag{5.135}$$

Therefore, the flowlines deviate towards the normal when they cross from a coarse (higher K) to fine (lower K) medium and deviate away from the normal when they cross from a fine (lower K) to coarse (higher K) medium and vice versa as shown in Figure 5.17.

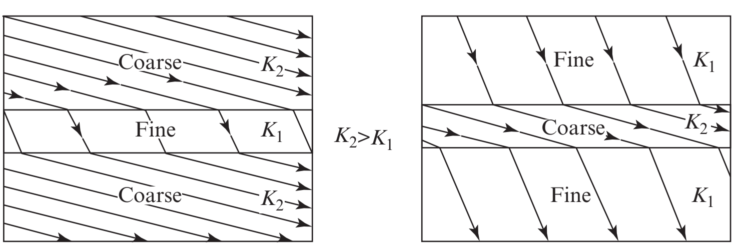

Figure 5.17 *Flow lines crossing different media*

SOLVED EXAMPLES

Example 5.1: Sketch the equivalent transformed sections in isotropic medium

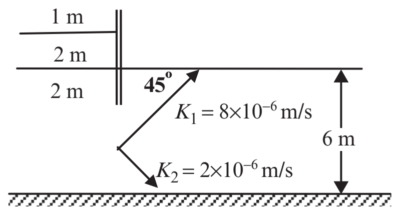

Figure 5.18 *Example 5.1*

Solution: This can be transformed in two ways (i) in K_1 direction or (ii) in K_2 direction.

Case 1: No change in dimensions along K_1 direction, but $\sqrt{K_1/K_2} = 2$, so there will be elongation (twice) along the K_2 direction. Draw a line parallel to K_1 through the point *O* (lower end of weir) and then draw normals on this reference line from all key points. There will be no change in the position of points on this line (e.g., a, *O*, *d*), but other points will move twice away from this reference line for example f' is the position of the point f (upper end of weir) where $f'f = 2f''f$. Similarly, other points will be placed as shown with prime and consequently bold lines joining points with prime in Figure 5.19 describe the transformed equivalent section, which is tilted in the isotropic medium.

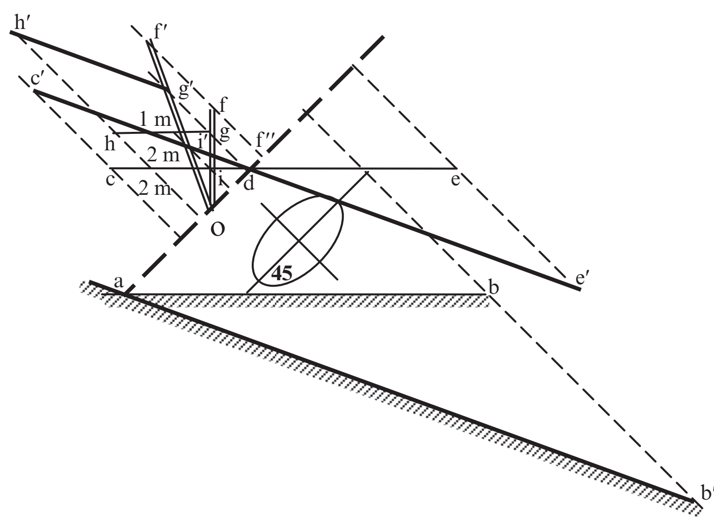

Figure 5.19 *Transformation in K_1 direction*

Case 2: No change in dimensions along K_2 direction, but $\sqrt{K_2 / K_1} = 0.5$, so there will be contraction (half) along the K_1 direction. Draw a line parallel to

K_2 through the point O and also draw normals on this reference line from all other points. The points will move half distance towards this reference line for example $b''b' = 0.5\ b''b$. Similarly, other points will be placed as shown with prime and consequently bold lines joining points with prime in Figure 5.20 describe the transformed equivalent section in the isotropic medium.

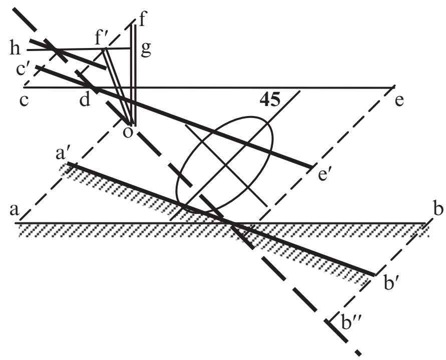

Figure 5.20 *Transformation in K_2 direction*

Example 5.2: Convert the following problem into an equivalent homogeneous and isotropic medium if

Layer	*Thickness*	*Hydraulic conductivity*
A	3 m	$K = 10\times10^{-6}$ m/s
B	2 m	$K = 5\times10^{-6}$ m/s

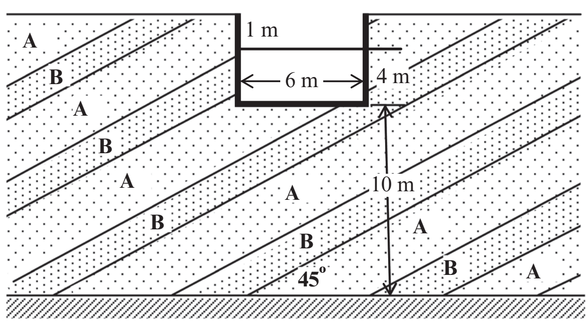

Figure 5.21 *Example 5.2*

Solution: Equivalent hydraulic conductivity in direction parallel to layers is

$$K_1 = \frac{3\times10\times10^{-6} + 2\times5\times10^{-6}}{3+2} = 8\times10^{-6}\ \text{m/s}$$

Equivalent hydraulic conductivity in direction normal to layers is

$$K_2 = \frac{3+2}{3/\left(10\times10^{-6}\right)+2/\left(5\times10^{-6}\right)} = 7.143\times10^{-6}\ \text{m/s}$$

Thus the problem is equivalent to as shown in Figure 5.22, which is similar to Example 5.1 and hence it can be solved following steps as mentioned in the solution for Example 5.1.

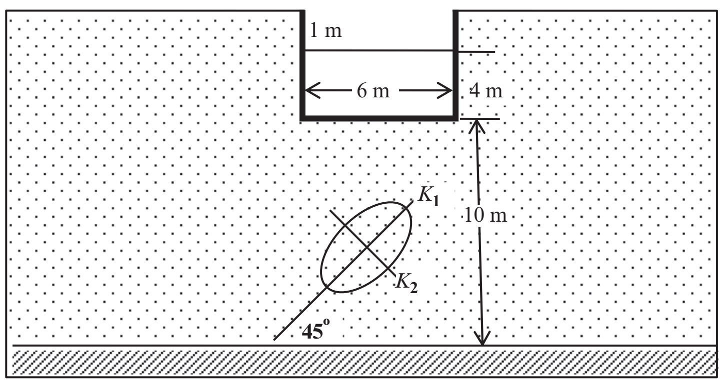

Figure 5.22 *Solution of Example 5.2*

PROBLEMS

5.1. If the laboratory coefficient of permeability of a sample of soil is 3.2×10^2 lpd/m^2 at 20°C, what would be the permeability value at 30°C?

5.2. An undisturbed soil sample has an oven-dry weight of 524.6g. After saturation with kerosene its weight is 628.2g. The saturated sample is then immersed in kerosene and displaces 256.3g. What is the porosity of the soil sample?

5.3. In a field test it was observed that a time of 5h was required for a tracer to travel from one observation well to another. The wells are 30m apart and the difference in their water table elevations is 50-cm. Samples of the aquifer between the wells indicate that the porosity is 15 percent. Compute (i) the coefficient of permeability of the aquifer assuming it to be homogeneous, (ii) the actual velocity of flow as indicated by the tracer, (iii) the seepage velocity, and (iv) Reynolds number for the flow assuming an average grain size of 1 mm and μ (water) at 27°C = 0.008 stroke.

5.4. In a homogenous isotropic confined aquifer of constant thickness of 20 m, effective porosity of 20 percent and permeability of 15 m/d, two observations well 1200 m apart indicate piezometric heads of 5.4 and 3.0 m, respectively, above msl. Assuming uniform flow, average grain diameter of sand 1 mm and kinematic viscosity of water = 0.01-cm^2/s, state (i) Whether Darcy's Law is applicable? and (ii) What is the average flow velocity in pores?

5.5. A confined aquifer is 18.5 m thick. The potentiometric surface elevations at two observation wells 822 m apart 25.96 and 24.62 m. If the horizontal hydraulic conductivity of the aquifer is 25 m/d, determine flow rate per unit width of the aquifer, specific discharge, and average linear velocity of the flow assuming steady unidirectional flow. Effective porosity is 0.25.

5.6. A 35-cm gravel packed well is pumped at a constant rate of 5000 m^3/h from a confined aquifer of thickness 50 m, having D_{10} = 0.23 mm and D_{50} = 0.6 mm. (i) What is the domain around the well for which Darcy's law is applicable, assuming that the law is valid up to R_e = 6? and (ii) if the gravel pack is 15-cm thick and has D_{10} = 1.5 mm and D_{50} = 3 mm, estimate the Reynolds's number and the seepage gradient at mid-pack.

5.7. Determine the hydraulic conductivity for an equivalent homogeneous and isotropic medium corresponding to the medium as shown in Figure: 5.23.

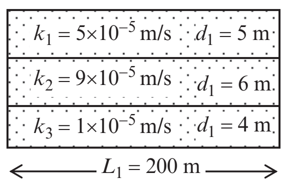

Figure 5.23 *Problem 5.7*

5.8. Sketch equivalent transformed sections in isotropic medium

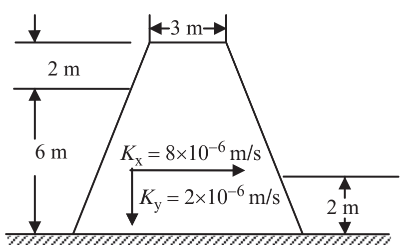

Figure 5.24 *Problem 5.8*

5.9. A confined aquifer has a constant thickness of 34 m and is stratified between two observation wells as shown in figure. Given the Piezometric surface elevations in the figure, determine the flow per unit width of the aquifer. What is the equivalent horizontal hydraulic conductivity of that section of confined aquifer between the observation wells?

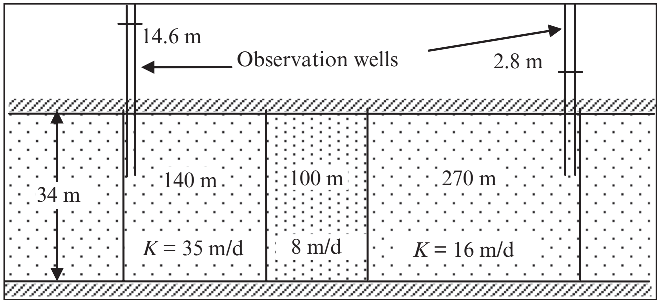

Figure 5.25 *Problem 5.9*

5.10. Convert the following problem into an equivalent homogeneous and isotropic medium.

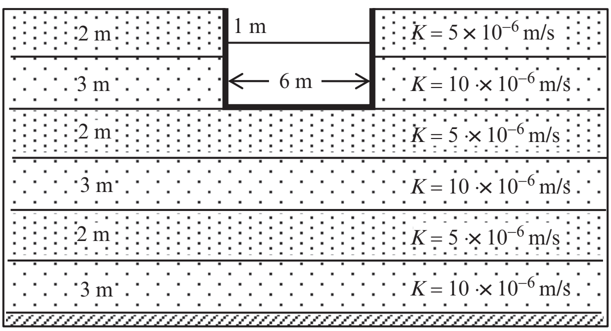

Figure 5.26 *Problem 5.10*

5.11. Convert the following problem into an equivalent homogeneous and isotropic medium if

Layer	*Thickness*	*Hydraulic conductivity*
A	3 m	$K = 10\times10^{-6}$ m/s
B	2 m	$K = 5\times10^{-6}$ m/s

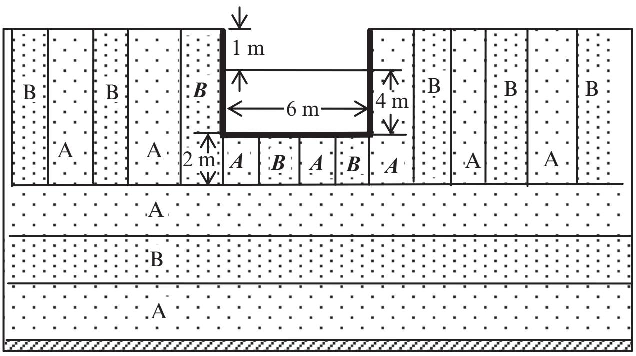

Figure 5.27 *Problem 5.11*

5.12. Convert the following problem into an equivalent homogeneous and isotropic medium

Layer	*Thickness*	*Hydraulic conductivity*
A	3 m	$K = 10\times10^{-6}$ m/s
B	2 m	$K = 5\times10^{-6}$ m/s

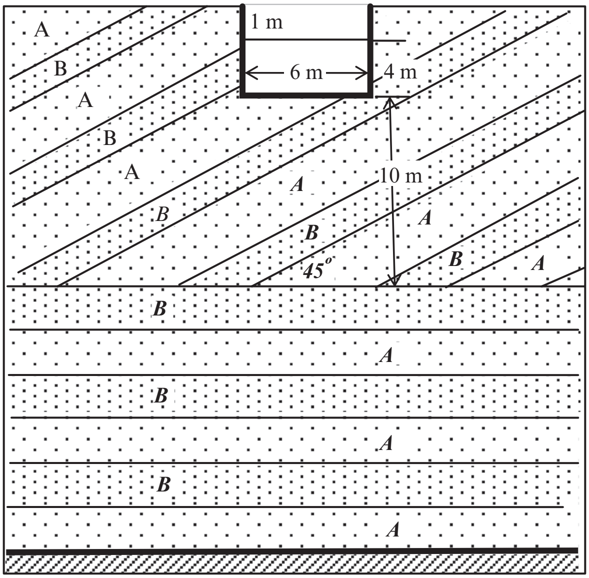

Figure 5.28 *Problem 5.12*

5.13. For a three layered porous media show that $K_x \geq K_y$ where K_x and K_y are hydraulic conductivities parallel and normal to layers respectively.

5.14. Starting from the *N–S* Equations obtain Darcy's law stating all the assumptions involved therein and defining velocity potential, intrinsic permeability, and hydraulic conductivity.

5.15. For a layered porous media show that $K_x/K_y \geq 1$ and $1/K_\alpha = \cos^2\alpha/K_x + \sin^2\alpha/K_y$; where K_x and K_y are hydraulic conductivities parallel and normal to layers respectively, and α is an angle with direction of layers.

5.16. Obtain the relation between groundwater flow directions if it occurs from one homogeneous and isotropic porous medium to another homogeneous and isotropic porous medium.

Chapter 6 Theory of Groundwater Flow

Groundwater in its natural state is invariably moving. This movement is governed by established hydraulic principles.

6.1 Governing Equations in Cartesian Coordinates

The differential equations for groundwater flow are developed from principles of mass conservation in a *representative elementary volume* (REV) of size Δx, Δy, and Δz (Figure 6.1). The mass conservation statement can be written as

mass inflow rate—mass outflow rate = change of mass storage with time

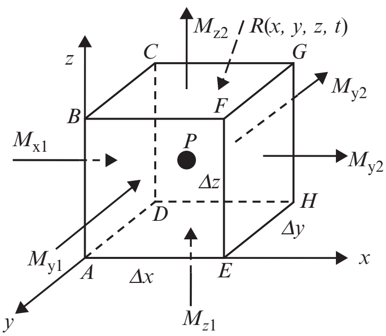

Figure 6.1 *Representative elementary volume*

A REV is defined as a volume exhibiting the average properties of the porous media around a point P (x, y, z), which is the center of the volume. For reference purposes, let's label the six faces of the REV as x_1 ($ABCD$), x_2 ($HGFE$), y_1 ($EFBA$), y_2 ($DCGH$), z_1 ($HEAD$), and z_2 ($GFBC$). Now, assume that the water mass fluxes through the six faces are M_{x1}, M_{x2}, M_{y1}, M_{y2}, M_{z1}, and M_{z2}, respectively. Furthermore, ρ_w is the density of water and η is the porosity in the REV, so that the initial mass within the REV is

$$M = \rho_w \eta \Delta x \Delta y \Delta z \tag{6.1}$$

Also, there exists a groundwater source of strength R (volumetric source rate per unit volume), hence the mass inflow rate (M_s) due to source is

$$M_s = \rho_w R(x, y, z, t) \Delta x \Delta y \Delta z \tag{6.2}$$

The mass conservation equation may be rewritten in mathematical terms as

$$M_{x1} - M_{x2} + M_{y1} - M_{y2} + M_{z1} - M_{z2} + M_s = \frac{\partial}{\partial t}\left(\rho_w \eta \Delta x \Delta y \Delta z\right) \tag{6.3}$$

The mass influx of water in the direction i is expressed as

$$M_i = \rho_w v_i \Delta A_i \tag{6.4}$$

where, v_i is the i (= x, y, and z) component of the Darcy velocity vector, and ΔA_i is the area perpendicular to the flow direction i. To obtain the mass outflow rates (M_{i2}) through the opposite face, we can use truncated Taylor's expansion series as

$$M_{i2} = M_i + \frac{\partial M_i}{\partial \mathrm{i}} \Delta i \tag{6.5}$$

Therefore, the mass inflow rate in the x-direction through the inflow face x_1 ($ABCD$) is

$$M_{x1} = \rho_w v_x \Delta y \Delta z \tag{6.6}$$

and the mass outflow rate through at the outflow face x_2 ($HGFE$) is

$$M_{x2} = M_{x1} + \frac{\partial M_{x1}}{\partial x} \Delta x \tag{6.7}$$

The net inflow rate into the REV in the x-direction is the difference between the inflow and the outflow rates would be

$$M_{x1} - M_{x2} = M_{x1} - \left(M_{x1} + \frac{\partial M_{x1}}{\partial x} \Delta x \right) = -\frac{\partial M_{x1}}{\partial x} \Delta x = -\frac{\partial \left(\rho_w v_x \right)}{\partial x} \Delta x \Delta y \Delta z \tag{6.8}$$

Similarly, the net flow rates into the REV in the y-and z-directions are

$$M_{y1} - M_{y2} = -\frac{\partial M_{y1}}{\partial y} \Delta y = -\frac{\partial \left(\rho_w v_y \right)}{\partial y} \Delta x \Delta y \Delta z \tag{6.9}$$

and

$$M_{z1} - M_{z2} = -\frac{\partial M_{z1}}{\partial z} \Delta z = -\frac{\partial \left(\rho_w v_z \right)}{\partial z} \Delta x \Delta y \Delta z \tag{6.10}$$

Total net inflow rate into the REV, which is equal to mass inflow rate minus mass outflow rate, become

$$M_{x1} - M_{x2} + M_{y1} - M_{y2} + M_{z1} - M_{z2} = -\left(\frac{\partial \left(\rho_w v_x \right)}{\partial x} + \frac{\partial \left(\rho_w v_y \right)}{\partial y} + \frac{\partial \left(\rho_w v_z \right)}{\partial z} \right) \Delta x \Delta y \Delta z \tag{6.11}$$

The change of mass in groundwater storage with time within the REV is

$$\frac{\partial M}{\partial t} = \frac{\partial \left(\rho_w \eta \Delta x \Delta y \Delta z \right)}{\partial t} \tag{6.12}$$

According to mass conservation, the net rate of water inflow is equal to the change in storage, thus collecting Eqs (6.2) and (6.11) and dividing both sides by volume of REV (i.e., $\Delta x \Delta y \Delta z$)

$$-\left(\frac{\partial \left(\rho_w v_x \right)}{\partial x} + \frac{\partial \left(\rho_w v_y \right)}{\partial y} + \frac{\partial \left(\rho_w v_z \right)}{\partial z} \right) + \rho_w R(x, y, z, t) = \frac{1}{\Delta x \Delta y \Delta z} \frac{\partial M}{\partial t} \tag{6.13}$$

By making a further assumption that the density of the fluid does not vary spatially, the density term on the left-hand side can be taken out as a constant so that Eqn. (6.13) becomes

$$\frac{\partial(v_x)}{\partial x}+\frac{\partial(v_y)}{\partial y}+\frac{\partial(v_z)}{\partial z}-R=-\frac{1}{\rho_w \Delta x \Delta y \Delta z}\frac{\partial M}{\partial t} \tag{6.14}$$

The right side of Eqn. (6.14) is related to the specific storage of an aquifer by

$$\frac{1}{\rho_w \Delta x \Delta y \Delta z}\frac{\partial M}{\partial t}=S_s\frac{\partial h}{\partial t} \tag{6.15}$$

where, S_s is the specific storage. Use of Darcy's law (momentum equation) for velocities v_x, v_y and v_z and Eqn. (6.15) in Eqn. (6.14) results

$$\frac{\partial}{\partial x}\left(K_x\frac{\partial h}{\partial x}\right)+\frac{\partial}{\partial y}\left(K_y\frac{\partial h}{\partial y}\right)+\frac{\partial}{\partial z}\left(K_z\frac{\partial h}{\partial z}\right)+R=S_s\frac{\partial h}{\partial t} \tag{6.16}$$

Equation (6.16) is the main equation of groundwater flow in saturated media. It can be written in many forms that apply to a variety of different conditions. Here are some of these alternative equations and the conditions under which they apply.

6.1.1 Without Source/Sink

If there is no source or sink in the control volume then $R(x, y, z, t) = 0$ and Eqn. (6.16) becomes

$$\frac{\partial}{\partial x}\left(K_x\frac{\partial h}{\partial x}\right)+\frac{\partial}{\partial y}\left(K_y\frac{\partial h}{\partial y}\right)+\frac{\partial}{\partial z}\left(K_z\frac{\partial h}{\partial z}\right)=S_s\frac{\partial h}{\partial t} \tag{6.17}$$

6.1.2 Steady-State flow

Under steady-state flow conditions RHS of Eqn. (6.16) becomes zero so

$$\frac{\partial}{\partial x}\left(K_x\frac{\partial h}{\partial x}\right)+\frac{\partial}{\partial y}\left(K_y\frac{\partial h}{\partial y}\right)+\frac{\partial}{\partial z}\left(K_z\frac{\partial h}{\partial z}\right)+R(x,y,z)=0 \tag{6.18}$$

with source and

$$\frac{\partial}{\partial x}\left(K_x\frac{\partial h}{\partial x}\right)+\frac{\partial}{\partial y}\left(K_y\frac{\partial h}{\partial y}\right)+\frac{\partial}{\partial z}\left(K_z\frac{\partial h}{\partial z}\right)=0 \tag{6.19}$$

without source. If the porous medium is homogeneous and isotropic ($K_x = K_y = K_z$), Eqn. (6.19) simplifies to the well-known Laplace equation

$$\frac{\partial^2 h}{\partial x^2}+\frac{\partial^2 h}{\partial y^2}+\frac{\partial^2 h}{\partial z^2}=0 \tag{6.20}$$

6.1.3 Unsteady State flow

The relevant equations for groundwater flow in isotropic and homogeneous medium for unsteady flow condition are

$$\frac{\partial^2 h}{\partial x^2}+\frac{\partial^2 h}{\partial y^2}+\frac{\partial^2 h}{\partial z^2}+\frac{R}{K}=\frac{S_s}{K}\frac{\partial h}{\partial t} \tag{6.21}$$

with source

$$\frac{\partial^2 h}{\partial x^2}+\frac{\partial^2 h}{\partial y^2}+\frac{\partial^2 h}{\partial z^2}=\frac{S_s}{K}\frac{\partial h}{\partial t} \tag{6.22}$$

without source.

6.1.4 Diffusion Form

Assuming constant specific storage and dividing both sides of Eqn. (6.16) by S_s, the equation is transformed into

$$\frac{\partial}{\partial x}\left(\frac{K_x}{S_s}\frac{\partial h}{\partial x}\right)+\frac{\partial}{\partial y}\left(\frac{K_y}{S_s}\frac{\partial h}{\partial y}\right)+\frac{\partial}{\partial z}\left(\frac{K_z}{S_s}\frac{\partial h}{\partial z}\right)+\frac{R}{S_s}=\frac{\partial h}{\partial t} \tag{6.23}$$

where, K_x/S_s, K_y/S_s, and K_z/S_s are called *hydraulic diffusivities* in the x-, y-, and z-directions, respectively. Writing the equation in this form shows that the groundwater flow equation is a form of diffusion equation in which the hydraulic diffusivities and hydraulic gradients in the x-, y-, and z-directions are the determining factors.

Multiplying both sides of Eqn. (6.16) by the aquifer thickness (b) gives

$$\frac{\partial}{\partial x}\left(T_x\frac{\partial h}{\partial x}\right)+\frac{\partial}{\partial y}\left(T_y\frac{\partial h}{\partial y}\right)+\frac{\partial}{\partial z}\left(T_z\frac{\partial h}{\partial z}\right)=S\frac{\partial h}{\partial t} \tag{6.24}$$

where, $K_x b = T_x$; $K_y b = T_y$; and $K_z b = T_z$ are transmissivities in the x-, y-, and z-directions and storativity $S = S_s b$. This form of the groundwater-flow equation is solved in MODFLOW.

6.2 Compressibility of Aquifers

To treat the compressibility of aquifers the following assumption are made

(i) The elemental volume is constrained in lateral directions and undergoes change in length only in z-direction.
(ii) The pore water is compressible.
(iii) The solid grains of the aquifer are incompressible but the pore structure is compressible.

Figure 6.2 shows a REV for a compressible aquifer.

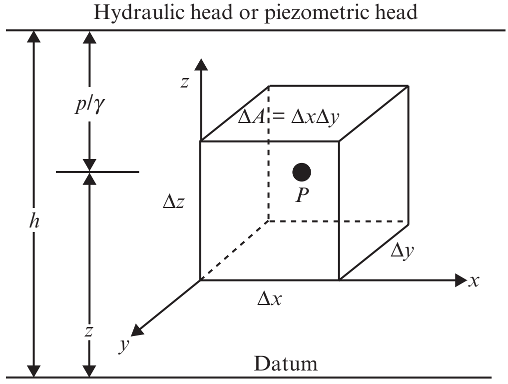

Figure 6.2 *REV for compressible aquifer*

Noting that $M = \rho_w \eta \Delta x \Delta y \Delta z$ from Eqn. (6.1) and as assumed above, the change in M with time happens as, η and Δz may vary due to vertical compression or expansion of the medium, and ρ_w may change in time as well as in space. But variations of the lateral dimensions of aquifers subject to variable flow are negligible because of the constraints of these aquifers by their surroundings. It follows that

$$\frac{\partial M}{\partial t} = \frac{\partial(\rho_w \eta \Delta z)}{\partial t}\Delta x \Delta y = \left[\rho_w \eta \frac{\partial(\Delta z)}{\partial t} + \rho_w \Delta z \frac{\partial \eta}{\partial t} + \eta \Delta z \frac{\partial \rho_w}{\partial t}\right]\Delta x \Delta y \tag{6.25}$$

It remains now to express the three terms in the right hand side of Eqn. (6.25) in terms of the compressibility α of the aquifer, the compressibility β of the fluid, and the pore pressure p.

6.2.1 Compressibility of Aquifer Material

Here the concept of vertical compressibility of the granular skeleton of the medium, treated as continuum, is introduced. $\alpha = 1/E_b$, where E_b is the bulk modulus of elasticity of this skeleton. The stress σ_z on the intergranular skeleton in the vertical direction is called intergranular pressure or stress. By definition of bulk modulus

$$E_b = -\frac{\textit{change in pressure}}{\textit{change in volume per unit volume}} = -\frac{d\sigma_z}{d(\Delta z)/\Delta z} = \frac{1}{\alpha} \tag{6.26}$$

So that

$$d(\Delta z) = -\alpha \, \Delta z \, d\sigma_z \qquad \Rightarrow \qquad \frac{\partial(\Delta z)}{\partial t} = -\alpha \, \Delta z \frac{\partial \sigma_z}{\partial t} \tag{6.27}$$

6.2.2 Compressibility of Voids

Volume of voids is $\eta \Delta x \Delta y \Delta z$ so the volume of solid grains $V_s = (1\text{-}\eta)\Delta x \Delta y \Delta z$ which may be considered as constant because the compressibility of the individual grains is considerably smaller than that of their skeleton and is also smaller than the compressibility of water. The total derivative of this quantity is zero, or

$$dV_s = d\left[(1-\eta)\Delta x \Delta y \Delta z\right] = 0 \tag{6.28}$$

Again Δx and Δy, the lateral dimensions of the volume element, do not change in comparison to the change in the vertical Δz. Therefore Δx and Δy in the above total derivative is treated as a constant, and only two terms remain, thus

$$\Delta z \, d(1-\eta) + (1-\eta) d(\Delta z) = 0 \qquad \Rightarrow \qquad d\eta = \frac{1-\eta}{\Delta z} d(\Delta z) \tag{6.29}$$

or

$$\frac{\partial \eta}{\partial t} = \frac{1-\eta}{\Delta z}\frac{\partial(\Delta z)}{\partial t} \tag{6.30}$$

This expression may be modified somewhat as

$$\frac{\partial \eta}{\partial t} = -(1-\eta)\,\alpha \frac{\partial \sigma_z}{\partial t} \tag{6.31}$$

This shows that the first and second terms are really not independent but that they express the effects of the same cause, namely, the vertical compression of the medium.

6.2.3 Compressibility of Fluid

To introduce the compressibility β of the fluid or the reciprocal of its bulk modulus of elasticity

$$\beta = -\frac{dV_f/V_f}{dp} \quad \Rightarrow \quad \frac{d(V_f)}{V_f} = -\beta\, dp \tag{6.32}$$

Here p is the pressure experience by water in the pores and is called *pore pressure* or neutral pressure.

From conservation of mass

$$\rho_w V_f = \rho_{w0} V_{f0} = const \tag{6.33}$$

In which ρ_{w0} and V_{f0} are constant reference values of density and elemental volume of fluid. Total differentiation of this equation gives

$$\rho_w\, d(V_f) + V_f\, d(\rho_w) = 0 \quad \Rightarrow \quad \frac{d(V_f)}{V_f} = -\frac{d(\rho_w)}{\rho_w} \tag{6.34}$$

Hence from Eqs (6.32) and (6.34)

$$\rho_w\, \beta\, dp = d(\rho_w) \quad \text{or} \quad \rho_w\, \beta \frac{\partial p}{\partial t} = \frac{\partial \rho_w}{\partial t} \tag{6.35}$$

At any depth intergranular pressure and pore pressure add to combined pressure. The combined pressure is numerically equal to the weight of all the matter that rests above per unit area if arching effects of the overlying strata are neglected. It follows that

$$\sigma_z + p = const \quad \Rightarrow \quad d\sigma_z = -dp \tag{6.36}$$

Therefore Eqn. (6.35) can be written as

$$\frac{\partial \rho_w}{\partial t} = -\rho_w\, \beta \frac{\partial \sigma_z}{\partial t} \tag{6.37}$$

6.2.4 Overall Compressibility

Making use of Eqs (6.27), (6.31) and (6.37) in Eqn. (6.25)

$$\frac{\partial M}{\partial t} = -\left[\rho_w \eta \alpha + \rho_w (1-\eta)\alpha + \eta \beta \rho_w\right] \Delta x \Delta y \Delta z \frac{\partial \sigma_z}{\partial t} = \rho_w \Delta x \Delta y \Delta z (\alpha + \eta\beta) \frac{\partial p}{\partial t} \tag{6.38}$$

We know that $h = \dfrac{p}{\rho_w g} + z + const$ or $p = \rho_w g (h - z) + const$; taking partial derivative

$$\frac{\partial p}{\partial x} = \rho_w g \frac{\partial h}{\partial x} + \frac{p}{\rho_w} \frac{\partial \rho_w}{\partial x} \tag{6.39}$$

$$\frac{\partial p}{\partial y} = \rho_w g \frac{\partial h}{\partial y} + \frac{p}{\rho_w} \frac{\partial \rho_w}{\partial y} \tag{6.40}$$

$$\frac{\partial p}{\partial z}=\rho_w g\left(\frac{\partial h}{\partial x}-1\right)+\frac{p}{\rho_w}\frac{\partial \rho_w}{\partial z} \tag{6.41}$$

$$\frac{\partial p}{\partial t}=\rho_w g\frac{\partial h}{\partial t}+\frac{p}{\rho_w}\frac{\partial \rho_w}{\partial t} \tag{6.42}$$

Using $dp=\dfrac{1}{\rho_w \beta}d\rho_w$ from Eqn. (6.35) in the above equations

$$\frac{\partial \rho_w}{\partial x}=\frac{1}{1-\beta p}\beta\rho_w^2 g\frac{\partial h}{\partial x} \tag{6.43}$$

$$\frac{\partial \rho_w}{\partial y}=\frac{1}{1-\beta p}\beta\rho_w^2 g\frac{\partial h}{\partial y} \tag{6.44}$$

$$\frac{\partial \rho_w}{\partial z}=\frac{1}{1-\beta p}\beta\rho_w^2 g\left(\frac{\partial h}{\partial x}-1\right) \tag{6.45}$$

$$\frac{\partial \rho_w}{\partial t}=\frac{1}{1-\beta p}\beta\rho_w^2 g\frac{\partial h}{\partial t} \quad \text{or} \quad \frac{\partial p}{\partial t}=\frac{1}{1-\beta p}\rho_w g\frac{\partial h}{\partial t} \tag{6.46}$$

Using Eqn. (6.46) in Eqn. (6.38)

$$\frac{\partial M}{\partial t}=\Delta x\Delta y\Delta z\left(\alpha+\eta\beta\right)\frac{1}{1-\beta p}\rho_w^2 g\frac{\partial h}{\partial t} \tag{6.47}$$

Comparing Eqs (6.15) and (6.47)

$$S_s=\frac{1}{1-\beta p}\rho_w g\left(\alpha+\eta\beta\right)\approx \rho_w g\left(\alpha+\eta\beta\right) \tag{6.48}$$

For practical values of p in groundwater flow and for bulk modulus β for water, the ratio $1/(1\text{-}\beta p)$ may be replaced by one as a first approximation. Two parts of specific storage in Eqn. (6.48) may be interpreted as

- $\rho_w g\alpha$ = water in storage released due to the compression of the intergranular skeleton per unit volume and per unit decline of head.
- $\rho_w g\eta\beta$ = water in storage released due to the expansion of the water per unit volume and per unit decline of head.

It may be observed that $\beta > 0$ for a decrease in pore pressure and a resulting expansion of the water. In the computation of S_s, the compressibility of water cannot be neglected because the term $\rho_w g\eta\beta$ may be of the same order of magnitude as the term $\rho_w g\alpha$. The decrease of the head h in a given point of a confined aquifer is generally a result of water withdrawal through pumpage and the accompanying decrease in pore pressure. Indeed the compressibility of aquifer material is relatively important only when the material is completely saturated with water and confined between impervious strata. When the flow is unconfined the compressibility of the material and the water are relatively unimportant compared to unsteady perturbations or vertical displacement of the free surface which affect the flow pattern.

6.3 Governing Equation Considering Compressibility

If flow is also compressible i.e. the density of the fluid varies spatially, then term on the left-hand side in Eqn. (6.13) can be expanded as

$$-\left(v_x\frac{\partial(\rho_w)}{\partial x}+v_y\frac{\partial(\rho_w)}{\partial y}+v_z\frac{\partial(\rho_w)}{\partial z}\right)-\rho_w\left(\frac{\partial(v_x)}{\partial x}+\frac{\partial(v_y)}{\partial y}+\frac{\partial(v_z)}{\partial z}\right)+\rho_w R$$

$$=\frac{1}{\Delta x\Delta y\Delta z}\frac{\partial M}{\partial t} \tag{6.49}$$

Use of Darcy's law for velocities v_x, v_y and v_z and Eqs (6.43), (6.44), and (6.45) in Eqn. (6.49) results

$$\frac{1}{1-\beta p}\beta\rho_w^2 g\left(K_x\left(\frac{\partial h}{\partial x}\right)^2+K_y\left(\frac{\partial h}{\partial y}\right)^2+K_z\frac{\partial h}{\partial z}\left(\frac{\partial h}{\partial z}-1\right)\right)+\rho_w R+$$

$$\rho_w\left(\frac{\partial}{\partial x}\left(K_x\frac{\partial h}{\partial x}\right)+\frac{\partial}{\partial y}\left(K_y\frac{\partial h}{\partial y}\right)+\frac{\partial}{\partial z}\left(K_z\frac{\partial h}{\partial z}\right)\right)=\frac{1}{\Delta x\Delta y\Delta z}\frac{\partial M}{\partial t} \tag{6.50}$$

Combining Eqs (6.47) and (6.50)

$$\frac{\beta\rho_w g}{1-\beta p}\left(K_x\left(\frac{\partial h}{\partial x}\right)^2+K_y\left(\frac{\partial h}{\partial y}\right)^2+K_z\frac{\partial h}{\partial z}\left(\frac{\partial h}{\partial z}-1\right)\right)+R+$$

$$\left(\frac{\partial}{\partial x}\left(K_x\frac{\partial h}{\partial x}\right)+\frac{\partial}{\partial y}\left(K_y\frac{\partial h}{\partial y}\right)+\frac{\partial}{\partial z}\left(K_z\frac{\partial h}{\partial z}\right)\right)=(\alpha+\eta\beta)\frac{\rho_w g}{1-\beta p}\frac{\partial h}{\partial t} \tag{6.51}$$

which is the most general governing equation as it considers compressibility of flow and aquifer, heterogeneity, anisotropy, and unsteady condition. Different particular cases can be deduced from it. Since 1—$\beta p \approx 1$

$$\beta\rho_w g\left(K_x\left(\frac{\partial h}{\partial x}\right)^2+K_y\left(\frac{\partial h}{\partial y}\right)^2+K_z\frac{\partial h}{\partial z}\left(\frac{\partial h}{\partial z}-1\right)\right)+R+$$

$$\left(\frac{\partial}{\partial x}\left(K_x\frac{\partial h}{\partial x}\right)+\frac{\partial}{\partial y}\left(K_y\frac{\partial h}{\partial y}\right)+\frac{\partial}{\partial z}\left(K_z\frac{\partial h}{\partial z}\right)\right)=\rho_w g(\alpha+\eta\beta)\frac{\partial h}{\partial t} \tag{6.52}$$

For incompressible flow $\beta = 0$ and Eqn. (6.52) reduces to Eqn. (6.16).

6.4 Dupuit—Forchhemeir Assumptions and 2-D Equations for Unconfined Flow

If there is no change of hydraulic head in the vertical direction, the relevant equations can be reduced to a two-dimensional groundwater flow equations by dropping z-directions terms. Consider the prism ABCDEF in Figure 6.3 in which the bottom is parallel to the direction of flow and the top surface is the water table. The datum plane for h coincides with the upper surface of the impervious stratum underlying the aquifer.

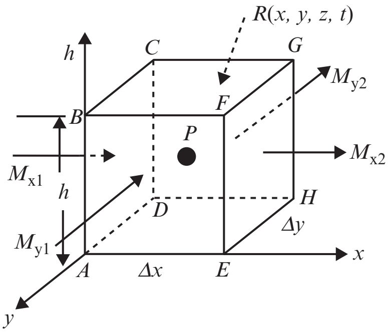

Figure 6.3 *REV for unconfined aquifer*

Applying mass balance for a control volume of size Δx, Δy in x-y plane, similar to confined aquifer except aquifer height h (equal to saturated thickness of aquifer = height of water table from the bed rock) in place of aquifer thickness b and additional inflow into REV through recharge rate R

$$M_{x1} - M_{x2} + M_{y1} - M_{y2} + \rho_w R\Delta x\Delta y = -\frac{\partial M_x}{\partial x}\Delta x - \frac{\partial M_y}{\partial y}\Delta y + \rho_w R\Delta x\Delta y = \frac{\partial M}{\partial t} \tag{6.53}$$

For an unconfined aquifer, direct analytical treatment is not possible. The difficulty arises from the fact that the water table in the 2-D case represents a flow line. The shape of the water table determines the flow distribution, but at the same time the flow distribution governs the water table shape. To obtain a solution, Dupuit assumed (i) the velocity of the flow to be proportional to the tangent of the hydraulic gradient instead of the sine, and (ii) the flow to be horizontal and uniform everywhere in a vertical section. These Dupuit–Forchhemeir assumptions, although permitting solution to be obtained, limit the application of the results. With these assumptions

$$M_x = \rho_w v_x h\Delta y; \quad M_y = \rho_w v_y h\Delta x; \quad v_x = -K_x\frac{\partial h}{\partial x}; \quad v_y = -K_y\frac{\partial h}{\partial y} \tag{6.54a-d}$$

For incompressible flow

$$\frac{\partial}{\partial x}\left(K_x h\frac{\partial h}{\partial x}\right) + \frac{\partial}{\partial y}\left(K_y h\frac{\partial h}{\partial y}\right) + R = S\frac{\partial h}{\partial t} \tag{6.55}$$

which can be written as

$$\frac{\partial}{\partial x}\left(K_x\frac{\partial h^2}{\partial x}\right) + \frac{\partial}{\partial y}\left(K_y\frac{\partial h^2}{\partial y}\right) + 2R = 2S\frac{\partial h}{\partial t} \tag{6.56}$$

For water table aquifer storage coefficient = specific yield ($S = S_y$). If medium is isotropic then $K_x = K_y = K$ and we have

$$\frac{\partial^2 h^2}{\partial x^2} + \frac{\partial^2 h^2}{\partial y^2} + \frac{2R}{K} = \frac{2S_y}{K}\frac{\partial h}{\partial t} \tag{6.57}$$

This relation is known as *Boussinesq Equation*. This equation can only be used when vertical hydraulic gradient is small and negligible. For general problems of flow unconfined aquifer, general equation should be used. If there is no recharge and flow is steady then

$$\frac{\partial^2 h^2}{\partial x^2} + \frac{\partial^2 h^2}{\partial y^2} = \nabla^2 h^2 = 0 \tag{6.58}$$

That is the Laplace equation in h^2 for unconfined flow.

6.5 Solution and Boundary Conditions

A governing partial differential equation has an infinite number of possible solutions, each of which corresponds to a particular case of flow through a porous medium domain. To obtain one particular solution (from infinite solutions) corresponding to a specific problem of interest, it is necessary to provide supplementary information e.g.

- Geometry of flow domain
- Values of physical coefficients
- Initial conditions
- Boundary conditions

The partial differential equation together with the supplementary information defines an individual problem leading to a particular solution. Different *boundary and initial conditions* lead to different solutions and hence these should be determined or assumed correctly on the basis of available information and past experience. *Initial conditions* include the specification of h at all points within the domain D at some initial time usually denoted as $t = 0$. This can be written schematically as specifying

$$h = f(x, y, z, 0) \tag{6.59}$$

For all points x, y, z inside D; f is a known function.

The various types of boundary conditions in flow through porous media are,

(i) *Boundary of prescribed head/potential or Dirichlet boundary or First type boundary*: The head h is prescribed for all points on this boundary S

$$h = f_1(x, y, z, t) \quad \text{on } S \tag{6.60}$$

where f_1 is a known function. A special case is

$$h = h_0 \quad \text{or} \qquad h = Const \qquad \text{on } S \tag{6.61}$$

wherein head is constant on the boundary or the boundary is an equipotential surface.

(ii) *Boundary of prescribed flux or Neumann boundary or Second type boundary*: On this type of boundary, the flux (derivative of head/potential) normal to the boundary surface is prescribed for all points i.e.

$$q_n = C\frac{\partial h}{\partial n} = f_2(x, y, z, t) \quad \text{on } S \tag{6.62}$$

where f_2 is a known function. A special case is an impervious or no flow boundary where the flux normal to the boundary vanishes everywhere.

(iii) *Semipervious Boundary or Cauchy boundary or Third type boundary or Mixed boundary*: On this type of boundary, a functional relationship between the flux and head/potential is prescribed i.e.

$$q_n = h(x, y, z, t) \quad \text{on } S \tag{6.63}$$

(iv) *Unsteady Phreatic Surface with Accretion*: The location and shape of the free surface are unknown; in fact, their determination constitutes part of the required solution. Since the pressure at all points of the phreatic surface S is atmospheric thus,

$$h(x, y, z, t) + Kz = Const \quad \text{on } S \tag{6.64}$$

That in fact gives at any time t a relationship between the coordinates of points of the phreatic surface. Therefore, it may be considered equivalent to $F(x, y, z, t) = Const$, describing the geometry of this surface,

$$F(x, y, z, t) = h(x, y, z, t) + Kz = Const \;\text{ on } S \tag{6.65}$$

The unsteady phreatic surface with accretion is a surface on which a certain property is maintained constant. For such a surface,

$$K_x\left(\frac{\partial h}{\partial x}\right)^2 + K_y\left(\frac{\partial h}{\partial y}\right)^2 + K_z\frac{\partial h}{\partial z}\left(\frac{\partial h}{\partial z} - 1\right) + R\left(1 - \frac{\partial h}{\partial z}\right) = \eta\frac{\partial h}{\partial t} \tag{6.66}$$

The difficulty with boundary condition Eqn. (6.65) stems from the fact that the distribution $h(x, y, z, t)$, and hence $F(x, y, z, t)$ is unknown before the problem is solved. In fact, in order to determine h we must know the boundary's location F and in order to know where this boundary is, we have to know h. Iterative techniques are used to overcome this difficulty in numerical techniques on the other hand analytical techniques are seldom capable to solve a problem with this complicated boundary condition Eqn. (6.66) except for some particular classes of problems.

(v) *Seepage Face*: Along a seepage face water emerges from the flow domain trickling downward to the adjacent body of water. The pressure along a seepage face is atmospheric pressure and hence similar to phreatic surface the boundary condition is,

$$h(x, y, z, t) + Kz = Const \quad \text{on } S \tag{6.67}$$

However the geometry of boundary S along the seepage face is known that is $F(x, y, z, t) = Const$, except for its upper limit which is exit point of unknown phreatic surface. The location of this point is part of the required solution. In unsteady flow the location of the upper limit of the seepage face varies with time.

(vi) *Surface of Discontinuity in Conductivity*: On any common point on the surface of discontinuity the elevation and pressure are same and also the flux across the boundary should be same from continuity requirement i.e.

$$h_1(x, y, z, t) = h_2(x, y, z, t) \;\text{ and }\; q_{n1} = q_{n2};\;\; K_1\frac{\partial h_1}{\partial n} = K_2\frac{\partial h_2}{\partial n} \tag{6.68}$$

where, n is distance measured along the normal to the boundary at the common point. Thus, two boundary conditions to be satisfied which requires simultaneous solution of two equations for h_1 and h_2.

There may be additional types of boundary conditions, for example if effect of capillary fringe is considered. Finally any problem of groundwater flow can be stated mathematically by

- Defining the flow domain; part of the boundary may be at infinity; sometimes the domain boundary is unknown a priority.
- Specifying the governing partial differential equation to be satisfied by h (other variables p, ϕ, ρ, or ψ can be used in place of h) at all points within the flow domain and $t > 0$.
- Specifying the boundary conditions that must be satisfied by h at all points of the boundary and at all times.
- Prescribing initial conditions at all the points of the flow domain, when the flow is unsteady.

Once a problem is mathematically formulated, it can be solved by an appropriate technique. A well posed mathematical problem satisfies *existence*, *uniqueness* and *stability* (three basic requirements) of the solution i.e. the solution must exist, the solution must be uniquely determined and the solution should depend continuously on the data (be stable). In majority of cases the governing partial differential equation, boundary conditions, domain geometry or material properties or their combination is not simple to be solved by analytical techniques and hence numerical techniques are adopted. Analytical solutions are possible for simple cases and few of such cases are dealt in the following section.

6.6 Analytical Solutions for Simple Groundwater Flow Problems

6.6.1 Steady Unidirectional Flow in Confined Aquifer

Let groundwater flows with a velocity u_x in the x-direction in a confined aquifer of uniform thickness b (Figure 6.4). Then for steady flow Laplace equation reduces into the following ordinary differential equation

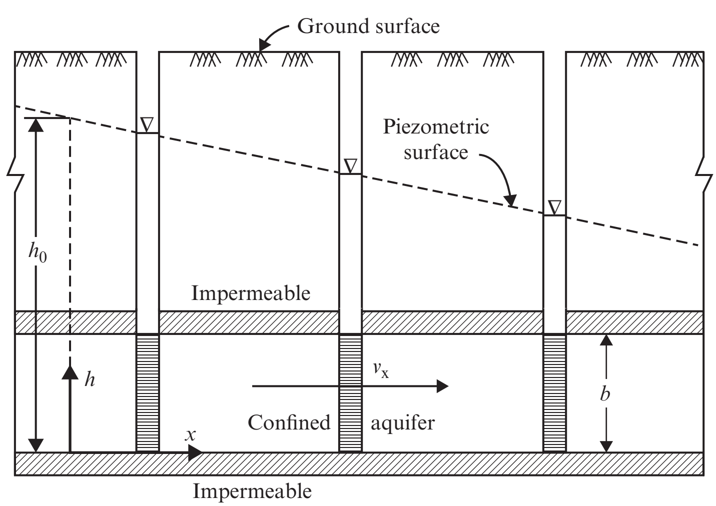

Figure 6.4 *Confined aquifer*

$$\frac{d^2h}{dx^2} = 0 \tag{6.69}$$

which has its solution

$$\frac{dh}{dx} = C_1 \quad \Rightarrow \quad h = C_1 x + C_2 \tag{6.70}$$

where, h is the head above a given datum and C_1 and C_2 are constants of integration. Assuming $h = h_0$ when $x = 0$ and $dh/dx = -(v_x/K)$ from Darcy's law, then, $C_2 = h_0$ and $C_1 = -\frac{v_x}{K}$

Therefore

$$h = -\frac{v_x x}{K} + h_0 \tag{6.71}$$

This states that the head decreases linearly with flow in the x-direction.

6.6.2 Steady Flow in a Varying Thickness Confined Aquifer

The governing equation for a steady groundwater flow in a homogeneous isotropic (wrt K) confined aquifer of varying thickness (Figure 6.5) in the x-direction becomes

$$\frac{\partial}{\partial x}\left(T_x \frac{\partial h}{\partial x}\right) = 0 \quad \Rightarrow \frac{d}{dx}\left(b_x \frac{dh}{dx}\right) = 0 \tag{6.72}$$

where the thickness of aquifer at section x is $b_x = b_0 - \frac{b_0 - b_1}{L} x$

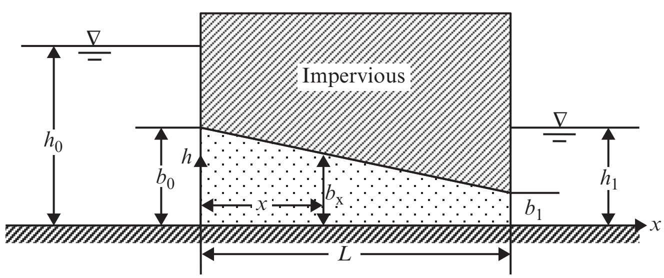

Figure 6.5 *Confined aquifer of varying thickness*

Integrating this ordinary differential equation

$$\frac{dh}{dx} = \frac{C_1}{b_x} \Rightarrow h = -\frac{C_1 L}{b_0 - b_1} \ln\left(b_0 - \frac{b_0 - b_1}{L} x\right) + C_2 \tag{6.73}$$

Boundary conditions $h = h_0$ at $x = 0$ and $h = h_1$ at $x = L$ can be used to find C_1 and C_2 so

$$C_1 = -\frac{h_0 - h_1}{L} \frac{b_0 - b_1}{\ln(b_0 / b_1)} \tag{6.74}$$

and

$$C_2 = h_0 - (h_0 - h_1) \frac{\ln b_0}{\ln(b_0 / b_1)} \tag{6.75}$$

Therefore,

$$h = h_0 - \frac{h_0 - h_1}{\ln(b_0 / b_1)}\left\{\ln b_0 - \ln\left(b_0 - (b_0 - b_1)x / L\right)\right\} \tag{6.76}$$

or

$$\frac{h_0 - h}{h_0 - h_1} = \frac{\ln(b_0 / b_x)}{\ln(b_0 / b_1)} = \frac{\ln b_0 - \ln b_x}{\ln b_0 - \ln b_1} \tag{6.77}$$

The discharge per unit width at any section x can be found by

$$q = A_x.v_x = b_x.1.(-)K\frac{dh}{dx} = -KC_1 = K\frac{h_0 - h_1}{L}\frac{(b_0 - b_1)}{(\ln b_0 - \ln b_1)} \tag{6.78}$$

This shows that q is independent of x as it should be from the continuity of flow.

Time to travel from upstream to downstream reservoir

$$v_s = \frac{v_x}{\eta} = \frac{dx}{dt} \qquad \Rightarrow dt = \frac{\eta dx}{v_x} \qquad \Rightarrow t = \frac{\eta}{KC_1}\int_0^L b_x dx = \frac{\eta L^2}{2K}\frac{b_0 + b_1}{h_0 - h_1}\frac{\ln b_0 - \ln b_1}{b_0 - b_1} \tag{6.79}$$

6.6.3 Steady Unidirectional Flow in Unconfined Aquifer

For steady unidirectional flow in an unconfined aquifer (Figure 6.6) without recharge, the governing equation reduces to

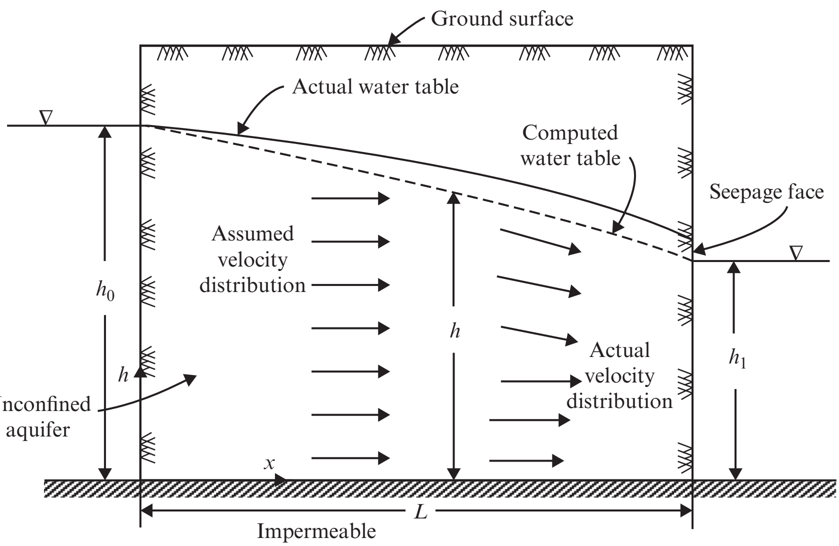

Figure 6.6 *Unconfined aquifer*

$$\frac{d^2h^2}{dx^2} = 0 \tag{6.80}$$

The integration of this ordinary differential equation renders

$$h^2 = C_1 x + C_2 \tag{6.81}$$

To determine integration constants, differentiate it

$$2h\frac{dh}{dx} = C_1 \tag{6.82}$$

Another expression of $h\frac{dh}{dx}$ is found in the flow rate per unit width q at any vertical section with Dupuit's assumptions as

$$q = -Kh\frac{dh}{dx} \qquad \Rightarrow h\frac{dh}{dx} = -\frac{q}{K} \tag{6.83}$$

Therefore, $C_1 = -2q/K$. The constant C_2 is determined by the condition that for $x = 0$, $h = h_0$. Therefore, $C_2 = h_0^2$. The equation of water table after substituting C_1 and C_2 in Eqn (6.81) becomes

$$h^2 = -\frac{2q}{K}x + h_0^2 \tag{6.84}$$

which indicates that the water table is parabolic in form. Neglecting the existence of a seepage face at the exit, that is, the condition that for $x = L$, $h = h_1$ may be used to determine q as

$$q = \frac{K}{2L}\left(h_0^2 - h_1^2\right) \tag{6.85}$$

The travel time between two points in the unconfined aquifer is

$$dt = \frac{\eta dx}{v_x} \qquad \Rightarrow t = \frac{2\eta}{KC_1}\int_{x1}^{x2} hdx == \frac{\eta}{q}\int_{x1}^{x2}\sqrt{h_0^2 - \frac{2q}{K}x}dx \tag{6.86}$$

In the direction of flow, the parabolic water table increases in slope and two Dupuit assumptions become increasingly poor approximations to the actual flow; therefore, the actual water table deviates more and more from the computed position in the direction of flow. The fact that the actual water table lies above the computed one is that the Dupuit flows are all assumed horizontal, whereas the actual velocities of the same magnitude have a downward vertical component so that a greater saturated thickness is for the same discharge. At the downstream boundary a discontinuity in flow forms because no consistent flow pattern can connect a water table directly to a downstream free water surface. The water table actually approaches the boundary tangentially above the water body surface and forms a seepage face. However, for flat slopes, where the sine and tangent are nearly equal, Dupuit's solution closely predicts the water table position except near the outflow. The solution also, accurately determines q or K for given boundary heads.

6.6.4 Steady Unidirectional Flow with Recharge in Unconfined Aquifer

For steady unidirectional flow in an unconfined aquifer with recharge as shown in Figure 6.7, the governing equation reduces to

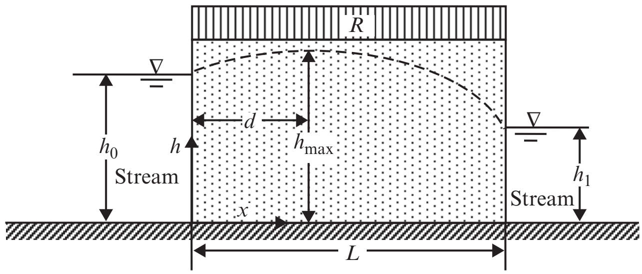

Figure 6.7 *Unconfined aquifer with recharge*

$$\frac{d^2h^2}{dx^2} + \frac{2R}{K} = 0 \tag{6.87}$$

The integration of this ordinary differential equation renders

$$2h\frac{dh}{dx} + \frac{2R}{K}x = C_1 \tag{6.88}$$

$$h^2 = -\frac{R}{K}x^2 + C_1x + C_2 \tag{6.89}$$

Boundary conditions $h = h_0$ at $x = 0$ and $h = h_1$ at $x = L$ can be used to find C_1 and C_2 so $C_2 = h_0^2$ and

$$C_1 = -\frac{h_0^2 - h_1^2}{L} + \frac{RL}{K} \tag{6.90}$$

Therefore,

$$h^2 = h_0^2 - \frac{R}{K}x^2 - \frac{h_0^2 - h_1^2}{L}x + \frac{RL}{K}x \tag{6.91}$$

which shows that water table varies elliptically. The water table first rises and after attaining h_{max} it falls. At h_{max} the water table slope is zero and known as *water divide line*. At the water divide line seepage discharge is zero and on one side of it the seepage is toward one stream and on the other side the seepage is toward the other stream. Thus, the location of the water divide line d can be computed using $dh/dx = 0$ condition as

$$d = \frac{KC_1}{2R} = \frac{L}{2} - \frac{K}{2RL}\left(h_0^2 - h_1^2\right) \tag{6.92}$$

$$h_{max}^2 = h_0^2 + \frac{R}{K}d\left(L-d\right) - \frac{h_0^2 - h_1^2}{L}d \tag{6.93}$$

The discharge per unit width at any section x can be found by

$$q = A_x.v_x = h.1.(-)K\frac{dh}{dx} = K\frac{h_0^2 - h_1^2}{2L} - \frac{RL}{2} + Rx \tag{6.94}$$

The above equation can be used at $x = 0$ and $x = L$ to find the base flows in the streams. It should be noted that total base flow into both streams is equal to the total recharge RL between the streams.

The travel time between two points for this case is

$$dt = \frac{\eta dx}{v_x} \qquad \Rightarrow t = 2\eta \int_{L1}^{L2} \frac{h}{2Rx - KC_1} dx \tag{6.95}$$

This is a complicated function difficult to integrate analytically, though it may be reduced into elliptical integral form and then the solution can be adopted from the standard formulae available in the literature (Byrd and Friedman 1971). For approximate computation of time, the variation in the head from water divide line to the stream may be assumed linear, which is equivalent to assumption of constant hydraulic gradient; for example, the travel time from water divide line to the left stream comes out.

$$dt = \frac{\eta dx}{-K \frac{dh}{dx}} \qquad \Rightarrow t = \frac{\eta}{K} \int_0^d \frac{d}{h_{max} - h_0} dx = \frac{\eta}{K} \frac{d^2}{h_{max} - h_0} \tag{6.96}$$

Similarly, travel time on the other side of the water divide line can be computed.

SOLVED EXAMPLES

Example 6.1: A confined aquifer (having three different materials) as shown in Figure 6.8 connects two reservoirs. If the upstream reservoir is polluted by a contaminant suddenly, how long will it take the contaminant to reach the downstream reservoir? Also, compute the flow rate. Use K_1 = 20 m/d, K_2 = 5 m/d, K_3 = 10 m/d, and the porosity of all three materials = 0.30.

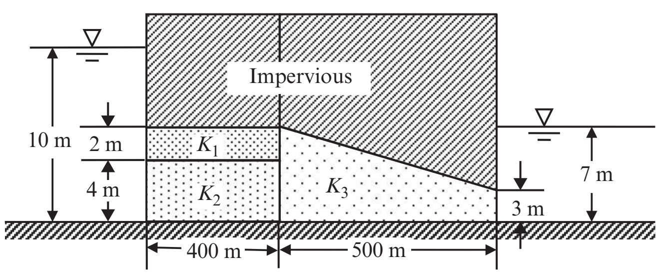

Figure 6.8 *Example 6.1*

Solution: Let assume *h'* be the unknown height of water table at the interface of three mediums. Steady discharge through the confined Medium 1 is

$$q_1 = A_x . v_x = b_x .1.(-)K_1 \frac{dh}{dx} = 2 \times 20 \times \frac{10 - h'}{400} = \frac{10 - h'}{10}$$

Steady discharge through the confined Medium 2 is

$$q_2 = 4 \times 5 \times \frac{10 - h'}{400} = \frac{10 - h'}{20}$$

Steady discharge through the confined variable thickness medium 3 is

$$q_3 = K_3 \frac{h' - h_1}{L_3} \frac{(b_0 - b_1)}{(\ln b_0 - \ln b_1)} = 10 \frac{h' - 7}{500} \frac{(6-3)}{(\ln 6 - \ln 3)} = \frac{3}{50 \ln 2}(h' - 7)$$

From continuity of flow

$$q_1 + q_2 = q_3 \qquad \Rightarrow \qquad \frac{10 - h'}{10} + \frac{10 - h'}{20} = \frac{3}{50 \ln 2}(h' - 7) \quad \Rightarrow h' = 8.9023$$

Hence, flow rate q_3 = 0.165 m^3/d.

Medium 1 and Medium 2 are parallel, but Medium 1 has hydraulic conductivity more than that in Medium 2, hence contaminant will move faster in Medium 1 in comparison to Medium 2. Therefore, the total time taken by the contaminant to reach from upstream to downstream reservoir will be

$$t = t_1 + t_3 = \frac{\eta_1 L_1}{v_{x1}} + \frac{\eta_3}{K_3 C_1} \int_0^{L3} b_x dx = \frac{\eta_1 L_1^2}{K_1 (h_0 - h')} + \frac{\eta_3 L_3^2}{2K_3} \frac{b_0 + b_1}{h' - h_1} \frac{\ln b_0 - \ln b_1}{b_0 - b_1}$$

$$t = \frac{0.3 \times 400^2}{20(10 - 8.9023)} + \frac{0.3 \times 500^2}{2 \times 10} \frac{6+3}{8.9023 - 7} \frac{\ln 6 - \ln 3}{6 - 3} = 2186.39 + 4099.20$$

t = 6285.59 days = 17.22 years.

Example 6.2: A canal is running parallel to and 450 m away from a river in an unconfined aquifer having hydraulic conductivity = 15 m/d and porosity = 0.35. The water surface elevations in the canal and river are 8 m and 10 m, respectively. The area between the canal and river receives an average infiltration of 1.5 m/year, (i) determine the daily discharge of groundwater into the canal and river, (ii) estimate the travel time from the water divide to canal and to river, and (iii) what should be recharge rate and water level in the canal if river is to remain free from contamination even if the area between the canal and river is contaminated?

Solution: Given data—h_1 = 10 m, h_2 = 8 m, L = 450 m, K = 15 m/d, and R = 1.5 m/year.

For flow of water through unconfined aquifer between two water bodies with recharge, the distance of water divide line from canal is given by

$$d = \frac{L}{2} - \frac{K}{2RL}\left(h_0^2 - h_1^2\right) = \frac{450}{2} - \frac{15 \times 365}{2 \times 1.5 \times 450}(64 - 100) = 371\text{m}$$

Using the relationship for head at water divide line

$$h_{\max}^2 = h_0^2 + \frac{K}{4R}\left(\frac{RL}{K} - \frac{h_0^2 - h_1^2}{L}\right)^2 = 64 + \frac{15 \times 365}{4 \times 1.5}\left(\frac{1.6 \times 450}{15 \times 365} - \frac{64 - 100}{450}\right)^2$$

Hence, $h_{\max} = 10.08513\,\text{m}$.

With help of discharge equation at any x

$$q_x = K \frac{h_0^2 - h_1^2}{2L} - \frac{RL}{2} + Rx = 15 \times \frac{64 - 100}{2 \times 450} - \frac{1.5 \times 450}{2 \times 365} + \frac{1.5x}{365}$$

Hence, discharge in the canal for $x = 0$ is $q_c = 1.52466\ \mathrm{m^3/d/m}$.

And similarly discharge (seepage) in river can be computed using $x = 450$ m, hence

$$q_r = 15 \times \frac{64-100}{2\times 450} - \frac{1.5\times 450}{2\times 365} + \frac{1.5\times 450}{365} = 0.32466\,\mathrm{m^3/d/m}$$

Now, velocity of seepage toward canal

$$v_c = \left(\frac{K}{\eta}\right)\left(\frac{\Delta h}{\Delta x}\right) = \left(\frac{15}{0.35}\right)\left(\frac{10.08513-8}{371}\right) = 0.24087\,\mathrm{m/d}$$

hence, travel time from water divide to canal

$$t_c = \frac{371}{0.24087} = 1540.24 \sim 1541\,\mathrm{days}.$$

Similarly, $v_r = \left(\frac{K}{\eta}\right)\left(\frac{\Delta h}{\Delta x}\right) = \left(\frac{15}{0.35}\right)\left(\frac{10.08513-10}{79}\right) = 0.04618\,\mathrm{m/d}$ and

hence travel time toward river is $t_r = \frac{79}{0.04618} = 1710\,\mathrm{days}$.

To make the river water free from contamination, the water divide line needs to be shifted to the river so that flow is unidirectional from river to canal. The location of water divide line is a function of hydraulic conductivity of the aquifer, recharge/infiltration rate, spacing, and water level elevations. As spacing between the canal and river is fixed and the hydraulic conductivity of the aquifer cannot be changed, there are two feasible options for shifting the water divide line at the river itself (i) changing recharge/infiltration rate or (ii) altering the water level elevations in the canal and river.

Adopting the first option $d = \frac{L}{2} - \frac{K}{2RL}\left(h_0^2 - h_1^2\right)$ or $450 = \frac{450}{2} - \frac{15(64-100)}{2\times\frac{R}{365}\times 450}$

so $R = 1.0274\,\mathrm{m/year}$. Thus, if recharge/infiltration rate is reduced from 1.5 to 1.0274 m/year, the water divide line shifts on the river.

In the second option $450 = \frac{450}{2} - \frac{15}{2\times\frac{1.5}{365}\times 450}\left(h_0^2 - 100\right)$; thus, $h_0 = 6.67237$ m

and hence by lowering the water level in canal from 8 m to 6.67 m the water divide line can be pushed to the river.

Hence, both the options, reduction of infiltration rate and lowering of level of water, in canal are reasonable to prevent the river from contamination.

Example 6.3: What will be the baseflow rates to both streams if $h_1 = 12$ m, $h_2 = 10$ m, $R = 1.6$ m/year, and $L = 500$ m for the groundwater flow problem case shown in Figure 6.9? Also, find the location of the steady groundwater divide line, the maximum elevation of the water table, and the travel time from groundwater divide line to the streams.

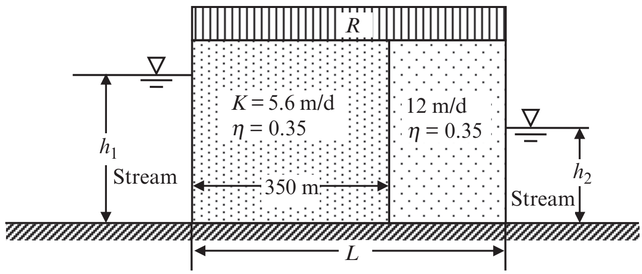

Figure 6.9 *Example 6.3*

Solution: The problem can be solved by different methods.

Method 1: Without medium transformation

Let assume h' be the unknown height of water table at the interface of two mediums. For steady unidirectional flow in an unconfined aquifer with recharge, we have

$$h^2 = h_0^2 - \frac{R}{K}x^2 - \frac{h_0^2 - h_1^2}{L}x + \frac{RL}{K}x\,; \quad \text{and} \quad d = \frac{L}{2} - \frac{K}{2RL}\left(h_0^2 - h_1^2\right);$$

$$h_{\max}^2 = h_0^2 + \frac{K}{4R}\left(\frac{RL}{K} - \frac{h_0^2 - h_1^2}{L}\right)^2; \quad \text{and} \quad q_x = K\frac{h_0^2 - h_1^2}{2L} - \frac{RL}{2} + Rx$$

For Medium 1, K_1 = 5.6 m/d; R = 1.6 m/year; L_1 = 350 m; h_0 = 12 m; and $h_1 = h'$; therefore,

$$h^2 = 12^2 - \frac{1.6x^2}{365 \times 5.6} + \left(\frac{1.6 \times 350}{365 \times 5.6} - \frac{12^2 - h'^2}{350}\right)x\,;$$

$$d = \frac{350}{2} - \frac{5.6 \times 365}{2 \times 1.6 \times 350}\left(12^2 - h'^2\right);$$

$$h_{\max}^2 = 12^2 + \frac{365 \times 5.6}{4 \times 1.6}\left(\frac{1.6 \times 350}{365 \times 5.6} - \frac{144 - h'^2}{350}\right)^2;$$

$$q_x = 5.6\frac{12^2 - h'^2}{2 \times 350} - \frac{1.6 \times 350}{365 \times 2} + \frac{1.6x}{365}$$

and hence

$$q_{350} = K\frac{h_0^2 - h_1^2}{2L} + \frac{RL}{2} = 5.6\frac{144 - h'^2}{700} + \frac{1.6 \times 350}{365 \times 2}$$

For Medium 2, K_2 = 12 m/d; R = 1.6 m/year; L_2 = 150 m; $h_0 = h'$; and h_1 = 10 m; therefore,

$$h^2 = h'^2 - \frac{1.6x^2}{365 \times 12} + \left(\frac{1.6 \times 150}{365 \times 12} - \frac{h'^2 - 10^2}{150} \right) x \, ;$$

$$q_x = 12 \frac{h'^2 - 10^2}{2 \times 150} - \frac{1.6 \times 150}{365 \times 2} + \frac{1.6x}{365}$$

and hence

$$q_0 = -K \frac{h_0^2 - h_1^2}{2L} + \frac{RL}{2} = -12 \frac{h'^2 - 100}{300} + \frac{1.6 \times 150}{365 \times 2}$$

Equating discharges at the interface of mediums

$$5.6 \frac{144 - h'^2}{700} + \frac{1.6 \times 350}{365 \times 2} = \left| -12 \frac{h'^2 - 100}{300} + \frac{1.6 \times 150}{365 \times 2} \right|$$

$$h'^2 = \frac{62479}{480} \qquad \text{or} \qquad h' = 11.409 \text{ m}$$

The baseflow in the streams are

$$q_{x=0} = \frac{RL_1}{2} - \frac{K_1 \left(h_0^2 - h'^2 \right)}{2L_1} = \frac{1.6 \times 350}{365 \times 2} - \frac{5.6 \times \left(12^2 - 130.165 \right)}{2 \times 350} = 0.6564$$

Hence, $q_{x=0} = 0.8025 \text{ m}^3/\text{d}$

$$q_{x=L} = \frac{RL_2}{2} - \frac{K_2 \left(h'^2 - h_1^2 \right)}{2L_2} = \frac{1.6 \times 150}{365 \times 2} - \frac{12 \times \left(130.165 - 10^2 \right)}{2 \times 150} = 1.5353$$

$$q_{x=L} = 1.389 \text{ m}^3/\text{d}$$

Let the maximum height of water table (water divide line) happens in the Medium 1, then its location (after using h' in relation for d for Medium 1) is

$$d = \frac{350}{2} - \frac{5.6 \times 365}{2 \times 1.6 \times 350} \left(12^2 - h'^2 \right) = 149.7474 \text{ m } (<350 \text{ m assumption OK})$$

and corresponding maximum height of the water table is

$$h_{\max}^2 = 12^2 + \frac{365 \times 5.6}{4 \times 1.6} \left(\frac{1.6 \times 350}{365 \times 5.6} - \frac{144 - h'^2}{350} \right)^2$$

Hence, $h_{\max} = 12.71$ m.

Method 2: With equivalent homogeneous medium transformation in main flow direction.

Here, we have steady unidirectional flow in an unconfined aquifer with recharge in x-direction only. Equivalent homogeneous medium in x-direction

$$K_x = \frac{350 + 150}{(350/5.6) + (150/12)} = 6.667 \text{ m/d}$$

Using given values (i.e., L = 500 m; h_0 = 12 m; h_1 = 10 m; K_x = 6.667 m/d; R = 1.6 m/year; and R/K = 1.6/365/6.667), the location of water divide line is

$$d=\frac{L}{2}-\frac{K}{2RL}\left(h_0^2-h_1^2\right)=\frac{500}{2}-\frac{6.667\times 365}{2\times 1.6\times 500}\left(12^2-10^2\right)=250-66.92=183.08\,\mathrm{m}$$

and the corresponding maximum height of water table is

$$h_{\max}^2=h_0^2+\frac{K}{4R}\left(\frac{RL}{K}-\frac{h_0^2-h_1^2}{L}\right)^2=144+\frac{6.667\times 365}{4\times 1.6}\left(\frac{1.6\times 500}{365\times 6.667}-\frac{144-100}{500}\right)^2$$

Hence, $h_{\max}$ = 12.886 m

$$C_1=\frac{2Rd}{K}=\frac{2\times 1.6\times 183.08}{6.667\times 365}=0.24075;\text{ therefore,}$$

$$h'^2=-\frac{R}{K}x^2+C_1x+C_2=-\frac{1.6\times 350^2}{6.667\times 365}+0.24075\times 350+144=147.7188$$

Thus, the height of water table at the interface is h' = 12.154 m

The flows in the ditches are

$$q_{x=0}=\frac{RL}{2}-K\frac{h_0^2-h_1^2}{2L}=\frac{1.6\times 500}{365\times 2}-6.667\frac{12^2-10^2}{2\times 500}=0.8025\ \mathrm{m^3/d}$$

$$q_{x=L}=\frac{RL}{2}+K\frac{h_0^2-h_1^2}{2L}=\frac{1.6\times 500}{365\times 2}+6.667\frac{12^2-10^2}{2\times 500}=1.389\ \mathrm{m^3/d}$$

Method 3: Through equivalent homogeneous and isotropic medium transformation.

Equivalent hydraulic conductivities in x-direction and y-direction are K_x = 6.667 m/d and K_y = 7.52 m/d, so the equivalent hydraulic conductivity for the isotropic medium is

$$K_e=\sqrt{K_xK_y}=\sqrt{6.667\times 7.52}=7.0807\ \mathrm{m/d}$$

Let us transform y-coordinate and leave x-coordinate unchanged. For Y-transformation

$$\frac{\partial}{\partial x}\left(K_x\frac{\partial h^2}{\partial x}\right)+\frac{\partial}{\partial y}\left(K_y\frac{\partial h^2}{\partial y}\right)+2R=0 \qquad \text{dividing by } K_x$$

$$\frac{\partial^2 h^2}{\partial x^2}+\frac{K_y}{K_x}\frac{\partial^2 h^2}{\partial y^2}+\frac{2R}{K_x}=0 \qquad \text{multiplying by } K_x/K_y$$

$$\frac{\partial^2\left(\sqrt{K_x/K_y}\,h\right)^2}{\partial x^2}+\frac{\partial^2\left(\sqrt{K_x/K_y}\,h\right)^2}{\partial\left(\sqrt{K_x/K_y}\,y\right)^2}+\frac{2R}{K_y}=0\Rightarrow \qquad \frac{\partial^2 h'^2}{\partial x^2}+\frac{\partial^2 h'^2}{\partial Y^2}+\frac{2R'}{K_e}=0$$

where, $h' = \sqrt{K_x/K_y}\,h$ and $R' = \sqrt{K_x/K_y}\,R$. For 1D flow the equation reduces to

$$\frac{\partial^2 h'^2}{\partial x^2} + \frac{2R'}{K_e} = 0$$

In Y-transformation all the dimensions along y-direction will bear a ratio

$$\frac{Y}{y} = \sqrt{K_x/K_y} = \sqrt{6.667/7.52} = 0.9416$$

Therefore, $h'_0 = 0.9416 \times 12 = 11.3$ m; $h'_1 = 0.9416 \times 10 = 9.416$ m; $R' = 0.9416 \times 1.6 = 1.50656$ m/year; and $\dfrac{R'}{K_e} = \dfrac{R}{K_y} = \dfrac{1.6}{365 \times 7.52}$ m; but dimensions along x-direction remain same i.e. $L' = 500$ m as shown in Figure 6.10.

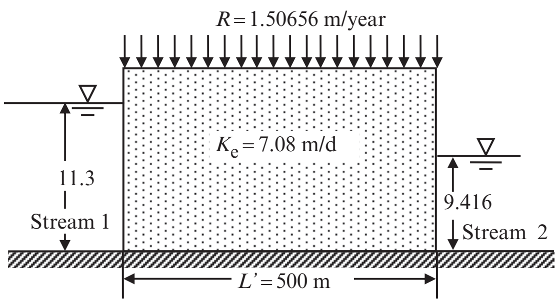

Figure 6.10 *Transformed Example 6.3*

Solution of equation $\dfrac{\partial^2 h'^2}{\partial x^2} + \dfrac{2R'}{K_e} = 0$ is

$$h'^2 = -\frac{R'}{K_e}x^2 + C_1 x + C_2 \quad \text{thus } C_2 = 11.3^2 \text{ and}$$

$$C_1 = -\frac{h_0'^2 - h_1'^2}{L} + \frac{R'L}{K_e} = -\frac{11.3^2 - 9.416^2}{500} + \frac{1.6 \times 500}{365 \times 7.52} = 0.213445$$

$$d = \frac{K_e C_1}{2R'} = \frac{365 \times 7.52 \times 0.213445}{2 \times 1.6} = 183.08 \text{ m}$$

$h_{max}'^2 = h_0'^2 + \dfrac{K_e}{4R'}\left(\dfrac{R'L}{K_e} - \dfrac{h_0'^2 - h_1'^2}{L}\right)^2 = 147.2051$ or $h'_{max} = 12.1328$ m so the corresponding maximum height of water table is $h_{max} = 12.1328/0.9416 = 12.886$ m.
At $x = 350$ m

$$h'^2 = -\frac{R'}{K_e}x^2 + C_1 x + C_2 = -\frac{1.6\times 350^2}{7.52\times 365} + 0.213445\times 350 + 11.3^2 = 130.963$$

or $h' = 11.444$ m

Hence, the height of water table at the interface is 11.444/0.9415 = 12.154 m. Relationship for discharge is

$$q_x = K_y\frac{h_0'^2 - h_1'^2}{2L} - \frac{RL}{2} + Rx = 7.52\frac{11.3^2 - 9.416^2}{2\times 500} - \frac{1.6\times 500}{2\times 365} + \frac{1.6}{365}x$$

$$= \frac{1.6}{365}x - 0.803$$

Therefore,

$$q_0 = -0.803; \qquad q_{500} = 1.389; \qquad q_{350} = 0.731 \text{ m}^3/\text{d/m}$$

Method 4: Similarly, this problem can also be solved by transforming x-coordinate and leaving y-coordinate unchanged. In this X transformation

$$\frac{\partial}{\partial x}\left(K_x\frac{\partial h^2}{\partial x}\right) + \frac{\partial}{\partial y}\left(K_y\frac{\partial h^2}{\partial y}\right) + 2R = 0 \qquad \text{dividing by } Ky$$

$$\frac{K_x}{K_y}\frac{\partial^2 h^2}{\partial x^2} + \frac{\partial^2 h^2}{\partial y^2} + \frac{2R}{K_y} = 0 \text{ for 1D flow the equation reduces to}$$

$$\frac{\partial^2 h^2}{\partial X^2} + \frac{2R'}{K_e} = 0 .$$

In this case, all the dimensions along x-direction will bear a ratio

$$\frac{X}{x} = \sqrt{K_y/K_x} = \sqrt{7.52/6.667} = 1.06205$$

Therefore, $L' = 531.025$, $R'L' = RL$ so $R' = 1.6/1.06205$ m/year and no change in depth dimensions.

Solution of equation $\frac{\partial^2 h^2}{\partial X^2} + \frac{2R'}{K_e} = 0$ yields

$$h^2 = -\frac{R'}{K_e}X^2 + C_1 X + C_2, \text{ thus } C_2 = 12^2 = 144 \text{ and}$$

$$C_1 = -\frac{h_0^2 - h_1^2}{L'} + \frac{R'L'}{K_e} = -\frac{12^2 - 10^2}{531.025} + \frac{1.6\times 531.025}{365\times 7.08\times 1.062} = 0.22668$$

$d' = \frac{K_e C_1}{2R'} = 194.44$ so location of water divide line d = 194.44/1.06205 = 183.08 m

$h_{\max}{}^2 = -\frac{R'}{K_e}d'^2 + C_1 d' + C_2 = 166.037$; hence, $h_{\max}$ = 12.886, which is maximum height of the water table. At X = 350 × 1.06205 = 371.7175 m

$h'^2 = -\frac{R'}{K_e}X^2 + C_1X + C_2 = 147.717$ or $h' = 12.154$ m, which is the height of water table at the interface.

Relationship for discharge is

$$q_x = K_e \frac{h_0^2 - h_1^2}{2L'} - \frac{R'L'}{2} + R'X = 7.0807 \frac{12^2 - 10^2}{2 \times 531.025} - \frac{1.6 \times 500}{2 \times 365} + \frac{1.6}{365 \times 1.062} X$$

therefore,

$$q_0 = -0.803; \qquad q_{500} = 1.389; \qquad q_{350} = 0.731 \text{ m}^3\text{/d/m}.$$

Example 6.4: In an irrigated field the steady-state water table is maintained at least 2 m below the ground surface by two parallel ditches as shown in Figure 6.11. Determine the minimum spacing between the ditches for this purpose and corresponding flow into ditches if h_0 = 8 m; h_1 = 4 m; K_1 = 10 m/s; K_2 = 20/11 m/s; and R = 5.256 m/year.

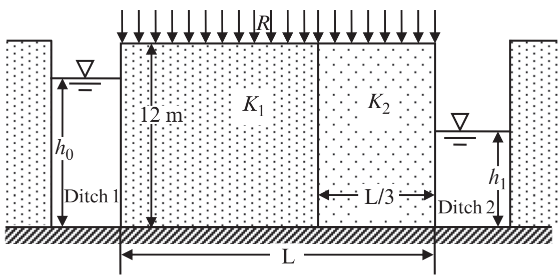

Figure 6.11 *Example 6.4*

Solution: With h_0 = 8 m; h_1 = 4 m; K_1 = 10 m/d; K_2 = 20/11 m/d; and R = 5.256 m/year.

Method 1: Without medium transformation

Let us assume that h' be the unknown height of water table at the interface of two mediums. For steady unidirectional flow in an unconfined aquifer with recharge

$$C_1 = -\frac{h_0^2 - h_1^2}{L} + \frac{RL}{K}; \; d = \frac{KC_1}{2R} = \frac{L}{2} - \frac{K}{2RL}\left(h_0^2 - h_1^2\right)$$

$$h_{\max}^2 = h_0^2 - \frac{R}{K}\left(\frac{KC_1}{2R}\right)^2 + C_1\frac{KC_1}{2R} = h_0^2 + \frac{KC_1^2}{4R} = h_0^2 + \frac{K}{4R}\left(\frac{RL}{K} - \frac{h_0^2 - h_1^2}{L}\right)^2$$

For Medium 1, K_1 = 10 m/d; R = 5.256 m/year = 0.0144 m/d; R/K = 0.0144/10;

$L_1 = 2L/3; h_0 = 8$ m; and $h_1 = h'$; therefore, $C_{21} = 64; C_{11} = -\frac{64 - h'^2}{2L/3} + \frac{0.0144 \times 2L}{10 \times 3}$;

and $q_{x=2L/3} = 10\frac{64 - h'^2}{4L/3} + \frac{0.0144L}{3}$

For Medium 2, K_2 = 20/11 m/d; R = 0.0144 m/d; R/K = 0.0144×11/20; $L_2 = L/3$; $h_0 = h'$; and $h_1 = 4$ m; therefore, $C_{22} = h'^2$; $C_{12} = -\dfrac{h'^2-16}{L/3} + \dfrac{0.0144\times 11L}{20\times 3}$; and $q_{x=2L/3} = -\dfrac{20}{11}\dfrac{h'^2-16}{2L/3} + \dfrac{0.0144L}{2\times 3}$

Equating discharges at the interface of mediums

$$10\frac{64-h'^2}{4L/3} + \frac{0.0144L}{3} = \left|-\frac{20}{11}\frac{h'^2-16}{2L/3} + \frac{0.0144L}{2\times 3}\right|$$

$$\frac{150}{11}h'^2 = \frac{640\times 12}{11} + \frac{2\times 0.0144L^2}{3} \quad \text{or} \quad h'^2 = \frac{256}{5} + \frac{0.0144\times 11L^2}{225}$$

$$\frac{210}{44L}h'^2 = \frac{24}{L}\frac{200}{11} + \frac{0.0144L}{2\times 3} \quad \text{or} \quad h'^2 = \frac{96\times 20}{21} + \frac{0.0144\times 11L^2}{3\times 105}$$

Let the maximum height of water table (water divide line) happen in the Medium 1, as the water table is maintained at least 2 m below the ground surface h_{max} = 10 m and hence

$$100 = 64 + \frac{10}{4\times 0.0144}\left(\frac{0.0144}{10}\frac{2L}{3} - \frac{64-h'^2}{2L/3}\right)^2$$

Eliminating h'

$$\sqrt{\frac{36\times 4\times 0.0144}{10}} = \frac{0.0144}{10}\frac{2L}{3} - \frac{96}{L} + \frac{3}{2L}\left(\frac{96\times 20}{21} + \frac{0.0144\times 11L^2}{3\times 105}\right)$$

$$\sqrt{\frac{36\times 4\times 0.0144}{10}} = \frac{0.0144}{10}\frac{2L}{3} - \frac{96}{L} + \frac{3}{2L}\left(\frac{256}{5} + \frac{0.0144\times 11L^2}{225}\right)$$

which yields L = 261.75 m and hence h' = 11.818 m. The water divide line lies at

$$d = \frac{KC_1}{2R} = \frac{10\times C_1}{2\times 0.0144} = 100 \text{ m } (< 2L/3 \text{ OK})$$

The flows in the ditches are

$$q_{x=0} = \frac{R}{2}\frac{2L}{3} - K_1\frac{h_0^2-h'^2}{4L/3} = \frac{0.0144\times 252.75}{3} - \frac{30\times\left(64-11.818^2\right)}{4\times 252.75} = 1.44\text{m}^3/\text{d}$$

$$q_{x=L} = \frac{R}{2}\frac{L}{3} + K_2\frac{h'^2-h_1^2}{2L/3} = \frac{0.0144}{2}\frac{252.75}{3} + \frac{20}{11}\frac{3\times\left(11.818^2-16\right)}{2\times 252.75} = 2.2\text{ m}^3/\text{d}$$

Method 2: With equivalent homogeneous medium transformation in main flow direction.

In this method, we have steady unidirectional flow in an unconfined aquifer with recharge in x-direction only. Equivalent homogeneous medium in x-direction (Figure 6.12)

$$K_x = \frac{2L/3 + L/3}{(2L/3/10) + (11L/3/20)} = \frac{3}{0.2 + 0.55} = 4 \text{ m/d}$$

R = 5.256 m/year = 0.0144 m/d; R/K = 0.0144/4; h_{max} = 10 m as the water table is maintained at least 2 m below the ground surface. Using relation for maximum height of water table

$$h_{max}^2 = h_0^2 - \frac{R}{K}\left(\frac{KC_1}{2R}\right)^2 + C_1\frac{KC_1}{2R} = h_0^2 + \frac{KC_1^2}{4R} = h_0^2 + \frac{K}{4R}\left(\frac{RL}{K} - \frac{h_0^2 - h_1^2}{L}\right)^2 \quad \text{or}$$

$$\sqrt{\left(h_{max}^2 - h_0^2\right)\frac{4R}{K}} = \frac{RL}{K} - \frac{h_0^2 - h_1^2}{L}$$

Using given values (i.e. h_0 = 8 m; h_1 = 4 m; h_{max} = 10 m; R/K = 0.0144/4)

$$\sqrt{36 \times 0.0144} = \frac{0.0144L}{4} - \frac{48}{L} \qquad \text{or} \qquad L^2 - 200L - \frac{4}{3}\times 10^4 = 0$$

therefore,
L = 252.75 m and h' = 9.116 m at $x = 2L/3$.
The flows in the ditches are

$$q_{x=0} = \frac{RL}{2} - K\frac{h_0^2 - h_1^2}{2L} = \frac{0.0144 \times 252.75}{2} - \frac{4 \times 48}{2 \times 252.75} = 1.44 \text{ m}^3\text{/d}$$

$$q_{x=L} = \frac{RL}{2} + K\frac{h_0^2 - h_1^2}{2L} = \frac{0.0144 \times 252.75}{2} + \frac{4 \times 48}{2 \times 252.75} = 2.2 \text{ m}^3\text{/d}$$

The location of water divide line is

$$d = \frac{L}{2} - \frac{K}{2RL}\left(h_0^2 - h_1^2\right) = \frac{252.75}{2} - \frac{4 \times 48}{2 \times 0.0144 \times 252.75} = 100 \text{ m}$$

Method 3: Through equivalent homogeneous and isotropic medium transformation.

Equivalent hydraulic conductivities in x-direction and y-direction are K_x = 4 m/d and K_y = 80/11 m/d, so the equivalent hydraulic conductivity for the isotropic medium is

$$K_e = \sqrt{K_x K_y} = \sqrt{80 \times 4/11} = 5.5936 \text{ m/d}$$

Let us transform x-coordinate and leave y-coordinate unchanged; thus, all the dimensions along x-direction will bear a ratio

$$\frac{X}{x} = \sqrt{K_y/K_x} = \sqrt{20/11} = 1.3484$$

Therefore, L' = 1.3484 L; $R'L' = RL$; $R' = R$/1.3484; R'/K_e = 0.0144/1.3484/5.5936 = 1.91× 10^{-3}; but dimensions along y-direction remain same, that is, h_0 = 8 m; h_1 = 4 m; h_{max} = 10 m; and consequently

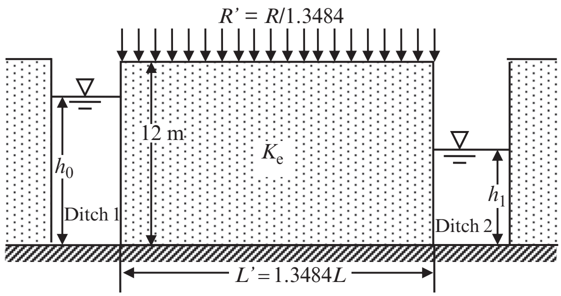

Figure 6.12 *Transformed Example 6.4*

$$\sqrt{\left(h_{\max}^2 - h_0^2\right)\frac{4R'}{K_e}} = \frac{R'L'}{K_e} - \frac{h_0^2 - h_1^2}{L'} \text{or } \sqrt{36\times 0.0144\times 11/20} = 1.91\times 10^{-3}L' - \frac{48}{L'}$$

or $$L'^2 - \frac{200}{\sqrt{11/20}}L' - \frac{4}{3}\times 10^4\,\frac{20}{11} = 0 \text{ therefore,}$$

$$L' = 252.75\times\sqrt{20/11}\text{ m and hence } L = 252.75\text{ m as in Method 2.}$$

The flows in the ditches are

$$q_{x=0} = \frac{R'L'}{2} - K_e\frac{h_0^2 - h_1^2}{2L'} = \frac{0.0144\times 252.75\sqrt{20/11}}{\sqrt{20/11}\times 2} - \frac{4\sqrt{20/11}\times 48}{2\times 252.75\sqrt{20/11}}$$
$$= 1.44\text{ m}^3/\text{d}$$

and $q_{x=L} = \dfrac{R'L'}{2} + K_e\dfrac{h_0^2 - h_1^2}{2L'} = 2.2\text{m}^3/\text{d}$, which are same as in Method 2.

The location of water divide line is

$$d' = \frac{L'}{2} - \frac{K_e}{2R'L'}\left(h_0^2 - h_1^2\right) = \frac{252.75\sqrt{20/11}}{2} - \frac{4\sqrt{20/11}\times 48}{2\times 0.0144\times 252.75}$$
$$= 100\sqrt{20/11}\text{m}$$

hence $d = 100$ m.

Similarly, this problem can also be solved by transforming y-coordinate bearing a ratio

$$\frac{Y}{y} = \sqrt{K_x/K_y} = \sqrt{11/20} = 0.7416$$

and leaving x-coordinate unchanged, thus, $L' = L$; $d' = d$; but $h_0 = 0.7416\times 8$ m; $h_1 = 0.7416\times 4$ m; $h_{\max} = 0.7416\times 10$ m, and so on.

PROBLEMS

6.1. Explain the Dupuit–Forchheimer assumptions and their limitations in steady unidirectional flow in an unconfined aquifer without recharge between two water bodies with vertical boundaries.

6.2. Using the mass conservation principle, show that

$$K\rho\left(\frac{\partial^2 h}{\partial x^2}+\frac{\partial^2 h}{\partial y^2}+\frac{\partial^2 h}{\partial z^2}\right)+K\beta\rho^2 g\left[\left(\frac{\partial h}{\partial x}\right)^2+\left(\frac{\partial h}{\partial z}\right)^2+\left(\frac{\partial h}{\partial z}\right)^2-\frac{\partial h}{\partial z}\right]$$

$$=\rho^2 g(\alpha+\eta\beta)\frac{\partial h}{\partial t}$$

6.3. Derive the general groundwater flow equation and then show that $S_s=\rho g(\alpha+\eta\beta)$, where ρ = mass density of seeping water, η = porosity of the porous medium and α and β are compressibility of the porous medium and water, respectively.

6.4. Explain the Dupuit–Forchheimer assumptions and their limitations in steady unidirectional flow in an unconfined aquifer without recharge between two water bodies with vertical boundaries.

6.5. In a basin consisting of 22 km^2 of plains, the maximum fluctuation of groundwater table is 3 m. Assuming a specific yield of 16 percent what is the probable groundwater storage?

6.6. An aquifer averages 50 m in thickness and is 100 ha in area. Determine the volume in ha-m of water available if (i) the aquifer is unconfined and is completely drained, (ii) the aquifer is confined and the piezometric head is lowered from 30 m to 10 m above the aquifer, and (iii) the aquifer is confined and the piezometric head is lowered 55 m which brings the water table 25 m below the confining layer. Assume S_y = 15 percent, and $S = 2\times10^{-4}$.

6.7. Artesian aquifer 30 m thick has a porosity of 26 percent and elastic modulus of 0.26 GN/m^2. Estimate the storage coefficient of the aquifer. What fraction of this is attributable to the expansibility of water? Bulk modulus of elasticity of water = 2.1GN/m^2.

6.8. Determine the storage coefficient of an aquifer from the following data: Porosity = 30 percent; thickness of aquifer = 25 m; bulk modulus of water, K_w = 2.1 GN/ m^2; modulus of elasticity of the soil skeleton, $E_s = 3\times10^8$ N/ m^2.

6.9. Determine the flow into a horizontal infiltration gallery 200 m long resting on an impervious strata 10 m below ground surface. The GWT in the area is 3 m bgl and drops at the face of the gallery to 8 m bgl in a length of 400 m. Permeability of the flow strata can be taken as 45 m/d. Give the equation of the phreatic surface.

6.10. A confined aquifer is 18.5 m thick. The potentiometric surface elevations at two observation wells 822 m apart are 25.96 m and 24.62 m. If the hydraulic conductivity and effective porosity of the aquifer are 25 m/d and 0.25, respectively, determine flow rate per unit width of the aquifer, specific discharge, and average linear velocity of the flow assuming steady unidirectional flow.

6.11. Calculate the fresh water flow in a coastal aquifer extending to length of 40 km along the coast, assuming an average permeability of 40 $m^3/d/m^2$, average thickness of aquifer of 20 m, and the piezometric gradient at 5 m/km.

6.12. A confined aquifer as shown in Figure 6.13 connects two reservoirs. If the upstream reservoir is polluted by a contaminant suddenly, how long will it take the contaminant to reach the downstream reservoir? Use the porosity of aquifer = 0.30, h_0 = 20 m, h_1 = 15 m, b_0 = 12 m, b_1 = 8 m, and L = 800 m.

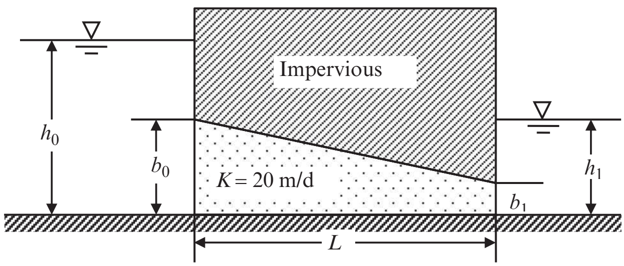

Figure 6.13 *Problem 6.12*

6.13. What will be the flow rate if K = 2 m/d in the seepage problem case as shown in the above case (Figure 6.13)?

6.14. What is the flow rate in the problem shown as Figure 6.14 ?

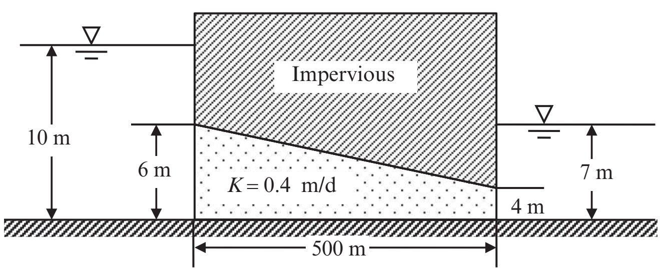

Figure 6.14 *Problem 6.14*

6.15. What will be the flow rate if h_0 = 20 m, h_1 = 15 m, b_0 = 10 m, L = 1000 m, d_1 = 2 m, d_2 = 8 m, K_1 = 1 m/d, K_2 = 20.7 m/d and θ = 30° for the seepage problem case shown in Figure 6.15?

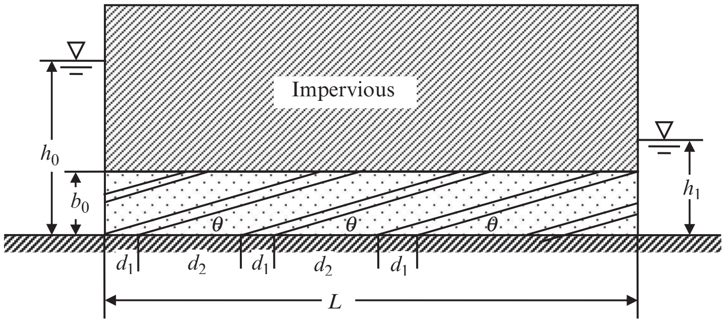

Figure 6.15 *Problem 6.15*

6.16. Derive the Boussinesq equation for flow in unconfined porous medium stating Dupuit's assumptions. Discuss the limitations of it in steady unidirectional flow in an unconfined aquifer between two water bodies with vertical boundaries. Also, compute the flow rate from the canal into the river in as shown in Figure 6.16.

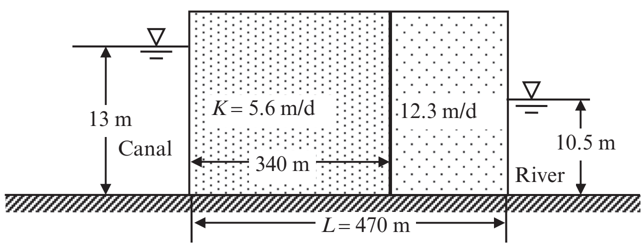

Figure 6.16 *Problem 6.16*

6.17. Derive the expressions for the location of steady water divide line, the maximum elevation of the water table, base flow rates to streams and the travel time from groundwater divide line to the streams for the case of flow in porous medium between two fully penetrating streams as shown in Figure 6.17.

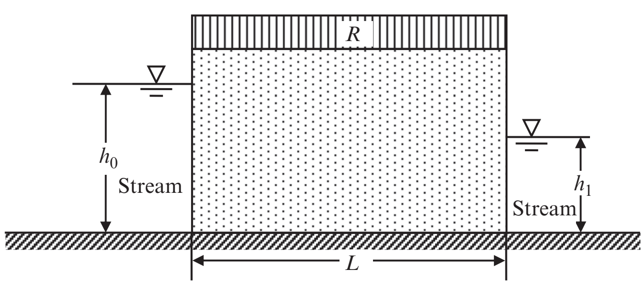

Figure 6.17 *Problem 6.17*

6.18. What will be the base flow rates to both streams if h_0 = 10 m, h_1 = 8.5 m, R = 1.6 m/year, and L = 460 m for the groundwater flow problem case shown in Figure 6.18? Also, find the location of the steady groundwater divide line, the maximum elevation of the water table, and the travel time from groundwater divide line to the streams.

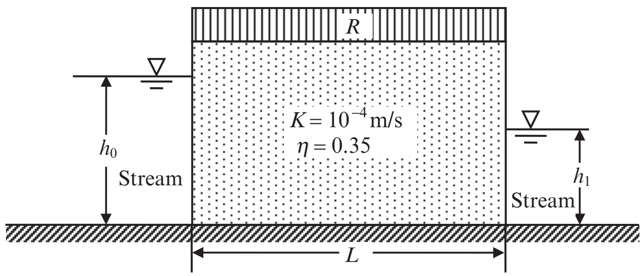

Figure 6.18 *Problem 6.18*

6.19. What will be the base flow rates to both streams if h_1 = 10 m, h_2 = 8 m, R = 2 m/year, and L = 500 m for the groundwater flow problem case shown in Figure 6.19? Also, find the location of the steady groundwater divide line and the maximum elevation of the water table.

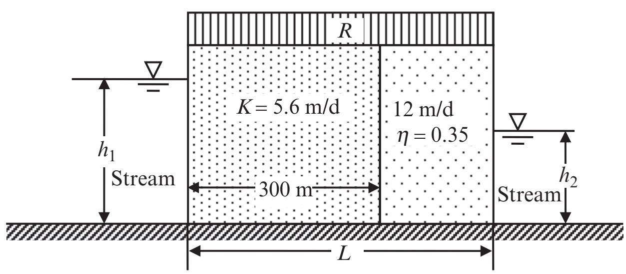

Figure 6.19 *Problem 6.19*

6.20. In an irrigated field the steady-state water table is maintained at least 4 m below the ground surface by two fully penetrating parallel drainage canals in an aquifer of hydraulic conductivity 1 m/d. The depth of bed rock is 10 m from NGL and depth of water in both canals is 3 m. Determine the optimal spacing between the canals and corresponding flow into canal if the daily recharge rate is 0.015 m.

6.21. In an irrigated field the steady-state water table is maintained at least 2 m below the ground surface by two parallel ditches as shown in Figure 6.20. Determine the optimal spacing between the ditches for this purpose and corresponding flow into ditches if h_0 = 7 m and h_1 = 4 m (use R = 5.475 m/year).

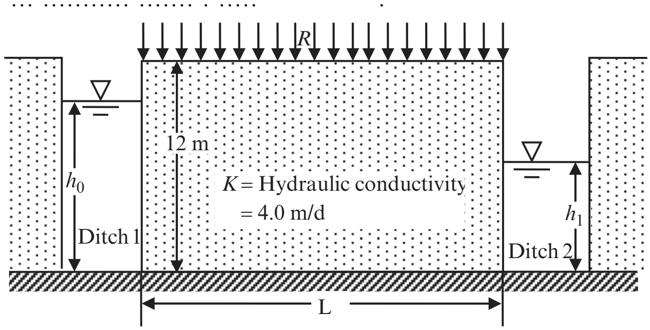

Figure 6.20 *Problem 6.21*

6.22. In an irrigated field the steady-state water table is maintained at 2 m below the ground surface by two parallel ditches spaced at 150 m as shown in Figure 6.21. Without transforming the medium, determine the water depth h_1 in ditch 2, location of water divide line and flow into ditches if h_0 = 10 m; K_1 = 4 m/d; K_2 = 8 m/d; and R = 3.65 m/year.

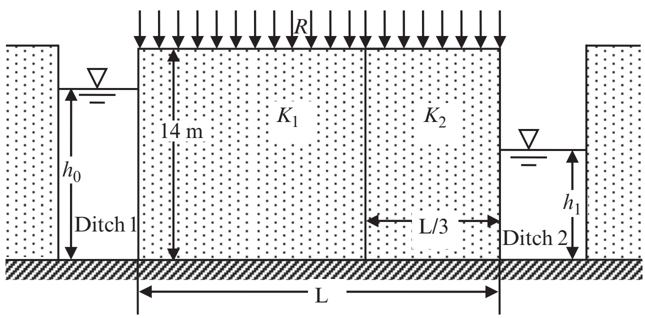

Figure 6.21 *Problem 6.22*

6.23. Solve the above Problem 6.22 by transforming medium into an equivalent homogeneous and isotropic medium.

Chapter

7 Contaminant Transport in Groundwater

7.1 Origins of Groundwater Contamination

Groundwater is more protected than surface water, but it can be contaminated from different sources. Water dissolves more things than any other substance; it is very susceptible to contamination or pollution. *Contamination* is a modification of physical, chemical, and biological properties of groundwater, restricting or preventing its use for various purposes. It can impair the use of water and can create hazards to public health through toxicity or the spread of disease. Generally, *contamination* and *pollution* terms are used as synonymous in groundwater. Sometimes, polluted term is used only if contamination crosses some limit to make groundwater unfit for a particular use. In contrast with surface water pollution, subsurface pollution is difficult to detect, and is even more difficult to control, and may persist for decades. *Groundwater pollution* is defined as the artificially induced degradation of natural groundwater quality. Alternatively, it may be defined as the undesirable changes in groundwater quality that make groundwater unfit for domestic consumption. During the last few decades, the quality of groundwater has deteriorated in many places due to the increased industrialization, urbanization and agricultural activities. Due to very long residence time, it takes several hundred to several thousand years for contaminated groundwater to be cleansed by natural recycling. With the growing recognition of the importance of groundwater resources, efforts are increasing to prevent, reduce, and eliminate groundwater pollution.

The possible pollutants in groundwater are many. They could be from *geogenic sources* or *anthropogenic sources*. Contamination from the dissolution of aquifer material is *geogenic*. Fluoride, arsenic, iron, and other heavy metals in groundwater are usually due to geogenic source contamination. *Anthropogenic sources* and causes of groundwater pollution are associated with human interventions and use of water. Most pollution stems from disposal of wastes on or into the ground. The principal anthropogenic sources and causes (continuous and/or accidental types) can be categorized as follows:

- Municipal – Sewer leakage, liquid waste, solid waste, and landfill,
- Industrial – Liquid waste, leakage, mining activity, and oil field brine,
- Agricultural – Return flows, fertilizers and pesticides, and animal waste,
- Miscellaneous – Salt water intrusion, acid rain, and deicing salts.

7.1.1 Municipal Sources

Sewer Leakage

Sanitary sewers are intended to be water tight; however, in reality, leakage of sewage into the ground is a common occurrence, especially from old/defective/damaged sewers. Sewer leakage can introduce high concentration of biochemical oxygen demand (BOD), chemical oxygen demand (COD), nitrate, organic chemicals, and possibly bacteria into groundwater. Heavy metals such as arsenic, cadmium, chromium, cobalt, copper, iron, lead, manganese, and mercury may enter into groundwater from industrial sewers.

Liquid Wastes

Wastewater in an urban area may originate from domestic uses, industries, or storm runoff. This wastewater without treatment or after treatment is discharged into surface waters or recharged into the ground, which can introduce bacteria, viruses, and inorganic and organic chemicals into groundwater. Furthermore, trace elements, heavy metals, stable organics, and by products of chlorination can enter into the aquifer through the disposed wastewater.

Solid Wastes

The land disposal of solid wastes creates a potential source of groundwater pollution. A *landfill* is an area serving as a depository of urban or municipal solid waste. It should be designed and constructed according to engineering specifications and then operated and monitored so that any *leachate* generated can be controlled and prevented from polluting groundwater. But many landfills are simply refuse dumps and leachates from them pollute groundwater (Figure 7.1). Main pollutants found in leachate are BOD, COD, iron, manganese, chloride, nitrate, hardness, and trace elements. The problem of pollution from landfills exaggerates where high rainfall and shallow water tables occur.

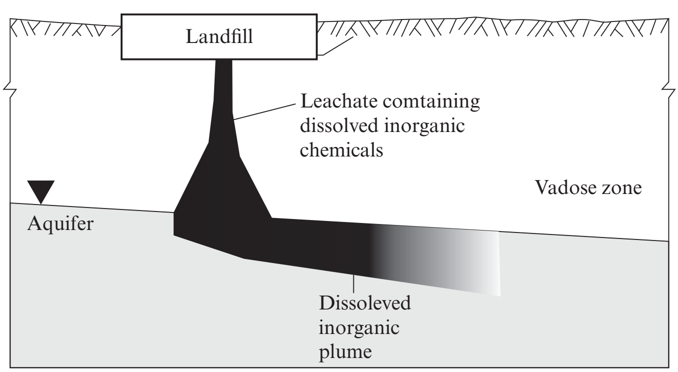

Figure 7.1 *Groundwater contamination from landfill site*

7.1.2 Industrial Sources

Liquid Wastes

The quality of the industrial waste water varies with type of industry and type of use. Groundwater pollution can occur where industrial wastewaters are discharged into pits, ponds, or lagoons, thereby enabling the wastes to migrate down to the water table.

Tank and Pipeline Leakage
Underground storage and transmission of a wide variety of fuels and chemicals are common practices for industrial and commercial installations. These tanks and pipelines are subject to structural failures so that subsequent leakage becomes a source of groundwater pollution. Petroleum and petroleum products are responsible for much of the pollution. Sometimes, radioactive wastes are stored in underground tanks; leakage from such cases can cause serious groundwater pollution problems.

Mining Activities
Mines can produce a variety of groundwater pollution problems. Pollution depends on the material being extracted and the milling process. Also, dewatering in the mining area is required since open pit and underground mines extend below the water table. Water so pumped may be highly mineralized and may reach to groundwater. Pollution of groundwater can also result from the leaching of old mine tailings and settling ponds. Oxygen may enter into aquifer during dewatering and it results in the oxidation of sulfide ores leading to acidic (H_2SO_4) water known as acid mine drainage, which contaminates aquifers.

Oil Field Brines
The production of oil and gas is usually accompanied by substantial discharges of wastewater in the form of brine. Constituents of brine include sodium, calcium, ammonia, boron, chloride, sulfate, trace metals, and high total dissolved solids. Oil field brine disposal in streams or evaporation ponds leads to brine polluted aquifer.

7.1.3 Agricultural Sources

Irrigation Return Flow
It is the part of irrigation water that is excess over the crop requirement and joins underlying groundwater. The salinity of irrigation return flow may be three to ten times that of the applied water resulting from the addition of salts by dissolution during the irrigation process, from salts added as fertilizers or soil amendments, and from the concentration of salts by evapotranspiration. Because irrigation is the primary use for water in arid and semiarid regions, irrigation return flow can be the major cause of groundwater pollution in such regions.

Animal Wastes
Where animals are confined within a limited area, large amounts of wastes are deposited on the ground. Storm runoff from such sites carries highly concentrated pollutants to surface and subsurface waters. Animal wastes may transport salts, organic loads, bacteria, and particularly nitrate–nitrogen into the groundwater.

Fertilizers and Soil Amendments
When fertilizers are applied to agricultural land, a portion usually leaches through the soil and to the water table. Phosphorus and potassium fertilizers are readily absorbed on soil particles and seldom constitute a pollution problem. But nitrogen in solution is only partially used by plants or absorbed by the soils, and it is the primary fertilizer pollutant. In addition to fertilizers, pesticides, and herbicides are also being extensively used. Soil amendments are applied to irrigated lands to

alter the physical or chemical properties of the soil. Lime, gypsum, and sulfur are widely used for this purpose; substantial amounts of these soil amendments may eventually leach to the groundwater, thereby increasing its salinity.

7.1.4 Miscellaneous Sources

Groundwater contamination may also be due to radioactive waste disposal, salt water intrusion, deep well disposal of liquid waste, thermal power plants, acid rains, road deicing salts, oil and chemical spills, runoff from urban/industrial set-ups, etc. Radioactive waste is generated in all the stages of the nuclear fuel cycle. This includes mining, refining, consumption, and waste disposal. The safe disposal of nuclear waste is a very difficult problem from the perspective of contamination. Generally, it is disposed in concrete/steel/iron containers buried underground in very low permeability (crystalline rocks, shales, and clay) unsaturated zones. Due to some or other reason radionuclides may enter groundwater flow system.

7.2 Classification of Groundwater Contamination

The nature and extent of groundwater contamination change with the type of chemicals and toxics wastes added to groundwater systems resulting from various anthropogenic activities. It is affected by degree of localization, loading history, and the kind of contaminants. All the sources and causes of pollution can also be classified based on their geometry as

- A *point source* originates from a singular location,
- A *line source* has a predominately linear alignment, and
- As *diffuse/area source* occupies an extensive area that may or may not be clearly defined.

The above classification sometimes is segregated into two categories: *point sources* and *nonpoint (area or distributed) sources*. The size of source may range from individual well to areas of 100 km^2 or more. Point sources include injection wells for disposal of liquid wastes, septic tanks, leaky sewer lines, storage tanks, landfills, waste disposal sites, spills (Figure 7.2), pipeline releases, chemical manufacturing locations,

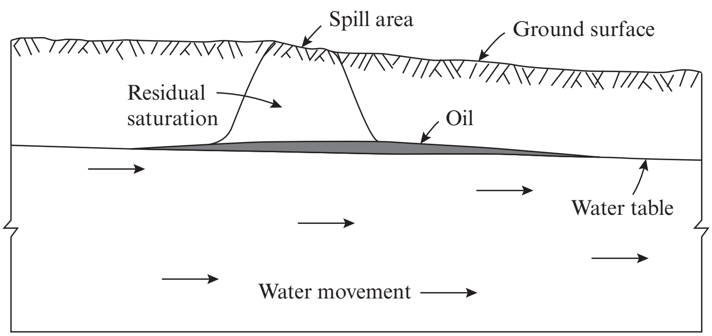

Figure 7.2 *Groundwater contamination from oil spill*

petroleum refining locations, wood treating facilities, and many others. Nonpoint sources include fertilizers on agricultural land, pesticides on agricultural land and forests, contaminants in rain, snow, and dry atmospheric fallout etc. In practice, the term point and nonpoint describe the degree of localization of the source. Classifying contamination sources according to their geometry are helpful because the source geometry significantly influences the plume evolution and helps in understanding the plume dynamics within the groundwater system using mathematical models.

Point source groundwater contamination problems can be divided into three main categories: (i) light nonaqueous phase liquids (LNAPLs), (ii) dense nonaqueous phase liquids (DNAPLs), and (iii) inorganic and other dissolved constituents. In the pure liquid form, LNAPLs are less dense than water and DNAPLs are denser than water. LANPL sites are caused by release of petroleum products or crude oil (Figure 7.3), whereas DNAPL sites have been caused by dry cleaning, automobile, wood preservation, asphalt operations, machining, electric circuit operation, aviation equipment, etc.; DNAPL contaminants (Figure 7.4) are troublesome. One litre of gasoline (LNAPL) can contaminate 1,000,000 L of groundwater. Inorganic and other dissolved constituents include metals and salts.

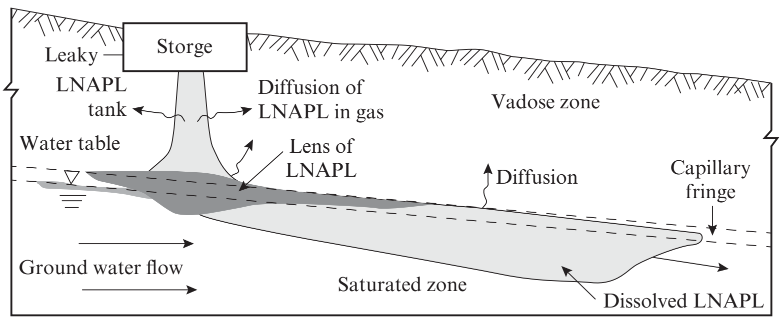

Figure 7.3 *Groundwater contamination from LNAPL*

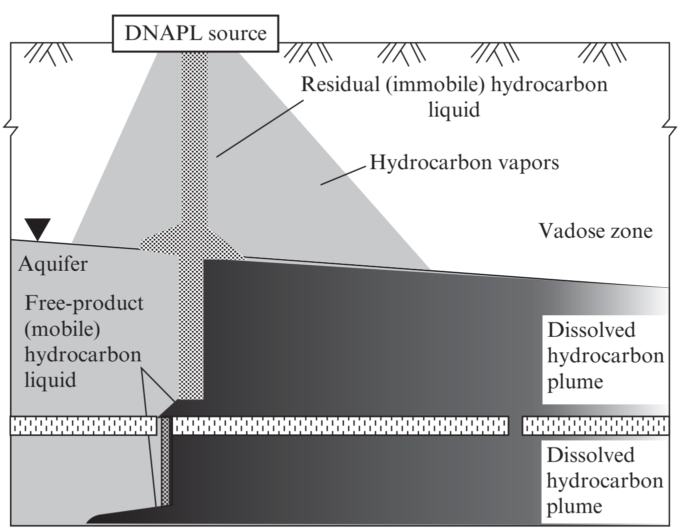

Figure 7.4 *Groundwater contaminations from DNAPL*

The contamination can be classified according to their type as follows:

- *Conservative* (*nonreactive*) and *nonconservative* (*reactive*)
- *Single phase* and *multiphase* (*immiscible*)
- *Unstratified* and *stratified*

This grouping categorizes the mechanism for contaminant transport within groundwater system and helps in selecting of a particular numerical model for solution. Conservative solute are nonreactive with the soil and/or native groundwater and do not undergo biological and radioactive decay. Chloride ion is an example of nonreactive or conservative solute.

Classification based on constituents and contaminants are as follows:

- *Inorganic contaminants* – carbon, chlorine, sulfur, nitrogen, fluorine, arsenic, metals, etc.
- *Organic contaminants*
- *Dissolved gases*
- *Particulate matters* including microorganisms

Groundwater may contain contaminants as dissolved elements and suspended particles depending on the source of groundwater contaminants, chemical and mineralogical composition of the rock formation in which groundwater flows and hydrogeological and geo-environmental conditions. Depending on the concentration of the dissolved constituents in groundwater, constituents are classified as

- Trace constituents
- Minor constituents
- Secondary constituents
- Major constituents

7.3 Transport Mechanism

Groundwater dissolves many different compounds, and most of these substances have the potential to contaminate large quantities of water. Once an aquifer is contaminated, it may be unusable for decades due to long residence time. Preventing contamination in the first place is by far the most practical solution to the problem of groundwater conservation. Then understanding the mechanism of contaminant transport in groundwater helps in management and restoration of contaminated aquifers. Distinguishing between the various flow mechanisms is still poorly understood, as the movement and interaction of contaminants with aquifer material and groundwater is a complex phenomenon. This limits our ability to model contaminant behavior. Efforts are hampered by a serious shortage of groundwater experts and a general lack of knowledge about how groundwater behaves.

A *transport mechanism* influences the migration of dissolved contaminant in saturated flow in granular aquifers. The different transport mechanisms are

- Advection
- Diffusion
- Dispersion
- Sorption
- Decay

- Physical, natural, or anthropogenic activities
- Hydrolysis, volatilization, and biotransformation
- Transport in aquifers with a pronounced bimodal permeability distribution
- Chemical reactions

The first three processes (advection, diffusion, and dispersion) are physically fundamental processes that govern the migration of contaminant in groundwater in the absence of any natural or anthropogenic stresses/activities. The relationship between advection and dispersion is used to determine the transport of mass in porous media. Generally the bulk transport of fluids, and solutes, is dominated by advection and dispersion. *Diffusion* is a process of mass transport in response to a concentration gradient. It is usually lumped in with the advective and dispersive behavior of fluids.

The solubility of a contaminant compound will determine the transport, fate, and toxicology of that compound in a groundwater system. The main characteristics of a system that may affect solubility are pH, sorption to solids, and temperature. *Sorption* is the exchange of molecules and ions between the solid phase and liquid phase. There are two types of associations among aqueous/liquid and solid phases: adsorption and absorption. *Adsorption* is the attachment of molecules and ions from the solute to the rock material, causing a decrease of concentration of solute. This is also referred to as a retardation of the contaminant transport. The *absorption* is the intermingling of solute molecules with the molecules of the solid phase and thus the absorption is the dissolution of a liquid material in a solid solvent. *Desorption* is the release of the molecules and ions from the solid phase to the solute.

7.3.1 Advection

Contaminant transport by the movement of a bulk of water is called *advection*. It is the main process conveying dissolved mass from one point to another. The driving force is the hydraulic gradient, hence the direction and rate of transport coincide with groundwater movement. The advection rate of transport is the same as the average linear velocity of the groundwater due to hydraulic gradient given by Darcy's law. Thus, 1-D steady state mass flux F_{xa} due to advection is

$$F_{\mathrm{xa}} = v_x \eta C = -K \frac{dh}{dx} C \tag{7.1}$$

where, F_{xa} = advective mass flux of the solute per unit area per unit time; v_{x} = advective transport or seepage velocity of groundwater in x direction; C = solute concentration (mass/volume); and η = porosity of the porous medium.

The actual transport velocity within the pore space remains unknown. If the advection is the sole transport process, then concentration changes in a control volume over time are equal to difference between advective inflows and outflows. In highly permeable materials, such as sand and gravel, advection is the dominant transport mechanism. During the evolution of most plumes, advection is the important transport mechanism. For unsteady case

$$\frac{\partial C}{\partial t} = -v_x \frac{\partial C}{\partial x} \tag{7.2}$$

Advective flow becomes more complex when the density and/or the viscosity of water change with solute concentration. Solutes with large density, introduce a larger vertical component of flow movement. Depending on the extent of contamination, migration behavior can be drastically changed, allowing contaminants to flow against the natural groundwater flow direction.

7.3.2 Diffusion

Diffusion is a net transport of molecules from a higher concentration to a lower concentration region by random molecular motion. The diffusion of a contaminant through groundwater in 1-D steady state case is given by Fick's first laws as

$$F_{\mathrm{xd}} = -D\eta \frac{dC}{dx} \tag{7.3}$$

where, F_{xd} = diffusive mass flux of the solute per unit area per unit time; D = molecular diffusion coefficient (m^2/s); and dC/dx = concentration gradient (mass/volume/distance). Diffusion coefficients for the major ions in groundwater are in order of 10^{-9} at 25°C. The negative sign indicates that the movement is from higher to lower concentrations. Molecular diffusion takes place even in a fluid at rest.

If the concentrations of contaminants in water change with time (unsteady state condition), Fick's second law may be applied

$$\frac{\partial C}{\partial t} = D\eta \frac{\partial^2 C}{\partial x^2} \tag{7.4}$$

where, $\partial C/\partial t$ = change in concentration with time (mass/volume/time).

Diffusion in porous media does not proceed at the rate it can in water because of the solid phase of the porous media and adsorption on the solids. In porous media, the ions follow longer pathways as they travel around mineral grains. Therefore, the diffusion process in groundwater is slower than in surface water. To apply Eqs (7.3) and (7.4) for groundwater, the porosity of the medium must be taken into account. Hence, an effective diffusion coefficient $D^* = \tau D$ is used to take this into account, where τ = empirical coefficient (<1) determined by experiments.

Even in the absence of hydraulic gradient (groundwater movement), contaminants diffuse in all directions. This causes a blurring of the boundary between contaminated groundwater and the surrounding groundwater. Also, the diffusion is dominant especially in rocks and soil with very low permeability where the water is moving very slow. If a solid waste is placed on a soil liner and both are saturated with water, contaminants from solid waste will diffuse into the soil liner even if there is no water flow. The concentration of contaminant C in the soil liner at distance x and time t can be calculated (Crank 1956) by

$$C(x,t) = C_0 \mathrm{erfc}\left(\frac{x}{2\sqrt{D^* t}}\right) \tag{7.5}$$

where, C_0 = concentration of contaminant in the solid waste; and erfc() = complementary error function. It may be noted that erfc(x) = 1–erf(x); $\mathrm{erf}(x) = \frac{2}{\sqrt{\pi}}\int_0^x e^{-\tau^2} d\tau$; $\mathrm{erfc}(x) = \frac{2}{\sqrt{\pi}}\int_x^\infty e^{-\tau^2} d\tau$ (see *Appendix C* for values of the error function).

7.3.3 Dispersion

Dispersion is defined as the dilution of contaminants because of being mixed with noncontaminated water. When the two fluids are brought into contact, there is a sharp interface at the beginning, which vanishes into the transition zone, as the difference between physical properties (concentration for instance) tend to be levelled with time. The spreading of contaminants due to dispersion and diffusion are similar in nature, although they are governed by different physical processes. The mechanism of dispersion is rather complex. A *contaminant plume* follows irregular pathways as it moves. A portion of the contaminant plume may find large pore spaces in which it can move quickly, whereas other portions have to pass through small pore spaces. Thus, there is difference in speed of an advancing plume that causes spreading out of the plume. The dispersion due to spreading out of plume happen both in longitudinal and transverse directions as shown in Figure 7.5, which indicates that contaminants spread in the direction of flow and in the lateral direction even though there is only one dimensional flow. The contaminant moves like plumes and these plumes are elliptical in shape and grow in direction of flow. As they grow in size the concentration go on decreasing from the initial value as shown in Figure 7.6.

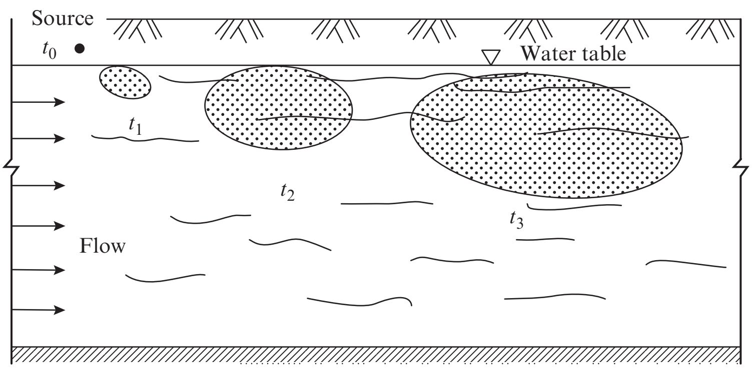

Figure 7.5 *Contaminant spread due to dispersion in longitudinal and transverse directions*

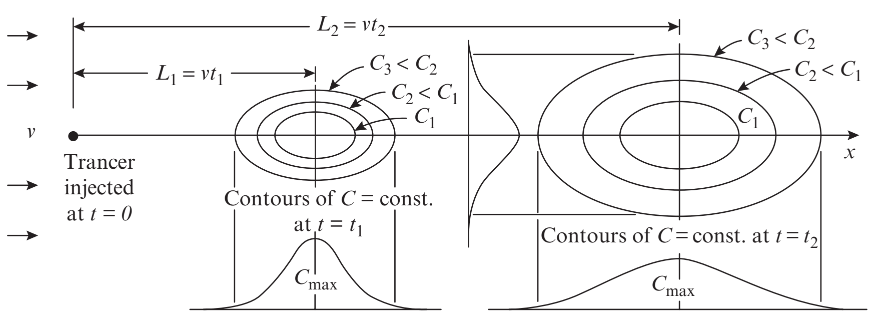

Figure 7.6 *Variation in contaminant concentration from point source as it moves*

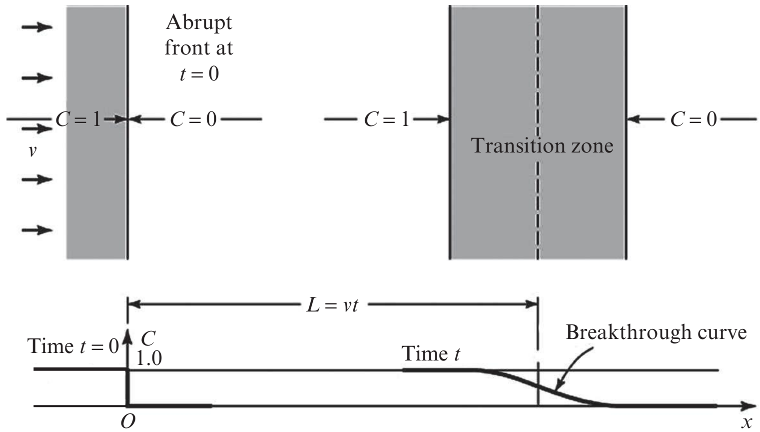

Figure 7.7 *Longitudinal spreading of contaminant from a sharp front due to dispersion*

Figure 7.7 shows the spreading of a conservative contaminants resulting from a sharp front. The relative concentration of contaminant varies in water with space and time. The plot of relative concentration at inlet/source with time is known as the *source loading curve*, whereas the plot of relative concentration at the outlet with time is known as the *breakthrough curve*. The breakthrough curve does not have sharp front as the source loading function. In reality, due to dispersion, the breakthrough curve will take the form of the S-shaped curve shown in Figure 7.8. Dispersion creates a zone of mixing/transition between the displacing fluid and the fluid being displaced. The size of *transition zone* increases as the advective front moves further from the source. The transport phenomena shown in Figures 7.7 and 7.8 are explained by dispersion and molecular diffusion, rather than by the advection mechanism only.

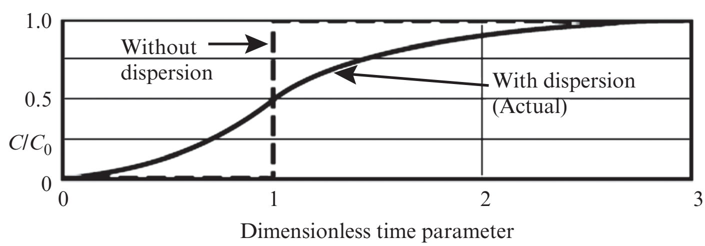

Figure 7.8 *Breakthrough curve due to dispersion in porous media*

Longitudinal dispersion occurs as the velocity distribution of a fluid flowing through a porous medium is not uniform due to geometry of pores and boundary effects of the solid matrix. *Mechanical dispersion* (sometimes called *convective diffusion*) is mixing that is caused by local variations in velocity around some mean velocity of flow, hence it is an advective process rather than a chemical process and happens due to flow and presence of a pore system through which flow takes place. The simultaneous action of the following mechanical phenomena (see Figure 7.9) result in mechanical dispersion:

- Fluid moves faster through the center of the pore than along the edges.
- Some portions of the fluid travel in longer pathways than other portions.
- The movement of fluid through larger pores travel faster than that in smaller pores.
- Heterogeneity of the aquifer causes the groundwater to move faster in some layers and slower in other layers.

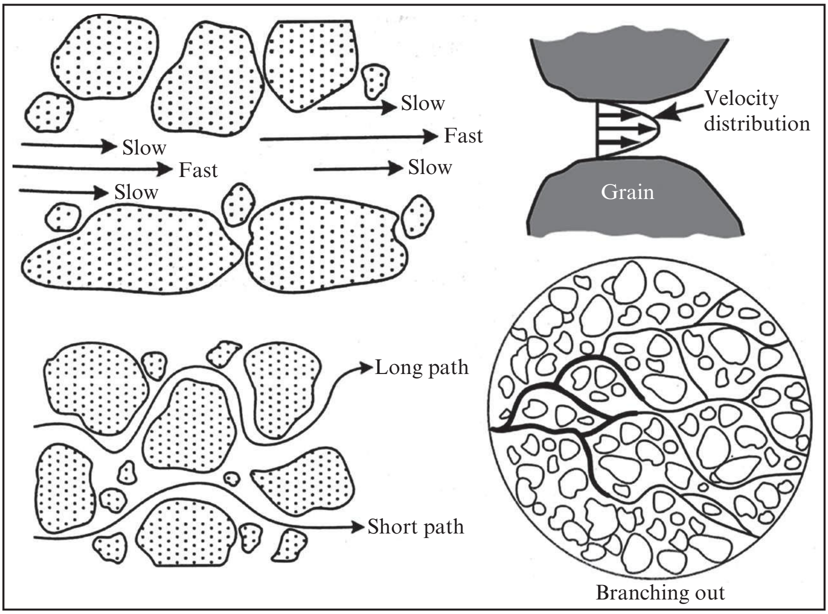

Figure 7.9 *Mechanical phenomena causing dispersion*

The main cause of the *transverse dispersion* is that flow paths branch out to the sides while passing through a porous medium as shown in Figure 7.9.

The mechanical dispersion D_m in uniform flow fields is given by

$$D_m = \alpha_L v_x \tag{7.6a}$$

where, α_L is the *longitudinal dynamic dispersivity*. It is a characteristics property of the porous medium and can be approximated by empirical relations for flow path length L, such as $\alpha_L = 0.83(\log L)^{2.414}$ or $0.0175L^{1.46}$ or $0.1L$.

Usually, molecular diffusion and mechanical dispersion take place coincidently in groundwater movement and hence they cannot be separated in groundwater flow. Actually, molecular diffusion is always present in dispersion and is a most important factor in regularizing the mechanical dispersion. The global effect results from simultaneous action of several physical–chemical phenomena, such as molecular diffusion and permeability contrasts of the porous medium. The *physicochemical dispersion* is molecular diffusion, which results from the chemical potential gradient. Chemical potential is correlated to the concentration. Clubbing together of molecular diffusion and mechanical dispersion is known as *hydrodynamic dispersion*. The longitudinal coefficient of hydrodynamic dispersion D_{hL} takes into account both the molecular diffusion and mechanical dispersion and thus for 1D flow

$$D_{hL} = D_m + D^* = \alpha_L v_x + \tau D \tag{7.6b}$$

Similarly, the transverse hydrodynamic dispersion D_{hT} can be computed as

$$D_{hT} = \alpha_T v_x + \tau D \tag{7.6c}$$

where, α_T is the transverse dynamic dispersivity, which is generally taken as 1/10–1/100 of the longitudinal dispersivity. Dispersion in transverse direction is much weaker process than in the longitudinal direction; however, the coefficients of longitudinal and transverse dispersion are nearly equal at low velocities when molecular diffusion is the dominant dispersive mechanism. The dominant process of mass transport is advection, moving aqueous chemical species along with fluid flow. Advection is important in terms of determining travel times and capture zones, while the diffusion plays an important role in the remediation of contaminants. It helps to dilute their concentration and to mix the contaminants with reactive compounds and microbes in the soil. Most of the contaminant modelling begin with advective transport, where the influences of dispersion and diffusion remain understated.

7.3.4 Decay

Nonconservative dissolved constituents change with time due to biological degradation, decay, chemical, or other reactions. The first-order kinetic equation describing decrease or increase of dissolved constituents in aqueous solution with time is given by

$$\frac{dC}{dt} = -\lambda C \tag{7.7}$$

where, λ = decay constant (1/time), which can be estimated from the half-life of the dissolved constituents or radioactive or the degraded contaminant $t_{1/2}$ as $\lambda = \ln 2 / t_{1/2} = 0.693 / t_{1/2}$. Solution of Eqn. (7.7) yields the concentration C at any time as

$$C = C_0 e^{-\lambda t} \tag{7.8}$$

7.4 GE for Contaminant Transport in Saturated Porous Media

The differential equation for contaminant transport in groundwater can be developed from principles of mass conservation in a REV of size Δx, Δy, and Δz (Figure 7.10) in homogeneous porous media of porosity η. The REV exhibits the average properties of the porous media around a point $P(x, y, z)$, which is the center of the volume. The mass conservation statement can be written as

[*Flux of the solute into REV*]− [*Flux of solute out of REV*] ± [*Loss or gain of solute mass due to reactions within REV*] = [*Net rate of change of mass of solute within REV*]

Let, C is the starting concentration of solute/contaminant [mass/volume] in the REV, so that the initial mass of contaminants within the REV is

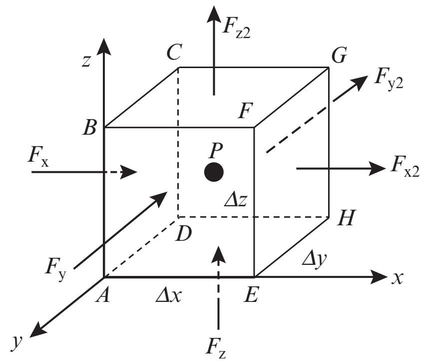

Figure 7.10 *Representative elementary volume*

$$M = C\eta\Delta x\Delta y\Delta z \tag{7.9}$$

hence the net rate of change of mass of contaminants within the REV would be

$$\frac{\partial M}{\partial t} = -\eta\frac{\partial C}{\partial t}\Delta x\Delta y\Delta z \tag{7.10}$$

Considering the nonreactive dissolved contaminant transport, the loss or gain of solute mass due to reactions within REV will be zero.

Now, assume that the contaminant mass fluxes per unit cross sectional area per unit time transported through the six faces are F_x, F_{x2}, F_y, F_{y2}, F_z, and F_{z2}. Use of truncated Taylor's expansion series gives

$$F_{x2} = F_x + \frac{\partial F_x}{\partial x}\Delta x\,; \quad F_{y2} = F_y + \frac{\partial F_y}{\partial y}\Delta y\,; \quad F_{z2} = F_z + \frac{\partial F_z}{\partial z}\Delta z \tag{7.11a-c}$$

Therefore, the net inflow rate into the REV in the *x*-direction would be the difference between the inflow and the outflow rates

$$\left(F_x - F_{x2}\right)\Delta y\Delta z = \left(F_x - F_x - \frac{\partial F_x}{\partial x}\Delta x\right)\Delta y\Delta z = -\frac{\partial F_x}{\partial x}\Delta x\Delta y\Delta z \tag{7.12}$$

Similarly, the net flow rates into the REV in the *y*- and *z*-directions are

$$\left(F_y - F_y - \frac{\partial F_y}{\partial y}\Delta y\right)\Delta x\Delta z = -\frac{\partial F_y}{\partial y}\Delta x\Delta y\Delta z \tag{7.13}$$

and

$$\left(F_z - F_z - \frac{\partial F_z}{\partial z}\Delta z\right)\Delta y\Delta x = -\frac{\partial F_z}{\partial z}\Delta x\Delta y\Delta z \tag{7.14}$$

Total net solute mass inflow rate into the REV, which is equal to solute mass flux into REV minus solute mass flux out of REV, becomes

$$= -\left(\frac{\partial F_x}{\partial x} + \frac{\partial F_y}{\partial y} + \frac{\partial F_z}{\partial z}\right)\Delta x\Delta y\Delta z \tag{7.15}$$

Conservation of mass implies that Eqn (7.10) is equal to Eqn (7.15), therefore

$$\left(\frac{\partial F_x}{\partial x}+\frac{\partial F_x}{\partial x}+\frac{\partial F_x}{\partial x}\right)\Delta x\Delta y\Delta z=\frac{\partial M}{\partial t}=-\eta\frac{\partial C}{\partial t}\Delta x\Delta y\Delta z \tag{7.16}$$

Dividing both sides by volume of REV (i.e., $\Delta x\Delta y\Delta z$)

$$\frac{\partial F_x}{\partial x}+\frac{\partial F_x}{\partial x}+\frac{\partial F_x}{\partial x}=-\eta\frac{\partial C}{\partial t} \tag{7.17}$$

Assume v_x, v_y, and v_z are components of the seepage velocity of groundwater in x, y, and z directions, respectively. The mass flux of solute is transported in x direction by advection and dispersion can be expressed as

Mass flux by advection $F_x = v_x\eta C$ (7.18a)

Mass flux by hydrodynamic dispersion $F_x = -\eta D_{hx}\left(\frac{\partial C}{\partial x}\right)$ (7.18b)

Therefore, total mass flux F_x transported in the x-direction per unit time becomes

$$F_x = v_x\,\eta C-\eta D_{hx}\frac{\partial C}{\partial x} \tag{7.19}$$

In a similar manner, F_y and F_z can be expressed as

$$F_y = v_y\,\eta C-\eta D_{hy}\frac{\partial C}{\partial x} \tag{7.20}$$

$$F_z = v_z\,\eta C-\eta D_{hz}\frac{\partial C}{\partial x} \tag{7.21}$$

Substituting F_x, F_y and F_z in Eqn. (7.17) yields

$$\left[\frac{\partial}{\partial x}\left(D_{hx}\frac{\partial c}{\partial x}\right)+\frac{\partial}{\partial y}\left(D_{hy}\frac{\partial c}{\partial y}\right)+\frac{\partial}{\partial z}\left(D_{hz}\frac{\partial c}{\partial z}\right)\right]-\left[\frac{\partial}{\partial x}\left(v_xC\right)+\frac{\partial}{\partial y}\left(v_yC\right)+\frac{\partial}{\partial z}\left(v_zC\right)\right]=\frac{\partial C}{\partial t} \tag{7.22}$$

For a homogeneous medium with v steady and uniform in space and time, in which the dispersion coefficients D_{hx}, D_{hy} and D_{hz} do not vary through space, then Eqn. (7.22) simplifies to

$$\left[D_{hx}\frac{\partial^2 C}{\partial x^2}+D_{hy}\frac{\partial^2 C}{\partial y^2}+D_{hz}\frac{\partial^2 C}{\partial z^2}\right]-\left[v_x\frac{\partial C}{\partial x}+v_y\frac{\partial C}{\partial y}+v_z\frac{\partial C}{\partial z}\right]=\frac{\partial C}{\partial t} \tag{7.23}$$

The terms in the first bracket represent dispersion–diffusion contribution, whereas the terms in the second bracket are corresponding to advection contribution. Contaminant transport is primarily one dimensional, where solute concentrations are horizontally and vertically well-mixed so that concentrations vary only in the longitudinal or downstream direction. In addition, if the solutes are conservative and the effects of dispersion are spatially constant in a steady uniform flow field, then Eqn. (7.23) reduces to

$$D_{hx}\frac{\partial^2 C}{\partial x^2}-v_x\frac{\partial C}{\partial x}=\frac{\partial C}{\partial t} \tag{7.24}$$

This is the constant-parameter advection–dispersion equation in one dimension. This simple form of advection–dispersion equation with given specific initial and boundary conditions describes spatial and temporal variations in solute concentration.

7.4.1 Solution by Ogata and Banks

Two input loading scenarios may be considered. Under the first scenario, a finite amount of mass is instantaneously released at the upstream boundary of the domain. This type of input function is applicable when the solutes of interest are introduced into the system over a short period of time, such as with a slug injection of dye. In the second input scenario, solutes are continuously released into the system at the upstream boundary. For the case of a continuous source of infinite duration, the initial and boundary conditions are

$$C(x,0)=0 \quad \text{for } x \geq 0 \tag{7.25a}$$

$$C(0,t)=C_0 \quad \text{for } t \geq 0 \tag{7.25b}$$

$$C(\infty,t)=0 \quad \text{for } t \geq 0 \tag{7.25c}$$

where, C_0 = concentration at the upstream boundary. Solution of Eqn. (7.24) with the boundary and initial conditions Eqn. 7.25 (a)–(c) is obtained by Ogata and Banks (1961) as

$$C(x,t)=\frac{C_0}{2}\left[\operatorname{erfc}\left\{\frac{x-v_x t}{2\sqrt{D_{hx}t}}\right\}+\exp\left(\frac{v_x x}{D_{hx}}\right)\operatorname{erfc}\left\{\frac{x+v_x t}{2\sqrt{D_{hx}t}}\right\}\right] \tag{7.26}$$

If a finite amount of mass (C_0 concentration) is instantaneously released at the upstream boundary of the domain, the solution becomes

$$C(x,t)=\frac{C_0}{2}\left[\operatorname{erfc}\left\{\frac{x-v_x t}{2\sqrt{D_{hx}t}}\right\}-\exp\left(\frac{v_x x}{D_{hx}}\right)\operatorname{erfc}\left\{\frac{x+v_x t}{2\sqrt{D_{hx}t}}\right\}\right] \tag{7.27}$$

Ogata and Banks (1961) observed that when the distance or time is large (i.e., $D_{hx}/v_x x < 0.002$) the omission of the second term in solution results in a maximum error of 3 percent. Therefore, for both cases the solutions reduces to

$$\frac{C(x,t)}{C_0}=\frac{1}{2}\left(\operatorname{erfc}\left\{\frac{x-v_x t}{2\sqrt{D_{hx}t}}\right\}\right) \tag{7.28}$$

This form of solution is a normal distribution function with expectation $v_x t$ and standard deviation $\sqrt{2D_{hx}t}$, at a given time at any x. A normal distribution function as labulated in Appendix C gives $\mathrm{P}_N(1)=0.8413$ and $\mathrm{P}_N(-1)=0.1587$. This property allows an easy computation of the standard deviation from the graph of concentration versus x, and very often the width of the transition zone is defined as difference between x at concentration 0.8413 and x at concentration 0.1587. Therefore, at a given time, the width of the transition zone (see Figure 7.11) is

$$2\sigma = x_{.16}-x_{.84}=2\sqrt{2D_{hx}t} \tag{7.29}$$

and D_{hx} is given by

$$D_{hx} = \frac{\left(x_{.16} - x_{.84}\right)^2}{8t} \tag{7.30}$$

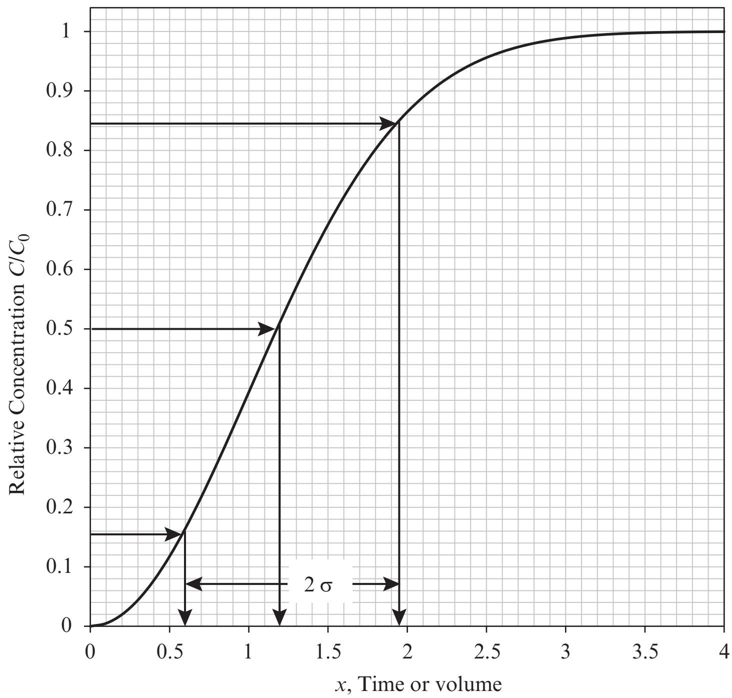

Figure 7.11 *Concentration profile for D_{hx} computation*

Measurements on concentration with time may be performed at a given x (for instance at the lower end of the porous medium). Assuming

$$X_i = \frac{x - v_x t_i}{\sqrt{2D_h t_i}} \tag{7.31}$$

and manipulating yields

$$\frac{\left(x - v_x t_{0.16}\right)}{\sqrt{2D_{hx} t_{0.16}}} - \frac{\left(x - v_x t_{0.84}\right)}{\sqrt{2D_{hx} t_{0.84}}} = 2 \tag{7.32}$$

Solving it for D_{hx} results

$$D_{hx} = \frac{1}{8}\left[\frac{\left(x - v_x t_{0.16}\right)}{\sqrt{t_{0.16}}} - \frac{\left(x - v_x t_{0.84}\right)}{\sqrt{t_{0.84}}}\right]^2 \tag{7.33}$$

If the transition zone is small with respect to the distance travelled from the upper end of the medium to the measurement points, then $\sqrt{t_{.16}} \approx \sqrt{t_{.84}} \approx \sqrt{t_{0.5}}$ and hence Eqn. (7.33) becomes

$$D_{hx} = \frac{1}{8t_{0.5}} v_x^{\,2} \left(t_{0.84} - t_{0.16}\right)^2 = \frac{1}{2} \sigma'^2 \, x v_x \tag{7.34}$$

where,

$$\sigma' = \frac{t_{.84} - t_{.16}}{2t_{.5}} \quad \text{and} \quad t_{0.5} = \frac{x}{v_x} \tag{7.35a,b}$$

This form may be convenient when, at the lower end of the medium, instead of time, injected volumes are measured. Injected volumes, per unit sectional area of porous medium, are related to time by $V_i = vt_i$. Thus, with C as the concentration at the lower end, the graph $\frac{C}{C_0}$ versus the injected volumes is roughly represented by a normal distribution function with standard deviation $(V_{0.84} - V_{0.16})/(2V_{0.5})$.

7.5 Transport of Reactive Pollutants

Within a control volume in an aquifer, there are several processes that act as sources and sinks for solute. These processes include decay, sorption, desorption, chemical reactions, and biological reactions. The one-dimensional transport equation for advection dispersion can be extended to include the effect of retardation of solute transport through sorption, chemical reactions, biological transformations, or radioactive decay by including source–sink term. In the sorption/desorption process, the net rate of reaction *rr* (change in concentration in groundwater caused by sorption and desorption) can be expressed as

$$rr = \left.\frac{\partial C}{\partial t}\right)_{\text{sorption}} = -\frac{\rho_b}{\eta}\frac{\partial \bar{C}}{\partial t} \tag{7.36}$$

where, ρ_b = bulk mass density of the porous media and $\bar{C}$ = concentration of the sorbed contaminants, which can be obtained by dividing the mass of sorbed solute by the mass of dry porous media. If the reaction is in equilibrium, the concentration of the sorbed contaminants is $\bar{C} = K_d C$, where K_d is equilibrium distribution coefficient (volume/mass); therefore,

$$\left.\frac{\partial C}{\partial t}\right)_{\text{sorption}} = -\frac{\rho_b}{\eta} K_d \frac{\partial C}{\partial t} \tag{7.37}$$

which gives the net rate of solute production based on a sorption/desorption reaction between a solute and the porous media within a control volume. Adsorption relationship that can be plotted as straight line on log-log paper is referred as Freundlich isotherm. Distribution coefficient assumes a linear Freundlich isotherm. Many contaminants that are of interest in groundwater studies meet these requirements. The advance of the contaminant front is retarded as a result of the transfer by sorption of the contaminant mass from groundwater to the solid part of the medium. The retardation of the front relative to bulk mass of water as it passes through the solids can be described by the retardation factor, R_a expressed as

$$R_a = 1 + \frac{\rho_b}{\eta} K_d \tag{7.38}$$

The retardation factor ranges from 1 to 10,000. A reactive solute will travel at slower rate than groundwater flow because of the adsorption. The velocity of the solute front v_c is

$$v_c = \frac{v}{R_a} \tag{7.39}$$

Not all contaminants that are adsorbed or desorbed follow the principal of the fast reactions. Reactions that are relatively slow in comparison to the average time travel of the contaminants are described by the kinetics. In case of biological degradation or decay is imposed on the solute, the net rate of solute production rs is expressed as

$$rs = \left.\frac{\partial C}{\partial t}\right)_{\text{decay}} = -\lambda\left(C + \frac{\rho_b}{\eta} K_d C\right) \tag{7.40}$$

Thus, the one-dimensional transport equation considering advection, dispersion, sorption, and decay becomes

$$D_{hx}\frac{\partial^2 C}{\partial x^2} - v_x\frac{\partial C}{\partial x} - \frac{\rho_b}{\eta} K_d \frac{\partial C}{\partial t} - \lambda\left(C + \frac{\rho_b}{\eta} K_d C\right) = \frac{\partial C}{\partial t} \tag{7.41}$$

which defines the change in storage of the contaminant in control volume.

Analytical solutions of the advection dispersion equation can be used for many applications, such as assessing the potential impacts of releases of contaminants to groundwater, estimating the potential exposure concentrations at different locations and providing tools for parameter estimation. Analytical solutions can also be used for locating the contamination sources and establishing the soil clean-up strategies using backward/inverse calculations.

For example, if the source release continues at a constant rate, the contaminant distribution appears as a plume that initially grows in length and width and eventually reaches a steady state distribution. Considering only advection and transverse dispersion (longitudinal dispersion negligible), in steady state the governing becomes

$$-D_{hy}\frac{\partial^2 C}{\partial y^2} + v_x\frac{\partial C}{\partial x} + \lambda C = 0 \tag{7.42}$$

If a constant mass release rate m occurs at the point $(x, y) = (0, 0)$ in an aquifer of thickness b having uniform flow field q, then the solution is

$$C(x,y) = \frac{m}{qb}\frac{1}{\sqrt{4\pi D_{hy} x / v_x}} \exp\left(\frac{-y^2}{4D_{hy} x / v_x}\right) \exp\left(\frac{-\lambda R_a x}{v_x}\right) \tag{7.43}$$

A simple solution (Bear 1979) for concentration distribution when water moves parallel to the contaminant moving front and $C = 0$ for $y \le 0$ and $C = C_0$ for $y > 0$ is

$$C = \frac{C_0}{2}\,\mathrm{erfc}\left(-\frac{y}{\sqrt{4D_{hy}t}}\right) \tag{7.44}$$

This solution is independent of x as well as advective velocity v_x and describes a normal distribution in the y direction.

Verruijit (1971) solved the case of steady state transverse dispersion without decay with boundary conditions

$$C = 0 \quad \text{at } x = 0 \text{ and } 0 < y < \infty \tag{7.45a}$$

$$C = C_0 \quad \text{at } x = 0 \text{ and } -\infty < y < 0 \tag{7.45b}$$

and large values of x. The solution is

$$C = \frac{C_0}{2}\,\mathrm{erfc}\left(\frac{y}{\sqrt{\alpha_T x}}\right) \tag{7.46}$$

This solution is independent of advective velocity v_x and describes a normal distribution in the y direction, with the width of the transition zone being proportional to $\sqrt{x}$. Lines of constant concentration are parabolas.

SOLVED EXAMPLES

Example 7.1: In a sedimentary basin groundwater has the electrical conductivity of 350 micro-siemens/cm. Find a rough estimate of total dissolved solids.

Solution: Electrical conductivity (EC) of any water shows its current carrying capacity. Generally ions are present in water in form of salt and other impurities. Field measurement of the total dissolved solids (TDS) is a difficult task. Because ions concentration present in water is also related to total dissolved solids present in it, a rough estimate can be made between TDS and EC by experimental studies using

TDS = empirical constant × EC $= 0.64 \times 350 = 224\ \mathrm{mg/l}$.

where empirical constant = 0.64 yields TDS in mg/l for EC in micro siemens/cm.

Example 7.2: A contaminant from a point source is continuously leached with a concentration of 115 mg/l. What concentration of the contaminant will reach in a stream after 4 years at 8 m distance from the point source? Assume diffusion coefficient and τ as 2.2×10^{-8} m²/s and 0.5, respectively.

Solution: Effective diffusion coefficient $D^* = \tau D = 0.5 \times 2.2 \times 10^{-8} = 1.1 \times 10^{-8}$ m²/s. Using Eqn. (7.5) for concentration for x = 8 m and t = 6 years

$$C = C_0 \operatorname{erfc}\left(\frac{x}{2\sqrt{D^* t}}\right) = 115 \times \operatorname{erfc}\left(\frac{8}{2\sqrt{1.1\times 10^{-8} \times 6 \times 365 \times 24 \times 3600}}\right)$$

Hence, $C = 115 \times \operatorname{erfc}(2.7726)$. From *Appendix C* $\operatorname{erfc}(2.7726) = 8.817\times 10^{-5}$, therefore

$$C(8\text{ m}, 6\text{ years}) = 115 \times 8.817 \times 10^{-5} = 0.01014\,\text{mg}/1.$$

Example 7.3: There is an unconfined aquifer, which is primary source of drinking water for a town. Hydraulic conductivity, porosity and hydraulic gradient in this aquifer are 5×10^{-5} m/s, 0.4 and 0.08, respectively. When a contaminant from a point source located at a distance 90 m from the town will affect the town in terms of water quality?

Solution: It is assumed that the contaminant is transported only by complete mixing and it has the same velocity as the groundwater. Therefore, $v = \frac{Ki}{\eta} = 5\times 10^{-5} \times \frac{0.08}{0.4} = 1.0\times 10^{-5}\,\text{m/s}$. Time required by contaminant to reach the town is $t = \frac{90}{10^{-5}}\,\text{s} = 104.1677\,\text{days}$.

Example 7.4: Groundwater flows through a cube of sandstone have side of 2m and comes out to the opposite face of the cube. Groundwater velocity is 4×10^{-5} m/s, porosity of sandstone is 0.15 and diffusion coefficient is $8\times 10^{-9}\,\text{m}^2\text{/s}$. Assume that tracer has concentrations 1.25×10^4 and $0.80\times 10^4\,\text{mg}/\text{m}^3$ at inflow and outflow faces respectively. Calculate mass flux due to advection and diffusion at outflow face.

Solution: Mass flux due to diffusion is given by $F_{dif} = -\eta D\frac{dC}{dx} = 0.15\times 8\times 10^{-9}$ $\times 0.45 \times \frac{10^4}{2} = 2.7\times 10^{-6}\,\text{mg/m}^2\text{/s}$. Similarly, mass flux due advection effect is given by

$F_{adv} = v_x \eta C = 4\times 10^{-5} \times 0.15 \times \frac{1.25+0.80}{2} \times 10^4 = 0.0615\,\text{mg/m}^2\text{/s}$; hence,

total mass flux per unit area becomes $F = F_{diff} + F_{adv} = 2.7\times 10^{-6} + 0.0615$ $= 0.061502\,\text{mg/m}^2\text{/s}$. Total mass flux out of an area of 4 m^2 is $F = 0.061502 \times 4 \times 24 \times 3600 \times 10^{-3} = 21.255$ g/d.

Example 7.5: Nitrobenzene (650 mg/l concentration) is being released in an aquifer having hydraulic conductivity 4×10^{-5} m/s, hydraulic gradient 0.002, and porosity 0.40. Assuming molecular diffusion for the nitrobenzene equal to $1.12\times 10^{-8}\,\text{m}^2\text{/s}$, compute the concentration of the contaminant after 2.5 years at 60 m away from the source.

Solution: Seepage velocity of groundwater in the aquifer $v_x = \dfrac{4\times10^{-5}\times0.0020}{0.40} =$ 2.0×10^{-7} m/s. Longitudinal dynamic dispersivity $\alpha_L = 0.83(\log(60))^{2.414} = 3.3304$ and longitudinal dispersion coefficient $D_L = \alpha_L v_x + D^* = 3.3304 \times 2 \times 10^{-7}$ $+ 1.12 \times 10^{-8} = 0.677 \times 10^{-7}$ m/s. Using Ogata and Banks (1961) solution Eqn. (7.26) for x = 60 m and $t = 2.5\,\text{years} = 2.5\times24\times3600\times365 = 7.884\times10^7$ s yields

$$C = \frac{650}{2}\left[\operatorname{erfc}\left\{\frac{60-2\times10^{-7}\times7.884\times10^7}{2\sqrt{0.677\times10^{-6}\times7.884\times10^7}}\right\}\right.$$

$$\left. +\exp\left(\frac{2\times10^{-7}\times60}{0.677\times10^{-7}}\right)\operatorname{erfc}\left\{\frac{60+2\times10^{-7}\times7.884\times10^7}{2\sqrt{0.677\times10^{-6}\times7.884\times10^7}}\right\}\right]$$

Therefore, $= \dfrac{650}{2}\left[\operatorname{erfc}(3.027)+\exp(17.7252)\operatorname{erfc}(5.2124)\right]$, using *Appendix C* for erfc

$$C = \frac{650}{2}\left[1.862\times10^{-5} + 49.8834\times10^6\times0\right] = 6.0515\times10^{-3}\ \text{mg/l}$$

PROBLEMS

7.1. What is contamination? What are sources and causes of groundwater contamination?

7.2. Describe the different classification of groundwater contamination.

7.3. What are differences between point source and nonpoint source of groundwater contamination?

7.4. Describe the different mechanisms of groundwater contamination.

7.5. What are differences between diffusion and dispersion?

7.6. Derive the governing equation of groundwater contamination.

7.7. Obtain Ogata and Banks solution for contamination transportation in groundwater?

7.8. An aquifer (porosity = 0.35) by a contaminant of diffusion coefficient 4×10^{-10} m^2/s. If the concentration gradient of the contaminant is 3×10^{-7} kg/l/m, calculate the diffusive flux.

7.9. Calculate the concentration of a contaminant 5 m away from the interface of a landfill and liner after 50 years if the initial concentration, diffuse coefficient, and τ are 150 mg/l, 2×10^{-8} m^2/s, and 0.5, respectively.

7.10. Calculate the concentration of a contaminant 400 m away in 20 years if the initial concentration, diffuse coefficient, and τ are 20 mg/l, 2×10^{-7} m^2/s, and 0.35 respectively. Assume the groundwater velocity is 5×10^{-7} m/s.

7.11. How far will a contaminant move in 2.5 years in an aquifer having hydraulic conductivity, hydraulic gradient, and porosity as 5×10^{-5} m/s, 0.1, and 0.35 respectively?

7.12. What is the total mass flux of a contaminant of 25 mg/l concentration out from a porous media of 2.5 m thick and 100 m wide having seepage velocity and porosity as 0.5 m/d and 0.25, respectively?

7.13. What is the total mass flux of a contaminant of 20 mg/l concentration out from a porous media of 2 m thick and 75 m wide having seepage velocity and porosity as 0.25 m/d and 0.3, respectively?

7.14. Compute the concentration of a contaminant after 2.5 years and 50 m away from a point source where the contaminant of 700 mg/l concentration is released in an aquifer having hydraulic conductivity, hydraulic gradient, and porosity as 5×10^{-5} m/s, 0.0015, and 0.35, respectively. Assume molecular diffusion of the contaminant is equal to 1.5×10^{-8} m^2/s.

7.15. Compute the concentration of a contaminant after 3 years and 75 m away from a point source where the contaminant of 500 mg/l concentration is released in an aquifer having hydraulic conductivity, hydraulic gradient, and porosity as 2.5×10^{-6} m/s, 0.04, and 0.25, respectively. Assume molecular diffusion of the contaminant is equal to 2×10^{-8} m^2/s.

7.16. Compute the time taken for a contaminant concentration to reach 10 percent of the initial concentration at 500 m away in 1-D flow neglecting decay process in an aquifer having hydraulic conductivity, hydraulic gradient, and porosity as 2 m/d, 0.06, and 0.2, respectively. Assume longitudinal coefficient of hydrodynamic dispersion of the contaminant is equal to 0.5 m^2/s.

7.17. Compute the time taken for a contaminant concentration to reach 20 percent of the initial concentration at 500 m away in 1-D flow neglecting decay process in an aquifer having hydraulic conductivity, hydraulic gradient, and porosity as 2.5 m/d, 0.075, and 0.3, respectively. Assume longitudinal coefficient of hydrodynamic dispersion of the contaminant is equal to 0.6 m^2/s.

Chapter

8 Groundwater Flow Solutions by Complex Analysis

8.1 General

Understanding of groundwater movement has always been an endeavour for engineers and mathematicians. The complexity of geological formations has added to the difficulty of understanding groundwater motion. Often mathematicians use complex functions and conformal mapping to find analytical solution to groundwater flow problems. The usefulness of conformal mapping in two-dimensional flow problems stems from the fact that solutions of Laplace's equation remain solutions when subjected to conformal transformation. The solution of a two-dimensional groundwater problem could be reduced to one seeking the solution of Laplace's equation subject to certain boundary conditions within a region R in the Z plane. Unless the region R is of a very simple shape, an analytical solution to Laplace's equation is generally very difficult. However by means of conformal mapping, it is often possible to transform the region R into a simpler region R_1, wherein Laplace's equation can be solved subject to the transformed boundary conditions. Once the solution has been obtained in region R_1, it can be carried back by the inverse transformation to the region R of the original problem. Hence, the crux of the problem finds a series of transformation that will map a region R conformally into a region R_1 so that R_1 will be of a simple shape, such as a rectangle or a circle.

8.2 Complex Numbers

Any number of the form $Z = X + iY$, in which X and Y are scalars and $i = \sqrt{-1}$ is the imaginary unit, is called a *complex number*. The real number X is called the real part of Z written as Re (Z) and the real number Y is called the imaginary part of Z written as Im (Z). A complex number $Z = X + iY$ can be taken as either the geometrical representation of a point with the Cartesian coordinates (X, Y) or as a position vector that radiates from the origin to this point. The Cartesian plane in complex analysis is called the *Argand diagram* or the *complex plane*, or simply the Z plane. The absolute value or the *modulus* of Z is given by the following equation:

$$\operatorname{mod} Z = |Z| = |X + iY| = \sqrt{X^2 + Y^2} \tag{8.1}$$

and *amplitude* or *argument* of Z by the following relation:

$$\arg Z = \theta = \tan^{-1}\frac{Y}{X} \tag{8.2}$$

Since X axis is normal to Y axis, it follows that two complex numbers can be equal if and only if their respective real and imaginary parts are equal.

The trigonometric representation and polar form of a complex number are

$$Z = r(\cos\theta + i\ \sin\theta)\ \text{ since }\ X = r\cos\theta; Y = r\sin\theta \tag{8.3a}$$

$$Z = re^{i\theta}\ \text{ since }\ e^{i\theta} = (\cos\theta + i\ \sin\theta) \tag{8.3b}$$

Therefore, $i = \sqrt{-1} = e^{i\pi/2}$ that means i has a modulus of unity and an argument $\pi/2$. We see that the multiplication of a complex number by i $\left(Zi = re^{i\theta}e^{i\pi/2} = re^{i(\theta+\pi/2)}\right)$ simply rotates the position vector through the angle $\pi/2$ without altering its modulus. The polar form is very convenient in taking logarithm of complex numbers, in multiplication and division of complex numbers and in deriving de Moivre′s theorem:

$$\ln Z = \ln\left(re^{i\theta}\right) = \ln|Z| + i\theta = \ln|Z| + i\arg Z \tag{8.4a}$$

$$Z_1Z_2 = r_1e^{i\theta_1}.r_2e^{i\theta_2} = r_1r_1e^{i(\theta_1+\theta_2)} \tag{8.4b}$$

$$Z^n = \left(re^{i\theta}\right)^n = r^n(\cos\theta + i\sin\theta)^n = r^ne^{in\theta} = r^n(\cos n\theta + i\sin n\theta) \tag{8.4c}$$

Therefore, if $r = 1$, then

$$(\cos\theta + i\sin\theta)^n = (\cos n\theta + i\sin n\theta) \tag{8.4d}$$

which is de Moivre′s theorem.

8.3 Complex Function

A *complex function* is a functional relationship between two complex variables. For example, $W = f(Z)$ is a complex function, if $W = Z^2$ then $\phi = X^2 - Y^2$; $\psi = 2XY$, where $W = \phi + i\psi$; in which ψ = stream function; and ϕ = velocity potential (m²/s) for a two-dimensional flow in XY plane given by the following equation:

$$\phi = -K\left(\frac{p_w}{\gamma_w} + Y\right) + C_1 \tag{8.5}$$

where, p_w = water pressure (Pa) at point (X, Y); γ_w = unit weight of water (N/m³); C_1 = arbitrary constant (m²/s); and Y = elevation head taken positive upward (m). The discharge velocities are defined by

$$u = \frac{\partial\phi}{\partial X} = \frac{\partial\psi}{\partial Y};\quad \text{and}\quad v = \frac{\partial\phi}{\partial Y} = -\frac{\partial\psi}{\partial X} \tag{8.6}$$

where, u = component of discharge velocity in X direction (m/s) and v = component of discharge velocity in Y direction (m/s).

Analytic, regular, or *holomorphic functions*: In general, the complex functions of interest in groundwater flow are analytic. If, at each point within a region of the Z plane, the function $W = f(Z)$ and its derivative dW/dZ are both single-valued and finite, then the function is said to be *analytic* within the region. An analytical function satisfies Cauchy–Riemann equations given by

$$\frac{\partial \phi}{\partial X} = \frac{\partial \psi}{\partial Y}; \qquad \text{and} \qquad \frac{\partial \phi}{\partial Y} = -\frac{\partial \psi}{\partial X} \tag{8.7}$$

and all the partial derivatives $\partial\phi/\partial X$, $\partial\phi/\partial Y$, $\partial\psi/\partial X$, and $\partial\psi/\partial Y$ are continuous within the region. If a function is analytical, it possesses derivatives not only of the first order but also of all orders. Thus, the existence and continuity of all partial derivatives of ϕ and ψ are assured if $W = f(Z)$ is analytical. Both the real (ϕ) and imaginary (ψ) parts of an analytical function satisfy Laplace's equation in two dimensions:

$$\frac{\partial^2 \phi}{\partial X^2} + \frac{\partial^2 \phi}{\partial Y^2} = 0; \qquad \text{and} \qquad \frac{\partial^2 \psi}{\partial X^2} + \frac{\partial^2 \psi}{\partial Y^2} = 0 \tag{8.8}$$

Any function that satisfies Laplace equation is called a *harmonic* function. Two harmonic functions such as ϕ and ψ so related that $W = \phi + i\psi$ is an analytical function, are called *conjugate harmonic functions*. If ϕ and ψ are conjugate harmonic functions, then the families of curves $\phi(X, Y) =$ constant and $\psi(X, Y) =$ constant are orthogonal to each other.

8.4 Mapping

The direct functional relationship $W = f(Z)$ may not be known, but the relationship of each of the complex variables Z and W with another complex variable may be known or established easily. The desired functional relationship is generally determined with the help of mapping. *Mapping* is the correspondence of a sequence of points from one plane into another plane.

Let $W = \phi + i\psi$ be an analytic function of $Z = X + iY$ and suppose that a complex number $X + iY$ is located at point P in the Z plane (Figure 8.1). As W is a function of Z, there must be some point Q in the W plane corresponding to the point P in the Z plane.

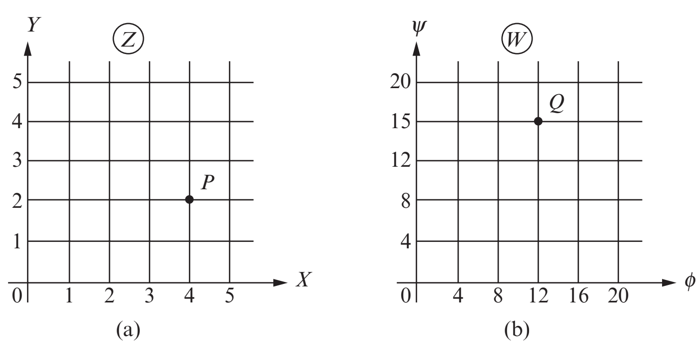

Figure 8.1 *Mapping*

In groundwater, commonly used mapping functions are conformal mapping, linear mapping, inverse mapping, velocity hodograph, Zhukovsky′s mapping, Schwarz–Christoffel transformation, etc. These mapping functions are described in the subsequent section following treatment used by Harr (1962).

8.5 Conformal Mapping

A transformation that possesses the property of preserving angles of intersection in magnitude and sense, and the approximate image of small shapes is said to be *conformal*.

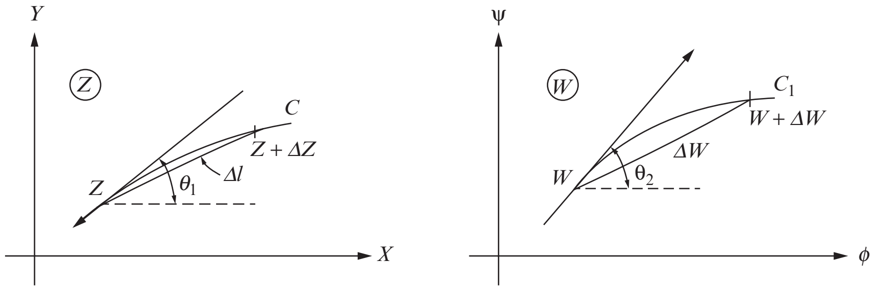

Figure 8.2 *Conformal mapping*

Let C (Figure 8.2) be a smooth curve through a point Z, and let C_1 be its image through point W under the transformation $W = f(Z)$ when $f(Z)$ is analytic at Z and $f'(Z) \neq 0$. As $f'(Z)$ must be a complex number, say $f'(Z) = A \exp i\alpha$, then from the definition of a derivative

$$f'(Z) = \frac{dW}{dZ} = \lim_{\Delta Z \to 0} \left(\frac{\Delta W}{\Delta Z} \right) \tag{8.9a}$$

we obtain the two equations:

$$\alpha = \arg f'(Z) = \lim_{\Delta Z \to 0} \left(\arg \frac{\Delta W}{\Delta Z} \right) = \theta_2 - \theta_1 \tag{8.9b}$$

$$A = \text{mod } f'(Z) = \lim_{\Delta Z \to 0} \left| \frac{\Delta W}{\Delta Z} \right| \tag{8.9c}$$

Salient Features of Conformal Mapping

Any two curve intersecting at a particular angle at point Z will, even after transformation, intersect at the same angle at W (the image of Z); that is, the sides of the angle at W are rotated in the same direction by the same amount α. Infinitesimal lengths in Z are magnified at W by a factor of $A = \text{mod} f'(Z)$. However, large figures in the Z plane may transform into shapes bearing little resemblance to the original, but the angles formed are preserved even in these cases of intersection in case of large figures. Points at which $f'(Z) = 0$ are termed as *critical or singular points* of the transformation where the angles are not preserved conformally. If $f'(Z)$ has n-fold zeros, angles are not preserved at the critical points but are multiplied $(n + 1)$ times.

8.6 Linear and Inverse Mapping Functions

Linear Mapping Function

The general form of linear mapping function is $W = aZ + b$ (where $a \neq 0$, a and b are any complex constants). This mapping is everywhere conformal, since $f'(Z) = a \neq 0$. This transformation represents a rotation through the angle arg a, a magnification (multiplication) by the factor $|a|$, and then a translation through the vector b. In the transformation, a region in the Z plane is transformed into a geometrically similar region in the W plane.

Inverse Mapping Function

The transformation $W = 1/Z$ provides a single valued correspondence between all points in the Z and W planes (see Figure 8.3). Taking $W = \rho\exp(i\alpha)$ and $Z = r\exp(i\theta)$, the transformation yields $\alpha = -\theta$ and $\rho = 1/r$.

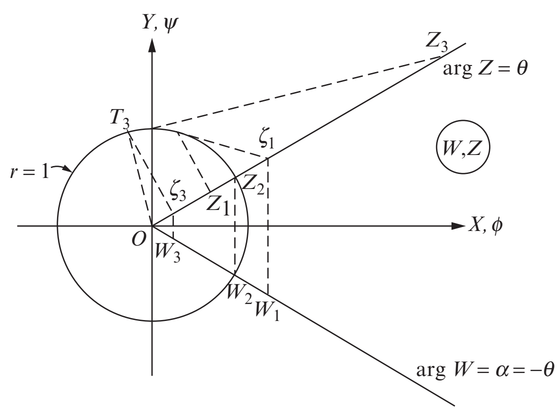

Figure 8.3 *Inverse function mapping*

Thus, the transformation yields $\arg W = -\arg Z$ and $|W||Z| = 1$, which implies that there is a simple reflection about the real axis and an inversion with respect to the unit circle $r = 1$. By a familiar theorem from geometry, a point and its inverse are related as follows: assume that the circle about point 0 represents the unit circle ($r = 1$) and that the point Z_3 is an exterior point in the Z plane ($r > 1$). From Z_3, construct the tangent to T_3 and drop a perpendicular to T_3 on the line ζ_3. ζ_3 is said to be the inverse of the point Z_3, and conversely. In the inversion process, the points $r = 1$ play a special role in that they define a circle of unit radius in the Z plane that maps into itself in the W plane. The points $r < 1$ in the Z plane (points interior to the unit circle) correspond to the points $\rho > 1$ (points exterior to the unit circle) in the W plane, or, in general, points exterior to the unit circle are mapped into its interior. In other words, the inversion process can be thought of as a reflection about the unit circle. In particular, points at the origin $Z = 0$ (or $W = 0$) are mapped into infinity $W = \infty$ (or $Z = \infty$), points at a circle of unit radius in the Z (or W) plane are mapped into itself in the W (or Z) plane, and points exterior to the unit circle in one plane are mapped into interior to the unit circle in the another plane and vice versa. In general, the reciprocal function transforms

(i) circles not passing through the origin into circles not through the origin
(ii) circles through the origin into straight lines not through the origin
(iii) straight lines through the origin into straight lines through the origin
(iv) straight lines not through the origin into circles through the origin

The inverse function can be used in transforming hodograph plane into inverse hodograph (dZ/dW) plane. The flow region in the inverse hodograph may be a polygon consisting only of straight-line boundaries.

8.7 Velocity Hodograph

Let the complex potential $W = \phi + i\psi$ be an analytical function of the complex variable Z, as $W = f(Z)$. Differentiation of W with respect to Z yields

$$\frac{dW}{dZ} = \frac{\partial \phi}{\partial X} + i\frac{\partial \psi}{\partial X} = \frac{\partial \psi}{\partial Y} - i\frac{\partial \phi}{\partial Y} = u - iv \tag{8.10}$$

The transformation of the region of flow from Z plane into the dW/dZ plane is called the *velocity hodograph*. The utility of the hodograph stems from the fact that although the shape of the free surface and the limit of the surface of seepage are not known initially in the Z plane, their hodographs are completely defined in the dW/dZ plane.

Generally, the various boundaries of a flow region in Z plane are transformed first into the $u + iv$ plane. Then the mirror reflections about u axis results into velocity hodograph, that is $u - iv$ plane. The various boundary relations of the hodograph are described in the following sections.

Impervious boundary

At an impervious boundary, the velocity vector is in the direction of the boundary. Therefore, designating the boundary at an angle α with the X-axis, in the hodograph plane we have $v/u = \tan \alpha$, which represents a straight line in the u–v plane, passing through the origin in a direction parallel to the impervious boundary.

Boundary of a reservoir

The boundary of a reservoir is an equipotential line, $\phi =$ constant; consequently, the velocity vector is perpendicular to the boundary. If the equation of the boundary is the straight line

$$Y = X \tan\alpha + b \tag{8.11a}$$

then in the hodograph plane the image of the boundary will be the straight line

$$v / u = -\cos\alpha \tag{8.11b}$$

which passes through the origin of the u–v plane and is normal to the reservoir boundary.

Free surface or Phreatic surface

Along the free surface $\phi + KY =$ constant. Differentiating this expression with respect to s, where s is along the free surface, and multiplying through by $\partial\phi/\partial s$, we obtain

$$(\partial\phi/\partial s)^2 + K(\partial\phi/\partial s)(dY/ds) = 0 \tag{8.12a}$$

Now, recognizing that $\partial\phi/\partial s$ is the velocity vector, and that

$$(\partial\phi/\partial s)^2 = u^2 + v^2 \text{ and } (\partial\phi/\partial s)(dY/ds) = v \tag{8.12b}$$

it follows that along the free surface

$$u^2 + v^2 + Kv = 0 \tag{8.12c}$$

Eqn. (8.12c) represents a circle, passing through the origin, with radius $K/2$ and centre at $(0, -K/2)$. It follows at once from Eqn. (8.12c) that the velocity vector at any point along the free surface can be obtained from the simple graphical construction shown in Figure 8.4. The angle β in this figure represents the angle between the tangent to the free surface at the point in question and the horizontal.

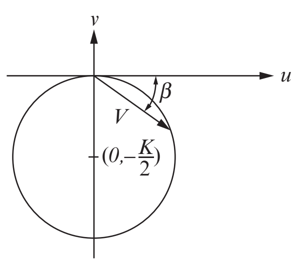

Figure 8.4 *Free surface mapping*

Surface of seepage

Along the surface of seepage, as in the case of the free surface, $\phi + KY =$ constant. Differentiating this expression with respect to n, the length along the surface, we have

$$\partial\phi/\partial n + K(dY/dn) = 0 \tag{8.13a}$$

Now, designating α as the angle that the surface of seepage makes with the X axis and recognizing that

$$\partial\phi/\partial n = u\cos\alpha + v\sin\alpha \quad \text{and } dY/dn = \sin\alpha \tag{8.13b}$$

we obtain

$$u\cos\alpha + v\sin\alpha + K\sin\alpha = 0 \text{ or } v = -u\cot\alpha - K \tag{8.13c}$$

Hence, if the surface of seepage is a straight line ($\alpha =$ constant) in the u–v plane, it will be represented as a straight line normal to the surface and passing through the point $(0, -K)$, the lowest point of the circle representing the image of the free surface.

Summary

The elementary boundaries transform into hodograph plane as follows:

- At an impervious boundary, the velocity vector is in the direction of the boundary; in *u*–*v* plane, a straight line passing through the origin and parallel to the impervious boundary represents the impervious boundary.
- Since a boundary of reservoir is an equipotential line, velocity vector is perpendicular to the boundary, hence in *u*–*v* plane a straight line passing through the origin and normal to the reservoir boundary represents the reservoir boundary.
- A line of seepage (phreatic line) is a streamline and along it $\phi + KY = const.$, in *u*–*v* plane a circle ($u^2 + v^2 + Kv = 0$) passing through the origin, with radius *K*/2 and centre at (0, −*K*/2) represents the phreatic line.
- A surface of seepage in *Z* plane, which is neither a streamline nor an equipotential line, is represented by a straight line normal to the seepage surface and passing through the point (0, −*K*) in the *u*–*v* plane.

Following these transformation properties, the velocity hodograph can be drawn for the physical flow region in the *Z* plane.

8.8 Zhukovsky Functions

A special mapping technique, of particular value when dealing with unconfined flow problems, makes the use of an auxiliary transformation called Zhukovsky′s function. Rewriting Eqn. (8.5) (the relationship between the velocity potential and the pressure) as

$$\phi + KY = -K\frac{p_w}{\gamma_w} + C_1 \tag{8.14a}$$

and defining $\theta_1 = -K\,p_w/\gamma_w$ and taking $C_1 = 0$, then

$$\phi + KY = \theta_1 \tag{8.14b}$$

Operating ∇^2 on this expression,

$$\nabla^2\theta_1 = \nabla^2(\phi + KY) = \nabla^2\phi = 0$$

This shows that θ_1 is a harmonic function of *X* and *Y*. Hence, its conjugate is the function

$$\theta_2 = \psi - KX \tag{8.14c}$$

Defining

$$\theta = \theta_1 + i\theta_2 \tag{8.14d}$$

We have

$$\theta = \phi + KY + i(\psi - KX) = W - iKZ \tag{8.15}$$

Any function of type Eqn. (8.15) that is, with its real or imaginary part differing from it by a constant multiplier is called a *Zhukovsky function*. Zhukovsky function for the free surface will have $\theta_1 = 0$ and $\theta_2 = -KX$, and hence in the θ plane, the free surface will have as its image the negative imaginary axis. Thus, the region of unconfined flow in the Z plane with an unknown position of phreatic line is transformed into an infinite strip in Zhukovsky′s θ plane. If the functional relationship between the θ plane and the W plane were determined, say $W = f(\theta)$, then making use of Zhukovsky function definition we would have $W = f(Z)$, and from which all pertinent seepage characteristics could be found.

8.9 Schwarz–Christoffel Transformation

Schwarz–Christoffel transformation is a method of mapping a polygon consisting of straight-line boundaries, from one plane onto the upper/lower half of another plane. The transformation can be considered as the mapping of a polygon from the Z plane onto a similar polygon in the t plane in such a manner that the sides of the polygon in the Z plane extend through the real axis of the t plane. This is accomplished by opening the polygon at some convenient point, say between A and E of Figure 8.5(a), and extending one side to $t = -\infty$ and the other to $t = +\infty$ (Figure 8.5b). In this operation, the sides of the polygon are bent into a straight line extending from $t = -\infty$ to $t = +\infty$ and are placed along the real axis of the t plane.

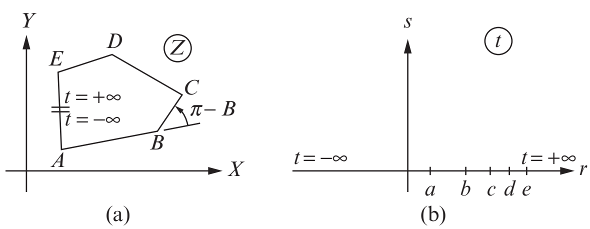

Figure 8.5 *Schwarz–Christoffel transformation*

This transformation can be considered as the mapping of a polygon from one plane onto a similar polygon in another plane in such a manner that the sides of the polygon in one plane extend through the real axis of another plane by opening the polygon at some point and extending one side to $-\infty$ and other to $+\infty$. Thus, the transformation maps conformally the region interior to the polygon into the entire upper/lower half of the auxiliary plane. The transformation that maps the Z plane conformally onto upper half of the auxiliary ζ plane is

$$\frac{dZ}{d\zeta} = C_1(\zeta - \beta_1)^{\alpha_1 - 1}(\zeta - \beta_2)^{\alpha_2 - 1}(\zeta - \beta_3)^{\alpha_3 - 1}\ldots \tag{8.16a}$$

$$Z = C_1\int_0^{\zeta} \frac{dt}{(t-\beta_1)^{1-\alpha_1}(t-\beta_2)^{1-\alpha_2}(t-\beta_3)^{1-\alpha_3}\ldots} + C_2 \tag{8.16b}$$

where, t is the dummy variable and C_1 and C_2 are complex constants. $\alpha_1, \alpha_2, \alpha_3, \ldots$ are the interior angles (fraction of π) of the polygon in the W plane, and $\beta_1, \beta_2, \beta_3, \ldots$

($-\infty < \beta_1 < \beta_2 < \beta_3 < \ldots < \infty$) are the points on the real axis of the ζ plane corresponding to the respective vertices. Any three of the values $\beta_1, \beta_2, \beta_3, \ldots$ can be chosen arbitrarily to correspond to three of the vertices of the given polygon. The (N-3) remaining values must then be determined so as to satisfy conditions of similarity. The interior angle at the point of opening may be regarded as π; hence, it takes no part in the transformation. Also the vertex of the polygon placed at infinity in the ζ plane does not appear in the transformation. Thus, by mapping a vertex of the flow region into one at infinity in the auxiliary plane omits vertex factor from the transformation and reduces one unknown.

8.10 Mapping Examples

8.10.1 Velocity Hodograph

Case 1: Draw velocity hodograph for seepage through an earth dam with a horizontal underdrain.

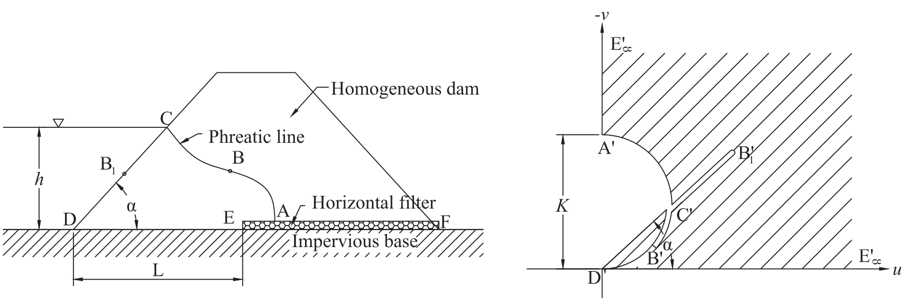

(a) Earth dam with a horizontal underdrain (b) Hodograph

Figure 8.6 *Velocity hodograph for an earth dam with a horizontal underdrain.*

Figure 8.6(a) shows an earth dam with a horizontal underdrawn. CB_1D is reservoir boundary (equipotential line); therefore in hodograph plane, it will be a straight line passing through origin and normal to the *u/s* slope of the dam. ABC is free surface (phreatic line) in the physical plane, therefore it maps along a circle of radius K with centre at (0, K/2) in the hodograph plane. Finally, DE is an impervious boundary (flow line), hence it maps a straight line passing through origin and parallel to the direction in physical seepage plane, that is, u-axis. The underdrawn AE is an equipotential line; hence, its mapping will be a straight line passing through origin and normal to the drain, that is, v-axis. Point E is a common point on equipotential and flow lines having angle $\alpha < \pi/2$; therefore, it is a singular point with infinite velocity. The slit at point B on the circumference of the circle is a consequence of the velocity at the point of inflection representing the minimum velocity along the free surface. Thus, in the hodograph plane Figure 8.6(b), the region of flow is bounded by the circle corresponding to the free surface, a straight line passing through the origin perpendicular to the *u/s* slope, the u-axis corresponding to the impervious base, and the v-axis corresponding to the underdrain.

Case 2: Draw the velocity hodograph for seepage from a trapezoidal canal.

Consider a trapezoidal channel of bed width b (m), depth of water y (m), side slope m (1 vertical: m horizontal), underlain by a drainage layer at a depth d (m) below the canal water surface, and passing through a homogeneous isotropic porous medium of hydraulic conductivity K (m/s) as shown in Figure 8.7. Let the physical plane is defined as $Z = X + iY$. Let us draw the velocity hodograph plane $(dW/dZ = u - iv)$ for the seepage domain $a'b'c'g'h'$ as hatched in Figure 8.7.

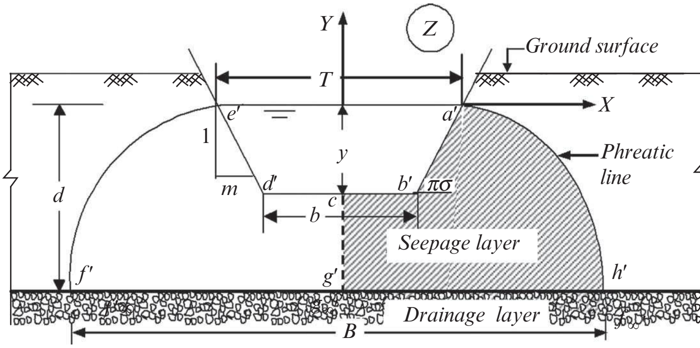

Figure 8.7 *Pattern of seepage from a trapezoidal canal with drainage layer at finite depth*

It is assumed that the water table is below the top of the drainage layer, and hence atmospheric pressure prevails at the bottom of the seepage layer and $g'h'$ is equipotential line. Being reservoir boundaries $a'b'$ and $b'c'$ are equipotential lines. Since $a'b'$, $b'c'$, and $g'h'$ are equipotential lines; therefore in hodograph plane, they will be straight lines passing through origin and normal to the direction in physical seepage plane. At b' seepage velocity is infinite, therefore point b' in hodograph plane goes to infinity. Point g' maps in between c' and h' in hodograph plane as the seepage velocity at there is less than at c'. $a'h'$ is the phreatic line in physical plane, therefore it maps along a circle of radius K with centre at (0, K/2) in the hodograph plane. Finally, $c'g'$ is a flow line (like impervious boundary), therefore it maps a straight line passing through origin and parallel to the direction in physical seepage plane. Therefore, the final velocity hodograph is $b_\infty'c'g'h'a'b_\infty'$ as shown in Figure 8.8.

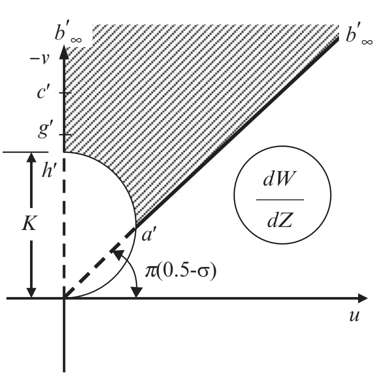

Figure 8.8 *Velocity hodograph for seepage from a trapezoidal canal*

8.10.2 Inverse Mapping

Draw an inverse hodograph plane for the case of seepage from a trapezoidal canal with drainage layer at finite depth (Figure 8.7) or inverse mapping of velocity hodograph plane of Figure 8.8. $a'h'$ is a circle of diameter K through the origin in the hodograph plane, therefore in the inverse plane it maps a straight line not through the origin that is, parallel to X axis at distance $1/K$. On the other hand $a'b'$, $b'c'$, $c'g'$, and $g'h'$ are straight lines through the origin in the hodograph plane, therefore these lines map into straight lines through the origin in the inverse hodograph plane. Thus the final inverse hodograph plane is $b'c'g'h'a'b'$ as shown in Figure 8.9.

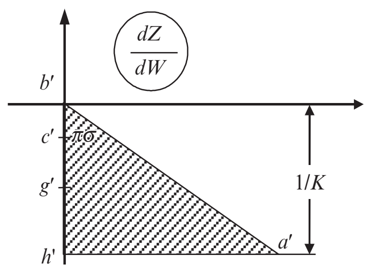

Figure 8.9 *Inverse mapping of hodograph*

8.10.3 Mapping in Complex Potential Plane

Defining complex potential $W = \phi + i\psi$ and as water table is below the top of the drainage layer and atmospheric pressure prevails at the bottom of the seepage layer, $g'h'$ is equipotential line. Also $a'b'c'$ is equipotential line and potential difference between $a'b'c'$ and $g'h'$ is Kd. On the other hand, $a'h'$ is last flow line (phreatic line) and $c'g'$ is middle flow line (due to symmetry of flow in vertical plane), therefore the difference between these two flow lines is $q_s/2$, where q_s is the total seepage per unit length of the canal. Therefore, the seepage domain in the physical plane is bounded by two flow lines and two equipotential lines, and hence the final mapping in complex potential $W = \phi + i\psi$ is a rectangle $c'g'h'a'$ as shown in Figure 8.10.

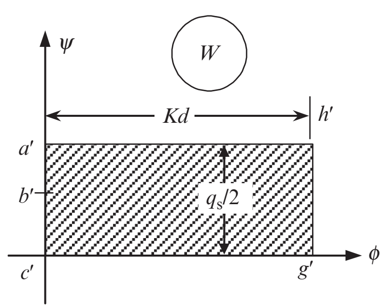

Figure 8.10 *Complex potential mapping*

8.10.4 Schwarz–Cristoffel Transformation

Find mapping of a semi-infinite strip through Schwarz–Cristoffel transformation.

Consider the conformal mapping of the semi-infinite strip $A\infty BC\ A\infty$ of width b (Figure 8.11a) onto the upper half of the ζ plane (Figure 8.11b) through Schwarz–Cristoffel transformation. The strip may be considered as a triangle with interior angles $B = \pi/2$, $C = \pi/2$, and $A = 0$. In mapping the points A_∞, B, and C arbitrarily on the points $\zeta = -\infty$, $\zeta = -1$, and $\zeta = 1$, respectively, conditions of symmetry places the fourth vertex at $\zeta = \infty$ and the Schwarz–Cristoffel transformation is

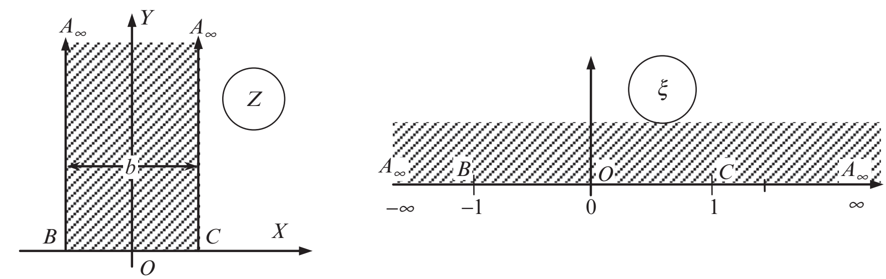

(a) Semi-Infinite strip (b) Upper half of auxiliary plane

Figure 8.11 *Schwarz–Cristoffel transformation of a semiinfinite strip*

$$\frac{dZ}{d\zeta} = C_1(\zeta - \beta_1)^{\alpha_1 - 1}(\zeta - \beta_2)^{\alpha_2 - 1}(\zeta - \beta_3)^{\alpha_4 - 1} \tag{8.17a}$$

$$Z = C_1\int_0^{\xi} \frac{dt}{(t-\beta_1)^{1-\alpha_1}(t-\beta_2)^{1-\alpha_2}(t-\beta_3)^{1-\alpha_3}} + C_2 \tag{8.17b}$$

Interior angles (fraction of π) of the polygon in the Z plane are $\alpha_1 = 0$, $\alpha_2 = 1/2$, and $\alpha_3 = 1/2$; and vertices on the real axis of the ζ plane $\beta_1 = -\infty$, $\beta_2, = -1$, and $\beta_3 = 1$. As the vertex A is placed at infinity in the ζ plane, it does not appear in the transformation. Therefore, Eqn. (8.17b) reduces to

$$Z = C_1\int_0^{\zeta} \frac{dt}{(t-1)^{1-1/2}(t+1)^{1-1/2}} + C_2 = C_1\int_0^{\zeta} \frac{dt}{\sqrt{t^2-1}} + C_2 \tag{8.18}$$

At the point O, $Z = 0$ as well as $\zeta = 0$, therefore $C_2 = 0$. Using the values at point C ($Z = b/2$ and $\zeta = 1$) in Eqn. (8.18):

$$\frac{b}{2} = C_1\int_0^1 \frac{dt}{\sqrt{t^2-1}} = -iC_1\int_0^1 \frac{dt}{\sqrt{1-t^2}} = -iC_1\left[\sin^{-1} t\right]_0^1 = -iC_1\frac{\pi}{2} \tag{8.19a}$$

Therefore,

$$C_1 = -\frac{1}{i}\frac{b}{\pi} = i\frac{b}{\pi} \tag{8.19b}$$

After substituting C_1 and C_2, Eqn. (8.18) becomes

$$Z = i\frac{b}{\pi}\int_0^{\zeta}\frac{dt}{\sqrt{t^2-1}} = \frac{b}{\pi}\sin^{-1}\zeta \tag{8.20a}$$

or

$$\zeta = \sin\frac{\pi Z}{b} \tag{8.20b}$$

8.10.5 Zhukovsky Function

Find Zhukovsky′s function mapping for the flow around an impervious sheetpile founded in an infinite depth of porous media.

Consider the flow around an impervious sheetpile founded in an infinite depth of porous media as shown in Figure 8.12(a). AB is an equipotential line (boundary of reservoir), whereas $OE\infty$ is a phreatic line (free surface). The corresponding W plane is shown Figure 8.12(b). The free surface satisfies the conditions $\psi = 0$ and $\phi + KY = 0$, consequently, Zhukovsky function for the free surface will have $\theta_1 = 0$ and $\theta_2 = -KX$, and hence in the θ plane the free surface will have its image the negative imaginary axis (Figure 8.12c). Along the sheetpile BCO, $\psi = 0$ and $X = 0$; hence $\theta_2 = 0$; its image is along the negative real axis in the θ plane. Finally along AB, where $\phi = -Kh_1$, $Y = 0$, and $-\infty \le \psi \le 0$, it will have $\theta_1 = -Kh_1$, and $-\infty \le \theta_2 \le 0$; its image is the line $BA\infty$ in Figure 8.12(c). Thus, the flow region in the Z plane with an unknown boundary OE (phreatic line) is transformed into an infinite strip in Zhukovsky′s θ plane as shown in Figure 8.12(c).

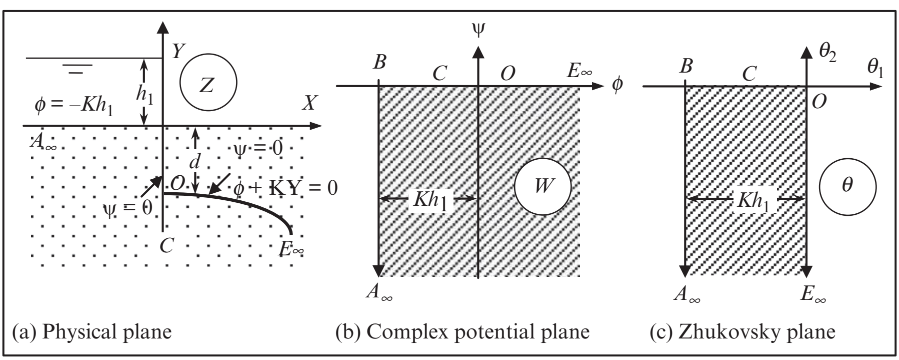

Figure 8.12 *Zhukovsky function mapping for flow around a sheetpile*

8.10.6 Schwarz–Cristoffel Transformation of Inverse Hodograph Plane

Figure 8.9 shows the inverse hodograph plane for the case of seepage from a trapezoidal canal with drainage layer at finite depth. The mapping is a polygon (triangle), and this polygon can be mapped onto a similar polygon in auxiliary plane in such a manner that the sides of the polygon extends through the real axis. This is accomplished by opening the polygon at a' point and extending one side to $-\infty$ and other to $+\infty$ and putting h' at 0, g' at γ, c' at β and b' at 1 as shown in Figure 8.13. Thus, the transformation maps conformally the region interior to the polygon of inverse hodograph into the entire lower half of the auxiliary plane (ζ plane) resulting.

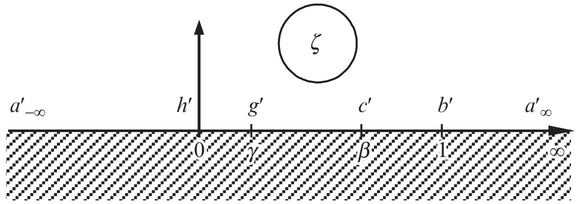

Figure 8.13 *Auxiliary plane*

$$\frac{dZ}{dW} = C_1 \int_0^{\zeta} \frac{dt}{(t-\beta_1)^{1-\alpha_1}(t-\beta_2)^{1-\alpha_2}(t-\beta_3)^{1-\alpha_3}(t-\beta_3)^{1-\alpha_3}} + C_2 \qquad (8.21)$$

where, interior angles of the polygon in the dZ/dW plane are $\alpha_1 = 1/2$, $\alpha_2 = 1$, $\alpha_3 = 1$, and $\alpha_4 = \sigma$; and vertices on the real axis of the ζ plane $\beta_1 = 0$, $\beta_2 = \gamma$, $\beta_3 = \beta$, and $\beta_1 = 1$. Therefore, Eqn. (8.21) reduces to

$$\frac{dZ}{dW} = C_1 \int_0^{\zeta} \frac{dt}{(t-1)^{1-\sigma}\sqrt{t}} + C_2 \qquad (8.22)$$

Constants C_1 and C_2 can be found by using values of dZ/dW and ζ at two points in dZ/dW plane and ζ plane. Using the values at point b' $(\zeta = 1;\ dZ/dW = 0)$ in Eqn. (8.22)

$$0 = C_1 \int_0^{1} \frac{dt}{(t-1)^{1-\sigma}\sqrt{t}} + C_2 \qquad (8.23a)$$

or

$$C_2 = -C_1 \int_0^{1} \frac{dt}{(t-1)^{1-\sigma}\sqrt{t}} \qquad (8.23b)$$

Combining Eqs (8.22) and (8.23b) at the point h' $(\zeta = 0;\ dZ/dW = -i/K)$,

$$-\frac{i}{K} = C_1 \int_0^{0} \frac{dt}{(t-1)^{1-\sigma}\sqrt{t}} - C_1 \int_0^{1} \frac{dt}{(t-1)^{1-\sigma}\sqrt{t}} \qquad (8.23c)$$

or

$$C_1 = \frac{i}{K} \Big/ \int_0^{1} \frac{dt}{(t-1)^{1-\sigma}\sqrt{t}} = \frac{-ie^{-i\pi\sigma}}{K\,B(1/2,\sigma)} \qquad (8.23d)$$

Since

$$\int_0^{1} \frac{dt}{(t-1)^{1-\sigma}\sqrt{t}} = \frac{1}{(-1)^{1-\sigma}} \int_0^{1} (1-t)^{\sigma-1}(t)^{1/2-1}\,dt = \frac{B(1/2,\sigma)}{(e^{-i\pi})^{1-\sigma}} \qquad (8.24)$$

where $B(1/2, \sigma)$ = complete Beta function, which can be expressed in terms of Gamma function (Γ) as (Abramowitz and Stegun, 1972):

$$B\left(\frac{1}{2},\sigma\right)=\frac{\Gamma(1/2)\Gamma(\sigma)}{\Gamma(0.5+\sigma)} \tag{8.25}$$

Selected values of gamma function are tabulated in *Appendix C*. After substituting C_1 and C_2, Eqn. (8.22) becomes

$$\frac{dZ}{dW}=\frac{-ie^{i\pi\sigma}}{K\,B(1/2,\sigma)}\int_1^{\zeta}\frac{dt}{(t-1)^{1-\sigma}\sqrt{t}} \tag{8.26}$$

8.10.7 Schwarz–Cristoffel Transformation of Complex Potential Plane

In the W plane, the mapping is a rectangle as shown in Figure 8.10, which can be mapped onto a similar polygon in auxiliary plane by opening the polygon at a' point and extending one side to $-\infty$ and other to $+\infty$ and putting h' at 0, g' at γ, c' at β and b' at 1 as shown in Figure 8.13. Thus, the transformation maps conformally the region interior of W plane into the entire lower half of the auxiliary plane (ζ plane) resulting

$$W=C_3\int_0^{\zeta}\frac{dt}{(t-\beta_1)^{1-\alpha_1}(t-\beta_2)^{1-\alpha_2}(t-\beta_3)^{1-\alpha_3}(t-\beta_3)^{1-\alpha_3}}+C_4 \tag{8.27a}$$

where, C_3 and C_4 are complex constants; interior angles (fraction of π) of the polygon in the W plane are $\alpha_1 = ½$, $\alpha_2 = ½$, $\alpha_3 = ½$, and $\alpha_4 = 1$; and vertices on the real axis of the ζ plane $\beta_1 = 0$, $\beta_2 = \gamma$, $\beta_3 = \beta$, and $\beta_1 = 1$. Therefore, Eqn. (8.27a) reduces to

$$W=C_3\int_0^{\zeta}\frac{dt}{\sqrt{t(t-\gamma)(t-\beta)}}+C_4 \tag{8.27b}$$

The constants C_3 and C_4 have been determined using the values at points c' $(\zeta=\beta;\, W=0)$ and g' $(\zeta=\gamma;\, W=Kd)$. After substituting C_3 and C_4, Eqn. (8.27b) becomes

$$W=\frac{Kd}{\displaystyle\int_\beta^{\gamma}\frac{dt}{\sqrt{t(t-\gamma)(t-\beta)}}}\int_\beta^{\zeta}\frac{dt}{\sqrt{t(t-\gamma)(t-\beta)}} \tag{8.28}$$

We know that

$$\int_\beta^{\gamma}\frac{dt}{\sqrt{t(t-\gamma)(t-\beta)}}=-i\int_\gamma^{\beta}\frac{dt}{\sqrt{t(t-\gamma)(\beta-t)}}=-i\frac{2}{\sqrt{\beta}}K\left(\sqrt{(\beta-\gamma)/\beta}\right) \tag{8.29}$$

where $K\left(\sqrt{(\beta-\gamma)/\beta}\right)$ = complete elliptical integral of the first kind with modulus $\left(\sqrt{(\beta-\gamma)/\beta}\right)$ (Byrd and Friedman, 1971). *Appendix C* tabulates values of complete elliptical integral of the first kind. Therefore,

$$W=i\,\frac{Kd\sqrt{\beta}}{2K\left(\sqrt{(\beta-\gamma)/\beta}\right)}\int_\beta^{\zeta}\frac{dt}{\sqrt{t(t-\gamma)(t-\beta)}} \tag{8.30}$$

SOLVED EXAMPLES

Example 8.1: Seepage below a Dam on Pervious Foundation

A simple example is given to find the functional relation between W and Z that is, $W = f(Z)$ for a two-dimensional steady flow in homogeneous isotropic domain using Schwarz–Christoffel conformal transformation. The relation can be obtained by mapping both W and Z plane onto an auxiliary ζ plane. The flow domain in Z plane, the corresponding complex potential W plane, and the auxiliary ζ plane are shown in the following Figure 8.14. The mapping of Z plane onto ζ plane is

$$Z = C_1 \int_0^{\zeta} dt + C_2 = C_1\zeta + C_2 \tag{8.31a}$$

Using values for point b' ($Z = 0$; $\zeta = 0$), $C_2 = 0$; and for point c' ($Z = b_1$; $\zeta = 1$), $C_1 = b_1$. Thus, the mapping becomes

$$Z = b_1\zeta \text{ or } \zeta = Z / b_1 \tag{8.31b}$$

Similarly, the mapping of W plane onto ζ plane is

$$W = C_1 \int_0^{\zeta} \frac{dt}{\sqrt{t(t-1)}} + C_2 = C_1 \sin^{-1}\sqrt{\zeta} + C_2 \tag{8.32a}$$

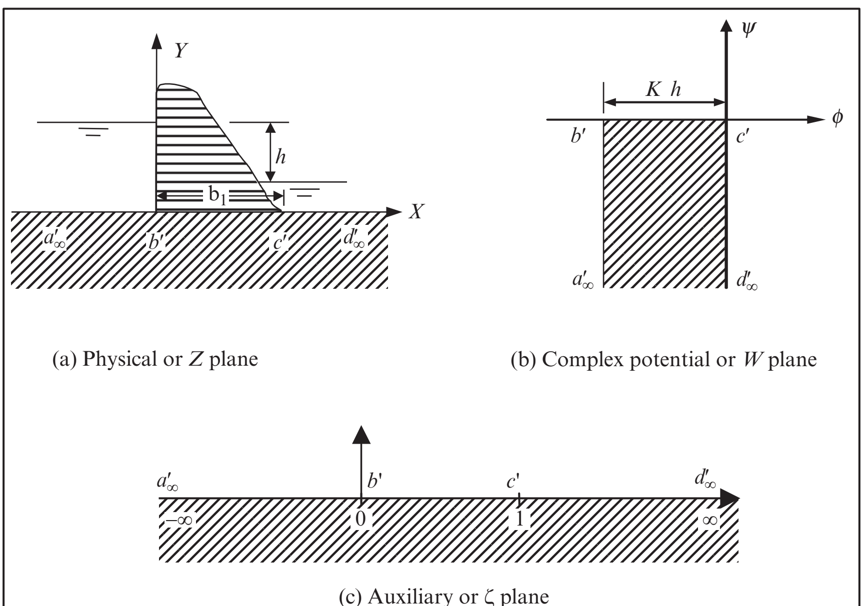

(a) Physical or Z plane

(b) Complex potential or W plane

(c) Auxiliary or ζ plane

Figure 8.14 *Seepage below a dam on pervious foundation*

Using values for point b' ($W = -Kh$; $\zeta = 0$), $C_2 = -Kh$; and for point c' ($W = 0$; $\zeta = 1$), $C_1 = 2Kh/\pi$. Thus the mapping is

$$W = \frac{2Kh}{\pi}\sin^{-1}\sqrt{\zeta} - Kh = -\frac{2Kh}{\pi}\cos^{-1}\sqrt{\zeta} \tag{8.32b}$$

or

$$\zeta = \cos^2\left(\frac{\pi W}{2Kh}\right) \tag{8.32c}$$

After eliminating ζ from Eqs (8.31b) and (8.32c), the required relation between W and Z planes is given by the following equation:

$$Z = b_1\cos^2\left(\frac{\pi W}{2Kh}\right) \tag{8.33a}$$

or

$$W = \frac{Kh}{\pi}\cos^{-1}\left(\frac{2Z}{b_1} - 1\right) \tag{8.33b}$$

For a simple problem like above, the direct functional relation can be obtained in explicit form. But, in general the direct relation between W and Z may not be possible. In such problems, relations between Z and ζ and between W and ζ are obtained. Using these relations, Z and corresponding W can be determined for a particular value of ζ.

Example 8.2: Seepage from Canals

The seepage loss from a canal is governed by

- hydraulic conductivity of the subsoils
- canal geometry
- hydraulic gradient between the canal and the aquifer underneath
- initial and boundary conditions.

The steady seepage discharge per unit length of canal q_s (m²/s) can be expressed in the following simplest form:

$$q_s = K(T + Ay) = KyF_s \tag{8.34}$$

where T = top width of canal (m), y = water depth in the canal (m), A = Vedernikov's parameter, and F_s = seepage function, which is a dimensionless function of canal geometry and boundary conditions. Depending on the geometry of the flow domain, one of the following boundary conditions may exist:

(i) porous medium underlain by an impermeable layer at a finite depth
(ii) porous medium underlain by a drainage layer at a finite depth, and water table is above the top of the drainage layer
(iii) porous medium underlain by a drainage layer at finite depth, and water table is below the top of the drainage layer
(iv) water table at a finite depth in a porous medium of infinite depth
(v) porous medium of infinite depth in which water table at infinite depth or a drainage layer and water table both at infinite depth

The seepage loss will be highest when the canal bed approaches a drainage layer containing the water table below its top surface. On the contrary, seepage is least when the water table approaches the water level in the canal. Thus for case, (iii) the seepage loss will be the largest. In most alluvial plains, the soils are stratified. In many cases, highly permeable layers of sand and gravel underlie a low permeable top layer of finite depth. In such case, the lower layers of sand and gravel act as a free drainage layer for the top seepage layer. The seepage from a canal running through such stratified strata is much more than those of a canal in a homogeneous seepage layer of very large depth. The difference in quantity of seepage becomes appreciable when the drainage layer lies at a depth less than twice the depth of water in the canal and the water table is below the top of the drainage layer. Further, the quantity of seepage becomes very large as the bed of the canal approaches the drainage layer.

Seepage from a Curvilinear Canal

Study of seepage from curved channels is equally important due to its applications in different areas. A semicircular channel is the most hydraulically efficient section. It is also the most economical section as it has the least cross-sectional area and wetted perimeter. Kozeny (Harr, 1962; Polubarinova Kochina, 1962; Muskat, 1982) investigated seepage from a curved channel using Zhukovsky function and found that resultant channel has trochoid shape. Verigin (Kovacs, 1981; Aravin and Numerov, 1965) analytically found approximate solution for a circular section in terms of a rapidly converging series. Ilyinskii and Kacimov (1992) found the optimal shape of a curved irrigation channel from the point of view of minimum seepage loss using inverse boundary value problem method. On the other hand, Kacimov (1991) investigated a curved drainage/recharge channel from the point of view of maximum drainage using mapping technique. Exact analytical solution for a semicircular channel is not achievable since its geometry maps in curvilinear shapes onto hodograph and inverse hodograph planes, for which Schwarz–Christoffel transformation is impossible. One possible way out is an inverse method where the shape of the unknown channel is searched as part of a solution. Using the inverse method, Chahar (2006) presented an exact solution for seepage from a curved channel whose boundary maps along a circle onto the hodograph plane. Pattern of seepage from an approximate semicircular channel in homogeneous and isotropic porous medium of infinite extend is shown in Figure 8.15(a). Due to vertical symmetry, the solution for the half domain ($a'b'c'f'a'$) is sought. In the velocity hodograph plane, the phreatic line $a'b'$ will map along a circle of radius K with centre at (0, K/2). Since a' lies at very large depth, the hydraulic gradient is unity and seepage velocity becomes K in vertically downward direction. The channel boundary $b'c'd'$ is an equipotential line, therefore the seepage velocity is normal to the boundary and in hodograph plane it will map a curvilinear path. However, the exact shape of the curve is not known. It is assumed that the channel boundary maps along a circle of diameter c in the hodograph plane. The inverse hodograph dZ/dW (Figure 8.15c) and the complex potential W (Figure 8.15d) for half of the physical flow domain have been drawn following steps described for the trapezoidal canal. The dZ/dW plane and W plane have been mapped onto the lower half of an auxiliary (ζ) plane (Figure 8.15e) using the Schwarz–Christoffel conformal transformation.

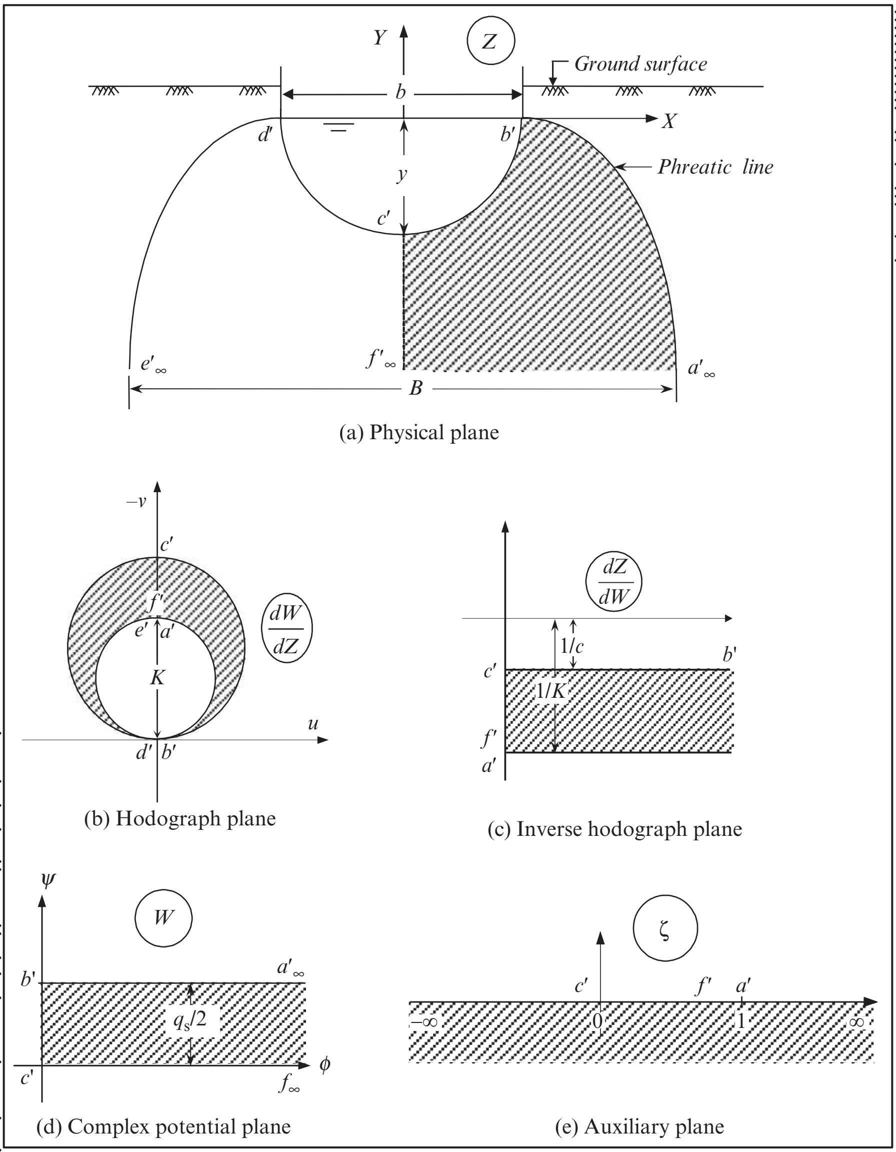

Figure 8.15 *Seepage from a curvilinear channel*

Mapping of Complex Potential Plane

Mapping of W plane onto ζ plane results in

$$W = C_1 \int_0^{\zeta} \frac{dt}{(t-1)\sqrt{t}} + C_2 \tag{8.35}$$

The C_1 and C_2 constants can be found by using values at point c' ($\zeta = 0$; $W = 0$) in Eqn. (8.35)

$$C_2 = 0 \tag{8.36}$$

and at the point b' ($\zeta = -\infty$; W $= iq_s/2$), therefore

$$\frac{iq_s}{2} = C_1 \int_0^{-\infty} \frac{dt}{(t-1)\sqrt{t}} = C_1 \int_0^{-\infty} \frac{-i\,dt}{(1-t)\sqrt{-t}} = iC_1 \int_0^{\infty} \frac{d\pi}{(1+\tau)\sqrt{\tau}} = iC_1\pi \tag{8.37}$$

and hence

$$C_1 = q_s/2\pi \tag{8.38}$$

Therefore,

$$W = \frac{q_s}{2\pi} \int_0^{\zeta} \frac{dt}{(t-1)\sqrt{t}} \tag{8.39}$$

In an infinite porous medium, both the points f' and a' are at infinity in Z plane as well as in W plane, and they map at $\zeta = 1$ in ζ plane. When the point $\zeta = 1$ is crossed (i.e. a' is approached from f') in ζ plane there is a jump of $q_s/2$ in the W plane mapping. Taking derivative of Eqn. (8.39),

$$\frac{dW}{d\zeta} = \frac{q_s}{2\pi(1-\zeta)\sqrt{\zeta}} \tag{8.40}$$

Mapping of Inverse Hodograph Plane

Mapping of dZ/dW plane onto ζ plane results in

$$\frac{dZ}{dW} = C_3 \int_0^{\zeta} \frac{dt}{\sqrt{t(t-1)}} + C_4 \tag{8.41}$$

where C_3 and C_4 = constants. Using the values at point c' ($\zeta = 0$; $dZ/dW = -i/c$)

$$\frac{-i}{c} = C_4 \tag{8.42}$$

At point a' ($\zeta = 1$; $dZ/dW = -i/K$)

$$\frac{-i}{K} = C_3 \int_0^{1} \frac{dt}{\sqrt{t(t-1)}} - \frac{i}{c} = -i\,C_3 \int_0^{1} \frac{dt}{\sqrt{t(1-t)}} - \frac{i}{c} = -i\,C_3\pi - \frac{i}{c} \tag{8.43}$$

Therefore,

$$C_3 = \frac{1}{\pi}\left(\frac{1}{K} - \frac{1}{c}\right) \tag{8.44}$$

Substituting values of C_3 and C_4 in Eqn. (8.41),

$$\frac{dZ}{dW} = \frac{1}{\pi}\left(\frac{1}{K} - \frac{1}{c}\right)\int_0^{\zeta} \frac{dt}{\sqrt{t(t-1)}} - \frac{i}{c} \tag{8.45}$$

Mapping of Physical Plane
Using Eqs (8.40) and (8.45),

$$\frac{dZ}{d\zeta} = \frac{dZ}{dW}\frac{dW}{d\zeta} = \left(\frac{1}{\pi}\left(\frac{1}{K} - \frac{1}{c}\right)\int_0^{\zeta} \frac{dt}{\sqrt{t(t-1)}} - \frac{i}{c}\right)\frac{q_s}{2\pi(1-\zeta)\sqrt{\zeta}} \tag{8.46}$$

Integrating it

$$Z = \frac{q_s}{2\pi^2}\left(\frac{1}{K} - \frac{1}{c}\right)\int_0^{\zeta}\left(\int_0^{t} \frac{dt}{\sqrt{\tau(\tau-1)}}\right)\frac{dt}{(1-t)\sqrt{t}} - \frac{i\,q_s}{2\pi c}\int_0^{\zeta} \frac{dt}{(1-t)\sqrt{t}} - i\,y \tag{8.47}$$

For $c'b'$ $(-\infty < \zeta \le 0)$

$$Z = \frac{q_s}{2\pi^2}\left(\frac{1}{K} - \frac{1}{c}\right)\int_0^{\zeta}\left(\int_0^{t} \frac{dt}{\sqrt{-\tau(1-\tau)}}\right)\frac{dt}{(1-t)i\sqrt{-t}} - \frac{i\,q_s}{2\pi c}\int_0^{\zeta} \frac{dt}{(1-t)i\sqrt{-t}} - i\,y \tag{8.48}$$

Eqn. (8.48) converts to

$$Z = \frac{q_s}{\pi c}\tan^{-1}\sqrt{-\zeta} - i\left(y - \frac{2q_s}{\pi^2}\left(\frac{1}{K} - \frac{1}{c}\right)\int_0^{\sinh^{-1}\sqrt{-\zeta}} \frac{\tau\,dt}{\cosh\tau}\right) \tag{8.49}$$

At the point b' ($\zeta = -\infty$; $Z = T/2$),

$$\frac{T}{2} = \frac{q_s}{\pi c}\tan^{-1}\infty - i\left(y - \frac{2q_s}{\pi^2}\left(\frac{1}{K} - \frac{1}{c}\right)\int_0^{\infty} \frac{\tau\,dt}{\cosh\tau}\right) \tag{8.50}$$

Equating real and imaginary parts,

$$T = \frac{q_s}{c} \quad\Rightarrow\quad q_s = Tc \quad\Rightarrow\quad c = \frac{q_s}{T} \tag{8.51}$$

and

$$y = \frac{2q_s}{\pi^2}\left(\frac{1}{K} - \frac{1}{c}\right)2G \qquad or \qquad \left(\frac{1}{K} - \frac{1}{c}\right) = \frac{\pi^2}{4G}\frac{y}{q_s} \tag{8.52}$$

where G = Catalan′s constant defined by

$$G = \frac{1}{2}\int_0^{\infty} \frac{\tau\,dt}{\cosh\tau} \tag{8.53}$$

It may be noted that the assumed diameter c of the circle in the hodograph plane is simply the maximum velocity of seepage (or seepage velocity at the centre c').Thus, Eqn. (8.51) reveals that the seepage from this class of curvilinear channels is simply top width times the maximum velocity at the centre of the channel.

Position of Phreatic Line

Equation of phreatic line $a'b'$ ($1 \le \zeta < \infty$) is given by the following equation:

$$Z = \int_{\infty}^{\zeta} \left(\frac{2}{\pi} \left(\frac{1}{K} - \frac{1}{c} \right) \cosh^{-1} \sqrt{\zeta} - \frac{i}{K} \right) \frac{q_s}{2\pi(1-t)\sqrt{t}} \, dt + \frac{T}{2} \tag{8.54}$$

which can be rewritten as follows:

$$Z = \frac{q_s}{\pi^2} \left(\frac{1}{K} - \frac{1}{c} \right) \int_{\infty}^{\zeta} \frac{\cosh^{-1} \sqrt{t}}{(1-t)\sqrt{t}} \, dt - \frac{i\, q_s}{2\pi K} \int_{\infty}^{\zeta} \frac{dt}{(1-t)\sqrt{t}} + \frac{T}{2} \tag{8.55}$$

After substituting values of q_s and c, Eqn. (8.55) can be manipulated into

$$Z = \frac{T}{2} + \frac{y}{2G} \int_{\cosh^{-1}\sqrt{\zeta}}^{\infty} \frac{\tau \, d\tau}{\sinh \tau} + i \left(T + \frac{\pi^2}{4G} y \right) \ln \tanh \left(\frac{\cosh^{-1} \sqrt{\zeta}}{2} \right) \tag{8.56}$$

Therefore, the parametric equations for the phreatic line are

$$X = \frac{T}{2} + \frac{y}{2G} \int_{\cosh^{-1}\sqrt{\zeta}}^{\infty} \frac{\tau \, d\tau}{\sinh \tau} \tag{8.57a}$$

$$Y = \left(T + \frac{\pi^2}{4G} y \right) \ln \tanh \left(\frac{\cosh^{-1} \sqrt{\zeta}}{2} \right) \tag{8.57b}$$

At $Y = -i\infty$ on the phreatic line that is, at the point a' ($\zeta = 1$), the phreatic line has vertical asymptote

$$X = \frac{T}{2} + \frac{\pi^2 y}{8G} \tag{8.58}$$

because

$$\int_{0}^{\infty} \frac{\tau \, d\tau}{\sinh \tau} = \frac{\pi^2}{4} \tag{8.59}$$

Also the width of the flow at infinity B can be obtained as follows:

$$B = 2X_{\infty} = T + \frac{\pi^2}{4G} y \tag{8.60}$$

Relationship for Channel Perimeter

The shape of the perimeter of the channel is given by Eqn. (8.49)

$$X + iY = \frac{T}{\pi} \tan^{-1} \sqrt{-\zeta} - i \left(y - \frac{y}{2G} \int_{0}^{\sinh^{-1}\sqrt{-\zeta}} \frac{\tau dt}{\cosh \tau} \right) \tag{8.61}$$

Equating real and imaginary parts

$$X = \frac{T}{\pi} \tan^{-1} \sqrt{-\zeta} \qquad \Rightarrow \qquad \sqrt{-\zeta} = \tan \left(\frac{\pi X}{T} \right) \tag{8.62a}$$

$$Y = -\left(y - \frac{y}{2G} \int_0^{\sinh^{-1}\sqrt{-\zeta}} \frac{\tau\, dt}{\cosh \tau} \right) \Rightarrow \frac{Y}{y} = \frac{1}{2G}\left(\int_0^{\sinh^{-1} \tan(\pi X/T)} \frac{\tau\, dt}{\cosh \tau} - 2G \right) \quad (8.62b)$$

Eqn. (8.62b) defines the shape of the channel perimeter in Cartesian coordinates.

Variation in Seepage Velocity

The distribution of the velocity of seeping water normal to the channel perimeter can be found by using Eqn. (8.87):

$$\frac{dZ}{dW} = \frac{1}{u - iv} = \frac{u + iv}{u^2 + v^2} = \frac{u + iv}{V^2} = \frac{2}{\pi}\left(\frac{1}{K} - \frac{1}{c} \right) \sinh^{-1} \sqrt{-\zeta} - \frac{i}{c} \quad (8.63)$$

Substituting value of c and equating imaginary and real parts gives

$$V = \frac{k\left(T/y + \pi^2/4G \right)}{\sqrt{\left((\pi \sinh^{-1}\sqrt{-\zeta})/2G \right)^2 + (T/y)^2}} \quad (8.64a)$$

Using Eqn. (8.62a) to eliminate ζ

$$V = \frac{k\left(T/y + \pi^2/4G \right)}{\sqrt{\left((\pi \sinh^{-1} \tan(\pi X/T))/2G \right)^2 + (T/y)^2}} \quad (8.64b)$$

Quantity of Seepage

At infinite depth, the hydraulic gradient becomes unity and the seepage velocity acquires a uniform magnitude equal to the hydraulic conductivity over a horizontal plane so the quantity of seepage can be given by the following equation:

$$q_s = KB \quad (8.65)$$

Using value of c from Eqn. (8.51) in Eqn. (8.52) or B from Eqn. (8.60) in Eqn. (8.65),

$$q_s = K\left(\frac{\pi^2}{4G} y + T \right) = Ky\left(\frac{\pi^2}{4G} + \frac{T}{y} \right) \quad (8.66)$$

Therefore, Vedernikov′s parameter and seepage function for this channel are, respectively,

$$A = \frac{\pi^2}{4G} \approx \pi(4 - \pi) \approx 2.69676 \quad (8.67a)$$

and

$$F_s = \frac{\pi^2}{4G} + \frac{T}{y} \quad (8.67b)$$

It is interesting to note that the Vedernikov′s parameter is identical to that of a slit (Chahar, 2001).

As per the comparison theorem, the value of q_s for any arbitrary channel is bounded from below and above by the following inequality:

$$q_i < q_s < q_c \tag{8.68}$$

where, q_i and q_c are seepage discharges from an arbitrary inscribed and an arbitrary comprising channel, respectively. A rectangular channel is selected as a comprising channel and a Kozeny′s trochoid channel as inscribed channel (see Figure 3.9). All the three channels have the same y and T but differ in their shape such that a monotonic deformation from one shape to another gives monotonic increase of the seepage losses according to Eqn. (8.68). The shape of the Kozeny′s trochoid can be given by the following parametric equations (Muskat, 1982):

$$Y = y\cos(\pi\psi/q_i) \tag{8.69a}$$

$$X + \psi/K = y\sin(\pi\psi/q_i) \tag{8.69b}$$

where, the quantity of seepage q_i is given by the following equation:

$$q_i = Ky(2 + T/y) \tag{8.69c}$$

Hence, the Vedernikov′s parameter for the trochoid channel is equal to 2. The main limitation of a trochoid channel is that it cannot be too deep. From Eqs (8.69a) and (8.69b),

$$\frac{dY}{dX} = \frac{\sin(\pi\psi/q_i)}{\cos(\pi\psi/q_i) - q_i/\pi Ky} = \frac{\sqrt{y^2 - Y^2}}{Y - q_i/\pi K} \tag{8.70}$$

At the central point $Y = y$, therefore $dY/dX = 0$ except when denominator is zero. In that case, dY/dX = indeterminate and the trochoid becomes self-intersecting and loses its usefulness. At this limiting case

$$y = \frac{q_i}{\pi K} = \frac{T + 2y}{\pi} \Rightarrow T = (\pi - 2)y \tag{8.71}$$

For a practical application of a trochoid shape T/y must be greater than $(\pi - 2)$. Figure 8.16 also compares the investigated curved channel and a self-intersecting case of a trochoid for $T/y = 1$. The present curved channel does not have such a limitation at any y and T (Figure 8.16).

Using these results, it can be verified that the following inequality is always true for any set of y and T:

$$2 + \frac{T}{y} < \frac{\pi^2}{4G} + \frac{T}{y} < \left(\left(\pi^2/4G\right)^{0.77} + \left(T/y\right)^{0.77} \right)^{1.3} \tag{8.72}$$

Approximate Semicircular Channel

The curved channel described by Eqn. (8.62b) possesses many interesting properties. It approximately represents a semiellipse with major and minor axes equal to T and $2y$, respectively, and vice versa. Actually, it always lies between an ellipse and a parabola, and it is any coordinate that is nearly exact to the

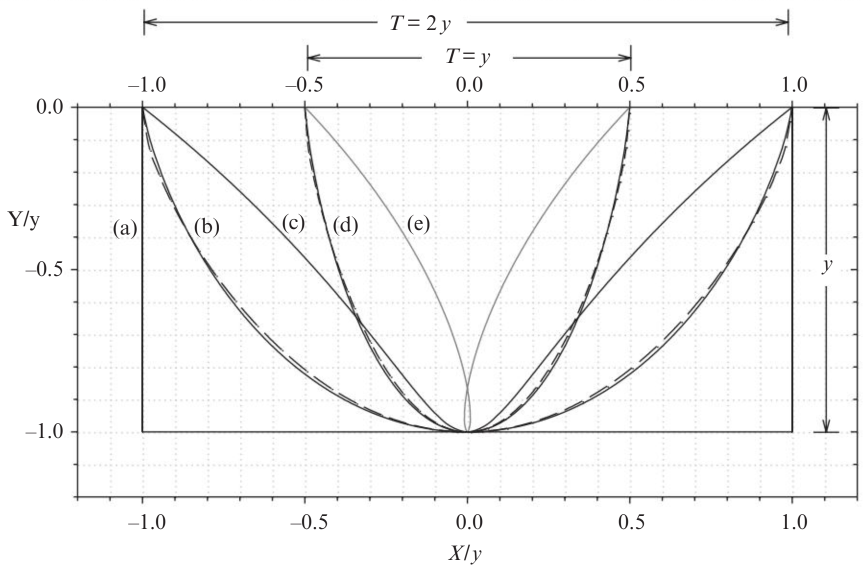

(a) Rectangular channel with $T / y = 2$
(b) Curved channel and average of parabolic and elliptical shape at $T / y = 2$
(c) Trochoid channel with $T / y = 2$
(d) Curved channel and average of parabolic and elliptical shape at $T / y = 1$
(e) Self intersecting trochoid at $T / y = 1$

Figure 8.16 *Comparison of seepage loss with other channel shapes*

average of coordinates of corresponding ellipse and parabola (see Figure 8.16 for $T/y=2$, $T/y=1$ and Table 1 for $T/y=3$). This channel is nonself-intersecting, and hence feasible from $T/y \to 0$ (slit—a very narrow and deep channel) to $T/y \to \infty$ (strip—a very wide and shallow channel). In fact, this is the basic shape of channel and highlights the importance of expressing seepage loss in terms of seepage function. It can be noted from Eqn. (8.67b) that the seepage function is a linear combination of seepage functions for a slit ($\pi^2/4G$) and a strip (T/y), respectively. On the other hand, the seepage functions for other channels are power combination of $\pi^2/4G$ and T/y. For example, the power is 1.3 for an inscribing triangular channel and 0.77 for a comprising rectangular channel (Swamee et al., 2000), whereas it is in between these limits for other feasible channels for same T/y.

A semicircle is a special case of a semiellipse, consequently adopting $T/y=2$, the curved channel can be approximated into a semicircular channel. Figure 8.17 shows a comparison with a semicircular channel. Both the channels closely match each other; the maximum error is being 6.3 percent. Taking $T/y = 2$ in Eqn. (8.64b),

$$\frac{V}{K} = \frac{\left(1+\pi^2/8G\right)}{\sqrt{\left((\pi \sinh^{-1} \tan(\pi X/T))/4G\right)^2 + 1}} \tag{8.73}$$

This variation in the velocity of seeping water normal to the channel perimeter is plotted in Figure 8.17. The maximum velocity at the deepest point ($X/T = 0$) of the channel perimeter is

$$\frac{V}{K} = 1 + \frac{\pi^2}{8G} = 2.3469 \tag{8.74}$$

Figure 8.17 also plots the phreatic lines by using $T/y = 2$ in Eqs (8.57a) and (8.57b). For an approximate semicircular channel, the vertical asymptote of the phreatic line, the width of the flow at infinity, and the quantity of seepage reduces to

$$\frac{X}{y} = \frac{T}{2y} + \frac{\pi^2}{8G} = 2.3469 \tag{8.75a}$$

$$B = y\left(\frac{T}{y} + \frac{\pi^2}{4G}\right) = 4.6938y \tag{8.75b}$$

and

$$q_s = 4.6938\,Ky \tag{8.75c}$$

respectively.

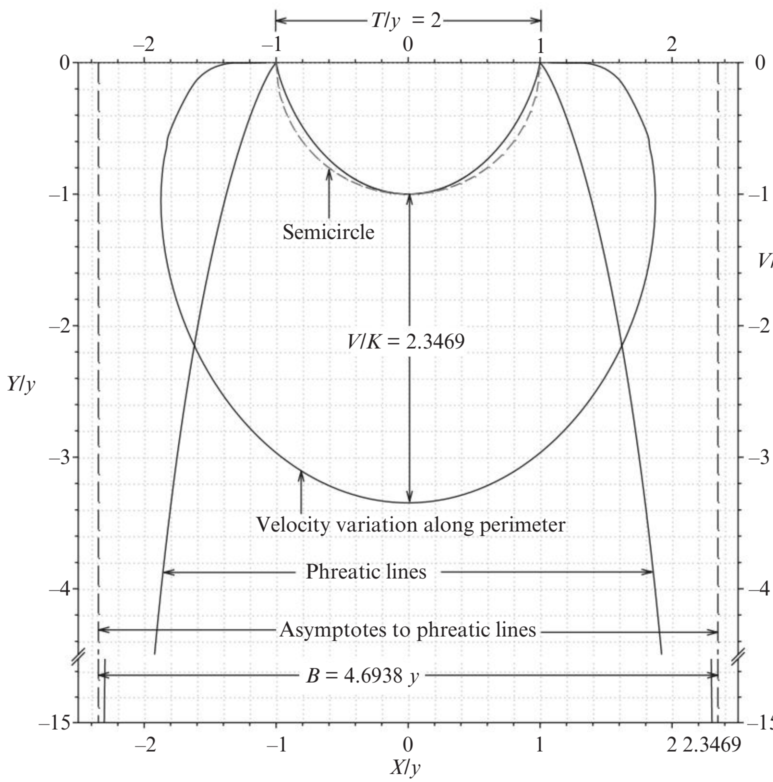

Figure 8.17 *Variation in seepage velocity and location of phreatic line for an approximate semicircular channel*

Example 8.3: Solution for a Trapezoidal Channel

Consider the pattern of seepage from the trapezoidal channel for which physical plane, inverse hodograph plane, complex potential plane and auxiliary plane are shown in Figure 8.7, Figure 8.9, Figure 8.10 and Figure 8.13 respectively. The seepage domain has symmetry about vertical axis Y, therefore half of the domain has been used in the analysis. The conformal mappings in various planes for this case have already been obtained in mapping examples. Differentiating Eqn. (8.30) with respect to ζ

$$\frac{dW}{d\zeta} = i\,\frac{Kd\sqrt{\beta}}{2K\left(\sqrt{(\beta-\gamma)/\beta}\right)}\frac{1}{\sqrt{\zeta(\zeta-\gamma)(\zeta-\beta)}} \tag{8.76}$$

Since $\dfrac{dZ}{d\zeta} = \dfrac{dZ}{dW}\dfrac{dW}{d\zeta}$, substitution of $\dfrac{dZ}{dW}$ from Eqn. (8.26) and $\dfrac{dW}{d\zeta}$ from Eqn. (8.76) results in

$$\frac{dZ}{d\zeta} = \frac{e^{i\pi\sigma}}{B(1/2,\sigma)}\frac{d\sqrt{\beta}}{2K\left(\sqrt{(\beta-\gamma)/\beta}\right)}\left(\int_1^{\zeta}\frac{dt}{(t-1)^{1-\sigma}\sqrt{t}}\right)\frac{1}{\sqrt{\zeta(\zeta-\beta)(\zeta-\gamma)}} \tag{8.77}$$

Integrating Eqn. (8.77) and applying the condition at h' ($\zeta = 0$; $Z = B/2 - id$) gives

$$Z = \frac{B}{2} - id + \frac{e^{i\pi\sigma}}{B(1/2,\sigma)}\frac{d\sqrt{\beta}}{2K\left(\sqrt{(\beta-\gamma)/\beta}\right)}\int_0^{\zeta}\left(\int_1^{t}\frac{d\tau}{(\tau-1)^{1-\sigma}\sqrt{\tau}}\right)\frac{dt}{\sqrt{t(t-\beta)(t-\gamma)}} \tag{8.78}$$

where, τ = another dummy variable. Eqn. (8.78) defines the physical domain of the seepage flow $a'b'c'g'h'a'$. Using Eqn. (8.78) at g' ($\zeta = \gamma$; $Z = -id$); c' ($\zeta = \beta$; $Z = -iy$); b' ($\zeta = 1$; $Z = b/2 - iy$); and a' ($\zeta = \infty$; $Z = b/2 + y\cot\pi\sigma$), and thereafter manipulation yields

$$\frac{B}{d} = \frac{\sqrt{\beta}}{K\left(\sqrt{(\beta-\gamma)/\beta}\right)B(1/2,\sigma)}\int_0^{\gamma}\frac{F_1(t,\sigma)dt}{\sqrt{t(\beta-t)(\gamma-t)}} \tag{8.79a}$$

$$\frac{d}{y} = \frac{K\left(\sqrt{(\beta-\gamma)/\beta}\right)B(1/2,\sigma)\big/\sqrt{\beta}}{K\left(\sqrt{(\beta-\gamma)/\beta}\right)B(1/2,\sigma)\big/\sqrt{\beta} - \dfrac{1}{2}\displaystyle\int_{\gamma}^{\beta}\frac{F_1(t,\sigma)dt}{\sqrt{t(\beta-t)(t-\gamma)}}} \tag{8.79b}$$

$$\frac{b}{y} = \frac{\displaystyle\int_{\beta}^{1}\frac{F_1(t,\sigma)dt}{\sqrt{t(t-\beta)(t-\gamma)}}}{K\left(\sqrt{(\beta-\gamma)/\beta}\right)B(1/2,\sigma)\big/\sqrt{\beta} - \dfrac{1}{2}\displaystyle\int_{\gamma}^{\beta}\frac{F_1(t,\sigma)dt}{\sqrt{t(\beta-t)(t-\gamma)}}} \tag{8.79c}$$

where,

$$F_1(t,\sigma) = \int_t^1\frac{dt}{(1-\tau)^{1-\sigma}\sqrt{\tau}} = B(1/2,\sigma) - B_t(1/2,\sigma) \tag{8.79d}$$

and $B_t(1/2, \sigma)$ = incomplete Beta function (Abramowitz and Stegun, 1972) defined as follows:

$$B_t\left(\frac{1}{2},\sigma\right)=\int_0^t \frac{dt}{(1-\tau)^{1-\sigma}\sqrt{\tau}}=2\sqrt{t}\ {}^2F_1\left(\frac{1}{2},1-\sigma;\frac{3}{2};t\right) \quad (8.79e)$$

in which ${}^2F_1$ = a Gauss hypergeometric series (Abramowitz and Stegun, 1972) given by

$${}^2F_1(a,b;c;t)=1+\frac{a.b}{c}t+\frac{a(a+1).b(b+1)}{c.(c+1).1.2}t^2+\frac{a(a+1)(a+2)b(b+1)(b+2)}{c.(c+1).(c+2).1.2.3}t^3+\ldots \quad (8.79f)$$

Position of Phreatic Line

The phreatic line $a'h'$ $(-\infty<\zeta<0)$ can be located by manipulating Eqn. (8.78) and separating real and imaginary parts as follows:

$$X=\frac{d\sqrt{\beta}}{2K\left(\sqrt{(\beta-\gamma)/\beta}\right)B(1/2,\sigma)}\left(\int_0^\gamma \frac{F_1(t,\sigma)dt}{\sqrt{t(\beta-t)(\gamma-t)}}-\int_0^\zeta \frac{F_3(t,\sigma)\,dt}{\sqrt{(-t)(\beta-t)(\gamma-t)}}\right) \quad (8.80a)$$

$$Y=d-\frac{d}{K\left(\sqrt{(\beta-\gamma)/\beta}\right)}F\left(\sin^{-1}\sqrt{\frac{\zeta}{\zeta-\gamma}},\sqrt{\frac{\beta-\gamma}{\beta}}\right) \quad (8.80b)$$

where, $F\left(\sin^{-1}\sqrt{\zeta(\zeta-\gamma)},\sqrt{(\beta-\gamma)/\beta}\right)$ = incomplete elliptical integral of the first kind with modulus $\sqrt{(\beta-\gamma)/\beta}$, and amplitude $\sin^{-1}\sqrt{\zeta/(\zeta-\gamma)}$ (Byrd and Friedman, 1971) and

$$F_3(t,\sigma)=\int_0^t \frac{d\tau}{(1-\tau)^{1-\sigma}\sqrt{-\tau}} \quad (8.80c)$$

Variation in Seepage Velocity

Manipulating Eqn. (8.26), equating real and imaginary parts and then squaring and adding results into

$$\frac{V}{K}=B(1/2,\sigma)\Big/\int_\zeta^1 \frac{dt}{(1-t)^{1-\sigma}\sqrt{t}} \quad (8.81)$$

which shows that at the corner of the canal the seepage velocity is infinity and the minimum seepage velocity along the bed of the canal occurs at the centre c' $(\zeta=\beta)$ which is equal to

$$\frac{V}{K}=B(1/2,\sigma)\Big/\int_\beta^1 \frac{dt}{(1-t)^{1-\sigma}\sqrt{t}} \quad (8.82)$$

Quantity of Seepage

Using the values at the point h' $(\zeta=0\,;\,W=Kd+iq_s/2)$ in Eqn. (8.30), we obtain

$$Kd+\frac{q_s}{2}i=\frac{i\ Kd\sqrt{\beta}}{2K\left(\sqrt{(\beta-\gamma)/\beta}\right)}\int_\beta^0 \frac{dt}{\sqrt{t(t-\gamma)(t-\beta)}}=\frac{Kd\sqrt{\beta}\int_0^\beta \frac{dt}{\sqrt{t(t-\gamma)(\beta-t)}}}{2K\left(\sqrt{(\beta-\gamma)/\beta}\right)} \quad (8.83)$$

Separating real and imaginary parts leads to

$$q_s = 2Kd\frac{K\left(\sqrt{\gamma/\beta}\right)}{K\left(\sqrt{(\beta-\gamma)/\beta}\right)} \tag{8.84}$$

Comparing with Eqn. (8.34),

$$F_s = 2\frac{d}{y}\frac{K\left(\sqrt{\gamma/\beta}\right)}{K\left(\sqrt{(\beta-\gamma)/\beta}\right)} \tag{8.85}$$

This involves two transformation parameters β and γ. Simultaneous solution of Eqs (8.79b) and (8.79c) for given channel dimension (b, y, and σ) and depth of the drainage layer (d) result in parameters β and γ. Using these values in Eqn. (8.85), the seepage function and then the quantity of seepage can be determined. Further, the seepage velocity can be computed by Eqn. (8.81). Moreover, these values can be used in Eqn. (8.79a) to find the width of seepage domain at the drainage layer. Finally, the phreatic line can be plotted using β and γin Eqs (8.80a) and (8.80b). However, these equations involve complicated integrals with implicit transformation variables. These integrals (complete and incomplete beta functions, complete and incomplete elliptical integrals, and remaining improper integrals) can be evaluated using numerical integration (Press et al., 1992) after converting the improper integrals into proper integrals.

Example 8.4: Seepage from a Rectangular Channel

A rectangular section is a special case of a trapezoidal section with vertical side slopes that is, $m = 0$, hence $\sigma = 0.5$. Since W plane mapping is identical to a trapezoidal channel, therefore the expressions for q_s and F_s remain unaltered as Eqs (8.84) and (8.85). Other expressions can be deduced using $\sigma = 0.5$. Thus, the transformation parameters β and γhave values different than a trapezoidal channel given by the simultaneous solution of the following equations:

$$\frac{d}{y} = \frac{\pi K\left(\sqrt{(\beta-\gamma)/\beta}\right)\Big/\sqrt{\beta}}{\pi K\left(\sqrt{(\beta-\gamma)/\beta}\right)\Big/\sqrt{\beta} - \int_{\gamma}^{\beta}\frac{\pi/2-\tan^{-1}\sqrt{t/(1-t)}}{\sqrt{t(\beta-t)(t-\gamma)}}dt} \tag{8.86a}$$

$$\frac{b}{y} = \frac{\int_{\beta}^{1}\frac{\pi-2\tan^{-1}\sqrt{t/(1-t)}}{\sqrt{t(t-\beta)(t-\gamma)}}dt}{\pi K\left(\sqrt{(\beta-\gamma)/\beta}\right)\Big/\sqrt{\beta} - \int_{\gamma}^{\beta}\frac{\pi/2-\tan^{-1}\sqrt{t/(1-t)}}{\sqrt{t(\beta-t)(t-\gamma)}}dt} \tag{8.86b}$$

Using Eqn. (8.86a) in Eqn. (8.84), the quantity of seepage from a rectangular canal becomes

$$q_s = \frac{2\pi K\, y\, K\left(\sqrt{\gamma/\beta}\right)\Big/\sqrt{\beta}}{\pi K\left(\sqrt{(\beta-\gamma)/\beta}\right)\Big/\sqrt{\beta} - \int_{\gamma}^{\beta}\frac{\pi/2-\tan^{-1}\sqrt{t/(1-t)}}{\sqrt{t(\beta-t)(t-\gamma)}}dt} \tag{8.87}$$

Example 8.5: Seepage from a Triangular Channel

A trapezoidal channel with zero bed width is a triangular channel. In the different mapping, the point b' coincides with the point c' and hence transformation variable β vanishes or $\beta = 1$. With this condition, various expressions for a trapezoidal channel become corresponding expression for a triangular channel. For example, using $\beta = 1$ in Eqn. (8.84),

$$q_s = 2Kd\frac{K\left(\sqrt{\gamma}\right)}{K\left(\sqrt{1-\gamma}\right)} \tag{8.88}$$

where,

$$\frac{d}{y} = \frac{K\left(\sqrt{1-\gamma}\right)B(1/2,\sigma)}{K\left(\sqrt{1-\gamma}\right)B(1/2,\sigma) - \frac{1}{2}\int_{\gamma}^{1}\frac{F_1(t,\sigma)\,dt}{\sqrt{t(1-t)(t-\gamma)}}} \tag{8.89}$$

Example 8.6: Seepage from a Trapezoidal Channel—Drainage Layer and Water Table at Infinite Depth

When drainage layer and water table both lies at infinite depth in homogeneous isotropic porous medium of infinite extent (see Figure 8.18a), the hodograph plane and inverse hodograph plane remain unaltered (as shown in Figures 8.8 and 8.9), but the mapping in the complex potential plane (W-plane) will be semiinfinite strip as shown in Figure 8.18(b). However, the points g' and h' both approach to each other in all the mapping planes and transformation variable γ vanishes from transformation after attaining value equal to zero (as shown in Figure 8.18c). The transformed equations with $\gamma = 0$ become

$$\frac{dZ}{dW} = \frac{i\,e^{i\pi\sigma}}{KB(1/2,\sigma)}\int_{1}^{\zeta}\frac{dt}{(t-1)^{1-\sigma}\sqrt{t}} \tag{8.90a}$$

$$W = \frac{i\,q_s\sqrt{\beta}}{2\pi}\int_{\beta}^{\zeta}\frac{dt}{t\sqrt{(t-\beta)}} \tag{8.90b}$$

$$Z = -iy + \frac{q_s\sqrt{\beta}}{2\pi}\frac{e^{i\pi\sigma}}{KB(1/2,\sigma)}\int_{\beta}^{\zeta}\left(\int_{1}^{t}\frac{d\tau}{(\tau-1)^{1-\sigma}\sqrt{\tau}}\right)\frac{dt}{t\sqrt{t-\beta}} \tag{8.90c}$$

Transformation variable β for this case is given by the following equation:

$$\frac{b}{y} = 2\int_{\beta}^{1}\left(\int_{t}^{1}\frac{d\tau}{(1-\tau)^{1-\sigma}\sqrt{\beta}}\right)\frac{dt}{t\sqrt{t-\beta}}\Bigg/\sin\pi\sigma\int_{1}^{\infty}\left(\int_{1}^{t}\frac{d\tau}{(\tau-1)^{1-\sigma}\sqrt{\tau}}\right)\frac{dt}{t\sqrt{t-\beta}} \tag{8.90d}$$

The width of seepage at infinite depth B can be expressed as follows:

$$\frac{B}{y} = \frac{2\pi B(1/2,\sigma)}{\sqrt{\beta}\sin\pi\sigma}\Bigg/\int_{1}^{\infty}\left(\int_{1}^{t}\frac{d\tau}{(\tau-1)^{1-\sigma}\sqrt{\tau}}\right)\frac{dt}{t\sqrt{t-\beta}} \tag{8.90e}$$

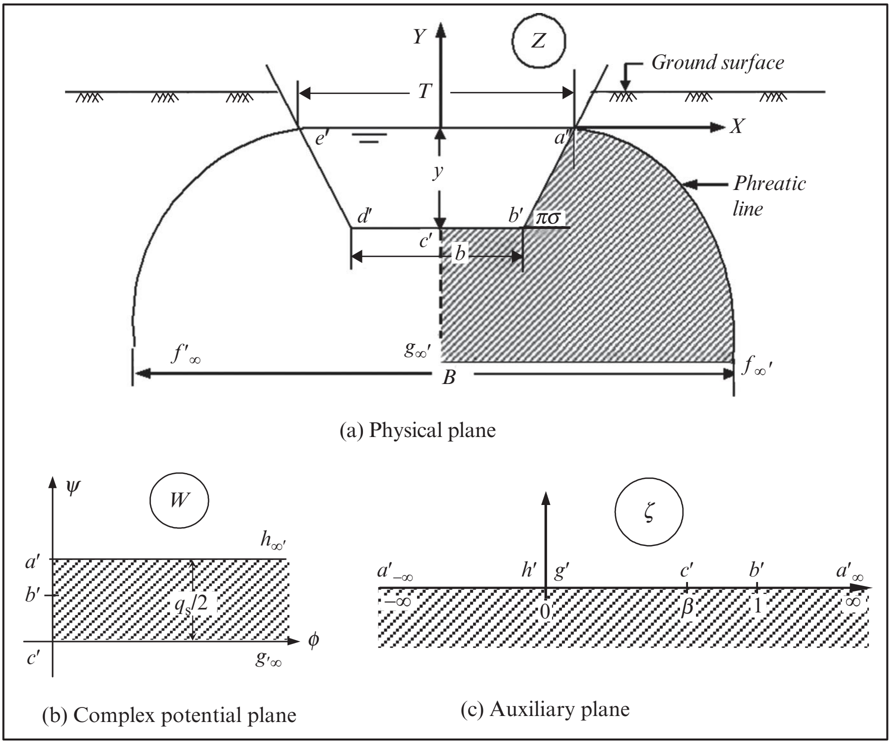

Figure 8.18 *Seepage from a trapezoidal canal with a drainage layer at infinite depth*

The expressions for the variation in the seepage velocity are identical to the case with drainage layer at shallow depth because inverse hodograph mapping is identical in both the cases. Substituting B from Eqn. (8.90e) in Eqn. (8.65), the expression for the quantity of seepage for this case becomes

$$q_s = \frac{2\pi K\, y\, B(1/2,\sigma)}{\sqrt{\beta}\sin\pi\sigma} \Bigg/ \int_1^\infty \left(\int_1^t \frac{d\tau}{(\tau-1)^{1-\sigma}\sqrt{\tau}} \right) \frac{dt}{t\sqrt{t-\beta}} \tag{8.91}$$

Rectangular Channel

With $\gamma = 0$ for a rectangular channel relation for the quantity of seepage changes to

$$q_s = \pi^2 Ky \Bigg/ \sqrt{\beta} \int_1^\infty \frac{\tan h^{-1}\sqrt{(t-1)/t}}{t\sqrt{(t-\beta)}}\, dt \tag{8.92}$$

For the present case, the transformation parameters β is given by the following equation:

$$\frac{b}{y} = \int_\beta^1 \frac{\pi/2 - \tan^{-1}\sqrt{t/(1-t)}}{t\sqrt{(t-\beta)}}\, dt \Bigg/ \int_1^\infty \frac{\tan h^{-1}\sqrt{(t-1)/t}}{t\sqrt{(t-\beta)}}\, dt \tag{8.93}$$

Triangular Channel

Using β = 1 in relations derived for a trapezoidal channel result into corresponding solutions for a triangular channel, for example

$$q_s = \frac{2\pi K\, y\, B(1/2,\sigma)}{\sin \pi\sigma} \Bigg/ \int_1^{\infty}\left(\int_1^{t}\frac{d\tau}{(\tau-1)^{1-\sigma}\sqrt{\tau}}\right)\frac{dt}{t\sqrt{t-1}} \tag{8.94}$$

Slit

A very narrow and deep polygon channel can be assumed as a slit. For a slit, the width at water surface (T) approaches zero, that is, $T/y \to 0$. This means $m \to 0$ (or $\sigma \to 0.5$) for a triangular section; $b/y \to 0$ (or $\beta \to 1$) for a rectangular channel; and both $m \to 0$ and $b/y \to 0$ for a trapezoidal channel. Thus Eqn. (8.86a) with $\beta = 1$ or Eqn. (8.79b) with $\sigma = 0.5$ results in

$$\frac{d}{y} = \pi K\left(\sqrt{1-\gamma}\right) \Bigg/ \int_{\gamma}^{1}\frac{\tan^{-1}\sqrt{t/(1-t)}}{\sqrt{t(1-t)(t-\gamma)}}\,dt \tag{8.95a}$$

Therefore, the seepage function for a slit with drainage layer at finite depth is

$$F_s = 2\pi K\left(\sqrt{\gamma}\right) \Bigg/ \int_{\gamma}^{1}\frac{\tan^{-1}\sqrt{t/(1-t)}}{\sqrt{t(1-t)(t-\gamma)}}\,dt \tag{8.95b}$$

If there is no drainage layer, Eqn. (8.95b) with $\gamma = 0$ yields

$$F_s = \pi^2 \Bigg/ \int_{0}^{1}\frac{\tan^{-1}\sqrt{t/(1-t)}}{t\sqrt{1-t}}\,dt = \frac{\pi^2}{4G} \approx \pi(4-\pi) \tag{8.95c}$$

Example 8.7: Simplified Solutions for Polygon Canals

The above described and other analytical solutions contain improper integrals and unknown implicit transformation variables. Also, these equations are highly implicit nonlinear in β and γ, hence the trial and error method is not convenient and accurate for such equations. These solutions have been simplified in ready to use explicit equation form for estimating the quantity of seepage conveniently from polygon canals.

Rectangular Section

The following equation for a rectangular canal can be fitted (Swamee et al 2001) through minimization of errors:

$$q_s = Ky\left\{\left(\frac{2.5(b/y)^{0.84}+0.45}{(d/y-1)^{0.69}}\right)^{2.38} + \left[(4\pi-\pi^2)^{0.77}+(b/y)^{0.77}\right]^{3.094}\right\}^{0.42} \tag{8.96a}$$

The involved error in the practical range ($0.1 \le y/b \le 2$) is less than 3.0 percent. This much error may be admissible in such type of problems, where uncertainty lies in fixing hydraulic conductivity and depth of drainage layer. As $d/y \to \infty$, (8.96a) reduces to

$$q_s = Ky\left((4\pi-\pi^2)^{0.77}+(b/y)^{0.77}\right)^{1.3} \tag{8.96b}$$

which gives q_s from a rectangular canal when drainage layer or water table is at very large depth (Swamee et al., 2000). The involved error in the practical range in Eqn. (8.96b) is < 0.5 percent and the maximum error is 1.0 percent for the whole range from slit to strip.

Triangular Section

Use of Eqn. (8.88) along with Eqn. (8.89) for computing seepage from a triangular canal can be simplified into

$$q_s = Ky\left\{\left(\frac{1.81m^{1.18}+2.1}{(d/y-1)^{0.26}}\right)^{9.35} + \left((4\pi-\pi^2)^{1.3}+(2m)^{1.3}\right)^{7.2}\right\}^{0.107} \quad (8.97a)$$

The errors involved in Eqn. (8.97a) are less than 2.0 percent in the practical range ($0.5 < m < 5$). As $d/y \to \infty$, Eqn. (8.97a) reduces to the following equation for seepage for infinite depth case:

$$q_s = Ky\left((4\pi-\pi^2)^{1.3}+(2m)^{1.3}\right)^{0.77} \quad (8.97b)$$

wherein the involved error in the practical range is < 0.9 percent and the maximum error is 1.8 percent for the whole range from slit to strip.

Trapezoidal Section

When the drainage layer is located at large depth, the following simplified expression can be used for computation of seepage from a trapezoidal canal:

$$q_s = Ky\left[\left((4\pi-\pi^2)^{1.3}+(2m)^{1.3}\right)^{\frac{0.77+0.462m}{1.3+0.6m}} + (b/y)^{\frac{1+0.6m}{1.3+0.6m}}\right]^{\frac{1.3+0.6m}{1+0.6m}} \quad (8.98)$$

which involves 1.4 percent error in the practical range ($0.5 < m < 5$ and $0.5 < b/y < 10$).

Example 8.8: Compute the quantity of seepage from a trapezoidal channel having bed width = 3.0 m, depth of flow = 2.0 m, and side slope = 1 Vertical: 1.5 Horizontal and passing through a porous medium having hydraulic conductivity = 3×10^{-6} m/s and underlain by a highly pervious drainage layer at a depth of 4.0 m.

Solution: For the given data, $b/y = 1.5$ and $d/y = 2.0$. Eqs (8.79b) and (8.79c) should be solved simultaneously to get β and γ. Since these equations are highly nonlinear and contain improper integrals; an indirect method has been used to find β and γ. The method consists of minimization of an objective function by Powell's conjugate search method (Press et al., 1992). The objective function defined as follows:

$$f(\beta,\gamma) = \left(\frac{d}{y} - f_1(\sigma,\beta,\gamma)\right)^2 + \left(\frac{b}{y} - f_2(\sigma,\beta,\gamma)\right)^2 \quad (8.99)$$

where $f_1(\sigma, \beta, \gamma)$ and $f_2(\sigma, \beta, \gamma)$ are right-hand sides of Eqn. (8.79b) and (8.79c), respectively. Since minimum of this function is zero and which could be attained only when both of the parts of the function reach zero values, and hence satisfy Eqs (8.79b) and (8.79c). After removing singularities and using Gaussian quadratures (96 points for weights and abscissa both for inner and outer integrals) for numerical integration (Abramowitz and Stegun, 2001), the function has been minimized for β and γ for given set of σ, b/y and d/y to get $\beta = 0.9354$ and $\gamma = 0.91466$. With these values and d/y in Eqn. (8.85) $F_s = 8.3658$ and finally from Eqn. (8.84) $q_s = 5.01948\times10^{-5}$ m³/s per metre run of the channel.

PROBLEMS

8.1. Show that irrespective of channel shape the complex potential plane (W-plane) is rectangular in shape for drainage layer at finite depth case while it is semiinfinite strip for homogeneous medium (drainage layer and water table both at finite depth) case.

8.2. Using Schwarz–Christoffel transformation, obtain an expression for the quantity of seeping water into a drainage ditch from a ponded land surface as shown in Figure 8.19.

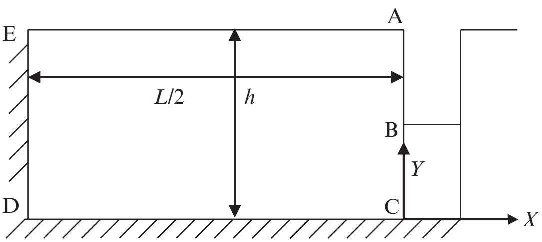

Figure 8.19 *Subsurface drainage by a ditch*

8.3. Construct velocity hodograph and its inversion for seepage through a triangular core in an earthen dam for the following cases (see Figure 8.20).

(i) $h_1 = h$; $h_2 = 0$; $\alpha < \pi/2$ and $\beta < \pi/2$.
(ii) $h_1 = h$; $h_2 = 0$; $\alpha < \pi/2$ and $\beta > \pi/2$.
(iii) $h_1 = h$; $h_2 = 0$; $\alpha > \pi/2$ and $\beta < \pi/2$.
(iv) $h_1 = h$; $0 < h_2 < h$; $\alpha < \pi/2$ and $\beta < \pi/2$.
(v) $h_1 = h$; $0 < h_2 < h$; $\alpha = \pi/2$ and $\beta < \pi/2$.
(vi) $0 < h_2 < h_1 < h$ (with seepage face); $\alpha < \pi/2$ and $\beta < \pi/2$.
(vii) $0 < h_2 < h_1 < h$ (with seepage face); $\alpha < \pi/2$ and $\beta > \pi/2$.
(viii) $0 < h_2 < h_1 < h$ (with seepage face); $\alpha > \pi/2$ and $\beta < \pi/2$.

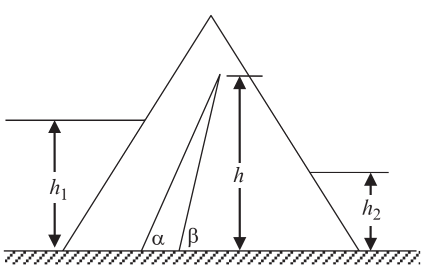

Figure 8.20 *Seepage through a zoned earthen dam*

8.4. Verify that different mappings for a case of seepage from a rectangular canal underlain by a drainage layer at shallow depth are as shown in Figure 8.21.

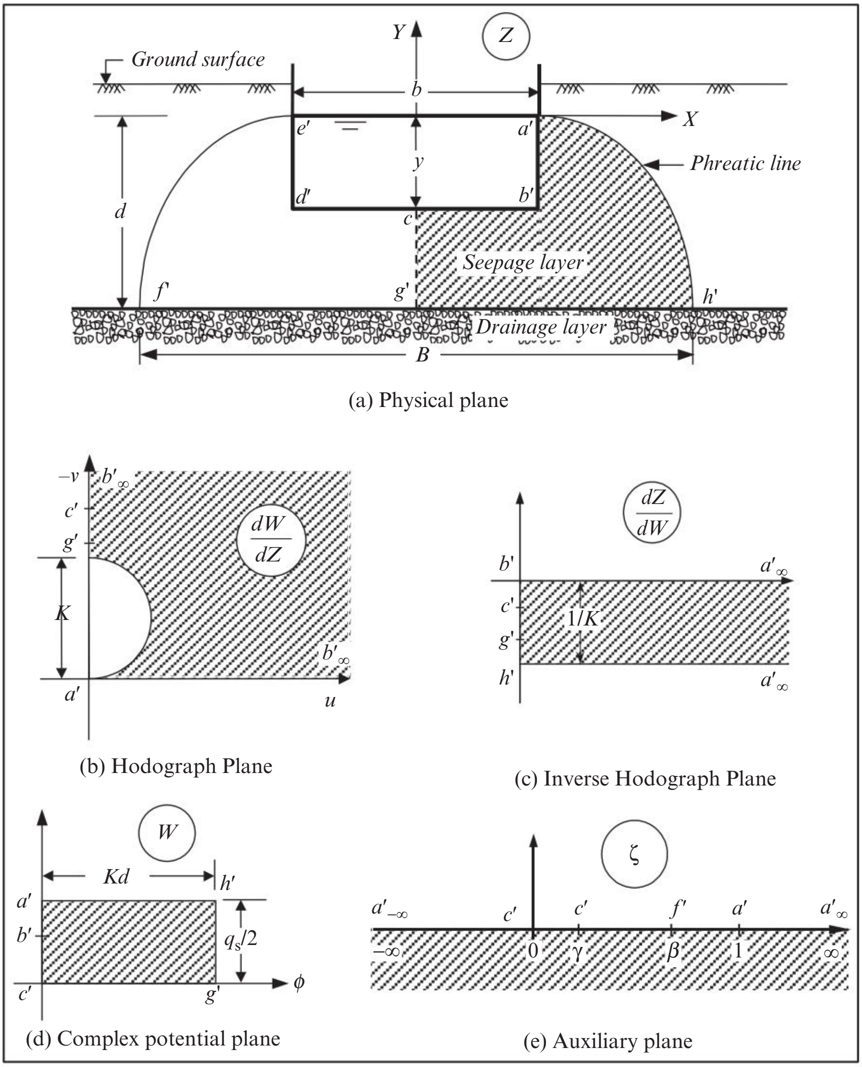

Figure 8.21 *Seepage from a rectangular canal underlain by a drainage layer*

8.5. Verify that different mappings for a case of seepage from a triangular canal passing through a homogeneous porous medium of infinite extent are as shown in Figure 8.22.

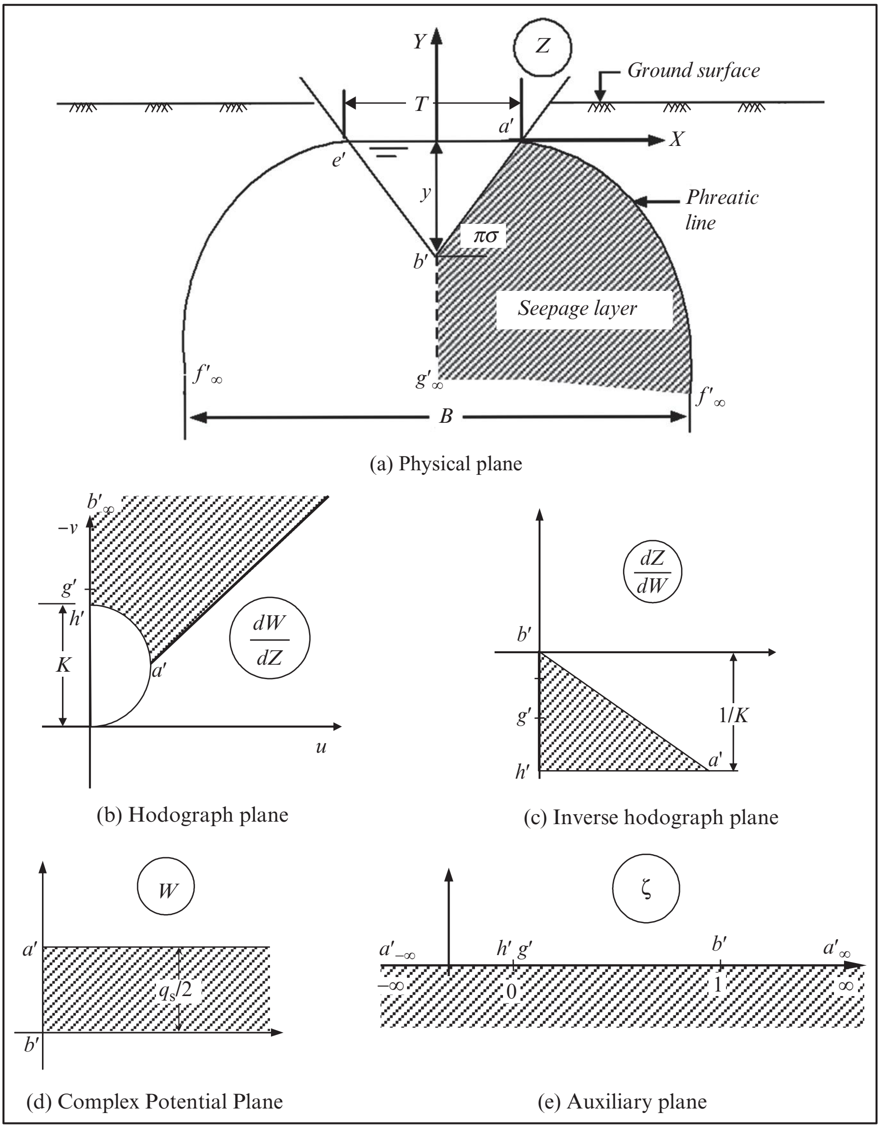

Figure 8.22 *Seepage from a triangular canal with a drainage layer at infinite depth*

8.6. Figure 8.23(a) shows the pattern of seepage from a curvilinear bottomed channel with drainage layer at shallow depth and the water table below the top of drainage layer, whereas in Figure 8.23(b), it is the corresponding complex potential plane (W-plane) for the physical seepage domain $a''a'b'c'f'$. If the W-plane is mapped onto the upper half of the auxiliary plane through Scwarz–Chritoffel transformation as shown in Figure 8.23(c), then verify that the quantity of seepage is given by the following equation:

$$q_s = 2Kd\frac{K\left(\sqrt{1-\alpha}\right)}{K\left(\sqrt{\alpha}\right)} \tag{8.100}$$

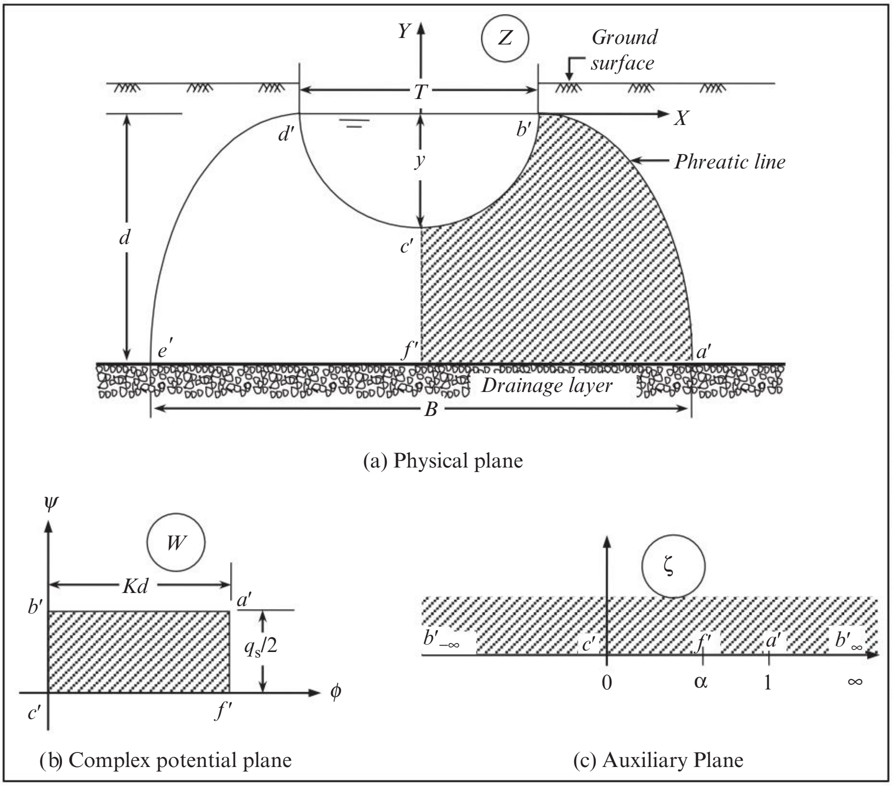

Figure 8.23 *Seepage from a curvilinear channel with a drainage layer*

8.7. Figure 8.24(a) shows the pattern of seepage from a curvilinear bottomed channel with drainage layer at shallow depth and the water table above the top of drainage layer. Verify that for the physical seepage domain $a''a'b'c'f'$, the hodograph plane and corresponding inverse hodograph plane mappings are as shown in Figure 8.24(b) and Figure 8.24(c).

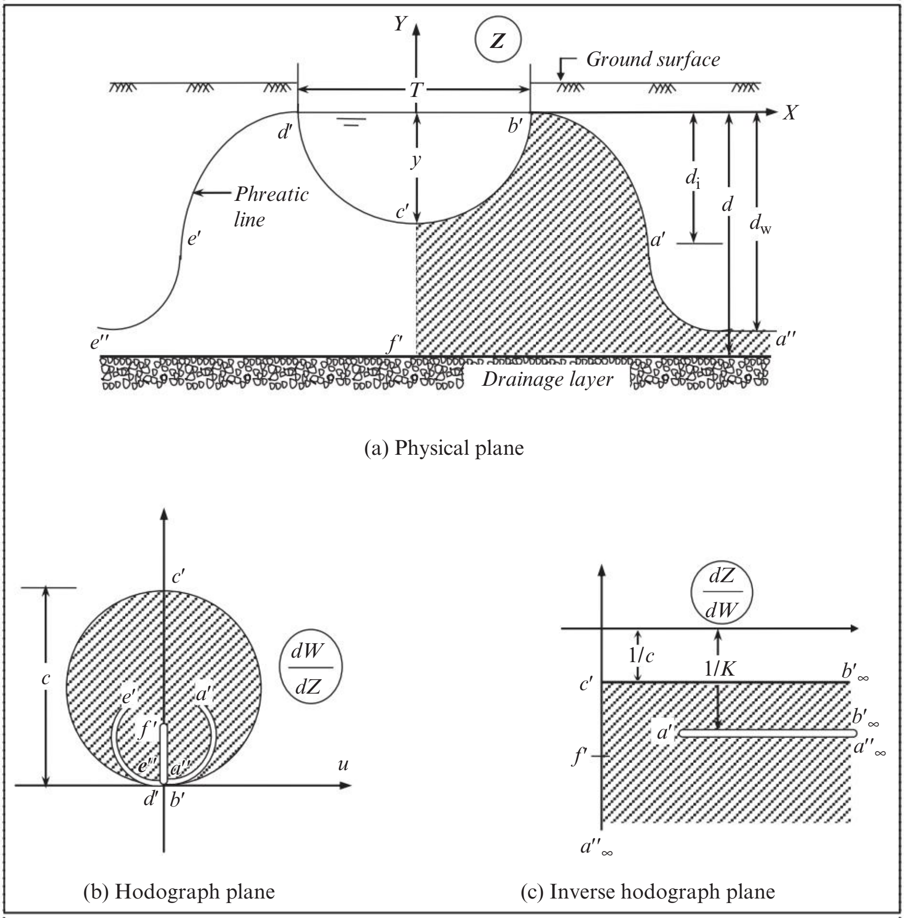

Figure 8.24 *Seepage from a curvilinear channel with water table above the top of a drainage layer*

Chapter 9 Flow through Unsaturated Porous Media

9.1 General

Flow through unsaturated medium is the link between surface water and groundwater. Certain important flow processes take place in unsaturated medium. Contaminants applied in various forms at the ground surface travel downward through soil-water zone, intermediate zone, and capillary zone before reaching to groundwater aquifer. Natural and artificial recharge of groundwater, evaporation of groundwater from soil or through plants, and infiltration are the other areas where unsaturated flow plays a significant role. Thus, study of flow through unsaturated medium is essential in the understanding, calculation, and prediction of replenishment of aquifers and movement and accumulation of contaminants. As discussed earlier in Chapter 1, in unsaturated flow, the pore space is filled partly by air and partly by water. If all the pores are filled by water ($\theta = \eta$), the medium is saturated. On the other hand, if a part of pores are filled by water and remaining by air, then $\theta < \eta$ and the medium is unsaturated. For unsaturated medium the *degree of saturation* that is, $S_e = \frac{V_w}{V_v} = \frac{\theta}{\eta}$ is less than 1 (or 100%). As water content declines (or degree of saturation decreases) and pores get partially filled with air, suction head increases (pressure head becomes more and more negative) and the hydraulic conductivity decreases. An unsaturated medium has *four phases*: solids, water, air, and air–water interface. The presence of even the smallest amount of free air renders a porous medium unsaturated. Even a small amount of air renders the pore fluid compressible. An equilibrium analysis can be applied to a multiphase system such as a saturated porous medium or an unsaturated porous medium. Each phase can be assumed to behave as independent, linear, and continuous in each of the three Cartesian coordinate directions. The total number of independent equilibrium equations will be three times the number of phases in a multiphase system. Equilibrium equations can be summed using the principle of superposition. For more details, Fredlund et al. (2012) may be referred. When two immiscible fluids are in contact, a discontinuity in pressure exits across the interface separating them. The magnitude of the pressure difference (known as *capillary pressure*) depends on the interface curvature at that point and the interface curvature itself depends on the degree of saturation. The negative value of the capillary pressure head is called tension or *suction head*. The most important state variables in an unsaturated porous medium are water content and suction pressure. The suction pressure is the partial pressure of the water vapour in equilibrium with the soil-water relative to the partial pressure of water vapour in equilibrium with free pure water. In field, the suction pressure may be difficult to measure. Several devices are available for measuring suction pressure in the unsaturated medium, for example, psychrometers, filter paper, tensiometers, null-type pressure plate, thermal conductivity sensors, pore fluid squeezer, etc. In groundwater hydrology applications, tensiometers are commonly adopted.

9.2 Suction Pressure

When the pore spaces of the unsaturated porous medium are partially filled with water, the water is attracted to the particle surfaces through electrostatic forces between the water molecules' polar bonds and particle surfaces. The pores in a soil are analogous to capillary tubes with small radii. Soil-water rises above the water table because of the capillaries created by the soil. The rise depends on the pore size distribution and also on the homogeneity and properties of soil. The height of *capillary rise* h_c can be approximated by (Bear 1979)

$$h_c = \frac{14.2}{d_{50}}\left(\frac{1-\eta}{\eta}\right)^{1.5} \tag{9.1}$$

or by (Polubarinova–Kochina 1962).

$$h_c = \frac{14.2}{d_{10}}\left(\frac{1-\eta}{\eta}\right) \tag{9.2}$$

where h_c, mean grain diameter (d_{50}) and effective particle diameter (d_{10}) are in centimeter. The capillary rise may be 2–5 cm in coarse sand, 12–35 cm in medium sand, 35–70 cm in fine sand, 70–105 cm in silt, and 2–4 m and more in clay.

Within capillary fringe, there is a gradual decrease in moisture content with height above the water table as shown in Figure 9.1. Just above the water table, the pores are practically saturated; and at higher levels, only the smaller connected pores contain water. In the capillary fringe, the pressure is less than atmospheric, and thus the capillary water has a negative pressure with respect to the air pressure. This *capillary pressure* depends on the air–water interface curvature corresponding to the moisture content at that point. Several methods are available for determining the relationship between the air–water interface curvature and capillary pressure. The interface is common boundary between air on one side and water on the other side. The air in pore spaces is at atmospheric pressure, therefore the water on the other side of interface in the pore space is at a pressure less than atmospheric. The negative value of the capillary pressure head of water in soil is known as *tension* or *suction head* ψ. The suction head of water measured in height but can also be thought of as energy per unit weight of the fluid. In unsaturated media, the part of the total energy possessed by the fluid due to soil suction forces is equal to suction head. The suction head vary with moisture content of the medium that is, highest when $\theta = 0$ and zero when $\theta = \eta$ soil is saturated. The water is held more tightly by the soil at lower water content and thus as the water content of a soil decreases, the pressure head becomes more negative or the suction/tension head increases. As more water is added to the porous medium, the air exits upward and the area of free surfaces diminishes within the medium, until the medium is saturated and there are no free surface within the pores and therefore no soil suction force. The effect of soil suction can be seen if a column of dry soil is placed vertically with its bottom in a container of water, moisture will be drawn up into the dry soil to a height above the water surface at which the soil suction and gravity forces are just equal.

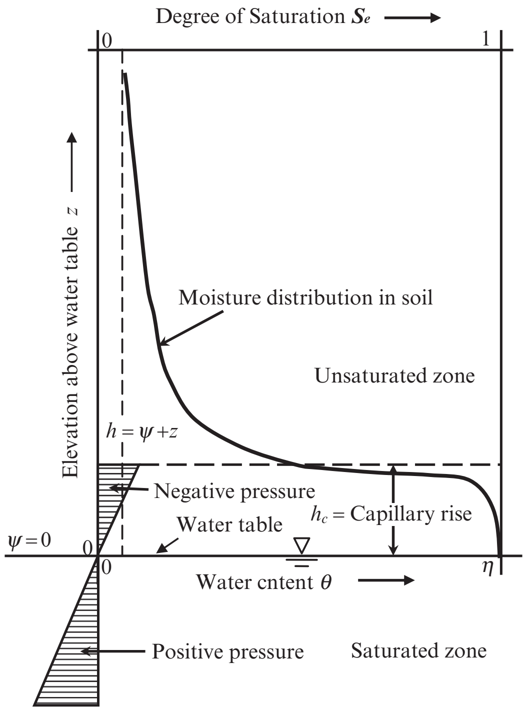

Figure 9.1 *Capillary rise, pressure, and moisture distribution in unsaturated zone*

The hydraulic head is the sum of elevation and pressure heads, that is, $h = z + p / \gamma$. The pressure head (p/γ) is positive in the saturated zone, negative in the unsaturated zone ($p/\gamma = \psi$), and zero at the water table. Therefore, the total energy head in unsaturated/vadose zone is

$$h = \psi + z \tag{9.3}$$

The negative pressure head in the unsaturated/vadose zones explains why water present in vadose zone cannot flow into wells. The pressure of water in unsaturated zones is negative due to the surface tension of the water in pores. A negative pressure cannot be measured with a piezometer. The pressure head of groundwater at a given point can be measured with a *piezometer*. A piezometer reads the head (known as piezometric head) in terms of the height of water column, which is the gauge pressure above the atmospheric pressure. Piezometers do not indicate true groundwater heads due to change in barometric pressure. The effect of barometric pressure change on the water table is reflected after a time lag due a very small air permeability of wet portions in vadose zone, whereas a piezometer immediately respond to any change in the atmospheric pressure. Temporary air pressure increases in vadose zones and resulting discrepancies between groundwater table positions and water levels in piezometers can also be caused by infiltration of water into surface soil over a large area. Piezometers can also give erroneous values if their bottom is placed in a compressible material (clay or fine textured soil).

To measure negative pore water pressures in vadose zone, tensiometers are generally used. The *tensiometer* consists of a high air entry porous ceramic cup connected to a pressure measuring device through a small diameter tube (see Figure 9.2). The tube is usually made from plastic or acrylic due to its low heat conduction and noncorrosive nature. The tensiometer is filled with water that is in contact with the water in the vadose zone through the pores of the membrane. After filling and sealing the tube, the ceramic cup can be inserted into a predrilled hole, but it should be kept immersed in water prior to its installation to avoid desaturation due to evaporation from the cup. It is important that there should be good contact between the cup and soil and soil particles should not be too large; otherwise, there will be inadequate continuity between the pore water in the soil and the water in the tensiometer tube. The water in the tensiometer will flow out through the porous cup into soil. As water flows out of the cup, the pressure in the sealed system declines until the negative pressure within the cup equals the pore water pressure in the surrounding unsaturated zone, thus equilibrium is achieved between the soil and the measuring system. If there is no vertical flow at a point in the vadose zone, the vadose water is in equilibrium with the water table and the negative pressure head at that point is equal to the height of that point above the water table.

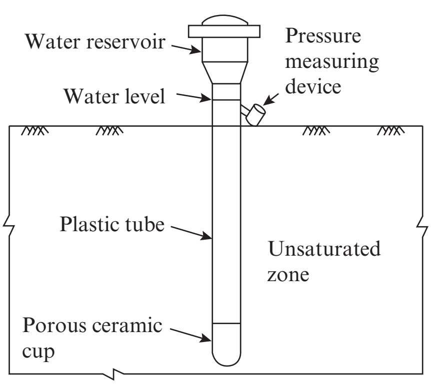

Figure 9.2 *Tensiometer*

9.3 Water Retention Characteristics

The relation between water content and the negative pressure head in a soil is called the *water retention characteristics*. It is generally in graphical form known as *water retention curve*. For uniform soil and no vertical flow, a plot of how the water content decreases with the distance above the water table yields the water characteristics of the soil material in the vadose zone. If a soil sample is initially saturated, then the moisture content θ_s is equal to porosity η. If it is allowed for free drainage (under gravitational force), a part of water (equal to gravitational water) will drain out and the sample becomes unsaturated having $\theta < \eta$ (or the degree of saturation $S_e < 1$) and pressure less than atmospheric. *Field capacity* θ_{FC} is the water content remaining in a unit volume of soil after gravity drainage has ceased after a period of rain or excess irrigation. It is a property of soil and depends on the soil structure, grain size distribution, etc. The moisture above the field capacity is generally not available for plants as the excess water above the field capacity quickly drains out under gravity. The water present in the soil water zone after gravitational drainage is used by plants and the suction pressure increases as plant roots extract soil moisture. After a certain limit of this suction pressure, after messure plant roots are not able to extract water for the survival of the plant and consequently the plant will die out. The soil moisture content below which plant cannot extract water and die is known as *wilting point*. The wilting point depends on the soil type, and type and age of plant. Thus, the *water available* for plants is the water holding capacity of soil that is equal to field capacity minus wilting point. The water below the field capacity cannot drain out under gravity since it is held in the pores due to capillary force. The water content between the field capacity and air dried soil is known as *capillary water*. Even the air-dried sample has some moisture, which remains adsorbed on the surface of soil particle and can be removed by drying in an oven; this water content is called *hygroscopic* or *adsorbed water*. Figure 9.3 shows these different types of water in unsaturated medium.

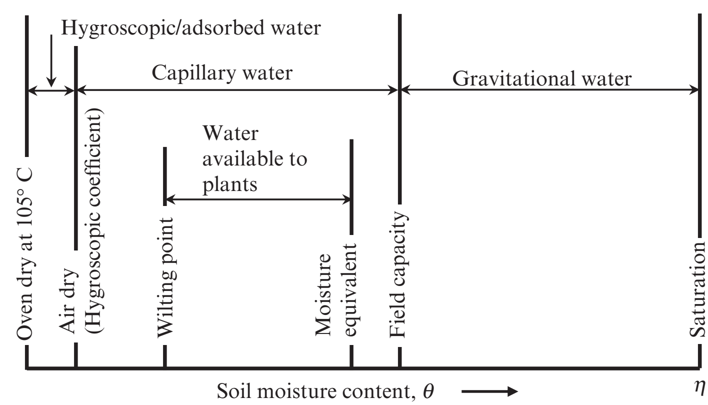

Figure 9.3 *Different moisture terms in unsaturated zone*

The complement of the field capacity that is, volume of water drained by gravity from a unit volume of saturated soil is called *effective porosity* and denoted by η_e, therefore $\eta_e = \eta - \theta_{FC}$. In the soil-water zone, water moves up or down due to water application, root uptake, and evaporation and hence equilibrium is seldom reached. The equilibrium moisture content (i.e. moisture content after gravity drainage ceased) depends on the elevation head above the water table.

At any point, once gravity drainage has ceased, a certain amount of moisture is retained. This retained moisture per unit volume of soil is defined as *retained moisture content* θ_r and its complementary component as the aerated porosity η_a, therefore $\eta_a = \eta - \theta_r$. Figure 9.4 shows these terms on a water retention curve. Both retained moisture and aerated porosity vary with elevation above the water table and with time, if water table changes its position.

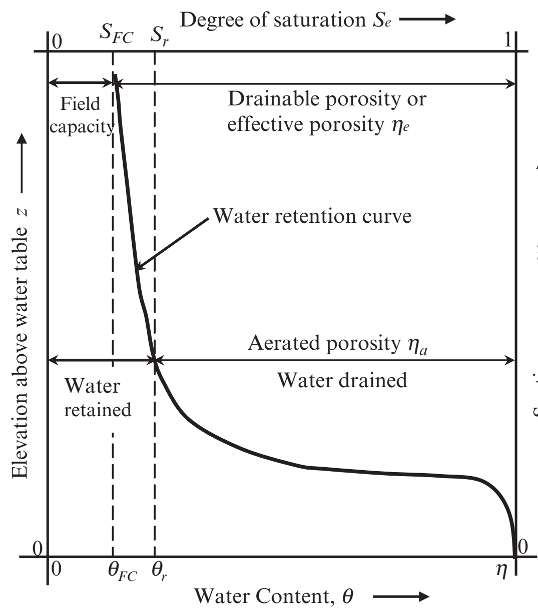

Figure 9.4 *A typical water retention curve*

Figure 9.5 depicts water retention curves for different soils. Water content decreases rapidly at *air-entry value*, where air becomes continuous in the pores. The air entry value or *bubbling pressure* is a function of the size of the largest opening between a set of particles. If this largest pore is relatively small, the air entry value will be relatively large. In uniform (poorly graded) soils, the water content usually decreases abruptly and significantly once the air entry value is reached (Figure 9.6). These soils have a well-defined capillary fringe, which is numerically equal to air entry value. In well-graded soils, the water content decreases gradually even after air entry value and hence the capillary fringe is higher but with a less distinct limit. If the vadose zone consists of layers of different soil materials, the suction head at equilibrium condition is still equal to the vertical distance above the water table, regardless of the layering. However, the water content at each point depends on the water characteristic of the particular soil material at that point. Thus, the water content distribution in the vadose zone of layered soils will be irregular/discontinuous. In the vadose zone, some fine-textured layers may be saturated, whereas coarse-textured materials above and below it may be unsaturated. A saturated fine-textured layer sandwiched

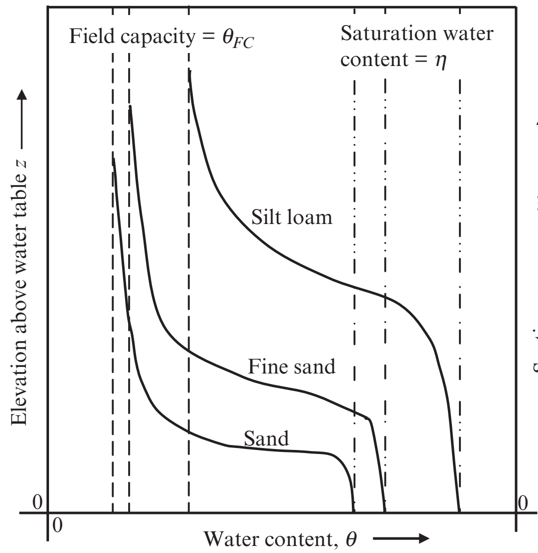

Figure 9.5 *Water retention curves for different soils*

between unsaturated materials acts as a barrier to air movement in the vadose zone. Thus, the equilibrium water content in the vadose zone does not always decrease with increasing distance above the water table and vadose zone term is preferred over the unsaturated zone.

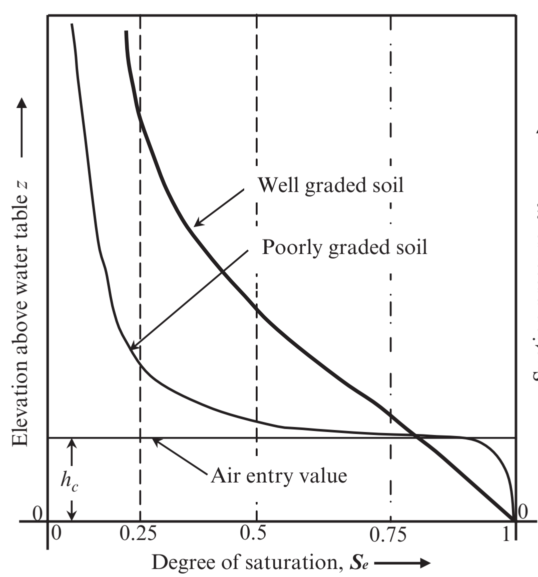

Figure 9.6 *Water retention curves for well- and poorly graded soils*

The equilibrium water content distribution above a static water table depends on whether the water table was falling or rising before reaching a constant level. Figure 9.7 depicts that the water content at a given negative pressure head is higher when this pressure head is reached by removing water from a

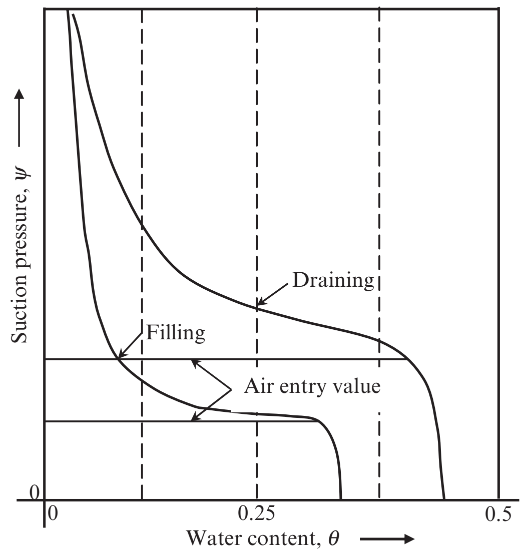

Figure 9.7 *Air entry (bubbling pressure) for draining and filling stages*

saturated soil (falling water table or drying/desorption case) than when this pressure is reached by adding water to an unsaturated soil (rising water table or wetting/sorption case). The drying and wetting curves form a closed loop called *hysteresis*, and this happens due to entrapped air that remains for some time in the soil pores after the soil has been wetted. It is possible to start the wetting process from any point on the drying curve or to start the dry process from any point on the wetting curve as shown in Figure 9.8. Depending on the starting point (history) of wetting/drying process, the hysteresis curve may be of main, primary, or scanning type. The hysteresis loop can be repeatedly traced. With increase in negative pressure in a saturated soil, air first enters the soil and becomes continuous in the soil pores (air entry value), whereas with decrease in negative pressure in unsaturated soil, water displaces the most of air and becomes continuous in the pores (*water entry value or air exit value*). For granular materials, the water entry value is half of air entry value, the capillary fringe in rising water table is about half of that in falling water table.

The water in the vadose zone may not be in complete equilibrium with the water table. Infiltration and downward movement of water from the soil surface, evaporation and water uptake by plants and fluctuations in water table always result into some vertical flow components in the vadose zone. Therefore, the negative pressure head is not equal to the distance above the water table, and it is not possible to plot soil water characteristic from the water content distribution in the vadose zone, and hence both the negative pressure using a tensiometer and water content using some method are simultaneously measured at a point in the vadose zone.

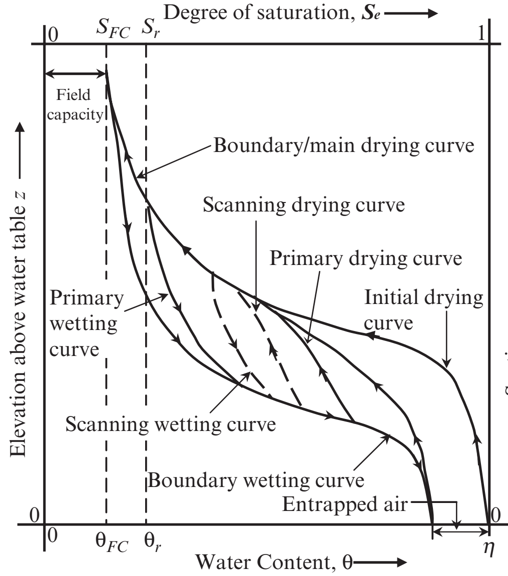

Figure 9.8 *Hysteresis curve*

As the water table drops, drainage of pore space takes place and air replaces water in the dewatered zone. The volume of water yielded by drainage of pores can be estimated by plotting the equilibrium water content above the water table at the beginning and at the end of a certain water table drop. The resulting two curves form an enclosed area and the total volume of water released by the pores is equal to the enclosed area of the curve as shown in Figures 9.9 and 9.10.

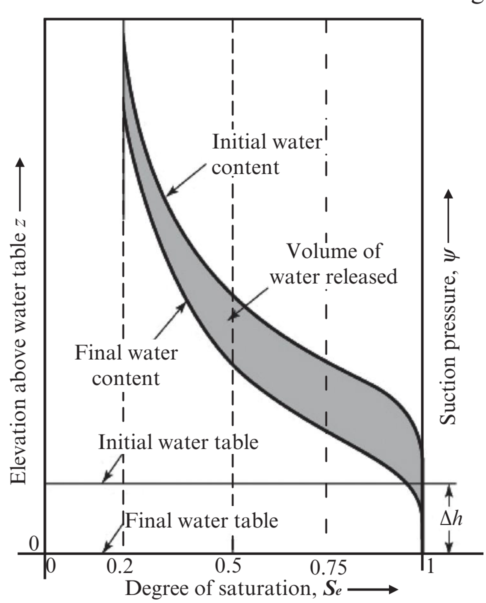

Figure 9.9 *Volume of water released due to change in water table*

The *specific yield*, which is volume of water yielded from a unit area of saturated medium per unit decline in head, is equal to the enclosed area of the curve divided by the water table drop (Figure 9.10). If the water table drops at high rate, the drainage of pore spaces may not be fast to deliver full specific yield, and it will continue for some time. This *apparent or instantaneous specific yield* depends on the rate of drop of water table, which in turn may vary with time and with distance from the groundwater collecting point. Thus as a result of fast drainage, the changes in the moisture distribution lag behind and reach a new equilibrium only after a certain time interval that depends on the type of soil. A time lag will also take place due to water table rise caused by infiltration. When the water table is rising or falling slowly, the changes in moisture distribution have sufficient time to adjust continuously and the time lag is negligible. The apparent specific yield (also called *drainable porosity*) is time dependent (see Figure 9.11) and takes into account the time lag in drainage due to faster drop in water table. The amount of water that unconfined aquifer can store per unit rise in water table and per unit area is called *fillable porosity*. The fillable porosity is less than the specific yield due to hysteresis. For unconfined aquifers, storage coefficient and specific yield are interchangeable.

Water content and suction head in an unsaturated porous medium are interrelated. Several empirical equations are available to compute the water content from known value of suction head and vice versa. For example, Gardener (1958) suggested

$$\theta = \frac{a\eta}{|\psi|^n + b} \Rightarrow \psi = \left[\frac{b}{a}\left(\frac{\eta}{\theta} - 1\right)\right]^{1/n} \tag{9.4}$$

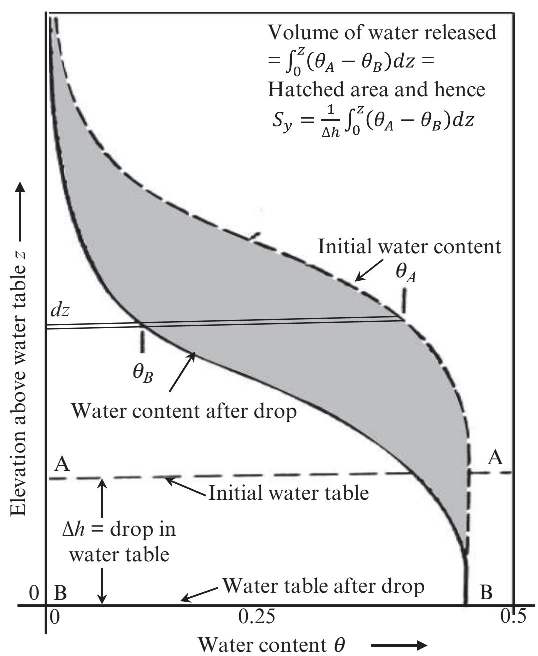

Figure 9.10 *Computation of volume of water and specific yield due to change in water table*

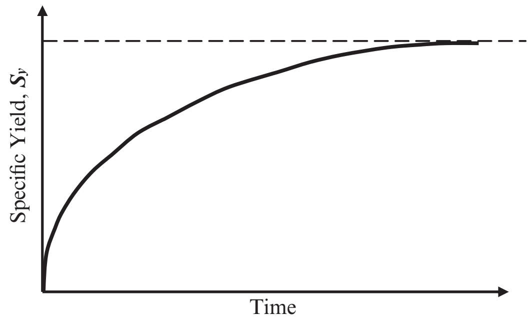

Figure 9.11 *Time-dependent (apparent) specific yield*

Brooks and Corey (1966) gave relation as follows:

$$\theta = \eta \text{ for } |\psi| < |\psi_{\text{aev}}| \tag{9.5}$$

and

$$S_{\text{e}} = \frac{\theta - \theta_{\text{r}}}{\eta - \theta_{\text{r}}} = \left(\frac{\psi}{\psi_{\text{aev}}}\right)^{-n} \Rightarrow \psi = \psi_{\text{aev}}\left(\frac{\eta - \theta_{\text{r}}}{\theta - \theta_{\text{r}}}\right)^{1/n} \text{ for } |\psi| \geq |\psi_{\text{aev}}| \tag{9.6}$$

where, ψ_{aev} = air-entry value or bubbling pressure and $n = 3 + 2/m$. McKee and Bumb (1984) expressed as follows:

$$S_{\text{e}} = \frac{\theta - \theta_{\text{r}}}{\eta - \theta_{\text{r}}} = \exp\left(\frac{a - \psi}{n}\right) \Rightarrow \psi = a - n\ln(S_{\text{e}}) \tag{9.7}$$

Van Genuchten (1980) proposed

$$\theta = \frac{\eta}{\left[|a\psi|^{n} + 1\right]^{m}} \Rightarrow \psi = \frac{1}{a}\left[\left(\frac{\eta}{\theta}\right)^{1/m} - 1\right]^{1/n} \tag{9.8}$$

Maulem (1976) suggested $m = (n - 1)/n$ and Burdine (1953) suggested $m = (n - 2)/n$ in Eqn. (9.8), therefore it reduces from 3 to 2 parameter relationship. In the above equations, a, b, n, and m are fitting parameters; θ_{r} = residual water content after soil thoroughly drained; and $\theta_{\text{s}} = \eta$ = saturated water content (porosity). The *residual water content* is the lower limit beyond which there is small change in water content even after application of extremely large changes in negative pressure head. It is an important parameter in *effective porosity* $\eta_{\text{e}} = \eta - \theta_{\text{r}}$ and *effective degree of saturation* S_{e}, hence $\theta = \theta_{\text{r}} + S_{\text{e}}\eta_{\text{e}}$. *Specific moisture capacity* (c_{m}) is defined as the change in moisture content divided by the change in suction head or $c_{\text{m}} = d\theta/d\psi$. It is the slope of water retention curve and can be computed using $\theta - \psi$ relations given in Eqs (9.4) through (9.8).

9.4 Hydraulic Conductivity Relations

In unsaturated soil, part of the pore channels are filled with air, which physically obstruct water movement, and hence water can flow only through the saturated finer pores or in films around the soil particles. The lower the value of θ, the lower the unsaturated hydraulic conductivity. For unsaturated medium, the hydraulic conductivity is not a constant, but it is strongly dependent on the moisture content or degree of saturation. When a medium is near saturation ($S_e = 1$), its hydraulic conductivity is maximum and is equal to the saturated hydraulic conductivity K. As the saturation decreases, the large pores drain first so that the flow takes place through the smaller ones. This causes both a reduction in the cross-sectional area available for flow and an increase in tortuosity of the flow paths. The combined effect causes a rapid reduction in the hydraulic conductivity as the water content decreases. As the water films become thinner, certain phenomena at the solid–water interface come into play, causing a further reduction in hydraulic conductivity. As the water content approaches the residual water content, the air phase becomes continuous and water phase is not continuous throughout the medium resulting to hydraulic conductivity near zero value. Thus, the hydraulic conductivity in an unsaturated medium will vary from zero at residual water content to K at water content equal to porosity/saturation. The ratio of hydraulic conductivity at any moisture content (K_θ or K_ψ) to the saturated hydraulic conductivity (K) is called the *relative hydraulic conductivity* (K_r) of the unsaturated medium that is, $K_r = K_\psi/K$, and it varies from 0 to 1 as depicted in Figure 9.12.

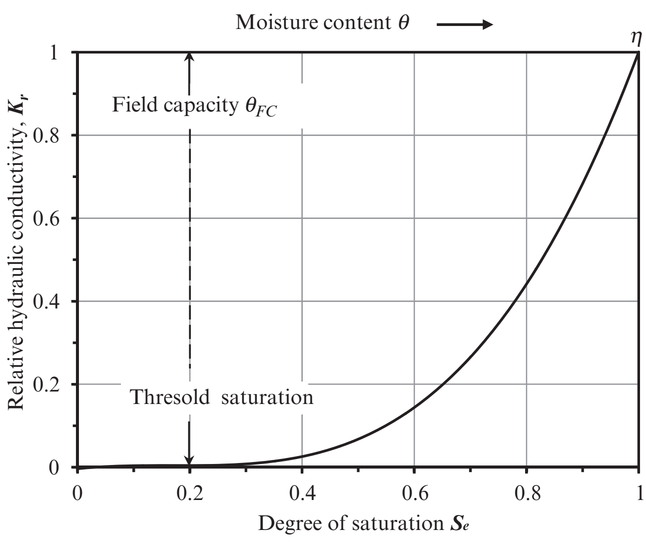

Figure 9.12 *Relative hydraulic conductivity of unsaturated medium*

The relative hydraulic conductivity depends on the type of soil. For clay, its range is large, but for sand the variation in the relative hydraulic conductivity is relatively smaller. Figure 9.13 compares this fact for clay, loam, and sand.

Unsaturated hydraulic conductivity is expressed as K_θ or K_h depending on whether it is considered a function of θ or ψ. While the relation between K_θ and θ is easy to interpret, the relation between K_ψ and ψ is more useful in flow analysis. Several methods and techniques are available to develop the relations between K_θ

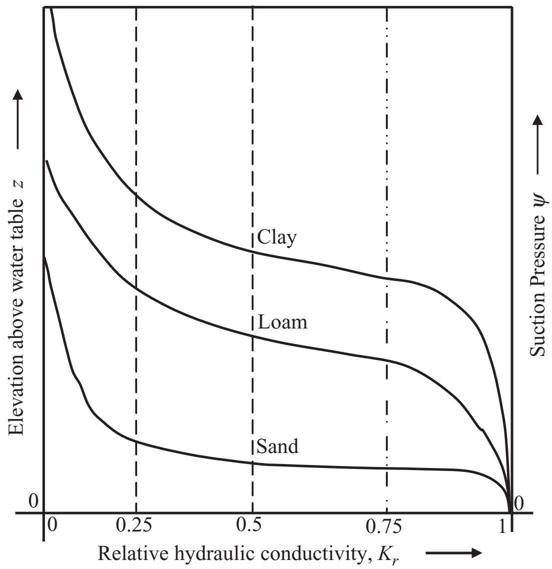

Figure 9.13 *Relative hydraulic conductivity of different soils*

and θ or between K_ψ and ψ. The relation between K_θ and θ is for a given material is free from hysteresis, but the relation between K_ψ and ψ is affected by hysteresis as relations between θ and ψ are hysteretic. The curve between K_ψ and ψ for wetting often remains below its drying counterpart even for $\psi > 0$. This means K after wetting will be less than K at saturation. The relation between K_ψ and ψ have been expressed by many investigators in empirical equations to facilitate analytical or numerical solution of unsaturated flow systems. Gardener (1958) equation is

$$K_\psi = \frac{a}{|\psi|^n + b} \tag{9.9}$$

where, a, b, and n are constants that decrease with decreasing particle sizes of the material. For $\psi = 0$, $K_\psi = a/b = K$, which is hydraulic conductivity at saturation. For convenient use in analytical purpose, it can used as follows:

$$K_\psi = K\exp(-a\psi) \tag{9.10}$$

Van Genuchten (1980) suggested $m = 1 - 1/n$ in the following equation:

$$K_\psi = K\frac{\left\{1-(a|\psi|)^{n-1}\left[1+(a|\psi|)^n\right]^{-m}\right\}^2}{\left[1+(a|\psi|)^n\right]^{m/2}} \tag{9.11}$$

Brooks and Corey (1966) put forward the following relation:

$$K_\psi = K\left(\frac{\psi_{\text{aev}}}{\psi}\right)^{2+3m} \tag{9.12}$$

for suction pressure greater than air-entry value ψ_{aev}.
As pointed earlier, the relation between K_θ and θ for a given material is free from hysteresis, so it is preferred. The relation for K_θ by Irmay (1954) is

$$K_\theta = K\left(\frac{\theta-\theta_{\text{FC}}}{\theta-\theta_{\text{FC}}}\right)^3 \tag{9.13}$$

Relation by Brooks and Corey (1964) for suction pressure greater than air-entry value ψ_{aev} is

$$K_\theta = K\left(S_{\text{e}}\right)^{3+2/m} = K\left(\frac{\theta-\theta_{\text{r}}}{\theta-\theta_{\text{r}}}\right)^{3+2/m} \tag{9.14}$$

Expression for K_θ given by Mualem (1976) is

$$K_\theta = K\left(S_{\text{e}}\right)^{3-2m} = K\left(\frac{\theta-\theta_{\text{r}}}{\eta-\theta_{\text{r}}}\right)^{3-2m} \tag{9.15}$$

Averjanov (1950) recommended the following equation:

$$K_\theta = K\left(S_{\text{e}}\right)^{3.5} = K\left(\frac{\theta-\theta_{\text{r}}}{\eta-\theta_{\text{r}}}\right)^{3.5} \tag{9.16}$$

Van Genuchten (1980) obtained the below equation:

$$K_\theta = K\left(\frac{\theta-\theta_{\text{r}}}{\eta-\theta_{\text{r}}}\right)^{1/2}\left\{1-\left[1-\left(\frac{\theta-\theta_{\text{r}}}{\eta-\theta_{\text{r}}}\right)^{1/m}\right]^m\right\}^2 \tag{9.17}$$

Campbell (1974) expression is applicable for suction pressure greater than air-entry value $\psi_{\text{aev.}}$

$$K_\theta = K\left(\frac{\theta}{\eta}\right)^n \tag{9.18}$$

Thus, hydraulic conductivity of unsaturated medium is nonlinear function of water content θ and varies with soil texture. It is higher for sandy soil than clayey soil though porosity is higher for clay; but at high suction head, the hydraulic conductivity may be higher for clay because the rate of change in suction head is higher for sandy soil than clayey soil.

9.5 Flow Equation in Unsaturated Porous Medium

For saturated flow, the only two forces involved are gravity and friction; but for unsaturated flow, the *suction force* binding water to soil particles through surface tension must also be included. Therefore, it is difficult to solve unsaturated flow equations. However, several useful mathematical models are available. Unsaturated flow is analyzed on the basis of Darcy's law, with added complication that K is dependent on the water content θ, which in turn is related to the suction head. The derivation of the partial differential equation for flow in unsaturated zone is similar to that in the saturated zone as derived in Chapter 6. Here also consider a representative elementary volume as shown in Figure 6.1 with initial water content θ. Therefore, the initial mass within the REV is

$$M = \rho_w \theta \Delta x \Delta y \Delta z \tag{9.19}$$

Following similar steps for mass conservation within REV, we obtain

$$-\left(\frac{\partial(\rho_w v_x)}{\partial x} + \frac{\partial(\rho_w v_y)}{\partial y} + \frac{\partial(\rho_w v_z)}{\partial z} \right) + \rho_w R(x, y, z, t) = \frac{1}{\Delta x \Delta y \Delta z} \frac{\partial M}{\partial t} \tag{9.20}$$

By making a further assumption that the density of the fluid does not vary spatially, and there is no external source/sink ($R = 0$) and substituting M from Eqn. (9.19) gives

$$\frac{\partial(v_x)}{\partial x} + \frac{\partial(v_y)}{\partial y} + \frac{\partial(v_z)}{\partial z} = -\frac{\partial \theta}{\partial t} \tag{9.21}$$

This is continuity equation for unsaturated flow system. The right-hand side of the equation can be written as follows:

$$\frac{\partial \theta}{\partial t} = (c_m + S_e S_s) \frac{\partial h}{\partial t} \tag{9.22}$$

where, c_m = specific moisture capacity, S_e = degree of saturation, and S_s = specific storage.

If water moves only in vertically downward direction through unsaturated porous medium and by choosing z axis along vertical downward direction, the flow becomes 1-D. Then Eqn. (9.21) reduces to

$$\frac{\partial \theta}{\partial t} + \frac{\partial v_z}{\partial z} = 0 \tag{9.23}$$

This is the continuity equation for one-dimensional unsteady flow in an unsaturated porous medium. This equation is applicable to flow at shallow depth below the land surface. At greater depth, such as in deep aquifers, changes in the water density and in the porosity can occur as the result of changes in fluid pressure, and these must also be accounted for in developing the continuity equation.

Darcy's law is also applicable to the unsaturated flow but with added complication that K is dependent on the water content θ, which in turn is related to the suction head ψ. In unsaturated flow systems, K_ψ and θ are continuously changing. Infiltration produces an increase in K_ψ and θ behind a downward moving front, whereas stopping the infiltration decreases K_ψ and θ in the wetted zone. Similarly, evaporation and uptake of water by plant roots reduce K_ψ and θ. In the unsaturated zone, the Darcy's equation can be written as follows:

$$v = -K_\psi \nabla h = -K_r \mathrm{K}\ \nabla h = -K_r \mathrm{K} \nabla(\psi + z) \tag{9.24}$$

where hydraulic conductivity tensor in the unsaturated medium is $K_\psi = K_r \mathrm{K}$, in which relative hydraulic conductivity varies $0 < K_r < 1$ and saturated hydraulic conductivity tensor K is given by Eqn. (5.34). Use of Darcy's law for velocities v_x, v_y, and v_z from Eqn. (9.24) in Eqn. (9.21) results

$$\frac{\partial}{\partial x}\left(K_r K_x \frac{\partial h}{\partial x}\right)+\frac{\partial}{\partial y}\left(K_r K_y \frac{\partial h}{\partial y}\right)+\frac{\partial}{\partial z}\left(K_r K_z \frac{\partial h}{\partial z}\right)=\frac{\partial \theta}{\partial t}=\left(c_m+S_e S_s\right)\frac{\partial h}{\partial t} \quad (9.25)$$

As $h=\psi+z$ so $\frac{\partial h}{\partial x}=\frac{\partial \psi}{\partial x};\frac{\partial h}{\partial y}=\frac{\partial \psi}{\partial y};$ and $\frac{\partial h}{\partial z}=\frac{\partial \psi}{\partial z}+1$. Therefore,

$$\frac{\partial}{\partial x}\left(K_r K_x \frac{\partial \psi}{\partial x}\right)+\frac{\partial}{\partial y}\left(K_r K_y \frac{\partial \psi}{\partial y}\right)+\frac{\partial}{\partial z}\left(K_r K_z \left(\frac{\partial \psi}{\partial z}+1\right)\right)=\frac{\partial \theta}{\partial t} \quad (9.26)$$

$$\frac{\partial}{\partial x}\left(K_{\psi x} \frac{\partial \psi}{\partial x}\right)+\frac{\partial}{\partial y}\left(K_{\psi y} \frac{\partial \psi}{\partial y}\right)+\frac{\partial}{\partial z}\left(K_{\psi z} \frac{\partial \psi}{\partial z}\right)+\frac{\partial K_{\psi z}}{\partial z}=\frac{\partial \theta}{\partial t} \quad (9.27)$$

Defining soil water diffusivity $D=K\frac{\partial \psi}{\partial \theta}$ (m²/s), Eqn. (9.27) reduces to

$$\frac{\partial}{\partial x}\left(D_x \frac{\partial \theta}{\partial x}\right)+\frac{\partial}{\partial y}\left(D_y \frac{\partial \theta}{\partial y}\right)+\frac{\partial}{\partial z}\left(D_z \frac{\partial \theta}{\partial z}+K_{\theta z}\right)=\frac{\partial \theta}{\partial t} \quad (9.28)$$

Eqs (9.25) through (9.28) are the different forms of main governing equation for unsteady unsaturated flow in porous media known as *Richards equation*. To solve Richard's equation, interrelations among water content, hydraulic conductivity, and suction pressure are needed. For steady flow, the right-hand side of the above equations is zero. For two-dimensional flow in a vertical plane (infiltration, seepage, etc.), the second term in Eqs (9.25) through (9.28) is zero. For one-dimensional vertical flow by choosing z-axis along vertical downward direction:

$$\frac{\partial \theta}{\partial t}=\frac{\partial}{\partial z}\left(D\frac{\partial \theta}{\partial z}+K_\theta\right) \quad (9.29)$$

which is the one-dimensional form of *Richards equation*.

The unsaturated flow equation is similar to the saturated flow equation, with soil moisture replacing porosity and unsaturated hydraulic conductivity is a function of suction head or water content. In unsaturated flow systems, K_ψ and θ continuously change. Values of soil water diffusivity can be obtained by graphically determining $\partial\psi/\partial\theta$ as the slope of the ψ-θ curve at a certain θ and multiplying this slope by K_θ belonging to the same θ. As D is θ dependent, the procedure must be repeated for a number of θ values.

Actually, unsaturated flow is a two-phase flow of water and air, however, only water phase flow is analysed and air is considered as part of the solid phase. Solution of unsaturated flow systems is a problem of solving the basic governing differential equation for a medium where the unsaturated hydraulic conductivity (K_θ or K_ψ) is a function of the water content, which changes with the suction head ψ. The flow equation for unsaturated medium are nonlinear, since K_θ or K_ψ, D and derivatives strongly depend on ψ or θ. Additional difficulties stem from (i) interrelations among K_θ or K_ψ, D, θ and ψ are experimental or empirical; (ii) interrelations are subjected to hysteresis; and (iii) boundaries are irregular and medium is inhomogeneous. These facts make it impossible for exact analytical solutions of unsaturated flow problems. Analytical solutions are preferable but are not possible so researchers have tried to obtain semianalytical or approximate solutions. Since soil water diffusivity is analogous to thermal diffusivity, the mathematics of heat flow can be used to for solving unsaturated flow with similar boundary conditions. Bouwer (1978) used a step function and critical pressure head to simplify solution for unsaturated systems. Some unsaturated problems can be solved using electric resistance network analogs. FDM, FEM, and other numerical methods are generally used to solve variety of unsaturated flow problems. These solutions include an iterative process, assuming an initial K_ψ solving for h, evaluating ψ at each point with Eqs (9.26) or (9.27) and determining the K_Ψ values corresponding to ψ. These K_Ψ values will differ from the initially assumed values. The procedure is repeated till the assumed K_ψ value agree with the computed K_Ψ value for ψ. In unsteady flow, θ must also be changed as ψ changes with time. This produces storage or release of pore water depending on whether ψ is increasing or decreasing.

9.6 Infiltration of Surface Water

9.6.1 Infiltration

Infiltration is the movement of water through the soil surface into the soil as distinguished from *percolation*, which is the movement of water within/through the soil. Infiltrated water replenishes soil moisture, recharges aquifers, and ultimately supports streamflows during dry periods. The infiltration process is complicated, because soils are different; the same soil behaves differently at different moisture conditions. During rainfall or irrigation, the upper soil layer will become saturated and water will start ponding and flowing on the surface. The distribution of soil moisture within the soil profile during the downward movement of water is illustrated in Figure 9.14. There are four moisture zones:

(i) *Saturation zone*: This is saturated layer just below the soil surface having almost constant water content, and it is only a few centimetres thick. It is followed by a *transition zone*, where water content decreases rapidly with depth. The transition zone is also a few centimetres thick only.

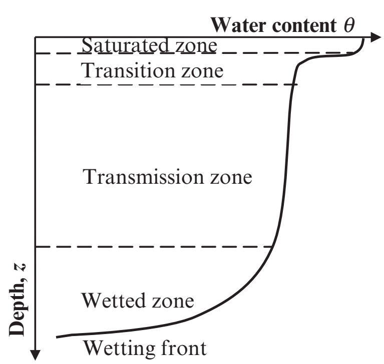

Figure 9.14 *Soil moisture movement*

(ii) *Transmission zone*: It is partially saturated layer of almost constant water content and gets thicker as wetting front moves down through soil column.
(iii) *Wetting zone*: In this zone, the water content decreases steeply with depth and soil wets as wetting zone moves down through the soil profile.
(iv) *Wetting front*: It is sharply defined leading edge of the wetting zone and moves down as water passes through the transmission zone.

The *infiltration rate f* is the rate at which water enters the soil at the surface. If water is ponded at the surface (an ample supply), then infiltration occurs at the *potential infiltration rate*, which is also called *infiltration capacity* f_c that is the maximum rate at which a given soil at a given time can absorb water. If the rate of supply is less than the potential rate, then the actual infiltration rate will be less than the potential rate and equal to the rate of supply of water. The infiltration capacity depends on a variety of factors: the two most important being soil type and water content in the upper soil layer. For example, a very wet soil will have a smaller infiltration capacity than a dry soil. Most infiltration equations describe the potential rate. The *cumulative infiltration rate F* is the accumulated depth of water infiltrated during a given time period and is equal to the integral of the infiltration rate over that period.

$$F(t) = \int_0^t f(\tau)d\tau \tag{9.30}$$

Conversely, the infiltration rate is the time derivative of the cumulative infiltration.

$$f(t) = \frac{dF(t)}{dt} \tag{9.31}$$

9.6.2 Horton Equation

If K and D are assumed constant that is, independent of θ, then Richard's equation becomes

$$\frac{\partial \theta}{\partial t} = D\frac{\partial^2 \theta}{\partial z^2} \tag{9.32}$$

Its solution is Horton's equation:

$$f(t) = f_c + \left(f_o - f_c\right)e^{-kt} \tag{9.33}$$

It implies that infiltration begins at some rate f_o and exponentially decreases until it reaches a constant rate f_c (saturated soil hydraulic conductivity). k is a decay constant ($1/T$). The actual rate of infiltration is also governed by the rate of supply.

Horton's model describes the decrease in infiltration capacity with time, assuming that infiltration always is maximum (i.e. at capacity). It is important to understand that it is not time, but rather the depth of infiltrated water that determines the infiltration capacity. Thus, Horton's equation cannot be used directly to calculate the rate of infiltration. Using Horton's equation directly, a reduction in infiltration capacity is made regardless of the amount of water that enters the soil. To overcome this problem, the integrated form of Horton's equation is used in practice.

$$F(t) = \int_0^t f_c + (f_o - f_c)e^{-ku}\,du = f_c t + \frac{f_o - f_c}{k}\left[1 - e^{-kt}\right] \tag{9.34}$$

$F(t_p)$ is the cumulative infiltration at time t_p if at all times supply rate is greater than or equal to the infiltration capacity. But such equation is transcendental for unknown t_p, must be solved iteratively. Using the obtained t_p value, the infiltration capacity available after time *t* can be determined using the original Horton's equation.

9.6.3 Phillip's Equation

In unsaturated flow systems, K_ψ and θ are continuously changing. Infiltration produces an increase in K_ψ and θ behind a downward moving front, while stopping the infiltration decreases K_ψ and θ in the wetted zone. Similarly, evaporation and uptake of water by plant roots reduce K_ψ and θ. Therefore, Phillip considered that *K* and *D* vary with θ. Using Boltzmann transformation $B(\theta) = z/\sqrt{t}$, we can get *dB* through change in *z* or in *t* that is,

$$dB = dz/\sqrt{t} \qquad \Rightarrow \qquad dz = \sqrt{t}dB \tag{9.35}$$

and

$$dB = z\left(-\frac{1}{2}t^{-3/2}\right)dt \qquad \Rightarrow \qquad dt = -\frac{2t^{3/2}}{z}dB \tag{9.36}$$

Substituting *dz* and *dt* in Richard's equation,

$$\frac{-zd\theta}{2t^{3/2}dB} = \frac{d}{\sqrt{t}dB}\left(D\frac{d\theta}{\sqrt{t}dB}\right) + \frac{dK}{d\theta}\frac{d\theta}{\sqrt{t}dB} \tag{9.37}$$

Simplifying

$$2\frac{d}{dB}\left(D\frac{d\theta}{dB}\right) = -\frac{d\theta}{dB}\left(\frac{z}{\sqrt{t}} + 2\sqrt{t}\frac{dK}{d\theta}\right) \tag{9.38}$$

After neglecting $\sqrt{t}\,dK/d\theta$ term, the above equation converts into an ordinary differential equation in *B* as follows:

$$2\frac{d}{dB}\left(D\frac{d\theta}{dB}\right) = -B\frac{d\theta}{dB} \tag{9.39}$$

Solution of this yield an infinite series for *F*(*t*) which can be approximated to

$$F(t) = St^{1/2} + Kt \tag{9.40}$$

Therefore,

$$f(t) = \frac{1}{2}St^{-1/2} + K \tag{9.41}$$

where *S* = sorptivity that is a function of soil suction potential ψ.

9.6.4 Green-Ampt Method

It is an exact analytical solution for an approximate physical model of infiltration. The wetting front is a sharp boundary dividing soil of moisture content θ_i below from saturated soil with moisture content η above. The wetting front has penetrated to a depth L in time t since infiltration began as shown in Figure 9.15. Water is ponded to a small depth h_0 on the soil surface. Consider a vertical column of soil of unit horizontal cross sectional area and let the soil moisture content increase from θ_i to η as the wetting front passes, therefore the increase in the water stored within the control volume as a result of infiltration is $L(\eta - \theta_i)$ for a unit cross section. By definition, this quantity is equal to F (the cumulative depth of infiltrated water into the soil). Hence,

$$F(t) = L(\eta - \theta_i) = L\Delta\theta \tag{9.42}$$

Apply Darcy's law between points 1 and 2 (located respectively at the ground surface and just on the dry side of the wetting front) to obtain

$$v = f = -K\frac{\partial h}{\partial z} = K\frac{h_1 - h_2}{z_2 - z_1} = K\frac{h_0 - (-\psi - L)}{L} \approx K\frac{\psi + L}{L} \tag{9.43}$$

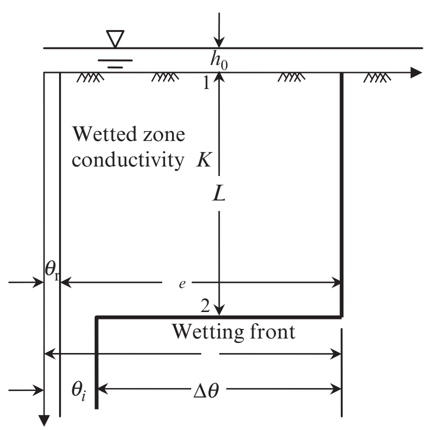

Figure 9.15 *Green-Ampt infiltration model*

since the velocity in the porous medium, v is equal to the rate at which water is entering from the ponded surface into the soil which is nothing but infiltration rate f. The head h_1, at the surface is equal to ponded depth h_0 and the head h_2 in the dry soil below the wetting front, equal $-\psi-L$. The ponded depth, h_0 is negligible compared to ψ and L. Eliminating L and substituting $f = dF/dt$

$$\frac{dF}{dt} = K\frac{\psi\Delta\theta + F}{F} \tag{9.44}$$

Separating variables and then integrating

$$\int_0^{F(t)} \left(1 - \frac{\psi\Delta\theta}{\psi\Delta\theta + F}\right) dF = \int_0^t K dt \tag{9.45}$$

results

$$F(t) = Kt + \psi\Delta\theta \ln\left(1 + \frac{F(t)}{\psi\Delta\theta}\right) \tag{9.46}$$

This is the Green-Ampt equation for cumulative infiltration. The infiltration rate can be obtained by taking derivative

$$\frac{dF}{dt} = K + \frac{\psi\Delta\theta}{1 + \dfrac{F(t)}{\psi\Delta\theta}} \frac{1}{\psi\Delta\theta} \frac{dF}{dt} \tag{9.47}$$

Rearranging for f

$$f(t) = K\left(1 + \frac{\psi\Delta\theta}{F(t)}\right) \tag{9.48}$$

The Green-Ampt equation is a nonlinear equation in terms of cumulative infiltration, F. Given K, t, ψ, and $\nabla\theta$, a trial value of F is substituted into the LHS of the equation, a new value is computed and the cycle repeated until satisfactory convergence.

9.6.5 Measurement of Infiltration

Information about the infiltration characteristics of the soil at a given location can be obtained by conducting controlled experiments on small area through *infiltrometers*. There are two types: (i) Flooding type — simple- and ring-type infiltrometers and (ii) rainfall simulator. The ring infiltrometer is a simple device that is used to measure the infiltration capacity of a soil. An open cylindrical ring is forced a few centimeters into the soil and filled with water. By measuring the rate at which the level of ponded water decreases, one can obtain an estimate of the infiltration capacity as a function of time. Because of high spatial variability, several measurements must be taken to get a reasonable estimate of the infiltration capacity of a soil. Horton infiltration capacity experiments with ring infiltrometers show that as the water content in the soil increases, infiltration capacity decreases.

SOLVED EXAMPLES

Example 9.1: Compute infiltration rate f after 34 min of infiltration into a soil having suction head = 16.7 cm, K = 0.65 cm/hr, porosity = 60 percent, and initial moisture content = 16 percent.

Solution: Using Green-Ampt Eqn. (9.46) with data $\Delta\theta = 0.6 - .16 = 0.44$; ψ = 16.7 cm; K = 0.65 cm/h; and t = 34/60 hr, the cumulative infiltration depth $F = \dfrac{0.65 \times 34}{60} + 16.7 \times 0.44 \times \ln\left(1 + \dfrac{F}{16.7 \times 0.44}\right)$, solving it by trial-and-error method yields F = 2.579 cm, therefore the infiltration rate will be $f = K\left(1 + \dfrac{\psi\Delta\theta}{F}\right) = 0.65\left(1 + \dfrac{16.7 \times 0.44}{2.579}\right) = 2.502$ cm/hr.

Example 9.2: Determine the soil water diffusivity for a soil at $\theta = 0.15$ in which $\theta_r = 0.05$, $\eta = 0.32$, saturated hydraulic conductivity = 5 m/d, $\psi = \left[\frac{1}{50}\left(\frac{\eta}{\theta}-1\right)\right]^{1/3}$, and $K_\theta = K\left(\frac{\theta-\theta_r}{\eta-\theta_r}\right)^{3.5}$.

Solution: From the given data, $K_\theta = 5\times\left(\frac{\theta-0.05}{0.27}\right)^{3.5} = 5\times\left(\frac{0.15-0.05}{0.27}\right)^{3.5}$

$= 0.1546$ m/d and $\psi = \left[\frac{1}{50}\left(\frac{0.32}{\theta}-1\right)\right]^{1/3}$, therefore $\frac{\partial\psi}{\partial\theta} = \frac{1}{3}\left[\frac{1}{50}\left(\frac{0.32}{\theta}-1\right)\right]^{-2/3}$

$\left(-\frac{0.32}{\theta^2}\times\frac{1}{50}\right) = \frac{1}{3}\left[\frac{1}{50}\left(\frac{0.32}{0.15}-1\right)\right]^{-2/3}\left(-\frac{0.32}{0.15^2}\times\frac{1}{50}\right) = -1.18382$, therefore

Diffusivity $D = K\frac{\partial\psi}{\partial\theta} = 0.1546\times1.18382 = 0.183\ \mathrm{m^2/d}$.

Example 9.3: An infiltration test was conducted using a double-ring infiltrometer (inner ring diameter = 20 cm) with the volume of water added to maintain constant level in the infiltrometer during different time intervals as tabulated below.

Time (min)	1	2	3	4	5	5	5	6	9	10	10	10	10
Volume (ml)	100	140	140	120	100	80	80	90	95	120	120	120	120

Determine the infiltration capacity.

Solution: Infiltration rates have been worked out in Table 9.1 and resultant graph is plotted as Figure 9.16. The infiltration capacity is 22.918 mm/hr.

Table 9.1 *Infiltration calculation*

S. No	*Time interval (min)*	*Volume added (ml)*	*Cumulative time (min)*	*Infiltration rate (mmlhr)*
1	1	100	1	190.9859
2	2	140	3	133.6902
3	3	140	6	89.12677
4	4	120	10	57.29578
5	5	100	15	38.19719
6	5	80	20	30.55775
7	5	80	25	30.55775
8	5	80	30	30.55775
9	6	90	36	28.64789
10	9	95	45	20.15963
11	10	120	55	22.91831

(*Continued*)

Table 9.1 Continued

S. No	Time interval (min)	Volume added (ml)	Cumulative time (min)	Infiltration rate (mmlhr)
12	10	120	65	22.91831
13	10	120	75	22.91831
14	10	120	85	22.91831

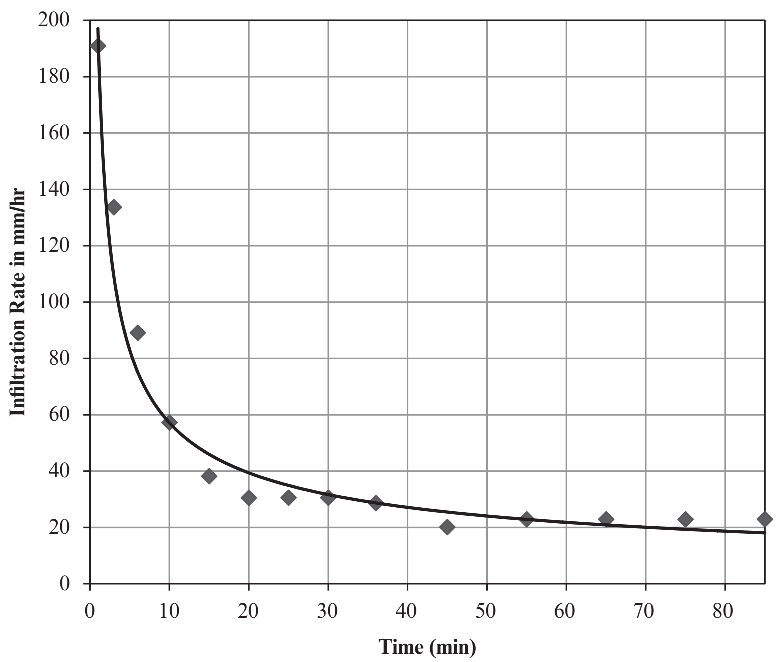

Figure 9.16 *Infiltration curve*

PROBLEMS

9.1. What are similarities and differences between governing equation for saturated and unsaturated media, explain?

9.2. Derive the governing flow equation for an unsaturated medium.

9.3. Derive Richards equation.

9.4. Write the continuity equation for a three-dimensional flow in an unsaturated medium.

9.5. Describe Green-Ampt infiltration model. Also derive its relation for the infiltration rate.

9.6. Using Darcy's law and continuity equation, derive Richards equation for unsteady flow through unsaturated porous media.

9.7. What is infiltration rate if ponding depth is 2 cm and rainfall rate is 40 cm/h, which lasted after 2 hour?

9.8. The porosity, water content, and residual water content in an unsaturated medium sample are 0.45, 0.25, and 0.05, respectively. Determine the effective porosity, degree of saturation, and effective degree of saturation.

9.9. Find the Horton's infiltration equation and cumulative infiltration at various times for the following data:

Time (h)	0.25	0.5	0.75	1.0	1.25	1.5	1.75	2.0
f (cm/h)	5.6	3.2	2.1	1.5	1.2	1.1	1.02	1.0

9.10. Determine cumulative infiltration and rate of infiltration at 0, 0.5, 1.0, 1.5, and 2.0 hr from Phillip's model using sorptivity $S = 5$ cm.h$^{-1/2}$ and hydraulic conductivity $K = 0.4$ cm/h.

9.11. Compute infiltration rate f and cumulative infiltration F after 1.352 hr of infiltration into a soil having suction head = 15 cm, hydraulic conductivity = 48 cm/d, porosity = 33 percent, and initial moisture content = 13 percent.

9.12. An infiltration test was conducted using a double ring infiltrometer (inner ring diameter = 20 cm) with the volume of water added to maintain constant level in the infiltrometer during different time intervals as tabulated below.

Time (min)	1	1	1	1	1	2	2	2	2	2	5	5	5
Vol. (ml)	100	80	60	50	40	80	70	60	60	50	120	120	110

Determine the infiltration capacity.

Chapter 10

GE in Radial Coordinates and Steady-State Solutions

10.1 General

Groundwater is the most important source of water for different purposes. Here, the main aim is to find and develop water supplies for the intended purpose. Wells form the most important mode of groundwater extraction from an aquifer. There are fundamentally two types of problems related to groundwater extraction from an aquifer. The first/forward problem involves prediction of the hydraulic head distribution in different scenarios, boundary conditions, and aquifer properties. The second/inverse problem comprises estimation of aquifer properties using observed values of hydraulic head and discharge. Well hydraulics deals both types of problems, but the study of well hydraulics is complicated. For every situation, such as the type of aquifer, the pattern of layering of aquifers, or the length of the screen in relation to the aquifer thickness, a different analytical solution is needed.

When a well is pumped, water is removed from the aquifer surrounding the well, and the water table or piezometric surface is lowered. The *drawdown* at a given point is the drop in the water table or piezometric surface elevation from its previous static level. A drawdown curve shows the variation of drawdown with distance from the well. In 3-D, the drawdown curve describes a conic shape known as the *cone of depression*. See Figure 10.1 for drawdown and cone of depression. In addition, the outer limit of the cone of depression defines the *area of influence* and its radial extent *radius of influence* of the well. Away from cone

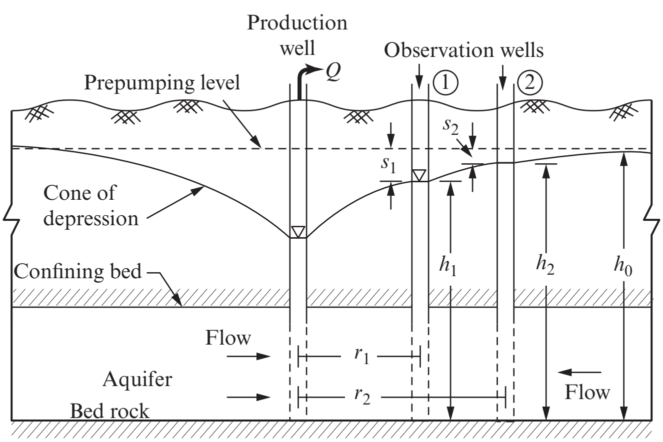

Figure 10.1 *Cone of depression due to pumping*

of depression or area of influence, drawdown caused by pumping is undetectable. The drawdown curve is steepest near the well; and farther away, it is flatter and beyond a certain distance (radius of influence), it is almost as flat as the original water table or piezometric surface. At constant rate of pumping, more water must be derived from the aquifer storage at greater distances leading to (i) expansion of cone of depression, (ii) increase in radius of influence, (iii) increment in drawdown at any point with the increase in the depth of the cone to provide the additional head required to move the water from greater distance, and (iv) more slow deepening and expansion of cone with time.

Initially, it is unsteady flow as the water table elevation at a given location near the well changes with time. On prolonged pumping, deepening or expansion of the cone during short intervals of pumping is barely visible, and it has been stablized, which may mislead that an equilibrium state (steady state) is reached, and the cone will not expand or deepen as pumping continues. Actually, the cone of depression continues to enlarge until the rate of pumping flow and the rate of inflow of groundwater into the aquifer from the recharge, leakage, or from outer edges of the zone of influence are balanced. Thus, the water discharged by a well under steady-state conditions comes from recharge or sources beyond the radius of influence, whereas the water discharged by a well under unsteady flow conditions comes from the aquifer storage within the radius of influence and sources beyond the radius of influence. After the pumping is stopped, the depleted storage in the cone of depression is replenished by groundwater inflow into the zone of influence called *recuperation* or *recovery* stage, which is an unsteady phenomenon. Recuperation time depends on the aquifer characteristics. In confined aquifers, the recovery takes place at a very rapid rate.

Prediction of well discharge is necessary for proper selection of the pump and power unit and of pumping depth. In some areas, it is possible to predict fairly accurately the performance of a new well based on the local experience. In other areas, the expected yield of the well must be calculated from the hydraulic properties of the aquifer. In the sections that follow, governing equations in radial coordinates have been derived, and these equations will subsequently be used for calculating well discharge for steady-state flow and for nonsteady or transient flow.

10.2 Governing Equations in Radial Coordinates

The shape of the cone of depression due to pumping of a well can be related by deriving a radial flow equation. To derive the radial flow equation, the groundwater flow is assumed to be two dimensional to a fully penetrating well. In such cases, the groundwater flow becomes *axisymmetric* about the well center. This means that the flow is independent of the angle θ in polar coordinates, and the head h is same along the perimeter of any circle concentric with the well. Such requirements are met only by a well centered on a circular island and fully penetrating a homogeneous and isotropic aquifer. If the complete penetration of the aquifer by the well is assumed, the flow is everywhere parallel to the bedrock and streamlines emanate symmetrically in all directions from the center of well.

For axisymmetric groundwater flow to wells, radial coordinates are preferred because the dimensional complexity is reduced by one degree, for example, 3-D flow reduces to 2-D and 2-D flow reduces to 1-D. Therefore, groundwater flow governing equations are usually dealt with in radial coordinates and not in Cartesian coordinates. Figure 10.2 shows plan of axisymmetric flow.

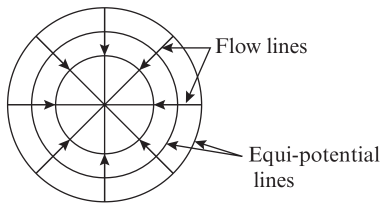

Figure 10.2 *Axisymmetrical flow*

10.2.1 Groundwater Flow in Confined Aquifer

Consider an isotropic-confined aquifer of uniform thickness b as shown in Figure 10.3.

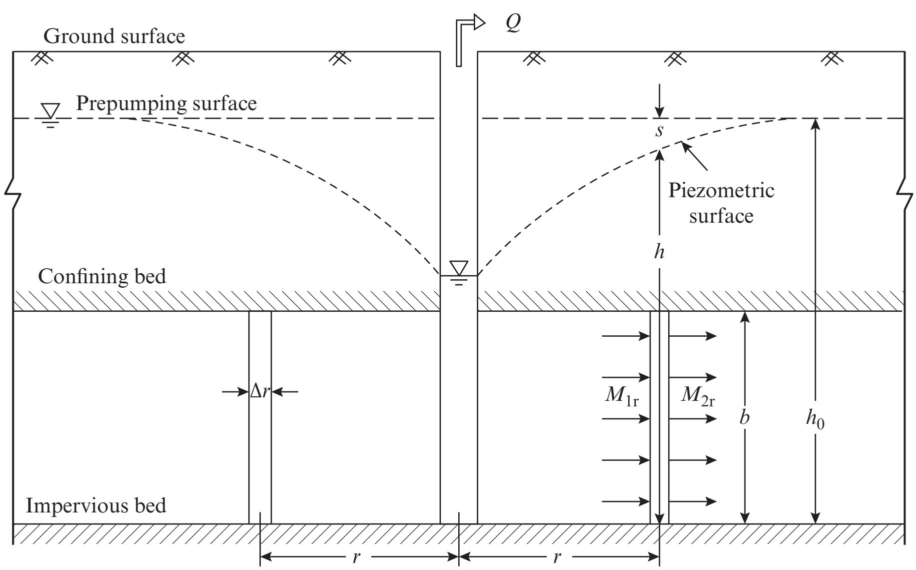

Figure 10.3 *Groundwater flow to fully penetrating well in confined aquifer*

Take representative elementary volume (REV) of annular cylindrical shape as shown in Figure 10.3, and let radius of median of annular space of thickness Δr is r. Also assume M_r to be the mass flux rate at the center of annular space in the outward direction, M_{1r} to be the mass flux rate at $r - \dfrac{\Delta r}{2}$, and M_{2r} to be the mass flux rate at a distance $r + \dfrac{\Delta r}{2}$ from the center of the cylinder. Therefore, by Taylor's series approximation,

$$M_{1r} = M_r - \frac{\partial M_r}{\partial r}\left(\frac{\Delta r}{2}\right) \tag{10.1}$$

and

$$M_{2r} = M_r + \frac{\partial M_r}{\partial r}\left(\frac{\Delta r}{2}\right) \tag{10.2}$$

Since M_{1r} is the inflow to annular space from the inner surface and M_{2r} is the outflow from annular space from the outer surface, therefore by applying mass balance (continuity equation) for the REV,

Inflow rate—outflow rate = rate of change in storage

$$M_{1r} - M_{2r} = \frac{\partial M}{\partial t} \tag{10.3}$$

$$M_r - \frac{\partial M_r}{\partial r}\left(\frac{\Delta r}{2}\right) - M_r - \frac{\partial M_r}{\partial r}\left(\frac{\Delta r}{2}\right) = \frac{\partial M}{\partial t} \tag{10.4}$$

$$-\frac{\partial M_r}{\partial r}\Delta r = \frac{\partial M}{\partial t} \tag{10.5}$$

The initial mass in storage of REV:

$$M = \rho_w \eta 2\pi r b \Delta r = \rho_w 2\pi r S h \Delta r \tag{10.6}$$

and mass flux rate at center of annular space in the outward direction:

$$M_r = \rho_w \upsilon_r A = \rho_w 2\pi r b \upsilon_r \tag{10.7}$$

where ρ_w is the mass density of water and S is the storage coefficient which is the property of aquifer.

$$-\frac{\partial}{\partial r}\left(\rho_w 2\pi r b v_r\right)\Delta r = \frac{\partial}{\partial t}\left(\rho_w 2\pi r S h \Delta r\right) \tag{10.8}$$

Using momentum equation, i.e. Darcy's law or $v_r = -K_r \dfrac{\partial h}{\partial r}$ and simplifying

$$\frac{\partial}{\partial r}\left(\rho_w r b K_r \frac{\partial h}{\partial r}\right) = \frac{\partial}{\partial t}\left(\rho_w S r h\right) \tag{10.9}$$

where K_r is the hydraulic conductivity at radial distance r. If the flow is incompressible, ρ_w is independent of space and time (may be put outside from differential operators). Therefore,

$$\frac{\partial}{\partial r}\left(r b K_r \frac{\partial h}{\partial r}\right) = S r \frac{\partial h}{\partial t} \tag{10.10}$$

As $K_r.b = T_r$ (transmissivity of aquifer), the Eqn (10.10) becomes

$$\frac{1}{r}\cdot\frac{\partial}{\partial r}\left(rT_{\mathrm{r}}\frac{\partial h}{\partial r}\right)=S\frac{\partial h}{\partial \mathrm{t}} \tag{10.11}$$

This is the general governing equation of confined aquifer when flow is incompressible. If the medium is homogeneous and isotropic, transmissivity is not the function of r, and it will come out from differential operator and thus,

$$\frac{1}{r}\cdot\frac{\partial}{\partial r}\left(r\frac{\partial h}{\partial r}\right)=\frac{S}{T}\frac{\partial h}{\partial \mathrm{t}} \tag{10.12}$$

Expanding RHS,

$$\frac{\partial^2 h}{\partial r^2}+\frac{1}{r}\frac{\partial h}{\partial r}=\frac{S}{T}\frac{\partial h}{\partial t} \tag{10.13}$$

This is the governing equation of groundwater flow in homogeneous and isotropic confined aquifer.

10.2.2 Groundwater Flow in Unconfined Aquifer

Consider a representative elementary volume of annular cylindrical shape at radial distance r in an isotropic unconfined aquifer as shown in Figure 10.4, and let R be recharge rate per unit area and h be height of water table at r. The thickness of annular space and mass fluxes are similar to the confined aquifer case. The mass balance in this case results as follows:

$$\rho_{\mathrm{w}}\,R\,2\pi\,r\Delta r-\frac{\partial M_{\mathrm{r}}}{\partial r}.\Delta r=\frac{\partial M}{\partial t} \tag{10.14}$$

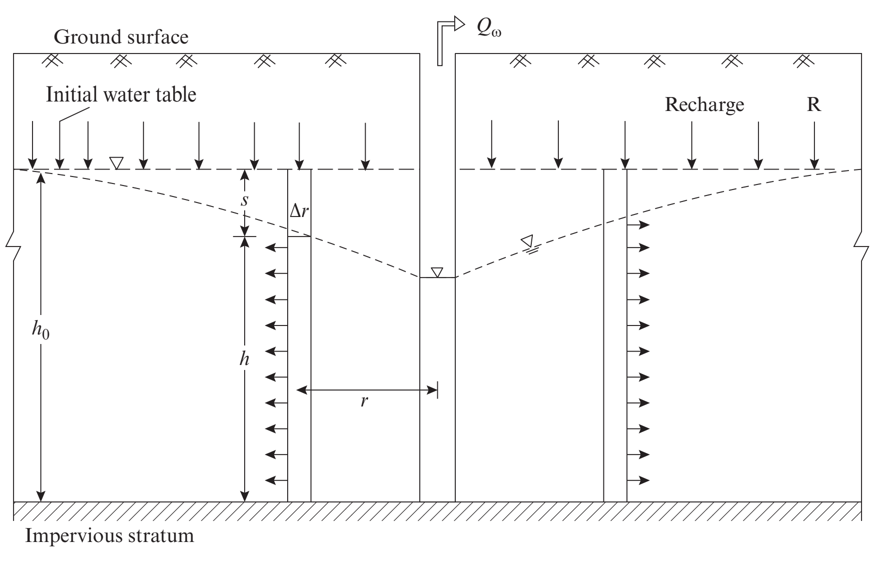

Figure 10.4 *Groundwater flow to fully penetrating well in unconfined aquifer*

Here, the reckoning of M_r is not straightforward. We need Duipit–Forchhemeir assumptions for this purpose, that is, the radial velocity v_r is horizontal and uniform throughout the height h and also hydraulic gradient is proportional to tangent, therefore

$$M_r = \rho_w 2\pi r h v_r = -\rho_w 2\pi r h K_r \frac{\partial h}{\partial r} \tag{10.15}$$

Using M_r from Eqn. (10.15) and M from definitions of storage coefficient, we obtain

$$R.\rho_w 2\pi r\Delta r + \frac{\partial}{\partial r}\left(\rho_w 2\pi rhK_r \frac{\partial h}{\partial r}\right)\Delta r = \frac{\partial}{\partial t}\left(\rho_w S.2\pi r\Delta r.h\right) \tag{10.16}$$

For incompressible flow,

$$Rr + \frac{\partial}{\partial r}\left(K_r hr\frac{\partial h}{\partial r}\right) = Sr\frac{\partial h}{\partial t} \tag{10.17}$$

which reduces to

$$\frac{1}{r}.\frac{\partial}{\partial r}\left(K_r r\frac{\partial h^2}{\partial r}\right) + 2R = 2S\frac{\partial h}{\partial t} \tag{10.18}$$

This is the general governing equation for incompressible flow of groundwater in inhomogeneous unconfined aquifer. For homogeneous medium, Eqn. (10.18) becomes

$$\frac{1}{r}.\frac{\partial}{\partial r}\left(r\frac{\partial h^2}{\partial r}\right) + \frac{2R}{K} = \frac{2S}{K}\frac{\partial h}{\partial t} \tag{10.19}$$

This is Boussinesq's equation in radial coordinates, which can also be rewritten as follows:

$$\frac{\partial^2 h^2}{\partial r^2} + \frac{1}{r}.\frac{\partial h^2}{\partial r} + \frac{2R}{K} = \frac{2S}{K}\frac{\partial h}{\partial t} \tag{10.20}$$

10.3 Steady-Flow Solutions

The equations derived above will be applied subsequently to obtain analytic solutions to particular groundwater flow problems. For solution to any problem, idealization of the aquifer and of the boundary conditions of the flow system is necessary. This idealization and simple boundary conditions make it possible to solve analytically without the use of mathematical techniques such as separation of variables, transforms, Green's functions, and conformal mapping. Results may only approximate field conditions; nevertheless, known deviations from assumptions frequently allow analytic solutions to be modified to obtain an answer that otherwise would not have been possible. Common assumptions regarding the aquifer are that it is homogeneous and isotropic. Often aquifers can be assumed to be infinite in areal extent; if not, boundaries are assumed to be (i) impermeable, such as underlying or overlying rock or clay layers, dikes, faults, or valley walls; or (ii) permeable, including surface water bodies in contact with the aquifer, ground surfaces where water emerges from underground and wells. Steady-state groundwater problems are relatively simpler. The steady state is an equilibrium condition whereby no changes occur with time. It seldom occurs in practice, but it may be approached after prolonged pumping of a well when piezometric surfaces or water tables decline at very slow rates. Expressions for steady-state radial flow into a well under confined and unconfined aquifer conditions are derived in the subsequent sections.

10.3.1 Steady Radial Flow to a Well in Confined Aquifer

It is assumed that

(i) aquifer is homogeneous and isotropic
(ii) aquifer is of uniform thickness and bedrock is horizontal
(iii) aquifer is of infinite areal extent, having no lateral inflow from surrounding water bodies,
(iv) well penetrates the entire aquifer, and its diameter is small
(v) well is pumped at constant rate Q, and the entire discharge is provided by the release of stored water and the water is instantaneously removed from the well
(vi) initially, the piezometric surface is horizontal

The radial flow to a fully penetrating well in a homogeneous and isotropic confined aquifer is everywhere horizontal; hence, the Dupuit's assumptions are not required. Using radial coordinates with the well as the origin, for steady radial flow Q to a well in homogeneous and isotropic confined aquifer, the governing equation (Eqn. 10.12) reduces to

$$\frac{1}{r}\cdot\frac{\partial}{\partial r}\left(r\frac{\partial h}{\partial r}\right)=0 \quad \Rightarrow \quad \frac{\partial}{\partial r}\left(r\frac{\partial h}{\partial r}\right)=0 \tag{10.21}$$

Here, h is a function of single variable r, the partial derivative can be replaced by total derivative, and hence

$$\frac{d}{dr}\left(r\frac{dh}{dr}\right)=0 \tag{10.22}$$

Integration leads to

$$r\frac{dh}{dr}=C_1 \tag{10.23}$$

And further integration yields

$$h=C_1\ln r+C_2 \tag{10.24}$$

From Darcy law, the well discharge at any distance r equals

$$-Q=A_r v_r=2\pi rb(-)K\frac{dh}{dr}\Rightarrow r\frac{dh}{dr}=\frac{Q}{2\pi bK} \tag{10.25}$$

Therefore, $C_1=Q/(2\pi bK)$. The constant C_2 is determined by one more condition at which h is known at any radial distance r. This may be one observation well or the pumped well itself or the radius of influence r_e. At $r=r_e$, $h=h_0$. Therefore,

$$h_0 = C_1 \ln r_e + C_2 \;\Rightarrow\; C_2 = h_0 - C_1 \ln r_e \tag{10.26}$$

Substituting C_1 and C_2 in Eqn. (10.24),

$$h = h_0 + \frac{Q}{2\pi Kb} \ln \frac{r}{r_e} \tag{10.27}$$

or

$$h = \frac{Q}{2\pi Kb} \ln r + \text{constant} \tag{10.28}$$

which shows that h varies logarithmically with r, and it increases indefinitely with increasing r. For extensive natural aquifers, values of r can be very large, but values of h are relatively small and are commonly limited by the elevation at which recharge enters the system. Therefore, from a practical standpoint, h approaches h_0 with distance from the well as the maximum h is the initial uniform head h_0. Thus, from a theoretical aspect steady radial flow in an extensive aquifer does not exist because the cone of depression must expand indefinitely with time. Equation (10.27) requires the concept of cylindrical boundaries at constant head, coaxial with the well, and at a distance r_e, but the form in Eqn. (10.28) avoids this requirement. The radius r_e is difficult to estimate as it is the vertical projection of a cylinder at constant head not affected by the pumping of the well. Consequently, Eqn. (10.28) is applicable only within reasonable distances from a well because the steady radial flow to a well is achieved only near the well and steady radial flow in infinite laterally extended aquifers is both theoretically and physically impossible.

From a practical standpoint, the drawdown s ($= h_0 – h$) rather than the head h is measured. In well problems, we are more interested in the drawdown than in absolute value of h, and in confined aquifer no special attention to the choice of the datum plane for elevation is required. Eqn. (10.27) can be written as follows:

$$h - h_o = \frac{Q}{2\pi bK} \ln\left(\frac{r}{r_e}\right) \;\Rightarrow\; h_o - h = \frac{Q}{2\pi bK} \ln\left(\frac{r_e}{r}\right) \tag{10.29}$$

or

$$s = \frac{Q}{2\pi bK} \ln\left(\frac{r_e}{r}\right) \tag{10.30}$$

Thus, the drawdown also varies with the logarithm of the distance from the well. Because any two points define the logarithmic drawdown curve, the method consists of measuring drawdowns in two observation wells at different distances from a well pumped at a constant rate (see Figure 10.5). Let in the first observation well at $r = r_1$, $h = h_1$ (or $s = s_1$), then from Eqn. (10.27) or Eqn. (10.30),

$$h_1 = h_0 + \frac{Q}{2\pi Kb} \ln \frac{r_1}{r_e} \quad \text{or} \quad s_1 = \frac{Q}{2\pi Kb} \ln \frac{r_e}{r_1} \tag{10.31}$$

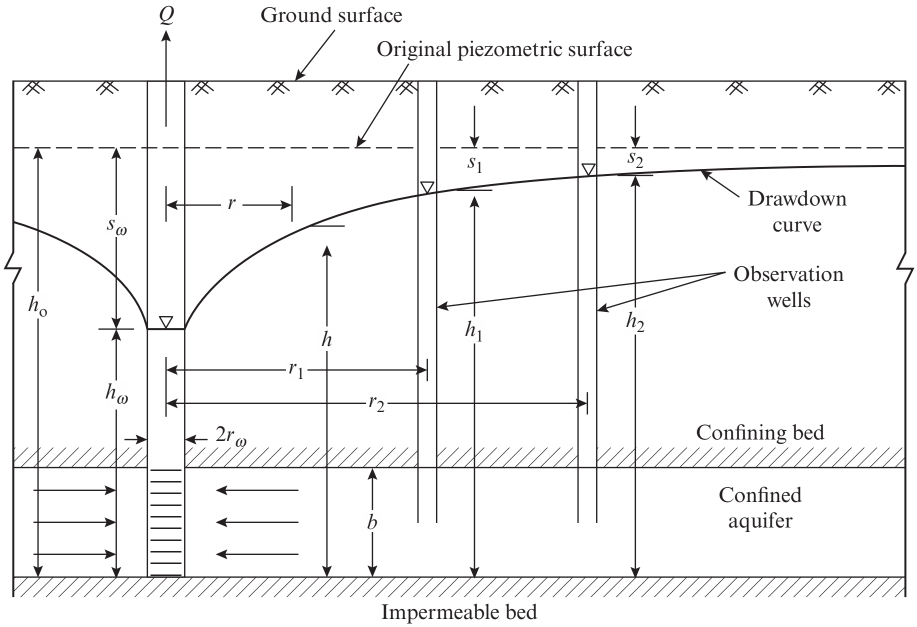

Figure 10.5 *Groundwater flow to fully penetrating well in confined aquifer*

Similarly, for the second observation well at $r = r_2$, $h = h_2$ (or $s = s_2$)

$$h_2 = h_0 + \frac{Q}{2\pi Kb}\ln\frac{r_2}{r_e} \text{ or } \quad s_2 = \frac{Q}{2\pi Kb}\ln\frac{r_e}{r_2} \tag{10.32}$$

Subtracting Eqn. (10.31) from Eqn. (10.32) gives relationship in terms of drawdowns/piezometric heads at two points as follows:

$$h_2 - h_1 = s_1 - s_2 = \frac{Q}{2\pi Kb}\ln\frac{r_2}{r_1} \tag{10.33}$$

To determine Q, the relation may be used as follows:

$$Q = 2\pi bK\frac{h_2 - h_1}{\ln(r_2/r_1)} = 2\pi bK\frac{s_1 - s_2}{\ln(r_2/r_1)} \tag{10.34}$$

and for the transmissivity, it corresponds to

$$T = Kb = \frac{Q}{2\pi(h_2 - h_1)}\ln(r_2/r_1) = \frac{Q}{2\pi(s_1 - s_2)}\ln(r_2/r_1) \tag{10.35}$$

This solution Eqn. (10.33), Eqn. (10.34), or Eqn. (10.35) is known as the *equilibrium* or *Thiem's equation*. It enables for the computation of steady discharge Q, hydraulic conductivity K, or transmissivity T, given one or the other, if values of h or s are measured in two observation wells. One of these two wells may be the well that is actually pumped. If the head or drawdown in the pumped well is h_w or s_w, then replace h_2 or s_2 by h_w or s_w and r_2 by the radius of the pumped well r_w in Thiem's equation to compute appropriate quantity. However, this should be used selectively only when other methods of analysis are not available because local hydraulic conditions in and near the well strongly influence the values of r_w, h_w, or s_w. It is difficult to define the radius of a well. Depending on the type of material comprising the aquifer formation, the well may be left as an uncased hole, or it may have a screen of various types with or without gravel pack. The well may be developed for enhancing its yield with different techniques. The increased transmissivity in the vicinity of a well reduces the drawdown and alters effective well radius. In addition, there are head losses due to change in velocity when water enters into well from the aquifer. Therefore, two observation wells should be used, close enough to the pumped well to have significant drawdowns that are easy to measure accurately.

10.3.2 Steady Radial Flow to a Well in Unconfined Aquifer

Figure 10.6 shows a fully penetrating well in an unconfined aquifer. Assumptions similar to confined aquifer are applicable for steady radial flow to a well in unconfined aquifer, but additional Dupuit–Forchhmeir assumptions are also required. The well completely penetrates to the horizontal base, and a concentric boundary of constant head surrounds the well. Using radial coordinates with the well as the origin, for steady radial flow without recharge (R = 0) in homogeneous and isotropic unconfined aquifer, the governing equation (Eqn. 10.19) reduces to

$$\frac{1}{r}\cdot\frac{\partial}{\partial r}\left(r\frac{\partial h^2}{\partial r}\right) = 0 \quad \Rightarrow \quad \frac{\partial}{\partial r}\left(r\frac{\partial h^2}{\partial r}\right) = 0 \tag{10.36}$$

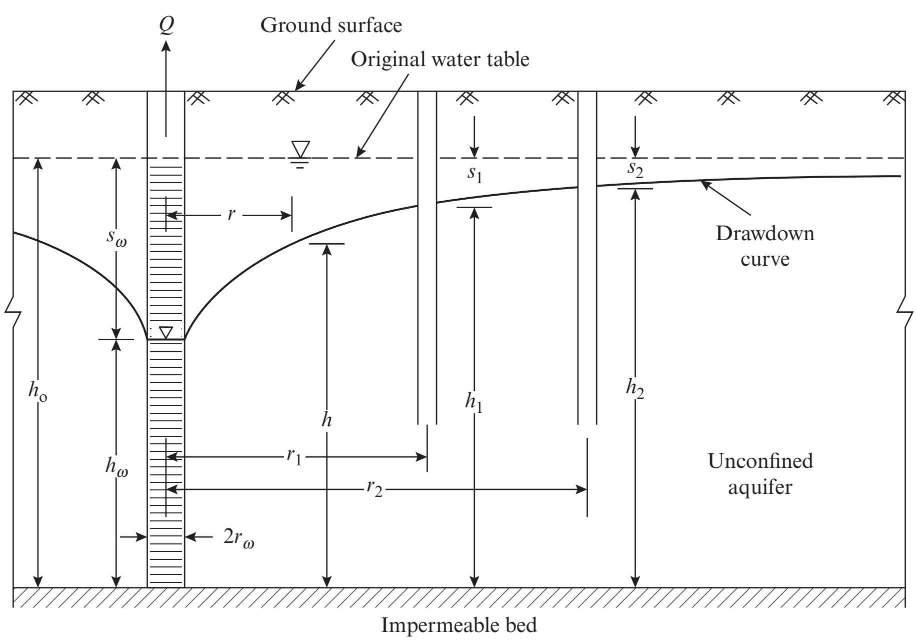

Figure 10.6 *Groundwater flow to fully penetrating well in unconfined aquifer*

In this case also h is a function of single variable r; the partial derivative can be replaced by total derivative, and hence

$$\frac{d}{dr}\left(r\frac{dh^2}{dr} \right) = 0 \tag{10.37}$$

Integrating successively leads to

$$r\frac{dh^2}{dr} = C_1 \tag{10.38}$$

and

$$h^2 = C_1 \ln r + C_2 \tag{10.39}$$

From Dupuit–Forchhmeir assumptions and Darcy law, the well discharge at any distance r equals

$$-Q = A_r v_r = 2\pi rh(-)K\frac{dh}{dr} \Rightarrow \ hr\frac{dh}{dr} = \frac{Q}{2\pi K} \Rightarrow \ r\frac{dh^2}{dr} = \frac{Q}{\pi K} \tag{10.40}$$

Therefore, $C_1 = Q/(\pi K)$. Similar to confined case, the constant C_2 can be determined by one more condition at which h is known at any radial distance r. Condition, when $r = r_e, \Rightarrow h = h_o$ yields

$$h_0^2 = C_1 \ln r_e + C_2 \ \Rightarrow \ C_2 = h_0^2 - C_1 \ln r_e \tag{10.41}$$

Using values of C_1 and C_2 in Eqn. (10.39),

$$h^2 = h_0^2 + \frac{Q}{\pi K}\ln\left(\frac{r}{r_e}\right) \tag{10.42}$$

or

$$h^2 = \frac{Q}{\pi K}\ln r + \text{constant} \tag{10.43}$$

Thus, the cone of depression must expand indefinitely with time, and hence a steady radial flow in an unconfined aquifer without recharge cannot establish in true sense. Eqn. (10.42) fails to describe accurately the drawdown curve near the well because the strong curvatures of the water table or the large vertical flow components contradict the Dupuit's assumptions. Also, this equation does not consider the existence of a seepage face above the water level in the well. The water level inside a pumped well h_w is always less than the height of water table adjacent to the well, even if head losses due to entry of water into the well are ignored (with head losses, it will be more less). This is because of development of a seepage face along the well perimeter where water moves out of the saturated material and then flows down along the saturated well perimeter face to the free water surface inside the well. Hall (1955) proposed the following equation for the height of seepage face h_{sf} (ignoring well losses):

$$h_{sf} = \frac{(h_2 - h_w)\left[1 - (h_w / h_2)^{2.4}\right]}{(1 + 5\mathrm{r}_w / h_2)\left[1 + 0.02\ln(\mathrm{r}_2 / \mathrm{r}_w)\right]} \tag{10.43b}$$

where h_2 at $r_2 = 500\ r_w$.

Because of the seepage face at the well and the occurrence of vertical flow components in the vicinity of the well, Eqn. (10.43) does not yield an accurate prediction of the water table height near the well. However, for $r > 1.5h_0$, the effects of the seepage face and vertical flow become negligible, therefore results based on the Dupuit's assumptions are accurate enough. In practice, drawdowns should be small in relation to the saturated thickness of the unconfined aquifer. In terms of drawdown,

$$h_0^2 - h^2 = \frac{Q}{\pi K}\ln\left(\frac{r_e}{r}\right) \Rightarrow (h_0 - h).(h_0 + h) = \frac{Q}{\pi K}\ln\left(\frac{r_e}{r}\right) \tag{10.44}$$

or

$$s(2h_0 - s) = \frac{Q}{\pi K}\ln\left(\frac{r_e}{r}\right) \tag{10.45}$$

If there are two observation wells ($r = r_1$, $h = h_1$; and $r = r_2$, $h = h_2$), then from Eqn. (10.42),

$$h_1^2 - h_0^2 = \frac{Q}{\pi K}\ln\left(\frac{r_1}{r_e}\right) \tag{10.46}$$

and

$$h_2^2 - h_0^2 = \frac{Q}{\pi K}\ln\left(\frac{r_2}{r_e}\right) \tag{10.47}$$

Therefore,

$$h_1^2 - h_2^2 = \frac{Q}{\pi K}\ln\left(\frac{r_1}{r_2}\right) \tag{10.48}$$

In terms of drawdown, the above equation can be written as follows:

$$(h_1 - h_2)(h_1 + h_2) = \frac{Q}{\pi K}\ln\left(\frac{r_1}{r_2}\right) \tag{10.49}$$

$$(s_2 - s_1)(2h_0 - s_1 - s_2) = \frac{Q}{\pi K}\ln\left(\frac{r_1}{r_2}\right) \tag{10.50}$$

Eqn. (10.48) or Eqn. (10.50) may be used to determine Q as follows:

$$Q = \pi K\frac{h_2^2 - h_1^2}{\ln(r_2 / r_1)} = \pi K\frac{(s_1 - s_2)(2h_0 - s_1 - s_2)}{\ln(r_2 / r_1)} \tag{10.51}$$

The transmissivity can be approximated with respect to average saturated thickness between two points, therefore

$$T = K\frac{h_1 + h_2}{2} = \frac{Q}{2\pi(h_2 - h_1)}\ln(r_2 / r_1) = \frac{Q}{2\pi(s_1 - s_2)}\ln(r_2 / r_1) \tag{10.52}$$

This equation is identical to Thiem's equation for confined aquifer. This means a steady discharge from well in an unconfined aquifer can be dealt with similar to confined aquifer case, provided the average transmissivity condition is adopted.

This is valid for a thick aquifer and small drawdown ($s << ho$). However, the unconfined aquifer transmissivity is generally defined based on the initial saturated thickness, that is, $T = Kh_0$, then rewriting Eqn. (10.48) as follows:

$$\left(s_2 - \frac{s_2^2}{2h_0}\right) - \left(s_1 - \frac{s_1^2}{2h_0}\right) = \frac{Q}{2\pi K h_0} \ln\left(\frac{r_1}{r_2}\right) \tag{10.53}$$

or

$$s'_1 - s'_2 = \frac{Q}{2\pi T} \ln\left(\frac{r_2}{r_1}\right) \tag{10.54}$$

where

$$s' = s - \frac{s^2}{2h_0} \tag{10.55}$$

This is called the *corrected drawdown*, which is the drawdown that would occur in an equivalent confined aquifer. It may be noted that an unconfined aquifer produces more drawdown than the equivalent confined aquifer. Thus, the observed drawdowns in an unconfined aquifer can be corrected using Eqn. (10.55), and then the unconfined aquifer converts into an equivalent confined aquifer. Hence the equilibrium, Theim, or other equations for the confined aquifer are applicable in terms of corrected drawdown.

10.3.3 Steady Radial Flow to a Well in Unconfined Aquifer with Uniform Recharge

This case is similar to the previous case of unconfined aquifer except uniform recharge. The recharge may be from rainfall, excess irrigation, or other surface water sources. All assumptions made in unconfined aquifer case are needed to get analytical solution for the present case. Using radial coordinates with the well as the origin, for steady radial flow in a fully penetrating well with recharge in homogeneous and isotropic unconfined aquifer, the governing equation (Eqn. 10.19) reduces to

$$\frac{1}{r} \cdot \frac{\partial}{\partial r}\left(r \frac{\partial h^2}{\partial r}\right) + \frac{2R}{K} = 0 \quad \text{or} \quad \frac{d}{dr}\left(r \frac{dh^2}{dr}\right) + \frac{2R}{K} r = 0 \tag{10.56}$$

Integrating it,

$$r \frac{dh^2}{dr} = -\frac{Rr^2}{K} + C_1 \tag{10.57}$$

or

$$\frac{dh^2}{dr} = -\frac{Rr}{K} + \frac{C_1}{r} \tag{10.58}$$

Integrating once more,

$$h^2 = -\frac{Rr^2}{2K} + C_1 \ln r + C_2 \tag{10.59}$$

At $r = r_e$; $h = h_o$, therefore

$$h_o^2 = -\frac{Rr_e^2}{2K} + C_1 \ln r_e + C_2 \tag{10.60}$$

and hence

$$C_2 = h_o^2 + \frac{Rr_e^2}{2K} - C_1 \ln r_e \tag{10.61}$$

For C_1 let us consider continuity equation for a cylinder of radius r

$$Q_w = Q + \pi r^2 R \tag{10.62}$$

where Q_w is well discharge (outflow), Q is inflow from cylindrical surface $2\pi rh$ $(= 2\pi rhK \frac{dh}{dr}$ from Darcy's law), and $\pi r^2 R$ is recharge (inflow) from the top surface. Therefore,

$$Q_w = 2\pi rhK \frac{dh}{dr} + \pi r^2 R \tag{10.63}$$

or

$$2rh\frac{dh}{dr} + \frac{Rr^2}{K} = \frac{Q_w}{\pi K} \tag{10.64}$$

Comparing Eqs (10.57) and (10.64),

$$C_1 = \frac{Q_w}{\pi K} \tag{10.65}$$

Plugging C_1 and C_2 in Eqn. (10.59) results to

$$h^2 = h_0^2 + \frac{Q_w}{\pi K}\ln r - \frac{Q_w}{\pi K}\ln r_e + \frac{Rr_e^2}{2K} - \frac{Rr^2}{2K} \tag{10.66}$$

or

$$h^2 = h_o^2 + \frac{R\left(r_e^2 - r^2\right)}{2K} - \frac{Q_w}{\pi K}\ln\frac{r_e}{r} \tag{10.67}$$

Eqn. (10.67) represents the shape of the piezometric surface corresponding to steady flow to a well in unconfined aquifer receiving uniform recharge. In this case, true steady-state condition is possible as at a particular radial distance, the well discharge is completely compensated by the recharge, and hence the cone of depression cannot extend beyond this distance (radius of influence) and acquires steady position. Under this condition,

$$Q_w = \pi r_e^2 . R \tag{10.68}$$

Therefore,

$$r_e = \sqrt{Q_w / \pi R} \tag{10.69}$$

This means the radius of influence is a function of the well discharge and recharge rate only. Combining Eqs (10.67) and (10.69), we obtain

$$h^2 = h_o^2 + \frac{Q_w - \pi r^2 R}{2\pi K} - \frac{Q_w}{2\pi K} \ln \frac{Q_w}{\pi r^2 R} \tag{10.70}$$

10.3.4 Steady Discharge from Several Wells in an Aquifer

The equations derived in the previous sections can be converted into Cartesian coordinate system, for example, when the center of the well is located at the point (x_w, y_w), then

$$r = \sqrt{(x - x_w)^2 + (y - y_w)^2} \tag{10.71}$$

Therefore, Eqn. (10.28) for confined aquifer in Cartesian coordinate system becomes

$$h = \frac{Q}{4\pi T} \ln\left\{(x - x_w)^2 + (y - y_w)^2\right\} + \text{constant} \tag{10.72}$$

and Eqn. (10.43) for unconfined aquifer becomes

$$h^2 = \frac{Q}{2\pi K} \ln\left\{(x - x_w)^2 + (y - y_w)^2\right\} + \text{constant} \tag{10.73}$$

When multiple wells are present in an aquifer, and they are spaced at distances smaller than their radius of influence, they affect each other's drawdown and discharge rate as shown in Figure 10.7.

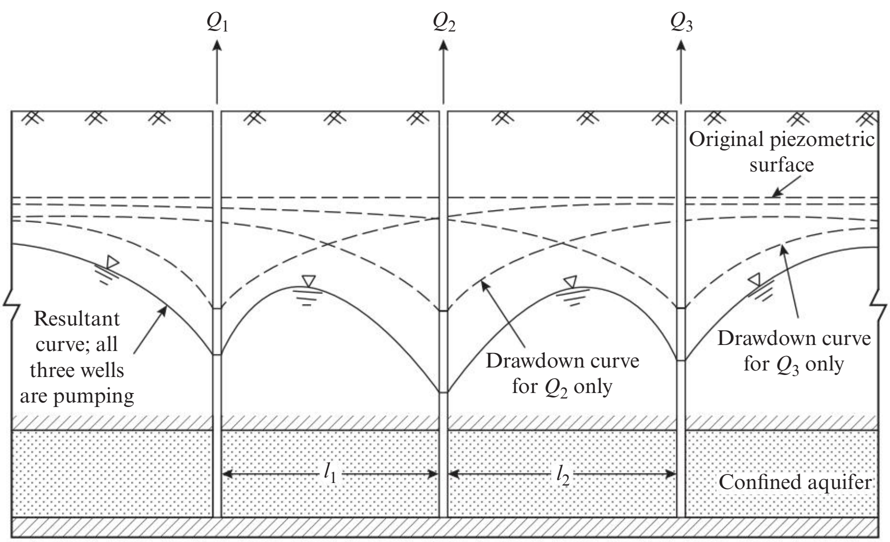

Figure 10.7 *Multiple wells in a confined aquifer*

The governing equations for steady flow both in confined and unconfined aquifers are Laplace type. As Laplace operator is a linear operator, superposition of solutions is applicable. Because of linearity of the Laplace operator, for several wells we can have

$$\nabla^2 h = \nabla^2 (h_1 + h_2 + h_3 + ..) = \nabla^2 h_1 + \nabla^2 h_2 + \nabla^2 h_3 + .. = 0 \tag{10.74}$$

where h is the resultant head due to several well and h_1, h_2, h_3, etc., are contributions from individual wells toward the resultant head. Therefore, the Laplace (governing) equation for individual wells can be solved separately, and then these values can be superimposed to get the final resultant head. Thus, for confined aquifer in case of multiple wells

$$h = \sum_{i=1}^{n} \frac{Q_i}{2\pi T_i} \ln r_i + \text{Constant} \tag{10.75}$$

For same homogeneous aquifer, $T_1 = T_2 = ... = T_i = T$, therefore

$$h = \frac{1}{2\pi T} \sum_{i=1}^{n} Q_i \ln r_i + \text{Constant} \tag{10.76}$$

Similarly, for unconfined aquifer

$$h^2 = \sum_{i=1}^{n} \frac{Q_i}{\pi K_i} \ln r_i + \text{Constant} \tag{10.77}$$

Eqn. (10.76) and Eqn. (10.77) in terms of Cartesian coordinates are

$$h = \frac{1}{4\pi T} \sum_{i=1}^{n} Q_i \ln\left[(x - x_{wi})^2 + (y - y_{wi})^2\right] + \text{Constant} \tag{10.78}$$

and

$$h^2 = \frac{1}{2\pi K} \sum_{i=1}^{n} Q_i \ln\left[(x - x_{wi})^2 + (y - y_{wi})^2\right] + \text{Constant} \tag{10.79}$$

10.3.5 Well in a Uniform Flow Field

Thus far, we have assumed that initially water table or piezometric surface is horizontal. If the water table or piezometric surface is not horizontal but has some slope, then groundwater will move with uniform velocity due to existing hydraulic gradient, and hence called *uniform flow field*. If a well is established in an aquifer having sloping/inclined water table (or piezometric surface) or uniform flow field and pumped, then

1. there is uniform flow because of hydraulic gradient due to sloping/inclined water table or piezometric surface.
2. there is radial flow toward well because of pumping.

These two effects can be considered by the method of superposition to get solution for steady-state discharge from a well in a uniform flow field.

Uniform flow

Consider a homogeneous and isotropic confined aquifer in which the initial piezometric surface is inclined. The inclined piezometric surface provides a hydraulic gradient, which leads to movement of groundwater. Align x-axis along the direction of the hydraulic gradient and y-axis normal to it in the horizontal plane (refer Figure 10.8). Thus, the uniform groundwater flow is 1-D (in x direction only). Therefore, from Darcy's law,

$$v_x = -Ki \text{ and } v_y = 0 \tag{10.80}$$

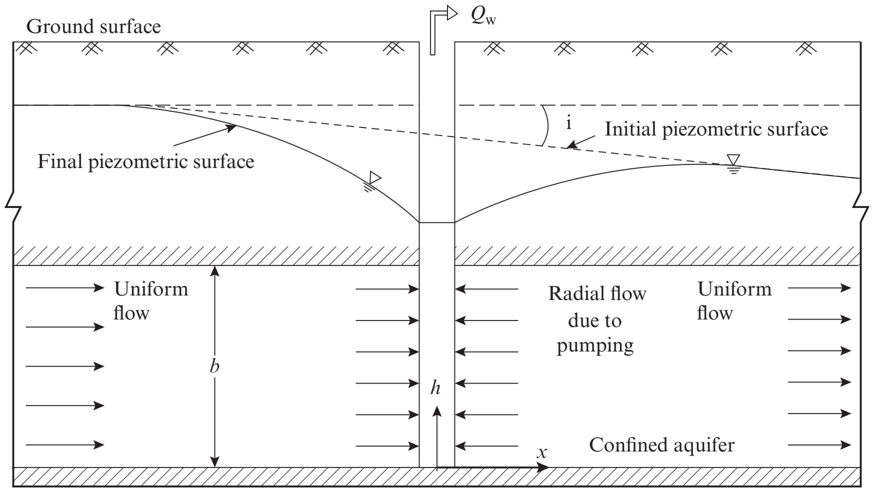

Figure 10.8 *Well in uniform flow field*

$$v_x = \frac{\partial \phi}{\partial x} = -Ki \quad \text{or} \quad \phi = -Kix + C_1 \tag{10.81}$$

and

$$v_x = \frac{\partial \psi}{\partial y} = -Ki \quad \text{or} \quad \psi = -Kiy + C_2 \tag{10.82}$$

As $\phi = -Kh + C$, Eqn. (10.81) gives

$$h = ix + C_3 \tag{10.83}$$

Eqn. (10.81) and Eqn. (10.83) show that the variation in velocity potential or head is linear in x-direction and stream lines vary linearly in y-direction as depicted in Figure 10.9.

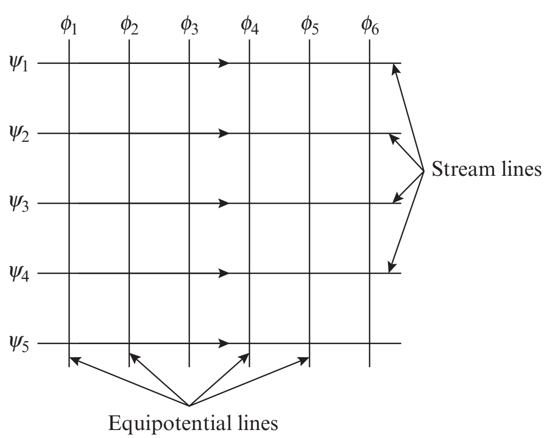

Figure 10.9 *Flownet for uniform flow*

Well Flow

At any radial distance r, the steady discharge Q from a well in confined aquifer of thickness b is

$$Q = -2\pi r b v_{\mathrm{r}} \quad \text{or} \quad v_{\mathrm{r}} = \frac{-Q}{2\pi r b} \tag{10.84}$$

where v_r is the radial velocity of groundwater toward well at distance r from the center of the well. Refer Figure 10.10 for writing Cauchy–Riemann conditions in radial coordinates. Since $\Delta y = r d\theta$ and $\Delta x = \Delta r$, it follows

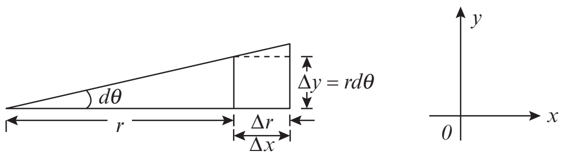

Figure 10.10 *Cartesian to radial coordinate system*

$$\frac{\partial \phi}{\partial r} = \frac{\partial \psi}{r \partial \theta} = v_{\mathrm{r}} \tag{10.85}$$

and

$$\frac{\partial \phi}{r \partial \theta} = -\frac{\partial \psi}{\partial r} = v_{\theta} \tag{10.86}$$

From Eqn. (10.84) and Eqn. (10.85),

$$\frac{\partial \phi}{\partial r} = \frac{-Q}{2\pi r b} \quad \text{or} \quad \phi = \frac{-Q}{2\pi b} \ln r + C_3 \tag{10.87}$$

Therefore, the velocity potential varies logarithmically as concentric circles around the well as shown dotted in Figure 10.11. From Eqn. (10.84) and Eqn. (10.86),

$$v_{\mathrm{r}} = \frac{\partial \psi}{r \partial \theta} = \frac{-Q}{2\pi r b} \quad \text{or} \quad \psi = \frac{-Q}{2\pi b} \theta + C_4 \tag{10.88}$$

This shows that streamlines vary linearly with θ. Figure 10.11 represents equipotential and streamlines for well flow.

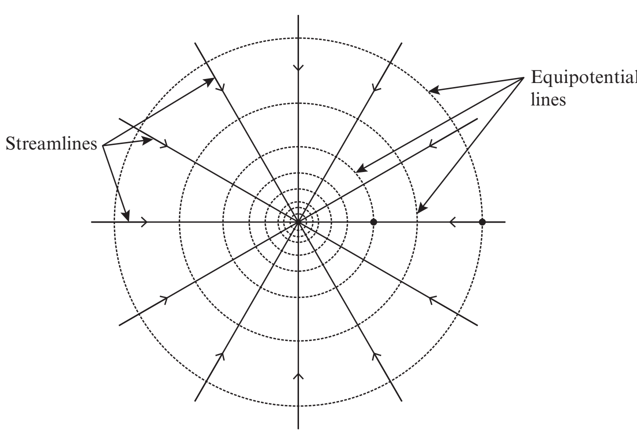

Figure 11.11 *Flownet for radial flow toward a well*

Well in Uniform Flow

The resultant groundwater flow pattern or flownet can be obtained by superimposing the above-derived relations for individual cases, thus

$$\psi = \psi_{uniform\ flow} + \psi_{well} = -Kiy + \left(\frac{-Q}{2\pi b}\right).\theta + C_5 \tag{10.89}$$

$$\phi = \phi_{uniform\ flow} + \phi_{well} = -Kix + \left(\frac{-Q}{2\pi b}\right).\ln r + C_6 \tag{10.90}$$

$$h = ix + \left(\frac{Q}{2\pi T}\right).\ln r + C_7 \tag{10.91}$$

In some part of the flow field, the velocity due to uniform flow and the radial velocity due to well pumping are in opposite directions. At a particular point, both these velocities may be equal in magnitude and opposite in direction, then the resultant velocity becomes zero, and that point is known as *stagnation point*. At the stagnation point, the net velocity is zero, therefore,

$$|v_x| = |v_r| \ \text{ or } \ |Ki| = \left|\frac{Q}{2\pi rb}\right| \ \text{ or } \ r = \left|\frac{Q}{2\pi Ti}\right| \tag{10.92}$$

This is the distance of stagnation point from the center of well.

Assuming $C_5 = 0$ and $\psi = 0$ for the resultant streamline passing through the stagnation point gives

$$Kiy = \left(\frac{-Q}{2\pi b}\right).\theta \ \text{ or } \ Kiy = \left(\frac{-Q}{2\pi b}\right).\tan^{-1}\frac{y}{x} \tag{10.93}$$

which yields

$$x = y\cot\left(\frac{2\pi Tiy}{-Q}\right) \tag{10.94}$$

This is a very important relationship for the streamline curve passing through the stagnation point. The curve defined by Eqn. (10.94) divides the flow field into two zones namely inside and outside as shown in Figure 10.12. The flow or streamlines outside this curve always bypass the well or never reach to the well, and thus the outside zone is beyond the influence area of the well. On the other side, the flow or streamlines inside this curve always reach to the well, and thus all the flow inside this curve is captured by the well, and hence known as *capture zone*. The capture zone geometry is important in locating new wells or managing existing wells for contaminant-free water supply. If any potential source of pollution is within capture zone, the pollutant will reach sooner or later in the water from the well. Therefore, all the sources of groundwater contamination should be located outside the capture zone of production wells. The other geometric properties of the capture zone are as follows:

At $x = 0$,

$$y\cot\left(\frac{2\pi Tiy}{-Q}\right) = 0 \ \text{ or } \ y = \pm\frac{Q}{4Ti} \tag{10.95}$$

At $y = 0$, there is stagnation point:

$$x = a = \frac{-Q}{2\pi Ti} \tag{10.96}$$

Therefore, Eqn. (10.95) and Eqn. (10.96) gives

$$y_{x=0} = \pm\frac{a\pi}{2} \tag{10.97}$$

For far-end points, as $r \to \infty$, $x \to -\infty$, and $\theta \to \pm\pi$; hence,

$$Kiy_l = \pm\left(\frac{Q}{2\pi b}\right).\pi \quad \text{or} \quad y_l = \pm\left(\frac{Q}{2Ti}\right) \quad \text{or} \quad y_l = \pm\pi a \quad \text{or} \quad y_l = \pm 2y_{x=0} \tag{10.98}$$

Thus, the water divide (capture zone curve) approaches asymptotically the lines $y = \pm\pi a$. Figure 10.12 shows the geometry of the capture zone.

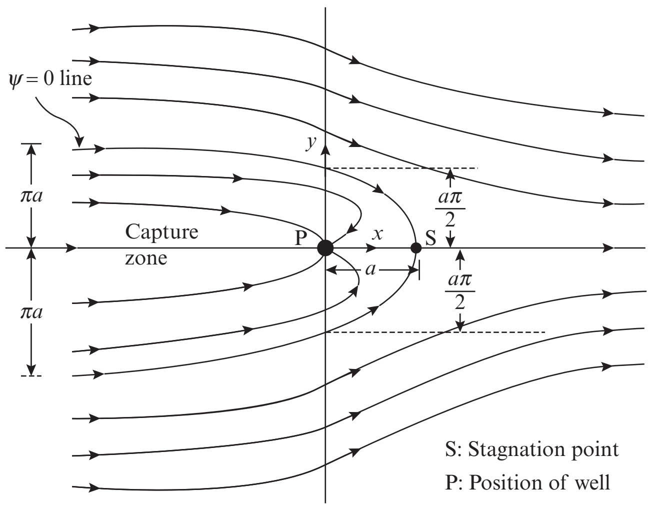

Figure 10.12 *Geometry of the capture for a well in uniform flow*

Combining Eqn. (10.94) and Eqn. (10.96) results in the equation of the capture zone in terms of the distance of the stagnation point as follows:

$$x = y\cot\left(\frac{y}{a}\right) \tag{10.99}$$

The orientation of the capture zone reverses (Figure 10.13) if the discharge well is replaced by a recharging well or the direction of uniform flow is opposite for the same discharging well.

10.3.6 Two Wells of Opposite Nature in Confined Aquifer

Consider two wells of equal strength but opposite nature in a homogeneous and isotropic aquifer of hydraulic conductivity K and uniform thickness b as shown in Figure 10.14. The first well discharges Q, whereas the second well

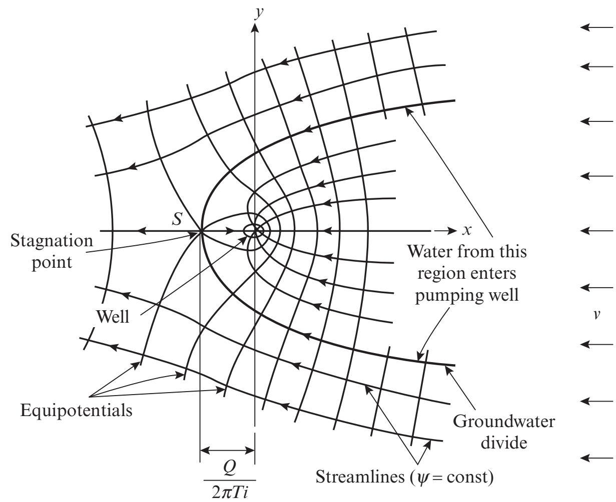

Figure 10.13 *Capture for a well in uniform flow in reverse direction*

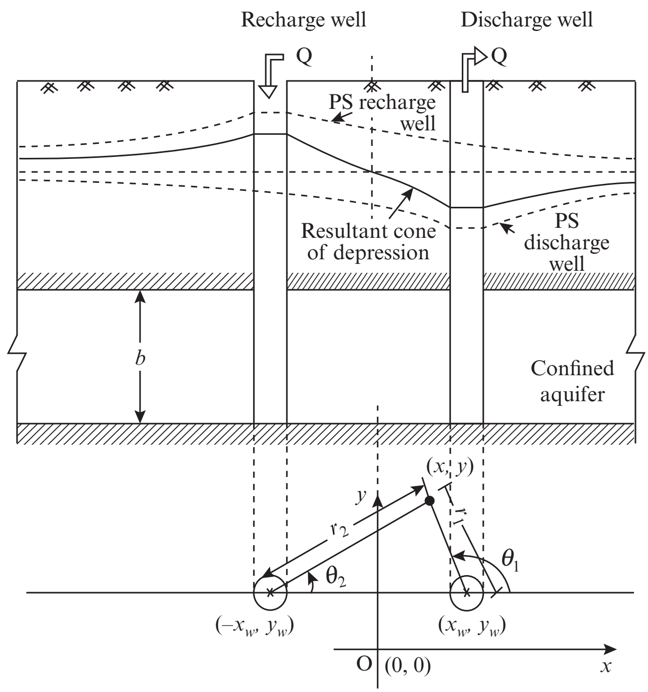

Figure 10.14 *Two wells in confined aquifer*

recharges Q. Let us take x and y coordinates in a horizontal plane with origin at the intersection of two vertical planes (one passing through the center of wells and the other normal to the first and passing through the midpoint between the wells). Therefore, if coordinate of the discharging well is (x_w, y_w), then the coordinate of the recharging well will be $(-x_w, y_w)$. The effect of steady pumping of both wells at any point (x, y) can be worked out by superimposing their individual heads at that point. Since

$$h_1 = \frac{Q}{4\pi T}\ln r_1^2 + C_1 = \frac{Q}{4\pi T}\ln\left\{(x-x_w)^2 + (y-y_w)^2\right\} + C_1 \tag{10.100}$$

and

$$h_2 = \frac{-Q}{4\pi T}\ln r_2^2 + C_2 = \frac{-Q}{4\pi T}\ln\left\{(x+x_w)^2 + (y-y_w)^2\right\} + C_2 \tag{10.101}$$

So

$$h = h_1 + h_2 = \frac{Q}{4\pi T}\ln\frac{r_1^2}{r_2^2} + C_3 = \frac{Q}{4\pi T}\ln\left\{\frac{(x-x_w)^2 + (y-y_w)^2}{(x+x_w)^2 + (y-y_w)^2}\right\} + C_3 \tag{10.102}$$

where, $r_1 \left(=\sqrt{(x-x_w)^2 + (y-y_w)^2}\right)$ and $r_2 \left(=\sqrt{(x+x_w)^2 + (y-y_w)^2}\right)$ are distances of the point (x, y) from the discharging and recharging wells, respectively. If the point is at a very large distance from the wells, then $r_1 \approx r_2$, and hence $h \rightarrow C_3 = h_0$ means steady flow is possible as the recharge well serves as a source of water. Let the radius of well r_w be very small in comparison with x_w $(r_w \ll x_w)$ and consider a point $(x = r_w + x_w; y = y_w)$, then Eqn. (10.102) reduces to

$$h = h_o - \frac{Q}{2\pi T}\ln\left\{\frac{2x_w}{r_w}\right\} \tag{10.103}$$

comparing with single well steady case, it may be interpreted as having radius of influence = 2 x_w.

The case can be analyzed for the resultant flownet. The velocity potential and stream function at the point (x, y) due to discharging well are

$$\phi_1 = -\left(\frac{Q}{2\pi b}\right).\ln r_1 + C_1 \tag{10.104}$$

and

$$\psi_1 = -\frac{Q}{2\pi b}\theta_1 + C_2 \tag{10.105}$$

where, θ_1 = angle of r_1 with x-axis. Similarly, the velocity potential and stream function at the point (x, y) due to recharging well are

$$\phi_2 = \left(\frac{Q}{2\pi b}\right).\ln r_2 + C_3 \tag{10.106}$$

$$\psi_2 = \frac{Q}{2\pi b}\theta_2 + C_4 \tag{10.107}$$

where, θ_2 = angle of r_2 with x-axis. Therefore, the resultant velocity potential and stream function at the point (x, y) due to both wells are

$$\phi = \phi_1 + \phi_2 = \left(\frac{Q}{2\pi b}\right).\ln\frac{r_2}{r_1} + C_5 \tag{10.108}$$

and

$$\psi = \psi_1 + \psi_2 = \frac{Q}{2\pi b}(\theta_2 - \theta_1) + C_6 \tag{10.109}$$

These equations in Cartesian coordinates are

$$\phi = \frac{Q}{4\pi b}.\ln\frac{(x+x_w)^2+(y+y_w)^2}{(x-x_w)^2+(y-y_w)^2}+C_5 \tag{10.110}$$

and

$$\psi = \frac{Q}{2\pi b}.\left\{\tan^{-1}\left(\frac{y+y_w}{x-x_w}\right)-\tan^{-1}\left(\frac{y-y_w}{x+x_w}\right)\right\}+C_6 \tag{10.111}$$

as $\theta_2 = \tan^{-1}\left(\frac{y-y_w}{x-x_w}\right)$; and $\theta_1 = \tan^{-1}\left(\frac{y-y_w}{x+x_w}\right)$.

Manipulating the resultant velocity potential, Eqn. (10.110) can be rewritten as follows:

$$\frac{(x+x_w)^2+(y-y_w)^2}{(x-x_w)^2+(y-y_w)^2} = e^{\left(\frac{4\pi b}{Q}\right).(\phi-C_5)} \tag{10.112}$$

For constant ϕ (equipotential line), the RHS is constant, let it be m, then

$$(x+x_w)^2+(y-y_w)^2 = m\left[(x-x_w)^2+(y-y_w)^2\right] \tag{10.113}$$

$$(1-m)x^2+2xx_w(1+m)+(1-m)x_w^2+(y-y_w)^2(1-m)=0 \tag{10.114}$$

or

$$\left(x-\frac{1+m}{m-1}x_w\right)^2+(y-y_w)^2 = x_w^2.\left(\frac{4m}{(m-1)^2}\right) \tag{10.115}$$

This represents a circle with center at $\left(\frac{1+m}{m-1}x_w, y_w\right)$ and of radius $=\frac{2x_w\sqrt{m}}{m-1}$. This means the circle grows with increasing value of m, and its center moves on the line joining centres of both wells ($y = y_w$). Thus, the resultant equipotential lines are in circular shape as shown dotted in Figure 10.15.

Similarly, the resultant stream function Eqn. (10.109) can be worked out as follows:

$$\theta_2-\theta_1 = \left(\frac{2\pi b}{Q}\right)(\psi-C_6) \tag{10.116}$$

Operating tangent on both sides,

$$\tan(\theta_2-\theta_1) = \tan\left(\frac{2\pi b}{Q}(\psi-C_6)\right) \tag{10.117}$$

For constant ψ (stream line), the RHS is constant, let it be n, then

$$\tan(\theta_2-\theta_1) = \frac{\tan\theta_2-\tan\theta_1}{1+\tan\theta_2.\tan\theta_1} = \frac{\left(\frac{y-y_w}{x+x_w}\right)-\left(\frac{y-y_w}{x-x_w}\right)}{1+\left(\frac{y-y_w}{x+x_w}\right).\left(\frac{y-y_w}{x-x_w}\right)} = n \tag{10.118}$$

$$\left(y-y_w\right).\left(x-x_w\right)-\left(y-y_w\right).\left(x+x_w\right)=n\left\{\left(x+x_w\right).\left(x-x_w\right)+\left(y-y_w\right)^2\right\} \quad (10.119)$$

$$x^2+\left(y-y_w\right)^2+\frac{2}{n}x_w\left(y-y_w\right)=x_w^2 \quad (10.120)$$

or

$$x^2+\left\{y-\left(y_w-\frac{x_w}{n}\right)\right\}^2=x_w^2+\frac{x_w^2}{n^2} \quad (10.121)$$

which is also an equation of circle having center at $\left(0,\left(y_w-\dfrac{x_w}{n}\right)\right)$ and radius $=\dfrac{x_w\sqrt{1+n^2}}{n}$. Also Eqn. (10.121) is satisfied by coordinates of both wells that are $\left(x_w,y_w\right)$ and $\left(-x_w,y_w\right)$. This means streamlines pass through the centers of recharging and discharging wells, and their center is always on the y-axis ($x = 0$). Thus, the resultant streamlines are circular in shape, having center on the y-axis and pass through centers of both the wells as shown in Figure 10.15.

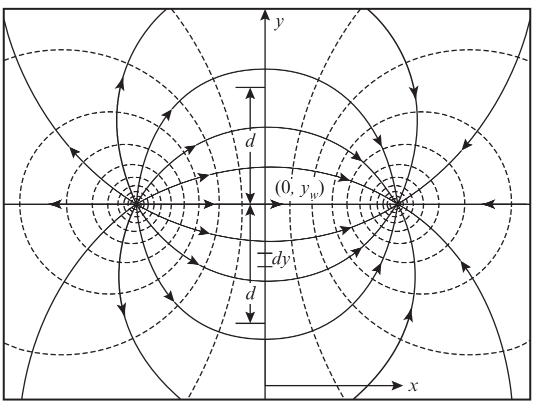

Figure 10.15 *Flownet—two wells of same strength and opposite nature*

Now to calculate discharge from one well to another well, take a strip of width dy normal to flow as shown in Figure 10.15. Elementary discharge through this strip is

$$dQ_s=v\ .b\,dy \quad (10.122)$$

and hence the total discharge through the strip of $2d$ width

$$Q_s=\int_{y_w-d}^{y_w+d}\left|\frac{\partial\phi}{\partial x}\right|_{x=0}.b\,dy \quad (10.123)$$

Partially differentiating Eqn. (10.110) w.r.t. to x,

$$\frac{\partial\phi}{\partial x}=\frac{\partial}{\partial x}\left\{\frac{Q}{4\pi b}\left[\frac{\left(x-x_w\right)^2+\left(y-y_w\right)^2}{\left(x+x_w\right)^2+\left(y-y_w\right)^2}\right]\right\} \quad (10.124)$$

Therefore,

$$\left|\frac{\partial \phi}{\partial x}\right|_{x=0} = \frac{Q}{4\pi b}\frac{4x_w}{x_w^2 + (y - y_w)^2} \tag{10.125}$$

and hence

$$Q_s = \frac{Q}{\pi b}\int_{y_w - d}^{y_w + d} \frac{x_w}{x_w^2 + (y - y_w)^2} b\,dy \tag{10.126}$$

or

$$Q_s = \frac{2Q}{\pi}\tan^{-1}\frac{d}{x_w} \qquad \text{or} \qquad \frac{Q_s}{Q} = \frac{2}{\pi}\tan^{-1}\frac{d}{x_w} \tag{10.127}$$

The practical application of this analysis of two-well system finds place when a discharging well is near a stream or water body apart from recharging well and recovery well system. Wells are established near water bodies for various purposes, such as

- bank filtration
- quality improvement
- recycling of water
- induced recharging of groundwater

The effect of the water body is equivalent to creating an image (well of same strength but opposite nature) of the actual discharging well. A well near a stream or water body can be dealt with replacing the stream or water body by an image well of same strength but opposite nature of the actual discharging well and then using the above solution. Eqn. (10.127) gives the stream contribution Q_s (the flow coming from the stream through $2d$ wide strip) in the total well discharge. If the width of strip d on both sides is considered very large, then

$$\frac{d}{x_w} \to \infty \quad \text{or} \quad \tan^{-1}\frac{d}{x_w} \to \frac{\pi}{2}$$

Therefore,

$$Q_s = Q \tag{10.128}$$

This means whole discharge from the pumping well is contributed by the stream. Actually, this should happen to attain steady-state condition.

10.3.7 Two Wells of Same Nature in Confined Aquifer

This case is similar to the previous one, except that both wells are discharging as shown in Figure 10.16. Therefore, the resultant head, velocity potential, and stream function at the point (x, y) due to both wells are

$$h = \left(\frac{Q}{2\pi T}\right).\ln r_1 r_2 + C_6 \tag{10.129}$$

$$\phi = \left(\frac{-Q}{2\pi b}\right).\ln r_1 r_2 + C_7 \tag{10.130}$$

and

$$\psi = \frac{-Q}{2\pi b}\left(\theta_2 + \theta_1\right) + C_8 \tag{10.131}$$

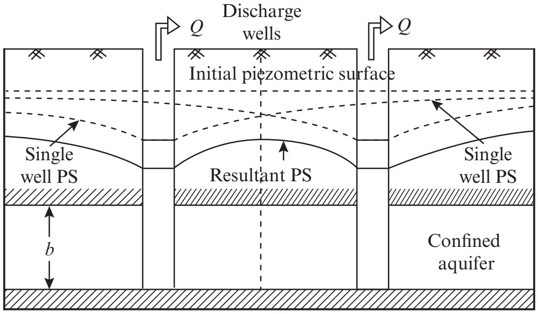

Figure 10.16 *Two well of same nature in confined aquifer*

Here, the streamlines are not circular but of hyperbolic shape. In this case, a stagnation point is created at the midpoint between the wells. The final flownet is shown in Figure 10.17. If the point is at a very large distance from the wells, then $r_1 \approx r_2$ and $\theta_2 \approx \theta_1$. Hence, the effect (head or drawdown) is twice as that of a single well. Apart from two production wells of same strength, this type of case happens when a discharging well is near a *barrier boundary*. The barrier boundary terminates the aquifer extension, and its effect is to create an image well of same

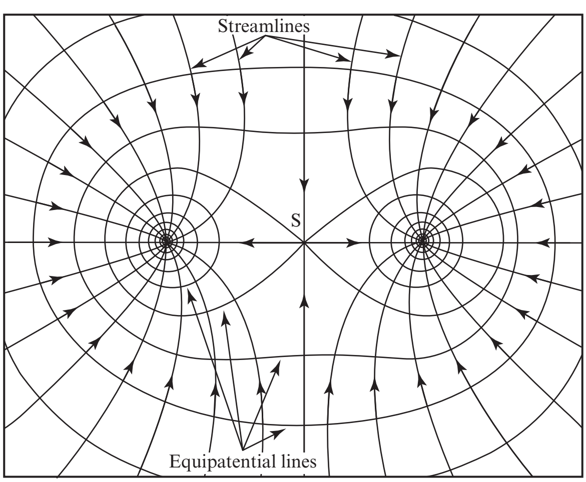

Figure 10.17 *Flownet for two wells of same strength and nature*

nature. Thus, if a well is situated near a barrier boundary, then the boundary can be replaced by an image well of same strength and same nature and problem can be solved considering two wells in the aquifer without the barrier boundary.

10.3.8 Two Wells in Uniform Flow Field

Consider two wells in a homogeneous and isotropic aquifer of hydraulic conductivity K and uniform thickness b in which the initial piezometric surface is inclined. The x–y coordinate system and its origin are chosen similar to two wells case. The first well at (x_w, y_w) is discharging well of strength Q_p, whereas the second well at ($-x_w$, y_w) is recharging well of strength Q_r. The hydraulic gradient or uniform flow due to the inclined piezometric surface is parallel to the vertical plane passing through the centers of wells. We have already derived relations for head, velocity potential, or stream function for a well or uniform flow field. The resultant head, velocity potential, or stream function at any point (x, y) can simply be obtained by superimposing the individual effects of three cases. For example, the resultant hydraulic head is

$$h = h_u + h_p + h_r \tag{10.132}$$

where, $h_u, h_p, \text{and}\, h_r$ are heads corresponding to uniform flow, pumping well, and recharging well, respectively. Using relevant equations,

$$h = ix + \frac{Q_p}{2\pi T}\ln r_2 - \frac{Q_r}{2\pi T}\ln r_1 + C \tag{10.133}$$

Similarly, the resultant velocity potential and stream function are

$$\phi = -Kix - \frac{Q_p}{2\pi b}\ln r_2 + \frac{Q_r}{2\pi b}\ln r_1 + C_1 \tag{10.134}$$

and

$$\psi = -Kiy - \frac{Q_p}{2\pi b}\theta_2 + \frac{Q_r}{2\pi b}\theta_1 + C_2 \tag{10.135}$$

At the stagnation point, the resultant velocity is zero, thus

$$|v_u| = |v_p| + |v_r| \text{ or } |Ki| = \left|\frac{Q_p}{2\pi b r_2}\right| + \left|\frac{Q_r}{2\pi b r_1}\right| \tag{10.136}$$

The location of the stagnation point depends on the strengths of discharging well Q_p, and recharging well Q_r, arrangement of wells, strength of uniform flow i, and direction of uniform flow. If d_s is the distance of stagnation point from the midpoint between the wells, then its distance r_2 from the discharging well and distance r_1 from the recharging well will be $(x_w + d_s)$, $(x_w - d_s)$, or $(d_s - x_w)$. The stagnation point may lie on the left-hand side of both wells $\{r_2 = (d_s - x_w) \text{and}\, r_1 = (x_w + d_s)\}$ on the right-hand side of both wells $\{r_2 = (x_w + d_s) \text{and}\, r_1 = (d_s - x_w)\}$, or in between of both wells. Further, the stagnation point in between of both wells may be near to the discharging well $\{r_2 = (x_w - d_s) \text{and}\, r_1 = (x_w + d_s)\}$ or near to the recharging well $\{r_2 = (x_w + d_s) \text{and}\, r_1 = (x_w - d_s)\}$. Therefore,

$$\left|Ki\right| = \left|\frac{Q_p}{2\pi b\left(x_w - d_s\right)}\right| + \left|\frac{Q_r}{2\pi b\left(x_w + d_s\right)}\right| \text{ or } \left|Ki\right| = \left|\frac{Q_p}{2\pi b\left(x_w + d_s\right)}\right| + \left|\frac{Q_r}{2\pi b\left(x_w - d_s\right)}\right| \tag{10.137}$$

Simplifying further for $Q_p = Q_r$,

$$Ki = \frac{-Q}{2\pi b}\left(\frac{2x_w}{x_w^2 - d_s^2}\right) \quad \text{or} \quad x_w^2 - d_s^2 = \frac{-Qx_w}{\pi Kbi} \tag{10.138}$$

or

$$d_s = \pm x_w\sqrt{1 - \frac{-Q}{\pi Tix_w}} \quad \text{or} \quad d_s = \pm x_w\sqrt{1 - a_{sw}} \tag{10.139}$$

where, parameter $a_{sw} = -Q/\pi Tix_w$. Thus, there are two stagnation points on the line joining wells and symmetric with respect to the midpoint as shown in Figure 10.18. It also shows two capture zones, one each for discharging well and recharging well. This arrangement is adopted in pump-and-treat system, wherein the polluted aquifer is pumped for treatment and then the treated water is used for recharging the same aquifer for future use.

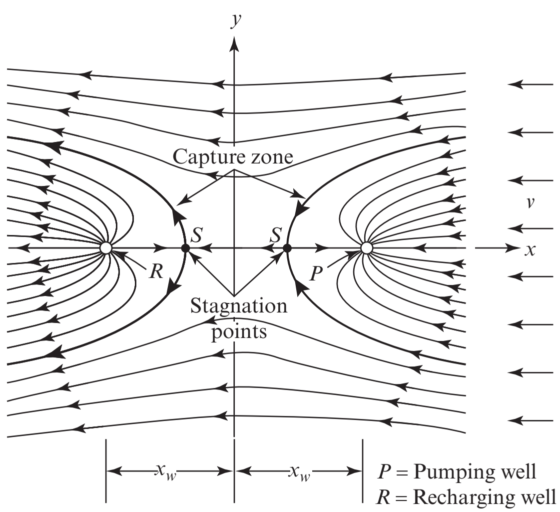

Figure 10.18 *Two wells in uniform flow field (two stagnation points)*

At the critical situation, these two stagnation points merge into one at the midpoint. For one stagnation point, d_s =0. Therefore,

$$a_{sw} = 1 \Rightarrow Q = \left|\pi Tix_w\right| \tag{10.140}$$

This is the required discharge to produce a single stagnation in an aquifer with T and i. Here, both the capture zones just touch each other as shown in Figure 10.19.

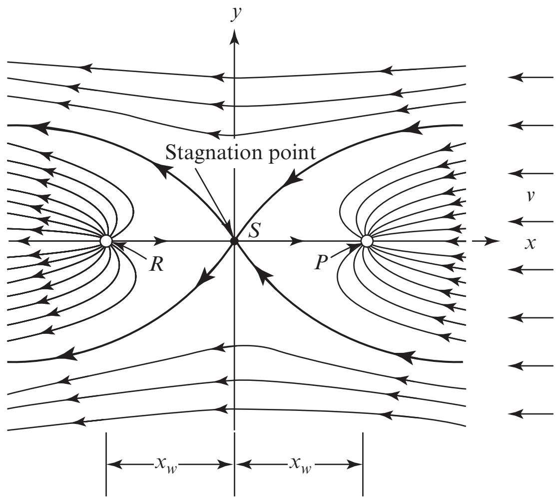

Figure 10.19 *Two wells in uniform flow field (single stagnation point)*

If $a_{sw} > 1$ or $Q > |\pi T i x_w|$, again there will be two stagnation points, but on the y-axis as shown in Figure 10.20.

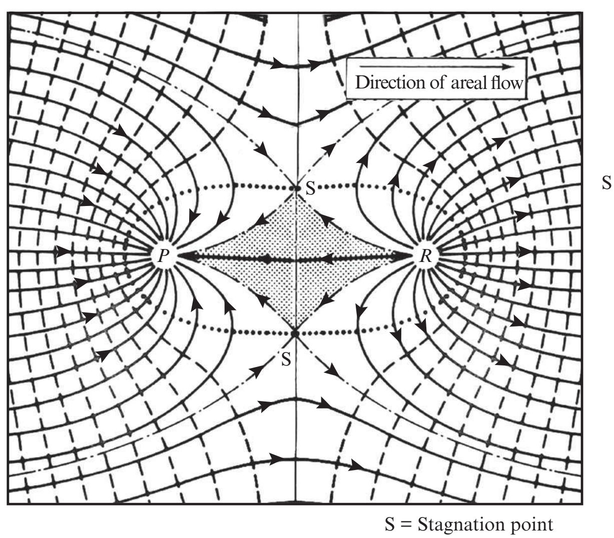

Figure 10.20 *Two wells in uniform flow—Two stagnation points with recirculation*

For this case, (see Figure 10.21)

$$|Ki| = \left|\frac{Q_p}{2\pi b r_2}\cos\theta_2\right| + \left|\frac{Q_r}{2\pi b r_1}\cos\theta_1\right| \tag{10.141}$$

Since

$$r_2^2 = r_1^2 = \left(x_w^2 + d_s^2\right); \ \cos\theta_1 = \frac{x_w}{r_1}; \quad \cos\theta_2 = \frac{x_w}{r_2} \tag{10.142}$$

Therefore, if $Q_p = Q_r$

$$Ki = \frac{-Q}{\pi b} \cdot \frac{x_w}{x_w^2 + d_s^2} \tag{10.143}$$

or

$$d_s = \pm x_w . \sqrt{\frac{-Q}{\pi T i x_w} - 1} \quad \text{or} \quad d_s = \pm x_w . \sqrt{a_{sw} - 1} \tag{10.144}$$

Therefore, some part of the capture zone of one well overlaps over the capture zone (Figure 10.21) of the other well.

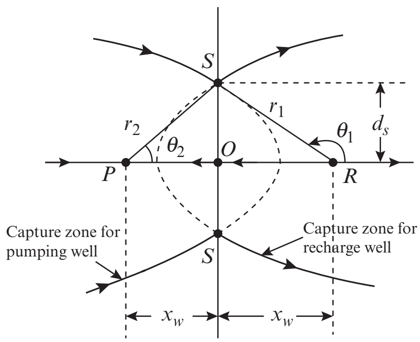

Figure 10.21 *Two stagnation points due to overlapped capture zone*

In this case, there is *recirculation* of flow between the wells due to overlapping capture zones as shown shaded part in Figure 10.20. To calculate the recirculation discharge Q_R, consider two streamlines in Figure 10.21 one passing through the stagnation point ψ_s and the other passing through the midpoint ψ_o. Therefore,

$$\psi_s - \psi_0 = \frac{Q_R}{2b} \tag{10.145}$$

Since

$$\psi_0 = -Kiy_w - \frac{Q_p}{2\pi b}(0) + \frac{Q_r}{2\pi b}(\pi) + C_2 \tag{10.146}$$

and

$$\psi_s = -Ki(y_w + d_s) - \frac{Q_p}{2\pi b}(\theta_2) + \frac{Q_r}{2\pi b}(\theta_1) + C_2 \tag{10.147}$$

Hence, for $Q_p = Q_r$,

$$\frac{Q_R}{2b} = \psi_s - \psi_0 = -Kid_s - \frac{Q}{2\pi b}\theta_2 + \frac{Q}{2\pi b}\theta_1 - \frac{Q}{2\pi b}.\pi \tag{10.148}$$

Since $\theta_1 + \theta_2 = \pi$

$$\frac{Q_R}{2b} = -Kid_s + \frac{Q}{2\pi b}(-2\theta_2) \tag{10.149}$$

Substituting values of d_s and θ_2

$$\frac{Q_R}{2b} = -Kix_w\sqrt{a_{sw}-1} - \frac{Q}{\pi b}\tan^{-1}\sqrt{a_{sw}-1} \tag{10.150}$$

In terms of absolute value of recirculation ratio, it becomes

$$\frac{Q_R}{Q} = \frac{2}{\pi}\left(a_{sw}\sqrt{a_{sw}-1} + \tan^{-1}\sqrt{a_{sw}-1}\right) \tag{10.151}$$

If the position of the wells is interchanged or the direction of the uniform flow is reversed, then the resultant flownet and capture zones are as shown in Figure 10.22. Also there is complete recirculation of flow between the wells as shaded in Figure 10.22. This means whatever water is pumped in the recharge well is completely recovered through pumping out of the discharge well without loss and without mixing with the adjoining aquifer groundwater. This is important in low-quality groundwater aquifers as the prevailing groundwater in the aquifer is bypassed and the good quality recharged water can only find the way to reach the recovery well. This configuration is preferred in *recharge-and-recovery system*, *recycling of treated waste water system*, *soil aquifer treatment recovery well system*, etc., where the main objective is to recover the whole treated water.

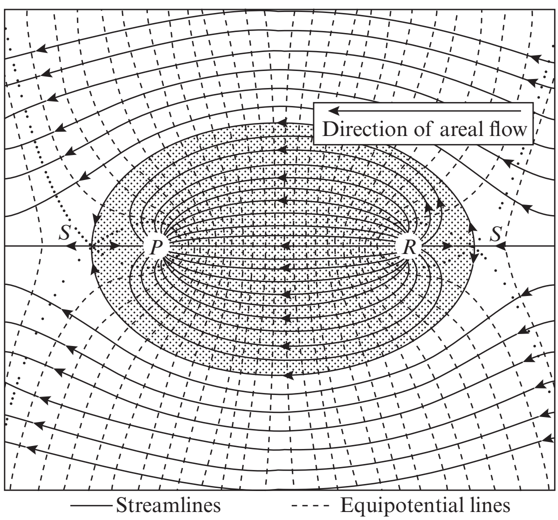

Figure 10.22 *Two wells in uniform flow—two stagnation points with complete recirculation*

In general, the direction of uniform flow may be oblique or the recharge rate may differ from the discharge rate, or there are more than two wells of different strength and nature in the flow field. In these practical cases, a similar analysis may be carried out. For example, if the direction of uniform flow makes an angle α with the x-axis, then the head, resultant velocity potential and stream function are

$$h = i\left(x\cos\alpha + y\sin\alpha\right) + \frac{Q_p}{2\pi T}\ln r_2 - \frac{Q_r}{2\pi T}\ln r_1 + C \tag{10.152}$$

$$\phi = -Ki\left(x\cos\alpha + y\sin\alpha\right) - \frac{Q_p}{2\pi b}\ln r_2 + \frac{Q_r}{2\pi b}\ln r_1 + C_1 \tag{10.153}$$

and

$$\psi = -Ki\left(y\cos\alpha - x\sin\alpha\right) - \frac{Q_p}{2\pi b}\theta_2 + \frac{Q_r}{2\pi b}\theta_1 + C_2 \tag{10.154}$$

If $Q_p < Q_r$, then the additional recharge will be leaked, whereas in case of $Q_p > Q_r$, the deficit amount comes from the aquifer water, hence there will be mixing. The pattern of flow for selected cases is shown in Figures 10.23–Figure 10.24.

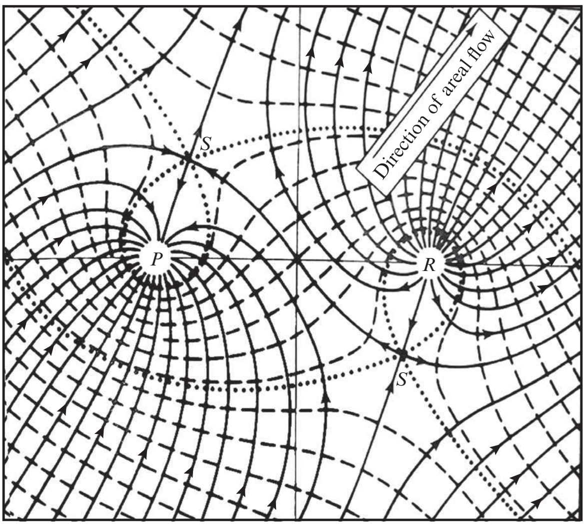

Figure 10.23 *Two wells in oblique direction of uniform flow*

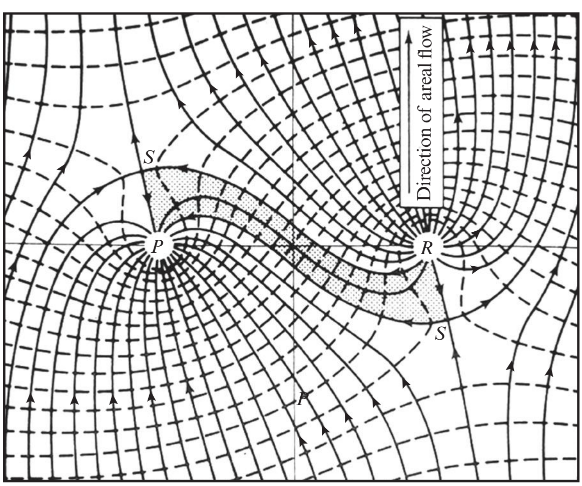

Figure 10.24 *Two wells of unequal strength with uniform flow in normal direction*

SOLVED EXAMPLES

Example 10.1: A farmer owns a farm of 200 m × 300 m size, in which the initial water table is 1.0 m below the ground level. The underlying aquifer has hydraulic conductivity 10^{-5} m/s and saturated thickness 20 m. The estimated recharge from irrigation return flow may be 5 cm/day. The farmer plans to maintain the water table atleast 3 m below the ground level by a pumping well at the center of a farm for better crop. Determine the steady-state minimum pumping rate required for this purpose.

Solution: Corner points are farthest from the well, and hence will have minimum drawdown within the farm due to the pumping well at the center. To maintain groundwater table at 3 m bgl, the required drawdown is 2 m at distance $r = \sqrt{100^2 + 150^2} = 180.28\,\text{m}$.

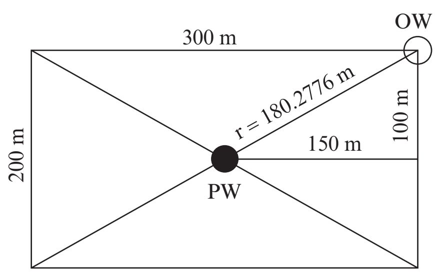

Figure 10.25 *Example 10.1*

Using Eqn. (10.70), wherein $h_0 = 20\,\text{m},\ h = 20 - 2 = 18\,\text{m},\ r = 180.28\,\text{m}$, $K = 10^{-5}\ \text{m/s},\ R = \dfrac{0.05}{24 \times 3600}\,\text{m/s}$, hence

$$18^2 = 20^2 + \frac{Q_w - \pi.180.28^2 \times 5.787 \times 10^{-7}}{2\pi.10^{-5}} - \frac{Q_w}{2\pi.10^{-5}} \ln \frac{Q_w}{\pi.180.28^2 \times 5.787 \times 10^{-7}}.$$

Solving by trial-and-error procedure yields Q_w = 84.4 lps and corresponding radius of influence $r_e = \sqrt{\dfrac{0.0844/\pi}{5.787} \times 10^{-7}} = 215.44\,\text{m}$.

Example 10.2: A well penetrates an unconfined aquifer of saturated thickness of 30 m completely. Under a steady pumping rate of 0.5 m³/s for a long time, the drawdown at distance of 50 m from the well was observed 3.0 m. If the hydraulic conductivity of the aquifer is 7.26×10⁻² m/s, determine the drawdown at distance of 150 m from the well.

Solution: Method I: Using equation $h_1^2 - h_2^2 = \dfrac{Q}{\pi K} \ln\left(\dfrac{r_1}{r_2}\right)$:

$$(25-3)^2-(25-s)^2=\frac{0.5}{\pi\times 7.26\times 10^{-2}}\ln\left(\frac{50}{150}\right)\Rightarrow s=2.945\,\text{m}$$

Method II: Using equivalent confined aquifer concept:

Equivalent observed drawdown $s_1' = 3-\dfrac{3^2}{2\times 25}=2.82\,\text{m}$

Using equation $s_1'-s_2'=\dfrac{Q}{2\pi T}\ln\left(\dfrac{r_2}{r_1}\right)$,

$$2.82-s_2' = \frac{0.5}{2\pi\times 7.26\times 10^{-2}\times 25}\ln\left(\frac{150}{50}\right)\Rightarrow s_2' = 2.77\ \text{m}$$

Converting this equivalent drawdown into corresponding unconfined aquifer drawdown,

$$2.77=s-\frac{s^2}{2\times 25}\ \Rightarrow\ s=2.945\,\text{m}$$

This is the same as obtained in Method I.

Example 10.3: A fully penetrating well operating under steady state in a confined aquifer of 50 m thickness produces hydraulic heads 82 m and 87 m at distances 100 m and 200 m, respectively, away from the well. Determine the radius of influence if the hydraulic head before pumping was 100 m.

Solution: Using Eqn. (10.32) for both point,

$$82=100+\frac{Q}{2\pi Kb}\ln\frac{100}{r_e}\ \text{and}\ 87=100+\frac{Q}{2\pi Kb}\ln\frac{200}{r_e}.$$

These conditions yield

$$\frac{18}{13}=\frac{\ln 100-\ln r_e}{\ln 200-\ln r_e}\ \Rightarrow 5\ln r_e = 18.\ln 200-13.\ln 100 \Rightarrow r_e = 1212.57\,\text{m}$$

Example 10.4: Two wells of 30-cm radius each are drilled 150 m apart in an unconfined aquifer having hydraulic conductivity 0.5 mm/s and saturated thickness 40 m. A discharge 100 lps from the first well and 125 lps from the second well are pumped for long time, then determine the steady-state position of water table in an observation well located 225 m from the first well and 300m from the second well. Assume the radius of influence 1000 m for each well as well as for both wells.

Solution: Using method of superposition for two wells in unconfined aquifer,

$$h^2=\frac{Q_1}{\pi K}\ln r_1+\frac{Q_2}{\pi K}\ln r_2+C$$

Substituting corresponding values

$$h^2=\frac{100\times 10^{-3}}{\pi\times 0.5\times 10^{-3}}\ln 225+\frac{125\times 10^{-3}}{\pi\times 0.5\times 10^{-3}}\ln 300+C$$

At radius of influence $40^2 = \dfrac{100\times10^{-3}}{\pi\times0.5\times10^{-3}}\ln1000+\dfrac{125\times10^{-3}}{\pi\times0.5\times10^{-3}}\ln1000+C$

yields C = 610.54 m², and hence h = 37.54 m. Thus, the water table in the observation well will be 37.54 m above datum or 2.46 m below the original water table.

Example 10.5: A 40-cm diameter well fully penetrates through a confined aquifer of thickness 15 m. Under a steady pumping rate at 35 lps, the drawdowns were 30 m in the pumping well, 5 m in the observation well 200 m away from pumping well, and 20 m in another observation well, which was 300 m away from the pumping well and at 135° with the first observation well. Estimate the inhomogeneity in the directions of the observation wells.

Solution: Given data for confined aquifer: r_w = 0.2 m, b = 15 m, Q = 35 lps = 35×10^{-3} m³/s, drawdown in pumping well = s_w = 30 m, s_1 = 5 m, r_1 = 200 m, s_2 = 20 m, r_2 = 300 m, and θ = 135° as shown in Figure 10.26

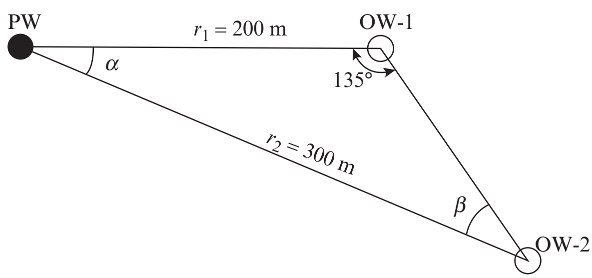

Figure 10.26 *Example 10.5*

Considering pumping well and observation well 1:

$$s_w - s_1 = \frac{Q}{2\pi T}\ln\frac{r_1}{r_w} \Rightarrow 30-5 = \frac{35x10^{-3}}{2\pi T}\ln(200/0.2) \Rightarrow T = 1.539\times10^{-3}\ \text{m}^2\text{/s}.$$

Therefore, $K = T/b = 1.026\times10^{-4}$ m/s in the direction of pumping well and observation well 1.

Considering pumping well and observation well 2:

$30-20 = \dfrac{35x10^{-3}}{2\pi T}\ln(300/0.2) \Rightarrow T = 4.074\times10^{-3}$ m²/s, so $K = 2.716\times10^{-4}$ m/s in the direction of pumping well and observation well 2 and at an angle of 16.87° with respect to observation well 1.

In Figure 10.26,

$$\frac{\sin135}{300} = \frac{\sin\alpha}{X} = \frac{\sin\beta}{200} = 2.357\times10^{-3}$$

Therefore,

$\beta = 28.13°$ and $\alpha = 16.87°$

Example 10.6: Water is pumped at a constant rate of 500 m^3/d from an unconfined aquifer whose thickness is 15 m and hydraulic conductivity is 5.5 m/day. Plot the water table profile under steady-state conditions if drawdown = 2.5 m at 50 m distance from pumping well.

Solution: Given data for unconfined aquifer: Q = 500 m^3/d, h_o = 15 m, K = 5.5 m/d, s = 2.5 m at r = 50 m. Using initial transmissivity, T = 5.5 × 15 = 82.5 m^2/day for solution $r > 1.5\, h_o$.

For unconfined aquifer Eqn. (10.54) $s_e = s - \dfrac{s^2}{2h_o} = \dfrac{Q}{2\pi T}\ln\left(\dfrac{r_e}{r}\right) \Rightarrow 2.5 - \dfrac{2.5^2}{2\times 15} = \dfrac{500}{2\pi\times 82.5}\ln\left(\dfrac{r_e}{50}\right)$ so r_e = 538 m. Therefore, water table profile relation, Eqn. (10.42), becomes $h^2 = 152 - \dfrac{500}{2\pi\times 82.5}\ln\left(\dfrac{538}{r}\right)$. Using this equation, the water table profile is plotted in Figure 10.27 for $r > 1.5\, h_o$ i.e. 22.5 m onward up to r_e

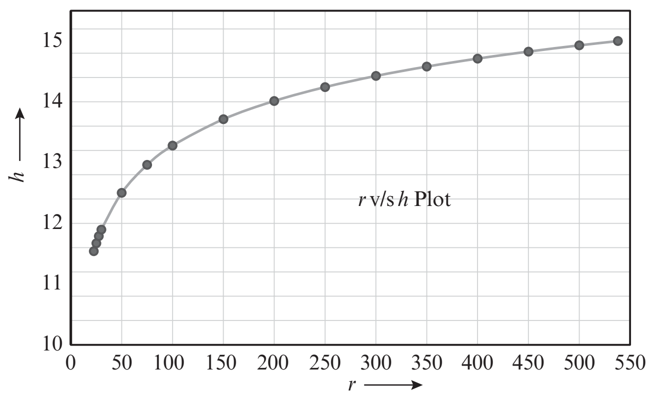

Figure 10.27 *Water table profile for Example 10.6*

Example 10.7: A municipal water supply well pumps at 10,000 m^3/day. The well is screened in a confined aquifer located from 25 m to 75 m below the ground level. The aquifer is formed with coarse sand having a hydraulic conductivity of 45 m/d. The potentiometric surface of the aquifer before the pumping started was 0.5 m for every 100 m. Estimate and plot the boundary of the capture zone. Will the toxic spill nearby the well, as shown in Figure 10.28, contaminate the well?

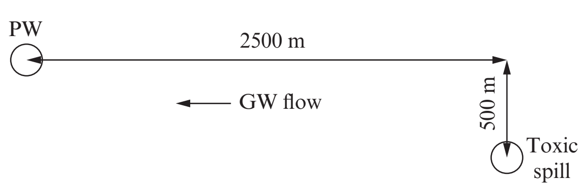

Figure 10.28 *Example 10.7*

Solution: Given data for confined aquifer under steady-state pumping: Q = 10,000 m³/d, i = 0.5/100 = 0.005, K = 45 m/day, b = 75–25 = 50 m. Therefore, T = 45×50 = 2250 m²/day. Location of stagnation point from Eqn. (10.96) is $= \dfrac{10000}{2\pi \times 2250 \times 0.005} = 141.47$ m, width of capture zone $= 2\pi \times 141.47 = 888.88$ m or half width of capture zone (one side of x-axis) = 444.44 m.

Using Eqn. (10.99) for boundary profile of the capture zone $x = y \cot\left(\dfrac{y}{141.47}\right)$. For different values of y, this equation gives values of x, those of which are tabulated and plotted in Figure 10.29.

y	x	y	x
0	–141.47	400	1231.162
50	–135.53	410	1650.708
100	–117.084	420	2406.808
150	–84.0025	421	2517.491
200	–31.6747	430	4197.783
250	49.73153	440	14011.43
300	183.8468	444	142395.5
350	443.9898		

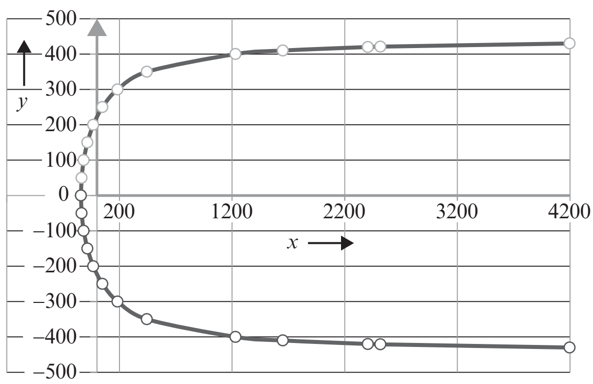

Figure 10.29 *Capture zone*

The toxic spill is at a distance of 500 m from x-axis, which is greater than 421 m. Therefore, the ground water coming to the well will not be contaminated.

Example 10.8: Three pumping wells are situated along a straight line as shown in Figure 10.30. The wells are screened throughout the thickness of the confined aquifer with hydraulic conductivity = 45 m/d and thickness = 40 m. Determine the allowable pumping rate common to all the wells so that the drawdown in any well shoud not be more than 1 m. Assume the diameter of the wells to be 30 cm and the radius of influence to be 1500 m.

Figure 10.30 *Examples 10.8*

Solution: Well 2 is critically located from drawdown point of view. Applying the method of superposition,

$$s = \sum_{i=1}^{n}\left[\frac{Q_i}{2\pi T}\ln\left(\frac{r_{ei}}{r_i}\right)\right] \Rightarrow s = \frac{Q}{2\pi T}\left[\ln\left(\frac{r_e}{r_{12}}\right)+\ln\left(\frac{r_e}{r_{22}}\right)+\ln\left(\frac{r_e}{r_{32}}\right)\right] = \frac{Q}{2\pi T}\ln\left(\frac{r_e^{\,3}}{r_{12}r_{22}r_{32}}\right)$$

Therefore,

$$Q = \frac{2\pi\times 45\times 40}{\ln\left[\dfrac{1500^3}{200\times 200\times 0.15}\right]} = 9.89\times 10^{-3}\ \text{m}^3/\text{s} = 9.89\ \text{lps}$$

PROBLEMS

10.1. Write the general governing equation for radial groundwater flow toward a well in confined aquifer. Give its Thiem's solution.

10.2. Obtain the relation $\frac{\partial^2 h^2}{\partial r^2} + \frac{1}{r}\frac{\partial h^2}{\partial r} + \frac{2R}{k} = \frac{2S}{k}\frac{\partial h}{\partial t}$ stating assumptions made for radial groundwater flow toward a well in an unconfined aquifer.

10.3. Derive the expressions for the equipotential lines and streamlines for a well near a stream.

10.4. Derive the expressions for the stagnation point and the width of flow contributing area (capture zone) of a well in a uniform flow field.

10.5. If a well near a stream as shown in Figure 10.31 is pumped at constant discharge under steady state, then derive expressions for (i) shape of equipotential lines and (ii) stream depletion rate (part of the pumped water taken from the stream) from the length 2 L.

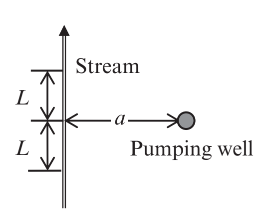

Figure 10.31 *Problem 10.5*

10.6. Drive an expression for stagnation points and recirculation ratio for two wells in uniform flow field as shown in Figure 10.32 and $Q_w > |\pi T i x_w|$. The aquifer transmmissivity $T = 0.003$ m²/s and the spacing between the wells $2\,x_w = 200$ m. Determine the position of stagnation points and value recirculation ratio if (i) $Q_w = 50$ l/s and $i = -0.03$, (ii) $Q_w = 50$ l/s, $i = 0.03$, and (iii) $Q_w = 20$ l/s and $i = -0.03$.

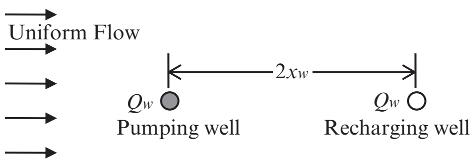

Figure 10.32 *Problem 10.6*

10.7. A confined aquifer of 35-m thickness is contaminated in area of 300-m wide and 600-m long along regional flow direction. The uniform flow gradient is 0.003 and the aquifer has hydraulic conductivity as 20 m/day. Determine the optimal pumping rate and location of the well to clean up the aquifer up to maximum extent.

10.8. A 30-cm diameter tube well taps a 25-m thick confined aquifer. Find the yield for a drawdown of 4.0 m if the hydraulic conductivity of the aquifer is 45 m/day. Assume the radius of influence of the well as 350 m. Also find the percentage change in yield if the diameter of the tubewell and drawdown are doubled while the other things remain the same.

10.9. A 40-cm diameter well in an unconfined aquifer of saturated thickness of 45 m yields 500 lpm under a drawdown of 3.0 m at the pumping well. What will be the discharge in a 30-cm well under a drawdown of 4.5 m? Assume the radius of influence to remain constant at 450 m in both cases.

10.10. A 40-cm diameter well fully penetrates through a confined aquifer of thickness 15 m. Under a steady pumping rate at 35 lps, the drawdowns were 30 m in the pumping well, 5 m in the observation well 200 m away from pumping well, and 20 m in another observation well, which was 300 m away from the pumping well and at 135° angle with the first observation well. Estimate the inhomogeneity in the directions of the observation wells.

10.11. A 45-cm diameter well in an unconfined aquifer of saturated thickness of 40 m yields 450 lpm under a drawdown of 3.2 m at the pumping well. What will be the discharge in a 30-cm diameter well under a drawdown of 4.5 m in the same aquifer? Assume the radius of influence to remain constant at 450 m in both cases.

10.12. A 45-cm well in an unconfined aquifer of saturated thickness of 45 m yields 600 lpm under a drawdown of 3.0 m at the pumping well. (i) What will be the discharge under a drawdown of 6.0 m? (ii) What will be the discharge in a 30-cm well under a drawdown of 3.0 m? Assume the radius of influence to remain constant at 500 m in both cases.

10.13. A 45-cm well penetrates an unconfined aquifer of saturated thickness of 30 m completely. Under a steady pumping rate for a long time, the drawdowns at two observation wells 15 and 30 m from the well are 5.0 and 4.2 m, respectively. If the hydraulic conductivity of the aquifer is 20 m/day, determine the discharge and the drawdown at the pumping well.

10.14. Determine the discharge and the drawdown at a pumping well of 45-cm diameter, if it fully penetrates an unconfined aquifer of saturated thickness of 32 m and hydraulic conductivity of 20 m/day and results the drawdowns of 7.0 and 6.2 m in two observation wells at 15 and 30 m from the well, respectively, under a steady pumping for a long time.

10.15. The discharge from a fully penetrating well operating under steady state in a confined aquifer of 35 m thickness is 3000 lpm. Values of drawdown at two observation wells 12 and 120 m away from the well are 3.0 and 0.30 m, respectively. Determine the hydraulic conductivity of the aquifer.

10.16. Three pumping wells 30-cm diameter each are placed along a straight line at spacing of 100 m in a confined aquifer of thickness 50 m and transmissibility 2000 m^2/day. What should be the steady-state pumping rate from each well so that the drawdown in each well will not exceed 1.0 m considering radius of influence of each well as 1000 m?

10.17. The foundation in a construction site is 4.5 m deep, whereas the position of the prevailing water table is 3.0 m below the ground surface. The site is to be dewatered up to 0.5 m below the foundation level by steady pumping of a well located at the cente of the site of 100 m×80 m in size. Determine the pumping rate if the initial saturated thickness and the hydraulic conductivity of the aquifer are 20 m and 80 m/day, respectively.

10.18. A 30-cm well penetrates 45m below the static water table. After a long period of pumping at a rate of 1200 lpm, the drawdown in the wells 20 and 45 m from the pumped well is found to be 3.8 and 2.4 m, respectively. Determine the transmissibility of the aquifer. What is the drawdown in the pumped well?

10.19. A 20-cm well completely penetrates an artesian aquifer. The length of the strainer is 15m. What is its yield for a drawdown of 3 m. Assume K = 35 m/day and R = 300 m. If the diameter of the well is doubled, find the percentage increase in the yield, the other conditions remaining the same.

10.20. If an artesian well produces 250 lpm with a drawdown of 3 m in the pumping well, what is the rate discharge with 4 m drawdown? Assume equilibrium conditions and negligible well losses.

10.21. A 30-cm well yielding 300 lpm under a drawdown of 2 m penetrates an aquifer 35 m thick. For the same drawdown, what would be the probable yield of (i) 20-cm well and (ii) 40-cm well? Assume a radius of influence of 500 m in all cases.

10.22. A circular island of 800 m radius has an effective rainfall of 6 mm/day. A central well of 30-cm diameter is pumped at a constant rate of 600 lpm. Hydraulic conductivity for the island aquifer is 20 m/day. The depth of sea around the island is 10 m. Determine the drawdown in the well and at the water divide.

10.23. Three pumping wells 30-cm diameter each are placed along a straight line at spacing of 100 m in a confined aquifer of thickness 50 m and transmissibility 2000 m^2/day. What should be the steady-state pumping rate from each well so that the drawdown in each well is 1.5 m considering radius of influence of each well as 1000 m?

10.24. Two tube wells of 20-cm diameter are spaced 120 m distance and penetrate fully a confined aquifer of 12 m thickness. Calculate the discharge when only one well is discharging under a depression head of 3 m. What will be the percentage decrease in the discharge of this well if both the wells are discharging under the depression head of 3 m? Assuming the radius of influence for each well as 200 m and hydraulic conductivity of the aquifer as 40 m/day.

10.25. A 1.5-m diameter well penetrates vertically through a 30-m thick confined aquifer. When the well is pumped at 115 m^3/h, the drawdown in wells at 15 m and 50 m away are 1.8 m and 0.9 m, respectively. What are the approximate head and drawdown in the pumped well for steady-state conditions? Also, compute the transmissivity of the aquifer and the radius of the influence of the pumping well. Take the initial piezometric level as 42 m above the datum.

10.26. Water is pumped at the rate of 3000 lpm from a 30-cm well fully penetrating a strip aquifer 1.5 km wide bounded by two field ditches. Assuming the transmissibility of the aquifer as 0.02 m^3/s, what is the drawdown at the well face if (i) the well is at the centre of the strip and (ii) the well is at 400 m from one ditch? What is the drawdown in an observation well in case (i) located at (300 and 400 m) with reference to pumping well?

Chapter 11 Unsteady State Solutions to Confined Aquifer Problems

Governing equations have been derived in Chapter 10 to relate well flow to drawdown in piezometric surface (or water table), transmissivity, and storativity of aquifers. Unsteady flow governing equations include the effect of time and they enable the calculation of the drop in piezometric surface or water table in relation to time since pumping began. The difficulty in solving groundwater problems depends on the degree to which the flow is three dimensional (3-D). It is practically impossible to solve analytically a natural 3-D groundwater flow problem unless axis symmetry makes it possible to convert into a 2-D form. In many cases, the regional groundwater flow can be considered coplanar or 2-D case. Even 2-D problems may be hard to solve because of difficult boundary conditions and inhomogeneity and anisotropy in the porous media. In some cases, the problem may be simplified by reducing the dimensionality of the problem to one. However, a significant error may be introduced in step-by-step simplification from 3-D to 1-D. If the problem is time dependent, it is more difficult to solve the problem due to additional dimension. However, *the additional dimension due to time is not as much difficult as additional dimension due to space*. The partial differential equations for groundwater flow have higher order derivatives with respect to space variables than with respect to the time variable. Therefore, in general it is easier to solve a 2-D unsteady flow than a 3-D steady flow problem.

11.1 Single-Well Solution

The governing equation derived in Chapter 10 can be solved with appropriate boundary and initial conditions for an unsteady problem of uniform discharge from a well in a confined aquifer. To make analytical solution possible, the derivation of equations relating well discharge to water level drawdown and hydraulic properties of aquifers is based on the following assumptions:

(i) Aquifer is homogeneous and isotropic,
(ii) Aquifer is of uniform thickness and bedrock is horizontal,
(iii) Aquifer is of infinite areal extent having no lateral inflow from surrounding water bodies,
(iv) Well penetrates the entire aquifer and its diameter is small,
(v) Well is pumped at constant rate Q and the entire discharge is provided by the release of stored water and the water is instantaneously removed from the well,
(vi) Initially the piezometric surface is horizontal.

The radial flow to a fully penetrating well in a homogeneous and isotropic confined aquifer is horizontal everywhere. The storage coefficient S is equal to the volume of water released from unit area of aquifer corresponding to unit decline in the head, accordingly

$$S = \frac{V}{\Delta A \Delta \text{h}} = \frac{\Delta Q . \Delta t}{r d\theta \, dr . \Delta h} \tag{11.1}$$

where ΔA is as shown in Figure 11.1; h is function of both space and time $h = h(r, \theta, t)$.

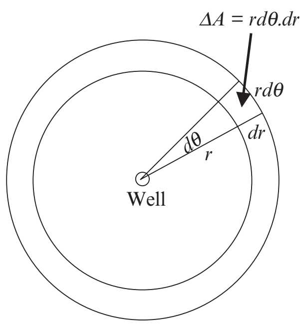

Figure 11.1 *Elementary area*

In general, the above equation for a discharging well in confined aquifer (see Figure 11.2) can be rewritten as

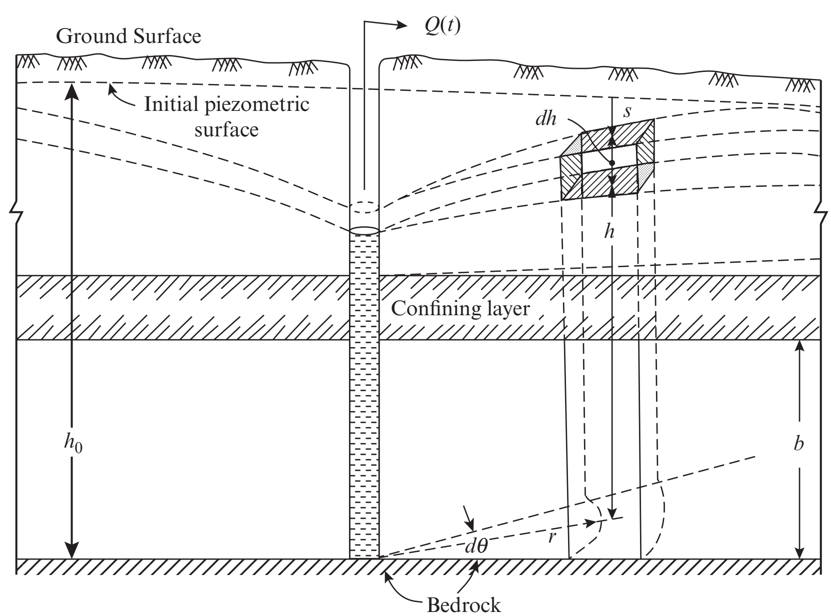

Figure 11.2 *Unsteady radial flow toward a well in confined aquifer*

$$dQ = -Srd\theta\, dr.\frac{\partial h(r,\theta,t)}{\partial t} \tag{11.2}$$

Therefore,

$$Q(t) = -\int_0^{2\pi}\int_{r_w}^{\infty} Sr\frac{\partial h(r,\theta,t)}{\partial t}\, d\theta dr = -2\pi S\int_{r_w}^{\infty} r\frac{\partial h(r,\theta,t)}{\partial t}\, dr \tag{11.3}$$

The distribution of head is radially symmetric in an aquifer of infinite extent tapped by a single well, and if Q and S are constant (see Figure 11.2), then

$$Q = -2\pi S\int_{r_w}^{\infty} r\frac{\partial h(r,t)}{\partial t}\, dr \;\Rightarrow\; \frac{Q}{2\pi S} = -\int_{r_w}^{\infty} r\frac{\partial h(r,t)}{\partial t}\, dr \tag{11.4}$$

This shows that for the right-hand side to be constant $r\partial h / \partial t$ should be constant; hence, the rate of decline of head must decrease continuously as the area affected by pumping (r) spreads out as time goes on, in order to make the integral a constant. Consequently, there can be no steady flow in a confined aquifer of infinite extent.

Also, at any radial distance r, the constant discharge from the continuity equation is

$$Q = Av_r = 2\pi rbK\frac{\partial h(r,t)}{\partial r} \Rightarrow r\frac{\partial h(r,t)}{\partial r} = \frac{Q}{2\pi T} \tag{11.5}$$

where, v_r = radial velocity at distance r from the center of well and $T = bK$ = transmissivity of the aquifer. Theis (1935) gave a solution for radial flow in homogeneous and isotropic confined aquifer based on the analogy with the conductive flow of heat to a sink in a plate. This radial flow in homogeneous and isotropic confined aquifer problem can be stated as:

Solve
$$\frac{\partial^2 h}{\partial r^2} + \frac{1}{r}\frac{\partial h}{\partial r} = \frac{S}{T}\frac{\partial h}{\partial t} \tag{11.6}$$

for the boundary conditions (for $t > 0$)

$$h(r,t) \to h_0 \quad \text{as } r \to \infty \tag{11.7}$$

$$r\frac{\partial h(r,t)}{\partial r} = \frac{Q}{2\pi T} \tag{11.8}$$

and the initial condition $(\text{for } t \le 0)$

$$h(r,0) \to h_0 \tag{11.9}$$

The initial condition states that the head in the aquifer was uniform till the pumping started, which is also an assumption as *initially the piezometric surface is horizontal everywhere*.

Theis's solution of the above problem is given by

$$h = h_0 - \frac{Q}{4\pi T}\int_u^{\infty}\left(\frac{e^{-x}}{x}\right)dx \tag{11.10}$$

The involved integral is only a function of the lower limit u, which is defined as

$$u = \frac{r^2 S}{4Tt} \tag{11.11}$$

It can be verified that Eqn. (11.10) is a solution of the problem stated in Eqs (11.6)–(11.9) by substitution of the expression for h in the governing differential equation. The exponential integral $\int_u^{\infty}\left(\frac{e^{-x}}{x}\right)dx$ is known as *Well Function* $W(u)$ in groundwater hydrology, that is,

$$W(u) = \int_u^{\infty}\left(\frac{e^{-x}}{x}\right)dx \tag{11.12}$$

In terms of well function, Eqn. (11.10) can be rewritten as

$$h = h_0 - \frac{Q}{4\pi T}.\,W(u) \tag{11.13}$$

or

$$s = \frac{Q}{4\pi T}.\,W(u) \tag{11.14}$$

Equations (11.13) and (11.14) are known as *Theis equation* or *non-equilibrium equation*. It is important to note that in Theis solution Eqn. (11.14), any arbitrary constant or radius of influence is not involved and it includes drawdown at single location unlike two drawdowns in Thies's steady-state equation. Although its derivation has been based on several assumptions as listed earlier, which are seldom justified in field tests, the nonequilibrium formula can be applied in determining the aquifer parameters and solving groundwater flow to confined aquifer problems.

Advantages of Theis non-equilibrium equation are

(i) both aquifer parameter (S and T) can be estimated;
(ii) only short duration pumping is required;
(iii) single observation well is sufficient;
(iv) estimation of aquifer parameters is economical by this method due to short duration pumping and single observation well requirement.

11.2 Computation of Well Function

The exponential integral has many applications in transient groundwater flow, hydrological problems, mathematical physics, and applied mathematics. Theis equation involves the exponential integral or well function; hence, its computation is prerequisite. The exponential integral cannot be evaluated analytically in terms of elementary functions; hence, certain numerical procedures must be used for its approximation. Mathematical tables have been developed to serve the practical needs. Many books contain such tables. *Appendix D* tabulates values of the well function. Figure 11.3 plots the well function.

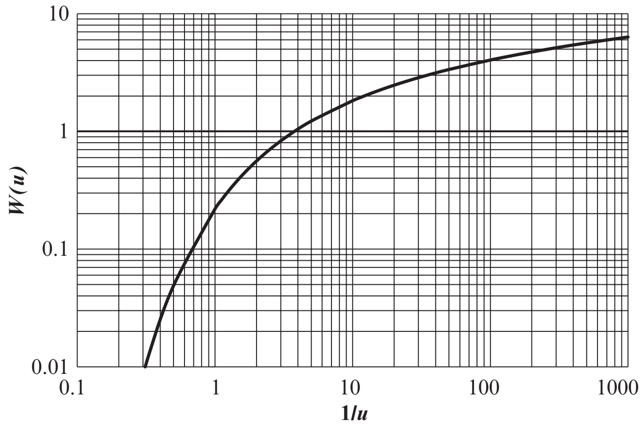

Figure 11.3 *Well function plot*

The well function behaves like a negative exponential for large values of the argument and like a logarithm for small values of the argument. The nonanalytic nature of the exponential integral has led to the development of various approximation methods; each is suitable for a limited range of argument u. The most widespread means of approximating an arbitrary function on a given interval is by polynomials of certain degree n. Unfortunately, it may often happen that for a desired accuracy a polynomial approximation would either be of prohibitively high degree or need to be partitioned into a sufficient number of piecewise approximations. Besides this drawback, nontrivial polynomials fail to approximate a function with singularities. To resolve all these difficulties, it is sometimes preferable to approximate a function using rational forms, which are the ratios of two polynomials, but these may be quite cumbersome to implement.

The problem now lies in how to choose an appropriate technique from a large number of available methods. Different methods are suitable for approximation of $W(u)$ in different ranges of argument u at a given accuracy. Among all these approximations, the series expansion based on expanding the exponential integral in power series is still the most widely used one for small values of u. The exponential integral or well function is only a function of u. It can be expressed as an infinite series as

$$W(u) = -.5772 - \ln u + u - \frac{u^2}{2.2!} + \frac{u^3}{3.3!} - \frac{u^4}{4.4!} + \dots \tag{11.15}$$

Thus, the well function can directly be computed using the series expansion but it is valid for $u > 0$ and there is a singularity in the well function at $u = 0$. Equation (11.15) is a convergent series for any finite value of u. However, the slow convergence rate for large argument u makes Eqn. (11.15) unsuitable for practical application. For instance, when u = 20 it is necessary to evaluate up to n = 75 terms in order to get an accuracy of only two significant figures. To avoid possible overflow and cancellation error, Eqn. (11.15) can be employed for $u < 4$.

Cooper Jacob (1946) used only the first two terms of the series as an approximate method of computation of the well function for small values of u. If $u < 10^{-2}$, the values of third term onwards in the series are negligible in comparison to the first two terms, therefore

$$W(u) = -0.5772 - \ln u = \ln e^{-0.5772} - \ln u = \ln \frac{1}{ue^{0.5772}} \tag{11.16}$$

or

$$W(u) = \ln\left(\frac{2.25Tt}{r^2S}\right) = 2.302\log\left(\frac{2.25Tt}{r^2S}\right) \tag{11.17}$$

Thus, from Eqn. (11.14) and Eqn. (11.17)

$$s = \frac{Q}{4\pi T}\ln\frac{1}{ue^{0.5772}} = \frac{Q}{4\pi T}\ln\left(\frac{2.25Tt}{r^2S}\right) = \frac{2.302Q}{4\pi T}\log\left(\frac{2.25Tt}{r^2S}\right) \tag{11.18}$$

For small value of u, that is $u < 10^{-2}$ Cooper–Jacob method avoids the interpolation or extrapolation of tabulated values of well function.

Although a small u can be mathematically due to any of the four parameters (i.e. r, S, T, and t) or their combination, the small u (< 0.01) in reality means large pumping times. Cooper–Jacob approximation is not useful in practical situations of early time pump test data collected from far-off observation wells. In geological formations involving petroleum, the lower transmissivity value will prohibit the use of Cooper–Jacob approximation. Beyond this range,the well function may be approximated (Singh 2008, 2010) by the following equations:

$$W(u) = \ln\left(\frac{625}{628\sqrt{\pi u}}\right) \quad \text{for } u < \frac{2}{69} \tag{11.19a}$$

$$W(u) = \left[e^{u}\left(\frac{241}{250}u + \frac{\pi}{3+\sqrt{2}}u^{1/4}\right)\right]^{-1} \quad \text{for } \frac{200}{23} \geq u \geq \frac{2}{69} \tag{11.19b}$$

$$W(u) = \ln\left(\frac{0.5614}{u}\right) \quad \text{for } u \leq 0.029 \tag{11.19c}$$

$$W(u) = \frac{e^{u}}{0.964u + 0.712u^{1/4}} \quad \text{for } u > 0.029 \tag{11.19d}$$

In addition, the evaluation of combined effects of a multiple well system including possible image wells may result in a relatively broad range of u due to the broad range of distance to wells. In practical applications, we often need to approximate $W(u)$ for a range of u broad enough such that using multiple approximation methods is required. The typical behavior makes developing a full-range straightforward approximation to calculate the well function a difficult task. ***Swamee-Ojha (1990)*** proposed an approximation for the well function for the full range of u as follows:

$$W(u) = \left(\left\{ \ln\left(\frac{1}{ue^{0.5772}} + 0.65 \right) + \ln(1+u) \right\}^{-7.7} + u^4 e^{7.7u} (2+u)^{3.7} \right)^{-0.13} \tag{11.20}$$

The maximum absolute error involved in the computed values of $W(u)$ using Eqn. (11.20) nowhere exceeds 1 percent, but the error in its derivative is higher. The derivative of the drawdown curve became more critical than the drawdown for slope-matching methods, and thus an accurate approximation of the well function should be able to accurately reproduce the derivative of the well function. For that purpose, ***Vatankhah (2014)*** further refined Swamee-Ojha's approximation as follows:

$$W(u) = \left(\left\{ \left(1 - 0.19u^{0.7}\right) \ln\left(\frac{1}{ue^{0.5772}} + 4 \right) \right\}^{-2} + \left(ue^u \frac{1.384+u}{0.444+u} \right)^2 \right)^{-0.5} \tag{11.21}$$

The maximum relative error in this approximation and its derivative are less than 0.2 and 0.22 percent, respectively.

11.3 Multiple Wells (Well Field) in a Confined Aquifer

Groundwater is often extracted by more than one well. For a large town or large water demand centers, a battery of wells is installed to meet the water requirement. A group of wells operating in a given area constitute a *well field*. As a well is pumped, a cone of depression forms and grows with time. Unless the periods of continuous operation are relatively short and/or the spacing of the wells in a well field is so great that their zones of influence do not effectively overlap, the discharge or drawdown of individual wells is affected by the neighboring wells. When multiple wells are present in an aquifer and they are spaced at distances smaller than their radius of influence, they affect each other's drawdown and discharge rate. Where the cones of depression of two nearby pumping wells overlap, the wells *interfere* with each other. Interference means that there is more drawdown than expected in each of the pumping wells because the water-level decline in a pumping well is not only due to its actual pumping but also due to drawdown caused by nearby wells causing increased drawdown and pumping lift. Therefore, multiple wells in an aquifer should be spaced as far apart as possible so that their areas of influence will produce a minimum interference with each other; but at the same time, they should be located such a manner that the cost of transporting the water to a central location of the well field is minimum. The spacing of wells is often dictated by practical considerations such as property boundaries and existing distribution pipe networks.

For a group of wells forming a well field, the head or drawdown at any point can be computed using the method of superposition. The principle of superposition can be applied for unsteady flow in confined aquifers because the parameters

T and S remain constant. In effect, the governing differential equation for confined aquifer is linear, making the solution additive. In a confined aquifer, well field consisting of N steadily discharging wells, each of the well separately satisfies the well boundary value problem, and the boundary condition at the face of each well is not influenced by the existence of the other wells. In case of unconfined aquifers, where T is a function of drawdown, the governing equation is nonlinear and superposition method is not applicable. From the principle of superposition, the drawdown at any point in the area of influence caused by the discharge of several wells is equal to the sum of the drawdowns caused by each well individually, thus for confined aquifer in case of multiple wells,

$$s = \sum_{i=1}^{N} s_i = \frac{1}{4\pi T}\sum_{i=1}^{N} Q_i W(u_i) \tag{11.22}$$

If the location of each of N wells is known and the drawdown/peizometric head at the end of a given period of continuous pumping is given, the discharge of each well can be obtained by solving the N linearly independent equations written for the drawdown for each well using Eqn. (11.22). For two wells at distance l in a confined aquifer,

$$s_{w1} = \frac{1}{4\pi T}\left\{Q_1 W\left(\frac{r_w^2 S}{4Tt}\right) + Q_2 W\left(\frac{l^2 S}{4Tt}\right)\right\} \text{ or } Q_1 W\left(\frac{r_w^2 S}{4Tt}\right) + Q_2 W\left(\frac{l^2 S}{4Tt}\right) = 4\pi T s_{w1} \tag{11.22a}$$

$$s_{w2} = \frac{1}{4\pi T}\left\{Q_2 W\left(\frac{r_w^2 S}{4Tt}\right) + Q_1 W\left(\frac{l^2 S}{4Tt}\right)\right\} \text{ or } Q_1 W\left(\frac{l^2 S}{4Tt}\right) + Q_2 W\left(\frac{r_w^2 S}{4Tt}\right) = 4\pi T s_{w2} \tag{11.22b}$$

These two linear equations in Q_1 and Q_2 can be solved. If $s_{w1} = s_{w2} = s_w$, then

$$Q_1 = Q_2 = 4\pi T s_w \,/\left\{W\left(\frac{l^2 S}{4Tt}\right) + W\left(\frac{r_w^2 S}{4Tt}\right)\right\} \tag{11.22c}$$

Similarly, for three wells forming an equilateral triangle of side l and producing same drawdown s_w at the face of each well

$$Q_1 = Q_2 = Q_3 = 4\pi T s_w \,/\left\{2W\left(\frac{l^2 S}{4Tt}\right) + W\left(\frac{r_w^2 S}{4Tt}\right)\right\} \tag{11.22d}$$

If $u = l^2 S / 4Tt < 0.01$, Cooper–Jacob approximation yields, $Q_1 = Q_2 = Q_3 = Q$ as follows:

$$Q = 4\pi T s_w \,/\left\{2\ln\left(\frac{2.25Tt}{l^2 S}\right) + \ln\left(\frac{2.25Tt}{r_w^2 S}\right)\right\} = 4\pi T s_w \,/\left\{3\ln\left(\frac{2.25Tt}{S}\right) - 2\ln\left(l^2 r_w\right)\right\} \tag{11.22e}$$

The discharge of equal strength wells forming a square for time having small u is

$$Q = \frac{4\pi T s_w}{\ln\left(\frac{2.25Tt}{r_w^2 S}\right) + 2\ln\left(\frac{2.25Tt}{l^2 S}\right) + \ln\left(\frac{2.25Tt}{2l^2 S}\right)} = \frac{4\pi T s_w}{4\ln\left(\frac{2.25Tt}{S}\right) - 2\ln\left(\sqrt{2}l^3 r_w\right)} \tag{11.22f}$$

When estimates of the drawdown are required, the influence of other wells operating in the area has to be included. If the locations and discharges of each of the wells in the area are known, the total drawdown at a desired location can be found by the method of superposition using Eqn. (11.22). Clearly, the number of wells and the geometry of the well field are important in determining drawdowns. The total drawdown in one pumped well caused by pumping other nearby wells can be obtained by using Eqn. (11.22). Consequently, the total additional head caused by well interference can be expressed in terms of the unknown intervening distances, the assumedly known hydraulic properties, and the parameters defining the geometry of the flow system.

The problem of spacing production wells is frequently encountered. The farther apart wells are spaced, the lesser their mutual interference, but the greater the cost of connecting pipeline and electrical equipment. Thus in a well field, the proper spacing of wells involves economics as well as aquifer-well hydraulics. If spacing between the wells is less, the interference will be more, but the cost of connecting pipelines and power installation will be less. The cost may be expressed as annual cost of lifting the water against the additional head caused by well interference and the cost of connecting pipelines between the wells and the power installation. Therefore, the total annual cost C can be expressed as follows:

$$C = C_1 l + C_2 \sum_{i=1}^{N} Q_i \int_0^{t_0} s_i \, dt \tag{11.22g}$$

where, C_1 is the capitalized cost per unit length of pipeline for maintenance, depreciation, original cost of pipe line, as well as taxes and interest on borrowed capital,etc.; C_2 is the cost to raise a unit volume of water a unit height, consisting largely of power charges, but also properly including some additional charges on the equipment; s_i is the total drawdown in the ith well caused by pumping all the other wells; l is the length of connecting pipe lines between wells and the power installation; N is the number of wells in operation; Q_i is the discharge of the ith well; and t_o is the period of continuous pumping.

The minimum cost will correspond to that point at which the first derivative of C with respect to l equals zero. By differentiating the above equation and equating the resulting expression to zero, the following relation is obtained:

$$\sum_{i=1}^{N} Q_i \int_0^{t_0} \frac{ds_i}{dl} dt = -\frac{C_1}{C_2} \tag{11.22h}$$

Hantush (1964) solved this equation to get the following relation for the optimal spacing l^* between the wells:

$$l^* = \frac{C_2}{\delta C_1}\frac{t_0}{2\pi T}\sum_{i=1}^{N} Q_i \sum_{j=1}^{N} Q_j \quad \text{for } j = i, Q_j = 0 \tag{11.22i}$$

where, δ represents the geometrical configuration of wells. For three wells Eqn. (11.22i) becomes as follows:

$$l^* = \frac{C_2}{\delta C_1}\frac{t_0}{pT}\left(Q_1Q_2 + Q_1Q_3 + Q_3Q_2\right) \tag{11.22j}$$

If wells have same discharge and form an equilateral triangle ($\delta = \sqrt{3}$), then

$$l^* = \frac{C_2}{C_1}\frac{\sqrt{3}\,t_0}{\pi T}Q^2 \tag{11.22k}$$

If wells have same discharge and located along a straight line at equidistant ($\delta = 2$), then

$$l^* = \frac{C_2}{C_1}\frac{3t_0}{2\pi T}Q^2 \tag{11.22l}$$

For two wells ($\delta = 1$), the optimal spacing is given by the following equation:

$$l^* = \frac{C_2}{C_1}\frac{t_0}{\pi T}Q^2 \tag{11.22m}$$

Similar analysis results in expressions for the optimum spacing parameter of various grouping of wells in different flow systems. Swamee et al., (1999) obtained optimal configurations of well fields by considering the minimum cost and the maximum reliability aspects for transporting the water to the center of the well field for its onward transmission to the treatment works. Theis (1957) derived the following equation for determining the optimum well spacing in the simple case of two wells pumping at the same rate from a thick and a really extensive aquifer

$$l^* = \frac{C_2}{C_1}\frac{55.16\times 10^8}{\pi T}Q^2 \tag{11.22n}$$

For small values of T and Q, spacing from Eqn. (11.22n) is of no practical significance. Because the effects of partial penetration are appreciable within a distance of about twice the saturated thickness of the aquifer from the well, it is generally advisable to space wells at least a distance of twice the saturated thickness apart in aquifers 30 m or less thick. Experience has shown that in the case of a multiple well system consisting of more than 2 wells, the proper spacing between wells is at least 80–100 m. Production wells should be spaced parallel to and as far away as possible from barrier boundaries and as near to the center of a buried valley as possible. Wells should be spaced on a line parallel to a recharge boundary and as close to the source of recharge as possible. The approximate permissible distance between production and disposal wells in a really extensive isotropic aquifer was suggested as $2Q/Ti$ by Theis (1941).

The total drawdown in one pumped well caused by pumping other nearby wells can be obtained using Eqn. (11.22). Consequently, the total additional head caused by well interference can be expressed in terms of the unknown intervening distances, the assumedly known hydraulic properties, and the parameters defining the geometry of the flow system.The maximum allowable drawdown in a well may be fixed by taking into account the field and constructional conditions rather than economic considerations. Physical limitations of the aquifer (depth, thickness, etc.), limitations of pump (suction lift, power rating, etc.) and depths of existing wells are important factors limiting the permissible drawdown in a well. In a well field for known pumping discharge and schedule of operation, the resultant drawdown at critical locations can be expressed by method of superposition using Eqn. (11.22). By equating this resultant drawdown with the permissible drawdown, the unknown spacing can be determined. Conversely, for the known location of the wells, the pumping discharges that produce the limiting drawdown can be calculated. For example, for a group of N wells pumping simultaneously from a confined aquifer and forming a circular battery of N-1 wells, with the maximum draw down occurring in the N-th well that is located at the center of the circular battery, the following is the relation:

$$W(u_r) = \left[4\pi T s_N - Q_N W(u_w)\right] / \sum_{i=1}^{N-1} Q_i \tag{11.22o}$$

where, s_N is the maximum permissible drawdown in the Nth well at the centre at end of a continuous period t_o of simultaneous pumping; $u_r = \dfrac{r^2 S}{4Tt_0}$; and $u_w = \dfrac{r_w^2 S}{4Tt_0}$. All the terms of the right-hand side are given, Eqn. (11.22o) yields value of $W(u_r)$. From table of the well function $W(u)$, the value of u_r corresponding to the known value of $W(u_r)$ can be obtained. Consequently, the value of r (radius of the circular battery) can be obtained.

11.4 Residual Drawdown

When pump is stopped, the water levels in pumping and observation wells begin to rise, which is known as *recovery* or *recuperation* of groundwater levels. After a long time, the levels completely recoup and acquire the initial water/piezometric levels in the aquifer. The drawdown during recovery period is called *residual drawdown* (See Figure 11.4). If a well is pumped for a known period of time and then stopped, the drawdown thereafter will be identically the same as if the discharge had been continued and a hypothetical recharge well with the same flow were superposed on the discharging well at the instant the pumping stopped.

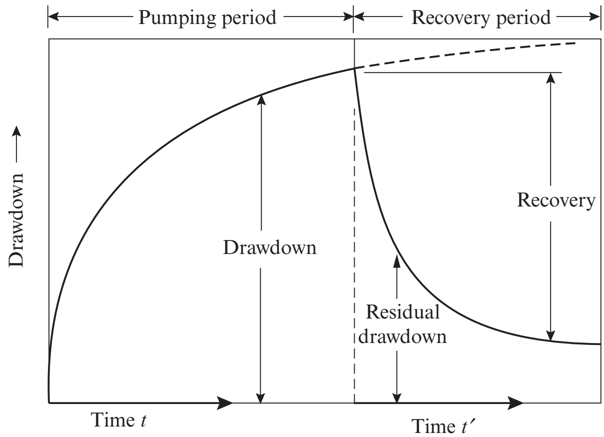

Figure 11.4 *Residual drawdown during recovery*

By method of superposition the residual drawdown s' will be

$$s' = s_{\mathrm{p}} + s_{\mathrm{R}} = \frac{Q}{4\pi T} W\left(u_{\mathrm{p}}\right) - \frac{Q}{4\pi T} W\left(u_{\mathrm{R}}\right) = \frac{Q}{4\pi T}\left(W\left(u_{\mathrm{p}}\right) - W\left(u_{\mathrm{R}}\right)\right) \qquad (11.23)$$

where, s_{p} = drawdown due to pumping well; s_{R} = drawdown due to hypothetical recharging well; $u_{\mathrm{p}} = \dfrac{r^2 S}{4Tt}$; $u_{\mathrm{R}} = \dfrac{r^2 S}{4Tt'}$; t = time since pumping started; and t' = time after pumping stopped. For small r and large t' both u_{p} and u_{R} may be small (less than 0.01), then Cooper–Jacob approximation for well function can be used to get residual drawdown

$$s' = \frac{Q}{4\pi T}\left[\ln\left(\frac{1}{u_{\mathrm{p}} e^{0.5772}}\right) - \ln\left(\frac{1}{u_{\mathrm{R}} e^{0.5772}}\right)\right] = \frac{Q}{4\pi T}\ln\left(\frac{u_{\mathrm{R}}}{u_{\mathrm{p}}}\right) = \frac{Q}{4\pi T}\ln\frac{t}{t'} \qquad (11.24)$$

Therefore, a plot between residual drawdown and logarithm of t/t' is a straight line as shown in Figure 11.5.

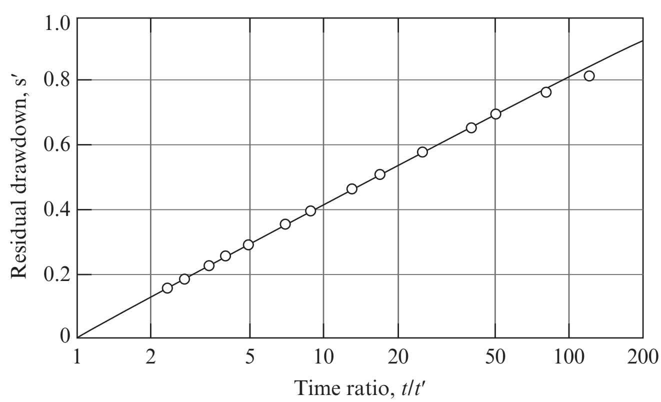

Figure 11.5 *Semilog plot of residual drawdown*

11.5 Wells Near Boundaries (Method of Images)

To develop/apply earlier solutions (steady/unsteady), one basic assumption as the aquifer of infinite areal extent was made. It is obvious that this type of aquifer cannot exist in reality and the aquifers have some boundaries; thus, very extensive aquifers are rarely encountered in nature. In general, discontinuities in geological formations caused by faults, hills, mountains, clay/impervious material, etc., or presence of water bodies (streams, lakes, sea, etc.) as shown in Figure 11.6 exist in aquifers. The first category is impervious boundary and second is equipotential/recharge boundary. There may be third type boundary as an interface between two different aquifers. These boundaries are assumed as abrupt discontinuities to simplify the mathematical treatment. Such boundaries are of interest whenever they are located within the zone of influence of considered wells. Therefore, solutions for wells near such boundaries are developed in the subsequent sections.

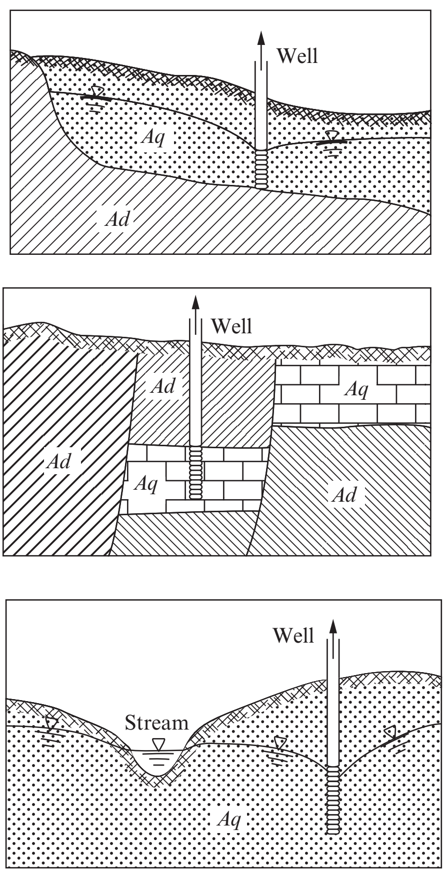

Aq = aquifer: *Ad* = aquiclude

Figure 11.6 *Different types of boundaries (Bear 1979)*

In general, well hydraulics theory cannot cope with the presence of one of these aquifer boundaries. However, it is possible to get rid of the boundary by adding imaginary/image wells. The *method of images* is most useful in the treatment of wells near straight line boundaries of the first and second types mentioned above. In method of images, the real bounded field of flow is replaced by a fictitious field with simpler boundary conditions, but in general, of a larger area. Image wells are located in the image domain such that the sought flow pattern produced in the real bounded flow domain by the real wells is the same as that produced in the same domain, now as part of the expanded real plus image domains by the ensemble of real and image wells. The location of the image well is a mirror image of the real well with respect to the straight line boundary. Although the boundary does not appear in the fictitious domain, the flow pattern still satisfies the original condition along that line. In addition, the ensemble of real and imaginary wells produces a flownet satisfying the appropriate continuity equation in the real domain.

11.5.1 Well Near a Recharge Boundary

If a water body is present near a well as shown in Figure 11.7(a), then it halts the spread of the cone of depression and influences the pattern of drawdown by providing a source of recharge to the aquifer. The drawdown at the observation well at early time corresponds to the drawdown change caused by the pumping well only and the cone of depression does not extend to the water body. Under continuous pumping, the cone of depression intersects the water body and hydraulic gradient develops between the water body and aquifer. Therefore, the water body recharges the aquifer as the cone of depression enlarges, and when the rate of recharge to the aquifer equals the rate of discharge from the well, the cone of depression becomes stable or equilibrium/steady condition occurs.

For dealing with such case, the recharge boundary can be removed by placing images of real wells with respect to the boundary as shown in Figure 11.7(b). Here an image well is opposite type as that of real well, that is, image well of a discharging well is recharging type and image well of a recharging well is discharging type. This image well operates simultaneously and at the same rate as the real well so that the build-up (due to recharging image well) and drawdown (due to real discharging well) of head along the line of boundary (water body) cancel each other. This creates a constant head along the water body. The resultant drawdowns in the aquifer can be calculated using the principle of superposition with one pumping well and other recharging well. Mathematically, the drawdown due to a single pumping well in a confined aquifer near a water body is

$$s = s_{\mathrm{p}} + s_{\mathrm{i}} = \frac{Q}{4\pi T}\left[W\left(u_{\mathrm{p}}\right) - W\left(u_{\mathrm{i}}\right)\right] \tag{11.25}$$

where s_{p} = drawdown due to pumping well; s_{i} = drawdown due to image well; $u_{\mathrm{p}} = \dfrac{r_{\mathrm{p}}^2 S}{4Tt_{\mathrm{p}}}$; and $u_{\mathrm{i}} = \dfrac{r_{\mathrm{i}}^2 S}{4Tt_{\mathrm{i}}}$. When u_1 and u_2 both are less that 10^{-2} then,

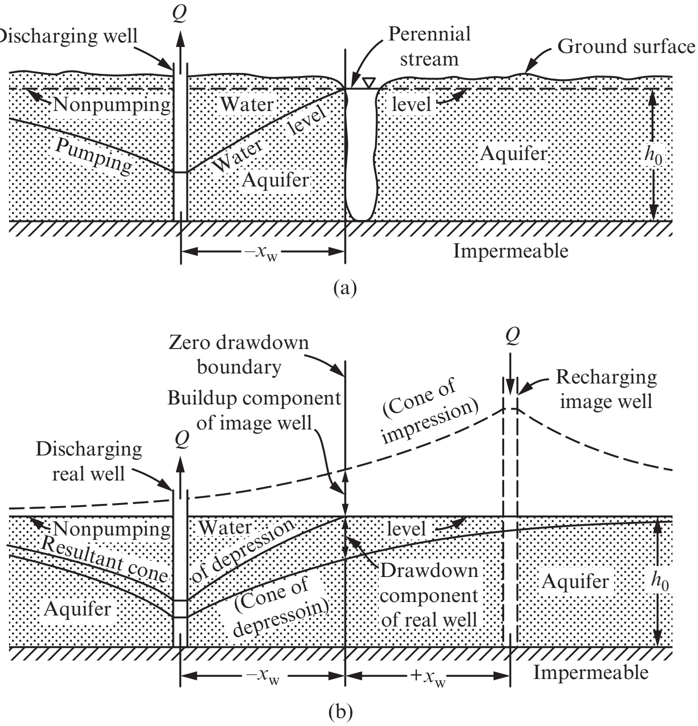

Figure 11.7 *Well near a stream or recharge boundary*

$$s = \frac{Q}{4\pi T}\left\{\ln\left(\frac{2.25Tt}{r_p^2 S}\right) - \ln\left(\frac{2.25Tt}{r_i^2 S}\right)\right\} = \frac{Q}{4\pi T}\ln\frac{r_i^2}{r_p^2} \tag{11.26}$$

This is independent of time and hence it is identical to steady case of two wells of same strength and opposite nature. In true sense it has not reached steady state; this happens due to Cooper–Jacob approximation for well function. If other approximation or more than first two terms of the series is used then it would be unsteady drawdown. In the Cartesian coordinate system the resultant drawdown at any point (x, y) is

$$s = \frac{Q}{4\pi T}\ln\frac{(x + x_w)^2 + (y - y_w)^2}{(x - x_w)^2 + (y - y_w)^2} \tag{11.27}$$

where (x_w, y_w) are coordinates of the pumping well. The water level in the wells will draw down initially only under the influence of the pumped well; after a time the effects of the recharge boundary will cause the time rate of drawdown to decrease and eventually reach equilibrium conditions when recharge equals the pumping rate. This produces a slope of equal but opposite sign on the drawdown curve, resulting in a horizontal asymptote as shown in Figure 11.8.

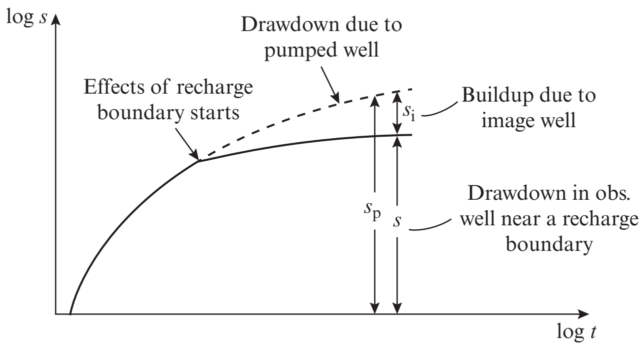

Figure 11.8 *Effect of recharge boundary on drawdown*

Considerable time elapses before a cone of depression stabilizes, water is no longer taken from storage within the aquifer, and new state of approximate equilibrium is established. The time required to reach approximate equilibrium in days, t_e, may be computed (Walton 1962) as follows:

$$t_e = \frac{487.6 x_w^2 S}{T \log(2x_w / r)^2} = \frac{487.6 x_w^2 S}{T \log\left[4x_w^2 / \left((x - x_w)^2 + (y - y_w)^2\right)\right]} \tag{11.27a}$$

11.5.2 Well Near an Impervious Boundary

Aquifers are not infinite in lateral extent because they can be cut by tight faults or they can end abruptly due to change in geology (see Figure 11.9). There is no groundwater flow across impermeable boundaries, hence they effectively halt the spread of the cone of depression and influence the pattern of drawdown resulting due to wells. The impervious boundary can be removed by placing images of real wells with respect to the boundary. Here, an image well is same type as that of real well, that is, image well of a discharging well is discharging type and image well of a recharging well is recharging type.

In the case of an impervious boundary, water cannot flow across the boundary as water is not contributed to the pumped well from the impervious formation. Because of impervious boundary there can be no flow across the boundary, the cone of depression resulting from the pumping well gets modified. The effect of the impermeable boundary to flow in some region of the aquifer is to accelerate the drawdown. To simulate an impermeable boundary, a discharging image well is created at an equal and opposite side from the real well with respect to the boundary. This creates the effect of no flow across the boundary. Drawdowns take place at an initial rate only due to the influence of the pumping well. As pumping continues the impervious boundary effects will begin, which are simulated by the image well. When the effects of the impervious boundary are realized, the time rate of drawdown will increase as shown in Figure 11.10, and the total discharge from the aquifer is equal to the pumping well and image well combined discharges causing the cone of depression of the real well to be deflected downward. The resultant drawdowns in the aquifer can be calculated using the principle of superposition with two pumping wells. Mathematically, the drawdown due to a single pumping well in a confined aquifer with an impervious boundary is

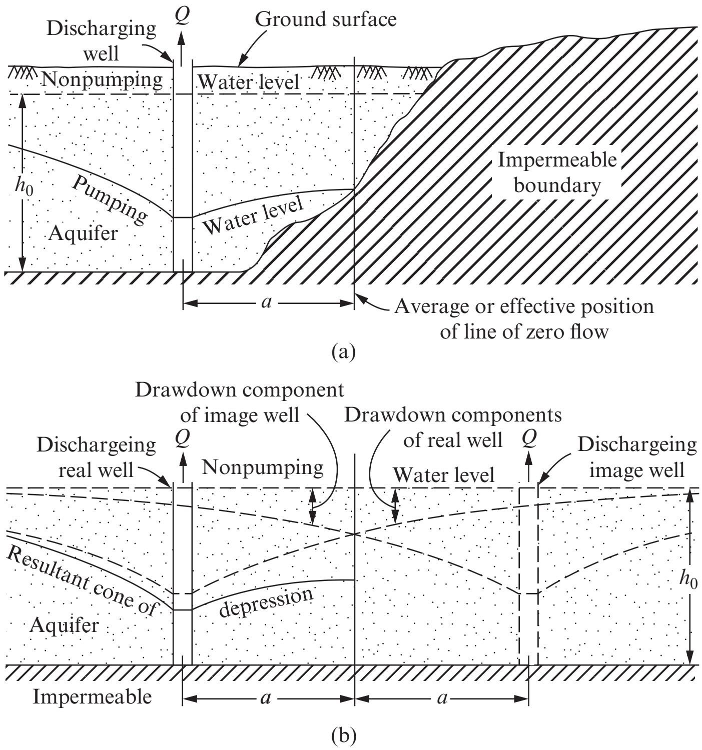

Figure 11.9 *Well near a barrier boundary (Todd and Mays 2005)*

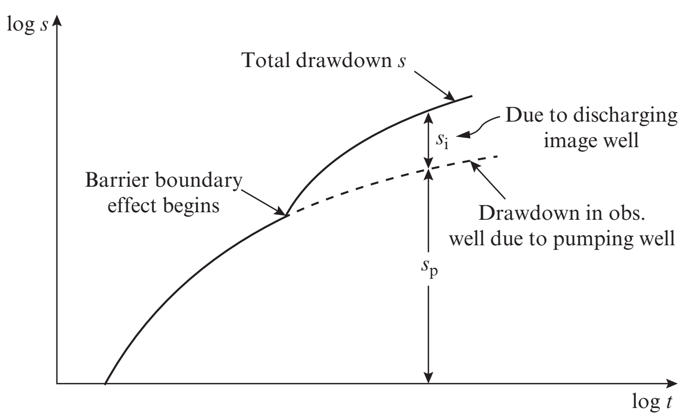

Figure 11.10 *Increased drawdown due to impervious boundary*

$$s = s_p + s_i \tag{11.28}$$

Aquifer test data in an aquifer with an impervious boundary can be used to estimate hydraulic parameters as well as the location of the boundary.

Let us consider the simple case of a single straight line impermeable boundary with a single pumping well. When an aquifer is bounded on one side by a straight line impermeable boundary, drawdowns due to pumping will be greater near the boundary. When the drawdown at the observation well is plotted with time, there are two distinct slopes as shown in Figures 11.10 and 11.11. The slope at early time corresponds to the drawdown change caused by the pumping well only. The slope at later times is different, in fact twice (see Figure 11.11), because drawdown is due to both the real well and the image well. The total drawdown at any point can be expressed as

$$s = s_p + s_i = \frac{Q}{4\pi T}\left[W(u_p) + W(u_i)\right] \tag{11.29}$$

where Q = constant pumping rate, $u_p = \dfrac{r_p^2 S}{4Tt_p}$, $u_i = \dfrac{r_i^2 S}{4Tt_i}$, r_p = distance of the point from the real pumping well, r_i = distance of the point from the image well, t_p = time since pumping started to produce drawdown s_p, and t_i = time taken by image well to produce drawdown s_i (see Figure 11.11).

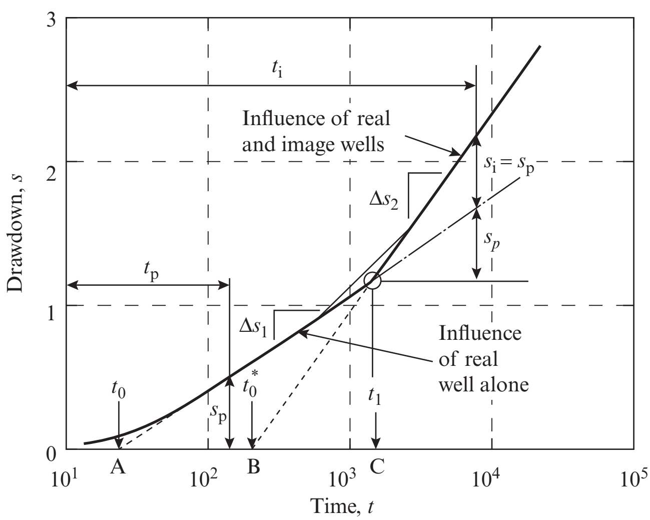

Figure 11.11 *Impervious boundary—law of times*

If we chose drawdowns at times t_p and t_i such that $s_p = s_i$, then

$$\frac{Q}{4\pi T}W(u_p) = \frac{Q}{4\pi T}W(u_i) \Rightarrow u_p = u_i \tag{11.30}$$

and hence

$$\frac{r_p^2 S}{4Tt_p} = \frac{r_i^2 S}{4Tt_i} \tag{11.31}$$

which reduces to

$$\frac{t_i}{r_i^2} = \frac{t_p}{r_p^2} \tag{11.32}$$

This relationship is known as *law of times*, which states that for a given aquifer, the times of occurrence of equal drawdown vary directly as the squares of distances from an observation well to a pumping well and corresponding image well. The law of times can be used to determine the distance from an image well to an observation well as

$$r_i = r_p \sqrt{\frac{t_i}{t_p}} \tag{11.33}$$

It is noted here that t_p = time since pumping started and before the barrier boundary is effective to produce drawdown s_p and t_i = time after pumping started and continued after the barrier boundary becomes effective taken by the image well to produce $s_i = s_p$.

11.5.3 Determining Location of a Boundary

Generally, the water body or recharging boundary near a well is visible. But impermeable subsurface boundaries such as faults or dikes may not be apparent. Well field in the vicinity of such hidden barrier boundary will perform far below the expected level. Therefore, detection of presence of any hidden subsurface impervious boundary is very important before establishing a well field. Fortunately the location and orientation of such boundaries can be identified from the observed drawdowns as follows:

- Observe drawdown in an observation well for a very long time.
- Plot these observed drawdown with logarithmic of time as shown in Figure 11.11.
- If the plot (except initial time period) is a continuous straight line, there is no recharging and barrier boundary within the influence area of the pumping well.
- If there is a break in the slope of the straight line, it shows the presence of a boundary.
- If the slope after the break becomes flatter, it indicates a recharging boundary. In this case, the resultant rate of drawdown is less and approaches a horizontal asymptote, as the recharging boundary produces a slope of equal but opposite sign on the drawdown curve.
- If the slope after the break becomes steeper, it indicates a barrier boundary. In this case, the resultant rate of drawdown in the observation well is double under the influence of an image pumping well due to the barrier boundary.
- Select an arbitrary drawdown s_p before the break in slope (under the influence of real well only) and note the corresponding time t_p as shown in Figure 11.11.

- Identify a point on the plot after the break having drawdown $2s_p$ above the break point (or s_p above the extended straight line prior to the break point) and note its time t_i. This is the time taken by the image well to produce equal drawdown.
- Use law of times to compute the distance of the observation well from the image well with help of known distance from the real well to the observation well r_p and above noted values of t_p and t_i as $r_i = r_p\sqrt{t_i / t_p}$.
- Draw a circle of radius r_i with center as the observation well. The distance r_i defines only the radius of a circle on which the image well lies (see Figure 11.12).
- Repeat the above steps for two more observation wells in order to define uniquely by intersection of three arcs the location of the image well.
- Join the real and image wells and draw perpendicular bisector. The impervious boundary lies along this perpendicular bisector (see Figure 11.12).

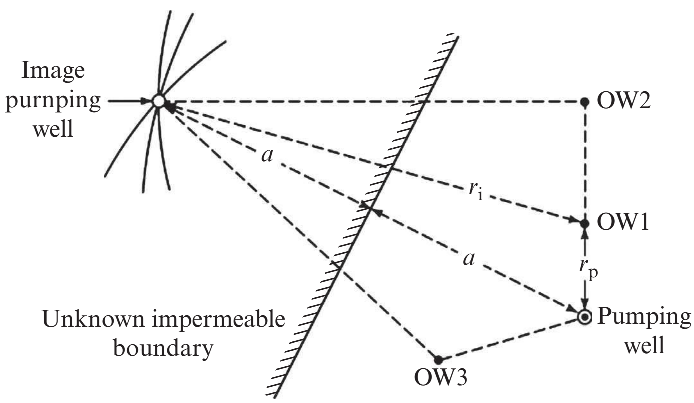

Figure 11.12 *Method of locating an impervious boundary*

Thus, at least three observation wells are required to locate uniquely the impervious boundary. Still more observation wells are preferred as some observation wells may lie in the silent zone (beyond impervious boundary) or outside the influence zone.

Generally the recharging boundary is visible. If it is hidden, still its effect on the well field is positive. Sometimes it is important to locate buried streams. The buried/lost streams may serve as lifeline by providing a good-quality groundwater source in arid regions where general groundwater is saline and surface water sources are absent. For locating buried stream, a method similar to the above mentioned for the barrier boundary can be adopted (see Figures 11.13(a) and 11.13(b)).

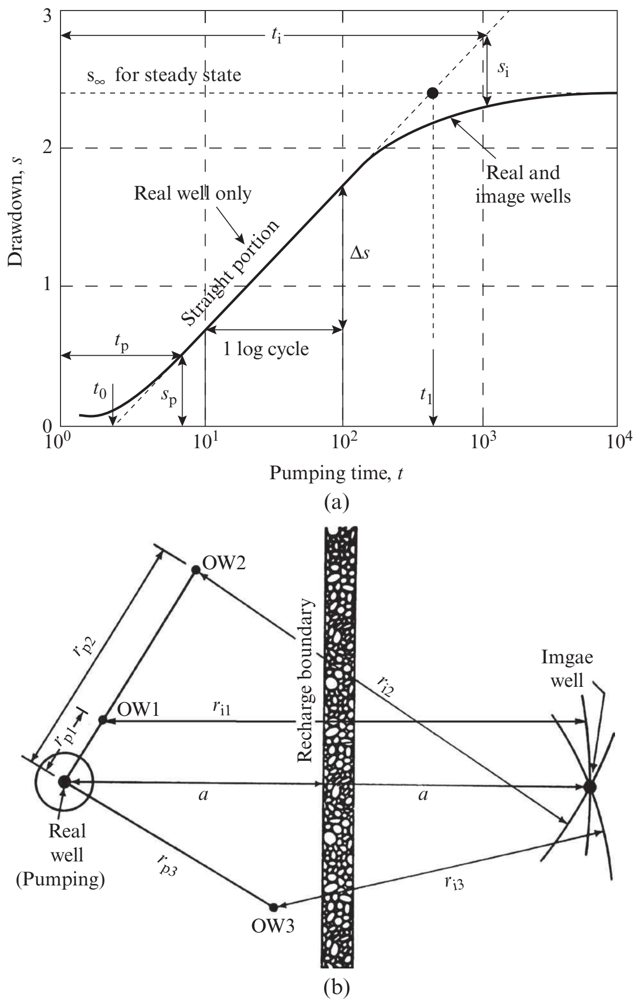

Figure 11.13 *Method of locating an recharge boundary*

11.5.4 Multiple Boundaries

Image theory is also applicable to the analysis of flow in an aquifer with multiple boundaries. Actual boundaries are replaced by an equivalent hydraulic system, which includes imaginary wells and permits solutions to be obtained from equations applicable only to extensive aquifers. With more than one boundary present, multiple image wells are needed to replace the boundaries. In locating the image well, each boundary should be considered to determine the type of image well and where it is located. In general, the number of image wells N_i required for two boundaries meeting at an angle θ is

$$N_i = \frac{360}{\theta} - 1 \tag{11.34}$$

As before actual boundaries are replaced by an equivalent hydraulic system, which is extensive areal extent and includes required number of image wells. If two boundaries are parallel to each other ($\theta = 0$), the number of images will be infinite as each successively added secondary image produces a residual effect at the opposite boundary. It is only necessary to add pairs of image wells until the next pair has negligible influence on the resultant drawdown. Examples of hydraulically equivalent aquifer systems bounded by different boundaries are shown in Figures 11.14–11.18 (Ferris et al 1962). In practice, two boundaries of the same type or different types may be encountered in valley between two hills (two impervious/barrier boundaries), stream originating from foothill (one barrier boundary and other recharge boundary), and near two streams/water bodies (two recharging boundaries). Once the hydraulically equivalent aquifer systems is ready, the method of superposition is used to compute the resultant drawdown.

For example, consider a pumping well near a tributary joining the main stream normally as shown in Figure 11.16b. Here $\theta = 90°$, hence there will be three image wells. The equivalent hydraulic system consists of one real pumping well, two recharging image wells, and one discharging image well. The resultant drawdown at any point (x, y)

$$s = s_1 + s_2 + s_3 + s_4 = \frac{Q}{4\pi T}\left[W(u_1) - W(u_2) + W(u_3) - W(u_4)\right] \tag{11.35}$$

which reduces to

$$s = \frac{Q}{4\pi T}\ln\left(\frac{r_1^2 r_3^2}{r_2^2 r_4^2}\right) \tag{11.36}$$

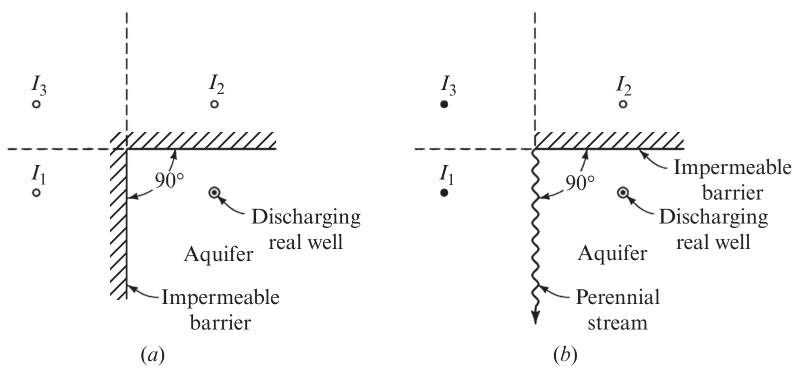

Figure 11.14 *Image wells for two perpendicular boundaries: (a) both impervious and (b) one recharge boundary and other barrier boundary*

In terms of Cartesian coordinates, the above equation can be written as follows:

$$s = \frac{Q}{4\pi T}\ln\frac{\left[(x-x_w)^2 + (y-y_w)^2\right]\left[(x+x_w)^2 + (y+y_w)^2\right]}{\left(\left[(x+x_w)^2 + (y-y_w)^2\right]\left[(x-x_w)^2 + (y+y_w)^2\right]\right.} \tag{11.37}$$

Figure 11.15 shows image wells for two impervious boundaries.

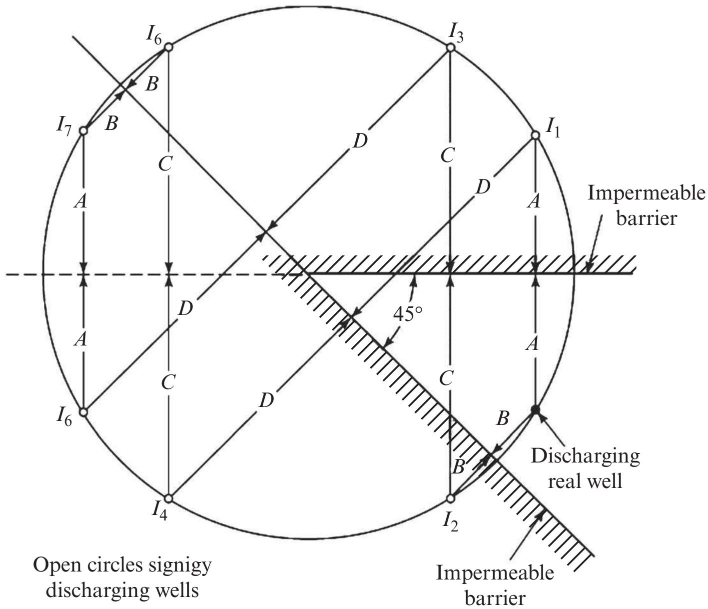

Figure 11.15 *Image wells for two impervious boundaries at 45°*

If a pumping well is located between two parallel rivers, then $\theta = 0°$; hence, there will be infinite number of images as shown in Figure 11.16c. The resultant drawdown for this case is

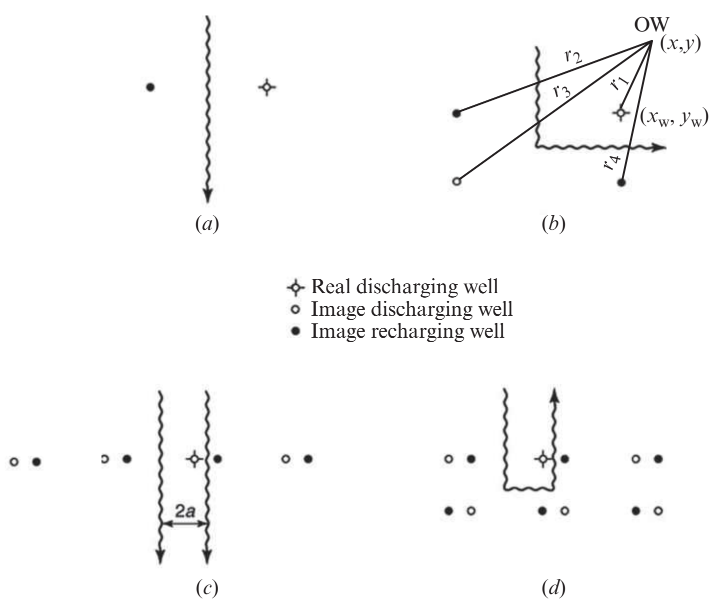

Figure 11.16 *Image wells for different configuration of a stream*

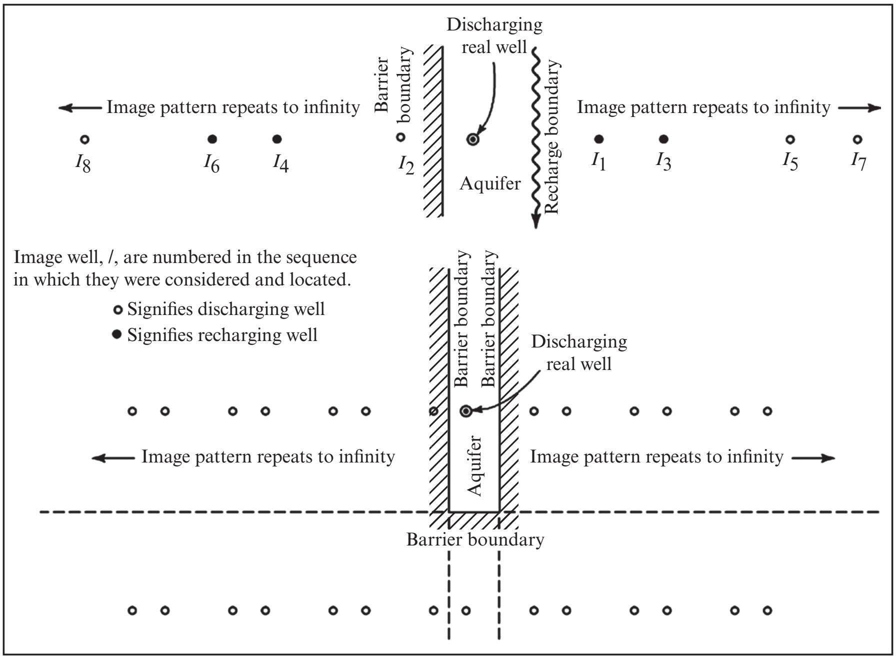

Figure 11.17 *Image wells for two parallel boundaries: (a) one recharge boundary and other barrier boundary and (b) both impervious*

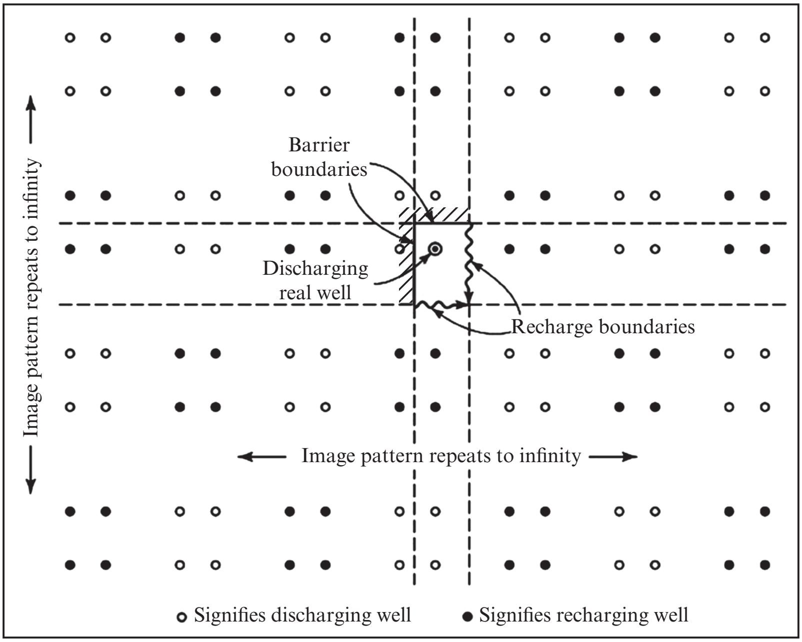

Figure 11.18 *Image wells for four perpendicular boundaries (Ferris et al., 1962)*

$$s = \frac{Q}{4\pi T} \sum_{n=-\infty}^{\infty} \ln \frac{\left(x - x_{\mathrm{w}} - 2nd\right)^2 + \left(y - y_{\mathrm{w}}\right)^2}{\left(x + x_{\mathrm{w}} - 2nd\right)^2 + \left(y - y_{\mathrm{w}}\right)^2} \tag{11.38}$$

which is equal to

$$s = \frac{Q}{4\pi T} \ln \frac{\cosh \frac{\pi\left(y - y_{\mathrm{w}}\right)}{2d} + \cosh \frac{\pi\left(x + x_{\mathrm{w}}\right)}{2d}}{\cosh \frac{\pi\left(y - y_{\mathrm{w}}\right)}{2d} - \cosh \frac{\pi\left(x + x_{\mathrm{w}}\right)}{2d}} \tag{11.39}$$

It gives approximate drawdown in the pumping well as

$$s_{\mathrm{w}} = \frac{Q}{4\pi T} \ln \frac{\pi r_{\mathrm{w}}}{2\mathrm{d} \sin\left(\pi x_{\mathrm{w}} / d\right)} \tag{11.40}$$

11.6 Stream Depletion

Many times wells are located near streams or waterbodies. If a stream is within the radius of influence of a well, a part of well discharge is contributed from the stream. Locations of well sites and design of wells are decided according to the stream contribution to the pumping. Due to discharge contribution in the pumping, the stream is depleted by same amount known as *stream depletion.* Determination of the stream contribution in the pumped water is important to ascertain the quality and quantity of the water that may be withdrawn through wells over long periods of time without critically depleting the available groundwater supply. As stream depletion also affects the stream stage and flow in the stream, its determination is important from the point of view of the legal rights of downstream users.

The discharge of a well near a stream is derived from storage in the aquifer as well as from infiltration from the stream. The infiltration of stream water into an aquifer is significant because of its effect on the quality and quantity of pumped water. Total rate of discharge of pumping through well near a stream is

$$Q_{\mathrm{w}} = Q_{\mathrm{R}} + Q_{\mathrm{A}} \tag{11.41}$$

where Q_{w} = discharge from a well, Q_{R} = river contribution in well discharge, and Q_{A} = aquifer storage contribution in well discharge. Let $\frac{Q_{\mathrm{R}}}{Q_{\mathrm{w}}} = P_{\mathrm{r}}$, which is known as *stream depletion rate* and it is the fraction of stream contribution rate in the total uniform discharge Q_{w} from a well that is steadily discharging from a homogeneous, uniform, isotropic aquifer hydraulically connected to a fully penetrating stream. Stream depletion rate was expressed by Theis (1941) as

$$P_{\mathrm{r}} = \frac{Q_{\mathrm{R}}}{Q_{\mathrm{w}}} = \frac{2}{\pi} \int_0^{\pi/2} e^{-\alpha \sec^2 \tau} d\tau \tag{11.42}$$

where, $\alpha = \dfrac{a^2 S}{4Tt}$ (dimensionless); a = effective distance between the pumping well and the recharging stream; and τ = dummy variable. It was also assumed in Eqn. (11.41) that the river stage does not change with time, which is valid when the flow in the river is much more than the quantity contributed by the river to pumping.

Equation (11.41) was expressed as a complementary error function by Glover and Balmer (1954) under confined conditions or unconfined conditions for ratios of drawdown to saturated thickness of up to 0.25 when the storage coefficient remains constant:

$$P_r = \operatorname{erfc}\sqrt{\alpha} \tag{11.43}$$

Appendix C may be referred for the complementary error function erfc ().

The total volume V (m^3), by which the stream is depleted by a continuously pumping well at constant discharge Q_w, can be found by

$$V = \int_0^t Q dt = Q_w t \tag{11.44}$$

Volume from river $V_R = \int_0^t Q_R dt$; because here Q_R is a function of time, hence it cannot be calculated straight forward and solution contains

$$V_R = \frac{2Q_w}{\pi}\int_0^t\left(\int_0^{\pi/2} e^{-\alpha\sec^2\tau d\tau}\right)dt \tag{11.45}$$

The fraction of stream contribution volume P_v in the total volume of water pumped from the well becomes

$$P_v = \frac{V_R}{V} = \frac{2}{\pi t}\left\{\int_0^t\left(\int_0^{\frac{\pi}{2}} e^{-\alpha\sec^2\tau} d\tau\right)dt\right\} \tag{11.46}$$

Hantush gave the solution for above equation as

$$P_v = 4i^2\operatorname{erfc}\left(\sqrt{\alpha}\right) \tag{11.47}$$

where, i^2erfc() = second repeated integral of the error function. Equation (11.47) is valid for confined or unconfined conditions when the ratio of drawdown to saturated thickness is less than 0.5. The values of the repeated integrals of the error functions are available in tabular form in Abramowitz and Stegun (1972) and *Appendix C* tabulates selected values of this function.

These methods to compute the rate of stream depletion rate and volume are not convenient, because they require computation of the complementary error function, interpolation from tables of probability integrals, or numerical integration. Swamee–Mishra–Chahar (2000) proposed the following simplified explicit solutions.

$$P_r = \left\{ \left[1 + 2\sqrt{\alpha/\pi} \right]^{2.75} + \left[e^{\alpha}\sqrt{\pi\alpha}\left(1 + \left(130\alpha e^{\alpha}\right)^{-.21}\right) \right]^{2.75} \right\}^{-.364} \qquad (11.48)$$

$$P_v = \left\{ \left[1 + 4\sqrt{\alpha/\pi} \right]^{2.6} + \left[\alpha e^{\alpha}\sqrt{\pi\alpha}\left(1 + 2.655\alpha\right)\right)^{-.97} \right]^{2.6} \right\}^{-0.385} \qquad (11.49)$$

Equations (11.48) and (11.49) are exact when $\alpha = 0$ or $\alpha \to \infty$. The maximum error involved in Eqn. (11.48) is 2.1 percent, occurring at $\alpha = 16$ and reduces to 1.5 percent in significant range of $P_r > 0.05$. On the contrary, the maximum error in use of Eqn. (11.49) is 0.7 percent, which occurs at $\alpha = 1.6$. A large α means early pumping, a high storage coefficient, low transmissivity, and a large distance from well to river. At the beginning of pumping, the aquifer contributes to the well discharge. For a higher storage coefficient and lower transmissivity, most of the water is taken from the aquifer storage. Also, when the distance from well to river is large, it is the aquifer that contributes more to the pumping. For a large α, the contribution of the stream in the pumping becomes insignificant. In the simplified method, interpolation from tables of complementary error functions for the rate of stream depletion and the second repeated integral of the error function for total volume of stream depletion is not required, nor is numerical integration necessary.

11.7 Unsteady Well Flow in Uniform Flow Field

As the method of superposition is applicable for unsteady flow toward a well in confined flow and for uniform flow, the resultant head or drawdown can be computed following methods similar to adopted for steady flow wells in uniform flow field as described in Chapter 10.

SOLVED EXAMPLES

Example 11.1: It is required to dewater a construction site 80 m by 80 m. The bottom of construction site will be 1.5 m below the initial water surface elevation. Four pumps are to be used of 0.5 m diameter at the four corners of the site. Transmissibility and storage coefficient of the aquifer are 1600 m²/d and 0.16, respectively (Figure 11.19). The site needs to be ready after one month of pumping. Determine the required pumping rate.

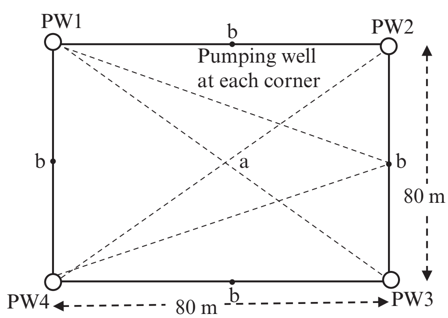

Figure 11.19 *Example 11.1*

Solution: Distance of point "a" from all four wells would be equal to $r=\sqrt{40^2+40^2}=56.6$ m or $r^2=3203.56$ m^2. At point "b" the distance will be same for wells 1 and 2, $r_1=40$ m, and for wells 3 and 4 $r_2=\sqrt{40^2+80^2}=89.44$ m, hence $r_1.r_2=3577.708$ m^2.

As $(r_1.r_2)_{\text{b}}>(r^2)_{\text{a}}$, the resultant drawdown at "b" will be less than at "a" so the point "b" is critical. For this case, $u_1=\dfrac{r_1^2S}{4Tt}=\dfrac{40^2\times 0.16}{4\times 1600\times 30}=0.001333$ and $u_2=\dfrac{r_2^2S}{4Tt}=\dfrac{89.44^2\times 0.16}{4\times 1600\times 30}=0.0067$, and both u_1 and $u_2<0.01$, hence Cooper–Jacob's approximation Eqn.(11.16) can be used.

As $T = 1600$ m^2/d and required minimum drawdown = 1.5 m at b,

hence $s_{\text{b}}=s_1+s_2+s_3+s_4=1.5$, substituting values $2\left\{\dfrac{Q}{4\pi T}(-0.5772-\ln u_1)\right\}$ $2\left\{\dfrac{Q}{4\pi T}(-0.5772-\ln u_1)\right\}$ or $1.5=\dfrac{(2\times Q)}{4\pi\times 1600}\{-0.5772-\ln 0.00133-0.5772$ $-\ln 0.0067\}\Rightarrow Q=1441$ m^3/d

Example 11.2: A production well and an injection well exist in a confined aquifer having a transmissivity of 150 m^2/d and a storativity of 5×10^{-4}. Water is pumped at 1900 m^3/d and injected at 800 m^3/d (Figure 11 20). Calculate the drawdown in the observation well after one year of pumping and injection.

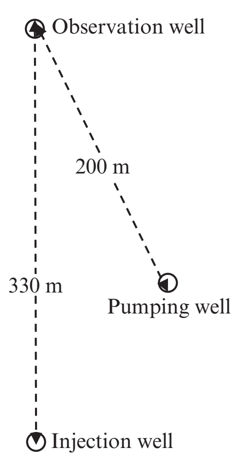

Figure 11.20 *Example 11.2*

Solution: Here t = 365 days, $u_{\text{p}} = \dfrac{(200)^2 \times 5\times10^{-4}}{4\times365\times150} = 9.132\times10^{-6}$, and

$u_{\text{i}} = \dfrac{(330)^2 \times 5\times10^{-4}}{4\times365\times150} = 2.486\times10^{-5}$, and both u_1 and $u_2 < 0.01$, hence Cooper–Jacob method of approximation can be used.

Thus, $W(u_{\text{p}}) = 11.0264$ and $W(u_{\text{i}}) = 10.025$ from Eqn. (11.17) and hence $s = \dfrac{Q_{\text{p}}}{4\pi T}W(u_{\text{p}}) = \dfrac{1900}{4\pi\times150}\times 11.0264 = 11.114\,\text{m}$ and $s_{\text{i}} = \dfrac{Q_{\text{i}}}{4\pi T}W(u_{\text{i}})$ $= \dfrac{800}{4\pi\times150}\times10.025 = 4.255$ m, which gives resultant draw down at the observation well $s = s_{\text{p}} - s_{\text{i}} = 11.114 - 4.255 = 6.86$ m.

Example 11.3: A well is pumping near an impervious boundary as shown in Figure 11.21 at rate of 0.03 m^3/s from a confined aquifer of 20 m thickness. The hydraulic conductivity and storability of the aquifer are 27.65 m/d and 3×10^{-5}, respectively. Determine the drawdown in the observation well after 10 hours of continuous pumping. What is the fraction of drawdown attributed by the barrier boundary?

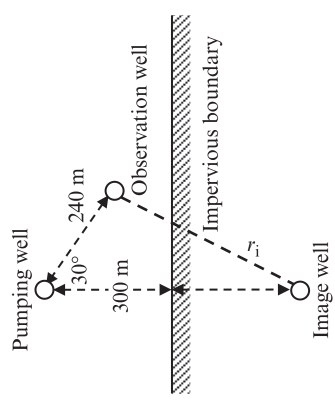

Figure 11.21 *Example 11.3*

Solution: An image well of same strength and same nature will be formed across the boundary at the same distance from the boundary as the pumping well. The drawdown in the observation well is due to the real pumping well and imaginary discharging well. Hence, the resultant drawdown is $s = \dfrac{Q}{4\pi T}W(u_{\text{p}}) + \dfrac{Q}{4\pi T}W(u_{\text{i}})$.

Given data: $Q = 0.03\,\text{m}^3/\text{s}$, $b = 20\,\text{m}$, $K = 27.65\,\text{m/d} = 3.2\times10^{-4}$ m/s or $T =$ $6.4\times10^{-3}\,\text{m}^2/\text{s}$, $S = 3\times10^{-5}$, $t = 10$ hours $= 36{,}000$ s, and $r_\text{i}^2 = 600^2 + 240^2 - 2\times$ $600\times240\times\cos30 \Rightarrow r_\text{i} = 410\,\text{m}$; therefore, $u_\text{p} = \frac{r_\text{p}^2 S}{4Tt} = \frac{(240)^2\times3\times10^{-5}}{4\times20\times3.2\times10^{-4}\times36000}$ $= 1.80\times10^{-3}$ and $u_\text{i} = \frac{r_\text{i}^2 S}{4Tt} = \frac{168185\times3\times10^{-5}}{4\times20\times3.2\times10^{-4}\times36{,}000} = 5.47\times10^{-3}$. Both u_p and u_i are $< 10^{-2}$, hence Cooper–Jacob approximation for well function is application, which yields $W(u_\text{p}) = \ln\frac{1}{u_p e^{0.5772}} = \ln\frac{1}{1.80\times10^{-3}e^{0.5772}} = 5.72$ and $W(u_\text{i}) =$ $\ln\frac{1}{5.47\times10^{-3}e^{0.5772}} = 4.63$.

Hence, drawdown at observation well is $s = \frac{Q}{4\pi T}\{W(u_\text{p}) + W(u_\text{i})\} =$ $\frac{0.03}{4\pi\times6.4\times10^{-3}}\times(5.72+4.63) = 3.86$ m . The drawdown attributed by barrier boundary is $s_\text{i} = \frac{Q}{4\pi T}W(u_\text{i}) = \frac{0.03}{4\pi\times6.4\times10^{-3}}\times4.63 = 1.73$ m , and hence the fraction of drawdown attributable to impermeable boundary is $\frac{s_\text{i}}{s} = \frac{1.73}{3.86} = 0.45 \Rightarrow 45\%$.

Example 11.4: Find out the drawdown in the observation well and percentage contribution in this drawdown by the impervious boundary as shown in Figure 11.22 after one day of pumping with constant flow rate 50 l/s from a confined aquifer having $S = 4\times10^{-5}$ and $T = 0.0064$ m²/s.

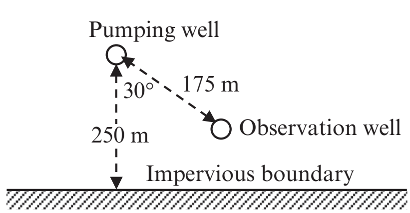

Figure 11.22 *Example 11.4*

Solution: Given data: $Q = 50\times10^{-3}$ m²/s, $T = 0.0064$ m²/s, $S = 4\times10^{-5}$, and $t = 12$ hours.

The well is near an impervious boundary, an image discharging well is formed, its distance from the observation well is $r_\text{i}^2 = 175^2 + 500^2 - 2\times175\times$ $500\times\cos30 = 129070.55$.

Hence, $u_\text{p} = \frac{r_\text{p}^2 S}{4Tt} = \frac{(175)^2\times4\times10^{-5}}{4\times0.0064\times12\times3600} = 1.108\times10^{-3}$ and $u_\text{i} = \frac{r_\text{i}^2 S}{4Tt} =$ $\frac{129070.55\times4\times10^{-5}}{4\times0.0064\times12\times3600} = 4.668\times10^{-3}$, thus both are <0.01: Cooper–Jacob approximation for the well function is suffice.

The resultant drawdown in the observation well is $s = s_p + s_i = 3.872 + 2.978 = 6.85\ \text{m}$. Therefore, the effect of the impervious boundary on the drawdown is $= \dfrac{2.978}{6.85} = 43.47\%$.

Example 11.5: A 0.5-m diameter well (200 m from a river as shown in Figure 11.23) is pumped at an unknown rate from a confined aquifer. The aquifer transmissivity is 432 m^2/d and S is 4×10^{-4}. After eight hours of pumping, the drawdown in observation well at 60 m from the river is 0.8 m. Compute the rate of pumping.

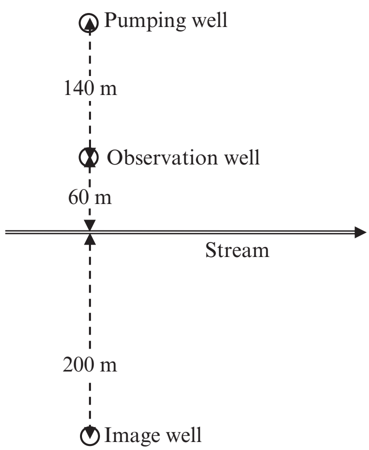

Figure 11.23 *Example 11.5*

Solution: Given data: r_w = 0.25 m, $T = 5.0\times10^{-3}$ m^2/s, $S = 4\times10^{-4}$, t = 8 hours = 28800 s, and drawdown = 0.8 m in observation well.

Here, the well is near a river so an image recharging well at 200 m from the river is put and the river is removed to create the equivalent hydraulic system. Therefore, the resultant drawdown is $= \dfrac{Q}{4\pi T}\left\{W\left(u_\text{p}\right) - W\left(u_\text{i}\right)\right\}$.

Using given data $u_\text{p} = \dfrac{r_\text{p}^2 S}{4Tt} = \dfrac{(140)^2 \times 4\times10^{-4}}{4\times28800\times5\times10^{-3}} = 1.36\times10^{-2}$; $u_\text{i} = \dfrac{r_\text{i}^2 S}{4Tt} = \dfrac{(260)^2\times4\times10^{-4}}{4\times28800\times5\times10^{-3}} = 4.69\times10^{-2}$.

Now for small value of u using Cooper–Jacob approximation $W(u_\text{p}) = -.5772 - \ln\left(1.36\times10^{-2}\right) = 3.79$ and $W\left(u_\text{i}\right) = -.5772 - \ln\left(4.69\times10^{-2}\right) = 2.54$. So $0.8 = \dfrac{Q}{4\pi T}(3.79 - 2.54)$, which gives $Q = \dfrac{0.8\times4\pi\times5\times10^{-3}}{1.25} = 0.04$ m^3/s.

It is to be noted that both u_p and u_i are > 10^{-2}, hence in place of Cooper–Jacob approximation, either Eqn. (11.19) by Swamee–Ojha or Eqn. (11.20) by Vatankhah should be used for the computation of the well functions.

Using Eqn. (11.19) by Swamee–Ojha $W(u_p) = 3.730312$ and $W(u_i) = 2.525443$. Thus, $0.8 = \frac{Q}{4\pi T}(3.730312 - 2.525443) \Rightarrow Q = \frac{0.8 \times 4\pi \times 5 \times 10^{-3}}{1.205} =$ 0.0417 m³/s and hence 4.3 percent error in discharge computation using Cooper–Jacob Method.

Example 11.6: A 0.6 diameter well (160 m from a river) is pumping at some rate from confined aquifer. The aquifer transmissivity is 368 m²/d and $S = 2 \times 10^{-4}$. After 10 hours of pumping, the drawdown in the observation well 80 m from the river is 1.0 m. Compute the drawdown in the pumping well. Assume configuration of pumping and observation wells are similar to Example 11.5.

Solution: Given data: r_w = 0.3 m, T = $368\ \text{m}^2/\text{d} = 4.26 \times 10^{-3}\ \text{m}^3/\text{s}$, $S = 2 \times 10^{-4}$, t = 10 hours = 36,000 s, and drawdown in observation well = 1.0 m.

Similarly to the previous problem $s = \frac{Q}{4\pi T}\{W(u_p) - W(u_i)\}$ and $u_p = 2.08 \times 10^{-3}$ and $u_i = 1.88 \times 10^{-2}$.

Using Vatankhah's equation $W(u_p) = 5.595075$ and $W(u_i) = 3.4119$.

Therefore, $1.0 = \frac{Q}{4\pi T}(5.595075 - 3.4119) \Rightarrow Q = 0.0245\ \text{m}^3/\text{s}$.

For computation of the drawdown in the pumping well $u_w = \frac{r_w^2 S}{4Tt} = \frac{(.3)^2 \times 2 \times 10^{-4}}{4 \times 36000 \times 4.26 \times 10^{-3}} = 2.93 \times 10^{-8}$ and $u_i = \frac{(360)^2 \times 2 \times 10^{-4}}{4 \times 36000 \times 4.26 \times 10^{-3}} = 4.22 \times 10^{-2}$, thus $W(u_w) = 16.7684$ and $W(u_i) = 2.62645$. Thus, drawdown is $s_w = \frac{0.268}{4\pi \times 4.26 \times 10^{-3}}\{16.7684 - 2.62645\} = 6.472\ \text{m}$.

Example 11.7: A well is pumping at an unknown rate from a confined aquifer. The diameter of the well is 0.6 m. After 8 hours of pumping, the drawdown in the observation well is 0.6 m and distance of observation well from the river is 60 m, and of pumping well is 120 m. What is the effect of the river on drawdown in the observation well and in pumping well? Assume configuration of pumping and observation wells are similar to Example 11.5

Solution: Given data: r_w = 0.4 m, t = 8 hours = 28,800 s, resultant drawdown = 0.6 m, $T = 432\ \text{m}^2/d = 5.0 \times 10^{-3}\ \text{m}^2/\text{s}$, and $S = 4 \times 10^{-4}$. Here, the well is near a recharge boundary so an image recharging well at 240 m from the river is required for the equivalent hydraulic system.

Using given data: $u_p = \dfrac{(120)^2 \times 4\times10^{-4}}{4\times28800\times5\times10^{-3}} = 10^{-2}$, and $u_i = \dfrac{(240)^2 \times 4\times10^{-4}}{4\times28800\times5\times10^{-3}} = 4\times10^{-2}$.

As $u_i > 0.01$, Swamee–Ojha relation for well function results $W(u_p) = 4.0339$ and $W(u_i) = 2.6778$.

Therefore, $s = \dfrac{Q}{4\pi T}\{4.0339 - 2.6778\} \Rightarrow Q = \dfrac{4\pi\times5\times10^{-3}}{1.3561}\times0.6 = 0.0278\,\text{m}^3/\text{s}$.

The effect of the river on the well is to decrease the drawdown. The drawdown contribution from river in the observation well $s_i = -\dfrac{Q}{4\pi T}W(u_i) = -\dfrac{0.0278\times2.6778}{4\pi\times5\times10^{-3}} = -1.185\,\text{m}$. Hence, the drawdown due to pumping alone $s_p = 0.6 - (-1.185) = 1.785$ m.

Example 11.8: A well in a confined aquifer having $S = 3\times10^{-5}$ and $T = 0.0048$ m^2/s is pumped with constant flow rate 40 l/s for 2 days and then it is stopped. Determine the percentage recovery after 5 hours of pump stopped in drawdown in the observation well which is 90 m from the pumping well.

Solution: Given data: $Q = 40\times10^{-3}$ m^2/s, $T = 0.0048$ m^2/s, $S = 3\times10^{-5}$, and $t = 2$ days.

Hence, $u_p = \dfrac{r_p^2 S}{4Tt} = \dfrac{(90)^2\times3\times10^{-5}}{4\times0.0048\times2\times24\times3600} = 7.324\times10^{-5} \Rightarrow W(u_p) = -.5772$ $-\ln(7.324\times10^{-5}) = 8.9445$, which yields $s = \dfrac{Q}{4\pi T}W(u_p) = \dfrac{40\times10^{-3}}{4\pi\times0.0048}\times8.9445$ $= 5.9315\,\text{m}$.

For residual drawdown $t = 53$ hours and $t' = 5$ days. Corresponding $u = \dfrac{(90)^2\times3\times10^{-5}}{4\times0.0048\times53\times3600} = 6.633\times10^{-5} \Rightarrow W(u) = 9.044$ and

$u' = \dfrac{(90)^2\times3\times10^{-5}}{4\times0.0048\times5\times3600} = 7.031\times10^{-4} \Rightarrow W(u') = 6.683.$ Hence, residual drawdown $s_R = \dfrac{Q}{4\pi T}\left[W(u) - W(u')\right] = \dfrac{40\times10^{-3}}{4\pi\times0.0048}\times(11.044 - 6.683) = 1.565\,\text{m}$.

Therefore, percent recovery $= \dfrac{5.9315 - 1.565}{5.9315} = 73.6\%$.

Example 11.9: A well as shown in Figure 11.24 in a confined aquifer having $S = 3\times10^{-5}$ and $T = 0.005$ m^2/s is pumped with constant flow rate 50 l/s for 3 days and then it is stopped. Determine the percentage recovery after 6 hours of pump stopped in drawdown in the observation well.

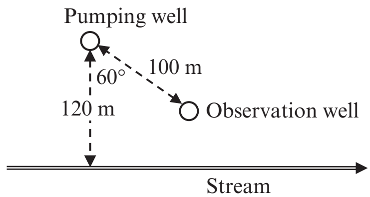

Figure 11.24 *Example 11.9*

Solution: Given data: $Q = 50\times10^{-3}$ m²/s, $T = 0.005$ m²/s, $S = 3\times10^{-5}$, and $t = 3$ days.

The well is near a stream, an image recharging well is formed, and its distance from the observation well is $r_2^2 = 100^2 + 240^2 - 2\times100\times240\times\cos 60 = 43600$.

Hence, $u_p = \dfrac{r_p^2 S}{4Tt} = \dfrac{(100)^2\times3\times10^{-5}}{4\times0.005\times3\times24\times3600} = 5.787\times10^{-5}$ and $u_R = \dfrac{r_R^2 S}{4Tt} = \dfrac{43600\times3\times10^{-5}}{4\times0.005\times3\times24\times3600} = 2.523\times10^{-4}$.

Considering first three terms of the exponential integral, the resultant drawdown after three days is $s = s_p - s_R = \dfrac{Q}{4\pi T}\left(-\ln u_p + u_p + \ln u_R - u_R\right) = \dfrac{50\times10^{-3}}{4\pi\times0.005}\left(\ln\dfrac{2.523\times10^{-4}}{5.787\times10^{-5}} + 5.787\times10^{-5} - 2.523\times10^{-4}\right) = 1.472\,\mathrm{m}$.

Residual drawdown after 6 hours is $s_R = \dfrac{Q}{4\pi T}\left[W(u_p) - W(u_p') - W(u_R) + W(u_R')\right]$, where $u_p = \dfrac{(100)^2\times3\times10^{-5}}{4\times0.005\times78\times3600} = 5.342\times10^{-5}$, $u_p' = \dfrac{(100)^2\times3\times10^{-5}}{4\times0.005\times6\times3600} = 6.994\times10^{-4}$, $u_R = \dfrac{43600\times3\times10^{-5}}{4\times0.005\times78\times3600} = 2.329\times10^{-4}$, and $u_R' = \dfrac{43600\times3\times10^{-5}}{4\times0.005\times6\times3600} = 3.028\times10^{-3}$ hence $S_R =$

$$\frac{Q}{4\pi T}\left[\ln\frac{u_p' u_R}{u_p u_R'} + u_p - u_p' - u_R + u_R'\right] = \frac{50\times10^{-3}}{4\pi\times0.005}\left[\ln\frac{6.944\times2.329}{5.342\times3.028} + 5.342\times10^{-5} - 6.944\times10^{-4} - 2.329\times10^{-4} + 3.028\times10^{-3}\right] = 0.0016\,\mathrm{m}.$$

Therefore, percent recovery $= \dfrac{1.472 - 0.0016}{1.472} \approx 100\%$ that mean after 6 hours the peizometric surface almost recouped.

Example 11.10: Determine the distance from the observation well of the image well if the distance of pumping well from the observation well is equal to 120 m, time after pumping started and before the barrier boundary became effective is 10 hours, and time at which drawdown of pumping well would be equal to image well is 15 hours.

Solution: The law of time can be used to determine the distance from an image well to the observation well using $r_i = r_p.\sqrt{t_i / t_p}$ where r_i = distance from image well to observation well, r_p= distance from pumping well to observation well, t_p = time after pumping started and before the barrier boundary is effective, t_i is time when $s_p = s_i$. Given that $r_p = 120\,\text{m}$, $t_p = 10\,\text{hours}$, and $t_i = 15\,\text{hours}$, thus $r_i = 120\sqrt{15/10} = 149.96\,\text{m}$.

Example 11.11: A well is located at 804.67 m from a stream. The aquifer between the well and stream has $T/S = 6.9677 \times 10^{-2}$ m²/s. Compute the fraction of stream depletion rate and volume due to continuous pumping of well for 12 months.

Solution: Given a = 804.67 m, t = 12 months = 24×360 × 3600 s, and T/S = 6.9677×10^{-2} m²/s, thus $\alpha = \dfrac{a^2 S}{4Tt} = \dfrac{804.67^2}{4\times 243603600\times 6.967710^{-2}} = 7.4691\times10^{-2}$.
For α = 0.074691, Glover and Balmer Eqn. (11.42) gives the stream depletion rate after 12 months P_r = 0.7008, while Swamee–Mishra–Chahar Eqn. (11.47) directly yields P_r = 0.6955 that means about 70 percent of pumped water would come from the stream. Similarly, for α = 0.074691, the interpolated values from the table of repeated integrals of the error function based on Hantush Eqn. (11.46) gives the stream depletion volume cumulated for 12 months P_v = 0.5201, while Swamee–Mishra–Chahar Eqn. (11.48) directly yields P_v = 0.5173 that means about 52 percent of pumped water volume during 12 months came from the stream. The results from the simplified equations of Swamee–Mishra–Chahar compare very well with exact solutions without needing numerical integration or interpolation from tables of complementary error functions for the rate of stream depletion and the second repeated integral of the error function for total volume of stream depleted.

PROBLEMS

11.1. Write the general governing equation for radial groundwater flow toward a well in confined aquifer. Give its Theis solution stating boundary conditions and assumptions involved. Why is this solution more advantageous than Thiem solution? Furthermore, describe step-by-step method of Cooper–Jacob for estimating S and T.

11.2. Derive the governing equation for unsteady radial flow toward a well in confined aquifer and then obtain its solution for drawdown. Also, deduce Cooper–Jacob's relations for estimating S and T.

11.3. Derive the expression for "law of time" and describe its physical significance.

11.4. A 25-cm well penetrates an artesian aquifer of 10 m thick. After 10 hours of pumping at the rate of 1100 lpm the drawdown in the well is 2.6 m and after 48 hours the drawdown is 2.85 m. Determine the transmissibility and storage coefficients of the aquifer. What is the hydraulic conductivity of the aquifer material? After what time will the drawdown be 4.1 m?

11.5. The drawdown is 2 m in an observation well 20 m away from a pumping well after 15 min of pumping. At what time the same drawdown will occur in another well 40 m away?

11.6. Using Cooper–Jacob approximation, compute the rate of piezometric drawdown around a pumping well with respect to time. If the well in an aquifer (S = 0.0215 and T = 0.0015 m^2/s) is pumped at a constant flow rate 50 l/s, what is the time to reach near-steady-state condition at 750 m from the pumping well? Assume that near-steady-state conditions are achieved when the drawdown rate falls below 1-cm/hour.

11.7. The drawdowns in an observation well 15 m away from the pumping well are 3 and 4 m after 10 and 100 min of pumping. What are the corresponding drawdowns in an observation well 150 m away from the pumping well?

11.8. The foundation in a construction site (80 m by 60 m) is 6 m deep while the position of the prevailing water table is 4 m below the ground surface. The site is to be dewatered upto the foundation level in one month using pumping wells one at each corner. Determine the required pumping rate if the transmissivity and the storage coefficient of the aquifer are 1600 m^2/d and 0.16, respectively.

11.9. The foundation in a construction site (60 m by 40 m) is 5 m deep while the position of the prevailing water table is 3.5 m below the ground surface. The site is to be dewatered upto 0.5 m below the foundation level in one month using pumping wells one at each corner and one at center. Determine the required pumping rate if the initial saturated thickness, the transmissivity and the storage coefficient of the aquifer are 20 m, 1600 m^2/d and 0.16, respectively.

11.10. The foundation in a construction site (70 m by 50 m) is 6 m deep while the position of the prevailing water table is 4.0 m below the ground surface. The site is to be dewatered upto 0.5 m below the foundation level in one month using pumping wells one at each corner. Determine the required pumping rate if the initial saturated thickness, the transmissivity, and the storage coefficient of the aquifer are 25 m, 1500 m^2/d, and 0.15, respectively.

11.11. Two pumping wells spaced at 1000 m fully penetrate the same aquifer having transmissibility of $2000\,\text{m}^3\text{/d}$ and storage coefficient of 4×10^{-4}. The pumping rate of one well is $1240\,\text{m}^3\text{/d}$ while it is $850\,\text{m}^3\text{/d}$ for the second well. When would the wells start interfering each other?

11.12. Determine the drawdown in the observation well and percentage contribution in this drawdown by the impervious boundary as shown in Figure 11.25 after 12 hours of pumping with constant flow rate 60 l/s from a confined aquifer having $S = 2 \times 10^{-5}$ and $T = 0.006$ m^2/s.

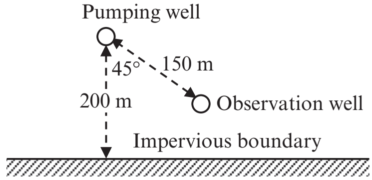

Figure 11.25 *Problem 11.12*

11.13. Give step-by-step method of locating an impervious boundary near a well. Also, determine the drawdown in the observation well and percentage contribution in this drawdown by the impervious boundary as shown in Figure 11.26 after 15 hours of pumping with constant flow rate 40 l/s from a confined aquifer having $S = 3 \times 10^{-5}$ and $T = 0.0048$ m²/s.

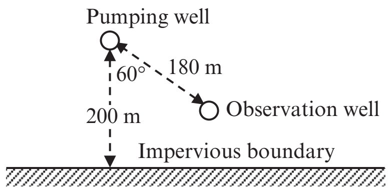

Figure 11.26 *Problem 11.13*

11.14. Analyze a problem of flow to a well near a stream. Also, determine the drawdown in the observation well after 8 hours of pumping with constant flow rate 50 l/s ($S = 0.0215$ and $T = 0.0015$ m²/s) in the problem as shown in Figure 11.27.

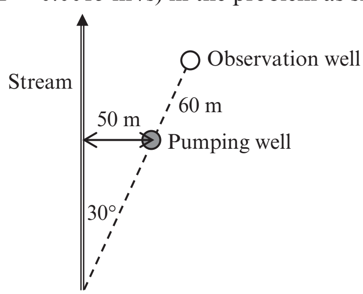

Figure 11.27 *Problem 11.14*

11.15. Draw images of the pumping well as shown in Figure 11.28. Also, determine the drawdown in the observation well after 8 hours of pumping with constant flow rate 50 l/s ($S = 0.0215$ and $T = 0.0015$ m²/s) if the impervious boundary is not present in the problem.

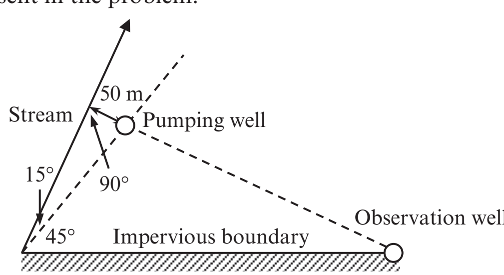

Figure 11.28 *Problem 11.15*

11.16. A well is to be established near a canal to intercept the seepage and prevent water logging in the reach of the canal where the seepage losses are found to be 105 lpd/km. What should be the distance of the well from the canal so that it does not induce extra seepage from the canal, and the discharge and spacing of tube well in this area. If a 30-cm tubewell is located at 250 m from the canal and pumped at rate of 5000 l/m, determine the time required to reach approximate equilibrium condition. Also, determine (i) the percentage of pumped water furnished by the canal after pumping of one month and (ii) the resultant drawdown in the tube well. Assume S = 0.11 and $T = 1.5 \times 10^8$ lpd/m for the underlying confined aquifer.

11.17. A tributary joins at right angles to a river and a pumping well is located near their confluence point. Show that the drawdown in an observation well will be independent of time.

11.18. A 30-cm well, located at a distance of 1 km from a recharge boundary, has been discharging at a constant rate from a water table aquifer. The coefficients of transmissibility and storage of the aquifer are 1.8×10^5 lpd/m and 0.2, respectively. Compute the time after which the water level in the well stabilizes.

11.19. Explain the theory of images as applied to groundwater hydrology. An aquifer is bounded by two converging boundaries at an angle of 36°, one being a barrier boundary and the other a recharge boundary. Compute the number of image wells and mark them neatly in a sketch.

11.20. Two wells PW1 and PW2 as shown in Figure 11.29 near a stream in a confined aquifer having $S = 3 \times 10^{-4}$ and $T = 0.0048$ m²/s are pumped with constant flow rates 40 l/s and 100 l/s, respectively. The diameter of each well is 20 cm. Determine the drawdown in the observation well after 3 days of pumping. Also, determine the discharge from PW1 and PW2 wells if the drawdown is 2 m in PW1 and 4 m in PW2 after 2 days of pumping in the above problem.

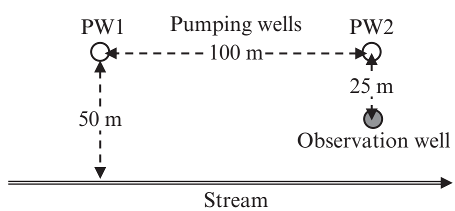

Figure 11.29 *Problem 11.20*

11.21. Determine the number of images for following cases with their location for a given pumping well in the aquifer. Also, derive the equation for drawdown. (i) Semi-infinite aquifer with recharge boundary on one side, (ii) two recharge straight boundaries meeting at 90°, and (iii) two unlike straight boundaries meeting at 90°.

11.22. A 30-cm well is discharging at the rate of 1000 lpm with a drawdown of 4.5 m. The transmissibility and storage coefficient of the aquifer are 0.015 m²/s and 0.001, respectively, and the aquifer is bounded by an aquiclude at a distance of 120 m from the well. Determine the drawdown after two days of pumping (i) at a distance of 80 m from the well toward the aquiclude and (ii) at a distance of 80 m on the opposite side of the well. What would be corresponding drawdowns under assumption of steady state conditions?

11.23. Two pumping wells, 1,000 m away fully penetrate the same aquifer. One of the wells pumps at a rate of $1{,}240\,\mathrm{m}^3/\mathrm{d}$. The second well pumps at a rate of $850\,\mathrm{m}^3/\mathrm{d}$. If the aquifer has a transmissibility of $2{,}000\,\mathrm{m}^3/\mathrm{d}$ and storage coefficient of 4×10^{-4}. When would the wells start interfering with each other?

11.24. A well field consists of three wells (each having r_w = 0.3 m) forming an equilateral triangle. The discharges of the wells are 2, 5, and 10 m^3/s, respectively, and all three wells are pumped for 2 weeks. The confined aquifer has a transmissibility of 0.005 m^2/s and storage coefficient of 10^{-4}. What would be (1) drawdown in the 10 m^3/s well if spacing = 50 m and (2) spacing if the permissible drawdown = 20 m?

Chapter 12

Unsteady-State Solutions to Special Cases

12.1 Single-Well Solution

In Chapter 11, it was assumed that a small diameter well fully penetrates the confined aquifer. In reality, the aquifer may be unconfined or leaky and the well may be partially penetrating or large diameter. This chapter deals with the following special cases of unsteady well flow problems to

1. wells in unconfined aquifer
2. wells in leaky aquifer
3. partially penetrating wells in confined aquifer
4. large diameter wells
5. flowing wells
6. multiple-layer aquifers
7. well losses

12.2 Unconfined Aquifer

Wells tapping unconfined or water table aquifers as shown in Figure 12.1 are called *water table wells*. They are also known as *gravity wells*. The unsteady-state behaviour of an unconfined aquifer is different from the earlier-dealt confined aquifer and extremely complicated because the position of the upper boundary of the flow, the water table is not known. The shape of the water table determines the distribution of flow underneath, whereas its shape in turn depends on that distribution. A further complication arises from the occurrence of the seepage face in such flow systems. The length of the seepage face is also unknown, as its upper terminal joins with the water table tangentially. In general, it is extremely difficult to satisfy analytically these boundary conditions. Accordingly, certain approximations are made such that flow systems may be described by conditions and differential equations that are amenable to relatively easy solutions with results that are sufficiently accurate for practical use.

When the discharge of a well is supplied from storage only, steady-state flow will theoretically never be attained, that is, the flow around the well is always transient and the zone of influence is always expanding. The flow appears to approach a steady state with time because the decline of water levels around the well decreases in magnitude with both time and distance from the well. Essential stability of flow in the immediate vicinity of pumping well may be reached within a relatively short time of pumping depending on the hydraulic properties of the aquifer. The area of essential stability expands continuously, and a considerable period of time may be required for the water levels in areas far from the pumped wells to reach approximate equilibrium.

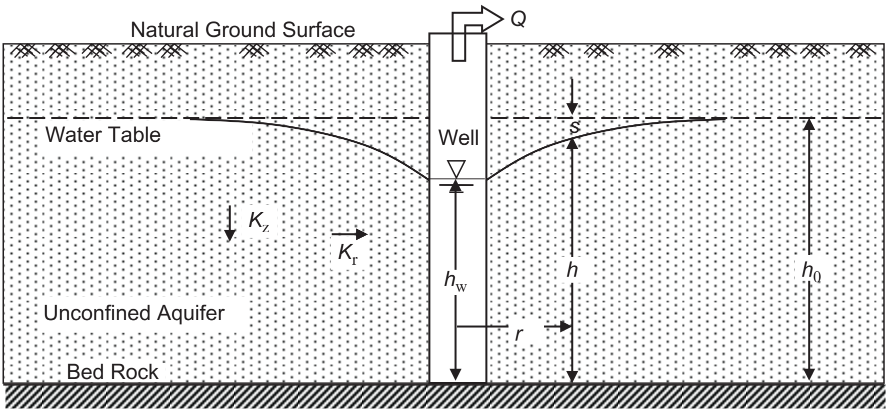

Figure 12.1 *Unconfined aquifer*

For near steady flow in an unconfined aquifer

$$2\int_0^h h(r,z)\,dz - h^2 = 2h\bar{h} - h^2 = h_0^{\,2} - \frac{Q}{\pi k}\ln\frac{r_e}{r} \Rightarrow h^2 \approx h_0^{\,2} - \frac{Q}{\pi k}\ln\frac{r_e}{r} \qquad (12.1)$$

The difference between h and $\bar{h}$ is not measurable at points for which $r > 1.5h$. Moreover, this difference is insignificant for smaller r as the water level in the well is increased. However, it fails to represent the water table near to the well. Within $r < 4r_w$, the shape of the water table may be approximated by

$$h^2 = h_0^{\,2} - \left(h_0^{\,2} - h_w^{\,2}\right)\left(\ln\frac{r_e}{r} / \ln\frac{r_e}{r_w}\right) \qquad (12.2)$$

This Dupuit–Forchheimer formula assumes purely horizontal flow and ignores the existence of the seepage face at the well surface. Still it gives fairly accurate results for the discharge. As the flow around the well in an infinite aquifer with no source of recharge is always transient, the zone of influence is always expanding, although the rate of its expansion is slow after a relatively long period of pumping, therefore estimation of actual radius of influence is not possible. Boulton (1951) showed that the ratio $2\pi K h_0\left(h_0 - h_w\right)/Q$ varies only slightly with r_w / h_0, and the height of seepage face h_{sf} for $r_w/h_0 < 0.1$ can be obtained as follows:

$$h_{sf} = \left(h_0 - h_w\right) - 3.75Q/(2\pi K h_0) \qquad (12.3)$$

and for r_w/h_0 of the order of 0.25, it can be obtained as follows:

$$h_{sf} = \left(h_0 - h_w\right) - 3.5Q/(2\pi K h_0) \qquad (12.4)$$

Generally, the solutions developed for confined aquifers are not applicable to unconfined aquifer problems because of the intricacies in their response to pumping mainly transmissivity changes with space and time as the water table declines during pumping and vertical flow components may be significant near the well invalidating the Dupuit–Forchheimer assumptions. However, if the point of interest is far away from the pumped well and the drawdown is less than 5 percent of the saturated thickness of the aquifer h_0, one can apply confined aquifer theory without too much error. A better approach is to correct/modify the observed unconfined aquifer drawdown into equivalent confined aquifer drawdown as follows. Based on the analogy of solutions for steady-state condition in confined and unconfined aquifers, the unsteady-state solution for an unconfined aquifer could be

$$h^2 = h_0^{\,2} - \frac{Q}{2\pi k} W(u) \text{ or } \frac{h_0^{\,2} - h^2}{2h_0} = \frac{Q}{4\pi T} W(u) \text{ or } s_\mathrm{e} = \frac{Q}{4\pi T} W(u) \qquad (12.5)$$

where, s_e is the drawdown in an equivalent confined aquifer. Relation between actual/observed drawdown in an unconfined aquifer s and equivalent drawdown is

$$s_\mathrm{e} = \frac{(h_0 - h)\times(h_0 + h)}{2h_0} = \frac{s(2h_0 - s)}{2h_0} = s - \frac{s^2}{2h_0} \qquad (12.6)$$

or

$$s = h_0 - \sqrt{h_0^{\,2} - 2h_0 s_\mathrm{e}} \qquad (12.7)$$

The equivalent drawdown can be used in solutions presented for a confined aquifer. In unconfined aquifer, a cone of depression forms under pumping, which decreases aquifer thickness and transmissivity because the upper boundary of the unconfined aquifer is the water table. In addition, the way in which water comes out of storage in the aquifer changes with time. Initially, the pumped water is released from storage due to compression of the aquifer matrix and expansion of the water. This *early time response* is similar to Theis solution for a confined aquifer. Thus, early time-drawdown data follow the Theis-type curve and storativity value is comparable to those for confined aquifers. As pumping continues, water comes from the slow gravity drainage of water from pores as the water table falls near the well. The pattern of drawdown depends on the vertical and horizontal hydraulic conductivities and the thickness of the aquifer. Drawdown data deviate from the Theis-type curve during this *delayed drainage*, and the drawdown is less than expected. Eventually, the contribution of water from the delayed drainage ceases and now the flow in aquifer is mainly radial and the time-drawdown data again follow the Theis-type curve. The storativity of the aquifer in this phase is equal to the specific yield S_y.

The equivalent drawdown approach is typically used with late-time drawdown data, once the contribution from *delayed yield* ceases. The delayed yield becomes negligible (Weeks 1969):

$$t = h_0 \frac{S_\mathrm{y}}{K_\mathrm{z}} \text{ if } \beta < 0.16 \qquad (12.8)$$

or

$$t = h_0 \frac{S_\mathrm{y}}{K_\mathrm{z}} \left(0.5 + 1.25\sqrt{\beta}\right) \text{ if } \beta \ge 0.16 \qquad (12.9)$$

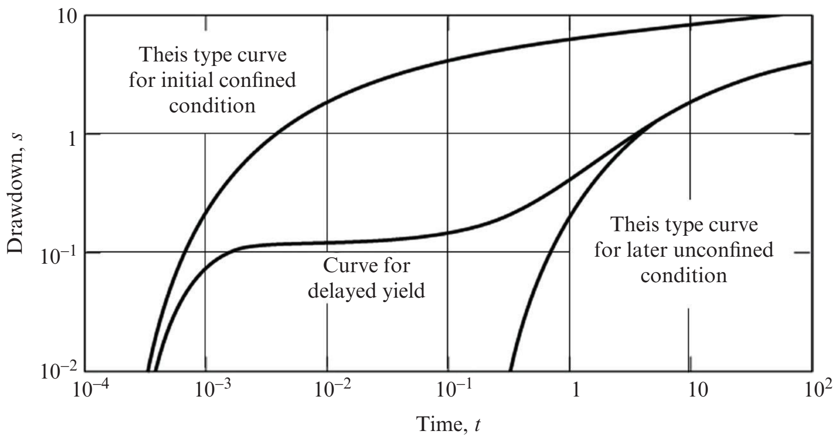

Figure 12 .2 *Effect of gravity drainage on drawdown in unconfined aquifer (Todd and mays, 2005)*

where beta is nondimensional parameter given by the following equation;

$$\beta = \frac{r^2}{h_0^2} \cdot \frac{K_z}{K_r} \tag{12.10}$$

where, K_r is the hydraulic conductivity in radial horizontal direction and K_z is the hydraulic conductivity in vertical direction of the anisotropic aquifer.

Boulton (1954, 1963, and 1970) studied the isotropic and homogeneous unconfined aquifer, resting on a horizontal impermeable bed, which is being drained by a fully penetrating well and well losses are zero. Radial flow component may be neglected in calculation of h for $h_w > h_0/2$ and contribution to the flow from aquifer compression except for very early period to get transient drawdown in an unconfined aquifer.

$$s = h_0 - h = \frac{Q}{2\pi K h_0}\left(1 + C_f\right)V\left(\tau, \rho\right) \tag{12.11}$$

where, $\tau = \dfrac{Kt}{S_y h_0}$; $\rho = \dfrac{r}{h_0}$; C_f is the correction factor that depends on τ, ρ, r_w, Q and h_0, and it varies from −0.3 to 0.16 and can be assumed zero for $r > 1.5h$ or $0.05 < \tau < 5$.

$$V\left(\tau, \rho\right) = \int_0^{\infty} \frac{1}{x} J_0\left(\rho x\right)\left[1 - \exp\left(-\tau x \tanh x\right)\right] dx \tag{12.12a}$$

is called Boulton's well function for an unconfined aquifer. Boulton (1954) completed values of $V(\tau, l)$ as tabulated in Appendix E. $V(\tau, l)$ may be approximately by

$$V\left(\tau,\rho\right) \approx \sinh^{-1}\left(1/\rho\right) + \sinh^{-1}\left(\tau/\rho\right) - \sinh^{-1}[(1+\tau)/\rho\,]\text{for } \tau < 0.05 \tag{12.12b}$$

$$V\left(\tau,\rho\right) \approx \sinh^{-1}\left(\tau/\rho\right) - \tau / \sqrt{1+\rho^2} \text{ for } \tau < 0.01 \tag{12.12c}$$

$$V\left(\tau,\rho\right) \approx \ln\left(2\tau/\rho\right) \text{ for } \tau < 0.01 \text{ and } \tau/\rho > 10 \tag{12.12d}$$

$$V\left(\tau,\rho\right) \approx 0.5W\left(\rho^2 / 4\tau\right) \text{ for } \tau > 5 \tag{12.12e}$$

If the aquifer is anisotropic the solution becomes

$$s = \frac{Q}{2\pi K h_0}\left(1 + C_f\right)V\left(\tau', \rho'\right) \tag{12.13}$$

where, $\tau' = \dfrac{K_z t}{S_y h_0}$ and $\rho' = \dfrac{r}{h_0}\sqrt{K_z / K_r}$

If the well losses are neglected, the drawdown in the pumping well can be approximated using $r = r_w$ for $\tau < 0.05$ in Eqs (12.11) and (12.12a). For $\tau > 5$, the expression reduces to

$$h_w^{\ 2} = h_0^{\ 2} - \frac{Q}{\pi K}\ln\left(1.5\sqrt{Kt / S r_w}\right) \tag{12.14}$$

For $0.05 < \tau < 5$, the drawdown in the pumped well can be computed as follows:

$$s_w = h_0 - h_w = \frac{Q}{2\pi K h_0}\left[m + \ln\left(h_0 / r_w\right)\right] \tag{12.15}$$

where, m is interpolated from the following data:

$\tau =$	5.0	2.0	0.2	0.05
$m =$	1.288	0.512	0.087	−0.043

Neumann (1972, 1973, 1974, and 1975) gave general solution for fully penetrating well in an unconfined aquifer as follows:

$$s = \frac{Q}{4\pi T}W\left(u_a, u_y, \beta\right) \tag{12.16}$$

where, $W\left(u_a, u_b, \beta\right)$ is the well function for the unconfined aquifer as tabulated in Appendix E and as shown in Figure 12.3 with definition

$$u_a = \frac{r^2 S}{4Tt} \tag{12.17a}$$

$$u_y = \frac{r^2 S_y}{4Tt} \tag{12.17b}$$

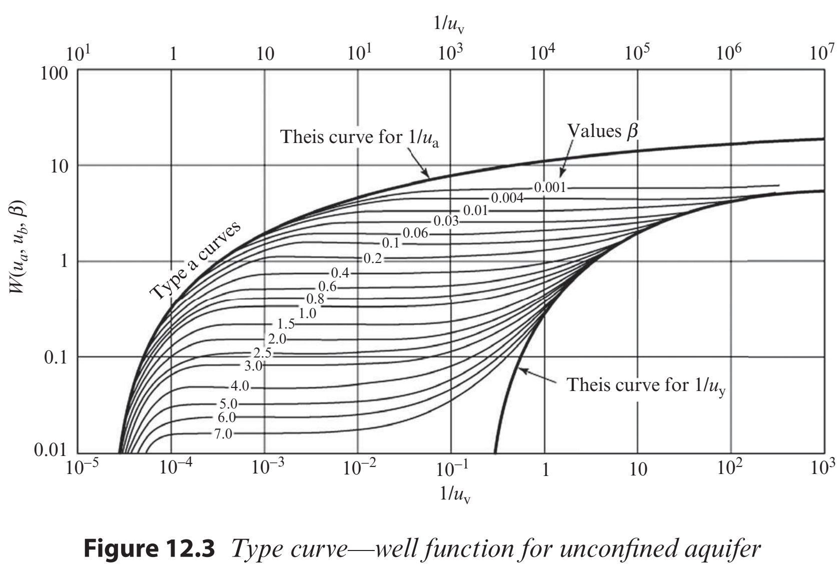

Figure 12.3 *Type curve—well function for unconfined aquifer*

12.3 Leaky Aquifer

Aquifers in nature are not always perfectly confined between completely impervious strata. Many aquifers are overlain by poorly pervious yet water transmitting strata as shown in Figure 12.4 which, over large contact areas, contribute significantly to the recharge of the aquifer. The semiconfining stratum may be overlain by other confined or unconfined aquifer or the semiconfining stratum itself (sands and gravels covered by loams and clays) may have a water table. Sometimes, water from the main aquifer seeps through underlying semipervious bed for certain duration and after changed head condition due to pumping, etc., the main aquifer is recharged from below. The seepage of water into and away from the main aquifer through the semiconfining strata is called *leakage*. Hantush and Jacob (1955) developed theory of the leaky aquifer.

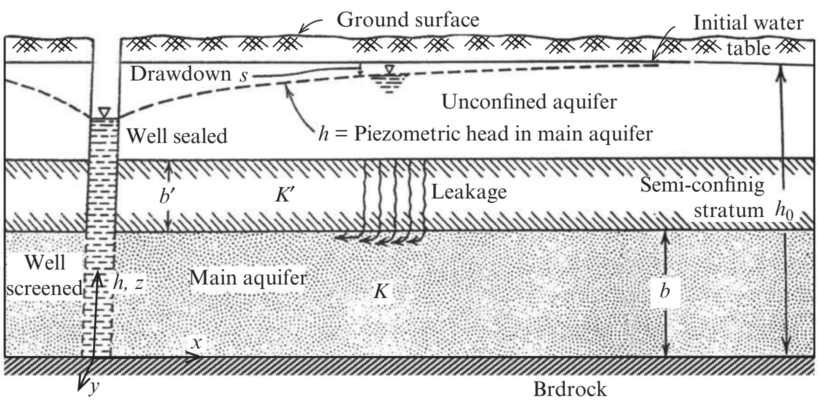

Figure 12.4 *Leaky aquifer (De Weist 1965)*

Consider a fully penetrating well in main/leaky aquifer as shown in Figure 12.4. The semiconfining top stratum is overlain by an unconfined aquifer in which the water table is horizontal and its capacity for lateral flow is sufficient to maintain essentially constant head in spite of the downward leakage into the main aquifer. This assumption of water table remains horizontal and unchanged will be valid during the first stages of pumping. The x–y plane coincides with the impervious bedrock and is also the datum plane for the head. Before pumping, the piezometric head h in the main aquifer is uniform and equal to the water table in the just above unconfined aquifer. After pumping is started, a cone of depression in the piezometric head develops, but the water table in the unconfined aquifer remains constant, thus a head difference is established between the top and bottom of the semiconfining stratum that will induce leakage through this stratum. Since the downward flow is proportional to the vertical difference between the water table and the piezometric surface, the rate of leakage decreases with increasing distance from the pumped well. The hydraulic conductivity K of the main aquifer is very very larger than the hydraulic conductivity K' of the semiconfining stratum; therefore, it is safe to assume that water seeps vertically through the semiconfining layer and is refracted over 90° to proceed horizontally in the main aquifer. Continuity equation for steady-state flow of water in aquifer is

$$\frac{\partial v_x}{\partial x}+\frac{\partial v_y}{\partial y}+\frac{\partial v_z}{\partial z}=0 \tag{12.18}$$

Due to leakage, velocity components are not uniform over the thickness of the main aquifer but are function of all coordinates, hence $v_x(x,y,z), v_y(x,y,z)$, and $v_z(x,y,z)$. The horizontal velocity components v_x and v_y vary according to their distance above bedrock, but if these changes are minor, average values of over the aquifer thickness b may be used which are as follows:

$$\bar{v}_x(x,y)=\frac{1}{b}\int_0^b v_x(x,y,z)\,dz \tag{12.19}$$

$$\bar{v}_y(x,y)=\frac{1}{b}\int_0^b v_y(x,y,z)\,dz \tag{12.20}$$

Similarly, the head h may be averaged over the aquifer thickness b as

$$\bar{h}(x,y)=\frac{1}{b}\int_0^b h(x,y,z)\,dz \tag{12.21}$$

Integrating the continuity equation with respect to z over the aquifer thickness

$$\int_0^b \frac{\partial v_x}{\partial x}dz+\int_0^b \frac{\partial v_y}{\partial y}dz+\int_0^b \frac{\partial v_z}{\partial z}dz=0 \tag{12.22}$$

We know that

$$\int_0^b \frac{\partial v_z}{\partial z}dz=v_z(b)-v_z(0) \tag{12.23}$$

where, $v_z(b)$ and $v_z(0)$ are vertical velocities at the top and bottom of the main aquifer, respectively. In the present case, $v_z(0)=0$ as the bedrock is impervious by assumption. For $v_z(b)$, using Darcy's law between the top and bottom of the semiconfining layer.

$$v_z(b)=-K'\left(\frac{\Delta h}{\Delta z}\right)=-\frac{K'\left(h_0-\bar{h}\right)}{b'} \tag{12.24}$$

Combining Eqs (12.22) and (12.23),

$$\int_0^b \frac{\partial v_x}{\partial x}dz+\int_0^b \frac{\partial v_y}{\partial y}dz+v_z(b)-v_z(0)=0 \tag{12.25}$$

Changing order of operators (first integration and then differentiation) results

$$\frac{\partial}{\partial x}\int_0^b v_x dz+\frac{\partial}{\partial y}\int_0^b v_y dz+v_z(b)=0 \tag{12.26}$$

Using Eqs (12.19) and (12.20) in Eqn. (12.26),

$$\frac{\partial}{\partial x}\left(b\bar{v}_x\right)+\frac{\partial}{\partial y}\left(b\bar{v}_y\right)+v_z(b)=0 \tag{12.27}$$

Now from Darcy's law $\bar{v}_x = -K_x \dfrac{\partial \bar{h}}{\partial x}$ and $\bar{v}_y = -K_y \dfrac{\partial \bar{h}}{\partial y}$ therefore,

$$\frac{\partial}{\partial x}\left(-bK_x \frac{\partial \bar{h}}{\partial x}\right) + \frac{\partial}{\partial y}\left(-bK_y \frac{\partial \bar{h}}{\partial y}\right) - \frac{K'\left(h_0 - \bar{h}\right)}{b'} = 0 \tag{12.28}$$

If the aquifer is homogeneous and isotropic,

$$-Kb\left(\frac{\partial^2 \bar{h}}{\partial x^2} + \frac{\partial^2 \bar{h}}{\partial y^2}\right) - \frac{K'\left(h_0 - \bar{h}\right)}{b'} = 0 \tag{12.29}$$

or

$$\nabla^2 \bar{h} + \frac{K'}{b'(Kb)}\left(h_0 - \bar{h}\right) = 0 \tag{12.30}$$

which can be rewritten in radial coordinates as follows:

$$\frac{\partial^2 \bar{h}}{\partial r^2} + \frac{1}{r}\frac{\partial \bar{h}}{\partial r} + \frac{K'}{b'(Kb)}\left(h_0 - \bar{h}\right) = 0 \tag{12.31}$$

This is the governing equation for steady condition in leaky aquifers. Comparison with the corresponding relationship for nonleaky confined aquifer, it shows that h is replaced by its average value h, and there is an additional linear term in h. Using similar analogy with unsteady governing equation for nonleaky confined aquifer dealt in the previous chapters, Eqn. (12.31) may be extended to include unsteady flow in leaky aquifer as follows:

$$\nabla^2 \bar{h} + \frac{K'}{b'(Kb)}\left(h_0 - \bar{h}\right) = \frac{S}{T}\left(\frac{\partial \bar{h}}{\partial t}\right) \Rightarrow \nabla^2 \bar{h} + \frac{h_0 - \bar{h}}{B^2} = \frac{S}{T}\left(\frac{\partial \bar{h}}{\partial t}\right) \tag{12.32}$$

or in radial coordinates

$$\frac{\partial^2 \bar{h}}{\partial r^2} + \frac{1}{r}\frac{\partial \bar{h}}{\partial r} + \frac{h_0 - \bar{h}}{B^2} = \frac{S}{T}\left(\frac{\partial \bar{h}}{\partial t}\right) \tag{12.33}$$

and in drawdown form

$$\nabla^2 s - \frac{s}{B^2} = \frac{S}{T}\left(\frac{\partial s}{\partial t}\right) \Rightarrow \frac{\partial^2 s}{\partial r^2} + \frac{1}{r}\frac{\partial s}{\partial r} - \frac{s}{B^2} = \frac{S}{T}\left(\frac{\partial s}{\partial t}\right) \tag{12.34}$$

where,

$$B = \sqrt{\frac{b'Kb}{K'}} \tag{12.35}$$

which is called *leakage factor*. In fact, a large leakage factor means that little leakage takes place, and vice versa. To quantify leakage directly, another coefficient is used, which is known as the *leakance* or *leakage coefficient* given by the following equation:

$$L = K'/b' = T/B^2 \tag{12.36}$$

The *leakage coefficient* is the quantity of water that flows across a unit area of the boundary between the main aquifer and its semiconfining bed, if the difference between the head in the main aquifer and recharging unconfined aquifer is unity.

Hantush and Jacob (1955) obtained an analytical solution of Eqn. (12.33) with appropriate boundary and initial conditions. The implicit assumptions involved in the governing equation and its solution are aquifer is homogeneous and isotropic; aquifer is of uniform thickness and bedrock is horizontal; aquifer is of infinite areal extent; well penetrates the entire aquifer and its diameter is small; flow is radial in the main aquifer; well is pumped at constant rate Q and the water is instantaneously removed from the well; initially the piezometric surface is horizontal and equal to the water table in the just above unconfined aquifer; semiconfining layer has uniform hydraulic conductivity and thickness; hydraulic conductivity of the main aquifer is very very larger than the hydraulic conductivity of the semiconfining stratum; water seeps vertically through the semiconfining layer and is refracted over 90° to proceed horizontally in the main aquifer; storage in the semiconfining layer is negligible; overlaid unconfined aquifer has water table horizontal, and its capacity for lateral flow is sufficient to maintain constant head despite the downward leakage into the main aquifer; leakage is linear with respect to head difference between the main aquifer and leakage supplying unconfined aquifer; and other boundary and initial conditions similar to no leaky confined aquifer.

The solution given by Hantush and Jacob (1955) is the following relation:

$$s = \frac{Q}{4\pi T} W\left(u, \frac{r}{B}\right) \tag{12.37}$$

where,

$$W\left(u, \frac{r}{B}\right) = \int_u^{\infty} \frac{1}{x} e^{\left(-x - \frac{r^2}{4B^2} \cdot \frac{1}{x}\right)} dx \tag{12.38}$$

which is a well function for leaky confined aquifers. Values of well function are extensively tabulated in literature. *Appendix F* tabulates values of the well function. Figure 12.5 plots the leaky aquifer well function.

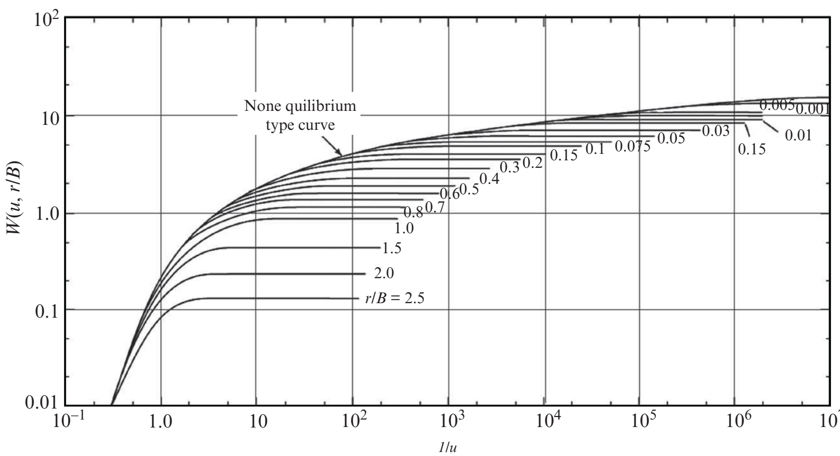

Figure 12.5 *Type curve—well function for leaky aquifer (Hantush 1956)*

Unlike Theis well function, the leaky aquifer well function is a family of curves, each for a separate r/B value. The different r/B curves represent differences in the amounts of leakage across the semiconfining bed. When $B \to \infty \Rightarrow \frac{r}{B} \to 0$ implies zero leakage or impervious confining bed leading to well function curve identical to Theis nonleaky aquifer curve. Curves with small r/B values indicate minor leakage, and hence minor deviation from the Theis curve. Curves with a large r/B value indicate significant leakage with a much greater deviation from the Theis curve. All curves for large pumping time approach horizontal asymptote; this means the drawdown acquires a maximum value corresponding to pumping rate and aquifer parameters and reaches into an equilibrium or steady condition. This is true in case of leaky aquifer as the cone of depression extends with pumping time; the leakage also increases, which ultimately balances the pumped water with the leakage. At steady state, the solution given in Eqn. (12.37) becomes (Jacob 1946).

$$s = \frac{Q}{2\pi T} K_0\left(\frac{r}{B}\right) \tag{12.39}$$

where, $K_0(r/B)$ is the modified Bessel function of the zero order and second kind. Eqn. (12.39) yields the maximum drawdown for the given pumping rate and aquifer parameters under equilibrium/steady condition. *Appendix C* tabulates $K_0(r/B)$ and Figure 12.6 plots $K_0(r/B)$.

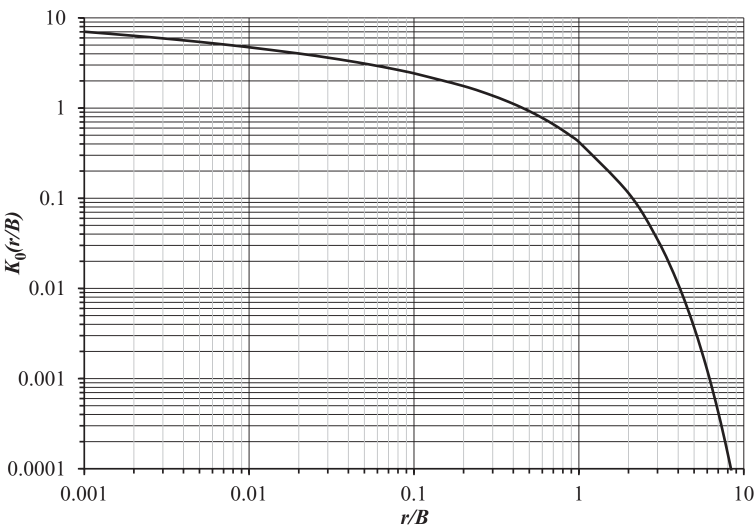

Figure 12.6 *Modified Bessel function of zero order and second kind*

The following relations may be useful in computations:

$$W(0,\rho) = 2K_0(\rho) \tag{12.40a}$$

$$W(u,0) = W(u) \tag{12.40b}$$

$$W(u,\rho) = 2K_0(\rho) - W\left(\rho^2/4u,\rho\right) \tag{12.40c}$$

$$W(u,\rho) \approx W(u) \quad \text{for } u > 2\rho \text{ or } u > 5\rho^2 \text{ and } \rho < 0.1 \tag{12.40d}$$

$$K_0(x) \approx \ln\left(\frac{1.12}{x}\right) \text{ for } x < 0.05 \tag{12.40e}$$

$$K_0(x) \approx \sqrt{\frac{\pi}{2x}}\left(1-\frac{1}{8x}\right)\frac{1}{e^x} \text{ for } x > 5 \tag{12.40f}$$

Wilson and Miller (1978) presented an asymptotic expansion derived using Laplace transforms:

$$W(u,r/B) = \sqrt{\frac{\pi B}{2r} e^{-r/B} erfc\left(\frac{2u - r/B}{2\sqrt{u}}\right)} \tag{12.41}$$

This equation involves 10 percent error for $r/B > 1$ and less than 1 percent for $r/B > 12$.

If the well is shut off after pumping for t_0, the drawdown will recover. The residual drawdown can be obtained as follows:

$$s_R = s_1 - s_2 = \frac{Q}{4\pi T}\left\{W\left(\frac{r^2 S}{4Tt}, \frac{r}{B}\right) - W\left(\frac{r^2 S}{4T(t-t_0)}, \frac{r}{B}\right)\right\} \tag{12.42}$$

For small value of u, we have $W(u,r/B) \to 2K_0(r/B)$. When both r/B and u are small, $W(u,r/B) \to 2\ln(1.12B/r)$, hence,

$$s = \frac{Q}{2\pi T}\ln\left(\frac{1.12B}{r}\right) \tag{12.43}$$

Hantush (1956) plotted drawdown data with logarithm of time and found the plot of s shape as shown in Figure 12.7, eventually attaining maximum drawdown s_{max} given by Eqn. (12.39). At the inflection point, the drawdown s_i is half of the maximum drawdown, that is

$$s_i = \frac{1}{2}s_{max} = \frac{Q}{4\pi T}K_0\left(\frac{r}{B}\right) \tag{12.44}$$

The slope at the inflection point can be derived as shown below. The slope at any point on a semilog plot of drawdown curve is

$$\frac{ds}{d(\log t)} = \frac{ds}{dt}\cdot\frac{dt}{d(\ln t)}(2.302) = 2.302t\frac{ds}{dt} \tag{12.45}$$

Since

$$s = \frac{Q}{4\pi T}\cdot\int_u^\infty \frac{1}{x} e^{\left(-x-\frac{r^2}{4B^2}\cdot\frac{1}{x}\right)} dx$$, taking derivative with respect to t

$$\frac{ds}{dt} = \frac{Q}{4\pi T}\left(0 - \frac{1}{u}e^{-u-\frac{r^2}{4B^2}\cdot\left(\frac{1}{u}\right)}\right)\frac{du}{dt} = -\frac{Q}{4\pi T}\frac{1}{u}e^{-u-\frac{r^2}{4B^2}\cdot\left(\frac{1}{u}\right)}\frac{du}{dt} \tag{12.46}$$

but

$$\frac{du}{dt} = \frac{d}{dt}\left(\frac{r^2 S}{4Tt}\right) = \frac{r^2 S}{4T}\left(-\frac{1}{t^2}\right) = -\frac{u}{t} \tag{12.47}$$

Hence,

$$\frac{ds}{dt} = \frac{Q}{4\pi T}\frac{1}{t}e^{-u-\frac{r^2}{4B^2}\cdot\left(\frac{1}{u}\right)} \tag{12.48}$$

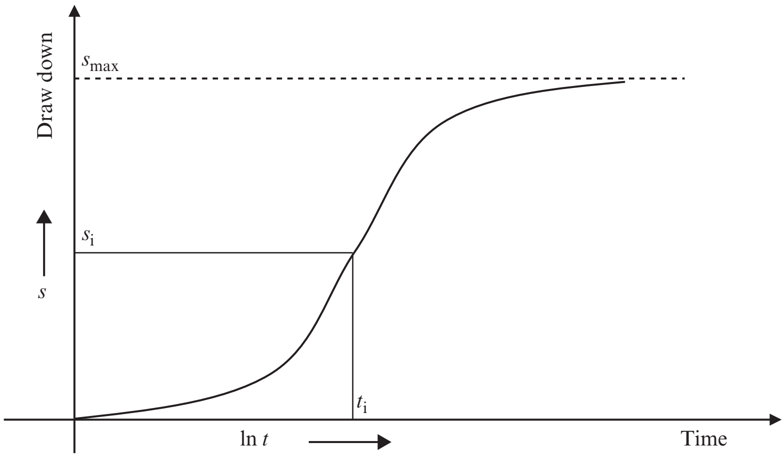

Figure 12.7 *Semilog plot of drawdown for leaky aquifer*

Therefore, slope at any point on semilog plot is

$$\frac{ds}{d(\log t)} = \frac{2.302Q}{4\pi T}e^{-u-\frac{r^2}{4B^2}\cdot\left(\frac{1}{u}\right)} \tag{12.49}$$

and hence the slope at the inflection point is

$$m_i = \frac{ds}{d(\log t)} = \frac{2.302Q}{4\pi T}e^{-u_i-\frac{r^2}{4B^2}\cdot\left(\frac{1}{u_i}\right)} \tag{12.50}$$

Differentiating Eqn. (12.50) further with respect to t

$$\frac{dm_i}{dt} = \frac{2.302Q}{4\pi T}e^{-u_i-\frac{r^2}{4B^2}\cdot\left(\frac{1}{u_i}\right)}\left[\left(-\frac{du_i}{dt}\right).-\frac{r^2}{4B^2}\left(-\frac{1}{u_i^2}\right).\frac{du_i}{dt}\right] \tag{12.51}$$

But

$$\frac{dm_i}{d(\log t)} = \frac{dm_i}{dt}.\frac{dt}{d(\ln t)}(2.302) = 2.302t\frac{dm_i}{dt} \tag{12.52}$$

At the inflection point,

$$\frac{\partial m_i}{\partial \log t} = 0$$

Hence from Eqs (12.51) and (12.52),

$$\frac{2.302^2 Qt}{4\pi T}e^{-u_i-\frac{r^2}{4B^2}\cdot\left(\frac{1}{u_i}\right)}\left[\frac{u_i}{t} + \frac{r^2}{4B^2}\left(-\frac{1}{u_i^2}\right).\frac{u_i}{t}\right] = 0 \tag{12.53}$$

which gives

$$u_i^2 = \frac{r^2}{4B^2} \Rightarrow u_i = \frac{r}{2B} \tag{12.54}$$

Therefore, Eqn. (12.50) becomes

$$m_i = \frac{2.302Q}{4\pi T}.e^{-\frac{r}{B}} \tag{12.55}$$

This property of the inflection point is used in estimating leaky aquifer parameters.

In the earlier solutions, it was assumed that the storage of the semiconfining bed is negligible. Hantush (1960) relaxed this assumption and obtained solution for leaky aquifer considering the storage of confining layers as follows:

$$s = \frac{Q}{4\pi T} H(u,\beta) \tag{12.56}$$

where,

$$H(u,\beta) = \int_u^\infty \frac{e^{-x}}{x} erfc\left(\frac{\beta\sqrt{u}}{\sqrt{x(x-u)}}\right) dx \tag{12.57}$$

$$\beta = \frac{r}{4}\left(\sqrt{\frac{K'S'}{b'TS}} + \sqrt{\frac{K''S''}{b''TS}}\right) \tag{12.58}$$

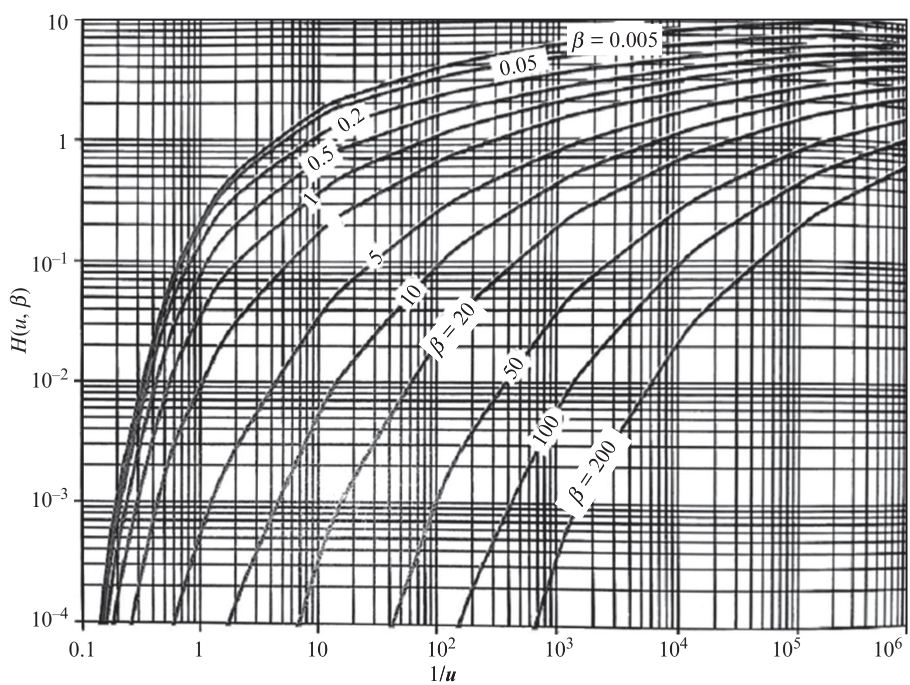

Figure 12.8 *Well function* $H(u,\beta)$ *for leaky aquifer with storage (Hantush 1960)*

where, T and S are transmissivity and storativity of main aquifer, respectively; K', S', and b' and K'', S'', and b'' are hydraulic conductivity, storativity, and thickness of upper- and lower-confining layers, respectively. *Appendix G* tabulates values of $H(u,\beta)$. Figure 12.8 plots the values of $H(u,\beta)$.

This solution is applicable for early time drawdown fulfilling

$$t < \frac{b'S'}{10K'} \text{ and } t < \frac{b''S''}{10K''} \tag{12.59}$$

$H(u,\beta)$ can be approximated (Singh 2008) by

$$H(u,\beta) \approx W(u) - \frac{4\beta}{\sqrt{\pi u}}\left(0.258 + \frac{0.693}{e^{\sqrt{u}}}\right) \text{ if } u > 10^4\beta^2 \tag{12.59a}$$

$$H(u,\beta) \approx \frac{1}{2}\ln\left(\frac{0.044}{u\beta^2}\right) \text{ if } u < 10^{-4}\beta^2 \text{ and } 10^{-5}/\beta^2 \tag{12.59b}$$

12.4 Partially Penetrating Well

Some aquifers are so thick that it is not justified to install a fully penetrating well. Instead, the aquifer has to be pumped by a *partially penetrating well*. Because partial penetration as shown in Figure 12.9 induces vertical flow components in the vicinity of the well, the general assumption that the well receives water from horizontal flow is not valid. Partial penetration causes the flow velocity in the immediate vicinity of the well to be higher than it would otherwise be, leading to an extra loss of head. This effect is strongest at the well face, and decreases with increasing distance from the well. It is negligible if measured at a distance that is 1.5–2 times greater than the saturated thickness of the aquifer, depending on the amount of penetration.

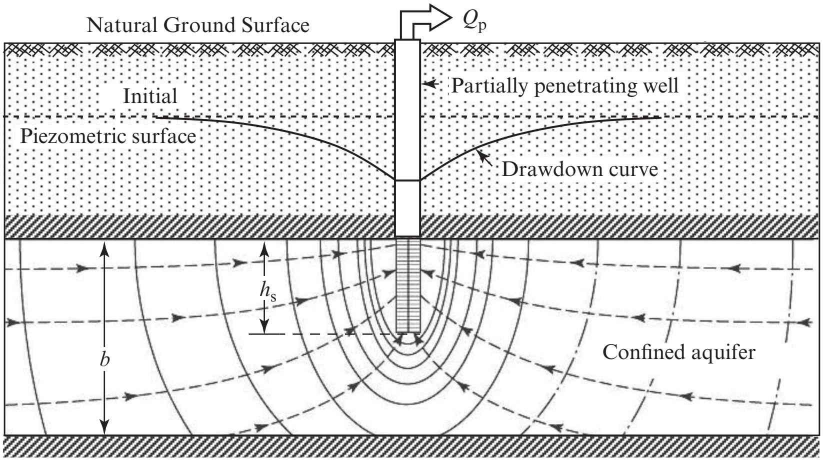

Figure 12.9 *Flow pattern in partially penetrating well*

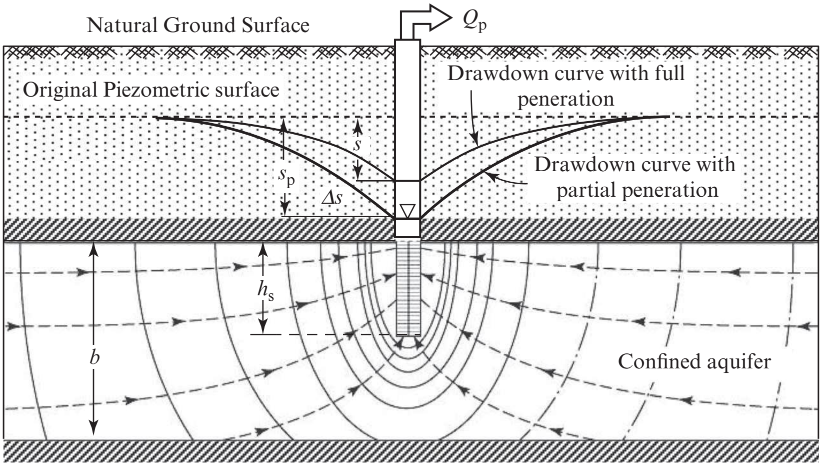

Figure 12.10 *Additional drawdown in well due to partial penetration*

If the aquifer has obvious anisotropy on the vertical plane, the effect is negligible at distances $r > 2b\sqrt{(K_r / K_z)}$. Hence, the standard methods of analysis cannot be used for $r < 2b\sqrt{(K_r / K_z)}$, unless allowance is made for partial penetration. For long pumping times ($t > bS/2K_z$), the effects of partial penetration reach their maximum value for a particular well/piezometer configuration and then remain constant. For confined aquifers under unsteady-state conditions, the Hantush modification of the Theis method or of the Jacob method can be used. For unconfined aquifers under unsteady-state conditions, the Neuman method can be used.

When the strainer of a well is not equal to the full thickness of the aquifer, the well is known as *partially penetrating well*. Generally, the thickness of the aquifer is large, and cost of drilling the well, casing, and strainer is also large. Hence, it is common to provide a strainer of short length than the aquifer thickness to save the cost as well as for practical considerations. Let height of strainer $= h_s$, and $h_s < b$, then well is partially penetrating and *penetration ratio* $p = h_s/b$ is less than one. In such case the flow toward the well will be three-dimensional because of vertical flow components as shown in Figure 12.9 and 12.10. Due to this the streamlines are no longer straight and parallel to the confining beds but they are curved and travel more distance to reach the well so there will be more resistance or head loss. Therefore, in a partially penetrating well for same rate of pumping $Q_p = Q$, the drawdown will be more than the fully penetrating well that is, $s_p > s$ as shown in Figure 12.10. On the other hand, if the partially penetrating well has drawdown equal to a fully penetrating well $s = s_p$, then the discharge from the partially penetrating well be less than the discharge from the fully penetrating well $Q_p < Q$, where Q_p and s_p are discharge and drawdown, respectively, for a partially penetrating well and Q and s are discharge and drawdown, respectively, for a fully penetrating well. Hence, in case of a partially penetrating well, the total drawdown can be expressed as follows:

$$s_p = s + \Delta s_{ap} \tag{12.60}$$

where, Δs_{ap} is additional drawdown due to partial penetration. The additional drawdown depends on the location and length of screen, distance of the observation well r, hydraulic conductivities in horizontal/radial and vertical directions, etc. For compressible leaking layer (with storage in confining beds), the general solution by Hantush (1961 and 1964) is

$$s_{\mathrm{p}} = \frac{Q}{4\pi K_{\mathrm{r}} b}\left\{W\left(u_{\mathrm{r}}, \frac{r}{B_{\mathrm{r}}}\right) + f\left(u_r, \frac{r}{B_{\mathrm{r}}}, \frac{r}{b}, \frac{l}{b}, \frac{d}{b}, \frac{z}{b}\right)\right\} \tag{12.61}$$

where, $u_{\mathrm{r}} = \dfrac{r^2 S}{4K_{\mathrm{r}} bt}$, $B_{\mathrm{r}}^2 = \dfrac{K_{\mathrm{r}} b}{K'/b'}$, $a = \sqrt{K_z / K_{\mathrm{r}}}$, l = depth of pumped well, d = length of blind pipe/casing so $h_s = l - d$ and $(l-d)/b$ = penetration ratio, z = depth of piezometer well, and

$$f = \frac{2b}{\pi(l-d)}\sum_{n=1}^{\infty}\frac{1}{n}\left(\sin\frac{n\pi l}{b} - \sin\frac{n\pi d}{b}\right)\cos\frac{n\pi z}{b} W\left(u_{\mathrm{r}}, \sqrt{\left(\frac{r}{B_{\mathrm{r}}}\right)^2 + \left(\frac{n\pi ar}{b}\right)^2}\right) \tag{12.62}$$

The solution for drawdown in nonleaky aquifer (when leakage is neglected) can be obtained by making $B_{\mathrm{r}} \to \infty$ or $K' \to 0$. Thus,

$$s_{\mathrm{p}} = \frac{Q}{4\pi K_{\mathrm{r}} b}\left\{W(u_{\mathrm{r}}) + f\left(u_{\mathrm{r}}, \frac{r}{b}, \frac{l}{b}, \frac{d}{b}, \frac{z}{b}\right)\right\} \tag{12.63}$$

For long pumping times in a nonleaky confined aquifer ($t > bS/2K_z$) or $u_{\mathrm{r}} < (K_z/K_{\mathrm{r}})(\pi r/b)^2/20$, the equation becomes independent of time (or $u_{\mathrm{r}} = 0$) and gets converted to

$$f = \frac{4b}{\pi(l-d)}\sum_{n=1}^{\infty}\frac{1}{n}\left(\sin\frac{n\pi l}{b} - \sin\frac{n\pi d}{b}\right)\cos\frac{n\pi z}{b} K_0\left(\frac{n\pi ar}{b}\right) \tag{12.64}$$

For long pumping times ($t > bS/2K_z$), the effects of partial penetration reach their maximum value for a particular well/piezometer configuration and then remain constant. For such steady state, $t \to \infty$ or $u_{\mathrm{r}} \to 0$. For large distance, $r > 1.5b.\sqrt{K_{\mathrm{r}} / K_z}$ may result $\beta > 4$ and the series of Eqn. (12.61) or f will be insignificant numerical value relative to that of the function $W(u_{\mathrm{r}}, r/B_{\mathrm{r}})$. Thus

$$s_{\mathrm{p}} = \frac{Q}{4\pi K_{\mathrm{r}} b} W\left(u_{\mathrm{r}}, \frac{r}{B_{\mathrm{r}}}\right) \tag{12.65}$$

and for nonleaky aquifer,

$$s_{\mathrm{p}} = \frac{Q}{4\pi K_{\mathrm{r}} b} W(u_{\mathrm{r}}) \tag{12.66}$$

Also the effects of partial penetration become unimportant even for r/b as small as $\sqrt{K_{\mathrm{r}} / K_z}$ provided $u_{\mathrm{r}} < 0.1(r/b)^2 (K_z/K_{\mathrm{r}})$. Eqs (12.65) and (12.66) are same as they would be for a fully penetrating well. In other words, the actual three-dimensional flow pattern changes to a radial type and is hardly distinguishable from that of a purely radial system at a distance from the pumped well equal to or greater than $r > 1.5b.\sqrt{K_r/K_z}$. Moreover, the flow will be as if the aquifer were isotropic with a conductivity equal to K_r.

At the face of well, the drawdown s_{pw} can be obtained with $r = r_w$ and $z = 0$. As $\frac{r_w}{B_r} \approx 0, t > \frac{Sb}{2K_z}$, and $(r_w/b)\sqrt{K_z/K_r}$ is small, the terms of second and higher powers of $(r_w/b)\sqrt{K_z/K_r}$ can be neglected. Generally, in practice, $(l/r_w)\sqrt{K_r/K_z} > 10$ and for $0 \le (l/b) \le 0.5$ the drawdown at the face of well becomes

$$s_{pw} = \frac{Q}{4\pi K_r b}\left\{W\left(u_w, \frac{r_w}{B_r}\right) + \frac{2b}{l}\left[\left(1-\frac{l}{b}\right)\ln\left(\frac{2l}{r_w}\sqrt{\frac{K_r}{K_z}}\right) - \frac{l}{b}\ln\frac{2b}{l} - \frac{0.423l}{b} + \ln\frac{2b+l}{2b-l}\right]\right\} \tag{12.67}$$

For a relatively short period of pumping $t < \frac{(2b-l-z)^2 S}{20K_z b}$, the drawdown in a piezometer at r from a partially penetrating well can be approximated (Hantush 1961a and 1961b) as follows:

$$s_p = \frac{Q}{8\pi K_r (l-d)}\left\{M(u_r,\beta_1) - M(u_r,\beta_2) + M(u_r,\beta_3) - M(u_r,\beta_4)\right\} \tag{12.68}$$

where $M(u,\beta) = \int_u^\infty \frac{e^{-x}}{x} erf\left(\beta\sqrt{x}\right)dx$, $M(u,-\beta) = -M(u,\beta)$, $\beta_1 = (l+z)/r$, $\beta_2 = (z+d)/r$, $\beta_3 = (l-z)/r$ and $\beta_4 = (d-z)/r$, The function $M(u,\beta)$ may be approximated by using the following equation:

$$M(u,\beta) \approx 2\left(\sinh^{-1}\beta - 2\beta\sqrt{\frac{u}{\pi}}\right) \text{ for } u < \frac{0.05}{\beta^2} < 0.01 \tag{12.69a}$$

$$M(u,\beta) \approx 2\left(\sinh^{-1}\beta - \beta\ \mathrm{erf}\left(\sqrt{u}\right)\right) \text{ for } u < \frac{0.05}{\beta^2} \tag{12.69b}$$

$$M(u,\beta) \approx W(u) \text{ for } u > 5/\beta^2 \tag{12.69c}$$

Eqn. (12.68) also gives the drawdown for the whole range of time in an infinitely deep aquifer ($b \to \infty$), and the well is screened throughout its depth of penetration ($d = 0$; $z = 0$). The drawdown at the well face becomes

$$s_{pw} = \frac{Q}{4\pi K_r l} M\left(u_w, \frac{al}{r_w}\right) \tag{12.70a}$$

If the aquifer isotropic, then $a = 1$; hence

$$s_{pw} = \frac{Q}{4\pi K_r l} M\left(u_w, \frac{l}{r_w}\right) \tag{12.70b}$$

Pumping at the same level, the yield of a partially penetrating well in an anisotropic aquifer will decrease with decreasing K_z/K_r other conditions being the same. The effect of anisotropy decreases as the well penetration increases. If K_z/K_r does not differ greatly from unity, the anisotropy will not be of particular consequence except for very small penetration. On the other hand, should K_z/K_r be very small, the anisotropy of the aquifer may cause an appreciable decrease in the yield of the partially penetrating well. If K_z vanishes, the flow toward the well becomes purely radial, confined to the part of the aquifer in which the well is screened.

The above expressions contain an infinite series and an exponential integral. Visocky (Walton 1970) used limited terms of the Hantush's solution for drawdown at the well face. Rewriting Eqn. (12.60) at the well face for nonleaky aquifer as follows:

$$s_{\text{pw}} = s_{\text{w}} + \Delta s_{\text{ap}} = \frac{Q}{4\pi T}\left[W(u_{\text{w}}) + \frac{4\pi T}{Q}\Delta s_{\text{ap}}\right] = \frac{Q}{4\pi T}\left[W(u_{\text{w}}) + 2\Delta s^{*}_{\text{ap}}\right] \quad (12.71)$$

where, Δs^{*}_{ap} is nondimensional additional drawdown. Visocky prepared plots between $\log_{10}\left(\frac{b}{r_{\text{w}}}\right)$ and Δs^{*}_{ap} and found that for $\frac{h_{\text{s}}}{b} > 20\%$ the plots were straight line as shown in Figure 12.11.

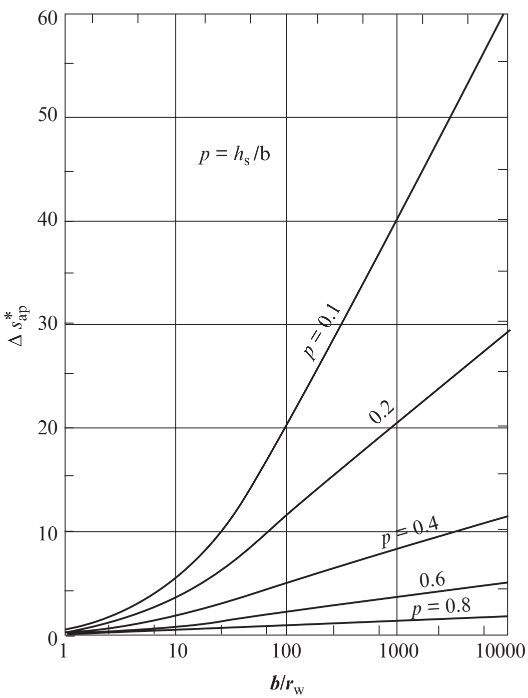

Figure 12.11 *Plot of additional drawdown at well face in partially penetrating well*

The equation of straight line is given by the following equation:

$$\Delta s_{\mathrm{ap}}^{*}=\frac{1-p}{p}\ln\left\{(1-p)\,p\frac{b}{r_{\mathrm{w}}}\right\} \tag{12.72}$$

Therefore,

$$s_{\mathrm{pw}}=\frac{Q}{4\pi T}\left[W\left(u_{\mathrm{w}}\right)+2\frac{1-p}{p}\ln\left\{(1-p)\,p\frac{b}{r_{\mathrm{w}}}\right\}\right] \tag{12.73a}$$

If u is small, then

$$s_{\mathrm{pw}}=\frac{Q}{4\pi T}\left[\ln\frac{2.25Tt}{r_{\mathrm{w}}^{2}S}+2\frac{1-p}{p}\ln\left\{(1-p)\,p\frac{b}{r_{\mathrm{w}}}\right\}\right] \tag{12.73b}$$

Hence, for steady-state condition, Visocky's solution becomes

$$s_{\mathrm{pw}}=\frac{Q}{2\pi T}\left\{\ln\left(\frac{r_{\mathrm{e}}}{r}\right)+\frac{1-p}{p}\ln\left[(1-p)\,p\left(\frac{b}{r_{\mathrm{w}}}\right)\right]\right\} \tag{12.74}$$

For generalization, if pumping rates through partially penetrating well and fully penetrating well are same $Q=Q_{\mathrm{p},}$ then

$$\frac{s}{s_{\mathrm{p}}}=\frac{s}{s+\Delta s_{\mathrm{ap}}}=\frac{\dfrac{Q}{4\pi T}W(u)}{\dfrac{Q}{4\pi T}W(u)+\Delta s_{\mathrm{ap}}}=\frac{W(u)}{W(u)+2\Delta s_{\mathrm{ap}}^{*}} \tag{12.75}$$

Similarly, for same drawdown $s=s_{\mathrm{p}}$, then

$$\frac{Q}{4\pi T}W(u)=\frac{Q_{\mathrm{p}}}{4\pi T}\left[W(u)+2\Delta s_{\mathrm{ap}}^{*}\right] \tag{12.76}$$

$$\frac{Q_{\mathrm{p}}}{Q}=\frac{W(u)}{W(u)+2\Delta s_{\mathrm{ap}}^{*}} \tag{12.77}$$

which is same as Eqn. (12.75), thus

$$\frac{Q_{\mathrm{p}}}{Q}=\frac{s}{s_{\mathrm{p}}} \tag{12.78}$$

This is called *performance* of the partially penetrating well. The *performance* or *efficiency* of the partially penetrating well is defined as the ratio of the flow Q_{p} from the partially penetrating well at a given drawdown to the flow Q that would be yielded at the same drawdown if the well were fully penetrating. For steady-state case, the performance is

$$\frac{s}{s_{\mathrm{p}}}=\frac{\ln\left(\dfrac{r_{\mathrm{e}}}{r}\right)}{\ln\left(\dfrac{r_{\mathrm{e}}}{r}\right)+\Delta s_{\mathrm{ap}}^{*}} \tag{12.79}$$

The efficiency of the partially penetrating well always exceeds the penetration ratio of the well that is,

$$\frac{Q_p}{Q} = \frac{s}{s_p} > \frac{h_s}{b} \tag{12.80}$$

This is because vertical flow components contribute additional inflow to the well. If the screen is at the top or bottom of the aquifer, the performance is same due to symmetry. If the screen is in the center of the aquifer, vertical flow components occur at both the top and bottom of the screen. To account for this, the aquifer is split midway along the symmetry line and the drawdown is computed for half of the aquifer and screen. Since the half sections of the well are symmetrical, the computed efficiency for the half section represents the efficiency or Q_p/Q value for the entire well. A special type of partially penetrating well is obtained when the intake portion of the well is divided over several screen sections separated by lengths of solid casing. The flow into such a well is greater than that into a well with the same total length of screen in one continuous section. Therefore, it is more advantageous to provide the screens of short lengths at several places rather than continuously at one place.

The solutions for drawdown for partially penetrating well in confined aquifer are also reasonable for unconfined aquifers particularly if the drawdown is small compared to the aquifer height and the well has been pumped for some time. For an unconfined aquifer, the modified equations for partial penetrating well are as follows

$$\Delta s_{ap}.2h_w = \frac{Q}{\pi K}\frac{1-p}{p}\ln\left\{(1-p)p\frac{b}{r_w}\right\} \tag{12.81a}$$

$$s_p^2 = s^2 + 2h_w \Delta s_{ap} \tag{12.81b}$$

where, $h_w = h_0 - s$ that is the saturated thickness at the well with full penetration. However, the effects of partial penetration become unimportant away from a pumping well. For

$$r > 1.5b.\sqrt{K_r / K_z} \tag{12.82}$$

the effect of partial penetration becomes negligible.

12.5 Large Diameter Wells

In earlier solutions, the diameter of the well consequently storage in the well was assumed small. But for many centuries, groundwater has been withdrawn from aquifers by means of large diameter wells and still large diameter wells are extensively used in different parts of the world especially in unconsolidated alluvial deposits or fissured rocks of shallow depths. Large-diameter wells are ideally suited for low-transmissivity aquifers and are different from small-diameter wells in the sense that there is a substantial contribution from well storage to the pumped discharge. Principally, large diameter wells have large storage volume ready for exploitation by direct pumping. Performance of a large diameter well has more problems in analysis and interpretations than a small diameter well. The larger the diameter, the greater the storage of the well, and therefore, at the time of need large quantities can be abstracted initially with no difficulty. But well storage has a distinctive effect on drawdown readings at early times during an aquifer test. In a large-diameter well during a short time period, the water is abstracted only from well storage. Therefore, consideration of storage should an integral part of solution in the case of large-diameter wells. When the abstraction rate is very low, the storage effects may be pronounced even in the case of borewells. Hantush (1964) proposed a well function $S(u,\rho)$ for obtaining drawdown in large diameter wells as follows:

$$s = \frac{Q}{4\pi T} S(u,\rho) \tag{12.83}$$

where $\rho = r / r_{\mathrm{w}}$ and r_{w} = radius of well screen. Hantush (1964) tabulated the values of the well function $S(u,\rho)$ for different values of u and ρ. For ρ = 1, it gives drawdown at the face of the well. This well function is for a constant pumping discharge and is in the form of an integral that involves Bessel's functions of zero order and first order of the first kind and second kind. This integral needs to be evaluated numerically to obtain a quantitative solution to a specific field problem. This solution includes all other assumptions of Theis solution as well as the drawdowns in the well and in the aquifer at the well face are equal at all times; the well loss is negligible; and the pumping discharge at all times is equal to the sum of discharges from the well storage and aquifer storage. Papadopulos and Cooper (1967) gave a well function $S(u_{\mathrm{w}},\rho)$ for obtaining drawdown in large diameter wells as follows:

$$s_{\mathrm{w}} = \frac{Q}{4\pi T} S(u_{\mathrm{w}},\rho') \tag{12.84}$$

where s_{w} = drawdown in well, $u_{\mathrm{w}} = \frac{r_{\mathrm{w}}^2 S}{4Tt}$, $\rho' = S\frac{r_{\mathrm{w}}^2}{r_{\mathrm{c}}^2}$, and r_{c} = radius of well casing. Papadopulos and Cooper (1967) tabulated (Appendix H) the values of the well function $S(u_{\mathrm{w}},\rho')$ for different values of u_{w} and ρ'. This well function also involves Bessel's functions of zero order and first order of the first kind and second kind.

In many situations, a constant pumping discharge is not observed in the case of large-diameter wells. A decrease in pumping discharge with increase in time is observed. Patel and Mishra (1983), Singh (2006), and Singh and Gupta (1986) proposed a kernel method for calculating drawdown in large diameter wells due to unsteady pumping discharge.

Swamee and Ojha (1995) approximated well functions of Hantush (1964) and Papadopulos and Cooper (1967) as the following:

$$S(u_{\mathrm{w}},1) = \left[\left(\ln\left(1+0.5615/u_{\mathrm{w}}\right)+2.93u_{\mathrm{w}}^{0.555}\right)^{-4} + \left(u_{\mathrm{w}}/0.83\right)^{1.76}\right]^{-0.25} \tag{12.85}$$

$$S(u_{\mathrm{w}},\rho') = \left[\left(\ln\left(1+0.5615/u_{\mathrm{w}}\right)+\frac{0.7u_{\mathrm{w}}^{0.41}}{\rho'^{0.25}}\right)^{-4} + \frac{u_{\mathrm{w}}^2}{\rho'\left(u_{\mathrm{w}}+0.45\rho'\right)}\right]^{-1} \tag{12.86}$$

Cimen (2001) proposed approximations for the drawdown in the well and in any observation well as follows:

$$S\left(u_{\mathrm{w}},\rho'\right)=\left[\frac{u_{\mathrm{w}}}{\rho'}-\frac{0.98}{0.5772+\ln u_{\mathrm{w}}}\right]^{-1} \tag{12.87}$$

$$s=\frac{Q}{4\pi T}\left(\frac{0.5772+\ln u_{\mathrm{w}}\rho^{2}}{0.98}\right)\left(\frac{u_{\mathrm{w}}}{\rho'}S\left(u_{\mathrm{w}},\rho'\right)-1\right) \tag{12.88}$$

Singh (2007) approximated well function by Papadopulos and Cooper (1967) as follows:

$$S\left(u_{\mathrm{w}},\rho'\right)=\frac{\rho'}{u_{\mathrm{w}}}\left[1+c_1\left(\rho'/u_{\mathrm{w}}\right)^{c_2}\right]^{-c_3} \tag{12.89a}$$

$$c_1=\frac{7}{5}\left(-\ln\rho'\right)^{-0.125}-1 \tag{12.89b}$$

$$c_2=\ln\sqrt{3}\left(-\ln\rho'\right)^{1/\pi} \tag{12.89c}$$

$$c_3=\left(\frac{37\pi}{90}\right)^{2}\left(-\ln\rho'\right)^{-10/33} \tag{12.89d}$$

For large diameter, early time data are required, therefore u_{w} is not small. For late time, the cumulative contribution from well storage to pumped volume of water up to that time can be considered negligible. The time beyond which the contribution from well storage to the pumped discharge can be considered negligible is given by the following equation:

$$t_{\mathrm{T}}=\frac{30Sr_{\mathrm{w}}^{2}}{T}\quad\text{or}\quad u_{\mathrm{wT}}=\frac{r_{\mathrm{w}}^{2}S}{4Tt_{T}}=\frac{\rho'}{100} \tag{12.90}$$

If $t > t_{\mathrm{T}}$ or $u_{\mathrm{w}} < u_{\mathrm{wT}}$ a large-diameter well technically behaves as a small-diameter well, and the equations and theory pertaining to small diameter wells are applicable to the diameter wells. For leaky aquifers, the well behaves as a small diameter well if,

$$t>\frac{30Sr_{\mathrm{w}}^{2}}{T}\left(1-\left(10r_{\mathrm{w}}/B\right)^{2}\right)\ \text{and}\ \frac{10r_{\mathrm{w}}}{B}<0.1 \tag{12.91}$$

In most cases, this time criterion applies almost for all time except for early few minutes from the start of pumping.

12.6 Flowing Well

Flowing wells are uncommon manifestation of geological activities. A permeable bed, sandwiched in between impermeable strata in a synclinal fold and exposed at the surface allowing recharge, contains water under pressure. Drilling through the upper confining bed can result in a flowing well. The water that flows from the flowing well is the outcome of an expansion of the water due to relief of pressure and compression of granular material of the aquifer and the included clayey beds. The drawdown at the flowing well, that is, the difference between the water level prevailing prior to the opening of the cap of the flowing well and the level of the threshold of the flowing well is constant, whereas the well discharge varies with time. The water yielding capacity depends on the pressure drop within the aquifer and the formation constants. The rate of flow from a flowing well Q for constant formation parameters for a homogeneous and infinite aquifer was given by Jacob and Lohman (1952) as follows:

$$Q = 2\pi T s_w G(\alpha) \tag{12.92}$$

where, s_w = constant draw down at the well, $\alpha = Tt/Sr_w^2$, t = time measured from the instant of cap opening of the well, and $G(\alpha)$ = well discharge function. Jacob and Lohman (1952) gave the following equation for $G(\alpha)$:

$$G(\alpha) = \frac{4\alpha}{\pi}\int_0^\infty xe^{-\alpha x^2}\left\{\frac{\pi}{2} + \tan^{-1}\left(\frac{Y_0(x)}{J_0(x)}\right)\right\}dx \tag{12.93}$$

where, J_0 and Y_0 are Bessel's functions of zero order of the kind and second kind, respectively. The solution thus is in form of an improper integral involving Bessel's functions. $G(\alpha)$ may be approximated for $\alpha < 0.05$.

$$G(\alpha) \approx 0.5 + \frac{1}{\sqrt{\pi\alpha}} \tag{12.94a}$$

and for $\alpha > 500$

$$G(\alpha) \approx \frac{2}{\ln(2.25\alpha)} \tag{12.94b}$$

Total production volume V up to time t is given by the following equation:

$$V = \int_0^t Q(\tau)d\tau = 8\pi T s_w t H(\alpha) \tag{12.95}$$

where, $H(\alpha)$ = well production function given by the following equation:

$$H(\alpha) = \int_0^\alpha G(\alpha)d\alpha \tag{12.96}$$

The yield of a flowing well within a given period of time between t_1 and t_2 as follows:

$$V = 2\pi T s_w \int_{t_1}^{t_2} G(\alpha)dt = 2\pi S s_w r_w^2\left(H(\alpha_2) - H(\alpha_1)\right) \tag{12.97}$$

Glover (1978) gave alternate solutions for $G(\alpha)$ and $H(\alpha)$ as a sum of infinite series involving Bessel's functions and their zeros. In these solutions, the aquifer was treated as an infinite aquifer until the disturbance produced by the flow from the well reaches the outer boundary of the aquifer. Thus, in a finite circular aquifer, for a flowing well located at the center of the aquifer, the solution of Glover (1978) is valid until the moving radius of influence, r_e, is less than the radius of the aquifer boundary. From the series solutions given by Glover (1978), it is possible to compute $G(\alpha)$ and $H(\alpha)$ with a limited number of terms for the known radius of the flowing well and valid assumed value of r_e.

The flowing well problem can also be solved by Duhamel's principle using discrete kernel coefficients derived from the Theis well function. Although this technique is simpler than analytical solutions of Jacob and Lohman (1952) and Glover (1978), it involves exponential integrals in generating discrete kernel coefficients and recursive expressions for $G(\alpha)$ and $H(\alpha)$. The improper integral involving Bessel's functions in Eqn. (12.93) cannot be evaluated by any of the ordinary means of integration. Using numerical methods, Jacob and Lohman (1952) and Glover (1978) tabulated $G(\alpha)$ and $H(\alpha)$ for a wide range. Appendix I lists values of flowing well function.

Swamee–Mishra–Chahar (2000) simplified the solution using numerical methods to avoid mathematical complexities of the solutions or inconvenience in interpolations of the tabulated values. The solutions are as follows:

$$G(\alpha) = \frac{1}{\sqrt{\pi\alpha}} + \frac{2}{\ln\left[(1+2.246\alpha)\left(1+30\alpha^{-0.45}\right)\right]} \tag{12.98}$$

$$H(\alpha) = \sqrt{\frac{4\alpha}{\pi}} + \frac{2\alpha\left(1+0.088\alpha^{-0.03}\right)}{\ln\left[(1+2.246\alpha)\left(1+30\alpha^{-0.45}\right)\right]} \tag{12.99}$$

The maximum error involved in Eqn. (12.98) is 2.32 percent at α = 0.03 with mean absolute error about 0.66 percent, while the maximum error in the use of Eqn. (12.99) is 2.45 percent at α = 0.5 and 400 with average absolute error = 0.77 percent. Singh (2007) also proposed similar equations for $\alpha > 100$ as follows:

$$G(\alpha) = \frac{2}{\ln(2.246\alpha)}\left[1+\left(\frac{11}{40000\alpha}\right)^{0.4}\right]^{-12} \tag{12.100}$$

$$H(\alpha) = \left[\frac{10\sqrt{\pi}}{9}\ln\alpha + \frac{5\pi}{99}\right]^{-1} \tag{12.101}$$

The maximum error involved in Eqn. (12.100) is 0.75 percent, while the maximum error involved in the use of Eqn. (12.101) is 0.7 percent. It is to be noted that relationships given by Swamee–Mishra–Chahar are applicable for full range of α ($0 < \alpha < \infty$), whereas Singh's equations are valid for restricted range of α (> 100). Therefore, the simplified solutions are good enough for practical purposes; and in these solutions, interpolations from the tables of the well discharge function and the well production functions are not required. Further, they do not require computations of the improper integrals involving Bessel's function.

12.7 Multilayer Aquifer

There are three types of multilayered systems:

(i) two or more aquifer systems separated by aquicludes;
(ii) two or more aquifers, each with its own hydraulic characteristics, separated by interfaces that allow unrestricted cross flow;
(iii) two or more aquifer layers separated by aquitards.

For the first type of system, if the pumping well pumps water from single aquifer layer at a time, then single-layered methods can be used. The transmissivity and storativity can be calculated for each layer individually. However, if the well fully penetrates the aquifer system, the single-layered methods cannot be used. For the second type of system, the response to pumping will be the same as that of a single-layered aquifer. The T and S are equal to the sum of the T and S of the individual layers. Therefore, single-layered methods can be applied, however, only the hydraulic characteristics of the equivalent aquifer system can be determined (Javandel and Witherspoon, 1969). For the third type of system, pumping one layer of the leaky system has measurable effects in layers other than the pumping layer. The resulting drawdown in each layer is a function of several parameters, which depend on the characteristics of the aquifer layers and the aquitards. If the pumping time period is short, and the effects of the drawdown in the unpumped layers can be considered negligible, then the methods for leaky single-layered aquifers can be used. A different method will need to be used for longer pump times. Various other analytical solutions have been derived for steady and unsteady-state flow to a well pumping a multilayered aquifer system.

Javandel and Witherspoon (1969) developed a solution for the drawdown in both layers of a confined two-layered aquifer system pumped by a well that is partially screened, either in the upper layer from the top downward, or in the underlying layer from the bottom upward as shown in Figure 12.12.

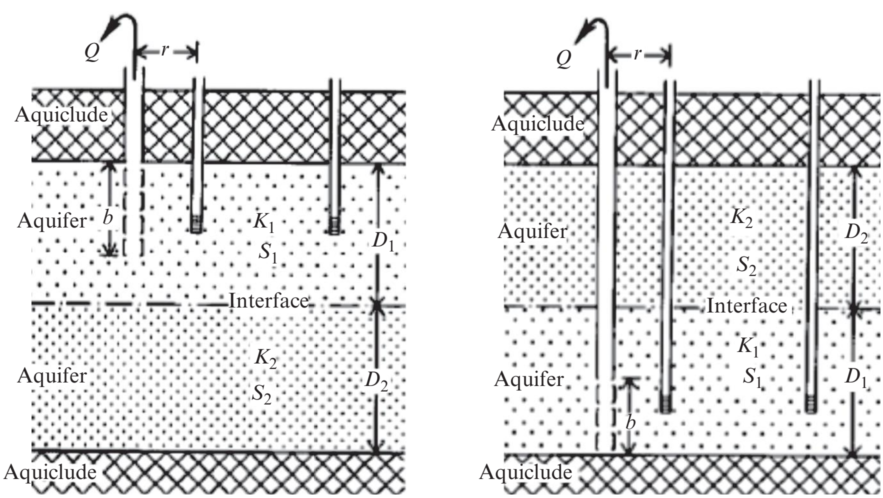

Figure 12.12 *Multilayer aquifer*

For small values of pumping time $t \le (D_1 - b)^2 / (10K_1D_1 / S_1)$, the drawdown equation for the pumped layer is the same as a confined single-layered aquifer that is pumped by a partially penetrating well. For large values of pumping time and with piezometers a fair distance away from the pumping well $r \geq 1.5\left(D_1 + K_2 D_2 / K_1\right)$, the partial penetration effects of the well can be ignored, hence

$$s = \frac{Q}{4\pi\left(K_1 D_1 + K_2 D_2\right)} W(u) = \frac{Q}{4\pi K D_{\text{eq}}} W(u) = \frac{Q}{4\pi T_{\text{eq}}} W(u) \tag{12.102}$$

$$u = \frac{r^2\left(S_1 + S_2\right)}{4t\left(K_1 D_1 + K_2 D_2\right)} = \frac{r^2 S_{\text{eq}}}{4t T_{\text{eq}}} \tag{12.103}$$

where, $T_{\text{eq}} = KD_{\text{eq}} = K_1 D_1 + K_2 D_2$ and $S_{\text{eq}} = S_1 + S_2$. The response of the two-layered system reflects the hydraulic characteristics of the equivalent single layered system. Following are the assumptions in addition to those involved in Theis solution:

(i) The system consists of two aquifer layers. Each layer has its own hydraulic characteristics, is of infinite areal extent, is homogeneous, isotropic, and of uniform thickness over the area influenced by the test. The interface between the two layers is an open boundary, that is, no discontinuity of potential or its gradient is allowed across the interface.
(ii) The pumped well does not penetrate the entire thickness of the aquifer system, but is partially screened, either in the upper layer from the top downward, or in the lower layer from the bottom upward (Figure 12.12).
(iii) The piezometers are placed at a depth that coincides with the middle of the well screen (Figure 12.12).
(iv) Drawdown data are available for small values of pumping time and for large values of pumping time. The late-time drawdown data are measured at $r \geq 1.5\left(D_1 + K_2 D_2 / K_1\right)$.

Since t is assumed to be large, u will be small. Therefore, Cooper–Jacob Method yields

$$s = \frac{Q}{4\pi T_{\text{eq}}} \ln\left(\frac{2.25 T_{\text{eq}} t}{r^2 S_{\text{eq}}}\right) \tag{12.104}$$

To analyze the late-time drawdown data, the Theis curve-fitting method can be used instead of the Cooper–Jacob method. If only one piezometer at the correct r is available, there may not be sufficient early time drawdown data to determine the hydraulic characteristics of the pumped layer. Therefore, only the combined T and S of the equivalent system can be determined.

12.8 Well Losses

In all earlier relations for the drawdown at the well face ($r = r_w$), the well losses were assumed to be zero. Actually, the drawdown at a well includes logarithmic drawdown and an additional loss caused by flow through the well screen and flow inside of the well to the pump. Total pumping lift is important in the selection of a suitable pump. The total lift includes the drawdown in the well s_w, which is the head loss in aquifer formation or *formation loss* and *well loss*, which is the loss in the screen or slots in the casing as shown in Figure 12.13.

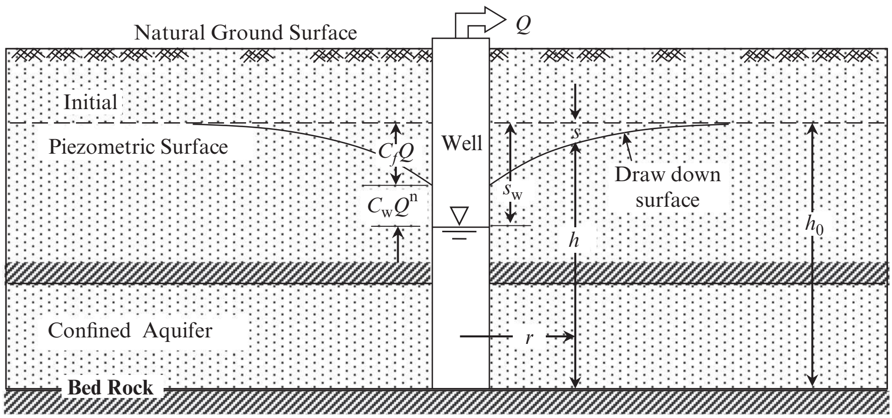

Figure 12.13 *Additional drawdown due to well losses*

Since the flow in the aquifer is laminar, the formation loss s_w varies linearly with Q. It also depends on the time; but if the pumping is continued for long time, s_w changes very little with time so the final s_w can be assumed a function of Q only. The flow through the well screen and in well itself is turbulent, therefore the well loss varies with some power of Q and thus the total loss or drawdown in the well is given by the following equation:

$$s_{\mathrm{wt}} = C_{\mathrm{f}} Q + C_{\mathrm{w}} Q^n \tag{12.105}$$

where C_f = formation loss constant, C_w = well loss constant, and n = exponent due to turbulence for which different values were suggested, for example $n = 2$ by Jacob (1947), $n = 2.5$ by Rorabough (1953), and $n = 3.5$ by Lennox (1966). Figure 12.14 plots variation in total loss and well loss with discharge. Values of n may be less than 2 if Q is relatively less, and full turbulence has not yet developed in the entire well entry flow. For very low values of Q, the flow may even be laminar through the screen and in the well itself, in which case C_w will be zero. The value of C_f could be calculated from one of the well flow equations developed in this and earlier chapters. The best way to estimate C_f, C_w, and n for a given well is by experiment. This can be done with the step drawdown test, where s_{wt} is measured for successively increasing values of Q. The step drawdown test gives information regarding the relation between Q and s_{wt} of a given well, which is important in selecting the optimum pump and depth of pumping. The test also shows how much head loss occurs in the aquifer and how much in and around the well. Excessive well losses indicate poor design and construction, poor development, or deterioration of the screen. Also, the C_f value can be used to estimate T of the aquifer, using the appropriate well flow equation relating s_w and Q.

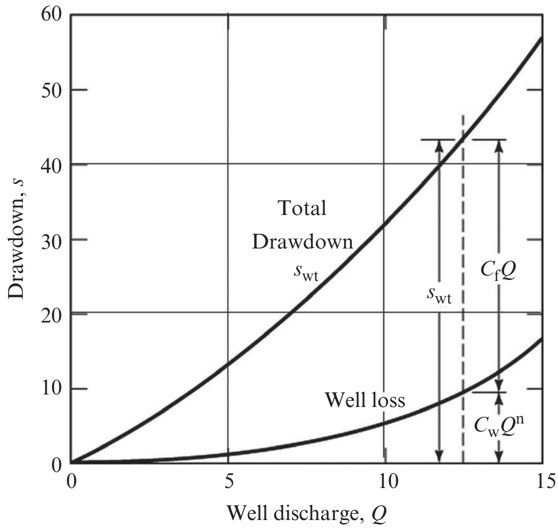

Figure 12.14 *Variation of well losses with discharge*

In Jacob (1947) method $n = 2$. Rewriting Eqn. (12.105), we obtain

$$\frac{s_{wt}}{Q} = C_f + C_w Q \tag{12.106}$$

Hence, a plot between Q and s_{wt}/Q is a straight line that yields C_f and C_w from its intercept and slope respectively. Rewriting Eqn. (12.105) for Rorabough (1953) method, we obtain

$$\frac{s_{wt}}{Q} - C_f = C_w Q^{n-1} \text{ or } \log\left(\frac{s_{wt}}{Q} - C_f\right) = \log C_w + (n-1)\log Q \tag{12.107}$$

Hence, a plot between log Q and log $(s_{wt}/Q - C_f)$ is a straight line with slope $(n - 1)$ and intercept C_w when $s_{wt}/Q - C_f = 1$. Since C_f is not known such a plot cannot be constructed. Hence, assume C_f and prepare such graphs till one result in a straight line as shown in Figure 12.15.

Clogging or deterioration of well screens can increase well losses in old wells. With proper design and development of new wells, well losses can be minimized. $C_w < 0.5$ for properly designed and developed well, $0.5 < C_w < 1.0$ for mild clogged screen or deteriorated wells, $1.0 < C_w < 4.0$ for severe clogged screen or deteriorated wells, and $C_w > 4.0$ difficult to restore well.

In steady state without well losses, Q varies inversely with $\ln(r_e/r_w)$, if all other variables are held constant. This means Q is not very sensitive to change in the well radius, for example, doubling a well radius increases the discharge only 10 percent. Because well losses vary with Q raised to power of two or more, the loss increases rapidly with increasing Q. The well loss can be minimized by providing sufficient screen or slot area and sufficient radius r_w. Larger r_w results into lower entry velocities and thus considerable reduction in well losses for example, doubling r_w will reduce entry velocity by half, which will reduce well losses by

75 percent if $n = 2$ and by 87.5 percent if $n = 3$. Thus, if well losses are considered, Q is sensitive to change in the well radius. The well loss can be substantial fraction of total drawdown when pumping rates are high.

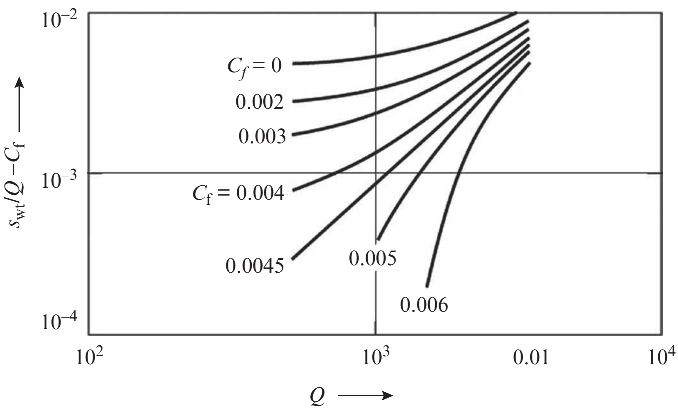

Figure 12.15 *Rorabough method for well losses estimation*

Specific capacity of a well is its discharge per unit drawdown, thus

$$\frac{Q}{s_{wt}} = \frac{1}{C_f + C_w Q} \tag{12.108}$$

Hence, the specific capacity decreases with increasing Q and t. This is a measure of the productivity of the well so a better well has higher specific capacity. Any significant decline in the specific capacity may be due to either reduction in transmissivity or increase in well losses (clogging or deterioration of well screens). *Well efficiency* E_w is another measure of well performance defined as the ratio of drawdowns at well face without and with well losses or ratio of specific capacities with and without considering well losses, and hence

$$E_w = \frac{s_w}{s_{wt}} = \frac{Q/s_{wt}}{Q/s_w} = \frac{C_f}{C_f + C_w Q} \tag{12.109}$$

Thus, the specific capacity or the well efficiency or the performance of a well is low, if the well losses are high. The drawdown due to well losses recovers very rapidly while due to formation loss recovers slowly once the pumping ceases. Where the well losses are large, the drawdown at the well face recovers rapidly, indicating less efficient well. For example, if after 1 hr of pumping, the drawdown recovers more than 90 percent within 5 min after pump is stopped, the well is inefficient due to rapid recovery caused by high well losses.

SOLVED EXAMPLES

Example 12.1: A 0.5-m diameter well (200 m from a river as shown in Figure 12.16) is pumping at an unknown rate from an unconfined aquifer. The aquifer has $h_0 = 20$ m, $T = 432$ m²/d, and $S = 4 \times 10^{-4}$. After 8 hr of pumping, the drawdown in observation well at 60 m from the river is 2 m, compute the rate of pumping.

Solution: Given data: $r_w = 0.25$ m, $T = 5.0 \times 10^{-3}$ m²/s, $S = 4 \times 10^{-4}$, $t = 8$ hr $=28,800$ s, and drawdown = 2 m in observation well. The equivalent drawdown $s' = s - \frac{S^2}{2h_0} = 2 - \frac{2^2}{2 \times 20} = 1.9$ m. Here, the well is near a river, therefore an image recharging well at 200 m from the river is put and the river is removed to create the equivalent hydraulic system. Therefore, the resultant drawdown is $= \frac{Q}{4\pi T}\left\{W\left(u_{\mathrm{p}}\right) - W\left(u_{\mathrm{i}}\right)\right\}$. Using the given data $u_{\mathrm{p}} = \frac{r_p^2 S}{4Tt}$ $= \frac{(140)^2 \times 4 \times 10^{-4}}{4 \times 28800 \times 5 \times 10^{-3}} = 1.36 \times 10^{-2}$; $u_{\mathrm{i}} = \frac{r_i^2 S}{4Tt} = \frac{(260)^2 \times 4 \times 10^{-4}}{4 \times 28800 \times 5 \times 10^{-3}} = 4.69 \times 10^{-2}$.

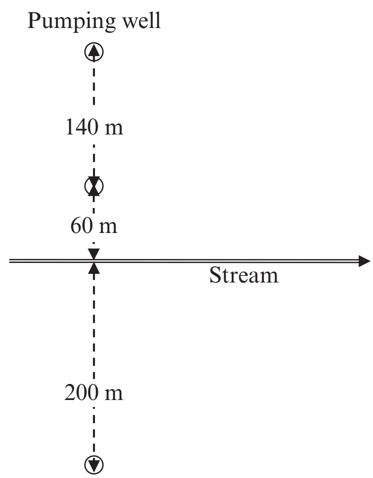

Figure 12.16 *Well near a river in unconfined aquifer*

Now for small value of u using Cooper–Jacob approximation $W(u_{\mathrm{p}}) = -.5772 - \ln(1.36 \times 10^{-2}) = 3.79$ and $W(u_{\mathrm{i}}) = -.5772 - \ln(4.69 \times 10^{-2}) = 2.54$. Hence, $1.9 = \frac{Q}{4\pi T}(3.79 - 2.54)$, which gives $Q = \frac{1.9 \times 4\pi \times 5 \times 10^{-3}}{1.25} = 0.095$ m³/s.

It is to be noted that both u_{p} and u_{i} were $> 10^{-2}$; therefore in place of Cooper–Jacob approximation, either Swamee-Ojha or Vatankhah equation should be used for the computation of the well functions. Using Swamee-Ojha's equation, $W\left(u_p\right) = 3.730312$ and $W\left(u_i\right) = 2.525443$. Therefore, $1.9 = \frac{Q}{4\pi T}$ $(3.730312 - 2.525443) \Rightarrow Q = \frac{1.9 \times 4\pi \times 5 \times 10^{-3}}{1.205} = 0.099$ m³/s, and hence 4.3 percent error in discharge computation using Cooper–Jacob Method.

Example 12.2: It is required to dewater a construction site 80 m by 80 m. The bottom of construction site will be 1.5 m below the initial water surface elevation. Four pumps are to be used of 0.5 m diameter at the four corners of the site. Transmissivity, storage coefficient, and initial saturated depth of the aquifer are T = 1,600 m²/d, S_y = 0.16, and h_0 = 30 m, respectively. The site needs to be ready after 1 month of pumping. Determine the required pumping rate.

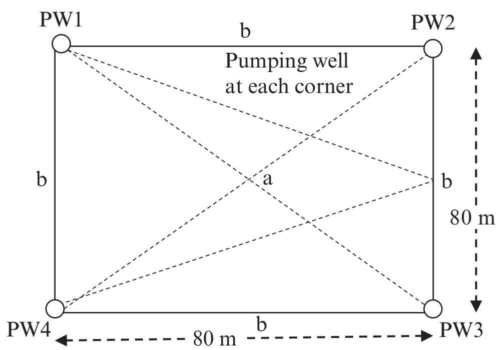

Figure 12.17 *Dewatering of construction site by four wells*

Solution: Refer Figure 12.17 for distance of point "a" from all four wells would be equal $r=\sqrt{40^2+40^2}=56.6\,\text{m}$ or $r^2=3203.56\,\text{m}^2$. At point "b" the distance will be same for well 1 and 2 $r_1=40\,\text{m}$ and for 3 and 4 $r_2=\sqrt{40^2+80^2}=89.44\,\text{m}$, hence $r_1.r_2=3577.708\,\text{m}^2$.

Since $(r_1.r_2)_b>(r^2)_a$, the resultant drawdown at b will be less than at a hence, the point "b" is critical. For this case, $u_1=\dfrac{r_1^2S}{4Tt}=\dfrac{40^2\times0.16}{4\times1600\times30}=0.001333$ and $u_2=\dfrac{r_2^2S}{4Tt}=\dfrac{89.44^2\times0.16}{4\times1600\times30}=0.0067$, and both u_1 and $u_2<0.01$. Therefore, Cooper–Jacob method of approximation can be used.

Since T = 1,600 m²/d and required minimum drawdown = 1.5 m at "b", its equivalent for confined aquifer $s'=1.5-\dfrac{1.5^2}{2\times30}=1.4625\,\text{m}$, hence $s_b=s_1+s_2+s_3+s_4=1.4625$, substituting values $2\left\{\dfrac{Q}{4\pi T}(-0.5772-\ln u_1)\right\}$ $+2\left\{\dfrac{Q}{4\pi T}(-0.5772-\ln u_2)\right\}=1.4625$ or $1.4625=\dfrac{(2\times Q)}{4\pi\times1600}\{-0.5772$ $-\ln0.00133-0.5772-\ln0.0067\}\Rightarrow Q=1405\,\text{m}^3/\text{d}$

Example 12.3: The foundation in a construction site (80 m × 100 m near a stream/water body) as shown in Figure 12.18 is 4.5 m deep, while the position of the prevailing water table is 3.0 m below the ground surface. The site is to be dewatered up to 0.5 m below the foundation level in 1 month using two pumping wells of equal strength at any two corners. Determine the optimal pumping rate if the initial saturated thickness, the transmissivity and the storage coefficient of the aquifer are 20 m, 1,600 m²/d, and 0.16, respectively.

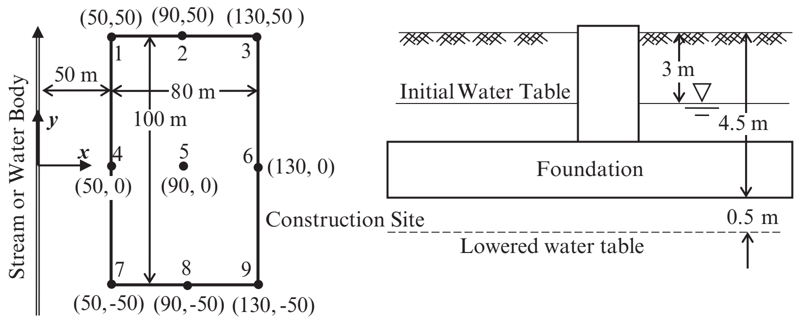

Figure 12.18 *Dewatering of construction site near a stream by two wells*

Solution: Given data: $h0$ = 20 m, T = 1,600 m²/d, S = 0.16, and t = 1 month = 24×3,600 =28,800 s. The minimum drawdown required = 4.5 + 0.5 − 3.0 = 2 m. The equivalent drawdown $s' = s - \dfrac{s^2}{2h_0} = 2 - \dfrac{2^2}{2\times 20} = 1.9$ m. The required two wells can be installed at any two out of four vertexes 1, 3, 7, and 9. These wells will be near a stream/waterbody, therefore two image recharging wells would be formed, and hence the equivalent hydraulic system would consist four (two real discharging and two image recharging) wells of equal strength. The critical point having resultant drawdown as minimum (= 1.9 m) may lie at 1, 2, 3, 4, 5, 6, 7, 8, or 9. The coordinates of vertexes and possible critical points are shown in Figure 12.18. The coordinates of the resulting image recharging wells will be same as the corresponding pumping well but with negative x coordinate. For example, if pumping wells are at (x_1, y_1) and (x_2, y_2), the resulting image recharging wells will be at $(-x_1, y_1)$ and $(-x_2, y_2)$, therefore the resultant drawdown at any point (x, y) will be $= \dfrac{Q}{4\pi T}\left\{W\left(u_{p1}\right) - W\left(u_{i1}\right) + W\left(u_{p2}\right) - W\left(u_{i2}\right)\right\}$ and the relevant distances will be $r_{p1}^2 = \left(x - x_1\right)^2 + \left(y - y_1\right)^2$; $r_{i1}^2 = \left(x + x_1\right)^2 + \left(y - y_1\right)^2$; $r_{p2}^2 = \left(x - x_2\right)^2$; and $r_{i2}^2 = \left(x + x_2\right)^2 + \left(y - y_2\right)^2$. Using Cooper–Jacob approximation, the resultant drawdown is $s_e = \dfrac{Q}{4\pi T}\ln\dfrac{r_{i1}^2 \times r_{i2}^2}{r_{p1}^2 \times r_{p2}^2} \Rightarrow Q = 4\pi \times 1600 \times 1.9 \times \left(\ln\dfrac{r_{i1}^2 \times r_{i2}^2}{r_{p1}^2 \times r_{p2}^2}\right)^{-1}$.

For different locations of pumping wells and critical points, the discharge can be computed, for example, if wells are at 1 (50,50) and 7 (50, −50) and drawdown at 3 (130,50): $r_{p1}^2 = (130-50)^2 + (50-50)^2 = 80^2$; $r_{i1}^2 = (130+50)^2 + (50-50)^2 = 180^2$; $r_{p2}^2 = (130-50)^2 + (50+50)^2 = 16400$; and $r_{i2}^2 = (130+50)^2 + (50+50)^2 = 42400$. Hence, $Q = 4\pi \times 1600 \times 1.9 \times \left(\ln \dfrac{180^2 \times 42400}{80^2 \times 16400}\right)^{-1} = 14854.52$ m³/d. Similarly, other values can be computed as listed in Table 12.1. It can be noted that the minimum drawdown occurs at point 1 for well locations at points 3 and 9 or 3 and 7 or 7 and 9; at point 3 for well locations at points 1 and 7; at point 7 for well locations at points 3 and 9 or 1 and 9 or 1 and 3; and at point 9 for well locations at points 1 and 7. The optimum location that requires minimum pumping is the minimum of maximum discharge for each case, therefore for the given problem, the best case is two wells is two wells located either at 1 and 7 or at 3 and 9 with Q = 14854.5 m³/d. By the same token, the least-efficient case is two wells located either at 1 and 3 or at 7 and 9, which requires pumping Q = 23251 m³/d.

Table 12.1 Discharge for different location of two wells

Drawdown at point	*Pumping wells located at*					
	1 and 7	*3 and 9*	*1 and 9*	*3 and 7*	*1 and 3*	*7 and 9*
1	NA	**14854.5**	NA	**16502.0**	NA	**23251.0**
2	11098.0	7601.1	9268.1	8789.6	6458.4	14963.0
3	**14854.5**	NA	10407.0	NA	NA	12739.0
4	11868.0	13979.0	12837.0	12837.0	12837.0	12837.0
5	11339.0	7583.1	9088.2	9088.2	9088.2	9088.2
6	13979.0	5729.8	8127.9	8127.9	8127.9	8127.9
7	NA	**14854.5**	**16502.0**	NA	**23251.0**	NA
8	11098.0	7601.1	8789.6	9268.1	14963.0	6458.4
9	**14854.5**	NA	NA	10407.0	12739.0	NA
Maximum, Q	**14854.5**	**14854.5**	**16502.0**	**16502.0**	**23251.0**	**23251.0**

Example 12.4: Determine the efficiencies of a partially penetrating well if the strainer is placed as shown in Figure 12.19. Use radius of influence = 120 m and diameter of well = 0.6 m.

For steady-state condition, the efficiency for a partially penetrating well from Eqn. (12.79) is $\dfrac{s}{s_\text{p}} = \dfrac{Q_p}{Q} = \dfrac{\ln\left(\dfrac{r_\text{e}}{r}\right)}{\ln\left(\dfrac{r_\text{e}}{r}\right) + \Delta s_{ap}^*}$. Given data r_e = 120 m; $r = r_\text{w}$ = 0.3 m;

and $b = 20$ m. Hence, $\ln\left(\frac{r_e}{r}\right) = \ln\left(\frac{120}{0.3}\right) = 5.9914$.

For Case 1: The screen is at the top of the aquifer with $p = \frac{h_s}{b} = \frac{10}{20} = 0.5$;

hence, using Eqn. (12.72) $\Delta s^*_{ap} = \frac{1-p}{p}\ln\left\{(1-p)p\frac{b}{r_w}\right\} = 2.8134$. Therefore,

Efficiency $\frac{s}{s_p} = \frac{5.9914}{5.9914 + 2.8134} = 0.6805$ or 68.05%.

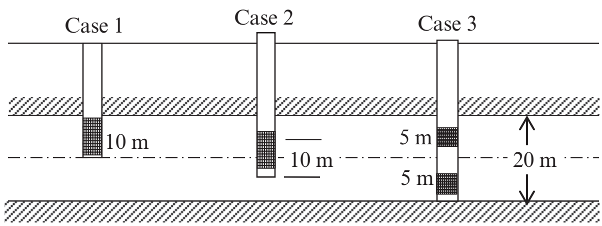

Figure 12.19 *Well screen at different locations in partially penetrating well*

For Case 2: The screen is at the center of the aquifer; vertical flow components occur at both the top and bottom of the screen. To account for this the aquifer is split midway along the symmetry line and the drawdown is computed for half of the aquifer (b = 10 m) and screen (h_s = 5 m). Since the half sections of the well are symmetrical, the computed efficiency for the half section represents the efficiency or Q_p/Q value for the entire well. Thus, $p = \frac{h_s}{b} = \frac{5}{10} = 0.5$, $\Delta s^*_{ap} = \frac{1-0.5}{0.5}\ln\left\{(1-0.5)0.5\frac{10}{0.3}\right\} = 2.1203$, therefore

Efficiency $\frac{s}{s_p} = \frac{5.9914}{5.9914 + 2.1203} = 0.7386$ or 73.86%

For Case 3: The screen is at two locations each at the center of half of the aquifer. In the same way as Case 2, the aquifer is split midway along the symmetry line and then again midway along the symmetry line through the screen and the drawdown is computed for one-quarter of the aquifer (b = 5 m) and screen (h_s = 2.5 m). Since these sections of the well are symmetrical, the computed efficiency represents the efficiency for the entire well. Thus, $p = \frac{h_s}{b} = \frac{2.5}{5} = 0.5$, $\Delta s^*_{ap} = \frac{1-0.5}{0.5}\ln\left\{(1-0.5)0.5\frac{5}{0.3}\right\} = 1.4271$, therefore

Efficiency $\frac{s}{s_p} = \frac{5.9914}{5.9914 + 1.4271} = 0.8076$ or 80.76%.

This shows that maximum efficiency in partially penetrating wells is achieved by distributing the given screen length at different locations. In addition, placing the well screen at the center of the aquifer yields higher efficiency in comparison with that placed at the same length screen at the top or bottom of the aquifer.

Example 12.5: A constant drawdown = 28.142 m was observed in a flowing well of radius 0.084 m in a confined aquifer having a transmissivity of 1.16×10^{-5} m²/s and a storativity of 3.88×10^{-5}. Calculate the discharge after half an hour and one and a half hour after opening the cap. Also compute the total production volume between this time interval.

Given data: s_w = 28.142 m, r_w = 0.084 m, $T = 1.16\times10^{-5}$ m²/s, and $S = 3.88\times10^{-5}$. Hence, at t_1 = 31.0 min, $\alpha_1 = 7.8576\times10^4$; and at t_2 = 91.0 min, $\alpha_2 = 2.3066\times10^5$. From Eqn. (12.98), $G(\alpha_1)$ = 0.165235, hence from Eqn. (12.92) discharge after half an hour = 3.39×10^{-4} m³/s and $G(\alpha_2)$ = 0.151921, hence discharge after one and half hour = 3.12×10^{-4} m³/s. From Eqn. (12.99), $H(\alpha_1) = 1.39465\times10^4$ and $H(\alpha_2) = 3.73984\times10^4$. Using Eqn. (12.97), the total production volume V = 1.139 m³.

PROBLEMS

12.1. The foundation in a construction site (60 m by 40 m) is 5 m deep, whereas the position of the prevailing water table is 3.5 m below the ground surface. The site is to be dewatered up to 0.5 m below the foundation level in 1 month using pumping wells one at each corner and one at centre. Determine the required pumping rate if the initial saturated thickness, the transmissivity and the storage coefficient of the aquifer are 20 m, 1,600 m²/d, and 0.16, respectively.

12.2. The foundation in a construction site (70 m by 50 m) is 6 m deep, whereas the position of the prevailing water table is 4.0 m below the ground surface. The site is to be dewatered up to 0.5 m below the foundation level in 1 month using pumping wells one at each corner. Determine the required pumping rate if the initial saturated thickness, the transmissivity and the storage coefficient of the aquifer are 25 m, 1,500 m²/d, and 0.15, respectively.

12.3. Find out the drawdown in the observation well and percentage contribution in this drawdown by the impervious boundary as shown in Figure 12.20 after 1 day of pumping with constant flow rate 60 l/s from an unconfined aquifer having $S_y = 2\times10^{-3}$ and h_0 = 28 m.

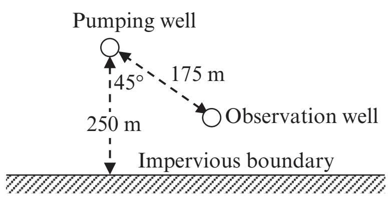

Figure 12.20 *Problem 12.3*

12.4. Determine the drawdown in the observation well after 15 hr of pumping with constant flow rate 75 l/s (Sy = 0.25 and h_0 = 20 m) in the problem shown in Figure 12.21.

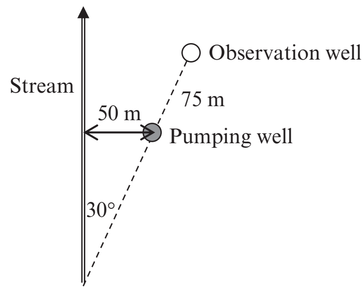

Figure 12.21 *Problem 12.4*

12.5. Determine the percentage recovery after 5 hr of pump stopped in drawdown in the observation well.

12.6. The foundation in a construction site (75 m by 50 m) is 6 m deep, whereas the position of the prevailing water table is 4.5 m below the ground surface. The site is to be dewatered up to 0.5 m below the foundation level in 1 month using pumping wells one at each corner. Determine the required pumping rate if the initial saturated thickness, the transmissivity and the storage coefficient of the aquifer are 20 m, 1,500 m^2/d, and 0.15, respectively.

12.7. The foundation in a construction site (70 m by 50 m) is 6 m deep, whereas the position of the prevailing water table is 4.0 m below the ground surface. The site is to be dewatered up to 0.5 m below the foundation level in 1 month using pumping wells one at each corner. Determine the required pumping rate if the initial saturated thickness, the transmissivity, and the storage coefficient of the aquifer are 25 m, 1,500 m^2/d, and 0.15, respectively.

12.8. Determine the efficiencies of a partially penetrating well if the strainer is placed as shown in Figure 12.22. Use radius of influence = 160 m and diameter of well = 0.5 m.

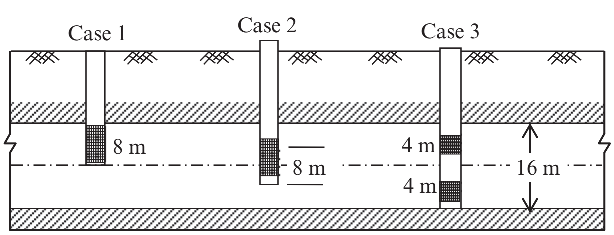

Figure 12.22 *Problem 12.8*

12.9. Discuss the effects of partial penetration of well on its drawdown and discharge with corresponding expressions.

12.10. Determine the efficiencies (under steady-state condition) of a partially penetrating well if the strainer is placed as shown in Figure 12.23. Use radius of influence = 120 m and diameter of well = 0.6 m.

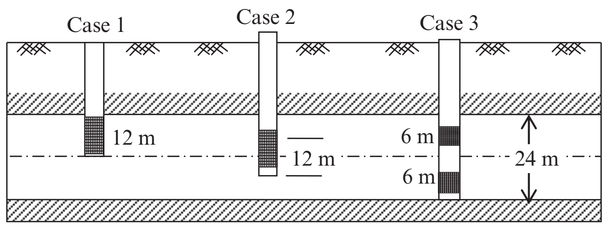

Figure 12.23 *Problem 12.10*

12.11. Compare the three partially penetrates cases as shown in Figure 12.24 with a fully penetrating well case where the 1.2 m diameter well is drilled in a confined aquifer of thickness 32 m. Comment on their relative efficiencies by evaluating their specific capacity (Q/s) for each case. Take the radius of influence for all cases as 200 m.

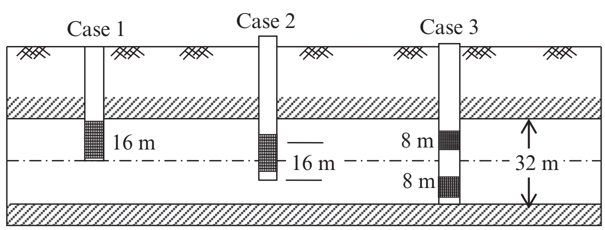

Figure 12.24 *Problem 12.11*

12.12. The foundation in a construction site (60 m by 100 m) is 4.5 m deep, whereas the position of the prevailing water table is 3.0 m below the ground surface. The site is to be dewatered up to 0.5 m below the foundation level in 1 month using pumping wells one at each corner. Determine the required pumping rate if the initial saturated thickness, the transmissivity, and the storage coefficient of the aquifer are 20 m, 1,600 m^2/d, and 0.16, respectively.

12.13. Show that in Hantush's method for leaky aquifer, $e^{r/B} K_0\left(r / B\right) = 2.3\, s_i / m_i$ and $u_i = r/2B$ where the subscript i denotes the values at inflection point.

12.14. The foundation in a construction site as shown in Figure 12.25 is 5.0 m deep, whereas the position of the prevailing water table is 2.5 m below the ground surface. The site is to be dewatered up to 0.5 m below the foundation level in 1 month using two pumping wells of equal strength at any two corners. Determine the optimal pumping rate if the initial saturated thickness, the transmissivity and the storage coefficient of the aquifer are 30 m, 1,500 m^2/d, and 0.15, respectively.

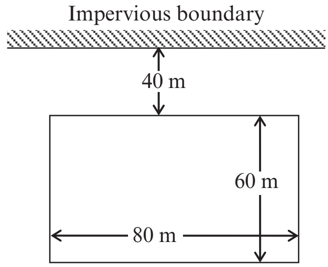

Figure 12.25 *Problem 12.14*

12.15. What is the effect of partial penetration on the drawdown in the well? A 30 cm well fully penetrating an artesian aquifer of 30 m depth and fully screened yields 1,800 lpm with a drawdown of 3m in the well. What will be the resulting drawdown when the screen extends from 7.5 to 22.5 m depth below the top of aquifer?

12.16. The coefficients of transmissibility and storage of a nonleaky artesian aquifer are 520 m^2/d and 1.21×10^{-3}, respectively. The aquifer is bounded on one side by a barrier boundary. A fully penetrating production well has been discharging at a constant rate of 2 m^3/min. The additional drawdown in an observation well 50 m away from the pumping well due to the effects of barrier boundary is found to be 0.5 m (i.e. the divergence in the Jacob's time-drawdown plot) for a pumping of 90 min. What should be the approximate distance of the pumping well from the barrier boundary.

12.17. An infinite nonleaky artesian has transmissibility of 600 m^2/d and storage coefficient 4×10^{-4}. Calculate the specific capacity of 30 cm fully penetrating well after 1 year of pumping at the rate of 1,600 m^3/d. Assume a well loss coefficients of 1,960 sec^2/m^5. What is the drawdown in the well after 1 year, assuming no replenishment? What is the well efficiency?

12.18. Discuss the effects of diameter of well on its drawdown and discharge with corresponding expressions.

12.19. A well is located in an unconfined aquifer with a vertical and horizontal hydraulic conductivity of 1.26 and 15.8 m/d, respectively. The value of specific storage is 0.00025 m^{-1}, and specific yield is 0.12. The aquifer's initial saturated thickness is 20.1 m and is pumped at a rate of 275 m^3/d. What is the drawdown at a distance of 7.0 m from the well after 1 and 50 day of pumping?

12.20. How and why are flowing wells found in the field? Explain.

12.21. How are multilayered aquifers treated? Explain.

Chapter 13

Estimation of Aquifer Parameters

13.1 General

The most important *aquifer parameters* are hydraulic conductivity K, transmissivity T, and storage coefficient S. They are the hydraulic properties of aquifers and soil materials that determine how fast water moves into, through and out of subsurface materials, and how piezometric surfaces or water tables are affected. In addition, identification of aquifer parameters is important for the development of mathematical models to predict the water and contaminant flow in an aquifer. Accurate prediction of ground water movement depends on how closely the pertinent aquifer parameters can be estimated. The aquifer parameters are important in design of drainage systems, agricultural water management schemes, optimum schemes of groundwater management, etc., and for predicting well yields, positions of water tables or piezometric surfaces, recharge rates of aquifers, water contents in vadose zones, surface–subsurface water relations, seepage from water bodies, groundwater contamination from waste disposal sites, etc. Any reliable method for aquifer parameter estimation that helps in simulating the actual behavior of natural aquifers is a valuable tool in groundwater management. Several techniques are available in the literature to estimate different aquifer parameters. These techniques may be classified under three categories: (i) pumping test techniques for saturated part of aquifer, (ii) slug test techniques for low transmissivity and/or poor quality groundwater aquifers, and (iii) auger hole, tensiometer, infiltration, etc., techniques for saturated/unsaturated zone. This chapter describes selected techniques for estimating aquifer parameters.

13.2 Pumping Test Techniques

Hydraulic properties of aquifers and associated layers can be determined by a *pumping test* that involves abstraction of water from a well at a controlled rate and observing, with respect to time, the water-level changes (the drawdown of the piezometric surface or water table) in the pumped well and/or in one or more observation wells at some distance from the pumped well. Pumping tests can also be designed to obtain information on the yield and drawdown of wells, for proper selection and positioning of pumps. The following information on aquifers and confining layers can be obtained from pumping tests:

(a) Transmissivity (and hydraulic conductivity if aquifer thickness is known), storage coefficient (specific yield in unconfined aquifers), leakage factor (of semiconfined aquifers), drainage factor (of semiunconfined aquifers), and hydraulic resistance (of confining layers),

(b) Distance, direction, and nature of barrier (impermeable) and recharge boundaries
(c) Lateral gradation, thickening, pinching, and interconnection of aquifers.

A properly designed test with one control well and a single observation well may suffice to obtain all the information needed pertaining to the aquifer and its boundary conditions in a limited area (Stallman, 1971). The following criteria may be followed.

Pumped or Control Well
The pumped well should be equipped with reliable power, pump, and discharge control equipment. The water discharged must be disposed away from the control well so that it cannot return to the aquifer during the test. This point is of special importance in testing shallow unconfined aquifers. It should be possible to measure depth to water before, during and after pumping. The diameter, depth, and position of all screens should be known.

Observation Wells
Observation wells for measuring drawdown may consist of existing wells or specially installed piezometers. Response of all observation wells to changing water stages should be tested by injecting a slug of water and measuring the head built up and decline of water level. Long abandoned wells tend to become clogged and unresponsive. Construction details of the observation well such as diameter, depth, and position of screen should be known. Radial distance from the control well to each of the observation wells must be known. At least three observation wells at different distances from the pumped well are desired, so that results can be averaged and/or erroneous data can be discarded. Observation wells may be located 10–100 m (or 100–300 m for thick aquifers) from the pumped well. A preferred arrangement consists of a pair of observation wells at distances of one, two, and four times the thickness of the aquifer from the pumped well. Each pair consists of a shallow well just reaching into the aquifer and a deep well extending to the bottom of the aquifer. Observation wells should be at a distance of at least 1.5 times the aquifer thickness from the pumped well in unconfined aquifers to avoid errors due to vertical flow components in the vicinity of the well. Financial constraints and the availability of existing wells (not at ideal locations) often force a compromise between what is theoretically desirable and what is practical. If water levels in observation wells are affected by factors other than the pumping well, observed drawdowns should be corrected.

Measurements During Test
Water levels are commonly measured with a steel tape from a well-defined measuring point that should not be changed during the test. Water-level recorders may be installed on observation wells. In wells not installed with recorders, water levels should be measured with sufficient frequency so that at least 10 measurements are taken in each logarithmic cycle in time. Discharge should be measured by anyone of the several methods. Besides, measurement of water levels and discharge, the temperature of water are observed and water samples are collected for quality determination, especially during tests on wells located in

areas facing salinity problems. The textural characteristic of the material in the zone of water-table fluctuation is of critical importance in making an evaluation of response to unconfined aquifers. Similarly, proper lithological logging of confining layers is of equal importance in predicting responses of aquifers adjacent to confining layers. The measurements should be made within acceptable tolerance levels of error (Stallman, 1971). The initial step toward correct analysis of aquifer test data comprises identification of water-level changes, in response to changes in the discharge at control well, from those caused by extraneous influences. Similarly, other aberrations, if any, in the levels are also identified and removed. If the pretest water level was constant, the drawdown data may be used straight away for further analyses. If the water level shows a declining or rising trend during pretest period, the trend should be extrapolated over the entire drawdown and recovery period for computation of drawdown and residual drawdown. Similarly, the drawdown curve has to be extrapolated through the recovery period for computation of recovery.

Interpretation of Test Data

A large number of analytic solutions are available for determining aquifer properties from pumping test data. The pumping test may be steady state or unsteady state or step drawdown test. In steady-state tests, long pumping is required and only T can be estimated; whereas in unsteady state pumping tests, the drawdowns are measured with respect to time and both S and T can be estimated, hence transient pumping tests are more common than steady-state tests. Different methods have been developed to cope with a wide variety of well and aquifer configurations, ranging from the simple homogeneous and isotropic aquifers to more complex situations involving anisotropy, barrier boundaries, leaky aquifers, fractured or porous medium, complete or partial penetration well, large-diameter well, etc. (Theis, 1935; Cooper–Jacob, 1946; Hantush, 1949, 1956, 1957, 1959, 1964; Hantush and Jacob, 1954, 1955, 1960; Boulton, 1963; Neuman and Witherspoon, 1968, 1969a, 1969b, 1972; Witherspoon et al., 1968; Şen, 1996, 2012). Some of these methodologies require a theoretical-type curve and matching to field data through a matching point, and then the aquifer parameter calculation equations are used for the numerical estimations. For the vast majority of the wells, reliable test data may not be available or parameter estimation methods involving curve matching or fitting straight lines may not be correctly applied where reliable data are available.

The application of these analytical methods requires both reliable test data and a good understanding of the assumptions inherent in the methods used. In pumping test analysis, the following assumptions and their applicability (unless differently stated) are involved (Santing, 1963):

1. Aquifer is homogeneous and isotropic.
2. Aquifer is of uniform thickness and bedrock is horizontal.
3. Aquifer is of infinite areal extent having no lateral inflow from surrounding water bodies.
4. Well penetrates the entire aquifer, therefore flow in the aquifer is everywhere horizontal radially toward the well.

5. The diameter well is small and the volume of water inside the well is negligible.
6. Well is pumped at constant rate Q, and the entire discharge is provided by the release of stored water and the water is instantaneously removed from the well.
7. Initially, the piezometric surface is horizontal.

These assumptions in actual field may not be valid due to various reasons. The aquifer is rarely homogeneous, isotropic, of uniform thickness, with horizontal bedrock, and of infinite areal extent. Alluvial and marine formations are stratified, and hard rocks are extremely heterogeneous and anisotropic. Transmissivity may not be constant, as in some cases changes in permeability may be brought about by chemical reaction and precipitation with time. Also, transmissivity in unconfined aquifer changes with continuous pumping, as drawdown is no longer small compared to the initial saturated thickness. Dupuit's assumption for unconfined aquifer may not be valid, as the flow is not horizontal and uniform near the steeper phreatic surface. If the vertical permeability of the semipervious layers is not far less than that of the aquifers, the flow through the aquifer does not remain horizontal, and neither the flow through the covering and underlying layers vertical. Slow release of water from falling water tables and irreversible compression of some formations do not justify a constant storage coefficient and instantaneous release from storage. Also, most confining layers are not continuous and have varying hydraulic resistance.

13.3 Confined Aquifer Parameters

The estimation of T or K with steady-state approach is based on the Thiem's equation, which requires equilibrium drawdowns s_1 and s_2 in two observation wells at distances of r_1 and r_2 from the pumped well corresponding to constant pumping rate Q. Theoretically, the drawdowns will never reach equilibrium, but the difference between drawdowns s_1–s_2 may reach near steady state after reasonable pumping time, and hence reasonably accurate estimate of T or K is possible. Once T is known, S can be determined using Theis equation if the drawdown s in one of the observation wells is measured at a certain time t.

The calculation of T and S with unsteady-state pumping test is based on the Theis equation, which requires observation of drawdowns with respect of time corresponding to constant pumping rate Q. As per Theis equation,

$$T = \frac{Q}{4\pi s} W(u) \tag{13.1}$$

$$S = 4Tu / \left(r^2 / t\right) \tag{13.2}$$

Since both u and $W(u)$ are functions of T and S; Eqs (13.1) and (13.2) cannot be solved directly and special techniques are needed.

13.3.1 Theis Curve Matching Method

Using Theis equation,

$$s = \frac{Q}{4\pi T} W(u) \Rightarrow \log s = \log \frac{Q}{4\pi T} + \log W(u) \tag{13.3}$$

$$\frac{t}{r^2} = \left(\frac{S}{4T}\right)\frac{1}{u} \Rightarrow \log \frac{t}{r^2} = \log \frac{S}{4T} + \log \frac{1}{u} \tag{13.4}$$

From Eqs (13.3) and (13.4), it is evident that functional relationship between $W(u)$ and $1/u$ must be similar to the relation between s and t/r^2, since $Q/4\pi T$ and $S/4T$ are constant. Thus, if log s is plotted against $\log(t/r^2)$ and $\log W(u)$ against log $1/u$ the resulting curves will be of the same shape, but horizontally and vertically offset by the constants $Q/4\pi T$ and $S/4T$. Theis suggested an approximate method for T and S based on a graphic method of superposition. A plot of $W(u)$ and $1/u$ (or u) on log–log paper is known as *type curve*. A drawdown plot is prepared on a separate sheet but on a same size and scale (same log–log paper). Both the plots are matched by keeping the coordinate axes of the two curves parallel and adjusted by moving horizontally and vertically until a position is found by trial whereby most of the plotted points of the observed drawdown data fall on a segment of the type curve. This procedure is called matching of curves. Any convenient point on the common overlapped part can be selected, and its coordinates are read to determine S and T. This method is known as *Theis curve matching method*. Three variations of the drawdown observations/plot are possible (i) time drawdown in a single observation well (s vs t), (ii) distance drawdown in several observation wells at a fixed time (s vs r^2), and (iii) general drawdown in several wells at different times (s vs t/r^2). The first scheme is more common. The steps in general drawdown scheme are as follows:

1. Prepare a type curve (plot of well function) on log–log paper between $W(u)$ and $1/u$ as shown in Figure 13.1.
2. Observe drawdowns in observation wells at regular intervals and draw a log–log graph between s and t/r^2 on a separate transparent paper with same size and scale as the type curve.
3. Overlay the transparent paper plot on the type curve keeping the co-ordinate axes of the two curves parallel and adjust by moving horizontally and vertically until a position is found by trial, whereby most of the plotted points of the observed drawdown data fall on a segment of the type curve. See Figure 13.1.
4. Select any convenient point on the matching curves (common overlapped part as in Figure 13.1), and read its coordinates s and t/r^2 and $W(u)$ and $1/u$.
5. Using these values $s, t/r^2, W(u)$, and $1/u$, determine the aquifer transmissivity by $T = \frac{Q}{4\pi s} W(u)$ and storage coefficient by $S = 4T(t/r^2)/(1/u)$.

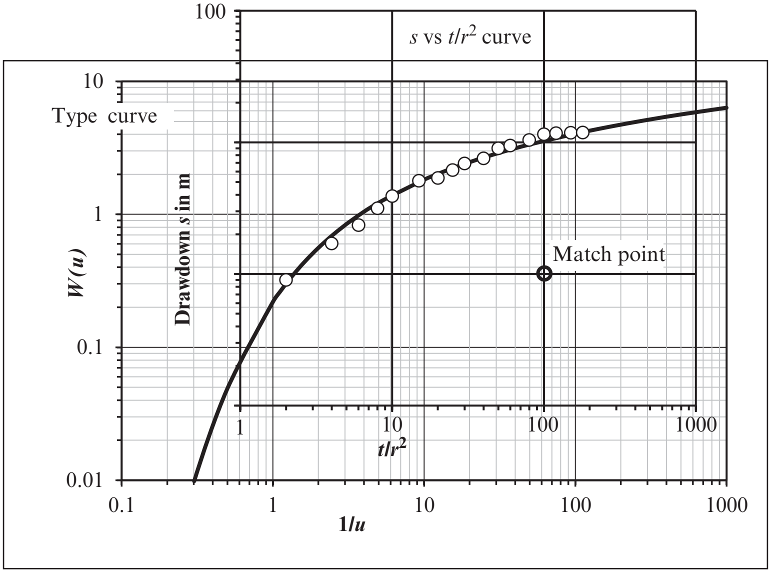

Figure 13.1 *Curve matching for time/general drawdown method*

In the most commonly used scheme, drawdowns are observed in a single observation well (r constant) with respect to time, and hence a log–log graph between s and t in place of s and t/r^2 is used. Rest steps are similar to the above case. The main drawback of Theis curve matching method is the subjectiveness and error of judgment involved in the match point.

13.3.2 Cooper–Jacob Method

For late time data, u is small, and hence Cooper–Jacob method can be used to approximate the drawdown as $s = \dfrac{2.302Q}{4\pi T}\log\left(\dfrac{2.25Tt}{r^2S}\right)$. Therefore, a plot between s and $\log\left(t/r^2\right)$ is a straight line (see Figure 13.2). If the straight line portion of the semilog plot between s and t/r^2 is extended, it intersects the abscissa (i.e. $s = 0$), and this condition ($s = 0$) implies that

$$0 = \frac{2.302Q}{4\pi T}\log\left(\frac{2.25Tt}{r^2S}\right) \tag{13.5}$$

Because $\dfrac{2.302Q}{4\pi T} \neq 0$, the log term must be zero so that

$$\frac{2.25T}{S}.\left(\frac{t}{r^2}\right)_0 = 1 \Rightarrow S = 2.25T\left(\frac{t}{r^2}\right)_0 \tag{13.6}$$

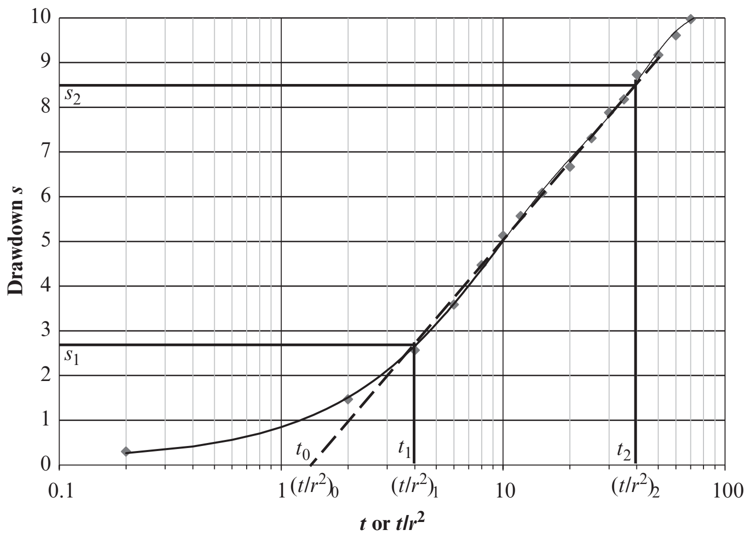

Figure 13.2 *Cooper–Jacob methods for time/general drawdown observation*

Taking the difference in drawdowns between one log cycle of t/r^2 in the straight line portion of the data curve

$$\Delta s = s_2 - s_1 = \frac{2.302Q}{4\pi T}\log\left\{\frac{2.25T}{S}10.\left(\frac{t}{r^2}\right)_1\right\} - \frac{2.302Q}{4\pi T}\log\left\{\frac{2.25T}{S}\left(\frac{t}{r^2}\right)_1\right\} = \frac{2.302Q}{4\pi T} \tag{13.7}$$

Thus,

$$T = \frac{2.302Q}{4\pi\Delta s} \tag{13.8}$$

Therefore, the estimation of aquifer parameters from this method consists of use of Eqn. (13.8) first to determine T and then to determine S using Eqn. (13.6). This method is widely used as it is more convenient, simple, and avoids matching of curves. The following steps are involved in this method. Depending on the available data, any one of three drawdown observation schemes (i.e. s vs t, s vs r, or s vs t/r^2) can be adopted In the first scheme, Eqn. (13.6) becomes

$$S = \frac{2.25T}{r^2}t_0 \tag{13.9}$$

where t_0 is the time for $s = 0$ that is the intersection point on the abscissa by the projection of straight line portion of the semilog plot between s and t as shown in Figure 13.2. The difference in drawdowns between one log cycle of t in the straight line portion of the data curve results into the same Eqn. (13.8) for T. The second scheme (distance drawdown in several observation wells at a fixed time) requires a plot between s and $\log r$, which will be straight line with negative slope as shown in Figure 13.3. In this case, Eqn. (13.6) changes to

$$S = \frac{2.25Tt}{r_0^2} \tag{13.10}$$

where r_0 is the distance for $s = 0$ by extension of straight line portion as shown in Figure 13.3. The difference in drawdowns between one log cycle of r in the straight line portion of the data curve results into

$$T = \frac{2.302Q}{2\pi\Delta s} \tag{13.11}$$

This equation enables the calculation of T, which when substituted along with t and r_0 in Eqn. (13.10) yields S.

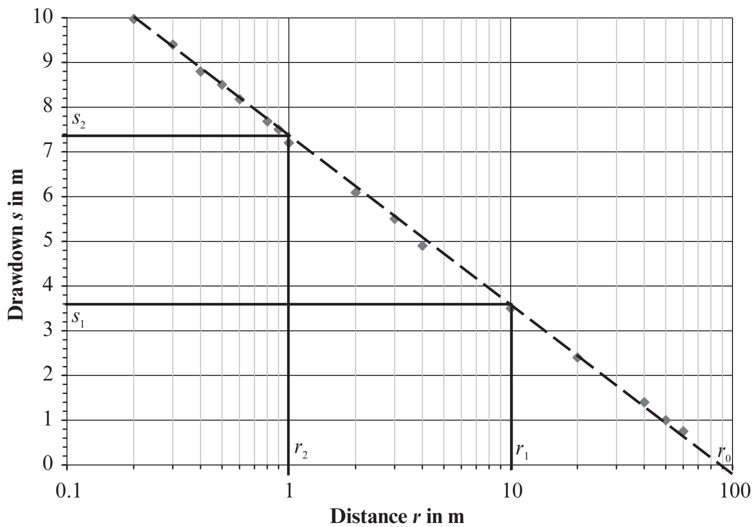

Figure 13.3 *Cooper–Jacob methods for distance drawdown observation*

The Cooper–Jacob method is valid for small u ($u < 0.01$) means longer pumping time and smaller r (observation well is not very far from the pumped well). For initial pumping time, u is not small; hence, the initial portion of the plot is curved and therefore should not be used. If r is relatively small, $u < 0.01$ may be attained after 1 hr of pumping for confined aquifers and after 12 hr for unconfined aquifers due to delayed yield.

Most often Cooper–Jacob straight line is used for aquifer parameter estimations from late time-drawdown data in cases of confined and unconfined aquifers. This straight line method is attractive because of its simplicity and straightforward calculations without tedious and dubious type-curve matching procedure. The warranty of the Cooper–Jacob method application depends on the fact that the late time-drawdown measurements fall along the final portion of the Theis-type curve. Another limitation is the subjective judgment of the limit up to which the data points should be considered in fitting a straight line, which requires trial and error.

13.3.3 Chow's Method

The curve matching method is inconvenient as it is involves subjectiveness/judgment of error in matching point. The Cooper–Jacob method cannot be used for early pumping time data. Chow (1952) developed a method that avoids curve matching and is unrestricted in its application. The observed drawdown data are plotted on a semilog paper similar to the Cooper–Jacob method (Figure 13.4).

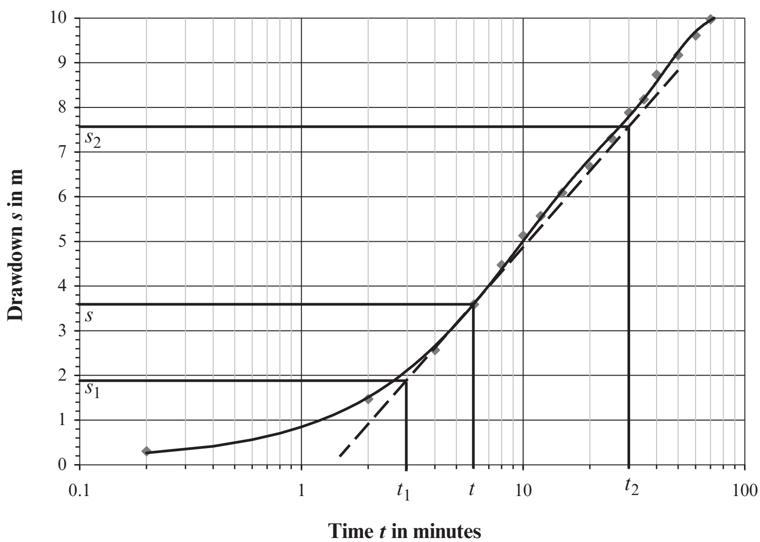

Figure 13.4 *Semilog plot of drawdown for parameter estimation by Chow's method*

Chow developed a function for this semilog plot as follows. The slope at any point on a semilog plot of drawdown curve is

$$\frac{ds}{d(\log t)} = 2.302t\frac{ds}{dt} \tag{13.12}$$

From Thies equation $s = \frac{Q}{4\pi T} \times \int_u^\infty \left(\frac{e^{-x}}{x}\right) dx$, taking derivative with respect to t

$$\frac{ds}{dt} = -\frac{Q}{4\pi T}\left(\frac{e^{-u}}{u}\right) \times \frac{du}{dt} \tag{13.13}$$

But $\frac{du}{dt} = -\frac{u}{t}$, hence

$$\frac{ds}{dt} = \frac{Q}{4\pi T}\left(\frac{e^{-u}}{u}\right) \times \frac{u}{t} = \frac{Q}{4\pi T}\left(\frac{e^{-u}}{t}\right) \tag{13.14}$$

Substituting Eqn. (13.14) in Eqn. (13.12) gives the slope as follows:

$$\frac{ds}{d(\log t)} = \frac{2.302Q}{4\pi T} e^{-u} \tag{13.15}$$

If we consider slope Δs for one log cycle on the tangent as shown in Figure 13.4, then

$$\Delta s = \frac{2.302Q}{4\pi T} e^{-u} \tag{13.16}$$

By dividing Theis equation with Eqn. (13.16) yields

$$\frac{s}{\Delta s} = \left(\frac{Q}{4\pi T} W(u)\right) / \left(\frac{2.302Q}{4\pi T} e^{-u}\right) = \frac{W(u) \times e^{u}}{2.302} = F(u) \tag{13.17}$$

which is function of u only. Chow(1952) plotted a curve for $F(u)$ as shown in Figure 13.5.

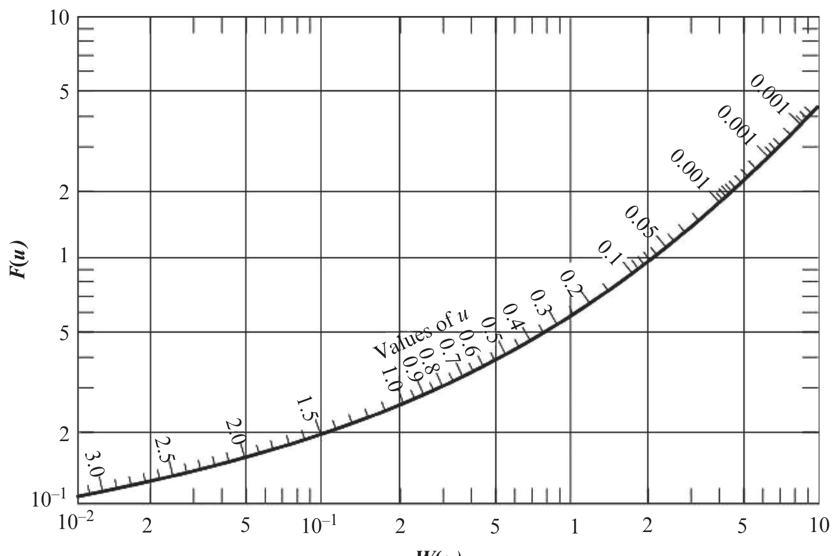

Figure 13.5 *Chow's function for parameter estimation*

If $F(u) > 2$, then

$$W(u) = 2.302\, F(u) \tag{13.18}$$

Hence, Chow's curve is not required; one can use Theis-type curve or table of well function.

The procedure for parameter estimation involves the following steps:

1. Prepare a plot between s and $\log t$.
2. Select any point on the curve and note down its s and t.
3. Draw a tangent at that point and determine Δs for the tangent line for one log cycle of time (Figure 13.4).

4. Using s and Δs, calculate $F(u) = s / \Delta s$.
5. Use Chow's plot or *Appendix J* for $F(u)$ and note down $W(u)$ and u for the above calculated value of $F(u)$.
6. Use $s = \frac{Q}{4\pi T} W(u)$ to find T with known values of $W(u)$, s and Q.
7. Finally, $u = \frac{r^2 S}{4Tt}$ gives S as r, t, u, and T are known.

13.3.4 Theis Recovery Method

Residual drawdown given by Theis (1935) for small u, as derived in Chapter 11 is

$$s_r = \frac{2.302Q}{4\pi T}\log\frac{t}{t'} \Rightarrow T = \frac{2.302Q}{4\pi s_r}\log\frac{t}{t'} \tag{13.19}$$

Therefore, the plot between residual drawdown and $\log(t / t')$ is straight line with slope $2.302Q / 4\pi T$. The difference in the residual drawdowns between one log cycle of t/t' is

$$\Delta s_r = \frac{2.302Q}{4\pi T} \Rightarrow T = \frac{2.302Q}{4\pi \Delta s_r} \tag{13.20}$$

From this equation T can be calculated, but S cannot be determined from recovery method. It is always preferred to continue the drawdown observation after pumping is stopped, as it does not require pumping cost but provides additional value of T, which cross checks its value estimated using other methods with pumping time data. Furthermore, this transmissivity value can be used to estimate S if drawdown s, in the observation well at the time of pump stopped is available as follows:

$$s = \frac{2.302Q}{4\pi T}\log\frac{2.25Tt_p}{r^2 S} \Rightarrow S = 2.25Tt_p / \left(r^2 \exp\left(\frac{4\pi Ts}{2.302Q}\right)\right) \tag{13.21}$$

where, t_p is total pumping time.

13.3.5 Singh Method

The curve-matching method proposed by Theis involves much subjectivity in judging the best match between the observed and theoretical curves, especially when only early drawdowns are considered. The Cooper–Jacob method cannot be applied to estimate aquifer parameters when for most of the data $u > 0.01$. In many cases of pump tests, substantial data have $u > 0.01$, especially when a pump test is for short duration and the observation well is at a large distance from the pumping well. Usually, the data pertaining to $u > 0.01$ are either neglected or considered unimportant. However, the early drawdown data are not corrupted by the effect of hydrological boundaries and interference of nearby wells. Also, because of certain factors such as pump failure and time and resource constraints, long duration pump tests sometimes are not feasible. Singh (2000) suggested a method for estimation of aquifer parameters from short duration pump-test data or initial data recorded during an abandoned pump test, which might otherwise be considered inappropriate for reliable estimation of the aquifer parameters. Singh (2000) defined u as follows:

$$u = \frac{S}{4T\alpha} \tag{13.22}$$

where, $\alpha = t / r^2$. Dividing Theis equation by α, we obtain

$$s' = \frac{s}{\alpha} = \frac{Q}{4\pi T\alpha} W(u) \tag{13.23}$$

Plot between s' and α is a bell-shaped curve for early drawdown data as shown in Figure 13.6.

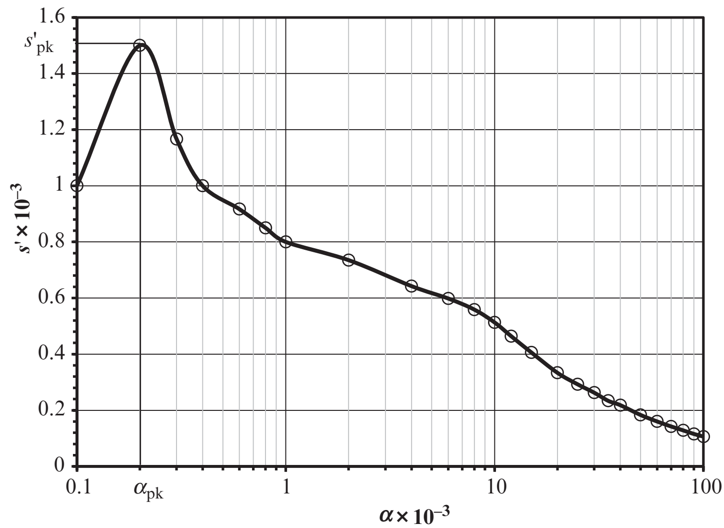

Figure 13.6 *Plot for Singh's method of parameter estimation*

Differentiating Eqn. (13.23) with respect to α gives the following:

$$\frac{ds'}{d\alpha} = \frac{Q}{4\pi T}\left(-\frac{W(u)}{\alpha^2} + \frac{1}{\alpha}\frac{dW(u)}{du}\frac{du}{d\alpha}\right) \tag{13.24}$$

But $\dfrac{du}{d\alpha} = -\dfrac{u}{\alpha}$ and $\dfrac{dW(u)}{du} = -\dfrac{e^{-u}}{u}$, therefore

$$\frac{ds'}{d\alpha} = \frac{Q}{4\pi T}\left(-\frac{W(u)}{\alpha^2} + \frac{e^{-u}}{\alpha^2}\right) \tag{13.25}$$

Equating it to zero gives the peak of bell-shaped curve for early drawdown data and hence for the peak

$$\frac{ds'}{d\alpha} = 0 \Rightarrow W(u) = e^{-u} \Rightarrow W(u) \times e^{u} = 1 \Rightarrow F(u) = \frac{1}{2.302} = 0.4343 \tag{13.26}$$

which yields

$$u_{pk} = \log e = \frac{1}{2.302} = 0.4343 \tag{13.27}$$

and

$$W\left(u_{pk}\right) = \frac{1}{e^{1/2.302}} = \frac{1}{1.5439} = 0.6477 \tag{13.28}$$

Chow's graph (Figure 13.5) can also be used to get these values approximately. A parameter with subscript pk denotes its value corresponding to the peak of s' and α curve. Therefore, the aquifer parameters can be obtained using these values as follows:

$$s_{pk} = \frac{Q}{4\pi T}0.6477 = \frac{Q}{19.4T} \Rightarrow T = \frac{Q}{19.4 s_{pk}} = \frac{0.6477}{4\pi}\frac{Q}{s'_{pk}\alpha_{pk}} \tag{13.29}$$

and

$$u_{pk} = \frac{S}{4T\alpha_{pk}} \Rightarrow \alpha_{pk} = \frac{S}{1.7372T} \Rightarrow S = 1.7372T\alpha_{pk} = \frac{0.2813}{\pi}\frac{Q}{s'_{pk}} \tag{13.30}$$

The procedure for parameter estimation involves the following steps:

1. Prepare a smooth curve between s' and α for early time drawdowns. The curve is bell shaped with a peak.
2. Read values of s'_{pk} and α_{pk} for the peak.
3. Determine T and S using Eqs (13.29) and (13.30), respectively.

This is a simple method for explicit determination of aquifer parameters using early drawdown data. The method does not require curve matching, initial guess of the parameters, or special care to check for $u < 0.01$. Also, less subjectivity is involved in locating the peak as compared to curve matching. This method requires only a few early drawdowns to estimate the aquifer parameters and still the estimates of the aquifer parameters are as good as those obtained by Theis curve matching using all data. Accuracy of the estimated aquifer parameters depends on accurate determination of the peak. At least one point should have $u > 0.4343$; however, more points in this range estimate more reliable aquifer parameters. This can be achieved by suitable placement of the observation well and fixing time intervals for drawdown measurement accordingly. In case of $u < 0.4343$ for all data, the resultant curve is not bell shaped (without peak) that means the observed data are not appropriate for this method. The pumping tests are designed such that the peak is observed by placing the observation well $r^2\alpha_{pk} > 2$ and by observing the drawdowns for $0.25t_{pk} \le t \le 5t_{pk}$ with smaller time intervals near t_{pk}. A semilog plot between s' and α with α on the log axis gives a better shape of the curve, especially when r is large. For time-drawdown data at a single observation well (r = constant), s/t is plotted against t (means $\alpha = t$), and the peak is identified. If $u < 0.4343$ (late drawdown observations), the peak could not be located on either s' and α (multiple observation wells) plot or s/t and t (single observation well) plot, the parameters can be obtained for $u < 0.01$ values using Cooper–Jacob method.

Later Singh (2008) developed a diagnostic curve of unimodal shape and a scaled well function for identifying the confined aquifer parameters from early drawdowns. It can be noted from Eqs (13.29) and (13.30) that s_{pk} and α_{pk} are the inverse measures of aquifer transmissivity and aquifer diffusivity (T/S), respectively, and hence s_{pk}/α_{pk} is an inverse measure of the storage coefficient. In terms of these peak parameters,

$$\frac{u}{u_{pk}} = \frac{S}{4T\alpha} / \frac{S}{4T\alpha_{pk}} = \frac{\alpha_{pk}}{\alpha} \Rightarrow u = 0.4343\frac{\alpha_{pk}}{\alpha} \tag{13.31}$$

$$\frac{s}{s_{pk}} = \frac{Q}{4\pi T}W(u) / \frac{Q}{4\pi T}0.6477 \Rightarrow \frac{s}{s_{pk}} = 1.5439W\left(\frac{0.4343\alpha_{pk}}{\alpha}\right) \tag{13.32}$$

$$\frac{s'}{s'_{pk}} = \frac{Q}{4\pi T\alpha}W(u) / \frac{Q}{4\pi T\alpha_{pk}}0.6477 = 1.5439\frac{\alpha_{pk}}{\alpha}W\left(\frac{0.4343\alpha_{pk}}{\alpha}\right) = w\left(\frac{\alpha}{\alpha_{pk}}\right) \tag{13.33}$$

where, $w(u)$ = scaled well function that is unimodal function with coordinates as (1, 1) at the peak. The unimodal curve between s' and α for early time drawdowns can be generalized by preparing other curve between s'/s'_{pk} and α/α_{pk}. This generalized curve has the coordinates of its peak as (1, 1) and is applicable for all values of Q and r, and hence it is termed the *diagnostic curve* because of its universal applicability for confined aquifers. In this method, the log–log curve between s' and α is matched with diagnostic-type curve between $w(\alpha/\alpha_{pk})$ and (α/α_{pk}) prepared on the same scale with a parallel shift of axes as shown in Figure 13.7.

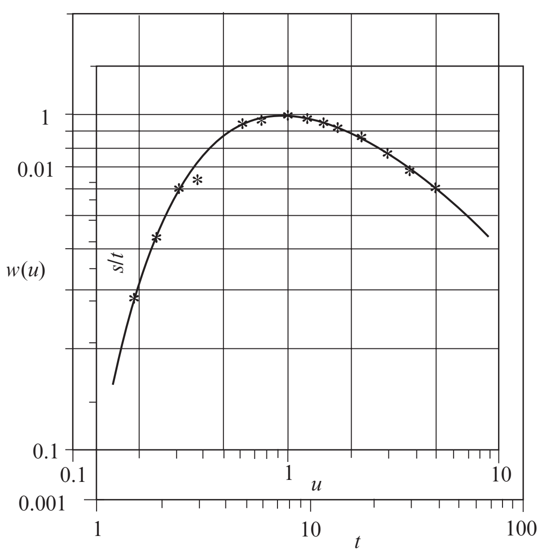

Figure 13.7 *Plot for Singh's (2008) method of parameter estimation*

The diagnostic curve can also be used for obtaining the drawdowns for other pumping discharges using $\frac{s_{pk1}}{s_{pk2}} = \frac{Q_1}{Q_2}$ or other observation points using $\frac{(t_{pk}/\alpha_{pk})_1}{(t_{pk}/\alpha_{pk})_2} = \frac{r_1^2}{r_2^2}$. The diagnostic curve may be viewed as an alteration of the Theis' curve. The unimodal shape of the diagnostic curve assists matching and reduces the personal errors to a considerable extent when compared to the Theis curve matching method; therefore, it is more accurate and less subjective than the Theis curve matching method. The diagnostic curve has a high diagnostic property, and it can easily identify the presence of boundaries and interference of wells.

13.3.6 Step and Intermittent Drawdown Tests

Step and intermittent drawdown tests are useful in determining the aquifer parameters and the efficiency of a pumped well. The intermittent drawdown tests involve a number of pumping and recovery cycles with variable pumping rates whereas step drawdown tests consist of a sequence of pumping periods of variable pumping rates and single recovery period at the end of pumping. Brisoy and Summers (1980) derived a solution for step and intermittent drawdown tests as follows

$$\frac{s}{Q_i} = \frac{1}{4\pi T}\ln\left[\beta_i(t)\frac{t-\tau_i}{t-\tau_i'}\right] \text{ for } t > \tau_i' \tag{13.34}$$

during recovery and

$$\frac{s}{Q_i} = \frac{1}{4\pi T}\ln\left[\frac{2.25T}{r^2 S}\beta_i(t)(t-\tau_i)\right] \text{ for } t > \tau_i \tag{13.35}$$

during pumping, where Q_i is the i^{th} pumping rate; and τ_i and τ'_i are the times when the i^{th} pumping rate starts and ends, respectively. For $i = 1$, $\beta_i(t) = 1$. For $i > 1$, $\beta_i(t)$ is given by the following equation:

$$\beta_n(t) = \Pi_{i=1}^{n-1}\left(\frac{t-\tau_i}{t-\tau_i'}\right)^{\frac{Q_i}{Q_n}} = \left(\frac{t-\tau_1}{t-\tau_1'}\right)^{\frac{Q_1}{Q_n}}\left(\frac{t-\tau_2}{t-\tau_2'}\right)^{\frac{Q_2}{Q_n}}\left(\frac{t-\tau_{n-1}}{t-\tau_{n-1}'}\right)^{\frac{Q_{n-1}}{Q_n}} \tag{13.36}$$

where, n = number of steps/times the variable pumping rates was adopted. The procedure for determining the transmissivity and storativity of an aquifer using step and intermittent drawdown tests can be divided into the following steps:

1. Calculate $\beta_i(t)$ at each step and measurement time using Eqn. (13.36) for the entire period.
2. Plot s/Q_i in linear scale versus adjusted time $\beta_i(t)(t-\tau_i)$ or $\beta_i(t)(t-\tau_i)/(t-\tau_i')$ on the logarithmic scale of semilog graph paper to get a straight line trend.
3. Select two points on the straight line separated by one log cycle to get $\Delta s/Q_i$.

4. Determine the transmissivity by $T = \dfrac{2.302}{4\pi\Delta(s/Q)}$.
5. Extend the straight line to the axis $s/Q_i = 0$ and read intercept $\beta_i(t_0)(t_0 - \tau_i)$ or $\beta_i(t_0)(t_0 - \tau_i)/(t_0 - \tau_i')$ as per the case.
6. Determine the storativity by $S = \dfrac{2.25T\beta_i(t_0)(t_0 - \tau_i)}{r^2}$.

13.4 Unconfined Aquifer Parameters

One of the assumptions in Theis solution is that the release of water from storage in the aquifer is in immediate response to the decline in head (drop of the water table or peizometric surface). For unconfined aquifers, this often is not true, because the rate of fall of the water table is faster than the rate at which pore water is released. When the water table is lowered by pumping, some pore water will drain immediately (early time response), and subsequent drainage takes some time and ultimately there may be synchronization between falling water table and pore water release (late time response). The rate of pore water release is also affected by the rate at which air can move into the zone draining zone. If such air movement is restricted, negative air pressures will develop, which will cause a delay in the release of pore water in response to a water table drop. Delayed yield also occurs in leaky aquifers that receive water from upper confining layers with a free water table. Pumping tests in unconfined aquifers should always be continued long enough so that the late response of *s*–*t* curve is adequately obtained.

Steady State: The estimation of T or K of unconfined aquifers with steady-state approach is based on the Thiem's equilibrium equation. It requires observation of equilibrium drawdowns s_1 and s_2 in two observation wells at distances of r_1 and r_2 from the pumped well corresponding to constant pumping rate Q. The average transmissivity between the two observation wells T_h can be computed using confined aquifer equation. Then, the transmissivity based on the initial saturated thickness h_0 can be corrected by $T = 2h_0T_h/(2h_0 - s_1 - s_2)$. Once T is known, S can be determined using method similar to a confined aquifer if the drawdown s in one of the observation wells is measured at a certain time t.

13.4.1 Corrected Distance Drawdown Method

The distance drawdown method for small u (late time) data can be applied to estimate parameters of an unconfined aquifer after modifying to equivalent drawdowns as follows:

1. Calculate equivalent drawdowns.
2. Plot the equivalent drawdowns s_e versus log r and fit a straight line
3. Note r_0 which is the distance for $s = 0$ by extension of straight line portion.
4. Also note the drawdown difference Δs for one log cycle of r in the straight line portion of the data.
5. Determine parameters $S = \dfrac{2.25Tt}{r_0^2}$ and $T = \dfrac{2.302Q}{2\pi\Delta s}$

13.4.2 Type Curve Matching Method

When a pumping test is performed in an unconfined aquifer, the water level initially drops relatively fast, then at a slower rate, and finally at faster rate as shown in Figure 12.2. The initial fast drop, which may occur only during the first few minutes of pumping, corresponds to release of water from storage (due to compression of aquifer material, decline in water table level, expansion of air in vadose zone/entrapped below water table, or decompression of water). In this period, response is similar to confined aquifer, and thus storativity corresponds to storage coefficient S. As water table continues to drop due to pumping more and more water is yielded by drainage of pore space which for longer pumping time (due to delayed yield) causes drawdown curve upward and follow a pattern corresponds to specific yield S_y. The following steps may be adopted in this procedure of parameter estimation of unconfined aquifers:

1. Prepare type curve on log–log paper as shown in Figure 12.3 using Neumann well function $W\left(u_a, u_y, \beta\right)$. The type curve consists of Type-A curves and Type-B curves connected by horizontal asymptotes and has different scales on horizontal coordinate axis for Type-A curves and Type-B curves.
2. Plot the observed drawdowns s versus time t on semitransparent log–log paper of same scale as type curve.
3. Superimpose s and t plot over the Type-B curves keeping axes parallel and till most of the data points follow the type curve. Select a convenient match point on the overlapped part and note values of $W\left(u_a, u_y, \beta\right), 1/u_y$, s and t as well as β of the matched curve.
4. Determine the transmissivity by $T = \dfrac{Q}{4\pi s} W\left(u_a, u_y, \beta\right)$ and specific yield by $S_y = \dfrac{4Ttu_y}{r^2}$.
5. Again superimpose s and t plot over the Type-A curves keeping axes parallel and till most of the data points follow the type curve of same β value. Select a convenient match point on the overlapped part and note values of $W\left(u_a, u_y, \beta\right), 1/u_a$, s and t.
6. Determine the transmissivity by $T = \dfrac{Q}{4\pi s} W\left(u_a, u_y, \beta\right)$ and storage coefficient by $S = \dfrac{4Ttu_a}{r^2}$. This value of transmissivity should be very close to that calculated from step (4).
7. Calculate horizontal hydraulic conductivity by $K_r = T / h_0$ and vertical hydraulic conductivity by $K_z = \dfrac{\beta K_r h_0^2}{r^2}$. Refer Schwartz and Zhang (2004) for more details.

Boulton (1963) presented a procedure for evaluating parameters for an unconfined aquifer based on the sigmoid relation between drawdown and time due to delayed yield. This procedure is similar to the Neumann method but for isotropic aquifer. The type curves are similar but for different parameter r/β', where

$$\beta' = \sqrt{T / \alpha S_y} \tag{13.37}$$

The resulting well function $w(u_{ay}, r/\beta')$ is called Boulton's well function for unconfined aquifer with delayed storage in which $u_{ay} = u_a$ for small values of t and $u_{ay} = u_y$ for large values of t. *Appendix E* tabulates the selected values of this well function. Theoretically, the type curves are valid only if S_y/S approaches infinity. In practice if this ratio is greater than 100, the mid segment of s versus t curve that forms the transition between the early and late response becomes essentially horizontal line. The value of s for the horizontal (where slope is zero) part of the s–t curve becomes

$$s = \frac{Q}{2\pi T} K_0 \left(\frac{r}{\beta'} \right) \tag{13.38}$$

If $S_y/S < 100$, the mid segment of s versus t curve is not horizontal. The storage coefficient S is applicable up to early pumping time t_A and in late pumping time after t_B when the delayed yield ceases and specific yield S_y prevails.

$$t_B = \alpha S_y \exp\left[-\alpha(t - t_A\right] \tag{13.39}$$

where, $1/\alpha$ is an empirical constant called delay index. It has dimension of time and is characteristic of the aquifer in question. The steps in this procedure of parameter estimation of unconfined aquifers are similar to the above-mentioned curve-matching method. This method also gives delay index α and the time that yield is no longer delayed and response starts similar to Theis curves for full release of pore water or specific yield.

13.4.3 Straight Line Method

Neumann (1975) proposed a simple method of determining parameters for an unconfined aquifer by straight line fit similar to Cooper–Jacob method, which may include the following steps:

1. Plot drawdown versus time on semilog graph paper. The plot indicates straight lines for early and late time data. If the drawdowns are not small in comparison to the saturated thickness of the aquifer, use modified equivalent drawdowns especially for the late time data.
2. Extend the straight trend of the late time segment of the s-log t curve till $s = 0$ on the horizontal axis and note down the corresponding time t_{0y}. Also note the drawdown difference Δs for one log cycle of time on this line.
3. Determine the transmissivity by $T = \dfrac{2.302Q}{4\pi\Delta s}$ and specific yield by $S_y = \dfrac{2.25Tt_{0y}}{r^2}$.
4. Extend the straight trend of the early time segment of the s-log t curve till $s = 0$ on the horizontal axis and note down the corresponding time t_{0a}.

Also note the drawdown difference Δs for one log cycle of time on this line.

5. Determine the transmissivity by $T = \dfrac{2.302Q}{4\pi\Delta s}$ and specific yield by $S = \dfrac{2.25Tt_{0a}}{r^2}$.
6. Fit a straight line through the intermediate part of the s-log t curve. The fitted line intercepts the late time straight line at t_β. Neumann (1975) showed that $\beta = 0.903u_\beta^{1.1053} = 0.903\left(\dfrac{r^2S}{4Tt_\beta}\right)^{1.1053}$, therefore the horizontal hydraulic conductivity $K_r = T/h_0$ and the vertical hydraulic conductivity $K_z = \dfrac{\beta K_r h_0^2}{r^2} = 0.903\dfrac{K_r h_0^2}{r^2}\left(\dfrac{r^2S}{4Tt_\beta}\right)^{1.1053}$. Refer Schwartz and Zhang (2004) for more details.

13.5 Leaky Aquifer Parameters

Jacob (1946), Hantush and Jacob (1955), and Hantush (1956, 1960, 1961, 1964) investigated different cases of a leaky aquifer. The additional assumptions involved in the analytical solutions for the leaky aquifers are the confining beds have a uniform hydraulic conductivity K' and thickness b'; flow is vertical in the confining bed and radial in the main confined aquifer; leakage across the confining bed comes from an aquifer whose head remains constant during pumping; etc. Various procedures are available for the estimation of parameters of leaky aquifers. Commonly used four methods are described in the subsequent sections.

13.5.1 Curve-Matching Technique

Jacob and Hantush (1955) solved the leaky aquifer problem as $s = \dfrac{Q}{4\pi T}W\left(u, \dfrac{r}{B}\right)$, when $B \to \infty, \Rightarrow \dfrac{r}{B} \to 0$, leakage coefficient $L_c = K'/b'$, leakage factor $B = \sqrt{\dfrac{Kbb'}{K'}} \Rightarrow L_c = \dfrac{Kb}{B^2} = \dfrac{T}{B^2}$ and hydraulic resistance of the confining layer $R_c = \dfrac{h_0 - b}{K'} = \dfrac{b'}{K'} = \dfrac{1}{L_c} = \dfrac{B^2}{T}$. The curve-matching method used for confined aquifer can be applied to leaky aquifer with modification suggested by Walton (1962). The leaky aquifer pump test also provides estimates on the vertical hydraulic conductivity of the confining bed K', which is one extra benefit. The steps are as follows:

1. Create type curves for the leaky aquifer well function $W\left(u, \dfrac{r}{B}\right)$ versus $1/u$ on log–log graph paper as in Figure 12.5 or Figure 13.8.

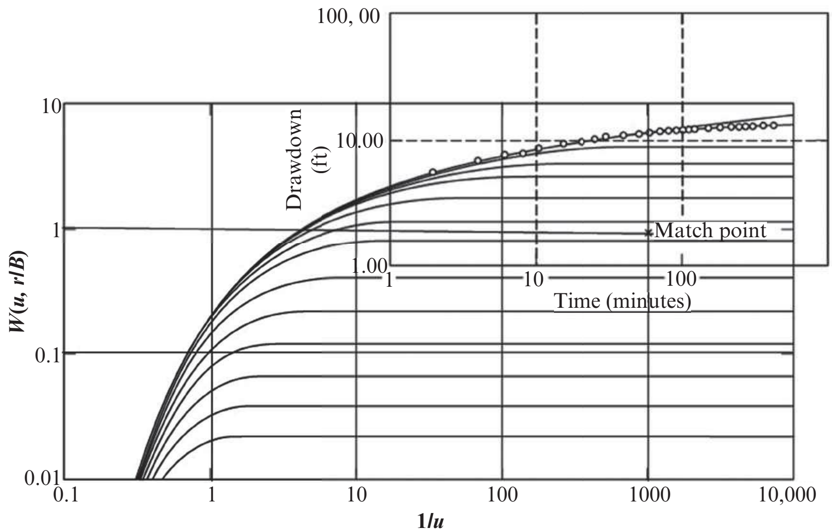

Figure 13.8 *Curve-matching leaky aquifer (Todd and Mays, 2005)*

2. Plot the observed drawdown against time on a transparent paper using log–log paper with same scale.
3. Move the plotted drawdown versus time data (transparent paper) on the type curves keeping axes parallel till most of the data fall on a type curve and thus find which of the family of type curves matches best. Read the r/B value for the matched curve.
4. Select a match point on the overlapped area as shown in Figure 13.8 (e.g. $W\left(u,\dfrac{r}{B}\right) = 1$ and $1/u = 10$, 100, or 1,000) and record the coordinates s and t.
5. Estimate the transmissivity by $T = \dfrac{Q}{4\pi s} W\left(u,\dfrac{r}{B}\right)$ and storage coefficient by $S = \dfrac{4Ttu}{r^2}$.
6. Calculate value of B from value of r/B as r is known.
7. Compute the leakage coefficient from $L_c = \dfrac{T}{B^2}$ or the vertical hydraulic conductivity of the confining bed from $K' = \dfrac{T}{B^2} b'$.

13.5.2 Hantush–Jacob Method

After long pumping time or when u is small the flow becomes steady and the following solution for drawdown by Hantush–Jacob (1955) applies

$$s = \frac{Q}{2\pi T} K_0\left(\frac{r}{B}\right) \tag{13.40}$$

Rewriting leakage factor equation as follows:

$$r = \sqrt{\frac{T}{K'/b'}}\frac{r}{B} \tag{13.41}$$

Therefore, the same functional relationship should exist between $K_0(r/B)$ and r/B and between s and r. Aquifer tests data from several observation wells under steady-state conditions are required. Parameters can be estimated as follows:

1. Prepare a type curve on log–log paper using Bessel's function $K_0(r/B)$ and r/B.
2. Plot the observed drawdowns, s, versus distance, t, on semitransparent log–log paper of same scale and size as type curve as shown in Figure 13.9.
3. Superimpose s and r plot over the type curve keeping axes parallel and till most of the data points fall on the type curve. Select a convenient match point anywhere in the overlapping portions of these two graphs and note values of $K_0(r/B)$, r/B, s, and r corresponding to the matched point.
4. Determine the transmissivity by $T = \frac{Q}{2\pi s}K_0\left(\frac{r}{B}\right)$ and leakage parameters by $B = \frac{r}{r/B}$ and $L_c = \frac{K'}{b'} = \frac{T}{r^2}\left(\frac{r}{B}\right)^2 = \frac{T}{B^2}$
5. Storage coefficient cannot be estimated by this method.

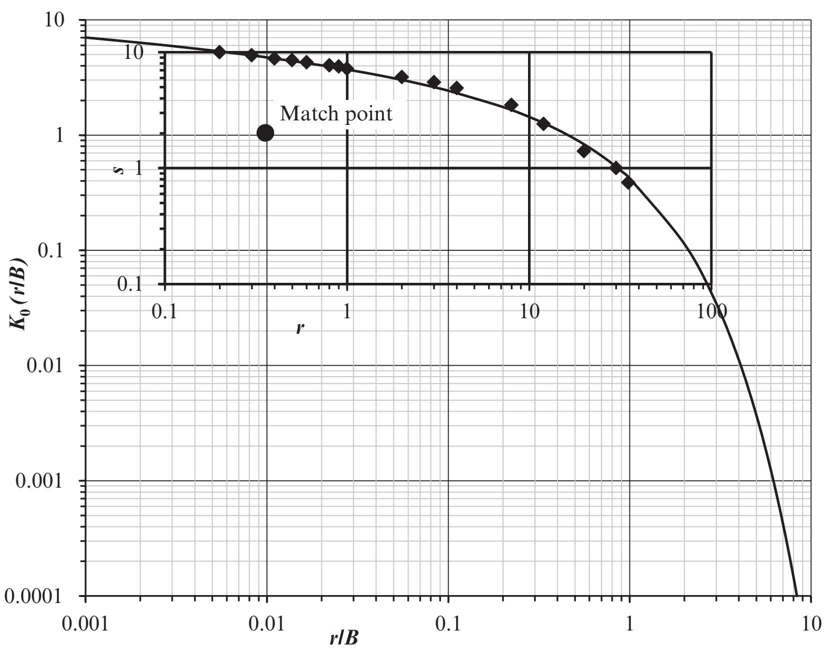

Figure 13.9 *Curve matching leaky aquifer (steady state)*

13.5.3 Hantush Method

When u is small and $\frac{r}{B} < 0.05$, then $s = \frac{Q}{2\pi T}\ln\left(\frac{1.12B}{r}\right) = \frac{Q}{2\pi T}\ln(1.12B) - \frac{Q}{2\pi T}\ln(r)$, $\Delta s = \frac{Q}{2\pi T}\ln\left(\frac{r_1}{r_2}\right)$, and $\frac{1.12B}{r_0} = 1$. Therefore, the plot between s and log r is a straight line with negative slope = $2.302Q/2\pi T$. The method consists of the following steps

1. Prepare a plot between s and log r, which is a straight line as in Figure 13.10.
2. Extend the straight line till the $s = 0$ axis and note r_0 (say $r_0 = 90$).
3. Determine $\Delta s = s_2 - s_1$ for one log cycle of r (say $r_1 = 10$ and $r_2 = 1$).
4. Calculate the transmissivity by $T = \frac{Q}{2\pi \Delta s}$ and the leakage parameters by $B = \frac{r_0}{1.12}$; $L_c = \frac{1.25T}{r_0^2}$; $R_c = \frac{r_0^2}{1.25T}$. However, the storage coefficient cannot be estimated.

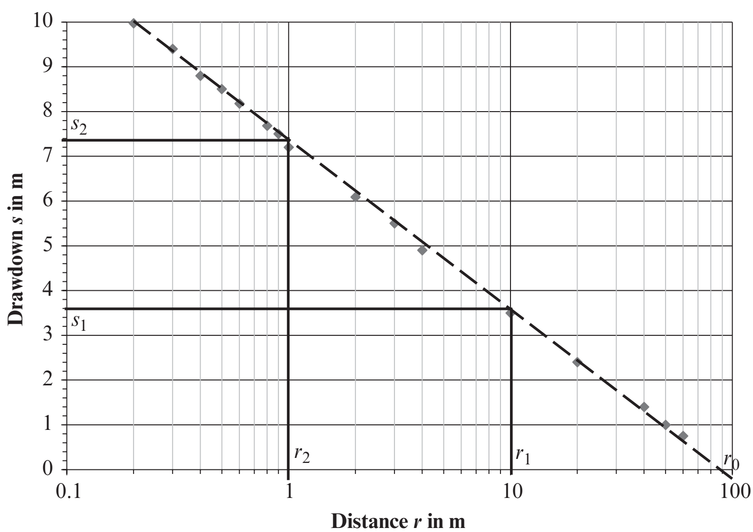

Figure 13.10 *Straight line method for leaky aquifer*

13.5.4 Hantush General Method

Hantush (1956) devised an elegant method to determine parameters of a leaky aquifer based on the semilog plot of drawdown versus time (Figure 13.11a). The important properties at the inflection point of this plot as derived in the previous chapter are $s_i = \frac{1}{2}s_{max} = \frac{Q}{4\pi T}K_0\left(\frac{r}{B}\right)$; $u_i = \frac{r}{2B}$; and $m_i = \frac{2.302Q}{4\pi T}.e^{-\frac{r}{B}}$; therefore,

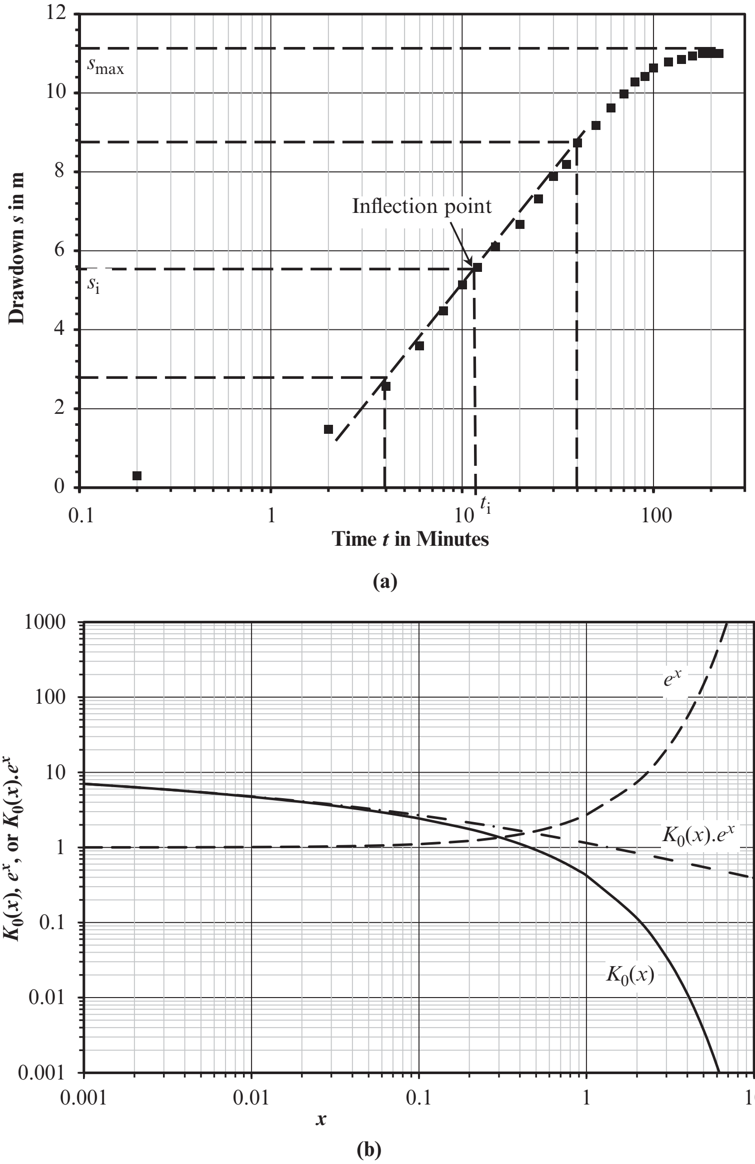

Figure 13.11 *Inflection point method for a leaky aquifer*

$$\frac{s_i}{m_i} = \frac{1}{2.302} K_0\left(\frac{r}{B}\right).e^{\frac{r}{B}} \Rightarrow 2.302\frac{s_i}{m_i} = K_0\left(x\right).e^x \qquad (13.42)$$

where, $x = r/B$. That means the ratio of drawdown to slope at the inflection point is independent of discharge and time of well pumping, and transmissivity and storage coefficient of the main aquifer. The step-by-step procedure is the following:

1. Pump the well and observe drawdown for long time till the drawdown in the observation well becomes steady.
2. Draw a graph as shown in Figure 13.11a between s and log t for log pumping time so that the later part of the graph becomes asymptotically horizontal. Note the maximum drawdown s_{max}. The difficulty in getting s_{max} by extrapolating the graph may be overcome by reading drawdowns in two or more observation wells.
3. Locate the inflection point on the drawdown curve, at which the drawdown is half of the maximum drawdown or $s_i = s_{max}/2$. Note the drawdown (s_i) and time (t_i) for the inflection point.
4. Determine the slope at the inflection point (m_i) by drawing a tangent and noting the drawdown difference on tangent line for one log cycle of time as shown in Figure 13.11a.
5. Calculate 2.302 s_i/m_i, which is equal to $K_0(x).e^x$.
6. Prepare a log–log plot of x (on horizontal axis) versus and $e^x, K_0(x)$, and $K_0(x).e^x$ (on vertical axis) as shown in Figure 13.11b.
7. Read value of x corresponding to $K_0(x).e^x$ as calculated in step 5 from the graph prepared in Step 6 and also read values of $K_0(x)$ and e^x for this value of x.
8. The leakage factor is given by $B = r/x$.
9. Determine the transmissivity by $T = \dfrac{Q}{4\pi s_i} K_0(x)$ or $T = \dfrac{2.302Q}{4\pi m_i} . \dfrac{1}{e^x}$.
10. Estimate the storage coefficient from $u_i = \dfrac{r^2 S}{4Tt_i} = \dfrac{r}{2B} = \dfrac{x}{2} \Rightarrow S = \dfrac{2Tt_i}{r^2} x$.
11. Finally, calculate the leakage coefficient by $L_c = \dfrac{K'}{b'} = \dfrac{T}{B^2}$.

Hantush (1956) devised another procedure to determine parameters of a leaky aquifer if drawdown observations with time are available in more than one observation wells. The steps in this procedure are the following:

1. Pump the well and observe drawdowns with time in all the observation wells.
2. Draw semilog graphs between s and log t for each observation well.
3. Determine the slope of the straight line portion of each curve by noting the change in drawdown Δs per log cycle of t.
4. Prepare a semilog plot between r (as ordinate) and log Δs (as abscissa).
5. Draw a best fit straight line and determine the slope of the straight line as the change Δr in r per log cycle of Δs.
6. Extend the straight line to abscissa yielding the intercept Δs_0 where $r = 0$.
7. Determine the transmissivity by $T = \dfrac{2.302Q}{4\pi\Delta s_0}$.
8. Calculate the leakage parameters by $B = \dfrac{\Delta r}{2.302}; L_c = \dfrac{T}{B^2}$.

9. Choose r (observation well), interpolate $K_0(r/B)$ from tabulated values of Bessel's function for known r/B, compute $s_i = \frac{Q}{4\pi T} K_0\left(\frac{r}{B}\right)$, read t_i corresponding to s_i from the graph between s and log t for that observation well (known r), and finally estimate the storage coefficient from $\frac{r^2 S}{4Tt_i} = \frac{r}{2B} \Rightarrow S = \frac{2Tt_i}{r^2}\frac{r}{B}$.

13.5.5 Hantush Curve-Fitting Method

When the aquitard is compressible, that is, the changes in aquitard storage are appreciable, Hantush (1959, 1964) solution $s = \frac{Q}{4\pi T} H(u, \beta)$ for $t < \frac{b'S'}{10K'}$ for a leaky aquifer with storage of semiconfining layer can be used for parameter estimation. Only the early time $t < \frac{b'S'}{10K'}$ drawdown data should be used so as to satisfy the assumption that the drawdown in the aquitard (or overlying unpumped aquifer) is negligible. The following steps may be followed:

1. Construct on log–log paper the family of type curves $H(u, \beta)$ versus $1/u$ for different value of β as shown in Figure 12.8.
2. On another semitransparent sheet of log–log paper of the same scale, plot s versus t for one of the observation wells.
3. Match the observed data plot with one of the type curves.
4. Select an arbitrary point on the overlapping portion of the two sheets and note the values of $H(u, \beta)$, $1/u$, s, and t for this point. Note the value of β on the selected-type curve.
5. Substitute the values of $H(u, \beta)$ and s and the known value of Q into equation $s = \frac{Q}{4\pi T} H(u, \beta)$
6. Calculate T.
7. Substitute the values of T, t, r, and u into equation $S = \frac{4Ttu}{r^2}$ and solve for S.
8. Substitute the values of β, T, S, r, and b' into equation $\beta = \frac{r}{4}\left(\sqrt{\frac{K'S'}{b'TS}}\right)$ and solve for $K'S'$.

It is difficult to obtain a unique match of the two curves because the shapes of the type curves change gradually with β (β values are practically indeterminate in the range $\beta = 0$–0.5, because the curves are very similar). As K' approaches zero or the ratio of the storativity of the aquitard and the storativity of the leaky aquifer is small ($S'/S < 0.01$), the effect of any storage changes in the aquitard on the drawdown in the aquifer is very small. In that case, and for small values of pumping time, the Theis formula can be used for parameter estimation.

Neuman and Witherspoon (1972) developed a method for determining the hydraulic characteristics of aquitards at small values of pumping time when the drawdown in the overlying unconfined aquifer is still negligible. The method is applicable for slightly leaky aquifer (Neuman and Witherspoon, 1968) as well as for a very leaky aquifer (Neuman and Witherspoon, 1972) provided $\beta < 1$ and $r < 100$ m. The different methods produce somewhat different results. This is due to inevitable inaccuracies in the observed and corrected or extrapolated data and especially, to the use of graphical methods. A lot of straight lines having to be fitted through observed and calculated data that do not fall exactly on a straight line. Consequently, there are slightly different positions possible for these lines, which are still acceptable as fitted straight lines, but give different values of the hydraulic parameters. The same difficulties are encountered when observed data plots have to be matched with a type curve or a family of type curves. In these cases too, slightly different matching positions are possible, with different match-point coordinates as a result, and thus different values for the hydraulic parameters. Most of the methods only require data from the pumped aquifer. But such data are not sufficient to characterize a leaky system (Neuman and Witherspoon, 1969b). The calculations should also be based on drawdown data from the aquitard; and if present, from the overlying unconfined unpumped aquifer, whose watertable will not remain constant, except for ideal situations, which are rare in nature. Moreover, the assumptions underlying the methods are not always entirely satisfied. One of the assumptions, for instance, is that the aquifer is homogeneous, isotropic, and of uniform thickness, but it will be obvious that for an aquifer made up of alluvial sand and gravel, this assumption is not usually correct and that its hydraulic characteristics will vary from one place to another.

13.6 Slug Test Techniques

Slug test is the cost effective and quickest method of estimating aquifer parameters. Pump tests are expensive to conduct as the installation and pumping costs of a well are high. In slug test, there is instantaneous change in head in a well away from some equilibrium position and then monitoring the return of the water level to the earlier equilibrium provides the head response with time data. For sudden change in water level in well a solid object (slug) is either inserted or removed from the well. This leads to sudden change in water level and after a while water level in well returns to a static level. The *response data* (head v/s time) is used to determine the hydraulic properties of the aquifer. The slug test is preferred or performed due to the following reasons:

(i) Slug test is simple, economical, and fast because installation and pumping of wells as well as observation wells are not required in the slug test.
(ii) Slug test is more suitable for obtaining parameters of contaminated aquifer because treatment and disposal of pumped out water is not required in the slug test as there is no pumping involved.
(iii) Pump tests cannot be performed for low transmissivity aquifers required for waste disposal or storage sites, but there is no problem in conducting

a slug test in low transmissivity cases, hence the slug test is one of the best options for a potential site for waste disposal or storage.

(iv) Slug test is also useful where continuous pumping at constant rate is difficult, where observation wells are not available, where there is interference from other wells, where the aquifer is not of infinite areal extent due to presence of boundaries, or where there are other disturbances that conflict with the basic conditions required for pumping tests.

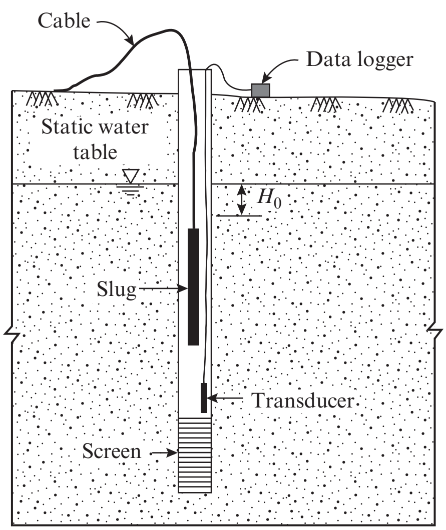

Figure 13.12 *Slug test arrangement*

Generally, a slug (piece of stainless steel pipe with both ends capped) is used for giving initial displacement to water level. The introduction of slug should be instantaneous or the time of introduction should be very less w.r.t to response of water level. For measuring heads and storing, the same pressure transducers are used as shown in Figure 13.12 if hydraulic conductivity of aquifer is large; but if it is small, then the electric tap can be used to measure the heads. Sometimes, slug test is also performed pneumatically if the well screen is air tight, which entails extra cost of making it airtight, but it has the following advantages:

- There is no need of handling water.
- Initial displacement of water level is very rapid.
- Both rising and falling (with vacuum) can be performed.

However, there are some limitations of slug tests, that is, it only evaluates a small portion of the aquifer adjacent to the well bore; it does not provide an evaluation of portions of the aquifer not screened by the well being tested; and slug test may be profoundly influenced by gravel or sand pack material in the bore hole adjacent to the well screen. A filter pack is installed around the well to avoid the vertical flow around the well and to overcome the chance of formation low permeability skin around the well. At least three sets (one with falling head and another with rising head) of slug tests should be performed at each well with different initial displacement of slug into the well to detect any presence of skin around the well.

13.6.1 Cooper-Bredhoeff-Papadopulos Method

With the slug test, the hydraulic conductivity or transmissibility of an aquifer is determined from the rate of rise of the water level in a well after a certain volume or slug of water is suddenly removed from the well. Conversely, a slug or a known volume of water may be introduced into the well over a short time period (instantaneously), causing the water level to rise to a maximum height H_0 above the initial water level and then the rate of fall of the water level in the well is observed. See Figure 13.13. The analytical solution for $H(t)$, the head above the original water level in well at any time t was obtained by Cooper et al. (1967) as follows:

$$\frac{H(t)}{H_0} = f(\beta, \alpha) \tag{13.43}$$

where, α and β are dimensionless storage and time parameters given by the following equation:

$$\alpha = \frac{r_s^2 S_s}{r_c^2} \text{ and } \beta = \frac{K_r bt}{r_c^2} = \frac{Tt}{r_c^2} \tag{13.44 a, b}$$

where, K_i = radial hydraulic conductivity, S_s = specific storage, r_c = radius of well casing, and r_s = radius of well screen. Assumptions involved in this solution are (i) the aquifer is confined but well may be fully and partially penetrating, (ii) the formation is homogeneous, (iii) flow of water is laminar and Darcy's law is applicable, (iv) there is instantaneous introduction of slug in the well, (v) boundary, if any, is at very large distance, and (vi) well losses are negligible.

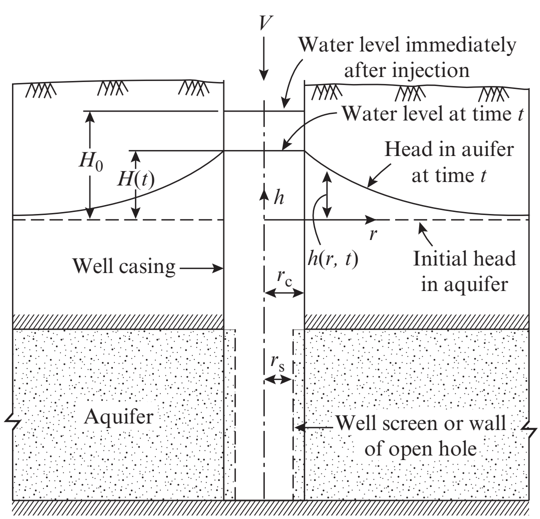

Figure 13.13 *Slug test schematic (Todd and Mays, 2005)*

Type curves for $\frac{H(t)}{H_0}$ versus β for different values of α are developed by Papadopulos et al. (1973) as shown in Figure 13.14.

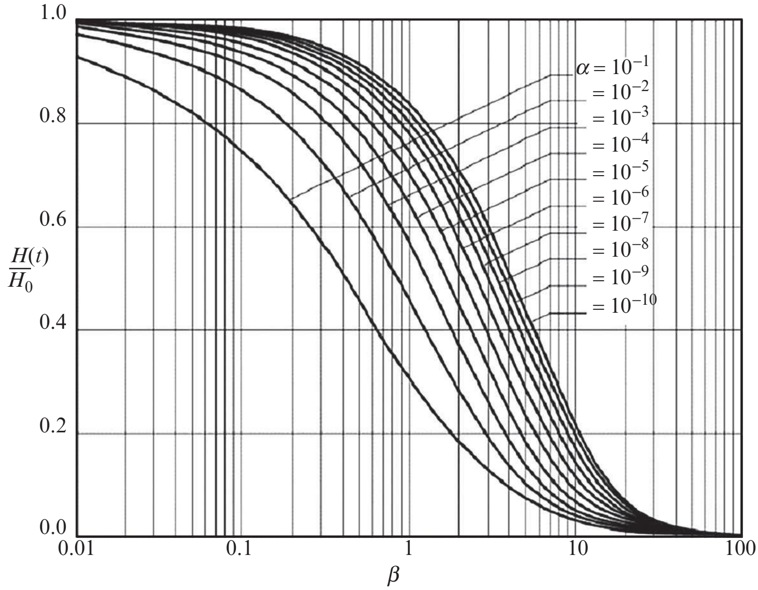

Figure 13.14 *Type curves for slug test by Cooper et al. (Todd and Mays, 2005)*

The following are the steps involved in this method:

1. Prepare Papadopulos et al. (1973) type curve on semilog graphs between $H(t)/H_0$ and β for different values of α.
2. Inset a slug instantaneously into the well and measure the maximum head H_0 above the initial water level.
3. Observe the head above the original water level in well $H(t)$ with respect to time.
4. Prepare a semilog plot on semitransparent paper between $H(t)/H_0$ and t on same scale and size as type curve.
5. Keeping axes parallel, find the best matched position of these two plots and select a match point on the overlapped area.
6. Note value of t, α, and β for the matched point.
7. Determine the transmissivity by $T = \frac{\beta r_c^2}{t}$ and specific storage by $S_s = \frac{\alpha r_c^2}{r_s^2}$.

13.6.2 Singh Method

Singh (2007) proposed an improved alternative procedure for parameter estimation by Cooper et al. (1967) method. In this method, explicit equations and diagnostic curve were developed for estimating the aquifer parameters. The rise or fall in water level of the well is plotted diagnostically on a double logarithmic graph and matched to one of the diagnostic curves plotted on the same scale with a parallel shift of axes, to estimate the aquifer parameters from the dual coordinates of a selected point on the matched portion of the graphs. The unimodal shape of the diagnostic curves and the guiding straight line facilitate the matching and limit the subjectivity. Singh (2007) developed unimodal diagnostic curves as follows. Multiplying Cooper et al. (1967) solution Eqn. (13.43) by t and substituting t in right hand side in terms of β gives

$$\frac{H(t)}{H_0}t = tf(\beta,\alpha) \Rightarrow \frac{H(t)}{H_0}t = \frac{r_c^2}{T}\beta f(\beta,\alpha) = \frac{r_c^2}{T}F(\beta,\alpha) \tag{13.45}$$

where, $F(\beta,\alpha) = \beta f(\beta,\alpha)$. The variation in F with β for any α is a unimodal curve. For different α, plots of F with β result in a family of unimodal curves known as diagnostic curves as shown in Figure 13.15.

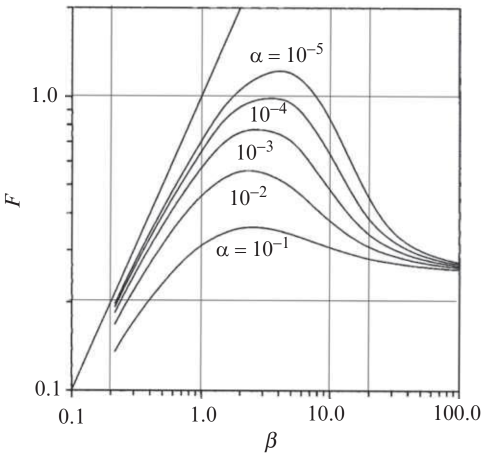

Figure 13.15 *Unimodal-type curves (Singh, 2007)*

Rewriting Eqn. (13.44b), we obtain

$$t = \frac{r_c^2}{T}\beta = \frac{r_s^2 S_s}{T}\frac{\beta}{\alpha} \tag{13.46}$$

This equation is similar to Eqn. (13.45), therefore functional form between $\frac{H(t)}{H_0}t$ and t is identical to that in between F and β for a fixed α. Therefore, the plot between $\frac{H(t)}{H_0}t$ and t is also a unimodal curve (Figure 13.16). At the peak of these curves,

$$F_{\text{pk}} = \frac{T}{r_c^2}\left(\frac{H}{H_0}t\right)_{\text{pk}} = \frac{T}{r_c^2}\frac{1}{H_0}H_{\text{pk}}t_{\text{pk}} \tag{13.47}$$

$$\beta_{\text{pk}} = \frac{T}{r_c^2}t_{\text{pk}} \tag{13.48}$$

Dividing Eqn. (13.47) by Eqn. (13.48) yields

$$\left(\frac{H}{H_0}\right)_{\text{pk}} = \frac{F_{\text{pk}}}{\beta_{\text{pk}}} = f(\alpha) \tag{13.49}$$

Singh (2007) gave the following explicit relation for Eqn. (13.49)

$$\ln\frac{1}{\alpha} = \frac{\pi\left(16+9\sqrt{\pi}\right)}{18}\left[\left(\frac{10}{\pi}\frac{H_{\text{pk}}}{H_0}\right)^{-50/9\sqrt{3}} - 1\right]^{-21/50} \tag{13.50}$$

$$F_{\text{pk}} = \frac{11\pi}{200}\left(\ln\frac{1}{\alpha}\right)^{9\sqrt{\pi}/20} \tag{13.51}$$

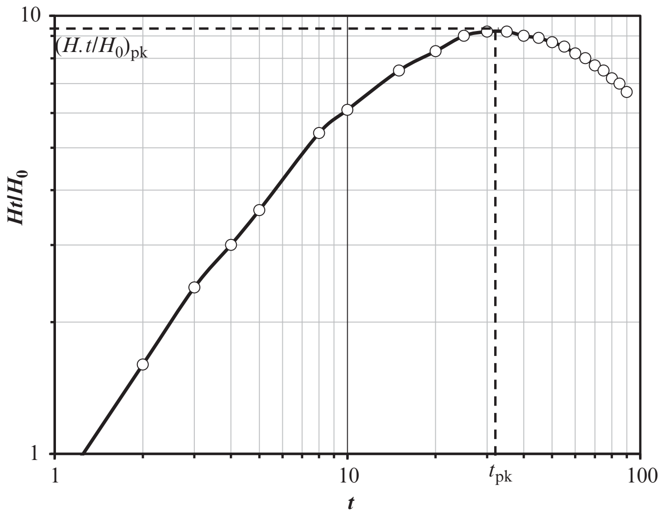

Figure 13.16 *Unimodal response*

The following steps may be adopted in this method:

1. Prepare a log-log plot for $\frac{H}{H_0}t$ versus t from the observed values and locate the peak to read $\left(\frac{H}{H_0}t\right)_{\text{pk}}$ and t_{pk} as in Figure 13.16.
2. Compute $\frac{H_{\text{pk}}}{H_0}$ from the ratio of $\left(\frac{H}{H_0}t\right)_{\text{pk}}$ and t_{pk}.
3. Estimate α using Eqn. (13.50) for known value of $\frac{H_{\text{pk}}}{H_0}$.
4. Estimate the storage coefficient by $S_s = \frac{r_c^2}{\alpha r_s^2}$ for already known value of α.

5. Calculate F_{pk} from Eqn. (13.51) and then determine the transmissivity by
$$T = F_{pk} r_c^2 / \left(\frac{H}{H_0} t \right)_{pk}$$

The estimates of the aquifer parameters based on a single point, that is, the peak, can be used to identify the nonideal conditions.

Curve-matching approach can also adopted in this method as follows:

1. Prepare diagnostic curves (unimodal F versus β curves for different α) on log–log scale.
2. Draw a straight line on the set of diagnostic curves having $F = \beta$.
3. Mark points $\frac{H}{H_0}t$ and t on semitransparent log–log paper on same scale and size as type curve and join them by a smooth unimodal curve and then also draw a straight line on it having $\frac{H}{H_0}t = t$.
4. Keeping axes parallel, find the best matched position of these two plots as shown in Figure 13.17. The unimodal shape of the diagnostic curves with sufficient curvature and guiding straight lines facilitate the matching. Straight lines on both graphs should also be made to coincide, while matching the graphs. The peaks of the diagnostic curves and guiding straight lines facilitate the matching and limit the subjectivity.

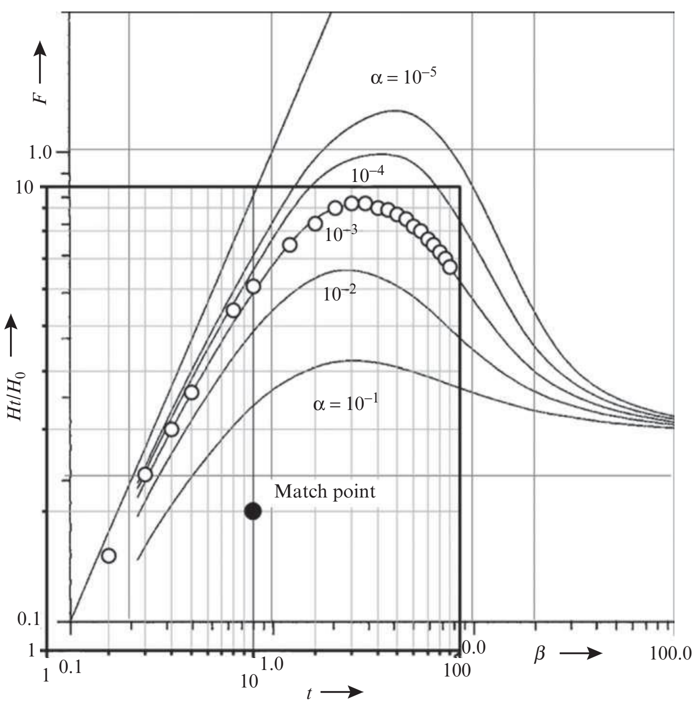

Figure 13.17 *Matching of diagnostic-type curves*

5. Select a match point on the overlapped area and read the coordinates of the selected point on the matched portion of a particular α curve that is, $F,\ \beta, \dfrac{H}{H_0}t$, and t.
6. Determine the transmissivity by $T = Fr_c^2 / \left(\dfrac{H}{H_0}t\right)$ or $T = \dfrac{\beta r_c^2}{t}$ and the storage coefficient by $S_s = \dfrac{r_c^2}{\alpha r_s^2}$.
7. The two estimates of the transmissivity should be the same provided the straight lines are also matched.
8. If the match point is so selected as to have $F = 1$ and $\beta = 1$, the estimate of the transmissivity is given by $T = \dfrac{\beta r_c^2}{t}$ or $T = r_c^2 / \left(\dfrac{H}{H_0}t\right)$.
9. The use of the diagnostic curves can easily identify nonideal conditions if the plotted points do not fall along an appropriate diagnostic curve with the guiding straight lines matched.

13.6.3 Hvorslev Method

Hvorslev method (Chirlin, 1989) considers that (i) the specific storage of aquifer is negligible, but head changes with time (a quasisteady-state flow condition); (ii) instantaneous introduction of slug is not necessary; and (iii) lateral constant head boundaries may be at finite distance from the well. Rewriting Theim's equation, we obtain

$$Q = \frac{2\pi K_r L_e H}{\ln\left(R_e / r_s\right)} \tag{13.52}$$

where, H is head difference between equilibrium position and head in well at time t; r_s is radius of the well screen; and L_e and R_e are effective length of well screen and effective radius of slug test at which head is dissipated respectively. It is assumed that drawdown of the water table around the well is negligible, flow above the water table (in the capillary fringe) can be ignored, head losses as water enters the well (well losses) are negligible, and the aquifer is homogeneous and isotropic. The rate of rise, dH/dt, of the water level in the well after suddenly removing a slug of water can be related to the inflow Q by

$$\frac{dH}{dt} = -\frac{Q}{\pi r_c^2} \tag{13.53}$$

where, r_c = inside radius of the casing, hence πr_c^2 = cross-sectional area of the well where the water level is rising. The minus sign in Eqn. (13.53) indicates that H decreases as t increases. If the water level is rising in the perforated section of the well, allowance should be made for the porosity outside the well casing if the hydraulic conductivity of the gravel envelope or developed zone is much higher than that of the aquifer. Substituting Q from Eqn. (13.52) into Eqn. (13.53),

$$\frac{dH}{dt} = -\frac{1}{\pi r_c^2}\frac{2\pi K_r L_e H}{\ln(R_e / r_s)} \Rightarrow \frac{dH}{H} = -\frac{1}{r_c^2}\frac{2K_r L_e}{\ln(R_e / r_s)}dt \tag{13.54}$$

Integrating it from $t = 0$ to t and $H = H_0$ to $H(t)$,

$$\ln\left[\frac{H(t)}{H_0}\right] = -\frac{2K_r L_e t}{r_c^2 \ln(R_e / r_s)} \Rightarrow 2.302 \log\left[\frac{H(t)}{H_0}\right] = -\frac{2K_r L_e t}{r_c^2 \ln(R_e / r_s)} \tag{13.55}$$

If a gravel pack around the screen is provided, the radius of the well screen should include the gavel pack zone and L_e is the length of the gravel pack zone as shown in Figure 13.18. The effective radius R_e, empirical value of which may be assumed equal to 200 r_s or L_e.

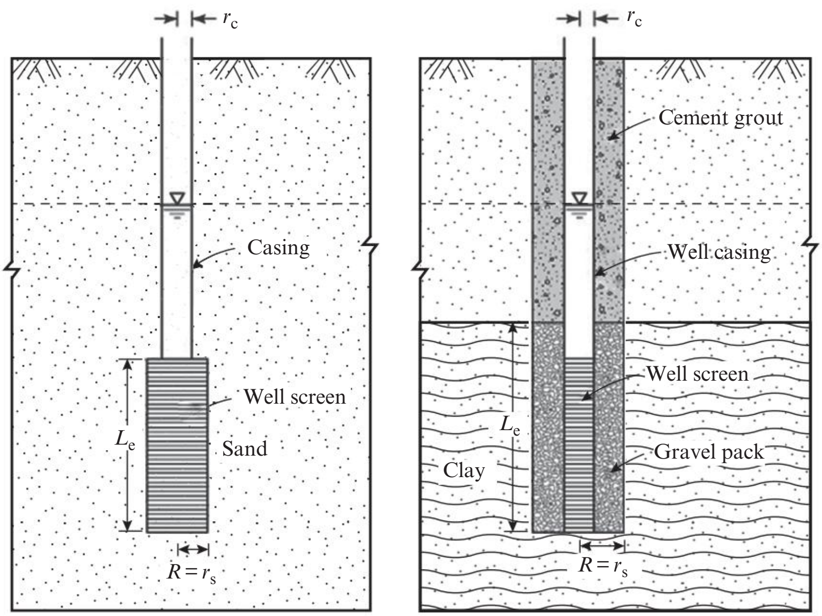

Figure 13.18 *Hvorslev method schematic (Todd and Mays, 2005)*

Equation (13.55) indicates that a plot between $\log(H(t)/H_0)$ and t is a straight line as shown in Figure 13.19 passing through $H(t)/H_0 = 1$ at $t = 0$. The slope of straight line on the semilog plot is equal to

$$\frac{2.302 \log[H(t_2)/H(t_1)]}{t_2 - t_1} = -\frac{2K_r L_e}{r_c^2 \ln(R_e / r_s)} \tag{13.56}$$

Thus,

$$K_r = \frac{r_c^2 \ln(R_e / r_s)}{2L_e}\frac{2.302 \log[H(t_1)/H(t_2)]}{t_2 - t_1} \tag{13.57}$$

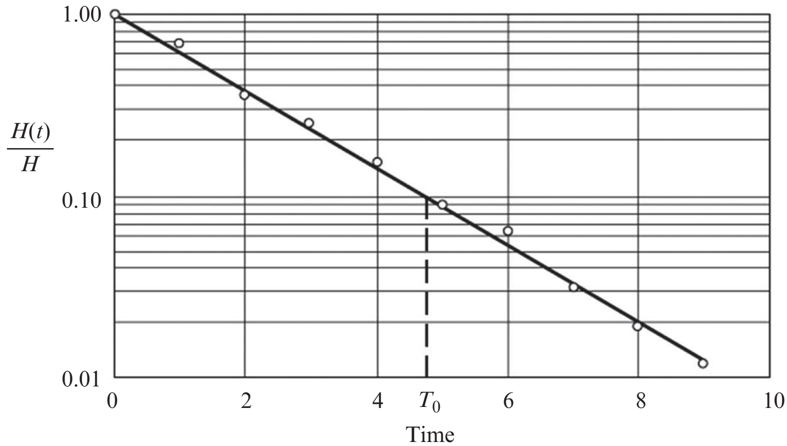

Figure 13.19 *Hvorslev method—time lag by straight line*

For one log cycle of $H(t)/H_0$ it reduces to

$$K_r = \frac{2.302 r_c^2 \ln(R_e / r_s)}{2L_e (t_2 - t_1)} \tag{13.58}$$

As the line passes through $H(t)/H_0 = 1$ at $t = 0$, hence $H(t_1)/H_0 = 1$ at $t_1 = 0$. Let $t = T_0$ after one log cycle of $H(t)/H_0$, therefore $t_2 = T_0$ and $H(t_2)/H_0 = 0.1$. Thus both Eqs (13.57) and (13.58) become

$$K_r = \frac{2.302 r_c^2 \ln(R_e / r_s)}{2L_e T_0} \tag{13.59}$$

As other parameters are known, the radial hydraulic conductivity K_r can be computed. Note that T_0 is the time after which head in the well reduces to one tenth of the initial head and it is known as *lag time*. Hence, Eqs (13.55) and (13.59) proves that the slope is simply $-2.302/T_0$. If the semilog plot is prepared on natural logarithm scale paper, the lag time is corresponding to 0.3679 times of the initial head and the slope of straight line $-1/T_0$ because

$$T_0 = \frac{2K_r L_e}{r_c^2 \ln(R_e / r_s)} \quad \text{and} \quad \ln\left[\frac{H(t)}{H_0}\right] = -1 \Rightarrow \frac{H(t)}{H_0} = e^{-1} = 0.3679 \tag{13.60}$$

The following steps may be followed for the hydraulic conductivity estimation:

1. Inset a slug into the well and measure the maximum head H_0 above the initial water level and then observe the head above the original water level in well $H(t)$ with respect to time.
2. Prepare a plot between log $H(t)/H_0$ and t and fit a straight line passing through $H(t)/H_0 = 1$ at $t = 0$.

3. Note value of lag time T_0, where $H(t)/H_0 = 0.1$.
4. Determine the hydraulic conductivity by $K_r = \dfrac{2.302 r_c^2 \ln(R_e / r_s)}{2L_e T_0}$.

However, the specific storage cannot be estimated by this method.

13.6.4 Bouwer and Rice Method

Bouwer and Rice (1976) developed a method for determining the hydraulic conductivity of an unconfined aquifer with a fully or a partially penetrating well. The method assumes that the effects of elastic storage mechanism are negligible, and the water table (or saturated thickness of the aquifer h_0) does not change during the test. Although streamlines in flow systems around slug tested wells contain both vertical and horizontal components, most of the head loss is dissipated in a horizontal direction. Therefore, the hydraulic conductivity K_r appears in the solution slug test solutions. Analytical solution given by Bouwer and Rice (1976) is

$$K_r = -\frac{r_c^2 \ln(R_e / r_s)}{2L_e} \times \frac{1}{t} \times \ln\left[\frac{H(t)}{H_0}\right] \qquad (13.61)$$

Equation (13.61) and the steps for estimation of K_r are identical to the earlier described Hvorslev method. However, if the effective radius R_e is considered an unknown parameter (rather than using empirical value equal to 200 r_s or L_e), it can be estimated by the following equation:

$$\ln\left(\frac{R_e}{r_s}\right) = \left[\frac{1}{\ln(L_w / r_s)} + \left(\frac{A + B\ln\left[(h_0 - L_w)/r_s\right]}{(L_e / r_s)}\right)\right]^{-1} \qquad (13.62)$$

for partially penetrating well ($h_0 > L_w$) and

$$\ln\left(\frac{R_e}{r_s}\right) = \left[\frac{1}{\ln(L_w / r_s)} + \frac{C}{(L_e / r_s)}\right]^{-1} \qquad (13.63)$$

for fully penetrating well. Here, L_w is the length of well below the water table and A, B, and C are function L_w / r_s, which can be read from the plot as shown in Figure 13.20. These values have less than 10- and 25-percent errors for $L_e > 0.4$ L_w and $L_e < 0.2$ L_w, respectively. The time t_{90} necessary for the water level in the well to rise 90 percent of H_0 is

$$t_{90} = 0.0527 \frac{r_c^2}{K_r L_e} \ln(R_e / r_s) \qquad (13.64)$$

If K_r and/or L_e are relatively large, t_{90} may be only a few seconds. Such fast water level rises can be measured with sensitive pressure transducers and fast strip-chart recorders.

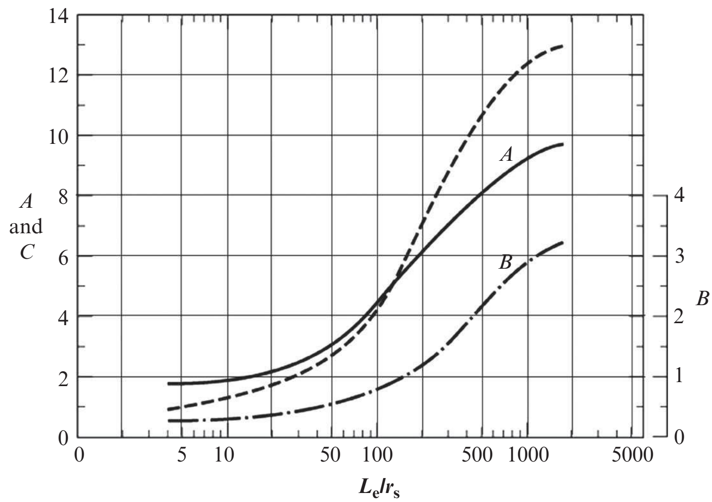

Figure 13.20 *Bouwer and Rice method*

The steps in determining the hydraulic conductivity using Bouwer and Rice (1976) method are as follows:

1. Inset a slug into the well and measure the maximum head H_0 above the initial water level, and then observe the head above the original water level in well $H(t)$ with respect to time.
2. Plot normalized head $H(t)/H_0$ on a log scale versus time t on a linear scale using semilog graph paper.
3. Calculate $\ln\left[\left(h_0 - L_w\right)/r_s\right]$ for partially penetrating well $(h_0 > L_w)$. If $\ln\left[\left(h_0 - L_w\right)/r_s\right] > 6$, set $\ln\left[\left(h_0 - L_w\right)/r_s\right] = 6$.
4. Read A, and B for partially penetrating well ($h_0 > L_w$) and C for fully penetrating well ($h_0 = L_w$) from the plot as shown in Figure 13.20
5. Calculate $\ln\left(\dfrac{R_e}{r_s}\right)$ using Eqn. (13.62) for partially penetrating well and Eqn. (13.63) for fully penetrating well.
6. Approximate the straight portion of the plotted curve by a straight line and extend the line to $t = 0$ and note H_1 there.
7. Read H_2 and t_2 at other point on the straight line.
8. Determine the hydraulic conductivity by $K_r = \dfrac{2.302 r_c^2 \ln\left(R_e / r_s\right)}{2L_e t_2} \log \dfrac{H_1}{H_2}$.

   Again the specific storage cannot be estimated by this method.

The method by Bouwer and Rice (1976) is simpler and quicker than the pumping test because observation wells and pumping the well are not needed. The portion of the aquifer on which hydraulic conductivity to be estimated, is approximately a cylinder with a radius of about R_e and a height slightly larger than L_e.

The transmissivity of the aquifer T can be obtained by $h_0 K_r$ assuming the aquifer is uniform. Although this technique is developed for an unconfined aquifer, it can also be used for a confined aquifer that receives water from an overlying confining layer (Bouwer, 1989). Many other methods of slug test for unconfined aquifers with different assumptions are also available.

13.7 Other Techniques

13.7.1 Auger Hole Method

The auger hole method is similar to the slug test for wells, but the water-level rise is measured in an unlined, cylindrical hole, and dug with an auger for the express purpose of measuring the hydraulic conductivity. In unstable soils, the hole may have to be lined with a screen to prevent caving of the wall. After the hole is dug and water level in the hole has reached equilibrium with the water table, a volume of water is removed usually with a bailer and the rate of rise of water level is measured. Various equations and charts are available to calculate the hydraulic conductivity from the rate of water level rise in the hole. Variations on the auger hole technique are two-well, four-well or multiple-well methods. The auger hole technique enables measurement of K in unconfined or perched aquifer. The K value obtained is essentially a point measurement and reflects mostly the hydraulic conductivity in a horizontal direction.

13.7.2 Piezometer Method

With the piezometer technique, a rigid pipe is driven or jetted into the soil. When the pipe has reached the desired depth, a cavity is augered out below the bottom of the pipe. After the water level in the pipe has reached equilibrium, a slug of water is rapidly removed and the subsequent rate of rise of the water level is measured. The K value of the soil around the cavity is calculated as follows:

$$K_r = -\frac{\pi r_c^2}{A_p t} \times \ln\left[\frac{H(t)}{H_0}\right] \tag{13.65}$$

where, A_p is a factor depends on the shape of the cavity and depth of the lower boundary. Piezometers normally are capable of measuring K at greater depths than the auger hole method. In unstable soils, the piezometer cavity may have to be lined with a perforated, screened section at the bottom of the pipe to prevent caving. The volume of soil on which is measured with this method is smaller than with other techniques, hence it is preferred where accurate point values of K is required, and it should not be used where objective is to measure K of extensive aquifer formation.

13.7.3 Core Sampling and Permeameter Technique

The oldest technique for measuring K of subsurface material is to collect a sample, place it in a permeameter in the laboratory, let water flow through it, and calculate K with Darcy's equation from the observed flow rate and head loss across the sample. But the sample becomes disturbed. The arrangement may be constant head or variable head permeameter. This disturbed sample permeameter technique yields reliable results only for uniform sands or other coarse materials consisting of relatively round particles. Better results are obtained with an undisturbed sample, but truly undisturbed samples of unconsolidated materials are almost impossible to obtain, no matter how sophisticated the core sampling techniques is used. The main disadvantages of the technique are disturbance of the material, the small size of the sample, and the possibility of leakage flow between the sample and permeameter wall. Core samples are usually taken in vertical bore holes so that the technique yields K_z. Horizontal samples for measuring K_r or K_h can be obtained by pushing the sampler horizontally into walls of pits.

13.7.4 Optimization Technique

The curve-matching method for estimation of aquifer parameters is subject to errors of judgment. For removing subjectiveness in parameter estimation, optimization techniques can be adopted. These techniques also need observed drawdowns through pumping test as they involve minimisation of errors between the observed and computed drawdowns. If s_{oi} is the observed drawdown at time t, during a pump test, the error in the ith observation e_i is

$$e_i = s_{oi} - s_{ci} \tag{13.66}$$

where, s_{ci} is the computed drawdown at time t, using appropriate expression (exact analytical or approximate) for case under consideration (confined, unconfined, or leaky aquifer). Many times the relative error is preferred which is

$$e_i = \frac{s_{oi} - s_{ci}}{s_{oi}} \tag{13.67}$$

Such expression involves aquifer parameters that are unknown so far. Therefore suitable initial values are assumed and the resulting errors are minimized by varying the aquifer parameters. To determine the aquifer parameters, the criteria function is summed to yield objective function F as follows:

$$F = \textstyle\sum_{i=1}^{N} e_i \tag{13.68}$$

with N being the total number of observed data to be minimized. In order to reduce observation errors, the following criteria function (Swamee and Ojha, 1990) can be used

$$f = \left(e_i^{-2} - e_c^{-2}\right)^{-p} \tag{13.69}$$

in which p = a positive number, and e_c = cutoff error. For a large value of e_i, the term e_i^{-2} drops out and f assumes a constant value e_c^{2p}. Thus, an erroneous observation cannot cross the limit e_c. Therefore, the errors fall into two categories that is, inherent errors (less than e_c) and removable errors (greater than e_c). On the other hand, for $e_c = \infty$ and $p = 1$, Eqn. (13.68) along with Eqn. (13.69) reduces to least square method

$$F = \Sigma_{i=1}^{N}\left(e_{\mathrm{i}}\right)^2 \tag{13.70}$$

This means, it consists of the minimisation of the sum-of-squares error for the entire data set. Further, for $e_c = \infty$ and $p = 0.5$, Eqn. (13.68) along with Eqn. (13.69) reduces to

$$F = \Sigma_{i=1}^{N}\left|e_{\mathrm{i}}\right| \tag{13.71}$$

The sum-of-squares error, however, gives undue importance to large errors that are associated with the later part of the pump test. Eqn. (13.71) is superior to Eqn. (13.70) as it does not give undue importance to large errors. Least-squares criterion serves a useful purpose in applying indirect methods of optimization as it yields differentiable objective function. In fact, any even power in Eqn. (13.69) results in a differentiable function. The power 2, being lowest, is most acceptable. If one selects p less than 0.5, it will give undue importance to small errors and with $p = 0$, the criteria collapse. Thus, the best value of p may be chosen as 0.5 for which the objective function becomes

$$F = \Sigma_{i=1}^{N}\left(e_{\mathrm{i}}^{-2} - e_{\mathrm{c}}^{-2}\right)^{-0.5} \tag{13.72}$$

Similarly, the objective function for least square method becomes

$$F = \Sigma_{i=1}^{N}\left(e_{\mathrm{i}}^{-2} - e_{\mathrm{c}}^{-2}\right)^{-1} \tag{13.73}$$

In the absence of any other information about the cut-off error, the very large value of $e_c = 10$ may be assumed to start with. Swamee and Ojha (1990) presented a procedure to arrive at appropriate value of e_c. The removable errors can be removed by using the appropriate value of e_c. For large value of e_c, the objective function F can be constructed as follows:

$$F = \Sigma_{i=1}^{N}\left(s_{\mathrm{oi}} - s_{\mathrm{ci}}\right)^2 \text{ or } F = \Sigma_{i=1}^{N}\left|\frac{s_{\mathrm{oi}} - s_{\mathrm{ci}}}{s_{\mathrm{oi}}}\right| \tag{13.74}$$

The function F can be minimized by using any standard method of unconstrained minimization like grid search, random search or Marquardt algorithm.

SOLVED EXAMPLES

Example 13.1: The following drawdowns (see Table 13.1) were observed when a fully penetrating 200 mm diameter well in 102 m thick confined aquifer is pumped at constant discharge 199 m^3/d:

Table 13.1 Pumping test data

Time (minutes)	*Drawdown (m)*	*Time (minutes)*	*Drawdown (m)*	*Time (minutes)*	*Drawdown (m)*
0	0	15	5.1	60	9.45
2	0.9	20	5.35	80	10.4
4	1.7	25	6.15	100	11.5
6	2.35	30	6.9	120	11.71
8	3.15	40	7.55	150	11.82
10	3.9	50	9	180	11.86

Estimate aquifer parameters.

Solution: Following the steps of Theis curve-matching method of parameter estimation Figure 13.21 was prepared. The selected match point has $s = 1$ m, $t = 100$ min, $W(u) = 0.37$, and $1/u = 62$. Therefore, $T = \frac{Q}{4\pi s} W(u) = \frac{199 \times 0.37}{4\pi \times 1} = 5.86$ m²/d and storage coefficient by $S = 4T(t/r^2)/(1/u) = \frac{4 \times 5.86 \times 100}{60 \times 24 \times 0.1 \times 0.1 \times 62} = 2.625.$ Thus, $K = T/b = 0.0574$ m/d and yield of the aquifer is not good.

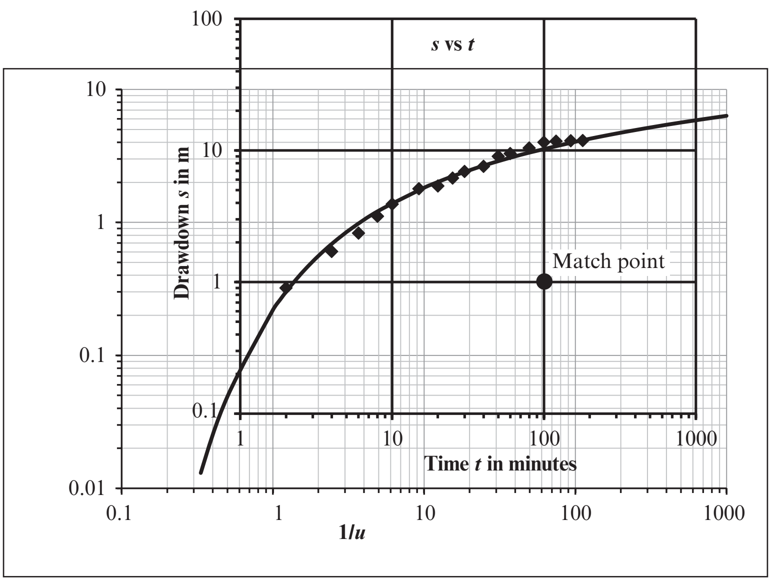

Figure 13.21 *Aquifer parameter estimation by curve matching*

Example 13.2: The following drawdowns (see Table 13.2) were observed when a fully penetrating 150 mm diameter well in 102-m-thick confined aquifer is pumped at constant discharge 165 lpm:

Table 13.2 Pumping test data 2

Time (minutes)	*Drawdown (m)*	*Time (minutes)*	*Drawdown (m)*	*Time (minutes)*	*Drawdown (m)*
0	0.00	8	23.38	25	39.88
1	4.95	9	25.30	30	42.07
2	9.52	10	27.25	45	44.65
3	12.85	12	29.46	60	46.35
4	15.32	14	31.28	75	47.48
5	18.06	16	33.12	90	48.08
6	19.65	18	34.43	105	49.32
7	21.42	20	36.37	120	50.05

Estimate aquifer parameters.

Solution: Following the steps of Cooper–Jacob method of parameter estimation a semilog plot between drawdown and time, which is a straight line, as shown in Figure 13.22 was prepared. For one log cycle determine $\Delta s = s_2 - s_1 = 27 - 2.5 = 24.5$ m (for $t = 1$ min $s_1 = 2.5$ m and for $t = 10$ min $s_2 = 27$ m). The straight line is extended to $s = 0$ where $t_0 = 0.85$ m. From Cooper–Jacob approximation $\Delta s = \dfrac{2.30Q}{4\pi T} \Rightarrow T = \dfrac{2.30 \times 165 \times 10^{-3} \times 60 \times 24}{4\pi \times 24.5} = 1.7749$ m^2/d and

$$S = \frac{2.25Tt_0}{r^2} \text{ or } S = \frac{2.25 \times 1.7749 \times .85}{60 \times 24 \times \left(\dfrac{150}{2}\right)^2} = 0.419.$$

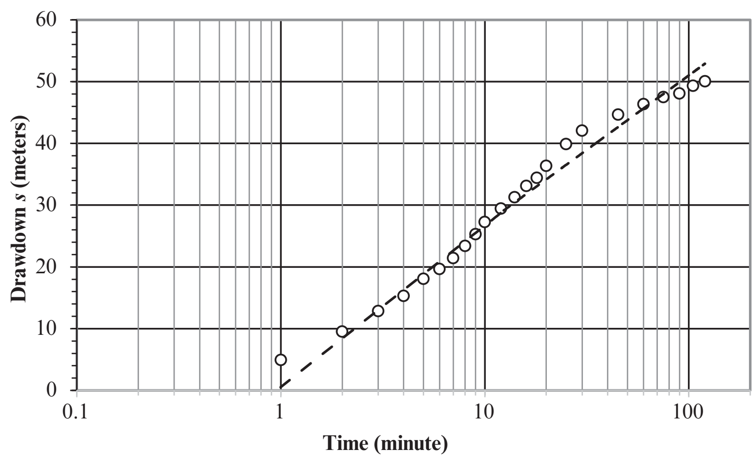

Figure 13.22 *Aquifer parameter estimation by Cooper–Jacob method*

Example 13.3: The following drawdowns (see Table 13.3) were observed when a fully penetrating 200 mm diameter well in 30 m thick confined aquifer is pumped at constant discharge = 250 m^3/d:

Table 13.3 Pumping test data 3

Time (min)	*Drawdown (m)*	*Time (min)*	*Drawdown (m)*	*Recovery time (min)*	*Residual drawdown (m)*
0	0	75	20.32	1	20.93
1	2.34	90	20.83	2	18.96
2	3.1	105	21.28	3	16.79
3	3.91	120	21.56	4	15.25
4	4.86	140	21.92	6	14.21
5	5.8	160	22.28	8	13.36
6	6.57	180	22.61	10	12.62
8	7.8	200	22.95	15	10.4
10	9.47	230	23.21	20	8.34
15	11.2	300	23.46	25	6.79
20	12.93	Pumping	Stopped	30	5.42
25	14.63	Recovery	Started	40	4.72
30	15.15			50	4.13
35	16.06			60	3.57
40	17.84			75	2.86
45	18.66			90	1.9
50	19.12			105	1.46
55	19.6			120	1.02
60	19.81			150	0.6

Estimate aquifer parameters from this recovery data.

Solution: A simple plot between drawdown and time since pumping started was drawn as shown in Figure 13.23.

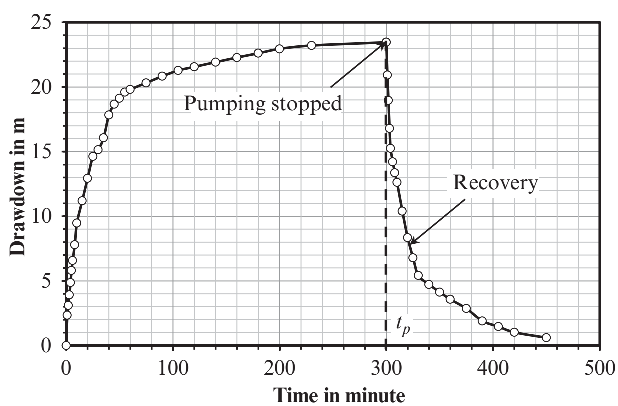

Figure 13.23 *Recovery of drawdown*

Table 13.4 is prepared for the given data.

Table 13.4 Theis recovery method

Time t (min)	*Recovery time t′ (min)*	*t/t′*	*Residual drawdown (m)*
300	0	-	23.46
301	1	301	20.93
302	2	151	18.96
303	3	101	16.79
304	4	76	15.25
306	6	51	14.21
308	8	38.5	13.36
310	10	31	12.62
315	15	21	10.4
320	20	16	8.34
325	25	13	6.79
330	30	11	5.42
340	40	8.5	4.72
350	50	7	4.13
360	60	6	3.57
375	75	5	2.86
390	90	4.33	1.9
405	105	3.86	1.46
420	120	3.5	1.02
450	150	3	0.6

A plot between residual drawdown and $\log(t/t')$ is drawn as shown in Figure 13.24, which is a straight line with slope $2.302Q/4\pi T$. The difference in the residual drawdowns between one log cycle of t/t' is 10.5 m hence,

$$\frac{2.302Q}{4\pi\Delta s_r} = \frac{2.302\times 250}{4\pi\times 10.5} = 4.36 \text{ m}^2\text{/d}$$

Storage coefficient value can be estimated if drawdown s, in the observation well at the time of pump stopped is available. In this case, it is 23.46 m for t_p = 300 min, therefore

$$S = 2.25Tt_p \Big/ \left(r^2 \exp\left(\frac{4\pi Ts}{2.302Q}\right)\right)$$

$$= \frac{2.25\times 4.36\times 300}{60\times 24\times 0.1\times 0.1}\exp\left(-\frac{4\pi\times 4.36\times 23.46}{2.302\times 250}\right) = 21.89$$

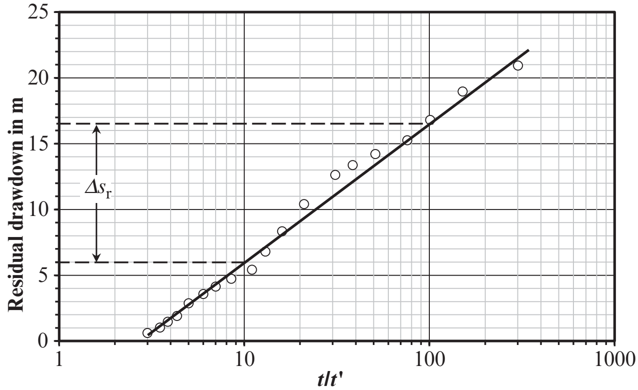

Figure 13.24 *Aquifer parameter estimation by recovery method*

Example 13.4: Estimate aquifer parameters from this recovery data if the following residual drawdowns (Table 13.5) were observed when a fully penetrating 150 mm diameter well in 159-m-thick confined aquifer is pumped at constant discharge = 200 lpm for 120 min and then pumping stopped:

Table 13.5 Pumping test data 4

Time t (min)	*Recovery time t′ (min)*	*t/t′*	*Residual drawdown (m)*
120	0		10.880
121	1	121.00	7.340
122	2	61.00	7.110
123	3	41.00	6.950
124	4	31.00	6.810
125	5	25.00	6.700
126	6	21.00	6.600
127	7	18.14	6.520
128	8	16.00	6.450
129	9	14.33	6.390
130	10	13.00	6.330
132	12	11.00	6.240
134	14	9.57	6.160
136	16	8.50	6.110
138	18	7.67	6.060
140	20	7.00	6.010
145	25	5.80	5.940

(*Continued*)

Table 13.5 (Continued)

Time t (min)	*Recovery time t′ (min)*	*t/t′*	*Residual drawdown (m)*
150	30	5.00	5.910
160	40	4.00	5.880
170	50	3.40	5.850
180	60	3.00	5.810
210	90	2.33	5.770
240	120	2.00	5.745

Solution: A plot between residual drawdown and $\log(t/t')$ is drawn as shown in Figure 13.25, which is a straight line with slope $2.302Q/4\pi T$. In the present case, $T = \dfrac{(2.302\times 200\times 10^{-3})}{4\pi\times(7.25-6.25)} = 0.0366\,\text{m}^2/\text{min} = 52.712\,\text{m}^2/\text{d}$.

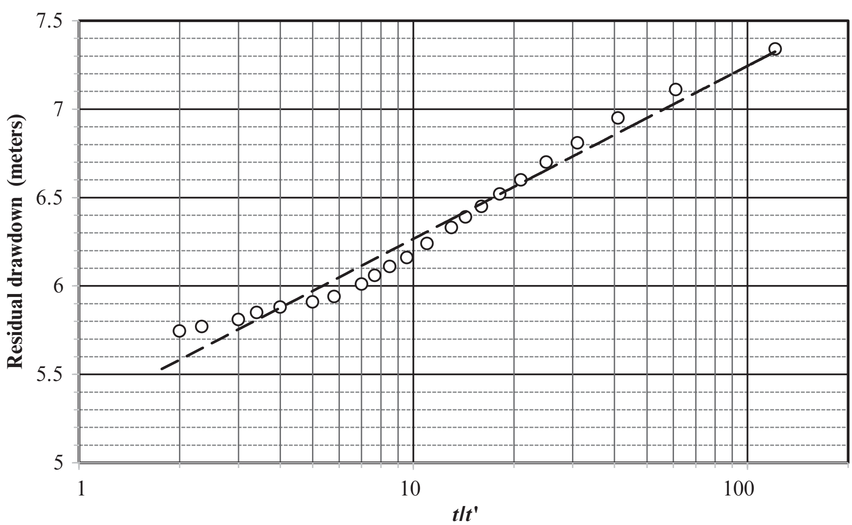

Figure 13.25 *Aquifer parameter estimation by recovery method*

Example 13.5: The following drawdowns (see Table 13.6) were observed in an observation well at 91.44 m when a well in confined aquifer is pumped at constant discharge = 8176 m^3/d:

Table 13.6 Pumping test data 5

Time (min)	*Drawdown (m)*	*Time (min)*	*Drawdown (m)*	*Time (min)*	*Drawdown (m)*
0	0	10	0.44196	200	0.902208
1	0.13716	30	0.615696	400	0.9906

(*Continued*)

Table 13.6 (Continued)

Time (min)	*Drawdown (m)*	*Time (min)*	*Drawdown (m)*	*Time (min)*	*Drawdown (m)*
2	0.225552	40	0.661416	600	1.039368
3	0.277368	50	0.70104	800	1.0668
4	0.316992	60	0.713232	1000	1.09728
6	0.368808	80	0.762	1440	1.161288
8	0.402336	100	0.813816		

Estimate aquifer parameters.

Solution: A semilog plot between time and drawdown was prepared as shown in Figure 13.26.

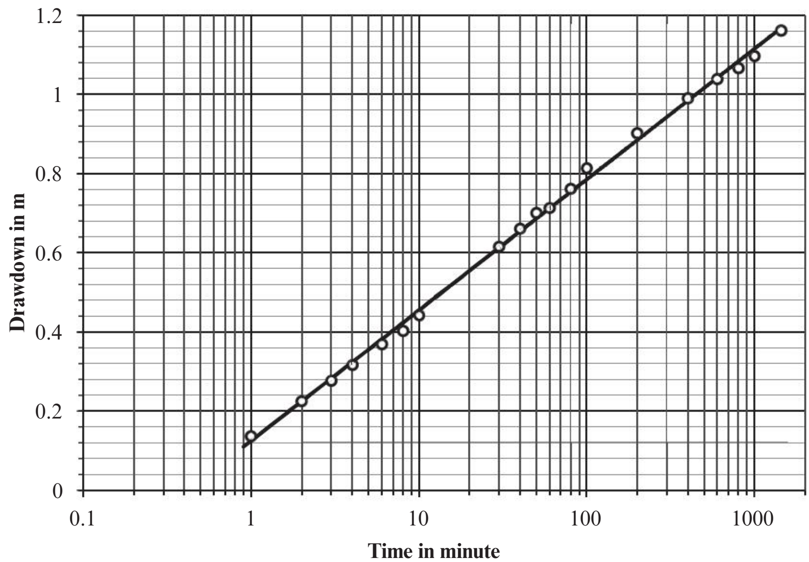

Figure 13.26 *Aquifer parameter estimation by recovery method*

Take a point on graph $(s,t) \rightarrow (1.04, 600)$ and draw a tangent at this point and determine Δs for one log cycle at this point, which yields $\Delta s = 1.1 - 0.78 = 0.32$. Therefore Chow's function $F(u) = \frac{s}{\Delta s} = \frac{1.04}{0.32} = 3.25$. Now from Chow's plot (Figure 13.5) for $F(u) = 3.25$, $W(u) = 7$ and $u = 0.0002$. Therefore, $s = \frac{Q}{4\pi T} W(u)$ results $T = \frac{8176 \times 7}{4\pi \times 1.04} = 4379$ m^2/d and $u = \frac{r^2 S}{4Tt}$ hence $S = \frac{0.0002 \times 4 \times 4379 \times 600}{91.44^2 \times 24 \times 60} = .000175$.

Example 13.6: The following response (see Table 13.7) was observed in a slug test in a 200-mm diameter bore hole and 300 mm diameter after gravel pack:

Table 13.7 Slug test data

Time (min)	H_t *(m)*	*H.t/H$_0$ (min)*	*Time (min)*	H_t *(m)*	*H.t/H$_0$ (min)*
0	1.0	0	35	0.26	9.2
1	0.86	0.8	40	0.225	9
2	0.82	1.6	45	0.20	8.9
3	0.78	2.4	50	0.17	8.7
4	0.75	3	55	0.15	8.5
5	0.72	3.6	60	0.14	8.2
8	0.67	5.4	65	0.12	8
10	0.61	6.1	70	0.11	7.7
15	0.5	7.5	75	0.1	7.5
20	0.42	8.3	80	0.09	7.2
25	0.36	9	85	0.08	7
30	0.31	9.2	90	0.07	6.7

Estimate aquifer parameters.

Solution: Given data: H_0 = 1.0 m, r_c = 0.1 m, and r_s = 0.15 m. A log–log plot between time and $H.t/H_0$ was prepared as shown in Figure 13.16, which is unimodal. The values at its peak are $(H.t/H_0)_{pk}$ = 9.2 min and t_{pk} = 32 min.

Therefore, $\dfrac{H_{pk}}{H_0} = \dfrac{9.2}{32}$, and hence $\ln\dfrac{1}{\alpha} = \dfrac{\pi\left(16+9\sqrt{\pi}\right)}{18}\left[\left(\dfrac{10}{\pi}\dfrac{H_{pk}}{H_0}\right)^{-50/9\sqrt{3}} - 1\right]^{-21/50}$

yields $\alpha = 0.000137$. Therefore, $S_s = \dfrac{r_c^2}{\alpha r_s^2} = \dfrac{0.1\times 0.1}{0.000137\times 0.15\times 0.15} = 3242.68$.

Using value of α in Eqn. (13.51), $F_{pk} = \dfrac{11\pi}{200}\left(\ln\dfrac{1}{\alpha}\right)^{9\sqrt{\pi}/20} = 0.9875$.

Therefore using Eqn. (13.47), the transmissivity by

$$T = F_{pk} r_c^2 \Big/ \left(\frac{H}{H_0}t\right)_{pk} = 0.9875\times\frac{0.1\times 0.1}{9.2} = 0.001 \text{ m}^2\text{/min} = 1.545 \text{ m}^2\text{/d}.$$

Using diagnostic curve by Singh (2007) for same data, Figure 13.17 was prepared and a match point was selected for which $F = 0.18$; $\beta = 0.81$; $\alpha = 10^{-4}$; $(H.t/H_0) = 2$ min and $t = 10$ min. Therefore, $T = Fr_c^2 \Big/ \left(\dfrac{H}{H_0}t\right) = \dfrac{0.18\times 0.1\times 0.1}{2} = 0.0009$ m²/min = 1.296 m²/d and the storage coefficient by $S_s = \dfrac{r_c^2}{\alpha r_s^2} = \dfrac{0.1\times 0.1}{0.0001\times 0.15\times 0.15} = 4444$. These values differ from earlier method due to error of judgment in curve matching.

PROBLEMS

13.1. Why is estimation of aquifer parameters important?

13.2. What are salient features of pumping test techniques?

13.3. Give the step-by-step method of aquifer parameter estimation by

a. Curve-matching method
b. Cooper–Jacob method
c. Chow's method
d. Theis recovery method
e. Curve matching method for unconfined aquifers.

13.4. Describe various methods and their advantages and disadvantages of aquifer parameter estimation for leaky aquifers.

13.5. What is a slug test? Where is it preferred?

13.6. Describe different slug test methods.

13.7. What are strong points of aquifer parameter estimation by optimization techniques?

13.8. The following drawdowns (see Table 13.8) were observed when a well in 14 m thick leaky aquifer is pumped at constant discharge = 761 m^3/d:

Table 13.8 Pumping test data (Swamee and Ojha, 1990)

r = 30 m		*r = 60 m*		*r = 90 m*		*r = 120 m*	
Time (days)	*Draw-down (m)*	*Time (days)*	*Draw-down (m)*	*Time (days)*	*Draw-down (m)*	*Time (days)*	*Draw-down (m)*
0	0	0	0	0	0		
0.0153	0.138	0.0188	0.081	0.0243	0.069	0.025	0.057
0.0181	0.141	0.0236	0.089	0.0306	0.077	0.0313	0.063
0.0229	0.15	0.0299	0.094	0.0375	0.083	0.0382	0.068
0.0292	0.156	0.0368	0.101	0.0468	0.091	0.05	0.075
0.0361	0.163	0.0472	0.109	0.0674	0.1	0.0681	0.086
0.0458	0.171	0.0667	0.12	0.0896	0.109	0.0903	0.092
0.066	0.18	0.0882	0.127	0.125	0.12	0.125	0.105
0.0868	0.19	0.125	0.137	0.167	0.129	0.167	0.113
0.125	0.201	0.167	0.148	0.208	0.136	0.208	0.122
0.167	0.21	0.208	0.155	0.25	0.141	0.25	0.125
0.208	0.217	0.25	0.158	0.292	0.142	0.292	0.127
0.25	0.22	0.292	0.16	0.333	0.143	0.333	0.129
0.292	0.224	0.333	0.164	-	-	-	-
0.333	0.228	-	-	-	-	-	-

Estimate aquifer parameters for the leaky aquifer.

13.9. The following drawdowns (see Table 13.9) were observed in an observation well at 300 m away when a well in confined aquifer is pumped at constant discharge = 500 m^3/d.

Table 13.9 Slug test data

Time (minutes)	*Drawdown (m)*	*Time (minutes)*	*Drawdown (m)*	*Time (minutes)*	*Drawdown (m)*
0	0	10.8	0.95	148.7	2.89
1	0.03	13.7	1.11	188.7	3.07
1. 3	0.05	17.4	1.27	239.5	3.26
1. 6	0.09	12.1	1.44	303.9	3.45
2	0.15	28.1	1.61	385.7	3.64
2. 6	0.22	35.6	1.79	489.4	3.83
3. 3	0.31	45.2	1.97	621	4.02
4. 2	0.41	57.4	2.15	788.1	4.21
5. 3	0.53	72.8	2.33	1000	4.39
6. 7	0.66	92.4	2.52	-	-
8. 5	0.8	117.2	2.7	-	-

Estimate aquifer parameters.

Chapter 14 Design, Development, and Maintenance of Water Wells

14.1 General

Water wells have been a source of water for people, animals, and crops since the earliest civilizations. These continue to play a significant role in the society, and there has been a huge increase in the use of water wells during the past two decades. Water well should have sufficient yield to meet the demand; the water quality should be suitable for the intended use of the well; the well should be reliable, requiring little maintenance; the construction and operating costs should not be excessive; and the well should not impact significantly on neighboring wells or on the environment. The aim of *well design* is to obtain the highest yield from an appropriately selected aquifer site, and the highest efficiency in terms of specific capacity. The well site should be selected to yield maximum water productivity from the aquifer. The design of a well must be done either before drilling or before manual construction begins, as it will govern the choice of well construction method. The choice of well type is also influenced by the required well discharge rate and by socioeconomic factors, such as manpower and materials, electricity supply, operation and maintenance logistics, and budgetary constraints. A successful well design takes into account the existing comprehensive information. Investment in a detailed groundwater investigation is repaid in a successful and long-lasting well. The well is then constructed and subsequently developed. The appropriate drilling and construction material should be identified suited to geology of site under drilling and well construction. Generally, wells are constructed by drilling. The action of drilling leads to some damage to the aquifer adjacent to the well, and it results in a reduction in the performance of the well. The entry of solids into the aquifer pores and the formation of mud cake produce plugging and clogging effects. The deleterious effects of drilling fall into two categories: (1) damage to the well face and (2) damage to the aquifer matrix. The relative degree of damages in these two categories will depend on the drilling technique used in well construction. The main purpose of *well development* is to repair the damage done to the aquifer and to restore the performance of the well. The secondary purpose is to develop the aquifer itself by increasing the transmissivity of the aquifer adjacent to the well to values actually greater than they were before drilling. The principal problem in developing a well is the removal of the filter cake from the well face and mud filtrate from the aquifer. Several methods are used to achieve optimum well efficiency through the well development.

The well should be properly logged and water production zones should be interpreted. In addition, the well should be protected against contamination and provided with appropriate casing, screen and pump set to reduce maintenance cost and increase life. A well in a fine, well-sorted aquifer should be equipped with a screen and an artificial gravel pack. The grain particle-size analysis data are used for evolving criteria for deciding gravel pack material that basically affects the efficiency of the well. The criteria for selection of the gravel pack for a well is decided based on uniformity coefficient of aquifer material. The screen sections are so designed so as to produce maximum water free of sand. *Properly designed, constructed and developed water wells have long life span and optimum water production capacity and efficiency*. Such wells create small drawdown and produce optimum water yield. Site selection and construction methods for wells have already been dealt with in Chapters 3 and 4, respectively.

In general, a water well is out of sight and receives little attention by way of monitoring or maintenance. However, it deteriorates over the years and needs periodic *maintenance*. The causes of the deterioration must be established through monitoring and diagnosis for effective maintenance. Well rehabilitation means bringing back a well to its original water-producing capacity. In the maintenance of wells, various activities are carried out with a view to retain the efficiency of wells. Wells should be pumped according to the designed discharge. Pumping a well at a rate higher than the prescribed rate gives rise to the problem of sand pumping, mechanical encrustation as well as some dewatering of aquifer which may cause subsidence around the well and damage well assembly. Pumps installed on wells should be well maintained. As soon as a decline in well yield of 10 to 15 percent is observed, the pump assembly should be pulled out and inspected for any wear and tear. Mechanical and chemical encrustations on intake portions of well screens also reduce specific capacity of wells and their life span. The chemical treatment of well becomes necessary when specific capacity of well diminishes. Wells are given acid treatment to overcome the problem of encrustation and chlorine treatment where wells are infected with problem of bacterial growth.

14.2 Well Design

An *ideal well design* must produce maximum water at minimum cost and should have maximum efficiency (minimal entrance losses) and long life. The well site should be ideally selected to yield maximum water productivity from aquifer. The yield potential of a well depends on hydrological conditions (rainfall, runoff, and recharge) of the area. If the yield potential of an area is not a limiting factor, a properly designed well provides the required quantity of water. Aquifers can be divided into three broad classes for the purposes of well design:

(i) crystalline aquifers
(ii) consolidated aquifers
(iii) unconsolidated aquifers

Groundwater occurs in crystalline aquifers in the secondary porosity. The secondary porosity due to weathering and fracturing decreases with depth; hence, there will be a depth beyond which the cost of drilling outweighs the increased yield of a borehole. This maximum depth will vary from place to place depending on the geology and geomorphology of the site. Generally, well screen is not required in crystalline aquifers. The design of a well in consolidated aquifers is similar to that in a crystalline aquifer because there is no well-defined base to the aquifer, and the groundwater flow in most consolidated aquifers is largely through fissures. The depth of the borehole needed for a target discharge will depend on the distribution and size of water-bearing fractures. In limestone aquifers, karstification process can produce very large conduits with excessive groundwater flow velocities. Well construction in such aquifers can be problematical. Even if a well is successfully completed in a karst aquifer, it may be vulnerable to rapid infiltration of pollutants from the surface. In addition, the erosion of sediment from the fracture walls by rapid flow along the fractures can damage pump and silt up surface storage. Well screens are required in water wells in unconsolidated aquifers to prevent formation collapse. The following are the basic design and construction principles for a well (Misstear et al, 2006):

- The location for the well should be selected after carrying out a systematic groundwater investigation as described in Chapters 3 and 4. There is little point in spending a lot of time and money in applying the design principles if the well site is not chosen carefully.
- The well should be of sufficient diameter, depth and straightness for the pump, and for monitoring and maintenance equipment.
- It should be stable and should not collapse.
- It should prevent excessive amounts of aquifer material (sand or clay particles) from entering the well during pumping.
- It should abstract from the aquifer zone of highest yield potential.
- The well should be efficient hydraulically, ensuring that the energy losses as water moves into and up the well are not excessive.
- The construction materials should resist corrosion and incrustation, thereby reducing maintenance or rehabilitation liabilities, and should not adversely affect water quality.
- The well and aquifer should be protected from contamination—mainly from the surface, but cross contamination between aquifers should also be avoided.
- The depth, diameter and construction materials for the well should be selected such that the cost of the well is reasonable. In extensive uniform aquifers, the design can be optimized on economic grounds.

The information needed for the design of a water well includes the following:

- Aquifer type and lithology: crystalline, consolidated, or unconsolidated
- Regional groundwater levels and hence aquifer condition: confined or unconfined

- Aquifer characteristics: depth, thickness, transmissivity, and hydraulic conductivity and storativity
- Aquifer boundaries: location of impermeable and recharge boundaries
- The available groundwater potential and recharge potential
- Groundwater quality: suitability for intended use, corrosion or incrustation potential, and pollution risk
- Details of geological formations that overlie the target aquifer(s): thickness, stability, and groundwater characteristics

The design of a well incorporates: *total depth*, *diameter*, *casing selection*, *screen selection*, *casing and screen installation*, and *gravel pack design*. The economy in well design may be achieved by avoiding overdesign and unnecessary expenditure, because the total depth of the well and the screen length are dictated by the aquifer geometry. Simple guidelines include (Misstear et al, 2006) the following:

- Do not drill deeper than necessary.
- Do not drill at larger diameter than necessary:
  – Do not design a gravel pack thicker than needed.
  – Do not design a screen or casing of greater diameter than necessary.
- Do not use expensive materials where cheaper ones will suffice.
- Do not use more screen than is necessary.

14.2.1 Open Well

The manually dug wells are rare in developed countries; but in developing countries, the dug wells are common source of groundwater supply. Dug wells are best suited to shallow and low-yielding aquifers, where they have a distinct advantage over a drilled well as the well acts as a reservoir and provides greater seepage face area in order to meet a peak demand which is much greater than the instantaneous aquifer yield. The well can be deepened to create a reservoir volume capable of meeting demand or holding the daily yield of the aquifer. They may be either circular or rectangular in shape. The circular shape is preferred in alluvial and other unconsolidated formations because of its greater structural strength and convenience in well sinking, whereas the rectangular shape may be preferred in hard rock formations as it has perimeter more than circular shape for same cross-sectional area. In stable rocks, the well is often left unlined. The lining of a dug well in unconsolidated formations is most commonly of concrete rings or masonry, which are made permeable below the water table.

The design of an open well includes the selection of its diameter, depth and lining. The diameter is selected on the basis of cost and practical considerations. The diameter is the main factor influencing the cost of construction and yield of the well. The diameter should be large enough to accommodate the well diggers, but it should not be wider than necessary. Excessive diameters will increase the volume of soil to be removed, the time needed to dig the well, the cost, and the risk of surface pollution. The depth depends on the thickness of the water-bearing formation, the depth of water table below the ground surface and allowable drawdown in the well and the minimum storage depth. The approximate depth of well may be the sum of the depth of water table below ground surface, maximum allowable drawdown (4–6 m) and minimum storage depth (about 2 m) at maximum drawdown.

14.2.2 Drilled Wells

The main factors in the design of a drilled well are the discharge rate required and the type of aquifer system being exploited. The maximum discharge rate dictates the diameter of well, the size of pumping system required and the minimum internal diameter of the pump chamber casing. Other parameters to be designed are screen, casing, and gravel pack. Chapter 4 (Section 4.6) deals with few aspects of well screen, casing, and gravel pack. The screen sections are designed to produce maximum sand-free water from pervious zones. They should have maximum open area and minimum entrance velocity. The screen openings should be selected based on results of grain size analysis of aquifer materials so as to not allow fine materials entering the well. The screen should be corrosive resistant, and the length of screen should be in proportion to type of aquifer and its saturated thickness. In unconfined aquifer, the screen is placed in its lower one-third saturated zone. The gravel pack design of well is decided based on grain size distribution curve. In crystalline and consolidated aquifers, the well can remain unlined. However, it is common to have 2–3 m (or more) of casing. The most common unconsolidated aquifers are alluvial deposits where water well design varies with the number of aquifers to be exploited and the depth of those aquifers.

Total Depth

In an aquifer of limited thickness, the well is normally fully penetrating to maximize yield. The depth of a well in a very thick aquifer is governed by the required discharge and by cost constraints. The thickness of aquifer to be drilled to give a design discharge can be estimated using Thiem's Eqn. (8.35) for drawdown in the pumped well s_w, and hence replacing $h_2 - h_1 = s_w$; $r_2 = r_e$ (radius of influence); and $r_1 = r_w$ (radius the pumped well); in it becomes

$$T = Kb = \frac{Q}{2\pi s_w} \ln \frac{r_e}{r_w} \tag{14.1}$$

The ratio r_e/r_w cannot be determined accurately during a pumping test unless data from several observation boreholes are available. Although this ratio may vary significantly, the $\log(r_e/r_w)$ is relatively insensitive to these variations. A number of approximations are available, for example (Misstear et al, 2006)

$$T = Kb = \frac{(1.22 \text{ or } 1.32)Q}{s_w} \tag{14.2}$$

The factor 1.22 is for ideal flow conditions and can be replaced by a higher factor such as 2.0 to allow for additional well drawdown resulting from partial penetration effects and well losses; and therefore for factor 2, the well depth b or the length of screen L_s comes out:

$$b = L_s = \frac{2Q}{Ks_w} \tag{14.3}$$

This equation assumes that the aquifer material is relatively uniform; it cannot be applied in very heterogeneous formations. In addition, well losses are actually proportional to the square of the discharge rate; therefore, the allowance for well losses included in the linear multiplier of 2.0 may not be adequate in the case of inefficient wells pumping at high discharge rates.

Diameter

Choice of proper well diameter is important because it affects the cost of well and its specific yield. A well may have different diameter from top to bottom. The diameter of the well should be such as to allow installation of pump suitable for the designed discharge with minimum loss of head. Thiem's equation,

$$s_w = \frac{Q}{2\pi Kb} \ln\frac{r_e}{r_w} \Rightarrow \ln\frac{r_e}{r_w} = \frac{2\pi Kbs_w}{Q} \Rightarrow r_w = r_e \exp\left(-C/Q\right) \tag{14.4}$$

indicates that all other factors remaining constant, the discharge is not much sensitive to diameter. The computed diameter using Eqn. (14.4) is indicative only as other requirements govern the diameter. The diameter of casing pipe is fixed considering permissible velocity (1.5–4.5 m/s) of water. A velocity of 2.5 to 3 m/s is most suitable. The drilled diameter is dictated by the casing pipe chosen for the well. The drilled hole at any depth should have a minimum diameter about 50 mm greater than the outer diameter of the casing and screen string, although larger clearances are required for grouting operations and installing a gravel pack. The casing in shallow wells is in one string, with an internal diameter giving sufficient clearance for the pump and monitoring/access tubes. The screen may be the same diameter as the casing or smaller. The latter can result in savings in capital costs. In deep wells, the casing and screen may be in several sections. The intermediate casing must be large enough for the screen to pass, and be small enough to pass through the pump chamber casing. The pump chamber again has to be large enough to accommodate the pump and monitoring/access tubes. The diameter of a borehole to be provided with gravel pack (which should be at least 75 mm thick) has to be at least 150 mm greater than the screen diameter. Table 14.1 lists diameters for well casings and screens.

Table 14.1 Minimum diameters for well casings and screens (USBR, 1977)

Well yield (m^3/d)	*Nominal pump chamber casing diameter (cm)*	*Surface casing diameter (cm)*		*Nominal screen diameter (cm)*
		Naturally developed wells	*Gravel-packed wells*	
<270	15	25	45	5
270–680	20	30	50	10
680–1,900	25	35	55	15
1,900–4,400	30	40	60	20
4,400–7,600	35	45	65	25
7,600–14,000	40	50	70	30
14,000–19,000	50	60	80	35
19,000–27,000	60	70	90	40

Gravel Pack Design

A gravel or sand pack is introduced around the screen of a water well to produce an envelope of material with enhanced permeability and stability adjacent to the screen as described in Chapter 4. The enhanced permeability reduces well losses and incrustation of the screen, whereas the physical stability reduces the amount of sediment drawn into the well by pumping. Two main kinds of gravel pack are used, natural and artificial, depending on the type of aquifer being drilled. A natural gravel pack is produced by development of the unconsolidated aquifer formation itself. Artificial gravel packs are used in unconsolidated aquifers where the aquifer material is either very fine or well sorted (i.e. of uniform grading). *Effective size* of formation D_{10} is the size at which 10 percent particles are finer (pass through) and 90 percent are coarser (retained). *Uniformity coefficient* represents variation in grain size of the formation material, and it is defined as the ratio of D_{60} (60% finer or 40% retained) to D_{10} (10% finer or 90% retained). For uniformly graded soils, it is less than 2 and its value is high for poorly graded and heterogeneous soils. *Gravel pack–aquifer (PA) ratio* may be defined as the ratio of D_{50} of gravel pack to D_{50} of aquifer material. PA ratio may be 4 to 5. For uniform aquifer, it may be between 9 and 12.5; and for graded aquifer, it may be between 12 and 15.5. Sometimes, PA is defined based on D_{30}.

For natural gravel pack, development techniques are used to draw the finer fraction of the unconsolidated aquifer through the screen, leaving behind a stable envelope of the coarser, and therefore more permeable, material of the aquifer. The development process produces a filter in which the coarsest particles are adjacent to the screen, with the grading reducing in size from the well face to the undisturbed formation at some distance from the borehole. An aquifer is suitable for a natural pack if it is coarse grained (D_{10} greater than 0.25 mm) and poorly sorted (uniformity coefficient = D_{60}/D_{10} > 3). Screens with very narrow slots are susceptible to blockage. A natural gravel pack design is not used for an aquifer when the D_{40} criterion requires a slot width of less than 0.5 mm, and hence an artificial pack would be appropriate.

Artificial gravel packs are used where the aquifer material is fine, well sorted or layered and heterogeneous. A significant advantage of the artificial pack is that, because the pack material is coarser than the geological formation, screens with larger slot sizes can be used. Artificial packs are useful in allowing thin-bedded heterogeneous aquifers to be screened much more safely than with direct screening and natural development. Their main advantages are (Misstear et al, 2006) as follows:

- They allow screens with larger slot sizes to be used, because the pack material is coarser than the formation.
- They reduce the risk of sand pumping and screen blockage.
- They increase the effective diameter of the well, since the gravel pack has a much higher permeability than the surrounding aquifer.
- They may reduce the required well development time.

Their disadvantages include the following:

- They require a larger drilling diameter to provide the required annular clearance for installing the pack.
- Suitable pack material is difficult to obtain in many situations.

Many designs of gravel pack have been proposed, relating the grain size distributions in the aquifer and pack. They generally differ only on points of detail concerning the gravel pack grading. Terzaghi and Peck (1948) criterion on filter design is most commonly used, which is

$$\frac{\text{Gravel pack } D_{15}}{\text{Aquifer } D_{85}} < 4 < \frac{\text{Gravel pack } D_{15}}{\text{Aquifer } D_{15}} \qquad (14.5)$$

The best approach is to specify a design envelope for a gravel pack, rather than a particular grading. The artificial gravel pack grain size distribution should be similar to that of the aquifer being screened, and should lie within an envelope defined by four and six times the aquifer grain size. Table 14.2 lists USBR-recommended criteria for selection of gravel pack material and corresponding screen slot sizes.

Table 14.2 Criteria for selection of gravel pack material (USBR, 1977)

Uniformity coefficient (U_c) of aquifer	*Gravel pack criteria*
<2.5	(a) U_c between 1 and 2.5 with the 50% size not greater than six times the 50% size of the aquifer (b) If (a) is not available, U_c between 2.5 and 5 with 50% size not greater than nine times the 50% size of the aquifer
2.5–5	(a) U_c between 1 and 2.5 with the 50% size not greater than nine times the 50% size of the formation (b) If (a) is not available, U_c between 2.5 and 5 with 50% size not greater than 12 times the 50% size of the aquifer

(*Continued*)

Table 14.2: Continued

Uniformity coefficient (U_c) of aquifer	*Gravel pack criteria*
>5	(a) Multiply the 30% passing size of the aquifer by 6 and 9 and locate the points on the grain-size distribution graph on the same horizontal line
	(b) Through these points, draw two parallel lines representing materials with $U_c < 2.5$
	(c) Select gravel pack material that falls between the two lines
Screen slot size in all three cases is ≤ 10 percent passing size of the respective gravel pack.	

A few millimetres (2–3 grain diameter) thick gravel pack can retain the formation in undisturbed conditions, but intentional disturbance of the pack and formation during well development needs a thicker pack to avoid sand pumping. A thick pack is also able to cope with unintentional thinning of the pack in cases where the screen is not adequately centred. The pack thickness should be not less than 75 mm and greater than 150 mm. Gravel packs much greater than 150 mm in thickness may create difficulties in development in removing mud cake and result in the higher cost due to the greater drilled diameter of the well. Artificial gravel packs, graded in size from the coarsest next to the screen to the finest next to the aquifer, may be proposed, but such a design is impractical for most field installations. In a conventional graded pack, installation by tremie pipe from the bottom of the hole upward (rather than by simply pouring the gravel in from the top) is done to avoid the different grain sizes in the pack settling at different rates leading to lamination in the pack and to ensure the gravel completely fills the annulus. The material used for a gravel pack should be natural, subrounded siliceous sand or gravel. Iron-rich sand or limestone gravel should be avoided, because solution and precipitation of iron or calcium salts are likely to cause problems.

Screen

The screen selection involves the length, diameter and type of screen to be used. The screen is usually more expensive than the casing; therefore, the efficient use of the screen can reduce the capital cost of a well. The screen should not extend above the lowest anticipated pumping water level. This avoids the upper section of the aquifer and screen becoming aerated as the aquifer is dewatered, and reduces the risk of incrustation of the screen and aquifer. A confined aquifer of limited thickness may have screen throughout. Keeping the total screen length at less than 100 percent of the aquifer thickness allows for casing to be set into the top of the aquifer and a bottom plug to be put at the bottom of the screen. Where the aquifer is unconfined, the choice of screen length is a tradeoff between a longer screen length giving a higher specific capacity and lesser drawdown, and resulting higher cost. Screen length may be selected equal to the lower one-third to one-half of a homogeneous unconfined aquifer. For a thick (e.g. more

than 30 m thick) homogeneous aquifer, Eqn. (14.2) can be applied to estimate the required screen length. If the aquifer is heterogeneous, the well design can incorporate short sections of screen placed opposite the most permeable layers, with appropriate screen slot sizes for each layer, and blank casing against the intervening aquicludes. The diameter of the screen should be at least 150 mm to allow ready access for workover tools in future maintenance operations. Screen diameters in excess of 300 mm are rarely needed on hydraulic grounds.
The open area of a screen governs the rate at which water can enter the well. The effective open area of the aquifer may be less than 10 percent, therefore the minimum screen open area of 10 percent is desirable. Once the open area exceeds 10 percent value, the hydraulic performances of the screens will be similar. In practice, about 50 percent of the initial open area may be blocked over time by pack or aquifer material; the concept of an effective screen open area is usually adopted in design. The open area, together with the diameter and length of the screen, determines the screen entrance velocity for a particular well discharge rate. The screen entrance velocity is one of the design considerations when examining potential well losses, and hence the hydraulic suitability of the well design. Chapter 4 (Section 4.6.2) provides additional information on screen types, and corresponding open areas.

Some screens are available with resin-bonded artificial gravel pack already installed. Although this screen and pack will act as a filter, it cannot be developed and may be susceptible to blockage. Similarly, small diameter screens suitable for observation boreholes can be purchased with a geotextile filter mesh wrapped around the slotted pipe. These can be convenient in situations where it is impractical to install an artificial gravel pack.

Slot Width

The width of slots in a screen should be selected with regard to the grain size of the aquifer or gravel pack. The screen slot size and pack grading are determined from a standard sieve analysis of lithological samples from the aquifer. In the development of a natural gravel pack, the screen should have slots that are wide enough to allow a certain proportion of fine material through for development of the pack. The size slot may be selected in range D_{30} to D_{70} (that will allow 30–70 percent of the aquifer material to pass through) depending on the formation material, the presence of caving formations above the aquifer, and the corrosiveness of the water. The slot choice for a screen in a very heterogeneous aquifer should be based on the analyses of the finer parts of the aquifer, not on average aquifer material. In a layered aquifer, the screen can be of multiple construction with a slot size to match each layer. The size of slots in artificially gravel packed wells should be between the D_{10} size and D_{40} size of the artificial gravel pack, the lower figure being preferred where the pack is uniform.

Gravel Pack Loss and Screen Entrance Loss

The head loss across the gravel pack Δh_g is given by (Misstear et al, 2006) the following equation:

$$\Delta h_{\mathrm{g}} = \frac{Q}{2\pi K_{\mathrm{hg}} L_{\mathrm{s}}} \ln \frac{r_{\mathrm{p}}}{r_{\mathrm{w}}} + \Delta h_{\mathrm{gg}} \tag{14.6}$$

where, K_{hg} is the horizontal hydraulic conductivity of the gravel pack, r_p is the radius of gravel pack, and Δh_{gg} is the correction factor for non-Darcian head losses in the gravel pack (related to the square of the discharge rate). The average velocity of water entering a screen v_e can be calculated using the following equation:

$$v_e = \frac{Q}{C_g \pi D L_s A_{eo}} \tag{14.7}$$

where, A_{eo} is the effective open area of the screen and C_g is the clogging coefficient (0.5 may be used to allow for long-term 50 percent blockages of the slots). Thus, the entrance velocity can be reduced by increasing the screen diameter, screen length or the open area. On the other hand, if minimum entrance velocity is prescribed, then for a given open area of the screen, the appropriate diameter and length of screen can be selected. Low entrance velocities are preferred to keep head losses in the screen to a minimum and to have benefits in terms of minimizing screen corrosion, incrustation and abrasion problems, and hence less well maintenance. The entrance velocity should not exceed 0.03 m/s. Walton (1970) suggested entrance velocity between 0.01 and 0.06 m/s with a low entrance velocity of 0.01 m/s for aquifers having a low hydraulic conductivity, where the screens are more prone to clogging. However, well efficiencies do not increase significantly if the open areas of the screen are increased above 3–5 percent and entrance velocity and screen open area are not critical design factors for most field situations.

The head loss across the screen slots Δh_e can be estimated using orifice formula:

$$\Delta h_e = \frac{1}{2g}\left(\frac{Q}{C_g \pi D L_s C_v C_c A_{eo}}\right)^2 = \frac{1}{2g}\left(\frac{v_e}{C_v C_c}\right)^2 \tag{14.8}$$

where, C_v and C_c are the velocity coefficient and the contraction coefficient, respectively. Using $C_v = 97$, $C_c = 0.67$, and $v_e = 0.03$ m/s results $\Delta h_e = 0.123$ mm, which very small in comparison with other head losses. If $v_e = 1.2$ m/s as upper limit is assumed, then $\Delta h_e = 0.2$ m, that is likely to be acceptable in many situations.

Materials

The materials most commonly used as casing and screen in wells are steel (mild or low carbon steel, carbon steel and stainless steel), plastic [polyvinyl chloride (PVC), acrylonitrile butadiene styrene (ABS), polyolefins and other plastics] and fiberglass [glass reinforced plastic (GRP)]. The choice is influenced by many factors, such as strength, jointing system, durability, chemical inertness, ease of handling, cost, local availability, and familiarity. The relative importance of the various factors will differ according to the type and purpose of the well. A temporary dewatering well will not require the same quality and durability of materials as a permanent water supply well. An observation borehole for sampling groundwater quality will require casing and screen materials that do not significantly absorb, or leach out, inorganic or organic contaminants being sampled, so as to minimize interference effects.

Strength: The material selected for casing and screen should have adequate radial compressive strength, longitudinal compressive strength, and longitudinal tensile strength. Radial compressive strength is needed to resist deformation (buckling) or collapse of the casing or screen due to earth pressures in unconsolidated formations, differential drilling fluid, or water pressures across the casing string, grouting pressures, and pressures caused by well development. The collapse resistance of a casing depends on its diameter, wall thickness, and the elastic properties (Young's modulus and Poisson's ratio) of the material. Longitudinal compressive strength is required to resist any longitudinal earth forces if the ground around the well is likely to subside, including forces resulting from consolidation of an artificial gravel pack. Longitudinal tensile strength is required to support the weight of the full casing string during installation. Additional loadings may act during removal of the casing and screen. These additional forces depend on the nature of the geology, the type, length and diameter of the casing and screen, the presence of a gravel pack, etc.

Jointing system: The type of jointing system affects the material strength as well as the ease with which the casing string can be installed or removed. The joints are normally the weakest part of the casing string, yet it must be strong enough to carry the full weight of the casing string. The jointing system should be such as to ensure a strong, straight, watertight, and durable connection between the lengths of casing. There is a huge variety of jointing systems available for steel and plastic casings. Threaded couplings can be used for both steel and plastic casings. Flush jointed casings are easier to install and pull back, but they may have less strength than external upset couplings because there is less effective thickness of material at the joint. Drawbacks of external upset couplings are that they require a larger drilled diameter to provide the same minimum annular clearance for installing the casing string, gravel pack and grout seal, and the casing string may be more difficult to pull out if the geological formation collapses on top of the joints before the full casing string has been installed. The threads come in a variety of shapes as V-shaped, square, round, and trapezoidal threads. Welded joints are used for steel casings, especially for some of the larger casing sizes. Plastic pipes can be solvent welded (glued) together. Such joints should be allowed to set before the casing string is lowered into the borehole. Spigot and socket with key locks, and variants of this system, are used for some plastic and fiberglass casings and can provide an effective and strong seal.

Durability: It is essential to select materials that resist corrosion. Electrochemical corrosion involves loss of metal into solution as a result of currents flowing between areas of different electrical potential in the well. Microbes that operate under anaerobic conditions also play a part in the corrosion process. Corrosion is to be avoided since it can lead to the following:

- Enlargement of screen openings and consequent sand pumping, leading to further abrasion of the well liner and pump
- Redeposition of corrosion products, leading to incrustation and blockage of scree openings and of the gravel pack and formation surrounding the well

- Perforation of the casing and casing joints, potentially allowing polluted water to enter the well
- Reduction in the strength of casing and screen through progressive removal of material, leading eventually to collapse of the well

Chemical inertness: The materials used for well construction should not leach chemicals into groundwater. When installing observation wells for monitoring groundwater quality, the construction materials should be nonreactive chemically. Mild or low carbon steel is not normally used because it is vulnerable to corrosion. Stainless steel is suitable, although expensive, for most monitoring applications, but it may not be appropriate where trace metals are present in the groundwater to be sampled. Unplasticized PVC offers a good balance between practicality and performance. PVC pipes should be jointed with leakproof threaded couplings and solvent welded joints should be avoided. PVC is not suitable where nonaqueous phase liquids are present. Fluoropolymers have high chemical inertness, but are more expensive and weaker than other plastics such as PVC and high density polyethylene (HDPE). They are therefore mainly suited to shallow, small diameter monitoring installations. Fluoropolymers or stainless steel may be used where organic contaminants are present and where monitoring is likely to be long term.

Casing: Steel is the most commonly used material for well casing because of its strength. Steel casing can be installed to great depths and pressure grouted. It can withstand fairly rough treatment on site, including driving and jacking. Even if an alternative material such as plastic is used for the main casing string, steel is almost always chosen for the surface conductor casing because of this robustness. The jointing system can be threaded couplings or butt welding. Steel casing is made in several grades and weights. The type of casing has to be chosen to suit local conditions: heavy, high-grade carbon steel is for use in deep wells, whereas lower grade steel is often used in shallow wells. Steel casings have much greater compressive and tensile strengths than plastic casings. The main disadvantage of steel is that it can be vulnerable to corrosion. Resistance to corrosion can be improved through the application of bituminous or other coating materials. Coated casing should be handled with care to avoid scratching or scraping it. The use of stainless steel is the best defence against corrosion, but it is expensive compared with plastic or fiberglass alternatives. Plastic (PVC, ABS, rubber-modified styrene, and polypropylene) is widely used in shallow aquifers because it is cheap and corrosion free. Plastic casings can be flush jointed (threaded), solvent welded, or spigot and socket connected. Fiberglass (GRP) casing is stronger than plastic casing and is corrosion resistant. Fiberglass lengths of water well casing are joined by external upset couplings with special mechanical key locks. The plastic and fiberglass casings are significantly weaker and more fragile than steel casings. Threads can be destroyed by abrasion and the casing cracked by shocks. The plastic and fiberglass casings should be handled carefully during transport and installation. These casings also deform more easily than steel, and they may be irreversibly crushed by external hydrostatic pressures during well development or maintenance operations. Plastic materials can also degrade when exposed to sunlight, and therefore pipes should always be covered during storage and transport. Because plastic casing bends easily, the casing string should be installed centrally in the well using centralizers. This will help the verticality and alignment of the well and also ensure a consistent annular clearance for the gravel pack. Plastic and fiberglass casings are much lighter than steel, which has considerable advantages in transport costs and ease of installation. The use of different materials often depends on local availability and practice.

Screen: Screens are manufactured to many designs in a wide range of materials. The choice of a particular screen type for a well will depend on a combination of factors: the strength and corrosion resistance, the slot design and open area, and cost. Chapter 4 (Section 4.6.2) provides additional information on screen materials. Mild steel screens are susceptible to corrosion and incrustation, whereas stainless steel screens are corrosion resistant, strong, and expensive.

Selection of screen and gravel pack

Misstear et al, (2006) summarised the criteria for selecting screen and gravel pack as following.

The need for a screen and pack will depend on the aquifer type:

- Crystalline aquifer: No screen or gravel pack is normally needed. However, if the main water-bearing zones are in unstable fractured or weathered rock, a screen with a formation stabilizer may be required.
- Consolidated aquifer: Screen and pack are often not required.
- Unconsolidated aquifer: Screen and gravel pack are needed. The choice of a natural or artificial gravel pack will depend on the aquifer grain size and its uniformity.

Screen diameter should be chosen such that

- head losses are small for the design discharge—the well upflow velocity should be less than 1.5 m/s.
- the screen is large enough to accommodate work over tools—a 150 mm minimum diameter is recommended for most water supply wells.
- cost is optimized.

Choice of screen material, screen length, and slot design depends on site conditions:

- If the aquifer is thick, then a long screen with limited (but greater than 10%) open area may be chosen. The screen length may be up to 90 percent of the full thickness of a confined aquifer, or the lower one-third of an unconfined aquifer. For a very extensive, uniform aquifer, Eqn. (14.1) can be used to calculate screen length, or the screen length can be optimized economically.
- If the aquifer is thin, then a screen with a large open area should be selected.
- If the aquifer is over 200 m deep, then a strong screen must be chosen; usually, carbon steel or stainless steel, but thick-walled plastic or fiberglass may be suitable in some situations.
- If the groundwater is corrosive, then corrosion-resistant screens should be used such as plastic, fiberglass, and stainless steel.

- If the groundwater is encrusting, then a screen with a large open area should be used to offset the effects of screen blockage.

Choice of gravel pack depends on the particle-size distribution (uniformity coefficient) of the aquifer formation:

- If the aquifer is poorly sorted (uniformity coefficient > 3), then a natural pack can be developed. The screen slot width should be the average D_{40} of the aquifer samples (based on the finest layer in a heterogeneous aquifer system). If the D_{40} size gives a slot width < 0.5 mm, then artificial gravel pack can be used to allow a larger slot width.
- If the aquifer is well sorted (uniformity coefficient < 3), then an artificial pack is needed. The screen slot width should be approximately the D_{10} of the gravel pack and not larger than D_{40}.

Optimization of Well Design

The most common unconsolidated aquifers are alluvial deposits. The well design in a thick, uniform, unconsolidated aquifer can be optimized because the aquifer geometry dictates neither the total depth nor the screen length in the well. The primary design aim in this situation is to obtain the required discharge rate at the lowest cost. The cost of the water pumped from a well depends on both the capital costs and running costs of the well. An increase in well depth and screen length increases the capital cost, whereas it will reduce the drawdown for a given design discharge, and hence the running (pumping) cost. Similarly, a decrease in well diameter will decrease the capital costs, but it may increase the running costs through increased well losses. Combining Eqs. (12.106) and (14.2), and substituting screen length for saturated thickness, we obtain

$$s_{\mathrm{wt}} = C_{\mathrm{f}}Q + C_{\mathrm{w}}Q^2 = \frac{1.22Q}{KL_{\mathrm{s}}} + C_{\mathrm{w}}Q^2 \tag{14.9}$$

When well losses are small, the relationship can be simplified by eliminating the second term in the equation. In addition, the multiplier in the first term from 1.22 may be increased to 2.0 to allow for some well losses plus additional drawdown due to partial penetration effects in a thick aquifer, which result to Eqn. (14.3). Thus, drawdown is inversely proportional to screen length for constant values of Q and K.

Capital cost of single-well installation C_{c} includes cost of drilling, casing, well screen, filter pack, sealing and well development, and pump system cost. Thus,

$$C_{\mathrm{c}} = C_0 + C_1 L_C + C_2 L_s + C_3 QH \tag{14.10}$$

where, C_0 is the fixed cost factor that includes cost of sealing, well development and others; C_1 is the cost of unit length of casing and drilling; C_2 is the cost of unit length of screen and filter pack; and C_3 is the multiplier so as to give C_3QH as cost of supply and installation of pump system. Length of casing and pumping head are function of s_{wt} and position of water table h_{w}.

The major factors that influence the annual pumping cost depend on the volume of water to be pumped, weight density of the water, hydraulic head, efficiency of the pump, and energy cost (Swamee and Sharma, 1990; Swamee, 1996; Sharma and Swamee, 2006; Moradi et al., 2003). The total cost of pumping consists of the capitalized electricity cost including the annual repair and maintenance cost. In addition, the pump should be replaced after its useful life is over. The annual recurring costs C_r can be expressed as follows:

$$C_r = C_4 + C_5 QH \tag{14.11}$$

where, C_4 and C_5 involve combined efficiency of the pump and prime mover and cost of the electricity per kilowatt hour. The future recurring costs must be discounted back to a present value C_{rp} using standard formulae for interest calculations as follows:

$$C_{rp} = C_6 \left(C_4 + C_5 QH\right) \tag{14.12}$$

where, C_6 is the present value conversion factor that takes care interest rate and pump life = $\{(1+r)^T - 1\} / \{r(1+r)^T\}$ in which r is the rate of interest, and T is the life of pump. For long life of pump, $C_6 = 1/r$. Therefore, total present cost will be

$$C_p = C_c + C_{rp} = C_0 + C_1 L_C + C_2 L_s + C_3 QH + C_6 \left(C_4 + C_5 QH\right) \tag{14.13}$$

Expressing L_c and H as function of s_{wt} and position of water table h_w results

$$C_p = C'_0 + C'_1 h_w + C'_2 L_s + C'_3 Q + C'_4 Q h_w + \frac{C'_5 Q}{K L_s} + \frac{C'_6 Q^2}{K L_s} \tag{14.14}$$

where C' are terms resulting from addition and multiplication of earlier constant C terms. Eqn. (14.14) represents the present value of capital and total recurring costs over the lifetime of well. If well losses term is also considered, then

$$C_p = C'_0 + C'_1 h_w + C'_2 L_s + C'_3 Q + C'_4 Q h_w + \frac{C'_5 Q}{K L_s} + \frac{C'_6 Q^2}{K L_s} + C'_7 Q^2 + C'_8 Q^3 \tag{14.15}$$

The optimum screen length and well depth can be determined from the least cost criteria. This can be achieved through partially differentiating Eqn. (14.14) with respect to any of the design variables (screen length L_s or well depth = L_c plus L_s) since at minima the first order derivatives must vanish. For example, the optimal value of L_s is

$$\frac{dC_p}{dL_s} = 0 \Rightarrow C'_2 - \frac{C'_5 Q}{K L_s^2} - \frac{C'_6 Q^2}{K L_s^2} \Rightarrow L_s = \sqrt{\frac{C'_5 Q + C'_6 Q^2}{C'_2 K}} \tag{14.16}$$

Similarly, optimal depth of well or other parameters can be computed.

Economic optimization of well design is especially relevant to a project in which large numbers of wells are to be constructed. In such case, optimization can be achieved by finding the layout of the well field that results in the minimum cost for transferring the water to a central location in the well field subjected to minimum interference between the wells. Swamee et al. (1999), Gaur et al. (2011; 2013) obtained optimal location of wells in a well field. In a well field, the total cost for new system of pumping wells consists of the cost of well installation, piping cost, and cost of pumping. The installation cost can be calculated by summing cost of one well Eqn. (14.14) for the number of wells N_w, that is $\sum_{i=1}^{N_w} Cp$. Here in all the wells are considered as of the same depth, diameter, and screen length. The piping cost depends on the location of wells along with many other factors. The cost for establishment of the pipeline depends on the cost of the earthwork, the cost of pipes, joining separate pipe sections together by welding, applying an outer insulation, and lowering the pipeline into a trench. The reference location consists of a water storage tank where water from all the wells will be stored and subsequently transported to the city. Considering, the piping length from the wells to a reference location only and all the pipes of the same diameter and material, the piping cost can be given as follows:

$$C_{\text{pn}} = C_7 \sum_{i=1}^{N_w} L_{\text{i}} \tag{14.17}$$

where, L_{i} is the pipe length for ith well and C_7 is the total cost for per meter piping. Equation (14.17) assumes that each well is directly connected to the reference location; therefore, L_{i} is the distance between the reference location and ith well. Therefore, the optimization problem can be stated as follows:

$$Minimize \sum_{i=1}^{N_w} \left[\left\{ C_0 + C_1 L_C + C_2 L_s + C_3 Q_i H_i + C_6 \left(C_4 + C_5 Q_i H_i \right) \right\} + C_7 L_i \right] \tag{14.18}$$

Subject to

$$Q_{i,\min} < Q_i < Q_{i,\max} \tag{14.19a}$$

$$\sum_{i=1}^{N_w} Q_{\text{i}} > Q_{\text{total}} \tag{14.19b}$$

$$s_{\text{wt}i} < s_{\text{wt,per}} \tag{14.19c}$$

$$\sqrt{(x - x_i)^2 + (y - y_i)^2} > d_{\text{w,per}} \tag{14.19d}$$

The first constraint prescribes the maximum and minimum discharge limit of a single well. The second constraint prescribes the minimum discharge limits by all wells. The third constraint was taken to limit the drawdown in individual well. The fourth constraint incorporates the minimum distance between the wells in order to provide a protective zone around the wells and avoid interference between wells. This optimization problem can be solved by a variety of methods (Swamee et al., 1999; Gaur et al., 2011; Gaur et al., 2013; etc.).

14.3 Well Development

A new well is developed to increase its specific capacity, prevent sand pumping, and obtain maximum economic well life by removing the finer material from the natural formations surrounding the screens. In addition, the drilling operation damages the natural aquifer by (i) incursion of drilling fluid, (ii) incursion of solids into the rock pores, and (iii) formation of mud cake on borehole wall against permeable zone. As a result, the hydraulic conductivity of formation material in the vicinity of the borehole is significantly and adversely altered. This damage is very severe in wells drilled in unconsolidated sediments by mud rotary method. If the well is to function efficiently, the formation damage must be repaired. The process of removing the finer material from the natural formations surrounding the well screen and/or repairing disturbed aquifer is termed as *well development*.

The objective of well development is to create a zone of enhanced porosity and hydraulic conductivity around the borehole, which will improve the well performance. This increase in well efficiency is a result of the decrease in the velocity of groundwater flow in the zone of enhanced porosity adjacent to the well screen. The flow velocity of groundwater in the natural aquifer is low and the flow is laminar. As groundwater approaches a pumping well, it has to flow through progressively smaller cross sections of aquifer; and therefore, the groundwater velocity can be high enough for the flow to become turbulent, which leads to increased drawdown in the well. The development increases porosity, leading to a proportional decrease in velocity in the zone where turbulent flow is most likely to occur. The development can improve the well performance, but it cannot produce additional groundwater resources from the aquifer as a whole because its effect is local to the well. The well development leads to the maximum capacity of the well due to the following:

- It corrects any damage to or clogging of the water-bearing formation due to drilling.
- It increases the porosity and hydraulic conductivity of the formation in the vicinity of the screen that maximizes well efficiency and specific capacity of the well.
- It clears the mud cake formed on the borehole wall against permeable zone.
- It removes the fine material from the formation in the vicinity of the well and stabilizes the sand formation around the screen so that well will yield desired quantity of water free of sand.

14.3.1 Factors Affecting Well Development

The length of time required for well development and the effect of development on the yield of well depend on the following factors:

- **Size and sorting characteristics of the aquifer material**: Formation material with large variance in size will require longer development time, whereas those with less variance in size can be developed fast.

- **Type of drilling mud**: The drilling mud results in incursion of more solids into the aquifer and formation of very thick mud cake on the borehole wall. Removal of mud cake from bore hole wall and fine materials from aquifer takes longer time.
- **Mixing of Additive**: Mixing of specially prepared mud additives in bentonite reduces the thickness of mud cake and solid incursion into aquifer, resulting in faster well development. The use of biodegradable organic polymer-based muds overcomes many of the problems associated with bentonite-based muds. However, it does not eliminate the need for development altogether. A filter cake is still produced, and formation incursion by fines from the formation being drilled also occurs. The breakdown of organic polymers can be accelerated by the use of additives such as chlorine. The organic polymer mud must be removed totally from the well, or it may act as food for bacteria and encourage infection and biofouling in the well. It must be ensured that polymer is not left behind the blind casing, where development cannot be effective.
- **Type of well screen**: The open area of screen is the key for access of developmental pressure to borehole wall and the aquifer. Screens with limited open area, such as slotted screens, prevent access to the formation surrounding the screen. As a result development is difficult, inefficient, and time-consuming. Continuous slot-type V-wire screens have large opening area with nonclogging slots, which ensure quick and better development.
- **Method of development**: The main intent in the development is to cause reversals of flow through screen openings that will rearrange the formation particles by breaking down bridging of groups of particles. Reversing the direction of flow by surging is effective as the outflow surge cycle breaks down bridging and inflow surge cycle moves the fine particles towards the screen and into the well. Techniques imparting high level of water pressure with surge reversal are much more efficient.

There are four main factors that will influence the choice of development method:

(i) Aquifer type: unconsolidated, consolidated, or crystalline
(ii) Well design: open hole or screened, plastic, or metallic screen
(iii) Drilling method and rig type: percussion, direct circulation rotary, reverse circulation rotary, or other method
(iv) Drilling fluid: bentonite mud, organic polymer, air, and water

Successful development of a poorly sorted, unconsolidated, aquifer will lead to the formation of a natural gravel pack. Development could remove up to 40 percent of the aquifer close to the screen, but because the effects of development will decrease away from the well face, the gravel pack will grade from a clean gravel against the screen, to the natural material as shown in Figure 14.1. Development will affect only the aquifer close to the well, usually within a meter of the screen. The development is beneficial even in artificial gravel-packed wells. The development of such a well should be undertaken with care, especially if the pack is thin, because too vigorous a development could mobilize the aquifer material to break through the pack and lead to sand pumping.

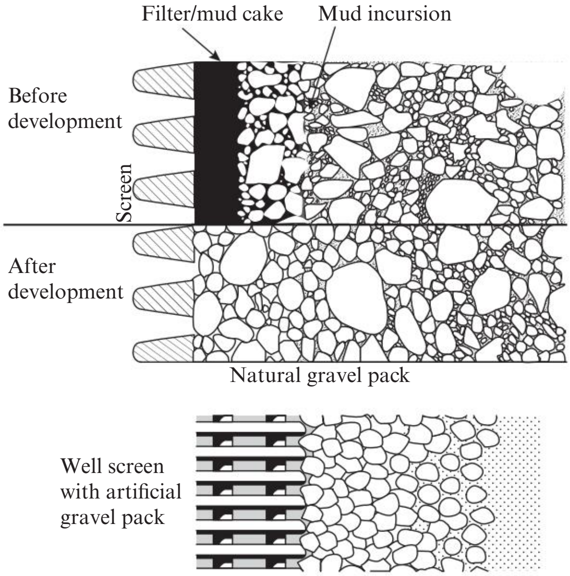

Figure 14.1 *Formation structure of developed well*

14.3.2 Development Methods

Depending on geological and hydrological environment, the development procedures are varied. Development relies on either physical or chemical methods to clean the well face and mobilize the material to be removed from the well. The physical methods include scratching, surging, and jetting, whereas the chemical methods include polyphosphate dispersion, and acidization. Use of explosive, bailing, and hydrofacturing are other methods of development. Where a well is constructed with plastic materials, great care needs to be taken to ensure that the more vigorous forms of well development do not damage the casing or screen. The best results are usually achieved by a combination of methods. The development techniques can be roughly divided into two groups:

(i) Dispersed method, in which development force is allowed to act on the entire screen length at one time, for example, overpumping, backwashing, mechanical surging, air development by surging and pumping, etc.
(ii) Concentrated method, in which the force is applied on a reduced section of the screen at one time, for example, air surging and lifting, high-velocity water jetting and air lifting, etc.

Interrupted Overpumping or Surge Pumping

The simplest method of removing fines from the formation is by overpumping. Pumping at a constant discharge rate greater than the design capacity may not be effective. Pumping at a constant rate, however high, will remove loose material initially, but because there is no surging, it could stabilize a situation of partial development. Development by pumping should be in a manner designed to induce surging; by pump is switched on for a few minutes and then switched off for a couple of hours. This sequence is repeated at different discharge rates in a series of steps from a low discharge to a discharge higher than the designed capacity. At each step pumping continued until the water clears, after which the power is shut off and water in the pump column surges back into the well. The discharge rate is then increased, and the procedure repeated until the final rate is the maximum capacity of the pump or well. This irregular and noncontinuous pumping agitates the fine material surrounding the well so that it can be carried into the well and pumped out. This procedure is advantageous because any well that can be pumped sand free at a high rate can be pumped sand free at a lower rate. The pump is normally set above the top of the screen, and development is primarily concentrated in the upper one-quarter section of screen length. Overpumping requires high-capacity pumping equipment that may not be available at reasonable cost. In addition, a well so developed may pump sand for several minutes each time the pump is started. Sand pumping will cause the pump to excessive wear and reduce its operating efficiency. A submersible pump is not good because, during development, debris is pumped which could damage the pump impellers. In addition, the pump discharge is not easily controlled; and if the screen is blocked, the pump could dewater the borehole. In such a case, the hydraulic pressure behind the screen could be great enough to collapse the screen. Development using a turbine pump without a nonreturn valve is a better choice. Air-lift pumping is very suitable for well development because there are no moving parts to be damaged by the debris drawn into the well. The rate of pumping can be controlled by the volume of air passed down the air line. Pumping can be stopped and started at short intervals by shutting off air from the compressor; this will induce surging. A gate valve on the discharge pipeline can also be used for surging, by allowing pressure in the pipe system to build up or release. When the gate valve is suddenly opened, there is a violent release of pressure and water is pulled through the screen as pumping begins. When the valve is closed, water is forced back through the screen as pressure builds up again. Surge pumping method of development is not recommended for developing shallow wells constructed with short length of screen. This development method by pumping is recommended as a finishing procedure after other well development techniques.

Backwashing

In backwashing method, a column of water is alternately lifted above the pumping water level and then allowed to fall back into the well. In this process, the pump is started, and as soon as the water is lifted to the surface, the pump is shut off. The water in the column pipe falls back into the well causing flow of water through the screen into the formation that breaks the bridge and agitates the sediment and removes the finer particles when pumping is restarted. The cycle of alternate starting and shutting off the pump is continued until the water is sand free. Some wells respond satisfactorily to backwashing method; but in most cases, satisfactory results are not obtained. In this method, the surging effect is concentrated near the top of the screen.

Mechanical Surging

Surging is a process in which the washing action is achieved by forcing water backward and forward through the material to be cleaned, that is, screen, gravel pack, and aquifer matrix. The simplest method of surging is to use a bailer, which acts like a piston in the well casing and will pull loose material into the well, where it can be removed in the bailer. Such a bailer, because of its loose fit in the casing and its flap valve, cannot push water back through the screen with any force. Instead of bailer, solid, vented, and spring-loaded surge blocks may be used. A solid surge block will provide a much more forceful surge (Figure 14.2). The block is 2–5 cm smaller than the well screen and has several flexible washers, sized to fit tightly in the well casing, and is fastened either to a rigid drill stem on a rotary rig or in a heavy tool assembly on a percussion rig. The block is put below the water level inside the well casing, but not in the screen, and is then rhythmically moved up and down on a stroke length of about 1 m. Water is forced out through the screen on the down stroke and pulled back through the screen on the up stroke. The down stroke causes backwash to break up any bridging that may occur, whereas the upstroke pulls dislodged sand grains into the well that is periodically cleaned out by bailing. The development should start gently to ensure that water can move through the screen, before becoming more vigorous to extend the effects into the aquifer. The suction caused by vigorous development of a blocked screen could damage the screen by making it collapse or deform, therefore care needs to be taken, especially in wells installed with plastic screen.

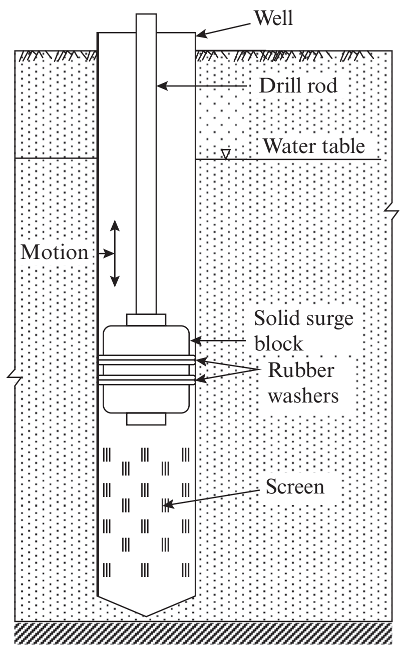

Figure 14.2 *Mechanical surging*

Surging is started above the screen to bring in the initial flow of sand, thus minimizing the sand locking. Surging is continued down to the bottom of the screen. After surging for several minutes at one setting, block is pulled out from the well. The sediments are pumped out of the well by air compressor or by bailer or sand pumps. The surging and cleaning is continued until no sand is pumped into the well. Total development time may range from about 4 hr for small wells to many days for large wells with long screens. Surge blocks are inexpensive tools that are convenient to use and do an effective job. The only drawback of using this method is that it does not permit pumping out sediments simultaneously while doing surging, thereby taking long time.

Air Development by Surging and Pumping

The most commonly adopted method of development of well is development with air. The method of development by compressed air comprises of pumping by air-lift method and surging. Water is alternately pumped from the well by air lift (pumping action) and then forced through the screen into the water bearing formation (surging action). This is accomplished by installing an air line inside an eductor (pumping) pipe. The development is started with lowering the eductor pipe nearly to the bottom of the screen and air line is lowered within the eductor pipe to the maximum possible depth the compressed air can handle. Air is turned on and the well is pumped until water is sand free, and then air supply is cut off to cause the air water mixed column in eductor pipe to fall back forcing flow of water through the screen into the formation that agitates the aquifer. The air is again turned on and pumping is continued until water is sand free. The process is repeated until no more sand is pulled into the well. The bottom of eductor pipe is then brought about 2 m above the bottom of the screen, and the development process is repeated. The process is continued until entire screen length is covered. At the end, the eductor pipe is lowered to the bottom of well and the sand, which has settled during development, is pumped out.

Air Surging and Lifting

The overpumping, backwashing and compressed air development technique usually develop only one-fourth of the top of aquifer screened. The surge block technique is an effective technique, but it also clears only about one-fourth of the top of aquifer. Well development is more difficult in the case of gravel-packed wells, long-screen wells, and wells tapping different aquifers. The concentration development techniques that focus on localized section of well screen are more effective way of well development.

Air surging and lifting tool consists of an eductor pipe, a discharge pipe fitted with a quick acting valve, screen isolator packers, etc. The packers isolate 1.4 to 1.5 m of screen length and facilitate full pressure of compressed air to individual screen section. The well development is carried out with the tool set at the bottom of the screen and compressed air allowed through air pipe installed inside the eductor pipe. The quick-acting valve is closed. The air pressure creates an outward flow from well to aquifer between the two packers producing efficient action. When the quick-acting valve is opened flow from aquifer to well occurs. When the discharge is comparatively clear, the quick-acting valve is closed and surging again takes place. Alternate surging and pumping is continued until the bottom zone is cleared. Similar sequence is repeated for the rest parts of the screen.

High-Velocity Water Jetting and Air Lifting

Air lift pumping with water jetting is an efficient well development technique in open rock holes and in wells containing screens with large percentage openings. Jetting washes the well face with high-pressure jets of water. Some pumping system having pumping rate greater than the jetting rate is incorporated so that there is a flow of water from the aquifer into the well. The drilling mud and fine sand are brought into the well, which are then pumped out. In this method, a high-velocity jet of fresh water is injected in the aquifer through well screen opening. The jetting tool has three or four nozzles at right angles to the drill string, so that the water jets are directed at the screen slots. The nozzle orifice should be as close to the well face as possible. The jet head is slowly rotated as it is raised and lowered past the section to be cleaned. The jetting should be done in short sections, and should start at the bottom of the screen (or open hole) and progress to the top. Fine-grained material from unconsolidated aquifers is carried into the well by the turbulent flow; in addition, the method is particularly effective in developing gravel-packed wells. The method works best with continuous slot screens having high open areas; it is less suited to louvre slot screens, because the shape of the louvre slots causes the water jets to deflect, thus dissipating some of their energy. The water used for jetting should be sand free to avoid abrasion of the screen. This method of well development is very effective in cleaning the screen or well face and removing filter cake, but it is less effective in restoring damaged aquifer matrix.

Use of Chemicals

Several chemicals can be used for well development, for example, polyphosphates (dispersants), dry ice, acids, etc. The development is done generally by contained air surging and lifting.

Dispersants: Adding polyphosphates to water in the well will aid the development process by other methods. The cohesiveness and plasticity of clay can be broken down by chemical dispersants (some form of polyphosphate or polyacrylamide). Chemical dispersants act as deflocculants and dispersants of clays and other fine-grained materials, thereby enabling the mud cake on the wall of a hole, and the clay fractions in an aquifer to be more readily removed by the development. The polyphosphate is mixed in appropriate proportion prior to introduction into the well. The polyphosphate is left in the hole for sufficient time to react, usually around 12 hr. This cause the individual flakes of the clay minerals to repel each other and so break up any clay flocs. The clay in the filter cake and in the mud filtrate becomes less cohesive, more dispersed, and is more easily removed by washing. After this reaction time, the well is pumped to try and remove all the spent phosphate, clay, and any other debris from the well. Phosphate is a nutrient for bacteria in groundwater, and any remaining in the well can promote bacterial growth and lead to biofouling problems. For this reason, if a polyphosphate dispersant is used, then a biocide such as chlorine or sodium hypochlorite solution should be added to the well after polyphosphate treatment. However, polyacrylamides do not contain phosphate, and hence do not promote biofouling, and their use is preferred. It should be borne in mind that the dispersed clay can slough over and block the well face, therefore mud dispersants are generally only recommended when there is a thick filter cake to be removed and where physical development methods have not been effective.

Dry Ice: Blocks of solid carbon dioxide (dry ice) are sometimes added to a well after acidizing and surging with compressed air to complete well development. The accumulation of gaseous carbon dioxide released by sublimation builds up a pressure within the well; upon release, this causes a burst of muddy water from the well.

Acid Treatment: In this method, acid solution is placed in contact with the water-bearing formation. The acid injected into the well penetrates along the fractures and widen openings and increase their permeability. Acid treatment can improve the performance of a well considerably in carbonate aquifers. Acid treatment involving the use of hydrochloric or sulfuric acid operates by dissolving the calcium carbonate from wall or from drilling debris forced into fissures. The acid treatment should contain an inhibitor to prevent the acid causing undue corrosion of steel casings. The use of strong acid can be a hazardous procedure and should only be undertaken by professional, competent personnel. The dose of acid is injected through a temporary line extending to a position near the bottom of the well and then the wellhead is sealed with a cap equipped with a safety valve. The solution is allowed to stand under pressure in the well for about 1 day. The dissolution of the limestone by the acid generates carbon dioxide, which builds up a pressure against the wellhead and forces the acid into the aquifer formation. The amount used will depend on the volume of water in the well and the amount of carbonate material to be removed. Hydrofluoric acid can be similarly used for rocks-containing silicates. Acidization of carbonates produces carbon dioxide, and measures should be taken to avoid this heavy gas filling any enclosed spaces, where it could asphyxiate people. A further problem with acidization is the disposal of the spent acid. The spent acid withdrawn from the well may have to be sent to a hazardous waste treatment facility. Normally, this procedure would be followed by one of the normal development methods.

Development of Wells in Bouldery Formations

The wells drilled in bouldery formations using percussion drilling method are usually developed in similar way as the wells drilled in alluvial formations by using rotary drilling method. Generally, bailing as initial development method and use of a partial surge block as the final development method are adopted for wells in bouldry formations.

Bailing as a Development Method: Bailer method is used to bring thick mud up from the bottom of the well to the top for its removal in the process of well development. When thick mud is removed, the mud water will become less thick and the mud wall, which had been intact during well drilling, will dissolve in places; and water will start flowing in from the aquifer. Continuous bailing from the well bottom for 1 to 2 days is carried out until entire screen portion is cleared. If the bailer is run up at considerable speed, it produces a negative pressure zone below the bailer. This causes water from aquifer to flow into well, bringing sand and finer materials that are then bailed out. The process is to be continued until the water sand and mud free.

Partial Surge Block Method: A partial surging block is a barrel-shaped steel block attached to the bailer. The aim of this method is to enhance effectiveness of screen development, by partially inducing strong flow of water into a selected portion of the screen, drawing fine sand particles from the aquifer into the well. The action is operated over the entire length of the screen. Through this action, the sand particles outside the screen are completely removed. A highly permeable gravel pack is created. Once the development at the bottom of the screen has been completed, the surging block is raised and operation repeated for the second screen from the bottom. This process is completed over entire section of screen and the accumulated sand from the bottom of the hole is removed with the bailer.

Development of Hard Rock Wells

Wells drilled in hard rocks may have poor yield, mainly due to the following effects:

- A borewell drilled in massive rock devoid of fractures
- Fractures filled with weathered material, thereby clogging the interconnections between the borewell and water-bearing fractures
- Closing of the horizontal fractures because of weight of overlying rocks

Well-drilling methods cause clogging of fractures in hard rock aquifers. The DTH drilling method can blow large quantities of fine drill cuttings into the fractures effecting fractures plugging. Any materials that clog the fractures must be removed by a development procedure. Air development method is generally used in DTH drilling wells. But air development is not effective in low-yielding borewells in hard rocks. The best technique to develop hard rock well is through chemical/acid treatment, explosive or hydro-fracturing followed by air surging and lifting.

Use of Acids: Acids can be used for both well and aquifer development in limestone or dolomite aquifers and in some semiconsolidated aquifers. Acid dissolves minerals and opens up the fractures and crevices in the formation around bore hole. Some of the acid is forced into cracks and fissures much away from the well bore. The acid dissolves some material naturally existing in the voids, thereby increasing the overall hydraulic conductivity of the aquifer. The acid also placed in the borehole by jetting. Utmost care should be taken in handling the acid.

Use of Explosives: Explosives blasting in rock wells can be adopted to develop and improve well specific capacity. Detonation of explosives in rock wells often increases yields by enlarging the hole, increasing rock fractures, and removing fine-grained deposits on the face of the well bore. Good results can be obtained if blasting procedures are appropriate for the rock type and the size and depth of the well. Small explosive charges of 15–45 kg are commonly used. Larger charges of 450 to 900 kg can be administered in igneous rock aquifers. However, use of explosives is very dangerous and should be used under expert supervision.

Hydrofracturing: Hydrofracturing is a development technique for opening up fractures in crystalline aquifers to increase well yield. It is a low-cost technique applied in stimulating poorly yielding hard rock wells. It involves injection of clean water at high pressure into borewell isolated by packers. Pressures range from around 5,000 kPa to more than 20,000 kPa, the pressure is used depending on the geology and on local experience. Once the pressure exceeds the in situ tectonic and local stresses in the rock, small existing fractures open up to increase their aperture. If no such fractures exist, new fractures will be initiated once the applied pressure exceeds the in situ stress and the tensile strength of the rock. The pressure is maintained after fracturing is initiated, in order to propagate the fracture some distance into the rock. Sometimes, sand/fine gravel grains or small beads are added to the injected water with the objective of propping open the fracture once the pressure is released. The injected water pressure widens, fractures and fines are removed by surging and lifting action. The widening up and clearing of existing fractures provide hydraulic connection between the well and the adjacent water-bearing fractures, thereby improving the yield. The packers are systematically moved within the well to hydrofracture-successive zones. The technique is very effective in poor-yielding well, less effective in moderate yielding and least effective in high-yielding aquifers. It is not effective in massive rock devoid of fractures as the technique does not create new fractures. It simply clears the new fractures and widens them. Hydrofracturing operation in pressure-sensitive rocks may lead to bore hole collapse. In low permeability carbonate aquifers, hydrofracturing may be carried out in combination with acidization in order to stimulate well yield.

Combined use of explosives and hydrofracturing is sometimes preferred to create new fractures or to increase the aperture of existing fractures in hard, fractured rock aquifers to enhance the yield. Combined use is applicable only in unlined, open boreholes. This method has the potential to create undesirable open fractures between the borehole and the surface (rendering the borehole vulnerable to surface contamination). In general, they should not be placed shallower than 30 m from the surface.

14.4 Well Maintenance and Rehabilitation

Timely maintenance overcomes many well problems, resulting in improved well performance and increased well life. Several things may cause to decrease the well yield, namely wear and tear of pump, drop in water table, interference due to nearby wells, clogging of screen, gravel pack and formation, etc. Water wells generally get inadequate maintenance due to out of sight—out-of-mind reason. The well screen being business end needs regular attention to keep it functioning properly. Good records of pumping rates, drawdown, power used, water quality, etc., should be maintained for deciding the type of maintenance procedures to be adopted for the best results.

14.4.1 Disinfecting the Well

Drilling operations may introduce bacteria into a well. After development and well testing, a disinfectant should be added to sterilize the well and to inhibit future biofouling problems. The most common disinfectants used are chlorine-based compounds such as chlorine gas and sodium hypochlorite. Chlorine compounds are strong oxidants, and care must be taken in their handling to avoid contact with skin, eyes, etc. Sodium hypochlorite is supplied in a solution containing between 5 and 12 percent available chlorine. It is added to the well, and then the water in the well is agitated using a surge block or other method so that the chlorine is distributed throughout the length of the well. The amount added should be such that the concentration of chlorine in the well after mixing will be at least 100 mg/l. In high pH groundwater, a stronger chlorine solution may be needed, since the effectiveness of chlorine treatment depends on the amount of hypochlorous acid produced in the well and this is retarded at high pH. The chlorine solution should be left in the well for at least 24 h and then removed by pumping. The chlorine-rich discharge water should not be discharged directly to streams or other surface waters. The well should be disinfected again after the production pump is installed and the headworks are complete. While chlorine and other disinfectant compounds are effective against bacteria, they are less effective in eliminating other microorganisms such as viruses and cryptosporidium. To minimize the risk of pollution from surface, it is better to choose the well site carefully, and to construct the well and the wellhead properly.

14.4.2 Well Protection

Proper sanitary precautions must be taken to protect the water quality of a well. Pollution sources may exist either above or below ground surface. Surface pollution can enter into a well either through the annular space outside of the casing or through the top of the well itself. To close avenues of access for undesirable water outside of the casing, the annular space should be filled with cement grout. Entry through the top of the well can be avoided by providing a watertight cover to seal the top of the casing. Seals may be made of metal or lead packing; asphaltic and mastic compounds are also satisfactory. Covers around the well should be made of concrete, should be elevated above the adjacent land level, and should slope away from the well. Whenever a new well is completed or an old well repaired, contamination from equipment, well materials, or surface water may be introduced into the well. Addition and agitation of a chlorine compound will disinfect the well. Following disinfection, the well should be pumped to waste until all traces of chlorine are removed. As a final check on the potability of the water, a sample should be collected and sent to a laboratory for bacteriological examination.

14.4.3 Well Monitoring

A well may underperform due to the following:

(i) Aquifer-related factors
(ii) Well-related factors
(iii) Pump-related factors

Proper design and construction of water wells minimizes problems with their future performance and reliability. If a well is not designed and constructed properly, the following problems commonly arise (Misstear et al, 2006):

- Poor gravel pack design and/or emplacement lead to sand pumping, and clogging or abrasion of the screen, pump, and headworks.
- Use of inappropriate materials in well design can deteriorate rapidly in corrosive groundwater, result in entry of poor-quality water to the well, or even result in well failure.

- Long screen sections may encourage mixing of different water types, leading to clogging.
- Bad drilling fluid control during drilling will result in clogging of the aquifer.
- Insufficient well development will lead to incomplete repair of the drilling damage.
- Poor installation of the casing string, with individual pipes not connected together correctly, may lead to enhanced corrosion and pitting of the pipe joints, sand pumping, entry of poor-quality water, and possibly structural failure of the well.
- Poor grouting of the upper casing string will allow the ingress of polluted water into the well from the ground surface.
- Inappropriate choice of pump and rising main materials for use in aggressive groundwater.
- Incorrect setting of pump; for example, a pump set in the well screen will increase the risk of fouling of both the screen and the pump.

An understanding of the limitations of the original design and construction can help in diagnosing the causes of the performance problems in a well system. The frequency of monitoring will depend to some extent on the use of the well and the monitoring facilities/capabilities available locally. Water level, discharge, and water-quality parameters are regularly monitored. Other important aids in monitoring and diagnosis include direct observation of the condition of the well and pumping plant, downhole CCTV and geophysical logging surveys, regular well pumping tests, pump efficiency measurements, and the availability of an observation borehole at some distance from the well.

14.4.4 Well Operation and Performance

Wells are best operated smoothly at relatively constant discharge rates, rather than pumped intermittently at higher discharges. Drawbacks associated with pumping a well intermittently include (Misstear et al, 2006) the following:

- It creates an opportunity for particles in the aquifer or gravel pack to mobilize each time the pump starts up, as frequent stopping and starting of the pump leads to surging of the well.
- The higher flow velocity associated with intermittent pumping may lead to greater particle migration than by pumping at a lower discharge for a longer period.
- Intermittent pumping gives a higher drawdown than continuous pumping for the same daily discharge, and thus creates a longer splash zone on the casing, where corrosion may be enhanced.
- Higher pumping rates increase the chance that water levels will fall close to the top of the screen, increasing the supply of oxygen, and hence the risk of clogging from biofouling or chemical incrustation.
- It requires a larger capacity pump and potentially a larger well than that needed for a continuously operating well; and hence, it involves greater capital costs.

- The operating costs of pumping a well intermittently will also tend to be greater, since the well loss component of drawdown increases in relation to the square of the discharge rate.
- Over pumping and falling groundwater levels in an unconfined aquifer may result in a significant decrease in aquifer transmissivity and hence in well yield.
- Lower pumping water levels may also lead to enhanced corrosion and biofouling as well as to increased pumping costs.

The factors affecting well performance can be categorized as follows:

(a) Physical
(b) Chemical
(c) Microbiological

Physical Factors

The main physical processes are clogging and abrasion. Clogging can result from drilling fluid and as a result of mixing of formation particles with the gravel pack material. Migration of aquifer and/or gravel pack material may lead to clogging of the screen slots. Sand pumping well may also result in clogging of the pump impellers and accumulation of sediment in the distribution and treatment system. In addition to clogging, the migration of particles into a well can lead to abrasion of the well, pump, and distribution system. The problems are usually greatest in the zones of highest flow velocity—the screen slots and the pump impellers.

Chemical Factors

The two main chemical processes that affect well system performance are incrustation and corrosion. They often occur together, and are also typically associated with microbiological activity. *Incrustation* may be of chemical or microbiological (biofouling) origin. The cause of incrustation is the change in physical and chemical conditions in the groundwater between the body of the aquifer and the well. In pumping wells, incrustation is mainly due to mixing of different water types at the well and degassing of carbon dioxide due to temperature and pressure changes at the pumping well. Incrustation can also occur from precipitation of calcium carbonate minerals. The incrustation and cementation by both iron and carbonate minerals may entrap and incorporate fine materials moving out of the aquifer under the influence of pumping. This can make a bad situation worse. The net result of incrustation, whether purely chemical or involving biofouling, is usually to impede groundwater flow in the aquifer in the vicinity of the well, in the gravel pack, or across the well screen. Incrustation increases the head losses, decreases the efficiency of well, puts greater stress on the structure of the well screen and increases the potential for sand pumping and abrasion. A water well can also deteriorate due to corrosion. The simplest form of *corrosion* is that of iron or steel exposed to oxygen and water. The main factors affecting corrosion are the nature of the metal corroded, the formation of corrosive microenvironments on the metal surface, the physical and chemical condition of the water, and microbiological activity. Other physicochemical factors that can strongly influence corrosion potential include salinity, temperature, dissolved gas content, and the presence of organic acids.

The corrosion can be severe in metal casings and screens where contrasting metals are present, or where there are physical imperfections in the materials.

Microbiological Factors

Microbes are involved in many of the processes that lead to clogging and corrosion of well systems. The most common problems in well systems result from iron-related biofouling, where the deposition of iron and other metals is mediated by bacteria. Many of the bacteria species are filamentous and occur in colonies, which develop biofilms. Where the biofilm accumulates sufficiently to cause problems of incrustation or corrosion in well systems, the process is usually known as biofouling. The rate of biofilm development depends on bacterial activity, nutrient availability, production of the biofilm coating materials, oxidation, degassing of CO_2, and biofilm shear forces relating to flow rate and turbulence. Corrosion in anaerobic conditions may be accelerated through the actions of sulfate-reducing bacteria.

14.4.5 Well Maintenance

Maintenance is an essential part of the well operation with the aim of keeping the well system at, or close to, its original level of performance. *Preventative maintenance* involves cleaning and other actions that are undertaken on the well system on a regular basis. In the maintenance of wells, a variety of activities are carried out to retain the efficiency of wells. It is advisable to maintain record of well drilling and constructional details. In addition, the technical and economic performance of wells can be maintained as well history sheet. The record eventually helps in rectification of errors and avoidance of mistakes in future. Wells should be pumped according to the designed discharge to avoid problems as described earlier. Sand pumping causes development of cavity around well screens, which would rupture and damage the well screen, therefore such cavities should be refilled with gravel in time. Pumps installed in wells should be well maintained. As soon as 10 to 15 percent decline in well yield of is observed, the pump assembly should be pulled out and inspected for any wear and tear. The well should be examined through sounding up to its bottom for any filling that might have taken place over time. Infilling of well screen sections choke the well and cause reduction in well yield.

The proper maintenance depends on having correct procedures in place for monitoring and diagnosis. One cause of decreased performance of a well is due to depletion of the groundwater in the storage of aquifer. This trouble can be overcome by decreasing pumping drafts, resetting the pump, or deepening the well. A second cause of well trouble results from faulty well design and construction, such as poor casing connections, improper screens, incomplete placement of gravel packs, and poorly seated wells. In many cases, it may be possible to repair the well, but sudden failures involving entrance of sand or collapse of a casing often require replacement of the entire well. The third cause of well failure is corrosion or incrustation of well screens. Corrosion may result from direct chemical action of the groundwater or from electrolytic action caused by the presence of two different metals in the well. The effects of corrosion can be minimized by selecting nonmetallic well screens or corrosion-resistant metal (such as nickel, copper, or stainless steel), and by providing cathodic protection. Incrustation is caused by precipitation on well screens of materials carried in solution by groundwater. The chemical (acid) treatment of well becomes necessary when specific capacity of well diminishes due to incrustation. Screens can be cleaned by adding hydrochloric acid (HCl) or sulfamic acid (H_2NSO_3H) to the well, followed by agitation and surging.

The maintenance activities should include the full well system—the aquifer, pumping plant, and headworks in addition to the well itself. If low-grade steel materials are used in a well system where the groundwater is corrosive, then corrosion and clogging problems will arise in the well, pump, and headworks, and it will not be possible to keep well performing at its original level, even if regular monitoring and maintenance are carried out. A screen with a large open area assists easy well maintenance. Where the main source of clogging is biological, biocides (chlorine, usually in the form of sodium, or calcium hypochlorite) can be used for well maintenance. In well maintenance, dispersing agents (some form of polyphosphate or polyacrylamide) may be used to assist in the removal of fines. However, phosphate is a nutrient for bacteria in groundwater and any remaining in the well after treatment could stimulate further biofouling problems. Acids and other chemicals used for well maintenance can be harmful to people and the environment if they are not used properly. Local health and safety guidelines should be followed when handling these chemicals.

If a well is not regularly maintained, then its performance may deteriorate appreciably as the screen and aquifer are totally blocked and any chemical incrustation or other fouling deposits are grown beyond limit. Such a deteriorated well may even be difficult for well restoration because it may not be possible to get water into the clogged gravel pack and/or aquifer to remove the clogging material. In addition, if an incrustation has aged and recrystallized it will be much harder than in its early state and will be much more difficult to break up and remove. The frequency with which preventative maintenance should be carried out depends on a number of factors and local experience. Taking a well out of supply can be costly and difficult, and maintenance operations themselves can be expensive, therefore it is necessary to strike some sort of balance between prevention and cure when developing a sensible preventative maintenance strategy. On hydraulic grounds, it is considered advisable to carry out cleaning operations in a well when the specific capacity has reduced to 80–85 percent of the original value, but other factors may influence the frequency of maintenance operations—for example, the local availability of the necessary expertise and equipment.

14.4.6 Well Rehabilitation

A well may yield decreasing quantities of water with time due to various reasons as described earlier. The regular maintenance is better in preserving the original well performance than occasional rehabilitation. *Well rehabilitation* is the process of trying to restore a well system to its original condition and performance after it has deteriorated significantly. It refers to the treatment of a well by mechanical, chemical, or other means to recover as much as possible of the lost yield. Commonly occurring problems of well sickness relate to sand pumping, clogging of intake well sections, screen plugging due to slime formation, and growth of organisms. The rehabilitation should be based on the diagnosis of the problem causing the reduction in condition or performance. In the well, the location of the clogging problem will have a strong bearing on the techniques used and their likely effectiveness. In a screened well, clogging of the screen slots is more accessible, and therefore easier to deal with, than clogging of the gravel pack and especially the aquifer beyond the pack. The upper part of the screen often experiences the most incrustation and biofouling and needs to be targeted in cleaning operations. The following are the well sickness problems and their remedial measures:

Sand pumping: The problem of sand pumping is often attributed to improper selection of screen opening size and gravel size as well as to suboptimal development of well. The problem is surmounted through lowering of appropriate size screen in existing screen where annular clearance of 50 mm is kept between existing and new screen slot for purpose of stabilizing of gravel.

Problem of decline in well yield: The reduction in well yield may be due to changes in aquifer characteristics, and interference of pumping wells in the neighborhood of well under rehabilitation. In the event of such situations, nothing can be done to rectify the situation.

Problem of chemical encrustation: Acids can dissolve and remove carbonates and hydroxides. If the incrustation is heavy, the treatment will be improved by use of wall scratchers and very high-pressure jetting to break up the carbonate and allow the acid better access. With hardened incrustation of ferric hydroxide, restoration has to depend on breaking up the cemented deposits by physical or hydraulic methods. Care has to be taken when using vigorous methods, not to damage the well and make the situation worse. Volume of acid twice the volume of water is added to well against screen section and then agitated through surge block. The solution is then pumped out. Hydrochloric and muriatic acids are used in treating chemical encrustations. Polyphosphates and hexa-meta-phosphates are also used in removing chemical encrustations. The process is one of mixing 2–4 kg of phosphates, 100–200 g of hypochlorite in 100 L of water standing in well and then surged for about 2 hr and allowed to rest for 24 hr before being pumped out.

Mechanical encrustation: This problem is common in wells tapping fine sand aquifer where twin problem of chemical and mechanical encrustations coexist. The phosphate treatment described above is best remedy of such situations.

Bacterial growth: Iron bacteria are a common feature in iron rich ground water. This can be treated through chlorination shocks. Doses of 100 to 200 mg are administered in giving chlorine shock treatment. The whole treatment process includes first a chlorine shock followed by acid treatment and then again followed by a repeat chlorine shock.

Structural collapse: The common structural problems include ruptures and collapse of well screens, and holes in well assembly. These features before correction are precisely identified and located through borehole CCTV camera device. Such features are corrected through application of smaller size liners inside blank portions in combination with packers.

Slime formation: Where slime-forming organisms block screens, particularly in recharge wells, treatment with chlorine gas or hypochlorite solutions can cure the problem. For improving yield of rock wells, acidizing or shooting with explosives is generally effective.

14.4.7 Maintenance of Dug Wells

A hand dug well is far more vulnerable to pollution than a drilled well as it is shallow and open to infiltration of polluted surface water, its lining and headworks are commonly badly finished so that spilled water or animal wastes can flow back into the well, its top is often left open allowing rubbish to fall in, and it may be badly situated with respect to pollution sources such as latrines and septic tanks. A hand-dug well can be protected from these hazards by using the following design criteria to limit pollution of groundwater.

- The well should be located up the hydraulic gradient from any latrines or point source of pollution. The minimum distance between the well and the pollution sources should be 30 m.
- The upper lining of the well must be impermeable, cemented in place, and should extend to the water table.
- The surface works of the well must shed spilled water away from the well, for example, by a surrounding concrete apron sloping away from the well.
- The surface works should be such that the water is used several metres away from the well, and not at the wellhead. Most importantly, animal troughs should be located away from the well.
- The surface works must prevent effluents from entering the well. A concrete apron should be constructed around the well, and securely keyed to the well lining.
- The surface works must prevent rubbish from entering the well. Ideally, the well should have a cover with a removable lid.
- The method used to lift water should discourage surface spillage and contact between contaminated private containers and the well water. A hand pump installed through a watertight well cover offers the least risk of spillage in comparison to bucket and windlass arrangement.
- The well should be disinfected on completion and then periodically thereafter.

14.4.8 Abandonment of Wells

A well may fail ultimately due to several reasons. If repair, restoration, and rehabilitation are not feasible or cost effective for the well, then it should be decommissioned or abandoned. Whenever a well is abandoned, it should be done properly by filling it with clay, concrete, or earth. If a well is not decommissioned properly, it can lead to a number of problems as follows:

(i) It may pose a physical danger to people and animals, especially an open well or a large diameter drilled well.

(ii) It may allow polluted surface water to enter the aquifer system.
(iii) It may allow poor-quality groundwater from one aquifer to contaminate another aquifer.
(iv) It may result in depletion of head and of the groundwater volume in an aquifer by leakage this aquifer into another aquifer. If the well is artesian, continued uncontrolled discharge may represent a serious wastage of aquifer resources.

To avoid such problems, the well should be decommissioned in an engineered manner so as to prevent the vertical movement of water from the surface to an aquifer or from one aquifer to another. The wellhead must be sealed so that it does not pose a risk to people or animals. The initial step in a well decommissioning is to find out as much as possible about the construction of the well: how deep it is, how it was lined, whether the casing was grouted, whether there is an artificial gravel pack around the screen, etc. The next step is to inspect the well. Visual inspection from the well top may give some clues as to the condition of well, and lowering a plumb bob or similar device can indicate if there are obstructions present that will need to be removed. However, a CCTV and logging survey will be necessary to identify the nature of any obstruction and to establish the condition of the casing and screen. It is essential that the presence of a poorly grouted casing does not compromise the effectiveness of the proposed well sealing operation. If there is a risk that the annulus between the casing string and the borehole wall will allow water to move vertically, then the casing string should be removed (if possible).

The approaches adopted for decommissioning a well will depend on the type and condition of the well and on the hydrogeology. A small diameter, shallow production well or exploration borehole is often backfilled with cement grout throughout its entire length, care being taken that the grout is emplaced from the bottom of the hole upward so as to avoid bridging. A larger diameter and deeper drilled well can be decommissioned by backfilling the aquifer sections of the hole with sand and gravel and by placing low permeability cement seals between the individual aquifer horizons. It is essential that the coarse material used for the backfill is clean and nonreactive. If the well being decommissioned is in a sensitive area or near an operating production well, disinfect the backfill material using a solution of hypochlorite before placing the backfill down the well being decommissioned. The backfill should be poured or pumped into the well using a tremie tube. In some situations, the amount of backfill material required could be very large, for example, for infilling a large diameter and deep well, or a deep well constructed in a highly fissured aquifer where significant quantities of sand and gravel backfill could be lost into the formation. In these situations, a very coarse aggregate can be used as backfill instead of sand and gravel, or the lowermost aquifer section can be left as open hole, with a bridging seal placed above this. Specialized cement-based devices are available for bridging seals.

SOLVED EXAMPLES

Example 14.1: Design a well for a discharge of 2,000 m^3/d, where a drawdown of 20 m is acceptable in a 150 m thick confined aquifer having the mean hydraulic conductivity 10 m/d. Uniformity coefficient of the aquifer material is 4.

Solution: Using Table 14.1 for 2,000 m^3/d, nominal pump chamber casing diameter = 30 cm; surface casing diameter for naturally developed well = 40 cm; gravel packed well = 60 cm and nominal screen diameter = 20 cm.

Required length of well screen using Eqn. (14.3) $L_s = \dfrac{2Q}{Ks_w} = \dfrac{2 \times 2000}{10 \times 20} = 20 \text{ m}$

Screen entrance velocity using $C_g = 0.5$ and $A_{eo} = 15\%$, in Eqn. (14.7):

$$v_e = \frac{Q}{C_g \pi D L_s A_{eo}} = \frac{2000}{0.5\pi 0.2 \times 20 \times 0.15} = 2122.1 \text{ m/d} = 1.47 \text{ m/min} = 0.0246 \text{ m/s},$$

which is within permissible (between 0.01 and 0.06 m/s) values.

Velocity in the well $v = \dfrac{4Q}{\pi D^2} = \dfrac{4 \times 2000}{\pi \times 0.2 \times 0.2} = 0.74 \text{ m/s}$, which is within permissible (less than 1.5 m/s) value.

Use Table 14.2 for design of the gravel pack. As uniformity coefficient of aquifer material is 4, select a gravel pack material having uniformity coefficient = 2 (between 1 and 2.5), and D_{50} of gravel pack ≤ 6 D_{50} of aquifer. Slot size of screen is ≤ D_{10} of gravel pack material.

PROBLEMS

14.1 What are basic design and construction principles for a well?

14.2 What information is required for the design of water well?

14.3 Describe the design steps for an open well.

14.4 How are diameters of different well components selected?

14.5 How is proper material for a well selected?

14.6 How are well screen and gravel pack selected? Mention the criteria and steps.

14.7 What problems may be faced if a well is not designed and constructed properly?

14.8 What is a well development? Why is it required? What are factors that affect the well development?

14.9 On what factors the life span of a well would depend. On what factors the optimum depth of well depends?

14.10 What purposes does a well gravel pack serve? Differentiate between natural gravel pack and artificial gravel pack. In what geological formations they are provided?

14.11 What are various well development methods that improve well yield?

14.12 What causes reduction in well yield? Which methods can restore well yield?

14.13 What are bad effects of pumping wells in excess of their designed capacity?

14.14 What are common well problems?

14.15 How is incrustation in wells treated?

14.16 Describe the conditions where different well development methods can and cannot be used.

14.17 What is hydrofracturing? Explain.

14.18 What are various well rehabilitation schemes?

14.19 What would happen if a well is not decommissioned properly? What is the sequence of steps in decommissioning of a well?

14.20 Find the length of the screen and other design parameters for a well to yield a discharge 2,000 lpm under a maximum drawdown of 15 m in a 150 m thick confined aquifer having the mean hydraulic conductivity 10 m/d.

Chapter 15 Managed Groundwater Recharge

15.1 Introduction

Water is a vital resource for all the living beings. In the past, availability of abundant fresh water had resulted in development of great civilizations. Before the industrial era, human activities were generally planned in tune with nature, that is, keeping in view the regeneration power of mother earth. Therefore, scarcity of renewable sources such as water was never felt. However, on account of the modern agricultural practices, unplanned industrial activities, growth in population, and urban lifestyle, the water resources have been indiscriminately exploited. Overexploitation of groundwater resource is a major concern all over the world. The problem is more serious in third-world countries such as India due to various reasons including population growth. The situation is aggravated further due to global warming. In arid regions where there are very few surface water sources, groundwater is the only source of water leading to groundwater mining. It has resulted in sharp fall of groundwater levels and the quality of water has severely deteriorated. The shortage of water is often associated with conflicts between different user groups leading to violent situations. Many times this water requirement for drinking and irrigation needs have led to violent protests as in the case of Raila, Bisalpur, and Gadsana in Rajasthan and Cauvery water dispute in Bangalore and other cities of Karnataka and Tamil Nadu. Erratic rainfall pattern and frequent monsoon failures add to this grim situation.

During the monsoon most of the rainfall is drained away even causing floods and there is hardly anyone to take this water. Flooding again causes significant loss of both property and life. Some places of the Northern plains such as Bihar are such examples. Surprisingly, this also occasionally happens in arid districts of Western Rajasthan such as Barmer in 2006 and Jodhpur in 2007. In arid parts of India, the construction of wells on the banks of ponds and other water bodies is a very old tradition. The water body collected rain water and helped in recharging the groundwater, which was extracted from the nearby wells during lean season. These water bodies were regularly de-silted, excavated, and maintained as a part of local culture and tradition and thus higher recharge rates were maintained. However, with growing population, changing community lifestyles, and piped water supply, these systems are being neglected and therefore are unable to cope up with the ever increasing demand in the present system of unplanned development and exploitation of nature and natural resources.

Although in the overall context, the situation regarding water availability is not all that grim, it becomes alarming due to unplanned industrial activities and fragmented vision of development. There is sufficient rainfall to satisfy the overall water requirements, but the temporal and spatial variation of rainfall causes drought and flood situation. This problem could be effectively tackled by storing the water during the period of abundance and using it during the time of scarcity. The conventional way of storing water has been with dams. However, good dam sites are becoming scarce. In addition, dams have various disadvantages, such as evaporation losses (about 2 m/year in warm, dry climates), sediment accumulation, potential of structural failure, increased malaria, schistosomiasis, and other human diseases; and adverse ecological, environmental, and sociocultural effects. New dams are often more and more difficult to build because of high cost and long-term environmental implications leading to public opposition. Consideration is being given to destroying some dams in the world. In the prevailing scenario of water-intensive activities (household, agriculture, and industrial etc.), artificial groundwater recharging offers an attractive technological solution. Artificial recharge is expected to become increasingly necessary in the future as growing population requires more water, which demands storage of more water during surplus availability of water. *Recharge* is defined as the downward flow of water reaching the water table, thus adding to the groundwater reservoir. The principal mechanism is downward percolation of soil water in excess of soil moisture deficit and evapotranspiration (infiltration excess). This may happen naturally or may be done artificially by human intervention. When the process of recharging occurs naturally, it is called natural recharge. *Natural recharge* is typically about 30–50 percent of precipitation in temperate humid climates, 10–20 percent of precipitation in Mediterranean type climates, and about 0–2 percent of precipitation in dry climates.

Artificial or *managed groundwater recharge* (MGR) systems are engineered systems where surface water is applied on or in the ground for infiltration and subsequent movement to aquifers to augment the groundwater resources. When the rate of extraction of groundwater is more than natural recharge, then artificial recharging of groundwater is required. Therefore, in most situations, artificial recharge projects not only serve as water-conservation mechanisms but also assist in overcoming problems associated with overdrafts. Artificial recharging is practiced to increase the availability as well as to improve the quality of water through soil-aquifer treatment (SAT) or geo-purification and to use aquifers as water conveyance systems. It also makes groundwater out of surface water where groundwater is traditionally preferred over surface water for drinking. To place water underground for further use requires that adequate amounts of water are available/collected for this purpose. In some localities, storm runoff is collected in ditches and basins for recharge. Elsewhere recharge water is imported into a region by pipelines or canals from a distant surface water source. A third possibility involves utilization of treated wastewater, which has yet to gain ground in India. The use of artificial recharge to enhance the availability and quality of groundwater has had increasing attention in recent years. In many countries in the world, artificial recharge schemes are being considered and in some areas artificial recharge has been common practice for many years. Recharging practices began in the nineteenth century in Europe, Sweden, Germany, and the Netherlands. California in the United States has a large number of artificial recharge projects. Traditional water harvesting in India dates back to Indus Valley Civilization and Mughal Period.

15.2 Objective and Purpose of MGR

MGR is adopted for conserving water as well as for overcoming problems associated with overdrafts. Its broad objectives are to maintain or augment the natural groundwater as an economic resource; provide subsurface storage for local or imported surface waters; coordinate operation of surface and groundwater reservoirs; reduce or stop significant land use subsidence; combat adverse conditions such as progressive lowering of groundwater levels, unfavorable salt balance, and saline water intrusion; provide treatment and storage for reclaimed wastewater for subsequent reuse; provide a localized subsurface distribution system for established wells; and conserve or extract energy in the form of hot or cold water. Therefore, managed recharge may be adopted to serve one or more of the abovementioned purposes. Also, the importance of MGR will increase in future due to inflated water requirement, hence more storage of water is needed in times of water surplus to be used in times of water shortage. The essential benefits of MGR can be classified under two categories: (i) relief of overdraft and (ii) use of groundwater basin as cyclic storage and distribution systems. By counteracting overdraft of groundwater basin, MGR may provide the following specific benefits:

1. Lower operating cost due to reduced pumping lifts for groundwater supplies.
2. Eliminate capital expenditure for deepening of wells or lowering of pump bowls.
3. Reduce incidence of premature abandonment of wells.
4. Prevent seawater intrusion in coastal aquifer.
5. Increase farm income as a result of augmented and dependable water supplies.
6. Increase municipal expansion resulting from augmented subsurface water supplies.
7. Prevent dewatering of all or part of the underground reservoir.

15.3 Methods of MGR

Artificial recharge is defined as the augmentation of the natural movement of surface water into aquifers by some method of construction, by spreading of water, or by artificially changing natural conditions. The total recharge is mainly influenced by contact area of recharge and contact time for recharge along with the infiltration rate and hence it can be enhanced by increasing contact area, contact time, or infiltration rate of surface water. A variety of methods have been developed to recharge groundwater artificially. Selection of methods depends on geomorphological condition, physiographic conditions, and availability of source water. Thus, the choice of a particular method is governed by local topographic, geologic, and soil conditions; the quality of water to be recharged; and the ultimate water use. In special circumstances, land value, water quality, or even climate may an important factor. An aquifer will be suitable for MGR if the following criteria are met:

1. Surface material should be highly permeable so as to allow water to percolate easily.
2. The unsaturated zone should possess a high vertical permeability and vertical flow of water should not be restrained by less permeable clayey layers.
3. Depth of water table should not be less than 7–10 m below ground level (bgl).
4. Aquifer transmissivity should be high enough to allow water to move rapidly from the mound created under the recharge basin. An adequate transmissivity for recharge is also a good indicator of the aquifer capacity to produce high well discharge and therefore easily to return the water stored.

All the available methods can be grouped under the following four major categories:

(a) direct surface techniques,
(b) direct subsurface techniques,
(c) combination surface—subsurface techniques,
(d) indirect techniques.

The different methods under these recharge techniques are listed below:

(a) Direct surface techniques

- flooding
- basins or percolation tanks
- stream augmentation
- ditch and furrow system
- over irrigation

(b) Direct subsurface techniques

- injection wells or recharge wells
- recharge pits and shafts
- dug well recharge
- bore hole flooding
- natural openings, cavity fillings

(c) Combination surface—subsurface techniques

- basin or percolation tanks with pit shaft or wells

(d) Indirect techniques

- induced recharge from surface water source
- aquifer modification

In the above listed techniques, one of the following three water application methods is adopted: (i) water infiltration into vadose zone from surface, (ii) water addition into vadose zone through shafts, pits, bore holes, etc., and (iii) water entry directly into aquifer through wells. Figure 15.1 shows these three water addition methods of artificial groundwater recharge.

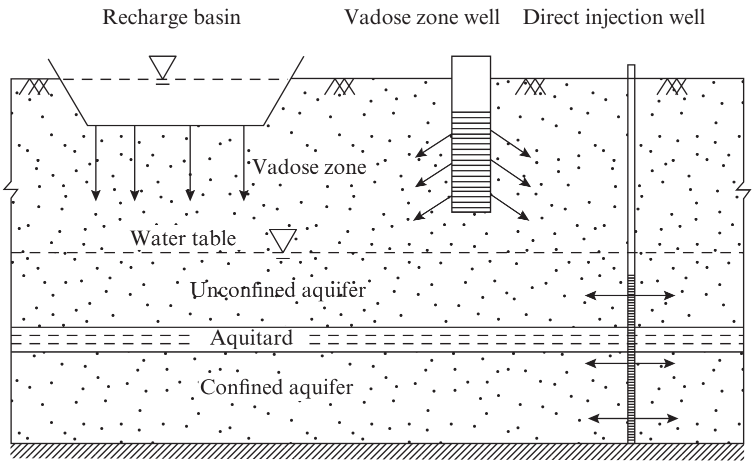

Figure 15.1 *Recharge water addition methods*

Artificial groundwater recharging is accomplished primarily through works designed to maintain infiltration rates, increase the wetted area, and increase the period of infiltration beyond what exists under natural conditions. The direct technique of recharge is preferred over indirect methods. The most widely practiced methods can be described as types of *surface water spreading* (increasing contact area). Surface water spreading systems for artificial recharge are divided into in-channel and off-channel systems. *In-channel systems* consist of dams placed across ephemeral or perennial streams to back the water up and spread it out, thus increasing the wetted area of the streambed or floodplain so that more water infiltrates into the ground and moves down to the groundwater. *Off-channel surface recharge systems* consist of specially constructed infiltration basins, lagoons, old gravel pits, flood-irrigated fields, perforated pipes, or any other facility where water is put or spread on the ground for infiltration into the soil and movement to underlying groundwater. Surface water spreading systems normally require permeable surface soils in order to get high infiltration rates and to minimize land requirements. In areas where permeable soil occur deeper down and the less permeable overburden is not very thick, the overburden can be removed so that the basin bottom is in the more permeable region. Vadose zones should be free from layers of clay or other fine-textured materials that unduly restrict downward flow and form perched groundwater that waterlogs the recharge area and reduces infiltration rates. Perched water can also form on aquatards where aquifers are semi-confined. Aquifers should be unconfined and sufficiently transmissive to accommodate lateral flow of the infiltrated water away from the recharge area without forming high groundwater mounds that interfere with the infiltration process. Also, soils, vadose zones, and aquifers should be free from undesirable contaminants that can be transported by the water and move to aquifers or other areas where they are not desired. The primary purpose of water spreading is to extend the time and the area over which water is recharged. The spreading methods may be classified as basin, stream channel, ditch and furrow, flooding and irrigation.

15.3.1 Basin Method

In basin recharge method, water is recharged by releasing it into basins formed by excavation or by the construction of containment dikes or small dams of dimensions varying from few meters to several hundred meters. The most common system consists of individual basins fed by pumped water from nearby surface water sources. Silt-free water avoids the problem of sealing basins during flooding. Basins require periodic scraping of the bottom surface when dry to preserve a percolation surface. Basins, because of their general feasibility and ease of maintenance, are the most favored method of artificial recharge from the surface. The design for basin recharge method is shown in Figure 15.2.

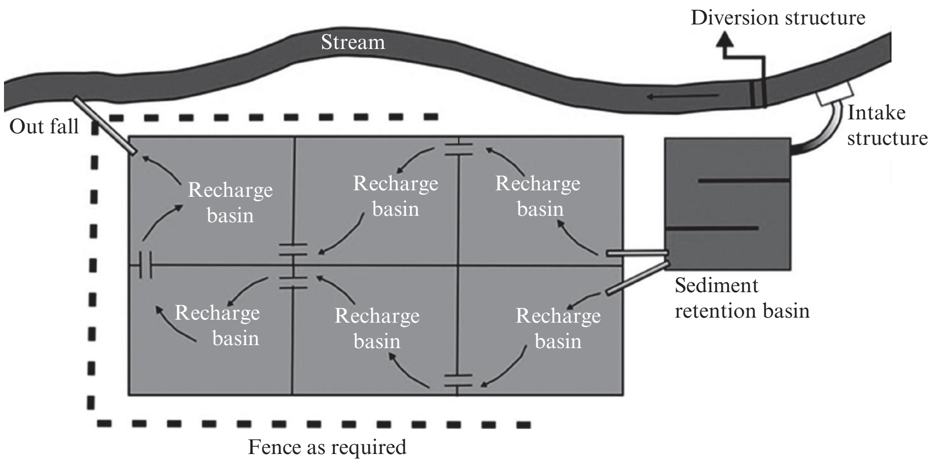

Figure 15.2 *Basin spreading recharge*

15.3.2 Stream Channel Method

Water spreading in a natural stream channel involves operations that increase the contact time and area over which water is recharged from a naturally losing channel. This method involves both upstream management of stream flow and channel modifications to enhance infiltration. Improvements of stream channels may include widening, leveling, scarifying, or ditching to increase infiltration. In addition, low check dams and dikes can be constructed across a stream where a wide bottom occurs; these act as weirs and distribute the water into shallow ponds occupying the entire streambed. The methods commonly used include

1. widening, leveling, scarifying, or construction of ditches in the stream channel
2. construction of L-shaped finger levees or hook levees in the river bed at the end of high stream flow season
3. low head check dams that allow flood waters to pass over them safely.

The channel is so modified that the flow gets spread over a wider area, resulting in increased contact with the streambed. The L-shaped finger levees can be constructed annually by bulldozer at the end of the high stream flow season. These structures are normally temporary, consisting of river-bottom material, and sometimes protected by vegetation, wire, or rocks. Such works quickly collapse when high stream flows occur; if permanent structures are placed in a channel, it is important that they do not create a flood hazard. Channel spreading can also be achieved without specific spreading works; for example, upstream reservoirs enable erratic runoff to be regulated and ideally limit stream flows to rates that do not exceed the absorptive capacity of downstream channels, so that they are entirely recharged into downstream reaches.

15.3.3 Ditch and Furrow Method

In the ditch and furrow method, water is distributed to a series of ditches, or furrows, that are shallow, flat bottomed, and closely spaced to obtain maximum water contact area. One of the following three basic layouts is generally employed: (i) contour, where the ditch follows the ground contour and by means of sharp switchbacks meanders back and forth across the land; (ii) tree shaped, where the main canal successively branches into smaller canals and ditches; and (iii) lateral, where a series of small ditches extend laterally from the main canal. Ditch widths range from 0.3 to 1.8 m. On very steep slopes, checks are sometimes placed in ditches to minimize erosion and to increase the wetted area. Gradients of major feeder ditches should be sufficient to carry suspended material through the system. Deposition of fine-grained material clogs soil surface openings. Although a variety of ditch plans are used, a particular plan should be tailored to the configuration of the local area. A collecting ditch is needed at the lower end of the site to convey excess water back into the main stream channel. The method is adaptable to irregular terrain but seldom provides water contact to more than about 10 percent of the gross area. Furrows used for irrigation may also serve for recharging without additional cost. The spacing between the ditches/furrows may be kept 3 m as this would help easy movement of person and animals and the land between the adjacent channels can be used for plantation of *Ber* (*Ziziphus mauritiana*), *Meetha Jaal* (*Salvadora oleoides*), Pomegranate (*Punica granatum*), *Amla* (*Emblica officinalis* or *Phyllanthus emblica*), *Baonli* (*Acacia jacquemontii*), *Khejri* (*Prosopis cineraria*), etc., which requires 2.5–3 m spacing. Such plantation on waste land is already being actively promoted by Central Arid Zone Research Institute (CAZRI), Jodhpur, and is a good source of income for rural people.

15.3.4 Flood Plain Recharge

In relatively flat topography, water may be diverted to spread evenly over a large area. In practice, canals and earth-distributing gullies are usually needed to release the water at intervals over the upper end of the flooding area. It is desirable to form a thin sheet of water over the land, which moves at a minimum velocity to avoid disturbing the soil. The highest infiltration rates occur on areas with undisturbed vegetation and soil covering. Compared with other spreading methods, flood-spreading costs are least for land preparation. To control the water at all times, embankments or ditches should surround the entire flooding area. To enhance efficiency, shallow pits and/or ditches are made manually or mechanically in the flood plain, before and/or even during the flooding. This recharging method is more suitable along the major rivers with well-developed flood plains, where recharged water can be easily recovered through a battery of tube wells, that is, *aquifer storage recovery* (ASR) method.

15.3.5 Irrigation Method

In irrigated areas, water is sometimes deliberately spread by irrigating cropland with excess water during monsoon period. The method requires no additional cost for land preparation because the distribution system is already installed. Even keeping irrigation canals full contributes to recharge by enhanced seepage from them. Where a large portion of the water supply is pumped, the method has the advantage of raising the water table and consequently reducing power costs. The main drawback of this method is possible reduction in crop yield due to the leaching action of the percolating water both in carrying salts from the root zone to groundwater and in removing soil nutrients.

15.3.6 Pit Method

A pit excavated into a permeable formation may serve as groundwater recharge system. Because the cost of excavation and removal of material is high, use of abandoned excavations, such as gravel pits, is preferred. In areas where shallow subsurface strata, such as hardpans and clay layers, restrict the downward movement of water, pits can effectively reach materials with higher infiltration rates. The geometry of a recharge pit is important to obtain the maximum infiltration rate as the steep sides provide a high silt tolerance. Silt usually settles to the bottom of the pit, leaving the walls relatively unclogged for continued infiltration of water. Silt-free water minimizes silt accumulation and periodic removal costs.

15.3.7 Percolation Tank/Pond

Percolation tank is an artificially created surface water body on highly permeable land areas, so that the surface runoff collected in the tank percolates and recharges the groundwater storage. The purpose of percolation tank is to conserve the surface runoff and divert the maximum possible surface water to the groundwater storage. In areas where land is available in and around the stream channel section, a small tank is created by means of earthen dams across the stream. The tank can also be located adjacent to the stream. The hydrogeological condition of site for percolation tank is of utmost importance. The soil/rocks coming under the submergence area should have high permeability. The aquifer zone getting recharged should extend downstream into the benefited area where adequate number of groundwater structures should be available to fully utilize the additional recharge. The size of the percolation tank depends on the catchment and rainfall characteristics as well as the percolation capacity of the strata in the tank bed. The water accumulated in the tank after monsoon should percolate at the earliest (normally before March). In case the percolation rate is not adequate, the impounded water is locked up and wasted more through evaporation losses, thus depriving the downstream area of the valuable resource.

15.3.8 Hill Toe Trenches

Hills generate sufficient quantity of runoff, which can be harvested and recharged through appropriate methods. Hill toe trenches can be constructed at the bottom of hill slopes as well as on sloping waste lands in both high and low rainfall areas. Trenches break the slope at intervals and reduce the velocity of surface runoff. The water retained in the trench help in conserving the soil moisture and groundwater recharge. Size and number of trenches depend on the rainfall and soil depth and normally they are 1–2 m wide and 1.5–2 m deep. The depth of trench is restricted in thin soil cover areas, and hence more trenches at closer intervals need to be constructed. Trenches may be continuous or interrupted and are constructed along the contours. Continuous trenches are used for moisture conservation in low rainfall area, whereas intermittent trenches are preferred in high rainfall area. The horizontal distance between two trenches should be less in steeply sloping areas. The hill toe trench for groundwater recharge is depicted in Figure 15.3.

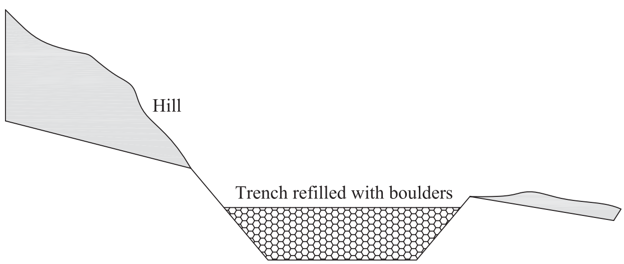

Figure 15.3 *Recharge from hill toe trench*

15.3.9 Gabion Structures

It is a kind of barrier commonly constructed across small stream to conserve stream flows. Practically no submergence beyond stream course happens in such structures. The boulders locally available are stored in a steel wire and put up across the stream to make a small dam by anchoring it to the streamside. The gabion structure is normally used in the streams with width of about 10–15 m and its height may be around 0.5 m. The excess water overflows this structure leaving some storage water to serve as source of recharge. Silt content of stream water deposited in interstices of boulders to make it more impermeable after some time. Such structures in Alwar (Rajasthan) have been very successful in recharging groundwater.

15.3.10 Check Dam/Anicut/Gully Bund/*Nala* Bund

Check dam, anicut, gully bund and nala bund are structures of smaller dimension across streams/*nalas* as shown in Figure 15.4 (CGWB 2007). They are constructed on a stream in areas where groundwater table fluctuation is very high and stream is influent. Average catchment area may be 20–50 ha. The objectives are to impound surface runoff coming from catchments, to reduce runoff velocity thereby minimizing erosion, and to facilitate percolation of stored water for increasing recharge to wells located downstream. Site conditions for locating check dams are the areas having medium slope (<2%). These are constructed on lower order streams generally up to third order. Soils and rock lithology and structure should be favorable for allowing percolation of water. The check dams and *nala* bunds always require a detailed study including measurement of the channel X-section, channel L-section, nature and thickness of bed material, and percent slope in stream bed. These are designed based on stream width and excess water is allowed to flow over the wall. The water stored in these structures is mostly confined to stream course and the height is normally around 2 m. Thus, a check dam or *nala* bund acts like a mini percolation tank with water storage confined to stream course. To avoid scouring from excess runoff, water cushions are provided at downstream side. The *nala*/stream bed should have soils with adequate permeability and good fracture development to facilitate groundwater recharge. To harness the maximum runoff in the stream, series of such check dams, small bunds, or weirs can be constructed to have recharge on a regional scale. For selecting a site for check dams/*nala* bunds the following aspects may be observed (CGWB 2013):

1. The total catchment of the *nala* should normally be between 40 and 100 ha though the local situations can be a guiding factor for this.
2. The annual rainfall in the catchment should be less than 1000 mm.
3. The width of *nala* bed should be at least 5 m and not exceed 15 m and the depth of bed should not be less than 1 m.
4. The lands downstream of check dam/bund should have groundwater demand.
5. The *nala*/stream bed should have soils with adequate permeability and good fracture development to cause groundwater recharge through ponded water.

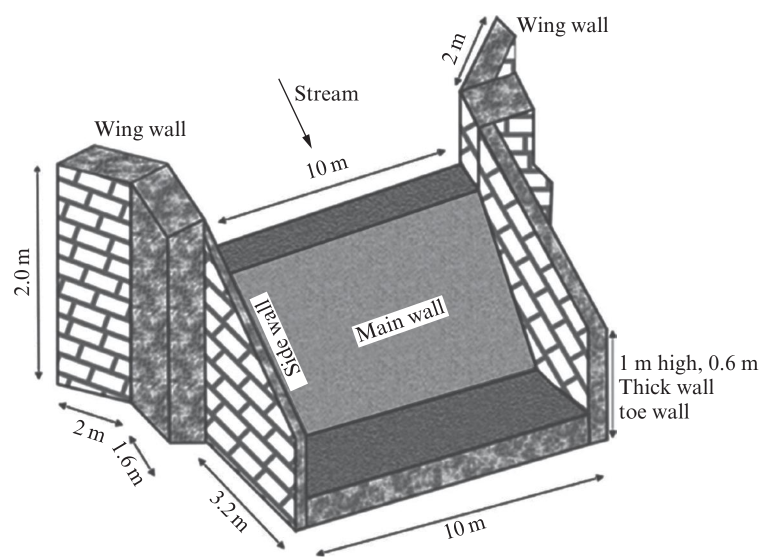

Figure 15.4 *Check dam or anicut*

15.3.11 Abandoned Quarries

In many parts of the country as a result of mining activity, quarries have been excavated and now after the completion or abandoning of such activities, abandoned quarries in the form of large cavity and depressions have been created. In mining areas for excavation of sand and rock material heavy pumping of groundwater has been made. The unused abandoned quarries can be utilized for groundwater recharge after making certain modifications. Revival and channelization of drainage around such abandoned quarries by construction of embankments and modifications in surface drainage toward these depressions will provide surface storage of rain water during monsoon period. Where the rocks are already weathered, fractured, and jointed, most of the water will automatically get recharged to groundwater. At places where fractured, weathered, and jointed rocks are not present, recharge shafts may be constructed for augmentation of groundwater recharge.

15.3.12 Recharge Shaft

Recharge shaft (Figure 15.5) is an artificial recharge structure that penetrates the overlying impervious horizon and provides affective access to surface water for recharging the phreatic aquifer. These structures are ideally suited for areas with deep water levels. In areas where low permeable sandy horizon is within shallow depths, a trench can be excavated to 3 m depth and back-filled with boulder and gravel. The trench can be provided with injection well to effectively recharge the deeper aquifers. The following are site characteristics and design guidelines:

- To be dug manually if the strata is of noncaving nature. If the strata are caving, proper permeable lining should be provided. The diameter of shaft should normally be more than 2 m to accommodate more water and to avoid eddies in the well.
- In the areas where source water carries silt, the shaft should be filled with boulder, gravel, and sand from bottom to have inverted filter. The uppermost sandy layer has to be removed and cleaned periodically.
- When water is put into the recharge shaft directly through pipes, air bubbles can choke the shaft. The injection pipe should therefore be lowered below the water level to avoid this.

15.3.13 Recharge Shaft in Water Bodies

Amongst the numerous water bodies, most of the water bodies are deteriorated and silted or filled with garbage or waste material. These ponds, lakes, and water bodies may be reclaimed and restored for storing the rain water during monsoon and augmenting the same to groundwater storages by constructing recharge shafts within or adjacent to them. The recharge shafts should be constructed in a way that only excess water is being recharged to groundwater and minimum water level is maintained in water bodies for their sustenance and environment. Before adopting such water bodies for enhancing groundwater recharge, these water bodies need to be restored by construction of proper bunds, cleaning of water bodies, excavation, and silt removal from the bottom of the ponds. Some of the tanks in Maharashtra and Karnataka have been converted into percolation tanks.

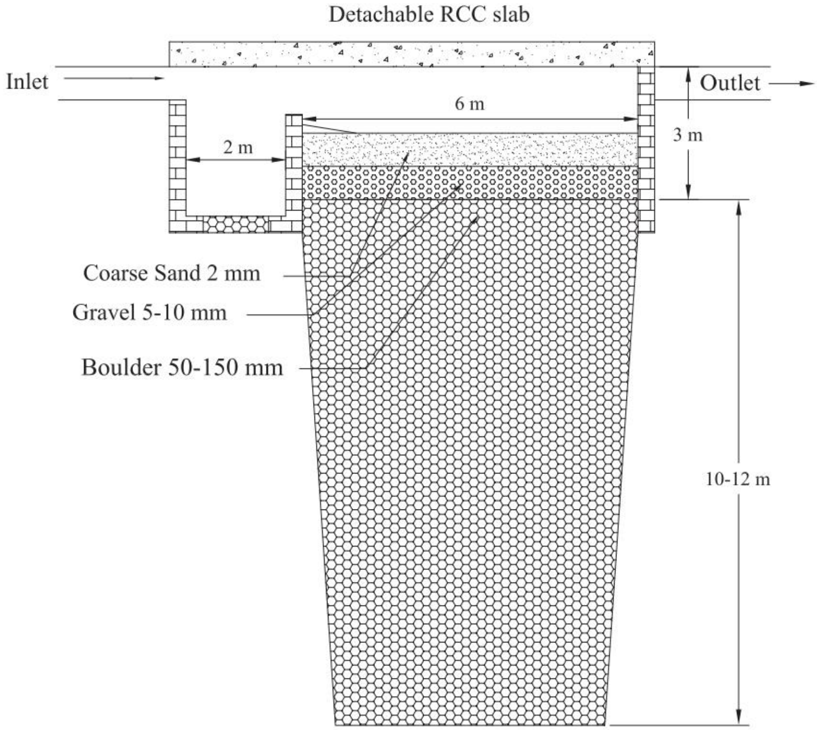

Figure 15.5 *Recharge shaft with bore hole*

15.3.14 Park-Type Structures

In urban agglomerate of residential colonies and institutional areas, parks are very common feature and can be fruitfully utilized for groundwater recharge. Runoff from the catchment of park as well as surrounding area may be diverted toward the location that is excavated in a basin-type depression to accommodate the runoff. The water is recharged through recharge shaft/recharge wells (Figure 15.6) or recharge pit depending on the hydrogeological conditions and depth of unconfined aquifer. The structure is used as rain water harvesting and recharge structure during monsoon and the same is used as a playground in other seasons.

15.3.15 Dug Well

There are thousands of dug wells that have either gone dry or the water levels have declined considerably. These dug wells (Figure 15.7) can be used as structures to recharge groundwater. The storm water, tank water, canal water, etc., can be diverted into these structures to recharge directly the dried aquifer. The recharge water is guided through a pipe to the bottom of well, below the water level to avoid scoring of bottom and entrapment of air bubbles in the aquifer. The quality of source water including the silt content should be such that the

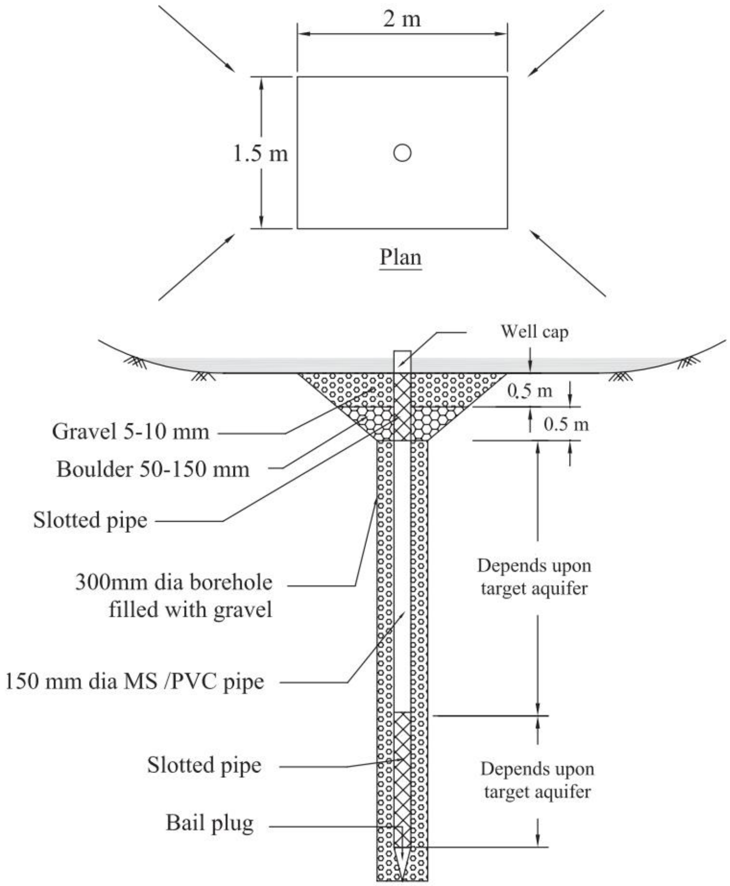

Figure 15.6 *Park-type recharge structure—sectional view*

quality of groundwater reservoir is not deteriorated. Water to be recharged should be passed through desilting chamber, filter media or their combination if it is not silt free. In rural areas, the rain water runoff can be channelized and recharged to dug wells through a filter. Open wells can easily be used for extraction as well as recharge wells for rooftop runoff as it has a big volume to store the instantaneous downpour and does not require pumping as in the case of injection wells. Abandoned well can very easily be converted to recharge well with a little cost input.

15.3.16 Abandoned Hand Pump and Tube Wells

Due to depletion in groundwater levels several tube wells and hand pumps became defunct. Still, these tube wells and hand pumps have proper connectivity with groundwater aquifers that got de-saturated with depletion of groundwater levels. These abandoned hand pumps and tube wells can be used as recharge wells after proper cleaning/development and constructing a recharge pit with desilting chamber along with them, thus an effective recharge through these wells may take place.

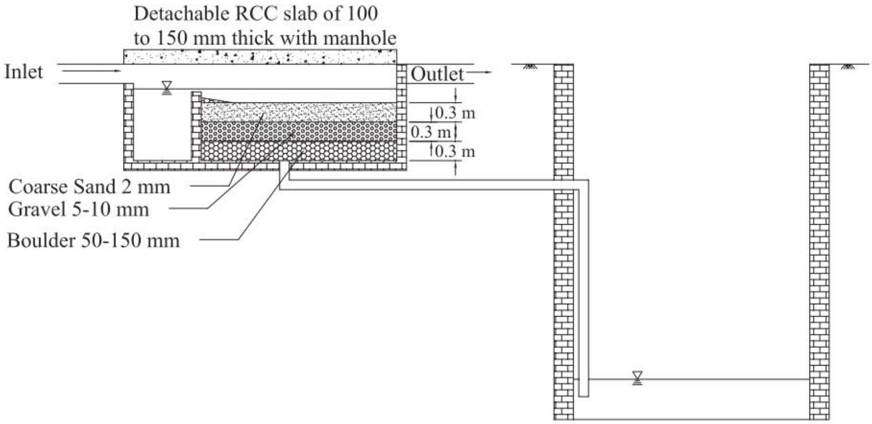

Figure 15.7 *Recharge through dug well*

15.3.17 Recharge or Injection Well Method

A *recharge well* admits water from the surface to freshwater aquifers. Recharge wells are also known as disposal wells and drain wells. Generally, *injection wells* are used to dispose brines and toxic industrial wastes to deep, saline water aquifers, but injection wells are also used for groundwater recharge. *Recharge* or *injection wells* are constructed where permeable soils and/or sufficient land area for surface infiltration are not available (such as economy of space in urban areas), vadose zones are not suitable for trenches, and aquifers are deep and/or confined. A recharge well is provided up to the water table and the recharge is done directly to aquifer as shown in Figure 15.8. Secondary sewage effluent can readily be used in surface infiltration systems for SAT, while effluent for injection and recharge wells should at least receive tertiary treatment as recharged water is directly put into aquifer so does not receive the SAT by vadose zone.

The flow in aquifer due to a recharge well is the reverse of a pumping well, but its construction may or may not be same. If water is admitted into a well, a cone of recharge will be formed that is similar in shape but is the reverse of a cone of depression surrounding a pumping well. The equation for the curve can be derived in a similar manner to that for a pumping well. The recharge capacity is less than the pumping capacity even if the recharge cone has dimensions equivalent to the cone of depression as the pumping and recharging differ by more than a simple change of flow direction. The following facts contribute in the discharging and recharging capacity difference:

1. Fine material present in the aquifer is carried through the coarser particles surrounding the well during the pumping from a well; on the contrary, any silt carried by water into a recharge well is filtered out and tends to clog the aquifer surrounding the well.
2. Recharge water may carry large amounts of dissolved air, tending to reduce the permeability of the aquifer by air binding.

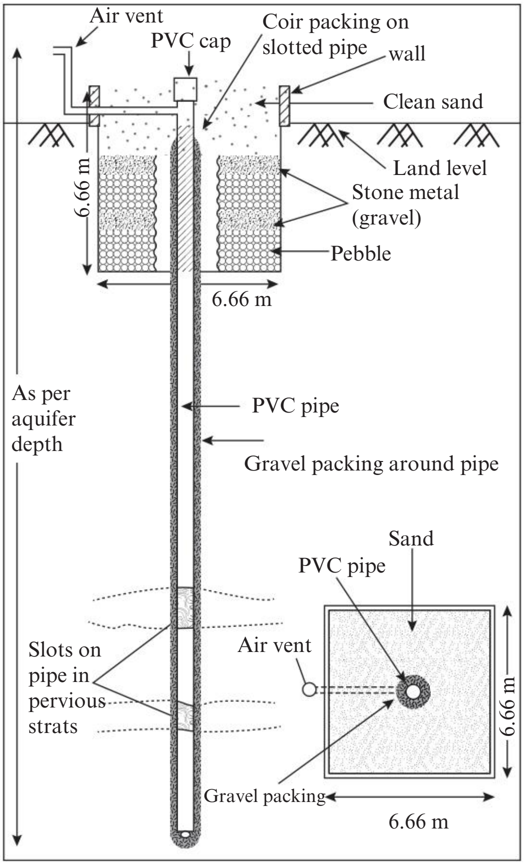

Figure 15.8 *A typical recharging well*

3. Recharge water may also contain bacteria, which can form growths on the well screen and the surrounding formation, thereby reducing the effective flow area.
4. Chemical constituents of the recharge water may differ sufficiently from the normal groundwater to cause undesired chemical reactions—for example, defloculation caused by reaction of high sodium water with fine soil particles.

These above-mentioned factors reduce recharge rates. Recharge wells serve as convenient means for the disposal of septic tank effluent, excess irrigation water, and surface runoff. Favorable recharge rates can be maintained by chlorination and deareation of recharged water and by well maintenance involving periodic pumping of the wells. Using the same well as pumping well and recharging well alternatively is the best strategy. This allows recharging when water demand is low and surplus water is available, and pumping when water demand is high like in the summer. Such storage and recovery wells may be used for municipal water supplies so that water-treatment plants do not have to meet peak demands but can be designed and operated for a lower average demand, which is financially attractive. Recharge wells are also feasible for temporary storage of fresh water in saline water aquifers through wells first recharged and latter pumped. The efficiency of the procedure increases with each recharge–storage–withdrawal cycle. The technique has application in flat coastal areas underlain by saline water aquifers where no surface reservoir sites are available to provide freshwater supplies on a year round basis. But for any recharge system, clogging is a major concern and it is much more typical in well as it cannot be scraped or dried. A well that is used only for recharging may become ineffective in 2–3 years, but frequent backwashing or alternate use as recharging and discharging of well reduces the chances of clogging and hence results in an effective life of the recharge well.

Injection well recharging a single aquifer or multiple aquifers can be constructed in a fashion similar to normal gravel-packed pumping well. The only difference is that cement sealing of the upper section of the well is done in order to prevent the injection pressures from forcing leakage of water through the annular space of borehole and well assembly. An injection pipe with opening against the aquifer to be recharged may be sufficient. However, in case of a number of permeable horizons separated by impervious rocks, a properly designed injection well may be constructed with slotted pipe against the aquifer to be recharged. In practice, the injection rates are limited by the physical characteristics of the aquifer. In the vicinity of well, the speed of groundwater flow may increase to the point that the aquifer is eroded, especially if it is made up of unconsolidated or semiconsolidated rocks. In confined aquifer, confining layers may fail if too great pressure is created under them. If this occurs, the aquifer will become clogged in the vicinity of the borehole and/or may collapse. The deeper the injection well, the thick overburden allows high injection pressures. High allowable injection pressures would result in reduced frequency of well redevelopment and lower maintenance costs. However, wherever possible surface infiltration methods should be adapted in place of injection wells, as clogging is a part and parcel to recharging and well redevelopment. The initial cost and running cost of injection wells are very high compared with the surface application methods.

15.3.18 Subsurface Dykes

A *subsurface dyke* or *groundwater dam* is a subsurface barrier across groundwater movement that retards the natural lateral groundwater flow of the system and stores water below ground surface to meet the demands during the period of need. The main purpose of groundwater dam is to arrest the flow of groundwater out of the sub-basin and increase the storage within the aquifer. By doing so the water levels in upstream of groundwater dam rises and saturates the otherwise dry part of aquifer as shown in Figure 15.9. The structure should be constructed up to bed rock, therefore depth to bed rock should not be very high. The subsurface dyke or underground dam has the following advantages: no submergence of land, no evaporation loss, no siltation in the reservoir, land acquisition not required, no potential disaster such as collapse of surface dams, and no hindrances to utilization of the land above the recharged aquifer/reservoir.

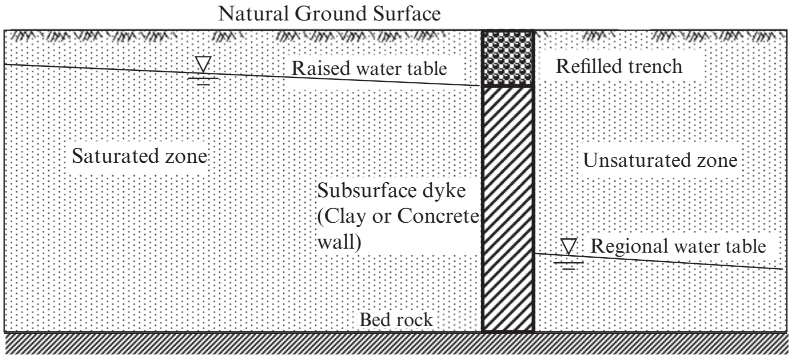

Figure 15.9 *Subsurface dyke*

15.3.19 Incidental Recharge Method

Incidental, or unplanned, recharge occurs where water enters the ground as a result of a human activity whose primary objective is unrelated to artificial recharge of groundwater. Included in this category is water from irrigation, cesspools, septic tanks, water mains, sewers, landfills, waste-disposal facilities, canals, and reservoirs. The quantity of incidental recharge in India is many times more than the planned artificial recharge. However, several of these sources introduce polluted wastes into the underground resulting in the degradation of the groundwater.

15.3.20 Induced Recharge Method

Direct methods of artificial recharge involve the conveyance of surface water to some point where it enters the ground. The method of *induced recharge* is accomplished by withdrawing groundwater at a location adjacent to a river or lake so that lowering of the groundwater level will induce water to enter the ground from the surface source. This is also known as *bank filtration*. Natural induced recharge occurs when intensive exploitation of groundwater close to river results in depression of groundwater level and water-inflow from the river. This phenomenon may also occur in semiarid climates where a depression of the piezometric level of an aquifer underlying a temporary river creates the empty space in the aquifer, which facilitates its recharge during floods. The induced recharge schemes have the following advantages:

1. Induced recharge furnishes water free of organic matter and pathogenic bacteria.
2. Because surface water commonly is less mineralized than groundwater, water obtained by induced infiltration, being a mixture of two water sources, possesses a higher quality than natural groundwater.
3. Induced infiltration where supplied by a perennial stream ensures a continuing water supply even though overdraft conditions may exist in nearby areas supplied only by natural recharge.

The induced recharge involves pumping water from an aquifer, which is hydraulically connected with surface water to induce recharge to the groundwater reservoir. Collector wells and infiltration galleries, used for obtaining very large water supplies from riverbeds, lakebeds, and waterlogged areas also function on the principle of induced recharge. The method is effective in unconsolidated formations of permeable sand and gravel hydraulically connected between stream and aquifer. The amount of water induced into the aquifer depends on the rate of pumping, permeability, type of well, distance from surface stream, and natural groundwater movement. It is important that the velocity of the surface stream be sufficient to prevent silt deposition from sealing the streambed. The factors important for controlling the design of schemes for induced recharge are quality of source water, hydraulic characteristics, thickness of aquifer material, distance of the pumping wells from the river, and pumping rates. In unconfined alluvium, the lower one-third of the wells may be screened. In highly fractured consolidated rocks, dug wells penetrating the entire thickness of the aquifer should be constructed with lining above the water table zone.

15.4 Features of MGR Systems

Groundwater is a major source of water supply for dinking, industrial, and agricultural purposes. Groundwater is being largely used for agricultural purposes in India. It is being overexploited in many areas and its quality is also deteriorating in the world in general and in India in particular. Resource management is the coupled approach of limiting the development and use of a resource in order to conserve it. Groundwater management has a somewhat broader scope, in that artificial recharge can be used to expand the amount of available water. Many approaches to bring groundwater withdrawals into balance are being adopted. *MGR* or *managed aquifer recharge (MAR)* is the infiltration or injection of water into an aquifer. The water can be withdrawn at a later date, left in the aquifer for environmental benefits, such as maintaining water levels in wetlands, or used as a barrier to prevent saltwater or other contaminants from entering the aquifer. As the water infiltrates or is injected into the soil, natural biological, chemical, and physical processes may assist in removing pathogens, chemicals, and nutrients from the water, and thus improve water quality. The following are the factors determining the effectiveness of MGR:

(i) environmental factors

(a) climate and hydrological criteria
(b) hydrogeological criteria
(c) topography and geomorphology
(d) source water considerations

(ii) physical and technical factors

(a) soil type (infiltrations capacity)
(b) source of water (river, canals, rainfall distribution, and intensity)
(c) subsurface storage capacity (geology, degree of confinement, permeability, groundwater flow, and quality)
(d) compatibility between quality of recharging and native waters

MGR may be used as a means of managing water from a number of sources, including storm water. MGR also makes water reuse possible where religious taboos exist against certain direct uses of "unclean" water. Water quality also does not deteriorate for decades of storage thus allowing the possibility of creating water bank. Many such projects of MGR are going on in Western countries where recharge quantities are much more than annual extraction thus creating a buffer zone for future unforeseen requirements. The ecological effects of MGR are generally positive, as besides improving the availability of water in aquifer, it provides moisture to the root zone for development of plant life. MGR helps in improving water levels/rejuvenating springs, lakes, ponds, and other water bodies that are fed by groundwater. MGR helps in maintaining a healthy salt balance in the aquifer and checking saline water intrusion. Overall, MGR improves the ecology of the area where it is practiced, but the impact on the ecology of the recharging source must be studied before undertaking any scheme of groundwater recharging. Any MGR activity must be planned without harming the ecology of the source of water such as stream or lake and adjoining area. The scope of MGR schemes can range in complexity and scale.

15.5 Artificial Recharge Strategy and Identification of Potential Areas

The approach to supporting the implementation of artificial recharge schemes should pay attention to groundwater monitoring, assessing the feasibility of schemes, developing support mechanism for implementing recharge schemes, promoting participation of stakeholders, etc. Induction of artificial recharge into farming sector is the need of the hour as it is the biggest user/stakeholder. Many farms have check dam, etc., the benefits of which have not been assessed and also it is not known whether these have any planned effects. Benefits of recharge would be high in alluvial aquifers and areas where farmers have no groundwater resource. Other potential recharge applications in industrial and mining sectors should be appreciated, encouraged, and promoted.

Satellite imageries are very useful in extracting several input parameters in planning, designing, execution, and monitoring of aquifer recharge systems. For example, it can be used to find catchment area, irrigable area, land use, soil type, drainage network, potential locations of recharge structures, etc. The viability of a MGR scheme is firstly dependent on the quality of water available to be used, or level of treatment required to achieve the necessary water quality. Storm water can contain contaminants such as oil, grease, metals, and pesticides, which build up on surfaces in urban areas. These come from sources such as pavement deterioration, wheel and brake-pad wear, vehicle emissions, and spills. MGR may improve water quality for a number of contaminants as a result of filtration in the aquifer, and through biochemical processes in the soil or aquifer. It is however noted that there are a number of contaminants that may not be removed by MGR, and that there exists the potential for MGR to cause contamination of the aquifer if improperly designed or managed. The potential for contamination of the soil or aquifer through which the water moves also requires consideration.

The aquifer characteristics must also be well understood and mapped before implementation of a MGR scheme. Knowledge of the aquifer characteristics is required to predict the flow and fate of injected water. Understanding and monitoring of the aquifer and injected water is required so that recovery bores can be located to ensure that sensitive receptors, such as bores, wetlands, and acid sulfate soils, are not affected. The quantity of water available for abstraction following MGR will be dependent on various factors, including the potential for impacts to the regional groundwater system. At times, due to either recovery efficiencies or environmental water allocations, the volume of water available to be recovered will be less than the volume of water that has been recharged to the aquifer in the scheme.

15.6 Source Water Availability and Assessment

Availability of source water is one of the basic prerequisites for taking up any MGR system. The source water available for MGR could be of the following types:

- *in situ* precipitation in the watershed
- nearby stream/spring/water body/surface water (canal) supplies located within the watershed/basin
- surface water supplies through trans-basin water transfer
- treated municipal/industrial wastewaters
- any other specific source(s)

The availability of water for MGR from all these sources may vary considerably from place to place. In any given situation, the following information may be required for a realistic assessment of the source water available for recharge:

1. the quantum of noncommitted water available for recharge
2. time for which the source water is available
3. quality of source water and the pretreatment required
4. conveyance system required to bring the water to the proposed recharge site

Rainfall and consequent runoff constitute the major sources of water for artificial recharge of groundwater. Rainfall is the primary source of recharge into the groundwater reservoir. For proper evaluation of source water availability, a thorough understanding of rainfall and runoff is essential. Collection and analysis of hydrometeorological and hydrological data have an important role to play in the assessment of source water availability for planning and design of MGR schemes. Rainfall-runoff modeling is done for estimating the runoff from any area and has its application in flood/drought forecasting, reservoir planning and operation, groundwater recharging, drainage design, etc. Direct measurement of runoff is a better option, but it is not possible to gauge all locations for runoff measurement. Hence, an indirect approach toward runoff estimation is more popular in the form of rainfall-runoff modeling as the data for rainfall are easily available. Runoff can be estimated using precipitation and some of the catchment characteristics. It is strongly dependent on soil, vegetation, and topographic characteristics of the catchment. Factors affecting runoff are as follows:

- precipitation: type, duration, amount, intensity, design storm event, etc.
- watershed/catchment: size, topography, shape, orientation, geology, interflow, soil, land use, etc.

These factors vary within a given catchment in spatial domain. Although there are many methods and models available in literature for the estimation of runoff, for example,

1. empirical relationships/rational method
2. peak discharge method (time of concentration)
3. tabular method (CN methods)
4. unit hydrograph method

Physically based distributed models on one side are based on physical theories but are very data intensive and complex, whereas empirical models are simple and require less data but they lack the strong scientific base. Selection of any particular method depends on many factors such as available data, purpose of modeling, catchment characteristics, etc. However, none of them are universally acceptable. Each model has its own advantages and disadvantages. Rational method for small catchments and soil conservation service (SCS) method for general catchments are based on easily available data and hence are the most widely used rainfall-runoff models. Where average percentage of runoff is not known, a figure of 10 percent of mean annual runoff for the catchment may be used as a guide. Rainfall on a return period of 1 in 10 years may be used in better estimation of runoff for a recharge structure.

15.6.1 Rational Method

The *rational method* is suitable for small size (<50 km^2) catchments, for example, rooftop, institutional area, industrial area, residential blocks, urban catchments, etc. It finds considerable application in rainwater harvesting, urban drainage designs, recharge structures, and design of small culverts and bridges. At the start of a rainfall event, the portions nearest the outlet contribute runoff first. As rain continues, farther and farther portions contribute runoff, until flow eventually arrives from all points on the watershed, *concentrating* at the outlet. For a rainfall of uniform intensity and very long duration over a catchment, the runoff increases as more and more flow from remote areas of the catchment reach the outlet. If the rainfall continues beyond the *time of concentration* ($t > t_c$), the runoff will be constant (Figure 15.10) and at the peak value (Q_p) equal to

$$Q_p = CiA \tag{15.1}$$

where i = rainfall intensity; A = catchment area; C = runoff coefficient = runoff/rainfall. The *runoff coefficient* represents the integrated effect of the catchment losses and hence depends on the nature of the surface, surface slope, and rainfall intensity. The rational formula assumes a homogeneous catchment surface. If the catchment is nonhomogeneous but can be divided into distinct subareas each

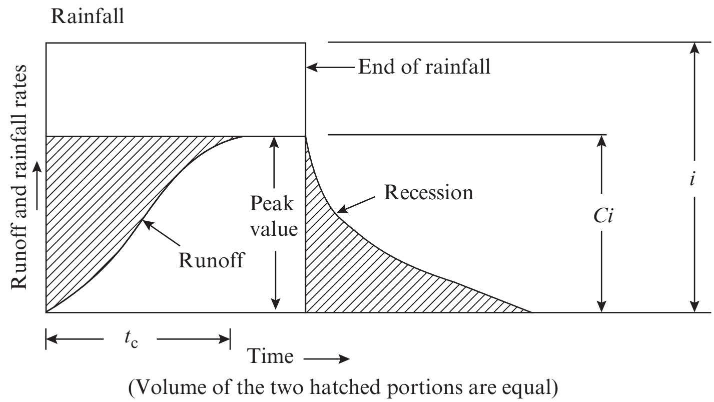

Figure 15.10 *Runoff hydrograph due to uniform rainfall*

having a different C, then the runoff from each subarea is calculated separately and merged in proper time sequence. If the rainfall is uniformly distributed over such a nonhomogeneous catchment for $t > t_c$, then a weighted equivalent runoff coefficient C_e can be determined and used.

$$C_e = \sum C_j A_j / A \tag{15.2}$$

Time of concentration is assumed to be independent of rainfall intensity. Watershed parameters that may affect t_c are (i) length of channel and overland flow plane, (ii) average slope of channel or watershed, and (iii) retardance or roughness characteristics of the watershed.

15.6.2 Water Available from Rooftop Rainwater Harvesting

A major portion of rainwater that falls on the earth's surface runs off into streams and rivers and finally into the sea. Natural recharge is restricted due to limited rainfall period of 4 months in monsoon and increased paved surface area. The concept of *rainwater harvesting* involves "tapping the rainwater where it falls." It is an outstanding method to conserve water and enhance availability of water for drinking, industrial, or groundwater recharge. The technique of rainwater harvesting consists of collecting the rain from localized catchment surfaces such as roofs, plain/sloping surfaces, etc., for either direct use or recharging the groundwater resources. The rooftop rain water can be conserved and used for recharge of groundwater. National water policy emphasizes the water conservation and water-harvesting practices. Government has been providing subsidy to promote the rooftop harvesting and encourages artificial groundwater recharge. This is also mandatory for all developers to adopt rainwater harvesting and artificial groundwater recharge if plot size exceeds a particular limit. Compared to other resources of development, rainwater harvesting is cheap to develop with high socioeconomic returns. Therefore, rain water harvesting coupled with artificial groundwater recharge is one of the sustainability elements in MGR. The rainwater harvesting process involves storing rainwater that falls within one's premises and re-using it after basic treatment. The treated rainwater is safe not just for cleaning and washing but also for cooking and personal consumption or groundwater recharge. Harvested rainwater in cities can mainly be used for recharging groundwater to facilitate in groundwater conservation. Several modular rainwater harvesting system are available in the market. Basic components of rainwater harvesting are

1. *catchment*: rooftop or a paved area
2. *initial conveyance system*: gravity-collection of the captured runoff water from the catchment area to storage using gutters, downspouts, and piping.
3. *debris removal systems*: includes first-flush diversion systems, filters, and screens designed to remove debris and dust from the captured rainwater before tank storage.
4. *storage containers*: most expensive component of a rainwater harvesting system. These containers could be placed on either surface or sub-surface as sumps.
5. *final conveyance system*: transfer of stored water to the end use utilizing gravity-stored or pressure pumping.
6. *water treatment and purification*: depending on the end-use of the storage water, appropriate water treatment systems.

The rainwater harvesting approach requires connecting the outlet of storm water drains and pipes from rooftop to divert the water to existing wells/tube wells/bore well or specially designed recharge wells. The urban housing complexes or institutional buildings have large roof area and can be utilized for harvesting rooftop rainwater. The main influencing factors in water-harvesting potentials are rainfall and catchment characteristics. Thus, the rainwater-harvesting potential depends on rainfall intensity and duration and on the area, kind, and surface features of the catchment and estimated using rational formula.

To design the recharge structure, peak intensity of rainfall and its duration has to be taken into account to assess the total volume of water, which shall be available during this period. This is most important as 80 percent of rainfall occurs in 3–5 rainstorms. The total volume of runoff likely to be generated during peak intensity can be estimated by runoff coefficient × rainfall intensity × catchment area × rainfall duration $= CiAt = Q_p t$. Runoff coefficient for rooftop, paved area, and grass area/open unpaved land catchments may be taken as 0.75–0.95, 0.60–0.85, and 0.1–0.2, respectively.

15.6.3 Soil Conservation Service or Curve Number Model

The SCS procedure (1998) was developed for rainfall–runoff relationships for small rural watershed areas. The procedure that is basically an empirical was developed to provide a rational basis for estimating the effects of land treatment and land use changes upon runoff resulting from storm rainfall. The SCS developed an index, known as runoff curve number (CN), to represent the combined hydrologic effect of soil, land use, agricultural land treatment class, hydrologic and antecedent soil moisture condition (AMC). The amount of rainfall in a period of 5 days before a particular storm starts is termed as AMC. Also, it refers to the water content present in the soil at a given time. The SCS developed three AMC conditions and labeled them as I (soils are dry, lowest runoff potential), II (the average condition), and III (the highest runoff potential). The watershed soil is practically saturated in AMC III. The relationship between rainfall and runoff for these three conditions is expressed as CN. Each storm in a rainfall series is assigned one of the three CNs according to antecedent moisture condition. The SCS also developed a soil classification system that consists of four hydrologic groups according to their minimum infiltration rate, which is obtained for a bare soil after prolonged wetting. The soil groups are identified by the letters A, B, C, and D.

The fundamental hypotheses of the SCS CN method are as follows:

1. Runoff starts after satisfying an initial abstraction I_a. This abstraction principally consists of interception, surface storage, and infiltration.
2. The ratio of actual retention of rainfall to the potential maximum retention (R_p) is equal to rainfall minus initial abstraction.

Mathematically,

$$\frac{R_a}{R_p} = \frac{R}{P - I_a} \tag{15.3}$$

where, R_a = actual retention = $P - Q - I_a$; R_p = potential maximum retention; R = runoff volume uniformly distributed over the drainage basin; P = mean rainfall over the drainage basin; and I_a = initial abstraction. The value of P, R, and R_p are given in depth dimensions. Eliminating R_a and solving for R

$$R = \frac{(P - I_a)^2}{(P - I_a) + R_p} \tag{15.4}$$

Equation (15.4) has two parameters: R_p and I_a. To remove the necessity for an independent estimation of initial abstraction, a linear relationship between I_a and R_p was suggested by SCS.

$$I_a = \eta R_p \tag{15.5}$$

where, η = initial abstraction ratio. SCS adopted $\eta = 0.2$ as a standard value thus

$$R = \frac{(P - 0.2R_p)^2}{P + 0.8R_p} \tag{15.6}$$

It is important to note that if $P \geq 0.2\ R_p$ then only runoff will occur, otherwise runoff be assumed as zero.

The parameter R_p depends on the characteristics of the soil–vegetation–land use (SVL) complex and antecedent soil-moisture conditions in a watershed. For each SVL complex, there is a lower limit and an upper limit of R_p. The SCS expressed R_p as a function of CN as

$$R_p = \frac{1000}{CN} - 10 \tag{15.7}$$

CN is a relative measure of retention of water for a given SVL complex and takes on values from 0 to 100. CN = 100 represents a condition of zero potential retention ($R_p = 0$), that is, an impermeable watershed. Conversely, CN = 0 represents a theoretical upper bound to the potential retention ($R_p = \infty$), that is, an infinitely abstracting watershed.

The CN value is determined from (i) SVL and (ii) AMC. The value of CN for AMC condition II and for a variety of land uses, soil treatment, or farming practices can be obtained from the table of runoff CNs for hydrologic soil-cover complexes. All the areas of a watershed do not fall under AMC II condition. A correction table for CN was developed by SCS to convert AMC II condition to AMC I and AMC III. Alternatively, the following equations can be used for conversion:

$$CN(\mathrm{I}) = \frac{4.2\, CN(\mathrm{II})}{10 - 0.058\, CN(\mathrm{II})} \tag{15.8}$$

and

$$CN\ (\mathrm{III}) = \frac{23\, CN(\mathrm{II})}{10 + 0.13\, CN(\mathrm{II})} \tag{15.9}$$

The CN values for normal antecedent moisture conditions (AMC II) for common land-use classes and soil types can be read from tables (Chow et al., 1988).

Limitations of SCS-CN method are the flowing

1. Equation (15.5) is valid only for $P \geq 0.2\ R_p$; otherwise $R = 0$.
2. The method does not consider the effect of variations in rainfall intensity and its duration.
3. The method does not properly predict I_a for shorter, more intense storms because I_a is assumed constant.
4. The method cannot be extended to properly predict infiltration within a storm.
5. The method assumes depth of infiltration R_p after which all rainfall becomes runoff.

15.7 Reuse and Recycling Wastewater

Treated wastewater reuse is conventionally carried out through direct application and/or mixed with fresh surface water wastewater in irrigation. Another way of reusing wastewater is through artificial recharge of the aquifer system with partially treated wastewater. Where soil and groundwater conditions are favorable, a high degree of upgrading can be achieved by allowing wastewater after necessary treatment to infiltrate into the soil and move down to the groundwater. The unsaturated zone then acts as a natural filter and can remove essentially all suspended solids, biodegradable materials, bacteria, viruses, and other microorganisms. Significant reductions in nitrogen, phosphorus, and heavy metals concentrations can also be achieved. Another advantage of artificial recharge over application of wastewater is the fact that water recovered from an artificial recharge system is not only clear and odor-free but also comes from a well, drain, or natural drainage to a stream or low area, rather than from a sewer or sewage treatment plant. Thus, the use of waste water for artificial recharge provides additional water source for water-scarce metrocities. However, the selection of possible locations for such schemes is controlled by a set of hydrogeological, planning, and environmental considerations. On top of these considerations is the availability and effectiveness of treatment plants. Hydrogeologically unsuitable areas and regions should be excluded from the artificial recharge through wastewater plans. Column experiments to be conducted to study the processes that take place during the infiltration of treated wastewater through the unsaturated zone and to estimate the attenuation capacity of the soil at the location selected for the experimental scale basin recharge. Also, for the purpose of the general selection of sites, two factors are taken into considerations. Firstly, the site should not be within or upstream of a groundwater-drinking community, and secondly, no recharge should be considered where groundwater is flowing into the river.

SAT Systems (Todd and Mays 2005)

Artificial recharge of treated wastewater has an important role to play in water reuse. Treated wastewater can be placed in recharge basins, allowing for infiltration into the ground for the recharge of aquifers. As the water moves through the soil and the aquifer, its quality further improves through physical, chemical, and biological processes that is known as SAT. SAT is based on the infiltration of treated wastewater into the soil and percolation through the vadose zone. Improvements in water quality can occur due to many different mechanisms, including infiltration, biological degradation, physical adsorption, ion exchange, and precipitation. SAT eliminates the undesired pipe-to-pipe or "toilet-to-tap" connection between the sewage-treatment plant and the water-supply system where municipal wastewater is used to augment drinking-water supplies. In this way, SAT is done to surface water and groundwater is made out of surface water. SAT makes potable-water reuse aesthetically and mentally much more acceptable to the public.

An SAT system (Figure 15.11) consists of five major components: (i) the pipeline that carries the treated wastewater from the wastewater treatment plant, (ii) the infiltration basins where the treated wastewater infiltrates into the ground, (iii) the soil immediately below the infiltration basins (vadose zone), (iv) the aquifer where water is stored for a long duration, and (v) the recovery well where water is pumped from the aquifer for potable or nonpotable reuse. The inputs for a SAT system are the soil type, water quality, operation schedule, and environment. The state of the SAT system, which controls the residence time of

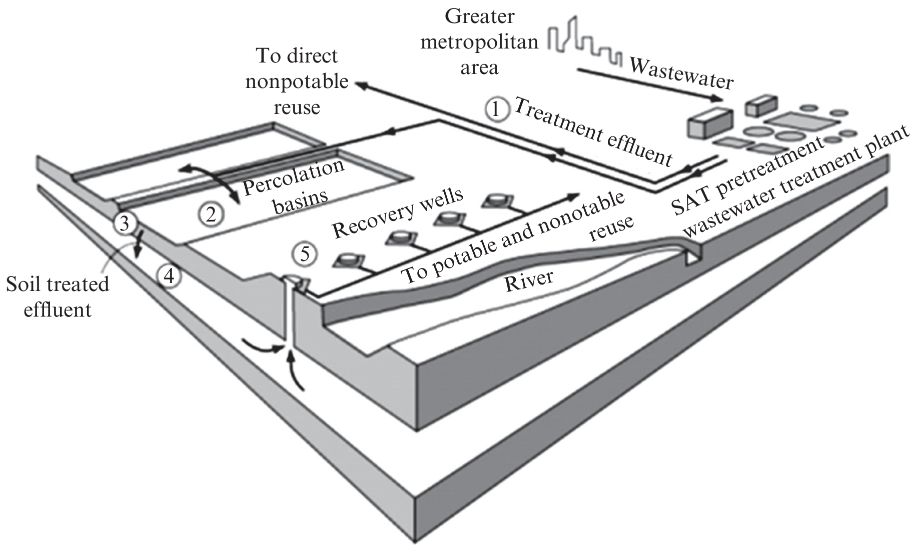

Figure 15.11 *SAT—recharge and recovery system (Todd and Mays 2005)*

water in the vadose zone and the level of microbial activity, includes the soil moisture profile, level of oxygen in the system, algal growth, and soil hydraulic conductivity. Level of oxygen is related to the microorganism distribution and oxygen-demanding substrates. Algal growth is related to clogging layer formation on the soil surface and effective soil hydraulic conductivity. Soil moisture is directly affected by soil type and the environment, and indirectly by the water quality, which affects algal growth and the soil hydraulic conductivity. Oxygen in the vadose zone is affected by the soil moisture profile, the water quality of treated effluent, the operation schedule, and the algal growth. Algal growth is affected by the water quality of treated effluent, the operation schedule, and the environment. Soil hydraulic conductivity is affected by algal growth, the soil type, and the environment. The critical outputs of the SAT system are the total infiltration, the total organic carbon removal efficiency, the nitrogen removal efficiency, and the pathogen removal efficiency. The total organic carbon removal efficiency is primarily affected by the amount of oxygen in the system through the organic oxidation process and the presence of acclimated microorganism. Nitrogen removal efficiency is dependent on oxygen levels and the availability of biodegradable organic carbon through the nitrification–denitrification process. Pathogen removal efficiency is dependent on the soil moisture profile and the soil hydraulic conductivity through the adsorption–inactivation process.

The major purification process in the SAT system are infiltration, organic biodegradation, physical adsorption/desorption, nitrification, denitrification, disinfection, ion exchange, and chemical precipitation/dissolution. SAT is a key component of overall water reuse strategies, providing for (i) mechanical filtration of suspended particles, (ii) biologically mediated transformation of organics and nitrogen, and (iii) physical–chemical retention of inorganic and organic dissolved constituents (e.g., phosphorus, potassium, and trace elements) from biologically treated wastewater. The removal of nitrogen, organic compounds, and biochemical oxygen demand can be a continuous biological process that is sustainable. Cyclic flooding and drying of the SAT infiltration basins is necessary to both improve infiltration rates and control aerobic/anoxic conditions in the soil. Basins are flooded until infiltration rates decrease due to development of a surface clogging layer. Most SAT-related treatment occurs in the upper strata of soil. Initially, unsaturated porous soils contain voids consisting of water and air. Accumulation of biofilm, algae, and suspended solids reduce the void space. The clogging layer development and reduced infiltration rates can dominate SAT system performance, adversely affecting the operation. Cyclic flooding/drying of the basins is necessary to renew hydraulic capacity. Cycle times also influence the transport of oxygen with depth in the vadose zone, causing cycle times to be critical for the control and efficiency of biological processes. Removal of trace metals, phosphorous, and refractory organics by abiotic mechanism can result in accumulation in the soil and eventual problem in future decades.

15.8 Recharge Mounds

Recharge mound is a local rise in groundwater table from natural or artificial recharge. It depends on the infiltration rate, shape and size of recharging area, duration of recharge, and aquifer properties. Mound geometries have been computed by various investigators based on complex mathematical analyses stemming from the generalized nonsteady groundwater flow equations. Most solutions are based on the assumptions of homogeneous and isotropic aquifer, the vertical recharge at a uniform rate, the top of the mound does not contact the bed of the spreading basin, and the height of the mound is small in relation to the initial saturated thickness.

15.8.1 Recharge Rates

Recharge volume depends on infiltration rate, contact area, and time. For a particular water-spreading system, the recharge volume in a certain duration is directly proportional to the infiltration rate. In surface-recharging systems, generally the infiltration rate decreases with time as shown in Figure 15.12. The initial decrease is due to dispersion and swelling of soil particles after wetting; the subsequent increase may be explained by elimination of entrapped air by solution in passing water; and the final decrease results from clogging of soil pores by microbial growths. Laboratory tests with sterile soil and water give nearly constant maximum recharge rates in the absence of microbial growths. Alternating wet and dry periods in surface recharging systems generally result in a greater recharge volume than does continuous spreading, despite lesser (about half) contact time. The reason is drying kills microbial growths and subsequent scarification of the soil surface is undertaken, both of which restore infiltration rate. Water containing silt or clay clog soil pores, leading to rapid reduction in recharge rates. The recharge rate also decreases as the mean particle size of the surface soil decreases. It can be increased by growing vegetation as well as by adding organic matter and certain chemicals. Furthermore, the recharge rate depends on the rate of subsurface lateral flow where less pervious strata lie below the recharging area. Therefore, an array of ditches/strips may result in the same volume of recharge as from the entire basin area.

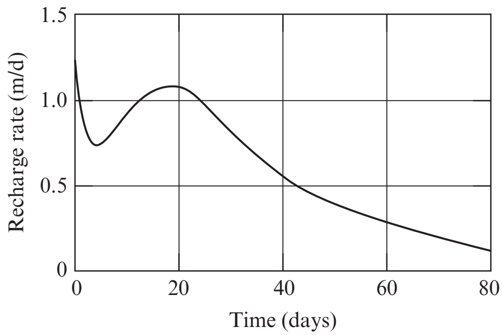

Figure 15.12 *Variation of recharge rate with time*

15 8.2 Perched Groundwater Mounds

A perched mound occurs when a mound is created abode a restricting layer (Figure 15.13). The height of a perched mound L_p, above a restrictive layer L_r, was given by Bouwer et al. (1964)

$$L_p = \frac{i/K_r - 1}{1 - i/K_s} L_r \tag{15.10}$$

where, K_r = hydraulic conductivity of the restricting layer, K_s = hydraulic conductivity of the soil above the restricting layer, i = infiltration rate and zero pressure head prevails at the bottom of the restricting layer. Often, i is much smaller than K_s because surface soils are finer textured that deeper soils. Also, there may be a clogging layer on the surface soil that reduces infiltration.

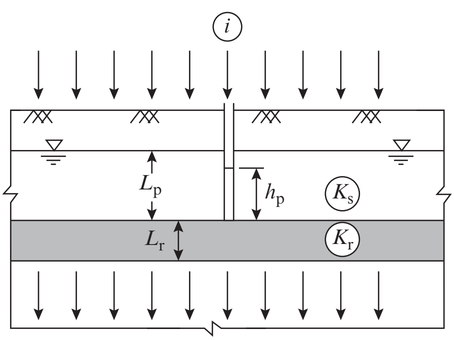

Figure 15.13 *Perched recharge mound*

The infiltration rate is often much larger than K_r. For these conditions

$$L_p = L_r \, i/K_r \tag{15.11}$$

L_p should be small enough so that the top of the perched mound is deep enough to avoid reduction in infiltration rates.

15.8.3 Steady-State Equations for Groundwater Mounds

For long strip basins (length of at least five times the width), groundwater flow away from the strip can be approximated as linear horizontal flow. Below an infiltration area, lateral flow can be assumed to increase linearly with distance from the center. Lateral flow can be assumed to be constant between the edge of the recharge system at a distance $W/2$ from the center and the constant control water table at a distance L_n from the edge. With these assumptions, Bouwer et al. (1964) developed an equation for the ultimate rise of a groundwater mound below the center of the recharge strip in the case of equilibrium between recharge and pumping from the aquifer (Figure 15.14):

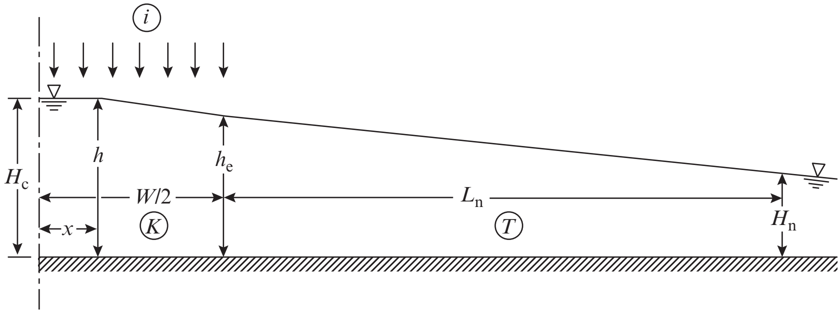

Figure 15.14 *Recharge mound beneath a strip-type basin*

$$H_c - H_n = \frac{iW}{2T}\left(\frac{W}{4} + L_n\right) \tag{15.12}$$

where H_c is the height of the groundwater mound in the center of the recharge area, H_n is the height of the groundwater table at the control area, i is the infiltration rate in the recharge area (total recharge divided by total area), W is the width of the recharge area, L_n is the distance between the edge of the recharge area and the control area, and T is the transmissivity of the aquifer.

For a round or square recharge area, the groundwater flow is in radial direction from the recharge area. Bouwer et al. (1964) used radial flow theory to develop an equation for the equilibrium height of the mound below the center of the recharge system, above the constant groundwater table at a distance R_n from the center of the recharge system.

$$H_c - H_n = \frac{iR^2}{4T}\left(1 + 2\ln\left(R_n/R\right)\right) \tag{15.13}$$

where, R is the radius or equivalent radius of the recharge area. These equations can be used to determine where groundwater should be recovered and to what depth groundwater levels should be pumped to keep the mound from rising too high. These equations can also be used to determine the dimensions of the recharge basins and to determine allowable recharge rates.

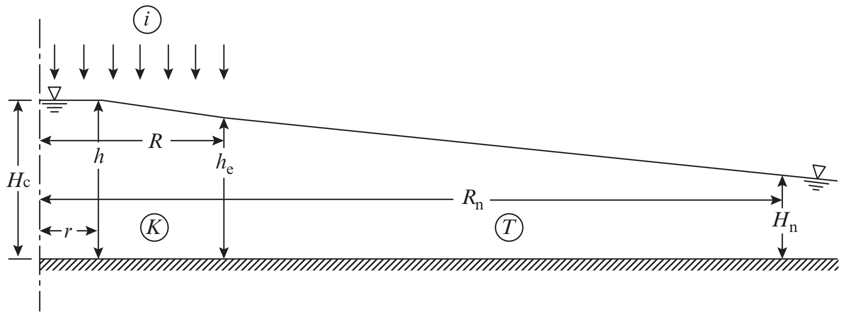

Figure 15.15 *Recharge mound beneath a circular basin*

15.8.4 Unsteady State Equations for Groundwater Mounds

The shape of a mound beneath a rectangular recharge area (Figure 15.16) can be expressed by dimensionless parameters. Hantush (1963) developed the following equation to determine the height of the water table as a function of location (x, y) and time t

$$h_{x,y,t} - H = \frac{v_a t}{4f}\left\{\begin{matrix} F\left[(W/2+x)n, (L/2+y)n\right] + F\left[(W/2+x)n, (L/2-y)n\right] \\ +F\left[(W/2-x)n, (L/2+y)n + F\left[(W/2-x)n, (L/2-y)n\right]\right] \end{matrix}\right\} \tag{15.14}$$

where, $h_{x,y,t}$ = height of the water table above the impermeable layer at x, y, and time t; t = time since the start of the recharge; H = original height of the water table above the impermeable layer; L = length of the recharge basin (in y direction); W = width of the recharge basin (in x direction); v_a = arrival rate at the water table of water from the infiltration basin; f = fillable porosity (1> f >0); $F(\alpha,\beta) = \int_0^1 erf\left(\alpha/\sqrt{\tau}\right).erf\left(\beta/\sqrt{\tau}\right)d\tau$; $n = 1/\sqrt{4tT/f}$; $\alpha = (W/2 \pm x)n$; $\beta = (L/2 \pm y)n$. The values of $F(\alpha, \beta)$ are tabulated in the *Appendix L*. Beneath the center of a square basin ($L = W$, $x = y = 0$), the equation reduces to

$$h_{x,y,t} - H = \frac{v_a t}{f}\left\{F\left[(W/2)n, (W/2)n\right]\right\} \tag{15.15}$$

Similar solutions are available for circular spreading basins and for basins above sloping water tables. If recharge ceases at time t_0, dissipation of the mound can be calculated by superposing hypothetically on the flow system at $t = t_0$ a rate of uniform discharge equal to that of the infiltration rate. The algebraic sum of the two mounds yields the mound shape at any time after the end of recharge. After a very long time, the mound disappears and the water table acquires its original position.

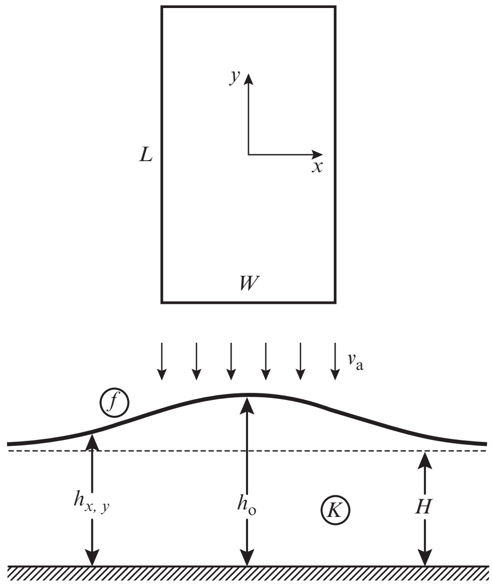

Figure 15.16 *Recharge mound beneath a rectangular basin*

15.8.5 Controls on Mound Growth

Under uniform recharge conditions, a mound will continue to grow until some control provides a limit. A *control* may be of potential type or lateral type. *Lateral control* occurs when the mound intersects a constant water elevation such as stream, lake, spring, or artificially maintained water table by pumping (Figure 15.17). For a large horizontal extent of this condition (existence of lateral control), the mound approaches an equilibrium with a constant recharge rate. On the contrary, in the absence of a lateral control the mound will keep on building until it reaches to the bottom of the recharging basin. This is the upper limit (potential limit) beyond which it can grow, thus the mound acquired its potential position. Henceforth, the mound away from the recharge basin continues to grow but as the head difference between the basin boundary (constant water surface) and far points go on decreasing due to continuous rising of the water table, and therefore the recharge rate diminishes with time in potential control conditions.

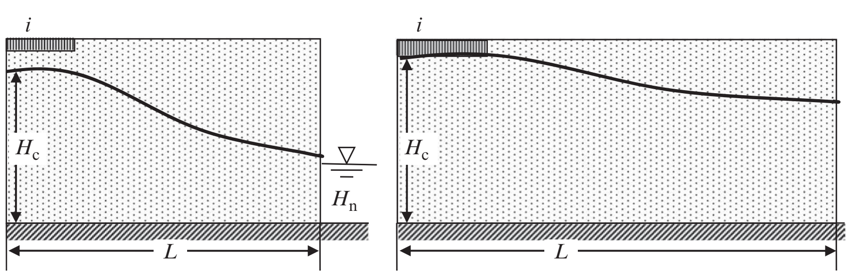

Figure 15.17 *Lateral control and potential control*

Based on other recharge experiments (i.e., fresh water recharge) in many of the western countries, the following intrinsic characteristics of the aquifer are recommended to ensure successful basin recharge operations.

1. A minimum of 18 m depth to the groundwater is required to allow for geo-purification processes (i.e., filtration, adsorption, etc.) before the infiltrating water reaches the groundwater. This depth also allows for groundwater mounding during the recharge process without affecting the infiltration process. The unsaturated zone must realize an infiltration rate not less than 0.25 m/d.
2. High values of saturated zone transmissivity and porosity are recommended to prevent water mounding below the basin bottom that can cause a decrease in infiltration rate and recharge capacity (effective porosity > 0.1 and transmissivity > 500 m^3/d).
3. Aquifer characteristics downstream the recharging sites must have good hydrogeological conditions to allow water recovery at the desired rates.

15.9 Recharge Scheme in Pal–Doli–Jhanwar Area

The study area comprising a total of 18 villages is located in the southwest of Jodhpur city. It has an aerial extent of 240 km^2. The satellite image of the area is shown in Figure 15.18 (see color Plate 5). The area has arid climate and erratic rainfall with high groundwater exploitation and favorable hydro-geological conditions. The mean annual rainfall is 372.6 mm, out of which 85 percent is received during the period from June to September. It is one of the highly groundwater-exploited area, and before the functioning of Rajasthan canal project it partly catered to water demand of Jodhpur as well as fulfilled the irrigation requirements of vegetables and cash crops. The depth of water table varies from 9 m to 62 m. Water yield from wells fitted with pump sets ranges from 70 to 200 m^3/d. The quality of groundwater in villages adjoining the hilly terrain is good for irrigation. It generally starts deteriorating in the areas away from outcrops and becomes saline to highly saline in the southern, southwest and western part of the study area.

Rainfall data from 1983 to 2004 have been used for runoff generation. The rainfall greater than 10 mm per day has been used for finding AMC conditions. Table 15.1 lists AMC conditions for year 2001. Considering the existing land use in the Pal–Doli–Jhanwar area, the runoff capabilities of the watersheds have been assessed by applying GIS methodology. The runoff has been generated by analysis of Landsat EMT plus satellite data. The satellite image of the study area of October 2000 with six band 28 m resolution has been acquired and has been processed on ERADAS. The GIS work has been done on ArcMap software. The satellite data have been classified using supervised classification and the land use has been classified in ten different classes as shown in Figure 15.19 (see color Plate 6).

Table 15.1 Daily rainfalls with AMC condition, year 2001

S. No.	*Date*	*Rain*	*Last 5 day rain*	*AMC condition*
1.	18 May	10	3	I
2.	19 May	17	13	II
3.	14 Jun	33.6	14.4	II
4.	17 Jun	11.5	42.1	III
5.	25 Jun	13.2	0	I
6.	26 Jun	18.2	13.2	II
7.	29 Jun	10.6	36.6	III
8.	2 Jul	49.4	15.8	II
9.	3 Jul	25.8	61	III
10.	9 Jul	13	6.4	I
11.	11 Jul	23	13.6	II
12.	12 Jul	10.2	36	III
13.	23 Jul	12.2	2.8	I
14.	24 Jul	12.7	15	II
15.	5 Aug	14.7	0	I
16.	11 Aug	21	3.2	I
17.	12 Aug	30.4	24.2	II

Table 15.2 Curve number of different classes for three AMC conditions

S.No.	*Class*	*Area (km^2)*	*AMC I*	*AMC II*	*AMC III*
1	Water	0.83	100	100	100
2	Plantation	4.67	44	65	81
3	Agricultural	27.33	45	66	82
4	Stream	9.06	27	47	67
5	Fallow	39.26	57	76	88
6	Settlement	2.34	69	84	92
7	Scrub	33.92	57	76	88
8	Waste	3.01	76	88	94
9	Road	0.27	69	84	92
10	Rocky	39.45	79	90	95

Then the CNs for each land use have been found (Table 15.2) using the land-use classification and soil type. The soil type have been selected by using soil information from Rocks and Minerals map of Jodhpur, Geological Survey of India, Jaipur, and field study. The CNs have been applied to the catchment for all the three AMC conditions and runoff maps have been generated (Figure 15.20, see color Plate 7).

Table 15.3 Annual runoff in MCM

S.No.	*Year*	*Runoff in MCM*	*S. No.*	*Year*	*Runoff in MCM*
1	1983	19.35	13	1995	40.12
2	1984	10.36	14	1996	21.46
3	1985	3.91	15	1997	7.61
4	1986	1.17	16	1998	25.35
5	1987	0.6	17	1999	4.44
6	1988	12.36	18	2000	0.58
7	1989	12.09	19	2001	6.9
8	1990	5.22	20	2002	0.64
9	1991	16.72	21	2003	10.65
10	1992	9.59	22	2004	4.91
11	1993	26.12		**Total**	249.77
12	1994	9.6		**Mean**	11.35

An average of this annual runoff has been calculated over a period of 22 years and this average runoff gives the total recharge potential of this area. The available average annual runoff from the selected area is about 11.35 MCM, but the annual variation is very high, so the recharging system warrants a storage reservoir of sufficient capacity to overcome these variations. The recharge system consisting of basins and ditches has been designed for two scenarios as shown in Figure 15.21 (see color Plate 8). One is for maximization of irrigation/recharge to groundwater and other is to allow some ecological flow in river and recharge the remaining water.

15.10 MAR in NCT of Delhi-Like Metro Cities

Rapid urbanization demands more water and leaves less pervious surface to groundwater recharge, which leads to quantity, quality, and sustainability-related water problems. Water supply in urban areas is mostly from surface sources such as natural or impounded reservoirs as well as from groundwater sources. As the population density is more, sources are planned and constructed to take care of the water requirements of the population throughout the year. Groundwater is in use in areas where the surface water supplies are either not reaching or are not adequate. Land use for constructed areas is more compared to open and barren land usage in urban areas. Therefore, small but effective recharge structures are required, which occupy smaller space and provide optimal recharge to groundwater. During rainy season, storm water drains exclusively containing rainwater flow up to brim. To harness the available runoff, trenches with recharge tube wells can be constructed inside the drain bed itself at a spacing of 100–300 m depending on the availability of runoff. The aquifer to be replenished is generally one which is already overexploited by tube well pumpage and the declining trend of water levels in the aquifer has set in. Because of the confining layers of low permeability, the aquifer cannot get natural replenishment from the surface and needs direct recharge through wells or shafts. Accordingly, the depth of recharge tube wells constructed inside the drain bed itself should reach the main aquifer to be recharged as shown in Figure 15.22. Depending upon the ratio of depth to slope of the drain walls, a small baffle wall of 0.6–1.0 m height is constructed to retain the water. The catchments should be maintained neat and clean, no mixing of sewerage and other water should be allowed, and open spaces around the storm water drains should be prevented from dumping of unwanted items and scrap material. Open storm water drains are covered with perforated detachable RCC slabs to maintain these drains and prevent pollution and contamination.

In urban areas mega structures, such as flyover, airports, stadium, metro, etc., cover huge area with concrete and prevents natural recharge to take place. Such giant civil structures generate large amount of surface runoff during the rains because of their runoff coefficient range varying from 0.6 to 0.8. To provide a conduit to rainwater to reach to aquifer certain recharge structures may be constructed in the vicinity of these mega civil structures. From the road surface lot of runoff goes waste through storm water drains. To harness this runoff, either trenches or shafts with recharge wells may be constructed in series along the road side at a spacing of 100–300 m depending on the availability of runoff. In

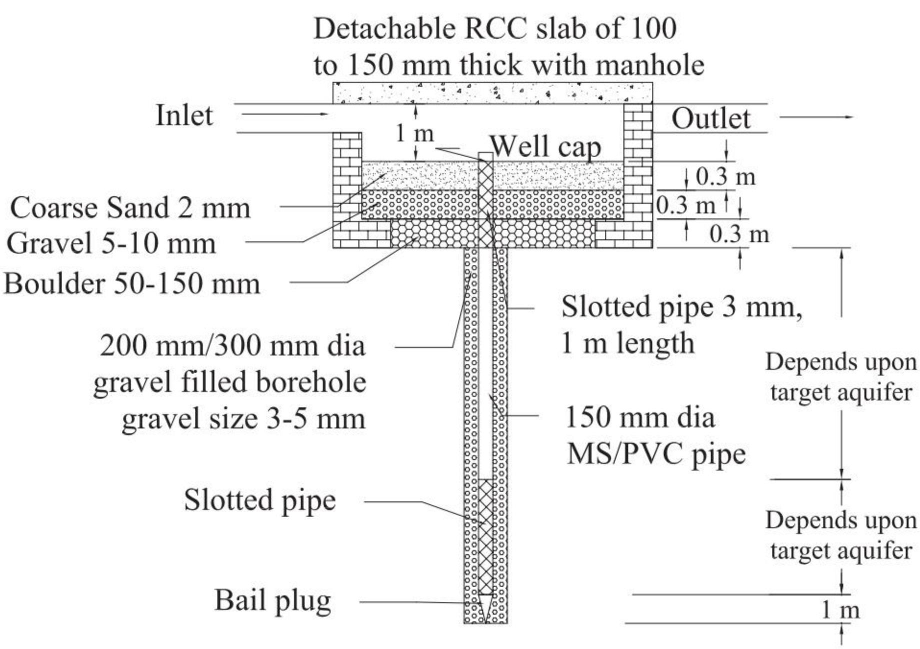

Figure 15.22 *Storm water recharge system*

Delhi, several flyovers generate enormous amount of surface runoff, which can be harvested by making shaft or trenches with recharge wells along the storm water drains. Similarly, the metro network in Delhi generates huge quantity of runoff, which can easily be harvested for recharging the groundwater. Trenches with length up to 20 m can be constructed with two or more than two recharge tube wells as shown in Figure 15.23. Generally, these trenches are recommended tapping runoff generated from whole campus/catchment of areas ranging from 10,000 to 40,000 m^2. As the runoff from the whole catchment consists of lot of silt, the same can be removed by constructing a desiltation chamber. The main advantage of recharge trenches is that they can recharge runoff generated from large areas.

BIS code on subsurface reservoirs may be consulted while constructing the recharge trenches. If the trenches are constructed in storm water drains where the polluted water is expected during the lean period or nonmonsoon months, a bypass arrangement may be made so that no polluted water enters into the recharge trenches.

Available water resources in NCT of Delhi are limited and limited quota of fresh water is being supplied to Delhi from the other states. The main issues related to groundwater in NCT of Delhi (CGWB 2014) are as follows:

1. High rate of population growth and high level of urbanization has resulted in over-development of groundwater resources.
2. In about 75 percent area of NCT, Delhi groundwater levels are declining at an alarming rate.
3. Out of 9 assessment units, 7 are overexploited and 2 are safe from groundwater development point of view.
4. Groundwater level has depleted by 8 m in the last 10 years in some areas.
5. Groundwater has been contaminated in several areas.
6. Major part is facing groundwater quality and quantity problems.

Overexploitation of groundwater has detrimental environmental consequences, and hence it needs to be effectively prevented by artificial groundwater recharge. The rainwater harvesting potential in Delhi is quite high, for example, average annual rainfall = 60 cm; considering runoff coefficient (rooftop/paved area) = 0.80 and efficiency due to evaporation and other losses = 0.8, the yearly rainwater harvesting yield/potential = 3840 m^3/ha. The rainwater harvesting and recharge pilots implemented in NCT Delhi (CGWB 2000) by utilizing runoff generated from rooftop, roads, paved area, and bare ground are

- Presidents Estate (Figure 15.24)
- Prime Minister's Office
- Shram Shakti Bhawan (Figure 15.25)
- Lodhi garden
- Safdarjung Hospital
- Tughlak Lane and surrounding areas
- Bunglow-5, Janpath Road
- Sena Bhawan
- Sultan Garhi Tomb (Figure 15.26)
- Kushk Nala artificial recharge project (Figure 15.27)

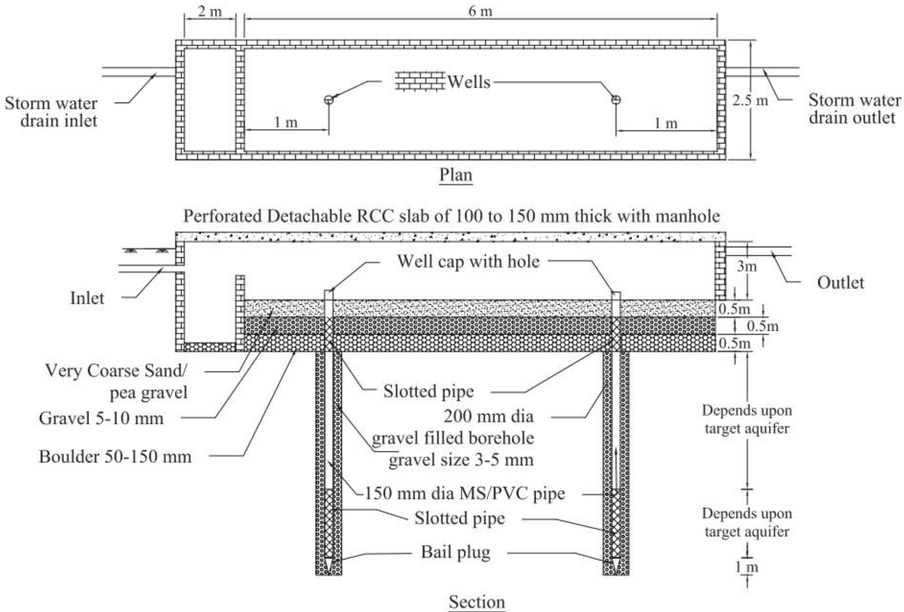

Figure 15.23 *Recharge trench with recharge wells*

In President Estate, runoff generated from 1.3 km^2 of area and drain of swimming pool are being recharged through two abandoned dug wells, one recharge shaft and two trenches with borewells. This has resulted in a rise in water levels ranging from 0.66 to 4.10 m. In Sharamshakti Bhawan, 3000 m^3 run-off is being recharged annually from 2001 through 3 set of trench and recharge wells system (Figure 15.25), which resulted in a rise in water levels ranging from 1.68 to 3.33 m in August 2007. Kushk Nala has a catchment area 5.59 km^2 and hence water availability is about 0.6 million m^3 per year, which is being recharged through 24 set of trench and recharge well systems (Figure 15.27) and resulted in a rise in water levels about 1 m annually. Similar trench and recharge wells system has been installed in Indira Gandhi International Airport premises. Rooftop rainwater harvesting scheme in Block-VI of IIT, Delhi campus, is recharging groundwater through construction of injection wells and abandoned dug well. It should be noted that about 830 m^3 of rainwater is recharged from the 1660 m^2 of roof area, which resulted in a rise in water level to the tune of about 2.29–2.87 m in 1 ha of area.

Summary: The artificial recharge is the augmentation of underground aquifers by some methods of construction or by artificially changing the natural conditions. Methods available are water spreading, recharge through pits and wells, and recharge from water bodies. The protection, management, and restoration of water bodies also help to recharge the groundwater. Artificial groundwater recharge from rainwater harvesting and treated waste water are also important

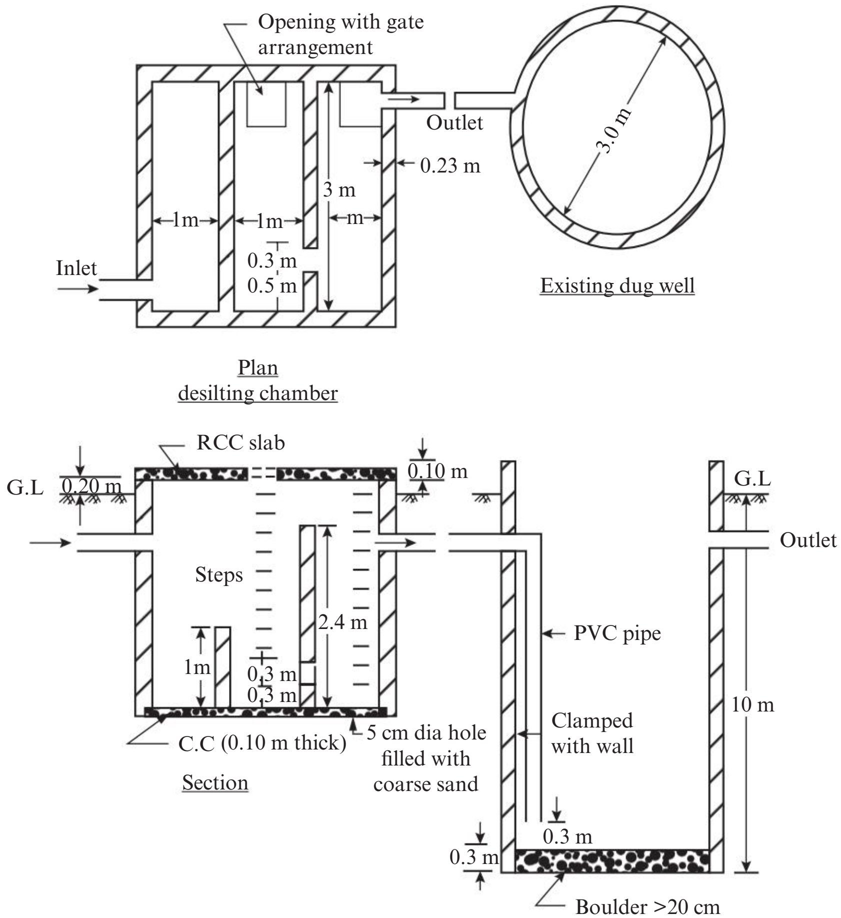

Figure 15.24 *Dug well recharge in President's Estate*

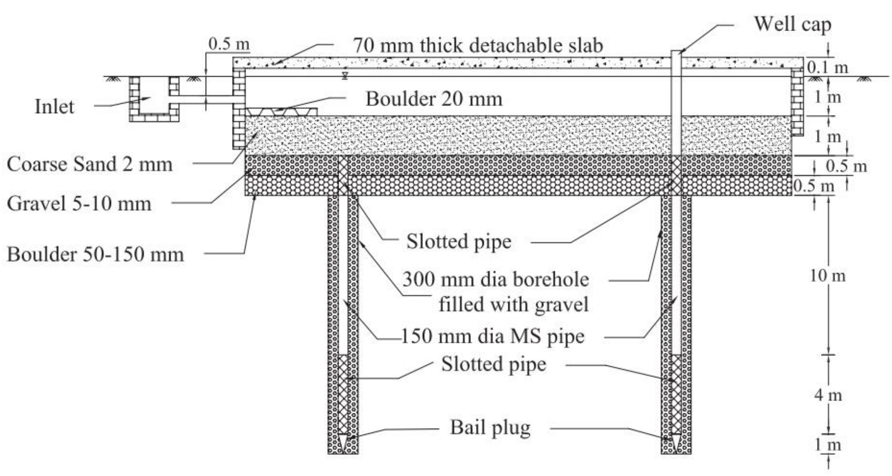

Figure 15.25 *Recharge shaft with injection well in Shram Shakti Bhawan*

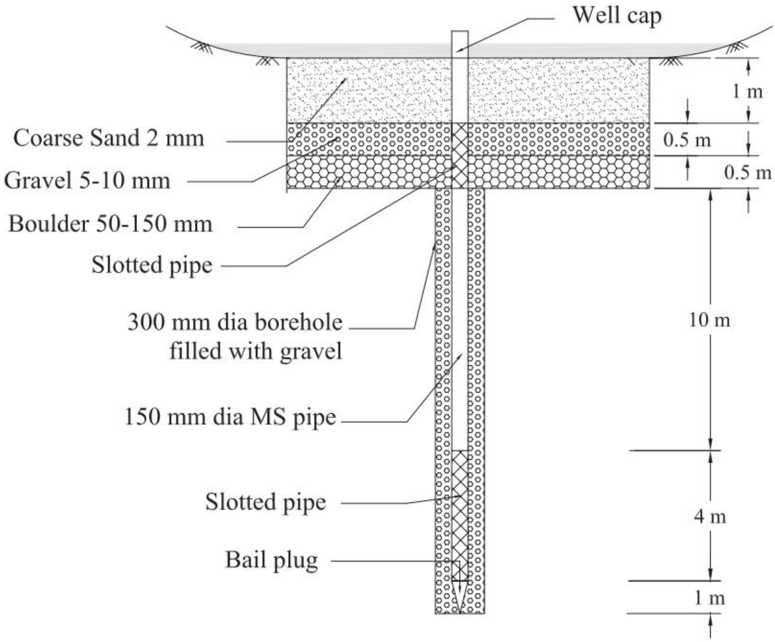

Figure 15.26 *Recharge well in Sultan Garhi Tomb*

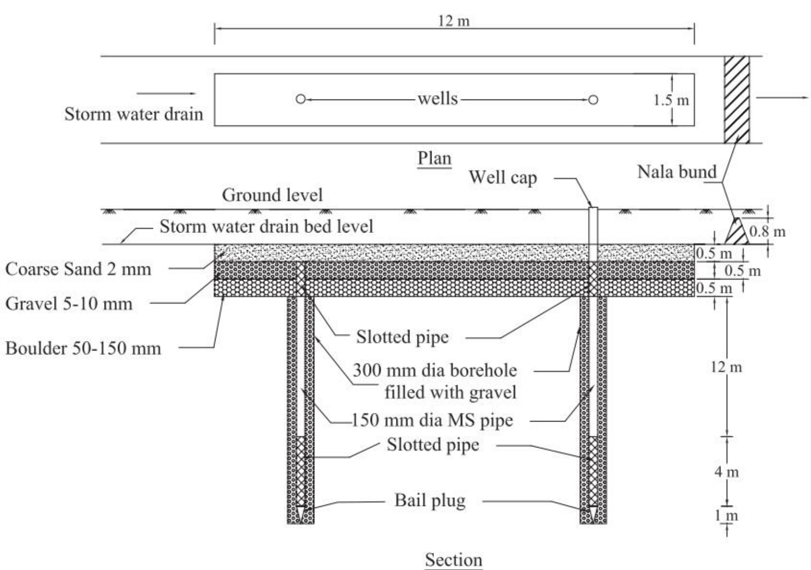

Figure 15.27 *Recharge scheme in Kushk Nala*

options. Use of aquifers as storage and distribution system of artificially recharged water is beneficial for rural population as it ensures availability of good quality water in remote areas not connected by surface distribution system. Depending on geomorphologic and physiographic conditions as well as conditions suitable for recharge, and availability of source water, suitable methods for water harvesting and artificial recharge can be used. Pilot testing of aquifer recharge systems is preferred to confirm whether they work satisfactorily and how they should best be managed before large projects are installed with considerable investment. Pilot testing is also desirable for simpler systems of basins, trenches, vadose zone wells, and aquifer wells, because their design, performance, and management depend to a large extent on local conditions of soil, hydrogeology, climate, and water quality. The golden rule in artificial recharge is to start at a small scale, learn as one goes, and expand as per requirement.

SOLVED EXAMPLES

Example 15.1: A restricting layer of 3.5 m is detected in the vadose zone. The top of the restricting layer is 8 m below the bottom of the recharge basin. The hydraulic conductivities of the restricting layer and soil above this are 0.03 m/d and 8 m/d. To maintain the recharge unimpeded, the water level should be at least 1 m below the top surface. Determine the maximum infiltration rate for the current situation.

Solution: Given data—$K_r = 0.03\,\text{m/d}$; $K_s = 8\,\text{m/d}$; $L_r = 3.5\,\text{m}$; maximum height of mound to keep unimpeded the recharge would be $L_p \le 8 - 1 = 7\,\text{m}$.

Using $L_p = \dfrac{L_r\left[\dfrac{i}{K_r} - 1\right]}{1 - \dfrac{i}{K_s}} \Rightarrow 7 \le \dfrac{3.5 \times \left[\dfrac{i}{0.03} - 1\right]}{1 - \dfrac{i}{8}} \Rightarrow i \le 0.0893\,\text{m/d}$, so as to keep the recharge rate free from interruption the recharge rate should be less than 0.0893 m/d.

Example 15.2: A lake is constructed artificially having plan area of 3000 m × 300 m. Saturated thickness of the aquifer is 30 m and depth of the bedrock is 45 m below the lake. The average transmissivity of the area is 1000 m²/d and leakage from lake is at about 0.5 m/d. Determine how far should the control be established from the center line of the lake assuming stead-state conditions and no natural groundwater gradient and if maximum permissible rise in groundwater mound above the bed rock limited to 45 m?

Solution: Given data—$W = 300\,\text{m}$, $L = 3000\,\text{m}$; Maximum rise in groundwater mound $H_c = 45\,\text{m}$; Thickness of the aquifer $H_n = 30\,\text{m}$; $T = 1000\,\text{m}^2/\text{d}$. As 3000/300 = 10, which is greater than 5, hence area can be treated as the strip recharge area. Using Eqn. (15.12) for the ultimate rise of a groundwater mound below the center of the recharge strip $H_c - H_n = \frac{iW}{2T}\left[\frac{W}{4} + L_n\right] \Rightarrow$ $45 - 30 = \frac{0.5\times 300}{2\times 1000}\left[\frac{300}{4} + L_n\right] \Rightarrow L_n = 125$. Thus, the control area should be established at 125 + 150 = 275 m from center line of the lake.

Example 15.3: A rectangular recharge basin has total area of $260\times 10^4\ \text{m}^2$ and transmissivity of the aquifer of this area is 800 m^2/d. If the maximum permissible rise in recharge mound above the original groundwater table is 22 m, then plot the permissible versus distance of the control area from center line of the recharge basin. Assume the original water table is maintained along the perimeter of the control area.

Solution: Area of the rectangular recharge basin $A = 260\times 10^4\ \text{m}^2$, hence equivalent radius $R = \sqrt{\frac{(260\times 10^4)}{\pi}} = 909.728\,\text{m}$. As given that maximum rise in water table = 22 m or $H_c - H_n = 22\,\text{m}$. Also, $T = 800\,\text{m}^2/\text{d}$. Using Eqn. (15.13) for the equilibrium height of the mound below the center of the recharge system, $H_c - H_n = \frac{iR^2}{4T}\left[1 + 2\ln\left(\frac{R_n}{R}\right)\right] \Rightarrow 22 = \frac{i\times 909.728^2}{4\times 8000}$ $\left[1 + 2\ln\left(\frac{R_n}{909.728}\right)\right] \Rightarrow i_{max} = \frac{0.0851}{\left[1 + 2\ln\left(\frac{R_n}{909.728}\right)\right]}$. With this equation maximum infiltration rate versus distance of control area from center line of recharge area values are tabulated and plotted (Figure 15.28) as below.

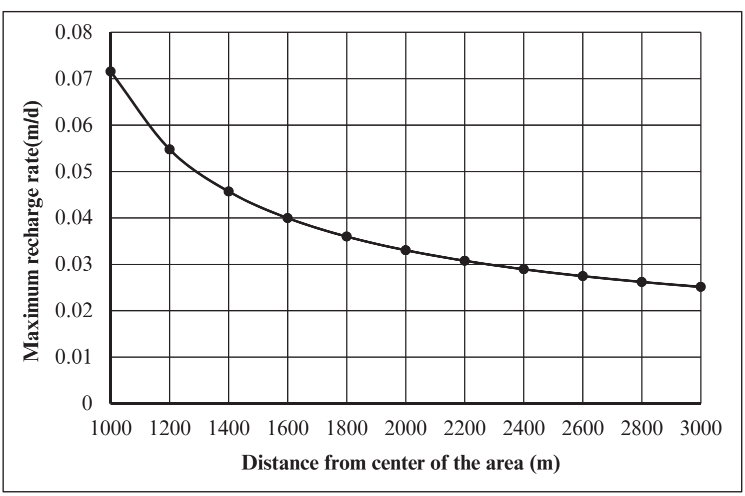

Figure 15.28 *Recharge rate versus distance plot*

R_n (m)	1000	1200	1400	1600	1800	2000	2200	2400	2600	2800	3000
i_{max} (mld)	0.072	0.055	0.046	0.040	0.036	0.033	0.031	0.029	0.027	0.026	0.025

Example 15.4: A small watershed consists of 1.5 km^2 of cultivated area (runoff coefficient $C = 0.20$), 2.5 km^2 under forest ($C = 0.10$), and 1 km^2 under grass cover ($C = 0.35$). There is a fall of 22 m in a water course length of 1.8 km length. The intensity duration relationship for the area may be taken as $i = 80\dfrac{T_r^{0.2}}{(t+13)^{0.46}}$ where i = rainfall intensity in cm/h, T_r = return period in years, and t = rainfall duration in minutes. Estimate the peak rate of runoff for a 25-year return period.

Solution: Length of the water course = 1.8 km = 1800 m and fall in the elevation = 22 m, hence slope S = 22/1800. Time of concentration can be computed by Kirpich formula $t_c = 0.0195L^{0.77}S^{-0.385} \Rightarrow t_c = 0.01951800^{0.77}$ $\left(\dfrac{22}{1800}\right)^{-0.385}$ = 34 minutes. As $i = 80\dfrac{T_r^{0.2}}{(t+13)^{0.46}} = 80\dfrac{25}{(34+13)^{0.46}} = 25.9$ cm/h

Further-more, $A_1 = 1.5$ km^2, $C_1 = 0.20$; $A_2 = 2.5$ km^2, $C_2 = 0.10$; and $A_3 = 1$ km^2, $C_3 = 0.35$ hence, using Eqn. (15.2) for equivalent runoff coefficient $C_e = \dfrac{0.2\times1.5+0.1\times2.5+1\times0.35}{1.5+2.5+1} = 0.18$. Therefore, the peak discharge $Q_p = 0.18\times0.259\times\dfrac{1}{3600}\times5.0\times10^6 = 64.75\,\text{m}^3/\text{s}$.

PROBLEMS

15.1 Compute the height of the perched mound above a restrictive layer of 3 m thick having hydraulic conductivity = 9 mm/d if the infiltration rate = 30 mm/d and hydraulic conductivity of the main aquifer = 2 m/d.

15.2. The thicknesses of the restrictive layer and the soil layer above the restricting layer are 3 m and 9.0 m, respectively, while their hydraulic conductivities are 0.02 m/d and 8.0 m/d, respectively. What can be recharge rate to keep the water table at least 1 m below the bottom of basin?

15.3. It is planned to recharge 60 MCM water annually from a recharge basin of 300 m × 30,000 m size into an aquifer having initial saturated thickness = 30 m and transmissivity = 2000 m^2/d. Determine the location of the control area if the recharge mound is restricted to 40 m.

15.4. A square recharge basin 1 km × 1 km is proposed in a locality where the initial saturated thickness of unconfined aquifer is 50 m and its transmissivity is 1000 m^2/d. If the maximum allowable rise in the water table over its original position is 20 m, compute (i) location of the control for recharge rate = 0.12 m/d and (ii) permissible recharge rate for control area at 5 km.

15.5. A circular recharge basin with a radius of 500 m will be established over an unconfined aquifer having transmissivity of 450 m^2/d and initial position of water table at 75 m bgl. If estimated recharge rate is 0.15 m/d and the control area is located at 1.5 km from the center of the basin, determine the final position of the water table below the center of the basin.

15.6. State the purpose and necessity of artificial recharge of groundwater. Also, describe recharge mound.

15.7. How does a well near a stream recharge groundwater? Describe methods of estimating recharge fractions in discharge and volume of pumped water from the well.

15.8. Why does the rate of recharge from a well diminish with time?

15.9. A basin 400 m × 3000 m is proposed to recharge 6×10^7 m^3 per year. The initial depth of water table = 45 m, saturated thickness of aquifer = 25 m, and transmissivity = 1825 m^2/d. If the maximum allowable rise in mound is 35 m, determine the location of production wells.

15.10. A basin 300 m × 2500 m is proposed to recharge 5×10^7 m^3 per year. The initial depth of water table = 40 m, saturated thickness of aquifer = 20 m, and transmissivity = 1800 m^2/d. If the maximum allowable rise in mound is 30 m, determine the location of production wells.

PLATE 5

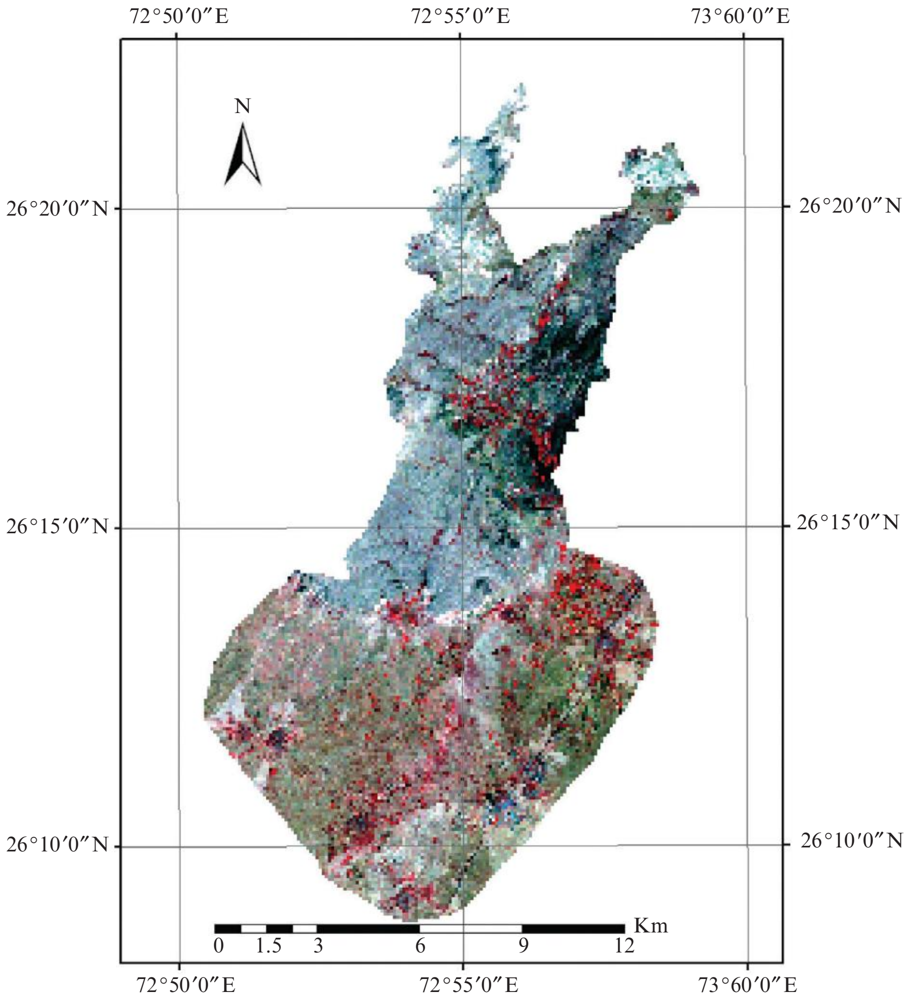

Figure 15.18 *Satellite image of Pal–Doli–Jhanwar area*

PLATE 6

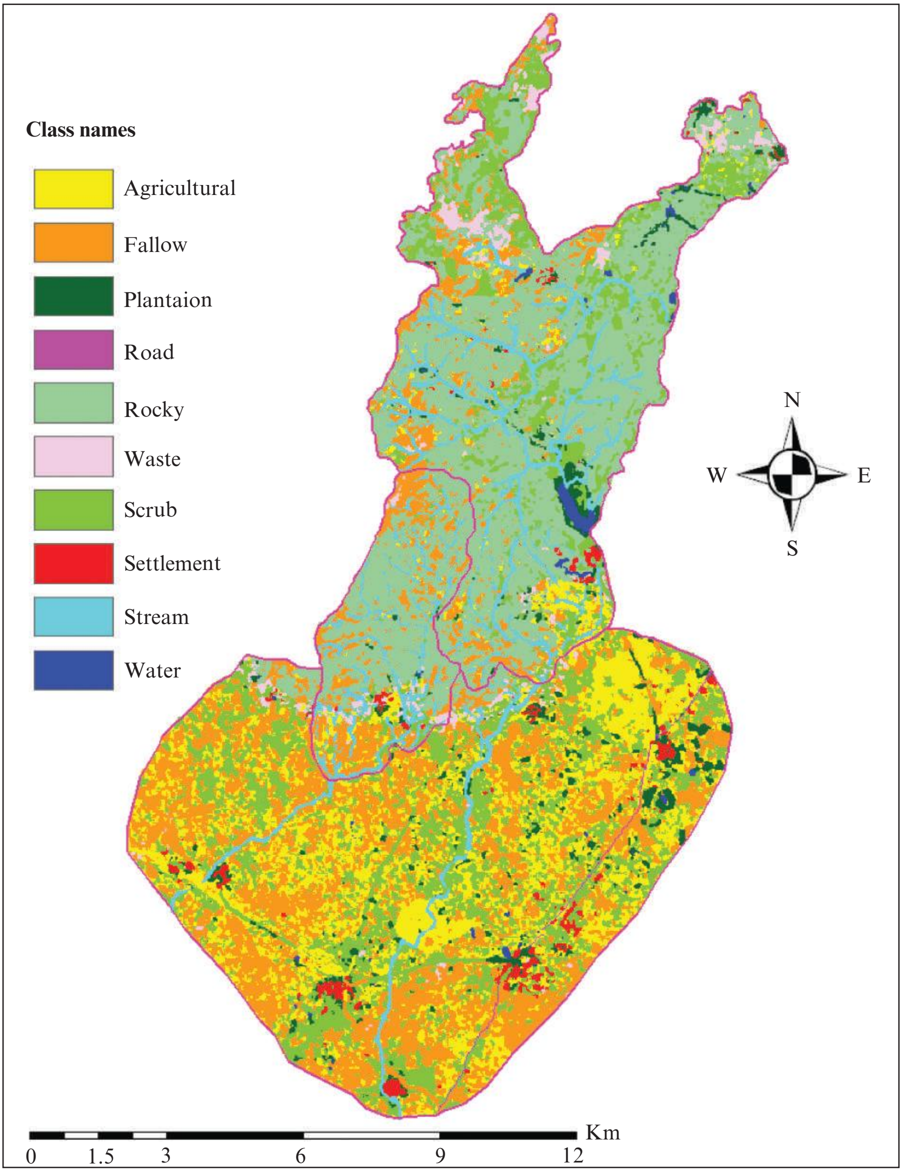

Figure 15.19 *Classified land-use image of the Pal–Doli–Jhanwar area*

PLATE 7

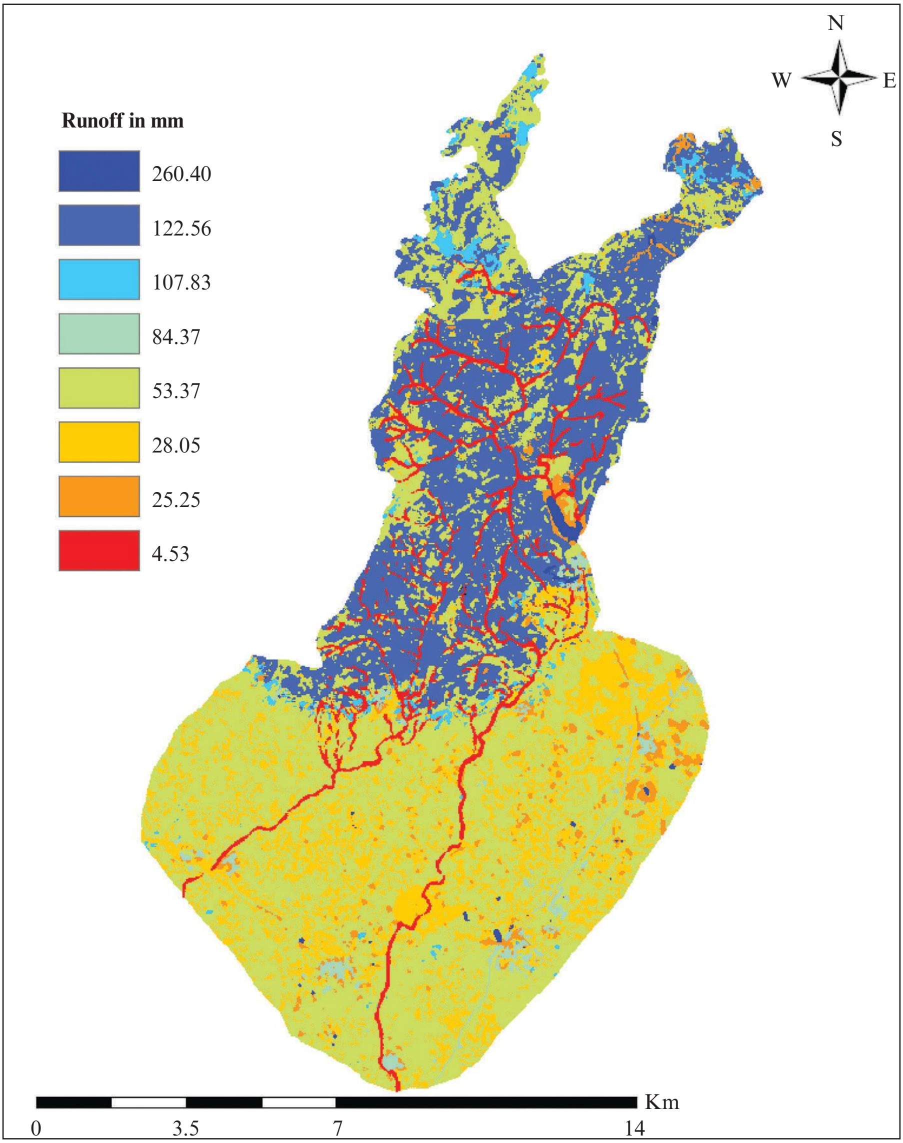

Figure 15.20 *Total depth of runoff in mm for year 2001*

PLATE 8

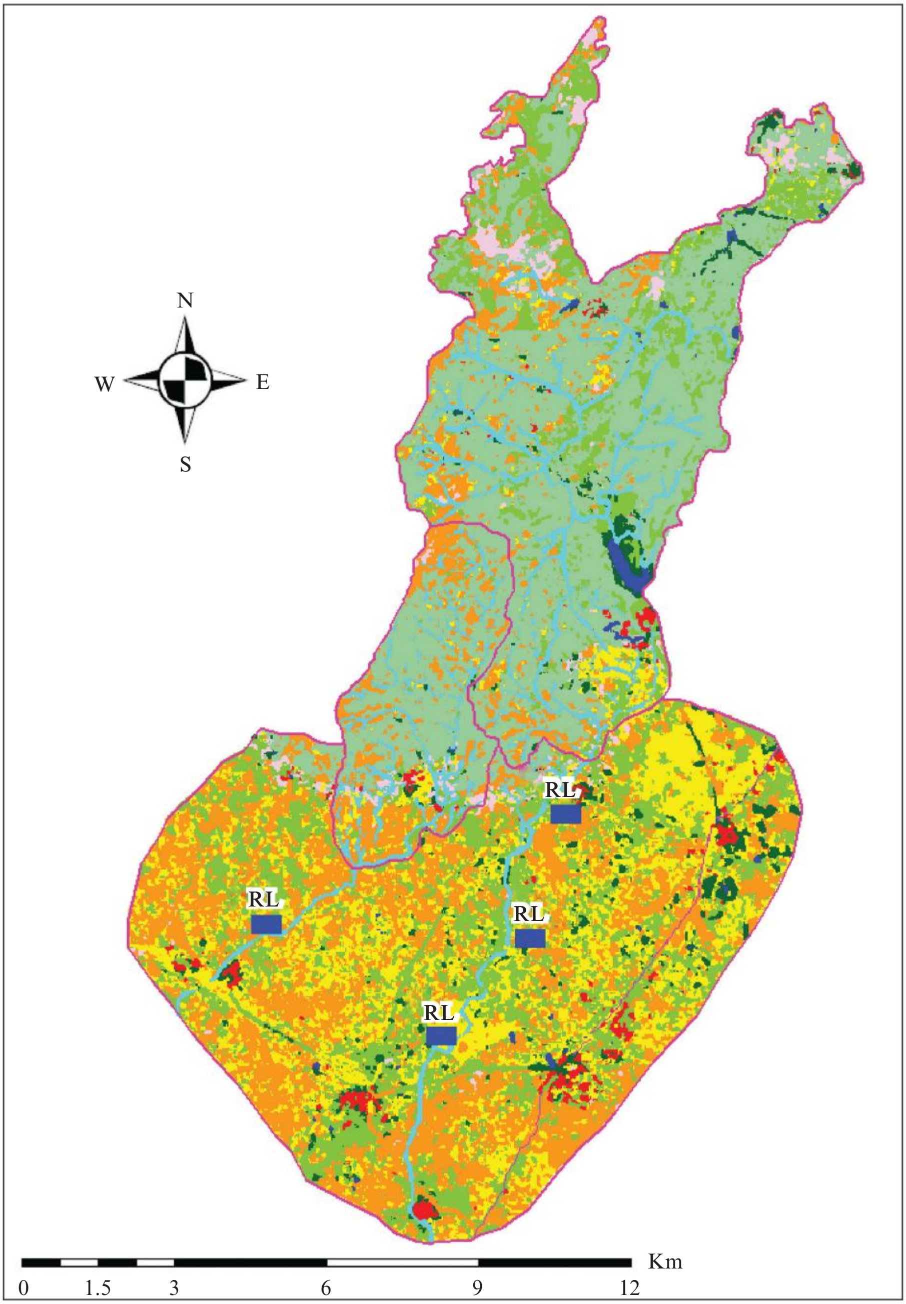

Figure 15.21 *Proposed recharge locations (RL)*

Chapter 16

Saline Water Intrusion In Aquifers

16.1 General

Saline/saltwater is the most common pollutant in fresh groundwater. *Intrusion of saline water* occurs where saline water displaces or mixes with freshwater in an aquifer. When freshwater heads are lowered by withdrawals through wells, the freshwater–saltwater contact migrates toward the point of withdrawals until a new balance is established. The movement of saltwater into zones previously occupied by freshwater is referred to as *saline water intrusion* or *saltwater encroachment*. Saltwater encroachment is a serious problem in some coastal area. This phenomenon can occur in deep aquifers with the upward advance of saline waters of geologic origin, in shallow aquifers from surface waste discharges, and in coastal aquifers from an invasion of seawater. In coastal areas, fresh groundwater derived from precipitation on the land comes in contact with and discharges in to the sea or in to estuaries containing brackish water. The relation between freshwater and saline water is controlled mainly by the differences in their densities. Thus, freshwater being less dense than the seawater tends to override or floats on the saline water. But at greater depths groundwater movement is much less, so that displacement of saline water is slower. As the occurrence of saline water intrusion is extensive and represents a special category of groundwater pollution, number of examples of salinity ingress/seawater intrusion exists all over the world including India. The basic concepts of salinity ingress/seawater intrusion is available in books by Todd and Mays (2005), Walton (1970), Freeze and Cherry (1979), etc. The intrusion of seawater is a complex phenomenon, controlled by several factors, such as heterogeneities in the subsurface, anisotropy in hydraulic properties, hydraulic gradient, salinity distribution, etc.; therefore, for optimal groundwater management in future, it is important to understand, conceptualize, and adequately characterize the aquifer systems from this point of view.

16.2 Occurrence of Saline Water Intrusion

Many fresh groundwater sources are in close proximity to the sea, saline lakes, brackish groundwater, or salty effluent wastes. Typically, shallow freshwater overlies saline water, but at greater depths brines are present. Many small oceanic islands are completely underlain with aquifers containing saline water; these pose special problem in meeting water supply demands. Saltwater intrusion into fresh groundwater formations generally results from activities of humans. Saline water in aquifers may be derived from any of the several sources:

1. encroachment of seawater in coastal areas
2. seawater that entered aquifers during past geologic time
3. salt in salt domes, thin beds, or disseminated in geologic formations
4. water concentrated by evaporation in tidal lagoons, playas, or other enclosed areas
5. return flows to streams from irrigated lands
6. domestic, commercial, and industrial saline waste

The mechanisms responsible for saline water intrusion fall into three categories: (i) reduction or reversal of groundwater gradients, which permits denser saline water to displace freshwater. This situation commonly occurs in coastal aquifers in hydraulic continuity with the sea when pumping of wells disturbs the natural hydrodynamic balance; (ii) destruction of natural barriers that separates fresh and saline waters, such as construction of coastal drainage canal that enables tidal water to advance inland and to percolate into a freshwater aquifer; and (iii) subsurface disposal of waste saline water, such as into disposal wells, landfills, or other waste repositories.

16.3 Ghyben–Herzberg Relation Between Fresh and Saline Waters

Ghyben and Herzberg independently found that saltwater occurred underground, not at sea level but at a depth below sea level of about 40 times the height of the freshwater above mean sea level (msl). This is attributed to a hydrostatic equilibrium existing between the two fluids of different densities. The hydrostatic balance between freshwater and saline water can be obtained by equating pressures on each side of a U-tube as shown in Figure 16.1. Thus,

$$\rho_s g z = \rho_s g(z + h_f) \tag{16.1}$$

where ρ_s is the density of the saline water, ρ_f is the density of the freshwater, z is the height of saline water column above the interface, and h_f is the height of freshwater column above the saline water level (Figure 16.1). Solving for z yields

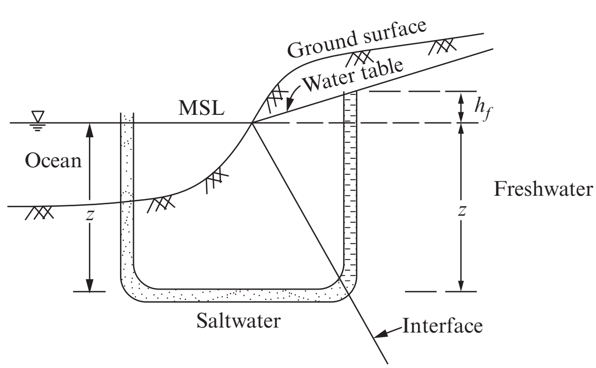

Figure 16.1 *Freshwater and saltwater equilibrium*

$$z = \frac{\rho_f}{\rho_s - \rho_f} h_f = \delta\, h_f \tag{16.2}$$

which is the Ghyben–Herzberg relation wherein $\delta = \rho_f / (\rho_s - \rho_f)$. For typical seawater conditions (ρ_s = 1025 kg/m^3 and ρ_f = 1000 kg/m^3) δ = 40, thus

$$z = 40 h_f \tag{16.3}$$

At the interface, it actually is a hydrodynamic rather than a hydrostatic balance because freshwater is flowing toward the sea. From density considerations alone, without flow, a horizontal interface would develop with freshwater everywhere floating above saline water. Where the flow is nearly horizontal, the Ghyben–Herzberg relation gives satisfactory results. However, near the shoreline, where vertical flow components become pronounced, significant errors in the position of the interface occur. For confined aquifers, the Ghyben–Herzberg relation can also be applied by replacing the water table by the piezometric surface. It is important to note that freshwater—saline water equilibrium requires that the water table or piezometric surface (i) lie above sea level and (ii) slope downward toward the ocean, otherwise, seawater will advance directly inland.

It may be noted that Ghyben–Herzberg relationship holds good only in case of homogeneous and isotropic aquifer in which freshwater is static and is in contact with tide-less sea or brackish water body. The thickness of the freshwater zone in a homogenous and isotropic aquifer is greater than that predicted by the Ghyben–Herzberg equation because both the seawater and freshwater are in motion (not static). On the contrary, in a stratified aquifer, the thickness of the freshwater lens is less than that predicted because of the head loss incurred as the freshwater moves across the least permeable beds.

16.4 Shape of the Freshwater–Saltwater Interface

Glover (Todd and Mays 2005) obtained solution for the shape of the interface using potential flow theory as

$$z^2 = \delta \frac{2qx}{K} + \left(\delta \frac{q}{K} \right)^2 \tag{16.4}$$

where K is the hydraulic conductivity of the aquifer and q is the freshwater flow per unit length of shoreline. The corresponding shape of the water table is given by

$$h_f = \sqrt{\frac{1}{1+\delta} \frac{2qx}{K}} \tag{16.5}$$

The width x_0 of the submarine zone through which freshwater discharge into the sea (see Figure 16.2) can be obtained for $z = 0$, yielding

$$x_0 = \delta \frac{q}{2K} \tag{16.6}$$

The depth of the interface z_0 beneath the shoreline (at $x = 0$) will be

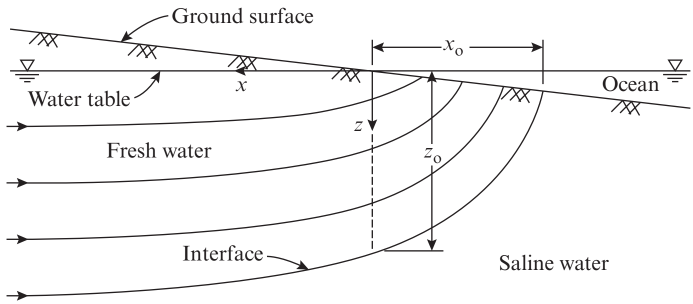

Figure 16.2 *Shape of freshwater—saltwater interface (Todd and Mays 2005)*

$$z_0 = \delta \frac{q}{K} = 2x_0 \tag{16.7}$$

In reality, a sharp interfacial boundary between freshwater and saline water does not occur under field conditions. Instead, a brackish transition zone of finite thickness separates the two fluids (Figure 16.3). This zone develops from dispersion by flow of the freshwater plus unsteady displacement of the interface by external influences such as tides, recharge, and pumping of wells. In general, the greatest thickness of transition zones are found in highly permeable coastal aquifers subject to heavy pumping. Where tidal action is the predominant mixing mechanism, the thickness of the transition zone is greatest near the shoreline. The salinity concentration varies from freshwater level to saltwater level in the transition zone. An important consequence of the transition zone and its seaward flow is the transport of saline water to the sea.

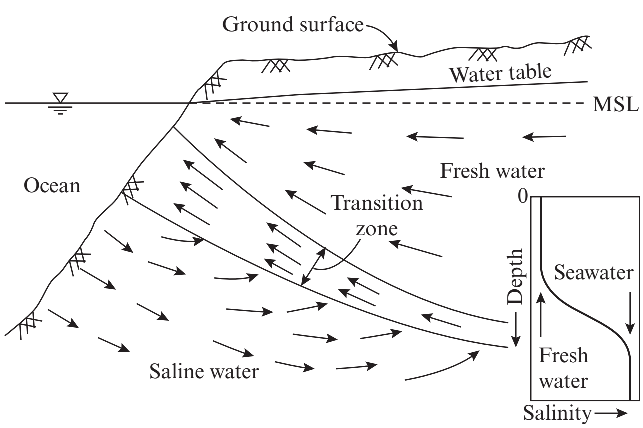

Figure 16.3 *Transition zone and salinity variation in transition zone*

16.5 Effect of Wells on Seawater Intrusion

The positions of freshwater–saltwater interface in isotropic homogeneous confined aquifer with a horizontal impervious base as shown in Figure 16.4 and with Ghyben–Herzberg assumption can be given as

$$x = \frac{(1+\delta)}{\delta^2}\frac{Kz^2}{2q} \tag{16.8}$$

Therefore, the length of the saltwater wedge (from shoreline to toe of the interface) becomes

$$L = \frac{(1+\delta)}{\delta^2}\frac{Kb^2}{2q} \tag{16.9}$$

where, b = depth to bedrock below MSL in unconfined aquifer or thickness of the confined aquifer.

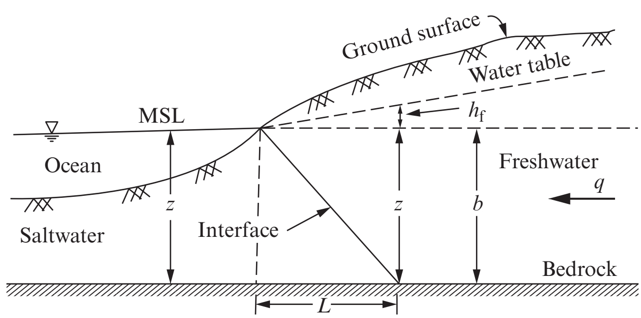

Figure 16.4 *Interface in aquifer with horizontal bedrock*

If a well is located near the coast line and pumped for freshwater, it affects the underlying interface. The well is near a water body (constant head boundary) in a uniform flow field (freshwater is moving toward the sea with discharge per unit shoreline = q). It is equivalent to two wells of equal strength and opposite nature in a uniform flow field; a stagnation point and corresponding capture zone will be formed for a particular well discharge. Strack (1976) considered the effect of a single well on seawater intrusion by assuming isotropic homogeneous aquifer with a horizontal impervious base and with horizontal freshwater flow and no flow in the saltwater zone. The relationship for the toe of the interface under steady conditions is

$$\frac{(1+\delta)}{\delta^2}\frac{Kb^2}{2q} = x + \frac{Q_w}{4\pi q}\ln\left(\frac{(x-x_w)^2+y^2}{(x+x_w)^2+y^2}\right) \tag{16.10}$$

or

$$\frac{(1+\delta)}{\delta^2}\frac{b^2}{2} = \frac{qx}{K} + \frac{Q_w}{4\pi K}\ln\left(\frac{(x-x_w)^2+y^2}{(x+x_w)^2+y^2}\right) \tag{16.11}$$

where, Q_w = steady well discharge, (x_w, 0) are the coordinates of the well with the origin at shoreline, and (x, y) are the coordinates of the toe of the interface as shown in Figure 16.5. The coordinates of the stagnation point (x_s, y_s) for this case (two wells of equal strength and opposite nature in a uniform flow field) are

$$x_s = x_w\sqrt{1-\frac{Q_w}{\pi q x_w}}; \qquad y_s = 0 \tag{16.12a, b}$$

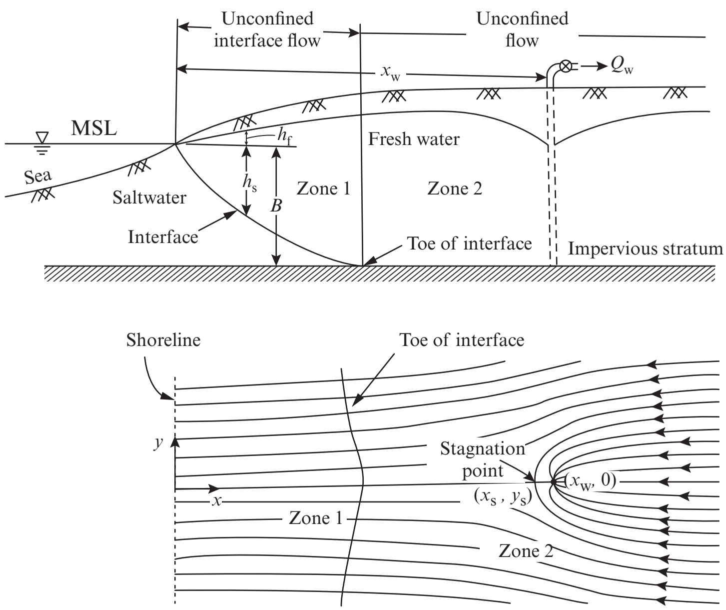

Figure 16.5 *Well in a coastal aquifer of finite thickness*

An unstable critical situation occurs when the toe of the interface passes through the stagnation point. Substituting $x = x_s$, and $y = y_s = 0$ in Eqn. (16.10)

$$\frac{(1+\delta)}{\delta^2}\frac{Kb^2}{2q} = x_s + \frac{Q_w}{4\pi q}\ln\left(\frac{(x_s - x_w)^2}{(x_s + x_w)^2}\right) = x_s + \frac{Q_w}{2\pi\, q}\ln\left(\frac{(x_w - x_s)}{(x_w + x_s)}\right) \tag{16.13}$$

Dividing by x_w and rearranging

$$\frac{(1+\delta)}{\delta^2}\frac{Kb^2}{qx_w} = 2\frac{x_s}{x_w} + \frac{Q_w}{\pi\, qx_w}\ln\left(\frac{(1-x_s/x_w)}{(1+x_s/x_w)}\right) \tag{16.14}$$

From Eqn. (16.12) $\dfrac{x_s}{x_w} = \sqrt{1-\dfrac{Q_w}{\pi\, qx_w}}$; therefore, the expression for computing the critical well discharge Q_w becomes

$$\frac{(1+\delta)}{\delta^2}\frac{Kb^2}{qx_w} = 2\sqrt{1-\frac{Q_w}{\pi\, qx_w}} + \frac{Q_w}{\pi qx_w}\ln\left(\frac{1-\sqrt{1-Q_w/\pi\, qx_w}}{1+\sqrt{1-Q_w/\pi qx_w}}\right) \tag{16.15}$$

or

$$\lambda = 2\sqrt{1-\mu} + \mu \ln\left(\frac{1-\sqrt{1-\mu}}{1+\sqrt{1-\mu}}\right) \tag{16.16}$$

where,

$$\mu = \frac{Q_w}{\pi q x_w} \tag{16.17}$$

and

$$\lambda = \frac{(1+\delta)}{\delta^2} \frac{Kb^2}{q x_w} \tag{16.18}$$

Equation (16.16) requires a trial and error solution for μ and hence for the critical discharge.

16.6 Effect of Tides on Seawater Intrusion

Tides cause saltwater to alternately invade and retreat from the freshwater zone, the result being a zone of diffusion across which salinity changes from that of freshwater to that of seawater. A part of the seawater that invades the freshwater zone is entrained in the freshwater and is flushed back to the sea by the freshwater as it moves to the sea to discharge. In coastal aquifers in contact with the ocean, sinusoidal fluctuations of groundwater levels occur in response to tides. If the sea level varies with a simple harmonic motion, a train of sinusoidal waves is propagated inland from the submarine outcrop of the aquifer. With distance, inland amplitudes of the waves decrease and the time lag of a given maximum increases. The problem has been solved by analogy to heat conduction in a semi-infinite solid subject to periodic temperature variations normal to the infinite dimension. For simplicity, consider the one-directional flow in a confined aquifer as shown in Figure16.6; the applicable differential equation governing the flow is

$$\frac{\partial^2 h}{\partial x^2} = \frac{S}{T}\frac{\partial h}{\partial t} \tag{16.19}$$

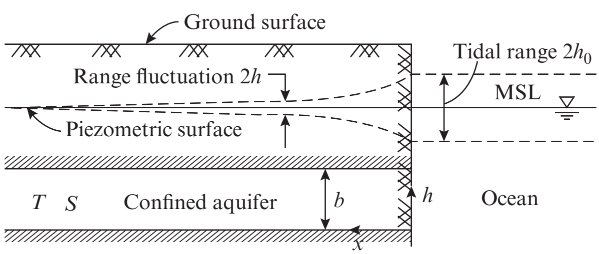

Figure 16.6 *Effect of tides in coastal confined aquifer*

where, h is the net rise or fall of the peizometric surface to the MSL, x is the distance inland from the outcrop, S is the storage coefficient of the aqifer, T is the transmissivity, and t is the time. If the amplitude of the tide is h_0, the applicable boundary conditions are

$$h = h_0 \sin \omega t \text{ at } x = 0 \text{ and } h = 0 \text{ at } x = \infty \tag{16.20}$$

where, ω is the angular velocity given by the following relation for a tidal period t_0

$$\omega = 2\pi/t_0 \tag{16.21}$$

The solution of the governing equation with above boundary conditions is

$$h = h_0 e^{-x\sqrt{\pi S/Tt_0}} \sin\left(2\pi\, t/t_0 - x\sqrt{\pi S / Tt_0}\right) \tag{16.22}$$

From this it follows that amplitude h_x of groundwater fluctuations at a distance x from the shore equals

$$h_x = h_0 e^{-x\sqrt{\pi S/Tt_0}} \tag{16.23}$$

The time lag t_L of a given maximum or minimum after it occurs in the ocean can be obtained by rewriting the part of equation as

$$\sin\left(2\pi\, t/t_0 - x\sqrt{\pi S / Tt_0}\right) = \sin \omega\left(t - \frac{x}{\omega}\sqrt{\pi S / Tt_0}\right) = \sin \omega\left(t - t_L\right) \tag{16.24}$$

Therefore,

$$t_L = \frac{x}{\omega}\sqrt{\pi S/Tt_0} = \frac{x\, t_0}{2\pi}\sqrt{\pi S/Tt_0} = x\sqrt{t_0 S/4\pi T} \tag{16.25}$$

The wave travel with a velocity

$$v_w = \frac{x}{t_L} = \sqrt{4\pi T/St_0} \tag{16.26}$$

and the wavelength is given by

$$L_w = v_w t_0 = t_0\sqrt{4\pi T/St_0} = \sqrt{4\pi Tt_0/S} \tag{16.27}$$

The ratio between the two consecutive amplitudes of each wave can be calculated as

$$\frac{h_x}{h_{x+L_w}} = \frac{h_0 e^{-x\sqrt{\pi S/Tt_0}}}{h_0 e^{-(x+L_w)\sqrt{\pi S/Tt_0}}} = e^{L_w\sqrt{\pi S/Tt_0}} = e^{\sqrt{4\pi Tt_0/S}\sqrt{\pi S/Tt_0}} = e^{2\pi} = 535.492 \tag{16.28}$$

Thus, there is a very strong damping in the wave amplitudes due to aquifer resistance, but the tidal effects may be propagated for a significant distance into aquifer due to larger wave lengths. Saline water flows into the aquifer during half of each cycle and out during the other half. By Darcy's law, the quantity of flow V per half cycle per unit length of coast is

$$V = \int_{-t_0/8}^{3t_0/8} q\, dt = \int_{-t_0/8}^{3t_0/8} vb.1\, dt = \int_{-t_0/8}^{3t_0/8} -Kb\left(\frac{\partial h}{\partial x}\right)_{x=0} dt = T\int_{-t_0/8}^{3t_0/8}\left(\frac{\partial h}{\partial x}\right)_{x=0} dt \tag{16.29}$$

where, q is the flow rate, b is aquifer thickness, and v is Darcy velocity. Differentiating Eqn. (16.22)

$$\frac{\partial h}{\partial x} = -h_0\sqrt{\pi S/Tt_0}\,e^{-x\sqrt{\pi S/Tt_0}}\left(\sin\left(2\pi t/t_0 - x\sqrt{\pi S/Tt_0}\right) + \cos\left(2\pi t/t_0 - x\sqrt{\pi S/Tt_0}\right)\right) \tag{16.30}$$

Thus, at $x = 0$,

$$\left(\frac{\partial h}{\partial x}\right)_{x=0} = -h_0\sqrt{\pi S/Tt_0}\left(\sin\left(2\pi t/t_0\right) + \cos\left(2\pi t/t_0\right)\right) \tag{16.31}$$

Therefore,

$$V = T\int_{-t_0/8}^{3t_0/8} h_0\sqrt{\pi S/Tt_0}\left(\sin\left(2\pi t/t_0\right) + \cos\left(2\pi t/t_0\right)\right)dt = h_0\sqrt{2STt_0/\pi} \tag{16.32}$$

The above analysis is also applicable as a good approximation to water table fluctuations of an unconfined aquifer if the range of fluctuations is small in comparison to the saturated thickness.

16.7 Upconing of Saline Water

Sometimes wells pump water from freshwater zone that is underlain by salt water. A situation like this is common in oceanic islands, elongated peninsulas, aquifers in arid/semiarid regions, or coastal aquifers. When an aquifer contains an underlying layer of saline water and is pumped by a well penetrating only the upper freshwater portion of the aquifer, a local rise of the interface below the well occurs, which is known as *upconing*. With continued pumping, an initially horizontal interface rises to successively higher levels until eventually it can reach the well (Figure 16.7). This requires shutting down the pumping because of the degrading influence of the saline water. When pumping is stopped, the denser saline water tends to settle downwards and return to its former position. Upconing is a complex phenomenon. Understanding this phenomenon is important in operation of wells for *skimming freshwater* from above saline water. From a water supply standpoint, it is important to determine the optimum location, depth, spacing, pumping rate, and pumping sequence that will ensure production of the largest quantity of freshwater while at the same time striving to minimize any underground mixing of the fresh saline water.

An approximate analytical solution for the upconing directly beneath a well as shown in Figure 16.7, based on the Dupuit assumptions and the Ghyben–Herzberg relation was given by Schmorak and Mercado (1969) as

$$z = \delta\frac{Q_w}{2\pi dK_x}\left(1 - \frac{2\delta\eta d}{2\delta\eta d + K_z t}\right) \tag{16.33}$$

where, z = rise of cone center; d = depth of the interface below the end of the well screen bottom prior to pumping; K_x = hydraulic conductivity in horizontal direction; K_z = hydraulic conductivity in vertical direction; η = porosity of aquifer; and t = time since start of pumping. For steady state ($t = \infty$), Eqn. (16.33) becomes

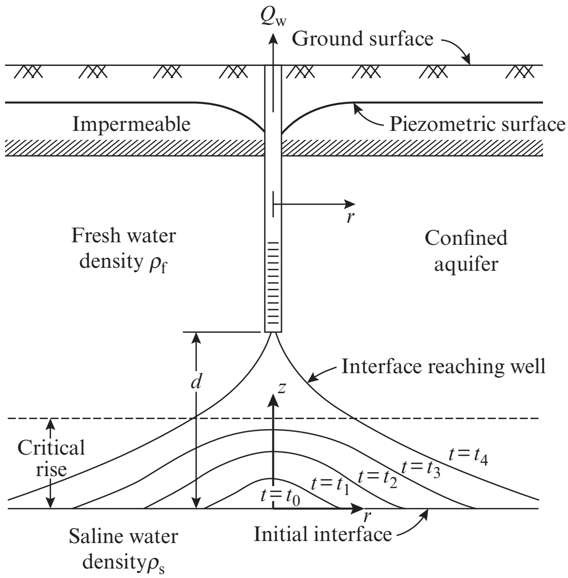

Figure 16.7 *Upconing (Todd and Mays 2005)*

$$z = \delta \frac{Q_w}{2\pi dK} \tag{16.34}$$

which is the ultimate or equilibrium height of the saline water cone below the well. This relation indicates an ultimate rise of the interface is directly proportional to the pumping rate. It holds only if the rise is limited. If the upconing exceeds a certain critical rise, it accelerates upward to the well. Up to a certain critical pumping rate, equilibrium with an upconed interface is possible. When the pumping rate is raised from one steady level to a higher steady level, a new equilibrium with a higher upconed interface is established. At the critical pumping rate, the interface is very unstable and the interface will immediately reach to the pumping well with any increase in pumping rate beyond critical value. The fast rising upconed interface is cusp-like form. When pumping stops, the upconed interface undergoes decay toward the initial steady-state interface prior to pumping. The critical rise may be taken z/d = 0.3–0.5. Adopting an upper limit of $z/d = 0.5$, the maximum permissible pumping rate without salt entering the well becomes

$$Q_w \leq \frac{\pi d^2 K}{\delta} \tag{16.35}$$

For anisotropic aquifers where the vertical permeability is less than the horizontal, a maximum discharge greater than that for the isotropic case is possible. If seaward flow of freshwater is taking place along with pumping, a stagnation point and a water divide (capture zone) are formed. The shape of water divide and the location of stagnation point depend on the location and length of well screen and rate of pumping and seaward freshwater movement. The determination of the exact shape of the upconed interface and the value of critical pumping rate as affected by various hydrological and geometrical parameters requires in principle the solution of the general 3-D flow problem.

Upconing of saltwater beneath pumping wells is a more imminent problem than lateral encroachment in most areas (Figure 16.8). One reason is that lateral encroachment must displace a volume of freshwater much larger than that displaced by upconing. In most places in semiarid parts of Gujarat and Rajasthan, saline water aquifers are overlain by other aquifers that contain freshwater and that serve as sources of water supply. When supply wells are drilled too deep or are pumped at too large a rate, upconing of the salt water may occur.

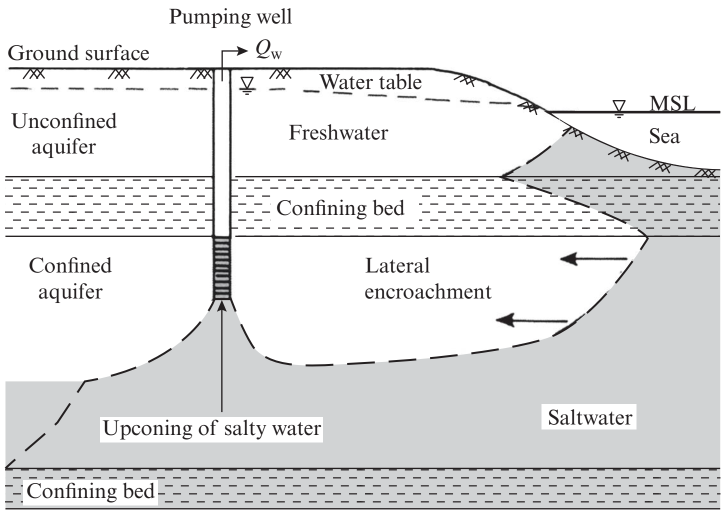

Figure 16.8 *Effect of pumping near to coast*

Most investigations of upconing, for simplicity, have assumed an abrupt interface between the two immiscible like fluids. But fresh and saline water are miscible, a mixing, or transition, zone having a finite thickness occurs. An interface can be considered as an approximation to the position of the 50 percent relative salinity in a transition zone. The water at the upper edge of the zone is essentially freshwater and moves accordingly. Upward movement of the freshwater attracts the transition zone; consequently, even with a relatively low pumping rate, no limiting critical rise exists above which saline water will not rise. It follows that with any rate of continuous pumping, some saline water must sooner or later reach a well. Upconing can be minimized by the proper design and operation of well. For given aquifer conditions, wells should be separated as far as possible vertically from the saline zone and pumped at a low uniform rate. *Scavenger wells*, which pump brackish or saline water from below the freshwater, can counteract upconing.

16.8 Freshwater–Saltwater Relations on Oceanic Islands

Most small oceanic islands are relatively permeable, consisting of sand, lava, coral, or lime stone, so that seawater is in contact with groundwater on all sides. Because fresh groundwater originates entirely from rainfall, only a limited quantity is available. A freshwater lens floats on the underlying saltwater; its thickness decreases from the center toward the coast as shown in Figure 16.9. From the Dupuit assumptions and the Ghyben–Herzberg relation, an approximate freshwater boundary can be determined for a circular island of radius r_0 receiving an effective recharge from rainfall at a rate R, as

$$Q = 2\pi rK(z + h_f)\frac{dh_f}{dr} \tag{16.36}$$

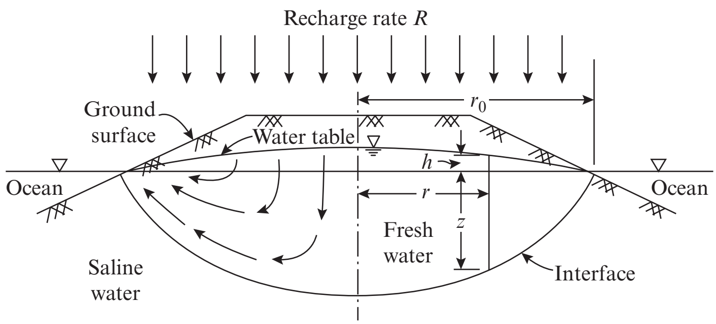

Figure 16.9 *Shape of freshwater—saltwater interface in oceanic island*

where, Q is the outward flow at radius r. As $Q = \pi r^2 R$ and $h_f = z/\delta$,

$$zdz = \frac{\delta^2}{(1+\delta)}\frac{Rrdr}{2K} \tag{16.37}$$

Integrating and applying boundary condition that $h = 0$ when $r = r_0$ yields

$$z^2 = \frac{\delta^2}{(1+\delta)}\frac{R(r_0^2 - r^2)}{2K} \tag{16.38}$$

Thus, the depth to saltwater at any location is a function of the rainfall recharge, the size of the island, and the hydraulic conductivity. This approximate solution is indistinguishable from more exact solution by potential theory. Tidal, atmospheric, and rainfall fluctuations together with dispersion create a transition zone along the interface in an oceanic island. The close proximity of this boundary zone to the water table can introduce saline water into a well by upconing. Therefore, care must be exercised in the development of groundwater supplies so that pumping causes a minimal disturbance to the freshwater—saltwater equilibrium. To avoid the danger of entrainment of saline water, island wells should be designed for minimum drawdown, just skimming freshwater from the top of the lens. If small diameter wells are employed, they should be shallow, dispersed, and pumped at low uniform rates. An infiltration gallery, consisting of a horizontal collecting tunnel at the water table, is advantageous in areas where water table is shallow and freshwater lenses are thin.

16.9 Identification of Seawater in Groundwater

Analysis of groundwater samples collected in zones of seawater intrusion may show a chemical composition differing from a simple proportional mixing of seawater and groundwater. Modification in the composition of seawater entering an aquifer can occur by three processes, namely, base exchange between the water and mineral of the aquifer, sulfate reduction, and substitution of carbonic or other week acid radicals and solution and precipitation. Only the last process can change the total salt concentration; however, the first two processes, which require maintenance of ionic balance, can alter the percentage by weight of different salt components and thereby the total dissolved solids in ppm.

For proper diagnosis of seawater intrusion as evidenced by temporary increases in the TDS, chloride bicarbonate ($Cl/[CO_3 + HCO_3]$) ratio may be used as a criterion to evaluate intrusion. Chloride is a dominant ion of ocean water, which is unaffected by the modification processes, and it normally occurs in small amounts in groundwater. On the contrary, HCO_3 is usually most abundant negative ion in groundwater and occurs in small amount in seawater. Although contaminants other than seawater can change a chloride–bicarbonate ratio, these would seldom be important in water collected from a well subject to intrusion.

16.10 Control of Saline Water Intrusion

Methods for controlling intrusion vary widely depending on the source of the saline water, the extent of the intrusion, local geology, water use, and economic factors. Table 16.1 lists selected methods for controlling saline water intrusion. Because as little as two percent of seawater in freshwater can render water not potable, considerable attention should be paid on methods to control seawater intrusion. The following sections describe methods for controlling saline water intrusion (Todd and Mays 2005).

Table 16.1 Methods for controlling saline water intrusion

Source or cause of intrusion	*Control methods*
Seawater in coastal aquifer	Modification of pumping pattern; artificial recharge; extraction barrier; injection barrier; and subsurface barrier
Upconing	Modification of pumping pattern; scavenger wells
Oil field brine	Elimination of surface disposal; injection well; plugging of abandoned wells
Defective well casing	Plugging of faulty wells
Surface infiltration	Elimination of source
Saline water zones in freshwater aquifers	Relocation and redesign of wells

16.10.1 Modification of Pumping Pattern

Changing the locations of the pumping wells, typically dispersing them in inland areas, can aid in reestablishing a stronger seaward hydraulic gradient. Also, reduction of pumping of existing wells can produce the same beneficial effect.

16.10.2 Artificial Recharge

Groundwater levels can be raised and maintained by artificial recharge, using surface spreading for unconfined aquifers and recharge wells for confined aquifers (Figure 16.10).

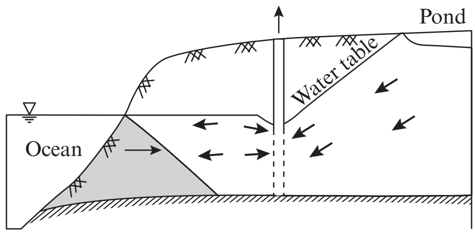

Figure 16.10 *Control through artificial recharge*

16.10.3 Extraction Barrier

An extraction barrier is created by maintaining a continuous pumping trough with a line of wells adjacent to sea. Seawater flows inland from the ocean to the trough, while freshwater within the basin flows toward the trough. The pumped water is brackish and normally is discharged into sea (Figure 16.11).

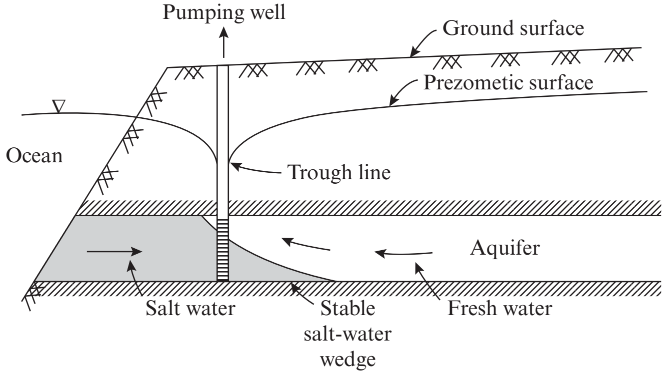

Figure 16.11 *Extraction barrier*

16.10.4 Injection Barrier

The method maintains a pressure ridge along the coast by a line of recharge wells. Injected water flows both seaward and landward. High-quality imported water is required for recharge into wells. A combination of injection and extraction barriers is feasible; this reduces both recharge and extraction rates but requires a large number of wells (Figure 16.12).

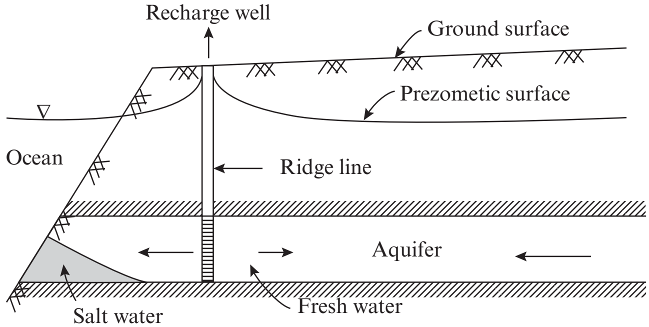

Figure 16.12 *Injection barrier*

16.10.5 Subsurface Barrier

Construction of an impermeable barrier parallel to the coast and through the vertical extent of the aquifer can effectively prevent the inflow of seawater into the basin. Materials to construct a barrier might include sheet piling, puddle clay, emulsified asphalt, cement grout, bentonite, plastics/geomembranes, etc. The main problems are lack of suitable site, high construction cost, less earthquake resistant, and prone to chemical erosion (Figure 16.13).

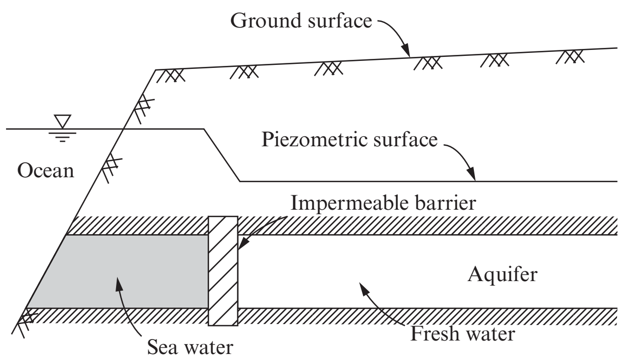

Figure 16.13 *Subsurface barrier*

16.11 Management of Coastal Aquifers

Coastal aquifers constitute an important source for water especially in arid and semiarid zones near the sea. The proximity of the sea requires special attention and special management techniques for the coastal aquifers. Coastal areas form environmentally sensitive terrain world over and generally have high population density. It also represents a complex zone where land and sea/ocean interact and the hydrologic regime varies from marine to estuarine to fluviatile. The coastal aquifers come in contact with the ocean at or seaward of the coastline and here, under natural conditions, fresh groundwater is discharged into the sea. In coastal areas, the groundwater is a vital component of the coastal zone resource that provides freshwater supply on sustained basis. With increased demands for groundwater in many coastal areas, however, the seaward flow of groundwater decreases or even gets reversed, causing seawater to enter and to penetrate inland in aquifers.

Groundwater discharge into the sea and the consequent migration of shorelines in the geological past has created different hydrogeological environments in the coastal tracts all over the world. The anthropogenic activities in coastal area interfere with the natural flow of groundwater, disturb the groundwater—seawater equilibrium, and reduce the freshwater discharge into the sea. This may trigger the seawater intrusion or upconing of saltwater. Effects are very slow and progress unnoticed until the time comes when a drastic salinity in groundwater is observed. The coastal groundwater resource needs to be exploited judiciously, used economically, and protected effectively from seawater intrusion, natural calamities, and pollution. The socioeconomic growth in the coastal tract essentially requires an overall management of the groundwater resources for the sustenance of its quality and quantity as well as the precautionary natural disaster preparedness and the remedial measures to tide over the calamites and make fresh groundwater available at shortest distance.

In coastal aquifers, the hydraulic gradient is generally toward the sea, which receives the excess of fresh groundwater. In the process an interface between seawater and freshwater is formed. This interface is disturbed if there is a heavy pumping of groundwater in coastal aquifers. Such a situation may also eventually lead to seawater ingress making the coastal aquifer totally unusable. The coastal aquifers are vulnerable to several factors. Overexploitation of groundwater may lead to permanent water-quality deterioration due to seawater intrusion. Similarly, the discharge of effluents from industries and the cyclonic inundation of coastal areas render the aquifers saline. These form grave social concern of the coastal region. Hence, protecting and preserving the quality and quantity of groundwater resource for its best use should be the goal for aquifer management in the coastal areas.

Seawater intrusion or the freshwater–saltwater interface can be maintained at a desired distance inland from the coast, if appropriate groundwater flow to the sea takes place. Groundwater being used for irrigation, there is a constant buildup of salt in the groundwater. Therefore, groundwater flow to the sea in the coastal tract is the main way to drain salt from the aquifer. Groundwater flow to the sea maintains and keeps the fresh saltwater interface at some desired distance from the coast and prevents saltwater encroachment and contamination of groundwater. There exists a relationship between the rate of freshwater discharge to the sea, and the extent of seawater intrusion. This makes seawater encroachment a management problem because the freshwater discharge to the sea is the difference between the rate of recharge (natural and artificial) and that of pumping. As the freshwater flow to the sea increases, the intrusion distance decreases. This means that the extent of seawater intrusion is a decision variable in the management of a coastal aquifer. It is controlled by controlling the fresh groundwater flow to the sea or alternatively by augmenting recharge and controlling pumping in the coastal strip. Overexploitation results in groundwater levels below sea level and consequently to saltwater intrusion and no drainage of the salt from the aquifer. Maintaining a seaward fresh groundwater flow will keep the interface at a desired distance from the coast. Artificial recharge in coastal areas is one of the most important and feasible option to keep the interface under control. Artificial recharge is the procedure of injecting freshwater into the freshwater aquifers to increase the amount of stored freshwater, slow down the depletion in storage, and increase the hydrostatic head and seaward hydraulic gradient and thus the velocity. There are a number of recharge procedures, such as recharge tanks/basins, channels, shafts, injection wells, hydraulic barriers, etc., but the major problem in implementing any artificial recharge scheme is to get the sufficient quantity of surface freshwater to be injected, cost involved in it, and the related social issues. The best possibility is to inject water from the same area during monsoon. In the coastal cities, it may be appropriate to take up rooftop rain water harvesting and artificial recharge of groundwater on a massive scale to combat the increasing stress on the fragile fresh groundwater system in these cities.

Groundwater management in coastal areas may require a precise understanding of the complex mechanism of the saline and freshwater relationship, so that the withdrawals are regulated to avoid upconing and to prevent migration of the seawater ingress further inland. The key to combat this problem is to maintain the proper balance between water being pumped from the aquifer and the amount of water recharging it. Constant monitoring of the saltwater interface is necessary in determining proper control measures. Other than the supply side or structural management measures, there is a need to implement various nonstructural measures in terms of regulation and control of groundwater withdrawal. Central Groundwater Authority, Ministry of Water Resources, is already vested with the power to control and regulate groundwater extraction in vulnerable areas. The notification for regulation in coastal areas may not be based on the vulnerability of the quality problem only. It should also account preventive measures for arresting seawater ingress of deeper aquifer and to maintain freshwater quality. Long-term water level behavior (say for the past 10 years) may be studied for the piezometric surface fluctuation for the premonsoon period and postmonsoon period. Technical expertise is required for construction of tube wells where sealing of brackish zones are required.

Coastal groundwater management requires integrating the studies on geomorphologic features, geological conditions, groundwater withdrawal and aquifer disposition, groundwater dynamics and resource estimation, quality interface identification, tidal water impact, subsurface drainage congestion, hazard-vulnerability and preparedness, conservation/recharge schemes including tank rehabilitation, simulations to predict aquifer stress, regulating the draft, protecting the upland recharge areas, and long-term impact of sea level changes due to global warming. There has to be a monitoring system to periodically check the groundwater quality. Seawater intrusion into the fresh groundwater body has to be controlled at the earliest for conservation of the resources along the coastal tract. To prevent/control saline water intrusion into coastal aquifers the following need to be considered: Accurate estimation of coastal fresh groundwater resource; monitoring of groundwater levels, piezometric surface, and chemical quality; mapping and characterization of shallow and deep aquifers, paleo-channels and impermeable clay barriers; mapping of areas/zones of recharge and their protection and estimation of rate of recharge; mapping of coastal sand dunes and their hydrogeological assessment; characterization of unsaturated zone capping the aquifers; study of hydrochemical processes involved in mixing of fresh groundwater with seawater; isotope studies for source of salinity in water, age, and aquifer recharge; study on effects of tides on groundwater quality; implementation of area specific economically and socially viable artificial recharge schemes; mathematical simulation of variable density/quality groundwater flow in coastal aquifers; study on offshore/submarine discharge of groundwater, etc. Additionally, the control mechanism also needs to be brought in place through area-specific control and regulation on groundwater withdrawal in coastal areas.

Groundwater modeling of coastal aquifers is a potent tool to understand hydrodynamics of coastal aquifers. The modeling can be effectively be used to study the present situation of freshwater–saltwater interface vis-à-vis the present groundwater development in the area. Such a study can thereafter lead to generation of different scenarios for predicting the effects of increased pumping in coastal aquifers as wells as impact of artificial recharge schemes to be implemented in the coastal areas. The groundwater modeling studies, however, require detailed information on the aquifer parameters, pumping patterns, and long-term data on water levels. Therefore, detailed studies in project mode, including groundwater exploration and evaluation of aquifer characteristics through pumping tests, are to be taken up. Also, a strong network of dedicated observation wells is required for high-frequency close grid monitoring.

16.12 Seawater Intrusion in India

Case Study by Sharma (2013)

Tamil Nadu, bounded by the Bay of Bengal on the east, has a shoreline of 998 km with varying widths of coastal tracts. It stretches from Pulicat Lake to Cape Comerin ranging in elevation between 2 and 30 m above msl with beach terraces and broad inter-terrace depressions. The coastal tract of Tamil Nadu is underlain by a sequential pile of unconsolidated alluvial sediments of Quaternary age. There are a number of aquifers down to depth of 750 m. Tiruvallur District in Tamil Nadu is underlain by the alluvial deposits of sands and clays in varying propositions. The thickness of the granular zones varies from place to place. Aquifers of Panjetti–Tamarapakkam–Minjur belt was developed on an intensive scale to augment the needs of Madras/Chennai city and industrial supplies, which has led to the decline in water levels and thus saline water intrusion between 1969 and 1983. The seawater intrusion studies carried out by the UNDP in Minjur area revealed that the interface had moved from 2 to 3.5 km as on 1969, to 8.5–9 km as on 1987, affecting part of Minjur well field, thereby rendering the groundwater unfit for drinking purposes. The UNDP study suggested that the pumping in Minjur well field be stopped and also recommended for artificial recharge of groundwater with reservoir or floodwater. Accordingly, a series of recharge tube wells for injection of freshwater were made in the east of Minjur on north–south direction parallel to the coast and established a freshwater ridge to arrest the interface movement further west. Despite reduction in the groundwater extraction, depletion of water table was noticed and the study by SG and SWRDC, WRO, Government of Tamil Nadu, indicated that the interface had moved to 13.5 km inland by 2000.

As one moves south to the coastal part of Kancheepuram district along Tiruvanmiyur–Covelong Kalpakkam Coastal Alluvial Tract, it is seen that sand dunes form a good repository of groundwater. A study carried out by CGWB in collaboration with BARC and MS Swaminathan Research Foundation revealed that formation water in the sand dunes extending down to 15 m, along the coast has freshwater and in the fractured basement, the water is brackish. The cause of salinity in the formation is not due to seawater intrusion but due to in situ salinity, as shown by the chemical and isotopic compositions of the groundwater. The seepage from Buckingham canal and backwater has also resulted in poor quality in the adjoining area. However, the landward hydraulic gradient in the northeastern part of the study area indicates a probable seawater ingress but has not been proved. In general, in the coastal tract of Tamil Nadu state, the poor quality of formation water is due to in situ salinity caused by depositional environment in major part of Tamil Nadu, and the deterioration of water quality due to seawater ingress has been reported mainly from Minjur area, north of Chennai city.

SOLVED EXAMPLES

Example 16.1: If density of freshwater = 1005 kg/m^3, density of saline water = 1030 kg/m^3, hydraulic conductivity of aquifer = 5 m/d, and depth of saline water from the well strainer prior to pumping = 50 m, determine (i) the position of the freshwater–saltwater interface if the well is pumped at rate of 1000 m^3/d and (ii) the maximum permissible pumping rate from the well without mixing saline water.

Solution: Given data $Q_w = 1000$ m^3/d; $K = 5$ m/d; $d = 50$ m; and $\delta = 40.2$, hence the rise in the freshwater–saltwater interface is $z = \delta \dfrac{Q_w}{2\pi dK} = \dfrac{40.2 \times 1000}{2 \times \pi \times 50 \times 5}$

$= 25.59$ m.

The maximum permissible pumping rate is $Q_w = \dfrac{\pi d^2 K}{\delta} = \dfrac{\pi \times 50 \times 50 \times 5}{40.2}$ $= 976.86$ m³/d.

Example 16.2: If density of freshwater = 1000 kg/m³, density of saline water = 1025 kg/m³, hydraulic conductivity of a coastal aquifer = 10 m/d, thickness of the aquifer = 50 m, and water levels in two monitoring wells at 1 km distance are 0.5 m and 1.0 m above msl, calculate the length of saltwater wedge.

Solution: Given data K = 10 m/d; b = 50 m; δ = 40; and $q = Kb\dfrac{dh}{dx}$ $= 10 \times 50 \times \dfrac{1.0-0.5}{1000} = 0.25$ m³/d/m; hence, the length of saltwater wedge is $L = \dfrac{1+\delta}{\delta^2}\dfrac{Kb^2}{2q} = \dfrac{1+40}{40^2}\dfrac{10 \times 50^2}{2 \times 0.25} = 1281.25$ m. By using Glover Equation

$$z^2 = \delta \frac{2qx}{K} + \left(\delta \frac{q}{K}\right)^2 \Rightarrow 50^2 = 40\frac{2 \times 0.25}{10}x + \left(40\frac{0.25}{10}\right)^2 \Rightarrow x = 1249.50 \text{ m}.$$

Example 16.3: In an unconfined coastal aquifer with hydraulic conductivity = 8 m/d and underlain by a horizontal impervious layer 50 m below msl, a fully penetrating well with a constant pumping rate of 400 m³/d is installed 800 m from the shoreline. If freshwater discharge toward sea is 1.5 m³/d/m, determine if brackish water occurs in the pumped water.

Solution: Given data K = 8 m/d; b = 50 m; δ = 40; Q_w = 400 m³/d and q = 1.5 m³/d/m, thus the position of the toe before pumping is $x = \dfrac{1+\delta}{\delta^2}\dfrac{Kb^2}{2q} = \dfrac{1+40}{40^2}\dfrac{8 \times 50^2}{2 \times 1.5} = 170.83$ m, and the position of the toe after the steady pumping is $\dfrac{(1+\delta)}{\delta^2}\dfrac{Kb^2}{2q} = x + \dfrac{Q_w}{4\pi q}\ln\left(\dfrac{(x-x_w)^2+y^2}{(x+x_w)^2+y^2}\right)$

$\Rightarrow 170.83 = x + \dfrac{400}{4\pi \times 1.5}\ln\left(\dfrac{(x-800)^2+0}{(x+800)^2+0}\right) \Rightarrow x = 218.38$ m. Thus, the toe of interface moved 218.38–170.83 = 47.55 m inland because of the well pumping at constant rate 400 m³/d. The brackish water will occur if well discharge is more than critical discharge, which is corresponding to the interface toe crossing the stagnation point. Equation (16.16) for critical pumping rate with $\lambda = \dfrac{(1+\delta)}{\delta^2}\dfrac{Kb^2}{qx_w} \Rightarrow \lambda = 170.83 \times 2/800 = 0.427$ yields

$0.427 = 2\sqrt{1-\mu} + \mu \ln\left(\dfrac{1-\sqrt{1-\mu}}{1+\sqrt{1-\mu}}\right)$, which after solving trial and error method

results to $\mu = 0.5625 \Rightarrow 0.5625 = \dfrac{Q_w}{\pi q x_w} = \dfrac{Q_w}{\pi \times 1.5 \times 800} \Rightarrow Q_w = 2120.57$ m³/d.

Stagnation point will be $x_s = x_w\sqrt{1-\mu} = 800 \times \sqrt{1-0.5625} = 529.15$ m and

$y_s = 0$ m. The toe of interface for pumping rate of 400 m^3/d is 218.38 m, which is quite short of stagnation point 529.15 m. Also, the pumping rate of 400 m^3/d is much below the critical discharge rate of 2120.57 m^3/d; thus, the toe will stabilize some distance away from the stagnation point or outside the capture zone of the pumping well. Thus, brackish water will not occur in the pumped water.

PROBLEMS

16.1. Give the solution for the shape and position of the saltwater—freshwater interface.

16.2. What do you understand by saltwater intrusion?

16.3. What are the causes of saline water encroachment?

16.4. What do you understand by upconing? Why it is important in pumping wells?

16.5. Derive the expression for the depth of saltwater interface in an oceanic island.

16.6. Derive expressions for amplitude in piezometric head, time lag, wavelength, damping ratio, and volume per cycle due to oceanic tides.

16.7. What are issues in coastal aquifer management?

16.8. What are the control measures for saltwater intrusion?

16.9. Determine the height of water table if a point on a steady interface is 30 m below sea level.

16.10. The freshwater–saltwater interface is located 45 m below MSL 500 m inland from the shoreline in an unconfined coastal aquifer. Determine the height of water table.

16.11. A homogeneous isotropic coastal aquifer with K = 15 m/d has a horizontal impervious base at 120 m below sea level. If uniform seaward freshwater flow rate is 8 m^3/m/d, determine the position of the toe of the interface for a well located at 800 m from the coast.

16.12. The steady-state freshwater–saltwater interface is located 30 m below MSL 100 m inland from the shoreline in an unconfined coastal aquifer. If the hydraulic conductivity of aquifer = 10 m/d, determine the freshwater discharge from aquifer into the sea using (i) Ghyben–Herzberg equation and (ii) Glover expression.

16.13. A partially penetrating well is installed in an unconfined coastal aquifer with hydraulic conductivity = 10 m/d and underlain by a horizontal freshwater–saltwater interface 25 m below the bottom of the well screen. If the well is pumped at constant rate of 300 m^3/h, how close can the saltwater face approach the well screen before the quality in the pumping well is affected?

16.14. Determine the maximum permissible pumping rate from a well without mixing saline water if density of freshwater = 1000 kg/m^3, density of saline water = 1025 kg/m^3, hydraulic conductivity of aquifer = 0.4 m/d, and depth of saline water from the well strainer prior to pumping = 10 m.

16.15. A well is drilled in an aquifer of hydraulic conductivity = 4 m/d with keeping the well strainer 20 m above the freshwater–saltwater interface. What is the maximum permissible discharge of the well to prevent saltwater mixing by limiting the upconing up to 10 m?

16.16. In a coastal aquifer with hydraulic conductivity = 4 m/d, the freshwater–saltwater interface is at a depth of 50 m below msl at a distance of 200 m inland from the shore. What is the rate of freshwater discharge into sea and the width of zone on the ocean bottom through which freshwater is seeping into ocean?

16.17. The freshwater–saltwater interface is found at a depth of 50 m below msl at a distanceof200minlandfromtheshoreinacoastalaquifer.Thehydraulicconductivityoftheaquiferis4m/d.Determinetherateoffreshwaterdischargeintoseaandthewidthofzoneontheoceanbottomthroughwhichfreshwaterisseepingintoocean?

16.18. In an unconfined coastal aquifer with hydraulic conductivity = 25 m/d and underlain by a horizontal impervious layer 40 m below msl, a fully penetrating well with a constant pumping rate of 800 m^3/d is installed 300 m from the shoreline. If freshwater discharge toward sea is 2.5 m^3/d/m, determine if brackish water occurs in the pumped water.

16.19. In an unconfined coastal aquifer with hydraulic conductivity = 28 m/d and underlain by a horizontal impervious layer 35 m below msl, a fully penetrating well with a constant pumping rate of 80 m^3/h is installed 300 m from the shoreline. If freshwater discharge toward sea is 5 m^3/d/m, determine (i) the location of the toe of the interface before the well installation; (ii) whether brackish water occurs in the pumped water; (iii) the new location of the toe after the well installation; and (iv) the location of stagnation point.

Chapter 17

Groundwater-Modeling Techniques

17.1 Introduction

Underground flow systems are more complex than the simple cases of one-dimensional or axisymmetric flow described in Chapters 5 through 13. These simple cases can be analyzed mathematically, but more complex systems with irregular boundaries, complex boundary conditions, anisotropic and inhomogeneous aquifer media, and several simultaneous discharge and recharge conditions can best be solved using modelling techniques. A *groundwater model* is used to simulate and describe real-world groundwater flow. A *model* may be defined as a simplified version of a real-world groundwater system that approximately simulates the relevant excitation–response relations of the real-world system or the relevant process happening inside the real system (Bear et al 1992). Another definition by Prickett (1979) is "Any system that can duplicate the response of a groundwater reservoir can be termed a model of the reservoir and the operation of the model and manipulation of the results is termed simulation." Due to increased exploitation of groundwater and continuously changing conditions of the groundwater system, there is a need for a better understanding of the functioning of groundwater reservoirs; for example (i) how groundwater levels are affected by pumping several wells in an aquifer; (ii) how drawdown around a well is affected by the proximity of barrier and recharge boundaries; (iii) how recharge is affected by water table depth and other subsurface conditions; (iv) how groundwater levels are affected by discharge (pumping from wells) and recharge (natural and artificial) in entire aquifer systems; (v) how flow systems are affected by anisotropy and inhomogeneity of the aquifer media; (vi) how salt water intrusion takes place and can be controlled; (vii) how surface, vadose, and subsurface waters interact; and so on. Various models for simulating groundwater flow are used to the extent that they simplify solution of groundwater problems. The groundwater is a hidden resource; the geometry of a real groundwater system is quite complex; and matrix characteristics and stresses imposed on the system vary widely in space and time. Therefore, analytical solutions for such systems are not possible and also the available analytically solutions derived on the basis of certain assumptions are restrictive in use. Therefore, the complex problem related to functioning of groundwater system can be solved with the aid of models that simulate the response of the real groundwater system. Model studies can be undertaken for the following purposes:

1. To understand the mechanism of operation of groundwater reservoirs
2. To predict the response of an aquifer under various possible scenarios that permit better management of existing well fields or design of an optimal configuration of wells and their pumping strategy in a new well field
3. To make planning and management decisions related to contaminants in real world very complex groundwater systems
4. To avoid irrevocable damaging and costly experimentation with real system
5. For analysis of no action alternatives
6. To carry out new research, for example, for verifying new solutions or for developing new empirical relations or semitheoretical laws, etc.
7. For instruction and demonstration

The three main characteristics that make the latest groundwater models very practical tools are as follows (Prickett 1979):

1. Models reproduce some aspect of the behavior of a complex natural system as they can solve extremely complex groundwater flow problems without making a large number of gross approximations.
2. Models are available to virtually everyone in the groundwater business. The days of specialty laboratories for complex groundwater model solving are over and the modelling tools are now in the hands of those doing the local work.
3. The model information as to how a problem was solved along with the exact assumptions used and the step-by-step solution of the problem that produced the results of the entire analysis can easily be transferred to another person.

Since real-world systems are very complex, a model cannot imitate all aspects of groundwater flow problems, therefore different types of groundwater models are available to address the variety of groundwater problems. They can be classified into various categories based on the principles involved in their designing. The right type of models has to be decided on the basis of the problem and on the hydrological quantities and properties that are to be simulated. The following are the main four categories of the groundwater models (Prickett 1979):

1. Physical models
2. Analog models
3. Model-based analytical formulas coupled with experience
4. Numerical models

The groundwater models may also be classified as *continuous models* or *discrete models*. Physical models and many analog models are continuous models, whereas electric network-based analog models and majority of numerical models are discrete models. The groundwater models are intellectual toys. A model should be selected based on the complexity of the problem, for example, the use of an overly sophisticated model is not justified for addressing a simple problem. There are many problems that can be solved by experience and application of formulas, and hence it is not appropriate to use modeling for such cases.

17.2 Physical Models

A *physical model* is a scaled-down model of a prototype aquifer. In the case of physical models, scale factor need to be chosen, which results in convenient model characteristics. These are conversion constants that relate the corresponding parameters and variables of the models to those of the aquifer. Among the physical models, a *sand tank* model is most commonly used for simulation of simple aquifer system. The sand tank model is a scale model of an aquifer with the boundaries scaled down and the absolute value and spatial distribution of the hydraulic conductivity modified. These models are constructed in water-tight columnar or wedge-shaped boxes made of wood, Perspex, or steel. A uniform hydraulic conductivity in the model can be achieved by placing coarse sand in small quantities under water and compacting consistently to remove air. Anisotropy can be attained by layers of different sands. Complex boundaries, three-dimensional systems, free surfaces such as water table and interfaces between different liquids are also possible in sand tank models. These models are being used since Darcy's time were more common in sixtieth 1960s and will continue to be used, especially in the area of groundwater quality and pollution research. The sand tank model can play a part in the area of dispersion, diffusion, ion exchange mechanisms, and heat transport phenomena (Prickett 1979). An unconfined condition can be represented by placing sand of uniform permeability, whereas a confined condition can be simulated by an impermeable layer over a permeable layer. For axisymmetric systems, such as the flow to a partially penetrating well in an unconfined aquifer, the model may be wedge shaped to represent a sector of the system; for two-dimensional flow systems in the vertical and horizontal planes, the model may be a narrow 5 –20-cm-wide rectangular box. Kimbler *et al*. (1975) used the sand tank model to study freshwater storage in saline water aquifers. Since visual identification of a water table is difficult, piezometers consisting of thin, transparent plastic tubes are placed at critical points for observing the water table or piezometric levels in the model. Piezometer tubes should be small in order to minimize modifications of the flow pattern. Sometimes dye is added at selected points to observe the flow field.

The sand tank model is created following the geometric similarity between model and prototype. The length scale/ratio L_r for the geometric similarity is

$$L_r = \frac{L_m}{L_p} \tag{17.1}$$

where, L_m and L_p are corresponding lengths in model and prototype, respectively. Since Darcy's law is applicable to both model and prototype, the velocity ratio v_r can be expressed as follows:

$$v_r = \frac{v_m}{v_p} = \frac{K_m i_m}{K_p i_p} \tag{17.2}$$

where, subscripts p, m, and r refer to the prototype, model, and ratio, respectively. For equal hydraulic gradient of model and prototype ($i_m = i_p$), Eqn. (17.2) yields

$$v_r = K_r \tag{17.3}$$

Applying Darcy's law to model and prototype, the ratio of flow for isotropic conditions is

$$Q_r = \frac{Q_m}{Q_p} = \frac{K_m A_m i_m}{K_p A_p i_p} = K_r L_r^2 \tag{17.4}$$

If transient flow systems are modelled, the prototype time t_p for the water table to rise or fall a certain distance can be calculated as follows:

$$t_p = t_m L_r \frac{K_m \eta_p}{K_p \eta_m} \tag{17.5}$$

For unsteady flow in phreatic aquifers, the time scale is given by the following relation:

$$Q_r = \frac{V_m t_p}{V_p t_m} = \frac{V_r}{t_r} = \frac{S_{yr} L_r^3}{t_r} \tag{17.6}$$

where, V is the volume in time t and specific yield S_y is related to $S_{yr} L_r^3 = V_r$ From Eqns. (17.4) and (17.6), we obtain

$$t_r = \frac{S_{yr} L_r}{K_r} \tag{17.7}$$

Drawbacks of sand models are as follows

1. Complex aquifer system cannot be easily represented in sand tank models.
2. Thickness of capillary zone depends on the porous medium; therefore for same material in model and prototype, it is disproportionately large in model in comparison to the vertical length scale. This yields an unrealistically high contribution of the flow above the water table to the total flow in the model.
3. Entrapment of air and organic growth are troublesome and require special treatment.

Well flow, seepage under hydraulic structures, artificial recharge, dispersion, sea water intrusion, etc., cases can be studied by sand tank models. The capillary effect may be reduced by using a coarse grained porous medium, but this could cause turbulent flow that invalidates Darcy's equation, however, the turbulent flow can be avoided by using a more viscous liquid in the model. In addition, the capillary effect is unimportant in confined aquifer modelling.

17.3 Analog Models

Analogs are devices with similar input–output or cause-and-effect relations as the prototype, but with different physical properties. Flow through porous medium obeys laws that are analogous to laws governing other physical systems. For example, viscous fluid flow, membrane deflection, heat flow, or flow of electric current are some of the physical phenomena that are analogous to and governed by similar mathematical formulae as groundwater flow in porous media. These analogies provide a variety of techniques for studying the movement of ground-water and models based on such analogy are termed as analog models. *Analog modeling* techniques had their heyday in the 1950s and 1960s, and now-a-days such models are hard to find. The versatility, availability, and convenience of the digital computer for solution of groundwater problems were the main reasons why analog models lost their popularity. One of the greatest advantages of the analog models is that time need not be discretized; otherwise, the necessity of using time increments in numerical modeling is always somewhat of an aggravation and source of possible error.

a. Viscous flow model
b. Membrane model
c. Thermal model
d. Electrical model

17.3.1 Viscous Flow Models

The movement of a viscous fluid flowing between two closely spaced parallel plates is analogous to that of two-dimensional groundwater flow in porous medium. Thus, this model is based on the analogy between two-dimensional flow of groundwater governed by Darcy's law and laminar flow of a viscous fluid between closely spaced plates stated by Poiseuille's law. The first viscous fluid model or parallel plate model based on this principle was developed by Hele–Shaw, and hence viscous fluid model is also referred as *Hele-Shaw model*. Hele–Shaw models can be vertical or horizontal to simulate two-dimensional aquifer flows. If the aquifer has a slope or uniform flow field, the Hele–Shaw model can be titled accordingly. Dyes can be injected to observe streamlines or path lines.

The mean velocity v_{m} for steady laminar flow of fluid between the plates is given by the following relation:

$$v_{\mathrm{m}} = -\frac{\rho_{\mathrm{m}} g b^2}{12\mu_{\mathrm{m}}} \cdot \frac{dh}{dx} = -C\frac{dh}{dx} \tag{17.8}$$

where, ρ_{m} is the model fluid density, μ_{m} is the model fluid viscosity, b is the spacing between the plates, and C is the $\rho_{\mathrm{m}} g b^2 / 12\mu_{\mathrm{m}}$ for a given spacing b. Poiseuille's Eqn. (17.8) is analogous to Darcy's law and hence C is the equivalent hydraulic conductivity K_{m} of the model. Thus,

$$K_{\mathrm{m}} = \frac{\rho_{\mathrm{m}} g b^2}{12\mu_{\mathrm{m}}} \tag{17.9}$$

Substituting the hydraulic conductivity by the intrinsic permeability k of the prototype, irrespective of fluid viscosities, the velocity ratio v_{r} of the model to prototype becomes

$$v_{\mathrm{r}} = \frac{v_{\mathrm{m}}}{v_{\mathrm{p}}} = \frac{K_{\mathrm{m}} i_{\mathrm{m}}}{K_{\mathrm{p}} i_{\mathrm{p}}} = \frac{\rho_{\mathrm{m}} g b^2 \mu_{\mathrm{p}}}{12\mu_{\mathrm{m}} \gamma_{\mathrm{p}} k} = \frac{\rho_{\mathrm{m}} \mu_{\mathrm{p}} b^2}{12\rho_{\mathrm{p}} \mu_{\mathrm{m}} k} = \frac{\rho_{\mathrm{r}} b^2}{12\mu_{\mathrm{r}} k} \tag{17.10}$$

where, $i_{\mathrm{m}} = i_{\mathrm{p}}$ i.e. hydraulic conductivities of model and prototype are assumed the same. Transparent sheets of glass or plastic are used to construct the model. Eqn. (17.10) shows that the equivalent hydraulic conductivity of the model is proportional to square of the spacing between plates, i.e. $K_{\mathrm{m}} \propto b^2$. Therefore, layers or zones of lower hydraulic conductivity or transmissivity can be simulated by locally reducing the spacing between the plates by pasting plastic strips to the inside of one or both walls. Layers of much lower *K*, such as aquitards, can be simulated by a horizontal strip that completely fills the space between the parallel plates that has vertical slots or perforations to let liquid through. Anisotropy can be simulated with narrow, parallel and closely spaced strips pasted to the inside of one or both walls to locally reduce *b*. This creates a directional hydraulic conductivity that is greater in the direction of the strips than normal to them. Liquid is added to or withdrawn from the model to simulate sources and sinks. Uniform flow rates such as infiltration of rainfall are simulated by an array of tubes. For horizontal models, storage is obtained by connecting vertical reservoirs to the fluid between the plates. Thus the following are advantages of viscous analog models:

1. The appropriate plate spacing and fluid can be selected to correspond to the permeability proposed to be introduced in the model.
2. Problem involving two-phase flow, such as sea water intrusion can be studied by using two liquids of different viscosities and specific weighs.
3. By injecting a suitable dye, the progressive movement of stream lines and interfaces can be studied.
4. Variation in thickness of the aquifer can be can be simulated by pasting synthetic rubber on the inner side of plates.
5. Water table aquifers are simulated using constant head reservoirs at one or both ends and creating a gradient by maintaining differences in the relative elevation of the water in the reservoirs.
6. Anisotropy can be represented using different scales for vertical and horizontal dimensions of the model.
7. Rainfall by sprinklers and groundwater abstractions can be simulated by an outlet tubes.

However, the viscous flow models cannot be used for three-dimensional flows and the expression for model hydraulic conductivity is not valid for large value of *b*.

17.3.2 Membrane Models

The *membrane model* based on the *Hooke's law* consists of a thin rubber membrane of negligible weight straight tight, under uniform tension, in a rigid frame. For small deflection of membrane, the component of tension, tangent to the deflected membrane surface and its slope, are related by $T_z = C.(dz/dx)$ which is analogous to Darcy's equation, and *dz*/*dx* is corresponding to the hydraulic gradient. Membrane models are useful in studying the drawdown effects produced by wells. Only two-dimensional steady-state problems can be solved with this model. Still, it is in vogue because of its simplicity of construction and operation. The surface of membrane represents the phreatic or piezometric surface. By exerting a small load on the membrane, drawdown cones produced by pumping wells can be reproduced. Composite drawdown cones of multiple-pumping wells can be simulated by simultaneously exerting loads at several points corresponding to well locations.

17.3.3 Thermal Models

The flow of heat in a uniform body of material satisfies the Laplace equation, and hence moves as a potential flow system in the same manner as groundwater. The steady heat flow equation is analogous to Darcy's law with thermal conductivity, flow of heat and temperature are analogous to hydraulic conductivity, flow rate and head in groundwater flow, respectively. Further, the diffusion equation governing the flow of heat in a homogeneous and isotropic body of material, given below, is similar to the partial differential equation describing the flow of groundwater in a similar medium.

$$\frac{\partial^2 \theta_{\mathrm{T}}}{\partial x^2}+\frac{\partial^2 \theta_{\mathrm{T}}}{\partial x^2}+\frac{\partial^2 \theta_{\mathrm{T}}}{\partial x^2}=\frac{\rho C_{\mathrm{p}}}{C}\left(\frac{\partial \theta_{\mathrm{T}}}{\partial t}\right) \tag{17.11}$$

where, θ_{T} is the temperature and C_{p} is specific heat. The ratio $\frac{C_{\mathrm{p}}}{C}$ is analogous to $\frac{S}{T}$. It may be noted that This equation is derived considering the heat flow analogy. The main advantage is it is the only available model that can handle continuously distributed transmissivity and storage properties for the nonsteady confined case, in three dimensions. However, the technique has not been widely applied because of practical problems of model design and instrumentation. In addition, no analogy exists for free surface problems and multiphase flow cannot be studied by this model.

17.3.4 Electric Analog Models

The most common analogs in the study of subsurface water movement are *electrical analogs* where current flow through resistors or conductive media simulates water flow through porous media and electric potentials correspond to total heads. The analogy is based on the similarity between *Ohm's law* and Darcy's law. The Ohm's law states that

$$I=-\sigma.\frac{dV}{dx} \tag{17.12}$$

where, I is the electric current per unit cross-sectional area, V is the voltage, and σ is the specific conductivity of the conductor. The equivalence between Darcy's law and Ohm's law rests in that I, σ, V, and $\frac{dV}{dx}$ represent v, K, h, and $\frac{dh}{dx}$, respectively. The flow lines of electric current and the lines of equal voltage in a conducting medium correspond to the flow lines and equipotential lines of the flow of liquid through the porous media, respectively. This suggests that if we were to force the water to flow at various rates through the porous medium, and electric currents of various strengths through the conducting medium, then the resulting gradients dh/dx and dV/dx, would be similar. Electric analog models can be divided into continuous media (electrolytic tanks, conducting sheets) or discrete/noncontinuous media (network analogs).

Continuous Media Electric Analogs

In the continuous-type system, an electrical conductive medium that is continuous in space, such as a conductive liquid or solid, forms the analog of the aquifer. The geometric shape of conductive medium is similar to the shape of aquifer and boundary conditions; sources and sinks are represented by electrical voltage and currents. Electrical measuring devices are incorporated to map the voltage distribution in the model. These models are best adapted for studying steady, two dimensional flows in the aquifers.

The *conductive liquid models*, also called *electrolytic tank models*, consist of the insulated shallow trough filled with an electrolyte such as weak chloride or copper sulphate solution. The boundaries of the trough are corresponding to scale down version of the aquifer. Changes in transmissivity of the aquifer are imparted by varying the depth of the electrolyte (horizontal systems) or the distance between walls (vertical systems). Layered horizontal systems can be represented using electrolytes of different densities in the tank. Potential boundaries are represented by conductor strips shaped to boundary profile and impervious boundaries are made of dielectric material (plastic, glass, etc.). Copper electrodes are immersed in the trough to create the equipotential surface and are imparted the requisite potential or voltage difference. Lines of constant potential drop can be traced by a probe connected to an oscilloscope, a voltmeter circuit and a pentagraph. Both equipotential lines and flow lines can be traced by reversing the conducting and nonconducting boundary surfaces. Water table or free surface boundaries can be determined by trial and error. This type of models are suitable for 2D steady-state situations; however, by appropriate model modifications, multiple and/or anisotropic aquifers can be studied. Figure 17.1 shows the electrical analogy of seepage under a dam.

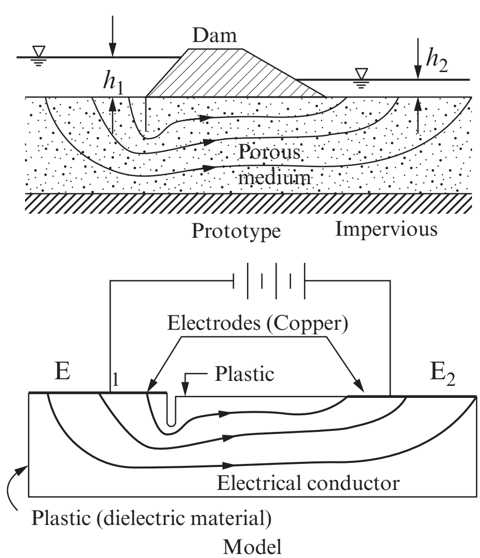

Figure 17.1 *Continuous Media Electric Analog Model*

Network/Discrete Analogs

In the discrete system, the aquifer is represented in the model by a large numbers of subareas with arrays of resistances or resistance capacitance networks (Walton and Prickett 1963). In *network analogs*, the flow medium is represented by a network of resistors and each node may be connected to electrical ground via a capacitor to simulate storage. The discrete models are based on Kirchhoff's current law:

1. At any junction of several branches of a circuit or a network, the algebraic sum of the current flowing toward the junction is zero, i.e. the total current flowing toward the junction is equal to the total current flowing out from it ($\sum I = 0$).
2. The algebraic sum of the product of current and resistance, i.e. the potential drop of each part of a closed circuit, is equal to the total emf present in the circuit ($\sum V = 0$).

The aquifer is represented by a large array of individual electric elements that form a scaled-down version of the aquifer (Bouwer 1967). Appropriate electric voltage and current sources are connected to the individual junctions or nodes of the model network to create sources, sinks, and external boundaries for the aquifer. Voltage measuring devices determine the voltage (equivalent head) distribution over the network. The pulse and waveform generators cause electric current to flow in the analog model at the appropriate times and in proportion to aquifer flow rates. The oscilloscope measures the time variations of potential levels in the model. Traces of the oscilloscope, actually time–voltage graphs, are analogous to time–drawdown graphs. A resistance network is adopted for steady-state flow conditions while a resistance-capacitance network is used for unsteady-state conditions. Electric resistors are made inversely proportional to aquifer transmissivity, whereas electric capacitors are made directly proportional to the aquifer storage. The analog is based on a finite difference grid superposed over a map of the aquifer. The analog model of the discretised aquifer with a scaled down array of electrical resistors and capacitors (Figure 17.2) can be achieved through the following scale factors:

$$c1 = \frac{Q}{Q_c}\frac{\mathrm{m}^3}{\mathrm{coulb}};\ c2 = \frac{h}{V}\frac{\mathrm{m}}{\mathrm{volt}};\ c3 = \frac{Q}{I}\frac{\mathrm{m}^3/\mathrm{day}}{\mathrm{amp}};\ c4 = \frac{t_\mathrm{d}}{t_\mathrm{s}}\frac{\mathrm{day}}{\mathrm{sec}};\ c5 = \frac{d}{\rho}\frac{\mathrm{m}}{\mathrm{cm}} \quad (17.13)$$

and values of resistors and capacitors:

$$R = \frac{c3}{c2T}\Omega;\ C = d^2 S\frac{c2}{c1}\,\text{farads} \quad (17.14)$$

The electric currents required to simulate individual pumping rate can be computed as follows:

$$I_1 = \frac{Q_1}{c3};\ I_2 = \frac{Q_2}{c3};\ I_3 = \frac{Q_3}{c3};\ I_n = \frac{Q_n}{c3} \quad (17.15)$$

It is noted that

$$T\left(h_1 + h_2 + h_3 + h_4 - 4h_0\right) = d^2 S\frac{\partial h_1}{\partial t} \quad (17.16)$$

is analogous to

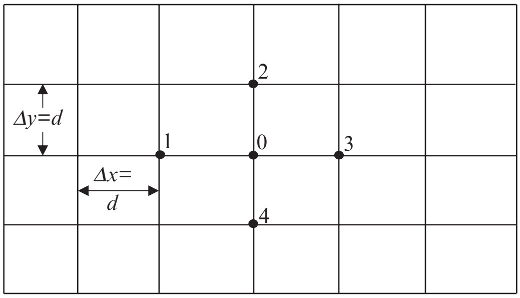

Space discretised confined aquifer

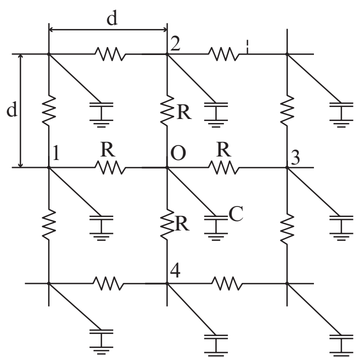

Equivalent electric network

Figure 17.2 *Discrete Electric Analog Model*

$$\frac{1}{R}\left(V_1 + V_2 + V_3 + V_4 - 4V_0\right) = C\frac{\partial V_1}{\partial t} \tag{17.17}$$

from Kirchoff's current law. The capacitance C is proportional to d^2S, it may vary as storage coefficient and the node spacing vary over the aquifer. Many times, the aquifer is divided into nonuniform grids rather than square grids of side d, e.g. grids are finer near the source or sink and wider away from them. In such cases, the network is subdivided to obtain a greater node density near the source or sink and diagonal resistors are used to obtain a smooth transition between the subdivided and regular network. For uniform media (homogeneous and isotropic aquifer), the corresponding values of resistance for square (small or large size) grids are same. A network may be constructed with plug in type resistors, which facilitates representation of uniform media in square and rectangular node patterns, and variable resistors for boundaries and layers or zones of different hydraulic conductivity or transmissivity. Variable resistors also make it possible to adjust resistance to head, as may be required for unsaturated flow or for flow in unconfined aquifers where the transmissivity varies linearly with the head.

Resistance network analogs can represent steady, 2D systems in horizontal or vertical planes and in axisymmetric systems. It is possible in resistance network analogs to simulate layered, homogeneous, or anisotropic media and to maintain the necessary input and output currents and boundary equipotentials. These analogs are simple to construct and operate. *Resistance-capacitance (RC) network analogs* can be used to study a variety of aquifer conditions, nonhomogeneous and anisotropic aquifer properties, 3D flow cases, etc. If RC analogs are used to model 2D flow systems in the vertical planes with a moving water table, capacitors are placed only at the top nodes representing the water table. RC analogs can be used to study the rise and fall of groundwater mounds below recharge basins, movement of water tables in tile drained land, groundwater-level trends in aquifers, etc. However, the network grid and resistors cannot be adjusted to properly represent the water table as it rises or falls. This can be somewhat overcome by selecting the network grid on the basis of the average water table height in the transient systems. RC analogs can be used to model an entire aquifer or groundwater basin simulating pumped wells and other discharges and recharges to predict future groundwater scenarios. Different groundwater pumping and recharge options can be simulated to develop criteria for optimum management of the groundwater resources. However, it is difficult to model nonlinear conditions of varying transmissivity in unconfined aquifers and two fluid flow problems.

17.4 Model-based Analytical Formulas Coupled with Experience

Analytical models generally require the solution of partial differential equation. Such models may be deterministic, stochastic, or it may be a combination of both. Deterministic models are used for solving regional groundwater problems involving cause and effect relationship of known systems and processes. Stochastic models which are based on probabilities of occurrence can be used in planning and decision-making processes for the groundwater resources and in evaluating the uncertainties of a system. Model-based analytical formulas coupled with experience are always one of the first to be applied in solving a groundwater problem. These models can greatly reduce the time and effort necessary in assembling a solution to a groundwater problem. In some cases, we do not need any other model other than experience coupled with use of available analytical formulas to get a solution to a problem such as Darcy's law, the Theis equation, generating solutions utilizing curve matching techniques, etc. This approach provides a rapid preliminary analysis of groundwater system utilizing a number of simplifying assumptions. These models cannot be used for solving problems with the irregularity of the domain's shape, the heterogeneity of the aquifer, and complex boundary conditions.

17.5 Numerical Models

Mathematical formulations, which consist of appropriate differential equations for the system, and their solutions, can be used as models for duplicating the hydrology and evaluating the response of groundwater reservoirs. *Analytical* *models* that consist of various analytical solutions of the differential equation of groundwater flow are applicable to relatively uniform aquifers with simple geometry for problems involving parts of aquifer of small areal extent, and have restricted use for problems of heterogeneous and extensive aquifers with irregular boundaries and multiple sources of recharge and discharge. In situations where simplified models are no longer adoptable to complex situations, numerical solutions of the partial differential equation are obtained using digital computers. *Numerical models* can also simulate more complicated problems with higher accuracy, utilizing more inputs, system parameters, and boundary conditions. *Numerical models* are used either for the simulation for the response of an aquifer to a deterministic pattern of groundwater withdrawal and recharge or for estimating the aquifer parameters by using historical data of aquifer response and excitation. The former is called a *direct* problem and the latter an *inverse* problem. Usually, a digital computer is programmed to solve the finite numbers of algebraic equations that define unknown values, e.g. hydraulic heads at specified nodes. Most of the numerical modeling was conceived in the past 40 years. Computer codes have become available and are being used by nearly all groundwater hydrologists.

Modeling starts by defining which processes are relevant and how they are represented within the model. Process identification can be easy for flow modeling and difficult for transport problems. The next issue is identification of model structure in terms of boundary conditions and parameter variability in space and time. Many assumptions and simplifications are also required. Depending on the type, description of reality that one is seeking (qualitative or quantitative) models can be conceptual or mathematical. A *conceptual model* is a qualitative description (verbal, figures, graphs, etc.) of some aspect of the behavior of a natural system. It may involve defining the origin of water (areas and processes of recharge) and the way it flows through and exits the aquifer. The conceptualization step of any modeling effort is somewhat subjective and dependent on the modeller's ingenuity, experience, scientific background and way of looking at the data. Thus, more than one description of the system may result from the conceptualization step. On the other hand, a *mathematical model* is an abstract description (based on variables, equations, etc.) of some aspect of the behavior of a natural system to aid quantification. Ideally, a model should be as simple as possible, but it should be capable to (i) represent the system information, (ii) reproduce observed system behavior, and (iii) represent features and processes key to the model's predictions. Thus a model should possess a minimal but functional complexity (simple as possible but not simpler) known as *parsimony*. Arriving at the right level of complexity is a matter of identifying what simplifications can be made without omitting something critical to the observed system and predicted system behaviors.

Both conceptual and mathematical models seek understanding. Conceptualization is the first step in modeling, and mathematical modeling helps in building firm conceptual models. In the next steps, the mathematical model is transformed into numerical model. The steps involved in numerical modelling are as follows:

1. The parameters characterizing the physical framework of the aquifer and the system conditions are identified.
2. The hydrogeological parameters are estimated using field data in specific points and interpolation/extrapolation is carried for their spatial distribution.
3. Understanding the physical behavior of the system in relation to cause and effect to formulate a conceptual model how the system operates.
4. A mathematical model is developed to describe the conceptual model by expressing the system condition using the groundwater flow equations along with associated boundary and initial conditions and appropriate simplifying assumptions. The model accuracy depends on the level of conceptualization and understanding of the groundwater system as well as the assumptions in the derivation of governing mathematical equations.
5. The mathematical model contains the same information as the conceptual model, and it is transformed to a numerical model and then solved by numerical methods to find the aquifer response in terms of head, pollutants concentrations, etc.
6. The numerical model is calibrated by fine-tuning parameters for predicting the behavior of a considered system by simulating the available field data.
7. The calibrated model is validated/verified with the selected observed data to eliminate errors resulting from the numerical approximations.
8. A sensitivity analysis is carried out to identify parameters that need to be estimated more accurately for minimizing modelling errors.
9. The final model is ready for application in assessment, planning, utilization, restoration, or management of groundwater resources.

Parameterization: The data requirement for constructing a groundwater flow/transport model requires all the parameters that constitute a groundwater flow equation at maximum number of points in space and time. Actual groundwater flow systems have mind-boggling complexity. The subsurface is a complex distribution of materials with transient fluxes of water. No matter how much effort is spent in drilling, sampling, and testing the subsurface, only limited information can be collected. In real-world situation, there may be various constraints including cost considerations. Hence, depending upon the objective of modeling and the accuracy desired the frequency of observation and the density of data requirement should be optimized. A good strategy is to start with a very simplified model with minimal data, carry out sensitivity analysis to identify critical data gaps, and gradually refine the model through expanding the database. The data required for modeling may be grouped under two broad categories: the data pertaining to physical framework of the system and data pertaining to hydrogeological framework.

Model conceptualization generally involves: (i) defining a simulation domain and the hydrogeological layers; (ii) dividing this domain into zones, each of which possesses a unique set hydraulic properties; (iii) collecting values of hydraulic properties for each material zone; (iv) determining the boundary conditions along the domain bounding surfaces; (v) determining the internal boundary conditions or stresses; (vi) collecting values of measured hydraulic head; and (vii) determining cells that are inactive or carry a constant head. Boundary conditions are often difficult to define along the sides, top, and bottom of the domain because hydraulic heads or inflow/outflow rates are generally poorly defined. To overcome this, the model boundaries may be placed along natural hydrogeologic boundaries (river, water divide line, hill, waterbody, etc.) or parallel to flowlines. Boundary condition along the top of the domain is more difficult due to inflow and outflow of water as functions of space and time. In transient models, the initial conditions are very complicated. The collected data provide only an incomplete picture of the actual system. Because of the inherent difficulty of characterizing model domain, substantial uncertainty is always introduced when creating the conceptual system.

In order to verify the accuracy of the solution, it is necessary to match the computed heads with heads measured at a number of points in the field. *Calibration* is a process of selecting/adjusting model parameters to achieve a good match between the predicted and measured hydraulic heads or other hydrogeologic data. Most commonly, calibration is accomplished by trial-and-error adjustment of model parameters. If a model is well calibrated, there may be some random deviation between simulated and observed data, but not systematic deviations. The choice of numerical values for model parameters is made during calibration, which consists of finding those values that grant a good reproduction of head and concentration data and are consistent with prior independent information. The calibration is rarely straightforward. Data may be from various sources with varying degrees of accuracy and levels of representativeness. Calibration or model tuning is required because groundwater systems are so poorly known. Calibration can be incomplete, tedious, and time consuming because many combinations of parameters have to be evaluated, and there are difficulties in taking into account the reliability of different pieces of information. Many software have automatic calibration procedures. Calibration or comparison may not be achieved due to problems in the system conceptualization or inappropriate parameter values, thus needs re-examination of model construction or data collection. There are hard-and-fast rules for what constitutes a good calibration except that errors should be small. Criteria may be based on mean error, mean absolute error, root-mean-square error, or other suitable guideline.

Once calibration is complete, a verification test is carried out to check that the model is valid representation of the hydrogeologic system. Commonly, model *verification/validation* involves using the calibrated model to simulate a hydrologic response that is known. Thus, the goal of model *validation* is to verify that the model is capable of simulating some historical hydrologic event for which field data are available. Generally, some additional refinement of parameters is necessary during validation. *Sensitivity analysis* refers to the assessment of the dependence between model inputs and outputs and, specially, how the latter respond to perturbations in the former. Analysing sensitivities is a good way to find out what additional forms of system information need to be collected.

After the model has been calibrated and validated, it is ready to be used for prediction; however, the predictions must be interpreted with caution. Even complex well calibrated-validated models are at best representation of the real flow system, since actual groundwater flow media are extremely complex and sparsely characterized. It may be noted that significant error and uncertainty are unavoidable in groundwater modelling due to errors in parameterization, conceptualization, and calibration. Predictability becomes a problem because groundwater systems are often so poorly characterized. It is usually unrealistic to find data sufficient to describe hydrologic processes in space and time. Thus, the model design depends on the informed judgement of the modeller rather than on real complete information. The calibration–validation process does not lead to a unique description of a hydrogeologic system. For poorly known system, a large number of different models can be developed without knowing which, if any, is correct. Thus, groundwater models are useful tools that should be used with full knowledge of their limitations.

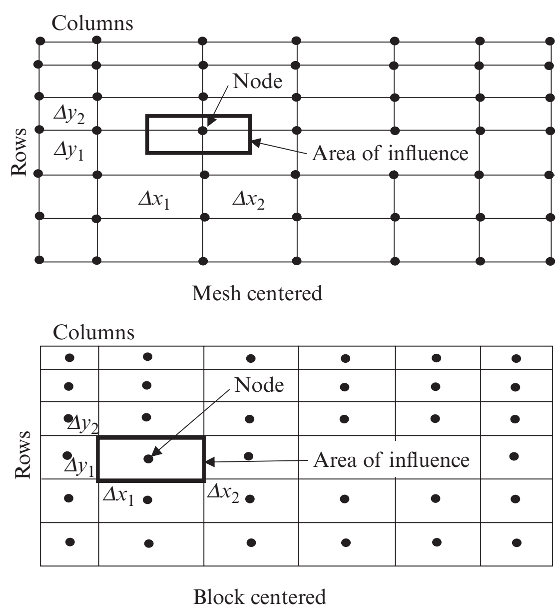

Figure 17.3 *2D Space discretization methods in FDM*

Numerical modelling solves the governing partial differential equation numerically. In case of numerical models, the continuous aquifer system parameters are first replaced by an equivalent set of discrete volumes. The time variable is also discretized. The model is solved only at these specified points in the space and time. These points are considered as discontinuous state variables for the entire domain. At these points, the governing partial differential equation is transformed into a set of algebraic equations in terms of discrete values of the state variables by utilising either finite difference form of the diffusion equation in finite difference method (FDM) or a set of difference equation from energy concepts derived by applying principle of vibrational calculus in finite element method (FEM). FDM and FEM techniques only differ from one another in the way the applicable differential equations are approximated and solved with a digital computer. FDM utilize a regular discretization, where an aquifer is subdivided into a series of rectangular grid blocks. For each grid, there is a single point, called a node, at which head is calculated. The node may be mesh centered or block centered (Figure 17.3). In 2D model, each model grid block is assumed to have a thickness; hence, it represents a volume of the aquifer. The spacing between the rows and columns may vary. The variable grid minimizes the number of nodes in a domain, but the change in size should be gradual for example the ratio in dimensions of two adjacent grids should be less than 1.5.

FEM permits a much more general arrangement (triangular, quadrilateral, etc.) of node points for easy modelling of irregular-shaped boundaries and geographical features. Each technique has its advantages and disadvantages, and neither one is the universal panacea for solving groundwater problems. Numerical models of the finite-difference and finite-element type are commonly available today to solve almost any type of groundwater problem. The popularity of FDM in groundwater modeling is due to its simplicity and the comfort of the user with mathematics involved. The model selection is a tradeoff between the computational burdens including boundary conditions, grid discretization, time steps, the model accuracy, and ways to avoid truncation errors and numerical oscillations. The performance and efficiency of a model depends upon how accurate the mathematical equations approximate the physical system being modeled, however a model is an approximation and not an exact simulation of real-world groundwater flow.

Finite Element Method: Flow systems are solved through an equivalent *variational functional* in finite element method, rather than through a finite difference solution of the differential flow equation. The flow system is considered as a general system of energy dissipation for which the head solution is found as the head distribution that minimizes the rate of energy dissipation. Thus, the solution of the differential flow equation is obtained by finding a solution that minimizes an equivalent variational function. With the finite element method, solution of differential equation is derived by an *integral approach* unlike the difference approach with the finite difference method. The first step in applying the finite element method is to derive an integral representation of partial difference equation. For obtaining a numerical solution, the aquifer is divided into a number of sub regions or finite elements, the shapes of which are determined by nodal distribution. Element shape may vary. Typically, they are triangular or quadrilateral for two-dimensional systems and tetrahedral or parallelepiped for three-dimensional systems. The irregular form of the elements facilitates representation of irregular boundaries. The element should have smallest dimensions where flow is concentrated as near pumping well. The parameters are kept constant for a given element, but may vary between elements. FEM with a fine mesh yields a more precise solution than coarse mesh, which leads to a lower precision. A fine mesh has more nodes and requires more computational effort to obtain a solution, thus it is a trade-off between the computational burden and the precision of modelling. After preparing the finite element mesh, the next step is to evaluate the integral formulation for the governing groundwater flow or solute transport equation. A system of algebraic equations is generated by implementation of the integral formulation over the domain. The method of *weighted residuals* (such as *Galekin's method*) is a most common approach that is widely used in groundwater modelling, in which an approximate solution is developed and by replacing the approximate solution into the governing equation, the residual at each node is determined. The weighted average of the residuals for each point is supposed to be equal to zero. The residual might have low value in some points while it has large value in the other points. Thus, minimizing the errors is achieved by integrating the weighted average of the error over the domain. The resultant large set of simultaneous equations can be solved by successive over relaxation, Gauss Seidel iteration, alternate direction implicit method, iterative alternating-direction implicit method or combination of these.

17.6 Finite Difference Method

In the FDM, the continuous problem domain is discretized so that the dependent variables are considered to exist only at discrete points. Derivatives are approximated by difference resulting in algebraic representation of partial differential equation. For example, the governing equation in radial coordinates

$$\frac{\partial^2 h}{\partial r^2} + \frac{1}{r}\frac{\partial h}{\partial r} = \frac{S}{T}\left(\frac{\partial h}{\partial t}\right) \tag{17.18}$$

involves first- and second-order derivatives with respect to space and first-order derivative with respect to time. These derivatives can be approximated using linear assumption or Taylor series expansion.

17.6.1 Linear Approximation

Consider h is a function of x, i.e. $h = f(x)$ as shown in Figure 17.4. For a small change in x, the variation in the function can be assumed linear. As x tends to very small, the approximation with linear assumption goes on reducing. Let $h_0 = f(x)_0$, $h_1 = f(x + \Delta x)$ and $h_{-1} = f(x - \Delta x)$ as shown in Figure 17.4. The slope of curve at x_0 or derivative can be approximated by finite difference as

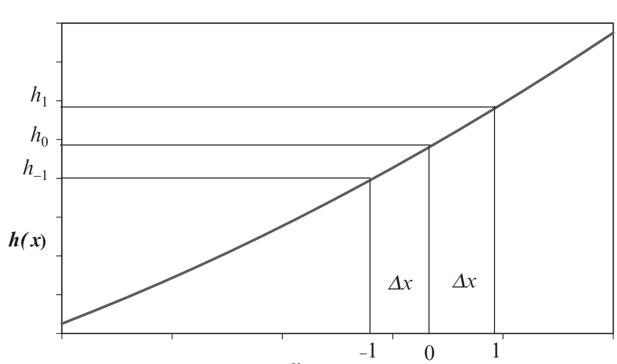

Figure 17.4 *Linear approximation of derivatives*

$$\frac{dh}{dx} = \frac{\Delta h}{\Delta x} = \frac{h_1 - h_0}{\Delta x} \tag{17.19}$$

through forward difference approximation,

$$\frac{dh}{dx} = \frac{\Delta h}{\Delta x} = \frac{h_0 - h_{-1}}{\Delta x} \tag{17.20}$$

through backward difference approximation, and

$$\frac{dh}{dx} = \frac{\Delta h}{\Delta x} = \frac{h_1 - h_{-1}}{2\Delta x} \tag{17.21}$$

by central difference approximation. The second-order derivative can be approximated as follows:

$$\frac{d^2h}{dx^2} = \frac{d}{dx}\left(\frac{dh}{dx}\right) = \frac{\Delta}{\Delta x}\left(\frac{dh}{dx}\right) = \frac{1}{\Delta x}\left\{\left(\frac{dh}{dx}\right)_{\frac{1}{2}} - \left(\frac{dh}{dx}\right)_{-\frac{1}{2}}\right\} = \frac{1}{\Delta x}\left\{\frac{h_1 - h_0}{\Delta x} - \frac{h_0 - h_{-1}}{\Delta x}\right\} \tag{17.22}$$

Therefore,

$$\frac{d^2h}{dx^2} = \frac{h_1 - 2h_0 + h_{-1}}{\Delta x^2} \tag{17.23}$$

17.6.2 Taylor Series Approximation

Using Taylor series expansion at forward space x around x_0

$$h_1 = h_0 + \frac{\Delta x}{1!}.\left(\frac{dh}{dx}\right)_0 + \frac{(\Delta x)^2}{2!}.\left(\frac{d^2h}{dx^2}\right)_0 + \frac{(\Delta x)^3}{3!}.\left(\frac{d^3h}{dx^3}\right)_0 + \ldots \tag{17.24}$$

which yields

$$\left(\frac{dh}{dx}\right)_0 = \frac{h_1 - h_0}{\Delta x} - \frac{(\Delta x)^1}{2!}.\left(\frac{d^2h}{dx^2}\right)_0 - \frac{(\Delta x)^2}{3!}.\left(\frac{d^3h}{dx^3}\right)_0 - \ldots = \frac{h_1 - h_0}{\Delta x} + \text{TE} \tag{17.25}$$

It is a forward difference approximation, where the involved truncation error is

$$\text{TE} = -\frac{(\Delta x)^1}{2!}.\left(\frac{d^2h}{dx^2}\right)_0 - \frac{(\Delta x)^2}{3!}.\left(\frac{d^3h}{dx^3}\right)_0 - \frac{(\Delta x)^3}{4!}.\left(\frac{d^4h}{dx^4}\right)_0 - \ldots \tag{17.26}$$

Using Taylor series expansion at backward space x around x_0

$$h_{-1} = h_0 - \frac{\Delta x}{1!}.\left(\frac{dh}{dx}\right)_0 + \frac{(\Delta x)^2}{2!}.\left(\frac{d^2h}{dx^2}\right)_0 - \frac{(\Delta x)^3}{3!}.\left(\frac{d^3h}{dx^3}\right)_0 + \ldots \tag{17.27}$$

which results

$$\left(\frac{dh}{dx}\right)_0 = \frac{h_0 - h_{-1}}{\Delta x} + \frac{(\Delta x)^1}{2!}.\left(\frac{d^2h}{dx^2}\right)_0 - \frac{(\Delta x)^2}{3!}.\left(\frac{d^3h}{dx^3}\right)_0 + \ldots = \frac{h_0 - h_{-1}}{\Delta x} + \text{TE} \tag{17.28}$$

It is a backward difference approximation, where the involved truncation error is

$$\text{TE} = \frac{(\Delta x)^1}{2!}.\left(\frac{d^2h}{dx^2}\right)_0 - \frac{(\Delta x)^2}{3!}.\left(\frac{d^3h}{dx^3}\right)_0 + \frac{(\Delta x)^3}{4!}.\left(\frac{d^4h}{dx^4}\right)_0 - \ldots \tag{17.29}$$

Subtracting Eqn. (17.27) from Eqn. (17.24) and manipulating

$$\left(\frac{dh}{dx}\right)_0 = \frac{h_1 - h_{-1}}{2\Delta x} - \frac{(\Delta x)^2}{3!}.\left(\frac{d^3h}{dx^3}\right)_0 - \frac{(\Delta x)^4}{5!}.\left(\frac{d^5h}{dx^5}\right)_0 - \ldots = \frac{h_0 - h_{-1}}{2\Delta x} + \text{TE} \quad (17.30)$$

It is a central difference approximation, where the involved truncation error is

$$\text{TE} = -\frac{(\Delta x)^2}{3!}.\left(\frac{d^3h}{dx^3}\right)_0 - \frac{(\Delta x)^4}{5!}.\left(\frac{d^5h}{dx^5}\right)_0 - \frac{(\Delta x)^6}{7!}.\left(\frac{d^7h}{dx^7}\right)_0 - \ldots \quad (17.31)$$

Adding Eqns. (17.24) and (17.27) and solving for second-order derivative results

$$\left(\frac{d^2h}{dx^2}\right)_0 = \frac{h_1 + h_{-1} - 2h_0}{(\Delta x)^2} - \frac{2(\Delta x)^2}{4!}\left(\frac{d^4h}{dx^4}\right)_0 - \frac{2(\Delta x)^4}{6!}\left(\frac{d^6h}{dx^6}\right)_0 - \ldots$$

$$= \frac{h_1 + h_{-1} - 2h_0}{(\Delta x)^2} + \text{TE} \quad (17.32)$$

where the involved truncation error is

$$\text{TE} = -\frac{2(\Delta x)^2}{4!}\left(\frac{d^4h}{dx^4}\right)_0 - \frac{2(\Delta x)^4}{6!}\left(\frac{d^6h}{dx^6}\right)_0 - \frac{2(\Delta x)^6}{8!}\left(\frac{d^8h}{dx^8}\right)_0 - \ldots \quad (17.33)$$

It can be noted that the first- and second-order derivative approximations are identical from both linear approximation and Taylor series expansion methods. But Taylor series expansion provides the estimation on the involved errors in form of truncation error. It is evident from the truncation error expressions that the error in the first-order derivative is proportional to grid size ($\Delta x/2$) in forward and backward approximations, whereas it is proportional to square of grid size ($\Delta x^2/6$) in central difference approximation; therefore, the error can be reduced by reducing the grid size more in central difference approximation than in forward and backward approximations, for example, by halving the grid size, the truncation errors can be reduced by one forth in central difference approximation in comparison to half in forward and backward approximations. In addition, the truncation error in central difference scheme involves - and higher-order derivatives, whereas the truncation errors in the backward and forward difference schemes involve second- and higher-order derivatives. Therefore, the central difference scheme is better approximation than the backward and forward difference schemes. Also, Eqns. (17.26) and (17.29) show that the truncation error in the backward difference approximation is less than in forward difference approximation. Similarly, if we compare the truncation errors in the first- and second-order derivatives, the truncation error is less in the second-order derivatives as it is proportional to square of grid size ($\Delta x^2/12$) and involves fourth- and higher-order derivatives.

Following the above-described approximation for the - and second- order derivatives, the equilibrium/steady-state governing equation in homogeneous and isotropic medium

$$\frac{\partial^2 h}{\partial r^2} + \frac{1}{r}\frac{\partial h}{\partial r} = 0 \quad (17.34)$$

will be rewritten in FDM as follows:

$$\frac{h_1 + h_{-1} - 2h_0}{(\Delta r)^2} + \frac{1}{r_0}\frac{h_1 - h_{-1}}{2\Delta r} = 0 \tag{17.35}$$

Thus, the problem in Eqn. (17.34) involving calculus has been transferred into algebraic problem in FDM Eqn. (17.35). The nature of the resulting algebraic system depends on the character of the problem posed by the original PDE. Equilibrium/steady-state problem usually results in a system of algebraic equations that must be solved simultaneously throughout the problem domain in conjunction with specified boundary values. Several considerations determine whether the solution so obtained will be a good approximation to exact solution of the original PDE. Among these considerations are truncation error, consistency, and stability.

As an alternative to uniform grid spacing r, the radial coordinate can be divided into grids increasing logarithmically. In the logarithmic scale, the grid spacing may be uniform or nonuniform. Transforming the radial distance variable by

$$a = \ln r \tag{17.36}$$

Hence,

$$da = \frac{1}{r}dr \Rightarrow dr = r\,da \tag{17.37}$$

Thus,

$$\frac{dh}{dr} = \frac{dh}{rda} \tag{17.38}$$

Similarly,

$$\frac{d^2h}{dr^2} = \frac{d}{dr}\left\{\frac{dh}{dr}\right\} = \frac{d}{dr}\left\{\frac{dh}{rda}\right\} = \frac{1}{r^2}\frac{d^2h}{da^2} - \frac{dh}{da}\left(\frac{1}{r^2}\right) \tag{17.39}$$

Substituting these in the governing equation yields

$$\frac{d^2h}{dr^2} + \frac{1}{r}\frac{dh}{dr} = \frac{1}{r^2}\frac{d^2h}{da^2} - \frac{dh}{da}\left(\frac{1}{r^2}\right) + \frac{1}{r}\frac{dh}{rda} = \frac{1}{r^2}\frac{d^2h}{da^2} = 0 \tag{17.40}$$

For uniform grid in logarithmic scale,

$$\Delta a = \ln r_2 - \ln r_1 = \ln r_3 - \ln r_2 = \ln r_4 - \ln r_3 = \ln r_5 - \ln r_4 \tag{17.41}$$

or

$$\frac{r_2}{r_1} = \frac{r_3}{r_2} = \frac{r_4}{r_3} = \frac{r_5}{r_4} \tag{17.42}$$

Therefore, the governing equation in radial coordinates with recharge

$$\frac{\partial^2 h}{\partial r^2} + \frac{1}{r}\frac{\partial h}{\partial r} + \frac{R}{T} = 0 \quad \text{or} \quad \frac{1}{r^2}\frac{d^2h}{da^2} + \frac{R}{T} = 0 \tag{17.43}$$

will be approximated in the finite difference scheme in the logarithmic uniform grid spacing by

$$\frac{h_1 + h_{-1} - 2h_0}{(\Delta a)^2} = -\left(\frac{R}{T}\right)_0 r_0^2 \tag{17.44}$$

This equation does not contain terms corresponding to first-order derivative approximations, therefore it has a smaller truncation error than nonlogarithmic spacing and is usually more suitable for analysing radial flow toward a well. In absence of recharge, this equation simplifies to

$$h_1 + h_{-1} - 2h_0 = 0 \tag{17.45}$$

which is independent of the grid spacing.

17.6.3 Finite Difference Approximations in Two or Three Dimensions

The governing equation for steady groundwater flow in homogeneous and isotropic medium in Cartesian coordinates is

$$\frac{\partial^2 h}{\partial x^2} + \frac{\partial^2 h}{\partial y^2} + \frac{\partial^2 h}{\partial z^2} + \frac{R}{T} = \nabla^2 h + \frac{R}{T} = 0 \tag{17.46}$$

Finite difference approximations of this equation in 3D can be derived directly using Taylor's series as described above at point 0 (Figure 17.5).

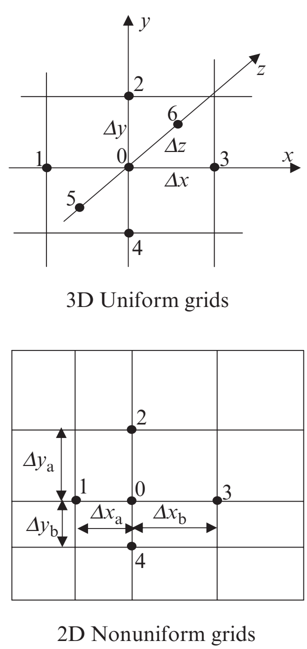

Figure 17.5 *2D and 3D discretization*

$$\frac{\partial^2 h}{\partial x^2}+\frac{\partial^2 h}{\partial y^2}+\frac{\partial^2 h}{\partial z^2}+\frac{R}{T}=\frac{h_1+h_3-2h_0}{(\Delta x)^2}+\frac{h_2+h_4-2h_0}{(\Delta y)^2}+\frac{h_5+h_6-2h_0}{(\Delta z)^2}+\left(\frac{R}{T}\right)_0 \quad (17.47)$$

Grids are not always uniformly spaced. Grid spacing can be varied depending on the spatial changes in hydraulic gradients and aquifer properties. It may preferably be closer in areas where there are large changes in transmissivity or gradient. Historic data on water are often available only at irregular spacing, so it is better to have a nonuniformly rather than a uniformly spaced grids. For nonuniform spacing of grids as shown in Figure 17.5, the finite difference approximation in 2D can be written as follows:

$$\left(\frac{\partial^2 h}{\partial x^2}\right)_0=\frac{2}{\Delta x_a+\Delta x_b}\left(\frac{h_1-h_0}{\Delta x_a}-\frac{h_0-h_3}{\Delta x_b}\right) \quad (17.48)$$

and

$$\left(\frac{\partial^2 h}{\partial y^2}\right)_0=\frac{2}{\Delta y_a+\Delta y_b}\left(\frac{h_2-h_0}{\Delta y_a}-\frac{h_0-h_4}{\Delta y_b}\right) \quad (17.49)$$

Substituting these approximations in the governing equation and multiplying each term by $(\Delta x_a+\Delta x_b)(\Delta y_a+\Delta y_b)/4$ results

$$\frac{\Delta y_a+\Delta y_b}{2}\left(\frac{h_1-h_0}{\Delta x_a}+\frac{h_3-h_0}{\Delta x_b}\right)+\frac{\Delta x_a+\Delta x_b}{2}\left(\frac{h_2-h_0}{\Delta y_a}+\frac{h_4-h_0}{\Delta y_b}\right)$$

$$=-\frac{(\Delta x_a+\Delta x_b)(\Delta y_a+\Delta y_b)}{4}\left(\frac{R}{T}\right)_0 \quad (17.50)$$

These expressions have a physical meaning. For unit thickness normal to x–y plane, the first term $\left(\frac{h_1-h_0}{\Delta x_a}\right)\left(\frac{\Delta y_a+\Delta y_b}{2}\right)$ is equivalent to head difference between nodes 0 and 1, divided the distance between the nodes and multiplied by the cross-sectional area normal to 0–1. Similar is the condition for other LHS terms. The RHS term denotes the volume centered around the node 0. Therefore the coefficients for nonuniform/graded grids in 1D, 2D, or 3D problems can be deduced from the cross-sectional area and distance between nodes.

In general, the transmissivity may vary due to a changing saturated depth or changing hydraulic conductivity and the grid spacing may also vary. The governing equation for steady groundwater flow in inhomogeneous and anisotropic medium in radial coordinates

$$\frac{\partial}{\partial r}\left(K_r b_r \frac{\partial h}{\partial r}\right)+\frac{K_r b_r}{r}\frac{\partial h}{\partial r}+R_r=0 \quad (17.51)$$

can be approximated in finite difference scheme as follows:

$$\frac{2}{\Delta r_a+\Delta r_b}\left(K_{ra}b_{ra}\frac{h_1-h_0}{\Delta r_a}-K_{ra}b_{ra}\frac{h_0-h_{-1}}{\Delta r_b}\right)+\frac{K_{r0}b_{r0}}{r_0}\frac{h_1-h_{-1}}{\Delta r_a+\Delta r_b}+R_{r0}=0 \quad (17.52)$$

If the governing equation in terms of a is used, then for variable grid spacing the above equation becomes

$$\frac{2}{\Delta a_a + \Delta a_b}\left(K_{ra}b_{ra}\frac{h_1 - h_0}{\Delta a_a} - K_{ra}b_{ra}\frac{h_0 - h_{-1}}{\Delta a_b}\right) + R_{r0}r_0^2 = 0 \tag{17.53}$$

17.6.4 Unsteady State

Finite difference form of general governing equation can be derived variously; the main difference is the manner in which the time and/or space derivative is approximated. In the backward difference form, the known values of heads at the previous time level are considered for approximating the time derivatives, wheareas in the forward difference scheme, the same is done by taking into account the difference between the known head values at present time level and the unknown values of head at the next time level as shown in Figure 17.6. For example, the governing equation for 1-D unsteady groundwater flow in Cartesian coordinates

$$\nabla^2 h = \frac{\partial^2 h}{\partial x^2} = \frac{S}{T}\left(\frac{\partial h}{\partial t}\right) = c\frac{\partial h}{\partial t} \tag{17.54}$$

involves second-order derivatives with respect to space and first-order derivative with respect to time. The finite difference approximation methods for space derivatives have already been described in the previous sections. Many approaches are available for the finite difference approximation for time derivatives. The continuous time is divided into discrete time steps in a similar manner to the discrete representation of continuous space as shown in Figure 17.6.

Since in a discrete time solution, the function is only defined at particular times, discrete time steps can be represented in additional dimension. The finite difference approximation of the space term (RHS of Eqn. 17.54) can be written as follows:

$$c\frac{\partial h}{\partial t} = c\frac{h_{0,t+\Delta t} - h_{0,t}}{\Delta t} \tag{17.55}$$

where the first suffix refers to the position in space and the second suffix refers to the time. The various finite difference approximations depend on the time at which $\nabla^2 h$ is defined. It is called a forward difference approximation in the case where $\nabla^2 h$ is defined at time *t*. Thus, in 1D space dimension with uniform grid spacing Δx the forward finite difference approximation of Eqn. (17.54) yields

$$\frac{h_{1,t} + h_{-1,t} - 2h_{0,t}}{(\Delta x)^2} = c\frac{h_{0,t+\Delta t} - h_{0,t}}{\Delta t} \tag{17.56}$$

It involves only one unknown $h_{0,t+\Delta t}$ solving for it

$$h_{0,t+\Delta t} = \frac{\Delta t}{c(\Delta x)^2}\left(h_{-1,t} - \left(2 - \frac{c(\Delta x)^2}{\Delta t}\right)h_{0,t} + h_{1,t}\right) \tag{17.57}$$

It can be noted that the function at time $t + \Delta t$ is expressed explicitly in terms of the known values of the function at time *t*, therefore it is an explicit scheme (Figure 17.6). The whole domain can be solved in *x–t* plane. The initial and boundary conditions must be satisfied as well as the differential equation. This scheme is conditionally stable.

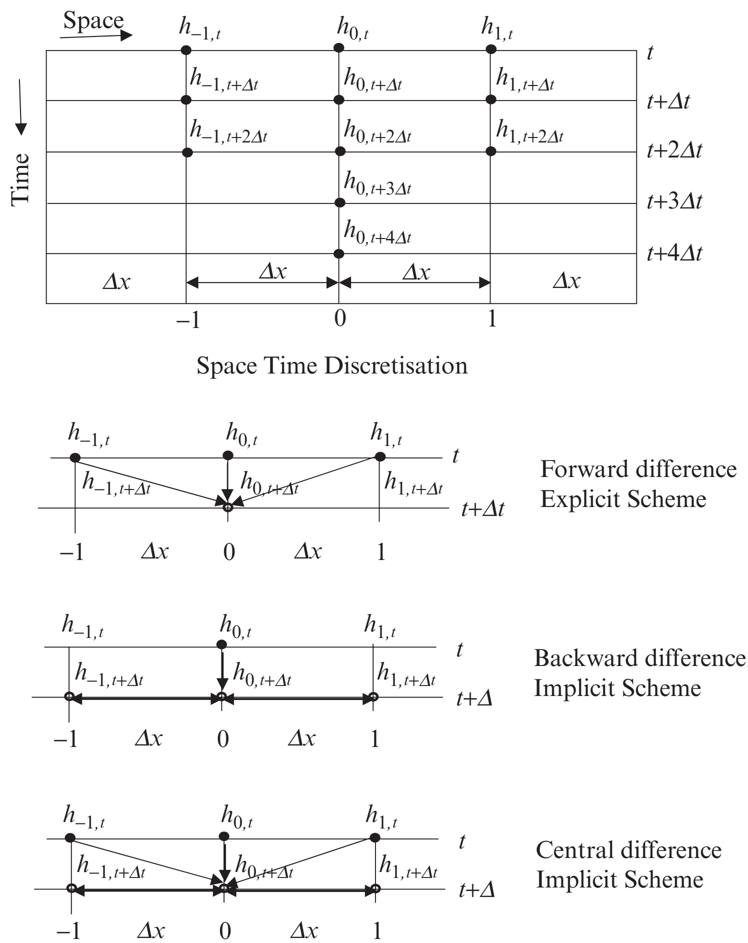

Figure 17.6 *Time space discretisation schemes*

When $\nabla^2 h$ is defined at time $t+\Delta t$ then the approximation is termed a backward difference (Figure 17.6). Similar to the earlier case, Eqn. (17.54) approximates to

$$\frac{h_{1,t+\Delta t} + h_{-1,t+\Delta t} - 2h_{0,t+\Delta t}}{(\Delta x)^2} = c\frac{h_{0,t+\Delta t} - h_{0,t}}{\Delta t} \tag{17.58}$$

Solving it for unknowns

$$h_{-1,t+\Delta t} - \left(2 + \frac{c(\Delta x)^2}{\Delta t}\right)h_{0,t+\Delta t} + h_{1,t+\Delta t} = -\frac{c(\Delta x)^2}{\Delta t}h_{0,t} \tag{17.59}$$

Here, explicit solution of unknowns is not possible. Similar equations have to be written for each space node at time $t+\Delta t$, which finally result into a system of linear equations and these simultaneous equations can be solved for all the unknowns. The unknowns are thus given implicitly. The solution is marched forward in time by solving the simultaneous equations at each time step and the technique is unconditionally stable.

The third alternate is to define $\nabla^2 h$ average of times t and $t+\Delta t$ (Figure 17.6), therefore

$$\frac{h_{1,t}+h_{-1,t}-2h_{0,t}}{2(\Delta x)^2}+\frac{h_{1,t+\Delta t}+h_{-1,t+\Delta t}-2h_{0,t+\Delta t}}{2(\Delta x)^2}=c\frac{h_{0,t+\Delta t}-h_{0,t}}{\Delta t} \tag{17.60}$$

Solving it for unknowns

$$h_{-1,t+\Delta t}-2\left(1+\frac{c(\Delta x)^2}{\Delta t}\right)h_{0,t+\Delta t}+h_{1,t+\Delta t}=-h_{1,t}+2\left(1-\frac{c(\Delta x)^2}{\Delta t}\right)h_{0,t}-h_{-1,t} \tag{17.61}$$

which is also an implicit scheme. This is a central difference approximation and known as the Crank–Nicholson method. If the LHS of the governing equation is nonlinear, then the discretization will also be nonlinear. Thus advancing in time will involve the solution of a system of nonlinear algebraic equations, although linearization is possible. Actually, the heads change between time step Δt, therefore the space derivatives of head are valid for small time steps only. The approximation can be improved by considering a weighted average of the approximations at times t and $t+\Delta t$ as follows:

$$(1-\alpha)\frac{h_{1,t}+h_{-1,t}-2h_{0,t}}{(\Delta x)^2}+\alpha\frac{h_{1,t+\Delta t}+h_{-1,t+\Delta t}-2h_{0,t+\Delta t}}{(\Delta x)^2}=c\frac{h_{0,t+\Delta t}-h_{0,t}}{\Delta t} \tag{17.62}$$

where α is a weighting parameter lies between 0 and 1. For $\alpha = 0$, it reduces to Eqn. (17.57) leading to explicit forward scheme implying that the value of space derivatives at the old time is the best approximation. For $\alpha = 1$, it reduces to Eqn. (17.59) leading to implicit backward difference scheme implying that the value of space derivatives at the future time is the best approximation. When $\alpha = 0.5$, the best value lies halfway between time step Δt and Eqn. (17.62) reduces to Eqn. (17.61) as the Crank–Nicholson scheme.

Finite difference approximations for both steady-state and unsteady-state problems lead to sets of simultaneous equations. The accuracy of the solution of the resultant equations depends on consistency, stability, and convergence. A finite difference scheme is consistent if it becomes the corresponding partial differential equation as the grid size and time step approach zero or truncation errors are zero. A numerical solution technique is stable if the error remains bounded. Certain criteria must be satisfied in order to achieve stability. A finite difference scheme is convergent if its solution approaches that of the partial differential equation as the grid-size approaches zero. Both consistency and stability are prerequisite to convergence.

The solution of the simultaneous equations, when the complete set has to be solved at each time step, can be a time-consuming procedure, even on a high-speed computer. The most convenient technique is the forward difference explicit procedure since it does not involve the solution of simultaneous equations. However, it suffers from two serious limitations namely stability and convergence. If the time step exceeds a critical value, unstable results are obtained, with the calculated functions showing wild fluctuations. The stability for a one-dimensional problem with constant coefficient using uniform grid spacing Δx can be achieved by the Courant condition as follows:

$$\frac{\Delta t}{c\left(\Delta x\right)^2} \leq \frac{1}{2} \tag{17.63}$$

With variable grid spacing or c (transmissivity and/or storage coefficient), the smallest time step anywhere within the domain is the critical condition. There is no stability criterion for the backward difference approximation. Difference between the analytical and numerical results can be caused by the finite difference approximation. The space discretization leads to certain errors but the nature of the forward difference time approximation, where the current value of the function depends only on the behaviour at the previous time step can lead to more serious errors. For example, the effect of a change in a condition at a boundary has no effect within the field until later time steps. Therefore, the convergence of the forward difference approximation is usually inferior to the backward difference approximation. The most important feature of the backward difference method is that the calculation is stable even if a large time step is adopted. Therefore, the implicit methods are generally preferred as the scheme is unconditionally stable, regardless of the size of time increment, whereas it is extremely small for achieving the stable solutions in the explicit methods. A time step that increases logarithmically is an economical choice when long time periods are being investigated. The central difference form is not widely applied, as the nonlinear aquifer problems generate nonlinear finite difference equations that are difficult to solve (Prickett 1975).

One-dimensional implicit problems can solved by means of Gaussian elimination of a tridiagonal matrix. Two-dimensional problems can be considered as a series of interconnected one-dimensional strips. During the first sub step, the grid is swept in the x direction, row by row, leading to a series of one-dimensional solutions, each with a tridiagonal matrix. In the second substep the equations are swept in the y direction. This alternating direction implicit (ADI) procedure is suitable for certain types of problems. It is an implicit method that does not involve the costly solution of a large number of simultaneous equations. A simple rearrangement of alternating direction technique leads to an explicit (ADE) formulation, which has a less stringent stability criterion than the standard explicit method. The ADE method is not suitable for the analysis of aquifers that are partly confined and partly unconfined. Other solution procedure is iterative and relaxation method known as the point successive overrelaxation (SOR) method. The speed of convergence in SOR is not sensitive to the choice of the overrelaxation parameter and nonlinearities can be included without difficulty in SOR method. The computational effort required for a time step of the ADI method is roughly eight times that for the explicit method and twice that for one iteration of the SOR technique. If SOR requires twenty iterations, the ADI becomes ten times efficient than SOR. The choice of method of solving the finite difference equations depends on the nature of the problem and the type of computational capability of the computer. Further, the following may be taken into considerations (i) simplicity of computer program, (ii) computational effort required, (iii) stability and convergence, and (iv) representation of internal and external boundaries.

17.6.5 Modflow

MODFLOW is a modular 3D, finite-difference groundwater flow model developed by the US Geological Survey (McDonald and Harbaugh, 1988). It is one of the most widely used groundwater simulation models. MODFLOW model can be downloaded freely from USGS Website. It gained broad acceptance because it is versatile, well tested, well documented, and in the public domain. It is designed to simplify model development and data input for groundwater modelling to develop maps, diagrams, and text files. In MODFLOW model, it is possible to simulate steady and unsteady flow in an irregularly shaped flow system in which aquifer layers can be confined, unconfined, or a combination of confined and unconfined. MODFLOW also has capability of solute transport modeling and parameter estimation. The partial–differential equation of groundwater flow used in MODFLOW is

$$\frac{\partial}{\partial x}\left\{K_{xx}\frac{\partial h}{\partial x}\right\}+\frac{\partial}{\partial y}\left\{K_{yy}\frac{\partial h}{\partial y}\right\}+\frac{\partial}{\partial z}\left\{K_{zz}\frac{\partial h}{\partial z}\right\}\pm R=S_s\frac{\partial h}{\partial t} \quad (17.64)$$

where, K_{xx}, K_{yy}, and K_{zz} are values of hydraulic conductivity along the x, y, and z coordinate axes, which are assumed to be parallel to the major axes of hydraulic conductivity; h is the potentiometric head; R is a volumetric flux per unit volume representing sources and/or sinks of water, with $R < 0.0$ for flow out of the groundwater system, and $R > 0.0$ for flow in (1/sec); S_s is the specific storage of the porous material (1/m); and t is time. The continuous groundwater flow system is discretized in space and time by divided into grids and layers in space and steps in time. The node may be mesh-centered or block-centered. A dense system of nodes can be provided around features of interest and sparse system otherwise. Eqn. (17.64) is converted into algebraic difference equations where the head in each node is a function of both space and time. Hydraulic conductivities, transmissivities, or thicknesses of any layer may differ spatially and may be anisotropic and the storage coefficient may be heterogeneous. Parameters of hydraulic conductivity, initial head, storage coefficient, top and bottom elevation, etc., are specified for each cell. Flow from external stresses such as flow to wells, real recharge, evapotranspiration, flow to drain, and flow to river bed can be simulated using different packages. Specified head, flux, and head dependent flux boundaries can easily be simulated. The number of stress periods over which the model is to be run and the time of their operation should be set. Several methods (e.g. slice successive overrelaxation (SSOR), strongly implicit procedure (SIP), preconditioned conjugate gradient (PCG) procedure, etc.) are available for solving the resulting set of algebraic equations; the user can choose the best one for a particular problem. Flow rate and cumulative volume, which are balanced from each type of inflow and outflow are computed for each time step. Care must be taken in selecting a time step size to avoid errors that can occur due to large time step particularly in the beginning. MODFLOW allows the user to increase the size of the time step as the simulation proceeds. Results can be analyzed in different ways. Prediction of head/drawdowns at pumping nodes is a problem because it is a cell averaged value rather than at the point. MODFLOW is built with a modular design that involves a main program and packages. The packages are groups of independent subroutines, which serve specific tasks. According to their functions, the packages fall into the following categories: (i) basic package; (ii) block-centered flow packages; (iii) solver packages such as SSOR, SIP, PCG, etc.; (iv) boundary condition (such as rivers, wells, recharge, drain, general head, evapotranspiration, etc.) packages; (v) and output control packages. For any solution, flow package and solver package are required. Boundary condition packages are optional. A default output is used if the output control is not specified. For user-friendly model creation and visualization of results various GUIs on MODFLOW are available for example groundwater modelling system (GMS), Visual MODFLOW, VFlex, etc. These are powerful graphical tools, wherein models can be built using digital maps and elevation models for reference and source data. They also make it possible to build a conceptual model using GIS feature objects. The conceptual model defines the boundary conditions, source/sinks, and material property zones for a model. The model data can then be automatically discretized to the model grid or mesh, which makes it possible to deal with large complex models in a simple and efficient manner.

17.7 Case Study

The case steady area was about 6 km south of Faridabad on the west of Delhi–Agra National Highway No. 2 and about 13 km away from the Delhi–Haryana border. The site was adjacent to Delhi–Kolkata railway line and was surrounded mostly by industrial units, which were small to medium scale in nature. The present groundwater level in the area is about 42 m bgl (154 mamsl) and the maximum thickness of top unconfined aquifer with fresh groundwater is about 62 m, leaving maximum saturated thickness of about 20 m, which varies spatially in the area. In view of the increasing stress on groundwater and proposed groundwater withdrawal in the area to the tune of 3000 m^3/d and to study the overall groundwater dynamics in the changed scenario a predictive groundwater simulation study was carried out in an area. In the study, Visual MODFLOW Version 4.2 was used, which is one of the most commonly used and internationally accepted standard modeling software for groundwater flow and transport modeling. The software uses MODFLOW code with Graphical User Interface (GUI), preprocessor, and postprocessor. The basic advantage of the software is its easy and user friendly menu driven operation. The data can be entered through the screen as well as it can be imported externally.

17.7.1 Model Conceptualization

For the purpose of detailed investigation, an area of 10 km × 10 km was selected. The area was explored by CGWB and map of exploratory wells drilled in study area and location of public/private wells in study area around the plant were available. The model domain falling within 10 km radius around the site had plain topography except in the North West where it had exposed Aravalli hills. The eastern part of the area was bounded by river Yamuna with regional easterly slope. The elevation varied from 216 m amsl at the North West portion to 190 m amsl at the eastern parts adjoining the river Yamuna.

The subsurface disposition of the litho units as compiled from the various drill logs was collated in the form of a fence diagram (See Figure 17.7, Color Plate 9). A perusal of the diagram indicates presence of a thin top soil gradually terminating into clay dominant zone underlain by alluvial sand with clay intercalations. The correlation of litholog data, cross sections, and fence diagrams indicates broadly two-layer aquifer system in the area within 135 m depth from the ground. Most ref the production wells in the area were tapping the aquifers down to the depth of 100–125 m bgl. The first aquifer (which is unconfined) was encountered in general within 80 m depth from the ground consisting of alluvial formation and the quality of groundwater in this aquifer was potable and being used heavily for drinking water supply, and hence the top aquifer was under stress for groundwater development. The second aquifer was considered up to the depth of 135 m from ground with an average alluvium thickness of 65 m with semi confined to confined conditions as it was separated by discontinuous thick clay/silt clay layer from the first aquifer. The groundwater in this aquifer was brackish to saline.

There was difficulty in deciding the model domain and boundary conditions due to absence of any physical boundary in the case study area. To overcome this, the groundwater flow direction and hydrogeological variations in the area were considered. Keeping in view the resultant flow direction and its gradient and location of the site (presence of Aravallis), part of the north western boundary of the model area was taken as no flow boundary. The river Yamuna (assumed effluent in this stretch) is not far away from the eastern boundary that was also the general flow direction, and hence lateral outflows of the model domain in the eastern and southern boundary was considered at the terminal end through General Head boundary at selected cells. The amount of water, i.e. the rate of inflow and outflow was arrived based on the Darcy's equation. Rest of the boundary of the model area was marked as no-flow boundary.

17.7.2 Model Design

Model design involved (i) spatial discretization of the model area and (ii) time discretization in terms of stress periods and time steps. The size of the cell is decided based on the objective of the study as well as availability of aquifer parameter data. A moderately fine grid size, with each cell measuring 250 m × 250 m has been found suitable for the area in view of the volumetric assessment of total inflow and out flow from the system and limited data availability of aquifer parameters and piezometric head values for all the layers. The entire model area (10 km × 10 km) was discretized into 40 columns and 40 rows i.e. 1600 cells of 250 m × 250 m. The top of the Layer one was generated from the reduced level (ground-level) data, by interpolation through Arc GIS and SURFER software; similarly, the bottom of all the layers were specified grid wise from the data available from the boreholes and cross sections and interpolated for all the active cells. The model domain and its boundary and 3D representation is shown in Figure 17.8 (Color Plate 10). The interpolated water level based on the field observations entered cell wise in the form of initial piezometric head (IPZ) for the layer 1represented the upper bound of the aquifer as shown in Figure 17.9 (See color Plate 10), the lower boundary was represented by the bottom of the layer. All the elevation of the layers were entered taking a standard datum.

17.7.3 Input Parameters

The aquifer parameters after steady-state calibration as hydraulic conductivity in x–y plane ($K_x = K_y$), hydraulic conductivity in vertical direction (K_z), and specific storage/specific yield (S_s/S_y) were 40–48 m/d, 4 m/d and 0.1–0.2, respectively, for aquifer layer 1 and 40 m/d, 4 m/d, and 2×10^{-5}, respectively, for aquifer layer 2. The water level /piezometric heads measured in the field at various observation wells was entered for both the layers by interpolating the field observations utilizing the Arc suit of software. The lumped data available for draft and recharge were distributed cell wise. The recharge as computed for the study area by using GEC methodology (CGWB, 2009) was distributed cell wise to the entire model domain for the layer 1. Similarly, the draft data available from the GEC computations were distributed to all cells evenly. Further, in order to accommodate the huge withdrawal 3000 m^3/d from the tube well in the area to meet the drinking and domestic water demand surrounding the area and an additional draft to the tune of 250 m^3/d (32 MLD) with annual increment of 2% was considered.

17.7.4 Model Calibrations

The model was calibrated initially for the steady state to firm up the aquifer parameters in view of the limited availability of aquifer parameters from the field. Number of trial runs was made by varying the hydraulic conductivity and storage parameters so as to achieve a good agreement between the observed and computed heads in space and time. After ensuring a reasonable match of contours of water level in spatial domain, the model was subjected to transient-state modeling for calibration and future predictions. In the transient modeling, the period of 365 days, i.e. one year has been further divided into two stress periods representing the monsoon and nonmonsoon cycles so as to accommodate the monsoon/rainfall recharge. The stress period one pertains to 90 days of monsoon period and reaming days of the year represents the nonmonsoon.

17.7.5 Model Predictions

The calibrated model was used for making future predictions. In order to simulate the impact of additional groundwater withdrawal in the area, two scenarios were generated. In Scenario I, the model was run for 10 years with the existing stress conditions of recharge and with an incremental groundwater withdrawal of 2% from layer one. In Scenario II, additional groundwater withdrawal of about 3000

m^3/d was imposed from the area. The model was run for ten years to observe the impact of additional withdrawal on the groundwater regime of the area. Further, in order to have a quantitative idea of various inputs and output from the system, the mass balance outputs in the form of histograms were obtained from the model after each run. The Table 17.1 lists the results.

Table 17.1 Prediction for 10 years

Prediction Time (Days)	*Drawdown Created (m)*		*Water Table (m Above Mean Sea Level)*		*Saturated Thickness Remaining (m)*	
	Scenario I	*Scenario II*	*Scenario I*	*Scenario II*	*Scenario I*	*Scenario II*
365	3	3.5	151.00	150.50	17	16.5
1825	7	8	147.00	146.00	13	12
3650	9.5	11	144.50	143.00	10.5	9

It may be concluded that after 10 years only 9–10 m of saturated thickness is left out in the top aquifer having fresh groundwater. In general, the decline is less in south eastern part and maximum in the north western part represented by Aravalli range. Any further drawdown may lead to increased exchange of water from the lower aquifer having saline water and may lead to up coning and mixing of saline water. In the layer 2, a similar decline in groundwater was observed. Hence, necessary measures may be taken for rain water harvesting and recharge of groundwater so as to provide sustainability of the aquifer with fresh water.

SOLVED EXAMPLES

Example 17.1: Solve the problem of flow through a confined aquifer having uniform leakage rate R from the aquitard as shown in Figure 17.10 using FDM.

Solution: Assume the origin at O for x and h at the centre. The flow is symmetrical in the confined aquifer, therefore use half of the domain for analysis. Let us divide the domain into four grids of Δx each, i.e. $\Delta x = L/4$. It is 1-D flow in a confined aquifer so governing equation is

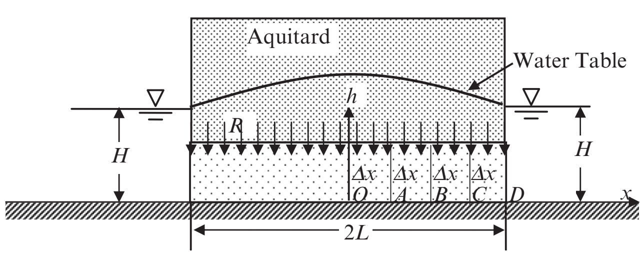

Figure 17.10 *1D flow in confined aquifer having uniform leakage*

$\frac{d^2h}{dx^2}+\frac{R}{T}=0$. Using central difference scheme for approximation of second-order derivative $\frac{d^2h}{dx^2}=\frac{h_1+2h_0-h_{-1}}{(\Delta x)^2}=\frac{h_1+2h_0-h_{-1}}{(\mathrm{L}/4)^2}$. Therefore, the FDM approximation of the governing equation becomes $h_1+2h_0-h_{-1}=-\frac{RL^2}{16T}$. This equation at node point O is

$$h_A-2h_O+h_A=-\frac{RL^2}{16T}\Rightarrow h_A=h_0-\left(\frac{Rl^2}{32T}\right)$$

Similarly, the FDM equations at the nodes A, B, and C become

$$h_B-2h_A+h_0=-\frac{RL^2}{16T}\Rightarrow h_B=h_0-\left(\frac{RL^2}{8T}\right)$$

$$h_C-2h_B+h_A=-\frac{RL^2}{16T}\Rightarrow h_c=h_0-\left(\frac{9}{32}\frac{RL^2}{T}\right)$$

$$h_D+h_B-2h_C=-\frac{RL^2}{16T}\Rightarrow h_c=\frac{h_D+h_B}{2}+\left(\frac{1}{32}\frac{RL^2}{T}\right)$$

Using $h_D=H$ from the boundary condition at D, and solving these equations yields

$$h_0=H+\frac{RL^2}{2T};h_A=H+\frac{15}{32}\frac{RL^2}{T};h_B=H+\frac{3}{8}\frac{RL^2}{T};\text{and}\,h_C=H+\frac{7}{32}\frac{RL^2}{T}$$

Now these are the heads at discrete points using numerical approximation, but let us check the accuracy of these results by comparing these to analytical solution.

The present case is a simple 1D flow with simple boundary conditions, therefore an analytical solution is possible. The solution of governing equation is $\frac{dh}{dx}=-\frac{R}{T}x+C1$ and $h=-\frac{R}{T}\frac{x^2}{2}+C1x+C2$. Now on applying boundary conditions, i.e. at $x=L\rightarrow h=H$ and $x=0\rightarrow\frac{dh}{dx}=0$, we get $C1=0$; and $C2=H-\frac{RL^2}{2T}$. Therefore, the solution becomes $h=H+\frac{R}{2T}\left(L^2-x^2\right)$. $\left(L^2-x^2\right)$. Therefore at O, $x=0\Rightarrow h_0=H+\frac{RL^2}{2T}$; at A, $x=\frac{L}{4}\Rightarrow h_A$ $=H+\frac{15}{32}\frac{RL^2}{T}$; $=H+\frac{15}{32}\frac{RL^2}{T}$; at B, $x=\frac{L}{2}\Rightarrow h_B=H+\frac{3}{8}\frac{RL^2}{T}$; and at C, $x=\frac{3L}{2}\Rightarrow h_c=H+\frac{7}{32}\frac{RL^2}{T}$. $=H+\frac{7}{32}\frac{RL^2}{T}$. These head values are identical as obtained using FDM.

Thus, it was observed that the FDM solution exactly matched with the analytical solution. This happened because of zero truncation errors when evaluated using $\text{TE} = -\frac{2(\Delta x)^2}{4!}\left(\frac{d^4h}{dx^4}\right)_0 - \frac{2(\Delta x)^4}{6!}\left(\frac{d^6h}{dx^6}\right)_0 - \frac{2(\Delta x)^6}{8!}\left(\frac{d^8h}{dx^8}\right)_0 - \ldots$ from analytical solution. Here, the exact solution is the second-order polynomial, but the truncation errors in FDM approximation of the governing equation of this problem through central difference method involve fourth- and higher-order derivatives, which are zero for second order polynomial function.

Example 17.2: Solve the same problem but with leakage rate R varying parabolically.

Solution: Here as in Figure 17.11 also, the flow is symmetrical, but leakage rate varies so the governing equation is $\frac{d^2h}{dx^2} = -\frac{R_x}{T}$ where $R_x = 0$ at $x = 0$; $R_x = \frac{3}{4} R_m$ at $x = \frac{1}{4} L$; $R_x = R_m$ at $x = \frac{1}{2} L$; $R_x = \frac{3}{4} R_m$ at $x = \frac{3}{4} L$; and $R_x = 0$ at $x = L$ for a parabolic variation in R_x with maximum value R_m. Therefore, FDM approximations of this equation at different nodes O, A, B, and C are

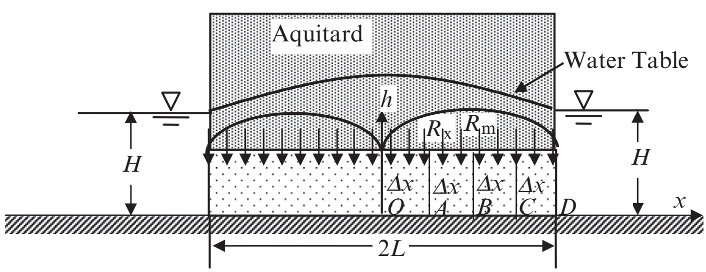

Figure 17.11 *1D flow in confined aquifer with parabolic leakage*

$$h_A - 2h_O + h_A = 0 \Rightarrow h_A = h_0$$

$$h_B - 2h_A + h_0 = -\frac{3}{4}\frac{R_m}{T}\frac{L^2}{16} \Rightarrow h_B = h_0 - \frac{3}{4}\frac{R_m}{T}\frac{L^2}{16}$$

$$h_C - 2h_B + h_A = -\frac{R_m}{T}\left(\frac{L^2}{16}\right) \Rightarrow h_C = h_0 - \frac{5}{32}\left(\frac{R_m}{T}\right)L^2$$

$$h_D + h_B - 2h_C = -\frac{3}{4}\frac{R_m}{T}\frac{L^2}{16} \Rightarrow h_C = \frac{h_D + h_B}{2} + \frac{3}{4}\frac{R_m}{T}\frac{L^2}{32} \Rightarrow h_C = \frac{h_D + h_0}{2}$$

Using $h_D = H$ and equating two equations for h_C gives $h_0 = H + \frac{5}{16}\left(\frac{R_m}{T}\right)L^2$. Therefore, plugging the value of h_0 in other equations result in $h_A = H + \frac{5}{16}\left(\frac{R_m}{T}\right)L^2$; $h_B = H + \frac{17}{64}\left(\frac{R_m}{T}\right)L^2$; and $h_C = H + \frac{5}{32}\left(\frac{R_m}{T}\right)L^2$.

Analytical solution of differential equation $\frac{d^2h}{dx^2} = -\frac{R_x}{T} = \frac{4R_m}{TL^2}\left(Lx - x^2\right)$ is $h = -\frac{4R_m}{L^2T}\left\{\frac{Lx^3}{6} - \frac{x^4}{12}\right\} + C1x + C2$ Applying boundary conditions $x = 0 \rightarrow \frac{dh}{dx} = 0$ and $x = L \rightarrow h = H,$ we get $C1 = 0$ and $C2 = H + \frac{R_m L^2}{3T}$. therefore the solution reduces to $h = -\frac{4R_m}{L^2T}\left\{\frac{Lx^3}{6} - \frac{x^4}{12}\right\} + H + \frac{R_m L^2}{3T}$ which is a fourth-order polynomial equation. Therefore, the heads at different nodes are as $h_0 = H + \frac{R_m L^2}{3T}$; $h_A = H + \frac{83}{256}\left(\frac{R_m L^2}{T}\right)$; $h_B = H + \frac{13}{48}\frac{R_m L^2}{T}$; and $h_c = H + \frac{121}{768}\frac{R_m L^2}{T}$.

It can be noted that here FDM solution does not match with the analytical solution due to involved truncation errors. The FDM computed head values are lower than the theoretical values. The truncation error is $\text{TE} = -\frac{2(\Delta x)^2}{4!}\left(\frac{d^4h}{dx^4}\right) - \frac{2(\Delta x)^4}{6!}\left(\frac{d^6h}{dx^6}\right)_0 - \ldots = \frac{1}{12}\frac{L^2}{16}\frac{4R_m}{TL^2}(2) = \frac{R_m}{24T},$ which is equivalent to a uniform reduction in recharge/leakage. Had the problem solved with RHS $= -\frac{R_x}{T} + \frac{R_m}{24T}$ in the FDM, the solution would be identical to the exact solution. Alternatively, with smaller mesh interval the truncation error becomes smaller and the numerical values become closer to the theoretical values.

Example 17.3: A well of 2 m diameter in a confined aquifer ($T = 200$ m²/d) is pumped under steady state such that the piezometric heads 20 m and 25 m are observed at the well face and 10 m away from the well centre respectively as shown in Figure 17.12. Solve the problem numerically and compare results with the corresponding analytical solution.

Solution: Let us consider only two uniform grids, i.e. $\Delta r = (10-1)/2 = 9/2 = 4.5$ m (Figure 17.12). From boundary conditions $h_A = 20$ m and $h_C = 25$ m, therefore only unknown piezometric head is h_B.

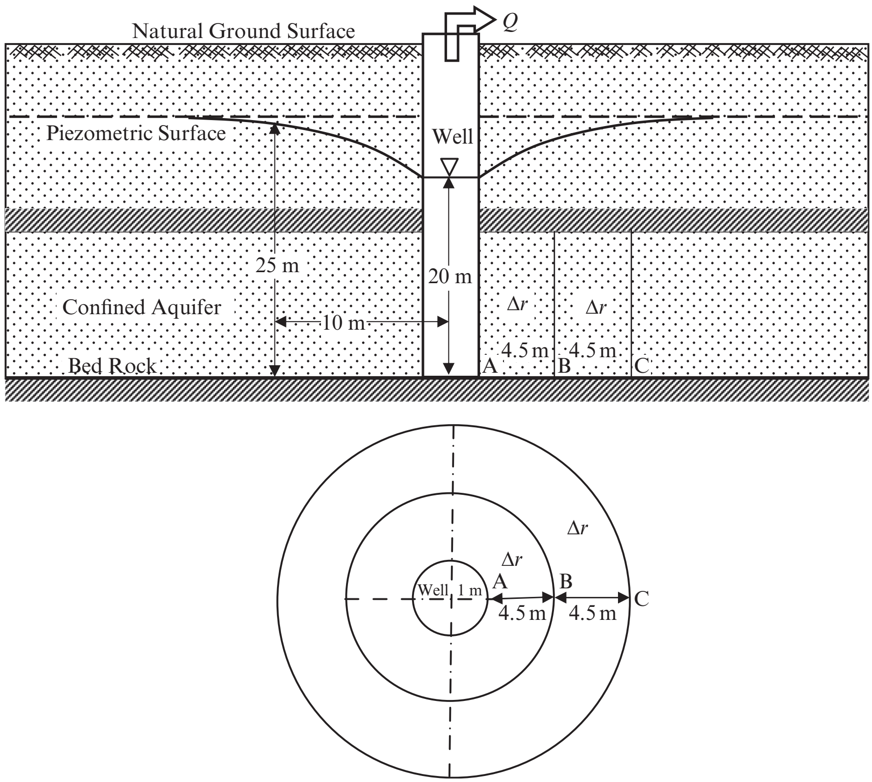

Figure 17.12 *Steady well discharge from a confined aquifer*

The steady-state governing equation in radial coordinates is $\frac{d^2h}{dr^2}+\frac{1}{r}\frac{dh}{dr}=0.$

The FDM approximation of this equation at B is $\frac{h_C+h_A-2h_B}{4.5^2}+\frac{1}{5.5}\frac{h_C-h_A}{9}=0 \Rightarrow \frac{20+25-2h_B}{4.5^2}+\frac{25-20}{9\times 5.5}=0 \Rightarrow h_B=23.523\,\text{m}.$

Analytical solution for steady flow in confined aquifer is $h=H+\frac{Q}{2\pi T}\ln\left(\frac{r}{r_e}\right)$,

but $r_1=1\,\text{m} \rightarrow h=20\,\text{m}$ and $r_2=10\,\text{m} \rightarrow h=25\,\text{m}$, hence $h_2-h_1=\frac{Q}{2\pi T}\ln\left(\frac{r_2}{r_1}\right)$

$\Rightarrow 5=\frac{Q}{2\pi T}\ln 10 \Rightarrow \frac{Q}{2\pi T}=\frac{5}{\ln 10}$; therefore, the analytical solution becomes $h=20+\frac{5}{\ln 10}\ln r.$ At node B, r = 5.5 m, hence $h_B=20+5\log 5.5=23.701\,\text{m}$, which is different from the FDM solved value.

Now let us divide the complete length into four grids, therefore $\Delta r = 9/4 = 2.25$ m as shown in Figure 17.13 . There will be three unknown heads viz. h_D at $r = 3.25$ m; h_B at $r = 5.5$ m and h_E at $r = 7.75$ m and two known heads from boundary condition viz. $h_A = 20$ m at $r = 1.0$ m and $h_C = 25$ m at $r = 10$ m.

The difference equations at the nodes D, B, and E are $\frac{h_A + h_B - 2h_D}{2.25^2} + \frac{1}{3.25} \times \frac{h_B - h_A}{2 \times 2.25} = 0$; $\frac{h_D + h_E - 2h_B}{2.25^2} + \frac{1}{5.50} \times \frac{h_E - h_D}{2 \times 2.25} = 0$; and $\frac{h_B + h_C - 2h_E}{2.25^2} + \frac{1}{7.75} \times \frac{h_C - h_B}{2 \times 2.25} = 0$. Solving these three equations simultaneously noting that $h_A = 20$ m and $h_C = 25$ m, we get $h_D = 22.4391\,\text{m}, h_B = 23.63095\,\text{m},;\text{and } h_E = 24.41484\,\text{m}$ From analytical solution, corresponding values are as $h_D = 20 + \frac{5}{\ln 10}\ln 3.25 = 22.56$ m;

$h_B = 20 + \frac{5}{\ln 10}\ln 5.5 = 23.702$ m; and $h_E = 20 + \frac{5}{\ln 10}\ln 7.75 = 24.447$ m.

Now the difference in between FDM and exact values of heads is reduced due to finer grid size. The truncation errors in approximation of second-order derivative is proportional to square of the grid size, therefore if two solutions are obtained using different grid size, then the truncation error for grid size half is only one-quarter of that for full grid size. As a result, the solution for finer grid is more accurate.

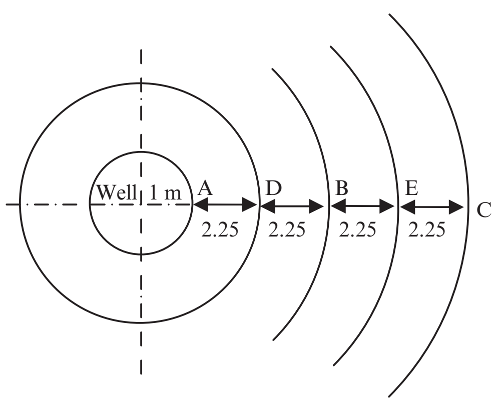

Figure 17.13 *Finer radial grids*

Example 17.4: Solve the same problem as shown in Figure 17.14 by finite difference method using logarithmic grid.

Solution: Now let us divide the complete length into four grids such that $\Delta a = \ln r_D - \ln r_A = \ln r_B - \ln r_D = \ln r_E - \ln r_B = \ln r_C - \ln r_E \Rightarrow \frac{r_D}{r_A} = \frac{r_B}{r_D} = \frac{r_E}{r_B} = \frac{r_C}{r_E}$

or $4\Delta a = \ln 10 - \ln 1 \Rightarrow \quad a = \frac{2.302}{4} = 0.5757$. Hence, $\ln r_D = \Delta a + \ln r_A \Rightarrow r_D$ $= e^{0.5757} = 1.7783\text{m}$; similarly, $r_B = e^{2\times 0.5757} = 3.1623\text{m}$; and $r_E = e^{3\times 0.5757} =$ 5.6234m. There will be three unknown heads viz. h_D at r = 1.7783 m; h_B at r = 3.1623 m; and h_E at r = 5.6234 m and two known heads from boundary condition viz. h_A = 20 m at r = 1.0 m and h_C = 25 m at r = 10 m.

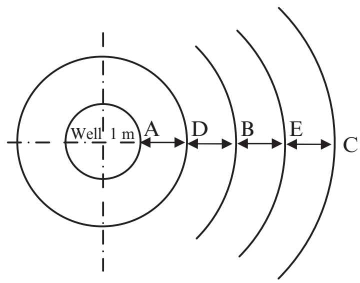

Figure 17.14 *Radial logarithmic grids*

In logarithmic grid spacing, the governing equations reduces to $\frac{d^2h}{da^2} = 0$, therefore finite difference equations are $\frac{h_B + h_A - 2h_D}{\Delta a^2} = 0 \Rightarrow h_B + h_A - 2h_D = 0$ $h_E + h_D - 2h_B = 0$; and $h_c + h_B - 2h_E = 0$. Solving these equations, we get $h_D = 21.25\,\text{m}, h_B = 22.50\,\text{m}$, and $h_E = 23.75\,\text{m}$.

Exact values from analytical solution are $h_D = 20 + \frac{5}{\ln 10}\ln e^{0.5757} = 21.25\text{m}$; $h_B = 20 + \frac{5}{\ln 10}\ln e^{2\times 0.5757} = 22.50\text{m}$, and $h_E = 20 + \frac{5}{\ln 10}\ln e^{3\times 0.5757} = 23.75\text{m}$.

m. These values are same as FDM solution values. Thus, in logarithmic grid, the FDM solution matched exactly with the analytical solution.

Example 17.5: Solve the same problem as shown in Figure 17.15 by finite difference method using nonuniform/graded grid.

Solution: Now let us divide the domain into three grids such that $\Delta r_1 = 2\text{m}$, $\Delta r_2 = 3\text{m}$, and $\Delta r_3 = 4\text{m}$. There will be two unknown heads viz. h_D at r = 6 m and h_B at r = 3.0 m and two known heads from boundary condition viz. h_A = 20 m at r = 1.0 m and h_C = 25 m at r = 10 m.

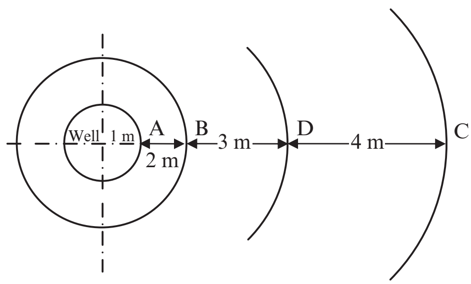

Figure 17.15 *Radial nonuniform grids*

Writing finite difference equations at nodes B and D results $\dfrac{\left\{\dfrac{h_D-h_B}{3}+\dfrac{h_A-h_B}{2}\right\}}{5/2}+\dfrac{1}{3}\cdot\dfrac{h_D-h_A}{5}=0$ and $\dfrac{\left\{\dfrac{h_C-h_D}{4}+\dfrac{h_B-h_D}{3}\right\}}{7/2}+\dfrac{1}{6}\cdot\dfrac{h_C-h_B}{7}$ =0. Applying boundary conditions and simplifying yields $5h_B-3h_D=40$ and $7h_D-3h_B=100$. Solving these two equations, we get h_b = 21.8181 m and $h_B=21.8181\,\text{m}$ and $h_c=23.6363\,\text{m}$. Exact values are $h_B=20+\dfrac{5}{\ln 10}\ln 3$ $=22.385\text{m}$ and $h_D=20+\dfrac{5}{\ln 10}\ln 6=23.891\text{m}$. It to be noted that the difference between numerical and analytical solutions is more in h_B and less in h_D, which shows that error in FDM solution is more at points near to the well in comparison to far-away points.

Example 17.6: Consider an unsteady flow in a confined aquifer of thickness 3 m shown in Figure 17.16 with initial heads at all grid points 5 m and for $t > 0$; h_1 = 5 m and h_5 = 1 m. Aquifer parameters are S = 0.03 and K = 0.5 m/d. Determine the spatial variation of piezometric head at different time steps assuming grid size $\Delta x = 3\,\text{m}$

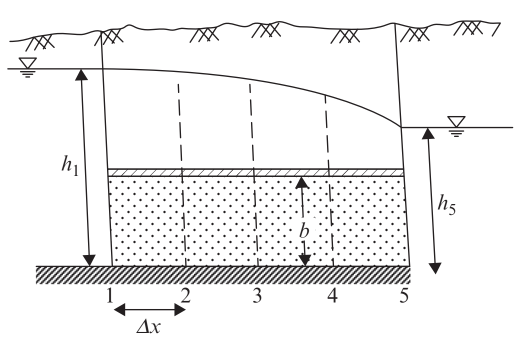

Figure 17.16 *Unsteady flow in a confined aquifer*

Solution: Aligning the x-axis in the direction of flow results into one-dimensional flow with governing equation $\frac{\partial^2 h}{\partial x^2} = \frac{S}{T}\frac{\partial h}{\partial t}$. Discretising this equation into algebraic difference equations using explicit scheme yields $\frac{(h_{i+1,j} + h_{i-1,j} - 2h_{i,j})}{(\Delta x)^2} = \frac{S}{T}\frac{h_{i,j+1} - h_{i,j}}{\Delta t}$ where i and j represent space and time steps/grids, respectively. Rewriting as $h_{i,j+1} = h_{i,j} + \frac{T\Delta t}{S\,\Delta x^2}(h_{i+1,j} + h_{i-1,j} - 2h_{i,j})$. For stability, Courant number should be limited to 0.5, hence $\frac{T\Delta t}{S\Delta x^2} < 0.5$

$$\Rightarrow \Delta t < 0.5\frac{S(\Delta x^2)}{T} \Rightarrow \Delta t < 0.5 \times 0.03 \times \frac{3^2}{0.5 \times 3} = 0.09\,\text{days}.$$

Therefore, let keep $\Delta t = 0.08\,\text{days} \Rightarrow \frac{T\Delta t}{S\,\Delta x^2} = 0.44$. Therefore, $h_{i,j+1} = h_{i,j} + 0.44(h_{i+1,j} + h_{i-1,j} - 2h_{i,j}) = 0.44(h_{i+1,j} + h_{i-1,j}) + 0.12h_{i,j}$. Thus for the first time step, $h_{2,1} = 0.44(h_{3,0} + h_{1,0}) + 0.12h_{2,0} = 0.44(5+5) + 0.12 \times 5 = 5\,\text{m}$; $h_{3,1} = 0.44(h_{4,0} + h_{2,0}) + 0.12h_{3,0} = 0.44(5+5) + 0.12 \times 5 = 5\,\text{m}$; $h_{4,1} = 0.44(h_{5,0} + h_{3,0}) + 0.12h_{4,0} = 0.44(5+5) + 0.12 \times 5 = 5\,\text{m}$; and $h_{4,1} = 1\,\text{m}$ from boundary condition. Similarly, for the second time step $2\,\Delta t = 0.08 \times 2\,\text{days}$: $h_{2,2} = 0.44(h_{3,1} + h_{1,1}) + 0.12h_{2,1} = 0.44(5+5) + 0.12 \times 5 = 5\,\text{m}$; $h_{3,1} = 0.44(h_{4,1} + h_{2,1}) + 0.12h_{3,1} = 0.44(5+5) + 0.12 \times 5 = 5\,\text{m}$; and $h_{4,2} = 0.44(h_{5,1} + h_{3,1}) + 0.12h_{4,1} = 0.44(1+5) + 0.12 \times 5 = 5\,\text{m}$. Similarly at other time periods, head can be calculated and corresponding values are listed in Table 17.2 . It can be noted that the solution is converging and after one day the variation in the peizometric head became almost linear, i.e. approached to the steady state analytical solution for flow through confined aquifer.

Table 17.2 Variation in computed head with time – stable results

Time step	*Time (days)*	h_1 *(m)*	h_2 *(m)*	h_3 *(m)*	h_4 *(m)*	h_5 *(m)*
0	0.08	5	5	5	5	5
1	0.16	5	5	5	5	1
2	0.24	5	5	5	3.24	1
3	0.32	5	5	4.226	3.029	1
4	0.4	5	4.659	4.040	2.663	1
5	0.48	5	4.537	3.706	2.537	1
6	0.56	5	4.375	3.557	2.375	1
7	0.64	5	4.290	3.397	2.290	1

(*Continued*)

Table 17.2: Continued

Time step	*Time (days)*	h_1 *(m)*	h_2 *(m)*	h_3 *(m)*	h_4 *(m)*	h_5 *(m)*
8	0.72	5	4.210	3.303	2.210	1
9	0.8	5	4.158	3.221	2.158	1
10	0.88	5	4.116	3.166	2.116	1
11	0.96	5	4.087	3.122	2.087	1
12	1.04	5	4.064	3.091	2.064	1

Now let us consider the time step $\Delta t = 0.12\,\text{days}$ for which $\dfrac{T\Delta t}{S\,\Delta x^2} = 0.67 > 0.5$, i.e. greater than the Courant stability requirement. For this time step $h_{i,j+1} = h_{i,j} + 0.67(h_{i+1,j} + h_{i-1,j} - 2h_{i,j}) = 0.67(h_{i+1,j} + h_{i-1,j})$ $-0.34h_{i,j,}$ and hence $h_{2,1} = 0.67(h_{3,0} + h_{1,0}) - 0.12h_{2,0} = 0.67(5+5) - 0.34 \times 5$ $h_{3,1} = 0.67(h_{4,0} + h_{2,0}) - 0.34h_{3,0} = 5\,\text{m}$; $h_{4,1} = 0.67(h_{5,0} + h_{3,0}) - 0.34h_{4,0}$ and $h_{5,1} = 1\,\text{m}$ from boundary condition. Similarly for the next time step, 2 $\Delta t = 0.12 \times 2\,\text{days}$: $h_{2,2} = 0.67(h_{3,1} + h_{1,1}) - 0.34h_{2,1} = 5\,\text{m}; h_{3,2} = 0.67\ (h_{4,1} + h_{2,1})$ $-0.34h_{3,1} = 5\,\text{m}$; and $h_{4,2} = 0.67(h_{5,1} + h_{3,1}) - 0.34h_{4,1} = 0.67(1+5) - 0.34 \times 5$ $= 2.32\,\text{m}$. Similarly at other time periods, head was calculated and corresponding values were listed in Table 17.3. It can be noted that the solution is unstable and nonconverging that is some values are negative and positive which are oscillating. This reveals the conditional stability of the explicit scheme.

Table 17.3 Variation in computed head with time – unstable results

Time step	*Time (days)*	h_1 *(m)*	h_2 *(m)*	h_3 *(m)*	h_4 *(m)*	h_5 *(m)*
0	0.08	5	5	5	5	5
1	0.16	5	5	5	5	1
2	0.24	5	5	5	2.32	1
3	0.32	5	5	3.204	3.231	1
4	0.4	5	3.797	4.425	1.718	1
5	0.48	5	5.024	2.191	3.051	1
6	0.56	5	3.110	4.665	1.100	1
7	0.64	5	5.419	1.234	3.422	1
8	0.72	5	2.335	5.503	0.334	1
9	0.8	5	6.243	–0.083	4.244	1
10	0.88	5	1.172	7.055	–0.829	1
11	0.96	5	7.678	–2.169	5.678	1
12	1.04	5	–0.714	9.686	–2.714	1

Plot of results are also shown in Figure 17.17 to compare them.

Discretiszing the governing equation into algebraic difference equations using implicit scheme yields . Taking $\Delta t = 0.08$ days , for the first time step: $(h_{i+1,j+1} + h_{i-1,j+1} - 2h_{i,j+1}) - 2.25h_{i,j+1} = -2.25h_{i,j}$, therefore $(h_{3,1} + h_{1,1} - 2h_{2,1})$ $-2.25h_{2,1} = -2.25h_{2,0} \Rightarrow h_{3,1} - 4.25h_{2,1} = -16.25$; $(h_{4,1} + h_{2,1} - 2h_{3,1}) - 2.25h_{3,1}$ $= -2.25h_{3,0} \Rightarrow h_{4,1} + h_{2,1} - 4.25h_{3,1} = -12.25$; $\left(h_{5,1} + h_{3,1} - 2h_{4,1}\right) - 2.25h_{4,1} = -2.25$ $\times h_{4,0} \Rightarrow h_{3,1} - 4.25h_{4,1} = -13.25$. Solving them simultaneously yields $h_{2,1} = 4.94$ m, $h_{3,1} = 4.75$ m, and $h_{4,1} = 4$ m. The piezometric heads at the subsequent time steps can be solved by following the similar procedure.

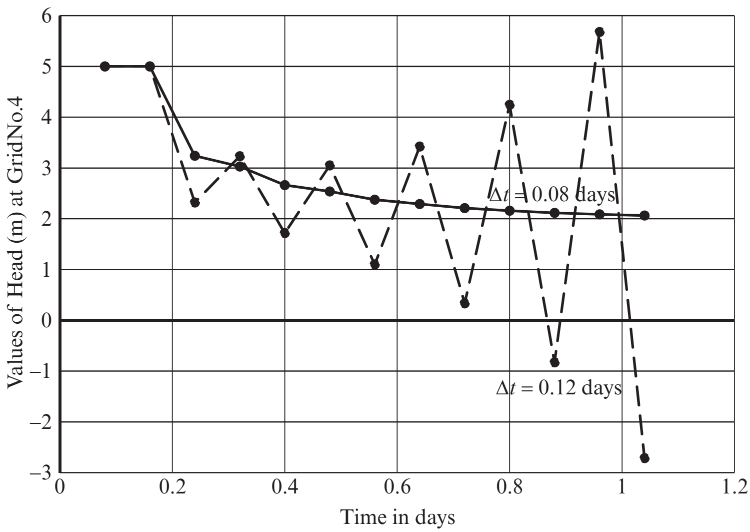

Figure 17.17 *Comparison of results using time step with and without meeting Courant condition*

Discretizing the governing equation using Crank Nicholson scheme and giving equal weightage to known and unknown heads results to.

$$0.5\frac{\left(h_{i+1,j+1} + h_{i-1,j+1} - 2h_{i,j+1}\right)}{\Delta x^2} + 0.5\frac{\left(h_{i+1,j} + h_{i-1,j} - 2h_{i,j}\right)}{\Delta x^2} = \frac{S}{T}\frac{h_{i,j+1} + h_{i,j} - 2h_{i,j+1}}{\Delta t} \Rightarrow$$

$$h_{i+1,j+1} - 2\left(1 + \frac{S\Delta x^2}{T\Delta t}\right)h_{i,j+1} = 2\left(1 - \frac{S\Delta x^2}{T\Delta t}\right)h_{i,j} - h_{i+1} - h_{i-1,j.}$$ Writing this equation for all nodes and at unknown time step and solving them simultaneously will give head at that time interval. Similarly, head values at other time steps can be calculated from pervious time interval. For example, at $\Delta t = 0.08$ days; $h_{3,1} + h_{1,1} - 6.50h_{2,1} = -2.50 \times h_{2,0} - h_{3,0} - h_{1,0} \Rightarrow h_{3,1} - 6.50h_{2,1} = -27.5$; $h_{4,1} + h_{2,1}$ $-6.50h_{3,1} = -2.50 \times h_{3,0} - h_{4,0} - h_{2,0} \Rightarrow h_{4,1} + h_{2,1} - 6.50h_{3,1} = -22.5$; and $h_{5,1} + h_{3,1}$

$-6.50h_{4,1} = -2.50 \times h_{4,0} - h_{5,0} - h_{3,0} \Rightarrow h_{3,1} - 6.50h_{4,1} = -23.5$ Solution for these three simultaneous equations yields $h_{2,1} = 4.98\,\text{m}, h_{3,1} = 4.90\,\text{m}$, and $h_{4,1} = 4.37\,\text{m}$. Similar procedure may be followed for the piezometric heads at the remaining time steps.

PROBLEMS

17.1. Why is modeling required in groundwater problems? Describe the objectives of the groundwater modeling. Also, classify various groundwater models.

17.2. What is a sand tank model? Describe in detail. What are its limitations and where is it preferred?

17.3. Describe in detail the working of a Hele–Shaw model. Discuss its application in different groundwater situations.

17.4. What is a finite difference in comparison to a derivative? How does a finite difference model a groundwater situation? Why are FDM so popular nowadays?

17.5. Describe the following:
a. Finite element model
b. Electric analog model
c. Thermal analog model

17.6. Why is groundwater modelling important? Describe Hele–Shaw model. What should be the spacing between the plates in Hele–Shaw model for modelling groundwater flow through a porous medium (hydraulic conductivity = 0.4 m/d) if the fluid used in the model has viscosity = 1.49 Pa.s and density = 1260 kg/m^3.

17.7. A well (30 cm diameter) in a confined aquifer is pumped such that the draw down difference of 4 m is created between the well and at a radial distance of 20.3 m. Solve the problem by finite difference method using regular mesh as well as logarithmic mesh. Also compare these results with the exact solution. What do you infer by comparing results?

17.8. A well (2 m diameter) in a confined aquifer ($T = 400$ m^2/d) is pumped such that the draw down difference of 5 m is created between the well and at a radial distance of 10 m. Solve the problem by finite difference method using the mesh as shown in Figure 17.18. Also, compare the results with analytical solution.

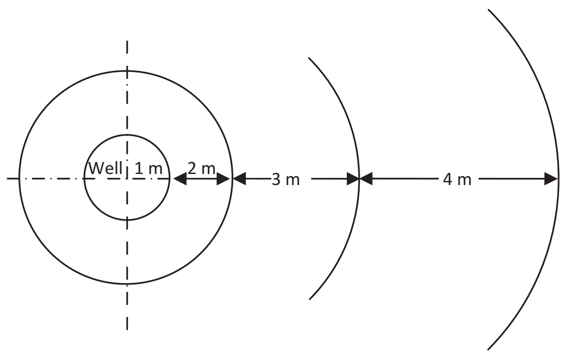

Figure 17.18 *Problem 17.8*

17.9. A well (2 m diameter) in a confined aquifer (T = 500 m^2/d) is pumped such that the draw down difference of 6 m is created between the well and at a radial distance of 10 m. Solve the problem by finite difference method using the logarithmic mesh. Also compare the results with analytical solution. What do you infer by comparing results?

17.10. Solve the problem as shown in Figure 17.19 by finite difference method if (i) $\Delta x1 = \Delta x2 = \Delta x3 = \Delta x4 = 25$ m; $K_A = 4$ m/d; $K_B = 5$ m/d; $K_C = 6$ m/d; $K_D = 4$ m/d; and (ii) $\Delta x1 = 10$ m; $\Delta x2 = 20$ m; $\Delta x3 = 30$ m; $\Delta x4 = 40$ m; $K_A = 4$ m/d; $K_B = 3$ m/d; $K_C = 2$ m/d; $K_D = 1$ m/d.

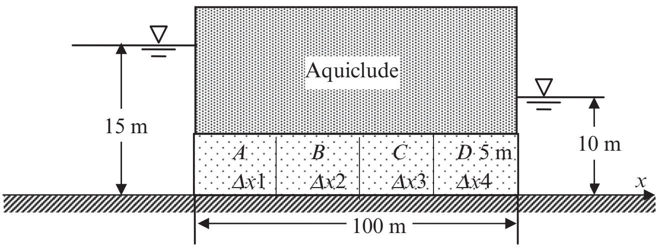

Figure 17.19 *Problem 17.10*

17.11. A well (2 m diameter) in a confined aquifer (T = 600 m^2/d) is pumped such that the draw down difference of 8 m is created between the well and at a radial distance of 16 m. Solve the problem by finite difference method using the mesh as shown in Figure 17.20. Also solve the same problem analytically and compare these results.

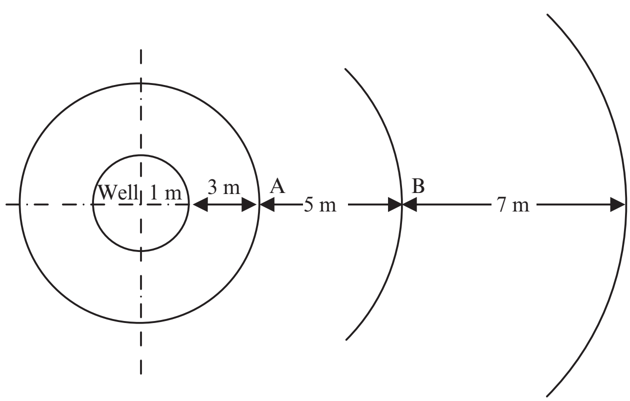

Figure 17.20 *Problem 17.11*

17.12. Is predicted head by FDM in an injection well likely to be lower or higher than the actual head? Explain, why?

17.13. A well (2 m diameter) in a confined aquifer (T = 500 m^2/d) is pumped such that the draw down difference of 6 m is created between the well and at a radial distance of 16 m. Find head at A and B by finite difference method using the mesh as shown in Figure 17.20. Also, solve the same problem using uniform mesh and logarithmic mesh and compare these results with analytical solution. What do you infer by comparing results?

17.14. Determine the spatial variation of piezometric head at different time steps assuming grid size $\Delta x = 3\,\text{m}$ for Figure 17.16 with aquifer thickness 6 m, $h_1 = 15$ m, $h_5 = 10$ m, and $K = 0.5$ m/d.

PLATE 9

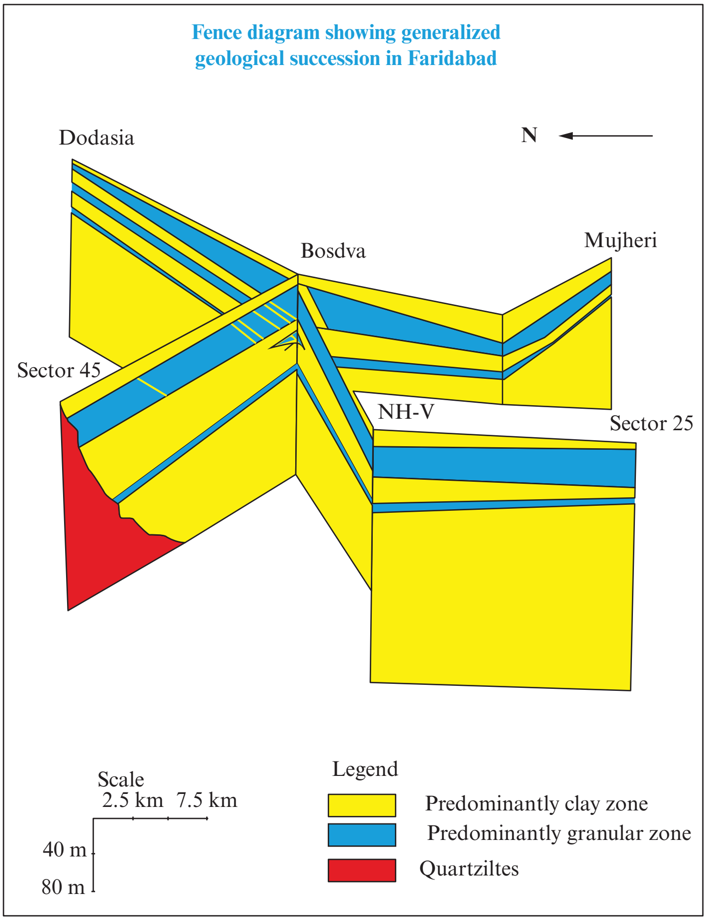

Figure 17.7 *Subsurface disposition of the litho units in the form of a fence diagram*

PLATE 10

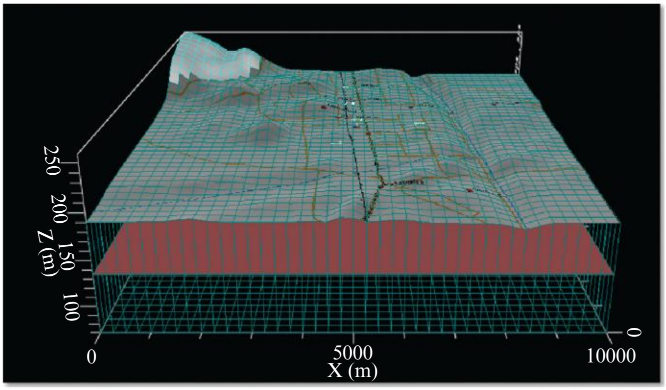

Figure 17.8 *3D Representation of Model Domain*

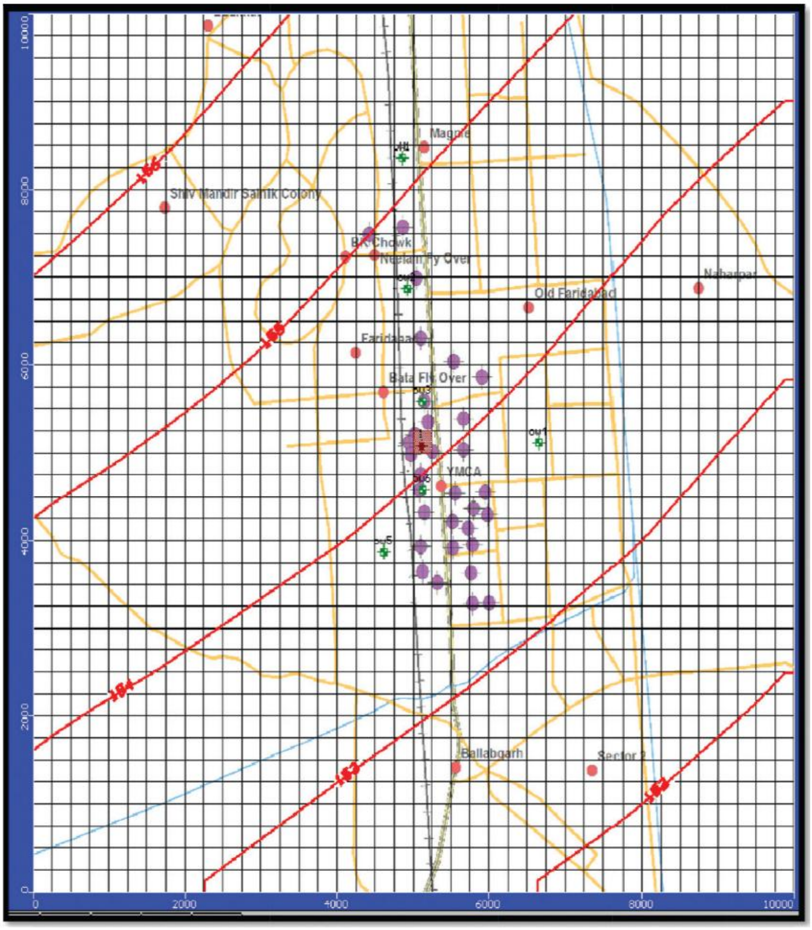

Figure 17.9 *Initial Piezometric Head of layer 1*

Chapter 18 Management of Groundwater Quantity

18.1 General

An aquifer is a large natural underground reservoir; therefore, *utilization of groundwater by one user affects the quantity of water available at other locations to all other users in that aquifer*. Groundwater is regarded as a renewable natural resource and is extracted from the aquifer just as other minerals. However, the quantity of groundwater in an aquifer is limited, and its production will not continue indefinitely with time. In effect, it can sustain only if there exists a balance between water recharged to the aquifer from surface sources and water pumped from the aquifer by wells. Development of groundwater begins with a few pumping wells scattered in an aquifer, and later more wells are added as demand increases. As wells become more numerous, development of the aquifer reaches and exceeds its natural recharge capability. Continued development thereafter without a management plan could eventually deplete the groundwater resource. An aquifer can be made to function beneficially and indefinitely through proper management by regulating inflow to and outflow from the aquifer. *The management of a groundwater implies development and utilization of aquifer water so as to obtain the maximum quantity of water to meet predetermined quality requirements at least cost*. To benefit all users, the development and utilization of groundwater from the entire aquifer should be planned and managed considering geologic, hydrologic, economic, legal, political, and financial aspects. In addition, optimum economic development of water resources in an area requires an integrated approach that coordinates the use of both surface water and groundwater resources. After evaluation of total water resources and preparation of alternative management plans, action decisions can then be made by appropriate public bodies or agencies.

Groundwater and surface water constitute a single unified source on a regional basis. A depletion of one can affect the other, and what is surface water today can be groundwater tomorrow and vice versa. Thus, a large-scale groundwater pumping depletes the surface water sources and baseflows to tributaries that may cause interstate water disputes. In addition, watershed development schemes such as check dams, terracing of fields, etc., reduce runoff resulting in depleted streamflows for downstream users. Thus, water used beneficially at head reaches might result in misdistribution at the regional level in the absence of a basin-level management approach. Therefore, a whole basin should be operated in an optimal manner as a system. For managing groundwater and making efficient use of it, a variety of strategies such as shifting of local water sources, changing pumping patterns, limiting pumpage, artificial recharge, reuse of wastewater and conjunctive use of groundwater and surface water, and their combinations are adopted.

18.2 Groundwater Quantity

Groundwater in aquifer storage is of no value unless it is used. If groundwater is regarded as a renewable natural resource, then only a certain quantity of water may be withdrawn annually from a groundwater basin. The maximum quantity of usable groundwater that is actually available from a groundwater basin on a perennial basis is limited by the possible deleterious side effects that can be caused by pumping and by the operation of the basin. The *safe yield* is a fixed quantity of extractable water basically limited to the average annual basin recharge. If groundwater is withdrawn at a rate exceeding the recharge, a mining yield exists. As a consequence, the aquifer storage is depleted and further continued mining results in overdrafting. The consequences of overdraft in terms of adverse impacts on water quantity, quality, land subsidence, and water rights have been mentioned earlier in Chapter 15. In arid areas, groundwater represents the only available water resource; almost any development of groundwater constitutes a mining yield. Such exploitation will continue in arid areas due the dire water needs and associated great benefits. With proper management and water conservation, such groundwater resources can be made to last from several decades to a few centuries.

The *perennial yield* of a groundwater basin defines the rate at which water can be withdrawn perennially under specified operating conditions without producing an undesired result. Any draft in excess of perennial yield is referred to as *overdraft*. Existence of overdraft implies that continuation of present water management practices will result in significant negative impacts on environmental, social, and/or economic conditions. The initial rate may exceed the perennial yield, thereby reducing the groundwater level. This planned overdraft furnishes water from storage at low cost and without creating any undesirable effects. In fact, reducing storage eliminates wasteful subsurface outflow of groundwater and losses to the atmosphere by evapotranspiration from high water table areas. After the groundwater level has been lowered to a predetermined depth, the perennial yield should be maintained. The efficient and economic production of water in a basin requires that all pumping, importations, and distributions of water in the system should be considered. The maximum quantity of groundwater perennially available if all possible methods and sources are developed for recharging the basin is called the *maximum perennial yield*. This yield can be increased by recharging (both naturally and artificially) the basin at enhanced rate.

Determination of the perennial yield of a groundwater basin requires analysis of the undesired results that may accrue if the extraction rate is exceeded. Economic considerations can govern perennial yield in basins where the cost of pumping groundwater becomes excessive due to lowered groundwater levels, necessitating deepening wells, lowering pump bowls, and installing larger pumps. Water quality can govern perennial yield if draft on a basin produces groundwater of inferior quality. A quality limitation on perennial yield depends on the minimum acceptable standard of water quantify, which in turn depends on the usage of the pumped water. Therefore, by lowering the quality requirement, the perennial yield can be increased. Legal considerations affect perennial yield if pumpage interferes with prior water right. Finally, if pumpage is responsible for land subsidence, a limitation on perennial yield can result. Determination of perennial yield where recharge is the limiting factor can be made based on the water balance equation. Basically, this implies that perennial yield is defined in terms of a rate at which groundwater can be withdrawn from a basin over a representative time period without producing a significant change in groundwater storage. Perennial yield of a groundwater basin tends to vary with time and with the level of groundwater development within a basin. In a virgin basin, where a balance exists between natural inflow and outflow and there is no pumping. If the water table is lowered, recharge from losing streams will be increased, discharge from gaining streams will be decreased, and evapotranspiration losses will be reduced. Conversely, a rise in water levels will have the opposite effects. Therefore, where recharge is sufficient, the greater the utilization of under groundwater, the larger the perennial yield. The perennial yield will increase by increasing pumpage and rearrangement of the pumping pattern. If the concentration of wells is shifted to near the recharge source, greater inflow can be induced.

18.3 Conjunctive Use

Surface and groundwater systems are two components of hydrologic cycle, which are in continuous dynamic interaction. Understanding the connectivity between surface and groundwater systems is required to plan and manage surface and groundwater resources. Independent development and management of surface and groundwater resources may lead to overallocation of resources and consequently adverse hydrological and environmental impacts. A river basin should be considered as a unit for analyzing interactions and interrelations between the surface water and groundwater systems for formulating the water management policy. Optimal beneficial use of water in a basin can be obtained by *conjunctive use*. Where surface water is available in addition to groundwater, these two sources are operated conjunctively. Conjunctive *use involves the coordinated and planned operation of both surface water and groundwater resources to meet water requirements along with water conservation*. Such a conjunctive use scheme provides a larger and more economic yield of water than can be obtained from the two sources operated independently. The limit to such an operation is governed by the ability to import and distribute water and also by the storage available for surface water and groundwater. FAO (1995) defined conjunctive use as harmonious combined use of two sources in order to maximize the economic and environmental effects of each and also to optimize the water demand and supply balance.

In a conjunctive use of surface water and groundwater resources, surface water storage supplies most annual water requirements, whereas the groundwater storage can be retained primarily for cyclic storage to cover years of subnormal precipitation. During periods of above-normal precipitation, surface water is utilized to the maximum extent possible and also artificially recharged into the ground to augment groundwater storage and raise groundwater levels. Conversely, during drought periods, limited surface water resources are supplemented by pumping groundwater, thereby lowering groundwater levels. The feasibility of the conjunctive use approach depends on operating a groundwater basin over a range of water levels; that is, there must be space to store recharged water; and, in addition, there must be water in storage for pumping when needed. Management by conjunctive use requires physical facilities for water distribution, artificial recharge, and pumping. The procedure requires careful planning to optimize use of available surface water and groundwater resources.

18.3.1 Concept of Conjunctive Use

Conjunctive use may be spontaneous or planned. The former involves the use of aquifer storage capacity to buffer the variability in surface water availability and flows. This enables greater water supply security, crop insurance, avoidance of groundwater depletion, etc., in regions of inadequate surface water supply. The planned conjunctive use optimally allocates and distributes surface water and groundwater to yield optimal outcomes in a basin, including control and/or reduce overdraft, water logging, and land salinity. Hydrogeological framework, climate, and geomorphological situation of a hydrologic region in relation to river and tributary basins as well as irrigation commands govern the prospects and potential for conjunctive use in agricultural irrigation. The alluvial plain aquifers having large groundwater storage potential are ideally situated for undertaking planned conjunctive use operations. As yet, there is hardly any planned (designed and operated) conjunctive use irrigation project in India. Although, several feasibility studies on conjunctive use in major irrigation commands have been undertaken and few investigative studies on conjunctive use have been conducted.

The conjunctive use benefits include economic gains, enhancements in agriculture productivity, expanded areas of irrigation, energy savings, water resources efficiency gains, and optimization of water infrastructure. The conjunctive use methods can be grouped into two broad categories: (i) passive or alternative conjunctive use system and (ii) comprehensive conjunctive use system. In either of the conjunctive use systems, the aquifer storage potential plays a significant role.

Alternative Conjunctive Use System

In this method, more surface water as available in storage reservoirs and or in streams is used, whereas groundwater remains in storage. In this method, groundwater is used in dry periods, while in wet period its use is minimal. Hence, the water supply demand is provisioned with the use of these two alternative sources for increasing capacity of water supply in lieu of constructing new dams. The stream-aquifer regime is included as subsystem of alternative conjunctive use system, where groundwater is used in complementing surface water in lean periods so as to maintain environmental flow in the stream. Overexploited aquifers connected with stream can change their relationship with previously effluent stream that is changed to influent, leading to storing of water in the aquifer. In addition, loss of water from canals and returns from overirrigation from crop-fields infiltrates and reaches aquifers, known as *incidental recharge*. The incidental recharge controls groundwater decline in large conjunctive use projects. However, the infiltrating water through silt–clay layers may cause situation of water logging and land salinization. The joint use of canal water, drainage water, and groundwater together can enhance efficiency as well as reduce deterioration of land salinity.

Comprehensive Conjunctive Use System

In this system, surface water is developed for managed aquifer recharge (MAR) and aquifer storage recovery (ASR), and as a result groundwater pumping is reduced. The availability of large storage capacity of aquifers that can retain huge volumes of recharge is core to comprehensive conjunctive use method. ASR comprises storage of water during periods of low demand for use in periods of high demand. The method is useful in areas where aquifers are confined and in close proximity to rivers. The ASR method is relatively expensive than water-spreading method of recharging.

Simulated and Integrated Models of Conjunctive Use

The conjunctive use is the management applied to optimize the water resources development, management, and conservation within the basin. The ultimate aim of the conjunctive use of surface water and groundwater is to maximize benefits through planned integration of two types of water sources providing optimal productivity and equity and water use efficiency outcomes. It consists of harmoniously combining the use of both sources of water in order to minimize the undesirable physical, environmental, and economical effects of each solution and to optimize the water balance in the basin. Conjunctive use plans can be based on benefit/cost analysis considering land use, crop pattern, water demand, meteorological, and hydrological conditions. The optimal conjunctive water management strategies can be developed using simulation–optimization models to determine the best spatially distributed balance between using surface water and groundwater. The conjunctive water use planning should increase the efficiency, reliability, and cost effectiveness of water use. In order to develop optimal policies, the conjunctive use planning can be formulated as an optimization model of the water resources system.

The aquifer integration with hydraulic system leads to improving water yield besides serving as buffer for low surface water availability. For water resources to be managed properly in a basin, the knowledge of water inflows and outflows and of total surface and groundwater balance is necessary. The conjunctive use systems require simulation and optimization models to represent groundwater surface water, vadose water, and stream–aquifer flow interchange as well as canal–aquifer water interchange/mixing over longer modeling time periods.

18.3.2 Conjunctive Use Planning

Three factors are considered in planning process with a view to optimizing the conjunctive use:

1. Availability of surface water and groundwater
2. Capital investment and operating cost
3. Energy requirements

The main objective of these factors is to produce maximum benefits per cubic meter of water used. A planned conjunctive use operation requires strong institutional setup, water policies, and regulations. The following points are beneficial in planned conjunctive use:

- Detailed knowledge and understanding of surface and groundwater systems
- A strong organizational and policy base
- Involvement of stakeholders at various stages of planning and management
- Public education and awareness

The following are the impediments to planned conjunctive use operations:

- Disjointed and disconnected responsibilities of water management between surface water and groundwater departments at various levels in governments
- Lack of information on conjunctive use management for use by planners, administrators, and politicians
- Inadequate knowledge of the degree to which groundwater is pumped by private users

18.4 Water Laws

The maximum quantity of water that can be extracted from an underground reservoir, and still maintain that supply unhindered, depends on the perennial yield. Until overdrafts are reduced to perennial yields in these basins, permanent damage or depletion of groundwater supplies will occur sooner or later. Groundwater overdrafts cause many problems, such as increased well pumping costs and water-quality issues. In areas of severe groundwater depletion, the earth's surface may also subside, causing cracks or fissures that can damage roads or building foundations. The main purpose of groundwater management is to determine who may pump groundwater and how much may be pumped. This includes identifying existing water rights and providing new ways for nonirrigation water users to initiate new withdrawals. If groundwater is treated as private property of a landowner, then the landowner has the right to pump water from a groundwater deposit beneath his land at any rate, as long as the withdrawal does not maliciously harm his neighbor. The groundwater management goals could be to control the severe overdraft and to provide a means to allocate the limited groundwater resources to most effectively meet the changing needs of the users.

Water management decisions and policies should have water laws as the fundamental basis to serve basic functions: (1) creation of supplemental private property rights in scarce resources and (2) imposition of public interest limitation on private use. Surface water law can be based on riparian or appropriation law, whereas groundwater allocation may be based on common or statutory law. *Riparian law* is based on the riparian policy, which states that the right to use water is considered real property, although the water itself is not the property of the landowner. *Appropriation law* states that the allocation of water rests on the proposition that the beneficial use of water is the basis, the measure, and the limit of the appropriative right: the first-in-time is prior in right. In order to appropriate water, the user only needs to demonstrate the availability of water in the source of supply, show intent to put the water to beneficial use, and give priority to more senior permit holders during times of shortage (Schmandt et al., 1976). Beneficial use of water under the law includes domestic consumption, livestock watering, irrigation, mining, power generation, municipal use, and other circumstances. Common law doctrines include absolute ownership, reasonable use, and correlative rights. These doctrines give equal rights to all landowners overlaying an aquifer. State water policies are based on surface and groundwater laws. If states cannot agree on apportionment in interstate waters even after involvement of central/federal government, then the courts have to intervene and settle the dispute by decree.

18.5 Groundwater Management Techniques

The development of groundwater resources involves planning in terms of an entire aquifer. The management objectives include providing an economic and continuous water supply to meet a continuous growing demand from an underground water resource. The optimal water supply to municipal, industrial, and agricultural water demands considering the physical, socioeconomic, and environmental constraints is the major objective of groundwater planning and management. The following planning problems are possible for a groundwater supply management (Yeh, 1992):

- The determination of an optimal pumping pattern such as location of pumping wells and their pumping rate to satisfy water demands
- The timing and staging of well field development (capacity expansion) considering future water demands
- The design of water transfer facilities for optimal allocation and distribution of water to demand points in the basin

Optimal policies for groundwater operation (such as optimal extraction, allocation, and aquifer recharge) can be determined by minimizing groundwater operation cost subject to physical, environmental, and socioeconomic constraints. The capacity expansion or timing and staging of well field development are common problems in groundwater system planning. Water demands in a well field increase with time and a capacity expansion planning capable of determining an optimal schedule is needed to expand system capacity according to increasing water demand. The capacity expansion model addresses the issue about how to expand the water supply system to meet the increasing demand with time. Groundwater allocation problem provides the optimal water distribution to different users with minimal effect on the environment and water users.

Here, the objective is to maximize the benefits of water supplied to different users from the total available water.

The groundwater management objective consists of providing an economic and continuous water supply from an aquifer to meet a growing demand of which only a small portion is renewable. Groundwater management models can be developed and used very effectively for groundwater management purposes. These models can be (a) *hydraulic management models* that are aimed at managing pumping and recharge or (b) *policy evaluation models* that can also consider the economics of water allocations. For groundwater planning and management, the following three techniques can be used:

1. Simulation
2. Optimization
3. Economic analysis

Aquifer simulation models can be used to examine the effects of various groundwater management strategies. The modeler specifies certain quantities, and the model predicts the technical and economic consequences of this choice. Groundwater management models may be used for optimization or as combined simulation optimization. Optimization techniques use mathematical expressions to describe a system and its response to the system inputs for various parameters. Constraints are used to define the limits of the design variables, and performance is evaluated through the use of objective functions. A set of values of the decision variables that simultaneously satisfy the constraints is a feasible solution. An optimal solution is a set of values of the decision variables that satisfy the constraints and provide an optimal value of the objective function. Economic analysis is required to identify the least-cost management strategy to meet specified hydraulic and water-quality restrictions in an aquifer. For example, one management strategy could be to fix the well locations and discharge rates to minimize the pumping cost to meet a known demand from a well field.

18.5.1 Simulation Models

Simulation models are realistic representation of the complex physical, economic, and social characteristics of a system utilizing the mathematical formulations. Such models are used to test the performance of a groundwater system under different design and operation scenarios. A simulation model cannot be used for optimal decision determination unlike an optimization model. However, groundwater models are highly nonlinear in objective function and constraints, and therefore cannot be handled by constrained optimization models, and hence the simulation model is used in the optimization process. The optimal scenario can be selected from the large number of simulation optimization results. Therefore, the simulation–optimization method is the most widely used method in groundwater planning and management.

Running of the numerical simulation models may be computational intensive and time-consuming. The physical model and mathematical description for a complex system can be very complicated to model and solve the system. If mathematical modeling is not possible for a complex groundwater system but a large number of observed data are available for the system, artificial neural networks (ANNs) model can be used to simulate the groundwater system. ANNs are very powerful and easy-to-use techniques. They can be trained to recognize patterns and can learn from their interaction with the environment. They are global nonlinear function approximates as their objective is to transform the inputs into meaningful outputs. A typical ANN structure is defined by three types of layers that consist of the different types of neurons, namely input neurons, output neurons, and hidden neurons. The hidden neurons connect the input layer neurons to the output layer. The hidden neurons can be arranged in one or more hidden layers. The choice of the number of hidden neurons/layers and the selection of ANN parameters play a key role in the ANN performance. Very less number of neurons in the hidden layer does not allow the network to produce accurate maps from the input to the desired output, whereas too many neurons can result in overfitting (ASCE Task Committee on Application of Artificial Neural Networks in Hydrology 2000). As there are no specific rules for the design and the architecture of an ANN, a trial-and-error procedure was adopted by Gaur et al. (2013). The back-propagation technique with Levenberg–Marquardt (L–M) method was used to train the ANN. A multilayer network with one hidden layer can be used to approximate almost any function if enough neurons are provided in the hidden layer; and hence, only one hidden layer can be adopted. The performance of the developed ANN model is measured on the basis of coefficient of correlation (R^2), RMSE, and Nash–Sutcliffe efficiency. The stopping criteria for the training can be defined on the basis of the specific maximum number of epochs and if the performance gradient falls below the minimum gradient. Numerous studies are available for addressing groundwater planning and management issues using ANN techniques.

18.5.2 Optimization Models

Optimization techniques assist in decision-making, which is the science of choice. The options from which the selection is made are known as alternatives, and the set of all possible alternatives is known as decision space. The limited alternatives are due to constraints that are the limitations from financial, technological, social, legal, quality, environmental, etc., considerations. The alternatives satisfying all constraints are called feasible. The goodness of any feasible alternative is characterized by criteria or objective function. If there is only one criterion, the problem is called the single-criterion optimization problem; otherwise, it is a multicriteria decision problem. Depending on the nature of the objective function and the constraints, an optimization problem can be classified as linear or nonlinear. The most simple single-criterion optimization problem with continuous variables is linear programming. Linear programming problems consist of a linear objective function and all the constraints are linear. Nonlinear programming problems have a nonlinear objective function and/or nonlinear constraints. Unconfined aquifers result in nonlinear programming problems. The optimization problem can be solved using different techniques depending on the nature of the problem. The commonly used optimization techniques are linear programming, nonlinear programming, dynamic programming, evolutionary methods, and others. Linear programming models, which can be solved by simplex method, have been extensively applied to optimal resource allocation problems. Many optimization problems may become too large to solve by available algorithms when a large-scale aquifer (especially an unconfined aquifer) is considered. Groundwater management models are often characterized as non-convex, nonlinear programming problems (Willis and Yeh, 1987). Most of the traditional optimization techniques are gradient-based, and the solutions from such methods produce local optimal values rather than global optimal solution. Therefore, application of gradient-based optimization techniques may be difficult in realistic problems related to wells' optimization. It is not always guaranteed that gradient-based methods will find out the global optimal solution in the case of highly nonlinear optimization problems. On the other side, global search methods are efficient to find out the global solution of the problem. Constraints in global optimization method can be incorporated into the formulation and do not require derivatives with respect to decision variables as in nonlinear programming (McKinney and Lin, 1994).

In recent years, applications of global search methods have been growing, and these methods have been applied to solve different kinds of groundwater quantity and quality management problems. Evolutionary methods (genetic algorithm, particle swarm optimization, ant colony optimization, firefly algorithm, simulation annealing, etc.) imitate natural systems and are based on heuristic search techniques. These methods require intensive computational efforts, but they are popular due to their easy applicability and ability to identify global optimum (Ritzel et al. 1994). Global search methods are more efficient and robust in comparison with other methods such as linear, nonlinear, and mixed integer. Katsifarakis and Petala (2006) applied simulation–optimization model to solve common problem in coastal aquifers' management, that is, maximization of groundwater extraction rate without saltwater intrusion. Hsiao and Chang (2002) solved groundwater management problems by considering well installation as fixed cost and pumping cost in objective function. GA integrated with constrained differential dynamic programming (CDDP) was applied to calculate optimal solutions for a groundwater resources planning problem while simultaneously considering fixed costs and time-varying pumping rates.

PSO is an efficient method for solving large nonlinear, complex global optimization problems and, in some cases, performs more efficiently compared with other evolutionary computation techniques (Eberhart and Kennedy, 1995). The PSO is a stochastic, swarm-based evolutionary computer algorithm for the solution of optimization problems. PSO is a member of the wide category of swarm intelligence-based methods that are suitable for solving global optimization problems. PSO is an evolutionary computation technique based on the simulation of simplified social models such as bird flocking, fish schooling, and the swarm theory (Kennedy et al., 2001). Its process can be simply compared with food-searching birds that consider two factors in order to achieve the goal: their own previous best experience and the best experience of all other members. This is also similar to human behavior in decision-making where people consider their own best past experience and the best experience of other people around them (Jarboui et al., 2008). In PSO, the system is initialized with a population of particles that represent the potential solution. In simple terms, each particle moves through a multidimensional search space, where the position of each particle is adjusted according to its own experience and that of its neighbors. In this process, each particle keeps track of its coordinates in the problem space, which are associated with the best solution (fitness) that it has achieved so far (the fitness value is also stored). Another "best" value that is tracked by the global version of the particle swarm optimizer is the overall best value, and its location, obtained so far by any particle in the population. To find the new position of each particle at each iteration (time step), a velocity term is computed on the basis of experience of particles. Gaur et al. (2011, 2013) used particle swarm optimization-based simulation–optimization model to solve two groundwater hydraulic management problems: (1) maximum pumping from an aquifer and (2) minimum cost to develop the new pumping well system.

18.5.3 Economy Consideration

The economic-based objective function of optimization model can be considered as maximizing the net benefit of water use. The optimization model can be constrained by the continuity equation, the hydraulic response equations, possible limitations on river runoff, pumping discharge volume from groundwater, allocated water discharge volume from surface water, groundwater table fluctuations, and appropriate well pumping rates at each planning period. In order to prevent excessive groundwater overdraft or water logging, constraints can be introduced to limit the head variation in each aquifer system.

A multiobjective planning problem considers economic, social, and environmental issues and conflicting objectives in groundwater management. A multicriteria optimization problem can be solved using sequential optimization, constraint method, weighting method, interactive fuzzy approach, etc.

Economic considerations play a significant role in making decision about groundwater resources planning, development, and management. Economic optimization can be achieved by finding the layout of the well field that results in the minimum cost for transferring the water to a central location in the well field subjected to minimum interference between the wells. Swamee et al. (1999) and Gaur et al. (2011, 2013) obtained optimal location of wells in a well field. In a well field, the total cost for new system of pumping wells consists of the cost of well installation, piping cost, and cost of pumping. The constraints included the maximum and minimum discharge limit of a single well, the minimum discharge limits by all wells, the maximum drawdown in individual well, and the minimum distance between the wells in order to provide a protective zone around the wells and avoid interference between wells. This optimization problem can be solved by a variety of methods (Swamee et al., 1999; Gaur et al., 2011, 2013; etc.).

The operation of groundwater systems is mostly a multiobjective problem, and hence some economic, hydraulic, water quality, or environmental objectives may conflict. The common conflict issue in groundwater systems planning and operation arises when the aquifer should supply water to different demand points for different purposes, and there are some constraints on groundwater table variations and groundwater quality. There are several alternative ways to solve conflict situations. The problem may be considered as a multiobjective optimization problem with the objectives of the different decision makers. Or, it can be solved as social choice problem with ranking or based on fairness requirements.

PROBLEMS

18.1. What do you mean by conjunctive use? Explain. What are benefits of conjunctive use, and why is it essential for countries such as India?

18.2. Why is groundwater management needed?

18.3. What are different water laws?

18.4. What are different yields? How are they computed?

18.5. Describe the groundwater management methods.

Chapter 19 Management of Groundwater Quality

19.1 General

Water is an essential precondition for life, and according to the United Nations, it is a human right to have access to clean water. However, in India millions of people are living without direct access to safe water; and based on the rapid population growth coupled with the fact that the water reserve is finite, it will be a very valuable and scarce resource within only a few years. Global changes such as population growth; climate variability; and ever-expanding industrialization and urbanization, often combined with pollution, severely affect water availability and lead to chronic water shortages in a growing number of regions. Therefore, preserving the quality and availability of fresh water resources has now become a pressing environment challenge. Growing pollution of water sources affects the availability of safe water besides causing environmental and health hazards. Mismanagement of water resources and low consciousness about overall scarcity and economic value of water are resulting in its wastage and inefficient use in major parts of India. Inequitable exploitation of groundwater without any consideration to its sustainability, large parts of India already became water stressed with a potential of causing societal challenges. All these require scientific planning, utilizing modern techniques, and analytical capabilities for a holistic management of groundwater-related problems.

Natural groundwater generally acquires dissolved constituents by dissolution of aquifer gases, minerals, and salts. All groundwater contains salts in solution that are derived from the location and past movement of the water. Consequently, soil zone and aquifer gases and the most soluble minerals and salts in an aquifer generally determine the chemical composition of groundwater in an aquifer. Lots of chemical changes take place in water as it travels through the hydrologic cycle from precipitation to groundwater. Recharge from precipitation introduces anthropogenically created trace elements into the groundwater. Precipitation reaching the earth contains only small amounts of dissolved mineral matter. After reaching the earth, the water contacts and reacts with the minerals of the soil and rocks. The quantity and type of mineral matter dissolved depend on the chemical composition and physical structure of the rocks as well as the hydrogen ion concentration and the redox potential of the water.

Groundwater is extensively developed for drinking, industrial, and irrigation purposes, and therefore its quality should be suitable (meet acceptable quality standards) for the corresponding purpose. *Color* in groundwater may be due to mineral or organic matter in solution. *Taste and odor* in water may be derived from bacteria, dissolved gases, mineral matter, or phenols. These can be established based on the maximum degree of dilution that can be distinguished from taste-free and odor-free water. *Turbidity* is a measure of the suspended and colloidal matter in water, such as clay, silt, organic matter, and microscopic organisms. The natural filtration produced by unconsolidated aquifers largely eliminates turbidity, but other types of aquifers can produce turbid groundwater. *Temperature* of groundwater is more or less constant. It is usually assumed to be at a value of 1°C–2°C greater than the annual average ambient air temperature for the region (Freeze and Cherry, 1979). In higher depths, greater than approximately 10 m, diurnal and seasonal variations of air temperature have minimal effects on groundwater. The uniformity of groundwater temperature is advantageous for water supply and industrial purposes, and underlying saline groundwater may be important because they offer potential benefits. The quality required of a groundwater supply depends on its purpose; thus, the need for drinking water, industrial water, and irrigation water varies widely. *Salinity*, *hardness*, and *silica* are three important parameters for industrial water. The overall quality and temperature of water should not fluctuate widely. In general, groundwater possesses uniform quality and temperature; it is preferred to surface water for industrial use. That is why the availability of groundwater of suitable quality often becomes a major consideration in selecting new industrial locations.

Carbon dioxide in solution, derived from the atmosphere and from organic processes in the soil, assists the solvent action of water as it moves underground. *Soluble salts* in groundwater originate primarily from solution of rock materials. *Sodium* and *calcium* are commonly cations; bicarbonate and sulfate are corresponding anions. *Bicarbonate*, usually the primary anion in groundwater, is derived from carbon dioxide released by organic decomposition in the soil. *Chloride* occurs to only a limited extent under normal conditions; important sources of chloride, however, are from sewage, connate water, and intruded seawater. Occasionally, *nitrate* is an important natural constituent; high concentrations may indicate sources of past or present pollution. The lack of productivity resulting from excess salt contents of the soil and water is called *badlands*.

Dissolved gases in groundwater can pose hazards if their presence goes unrecognized. Most *pathogenic bacteria* found in water are indigenous to the intestinal tract of animals and humans; the presence of these in groundwater is tantamount to its contact with sewage sources. Because bacteria of the coliform group are relatively easy to isolate and identify, standard tests to determine their presence or absence in a water sample are taken as a direct indication of the safety of the water for drinking purposes. *Coliform* test results are reported as the most probable number (MPN) of coliform group organisms in a given volume of water. *To establish groundwater quality, measures of chemical, physical, biological, and radiological constituents should be performed*. The resultant data are then analyzed to verify its standards. Tables may be difficult to interpret results of multianalyses of chemical quality of groundwater. To overcome this, graphic representations are useful for display, comparing analyses, and emphasizing similarities and differences. Graphs can also aid in detecting the mixing of water of different compositions and in identifying chemical processes occurring as groundwater moves. *The main graphic techniques used in groundwater* *quality include bar charts, radiating vectors, pattern/Stiff diagrams, circular/pie diagrams, trilinear/Piper diagram, semilogarithmic/Schoeller diagram*, etc.

Population increase and lack of surface water supplies have increased the demand for groundwater usage. Groundwater may be polluted due to many activities, including leaching from municipal and chemical landfills, accidental leaking of chemicals or waste materials, and improper underground injection of liquid wastes from septic tank systems. *Groundwater pollution* is the artificially induced degradation of natural groundwater quality due to disposal of wastes on or into the ground. Entry of pollutants into shallow aquifers occurs by percolation from ground surface, through wells, from surface waters, and by saline water intrusion. When a contaminant enters from ground surface, depending on the type of the contaminant, a portion of it may be adsorbed, volatilized, degraded by microorganisms, or uptaken by plants, and the rest of that may reach the underlying aquifers. Therefore, the amount that reaches the underlying aquifer is significantly less than the initial amount. But this reduced amount of contaminant can still cause quality problems for the underlying aquifer. Further, some toxics and chemicals as well as some dissolved contaminants are not degraded or adsorbed, and almost all of what is applied to the field will reach the aquifer. The sources and causes of groundwater pollution are closely associated with human use of water. It is difficult to detect, and is even more difficult to control, and may persist for decades. It can create hazards to public health through toxicity or the spread of disease. Thus, it is important to prevent, reduce, and eliminate groundwater pollution. The principal sources and causes of groundwater pollution and their classification are dealt with in Chapter 7.

An important aspect of groundwater pollution is the fact that it may persist underground for years, decades, or even centuries. This is in marked contrast to surface water pollution. Reclaiming polluted groundwater is usually much more difficult, time-consuming, and expensive than reclaiming polluted surface water. Underground *pollution control* is achieved primarily by regulating the pollution source, and secondarily by physically entrapping and, when feasible, removing the polluted water from the underground. Various technologies are available to prevent, abate, or clean up polluted groundwater. To protect groundwater resources, institutional tools (i.e. regional groundwater management, land zoning, effluent charges/credits, guidelines, aquifer standards, and criteria) are required. Regional management of groundwater is an effective approach in prevention of long-term quality and quantity polluting activities. Public education on proper use of agricultural fertilizers, pesticides, herbicides, chemicals, waste disposal guidelines, etc., and regulatory enforcement are very useful to prevent polluting activities as overuse or abuse of chemicals, excessive groundwater withdrawal, etc. *Land zoning* is related to optimum site selection and disallows industrial or waste disposal activities in groundwater recharge areas. Economic incentives and credits to facilities those improve the groundwater resources result in protecting groundwater resources; while, by applying charges to potential polluting activities leads to less pollution load to groundwater resources. Establishing guidelines or standards for construction and operation of groundwater polluting activities and establishment and application of groundwater quality standards and criteria for aquifers are the most effective tools to protect aquifers. Once aquifer gets contaminated, it should be restored. Remediation of contaminated groundwater may be achieved by adopting three major strategies: (1) containment of groundwater, (2) groundwater extraction, and (3) treatment of contaminated groundwater.

19.2 Groundwater Contaminants

Water is the essential commodity for life to survive. The quality of groundwater is as important as its quantity. The quality of water has been under serious threat, which in turn puts a question mark on the health of living beings. The natural quality of groundwater depends largely on local geological characteristics and climatic conditions. Changes in atmospheric composition and soil chemistry and human activities that directly alter the physical or chemical conditions of soil layers can contribute to the changes in the quality of groundwater. In higher temperatures, more thermal energy is available, and in consequence, reaction rates increase. Heat may affect groundwater contaminants as it (1) changes the equilibrium and kinetics of precipitation and the dissolution of minerals and (2) changes the rates of biological transformation processes.

19.2.1 Inorganic Contaminants

Adsorption processes influence occurrence and mobility of the heavy metals in groundwater. The most common nonmetals that may occur in groundwater are carbon, chlorine, sulfur, nitrogen, fluorine, arsenic, selenium, phosphorus, and boron. *Carbon*, *chlorine*, and *sulfur* may exist in high concentrations in dissolved forms in most natural and contaminated groundwater systems. *Arsenic* and its compounds have been used as insecticides and herbicides for a long time and can be found in groundwater systems influenced by agricultural activities. Arsenic is a human health concern because it can lead to skin, bladder, and other cancers. It is found in groundwater in many parts of India. It is a naturally occurring element in rocks, soils, and water in contact with them. *Nitrogen* is mostly from agricultural activities and the disposal of sewage on or beneath the land surface. Nitrogen may exist in groundwater in different forms such as nitrate (NO_3), ammonium (NH_4^-), ammonia (NH_3), nitrite (NO_2^-), nitrogen (N_2), nitrous oxide (N_2O), and organic nitrogen. *Fluoride* is used as a municipal water-supply additive in many cities due to its beneficial effects on dental health. It is also a natural constituent of groundwater. *Phosphorus* causes accelerated growth of algae and aquatic vegetation; but, it is not a harmful constituent in drinking water. The main sources of phosphorus are the widespread use of fertilizers and the disposal of sewage on land.

19.2.2 Dissolved Gasses

Groundwater contains dissolved gases (mainly carbon dioxide, oxygen, nitrogen, methane, and hydrogen sulfide) derived from natural sources. The natural gases, mostly originating from the atmosphere, involved in the geochemical cycle of groundwater are carbon dioxide, oxygen, and nitrogen. Oxygen plays a significant role in microbiological activities depending on aerobic, anoxic, or anaerobic conditions. Carbon dioxide dissolves in water and forms carbonic acid. This acid can be dissociated from bicarbonate (HCO_3–) and carbonate (CO_3^{2-}) ions. The carbonate plays an important role in groundwater composition through precipitation reactions. Carbonic acid cycle influences the pH and buffering capacity of precipitation. Water at equilibrium with atmospheric CO_2 will have a pH of approximately 5.7, which can be used as a benchmark in the evaluation of the effects of atmospheric constituents. *Nitrogen* and *sulfur oxides* (NOx and SOx) may cause the production of strong acids, such as HNO_3 and H_2SO_4. Many natural processes, such as volcanic and microbiological activity, release NOx and SOx into the atmosphere. Biochemical processes produce dissolved gases in groundwater like the flammable gases methane, and hydrogen sulfide. *Hydrogen sulfide* rarely accumulates to dangerous proportions and has a distinctive rotten-egg odor. *Methane* is produced by the decomposition of buried plant and animal matter in unconsolidated and geologically young deposits. It is a colorless, tasteless, and odorless gas that can cause serious problems in terms of fires and explosions. Groundwater containing 1–2 mg/l of methane can produce an explosion in a poorly ventilated air space. The minimum concentration of methane in water sufficient to produce an explosive mixture depends on the temperature, pressure, quantity of water pumped, and volume of air into which the gas evolves. Many times people suffocate in dug wells and pump pits where high methane concentrations accumulate. Safety measures include analyses to detect the presence of the gas, restricting people from entering dug wells and pump pits where methane gas may be present, aeration of water before use, and ensuring adequate ventilation where the water is being used.

19.2.3 Particles

Constituents that exist in the solid phase either within or apart from the groundwater are referred to as *particulate matters*. Generally, constituents with a size of 10 nm or greater are considered as particles in groundwater system. Microorganisms are also important particulate contaminants in groundwater systems. Microbial contaminants in groundwater can be categorized into viruses, bacteria, and protozoan cysts. All these microorganisms move in groundwater systems, and the larger microorganisms generally move slower than viruses. The size of bacteria generally ranges from about 0.5–3 μm. Protozoan cysts are more difficult to inactivate than either bacteria or viruses. They might be found in higher concentrations in groundwater supplies that are under the direct influence of surface waters. The main effect of microorganisms on groundwater contaminants is that they catalyze the important redox reactions in groundwater.

19.3 Soluble Salts in Groundwater

All groundwater contains salts in solution. The type and concentration of salts depend on the environment, movement, and source of the groundwater. Ordinarily, higher concentrations of dissolved constituents are found in groundwater than in surface water because of the greater exposure to soluble materials in geologic strata. Soluble salts in groundwater originate primarily from solution of rock materials. Salts are added to groundwater passing through soils by soluble products of soil weathering and of erosion by rainfall and flowing water. As groundwater moves underground, it tends to develop a chemical equilibrium by chemical reactions with its environment. Such equilibrium in groundwater plays an important role in artificial recharge, movement of pollutants, and clogging of wells. The equilibrium achieved by the various chemical reactions under the slow movement and long residence time of groundwater within an aquifer produces a stable quality. In general, quality variations in groundwater are more noticeable in shallow aquifers due to waste disposal, freezing, and seasonal variations in quality and quantity of recharge and quantity of discharge.

In limestone terrains, calcium and bicarbonate ions are added to the groundwater by solution. An important source of salinity in groundwater in coastal regions is airborne salts originating from the air–water interface over the sea. The deposition decreases inland, varying exponentially with distance from the sea. In arid regions, where surface runoff is small and evapotranspiration is large, airborne salt deposition becomes intensified several fold in groundwater. In specifying the quality, characteristics of groundwater, chemical, physical, and biological analyses are normally required. The characteristics of water that affect water quality depend both on substances dissolved in water and on certain properties. Natural inorganic constituents commonly dissolved in water that are most likely to affect water use include bicarbonate, carbonate, calcium, magnesium, chloride, flouride, iron, manganese, sodium, and sulfate.

Salinity varies with specific surface area of aquifer materials, solubility of minerals, and contact time. Salinity is higher where groundwater movement is slower; hence, it generally increases with depth. Generally, bicarbonate salts dominate in shallow depths, whereas chloride salts dominate in deeper depths in aquifers. Excess irrigation water percolating to the water table may contribute to substantial quantities of salt. Water passing through the root zone of cultivated areas usually contains salt concentrations several times that of the applied irrigation water. In addition, soluble soil materials, fertilizers, and selective absorption of salts by plants will modify salt concentrations of percolating waters. Factors governing the increase include soil permeability, drainage facilities, amount of water applied, crops, and climate. High evapotranspiration process tends to concentrate salts in groundwater. Similarly, poorly drained areas often contain high salt concentrations. Some regions contain leftovers of sedimentary deposition of salty nature. Thus, high salinities may be found in soils and groundwater of arid climates where leaching by rainwater is not effective in diluting the salt solutions.

The groundwater in natural systems generally contains less than 1,000 mg/l dissolved solids, unless groundwater has encountered a highly soluble mineral, been concentrated by evapotranspiration, or been geothermally heated. *Total dissolved solids* (TDS) can quickly be determined by measuring the electrical conductance of a groundwater sample. Groundwater is treated as *fresh water* if TDS is less than 1,000 mg/l. When TDS is in high concentrations, groundwater becomes unusable for ordinary water-supply purposes. The groundwater is called *hard/brackish* if TDS is in between 1,000 and 10,000 mg/l. Any groundwater containing more than 10,000 mg/l TDS is termed *saline groundwater*. If TDS concentration in groundwater exceeds 1,00,000 mg/l, it is called *brine*. Chapter 16 deals with analysis and management of saline water.

The solubility of a contaminant compound will determine the transport, fate, and toxicology of that compound in a groundwater system. The main characteristics of a system, which may affect solubility, are pH, sorption to solids, and temperature. There are two types of associations among aqueous and solid phases: (1) *adsorption*—the accumulation of material at a water–solid interface and (2) *absorption*—the intermingling of solute molecules with the molecules of the solid phase (or the dissolution of a liquid material in a solid solvent). It is difficult to distinguish between the two processes. *Sorption* is a combined term for both adsorption and absorption. There are three types of sorptions for groundwater systems as follows:

1. Physisorption
2. Chemisorption
3. Ion exchange

Chemical precipitation may remove ions in solution by forming insoluble compounds. Precipitation of calcium carbonate and release of dissolved carbon dioxide may result from a decrease in pressure and/or an increase in temperature. Ferrous iron in solution oxidizes on exposure to air and is deposited as ferric hydroxide. *Ion exchange* involves the replacement of ions adsorbed on the surface of fine-grained materials in aquifers by ions in solution. Ion exchange causes changes in the physical properties of soils and assists in softening groundwater naturally. Sodium contents in groundwater cause deflocculation and reduction of permeability. While in the case, where calcium is the dominant cation, the exchange occurs in the reverse direction, creating a flocculated and more permeable soil. The soil texture and drainability can be improved by adding gypsum ($CaSO_4$) to a soil. In presence of certain bacteria, chemical reduction of oxidized sulfur ions to sulfate ions or to the sulfide state occurs frequently in groundwater.

Under certain conditions, a chemical bond is formed between the solute and a solid surface. Ion exchange occurs due to an electrostatic interaction between the solute and a solid surface. In physisorption and ion exchange processes, the forces responsible for the attraction of a solute to the solid are relatively weak. Therefore, these processes tend to be readily reversible. The selectivity order in ion exchange for some common cations is

$$Ba^{2+} > Sr^{2+} > Ca^{2+} > Mg^{2+} > Cs^{+} > K^{+} > Na^{+} > Li^{+}$$

Ions will replace those ions on their right in the selectivity order. As an example, Ca^{2+} will replace Na^{+}.

Hardness forms a scale not so good for household purposes. Hardness results from the presence of divalent metallic cations, of which calcium and magnesium are the most abundant in groundwater. The hard water tends to originate in areas where thick topsoils overlie limestone formations. Hardness is derived from the solution of carbon dioxide and the solution of insoluble carbonates in the soil and in limestone formations to convert them into soluble bicarbonates at low pH conditions. Impurities in limestone, such as sulfates, chlorides, and silicates, become exposed to the solvent action of water as the carbonates are dissolved so that they also pass into solution. Hardness H_T may be expressed as the equivalent of calcium carbonate given by the following equation:

$$H_T = \mathrm{Ca} \times \frac{\mathrm{CaCO_3}}{\mathrm{Ca}} + \mathrm{Mg} \times \frac{\mathrm{CaCO_3}}{\mathrm{Ca}} = 2.5\mathrm{Ca} + 4.1\mathrm{Mg} \tag{19.1}$$

Groundwater is considered soft, hard, and very hard if the hardness as $CaCO_3$ (mg/l) is less than 75, in between 150 and 300, and greater than 300, respectively.

The quality of groundwater should be suitable for both the plant and the soi1. Salts may affect plant growth physically and chemically. Effects of salts on soils, causing changes in soil structure, permeability, and aeration, indirectly affect plant growth. Salt tolerance of different plants varies widely. Drainage is also an important factor that affects crop growth under application of salty groundwater. If a soil is open and well drained, crops may be grown on it with the application of saline groundwater; but, on the contrary, a poorly drained soil may fail to produce a good crop production even under application of good-quality water. Poor drainage permits salt concentrations in the root zone to build up to toxic proportions, and hence adequate drainage is required for maintaining a favorable salt balance (i.e. TDS inflow by groundwater < TDS outflow with drainage water). Sodium reacts with soil to reduce its permeability. When high-sodium water is applied to a soil, the number of sodium ions combined with the soil increases, while an equivalent quantity of calcium or other ions is displaced. These reactions cause deflocculation and reduction of permeability. *Alkali soils* contain a large proportion of sodium with carbonate as the predominant anion. *Saline soils* contain a large proportion of sodium with chloride or sulfate as the predominant anion. Both types of sodium saturated soil hardly support plant growth. Sodium content (or soluble-sodium percentage) is expressed by

$$\%\mathrm{Na} = \frac{\mathrm{Na} + \mathrm{K}}{\mathrm{Ca} + \mathrm{Mg} + \mathrm{Na} + \mathrm{K}} \times 100 \tag{19.2}$$

Alternatively, *sodium adsorption ratio* (SAR) is used, which is defined by

$$\mathrm{SAR} = \frac{\mathrm{Na}}{\sqrt{(\mathrm{Ca} + \mathrm{Mg})/2}} \tag{19.3}$$

All ionic concentrations in Eqs (19.2) and (19.3) are expressed in milliequivalents per liter. Boron is necessary in very small quantities for normal growth of all plants; but in larger concentrations, it becomes toxic. In classifying quality of groundwater for irrigation, it is also important to take cognizance of the salt distribution within the soil.

19.4 Sources of Groundwater Contamination

Chapter 7 describes various sources of groundwater contamination. The following is the summary of sources of groundwater contamination (Karamouz et al 2011):

1. Groundwater quality problems that originate on the land surface
   - Infiltration of polluted surface water
   - Land disposal of either solid or liquid wastes
   - Dumps
   - Disposal of sewage and water-treatment plant sludge
   - Deicing salt usage and storage
   - Animal feedlots
   - Fertilizers and pesticides
   - Accidental spills
   - Particulate matter from airborne sources
2. Groundwater quality problems that originate in the ground above the water table
   - Septic tanks, cesspools, and privies
   - Holding ponds and lagoons
   - Sanitary landfills
   - Waste disposal in excavations
   - Leakage from underground storage tanks
   - Leakage from underground pipelines
   - Artificial recharge
3. Groundwater quality problems that originate in the ground below the water table
   - Waste disposal in well excavations
   - Drainage wells and canals
   - Well disposal of wastes
   - Underground storage
   - Exploratory wells
   - Groundwater development

19.5 Groundwater Pollution Control

Pollutants in groundwater tend to be removed or reduced in concentration with time and with distance traveled. Mechanisms involved include filtration, sorption, chemical processes, microbiological decomposition, and dilution. The rate of pollution attenuation depends on the type of pollutant and on the local hydrogeologic situation. Radioactive decay, based on the half-life of a radioisotope, acts as an attenuation mechanism for radioactive pollutants. Attenuation mechanisms tend to localize groundwater pollution near its source; they also are responsible for the interest in groundwater recharge as a water reclamation technique.

19.5.1 Chemical Process

Precipitation of calcium, magnesium, bicarbonate, and sulfate can occur in groundwater where appropriate ions in sufficient quantities are present in solution. Precipitation of trace elements (such as arsenic, barium, cadmium, copper, cyanide, fluoride, iron, lead, mercury, molybdenum, radium, zinc, etc.) may also take place. *Chemical precipitation* is a major attenuation mechanism in arid regions, where moisture in the unsaturated zone is minimal. In the zone above the water table, oxidation of organic matter acts as an important attenuation mechanism. Complex organic compounds are oxidized stepwise to more simple organic compounds until CO_2 and H_2O are formed along with numerous inorganic ions and compounds. Both oxidation and reduction reactions can occur underground in conjunction with other mechanisms, leading to precipitates, deposits of insoluble trace metals, and gases.

19.5.2 Dilution

Pollutants in groundwater flowing through porous media tend to become diluted in concentration due to hydrodynamic dispersion. The volume affected increases and the concentration decreases with distance traveled due to longitudinal and lateral spreading of a pollutant within the aquifer. Dilution is the most important attenuation mechanism for pollutants after they reach the water table. Maximum attenuation requires an adequate distance to the water table and the presence of fine-grained geologic materials, such as silt and clay. Pollutant attenuation below the water table occurs more slowly with dilution serving as the principal mechanism.

19.5.3 Partitioning Process

Since contaminants move through soil layers to reach groundwater, it is important to know how much of the pollutant is adsorbed to the soil particles and how much is in solution or can potentially be dissolved into pore water. In the dissolved phase, the pollutants can be transported to aquifers and surface waters. The term *partitioning* is used to divide the total pollutant mass between the particulate (adsorbed on particulate matter) and dissolved fractions. Adsorption of the contaminant into the particulate form immobilizes contaminants and makes them biologically unavailable in most cases. Dissolved or dissociated (ionized) contaminants are mobile with soil pore water. The master variables that affect the interactions between the soluble and particulate fractions of the contaminant are the pH, the anion–cation composition of the soil–pore water solution, and the particulate and dissolved organic carbon (Salomons and Stol, 1995). Hydrophilic or water-soluble compounds have higher bioavailability and leach more easily into groundwater. On the other hand, hydrophobic or water-insoluble compounds are immobile, and they accumulate in soils. For describing the proportion between the dissolved (ionized) and adsorbed (precipitated) particulate fractions, among several proposed mathematical formulations of adsorption equilibrium (isotherms), the Langmuir, Freundlich, and linear isotherms are most widely used.

19.5.4 Retardation

In porous media, organic chemicals move more slowly than dissolved contaminants since they are retarded by adsorption. Adsorption may be incorporated in groundwater contaminant transport calculations through retardation factor, which is an empirical term derived from partitioning coefficient. *Retardation factor R* is a ratio of total chemicals to dissolved chemicals. The chemical solute moves only in dissolved phase and the adsorbed phase is not moving. Retardation factor is also equal to the ratio of the velocity of water to the velocity of the solute. The downward velocity of water/or dissolved phase is equal to infiltration rate divided by the soil water content. Therefore, how fast a solute moves downward in the unsaturated zone can be determined. To determine how far the solute goes downward, assume a depth of water, d, is added to the soil at a constant water content, θ. Then, the depth to which the water moves down, D, is equal to d/θ. If this water contains a chemical with a constant concentration, the chemical moves downward to the depth D' given by the following equation:

$$D' = \frac{D}{R} = \frac{d}{\theta R} \tag{19.4}$$

19.5.5 Natural Losses of Contaminants

The contaminants applied to a field may be removed from soil before reaching aquifers by volatilization, biological degradation, and plant uptake.

Volatilization

Volatilization is the loss of chemicals in vapor form from soil or water surfaces to the atmosphere. The potential of volatilization is mainly related to the saturated vapor pressure of the chemical in the air above the interface. In porous media, volatilization applies particularly to reactions involving nitrate and sulfate. Volatilization does not occur from submerged aquatic sediments. The relation between the vapor density and corresponding concentration of the chemical (C_d) in water solution can be computed by Henry's law:

$$C_d = K_H C_g \tag{19.5}$$

where, K_H = Henry's constant for the chemical (dimensionless) and C_g = the vapor density of the chemical (μg/l).

Biological Degradation

Most pathogenic microorganisms in the soil do not flourish in the soil, and hence are subject to ultimate destruction, the timing of which depends on different species and environmental conditions. Bacteria and viruses move slower through a porous media than water and can be removed in short distance if reasonable amounts of silt and clay are present. Some microorganisms or fungi can also cause biotransformation of chemicals. These organisms require energy and organic carbon source as well as nutrients for their growth. The breakdown of a chemical by microorganisms to more simple compounds (e.g. carbon dioxide, water, methane, ammonium, and other simple by-products) is known as biological degradation. The degradation rate of chemicals can be calculated using he first-order reaction as follows:

$$C_t = C_0 e^{-\kappa t} \tag{19.6}$$

where, C_t and C_0 are the chemical masses at time t and 0, respectively; K is the overall degradation coefficient (per day); and t = time (day). The half-life of organic chemicals, which is the time required for 50 percent degradation of the original chemical in the soil, or their persistence in the soil is computed as follows:

$$t_{1/2} = -\frac{\ln 0.5}{\kappa} = \frac{0.693}{\kappa} \tag{19.7}$$

Plant Uptake

Plants uptake nutrients and some chemicals and immobilize them. The nutrient and chemical uptake process is a part of the overall transpiration process of plants. Nutrients and chemicals are transported into plant tissues from the dissolved or ionic pool of chemicals in pore water. Therefore, chemical and nutrient adsorbed on soil particles or precipitated in soils are not removed from the system by plant uptake. These adsorbed pollutants must first be transferred into pore water by disruption or dissolution.

19.5.6 Source Control Techniques

The best solution to pollution is prevention. Source control techniques represent attempts to minimize or prevent groundwater pollution before a potential polluting activity is initiated. Source control strategies are applied to the design of new facilities although some of the strategies can be used as pollution reduction tools for existing facilities. The following are some common types of source control strategies that can be applied to prevent groundwater pollution at waste disposal facilities (Karamouz et al 2011):

1. Volume reduction strategies
   - A. Recycling
   - B. Resource recovery
     - Materials recovery
     - Waste-to-energy conversion
   - C. Centrifugation
   - D. Filtration
   - E. Sand drying beds
2. Physical/chemical alteration strategies
   - A. Chemical fixation
     - Neutralization
     - Precipitation
     - Chelation
     - Cementation
     - Oxidation–reduction
     - Biodegradation
   - B. Detoxification
     - Thermal
     - Chemical—ion-exchange, pyrolysis, etc.
     - Biological—activated sludge, aerated lagoons, etc.
   - C. Degradation
     - Hydrolysis
     - Dechlorination

  - Photolysis
  - Oxidation

D. Encapsulation
E. Waste segregation
F. Co-disposal
G. Leachate recirculation

The advantages of source control strategies include the following:

- Enhancing groundwater quality by reducing the pollution load applied to the aquifer.
- Reducing the stabilization time of waste disposal facilities.
- Decreasing the cost of aquifer restoration and groundwater treatment.

All source control strategies require extensive monitoring and recordation. The disadvantages of source control strategies are the following:

- It is hard to convince industries to apply these strategies because of the lack of public knowledge about the environmental hazards.
- Installation and maintenance costs.
- Monitoring and skilled operator requirements.

19.5.7 Surface Water Control, Capping, and Liners

Surface water control, capping, and liners are preventive measures that are usually used in conjunction with each other. The amount of surface water infiltrating into ground is minimized using surface water control techniques. By capping of a site, the infiltration of any surface water or direct precipitation coming onto a site is reduced. Impermeable liners provide groundwater protection by inhibiting downward flow of leachate and other pollutants by adsorption processes.

19.5.8 Sheet Piling

In sheet piling, a thin impermeable permanent barrier for flow is created by driving lengths of steel as shown in Figure 19.1 that connect together into the

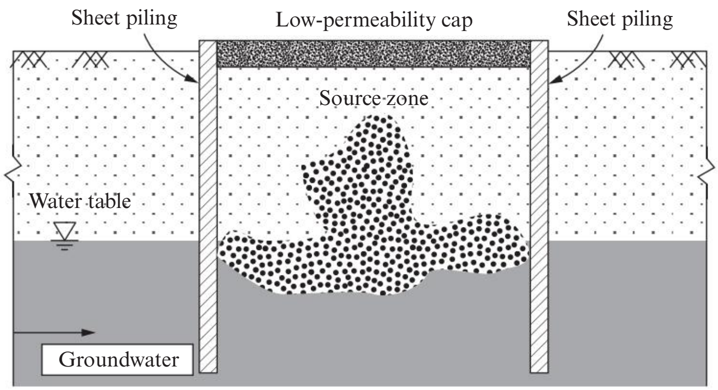

Figure 19.1 *Sheet piling (Todd and Mays 2005)*

ground. Construction of sheet piles is easy and may be economical as excavation is not required. There is no maintenance required after construction. However, driving piles through ground containing boulders is difficult. Certain chemicals may attack the steel pile. As the size of a project increases, application of sheet piling becomes uneconomical.

19.5.9 Grouting

Grouting can be used for groundwater pollution control. Grouting is limited to granular types of soils that have a pore size large enough to accept grout fluids under a pressure. Highly layered soil profiles, the presence of high water table, and rapidly flowing groundwater are not suitable for grouting.

19.5.10 Slurry Walls

One of the most widely used techniques for containment is the soil-bentonite slurry wall. Slurry walls encapsulate an area to prevent groundwater pollution and restrict the movement of contaminated groundwater as shown in Figure 19.2. This method is an effective way of isolating hazardous waste and preventing migration of pollutants. Slurry walls can either be placed up-gradient from a waste site to prevent flow of groundwater into the site, or it can be placed around a site to prevent movement of polluted groundwater away from a site. The construction methods for slurry walls are simple, and adjacent areas are not usually affected by groundwater drawdown. In this method, a trench is first excavated around an area. This trench is then filled with an impermeable material. If bentonite is used in the slurry wall, it will not deteriorate with age. Slurry walls have low maintenance requirements, and they are typically the most economical ones. They eliminate risks due to pump breakdowns or power failure.

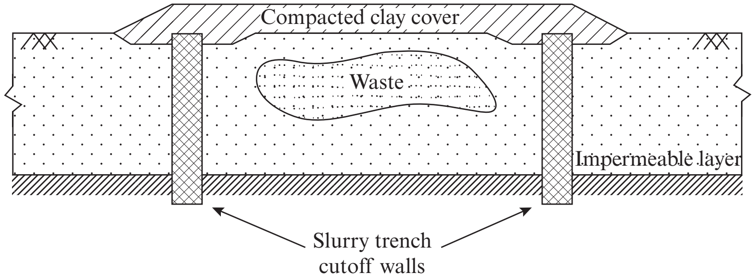

Figure 19.2 *Slurry walls (Karamouz et al 2011)*

19.5.11 Groundwater Extraction Systems

Groundwater extraction systems, the most common being extraction well systems and extraction trench systems, are a combination of subsurface components and above-ground components. The subsurface components are the wells or trenches, which provide access to the contaminated water; the above-ground components are used to regulate and monitor the extraction process.

The use of well systems is one of the most common methods of groundwater pollution control. In this method, the subsurface hydraulic gradient is manipulated through injection or withdrawal of water. Here, the movement of water phase is controlled directly and concentration of pollutants in the subsurface water is controlled indirectly. There are three main classes of well systems namely, well point systems, deep well systems, and pressure ridge systems. All of them require the installation of several wells at selected sites. These wells are then pumped (or injected) at specified rates so as to make the movement of the water phase and associated pollutants. Well systems are also known as plume management, and it is the most assured means of controlling contaminants in groundwater. Well systems can be installed readily, can include recharge of aquifer, and have high design flexibility. However, operation and maintenance costs are high, require continued monitoring, and may require surface treatment prior to discharge of water mixed with pollutants.

Interceptor systems consist of a trench excavated below the water table, a perforated pipe placed at the bottom, and backfilled with coarse material. The trench creates a continuous zone of depression. Interceptor systems are preventive measures (leachate collection systems) or abatement measures (interceptor drains). Interceptor systems provide a means of collecting leachate without the use of impervious liners and since flow to underdrains is by gravity, operation costs are relatively cheap. Design of underdrains is flexible, and construction methods are simple. However, these systems are (i) not suitable for poorly permeable soils; (ii) not feasible beneath an existing site; (iii) not useful for deep disposal sites; and (iv) less efficient than well-point systems. In addition, interceptor systems require continuous and careful monitoring to assure adequate leachate collection.

19.6 Treatment of Contaminated Aquifer

The type of treatment required for site-specific contaminated groundwater depends on the contaminants being removed. Due to the number of chemicals that potentially exist in groundwater as contaminants, the treatment can be simple or extremely complex. Groundwater treatment technologies can be classified as in situ or ex situ. *In situ treatment techniques* either render a contaminant nontoxic through treatment or enhance extraction of the contaminant from the aquifer. *Ex situ treatment techniques* treat groundwater that has been extracted from the aquifer. Different in situ and ex situ techniques are listed in Table 19.1. In situ treatment technologies are generally designed to perform one or more of the following functions: Remove contaminant source zone; restore aquifer; and prevent or minimize continued contaminant migration. In situ treatment techniques can be biological remediation (bioremediation) techniques, volatization processes, and chemical and physical processes. *Bioremediation* is the biological degradation of contaminants using naturally occurring microbes in the soil. *Volatization processes* transfer the chemical from of the liquid state to the gaseous state (vapor phase), because vapor phase contaminants are typically easier to remediate. Aquifer materials are significantly more permeable to vapors than to liquids, making vapors easier to remove from the aquifer.

Table 19.1 Treatment techniques (Todd and Mays 2005)

In situ	*Process description*
Bioremediation	Biological degradation of contaminants using naturally occurring microbes in soil
Soil vapor extraction	Volatization of contaminants that are present in the vadose zone
Air sparging	Volatization of contaminants in the saturated zone
Permeable reaction barriers	Physical or chemical treatment in a trench
Vacuum vapor extraction	Volatization, within a well, of contaminants from saturated zone
Density driven convection	Enhanced bioremediation using single-well driven convection system in aquifer.
Ex situ	***Process description***
Bioreactor	Biological degradation of contaminants (activated sludge, fixed-film biological reactor, biophysical treatment)
Slurry-phase biological treatment	Variation on bioreactor in which contaminants are treated in a slurry form
Air stripping	Volatization of contaminants
Carbon adsorption	Adsorption of contaminants to activated carbon
Ion exchange	Exchange-type attachment of contaminants to ion-exchange resin
Alkaline precipitation	Alteration of water quality (usually pH adjustment) such that concentration exceeds the compound's solubility limit, causing precipitation
Membrane	Separation of solids from water using membranes (reverse osmosis, ultrafiltration)
Wetlands treatment	Uptake of contaminants by wetland features
Electrokinetic decontamination	Desorption of contaminants by "acidic front" of groundwater caused by hydrolysis of the groundwater

In situ techniques can be divided into the following three categories (Todd and Mays 2005):

1. Source zone treatment technologies
   - Free-product recovery
   - Excavation and disposal or above-ground treatment
   - In situ soil venting

- Bioventing
- In situ air sparging
- Enhanced in situ soil venting with soil heating and/or soil fracturing
- In-situ vitrification
- Phytoremediation
- Groundwater pump and treatment systems

2. Aquifer restoration techniques
- Groundwater pump-and-treat systems
- Natural attenuation
- In situ air sparging
- Enhanced bioremediation

3. Contaminant migration prevention
- Natural attenuation
- Groundwater pump-and-treat systems
- In situ reaction walls
- In situ air sparging curtains
- Infiltration barriers
- In situ contaminant options (grout walls, sheet piling walls, etc.)

Source zone treatment technologies treat the cause of the groundwater contamination so that they target the removal and destruction of the residual contaminants in the soil that are the source. *Aquifer restoration* technologies are employed before, during, or after source zone treatment to target the treatment of dissolved contaminant plumes. *Contaminant migration prevention* technologies are employed at sites where the source zone location is unknown and/or there are no practicable source zone and aquifer restoration options in order to minimize future impacts of contaminants on groundwater.

19.6.1 Air Sparging

In situ *air sparging* is primarily used to remove volatile organic carbons (VOCs) from the saturated subsurface. The removal process is done through stripping VOCs by injecting air into the saturated zone to promote contaminant partitioning from the liquid to the vapor phase as shown in Figure 19.3. In air stripping, a substance is transferred from the solution in water to solution in a gas, and then it is transferred to atmosphere. Since injected air, oxygen, can induce the activity of indigenous microbes, air sparging can be effective in increasing the rate of natural aerobic biodegradation. In addition, by injecting a nonoxygenated gaseous carbon source, anaerobic environments can be created to provide denitrification conditions for nitrate removal from the groundwater. Air sparging is relatively inexpensive and easy to implement. It is one of the most practiced engineered technologies for in situ groundwater remediation. However, the presence and distribution of preferential airflow pathways, the degree of groundwater mixing, and potential precipitation and clogging of the soil formation by inorganic compounds are important aspects to be taken into consideration in designing air sparging system.

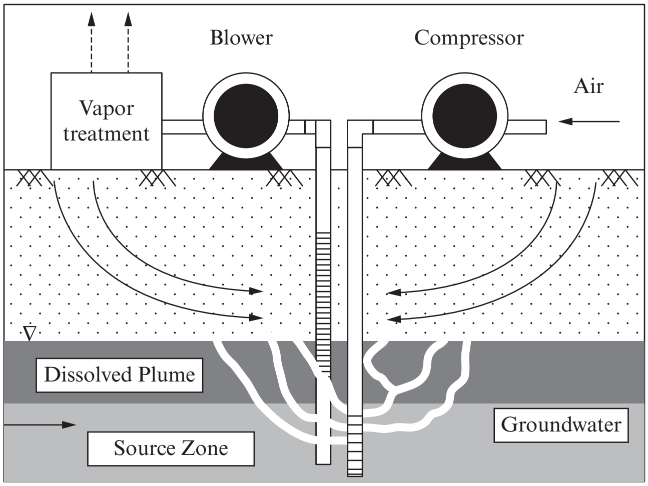

Figure 19.3 *Air sparging (Todd and Mays 2005)*

19.6.2 Carbon Adsorption

Activated carbon adsorption is a successful way for removing organics from contaminated groundwater. Organic molecule can be held on the surface of activated carbon by physical and/or chemical forces. Due to the balance between the forces that keep the compound in solution and the forces that attract the compound to the carbon surface, the quantity of a compound that can be adsorbed by activated carbon is determined.

19.6.3 Thermal Technologies

Soil and groundwater zones contaminated by chlorinated solvents, volatile and semivolatile organic contaminants, pesticides, fuels, oils, and lubricants can be remediated by in situ *thermal heating* methods. A thermal heating system typically consists of a series of injection and extraction wells. The injection wells are usually placed in clean areas around the source zone, if possible, to minimize the risk of contaminant spreading. The hot water, steam, or hot air is injected into the subsurface to dissolve, vaporize, and mobilize contaminants that are then recovered. Then, mobilized contaminants are extracted from the subsurface using vapor and liquid extraction equipment. Extracted vapors and liquids are then treated using conventional aboveground treatment technologies. In all thermal technologies, the viscosity of nonaqueous phase liquids (NAPLs) is lowered, and the vapor pressure and solubility of VOCs are increased. In consequence, the removal of NAPL is enhanced.

19.6.4 Bioremediation Techniques

Bioremediation can be achieved by adding some microorganisms artificially to remove organic chemicals. Bioremediation enhances growth and reproduction of microorganisms, which are capable of degrading the chemicals. Bioremediation technologies reduce the cost and time required to clean up aquifers. These technologies rely on natural processes to treat contaminants and are usually less expensive as they do not require waste extraction or excavation. The following are factors that affect aquifer bioremediation: Hydraulic conductivity; soil structure and stratification; groundwater mineral content; groundwater pH; groundwater temperature; and microbial presence.

19.6.5 Adding Chemicals and In Situ Chemical Oxidation

Adding chemicals to contaminated aquifers is one the effective ways for the removal of inorganic compounds. Sulfides remove the most inorganics, with the exception of arsenic (because of the low solubility of sulfide compounds). But the side effect is that sulfide sludge might be oxidized to sulfate when exposed to air, resulting in resolubilization of the metals. Carbonates may be used, but conditions are difficult to control in actual site. Hydroxides have the best performance for the removal of inorganics and metals. In in situ chemical oxidation method, groundwater or soil contaminants are transformed into less harmful chemical species by the introduction of a chemical oxidant into the subsurface. In the remediation of contaminated groundwater, oxidants (permanganate, hydrogen peroxide, or ozone), and potential amendments are directly injected into the source zone and down-gradient plume. The oxidant chemicals react with the contaminants and produce harmless substances such as carbon dioxide, water, etc. This technique is a suitable method for removing BTEX, MTBE, TPH, chlorinated solvents, PAHs, PCBs, chlorinated benzenes, phenols, and organic pesticides.

19.6.6 Permeable Reactive Barriers

Permeable reactive barriers are barriers to the contaminant. In this method, reactive materials are placed using trenches or by injecting reactive materials in the subsurface across the path of a plume of contaminated groundwater to create a passive treatment system. These barriers may contain metal-based catalysts for degrading volatile organics, nutrients, and oxygen for microorganisms to enhance biodegradation or other agents. The barrier can be a precipitation wall or a sorption wall. The former reacts with the contaminants to form insoluble products, which may remain in the wall and the latter adsorbs contaminants to the wall surface. When the polluted groundwater passes through these materials, treated water comes out from the other side. Figure 19.4 sketches a plume being treated by a permeable reactive barrier.

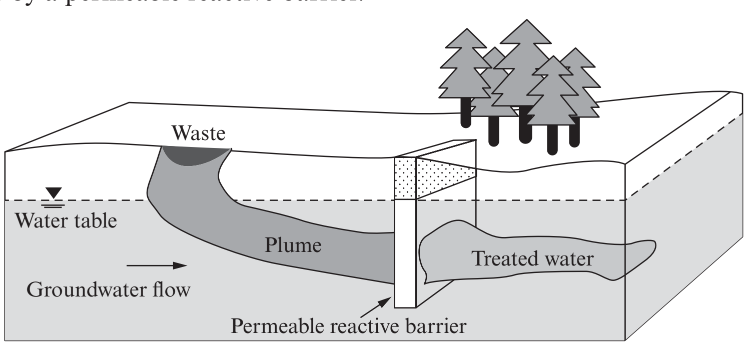

Figure 19.4 *Permeable reactive barrier (Karamouz et al 2011)*

19.7 Restoration of Contaminated Aquifer

Development of appropriate methodologies for aquifer cleanup and restoration is required to meet the increased demand for groundwater usage. *Remediation/* restoration refers to the reduction of risk caused by exposure to contaminated groundwater, wherein it is tried to find to protect human health and the environment and to restore groundwater meeting appropriate standards. One of the following remediation goals may be identified (Todd and Mays 2005):

- *Complete restoration*, which involves removal of all contaminants from the contaminated aquifer;
- *Nondegradation*, which involves removal of contaminants that exceed either the detection limits of available analytical equipment or background concentrations;
- *Remediation to health-based standards*, which involves removal of contaminants that are present at a concentration that could cause adverse health effects;
- *Remediation to the limits of technology-based standards*, which involves the use of the best available technology to remove as much of the contaminants as possible;
- *Partial-use restrictions* (or *institutional controls)*, such as legal restrictions on the use of groundwater in areas where groundwater has been contaminated, or physical barriers to prevent access to contaminated media;
- *Containment*, which involves the use of engineered systems for preventing migration of the contaminants to locations where receptors could be exposed to the contaminants.

Table 19.2 lists advantages and disadvantages of each of the above remediation goals. Once a remediation goal is selected, a remedy must be implemented to achieve the goal.

19.7.1 Stabilization/Solidification Strategies

Stabilization refers to immobilization by chemical reaction or entrapping, whereas *solidification* means the production of a solid, monolithic mass with enough integrity to be easily transported. When a material is chemically stabilized, a substance that is more resistant to leaching and also more amenable to the solidification process is provided. By chemically fixing the hazardous waste constituents, their release will be minimized in the event of a breakdown of the solid matrix. By structurally isolating, the waste material in a solid matrix prior to landfilling, the threat to groundwater from land disposal of waste materials can be reduced. This process is more important for hazardous and radioactive waste disposal. In this process, the waste in a solid matrix is chemically fixed. This reduces the exposed surface area and minimizes leaching of toxic constituents. In immobilization process, toxic components chemically react to form compounds immobile in the environment and/or the toxic material in an inert stable solid entrap. pH adjustment is the simplest stabilization process. In most industrial sludge, toxic metals are precipitated as amorphous hydroxides

Table 19.2 Different remediation goals (Todd and Mays 2005)

Goal	Advantages	Disadvantages
Complete restoration	Eliminates all risk	Likely impossible
Nondegradation	Reduction of contaminants to lowest level measurable	Extremely difficult, expensive, and time-consuming for many contaminants and hydrogeologic settings
Health-based standards	Designed to prevent measurable impacts to human health or environment	Difficult to defineand may not accurately address all possible health impacts of exposure to contaminated groundwater
Technology-based standards	Allows treatment to the best capabilities of current technology	May not reduce risk to a level that is protective of human health and the environment
Partial-use restrictions	Prevents contact between contaminants and receptors in a cost-effective manner	Leaves contaminants that could cause risk if partial use restrictions are ineffective
Containment	Relatively predictable and reliable; typically less costly than other remediation approaches	Leaves contamination that could migrate if containment system fails

Increasing flexibility
Increasing cost
Increasing protection

that are insoluble at an elevated pH. By carefully selecting stabilization system of suitable pH, the solubility of any metal hydroxide can be minimized. Certain metals can also be stabilized by forming insoluble carbonates or sulfides. By encapsulation, stabilized wastes can be solidified into a solid mass. By stabilization/solidification processes, a material is produced which does not pose a threat to the land on which it is disposed. Solidification may be done through the addition of cement, lime, pozzolanic materials, organic polymer, etc.; by embedding wastes in thermoplastic materials such as bitumen, paraffin, or polyethylene; by encapsulation of wastes in an inactive coating; by treatment of the wastes to produce a cementitious product; or by formation of a glass by fusion of wastes with silica. There is no optimum stabilization/solidification process applicable to every type of hazardous waste.

19.7.2 Hydraulic Containment of Groundwater

Hydraulic containment can be used at sites where the contaminant source cannot be removed, such as at landfills or in bedrock with dense nonaqueous phase liquids (DNAPLs). The most widely used types of hydraulic containment are physical barriers and hydraulic barriers. *Physical barriers* are vertical features in the ground that are barriers to the flow of groundwater. They can be *nonselective* *physical barriers*, which obstruct the flow of all groundwater, or *selective physical barriers*, which obstruct only the migration of target contaminants. Cutoff walls, which limit migration of groundwater by forming a physical barrier to the flow, are the oldest and most commonly used. Soil-bentonite slurry walls are the most commonly used in geotechnical and environmental remediation projects. *Hydraulic barriers* create a depression in the piezometric surface of groundwater, acting as a barrier beyond which groundwater within the zone of influence of the barrier should not flow. They can be formed using trenches, wells, or other methods that remove groundwater. Other options for hydraulic containment include horizontal drains, geomembranes, and well points.

19.7.3 Use of Capture Zone in Treatment

The *capture zone* of an extraction well or drain is the portion of the subsurface containing groundwater that will ultimately discharge to the well. The shape of the capture zone depends on the natural hydraulic gradient as well as the pumping rate and transmissivity as analyzed in Chapter 10. The shape of capture zone is given by the following equation:

$$x = y\cot\left(\frac{2\pi Tiy}{-Q}\right) \text{ or } y = \pm\frac{Q}{2Ti} - \frac{Q}{2\pi Ti}\tan^{-1}\frac{y}{x} = \pm\frac{Q}{2Ti} - \frac{Q}{2\pi Ti}\varphi \quad (19.8)$$

where, φ is the angle between a horizontal line through the well and any point (x, y) on the capture zone curve. There have been many models developed to determine capture zones for different conditions (Javandel and Tsang 2001; Haitjema et a1., 2005).

The extent of pollution in groundwater from a point source decreases as pollutants move away from the source until a harmless or very low concentration level is reached. Because each constituent of a pollution source may have a different attenuation rate, the distance to which pollutants travel will vary with each quality component. Pollutants, once entrained in the saturated groundwater flow, tend to form *plumes* of polluted water extending downstream from the pollution source until they attenuate to a minimum quality level. The shape and size of a plume depend on the local geology, the groundwater flow, the type and concentration of pollutant, the continuity of waste disposal, and any human modifications of the groundwater system, such as pumping wells. Where groundwater is moving relatively rapidly, a plume from a point source tends to be long and thin; but where the flow rate is low, the pollutant tends to spread more laterally to form a wider plume. Ogata and Banks (1961) obtained analytical solution for a plume as given by Eqn. (7.26). *Peclet number* ($P_e = v_x x/D_{hx}$) is a measure of the ratio of the rate of transport by advection to the rate of transport by diffusion. Large Peclet numbers ($P_e > 100$) indicate that advection dominates. When advection dominates, the second term on the right-hand side of Eqn. (7.26) becomes negligible and reduces to Eqn. (7.28). By superimposing a plume onto a capture zone, it can be determined whether or not the well of interest is sufficient to extract the entire plume as shown in Figure 19.5. This can also be used to specify the location of the well.

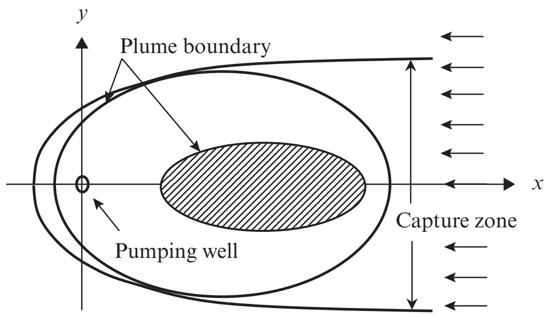

Figure 19.5 *Plume superimposed onto a capture zone of a single well*

Irregularly shaped plumes can be created by local influences such as pumping wells and non-uniformities in permeability. Plumes tend to become stable areas if there is a constant input of waste into the ground. This occurs for two reasons: enlargement as pollutants continue to be added at a point source is counterbalanced by attenuation mechanisms, or the pollutant reaches a location of groundwater discharge, such as a stream, and emerges from the underground. When a waste is first released into groundwater, the plume expands until a quasiequilibrium stage is reached. If sorption is important, a steady inflow of pollution will cause a slow expansion of the plume as the earth materials within it reach a sorption capability limit. An approximately stable plume will expand or contract generally in response to changes in the rate of waste discharge. Figure 19.6 shows changes in plumes and corresponding causing factors.

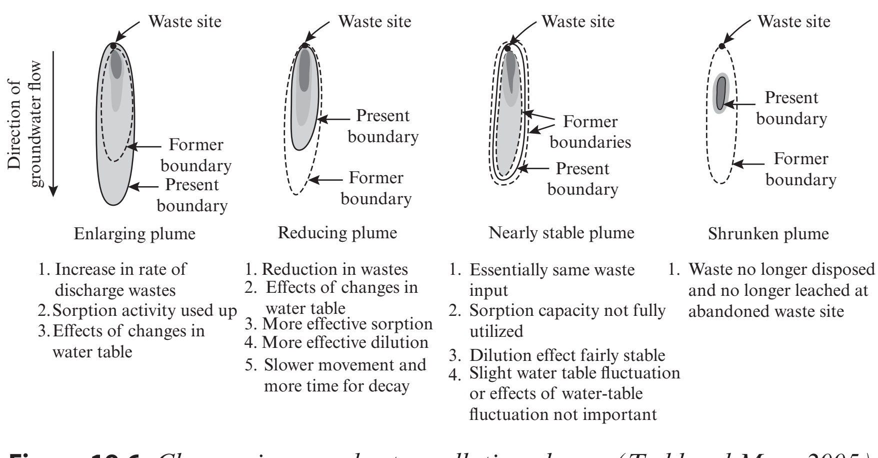

Figure 19.6 *Changes in groundwater pollution plumes (Todd and Mays 2005)*

To clean a plume by a single well, the well should be located far down gradient from the plume. This condition results in the pumping out of a large volume of clean groundwater before the contaminated plume reaches the well and consequent significant cost of pumping. To overcome this, more extraction wells may be installed closer to the head of the plume. Capture-zone type curves for a series of n optimally placed wells were derived by Javandel and Tsang (1986) by assuming each well pumping at the same rate, Q, and the wells aligned along the y-axis. The maximum optimal spacing between wells prevents any flow from passing between them. Therefore, the optimized distance between two wells is $Q/(nTi)$. Locating wells with this distance apart from each other provides the possibility of capturing a plume as wide as $Q/(Ti)$ along the y-axis and as wide as $2Q/(Ti)$ along the x-axis, i.e., far up-gradient from the wells, (see Figure 19.7). A general form for the positive half of the capture zone for n optimally spaced wells is

$$y = \frac{Q}{2Ti}\left(n - \frac{1}{\pi}\sum_{j=1}^{n}\varphi_j\right) \tag{19.9}$$

where φ_j is the angle between a horizontal line through the jth well and a spot on the capture zone curve. It is assumed in this equation that the wells have been arranged symmetrically along the y-axis.

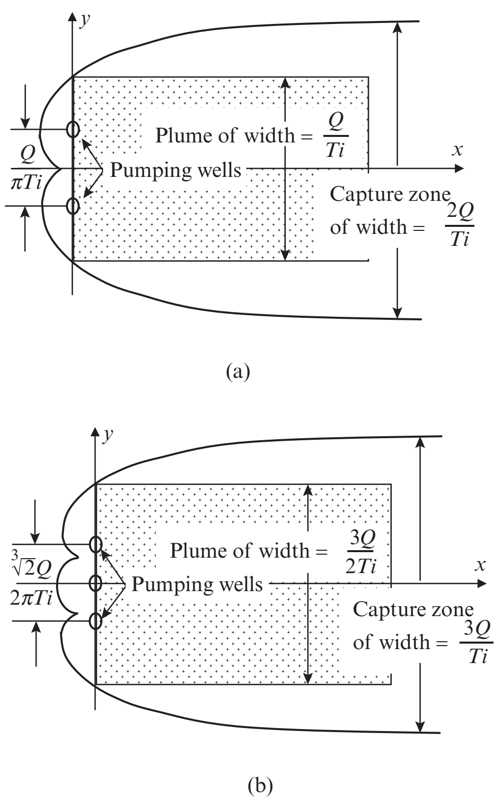

Figure 19.7 *Capture-zone curves for optimally spaced wells (a) two wells and (b) three wells*

19.7.4 Pump-and-Treat Remediation Strategies

Pump and treat is the most widely used groundwater remediation technology and is an important component of groundwater remediation efforts (USEPA, 2007). Pump-and-treat system is primarily used (USEPA, 1996) to (1) control the movement of contaminated groundwater and prevent the continued expansion of the contaminated zone (hydraulic containment) and to (2) reduce the dissolved contaminant concentrations in groundwater in a degree that complies with cleanup standards (treatment). This technology is considered as effective practices for aquifer remediation, although it cannot reduce contaminants to levels required by health-based standards. However, the pump-and-treat system, combined with in situ restoration technologies, can result in the full restoration at some sites. The following observations are made for characterizing sites for pump and treatment design (Cohen 1997):

- Nature, extent, and distribution of contaminants in source areas and downgradient plumes;
- Potential receptors and risks posed by contaminated groundwater;
- Hydrogeologic and contaminant properties that affect containment, restoration, and system design in different site areas.

Important goals for contaminant characterization data include (Cohen 1997) the following:

- Delineating contaminant source areas and release characteristics;
- Defining the nature and extent (horizontal and vertical) of contamination;
- Characterizing contaminant transport pathways, processes, and rates;
- Estimating risks associated with contaminant transport;
- Assessing aquifer restoration potential.

Conventional pump-and-treat systems extract the contaminated groundwater and treat it on the surface before discharging or reinjection. Conflicting objectives for restoration may generally include the following: (1) reducing contaminant concentrations to cleanup standards, (2) maximizing mass removal, (3) minimizing cleanup time, and (4) minimizing costs. The strategies for managing groundwater contamination using pump-and-treat technology (Cohen 1997) include (1) hydraulic/physical containment, (2) groundwater quality restoration, and (3) mixed objective strategies. The selected management strategy depends on site-specific hydrogeology and contaminant conditions, and remediation goals. Figure 19.8 illustrates NAPL and DNAPL contamination management strategies using pump-and-treat technology.

Groundwater cleanup is typically more difficult to achieve than hydraulic containment; however, for sites where the contaminative source has been removed or contained, pump-and-treat technology may be used for cleanup of a dissolved plume as shown in Figure 19.9. For better results for aquifer restoration, the pump-and-treat technology combined with hydraulic containment may be used. The design of pump-and-treat systems involves optimizing well locations, depths, and injection/extraction rates to maintain an effective hydraulic sweep through the contamination zone; minimize stagnation zones, flush pore

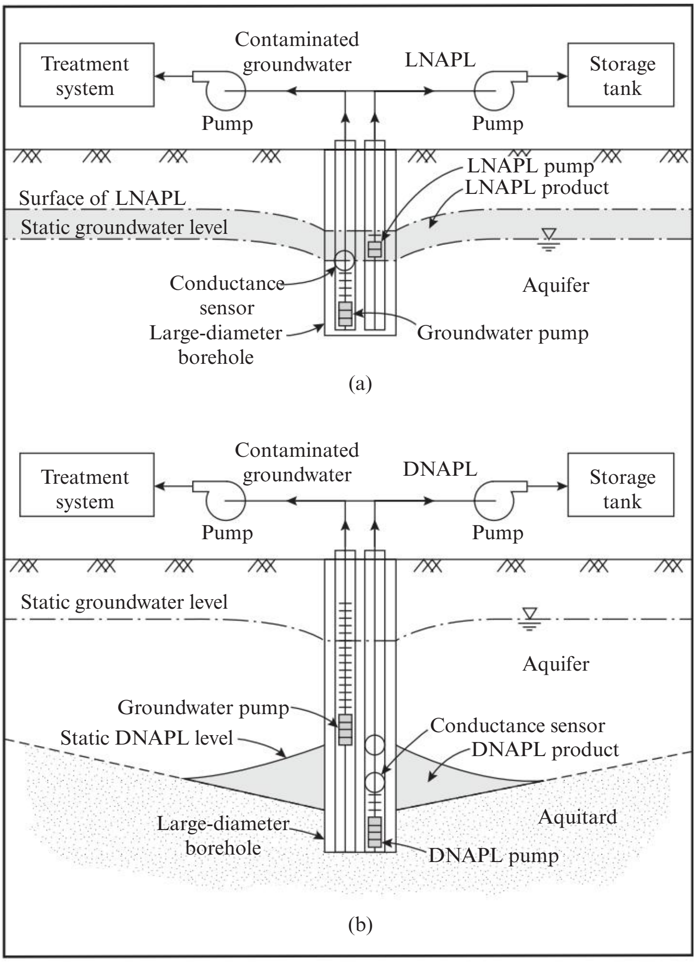

Figure 19.8 *Pump-and-treat arrangements for (a) LNAPL system and (b) DNAPL system (Todd and Mays 2005)*

volumes through the system; and contain contaminated groundwater. Figure 19.9 shows three strategies namely down-gradient pumping, source control with down-gradient pumping, and source control with mid-plume and down-gradient pumping. The down-gradient pumping results in expansion of the plume, making it more difficult to achieve cleanup. The other two strategies are more effective, with the source control clearly being important in preventing continued off-site migration. The third strategy with source control, mid-plume, and down-gradient pumping reduces the flow path and travel time of the contaminants to extraction wells and diminishes the impact of processes that cause tailing. There may be various pumping schemes to achieve the optimal cleanup. The pump-and-treat systems may be required to operate for long duration in order to clean up and contain contaminated groundwater, because of the slow contaminant transport and interphase transfer.

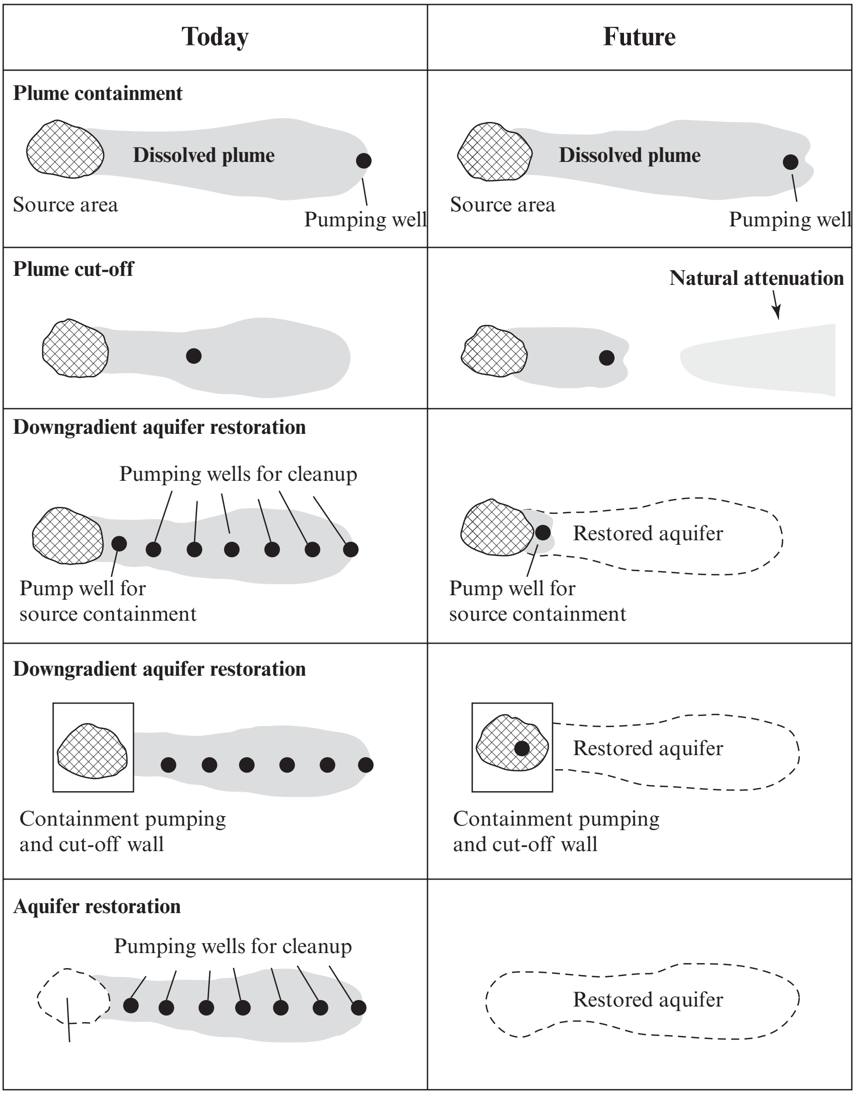

Figure 19.9 *Aquifer restoration by pump and treat systems (Todd and Mays 2005)*

19.8 Monitoring of Groundwater Quality

Availability and access to safe water and sanitation facilities are essential for health considerations. Bacterial diarrhea and epidemics of cholera and typhoid are often transmitted through drinking water. There may be chemical water quality problems. Increasing concentrations of pesticides and fertilizers in groundwater are taking place in shallow unprotected aquifers. Aquifers suspected to be polluted or the ones likely to become contaminated must be monitored. As soon as some concentrations of a pollutant are observed in the aquifer or unsaturated zone, restoration programs or reformatory actions may be set to protect the aquifer against contamination. Therefore, a system that enables detection of contaminants in water quality and its immediate remedy is must. To protect a groundwater resource against pollution, a water quality monitoring is necessary. The purpose of water quality monitoring is to define the physical, chemical, and biological characteristics of water. The ultimate goal of groundwater quality monitoring is to ensure that it is safe. Monitoring involves sampling and analyses of groundwater quality, determination of groundwater levels and flow directions, measurements of moisture in the unsaturated zone, evaluations of wastes and other materials contributing to subsurface pollution, geophysical surveys, and so on. The following are the purposes of groundwater quality monitoring (Houlihan and Lucia 1999):

- *Detection monitoring* to detect an impact to groundwater quality;
- *Assessment monitoring* to assess the nature and extent of contaminants and collect data for designing remediation;
- *Corrective action monitoring* to assess the impact of a particular remediation design; and
- *Performance monitoring* to evaluate the effectiveness of an element of a groundwater remediation system.

Monitoring is one of the most important steps of water quality management. Potential sources of contamination and the aquifers of concern should be evaluated before developing a monitoring strategy. A groundwater monitoring plan is a site-specific one. There is a need on optimal design of monitoring networks and extraction of suitable information from collected data. The restoration of contaminated groundwater is very complex and costly. Therefore, it is always desirable to prevent groundwater against becoming contaminated. In this regard, it must be determined if groundwater contamination is likely to occur in the future so that reformatory action could be taken early enough to prevent contamination from reaching the water table. For example, a groundwater monitoring system might be installed to detect leaks from the facilities when a landfill or a lagoon is constructed. The main purpose of monitoring vadose zone is to detect leaks from overlain facilities prior to the time that the contaminant reaches the water table. This way, reformatory actions could be accomplished to avoid contamination of groundwater. Sanders et al. (1987) proposed general guidelines for the establishment of a monitoring system as follows:

1. Evaluate information expectations
   - Water quality concerns
   - Information goals
   - Monitoring objectives
2. Establish statistical design criteria
   - Development of hypotheses
   - Selection of statistical methods

3. Design monitoring network
    - Where to sample
    - What to measure
    - How frequently to sample
4. Develop operation plans and procedures
    - Sampling procedures
    - Laboratory analysis procedures
    - Quality control procedures
    - Data storage and retrieval
5. Develop information reporting procedures
    - Types and liming of repol1s
    - Reporting formats
    - Distribution of information
    - Monitoring program evaluation

Identifying the information to be obtained and statistical methods for converting the data to useful information are considered in the first two steps. The third step deals with monitoring network design. Monitoring operation plans are specified in the fourth step. In the fifth step, the information related to original monitoring objectives is determined.

The strategy of well selection involves spatially distributed monitoring wells within each hydrogeological unit in an area, and such wells are located at various depths along and across flow paths in each type of lithostratigraphic units as aquifers. Water quality monitoring is to function as an early warning system and to provide information for remedial actions. Water quality monitoring can be classified under two categories: (1) background monitoring to characterize the initial stage of a system and (2) specific monitoring to deal with systems, where significant exploitation has taken place.

19.8.1 Background Monitoring

Background monitoring is a long-term effort. It commences with inventory of existing information such as land use, topography, extent, thickness, structure of the geological units, and their hydraulic properties. Based on the analysis of the data, different groundwater systems can be identified. These are defined by the occurrence and types of aquifers and aquitards, positive and negative boundaries, and aerial distribution of recharge, heads, leakage and seepage areas, flow direction, and general chemical composition. Groundwater monitoring may be based on existing observation wells only. Monitoring data should be thoroughly analyzed. Geostatistics may help to improve upon the sampling density and frequency. The analysis will bring out the general characteristics of the groundwater system in an area. The background monitoring data may be used to provide baseline information regarding spatial variations in water quality and understand potential development constraints and benefits.

19.8.2 Specific Monitoring

Based on information of the background monitoring data, the specific monitoring system is designed. The specific monitoring aims at study of hydrochemical changes affecting water use and well installation. Knowledge and understanding of well-field performance requires thorough understanding of the groundwater distribution and head changes. Consequent to abstraction, the monitoring wells network should be so designed as to provide quality changes consequent to extracting of groundwater. Based on this information, a numerical model may be developed that will act as an early warning system showing changes in groundwater quality in space and time due to the stressed imposed upon the aquifer system and providing information for necessary remedial actions.

19.8.3 Protection against Groundwater Contaminations

Elimination of contaminated groundwater is both difficult and costly proposition. The disposal and recycling of waters may alone help in reducing/minimizing the contaminants to groundwater, and therefore preventive actions take precedence over costly aquifer clean-up measures. Second, the public awareness and education as nonregulatory measures can also help decrease the contamination to groundwater. In addition, regulatory measures and safe drinking water acts help in controlling the contaminations to groundwater.

Normally, the protection plans need to be set up for groundwater monitoring network. Prerequisites to developing aquifer protection plan include: (i) preparation of aquifer sensitivity maps, (ii) groundwater-level contour maps, and (iii) length to groundwater maps. With a view to foster better groundwater management, especially quality at local and national levels, the suggestive measures may be to adopted:

- Conjunctive use of surface water and groundwater
- Rainwater harvesting and artificial recharge should be adopted for dilution of water contaminants.
- Development of deeper aquifers (uncontaminated and sustainable) and with proper well design should be taken up.
- Treatment of groundwater with quality problem and stress on R&D related to scientific and proper disposal of industrial effluents, and domestic and municipal sewages.
- Regular monitoring of groundwater quality to be carried out, especially in problematic areas.
- Public awareness programs should be organized periodically to make people and industry aware of the deterioration of quality.

19.9 Groundwater Risk and Disaster Management

Water is a renewable natural resource that cleanses and redistributes itself through natural cycles. Increasing demands for water, the fact that there is no substitute for this essential resource, and decreasing water availability due to overuse, pollution, and inefficient water management lead to water disaster worldwide in general and in developing countries in particular where the social infrastructure is not sufficient. The rapid expansion of water sectors and inadequate institutional and infrastructural setups are worsening these problems. Climate changes are also exaggerating the problem. Therefore, the need for disaster planning and management is growing fast. Disasters are described as the realization of risk. Both natural and man-made hazards and vulnerability are changing as well as our adaptive capacity due to climate change and our more interconnected complex world.

19.9.1 Groundwater Risk Assessment

Risk assessment includes the impact of groundwater pollution on human health. There are two basic elements associated with risk assessment: risk quantification/estimation and risk evaluation. In risk quantification, the hazard is defined, and the initiating events that would cause the hazard are identified. Further, the response and consequences to the receptor system is evaluated, and probabilities of occurrence are determined. Risk is the overlay and intersection of the probable hazards and vulnerabilities. Risk assessment is a process to measure and estimate the probable adverse effects of past, existing, and/or future hazards to human and ecological entities. Risk assessment can be used as a tool in evaluating the potential impacts on public health of hazardous materials in remote or disposal facilities. It may be done in the following steps (Karamouz et al., 2011):

- *Hazard identification* determines the linkage between a particular chemical to particular health effects, such as cancer or birth defects. As the availability of human data is so often scarce, this step focuses on the toxicity of a chemical in animals or other test organisms.
- *Dose-response assessment* describes the relationship between the dose of an administered or received agent and the occurrence of an adverse health effect. Some conditions such as the response characteristics of being carcinogenic or not and the experiment condition of being a one-time acute test or a long-term chronic test lead to a diversity of response relationships for any given agent. In this assessment, a method of extrapolating animal data to humans is included.
- *Exposure assessment* determines the size of the population exposed to the toxicant under consideration, the duration of the exposure, and the concentration of the toxicant. Factors such as the age and health of the subjected population, the likelihood that members of the population might be pregnant, and whether or not synergistic effects might occur due to exposure to multiple toxicants should be considered.
- *Risk characterization* contains the preceding three steps that estimate the magnitude of the public-health problem. In this step, the data collected in the previous steps are combined to generate a statement of risk. The final statement of risk can be qualitative or qualitative.

The risk could entail the hazard of the intentional contamination of a well. Even though the hazard of groundwater contamination by terrorist acts is low compared to surface water, the vulnerability is higher due to out of sight of groundwater and the widespread movement of the contaminants. It is a much slower process, but, once contaminated, it will be very difficult to capture, monitor, and remediate the long-lasting effects.

19.9.2 Environmental Risk Analysis

The following are four major approaches for environmental risk analysis (Karamouz et al., 2011):

1. *Stochastic/statistical approach*: In this approach, large amounts of data are obtained under a variety of conditions. Then, the correlations between the input of a certain material and its observed concentrations and effects are determined in various environmental compartments.
2. *Model ecosystem approach*: In this approach, a physical model of a given environmental situation is constructed. A chemical is then applied to the model. The fate and effects of the chemical are observed through the model.
3. *Deterministic approach*: A simple mathematical model is used in this approach to describe the rates of individual transformations and the transport of the chemical in the environment.
4. *Baseline chemical approach*: In this approach, transformations, transports, and effects are measured as in the deterministic approach. Then, the results are compared with data on chemicals of known degrees of risk.

19.9.3 Groundwater Risk Management

A set of policies, procedures, and practices applied to minimize disaster risks at all levels and locations is called risk management. The aim of risk management is to increase awareness, assessment, analysis, evaluation, and management measures. The framework of risk management includes legal provisions defining the responsibilities for disaster damage and long-term social impacts and losses. In risk management, administrative decisions, technical measures, and the participation of the public should protect water-supply and sanitation facilities from natural disasters. The following actions are required to be performed for risk assessment and disaster formulation (Karamouz et al., 2011):

- Risk awareness and assessment including hazard analysis and vulnerability/capacity analysis
- Knowledge development (education, training, research, and information)
- Institutional frameworks (organizational, policy, legislation, and community action)
- Application of measures such as environmental management, land use and urban planning, protection of critical facilities, application of science and technology, partnership and networking, and financial instruments
- Using early-warning systems including forecasting, public notification of warnings, and preparation measures

Thus, risk management includes preventive, organizational, and technical activities with the aim of preparing the society for disasters and decreasing their consequences. In general, in groundwater risk management, the preventive control and protection of drinking water supplies and the relevant technical devices (e.g. pumping stations) are taken into account with the aim of reducing the impact of disasters on water supply and distribution systems as much as possible.

19.9.4 Groundwater Risk Mitigation

Risk mitigation can be structural and nonstructural measures used to limit the adverse impacts of natural and technological hazards as well as environmental degradation. These measures include the following:

- Switch off polluted wells to avoid infectious diseases.
- Activate emergency water resources, such as deep wells, springs, etc.
- Provide water in mobile tanks in case of no local emergency water resources.
- Make people aware of the location of emergency water resources.
- Ration water in case of water scarcity threats.
- Take immediate actions for the restoration of the affected water supply systems after the hazard.

19.9.5 Groundwater Disaster Management

Disaster is the realization of the risk. Many regional problems are the direct result of regional climates, geography, and hydrology. Others are as a result of human activities and mismanagement. Groundwater is less vulnerable to short-term natural disasters such as floods, but it is more vulnerable toward long-term man-induced disasters such as overexploitation, gradual drawdown, and widespread contamination. Droughts and floods are natural water disasters. Drought is the deficit of water that is required to meet basic demands. Drought also causes inadequate recharge of groundwater. Floods are the result of excess runoff. Besides the quantity of water, its quality could also be the cause of a water disaster. Disaster management includes all activities, programs, and measures that can be attended to before, during, and after a disaster with main purposes of avoiding a disaster, reducing its impacts, and recovering from its losses. To effectively address disaster prevention, preparedness, emergency response, recovery and mitigation, and national and local institutional and technical capacity building are required. Institutional capacity building includes governmental authorities, the legal framework, control mechanisms, the availability of human resources and public participation, awareness, and education.

19.9.6 Disaster Indices

The most common indicators to measure the relative level of water disaster are reliability, resiliency, and vulnerability. System performance indices identify optimal situations. To assess the performance of a system, the mean and standard deviation of the outputs of the system are evaluated. To evaluate the probability of failure and system performance, reliability is one of the reasonable indices that can be used. Once failure occurs in a system, the time taken for the system to recover from the failure is described by resiliency. *Resiliency* is a measure of the persistence of systems and of their ability to absorb changes and disturbances and still maintain the same relationships between populations and state variables. It may also be defined as the speed with which a system disturbed from equilibrium recovers some proportion of its equilibrium. In general, resiliency can be considered as a tendency to stability and a resistance to perturbation. However, there is no general and overall accepted definition for resiliency. Depending on the field of application, the definition and formulation of resiliency may vary and be specialized. The distance of the failed state from the desired condition in a historical time series describes the vulnerability of the corresponding system. *Vulnerability* can be considered as the maximum distance from the desired situation, the expected value of system failure cases, or the probability of failure occurrence. The vulnerability of groundwater in general and natural terms depends on the geological setting of the groundwater system. The deeper the hydrogeological structure and the older the groundwater, the lower its vulnerability. Therefore, the deeply confined aquifers have a lower vulnerability than unconfined aquifers.

19.9.7 Drought

Droughts could be a disaster with the longest effects and intense social and environmental impacts. *Drought* is referred to as a sustained and extensive occurrence of low-flow thresholds on natural water availability. The response of groundwater systems to drought events and their performance under drought conditions is important. When drought affects groundwater systems, first groundwater recharge and later groundwater levels, and eventually groundwater discharge decreases. The characteristics of the droughts, such as duration, severity, and frequency, are changed by the groundwater system. Therefore, droughts have different impacts on the groundwater levels and discharge rather than groundwater recharge. Effective drought management depends on drought indicators and triggers. Drought indicators can be defined as variables for detecting and characterizing drought conditions. They describe the magnitude, duration, severity, and spatial extent of drought. Typical indicators are based on meteorological and hydrological variables, such as precipitation, stream flows, soil moisture, reservoir storage, and groundwater levels. When several indicators are synthesized into a single indicator on a quantitative scale, the result is called a drought index. In creating drought indices, how each indicator is combined and weighted in the index, and how an arbitrary index value relates to geophysical and statistical characteristics of drought are some challenging issues. Indicator thresholds to define and activate levels of drought responses are called drought triggers. Determining indicators and triggers and using them in a drought management plan become more challenging due to the complexity of drought. Threshold values of an indicator that identify a drought level are called drought triggers. They determine when management actions should begin and end. Triggers specify the indicator value, the time period, the spatial scale, and the drought level. Drought levels (phases, stages) are categorized as mild, moderate, and severe, extreme drought or stages 1, 2, and 3 droughts corresponding respectively to the local conditions of a drought watch, warning, or emergency.

Groundwater availability is influenced by drought in two ways: (1) recharge from precipitation on the aquifer outcrop and infiltration of surface water are reduced and (2) groundwater pumping is increased to make up for surface water supplies that are more susceptible to drought conditions. To manage district groundwater resources in droughts, the district's vulnerability to drought is evaluated and triggering criteria for specific management zones are defined. Then, drought response goals and measures are determined. Drought vulnerability maps are central to the optimum use of groundwater during drought. Regions that are more vulnerable to groundwater drought are pointed out by these maps. Some regions are more vulnerable to groundwater droughts than others.

19.9.8 Flood

Floods continue to be the most destructive natural hazard in terms of short-term damages and economic losses to a region. The main impacts of floods on groundwater systems can be summarized as follows:

- Infiltration of flood water directly into the aquifer
- Infiltration of overland flow into sewer systems and from the sewer system into the groundwater
- Increasing inflow from the recharge areas
- Transferring contaminants from the ground surface to the underlying aquifers

The aim of groundwater flood hazard maps is to indicate areas with need of protection of underground structures against groundwater flood.

19.9.9 Widespread Contamination

Groundwater contamination can occur when a source releases contaminants into the environment. Urban life, agricultural, and industrial activities pose potential hazards to groundwater quality. Harmful microorganisms often enter groundwater from leaking sewers and latrines. A wide range of pollutants including bacteria and other microorganisms, major inorganic ions, heavy metals, and a wide range of organic chemicals could contaminate groundwater. The risk of contamination is especially serious when many people or industries depend on the aquifer for their water. The vulnerability of an aquifer to different pollutants is related to the hydraulic characteristics of the aquifer and the characteristic of contaminant attenuation. The challenges facing engineers to protect groundwater include mechanisms by which pollutants enter groundwater, predictions of the transport of pollutants, and protective measures and legal enforcement issues. For protecting groundwater from contamination, it is important to develop techniques for predicting which areas are more likely than others to become contaminated as a result of human activities at the land surface. Once identified, areas prone to contamination could be subjected to certain use restrictions or targeted for greater attention. Groundwater vulnerability is a concept not a measurable property, which depends on the following:

- The travel time of infiltrating water carrying contaminants
- The proportion of contaminants that reaches groundwater
- The contaminant attenuation capacity of the geological materials through which the contaminated water travels

All of the existing aquifer vulnerability assessment methods can be grouped into three major categories: overlay and index methods, process-based methods, and statistical methods. The DRASTIC method is an experimental method, which follows the category of overlay and index methods. DRASTIC is an acronym for the thematic maps required for the model as follows:

- Depth to water table
- Recharge (aquifer)
- Aquifer media
- Soil media
- Topography
- Impact of vadose zone media
- Conductivity (hydraulic) of the aquifer

The above-listed factors are considered in DRASTIC model. The DRASTIC model defines ranges and ratings for the classes associated with each of the above thematic maps as well as weights for each thematic map. The significant media types/classes that have bearing on the vulnerability in each map are the ranges, which have associated ratings on a 1–10 scale. The relative importance of each of the above thematic maps on vulnerability is considered as its weight. Thus, the aquifer vulnerability DRASTIC model is a standardized system that evaluates groundwater pollution potential of hydrogeologic settings.

SOLVED EXAMPLES

Example 19.1: A pesticide is applied with a 5 cm water depth to an agricultural field in which the soil water content and bulk density are 0.30 and 1,600 kg/m^3, respectively. Assuming the retardation coefficient 7.0, what fraction of the total chemical may reach the groundwater? How far can the dissolved portion go downward in a day? If the water table depth is 3 m, how long does it take for the chemical to reach the water table? Assume the soil water content remains constant.

Solution: The fraction of the total chemical that may reach the groundwater = Dissolved fraction = $1/R$ = 1/7 = 0.143 = 14.3 percent. The depth to which the chemical reaches:

$D' = \dfrac{d}{\theta R} = \dfrac{5}{0.3 \times 7} = 2.38$ cm. Therefore, the time required for the pesticide to reach the water table at the depth of 3 m is $t = \dfrac{3 \times 100}{2.38} = 126$ days, that is, the chemical will reach the water table after 126 days.

Example 19.2: A pesticide (having decay factor 0.04 per day) is applied to an agricultural field at a rate of 1.25 kg/ha. This field is irrigated at a rate of 3 cm/d and the crop water use is 0.4 cm/d. Assuming soil water content remains constant at 0.3, the retardation coefficient is 5, and the water table depth is 4 m. Determine the load of dissolved pesticide that reaches to the water table.

Solution: The fraction of the total chemical that may reach the groundwater = Dissolved fraction = $1/R$ = 1/5 = 0.2 = 20 percent. Therefore, adsorbed fraction = 100 − 20 = 80 percent. Out of 3 cm/d water that is applied to the field, 0.4 cm/d is used by the crop. Therefore, the depth to which water reaches in a day is $D = \frac{d}{\theta} = \frac{3-.4}{0.3} = 8.67$ cm. Thus, the depth to which the pesticide reaches in a day is $D' = \frac{D}{R} = \frac{8.67}{5} = 1.733$ cm. Therefore, the time required for the pesticide to reach the water table at the depth of 4 m is $t = \frac{4\times 100}{1.733} = 230.77$ days. Finally, the concentration of dissolved pesticide that will remain in water when it reaches the water table is

$$C_t = C_0 e^{-kt} = 1.25\times e^{-0.04\times 230.77} = 1.22\times 10^{-4}\ \text{kg/ha}.$$

Example 19.3: A confined aquifer (thickness = 25 m, hydraulic conductivity = 1.5×10^{-3} m/s) has been contaminated in 60 m normal to the regional flow (hydraulic gradient = 0.001). To totally clean up the aquifer from the plume, determine the optimal location of pumping wells for (1) a single well pumped out at 0.003 m^3/s, (2) two wells, and (3) three wells.

Solution:

(1) Single well: The width of the capture zone along the y-axis is given by Eqn. (10.97) as $2y_{x=0} = a\pi = \frac{Q}{2Ti} = \frac{0.003}{2\times 25\times 1.5\times 10^{-3}\times 0.001} = 40\,\text{m}$. The total width of the capture zone at infinity will be 80 m. The location of the well should be some distance downgrading from the front edge to encompass the 60 m wide plume within the capture zone. Considering y = 30 m, Eqn. (19.8) yields
$$x = y\cot\left(\frac{2\pi Tiy}{-Q}\right) = 30\times\cot\left(\frac{2\pi\times 25\times 1.5\times 10^{-3}\times 0.001}{0.003}\right) = 30\,\text{m}.$$
Therefore, the single-pumping well should be placed in line with the oncoming plume and 30 m ahead of it.

(2) Two wells: Both wells are placed along y-axis, so n =2, φ_1 = π/2 and φ_2 = π/2; therefore, Eqn. (19.9) reduces for the width of the capture zone along the y-axis as $2y_{x=0} = \frac{Q}{Ti}(2-0.5-0.5) = \frac{Q}{Ti}$. The plume width

along the y-axis (also the leading edge of the plume) is 60 m, therefore $\frac{Q}{Ti} = \frac{Q}{25\times1.5\times10^{-3}\times0.001} = 60 \Rightarrow Q = 0.00225\ \text{m}^3/\text{s}$. Therefore, each well should have the pumping rate of 0.00225 m^3/s. The optimal spacing between the wells is given by $\frac{Q}{\pi Ti} = \frac{0.00225}{\pi\times25\times1.5\times10^{-3}\times0.001} = 19.1\ \text{m}$. If the length of the plume is 600 m and the aquifer porosity is 0.4, then the total volume of contaminated water within the plume = $0.4\times60\times25\times600 = 3{,}60{,}000\ \text{m}^3$. Therefore, the time to pump out the total contaminated groundwater would be $t = \frac{360000}{2\times0.00225\times3600\times24\times365} = 2.537$ year. However, it would take much longer to pump out the whole plume due to retardation and extra uncontaminated water to be removed with contaminated water.

(3) Three wells: All wells are placed along y-axis so $n = 3$, $\varphi_1 = \pi/2$, $\varphi_2 = \pi/2$, and $\varphi_3 = \pi/2$, therefore Eqn. (19.9) reduces for the width of the capture zone along the y-axis as $2y_{x=0} = \frac{Q}{Ti}(3-0.5-0.5-0.5) = \frac{3Q}{2Ti}$. The plume width along the y-axis (also the leading edge of the plume) is 60 m, therefore $\frac{3Q}{2Ti} = \frac{3Q}{2\times25\times1.5\times10^{-3}\times0.001} = 60 \Rightarrow Q = 0.0015\ \text{m}^3/\text{s}$. Therefore, each well should have the pumping rate of 0.0015 m^3/s. The optimal spacing between the wells is given by $\frac{\sqrt[3]{2}Q}{\pi Ti} = \frac{\sqrt[3]{2}\times0.0015}{\pi\times25\times1.5\times10^{-3}\times0.001} = 16\ \text{m}$. The time to pump out the total contaminated groundwater would be same, that is, $t = \frac{360000}{3\times0.0015\times3600\times24\times365} = 2.537$ year.

PROBLEMS

19.1. What are different groundwater contaminants?

19.2. How are soluble salts in groundwater critical?

19.3. Why is groundwater quality management needed?

19.4. What are different sources of groundwater contamination?

19.5. What are various methods of groundwater pollution control?

19.6. Describe and compare different techniques of treatment of contaminated aquifers?

19.7. Why is restoration of contaminated aquifer important?

19.8. What are different remediation goals and what are their advantages and disadvantages?

19.9. Describe the aquifer restoration techniques.

19.10. What is a pump and treat systems? How is contaminated aquifer restored using pump and treat systems?

19.11. What fraction of the total contaminant may reach the underlying unconfined aquifer if water table is at 1.8 m below the soil surface? Assume that the soil water content and bulk density are 0.35 and 1,540 kg/m^3, respectively. The partitioning coefficient is 0.98. In addition, determine how far the dissolved portion can go downward in a day. In addition, compute how long it takes for the contaminant to reach groundwater? Assume that the irrigation rate is 2 cm/d and crop water use is 0045 cm/d.

19.12. A chemical is applied to an agricultural field. Determine the load of the dissolved portion of the chemical that reaches groundwater if application rate of the chemical is 3.2 kg/ha, irrigation rate is 1.5 cm/d, crop water use is 0.38 cm/d, soil water content is 0040, and partitioning coefficient is 0.89.

19.13. How is monitoring important in groundwater quality management?

19.14. A confined aquifer (thickness = 35 m, hydraulic conductivity = 1,200 m/d) has been contaminated in 75 m normal to the regional flow (hydraulic gradient = 0.0008). To totally clean up the aquifer from the plume, determine the optimal location of pumping wells for (1) a single well pumped out at 2,200 m^3/d, (2) two wells, and (3) three wells.

Appendices

Appendix A: *Groundwater Resources Availability, Utilization and Stage of Development in India (CGWB 2011)*

Appendix B: *Categorization of groundwater assessment units (CGWB 2011)*

Appendix C: *Error Function, Normal distribution, complete elliptic integral, and modified Bessel's function*

Appendix D: *Theis well function W(u)*

Appendix E: *Well function for an unconfined aquifer*

Appendix F: *Hantush (1956) Well Function W(u, r/B) for a leaky aquifer*

Appendix G: *Hantush (1956) well function H(u,β) for a leaky aquifer*

Appendix H: *Papadopulos and Cooper (1967) well function* $S\left(u_w, \rho'\right)$ *for large diameter wells*

Appendix I: *Flowing well function*

Appendix J: *Chow's (1952) Function F(u)*

Appendix K: *Values for slug test type curves by Papadopulos et al (1973)*

Appendix L: *Values of Hantush (1963) recharge mound function*

$$F(\alpha,\beta) = \int_0^1 erf\left(\alpha/\sqrt{\tau}\right).erf\left(\beta/\sqrt{\tau}\right)d\tau$$

Appendix A: *Groundwater Resources Availability, Utilization and Stage of Development in India (CGWB 2011)*

Sl. No.	States/Union Territories	Annual replenishable ground water resource					Natural discharge during non–monsoon season
		Monsoon season		Non–monsoon season		Total	
		Recharge from rainfall	Recharge from other sources	Recharge from rainfall	Recharge from other sources		
1	2	3	4	5	6	7	8
	States						
1	Andhra Pradesh	15.12	6.52	5.49	6.70	33.83	3.07
2	Arunachal Pradesh	3.41	0.0003	1.04	0.0004	4.45	0.45
3	Assam	18.95	2.20	8.62	0.59	30.35	2.537
4	Bihar	18.92	3.92	3.40	2.38	28.63	2.42
5	Chhattisgarh	9.85	0.56	0.91	0.90	12.22	0.64
6	Delhi	0.11	0.10	0.02	0.08	0.31	0.02
7	Goa	0.135	0.008	0.006	0.072	0.221	0.088
8	Gujarat	12.21	2.76	0.00	3.46	18.43	1.08
9	Haryana	3.53	2.69	1.01	3.25	10.48	0.68
10	Himachal Pradesh	0.40	0.02	0.12	0.04	0.59	0.06
11	Jammu & Kashmir	1.45	1.69	0.36	0.19	3.70	0.37
12	Jharkhand	4.46	0.14	1.11	0.26	5.96	0.55
13	Karnataka	6.30	4.28	2.73	3.51	16.81	2.00
14	Kerala	4.77	0.06	0.64	1.15	6.62	0.59
15	Madhya Pradesh	27.49	1.10	0.80	4.56	33.95	1.70
16	Maharashtra	22.04	2.67	1.90	9.12	35.73	1.93
17	Manipur	0.24	0.01	0.19	0.01	0.44	0.04
18	Meghalaya	1.0191	0.0000	0.2152	0.0000	1.2343	0.1234
19	Mizoram	0.03	Negligible	0.02	Negligible	0.044	0.004
20	Nagaland	0.28	–	0.14	–	0.42	0.04
21	Orissa	11.29	2.53	1.33	2.63	17.78	1.09
22	Punjab	5.86	10.57	1.34	4.78	22.56	2.21
23	Rajasthan	8.76	0.67	0.32	2.11	11.86	1.07
24	Sikkim	–	–	–	–	–	–
25	Tamil Nadu	7.54	11.05	2.16	2.18	22.94	2.29
26	Tripura	1.66	0	0.73	0.57	2.97	0.23
27	Uttar Pradesh	40.78	11.37	5.41	17.70	75.25	6.68
28	Uttarakhand	1.26	0.24	0.20	0.46	2.17	0.10
29	West Bengal	18.17	2.16	5.43	4.74	30.50	2.92
	Total States	**246.05**	**67.32**	**45.63**	**71.45**	**430.45**	**34.99**
	Union Territories						
1	Andaman & Nicobar	0.245	–	0.065	–	0.310	0.012
2	Chandigarh	0.015	0.001	0.005	0.001	0.022	0.002
3	Dadara & Nagar Havel	0.043	0.003	0.009	0.005	0.059	0.003
4	Daman & Diu	0.010	0.001	0.000	0.002	0.012	0.001
5	Lakshdweep	–	–	–	–	0.0105	0.0070
6	Puducherry	0.086	0.056	0.008	0.022	0.171	0.017
	Total Uts	**0.40**	**0.06**	**0.09**	**0.03**	**0.59**	**0.04**
	Grand Total	**246.45**	**67.38**	**45.71**	**71.48**	**431.03**	**35.03**

Net annual ground water availability	Annual ground water draft			Projected demand for domestic and industrial uses up to 2025	Ground water availability for future irrigation use	Stage of ground water development (%)
	Irrigation	Domestic and industrial uses	Total			
9	10	11	12	13	14	15
30.76	12.61	1.54	14.15	2.69	15.89	46
4.01	0.002	0.001	0.003	0.01	4.00	0.07
27.81	5.333	0.69	6.026	0.977	21.50	22
26.21	9.79	1.56	11.36	2.56	13.85	43
11.58	3.08	0.52	3.60	0.64	7.85	31
0.29	0.14	0.26	0.40	0.26	0.01	138
0.133	0.014	0.030	0.044	0.037	0.082	33
17.35	11.93	1.05	12.99	1.47	5.32	75
9.80	11.71	0.72	12.43	0.79	–2.70	127
0.53	0.23	0.08	0.31	0.08	0.22	58
3.33	0.15	0.58	0.73	0.82	2.35	22
5.41	1.17	0.44	1.61	0.62	3.62	30
14.81	9.01	1.00	10.01	1.26	6.18	68
6.03	1.30	1.50	2.81	1.71	3.02	47
32.25	16.66	1.33	17.99	1.83	13.76	56
33.81	15.91	1.04	16.95	2.00	16.32	50
0.40	0.0033	0.0007	0.0040	0.05	0.35	1
1.1109	0.0015	0.0002	0.0017	0.0964	1.0131	0.15
0.039	0.000	0.0004	0.0004	0.0008	0.039	1
0.38	–	0.008	0.008	0.01	0.36	2.14
16.69	3.47	0.89	4.36	1.27	11.94	26
20.35	33.97	0.69	34.66	0.95	–14.57	170
10.79	12.86	1.65	14.52	1.84	0.75	135
0.046	0.003	0.007	0.010	0.012	0.031	21
20.65	14.71	1.85	16.56	1.97	4.70	80
0.09	0.07	0.16	0.23	2.42	6	
46.00	3.49	49.48	5.36	17.22	72	
2.07	1.01	0.03	1.05	0.08	0.98	51
27.58	10.11	0.79	10.91	1.02	16.75	40
395.52	**221.29**	**21.83**	**243.14**	**30.65**	**153.26**	**61**
0.298	0.0006	0.010	0.011	0.015	0.283	4
0.020	0.000	0.000	0.000	0.000	0.020	0.000
0.056	0.001	0.007	0.009	0.009	0.047	15
0.011	0.008	0.003	0.011	0.004	–0.001	99
0.0035	0.0000	0.0026	0.0026	0.0000	0.0000	74
0.154	0.121	0.029	0.150	0.032	0.050	98
0.54	**0.13**	**0.05**	**0.18**	**0.06**	**0.40**	**34**
396.06	**221.42**	**21.89**	**243.32**	**30.71**	**153.66**	**61**

Appendix B: *Categorization of groundwater assessment units (CGWB 2011)*

Sl.No.	States/Union Territories	Total No. of assessed units	Safe		Semi–critical		
			Nos.	%	Nos.	%	
	States						
1	Andhra Pradesh	1108	867	78	93	8	
2	Arunachal Pradesh	16	16	100	0	0	
3	Assam	23	23	100	0	0	
4	Bihar	533	529	99	4	1	
5	Chhattisgarh	146	132	90	14	10	
6	Delhi	27	2	7	5	19	
7	Goa	11	11	100	0	0	
8	Gujarat	223	156	70	20	9	
9	Haryana	116	18	16	9	8	
10	Himachal Pradesh	8	6	75	0	0	
11	Jammu & Kashmir	14	14	100	0	0	
12	Jharkhand	208	200	96	2	1	
13	Karnataka	270	154	57	34	13	
14	Kerala	152	126	83	22	14	
15	Madhya Pradesh	313	224	72	61	19	
16	Maharashtra	353	324	92	19	5	
17	Manipur	8	8	100	0	0	
18	Meghalaya	7	7	100	0	0	
19	Mizoram	22	22	100	0	0	
20	Nagaland	8	8	100	0	0	
21	Orissa	314	308	98	0	0	
22	Punjab	138	23	17	2	1	
23	Rajasthan	239	31	13	16	7	
24	Sikkim	4	4	100	0	0	
25	Tamil Nadu	386	136	35	67	17	
26	Tripura	39	39	100	0	0	
27	Uttar Pradesh	820	605	74	107	13	
28	Uttarakhand	17	11	65	5	29	
29	West Bengal	269	231	86	38	14	
	Total States	**5792**	**4235**	**73**	**518**	**9**	
	Union Territories						
1	Andaman & Nicobar	33	33	100	0	0	
2	Chandigarh	1	1	100	0	0	
3	Dadra & Nagar Haveli	1	1	100	–	–	
4	Daman & Diu	2	0	0	1	50	
5	Lakshdweep	9	5	56	4	44	
6	Puducherry	4	2	50	0	0	
	Total Union Territories	**50**	**42**	**84**	**5**	**10**	
	Grand Total	**5842**	**4277**	**73**	**523**	**9**	

	Critical		*Over–exploited*		*Remarks*
	Nos.	*%*	*Nos.*	*%*	
	26	2	84	8	38 – salinity affected
	0	0	0	0	
	0	0	0	0	
	0	0	0	0	
	0	0	0	0	
	0	0	20	74	
	0	0	0	0	
	6	3	27	12	14 – salinity affected
	21	18	68	59	
	1	13	1	13	
	0	0	0	0	
	2	1	4	2	
	11	4	71	26	
	3	2	1	1	
	4	1	24	8	
	1	0	9	3	
	0	0	0	0	
	0	0	0	0	
	0	0	0	0	
	0	0	0	0	
	0	0	0	0	6 – salinity affected
	3	2	110	80	
	25	10	166	69	1 – salinity affected
	0	0	0	0	
	33	9	139	36	11 – salinity affected
	0	0	0	0	
	32	4	76	9	
	1	6	0	0	
	0	0	0	0	
	169	**3**	**800**	**14**	
	0	0	0	0	
	0	0	0	0	
	–	–	–	–	–
	0	0	1	50	
	0	0	0	0	
	0	0	1	25	1 – salinity affected
	0	**0**	**2**	**4**	
	169	**3**	**802**	**14**	**71 – salinity affected**

Appendix C : *Error Function, Normal distribution, complete elliptic integral, and modified Bessel's function*

x	e^x	$erf(x)$	$erfc(x)$	$Z_N(x)$	$P^1_N(x)$	$\Gamma(x)$	$i^2.erfc(x)$	$K(x)$	$K_0(x)$
0.00	1	0	1	0.39894	0	∞	0.25	π/2	∞
0.001	1.00100	0.00113	0.99887	0.39894	0.00040	9.994E2	0.24944	1.57080	7.02369
0.01	1.01005	0.01128	0.98872	0.39892	0.00399	9.943E1	0.24441	1.57080	4.72124
0.02	1.02020	0.02256	0.97744	0.39886	0.00798	4.944E1	0.23891	1.57100	4.02846
0.03	1.03045	0.03384	0.96616	0.39876	0.01197	3.278E1	0.23352	1.57110	3.62353
0.04	1.04081	0.04511	0.95489	0.39862	0.01595	2.446E1	0.22822	1.57140	3.33654
0.05	1.05127	0.05637	0.94363	0.39844	0.01994	1.947E1	0.22302	1.57180	3.11423
0.06	1.06184	0.06762	0.93238	0.39822	0.02392	1.614E1	0.21791	1.57220	2.93288
0.07	1.07251	0.07886	0.92114	0.39797	0.02790	1.377E1	0.21289	1.57270	2.77982
0.08	1.08329	0.09008	0.90992	0.39767	0.03188	1.200E1	0.20797	1.57330	2.64749
0.09	1.09417	0.10128	0.89872	0.39733	0.03586	1.062E1	0.20314	1.57400	2.53102
0.10	1.10517	0.11246	0.88754	0.39695	0.03983	9.51351	0.19839	1.57470	2.42707
0.11	1.11628	0.12362	0.87638	0.39654	0.04380	8.61269	0.19374	1.57560	2.33327
0.12	1.12750	0.13476	0.86524	0.39608	0.04776	7.86325	0.18917	1.57650	2.24786
0.13	1.13883	0.14587	0.85413	0.39559	0.05172	7.23024	0.18469	1.57750	2.16950
0.14	1.15027	0.15695	0.84305	0.39505	0.05567	6.68869	0.18030	1.57860	2.09717
0.15	1.16183	0.16800	0.83200	0.39448	0.05962	6.22027	0.17599	1.57970	2.03003
0.16	1.17351	0.17901	0.82099	0.39387	0.06356	5.81127	0.17176	1.58100	1.96742
0.17	1.18530	0.18999	0.81001	0.39322	0.06749	5.45117	0.16762	1.58230	1.90880
0.18	1.19722	0.20094	0.79906	0.39253	0.07142	5.13182	0.16355	1.58380	1.85371
0.19	1.20925	0.21184	0.78816	0.39181	0.07535	4.84676	0.15957	1.58530	1.80179
0.20	1.22140	0.22270	0.77730	0.39104	0.07926	4.59084	0.15566	1.58690	1.75270
0.21	1.23368	0.23352	0.76648	0.39024	0.08317	4.35989	0.15184	1.58860	1.70619
0.22	1.24608	0.24430	0.75570	0.38940	0.08706	4.15048	0.14809	1.59030	1.66200
0.23	1.25860	0.25502	0.74498	0.38853	0.09095	3.95980	0.14441	1.59220	1.61994
0.24	1.27125	0.26570	0.73430	0.38762	0.09483	3.78550	0.14081	1.59420	1.57983
0.25	1.28403	0.27633	0.72367	0.38667	0.09871	3.62561	0.13728	1.59620	1.54151
0.26	1.29693	0.28690	0.71310	0.38568	0.10257	3.47845	0.13383	1.59840	1.50484
0.27	1.30996	0.29742	0.70258	0.38466	0.10642	3.34260	0.13044	1.60070	1.46971
0.28	1.32313	0.30788	0.69212	0.38361	0.11026	3.21685	0.12713	1.60300	1.43600
0.29	1.33643	0.31828	0.68172	0.38251	0.11409	3.10014	0.12389	1.60550	1.40361
0.30	1.34986	0.32863	0.67137	0.38139	0.11791	2.99157	0.12071	1.60800	1.37246
0.31	1.36343	0.33891	0.66109	0.38023	0.12172	2.89034	0.11760	1.61070	1.34247
0.32	1.37713	0.34913	0.65087	0.37903	0.12552	2.79575	0.11456	1.61350	1.31356
0.33	1.39097	0.35928	0.64072	0.37780	0.12930	2.70721	0.11158	1.61640	1.28567
0.34	1.40495	0.36936	0.63064	0.37654	0.13307	2.62416	0.10867	1.61940	1.25873
0.35	1.41907	0.37938	0.62062	0.37524	0.13683	2.54615	0.10582	1.62250	1.23271
0.36	1.43333	0.38933	0.61067	0.37391	0.14058	2.47273	0.10303	1.62580	1.20754
0.37	1.44773	0.39921	0.60079	0.37255	0.14431	2.40355	0.10030	1.62910	1.18317
0.38	1.46228	0.40901	0.59099	0.37115	0.14803	2.33826	0.09763	1.63260	1.15958
0.39	1.47698	0.41874	0.58126	0.36973	0.15173	2.27655	0.09503	1.63620	1.13671
0.40	1.49182	0.42839	0.57161	0.36827	0.15542	2.21816	0.09248	1.64000	1.11453

(*Continued*)

Appendix C : (Continued)

x	e^x	$erf(x)$	$erfc(x)$	$Z_N(x)$	$P^1_N(x)$	$\Gamma(x)$	$i^2.erfc(x)$	$K(x)$	$K_0(x)$
0.41	1.50682	0.43797	0.56203	0.36678	0.15910	2.16284	0.08998	1.64390	1.09301
0.42	1.52196	0.44747	0.55253	0.36526	0.16276	2.11037	0.08755	1.64790	1.07212
0.43	1.53726	0.45689	0.54311	0.36371	0.16640	2.06055	0.08517	1.65210	1.05182
0.44	1.55271	0.46623	0.53377	0.36213	0.17003	2.01319	0.08284	1.65640	1.03209
0.45	1.56831	0.47548	0.52452	0.36053	0.17364	1.96814	0.08056	1.66090	1.01291
0.46	1.58407	0.48466	0.51534	0.35889	0.17724	1.92523	0.07834	1.66550	0.99426
0.47	1.59999	0.49375	0.50625	0.35723	0.18082	1.88433	0.07617	1.67030	0.97610
0.48	1.61607	0.50275	0.49725	0.35553	0.18439	1.84531	0.07405	1.67530	0.95842
0.49	1.63232	0.51167	0.48833	0.35381	0.18793	1.80805	0.07199	1.68040	0.94120
0.50	1.64872	0.52050	0.47950	0.35207	0.19146	1.77245	0.06996	1.68580	0.92442
0.51	1.66529	0.52924	0.47076	0.35029	0.19497	1.73842	0.06799	1.69130	0.90806
0.52	1.68203	0.53790	0.46210	0.34849	0.19847	1.70584	0.06607	1.69700	0.89212
0.53	1.69893	0.54646	0.45354	0.34667	0.20194	1.67466	0.06419	1.70290	0.87656
0.54	1.71601	0.55494	0.44506	0.34482	0.20540	1.64477	0.06235	1.70900	0.86138
0.55	1.73325	0.56332	0.43668	0.34294	0.20884	1.61612	0.06056	1.71540	0.84657
0.56	1.75067	0.57162	0.42838	0.34105	0.21226	1.58864	0.05882	1.72190	0.83210
0.57	1.76827	0.57982	0.42018	0.33912	0.21566	1.56226	0.05712	1.72870	0.81798
0.58	1.78604	0.58792	0.41208	0.33718	0.21904	1.53693	0.05545	1.73580	0.80418
0.59	1.80399	0.59594	0.40406	0.33521	0.22240	1.51259	0.05383	1.74310	0.79070
0.60	1.82212	0.60386	0.39614	0.33322	0.22575	1.48919	0.05226	1.75080	0.77752
0.61	1.84043	0.61168	0.38832	0.33121	0.22907	1.46669	0.05072	1.75870	0.76464
0.62	1.85893	0.61941	0.38059	0.32918	0.23237	1.44504	0.04921	1.76690	0.75204
0.63	1.87761	0.62705	0.37295	0.32713	0.23565	1.42420	0.04775	1.77540	0.73972
0.64	1.89648	0.63459	0.36541	0.32506	0.23891	1.40413	0.04633	1.78420	0.72767
0.65	1.91554	0.64203	0.35797	0.32297	0.24215	1.38480	0.04494	1.79350	0.71587
0.66	1.93479	0.64938	0.35062	0.32086	0.24537	1.36616	0.04358	1.80300	0.70433
0.67	1.95424	0.65663	0.34337	0.31874	0.24857	1.34820	0.04227	1.81300	0.69303
0.68	1.97388	0.66378	0.33622	0.31659	0.25175	1.33088	0.04098	1.82350	0.68197
0.69	1.99372	0.67084	0.32916	0.31443	0.25490	1.31418	0.03973	1.83430	0.67113
0.70	2.01375	0.67780	0.32220	0.31225	0.25804	1.29806	0.03852	1.84570	0.66052
0.71	2.03399	0.68467	0.31533	0.31006	0.26115	1.28250	0.03733	1.85760	0.65012
0.72	2.05443	0.69143	0.30857	0.30785	0.26424	1.26747	0.03618	1.87000	0.63994
0.73	2.07508	0.69810	0.30190	0.30563	0.26730	1.25297	0.03505	1.88300	0.62996
0.74	2.09594	0.70468	0.29532	0.30339	0.27035	1.23895	0.03396	1.89670	0.62017
0.75	2.11700	0.71116	0.28884	0.30114	0.27337	1.22542	0.03290	1.91100	0.61058
0.76	2.13828	0.71754	0.28246	0.29887	0.27637	1.21234	0.03187	1.92610	0.60118
0.77	2.15977	0.72382	0.27618	0.29659	0.27935	1.19969	0.03086	1.94200	0.59196
0.78	2.18147	0.73001	0.26999	0.29431	0.28230	1.18747	0.02988	1.95870	0.58292
0.79	2.20340	0.73610	0.26390	0.29200	0.28524	1.17566	0.02893	1.97650	0.57405
0.80	2.22554	0.74210	0.25790	0.28969	0.28814	1.16423	0.02801	1.99530	0.56535
0.81	2.24791	0.74800	0.25200	0.28737	0.29103	1.15318	0.02711	2.01530	0.55681
0.82	2.27050	0.75381	0.24619	0.28504	0.29389	1.14249	0.02623	2.03660	0.54843
0.83	2.29332	0.75952	0.24048	0.28269	0.29673	1.13216	0.02538	2.05930	0.54021
0.84	2.31637	0.76514	0.23486	0.28034	0.29955	1.12216	0.02456	2.08370	0.53215

(*Continued*)

Appendix C : (Continued)

x	e^x	$erf(x)$	$erfc(x)$	$Z_N(x)$	$P^1_N(x)$	$\Gamma(x)$	$i^2.erfc(x)$	$K(x)$	$K_0(x)$
0.85	2.33965	0.77067	0.22933	0.27798	0.30234	1.11248	0.02376	2.10990	0.52423
0.86	2.36316	0.77610	0.22390	0.27562	0.30511	1.10312	0.02298	2.13830	0.51645
0.87	2.38691	0.78144	0.21856	0.27324	0.30785	1.09407	0.02222	2.16910	0.50882
0.88	2.41090	0.78669	0.21331	0.27086	0.31057	1.08531	0.02149	2.20270	0.50132
0.89	2.43513	0.79184	0.20816	0.26848	0.31327	1.07683	0.02077	2.23960	0.49396
0.90	2.45960	0.79691	0.20309	0.26609	0.31594	1.06863	0.02008	2.28050	0.48673
0.91	2.48432	0.80188	0.19812	0.26369	0.31859	1.06069	0.01941	2.32630	0.47963
0.92	2.50929	0.80677	0.19323	0.26129	0.32121	1.05302	0.01876	2.37810	0.47265
0.93	2.53451	0.81156	0.18844	0.25888	0.32381	1.04559	0.01813	2.43750	0.46580
0.94	2.55998	0.81627	0.18373	0.25647	0.32639	1.03840	0.01751	2.50690	0.45906
0.95	2.58571	0.82089	0.17911	0.25406	0.32894	1.03145	0.01692	2.59000	0.45245
0.96	2.61170	0.82542	0.17458	0.25164	0.33147	1.02473	0.01634	2.69310	0.44594
0.97	2.63794	0.82987	0.17013	0.24923	0.33398	1.01823	0.01578	2.82800	0.43955
0.98	2.66446	0.83423	0.16577	0.24681	0.33646	1.01195	0.01523	3.02100	0.43327
0.99	2.69123	0.83851	0.16149	0.24439	0.33891	1.00587	0.01471	3.35660	0.42710
0.992	2.69662	0.83935	0.16065	0.24391	0.33940	1.00468	0.01460	3.46570	0.42587
0.994	2.70202	0.84020	0.15980	0.24342	0.33989	1.00350	0.01450	3.60700	0.42465
0.996	2.70743	0.84103	0.15897	0.24294	0.34037	1.00232	0.01440	3.80710	0.42344
0.998	2.71285	0.84187	0.15813	0.24245	0.34086	1.00116	0.01430	4.15070	0.42223
0.999	2.71556	0.84229	0.15771	0.24221	0.34110	1.00058	0.01425	4.49560	0.42163
1.00	2.71828	0.84270	0.15730	0.24197	0.34134	1.00000	0.01420	8	0.42102
1.01	2.74560	0.84681	0.15319	0.23955	0.34375	0.99433	0.01370		0.41506
1.02	2.77319	0.85084	0.14916	0.23713	0.34614	0.98884	0.01322		0.40919
1.04	2.82922	0.85865	0.14135	0.23230	0.35083	0.97844	0.01231		0.39774
1.06	2.88637	0.86614	0.13386	0.22747	0.35543	0.96874	0.01145		0.38667
1.08	2.94468	0.87333	0.12667	0.22265	0.35993	0.95973	0.01065		0.37597
1.10	3.00417	0.88021	0.11979	0.21785	0.36433	0.95135	0.00989		0.36560
1.15	3.15819	0.89612	0.10388	0.20594	0.37493	0.93304	0.00821		0.34112
1.20	3.32012	0.91031	0.08969	0.19419	0.38493	0.91817	0.00679		0.31851
1.25	3.49034	0.92290	0.07710	0.18265	0.39435	0.90640	0.00560		0.29760
1.30	3.66930	0.93401	0.06599	0.17137	0.40320	0.89747	0.00459		0.27825
1.35	3.85743	0.94376	0.05624	0.16038	0.41149	0.89115	0.00376		0.26031
1.40	4.05520	0.95229	0.04771	0.14973	0.41924	0.88726	0.00306		0.24366
1.45	4.26311	0.95970	0.04030	0.13943	0.42647	0.88566	0.00248		0.22819
1.50	4.48169	0.96611	0.03389	0.12952	0.43319	0.88623	0.00201		0.21381
1.55	4.71147	0.97162	0.02838	0.12001	0.43943	0.88887	0.00162		0.20042
1.60	4.95303	0.97635	0.02365	0.11092	0.44520	0.89352	0.00130		0.18795
1.70	5.47395	0.98379	0.01621	0.09405	0.45543	0.90864	0.00082		0.16550
1.80	6.04965	0.98909	0.01091	0.07895	0.46407	0.93138	0.00051		0.14593
1.90	6.68589	0.99279	0.00721	0.06562	0.47128	0.96177	0.00032		0.12885
2.00	7.38906	0.99532	0.00468	0.05399	0.47725	1	0.00019		0.11389
3.00	2.009E1	0.99998	2.2E−5	0.00443	0.49865	2	4.9E−07		0.03474
4.00	5.460E1	1	1.54E−8	0.00013	0.49997	6	2.1E−10		0.01116
5.00	1.484E2	1	1.5E−12	0.00000	0.50000	24	1.4E−14		0.00369
∞	∞	1	0	0	0.5	∞	0		0

Note:

$\text{erf}(x) = \frac{2}{\sqrt{\pi}}\int_0^x e^{-\tau^2}\,d\tau$; $\text{erfc}(x) = \frac{2}{\sqrt{\pi}}\int_x^\infty e^{-\tau^2}\,d\tau$; erfc($x$) =1 –erf($x$); erf(–$x$) = –erf($x$); erfc(–$x$) = 2 –erfc($x$) = 1+ erf($x$); $\text{erf}(-\infty) = 2$; for x< 0.1, $\text{erf}(x) \approx \frac{2x}{\sqrt{\pi}}$; for x> 9, $\text{erfc}(\sqrt{x})e^x \approx \frac{1}{\sqrt{\pi x}}$; $\int_0^\infty \text{erfc}(\tau)\,d\tau = \frac{1}{\sqrt{\pi}}$; $i^n.\text{erfc}(x) = \int_x^\infty i^{n-1}.\text{erfc}(\tau)\,d\tau$; $i^{-1}.\text{erfc}(x) = \frac{2}{\sqrt{\pi}}e^{-x^2}$; $i^0.\text{erfc}(x) = \text{erfc}(x)$; $i^1.\text{erfc}(x) = \frac{1}{\sqrt{\pi}}e^{-x^2} - x.\text{erfc}(x)$; $i^2.\text{erfc}(x) = \frac{1}{4}\left(\text{erfc}(x) - 2x.i^1.\text{erfc}(x)\right)$; $i^n\,\text{erfc}(0) = 1/\left[2\Gamma(1+n/2)\right]$; $2ni^n$ erfc $(x) = i^{n-2}\,\text{erfc}(x) - 2xi^{n-1}\,\text{erfc}(x)$; $\int_{-a}^{a}\text{erf}(\tau)\,d\tau = 0$; $\int_{-a}^{a}\text{erfc}(\tau)\,d\tau = 2a$; Also $y = i^n$. $\text{erfc}(x)$ is the solution of the differential equation $\frac{d^2y}{dx^2} + 2x\frac{dy}{dx} - 2ny = 0$.

Standard normal distribution function $\text{P}_N(x) = \frac{1}{\sqrt{2}}\int_{-\infty}^{x} e^{-\tau^2/2}d\tau = \frac{1}{2} + \frac{1}{\sqrt{2}}\int_0^x e^{-\tau^2/2}d\tau = \frac{1}{2} + P_N'(x)$ gives probability of a variate with mean 0 and standard deviation 1, where $P_N'(x) = \frac{1}{\sqrt{2}}\int_0^x e^{-\tau^2/2}d\tau$ $\quad \text{P}_N(x) = \frac{1}{2}\left[1 + \text{erf}\left(x/\sqrt{2}\right)\right]$ and corresponding probability density function is $\text{Z}_N(x) = \frac{1}{\sqrt{2}}e^{-x^2/2}$. Standard normal distribution is symmetric about x = 0, so $\text{Z}_N(-x) = \text{Z}_N(x)$; $\text{P}_N(-x) = 1 - \text{P}_N(x)$ and $P_N'(-x) = -P_N'(x)$. Thus $\text{Z}_N(x)$ is the ordinate of the standard normal curve at x, and $\text{P}_N(x)$ and $P_N'(x)$ are the area under the standard normal curve from -∞ to x, and 0 to x respectively.

$\Gamma(x) = \int_0^\infty e^{x-1}e^{-\tau}d\tau$ = Gamma function, where $\Gamma(x+1) = x\Gamma(x)$;
$\Gamma(x).\Gamma(1-x) = \frac{\pi}{\sin \pi x}$; $2^{2x-1}\Gamma(x).\Gamma\left(x + \frac{1}{2}\right) = \sqrt{\pi}.\Gamma(2x)$; and $\Gamma(1/2) = \sqrt{\pi}$

$K_0(x)$ = modified Bessel function of the zero order and second kind.

$K(x)$ = complete elliptical integral of the first kind = $\int_0^{\pi/2}\frac{d\tau}{\sqrt{1 - x.\sin^2\tau}}$

Appendix D : *Theis well function $W(u)$*

$n\rightarrow$ $m\downarrow$	10^{-15}	10^{-14}	10^{-13}	10^{-12}	10^{-11}	10^{-10}	10^{-9}	10^{-8}	10^{-7}	10^{-6}	10^{-5}	10^{-4}	10^{-3}	10^{-2}	10^{-1}	1
1.0	33.962	31.659	29.356	27.054	24.751	22.449	20.146	17.844	15.541	13.238	10.936	8.6332	6.3315	4.0379	1.8229	2.19E–1
1.5	33.556	31.254	28.951	26.648	24.346	22.449	19.741	17.438	15.135	12.833	10.530	8.2278	5.9266	3.6374	1.4645	1.00E–1
2.0	33.268	30.966	28.663	26.361	24.058	22.043	19.453	17.150	14.848	12.545	10.243	7.9402	5.6394	3.3547	1.2227	4.89E–2
2.5	33.045	30.743	28.440	26.138	23.835	21.756	19.230	16.927	14.625	12.322	10.019	7.7172	5.4167	3.1365	1.0443	2.49E–2
3.0	32.863	30.560	28.258	25.955	23.653	21.532	19.047	16.745	14.442	12.140	9.8371	7.5348	5.2349	2.9591	0.9057	1.31E–2
3.5	32.709	30.406	28.104	25.801	23.499	21.350	18.893	16.591	14.288	11.986	9.6830	7.3807	5.0813	2.8099	0.7942	6.97E–3
4.0	32.575	30.273	27.970	25.668	23.365	21.196	18.760	16.457	14.155	11.852	9.5495	7.2472	4.9482	2.6813	0.7024	3.78E–3
4.5	32.458	30.155	27.852	25.550	23.247	21.062	18.642	16.339	14.037	11.734	9.4317	7.1295	4.8310	2.5684	0.6253	2.07E–3
5.0	32.352	30.050	27.747	25.444	23.142	20.945	18.537	16.234	13.931	11.628	9.3263	7.0242	4.7261	2.4679	0.5598	1.15E–3
5.5	32.257	29.954	27.652	25.349	23.047	20.839	18.441	16.139	13.836	11.533	9.2310	6.9289	4.6313	2.3775	0.5034	6.41E–4
6.0	32.170	29.867	27.565	25.262	22.960	20.744	18.354	16.052	13.149	11.447	9.1440	6.8420	4.5448	2.2953	0.4544	3.60E–4
6.5	32.090	79.787	27.485	25.182	22.879	20.657	18.274	15.972	13.669	11.367	9.0640	6.7620	4.4652	2.2201	0.4115	2.03E–4
7.0	32.016	29.713	27.411	25.108	22.805	20.503	18.200	15.898	13.595	11.292	8.9899	6.6879	4.3916	2.1508	0.3738	1.16E–4
7.5	31.947	29.644	27.342	25.039	22.736	20.434	18.131	15.828	13.526	11.223	8.9209	6.6190	4.3231	2.0867	0.3403	6.58E–5
8.0	31.882	29.580	27.277	24.974	22.672	20.369	18.067	15.764	13.461	11.159	8.8563	6.5545	4.2591	2.0269	0.3106	3.76E–5
8.5	31.822	29.519	27.216	24.914	22.611	20.309	18.006	5.703	13.401	11.098	8.7957	6.4939	4.1990	1.9711	0.2840	2.16E–5
9.0	31.764	29.462	27.159	24.857	22.554	20.251	17.949	15.646	13.344	11.041	8.7386	6.4368	4.1423	1.9187	0.2602	1.24E–5
9.5	31.710	29.408	27.105	24.802	22.500	20.197	17.895	15.592	13.290	10.987	8.6845	6.3828	4.0887	1.8695	0.2387	7.10E–6
10	31.659	29.356	27.054	24.751	22.449	20.146	17.844	15.541	13.238	10.936	8.6332	6.3315	4.0379	1.8229	0.2194	1.00E–6

Note: $u = m \times n$

Appendix E: *Well function for an unconfined aquifer*

(a) Boulton's (1954) well function $V(\tau, \rho)$ for an unconfined aquifer

		10^{-3}									10^{-2}									
	$\tau \backslash \rho$	1	2	3	4	5	6	7	8	9	1	2	3	4	5	6	7	8	9	10
10^{-2}	1	2.99	2.30	1.90	1.64	1.42	1.28	1.15	1.04	0.950	0.875	0.474	0.322	0.240	0.192	0.158	0.135	0.118	0.104	0.093
	2	3.68	2.97	2.58	2.30	2.09	1.92	1.76	1.64	1.52	1.42	0.860	0.610	0.468	0.378	0.316	0.270	0.236	0.210	0.187
	3	4.08	3.40	3.00	2.70	2.46	2.28	2.13	2.00	1.88	1.79	1.18	0.860	0.675	0.555	0.465	0.400	0.350	0.310	0.278
	4	4.35	3.68	3.26	2.98	2.75	2.58	2.42	2.29	2.17	2.06	1.42	1.07	0.850	0.710	0.600	0.525	0.460	0.410	0.368
	5	4.58	3.90	3.49	3.20	2.96	2.79	2.64	2.50	2.38	2.28	1.60	1.24	1.010	0.850	0.725	0.630	0.560	0.500	0.450
	6	4.76	4.06	3.65	3.36	3.15	2.96	2.80	2.68	2.56	2.45	1.78	1.40	1.15	0.970	0.840	0.735	0.650	0.585	0.530
	7	4.92	4.20	3.80	3.51	3.30	3.12	2.96	2.82	2.70	2.60	1.91	1.54	1.28	1.09	0.950	0.835	0.740	0.670	0.610
	8	5.08	4.34	3.94	3.65	3.42	3.24	3.09	2.95	2.84	2.72	2.04	1.65	1.39	1.20	1.04	0.925	0.825	0.750	0.680
	9	5.18	4.47	4.05	3.75	3.54	3.35	3.20	3.05	2.95	2.84	2.14	1.75	1.50	1.29	1.14	1.02	0.910	0.825	0.750
10^{-1}	1	5.24	4.54	4.14	3.85	3.63	3.45	3.30	3.15	3.04	2.94	2.25	1.85	1.58	1.38	1.22	1.09	0.985	0.890	0.815
	2	5.85	5.15	4.78	4.50	4.28	4.10	3.93	3.80	3.66	3.56	2.87	2.46	2.20	1.98	1.80	1.65	1.52	1.42	1.32
	3	6.24	5.50	5.12	4.85	4.61	4.43	4.28	4.14	4.01	3.90	3.24	2.84	2.54	2.32	2.14	1.98	1.85	1.74	1.64
	4	6.45	5.75	5.35	5.08	4.85	4.67	4.50	4.38	4.26	4.15	3.46	3.05	2.76	2.54	2.36	2.20	2.07	1.96	1.86
	5	6.65	6.00	5.58	5.25	5.00	4.85	4.70	4.55	4.45	4.30	3.65	3.24	2.95	2.72	2.52	2.38	2.24	2.14	2.03
	6	6.75	6.10	5.65	5.40	5.15	4.98	4.82	4.68	4.56	4.45	3.76	3.37	3.09	2.85	2.67	2.50	2.38	2.26	2.16
	7	6.88	6.20	5.80	5.50	5.25	5.08	4.92	4.80	4.68	4.55	3.90	3.50	3.20	2.99	2.80	2.64	2.50	2.38	2.28
	8	7.00	6.25	5.85	5.60	5.35	5.20	5.00	4.90	4.80	4.65	3.96	3.55	3.26	3.05	2.86	2.71	2.58	2.46	2.36
	9	7.10	6.35	6.00	5.70	5.50	5.30	5.12	5.00	4.90	4.75	4.05	3.65	3.36	3.15	2.96	2.80	2.66	2.55	2.45
1	1	7.14	6.45	6.05	5.75	5.55	5.35	5.20	5.05	4.95	4.83	4.10	3.74	3.45	3.22	3.04	2.90	2.75	2.64	2.54
	2	7.60	6.88	6.45	6.15	5.92	5.75	5.60	5.50	5.35	5.25	4.59	4.18	3.90	3.68	3.50	3.34	3.20	3.09	2.97
	3	7.85	7.15	6.70	6.45	6.20	6.00	5.85	5.75	5.60	5.50	4.82	4.42	4.12	3.90	3.72	3.57	3.45	3.31	3.20
	4	8.00	7.28	6.85	6.58	6.35	6.15	6.00	5.90	5.75	5.70	4.95	4.55	4.26	4.04	3.86	3.70	3.59	3.46	3.36
	5	8.15	7.35	7.00	6.65	6.50	6.25	6.10	6.00	5.65	5.80	5.05	4.68	4.40	4.19	4.00	3.85	3.71	3.60	3.49
	6	8.20	7.50	7.10	6.75	6.55	6.35	6.20	6.10	5.95	5.85	5.20	4.78	4.50	4.26	4.09	3.92	3.80	3.69	3.59
	7	8.25	7.55	7.15	6.85	6.62	6.40	6.30	6.20	6.05	5.95	5.25	4.85	4.38	4.35	4.18	4.00	3.90	3.78	3.66
	8	8.30	7.60	7.20	6.90	6.70	6.50	6.35	6.25	6.10	6.05	5.30	4.92	4.18	4.40	4.25	4.10	3.95	3.82	3.74
	9	8.32	7.65	7.25	7.00	6.75	6.55	6.40	6.30	6.15	6.10	5.35	5.00	4.70	4.49	4.30	4.15	4.00	3.90	3.80
	10	8.35	7.75	7.35	7.05	6.80	6.60	6.45	6.35	6.20	6.14	5.40	5.02	4.80	4.52	4.35	4.19	4.05	3.92	3.84

		10^{-1}									1				
	$\tau \backslash \rho$	1	2	3	4	5	6	7	8	9	1	2	3	4	5
10^{-2}	1	0.093	0.0430	0.0264	0.0180	0.0132	0.0100	0.0078	0.0062	0.0049	0.0040	0.00057	0.00015		
	2	0.187	0.0865	0.0530	0.0365	0.0268	0.0205	0.0160	0.0125	0.0100	0.0081	0.00118	0.00020	0	0
	3	0.278	0.130	0.0800	0.0550	0.0405	0.0310	0.0240	0.0190	0.0150	0.0122	0.00184	0.00032		
	4	0.368	0.174	0.107	0.0735	0.0540	0.0415	0.0322	0.0255	0.0202	0.0165	0.00244	0.00043	0	0
	5	0.450	0.215	0.133	0.0920	0.0675	0.0520	0.0400	0.0320	0.0255	0.0206	0.00305	0.00055		
	6	0.530	0.257	0.160	0.110	0.0810	0.0610	0.0478	0.0380	0.0305	0.0250	0.00365	0.00065	0	0
	7	0.610	0.298	0.186	0.130	0.0950	0.0725	0.0565	0.0450	0.0360	0.0292	0.00430	0.00078		
	8	0.680	0.340	0.214	0.148	0.108	0.0825	0.0645	0.0510	0.0412	0.0336	0.00500	0.00090	0	0
	9	0.750	0.378	0.236	0.164	0.122	0.0930	0.0730	0.0585	0.0470	0.0380	0.00570	0.00105		
10^{-1}	1	0.815	0.415	0.260	0.180	0.134	0.103	0.0805	0.0640	0.0515	0.0420	0.00635	0.00118	0	0
	2	1.32	0.750	0.500	0.359	0.268	0.208	0.165	0.132	0.107	0.0880	0.0145	0.00278		
	3	1.64	1.02	0.700	0.515	0.392	0.308	0.246	0.200	0.164	0.135	0.0238	0.00490	0	0
	4	1.86	1.22	0.870	0.650	0.510	0.405	0.328	0.268	0.220	0.182	0.0350	0.00750	0.00160	0.00038
	5	2.03	1.37	1.00	0.770	0.610	0.490	0.400	0.330	0.275	0.230	0.0450	0.0104	0.00240	0.00056
	6	2.16	1.49	1.12	0.875	0.700	0.570	0.468	0.390	0.325	0.276	0.0580	0.0138	0.00320	0.00080
	7	2.28	1.60	1.22	0.965	0.775	0.640	0.525	0.445	0.375	0.320	0.0715	0.0175	0.00425	0.00108
	8	2.36	1.69	1.30	1.04	0.850	0.715	0.600	0.500	0.425	0.364	0.084C	0.0212	0.00525	0.00140
	9	2.45	1.75	1.38	1.11	0.920	0.775	0.650	0.550	0.475	0.404	0.0980	0.0260	0.00630	0.00165
1	1	2.54	1.85	1.45	1.18	0.975	0.825	0.700	0.595	0.510	0.444	0.113	0.0310	0.00840	0.00235
	2	2.97	2.29	1.88	1.60	1.38	1.22	1.07	0.950	0.840	0.750	0.259	0.0950	0.0330	0.0115
	3	3.20	2.50	2.10	1.82	1.60	1.42	1.28	1.15	1.05	0.960	0.388	0.165	0.0700	0.0275
	4	3.36	2.66	2.25	1.97	1.75	1.58	1.42	1.30	1.20	1.10	0.495	0.235	0.112	0.0535
	5	3.49	2.78	2.38	2.09	1.87	1.69	1.54	1.42	1.30	1.21	0.580	0.300	0.150	0.0715
	6	3.59	2.90	2.47	2.18	1.95	1.78	1.65	1.52	1.40	1.30	0.660	0.360	0.195	0.0990
	7	3.66	2.96	2.55	2.25	2.04	1.85	1.70	1.58	1.48	1.38	0.730	0.415	0.230	0.125
	8	3.74	3.00	2.60	2.32	2.11	1.94	1.79	1.66	1.55	1.44	0.790	0.465	0.272	0.155
	9	3.80	3.09	2.67	2.39	2.17	2.00	1.85	1.72	1.60	1.50	0.850	0.515	0.307	0.182
	10	3.84	3.12	2.74	2.45	2.24	2.05	1.90	1.77	1.65	1.55	0.890	0.550	0.340	0.210

Appendix E : (Continued)

(b) Neumann (1975) well function $W(u_a, u_y, \beta)$ for an unconfined aquifer

$1/u_y$	u_y	β								
		0.001	0.01	0.06	0.2	0.6	1	2	4	6
0.4	2.5	0.0248	0.0241	0.023	0.0214	0.0188	0.017	0.0138	0.01	0.01
0.8	1.25	0.145	0.14	0.131	0.119	0.0988	0.0849	0.0603	0.0317	0.0174
1.4	0.71429	0.358	0.345	0.3178	0.279	0.217	0.175	0.107	0.0445	0.021
2.4	0.41667	0.662	0.633	0.57	0.483	0.343	0.256	0.133	0.0476	0.0214
4	0.25	1.02	0.963	0.849	0.688	0.438	0.3	0.14	0.0478	0.0215
8	0.125	1.57	1.46	1.23	0.918	0.497	0.317	0.141	0.0478	0.0215
14	0.07143	2.05	1.88	1.51	1.03	0.507	0.317	0.141	0.0478	0.0215
24	0.04167	2.52	2.27	1.73	1.07	0.507	0.317	0.141	0.0478	0.0215
40	0.025	2.97	2.61	1.85	1.08	0.507	0.317	0.141	0.0478	0.0215
80	0.0125	3.56	3	1.92	1.08	0.507	0.317	0.141	0.0478	0.0215
140	0.007143	4.01	3.23	1.93	1.08	0.507	0.317	0.141	0.0478	0.0215
240	0.004167	4.42	3.37	1.94	1.08	0.507	0.317	0.141	0.0478	0.0215
400	0.0025	4.77	3.43	1.94	1.08	0.507	0.317	0.141	0.0478	0.0215
800	0.00125	5.16	3.45	1.94	1.08	0.507	0.317	0.141	0.0478	0.0215
1400	0.000714	5.4	3.46	1.94	1.08	0.507	0.317	0.141	0.0478	0.0215
2400	0.000417	5.54	3.46	1.94	1.08	0.507	0.317	0.141	0.0478	0.0215
4000	0.00025	5.59	3.46	1.94	1.08	0.507	0.317	0.141	0.0478	0.0215
8000	0.000125	5.62	3.46	1.94	1.08	0.507	0.317	0.141	0.0478	0.0215

(Continued)

Appendix E: (Continued)

$1/u_y$	u_y	β								
		0.001	0.01	0.06	0.2	0.6	1	2	4	6
0.014	71.42857							0.145	0.0509	0.0.39
0.024	41.66667		3.46	1.94	1.09	0.512	0.323	0.147	0.0532	0.0257
0.04	25.00000	5.62	3.46	1.94	1.09	0.516	0.327	0.152	0.0568	0.0286
0.08	12.50000	5.62	3.46	1.94	1.09	0.524	0.337	0.162	0.0661	0.0362
0.14	7.14286	5.62	3.46	1.94	1.1	0.537	0.35	0.178	0.0806	0.0486
0.24	4.16667	5.62	3.46	1.95	1.11	0.557	0.374	0.205	0.106	0.0714
0.4	2.50000	5.62	3.46	1.96	1.13	0.589	0.412	0.248	0.149	0.113
0.8	1.25000	5.62	3.46	1.98	1.18	0.667	0.506	0.357	0.266	0.231
1.4	0.71429	5.63	3.47	2.01	1.24	0.78	0.642	0.517	0.445	0.419
2.4	0.41667	5.63	3.49	2.06	1.35	0.954	0.85	0.763	0.718	0.703
4	0.25000	5.63	3.51	2.13	1.5	1.2	1.13	1.08	1.06	1.05
8	0.12500	5.64	3.56	2.31	1.85	1.68	1.65	1.63		
14	0.07143	5.65	3.63	2.55	2.23	2.15				
24	0.04167	5.67	3.74	2.86	2.68	2.65				
40	0.02500	5.7	3.9	3.24	3.15					
80	0.01250	5.76	4.22	3.85	3.82					
140	0.00714	5.85	4.58	4.38						
240	0.00417	5.99	5	4.91						
400	0.00250	6.16	5.46							
800	0.00125	6.47	6.11							
1000	0.00100	6.6	6.5							

(c) Boulton's (1963) well function $W\left(u_{ay}, r/\beta'\right)$ *for an unconfined aquifer with delayed storage*

r/β'	$1/u_a$	$W(u_a, r/\beta')$	r/β'	$1/u_y$	$W(u_y, r/\beta')$
0.01	1.00E + 01	1.8200	0.01	4.00E + 02	9.4500
0.01	1.00E + 02	4.0400	0.01	4.00E + 03	9.5400
0.01	1.00E + 03	6.3100	0.01	4.00E + 04	10.2300
0.01	5.00E + 03	7.8200	0.01	4.00E + 05	12.3100
0.01	1.00E + 04	8.4000	0.01	4.00E + 06	14.6100
0.01	1.00E + 05	9.4200	0.1	4.00E + 00	4.8600
0.01	1.00E + 06	9.4400	0.1	4.00E + 01	4.9500
0.1	1.00E + 01	1.8000	0.1	4.00E + 02	5.6400
0.1	5.00E + 01	3.2400	0.1	4.00E + 03	7.7200
0.1	1.00E + 02	3.8100	0.1	4.00E + 04	10.0100
0.1	2.00E + 02	4.3000	0.2	4.00E – 01	3.5100
0.1	5.00E + 02	4.7100	0.2	4.00E + 00	3.5400
0.1	1.00E + 03	4.8300	0.2	2.00E + 01	3.6900
0.1	1.00E + 04	4.8500	0.2	4.00E + 01	3.8500
0.2	5.00E + 00	1.1900	0.2	1.50E + 02	4.5500
0.2	1.00E + 01	1.7500	0.2	4.00E + 02	5.4200
0.2	5.00E + 01	2.9500	0.316	4.00E – 01	2.6600
0.2	1.00E + 02	3.2900	0.316	4.00E + 00	2.7400
0.2	5.00E + 02	3.5000	0.316	4.00E + 01	3.3800
0.2	1.00E + 03	3.5100	0.316	4.00E + 02	5.4200
0.316	1.00E + 00	0.2160	0.316	4.00E + 03	7.7200
0.316	2.00E + 00	0.5440	0.4	1.00E – 01	2.2300
0.316	5.00E + 00	1.1530	0.4	1.00E + 00	2.2600
0.316	1.00E + 01	1.6550	0.4	5.00E + 00	2.2400
0.316	5.00E + 01	2.5040	0.4	1.00E + 01	2.5500
0.316	1.00E + 02	2.6230	0.4	3.75E + 01	3.2000
0.316	1.00E + 03	2.6480	0.4	1.00E + 02	4.0500
0.4	1.00E + 00	0.2130	0.6	4.44E – 01	1.5860
0.4	2.00E + 00	0.5340	0.6	2.22E + 00	1.7070
0.4	5.00E + 00	1.1140	0.6	4.44E + 00	1.8440
0.4	1.00E + 01	1.5640	0.6	1.67E + 01	2.4480
0.4	5.00E + 01	2.1810	0.6	4.44E + 01	3.2550
0.4	1.00E + 02	2.2250	0.8	2.50E – 02	1.1330
0.4	1.00E + 03	2.2290	0.8	2.50E – 01	1.1580
0.6	1.00E + 00	0.2060	0.8	1.25E + 00	1.2640
0.6	2.00E + 00	0.5040	0.8	2.50E + 00	1.3870
0.6	5.00E + 00	0.9960	0.8	9.37E + 00	1.9380
0.6	1.00E + 01	1.3110	0.8	2.50E + 01	2.7040
0.6	2.00E + 01	1.4930	1.0	4.00E – 02	0.8440
0.6	5.00E + 01	1.5530	1.0	4.00E – 01	0.9010
0.6	1.00E + 02	1.5550	1.0	4.00E + 00	1.3560

(Continued)

Appendix E: (Continued)

r/β'	$1/u_a$	$W(u_a, r/\beta')$	r/β'	$1/u_y$	$W(u_y, r/\beta')$
0.8	5.00E – 01	0.0460	1.0	4.00E + 01	3.1400
0.8	1.00E + 00	0.1970	1.5	7.11E – 02	0.4440
0.8	2.00E + 00	0.4660	1.5	3.55E – 01	0.5090
0.8	5.00E + 00	0.8570	1.5	7.11E – 01	0.5870
0.8	1.00E + 01	1.0500	1.5	2.67E + 00	0.9630
0.8	2.00E + 01	1.1210	1.5	7.11E + 00	1.5690
0.8	5.00E + 01	1.1310	2.0	4.00E – 02	0.0239
1.0	5.00E – 01	0.0444	2.0	2.00E – 01	0.2830
1.0	1.00E + 00	0.1855	2.0	4.00E – 01	0.3370
1.0	2.00E + 00	0.4210	2.0	1.50E + 00	0.6140
1.0	5.00E + 00	0.7150	2.0	4.00E + 00	1.1110
1.0	1.00E + 01	0.8190	2.5	2.56E – 02	0.1321
1.0	2.00E + 01	0.8410	2.5	1.28E – 01	0.1617
1.0	5.00E + 01	0.8420	2.5	2.56E – 01	0.1988
1.5	5.00E – 01	0.0394	2.5	9.60E – 01	0.3990
1.5	1.00E + 00	0.1509	2.5	2.56E + 00	0.0798
1.5	1.25E + 00	0.1990	3.0	1.78E – 02	0.0743
1.5	2.00E + 00	0.3010	3.0	8.89E – 02	0.0939
1.5	5.00E + 00	0.4130	3.0	1.78E – 01	0.1189
1.5	1.00E + 01	0.4270	3.0	6.67E – 01	0.2618
1.5	2.00E + 01	0.4280	3.0	1.78E + 00	0.5771
2.0	3.33E – 01	0.0100			
2.0	5.00E – 01	0.0335			
2.0	1.00E + 00	0.1140			
2.0	1.25E + 00	0.1440			
2.0	2.00E + 00	0.1940			
2.0	5.00E + 00	0.2270			
2.0	1.00E + 01	0.2280			
2.5	5.00E – 01	0.0271			
2.5	1.00E + 00	0.0803			
2.5	1.25E + 00	0.9610			
2.5	2.00E + 00	0.1174			
2.5	5.00E + 00	0.1247			
2.5	1.00E + 01	0.1247			
3.0	5.00E – 01	0.0210			
3.0	1.00E + 00	0.0534			
3.0	1.25E + 00	0.6070			
3.0	2.00E + 00	0.0681			
3.0	5.00E + 00	0.0695			
3.0	1.00E + 01	0.0695			

Note: $W\left(u_{ay}, r/\beta'\right) = W\left(u_a, r/\beta'\right)$ for small values of t (early pumping period)

and $W\left(u_{ay}, r/\beta'\right) = W\left(u_y, r/\beta'\right)$ for large values of t (late pumping period).

Appendix F: *Hantush (1956) well function W(u, r/B) for a leaky aquifer*

r/B \ u	0	0.001	0.002	0.003	0.004	0.005	0.006	0.007	0.008	0.009	0.01
0	00	14.0474	12.6611	11.8502	11.2748	10.8286	10.4640	10.1557	9.8887	9.6532	9.4425
.000001	13.2383	13.0031	12.4417	11.8153	11.2711	10.8283	10.4640	10.1557	9.8887	9.6532	9.4425
.000002	12.5451	12.4240	12.1013	11.6716	11.2259	10.8174	10.4619	10.1554	9.8886	9.6532	9.4425
.000003	12.1397	12.0581	11.8322	11.5098	11.1462	10.7849	10.4509	10.1523	9.8879	9.6530	9.4425
.000004	11.8520	11.7905	11.6168	11.3597	11.0555	10.7374	10.4291	10.1436	9.8849	9.6521	9.4422
.000005	11.6289	11.5795	11.4384	11.2248	10.9642	10.6822	10.3993	10.1290	9.8786	9.6496	9.4413
.000006	11.4465	11.4053	11.2866	11.1040	10.8764	10.6240	10.3640	10.1094	9.8686	9.6450	9.4394
.000007	11.2924	11.2570	11.1545	10.9951	10.7933	10.5652	10.3255	10.0862	9.8555	9.6382	9.4361
.000008	11.1589	11.1279	11.0377	10.8962	10.7151	10.5072	10.2854	10.0602	9.8398	9.6292	9.4313
.000009	11.0411	11.0135	10.9330	10.8059	10.6416	10.4508	10.2446	10.0324	9.8219	9.6182	9.4251
.00001	10.9357	10.9109	10.8382	10.7228	10.5725	10.3963	10.2038	10.0034	9.8024	9.6059	9.4176
.00002	10.2426	10.2301	10.1932	10.1332	10.0522	9.9530	9.8386	9.7126	9.5781	9.4383	9.2961
.00003	9.8371	9.8288	9.8041	9.7635	9.7081	9.6392	9.5583	9.4671	9.3674	9.2611	9.1499
.00004	9.5495	9.5432	9.5246	9.4940	9.4520	9.3992	9.3366	9.2653	9.1863	9.1009	9.0102
.00005	9.3263	9.3213	9.3064	9.2818	9.2480	9.2052	9.1542	9.0957	9.0304	8.9591	8.8827
.00006	9.1440	9.1398	9.1274	9.1069	9.0785	9.0426	8.9996	8.9500	8.8943	8.8332	8.7673
.00007	8.9899	8.9863	8.9756	8.9580	8.9336	8.9027	8.8654	8.8224	8.7739	8.7204	8.6625
.00008	8.8563	8.8532	8.8439	8.8284	8.8070	8.7798	8.7470	8.7090	8.6661	8.6186	8.5669
.00009	8.7386	8.7358	8.7275	8.7138	8.6947	8.6703	8.6411	8.6071	8.5686	8.5258	8.4792
.0001	8.6332	8.6308	8.6233	8.6109	8.5937	8.5717	8.5453	8.5145	8.4796	8.4407	8.3983

(Continued)

Appendix F: (Continued)

u \ r/B	0	0.001	0.002	0.003	0.004	0.005	0.006	0.007	0.008	0.009	0.01
.0002	7.9402	7.9390	7.9352	7.9290	7.9203	7.9092	7.8958	7.8800	7.8619	7.8416	7.8192
.0003	7.5348	7.5340	7.5315	7.5274	7.5216	7.5141	7.5051	7.4945	7.4823	7.4686	7.4534
.0004	7.2472	7.2466	7.2447	7.2416	7.2373	7.2317	7.2249	7.2169	7.2078	7.1974	7.1859
.0005	7.0242	7.0237	7.0222	7.0197	7.0163	7.0118	7.0063	6.9999	6.9926	6.9843	6.9750
.0006	6.8420	6.8416	6.8403	6.8383	6.8353	6.8316	6.8271	6.8218	6.8156	6.8086	6.8009
.0007	6.6879	6.6876	6.6865	6.6848	6.6823	6.6790	6.6752	6.6706	6.6653	6.6594	6.6527
.0008	6.5545	6.5542	6.5532	6.5517	6.5495	6.5467	6.5433	6.5393	6.5347	6.5295	6.5237
.0009	6.4368	6.4365	6.4357	6.4344	6.4324	6.4299	6.4269	6.4233	6.4192	6.4146	6.4094
.001	6.3315	6.3313	6.3305	6.3293	6.3276	6.3253	6.3226	6.3194	6.3157	6.3115	6.3069
.002	5.6394	5.6393	5.6389	5.6383	5.6374	5.6363	5.6350	5.6334	5.6315	5.6294	5.6271
.003	5.2349	5.2348	5.2346	5.2342	5.2336	5.2329	5.2320	5.2310	5.2297	5.2283	5.2267
.004	4.–9482	4.9482	4.9480	4.9477	4.9472	4.9467	4.9460	4.9453	4.9443	4.9433	4.9421
.005	4.7261	4.7260	4.7259	4.7256	4.7253	4.7249	4.7244	4.7237	4.7230	4.7222	4.7212
.006	4.5448	4.5448	4.5447	4.5444	4.5441	4.5438	4.5433	4.5428	4.5422	4.5415	4.5407
.007	4.3916	4.3916	4.3915	4.3913	4.3910	4.3908	4.3904	4.3899	4.3894	4.3888	4.3882
.008	4.2591	4.2590	4.2590	4.2588	4.2586	4.2583	4.2580	4.2576	4.2572	4.2567	4.2561
.009	4.1423	4.1423	4.1422	4.1420	4.1418	4.1416	4.1413	4.1410	4.1406	4.1401	4.1396
.01	4.0379	4.0379	4.0378	4.0377	4.0375	4.0373	4.0371	4.0368	4.0364	4.0360	4.0356
.02	3.3547	3.3547	3.3547	3.3546	3.3545	3.3544	3.3543	3.3542	3.3540	3.3538	3.3536
.03	2.9591	2.9591	2.9591	2.9590	2.9590	2.9589	2.9589	2.9588	2.9587	2.9585	2.9584
.04	2.6813	2.6812	2.6812	2.6812	2.6812	2.6811	2.6810	2.6810	2.6809	2.6808	2.6807

.05	2.4679	2.4679	2.4679	2.4679	2.4678	2.4678	2.4678	2.4677	2.4676	2.4676	2.4675
.06	2.2953	2.2953	2.2953	2.2953	2.2952	2.2952	2.2952	2.2952	2.2951	2.2950	2.2950
.07	2.1508	2.1508	2.1508	2.1508	2.1508	2.1508	2.1508	2.1507	2.1507	2.1506	2.1506
.08	2.0269	2.0269	2.0269	2.0269	2.0269	2.0269	2.0269	2.0268	2.0268	2.0268	2.0267
.09	1.9187	1.9187	1.9187	1.9187	1.9187	1.9187	1.9187	1.9186	1.9186	1.9186	1.9185
.1	1.8229	1.8229	1.8229	1.8229	1.8229	1.8229	1.8229	1.8228	1.8228	1.8228	1.8227
.2	1.2227	1.2226	1.2226	1.2226	1.2226	1.2226	1.2226	1.2226	1.2226	1.2226	1.2226
.3	0.9057	0.9057	0.9057	0.9057	0.9057	0.9057	0.9057	0.9057	0.9056	0.9056	0.9056
.4	0.7024	0.7024	0.7024	0.7024	0.7024	0.7024	0.7024	0.7024	0.7024	0.7024	0.7024
.5	0.5598	0.5598	0.5598	0.5598	0.5598	0.5598	0.5598	0.5598	0.5598	0.5598	0.5598
.6	0.4544	0.4544	0.4544	0.4544	0.4544	0.4544	0.4544	0.4544	0.4544	0.4544	0.4544
.7	0.3738	0.3738	0.3738	0.3738	0.3738	0.3738	0.3738	0.3738	0.3738	0.3738	0.3738
.8	0.3106	0.3106	0.3106	0.3106	0.3106	0.3106	0.3106	0.3106	0.3106	0.3106	0.3106
.9	0.2602	0.2602	0.2602	0.2602	0.2602	0.2602	0.2602	0.2602	0.2602	0.2602	0.2602
1.0	0.2194	0.2194	0.2194	0.2194	0.2194	0.2194	0.2194	0.2194	0.2194	0.2194	0.2194
2.0	0.0489	0.0489	0.0489	0.0489	0.0489	0.0489	0.0489	0.0489	0.0489	0.0489	0.0489
3.0	0.0130	0.0130	0.0130	0.0130	0.0130	0.0130	0.0130	0.0130	0.0130	0.0130	0.0130
4.0	0.0038	0.0038	0.0038	0.0038	0.0038	0.0038	0.0038	0.0038	0.0038	0.0038	0.0038
5.0	0.0011	0.0011	0.0011	0.0011	0.0011	0.0011	0.0011	0.0011	0.0011	0.0011	0.0011
6.0	0.0004	0.0004	0.0004	0.0004	0.0004	0.0004	0.0004	0.0004	0.0004	0.0004	0.0004
7.0	0.0001	0.0001	0.0001	0.0001	0.0001	0.0001	0.0001	0.0001	0.0001	0.0001	0.0001
8.0	0	0	0	0	0	0	0	0	0	0	0

Appendix F

u \ r/B	0.01	0.015	0.02	0.025	0.03	0.035	0.04	0.045
0	9.4425	8.6319	8.0569	7.6111	7.2471	6.9394	6.6731	6.4383
.000001	9.4425	8.6319	8.0569	7.6111	7.2471	6.9394	6.6731	6.4383
.000002	9.4425	8.6319	8.0569	7.6111	7.2471	6.9394	6.6731	6.4383
.000003	9.4425	8.6319	8.0569	7.6111	7.2471	6.9394	6.6731	6.4383
.000004	9.4422	8.6319	8.0569	7.6111	7.2471	6.9394	6.6731	6.4383
.000005	9.4413	8.6319	8.0569	7.6111	7.2471	6.9394	6.6731	6.4383
.000006	9.4394	8.6319	8.0569	7.6111	7.2471	6.9394	6.6731	6.4383
.000007	9.4361	8.6319	8.0569	7.6111	7.2471	6.9394	6.6731	6.4383
.000008	9.4313	8.6318	8.0569	7.6111	7.2471	6.9394	6.6731	6.4383
.000009	9.4251	8.6316	8.0569	7.6111	7.2471	6.9394	6.6731	6.4383
.00001	9.4176	8.6313	8.0569	7.6111	7.2471	6.9394	6.6731	6.4383
.00002	9.2961	8.6152	8.0558	7.6111	7.2471	6.9394	6.6731	6.4383
.00003	9.1499	8.5737	8.0483	7.6101	7.2470	6.9394	6.6731	6.4383
.00004	9.0102	8.5168	8.0320	7.6069	7.2465	6.9394	6.6731	6.4383
.00005	8.8827	8.4533	8.0080	7.6000	7.2450	6.9391	6.6730	6.4383
.00006	8.7673	8.3880	7.9786	7.5894	7.2419	6.9384	6.6729	6.4383
.00007	8.6625	8.3233	7.9456	7.5754	7.2371	6.9370	6.6726	6.4382
.00008	8.5669	8.2603	7.9105	7.5589	7.2305	6.9347	6.6719	6.4361
.00009	8.4792	8.1996	7.8743	7.5402	7.2222	6.9316	6.6709	6.4378
.0001	8.3983	8.1414	7.8375	7.5199	7.2122	6.9273	6.6693	6.4372
.0002	7.8192	7.6780	7.4972	7.2898	7.0685	6.8439	6.6242	6.4143
.0003	7.4534	7.3562	7.2281	7.0759	6.9068	6.7276	6.5444	6.3623
.0004	7.1859	7.1119	7.0128	6.8929	6.7567	6.6088	6.4538	6.2955
.0005	6.9750	6.9152	6.8346	6.7357	6.6219	6.4964	6.3626	6.2236
.0006	6.8009	6.7508	6.6828	6.5988	6.5011	6.3923	6.2748	6.1512
.0007	6.6527	6.6096	6.5508	6.4777	6.3923	6.2962	6.1917	6.0807
.0006	6.5237	6.4858	6.4340	6.3695	6.2935	6.2076	6.1136	6.0129
.0009	6.4094	6.3757	6.3294	6.2716	6.2032	6.1256	6.0401	5.9481
.001	6.3069	6.2765	6.2347	6.1823	6.1202	6.0494	5.9711	5.8864
.007	5.6271	5.6118	5.5907	5.5638	5.5314	5.4939	5.4516	5.4047
.003	5.2267	5.2166	5.2025	5.1845	5.1627	5.1373	5.1064	5.0762
.004	4.9421	4.9345	4.9240	4.9105	4.8941	4.8749	4.8530	4.8286
.005	4.7212	4.7152	4.7068	4.6960	4.6829	4.6675	4.6499	4.6302
.006	4.5407	4.5357	4.5287	4.5197	4.5088	4.4960	4.4814	4.4649
.007	4.3882	4.3839	4.3779	4.3702	4.3609	4.3500	4.3374	4.3233
.008	4.2561	4.2524	4.2471	4.2404	4.2323	4.2228	4.2118	4.1994
.009	4.1396	4.1363	4.1317	4.1258	4.1186	4.1101	4.1004	4.0894

	0.05	0.055	0.06	0.065	0.07	0.075	0.08	0.085	0.09	0.095	0.10
	6.2285	6.0388	5.8658	5.7067	5.5596	5.4228	5.2950	5.175	5.0620	4.9553	4.8541
	6.2285	6.0388	5.8658	5.7067	5.5596	5.4228	5.2950	5.175	5.0620	4.9553	4.8541
	6.2285	6.0388	5.8658	5.7067	5.5596	5.4228	5.2950	5.175	5.0620	4.9553	4.8541
	6.2285	6.0388	5.8658	5.7067	5.5596	5.4228	5.2950	5.175	5.0620	4.9553	4.8541
	6.2285	6.0388	5.8658	5.7067	5.5596	5.4228	5.2950	5.175	5.0620	4.9553	4.8541
	6.2285	6.0388	5.8658	5.7067	5.5596	5.4228	5.2950	5.175	5.0620	4.9553	4.8541
	6.2285	6.0388	5.8658	5.7067	5.5596	5.4228	5.2950	5.175	5.0620	4.9553	4.8541
	6.2285	6.0388	5.8658	5.7067	5.5596	5.4228	5.2950	5.175	5.0620	4.9553	4.8541
	6.2285	6.0388	5.8658	5.7067	5.5596	5.4228	5.2950	5.175	5.0620	4.9553	4.8541
	6.2285	6.0388	5.8658	5.7067	5.5596	5.4228	5.2950	5.175	5.0620	4.9553	4.8541
	6.2285	6.0388	5.8658	5.7067	5.5596	5.4228	5.2950	5.175	5.0620	4.9553	4.8541
	6.2285	6.0388	5.8658	5.7067	5.5596	5.4228	5.2950	5.175	5.0620	4.9553	4.8541
	6.2285	6.0388	5.8658	5.7067	5.5596	5.4228	5.2950	5.175	5.0620	4.9553	4.8541
	6.2285	6.0388	5.8658	5.7067	5.5596	5.4228	5.2950	5.175	5.0620	4.9553	4.8541
	6.2285	6.0388	5.8658	5.7067	5.5596	5.4228	5.2950	5.175	5.0620	4.9553	4.8541
	6.2285	6.0388	5.8658	5.7067	5.5596	5.4228	5.2950	5.175	5.0620	4.9553	4.8541
	6.2285	6.0388	5.8658	5.7067	5.5596	5.4228	5.2950	5.175	5.0620	4.9553	4.8541
	6.2284	6.0388	5.8658	5.7067	5.5596	5.4228	5.2950	5.175	5.0620	4.9553	4.8541
	6.2283	6.0388	5.8658	5.7067	5.5596	5.4228	5.2950	5.175	5.0620	4.9553	4.8541
	6.2282	6.0388	5.8658	5.7067	5.5596	5.4228	5.295	5.175	5.0620	4.9553	4.8541
	6.2173	6.0338	5.8637	5.7059	5.5593	5.4227	5.2949	5.1750	5.0620	4.9553	4.8541
	6.1848	6.0145	5.8527	5.6999	5.5562	5.4212	5.2942	5.1747	5.0619	4.9552	4.8541
	6.1373	5.9818	5.8309	5.6860	5.5476	5.4160	5.2912	5.1730	5.0610	4.9547	4.8539
	6.0821	5.9406	5.8011	5.6648	5.5330	5.4062	5.2848	5.1689	5.0585	4.9532	4.8530
	6.0239	5.8948	5.7658	5.6383	5.5134	5.3921	5.2749	5.1621	5.0539	4.9502	4.8510
	5.9652	5.8468	5.7274	5.6081	5.4902	5.3745	5.2618	5.1526	5.0471	4.9454	4.8478
	5.9073	5.7982	5.6873	5.5755	5.4642	5.3542	5.2461	5.1406	5.0381	4.9388	4.8430
	5.8509	5.7500	5.6465	5.5416	5.4364	5.3317	5.2282	5.1266	5.0272	4.9306	4.8368
	5.7965	5.7026	5.6058	5.5071	5.4075	5.3078	5.2087	5.1109	5.0133	4.9208	4.8292
	5.3538	5.2991	5.2411	5.1803	5.1170	5.0517	4.9848	4.9166	4.8475	4.7778	4.7079
	5.0408	5.0025	4.9615	4.918	4.8722	4.8243	4.7746	4.7234	4.6707	4.6169	4.5622
	4.8016	4.7722	4.7406	4.7068	4.6710	4.6335	4.5942	4.5533	4.5111	4.4676	4.4230
	4.6084	4.5846	4.559	4.5314	4.5022	4.4713	4.4389	4.4050	4.3699	4.3335	4.2960
	4.4467	4.4267	4.4051	4.3819	4.3573	4.3311	4.3036	4.2747	4.2446	4.2134	4.1812
	4.3077	4.2905	4.2719	4.2518	4.2305	4.2078	4.1839	4.1588	4.1326	41053	4.0771
	4.1857	4.1707	4.1544	4.1368	4.1180	4.0980	4.0769	4.0547	4.0315	40073	3.9822
	4.0772	4.0638	4.0493	4.0336	4.0169	3.9991	3.9802	3.9603	3.9395	3.9178	3.8952

(Continued)

Appendix F: (Continued)

u \ r/B	0.01	0.015	0.02	0.025	0.03	0.035	0.04	0.045
.01	4.0356	4.0326	4.0285	4.0231	4.0167	4.0091	4.0003	3.9905
.02	3.3536	3.3521	3.3502	3.3476	3.3444	3.3408	3.3365	3.3317
.03	2.9584	2.9575	2.9562	2.9545	2.9523	2.9501	2.9474	2.9444
.04	2.6807	2.6800	2.6791	2.6779	2.6765	2.6747	2.6727	2.6705
.05	2.4675	2.4670	2.4662	2.4653	2.4642	2.4628	2.4613	2.4595
.06	2.2950	2.2945	2.2940	2.2932	2.2923	2.2912	2.2900	2.2885
.07	2.1506	2.1502	2.1497	2.1491	2.1483	2.1474	2.1464	2.1452
.08	2.0267	2.0264	2.0260	2.0255	2.0248	2.0240	2.0231	2.0221
.09	1.9163	1.9183	1.9179	1.9174	1.9169	1.9162	1.9134	1.9146
.1	1.8227	1.8225	1.8222	1.8218	1.8213	1.8207	1.8200	1.8193
.2	1.2226	1.2225	1.2224	1.2222	1.2220	1.2218	1.2215	1.2212
.3	0.9056	0.9056	0.9055	0.9054	0.9053	0.9052	0.9050	0.9049
.4	0.7024	0.7023	0.7023	0.7022	0.7022	0.7021	0.7020	0.7019
.5	0.5598	0.5597	0.5597	0.5597	0.5596	0.5596	0.5595	0.5594
.6	0.4544	0.4544	0.4543	0.4543	0.4543	0.4542	0.4542	0.4542
.7	0.3738	0.3738	0.3737	0.3737	0.3737	0.3737	0.3736	0.3736
.8	0.3106	0.3106	0.3106	0.3106	0.3105	0.3105	0.3105	0.3105
.9	0.2602	0.2602	0.2602	0.2602	0.2601	0.2601	0.2601	0.2601
1.0	0.2194	0.2194	0.2194	0.2194	0.2193	0.2193	0.2193	0.2193
2.0	0.0489	0.0489	0.0489	0.0489	0.0429	0.0489	0.0489	0.0489
3.0	0.0130	0.0130	0.0130	0.0130	0.0130	0.0130	0.0130	0.0130
4.0	0.0038	0.0038	0.0038	0.0038	0.0038	0.0038	0.0038	0.0038
5.0	0.0011	0.0011	0.0011	0.0011	0.0011	0.0011	0.0011	0.0011
6.0	0.0004	0.0004	0.0004	0.0004	0.0004	0.0004	0.0004	0.0004
7.0	0.0001	0.0001	0.0001	0.0001	0.0001	0.0001	0.0001	0.0001
8.0	0	0	0	0	0	0	0	0

0.05	0.055	0.06	0.065	0.07	0.075	0.08	0.085	0.09	0.095	0.10
3.9795	3.9675	3.9544	3.9403	3.9252	3.9091	3.892	3.8741	3.8552	3.8356	3.8150
3.3264	3.3205	3.3141	3.3071	3.2997	3.2917	3.2832	3.2742	3.2647	3.2547	3.2442
2.9409	2.9370	2.9329	2.9284	2.9235	2.9183	2.9127	2.9069	2.9007	2.8941	2.8873
2.6680	2.6652	2.6622	2.6589	2.6553	2.6515	2.6475	2.6432	2.6386	2.6338	2.6288
2.4576	2.4554	2.4531	2.4505	2.4478	2.4448	2.4416	2.4383	2.4347	2.4310	2.4271
2.2870	2.2852	2.2833	2.2812	2.2790	2.2766	2.2740	2.2713	2.2684	2.2654	2.2622
2.1439	2.1424	2.1408	2.1391	2.1372	2.1352	2.1331	2.1308	2.1284	2.1258	2.1232
2.0210	2.0198	2.0184	2.0169	2.0153	2.0136	2.0118	2.0099	2.0078	2.0054	2.0034
1.9136	1.9125	1.9114	1.9101	1.9087	1.9072	1.9056	1.9040	1.9022	1.9003	1.8983
1.8184	1.8175	1.8164	1.8153	1.8141	1.8128	1.8114	1.8099	1.8084	1.8067	1.8050
1.2209	1.2205	1.2201	1.2198	1.2192	1.2186	1.2181	1.2175	1.2168	1.2162	1.2155
0.9047	0.9045	0.9043	0.9040	0.9038	0.9035	0.9032	0.9029	0.9025	0.9022	0.9018
0.7018	0.7016	0.7015	0.7014	0.7012	0.7010	0.7008	0.7006	0.7004	0.7002	0.7000
0.5594	0.5593	0.5592	0.5591	0.5590	0.5588	0.5587	0.5586	0.5584	0.5583	0.5581
0.4541	0.4540	0.4540	0.4539	0.4538	0.4537	0.4536	0.4535	0.4534	0.4533	0.4532
0.3735	0.3735	0.3734	0.3734	0.3733	0.3733	0.3732	0.3732	0.3731	0.3730	0.3729
0.3104	0.3104	0.3104	0.3103	0.3103	0.3102	0.3102	0.3101	0.3101	0.3100	0.3100
0.2601	0.2600	0.2600	0.2600	0.2599	0.2599	0.2599	0.2598	0.2598	0.2597	0.2597
0.2193	0.2193	0.2192	0.2192	0.2192	0.2191	0.2191	0.2191	0.2191	0.2190	0.2190
0.0489	0.0489	0.0489	0.0489	0.0489	0.0489	0.0489	0.0489	0.0489	0.0488	0.0488
0.0130	0.0130	0.0130	0.0130	0.0130	0.0130	0.0130	0.0130	0.0130	0.0130	0.0130
0.0038	0.0038	0.0038	0.0038	0.0038	0.0038	0.0038	0.0038	0.0038	0.0038	0.0038
0.0011	0.0011	0.0011	0.0011	0.0011	0.0011	0.0011	0.0011	0.0011	0.0011	0.0011
0.0004	0.0004	0.0004	0.0004	0.0004	0.0004	0.0004	0.0004	0.0004	0.0004	0.0004
0.0001	0.0001	0.0001	0.0001	0.0001	0.0001	0.0001	0.0001	0.0001	0.0001	0.0001
0	0	0	0	0	0	0	0	0	0	0

(Continued)

Appendix F: (Continued)

r/B \ u	0.1	0.15	0.2	0.25	0.3	0.35	0.4	0.45	0.5
0	4.8541	4.0601	3.5054	3.0830	2.7449	2.4654	2.2291	2.0258	1.8488
.0001	4.8541	4.0601	3.5054	3.0830	2.7449	2.4654	2.2291	2.0258	1.8488
.0002	4.8541	4.0601	3.5054	3.0830	2.7449	2.4654	2.2291	2.0258	1.8488
.0003	4.8541	4.0601	3.5054	3.0830	2.7449	2.4654	2.2291	2.0258	1.8488
.0004	4.8539	4.0601	3.5054	3.0830	2.7449	2.4654	2.2291	2.0258	1.8488
.0005	4.8530	4.0601	3.5054	3.0830	2.7449	2.4654	2.2291	2.0258	1.8488
.0006	4.8510	4.0601	3.5054	3.0830	2.7449	2.4654	2.2291	2.0258	1.8488
.0007	4.8478	4.0600	3.5054	3.0830	2.7449	2.4654	2.2291	2.0258	1.8488
.0008	4.8430	4.0599	3.5054	3.0830	2.7449	2.4654	2.2291	2.0258	1.8488
.0009	4.8368	4.0598	3.5054	3.0830	2.7449	2.4654	2.2291	2.0258	1.8488
.001	4.8292	4.0595	3.5054	3.0830	2.7449	2.4654	2.2291	2.0258	1.8488
.002	4.7079	4.0435	3.5043	3.0830	2.7449	2.4654	2.2291	2.0258	1.8488
.003	4.5622	4.0092	3.4969	3.0821	2.7448	2.4654	2.2291	2.0258	1.8488
.004	4.4230	3.9551	3.4806	3.0788	2.7444	2.4654	2.2291	2.0258	1.8488
.005	4.2960	3.8821	3.4567	3.0719	2.7428	2.4651	2.2290	2.0258	1.8488
.006	4.1812	3.8284	3.4274	3.0614	2.7398	2.4644	2.2289	2.0258	1.8488
.007	4.0771	3.7529	3.3947	3.0476	2.7350	2.4630	2.2286	2.0257	1.8488
.008	3.9822	3.6903	3.3598	3.0311	2.7284	2.4608	2.2279	2.0256	1.8488
.009	3.8952	3.6302	3.3239	3.0126	2.7202	2.4576	2.2269	2.0253	1.8487
.01	3.8150	3.5725	3.2875	2.9925	2.7104	2.4534	2.2253	2.0248	1.8486
.02	3.2442	3.1158	2.9521	2.7658	2.5688	2.3713	2.1809	2.0023	1.8379
.03	2.8873	2.8017	2.6896	2.5571	2.4110	2.2578	2.1031	1.9515	1.8062
.04	2.6288	2.5655	2.4816	2.3802	2.2661	2.1431	2.0155	1.8869	1.7603
.05	2.4271	2.3776	2.3110	2.2299	2.1371	2.0356	1.9283	1.8181	1.7075
.06	2.2622	2.2218	2.1673	2.1002	2.0227	1.9369	1.8452	1.7497	1.6524
.07	2.1232	2.0894	2.0435	1.9867	1.9206	1.8469	1.7673	1.6835	1.5973
.08	2.0034	1.9745	1.9351	1.8861	1.8290	1.7646	1.6947	1.6206	1.5436
.09	1.8983	1.8732	1.8389	1.7961	1.7460	1.6892	1.6272	1.5609	1.4918
0.1	1.8050	1.7829	1.7527	1.7149	1.6704	1.6198	1.5644	1.5048	1.4422
0.2	1.2155	1.2066	1.1944	1.1789	1.1602	1.1387	1.1145	0.0879	1.0592
0.3	0.9018	0.8969	0.8902	0.8817	0.8713	0.8593	0.8457	0.8306	0.8142
0.4	0.7000	0.6969	0.6927	0.6874	0.6809	0.6733	0.6647	0.6551	0.6446
0.5	0.5581	0.5561	0.5532	0.5496	0.5453	0.5402	0.5344	0.5278	0.5206
0.6	0.4532	0.4518	0.4498	0.4472	0.4441	0.4405	0.4364	0.4317	0.4266
0.7	0.3729	0.3719	0.3704	0.3685	0.3663	0.3636	0.3606	0.3572	0.3534
0.8	0.3100	0.3092	0.3081	0.3067	0.3050	0.3030	0.3008	0.2982	0.2953
0.9	0.2597	0.2591	0.2583	0.2572	0.2559	0.2544	0.2527	0.2507	0.2485
1.0	0.2190	0.2186	0.2179	0.2171	0.2161	0.2149	0.2135	0.2120	0.2103
2.0	0.0488	0.0488	0.0487	0.0486	0.0485	0.0484	0.0482	0.0480	0.0477
3.0	0.0130	0.0130	0.0130	0.0130	0.0130	0.0130	0.0129	0.0129	0.0128
4.0	0.0038	0.0038	0.0038	0.0038	0.0038	0.0038	0.0038	0.0037	0.0037
5.0	0.0011	0.0011	0.0011	0.0011	0.0011	0.0011	0.0011	0.0011	0.0011
6.0	0.0004	0.0004	0.0004	0.0004	0.0004	0.0004	0.0004	0.0004	0.0004
7.0	0.0001	0.0001	0.0001	0.0001	0.0001	0.0001	0.0001	0.0001	0.0001
8.0	0	0	0	0	0	0	0	0	0

0.55	0.6	0.65	0.7	0.75	0.8	0.85	0.9	0.95	1.0
1.6981	1.5550	1.4317	1.3210	1.2212	1.1307	1.0485	0.9735	0.9049	0.8420
1.6981	1.5550	1.4317	1.3210	1.2212	1.1307	1.0485	0.9735	0.9049	0.8420
1.6981	1.5550	1.4317	1.3210	1.2212	1.1307	1.0485	0.9735	0.9049	0.8420
1.6981	1.5550	1.4317	1.3210	1.2212	1.1307	1.0485	0.9735	0.9049	0.8420
1.6981	1.5550	1.4317	1.3210	1.2212	1.1307	1.0485	0.9735	0.9049	0.8420
1.6981	1.5550	1.4317	1.3210	1.2212	1.1307	1.0485	0.9735	0.9049	0.8420
1.6981	1.5550	1.4317	1.3210	1.2212	1.1307	1.0485	0.9735	0.9049	0.8420
1.6981	1.5550	1.4317	1.3210	1.2212	1.1307	1.0485	0.9735	0.9049	0.8420
1.6981	1.5550	1.4317	1.3210	1.2212	1.1307	1.0485	0.9735	0.9049	0.8420
1.6981	1.5550	1.4317	1.3210	1.2212	1.1307	1.0485	0.9735	0.9049	0.8420
1.6981	1.5550	1.4317	1.3210	1.2212	1.1307	1.0485	0.9735	0.9049	0.8420
1.6981	1.5550	1.4317	1.3210	1.2212	1.1307	1.0485	0.9735	0.9049	0.8420
1.6981	1.5550	1.4317	1.3210	1.2212	1.1307	1.0485	0.9735	0.9049	0.8420
1.6981	1.5550	1.4317	1.3210	1.2212	1.1307	1.0485	0.9735	0.9049	0.8420
1.6981	1.5550	1.4317	1.3210	1.2212	1.1307	1.0485	0.9735	0.9049	0.8420
1.6981	1.5550	1.4317	1.3210	1.2212	1.1307	1.0485	0.9735	0.9049	0.8420
1.6981	1.5550	1.4317	1.3210	1.2212	1.1307	1.0485	0.9735	0.9049	0.8420
1.6981	1.5550	1.4317	1.3210	1.2212	1.1307	1.0485	0.9735	0.9049	0.8420
1.6981	1.5550	1.4317	1.3210	1.2212	1.1307	1.0485	0.9735	0.9049	0.8420
1.6931	1.5550	1.4317	1.3210	1.2212	1.1307	1.0485	0.9735	0.9049	0.8420
1.6883	1.5530	1.4309	1.3207	1.2210	1.306	1.0484	0.9735	0.9049	0.8420
1.6695	1.5423	1.4251	1.3177	1.2195	1.299	1.0481	0.9733	0.9048	0.8420
1.6379	1.5213	1.4117	1.3094	1.2146	1.270	1.0465	0.9724	0.9044	0.8418
1.5985	1.4927	1.3914	1.2955	1.2052	1.210	1.0426	0.9700	0.9029	0.8409
1.5551	1.4593	1.3663	1.2770	1.1919	1.1116	1.0362	0.9657	0.9001	0.8391
1.5101	1.4232	1.338	1.2551	1.1754	1.0993	1.0272	0.9593	0.8956	0.8360
1.4650	1.3860	1.3078	1.2310	1.1564	1.0847	1.0161	0.9510	0.8895	0.8316
1.4206	1.3486	1.2766	1.2054	1.1358	1.0682	1.0032	0.9411	0.8819	0.8759
1.3774	1.3115	1.2451	1.1791	1.1140	1.0505	0.9890	0.9297	0.8730	0.8190
1.0286	0.9964	0.9629	0.9284	0.8932	0.8575	0.8216	0.7857	0.7501	0.7148
0.7964	0.7775	0.7577	0.7362	0.7154	0.6932	0.6706	0.6476	0.6244	0.6010
0.6332	0.6209	0.6080	0.5943	0.0580	0.5653	0.5501	0.5345	0.5186	0.5024
0.5128	0.5044	0.4955	0.4860	0.0476	0.4658	0.4550	0.4440	0.4326	0.4210
0.4210	0.4150	0.4086	0.4018	0.3946	0.3871	0.3793	0.3712	0.3629	0.3543
0.3493	0.3449	0.3401	0.3351	0.0329	0.3242	0.3183	0.3123	0.3060	0.2996
0.2922	0.2889	0.2853	0.2815	0.0277	0.2732	0.2687	0.2641	0.2592	0.2543
0.2461	0.2436	0.2408	0.2378	0.0234	0.2314	0.2280	0.2244	0.2207	0.2168
0.2085	0.2065	0.2043	0.2020	0.1995	0.1970	0.1943	0.1914	0.1885	0.1855
0.0475	0.0473	0.0470	0.0467	0.0463	0.0460	0.0456	0.0452	0.0446	0.0444
0.0128	0.0127	0.0127	0.0126	0.0125	0.0125	0.0124	0.0123	0.0123	0.0122
0.0037	0.0037	0.0037	0.0037	0.0037	0.0037	0.0036	0.0036	0.0036	0.0036
0.0011	0.0011	0.0011	0.0011	0.0011	0.0011	0.0011	0.0011	0.0011	0.0011
0.0004	0.0004	0.0004	0.0004	0.0004	0.0004	0.0004	0.0004	0.0004	0.0004
0.0001	0.0001	0.0001	0.0001	0.0001	0.0001	0.0001	0.0001	0.0001	0.0001
0	0	0	0	0	0	0	0	0	0

(Continued)

Appendix F: (Continued)

u \ r/B	1.0	1.5	2.0	2.5	3.0	3.5	4.0	4.5	5.0	6.0	7.0	8.0	9.0
0	0.8420	0.4276	0.2278	0.1247	0.0695	0.0392	0.0223	0.0128	0.0074	0.0025	0.0008	0.0003	0.0001
.01	0.8420	0.4276	0.2278	0.1247	0.0695	0.0392	0.0223	0.0128	0.0074	0.0025	0.0008	0.0003	0.0001
.02	0.8420	0.4276	0.2278	0.1247	0.0695	0.0392	0.0223	0.0128	0.0074	0.0025	0.0008	0.0003	0.0001
.03	0.8420	0.4276	0.2278	0.1247	0.0695	0.0392	0.0223	0.0128	0.0074	0.0025	0.0008	0.0003	0.0001
.04	0.8418	0.4276	0.2278	0.1247	0.0695	0.0392	0.0223	0.0128	0.0074	0.0025	0.0008	0.0003	0.0001
.05	0.8409	0.4276	0.2278	0.1247	0.0695	0.0392	0.0223	0.0128	0.0074	0.0025	0.0008	0.0003	0.0001
.06	0.8391	0.4276	0.2278	0.1247	0.0695	0.0392	0.0223	0.0128	0.0074	0.0025	0.0008	0.0003	0.0001
.07	0.8360	0.4276	0.2278	0.1247	0.0695	0.0392	0.0223	0.0128	0.0074	0.0025	0.0008	0.0003	0.0001
.08	0.8316	0.4275	0.2278	0.1247	0.0695	0.0392	0.0223	0.0128	0.0074	0.0025	0.0008	0.0003	0.0001
.09	0.8259	0.4274	0.2278	0.1247	0.0695	0.0392	0.0223	0.0128	0.0074	0.0025	0.0008	0.0003	0.0001
.1	0.8190	0.4271	0.2278	0.1247	0.0695	0.0392	0.0223	0.0128	0.0074	0.0025	0.0008	0.0003	0.0001
.2	0.7148	0.4135	0.2268	0.1247	0.0695	0.0392	0.0223	0.0128	0.0074	0.0025	0.0008	0.0003	0.0001
.3	0.6010	0.3812	0.2211	0.1240	0.0694	0.0392	0.0223	0.0128	0.0074	0.0025	0.0008	0.0003	0.0001
.4	0.5024	0.3411	0.2096	0.1217	0.0691	0.0392	0.0223	0.0128	0.0074	0.0025	0.0008	0.0003	0.0001
.5	0.4210	0.3007	0.1944	0.1174	0.0681	0.0390	0.0223	0.0128	0.0074	0.0025	0.0008	0.0003	0.0001
.6	0.3543	0.2630	0.1774	0.1112	0.0664	0.0386	0.0222	0.0128	0.0074	0.0025	0.0008	0.0003	0.0001
.7	0.2996	0.2292	0.1602	0.1040	0.0639	0.0379	0.0221	0.0127	0.0074	0.0025	0.0008	0.0003	0.0001
.8	0.2543	0.1994	0.1436	0.0961	0.0607	0.0368	0.0218	0.0127	0.0074	0.0025	0.0008	0.0003	0.0001
.9	0.2168	0.1734	0.1281	0.0881	0.0572	0.0354	0.0213	0.0125	0.0073	0.0025	0.0008	0.0003	0.0001
1.0	0.1855	0.1509	0.1139	0.0803	0.0534	0.0338	0.0207	0.0123	0.0073	0.0025	0.0008	0.0003	0.0001
2.0	0.0444	0.0394	0.0335	0.0271	0.0210	0.0156	0.0112	0.0077	0.0051	0.0021	0.0008	0.0003	0.0001
3.0	0.0122	0.0112	0.0100	0.0086	0.0071	0.0057	0.0045	0.0034	0.0025	0.0012	0.0006	0.0003	0.0001
4.0	0.0036	0.0034	0.0031	0.0027	0.0024	0.0020	0.0016	0.0013	0.0010	0.0006	0.0003	0.0002	0.0001
5.0	0.0011	0.0010	0.0010	0.0009	0.0008	0.0007	0.0006	0.0005	0.0004	0.0002	0.0001	0.0001	0
6.0	0.0004	0.0003	0.0003	0.0003	0.0003	0.0002	0.0002	0.0002	0.0002	0.0001	0.0001	0	0
7.0	0.0001	0.0001	0.0001	0.0001	0.0001	0.0001	0.0001	0.0001	0.0001	0	0	0	0
8.0	0	0	0.0000	0	0	0	0	0	0	0	0	0	0

Appendix G: *Hantush (1956) well function $H(u,\beta)$ for a leaky aquifer*

u	β							
	0.03	*0.1*	*0.3*	*1*	*3*	*10*	*30*	*100*
1×10^{-9}	12.3088	11.1051	10.0066	8.8030	7.7051	6.5033	5.4101	4.2221
2	11.9622	10.7585	9.6602	8.4566	7.3590	6.1579	5.0666	3.8839
3	11.7593	10.5558	9.4575	8.2540	7.1565	5.9561	4.8661	3.6874
5	11.5038	10.3003	9.2021	7.9987	6.9016	5.7020	4.6142	3.4413
7	11.3354	10.1321	9.0339	7.8306	6.7337	5.5348	4.4487	3.2804
1×10^{-8}	11.1569	9.9538	8.8556	7.6525	6.5558	5.3578	4.2737	3.1110
2	10.8100	9.6071	8.5091	7.3063	6.2104	5.0145	3.9352	2.7858
3	10.6070	9.4044	8.3065	7.1039	6.0085	4.8141	3.7383	2.5985
5	10.3511	9.1489	8.0512	6.8490	5.7544	4.5623	3.4919	2.3662
7	10.1825	8.9806	7.8830	6.6811	5.5872	4.3969	3.3307	2.2159
1×10^{-7}	10.0037	8.8021	7.7048	6.5032	5.4101	4.2221	3.1609	2.0591
2	9.6560	8.4554	7.3585	6.1578	5.0666	3.8839	2.8348	1.7633
3	9.4524	8.2525	7.1560	5.9559	4.8661	3.6874	2.6469	1.5966
5	9.1955	7.9968	6.9009	5.7018	4.6141	3.4413	2.4137	1.3944
7	9.0261	7.8283	6.7329	5.5346	4.4486	3.2804	2.2627	1.2666
1×10^{-6}	8.8463	7.6497	6.5549	5.3575	4.2736	3.1110	2.1051	1.1361
2	8.4960	7.3024	6.2091	5.0141	3.9350	2.7857	1.8074	0.8995
3	8.2904	7.0991	6.0069	4.8136	3.7382	2.5984	1.6395	0.7725
5	8.0304	6.8427	5.7523	4.5617	3.4917	2.3661	1.4354	0.6256
7	7.8584	6.6737	5.5847	4.3962	3.3304	2.2158	1.3061	0.5375
1×10^{-5}	7.6754	6.4944	5.4071	4.2212	3.1606	2.0590	1.1741	0.4519
2	7.3170	6.1453	5.0624	3.8827	2.8344	1.7632	0.9339	0.3091
3	7.1051	5.9406	4.8610	3.6858	2.6464	1.5965	0.8046	0.2402
5	6.8353	5.6821	4.6075	3.4394	2.4131	1.3943	0.6546	0.1685
7	6.6553	5.5113	4.4408	3.2781	2.2619	1.2664	0.5643	0.1300
1×10^{-4}	6.4623	5.3297	4.2643	3.1082	2.1042	1.1359	0.4763	963(−4)

(*Continued*)

Appendix G: (Continued)

u	β							
	0.03	*0.1*	*0.3*	*1*	*3*	*10*	*30*	*100*
2	6.0787	4.9747	3.9220	2.7819	1.8062	0.8992	0.3287	494(−4)
3	5.8479	4.7655	3.7222	2.5937	1.6380	0.7721	0.2570	315(−4)
5	5.5488	4.4996	3.4711	2.3601	1.4335	0.6252	0.1818	166(−4)
7	5.3458	4.3228	3.3062	2.2087	1.3039	0.5370	0.1412	103(−4)
1×10^{-3}	5.1247	4.1337	3.1317	2.0506	1.1715	0.4513	0.1055	390(−5)
2	4.6753	3.7598	2.7938	1.7516	0.9305	0.3084	551(−4)	169(−5)
3	4.3993	3.5363	2.5969	1.5825	0.8006	0.2394	355(−4)	713(−6)
5	4.0369	3.2483	2.3499	1.3767	0.6498	0.1677	190(−4)	205(−6)
7	3.7893	3.0542	2.1877	1.2460	0.5589	0.1292	120(−4)	821(−7)
1×10^{-2}	3.5195	2.8443	2.0164	1.1122	0.4702	955(−4)	695(−5)	274(−7)
2	2.9759	2.4227	1.6853	0.8677	0.3214	487(−4)	205(−5)	226(−8)
3	2.6487	2.1680	1.4932	0.7353	0.2491	308(−4)	888(−6)	0
5	2.2312	1.8401	1.2535	0.5812	0.1733	160(−4)	261(−6)	0
7	1.9558	1.6213	1.0979	0.4880	0.1325	982(−5)	106(−6)	0
1×10^{-1}	1.6667	1.3893	.9358	0.3970	966(−4)	552(−5)	365(−7)	0
2	1.1278	0.9497	.6352	0.2452	468(−4)	149(−5)	307(−8)	0
3	0.8389	0.7103	.4740	0.1729	281(−4)	592(−6)	0	0
5	0.5207	0.4436	.2956	0.1006	130(−4)	151(−6)	0	0
7	0.3485	0.2980	.1985	646(−4)	714(−5)	534(−7)	0	0
1×1	0.2050	0.1758	.1172	365(−4)	337(−5)	151(−7)	0	0
2	458(−4)	395(−4)	264(−4)	760(−5)	487(−6)	0	0	0
3	122(−4)	106(−4)	707(−5)	196(−5)	102(−6)	0	0	0
5	108(−5)	934(−6)	624(−6)	167(−6)	672(−8)	0	0	0
7	109(−6)	941(−7)	629(−7)	165(−7)	0	0	0	0
1×10	391(−8)	339(−8)	227(−8)	0	0	0	0	0

Appendix H: *Papadopulos and Cooper (1967) well function* $S(u_w, \rho')$ *for large diameter wells*

u_w	$\rho' = 10^{-1}$	$\rho' = 10^{-2}$	$\rho' = 10^{-3}$	$\rho' = 10^{-4}$	$\rho' = 10^{-5}$
10	9.755×10^{-3}	9.976×10^{-4}	9.998×10^{-5}	1.000×10^{-5}	1.000×10^{-6}
1	9.192×10^{-2}	9.914×10^{-3}	9.991×10^{-4}	1.000×10^{-4}	1.000×10^{-5}
5×10^{-1}	1.767×10^{-1}	1.974×10^{-2}	1.997×10^{-3}	2.000×10^{-4}	2.000×10^{-5}
2×10^{-1}	4.062×10^{-1}	4.890×10^{-2}	4.989×10^{-3}	4.999×10^{-4}	5.000×10^{-5}
1×10^{-1}	7.336×10^{-1}	9.665×10^{-2}	9.966×10^{-3}	9.997×10^{-4}	1.000×10^{-4}
5×10^{-2}	1.260	1.896×10^{-1}	1.989×10^{-2}	1.999×10^{-3}	2.000×10^{-4}
2×10^{-2}	2.303	4.529×10^{-1}	4.949×10^{-2}	4.995×10^{-3}	5.000×10^{-4}
1×10^{-2}	3.276	8.520×10^{-1}	9.834×10^{-2}	9.984×10^{-3}	1.000×10^{-3}
5×10^{-3}	4.255	1.540	1.945×10^{-1}	1.994×10^{-2}	2.000×10^{-3}
2×10^{-3}	5.420	3.043	4.725×10^{-1}	4.972×10^{-2}	4.998×10^{-3}
1×10^{-3}	6.212	4.545	9.069×10^{-1}	9.901×10^{-2}	9.992×10^{-3}
5×10^{-4}	6.960	6.031	1.688	1.965×10^{-1}	1.997×10^{-2}
2×10^{-4}	7.866	7.557	3.523	4.814×10^{-1}	4.982×10^{-2}
1×10^{-4}	8.572	8.443	5.526	9.340×10^{-1}	9.932×10^{-2}
5×10^{-5}	9.318	9.229	7.631	1.768	1.975×10^{-1}
2×10^{-5}	10.24	10.20	9.676	3.828	4.861×10^{-1}
1×10^{-5}	10.93	10.87	10.68	6.245	9.493×10^{-1}
5×10^{-6}	11.63	11.62	11.50	8.991	1.817
2×10^{-6}	12.55	12.54	12.49	11.74	4.033
1×10^{-6}	13.24	13.24	13.21	12.91	6.779
5×10^{-7}	13.93	13.93	13.92	13.78	10.13
2×10^{-7}	14.85	14.85	14.84	14.79	13.71
1×10^{-7}	15.54	15.54	15.54	15.51	15.13
5×10^{-8}	16.23	16.23	16.23	16.22	16.05
2×10^{-8}	17.05	17.05	17.05	17.14	17.08
1×10^{-9}	17.84	17.84	17.84	17.84	17.81
5×10^{-9}	18.54	18.54	18.54	18.54	18.51
2×10^{-9}	19.45	19.45	19.45	19.45	19.40
1×10^{-9}	20.15	20.15	20.15	20.15	20.15

Appendix I: *Flowing well function*

(a) Jacob and Lohman (1952) flowing well function $G(\alpha)$

α	$\times 10^{-4}$	$\times 10^{-3}$	$\times 10^{-2}$	$\times 10^{-1}$	$\times 1$	$\times 10$	$\times 10^{2}$	$\times 10^{3}$	$\times 10^{4}$	$\times 10^{5}$	$\times 10^{6}$	$\times 10^{7}$	$\times 10^{8}$	$\times 10^{9}$	$\times 10^{10}$	$\times 10^{11}$
1	56.9	18.34	6.13	2.249	0.985	0.534	0.346	0.251	0.1964	0.1608	0.1360	0.1177	0.1037	0.0927	0.0838	0.0764
2	40.4	13.11	4.47	1.716	0.803	0.461	0.311	0.232	0.1841	0.1524	0.1299	0.1131	0.1002	0.0899	0.0814	0.0744
3	33.1	10.79	3.74	1.477	0.719	0.427	0.294	0.222	0.1777	0.1479	0.1266	0.1106	0.0982	0.0882	0.0801	0.0733
4	28.7	9.41	3.30	1.333	0.667	0.405	0.283	0.215	0.1733	0.1449	0.1244	0.1089	0.0968	0.0872	0.0792	0.0726
5	25.7	8.47	3.00	1.234	0.630	0.389	0.274	0.210	0.1701	0.1426	0.1227	0.1076	0.0958	0.0864	0.0785	0.0720
6	23.5	7.77	2.78	1.160	0.602	0.377	0.268	0.206	0.1675	0.1408	0.1213	0.1066	0.0950	0.0857	0.0779	0.0716
7	21.8	7.23	2.60	1.103	0.580	0.367	0.263	0.203	0.1654	0.1393	0.1202	0.1057	0.0943	0.0851	0.0774	0.0712
8	20.4	6.79	2.46	1.057	0.562	0.359	0.258	0.200	0.1636	0.1380	0.1192	0.1049	0.0937	0.0846	0.0770	0.0709
9	19.3	6.43	2.35	1.018	0.547	0.352	0.254	0.198	0.1621	0.1369	0.1184	0.1043	0.0932	0.0842	0.0767	0.0706
10	18.3	6.13	2.25	0.985	0.534	0.346	0.251	0.196	0.1608	0.1360	0.1177	0.1037	0.0927	0.0838	0.0764	0.0704

Appendix I: (Continued)

(b) Hantush (1959) flowing well function $G(\alpha, r_w/B)$ for a confined aquifer with leakage

α \ r_w/B	0	1×10^{-5}	2×10^{-5}	4×10^{-5}	6×10^{-5}	8×10^{-5}	10^{-4}	2×10^{-4}	4×10^{-4}	6×10^{-4}	8×10^{-4}	10^{-3}	2×10^{-3}	4×10^{-3}	6×10^{-3}	8×10^{-3}	10^{-2}
1×10^2	0.346	0.346	0.346	0.346	0.346	0.346	0.346	0.346	0.346	0.346	0.346	0.346	0.346	0.346	0.346	0.346	0.346
2	0.311	0.311	0.311	0.311	0.311	0.311	0.311	0.311	0.311	0.311	0.311	0.311	0.311	0.311	0.311	0.312	0.312
3	0.294	0.294	0.294	0.294	0.294	0.294	0.294	0.294	0.294	0.294	0.294	0.294	0.294	0.294	0.294	0.295	0.295
4	0.283	0.283	0.283	0.283	0.283	0.283	0.283	0.283	0.283	0.283	0.283	0.283	0.283	0.283	0.283	0.284	0.285
5	0.274	0.274	0.274	0.274	0.274	0.274	0.274	0.274	0.274	0.274	0.274	0.274	0.274	0.274	0.275	0.275	0.276
6	0.268	0.268	0.268	0.268	0.268	0.268	0.268	0.268	0.268	0.268	0.268	0.268	0.268	0.268	0.268	0.269	0.271
7	0.263	0.263	0.263	0.263	0.263	0.263	0.263	0.263	0.263	0.263	0.263	0.263	0.263	0.263	0.263	0.264	0.266
8	0.258	0.258	0.258	0.258	0.258	0.258	0.258	0.258	0.258	0.258	0.258	0.258	0.258	0.258	0.259	0.260	0.261
9	0.254	0.254	0.254	0.254	0.254	0.254	0.254	0.254	0.254	0.254	0.254	0.254	0.254	0.255	0.256	0.257	0.258
1×10^3	0.251	0.251	0.251	0.251	0.251	0.251	0.251	0.251	0.251	0.251	0.251	0.251	0.251	0.252	0.252	0.254	0.255
2	0.232	0.232	0.232	0.232	0.232	0.232	0.232	0.232	0.232	0.232	0.232	0.232	0.232	0.233	0.234	0.236	0.239
3	0.222	0.222	0.222	0.222	0.222	0.222	0.222	0.222	0.222	0.222	0.222	0.222	0.222	0.223	0.225	0.227	0.231
4	0.215	0.215	0.215	0.215	0.215	0.215	0.215	0.215	0.215	0.215	0.215	0.215	0.215	0.216	0.219	0.222	0.226
5	0.210	0.210	0.210	0.210	0.210	0.210	0.210	0.210	0.210	0.210	0.210	0.210	0.210	0.212	0.215	0.218	0.222
6	0.206	0.206	0.206	0.206	0.206	0.206	0.206	0.206	0.206	0.206	0.206	0.206	0.206	0.208	0.211	0.215	0.220
7	0.203	0.203	0.203	0.203	0.203	0.203	0.203	0.203	0.203	0.203	0.203	0.203	0.203	0.205	0.209	0.213	0.219
8	0.201	0.201	0.201	0.201	0.201	0.201	0.201	0.201	0.201	0.201	0.201	0.201	0.201	0.203	0.207	0.212	0.218
9	0.198	0.198	0.198	0.198	0.198	0.198	0.198	0.198	0.198	0.198	0.198	0.198	0.198	0.201	0.205	0.210	0.217
1×10^4	0.196	0.196	0.196	0.196	0.196	0.196	0.196	0.196	0.196	0.196	0.196	0.196	0.197	0.200	0.204	0.209	0.216
2	0.185	0.185	0.185	0.185	0.185	0.185	0.185	0.185	0.185	0.185	0.185	0.185	0.185	0.190	0.197	0.205	0.213
3	0.178	0.178	0.178	0.178	0.178	0.178	0.178	0.178	0.178	0.178	0.178	0.178	0.179	0.186	0.194	0.203	0.212
4	0.173	0.173	0.173	0.173	0.173	0.173	0.173	0.173	0.173	0.173	0.173	0.173	0.176	0.183	0.193	0.202	0.212
5	0.170	0.170	0.170	0.170	0.170	0.170	0.170	0.170	0.170	0.170	0.170	0.170	0.173	0.181	0.192	0.202	0.212

(Continued)

Appendix I: (Continued)

α \ r_w/B	0	1×10^{-5}	2×10^{-5}	4×10^{-5}	6×10^{-5}	8×10^{-5}	10^{-4}	2×10^{-4}	4×10^{-4}	6×10^{-4}	8×10^{-4}	10^{-3}	2×10^{-3}	4×10^{-3}	6×10^{-3}	8×10^{-3}	10^{-2}
1×10^{6} 6	0.168	0.168	0.168	0.168	0.168	0.168	0.168	0.168	0.168	0.168	0.168	0.168	0.171	0.180	0.192	0.202	0.212
7	0.166	0.166	0.166	0.166	0.166	0.166	0.166	0.166	0.166	0.166	0.166	0.167	0.170	0.179	0.191	0.202	0.212
8	0.164	0.164	0.164	0.164	0.164	0.164	0.164	0.164	0.164	0.164	0.164	0.165	0.169	0.179	0.191	0.202	0.212
9	0.163	0.163	0.163	0.163	0.163	0.163	0.163	0.163	0.163	0.163	0.163	0.164	0.168	0.179	0.191	0.202	0.212
1×10^{5}	0.161	0.161	0.161	0.161	0.161	0.161	0.161	0.161	0.161	0.162	0.162	0.162	0.167	0.178	0.191	0.202	0.212
2	0.152	0.152	0.152	0.152	0.152	0.152	0.152	0.152	0.153	0.153	0.154	0.155	0.163	0.177	0.191	0.202	0.212
3	0.148	0.148	0.148	0.148	0.148	0.148	0.148	0.148	0.148	0.149	0.150	0.152	0.162	0.177	0.191	0.202	0.212
4	0.145	0.145	0.145	0.145	0.145	0.145	0.145	0.145	0.145	0.146	0.147	0.150	0.162	0.177	0.191	0.202	0.212
5	0.143	0.143	0.143	0.143	0.143	0.143	0.143	0.143	0.143	0.144	0.145	0.148	0.161	0.177	0.191	0.202	0.212
6	0.141	0.141	0.141	0.141	0.141	0.141	0.141	0.141	0.142	0.143	0.144	0.147	0.160	0.177	0.191	0.202	0.212
7	0.140	0.140	0.140	0.140	0.140	0.140	0.140	0.140	0.140	0.141	0.143	0.146	0.160	0.177	0.191	0.202	0.212
8	0.138	0.138	0.138	0.138	0.138	0.138	0.138	0.138	0.139	0.141	0.143	0.145	0.160	0.177	0.191	0.202	0.212
9	0.137	0.137	0.137	0.137	0.137	0.137	0.137	0.137	0.138	0.14	0.142	0.144	0.160	0.177	0.191	0.202	0.212
1×10^{6}	0.136	0.136	0.136	0.136	0.136	0.136	0.136	0.137	0.138	0.139	0.141	0.144	0.159	0.177	0.191	0.202	0.212
2	0.130	0.130	0.130	0.130	0.130	0.130	0.130	0.131	0.133	0.135	0.139	0.143	0.159	0.177	0.191	0.202	0.212
3	0.127	0.127	0.127	0.127	0.127	0.127	0.127	0.127	0.13	0.134	0.138	0.142	0.158	0.177	0.191	0.202	0.212
4	0.124	0.124	0.124	0.124	0.124	0.124	0.124	0.125	0.129	0.134	0.138	0.142	0.158	0.177	0.191	0.202	0.212
5	0.123	0.123	0.123	0.123	0.123	0.123	0.123	0.124	0.128	0.133	0.138	0.142	0.158	0.177	0.191	0.202	0.212
6	0.121	0.121	0.121	0.121	0.121	0.121	0.121	0.123	0.128	0.133	0.138	0.142	0.158	0.177	0.191	0.202	0.212
7	0.120	0.120	0.120	0.120	0.120	0.120	0.120	0.122	0.127	0.133	0.138	0.142	0.158	0.177	0.191	0.202	0.212
8	0.119	0.119	0.119	0.119	0.119	0.119	0.119	0.121	0.127	0.133	0.138	0.142	0.158	0.177	0.191	0.202	0.212
9	0.118	0.118	0.118	0.118	0.118	0.118	0.118	0.121	0.127	0.133	0.138	0.142	0.158	0.177	0.191	0.202	0.212
1×10^{7}	0.118	0.118	0.118	0.118	0.118	0.118	0.118	0.117	0.126	0.133	0.138	0.142	0.158	0.177	0.191	0.202	0.212
2	0.114	0.114	0.114	0.114	0.114	0.114	0.114	0.116	0.126	0.133	0.138	0.142	0.158	0.177	0.191	0.202	0.212
3	0.111	0.111	0.111	0.111	0.111	0.111	0.112	0.116	0.126	0.133	0.138	0.142	0.158	0.177	0.191	0.202	0.212
4	0.109	0.109	0.109	0.109	0.109	0.110	0.111	0.116	0.126	0.133	0.138	0.142	0.158	0.177	0.191	0.202	0.212
5	0.108	0.108	0.108	0.108	0.108	0.109	0.11	0.116	0.126	0.133	0.138	0.142	0.158	0.177	0.191	0.202	0.212
6	0.107	0.107	0.107	0.107	0.108	0.109	0.11	0.116	0.126	0.133	0.138	0.142	0.158	0.177	0.191	0.202	0.212

7	0.106	0.106	0.106	0.106	0.107	0.108	0.109	0.116	0.126	0.133	0.138	0.142	0.158	0.177	0.191	0.202	0.212
8	0.105	0.105	0.105	0.105	0.106	0.108	0.109	0.116	0.126	0.133	0.138	0.142	0.158	0.177	0.191	0.202	0.212
9	0.104	0.104	0.104	0.105	0.106	0.107	0.108	0.116	0.126	0.133	0.138	0.142	0.158	0.177	0.191	0.202	0.212
1×10^{8}	0.104	0.104	0.104	0.104	0.105	0.106	0.108	0.116	0.126	0.133	0.138	0.142	0.158	0.177	0.191	0.202	0.212
2	0.100	0.1000	0.101	0.102	0.103	0.105	0.107	0.116	0.126	0.133	0.138	0.142	0.158	0.177	0.191	0.202	0.212
3	0.0982	0.0982	0.086	0.100	0.103	0.105	0.107	0.116	0.126	0.133	0.138	0.142	0.158	0.177	0.191	0.202	0.212
4	0.0968	0.0968	0.0974	0.0994	0.102	0.105	0.107	0.116	0.126	0.133	0.138	0.142	0.158	0.177	0.191	0.202	0.212
5	0.0958	0.0958	0.0966	0.0989	0.102	0.105	0.107	0.116	0.126	0.133	0.138	0.142	0.158	0.177	0.191	0.202	0.212
6	0.0950	0.0951	0.0959	0.0986	0.102	0.105	0.107	0.116	0.126	0.133	0.138	0.142	0.158	0.177	0.191	0.202	0.212
7	0.0943	0.0944	0.0954	0.0984	0.102	0.105	0.107	0.116	0.126	0.133	0.138	0.142	0.158	0.177	0.191	0.202	0.212
8	0.0937	0.0939	0.0949	0.0982	0.102	0.105	0.107	0.116	0.126	0.133	0.138	0.142	0.158	0.177	0.191	0.202	0.212
9	0.0932	0.0934	0.0946	0.0981	0.102	0.105	0.107	0.116	0.126	0.133	0.138	0.142	0.158	0.177	0.191	0.202	0.212
1×10^{9}	0.0927	0.0930	0.0943	0.0980	0.102	0.105	0.107	0.116	0.126	0.133	0.138	0.142	0.158	0.177	0.191	0.202	0.212
2	0.0899	0.0906	0.0927	0.0977	0.102	0.105	0.107	0.116	0.126	0.133	0.138	0.142	0.158	0.177	0.191	0.202	0.212
3	0.0883	0.0893	0.0920	0.0976	0.102	0.105	0.107	0.116	0.126	0.133	0.138	0.142	0.158	0.177	0.191	0.202	0.212
4	0.0872	0.0885	0.0917	0.0976	0.102	0.105	0.107	0.116	0.126	0.133	0.138	0.142	0.158	0.177	0.191	0.202	0.212
5	0.0864	0.0880	0.0916	0.0976	0.102	0.105	0.107	0.116	0.126	0.133	0.138	0.142	0.158	0.177	0.191	0.202	0.212
6	0.0857	0.0876	0.0915	0.0976	0.102	0.105	0.107	0.116	0.126	0.133	0.138	0.142	0.158	0.177	0.191	0.202	0.212
7	0.0851	0.0873	0.0915	0.0976	0.102	0.105	0.107	0.116	0.126	0.133	0.138	0.142	0.158	0.177	0.191	0.202	0.212
8	0.0846	0.0870	0.0915	0.0976	0.102	0.105	0.107	0.116	0.126	0.133	0.138	0.142	0.158	0.177	0.191	0.202	0.212
9	0.0842	0.0869	0.0914	0.0976	0.102	0.105	0.107	0.116	0.126	0.133	0.138	0.142	0.158	0.177	0.191	0.202	0.212
1×10^{10}	0.0838	0.0867	0.0914	0.0976	0.102	0.105	0.107	0.116	0.126	0.133	0.138	0.142	0.158	0.177	0.191	0.202	0.212
2	0.0814	0.0862	0.0914	0.0976	0.102	0.105	0.107	0.116	0.126	0.133	0.138	0.142	0.158	0.177	0.191	0.202	0.212
3	0.0861	0.0860	0.0914	0.0976	0.102	0.105	0.107	0.116	0.126	0.133	0.138	0.142	0.158	0.177	0.191	0.202	0.212
4	0.0792	0.0860	0.0914	0.0976	0.102	0.105	0.107	0.116	0.126	0.133	0.138	0.142	0.158	0.177	0.191	0.202	0.212
5	0.0785	0.0860	0.0914	0.0976	0.102	0.105	0.107	0.116	0.126	0.133	0.138	0.142	0.158	0.177	0.191	0.202	0.212
6	0.0779	0.0860	0.0914	0.0976	0.102	0.105	0.107	0.116	0.126	0.133	0.138	0.142	0.158	0.177	0.191	0.202	0.212
7	0.0774	0.0860	0.0914	0.0976	0.102	0.105	0.107	0.116	0.126	0.133	0.138	0.142	0.158	0.177	0.191	0.202	0.212
8	0.0770	0.0860	0.0914	0.0976	0.102	0.105	0.107	0.116	0.126	0.133	0.138	0.142	0.158	0.177	0.191	0.202	0.212
9	0.0767	0.0860	0.0914	0.0976	0.102	0.105	0.107	0.116	0.126	0.133	0.138	0.142	0.158	0.177	0.191	0.202	0.212
10	0.0764	0.0860	0.0914	0.0976	0.102	0.105	0.107	0.116	0.126	0.133	0.138	0.142	0.158	0.177	0.191	0.202	0.212

Appendix J: *Chow's (1952) Function F(u)*

u	*W(u)*	*F(u)*	*u*	*W(u)*	*F(u)*	*u*	*W(u)*	*F(u)*
5.0E–05	9.3263	4.051	2.0E–03	5.6394	2.460	8.0E–02	2.0269	0.956
6.0E–05	9.1440	3.972	3.0E–03	5.2349	2.280	9.0E–02	1.9187	0.913
7.0E–05	8.9899	3.905	4.0E–03	4.9482	2.160	1.0E–01	1.8229	0.874
8.0E–05	8.8563	3.847	5.0E–03	4.7261	2.070	2.0E–01	1.2227	0.647
9.0E–05	8.7386	3.796	6.0E–03	4.5448	1.990	3.0E–01	0.9057	0.532
1.0E–04	8.6332	3.750	7.0E–03	4.3916	1.920	4.0E–01	0.7024	0.455
2.0E–04	7.9402	3.449	8.0E–03	4.2591	1.870	5.0E–01	0.5598	0.401
3.0E–04	7.5348	3.273	9.0E–03	4.1423	1.820	6.0E–01	0.4544	0.360
4.0E–04	7.2472	3.148	1.0E–02	4.0379	1.770	7.0E–01	0.3738	0.327
5.0E–04	7.0242	3.051	2.0E–02	3.3547	1.490	8.0E–01	0.3106	0.301
6.0E–04	6.8420	2.972	3.0E–02	2.9591	1.330	9.0E–01	0.2602	0.276
7.0E–04	6.6879	2.905	4.0E–02	2.6813	1.210	1.0E+00	0.2194	0.259
8.0E–04	6.5545	2.847	5.0E–02	2.4679	1.130	2.0E+00	4.89E–02	0.157
9.0E–04	6.4368	2.796	6.0E–02	2.2953	1.060	3.0E+00	1.31E–02	0.117
1.0E–03	6.3315	2.750	7.0E–02	2.1508	1.000	4.0E+00	3.78E–03	0.090
2.0E–03	5.6394	2.460	8.0E–02	2.0269	0.956	5.0E+00	1.15E–03	0.073

$F(u) = \dfrac{e^u}{2.302}\displaystyle\int_u^{\infty}\left(\dfrac{e^{-\tau}}{\tau}\right)d\tau$; and if $u < 10^{-3}$, then $F(u) = W(u)/2.302$

Appendix K: *Values for slug test type curves by Papadopulos et al (1973)*

$\beta = Tt/r_c^2$	H/H_0				
	$\alpha = 10^{-1}$	$\alpha = 10^{-2}$	$\alpha = 10^{-3}$	$\alpha = 10^{-4}$	$\alpha = 10^{-5}$
1.00×10^{-3}	0.9771	0.9920	0.9969	0.9985	0.9992
2.15×10^{-3}	0.9658	0.9876	0.9949	0.9974	0.9985
4.64×10^{-3}	0.9490	0.9807	0.9914	0.9954	0.9970
1.00×10^{-2}	0.9238	0.9693	0.9853	0.9915	0.9942
2.15×10^{-2}	0.8860	0.9505	0.9744	0.9841	0.9888
4.64×10^{-3}	0.8293	0.9187	0.9545	0.9701	0.9781
1.00×10^{-1}	0.7460	0.8655	0.9183	0.9434	0.9572
2.15×10^{-1}	0.6289	0.7782	0.8538	0.8935	0.9167
4.64×10^{-1}	0.4782	0.6436	0.7436	0.8031	0.8410
1.00×10^{0}	0.3117	0.4598	0.5729	0.6520	0.7080
2.15×10^{0}	0.1665	0.2597	0.3543	0.4364	0.5038
4.64×10^{0}	0.07415	0.1086	0.1554	0.2082	0.2620
7.00×10^{0}	0.04625	0.06204	0.08519	0.1161	0.1521
1.00×10^{1}	0.03065	0.03780	0.04821	0.06355	0.08378
1.40×10^{1}	0.02092	0.02414	0.02844	0.03492	0.04426
2.15×10^{1}	0.01297	0.01414	0.01545	0.01723	0.01999
3.00×10^{1}	0.009070	0.009615	0.01016	0.01083	0.01169
4.64×10^{1}	0.005711	0.005919	0.006111	0.006319	0.006554
7.00×10^{1}	0.003722	0.003809	0.003884	0.003962	0.004046
1.00×10^{2}	0.002577	0.002618	0.002653	0.002688	0.002725
2.15×10^{2}	0.001179	0.001187	0.001194	0.001201	0.001208

Appendix L: *Values of Hantush (1963) recharge mound function* $F(\alpha,\beta)=\int_0^1 erf\left(\alpha/\sqrt{\tau}\right).erf\left(\beta/\sqrt{\tau}\right)d\tau$

α \ β	0.02	0.04	0.06	0.08	0.10	0.14	0.18	0.22	0.26	0.30	0.34	0.38	0.42	0.46	0.50	0.54	0.58	0.62
0.02	0.0041	0.0073	0.0101	0.0125	0.0146	0.0184	0.0216	0.0243	0.0267	0.0288	0.0306	0.0322	0.0337	0.0349	0.0361	0.0371	0.0380	0.0387
0.04	0.0073	0.0135	0.0188	0.0236	0.0278	0.0353	0.0416	0.0470	0.0518	0.0559	0.0596	0.0628	0.0657	0.0683	0.0705	0.0725	0.0743	0.0759
0.06	0.0101	0.0188	0.0266	0.0335	0.0398	0.0509	0.0602	0.0684	0.0754	0.0817	0.0871	0.0920	0.0963	0.1001	0.1035	0.1065	0.1091	0.1115
0.08	0.0125	0.0236	0.0335	0.0425	0.0508	0.0652	0.0776	0.0884	0.0978	0.1060	0.1133	0.1197	0.1254	0.1305	0.1350	0.1389	0.1425	0.1456
0.10	0.0146	0.0278	0.0398	0.0508	0.0608	0.0786	0.0939	0.1072	0.1188	0.1290	0.1381	0.1461	0.1532	0.1595	0.1650	0.1700	0.1744	0.1783
0.14	0.0184	0.0353	0.0509	0.0652	0.0786	0.1025	0.1232	0.1414	0.1573	0.1714	0.1839	0.1941	0.2048	0.2135	0.2212	0.2281	0.2343	0.2397
0.18	0.0216	0.0416	0.0602	0.0776	0.0939	0.1232	0.1490	0.1716	0.1916	0.2094	0.2251	0.2391	0.2515	0.2626	0.2724	0.2812	0.2890	0.2959
0.22	0.0243	0.0470	0.0684	0.0884	0.1072	0.1414	0.1716	0.1984	0.2222	0.2433	0.2621	0.2789	0.2938	0.3071	0.3189	0.3295	0.3389	0.3472
0.26	0.0267	0.0518	0.0754	0.0978	0.1188	0.1573	0.1916	0.2222	0.2494	0.2737	0.2954	0.3147	0.3320	0.3474	0.3612	0.3735	0.3844	0.3941
0.30	0.0288	0.0559	0.0817	0.1060	0.1290	0.1714	0.1094	0.2433	0.2737	0.3009	0.3252	0.3470	0.3665	0.3839	0.3995	0.4134	0.4257	0.4368
0.34	0.0306	0.0596	0.0871	0.1133	0.1391	0.1839	0.2251	0.2621	0.2954	0.3252	0.3520	0.3761	0.3976	0.4169	0.4341	0.4495	0.4633	0.4756
0.38	0.0322	0.0628	0.0920	0.1197	0.1461	0.1949	0.2391	0.2789	0.3147	0.3470	0.3761	0.4022	0.4256	0.4466	0.4654	0.4823	0.4973	0.5108
0.42	0.0377	0.0657	0.0963	0.1254	0.1532	0.2048	0.2515	0.2938	0.3320	0.3665	0.3976	0.4256	0.4508	0.4734	0.4937	0.5119	0.5281	0.5427
0.46	0.0349	0.0683	0.1001	0.1305	0.1595	0.2135	0.2626	0.3071	0.3474	0.3839	0.4169	0.4466	0.4734	0.4975	0.5161	0.5385	0.5559	0.5715
0.50	0.0361	0.0705	0.1035	0.1350	0.1650	0.2212	0.2724	0.3189	0.3612	0.3995	0.4341	0.4654	0.4937	0.5191	0.5420	0.5626	0.5810	0.5975
0.54	0.0371	0.0725	0.1065	0.1389	0.1700	0.2281	0.2812	0.3295	0.3735	0.4134	0.4495	0.4823	0.5119	0.5385	0.5626	0.5842	0.6036	0.6209
0.58	0.0380	0.0743	0.1091	0.1425	0.1744	0.2343	0.2890	0.3389	0.3844	0.4257	0.4633	0.4973	0.5281	0.5559	0.5810	0.6036	0.6238	0.6420
0.62	0.0387	0.0759	0.1115	0.1456	0.1783	0.2397	0.2959	0.3472	0.3941	0.4368	0.4756	0.5108	0.5427	0.5715	0.5975	0.6209	0.6420	0.6609
0.66	0.0394	0.0773	0.1136	0.1484	0.1718	0.2445	0.3020	0.3547	0.4027	0.4466	0.4865	0.5227	0.5556	0.5854	0.6122	0.6364	0.6582	0.6778
0.70	0.0401	0.0785	0.1154	0.1509	0.1849	0.2488	0.3075	0.3612	0.4104	0.4553	0.4962	0.5334	0.5672	0.5977	0.6254	0.6503	0.6728	0.6929
0.74	0.0406	0.0796	0.1117	0.1531	0.1876	0.2526	0.3123	0.3671	0.4172	0.4630	0.5048	0.5429	0.5774	0.6087	0.6371	0.6627	0.6857	0.7064
0.78	0.0411	0.0806	0.1185	0.1550	0.1900	0.2559	0.3166	0.3722	0.4232	0.4699	0.5125	0.5513	0.5865	0.6185	0.6475	0.6736	0.6972	0.7184
0.82	0.0415	0.0814	0.1198	0.1567	0.1921	0.2589	0.3203	0.3768	0.4286	0.4760	0.5192	0.5587	0.5946	0.6272	0.6567	0.6834	0.7074	0.7291
0.86	0.0419	0.0822	0.1209	0.1582	0.1940	0.2615	0.3237	0.3808	0.4333	0.4813	0.5252	0.5653	0.6017	0.6348	0.6648	0.6920	0.7165	0.7386
0.90	0.0422	0.0828	0.1219	0.1595	0.1957	0.2638	0.3266	0.3844	0.4374	0.4860	0.5305	0.5711	0.6080	0.6416	0.6721	0.6996	0.7245	0.7469

0.94	0.0425	0.0834	0.1228	0.1607	0.1971	0.2658	0.3292	0.3875	0.4411	0.4902	0.5351	0.5762	0.6136	0.6476	0.6784	0.7063	0.7316	0.7543
0.98	0.0428	0.0839	0.1236	0.1617	0.1984	0.2676	0.3314	0.3902	0.4442	0.4938	0.5392	0.5807	0.6184	0.6528	0.6840	0.7123	0.7378	0.7608
1.00	0.0429	0.0842	0.1239	0.1622	0.1990	0.2684	0.3324	0.3914	0.4457	0.4955	0.5410	0.5827	0.6206	0.6552	0.6865	0.7150	0.7406	0.7638
1.20	0.0437	0.0858	0.1263	0.1654	0.2030	0.2740	0.3396	0.4001	0.4558	0.5070	0.5540	0.5969	0.6362	0.6719	0.7044	0.7339	0.7605	0.7846
1.40	0.0441	0.0866	0.1275	0.1669	0.2049	0.2767	0.3431	0.4043	0.4608	0.5127	0.5603	0.6039	0.6438	0.6801	0.7132	0.7432	0.7704	0.7949
1.80	0.0444	0.0871	0.1283	0.1680	0.2062	0.2785	0.3454	0.4071	0.4641	0.5165	0.5645	0.6086	0.6489	0.6856	0.7190	0.7494	0.7769	0.8018
2.00	0.0444	0.0871	0.1284	0.1681	0.2064	0.2787	0.3457	0.4075	0.4645	0.5169	0.5651	0.6092	0.6495	0.6863	0.7198	0.7502	0.7778	0.8027
2.20	0.0444	0.0872	0.1284	0.1682	0.2065	0.2788	0.3458	0.4076	0.4646	0.5171	0.5653	0.6094	0.6497	0.6865	0.7200	0.7505	0.7781	0.8030
2.50	0.0444	0.0872	0.1284	0.1682	0.2065	0.2788	0.3458	0.4077	0.4647	0.5172	0.5653	0.6095	0.6498	0.6867	0.7202	0.7506	0.7782	0.8032
3.00	0.0444	0.0872	0.1284	0.1682	0.2065	0.2789	0.3458	0.4077	0.4647	0.5172	0.5654	0.6095	0.6499	0.6867	0.7202	0.7506	0.7782	0.8032

Appendix L: (Continued)

α \ β	*0.66*	*0.70*	*0.74*	*0.78*	*0.82*	*0.86*	*0.90*	*0.94*	*0.98*	*1.00*	*1.20*	*1.40*	*1.80*	*2.00*	*2.20*	*2.50*	*3.00*
0.02	0.0394	0.0401	0.0406	0.0411	0.0415	0.0419	0.0422	0.0425	0.0428	0.0429	0.0437	0.0441	0.0444	0.0444	0.0444	0.0444	0.0444
0.04	0.0773	0.0785	0.0796	0.0806	0.0814	0.0822	0.0828	0.0834	0.0839	0.0842	0.0858	0.0866	0.0871	0.0871	0.0872	0.0882	0.0882
0.06	0.1136	0.1154	0.1171	0.1185	0.1198	0.1209	0.1219	0.1228	0.1236	0.1239	0.1263	0.1275	0.1283	0.1284	0.1284	0.1284	0.1284
0.08	0.1484	0.1509	0.1531	0.1550	0.1567	0.1582	0.1595	0.1606	0.1617	0.1622	0.1654	0.1669	0.1680	0.1681	0.1682	0.1682	0.1682
0.10	0.1818	0.1849	0.1876	0.1900	0.1921	0.1940	0.1957	0.1971	0.1984	0.1990	0.2030	0.2049	0.2062	0.2064	0.2065	0.2065	0.2065
0.14	0.2445	0.2488	0.2526	0.2559	0.2589	0.2615	0.2638	0.2658	0.2676	0.2684	0.2740	0.2777	0.2785	0.2787	0.2788	0.2788	0.2788
0.18	0.3020	0.3075	0.3123	0.3166	0.3203	0.3237	0.3266	0.3292	0.3314	0.3224	0.3396	0.3431	0.3454	0.3457	0.3454	0.3454	0.3454
0.22	0.3547	0.3612	0.3671	0.3722	0.3768	0.3808	0.3844	0.3875	0.3902	0.3914	0.4001	0.4043	0.4071	0.4075	0.4076	0.4077	0.4077
0.26	0.4027	0.4104	0.4172	0.4232	0.4286	0.4333	0.4374	0.4411	0.4442	0.4457	0.4558	0.4608	0.4641	0.4645	0.4646	0.4647	0.4647
0.30	0.4466	0.4553	0.4630	0.5699	0.5760	0.4813	0.4860	0.4902	0.4938	0.4955	0.5070	0.5127	0.5165	0.5159	0.5171	0.5172	0.5172

(Continued)

Appendix L: (Continued)

α \ β	*0.66*	*0.70*	*0.74*	*0.78*	*0.82*	*0.86*	*0.90*	*0.94*	*0.98*	*1.00*	*1.20*	*1.40*	*1.80*	*2.00*	*2.20*	*2.50*	*3.00*
0.34	0.4865	0.4962	0.5048	0.5125	0.5192	0.5252	0.5305	0.5351	0.5392	0.5410	0.5540	0.5603	0.5645	0.5651	0.5653	0.5653	0.5654
0.38	0.5227	0.5334	0.5429	0.5213	0.5587	0.5653	0.5711	0.5762	0.5807	0.5827	0.5969	0.6039	0.6086	0.6092	0.6094	0.6095	0.6095
0.42	0.5556	0.5672	0.5774	0.5865	0.5946	0.6017	0.6080	0.6136	0.6184	0.6206	0.6362	0.6438	0.6489	0.6495	0.6497	0.6498	0.6499
0.46	0.5854	0.5977	0.6087	0.6185	0.6272	0.6348	0.6416	0.6476	0.6528	0.6552	0.6719	0.6801	0.6856	0.6863	0.6865	0.6867	0.6867
0.50	0.6122	0.6254	0.6371	0.6475	0.6567	0.6648	0.7721	0.6784	0.6840	0.6865	0.7044	0.7132	0.7190	0.7198	0.7200	0.7202	0.7202
0.54	0.6364	0.6503	0.6627	0.6736	0.6834	0.6920	0.6996	0.7063	0.7123	0.7150	0.7379	0.7432	0.7494	0.7502	0.7505	0.7506	0.7506
0.58	0.6482	0.6728	0.6857	0.6972	0.7074	0.7165	0.7245	0.7316	0.7378	0.7406	0.7605	0.7704	0.7799	0.7778	0.7781	0.7782	0.7782
0.62	0.6778	0.6929	0.7064	0.7784	0.7291	0.7386	0.7469	0.7543	0.7608	0.7638	0.7846	0.7949	0.8018	0.8027	0.8030	0.8032	0.8032
0.66	0.7953	0.7110	0.7250	0.7375	0.7486	0.7584	0.7671	0.7748	0.7816	0.7846	0.8064	0.8171	0.8243	0.8252	0.8255	0.8257	0.8257
0.70	0.7110	0.7272	0.7417	0.7546	0.7660	0.7762	0.7852	0.7932	0.8002	0.8034	0.8259	0.8370	0.8445	0.8454	0.8458	0.8460	0.8460
0.74	0.7250	0.7414	0.7566	0.7698	0.7816	0.7921	0.8014	0.8096	0.8168	0.8201	0.8434	0.8549	0.8627	0.8636	0.8640	0.8642	0.8642
0.78	0.7375	0.7546	0.7698	0.7834	0.7956	0.8063	0.8159	0.8243	0.8317	0.8351	0.8591	0.8710	0.8789	0.8799	0.8803	0.8805	0.8805
0.82	0.7486	0.7660	0.7816	0.7956	0.8080	0.8190	0.8288	0.8374	0.8450	0.8485	0.8731	0.8853	0.8935	0.8945	0.8949	0.8951	0.8951
0.86	0.7584	0.7762	0.7921	0.8063	0.8190	0.8302	0.8402	0.8491	0.8569	0.8604	0.8855	0.8980	0.9065	0.9075	0.9079	0.9081	0.9081
0.90	0.7671	0.7852	0.8014	0.8159	0.8288	0.8402	0.8504	0.8594	0.8674	0.8710	0.8966	0.9094	0.9180	0.9191	0.9195	0.9187	0.9187
0.94	0.7748	0.7932	0.8096	0.8243	0.8374	0.8491	0.8594	0.8686	0.8767	0.8803	0.9064	0.9195	0.9282	0.9294	0.9298	0.9300	0.9300
0.98	0.7816	0.8002	0.8168	0.8317	0.8450	0.8569	0.8674	0.8767	0.8849	0.8886	0.9151	0.9284	0.9373	0.9384	0.9389	0.9391	0.9391
1.00	0.7846	0.8034	0.8201	0.8351	0.8485	0.8604	0.8710	0.8803	0.8886	0.8924	0.9191	0.9324	0.9414	0.9426	0.9430	0.9432	0.9433
1.20	0.8064	0.8259	0.8434	0.8591	0.8731	0.8855	0.8966	0.9064	0.9151	0.9191	0.9472	0.9614	0.9709	0.9722	0.9726	0.9728	0.9729
1.40	0.8171	0.8370	0.8549	0.8710	0.8853	0.8980	0.9094	0.9195	0.9284	0.9324	0.9614	0.9759	0.9858	0.9871	0.9875	0.9878	0.9878
1.80	0.8243	0.8445	0.8627	0.8789	0.8935	0.9065	0.9180	0.9282	0.9373	0.9414	0.9709	0.9858	0.9959	0.9972	0.9972	0.9879	0.9980
2.00	0.8252	0.8454	0.8636	0.8799	0.8945	0.9075	0.9191	0.9594	0.9384	0.9426	0.9722	0.9871	0.9972	0.9985	0.9990	0.9992	0.9934
2.20	0.8255	0.8458	0.8640	0.8803	0.8949	0.9079	0.9195	0.9298	0.9389	0.9430	0.9726	0.9875	0.9977	0.9990	0.9995	0.9997	0.9998
2.50	0.8257	0.8460	0.8642	0.8805	0.8951	0.9081	0.9197	0.9300	0.9391	0.9432	0.9728	0.9878	0.9979	0.9992	0.9997	1.0000	1.0000
3.00	0.8257	0.8460	0.8642	0.8805	0.8951	0.9081	0.9197	0.9300	0.9391	0.9433	0.9729	0.9878	0.9980	0.9993	0.9998	1.0000	1.0000

Bibliography

Bear, J. (1979). *Hydraulics of groundwater*, McGraw-Hill, New York.

Bouwer, H. (1978). *Groundwater hydrology,* McGraw Hill, New York.

De Wiest, R. J. M. (1965). *Geohydrology*, John Wiley & Sons, New York.

Hantush, M. S. (1964). "Hydraulics of wells." In: V. T. Chow ed., *Advances in hydroscience,* Academic Press, New York, 281–432.

Harr, M. E. (1962). *Groundwater and seepage*, McGraw Hill, New York.

Karamouz, M., Ahmadi, A., and Akhbari, M. (2011). *Groundwater hydrology: engineering planning and management,* CRC Press, Taylor & Francis Group, New York.

Misstear, B., Banks, D., and Clark, L. (2006). *Water wells and boreholes,* John Wiley & Sons, New York.

Schwartz, F. W., and Zhang, H. (2004). *Fundamentals of ground water,* John Wiley & Sons, New York.

Todd, D. K., and Mays, L. W. (2005). *Groundwater hydrology,* John Wiley & Sons, New York.

The complete bibliography can freely be accessed and downloaded from website http://www.mhhe.com/chahar/gh1

Index

T

U

V

W

Z